

UCLA

UCLA Electronic Theses and Dissertations

Title

Merging ozone and copper catalysis for C(sp³)–N bond coupling

Permalink

<https://escholarship.org/uc/item/1jz811s4>

Author

Moreno, Jose Antonio

Publication Date

2024

Peer reviewed|Thesis/dissertation

UNIVERSITY OF CALIFORNIA

Los Angeles

Merging ozone and copper catalysis for

C(sp³)-N bond coupling

A dissertation submitted in partial satisfaction of the

requirements for the degree Doctor of Philosophy

in Chemistry

by

Jose Antonio Moreno

2024

© Copyright by

Jose Antonio Moreno

2024

ABSTRACT OF THE DISSERTATION

Merging ozone and copper catalysis for

C(sp³)-N bond coupling

by

Jose Antonio Moreno

Doctor of Philosophy in Chemistry

University of California, Los Angeles, 2024

Professor Ohyun Kwon, Chair

This dissertation describes the development of a dealkenylative approach toward C(sp³)-N bond coupling which leverages the copper-catalyzed decomposition of hydroperoxyacetals, obtained by Criegee ozonolysis of alkenes, to produce alkyl radicals which subsequently undergo copper-mediated cross coupling with a variety of nitrogen nucleophiles. These methodologies allow for a diverse range of alkene substrates, many derived from naturally occurring and renewable terpenes, to be coupled with nitrogen nucleophiles to rapidly access several classes of valuable nitrogen-containing products of interest to the pharmaceutical, chemical biology, and materials chemistry sectors. This work provides a foundation for further development of transition metal-catalyzed deconstructive cross-coupling and establishes a novel paradigm for alkene reactivity as they relate to C(sp³)-N bond formation. The operational simplicity, cost-effective and accessible catalyst system, and novel reactivity suggest these methodologies could see widespread implementation in various industries, academic research, and total synthesis campaigns.

Chapter One provides background information on the chemistry and reactivity that underpins the dealkenylative functionalization platform and establishes the context of the dissertation work in the broader historical context of ozonolysis and peroxide decomposition by transition metals. Despite the rich history in this area, its exploitation for cross-coupling chemistry went relatively unreported until recently. A perspective on traditional and modern approaches to C–N bond formation will also be described, with a focus on modern C–N copper-catalyzed coupling of relevance to the current study.

Chapter Two describes the development of the aminodealkenylation reaction, wherein an alkene $C(sp^3)$ – $C(sp^2)$ σ -bond is used to construct a new $C(sp^3)$ –N bond with nitrogen nucleophiles. The unprecedented disconnections enabled by this deconstructive methodology allowed for rapid and economical access to pharmaceutical intermediates, enantiopure chiral amines, terpene-nucleoside conjugates as well as a novel, single-step nucleoside N-methylation protocol.

Chapter Three describes mechanistic studies undertaken to unravel the role of the copper catalyst in the aminodealkenylation reaction. Data from kinetic profiling experiments, control experiments, and spectral data are discussed as they relate to the proposed mechanism. The identification of the copper catalyst operating by a previously undescribed cooperative copper ion-pair mechanism will be highlighted.

Chapter Four discusses the development of the azide variant of the dealkenylation reaction manifold, dubbed azidodealkenylation. The application of this methodology toward the conversion of terpenes to pseudoalkaloid lactams will be detailed. Azidation strategies and their relevance will be generally discussed to provide context into the significance of the current work.

The dissertation of Jose Antonio Moreno is approved.

Miguel A. García-Garibay

William M. Gelbart

Yves F. Rubin

Ohyun Kwon, Committee Chair

University of California, Los Angeles

2024

“Quisieron enterrarnos, pero no sabían que éramos semilla”

-Ernesto Cardenal

To my parents, Patricia and Joaquin, with love and gratitude.

TABLE OF CONTENTS

Abstract of the Dissertation	ii
Committee Page	iv
Dedication Page	v
Table of Contents	vi
List of Figures	x
List of Schemes	xiv
List of Tables	xv
List of Abbreviations	xvi
Acknowledgements	xix
Biographical Sketch	xxvii
CHAPTER 1: History and development of metal-peroxide redox chemistry and copper mediated C–N coupling	1
1.1. Abstract	1
1.2. Introduction	1
1.3. History and development of metal-peroxide redox chemistry	2
1.4. Criegee ozonolysis and early applications of peroxide redox chemistry	7
1.5. The development of copper-mediated C–N coupling	10
1.6. Modern copper-peroxide redox chemistry for formation of C–N bonds	17
1.7. Conclusion	22
1.8. References	23
CHAPTER 2: Aminodealkenylation: Ozonolysis and Copper Catalysis Convert C(sp ³)–C(sp ²) Bonds to C(sp ³)–N Bonds	36

2.1. Abstract	36
2.2. Introduction.....	36
2.3. Reaction Design.....	39
2.4. Reaction Scope.....	40
2.5. Applications of aminodealkenylation: Chiral primary amines, N-methylation protocol, and terpene-nucleosides	46
2.6. Experimental	51
2.6.1. Materials and Methods.....	51
2.6.2. Substrate Preparation	52
2.6.3. Detection of side products under unoptimized conditions.....	56
2.6.4. Reaction Optimization	59
2.6.5. Experimental Procedures and Characterization Data	72
2.6.6. NMR Spectra Relevant to Chapter 2	195
2.7. References.....	350
 CHAPTER 3: Mechanism of aminodealkenylation: the unexpected role of CuCl 1,10- phenanthroline complex as a cooperative ion pair catalyst system	 365
3.1. Abstract	365
3.2. Mechanism studies.....	365
3.3. Synthesis of Cu Complexes	369
3.4. Control Experiments	371
3.5. UV–Vis Spectroscopy.....	373
3.6. Kinetic Studies	375
3.6.1. General considerations and procedures for the ReactIR reaction setup	375

3.6.2. Determination of the reaction order of (CuCl + Phen) catalyst	378
3.6.3. Determination of the reaction order of phthalimide	382
3.6.4. Determination of the reaction order of peroxide (alkene)	385
3.6.5. Determination of the reaction order of [(Phen) ₂ Cu]BF ₄	389
3.6.6. Determination of the reaction order of (CuCl + Et ₄ NCl).....	395
3.6.7. Determination of the reaction order of phenanthroline.....	402
3.6.8. Effect of chloride	408
3.7. TEMPO Trap Experiment.....	410
3.8. Mechanistic Discussion	412
3.8.1. Discussion of the mechanism.....	412
3.8.2. Rate law derivation and explanation of the reaction orders obtained in Section 3.6	420
3.9. Conclusion	427
3.10. References.....	429
CHAPTER 4: Azidodealkenylation.....	434
4.1. Abstract	434
4.2. Introduction.....	434
4.3. Results and Discussion	439
4.3.1. Scope of exomethylene alkenes	442
4.3.2. Reductive Cyclization of Azidoesters.....	443
4.4. Mechanism of dealkenylative azidation.....	445
4.5. Conclusion	446
4.6. References.....	448

4.7. Materials and Methods.....	456
4.7.1. Substrate Preparation	458
4.8. Experimental Procedures and Characterization Data	459
4.8.1. General procedure for azidation.....	459
4.8.2. Characterization data	460
4.8.3. General procedure for reduction	463
4.8.4. Characterization data	464
4.8.5. NMR Spectra Relevant to Chapter 4	466
4.9. References relevant to substrate preparation	474

LIST OF FIGURES

Figure 1.1 Discovery and early uses of hydrogen peroxide.....	3
Figure 1.2 Thermal decomposition of diacyl peroxides and formation of trityl radical.....	5
Figure 1.3 Mechanism of ozonolysis	8
Figure 1.4 Early metal-peroxide redox functionalization	10
Figure 1.5 Ullman & Goldberg C–N coupling	12
Figure 1.6 Chan-Lam coupling	13
Figure 1.7 Copper catalyzed N-alkylations	18
Figure 1.8 Recent C–N bond formation using peroxides and copper.....	20
Figure 2.1 Concept and development of dealkenylative C(sp ³)–N bond coupling	38
Figure 2.2 Substrate scope of nitrogen nucleophiles.	42
Figure 2.3 Scope of Alkenes	45
Figure 2.4 Application of dealkenylative C(sp ³)–N bond coupling in bioactive compound synthesis.....	49
Figure 2.5: Substrates used in aminodealkenylation reactions	53
Figure 2.6 Preliminary results and side products of copper-catalyzed aminodealkenylation.....	57
Figure 2.7 Preliminary mechanistic explanation for the formation of the byproducts	59
Figure 2.8 Graphical guide for a large-scale reaction.....	77
Figure 2.9 Graphical guide for the 20-mmol-scale synthesis of m ^{6,6} A.....	180
Figure 2.10 ¹ H NMR spectrum of the m ^{6,6} A sample prepared without column chromatography	182
Figure 2.11 Previous routes for the synthesis of enantiopure 3-indazolyl-2-methylpropanols ..	186
Figure 2.12 Previous routes for the synthesis of enantiopure 4-methyl-3-cyclohexenamine.....	187

Figure 2.13 Previous route for the synthesis of 5-amino-3-methylpentan-1-ol.....	188
Figure 2.14 Previous route for the synthesis of (<i>S</i>)-2-(4-methylcyclohex-3-en-1-yl)isoindoline-1,3-dione.....	189
Figure 2.15 Previous routes for the synthesis of (1 <i>R</i> ,3 <i>R</i> ,4 <i>R</i>)-3-hydroxy-4-methylcyclohexan-1-aminium chloride	190
Figure 2.16 Previous routes for the synthesis of m ⁶ A and D ₃ -m ⁶ A.....	191
Figure 2.17 Previous routes for the synthesis of m ^{6,6} A	192
Figure 2.18 Previous routes for m ⁶ dA synthesis.....	192
Figure 2.19 Previous routes for the synthesis of m ⁴ C.....	193
Figure 2.20 Previous routes for the synthesis of m ⁴ dC.....	194
Figure 3.1 (A) Comparison of different copper complexes. (B) Kinetic studies. (C) Proposed mechanism	367
Figure 3.2 Crystals of complex 3-2.....	371
Figure 3.3 UV–Vis absorption spectra of copper complexes	374
Figure 3.4 UV–Vis absorption spectra of copper salt, phthalimide and ammonium salts.....	375
Figure 3.5 Reaction setup before addition of the peroxide solution.	378
Figure 3.6 VTNA to determine the reaction order of (CuCl + Phen) on 3-15 generation.....	380
Figure 3.7 VTNA to determine the reaction order of (CuCl+ Phen) on MeOAc generation.	381
Figure 3.8 VTNA to determine the reaction order of phthalimide on 3-15 generation.	384
Figure 3.9 VTNA to determine the reaction order of phthalimide on MeOAc generation.	384
Figure 3.10 VTNA to determine the reaction order of peroxide on 3-15 generation.	388
Figure 3.11. VTNA to determine the reaction order of peroxide on MeOAc generation.....	388

Figure 3.12 VTNA to determine the reaction order of complex 3-5 on 3-15 generation (from 0.5 mol % to 4.0 mol %) using 2.0 mol % of (CuCl + TEACl).	392
Figure 3.13 VTNA to determine the reaction order of complex 3-5 on MeOAc generation (from 0.5 to 4.0 mol %) using 2.0 mol % of (CuCl + TEACl).....	392
Figure 3.14 VTNA to determine the reaction order of complex 3-5 on 3-15 generation (from 0 to 0.5 mol %) using 2.0 mol % of (CuCl + TEACl).	393
Figure 3.15 VTNA to determine the reaction order of complex 3-5 on MeOAc generation (from 0 to 0.5 mol %) using 2.0 mol % of (CuCl + TEACl).	394
Figure 3.16 VTNA to determine the reaction order of (CuCl + Et ₄ NCl) (from 2.0 to 4.0 mol %) on 3-15 generation using 2.0 mol % of [(Phen) ₂ Cu]BF ₄	398
Figure 3.17 VTNA to determine the reaction order of (CuCl + Et ₄ NCl) (from 2.0 to 4.0 mol %) on MeOAc generation using 2.0 mol % of [(Phen) ₂ Cu]BF ₄	398
Figure 3.18 VTNA to determine the reaction order of (CuCl + Et ₄ NCl) (from 1.0 to 2.0 mol %) on 3-15 generation using 0.5 mol % of [(Phen) ₂ Cu]BF ₄	400
Figure 3.19 VTNA to determine the reaction order of (CuCl + Et ₄ NCl) (from 1.0 to 2.0 mol %) on MeOAc generation using 0.5 mol % of [(Phen) ₂ Cu]BF ₄	401
Figure 3.20 VTNA to determine the reaction order of phenanthroline (from 2.0 to 4.0 mol %) on 3-15 generation using 4.0 mol % of CuCl.	404
Figure 3.21 VTNA to determine the reaction order of phenanthroline (from 2.0 to 4.0 mol %) on MeOAc generation using 4.0 mol % of CuCl.....	405
Figure 3.22 VTNA to determine the reaction order of phenanthroline (from 4.0 to 8.0 mol %) on 3-15 generation using 4.0 mol % of CuCl.	405

Figure 3.23 VTNA to determine the reaction order of phenanthroline (from 4.0 to 8.0 mol %) on MeOAc generation using 4.0 mol % of CuCl.....	406
Figure 3.24 Reaction profile using 4.0 mol % of complex 3-5 in the absence and presence of chloride anions.....	410
Figure 3.25 Proposed mechanism with known reaction constants	414
Figure 3.26 Color changes of the reaction when using CuCl + Phen, [CuCl ₂] ⁻ , or [(Phen) ₂ Cu] ⁺	414
Figure 3.27 Redox processes between copper dichloride species and peroxides	416
Figure 3.28 Copper dichloride–catalyzed decomposition of the peroxide	418
Figure 3.29 Mass spectral (MS) evidence for the generation of the peroxide H.....	419
Figure 3.30 Proposed reaction pathways of the alkyl radical B	423
Figure 3.31 Proposed phenanthroline dissociation from Cu-8 and association to Cu-2.....	426
Figure 4.1: a. Medicinally important aliphatic azides b. Traditional azide synthesis c. Modern azide synthesis.	436
Figure 4.2 Methylidene Cycloalkene Substrate Scope	442
Figure 4.3 Reductive Cyclization of Azidoesters	444

LIST OF SCHEMES

Scheme 1.1 Metal mediated beta-scission	6
Scheme 1.2 Thermal decomposition of hydroperoxide	6
Scheme 1.3 Mechanism of asymmetric copper-catalyzed C–N coupling by Fu and Peters.....	16
Scheme 1.4 Dialkyl peroxides as alkyl radical precursors	18
Scheme 1.5 Mechanism of ring expansion/cross-coupling cascade by Guo & Duan	21
Scheme 4.1: Reaction design of dealkenylative azidation & reductive cyclization	438
Scheme 4.2 Proposed mechanism of dealkenylative azidation	446

LIST OF TABLES

Table 2.1 Survey of the reaction solvents	61
Table 2.2 Survey of the copper salts	63
Table 2.3 Ligand Survey	65
Table 2.4 Alkene to amine ratio screen	66
Table 2.5 Relationship between the Criegee ozonolysis and the overall product yield	69
Table 2.6 Impact of ligands on diastereoselectivity	71
Table 3.1 Comparison of different Cu complexes	372
Table 4.1 Cu(I) Salt Optimization	439
Table 4.2 Optimization of catalyst loading and solvent	440
Table 4.3 Impacts of ligand, reaction scale and N ₃ source	441

LIST OF ABBREVIATIONS

AMS	alpha-methylstyrene
aq	aqueous
Ar	aryl
br	broad
Boc	tert-butyloxycarbonyl
Bz	benzoyl
Bu	butyl
CAM	cerium ammonium molybdate
Cbz	benzyloxycarbonyl
cm	centimeter
d	doublet
DART	direct analysis in real time
DCE	dichloroethane
DCM	dichloromethane
d.r.	diastereomeric ratio
e.e.	enantiomeric excess
EtOAc	ethyl acetate
ESI	electrospray ionization
Et	ethyl
Et ₂ O	diethyl ether
FCC	flash column chromatography
Fmoc	9-Fluorenylmethyloxycarbonyl

g	gram
hr	hour
HAD	hydrogen atom donor
HAT	hydrogen atom transfer
HPLC	high-performance liquid chromatography
HRMS	high-resolution mass spectrometry
Hz	hertz
IR	infrared radiation
i-Pr	isopropyl
L	liter
LAH	lithium aluminum hydride
m	multiplet
mCPBA	meta-chloroperoxybenzoic acid
Me	methyl
MeCN	acetonitrile
MeOH	methanol
mg	milligram
MHz	megahertz
min	minute
mL	milliliter
mm	millimeter
mmol	millimole
MMPP	magnesium monoperoxyphthalate

MP	melting point
Ms	methanesulfonyl (mesyl)
m/z	mass-to-charge ratio
NMR	nuclear magnetic resonance
NR	no reaction
Ph	phenyl
phen	1,10-phenanthroline
ppm	parts per million
Pr	propyl
Py	pyridyl
q	quartet
quint	quintet
R _f	retention factor
r.r.	regioisomeric ratio
rt	room temperature
s	singlet
SET	single electron transfer
t	triplet
temp	temperature
THF	tetrahydrofuran
TLC	thin-layer chromatography
Ts	toluenesulfonyl (tosyl)
UV	Ultraviolet

ACKNOWLEDGEMENTS

First I would like to thank my thesis advisor, Professor Ohyun Kwon. You have taught me so much during our time together and for that I am forever grateful. Your lab has provided so many opportunities for me to grow as a scientist and a person. Thank you for all you have done and continue to do for me and the next generation of chemists you will undoubtedly inspire.

To the esteemed members of my committee, Professor Miguel Garcia-Garibay, Professor William Gelbart, and Professor Yves Rubin – I appreciate your time and efforts during my PhD journey. Thank you for always being a source of support, guidance and inspiration.

As I reflect on the path that led me here, there are so many people who have inspired and helped me on the way. I must thank my Mom and Dad, Patrica & Joaquin, for doing all they could to allow me to achieve my dreams of being a scientist and helping the world. You both worked in the fields most your lives doing back-breaking work to provide for me and the family. I still remember my mom telling me, “You can work hard in the fields or you can work hard in school but people like us, we don’t have a choice. *We have* to work hard”. I acknowledge and am so very grateful for your sacrifice – your actions and words inspire my work ethic to this day.

Thank you for everything, I love you!

To my brothers and sisters, Ralphie, Rubin, Alonso, Zenayda, Francisco, Lucy, Nico, Chico, Patty thank you from the bottom of my heart for the immense love and support throughout the years. From Lucy taking me to preschool every morning to Patty helping me navigate my first semester of community college, you all have been there for me in so many ways at many points along my path. Your nerdy little brother is finally a doctor! We did it!! To my nieces and nephews, I hope I can serve as inspiration as to what is possible with dedication and hard work. To my Tia Ramona, thank you for all the love you’ve shown me. I still have warm memories of

you reading books to me when I was very small. You are a big reason why I loved to read as a kid, and *the* reason I learned to read in Spanish! Your patience and encouragement helped prime me to do well in school and in life. Thank you Tia! To my late Tia Victoria, you always had stacks of amazing books for me to read and you further fueled my passion for reading. You once sent me a check to help me buy one of my books at UC Davis. I was working full time in lab and taking classes, so money was tight and I was eating ramen noodles for just about every meal back then, so your support meant so much to me. Love you and Tio Don both, and you're deeply missed Tia Vicky. To my Tia Tina, thank you for helping me see the world and planning the best trips for the family! I have such great memories of us, and you helped me understand the wider context of the world that I would have otherwise not been able to grasp. Love you! To my Tia Mona and Tio Abel, thank you for bringing me into your church and helping me grow to be a good person. You two introduced me to one of my greatest passions in life – the guitar and music! To this day it's one of my favorite ways to destress and have fun. Thank you both for such a wonderful gift. A big thank you to my cousin, Marc! My life would be much different without you man. You allowed me to experience higher education at a university for the first time – I'm not sure I would have been able to attend UCB without you opening your home to me. You were my first role model, the first family member I learned had a doctorate, and a shining example of what was attainable. I am extremely proud of all that you've accomplished and inspired by what you continue to do. Much love Marc, thank you!

To my partner Jason – thank you for always being my best friend and loudest supporter. You reminded me of my strength when I doubted myself and you've been my shelter through the storms. While we've weathered a number of historical moments together, we have basked in some of the best moments of my life and I couldn't think of anyone I'd rather have by my side

through it all. I would not be where I am today without your unwavering love and support. You are such an amazing, caring person, a certified goofball, and my favorite human. I am honored to call you my partner and I look forward to continuing to build a wonderful future hand-in-hand with you. I love you babes!

To my friends, my chosen family, so many of you have helped me on this journey in countless ways. To my best friend Eric Hjelm, where do I begin? Through example, you showed me what was possible. I remember you taking the 6 a.m. bus every day, even after playing D&D all night, to get to classes in Merced. The next semester, I did the same. You moved to Merced to be closer to school and the next semester I moved in with you. You've been instrumental in my success and you've always believed in me. Unprompted you bought me my first laptop to help with school. Years later you took me shopping for nice clothes for my grad school interview and you and Sally drove me to Irvine to get to my visitation. My brother, I'm so honored to call you my friend. You are a phenomenal human and the epitome of "homies help homies, always". Thank you for all the deep talks, late night skates around town, and for constantly fireballing the party. Love you man! Sally, I still remember sitting next to you in our first organic chemistry class and we've both been in college nearly constantly since. You've remained a shining example of dedication and perseverance, and its been an inspiration to see all that you've accomplished. Thank you for being such a wonderful friend, for all the fun game nights, and all you have done to help me get to this point. Love yooouuuu! To Carolina, my forever vecina regardless of how far apart we actually are, my sister from another mister – I love you so so much, thank you for everything! You've been a constant source of support, guidance, inspiration, amazing music, photos, and my most fun memories. You are always there for me no matter what and I truly appreciate you. To the rest of the Nava clan, thank you for taking me in as family. To Ale, you

are one of the sweetest and most hilarious people I've had the pleasure of getting to know. Thank you for all your help with my pup Jelly, it really meant so much to me. Love you! Thank you to Thelma for all the love, good food, and the dishes she gave me for my new place in Davis. Thank you to Alejandro for all the laughs and fun music, to Tio Pancho for the asada and Modelos, and Chelly, who makes the BEST tea. To the Libby clan, Aaron, you so quickly became one of my favorite people and I really appreciate all the fun times we've shared, especially during grad school – doing things with you and Caro was always such a welcomed reset. To Aelish, I adore you, thanks for always being such a sweetheart. Thank you to Raquel for being one of my oldest and steadfast friends and honorary sibling. Near or far it is constant laughter whenever you and I talk. We learned so much from each other growing up, and I wouldn't change a thing. Love ya Rux! Thanks to Gracie for enduring our shenanigans throughout the years. To my dearest friend Monica, thank you for being such a smart cookie and for helping me organize my first class as an instructor. Your guidance was instrumental to my success and I appreciate you and your friendship. Misty, thank you for giving me the courage to dive back into school. I still remember staying up late at the kitchen table doing o-chem problems and quizzing each other on the whiteboard. Thank you *so* much for encouraging me to keep going and for being all around amazing. Seeing you achieve your PharmD was inspirational for me on my own journey. Much love! Thank you to Merly, who has been an amazing friend throughout the years. You've always been willing to help me whenever you could and I truly appreciate your kindness. Thank you for visiting me regardless of how far away I was, for picking me up to hang out, and for being quite the meme queen. My shortest supporter, I love you! To Mel and Gibb, thank you both for all the evenings we spent chatting and laughing away together online. You both were there celebrating my successes and commiserating with me along the way and made life a lot less lonely for Jason

and me, especially during the pandemic. I truly appreciate your guys' friendship, and Mel's pozole, and I can't wait till we hang out in person again. Love you two. Huge thanks to my friends Brandon and Joe for all the game nights, good food, and great laughs we shared. I would be much less sane without your guys' friendship, love y'all! To the Volz, from the bottom of my heart, thank you for your love, kindness, and for some of the best memories I have! I would not be where I am today without your support - much love to you Charlie, Michelle, and Eliana. Thank you to my family & friends who supported and encouraged me along the way: Richard, Monica, Tony, Kevin, Andre, Jackie, Jenny, Adam, Danny, Roland, Eric A., Jianna, Chris K., Vida, Antwon, Esteban (RIP), Swanna, Jace, Walker, Connor, Jess, Luke, Sonia, Dolsia, Matt, Brandy, and Karen Deeming.

Thank you to the Hiking My Feelings fam, Sydney and Barry, and everyone I had the pleasure of meeting at the inaugural Sequoia Hike and Heal weekend. Your kindness, wisdom, and wonderful energy under those giant trees was revitalizing and reminded me to get out in nature. Thank you to my esteemed colleagues over at UCLA. In particular I would like to thank Dr. Zhiqi He, a brilliant scientist with whom I had the honor of working with for several years. Aside from sharing your experimental prowess with me, thank you for all the wisdom and encouragement you provided. I will look fondly back on all the time in lab we spent together. I would also like to thank Dr. Manisha Swain for your time, patience in helping me when I first joined the lab, and for all the fun conversations and laughs we shared. Your hard work and dedication are truly an inspiration. Thank you to Dr. Changmin Xie for all your help with the synthesis of Efsevin, and for being a source of wisdom. To my lab mates turned friends, Dr. Ruoxi Wang, Tom, Jacob, Jeremy, Brady, Elizabeth, Aris, Betsy, Lorena, and Cameron, thank you for your kindness, wisdom, support and all the hilarity we have shared. I truly wish you all

the very best in all you do. To my professors, Prof. Merlic, Prof. Sletten, Prof. Houk, Prof. Jung thank you for all you have done to further my education. To my friends outside of lab, thank you for all your help throughout the program – Roberto, Asher, Helen, and Mariah, I am so thankful for you and lucky to call you all friends. Wishing you all the very best! To my folks at UC Davis: Thank you to my undergrad PI, Dr. Jared Shaw – you were such a great example of collaborative leadership. Thanks for giving me the opportunity to be a part of your lab, for teaching a killer synthesis class, your help with SACNAS and for helping me navigate graduate school as a first generation student. To my undergraduate mentors Lucas, Anna, and Nicole I learned so much from you all, thank you so much for your guidance and patience as I was finding my way in lab for the first time. I appreciate you all! Thank you to the wonderful folks with the MURPPS program, including Lolita Atkins, wishing you the best with your PhD! Big thanks to Dr. Valentine Taufour, Dr. Richard Scalettar and Dr. Annaliese Franz for all you've done for the program! To my previous roomies, Joseph and Efren – y'all are amazing, and I'm always rooting for you guys! Thank you to the brothers of Gamma Zeta Alpha, Theta chapter, for inspiring me to reach the top of the pyramid. The brotherhood and encouragement toward academic excellence really helped shape my experience at UCD – thank you bros!

Thank you to everyone at Aqua Metrology Systems for the opportunity to be a part of your team and help create a solution for safer drinking water. Thank you to my supervisor, who I now consider a good friend, Vlad, for all that you taught me during my time there. You are a brilliant scientist, and a patient teacher. Our work together remains as one of my crowning achievements. Enormous thank you to Michael West for allowing me to be his roommate during my tenure at AMS. Thank you for your incredible hospitality, for teaching me how to drive a manual transmission, and for being such a joy to live with. I wish you, Vlad, Rick, and the rest of the

AMS team much success. Huge shoutout to the wonderful folks at the San Luis Reservoir that I had the pleasure of working with. Cheryl, Rosie – some of my best memories were working with you two. Thank you for all you taught me and for all the times you made me cry laughing. To Rangers Nate and Chris – thanks for being awesome guys to work with and for encouraging me get on to bigger things. To my high school chemistry teacher, Mr. Leonardo, thank you for always making me feel welcome in class, and for stoking my interest in chemistry. To Dr. Lana Jordan, the best physics professor around – thank you for providing a welcoming space for your students and for being such a phenomenal educator. You have remained an inspiration for me for how I approach educating others, thank you!

Chapters 2 & 3 are a version of He, Z.; Moreno, J. A.; Swain, M.; Wu, J.; Kwon, O.

Aminodealkenylation: Ozonolysis and Copper Catalysis Convert C(sp³)-C(sp²) Bonds to C(sp³)-N Bonds. *Science* **2023**, *381* (6660), 877–886. He, Z. and Kwon, O. were responsible for preparing the manuscript. He, Z., Moreno, J. A., Swain, M. and Wu, J conducted the experiments.

Chapter 4 contains unpublished results that are to be contained in a manuscript under preparation to be published as: Dealkenylative Azidation. Moreno, J. A.; Bunnell, T.; Kwon, O.

BIOGRAPHICAL SKETCH

Education

- Ph. D., Chemistry, University of California, Los Angeles, CA. (projected December 2024)
- M.S., Chemistry, University of California, Los Angeles, CA. 2021
- B.S., Pharmaceutical Chemistry, University of California, Davis, CA. 2018
- A.S. Biological Sciences; A.S. Chemistry, Merced College, Merced, CA. 2015

Research Training

- Graduate Research Assistant: University of California, Los Angeles, CA
Advisor: Prof. Ohyun Kwon; 2019-Present
 - Development of dealkenylative azidation platform for the conversion of terpenes to pseudoalkaloid lactams
 - Achieved the first copper-catalyzed amination variant of the dealkenylation reaction
 - Established the previously undescribed synergistic cooperative copper ion pair role in the mechanism of aminodealkenylation
 - Synthesis of efsevin, a small molecule agonist of mitochondrial outer membrane protein VDAC2
- Research Intern: Aqua Metrology Systems Ltd., Sunnyvale, CA
Supervisor: Dr. Vladamir Dozortsev; Summer 2017
 - Provided the theoretical understanding of the electrochemical requirements and optimal electrode design for selective production of stannous ions from tin electrodes in aqueous media
 - Designed, built and patented a flow-through electrochemical stannous generator to treat Cr(VI) contamination in drinking water.
- Undergraduate Research Assistant: University of California, Davis, CA.
Advisor: Prof. Jared T. Shaw; 2016-2018
 - Developed a predictive stereochemical model for nucleophilic additions to alpha-chiral N-sulfonyl imines
 - Synthesized and assayed an analog library of a lead antibiotic compound targeting the bacterial cell division protein, FtsZ

Teaching Experience

- Teaching assistant, UCLA Department of Chemistry and Biochemistry, 2019-2024
- Biochemistry instructor, UC Davis Health – Prep Médico Program, Summer 2018

Honors and Awards

University of California, Los Angeles

- UCLA Doctoral Student Travel Grant (2023)
- Michael E. Jung Excellence in Teaching Award (2022)

University of California, Davis

- Provost's Undergraduate Fellowship Award (2017)

Publications

1. Champion O.; Maïga S.; Antier C.; Dousset C.; Moreau-Aubry A.; Bellanger C.; Guillonnet F.; **Moreno J. A.**; Kwon O.; Lilli N.L.; Moreau P.; Chiron D.; Pellat-Deceunynck C.; Touzeau C.;

- Gomez-Bougie P. VDAC2 primes Myeloma cells for BAK-dependent apoptosis and represents a novel therapeutic target. *Leukemia* **2024**, Submitted.
- Schröder, I.; Kolodziej, C. M.; **Moreno, J. A.**; Merlic, C. A. Lessons Learned—Explosion and Fires Resulting from Quenching Lithium, Lithium Nitride, and Sodium. *ACS Chem. Health Saf.* **2024**, <https://doi.org/10.1021/acs.chas.4c00069>.
 - He, Z.; **Moreno, J. A.**; Swain, M.; Wu, J.; Kwon, O. Aminodealkenylation: Ozonolysis and Copper Catalysis Convert C(sp³)–C(sp²) Bonds to C(sp³)–N Bonds. *Science* **2023**, *381*, 877–886.
 - Hagiwara, H.; Watanabe, M.; Fujioka, Y.; Kadosaka, T.; Koizumi, T.; Koya, T.; Nakao, M.; Kamada, R.; Temma, T.; Okada, K.; **Moreno, J. A.**; Kwon, O.; Sabe, H.; Ohba, Y.; Anzai, T. Stimulation of the Mitochondrial Calcium Uniporter Mitigates Chronic Heart Failure Associated Ventricular Arrhythmia in Mice. *Heart Rhythm* **2022**, *19*, 1725–1735.
 - Moore, L. C.; Lo, A.; Fell, J. S.; Duong, M. R.; **Moreno, J. A.**; Rich, B. E.; Bravo, M.; Fetting, J. C.; Souza, L. W.; Olmstead, M. M.; Houk, K. N.; Shaw, J. T. Acyclic Stereocontrol in the Additions of Nucleophilic Alkenes to α -Chiral *N*-Sulfonyl Imines. *Chem. Eur. J.* **2019**, *25*, 12214–12220.
 - Moreno, J. A.**; Dozortsev, V.; Bacon, R. Stannous – Literature Review [White paper]. Aqua Metrology Systems Ltd., **2020**, http://www.aquametrologysystems.com/wp-content/uploads/2020/01/AMS_RD_Stannous_Literature_Review.pdf
 - Moreno, J. A.**; Dozorsev, V.; Bacon, R. Treatment of Aqueous Matrices Using Electrolysis to Produce Soluble Tin Metal. **2018**. (PCT/US18/40836),

Presentations/Posters

- “Dealkenylative Amination” Poster presentation at the Amgen Young Investigator Award Symposium, Amgen, Thousand Oaks CA, October 2024.
- “Aminodealkenylation” Poster presentation at the M. Frederick Hawthorne Symposium, UCLA, Los Angeles CA, December 2023.
- “Dealkenylative Amination of Alkene C(sp³)–C(sp²) σ -Bonds through tandem Ozonolysis–Copper Catalysis”, Oral presentation at the American Chemical Society Conference, San Francisco, CA, August 2023.
- “Acyclic Stereocontrol in Nucleophilic Additions to α -Chiral *N*-Sulfonyl Imines” Oral presentation at the Larock Undergraduate Research Conference. UC Davis, Davis, CA, May 2018.
- “Reactivity and Stereoselectivity of Nucleophilic Additions to α -Chiral *N*-Sulfonyl Imines” Poster presentation at the 29th Annual Undergraduate Research, Scholarship & Creative Activities Conference. UC Davis, Davis, CA, April 2018.
- “Synthesis of Small Molecule Inhibitor Analogs of Bacterial Cell Division Protein FtsZ” Oral presentation at Larock Undergraduate Research Conference. UC Davis, Davis, CA, May 2017.

CHAPTER 1: History and development of metal-peroxide redox chemistry and copper mediated C–N coupling

1.1. Abstract

The formation and decomposition of organic peroxides by transition metals has a rich history which spans over a century. The synthesis of peroxides, identification and characterization of organic radical species, and understanding modes of peroxide decomposition were integral to the development of metal-peroxide redox chemistry as a viable functionalization strategy. Similarly, copper mediated nitrogen atom functionalization has a storied history which has provided the basis for the development of modern strategies to install nitrogen-carbon bonds. Taken together these concepts form the foundation from which dealkenylative amination and azidation methodologies were developed therefore, a detailed discussion on these topics is provided.

1.2. Introduction

In 2018 the lab of Ohyun Kwon at UCLA realized a brilliant method to replace the C(sp³)–C(sp²) sigma-bond of alkenes with a C(sp³)–H bond, for which there was very little precedent in the literature.¹ Realizing the potential of this transformation, the group developed a robust platform to deconstructively remove the alkene moiety and functionalize the former allylic C(sp³) center. The seminal publication on this work was dubbed hydrodealkenylation, a name rooted in the precedent for replacing the methyl group of toluene with hydrogen to form benzene, hydrodealkylation.² Eschewing the high temperature and pressures required for the latter process, hydrodealkenylation employed a mild and operationally simple reaction sequence that was inspired by earlier work from the laboratory of Stewart Schrieber.³ Noting this inspiration, some in the synthetic organic community viewed hydrodealkenylation as an exploration of so-called, “Schrieber chemistry”. While true that the venerable Schrieber popularized metal-peroxide redox chemistry in 1980

through its employment in the total synthesis of (\pm)-recifeiolide, the astute reader is encouraged to peruse the following sections discussing the deep history of this chemistry to determine whether the eponym is appropriately placed. Nevertheless, the dealkenylative functionalization platform was further developed to install various C(sp³) bonded functionalities from the C(sp³)–C(sp²) sigma-bond of olefins through the Fe(II) mediated fragmentation of alkene-derived peroxides.^{4–7} The latest extension of this methodology, and the subject of the current dissertation work, being dealkenylative amination (Chapter 2) and dealkenylative azidation (Chapter 4). While a definitive discussion of metal-peroxide redox chemistry as it relates to dealkenylation has been reviewed by esteemed colleagues in the Kwon lab, it is in the context of the early dealkenylation work which used Fe(II) to reduce the alkene-derived peroxides.⁸ In contrast, the current dissertation work on dealkenylation is the first to employ catalytic Cu(I) to achieve C(sp³)–N bond formation. As such, the discussion on the history and reactions of peroxides with an emphasis on copper will be succinctly summarized as a vehicle to introduce the principles of chemical reactivity necessary for the reader to gain a chemical understanding which underpin the dealkenylative amination and azidation work as well as establish the larger context to which these works are placed.

1.3. History and development of metal-peroxide redox chemistry

The chemical history of peroxides begins with the discovery of the simplest peroxide, hydrogen peroxide, H₂O₂, in 1818 by French chemist Louis Thenard.⁹ He accomplished this through the reaction of barium peroxide with different acids including nitric, hydrochloric, and sulfuric acids. In this very same report Thenard provided one of the earliest qualitative descriptions of the combination of a copper oxide with his crude hydrogen peroxide, noting a color change from dark brown to olive green. It is likely that Thenard was describing a now well-understood process but unknown at the time by which cuprous ions, Cu(I), which can appear red in solution are oxidized

by peroxides to cupric ions, Cu(II) which can appear green in solution. The chemistry underlying this qualitative description occurs through a single electron transfer (SET) from copper (I) to the weak peroxide O–O bond (BDE=50 kcal/mol). Of the metals known to undergo similar SET reactivity with peroxides, ferrous ions, Fe(II), are perhaps one of the earliest and most heavily investigated. One of the first reactions of hydrogen peroxide and ferrous ions, Fe(II), was reported in 1844 by Schönbein, where he described the observation of elemental iodine from a solution of potassium iodide and hydrogen peroxide catalyzed by the addition of the red component of blood.¹⁰ This observation can be explained by the action of heme iron reacting with hydrogen peroxide by a SET mechanism, and the subsequent reduction of iodide ions to elemental iodine. In 1868 Parnell gave another qualitative descriptions of the action of ferrous sulfate, hydrogen peroxide and organic acids, as well as cupric oxide, Cu(II)O, in an ammoniacal solution with hydrogen peroxide.¹¹ However, one of the most prominent chemists to investigate early hydrogen peroxide chemistry was Henry Fenton. As an undergraduate, Fenton was the first to describe the enhanced

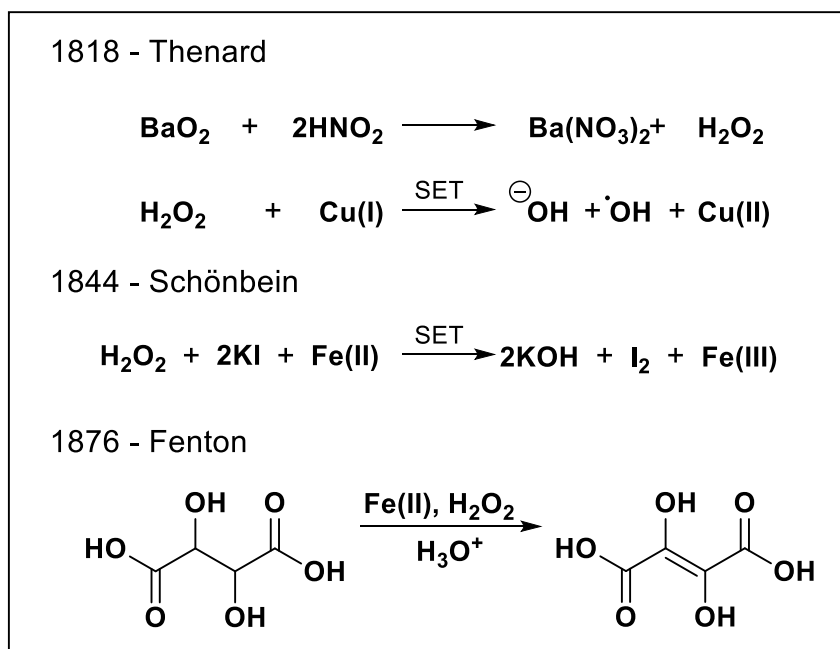


Figure 1.1 Discovery and early uses of hydrogen

oxidizing capacity of hydrogen peroxide and ferrous ions in an acidic aqueous solution, now known as Fenton's reagent, on tartaric acid in a letter to the editor of *Chemical News* in April of 1876.¹² Eighteen years later he repeated the experiment with catalytic iron and identified the product of the acid oxidation, a previously unknown compound, dihydroxy maleic acid (Figure 1.1, bottom).^{13,14} The utility of Fenton's reagent was also central to early carbohydrate chemistry as Otto Ruff described its action on the sugar D-glucose converting it to D-arabinose in 1898.¹⁵ The Ruff degradation, as it has come to be known, was extensively used by Nobel laureate Emil Fischer, for which his projections are eponymous, to determine the structure of sugars.¹⁶ Until the seminal work on organic peroxide synthesis by Brodie in 1858, studies of peroxides were mostly limited to the use of hydrogen peroxide, H₂O₂.¹⁷

Brodie's report on the synthesis of dibenzoyl peroxide from sodium peroxide and benzoyl chloride opened the field for further study into the reactivity of such organic peroxides. His investigations into the nature of the peroxides usually involved heating, albeit with explosive results. However, the characterization of the products from such thermal detonations were hampered by the available tools of the time, so progress was incremental. Despite this, Brodie in 1864 was able to identify CO₂ and small amounts of benzoic acid from the thermolysis of dibenzoyl peroxide heated to decomposition in sand although the process by which this occurred was still speculative at the time (Figure 1.2, top).¹⁸ A critical piece of chemical understanding necessary to describe such a processes was still in its infancy – radicals. Indeed it was the serendipitous reports regarding the nascent concept of radicals published in 1851 by Frankland¹⁹ which allowed Brodie to consider their role in peroxide chemistry.^{19,20} While Brodie published a series of reports on the topic of peroxides and radicals^{18,21,22}, it was not until several years later that the first organic radical was synthesized and characterized.

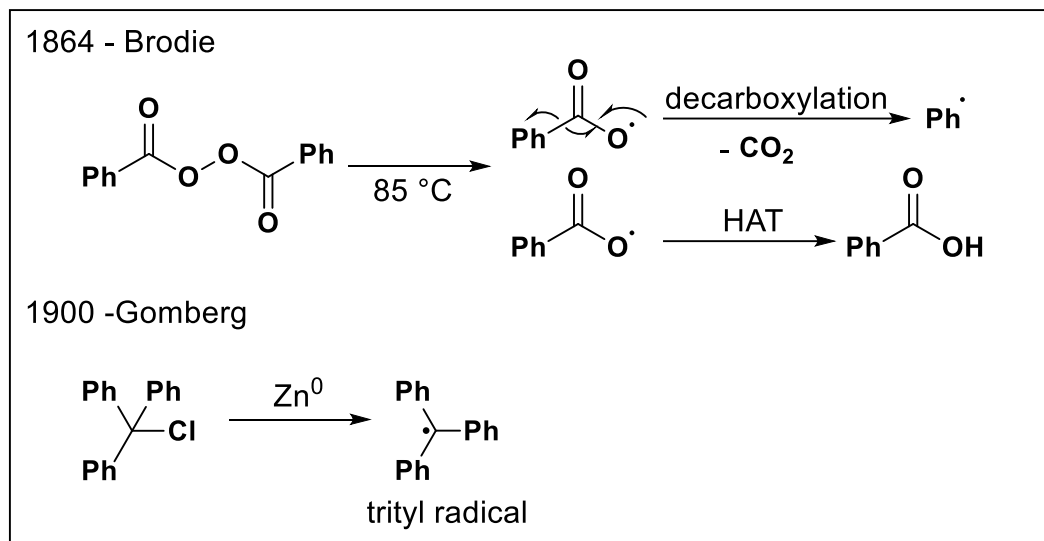
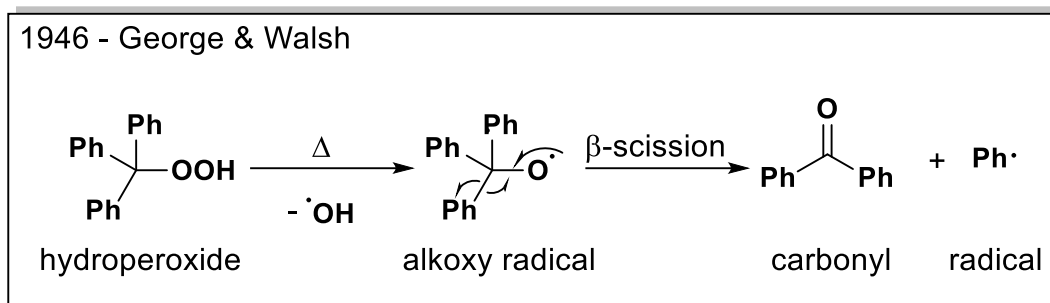


Figure 1.2 Thermal decomposition of diacyl peroxides and formation of trityl

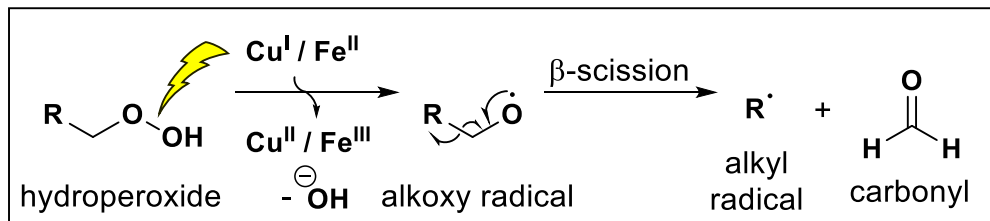
The isolation of the first organic radical was accomplished by Gomberg at the turn of the 19th century, who synthesized and characterized the stabilized trityl radical from the reaction of triphenylmethyl chloride with zinc metal (Figure 1.2 bottom).²³ This discovery provided evidence for open-shell species that had only been proposed to be involved in various chemical processes. It was not until three decades later in 1932 that Haber and Weiss formally proposed the mechanism by which peroxides are decomposed by ferrous salts, based on previous studies by Haber and Willstatter on the ferric-containing catalase enzyme with hydrogen peroxide.^{24,25} In addition to metal-mediated peroxide decomposition, the thermal decomposition of peroxides was being well-established with explorations of thermolysis of acyl peroxides by the group of Gellisen and Hermans.²⁶⁻²⁹ They were able to further clarify observations made by Brodie, and went on to identify products such as biphenyl from the homocoupling of phenyl radicals produced from the thermolysis of dibenzoyl peroxide and subsequent decarboxylation. This investigation was generalized to include organic peroxide synthesis and their thermolysis in the seminal series by Milas beginning in 1930's.³⁰ Taken together these studies contributed to a growing body of

evidence from which a clearer picture of the reactivity patterns of peroxide decomposition began to emerge.



Scheme 1.2 Thermal decomposition of hydroperoxide

In the context of peroxide redox chemistry, another important mechanistic aspect of their decomposition was being reported on in 1946 by George and Walsh – beta-scission (Scheme 1.1).³¹ While the evidence for this process was observed in many previous studies, it was George and Walsh who formalized it in their study. In their case beta-scission occurred through the thermal homolysis of tertiary hydroperoxides however this process also arises from the single electron transfer (SET) from a metal, usually Fe(II) or Cu(I), to the O–O bond of an organic peroxide to generate hydroxide and an oxygen-centered radical (Scheme 1.2). This O-centered radical can trigger a homolytic fragmentation of an adjacent sigma bond to form a carbonyl and provide an alkyl radical. This work by George and Walsh cemented radical processes into the understanding of how peroxides fragment. With Rudolf Criegee concurrently disclosing investigations regarding



Scheme 1.1 Metal mediated beta-scission

the organic hydroperoxides produced from ozonolysis and the mechanism of this process, transition metal-peroxide redox chemistry enjoyed a renaissance during the mid-19th century.

1.4. Criegee ozonolysis and early applications of peroxide redox chemistry

During his career Criegee investigated several oxidation processes of organic compounds and was the first to characterize several of the organic peroxides produced from auto-oxidation.^{32,33} He also became interested in the mechanism of peroxide formation, the route by which the di- and trimeric cyclic peroxides from cyclohexanone and hydrogen peroxide were formed.³⁴ Criegee was also able to isolate and characterize the first alpha-methoxy hydroperoxide from the ozonolysis of the alkene 9,10-octalin in methanol, a procedure now known as Criegee ozonolysis.³⁵ Perhaps the most significant contribution to the field was Criegee's mechanism of olefin ozonolysis.

While Schönbein was credited with the discovery of ozone in 1840's,³⁶ it was Harries who, beginning in 1903, published extensively on the subject and established the synthetic utility of ozone, demonstrating its analytical use for the structural determination of alkenes.³⁷⁻³⁹ Harries made attempts to determine the mechanism of the reaction, but ultimately was not successful. Gradually aspects of this mechanism began to unravel. First proposed by Staudinger⁴⁰, the constitution of the 1,2,4-trioxolane ozonide formed from alkene ozonolysis was later confirmed by Pummerer⁴¹ and Rieche⁴² in 1938 and 1942, respectively. What remained unclear until Criegee's proposal was the mechanism by which the ozonide formed concurrent with cleavage of the C-C bond.

The mechanism of ozonolysis was published by Criegee two years before his death in 1975.⁴³ As shown in Figure 1.3, ozone can be conceived as a 1,3-dipole that, in the presence of an alkene, incorporates into the substrate through a 1,3-dipolar cycloaddition to produce a primary ozonide, otherwise known as molozonide. The primary ozonide is unstable and rapidly performs a cycloreversion to break the remaining sigma bond of the former alkene to produce a carbonyl fragment and a zwitterionic carbonyl oxide fragment. Reactions conducted in non-participating

solvents, for example DCM, allow for the carbonyl oxide and carbonyl fragments to recombine in another [3+2] cycloaddition to form the secondary ozonide, also known as a 1,2,4-trioxolane. However, when alcohols are used as the solvent medium, they can participate in the reaction and will nucleophilically add to the electrophilic carbon of the carbonyl oxide to form, after proton transfer, a hydroperoxyacetal.

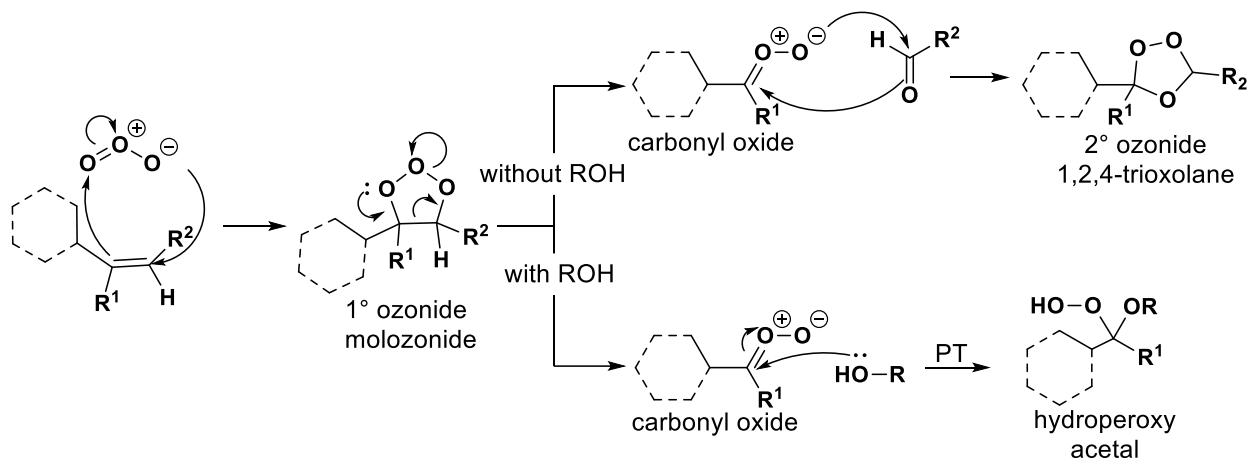


Figure 1.3 Mechanism of ozonolysis

Establishing the synthetic utility of peroxide redox chemistry, many groups began exploring metal salts to fragment peroxides. Works by Hawkins⁴⁴, Rust and De La Mare⁴⁵, and Kochi⁴⁶ explored the action of FeSO₄ on peroxide decomposition but of particular relevance to the dissertation work herein described are the early studies of copper on peroxide decomposition. Some of the earliest reports of CuCl being investigated with hydroperoxides are from Kharash and Fono, who in 1958 reported that just a 1% solution of the copper salt was sufficient to catalyze the reduction of various peroxides.⁴⁷ Indeed, copper was intriguing researchers at the time with Kharash and Fono in another 1959 report speculating on the metal's homolytic nature in regards to the Ullmann reaction which uses copper to couple amine nucleophiles to aromatic halides.⁴⁸ In this same report the authors note the ability of copper to coordinate and bind alkyl radicals, proposing the term "free radical trapper" to describe this ability. Kharash and others continued to systematically investigate

copper in the context of metal-peroxide redox chemistry in the late 1950's and '60's, which obviated the thermolysis of peroxides for reactivity.^{49,50} One of the first examples of this chemistry being exploited to form C–N bonds come from Minisci, who in 1959 reported the decomposition of cyclohexyl geminal hydroxyhydroperoxide using ferrous sulfate heptahydrate and sodium azide to achieve the corresponding ring opened 6-azidohexanoic acid in 50% yield (Figure 1.4, top).⁵⁰ Other early adopters using this chemistry for functionalization including Kochi⁵¹ and Kumamoto, who went on to work with De La Mare and Rust at Shell oil company. While at Shell they published one of the earliest reports of a synthetic method utilizing iron and copper chlorides on alkyl hydroperoxides for preparative scale synthesis of alkyl chlorides (Figure 1.4, middle).⁵² In a subsequent publication that noted the effects the counter anion of the metal salts had on product formation, favoring unsaturated products when using Fe(II)SO₄ in addition to Cu(II)SO₄.⁵³ A similar platform for functionalization was employed in the mid 1970's by the Green and Cekovic, who investigated the formation of olefins arising from the 1,5-hydrogen atom transfer (HAT) of alkoxy radicals derived from the Fe(II)SO₄ mediated decomposition of alkylhydroperoxides in the presence of Cu(II)(OAc)₂ (Figure 1.4, bottom).⁵⁴ Cekovic later went on to leverage this chemistry to functionalize the alkyl radicals after HAT through interception and ligand transfer with Cu(II)X₂

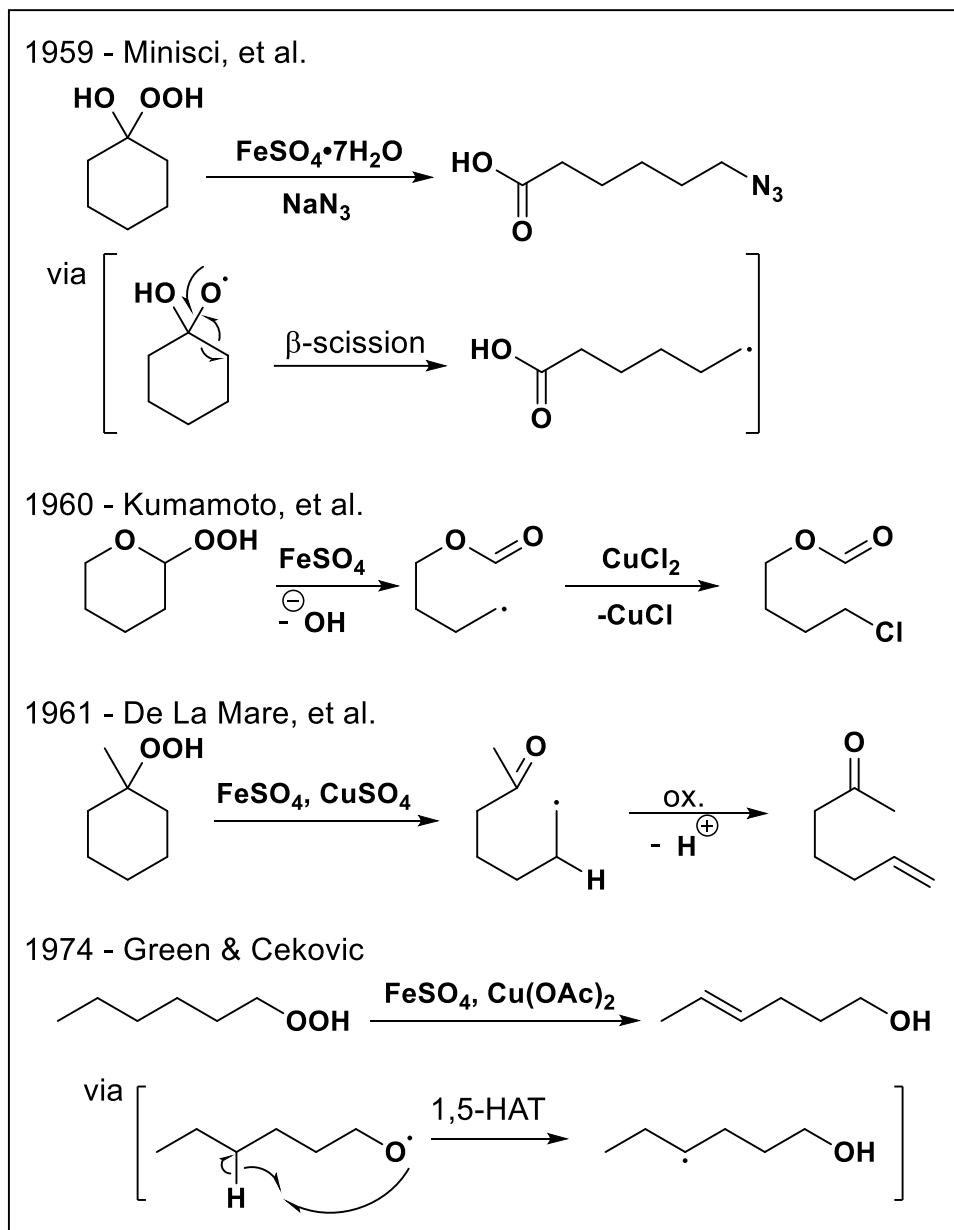


Figure 1.4 Early metal-peroxide redox functionalization

reagents including delta-functionalizations with Cl, Br, I, N₃, and thiocyanates.⁵⁵ However, it would not be until 1980 that peroxide redox chemistry would be applied in the context of total synthesis.

1.5. The development of copper-mediated C–N coupling

Biology often serves as a source of knowledge to understand chemical reactivity, as in the case of Haber and coworkers who proposed the mechanism for peroxide decomposition by ferrous salts

based on Haber's previous studies on the ferric-containing catalase enzyme (*vide supra*), and an inspiration for chemists to emulate chemical transformations *in vitro*. Copper is present in several enzymes of biological importance – catalyzing electron transfers, redox reactions, and activation of a variety of substrates as mono-, or polynuclear metalloproteins. One such enzyme, zinc copper superoxide dismutase, protects cells from oxidative damage by catalyzing the reduction of superoxide (O_2^-) from SET of Cu(I) to form hydrogen peroxide.⁵⁶ Copper with a ground state electronic valence configuration $[4s^1 3d^{10}]$ can access several oxidation states, including 0, +1, +2, and +3. An interesting consequence of the odd oxidation states available to the metal is the ability to not only engage in polar, two-electron, processes but also single-electron chemistry as evidenced by the superoxide dismutase chemistry. This, along with its ability to coordinate heteroatoms as a Lewis acid, has allowed it to be used for more than a century by chemists to form C–C and C–heteroatom bonds and by nature in enzymes for much, much longer. Of the earliest work by chemists in this area, pioneering work by Ullmann and coworkers is often credited as establishing the foundation of copper-mediated C–N coupling.

The development of copper-mediated C–N coupling was preceded by using the metal for C–C coupling. Namely Glaser, in 1869, reported the homocoupling of terminal acetylenes under the action of copper (I) chloride, and ammonium hydroxide in ethanol.⁵⁷ It was not until over 30 years later that, in 1901, Ullmann and Goldberg reported the first biaryl synthesis utilizing aryl halides as substrates under the action of stoichiometric amounts of copper powder at $>200\text{ }^\circ\text{C}$.⁵⁸ Two years later the authors expanded the scope of this coupling, reporting in 1903 one of the earliest instances of C–N coupling.⁵⁹ They accomplished this by using the electron-deficient *o*-chlorobenzoic acid, with copper powder in refluxing aniline to produce the diarylamine, phenylanthranilic acid. The Ullmann group showed that copper could be used catalytically in their 1905 publication creating

biaryl ethers from phenols and aryl halides.⁶⁰ A year later the Goldberg group extended this methodology, reporting the first instance of copper-catalyzed amidation of aryl bromides.⁶¹

With respect to the mechanism, the Ullmann C–C coupling reaction for biaryl synthesis proceeds by oxidative addition of copper to the aryl–halide bond, SET from another equivalent of Cu(0) to Ar–Cu(II)–X to form the active Ar–Cu(I), which then performs another oxidative addition into the second equivalent of the aryl halide which is proceeded by reductive elimination to form the product. The C–heteroatom variant has undergone intense investigation, even into the 21st century, and is still debated. Due to the variable oxidation states and wide range of reactivity copper can engage in, mechanisms proposed include radical-based mechanisms, metathesis-type reactions, aromatic nucleophilic substitution, and more classical cross-coupling mechanisms depending on

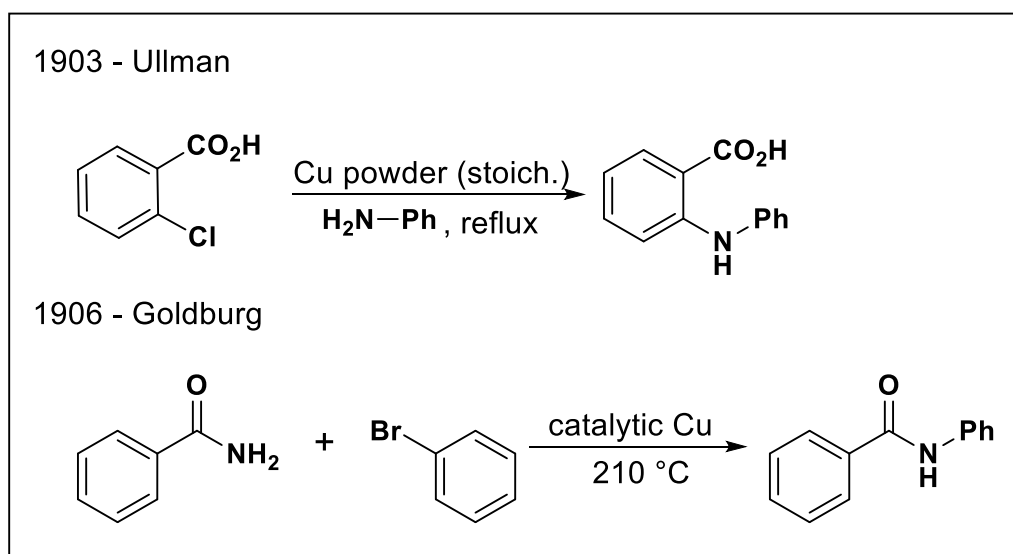


Figure 1.5 Ullman & Goldberg C–N coupling

the reaction conditions. The discussion on the proposed mechanisms is brilliantly covered elsewhere⁶² and while the exact details and support for the various mechanisms will not be discussed here further, a salient feature of this reaction includes detailed work from Paine in 1987 revealing that soluble cuprous ions are responsible for the observed reactivity.⁶³ Owing to the high

temperatures required for the Ullmann reaction, early efforts to improve the reaction were focused on utilizing less harsh conditions. To this end Chan and Lam both reported in 1998 a much milder method for forming aryl amines. By using an aryl boronic acid with an amine coupling partner, aryl amines were synthesized at room temperature (Figure 1.6).^{64,65} Other explorations into milder reaction conditions manifested in an extensive exploration of ligated copper species.

In the early 1980's and 90's the concept of ligated copper catalysis had begun to be explored in works by Bryant and Capdevielle. Reports on the rate acceleration observed by copper ligated with esters on the methanolysis of aryl iodides to produce aryl ethers which took place at much lower temperatures were disclosed in a patent by Bryant and later in the literature by Capdevielle.^{66,67} These pioneering works provided precedent for further exploration into other copper catalyst complexes, such as the works of Goodbrand. In 1999 the group reported a copper(I) and 1,10-phenanthroline (1,10-phen or simply, phen) catalyst system for the bisarylation of aryl amines via the Ullmann condensation.⁶⁸ The ligated copper allowed for this reaction to be conducted at temperatures as low as 98 °C, conditions that were much milder than the original Ullmann protocol. Among the ligand development that occurred during this period included extensive work by the Buchwald group who disclosed ethylene glycol⁶⁹, delocalized enolates^{70,71}, and diamine ligands^{72,73} for amine arylations and amide allylations, the Fu group who disclosed 1,1'-bi-2-

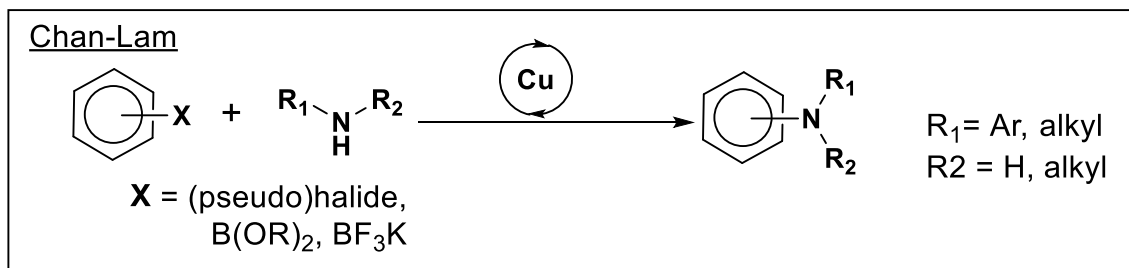


Figure 1.6 Chan-Lam coupling

naphthol (BINOL) ligated copper for arylamine alkylation⁷⁴, among many others including

phosphine based ligands.⁷⁵ Among the many ligands, the copper(I)-1,10-phen scaffolds remained a privileged catalyst combination.

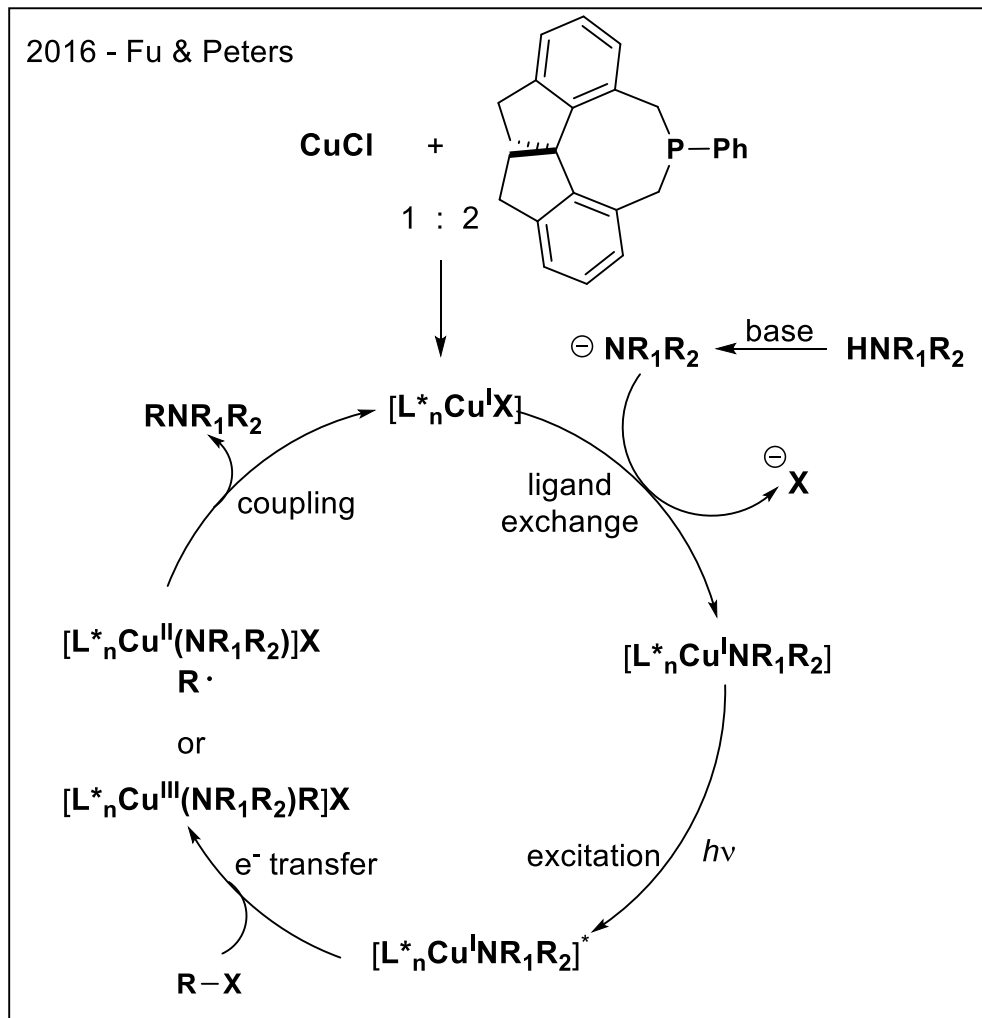
The copper(I)-1,10-phen complex was thoroughly studied by the Hartwig group in the context of their copper-catalyzed amidation and imidation of unactivated alkenes and aryl halides protocol.^{76,77} The Hartwig group was successful at synthesizing and characterizing complexes of copper(I) with phenanthroline ligands as well as mixed copper-1,10-phen-phthalimide complexes. Taken together the Hartwig studies represent a milestone in defining a catalytically active copper complex and its associated reactivity. An interesting result from this work showed that in polar solvents these complexes can speciate into an ionic form with the general formula $[L_2Cu]^+$ and $[CuX_2]^-$, where L is a donor N,N-ligand and X is an anionic amidate ligand. They accomplished this assignment after solid state and solution structural elucidation of the complexes by using conductivity measurements in solvents of varying polarity. These results showed substantial ionic character in DMSO, some ionic character in THF and primarily the neutral form of the complex in non-polar solvents such as benzene. The ability for a copper complex to speciate into this tight ion pair consisting of distinct cationic and anionic complexes can be taken as another factor confounding previous attempts to understand the nature of active copper complexes in the C–N coupling mechanisms.

The rise of ligated copper catalysis in the modern era has provided somewhat of a renaissance beyond its roots as the metal of choice for the Ullmann coupling. The use of copper for C–N coupling has rivaled that of palladium, and in fact has several advantages. Copper is earth abundant making it more affordable, with respect to active pharmaceutical ingredient (API) synthesis where metal-mediated coupling is extensively used, copper it is less immunotoxic than palladium and thus requires less intensive trace metal removal.⁷⁸ Furthermore, copper can engage in unique

reactivity not easily reproduced with palladium catalysis and it can be modulated or change reactivity based on the identity of the ligands. A unique advantage is the ability for copper to produce radicals by homolysis of weak hetero, for instance through photochemistry or through metal-peroxide redox chemistry, and subsequently engage them in the bond formation step.

In a recent example, Greg Fu and Jonas Peters have been prominent in asymmetric copper-catalyzed photochemistry to form C–N bonds. In a joint investigation they showcased the versatility of copper by employing indoles and carbazoles as substrates, which in the presence of base, become ligated to copper to form photoactive complexes.⁷⁹ As depicted in Scheme 1.3, under visible light irradiation the excited state photoactive Cu(I) complex delivers an electron to a racemic alkyl halide substrate to provide an alkyl radical. The alkyl radical is coupled to the

nitrogen nucleophile through an inner-sphere Cu(III) complex, or through an outer sphere Cu(II) complex. By employing a chiral phosphine ligand, this coupling is rendered asymmetric providing enantioenriched tertiary C–N coupled products and regenerating the starting catalyst.



Scheme 1.3 Mechanism of asymmetric copper-catalyzed C–N coupling by Fu and Peters

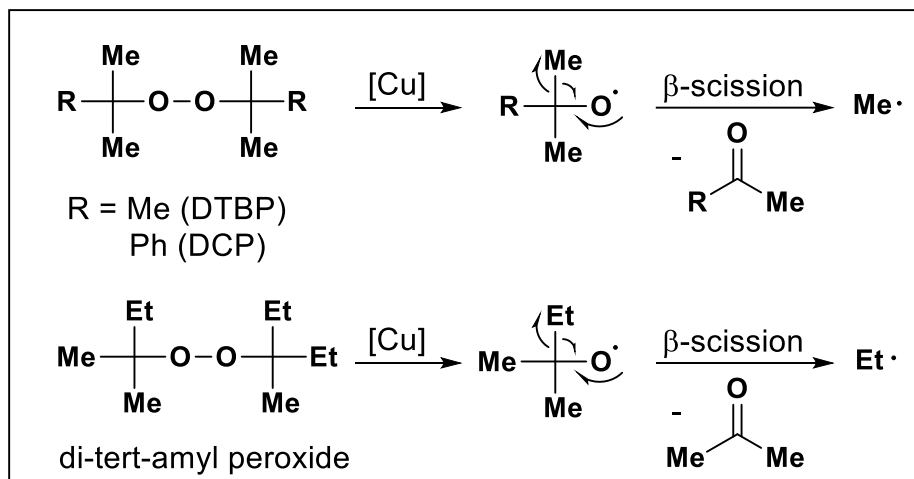
While the brevity of this section does not provide an exhaustive survey of the fascinating chemistry that copper participates in, the illustrative examples presented should serve to not only establish the rich history and robust precedent for which copper has been used for C–N coupling but also as a testament to unique chemistry and mechanistic scenarios involved in this chemistry. The following detailed reviews are recommended for readers whose interest has been piqued by

Ullmann chemistry^{62,75}, development of ligated copper species⁸⁰, and modern C–N coupling involving copper^{81–83}.

1.6. Modern copper-peroxide redox chemistry for formation of C–N bonds

Stewart Schrieber left an indelible mark on the synthetic organic community as he showcased metal-peroxide redox chemistry in a highly efficient final step in the total synthesis of (±)-recifeiolide.³ While this chemistry was known in the literature, Schrieber brilliantly demonstrated for the modern audience a few approaches to peroxide synthesis, including condensation and Criegee ozonolysis, Fe(II) and Cu(II) mediated peroxide decomposition products such as halides and olefins, application of this chemistry to natural products to create chiral building blocks, and provided a mechanistic proposal for the highly regio- and stereoselective formation of the olefin of his macrolactone target. This work was highly influential, spawning several synthetic campaigns utilizing the very same sequence of Criegee ozonolysis and metal-mediated decomposition of the thus formed alpha-alkoxy hydroperoxide of the terpene carvone to access enantiopure 6-methylcyclohex-2-enone.^{84–91} While true that Schrieber's work did not involve C–N bond formation, it is undeniable that he helped set the stage for a new generation of organic chemists to become acquainted with these technologies from which future developments in this area sprang. Despite being widely employed, novel applications of this methodology did not appear until over three decades later.

Beginning in 2013 with Chen and coworkers, researchers began to access simple methyl and ethyl radicals from the copper-catalyzed decompositions of available dialkyl peroxides which form via beta-scission as shown in Scheme 1.4 for the N-alkylation of nitrogen containing compounds.⁹² Chen and coworkers took inspiration from earlier work in this vein which employed metals other than copper such as Ni⁹³, Fe⁹⁴, and even Pd⁹⁵. The group employed



Scheme 1.4 Dialkyl peroxides as alkyl radical precursors

applied the copper (I) chloride catalyzed decomposition of dicumyl peroxide (DCP) at elevated temperatures (130 °C) to achieve mono-methylation of primary amides (Figure 1.7, top). A similar reaction manifold was used by the Yu group in 2015 with copper catalyzed decomposition di-tertbutyl peroxide and di-tert-amyl peroxide for the methylation and ethylation, respectively, of sulfoximines (Figure 1.7, bottom).⁹⁶ While valuable, these protocols were limited to primary alkyl radicals able to be accessed by the simple dialkyl peroxides available.

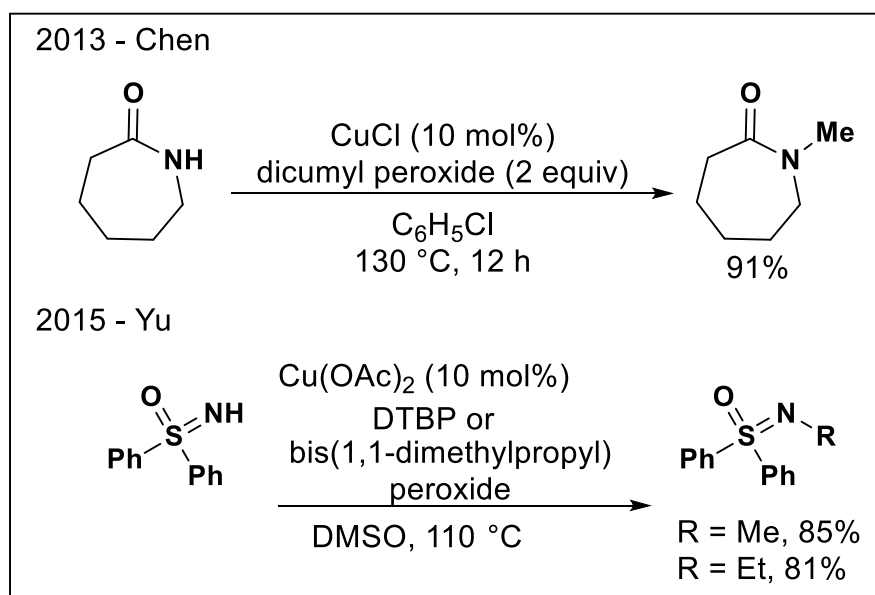


Figure 1.7 Copper catalyzed N-alkylations

To overcome the limitation of alkyl radicals that could be released by available dialkyl peroxides, the laboratory of Maruoka in 2017 introduced alkylsilyl peroxides, which could be accessed in low to moderate yields from readily available alcohols, as alkyl radical precursors (Figure 1.8, top).⁹⁷ Utilizing a catalytic copper-phenanthroline complex it was found the alkylsilyl peroxides reacted identically to dialkyl peroxides, undergoing O–O cleavage and beta-scission to provide an expanded range of primary and secondary alkyl radicals which were coupled to primary amides in moderate to quantitative yields.⁹⁸ That same year Maruoka and coworkers demonstrated yet another silicon-containing alkyl radical precursor, bis(trialkylsilyl) peroxides (Figure 1.8, middle).⁹⁹ These reagents were employed using the same Cu complex to alkylate primary amides and aryl amines, albeit in moderate to low yields. Interestingly it was proposed the bis(trialkylsilyl) peroxides do not provide alkyl radicals through beta-scission like their alkyl counterparts. Instead HRMS evidence suggested the siloxyl radical adds to the silicon center of another molecule of bis(trialkylsilyl) peroxide with a concomitant release of the alkyl radical for C–N coupling. Another significant advancement in this area of Cu-peroxide C–N coupling came from the group of Gui.

The Gui lab provided a brilliant methodology to access a striking variety of radicophiles that could be coupled to alkyl radicals derived from fused bi- and tricyclic furan precursors (Figure 1.8, bottom).¹⁰⁰ The group relied on the Diels-Alder cycloaddition of singlet oxygen with the furan motif in methanol to provide hydroperoxide intermediates. These intermediates were fragmented using Fe(II), which after beta-scission ruptured the conjoined ring to provide a butanolide tethered to a carbon chain with an alkyl radical at the distal end. The group used a variety of conditions to couple the alkyl radical with an exhaustive list of radicophiles, including the use of Cu(II) azide in an example of Cu mediated C–N coupling. Another recent work

involving the alkoxy radical triggered ring opening of bicyclic systems comes from the Guo and Duan group.¹⁰¹ The authors utilize the tautomerization of alpha-hydroxyalkylketones to form hemiketals which are activated by acid and hydrogen peroxide to form hemiketal hydroperoxides

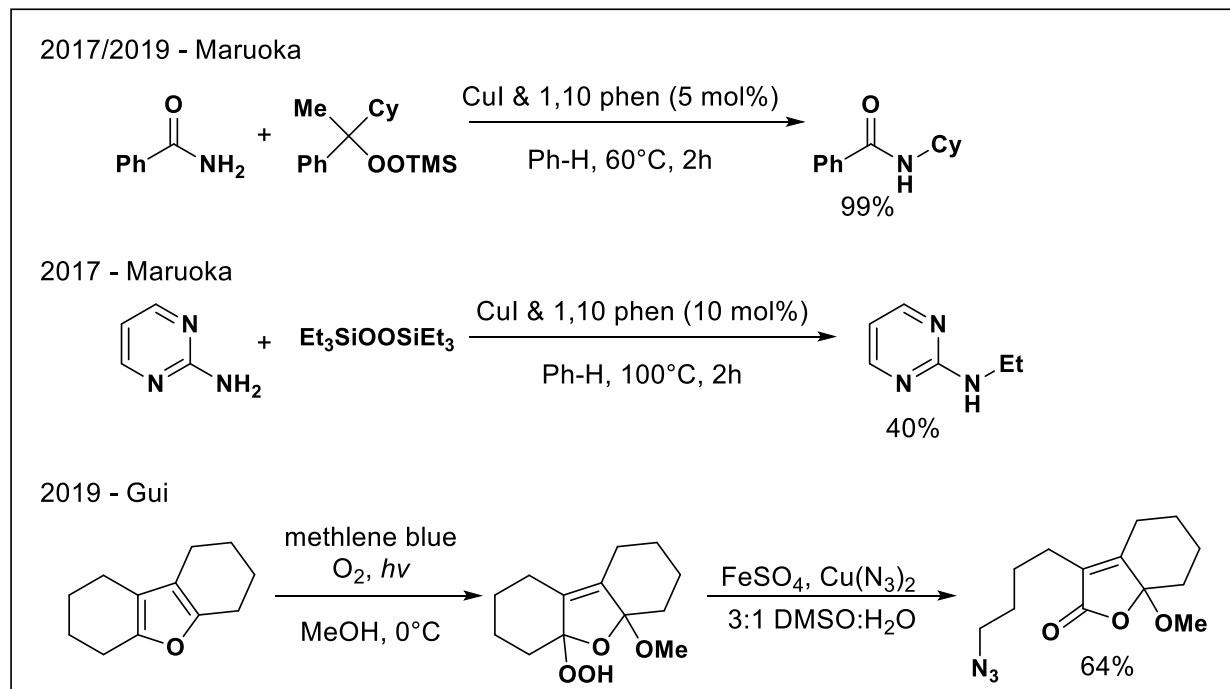
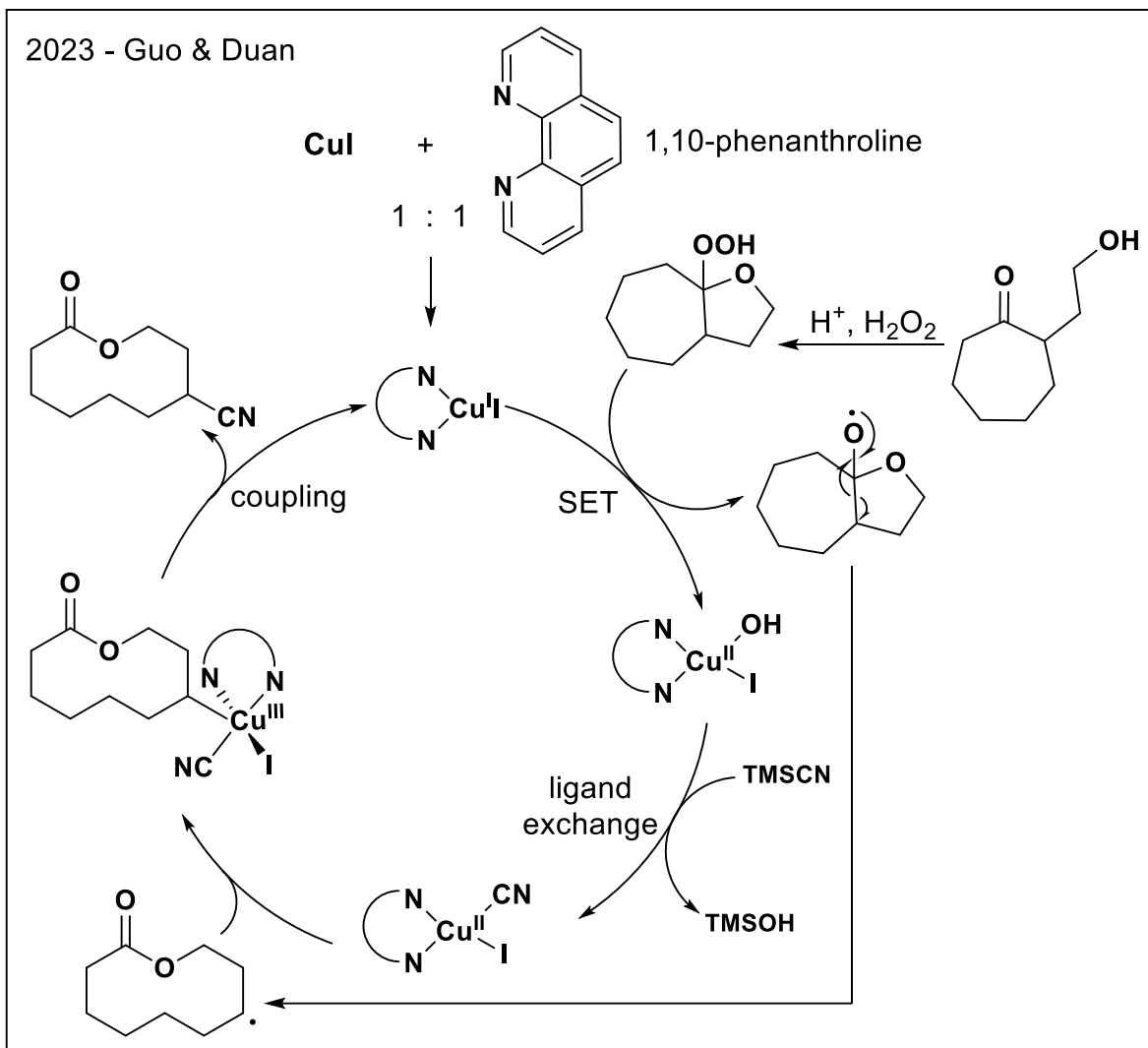


Figure 1.8 Recent C–N bond formation using peroxides and copper

(Scheme 1.5). Under optimized conditions the researchers found 5% of Cu(I)-phen complex was sufficient to fragment the bicyclic ring to simultaneously form medium to large lactones and provide an alkyl radical. The authors demonstrated the alkyl radical could be coupled with azides in the presence of TMSN₃ as well as other functionalities such as CN, SCN, and halogens. The catalytic cycle for the cyanation procedure was studied by DFT done by Ken Houk's group at UCLA, which supported the metalation of the alkyl radical by a Cu(II)CN complex to form Cu(III), which undergoes reductive elimination to form the coupled product and regenerate the starting [PhenCu(I)X] complex. Other recent examples which enabled unprecedented diversity in coupling partners include the work of Ouyang and Li.



Scheme 1.5 Mechanism of ring expansion/cross-coupling cascade by Guo & Duan

In 2021 the group of Ouyang and Li disclosed a method for N-alkylation of a wide range of nitrogen nucleophiles using diacyl peroxides under copper catalysis.¹⁰² The researchers were able to access primary radicals, after fragmentation and decarboxylation of the diacyl peroxides, using a copper-phen complex for coupling with N-nucleophiles including N-heterocycles, carbazoles, sulfonamides and anilines with excellent functional group tolerance. To access secondary alkyl radicals for coupling, photoredox with an Ir catalyst was required in addition to the copper catalyst. Limitations included amidation products when using aliphatic amines or when tertiary alkyl

radicals were attempted to be coupled. The scope of N-nucleophiles is truly a strength of this methodology and an inspiration to our own work in dealkenylative amination.

1.7. Conclusion

Researchers the world over have contributed to advancing our understanding of peroxides, their reactivity and methods to leverage such phenomena in predictable and useful ways. Likewise, exploiting the unique reactivity of copper to form valuable carbon-nitrogen bonds has drastically advanced over the century since Ullmann and Goldberg's seminal reports. The marriage of the two fields has undoubtedly provided fruitful technologies and novel tools by which chemists will surely take inspiration from and build their own advancements upon. Metal-peroxide redox chemistry has irrevocably shifted the paradigm of how organic chemists approach synthesis, offering new avenues of reactivity through radical processes providing access to novel molecules by way of deconstructive methods which simultaneously remodel and functionalize substrates in short order. These technologies will surely become part of the modern chemist's toolkit for some time to come and time will only tell what exciting advancements will continue to be made in this area.

1.8. References

- (1) Smaligo, A.; Swain, M.; Quintana, J.; Tan, M.; Kim, D.; Kwon, O. Hydrodealkenylative C(Sp³)-C(Sp²) Bond Fragmentation. *Science* **2019**, *364* (6441), 681-+. <https://doi.org/10.1126/science.aaw4212>.
- (2) Griesbaum, K.; Behr, A.; Biedenkapp, D.; Voges, H.; Garbe, D.; Paetz, C.; Collin, G.; Mayer, D.; Höke, H. Hydrocarbons. In *Ullmann's Encyclopedia of Industrial Chemistry*; Wiley-VCH, Ed.; Wiley, 2000. https://doi.org/10.1002/14356007.a13_227.
- (3) Schreiber, S. L. Fragmentation Reactions of .Alpha.-Alkoxy Hydroperoxides and Application to the Synthesis of the Macrolide (+.-)-Recifeiolide. *J. Am. Chem. Soc.* **1980**, *102* (19), 6163–6165. <https://doi.org/10.1021/ja00539a041>.
- (4) Smaligo, A.; Kwon, O. Dealkenylative Thiylation of C(Sp³)-C(Sp²) Bonds. *Org. Lett.* **2019**, *21* (21), 8592–8597. <https://doi.org/10.1021/acs.orglett.9b03186>.
- (5) Swain, M.; Sadykhov, G.; Wang, R.; Kwon, O. Dealkenylative Alkenylation: Formal σ -Bond Metathesis of Olefins. *Angew Chem Int. Ed.* **2020**, *59* (40), 17565–17571. <https://doi.org/10.1002/anie.202005267>.
- (6) Swain, M.; Bunnell, T.; Kim, J.; Kwon, O. Dealkenylative Alkynylation Using Catalytic FeII and Vitamin C. *J. Chem. Soc.* **2022**, *144* (32), 14828–14837. <https://doi.org/10.1021/jacs.2c05980>.
- (7) Smaligo, A. J.; Wu, J.; Burton, N. R.; Hacker, A. S.; Shaikh, A. C.; Quintana, J. C.; Wang, R.; Xie, C.; Kwon, O. Oxodealkenylative Cleavage of Alkene C(Sp³)-C(Sp²) Bonds: A Practical Method for Introducing Carbonyls into Chiral Pool Materials. *Angew Chem Int Ed* **2020**, *59* (3), 1211–1215. <https://doi.org/10.1002/anie.201913201>.

- (8) Dehnert, B.; Dworkin, J.; Kwon, O. Dealkenylative Functionalizations: Conversion of Alkene C(Sp³)-C(Sp²) Bonds into C(Sp³)-X Bonds via Redox-Based Radical Processes. *Synthesis-Stuttgart* **2024**, *56* (01), 71–86. <https://doi.org/10.1055/a-2044-4571>.
- (9) de Morveau, L. B. G.; Gay-Lussac, J. L.; Arago, F.; Chevreul, M. E.; Berthelot, M.; Mascart, É. É. N.; Haller, A. *Annales de Chimie et de Physique*; Landmarks II, scientific journals; Masson., 1818.
- (10) Rubin, M. B. The History of Ozone. The Schönbein Period, 1839–1868. *Bull. Hist. Chem* **2001**, *26* (1), 40–56.
- (11) Parnell, J. XXXVIII.—On the Reducing Action of Peroxide of Hydrogen and Carboic Acid. *J. Chem. Soc.* **1868**, *21* (0), 356–357. <https://doi.org/10.1039/JS8682100356>.
- (12) Wardman, P.; Candeias, L. P. Fenton Chemistry: An Introduction. *Radiation Research* **1996**, *145* (5), 523. <https://doi.org/10.2307/3579270>.
- (13) Fenton, H. J. H. XLI.—The Constitution of a New Dibasic Acid, Resulting from the Oxidation of Tartaric Acid. *J. Chem. Soc., Trans.* **1896**, *69* (0), 546–562. <https://doi.org/10.1039/CT8966900546>.
- (14) Fenton, H. J. H. LXXIII.—Oxidation of Tartaric Acid in Presence of Iron. *J. Chem. Soc., Trans.* **1894**, *65* (0), 899–910. <https://doi.org/10.1039/CT8946500899>.
- (15) Ruff, O. Ueber Die Verwandlung Der *d*-Gluconsäure in *d*-Arabinose. *Ber. Dtsch. Chem. Ges.* **1898**, *31* (2), 1573–1577. <https://doi.org/10.1002/cber.18980310250>.
- (16) Fischer, E. Ueber Die Configuration Des Traubenzuckers Und Seiner Isomeren. *Ber. Dtsch. Chem. Ges.* **1891**, *24* (1), 1836–1845. <https://doi.org/10.1002/cber.189102401311>.
- (17) Brodie, B. C. Ueber Die Bildung Der Hyperoxyde Organischer Säureradicale. *Justus Liebigs Ann. Chem.* **1858**, *108* (1), 79–83. <https://doi.org/10.1002/jlac.18581080117>.

- (18) Brodie, B. C. XXXII.—The Organic Peroxides Theoretically Considered. *J. Chem. Soc.* **1864**, 17 (0), 281–294. <https://doi.org/10.1039/JS8641700281>.
- (19) Frankland, E. XXVII.—Researches on the Organic Radicals. *Q. J. Chem. Soc.* **1851**, 3 (4), 321–347. <https://doi.org/10.1039/QJ8510300321>.
- (20) Kolbe, H. XXXII.—On the Chemical Constitution and Nature of Organic Radicals. *Q. J. Chem. Soc.* **1851**, 3 (4), 369–405. <https://doi.org/10.1039/QJ8510300369>.
- (21) Brodie, B. C. S. XLI.—On the Oxidation and Disoxidation Effected by the Alkaline Peroxide. *J. Chem. Soc.* **1863**, 16 (0), 316–342. <https://doi.org/10.1039/JS8631600316>.
- (22) Brodie, C. XXXI.—On the Peroxides of the Radicals of the Organic Acids. *J. Chem. Soc.* **1864**, 17 (0), 266–281. <https://doi.org/10.1039/JS8641700266>.
- (23) Gomberg, M. AN INSTANCE OF TRIVALENT CARBON: TRIPHENYLMETHYL. *J. Am. Chem. Soc.* **1900**, 22 (11), 757–771. <https://doi.org/10.1021/ja02049a006>.
- (24) Haber, F.; Weiss, J. Über die Katalyse des Hydroperoxydes. *Naturwissenschaften* **1932**, 20 (51), 948–950. <https://doi.org/10.1007/BF01504715>.
- (25) Haber, F.; Willstätter, R. Unpairedness and Radical Chains in the Reaction Mechanism of Organic and Enzymic Process. *Ber Deutsch Chem Ges* **1931**, 64, 2844–2856.
- (26) Gelissen, H.; Hermans, P. H. Über Neue Synthesen Mittels Organischer Peroxyde, I. Mitteilung: Die Einwirkung Des Dibenzoylperoxyds Und Einiger Seiner Derivate Auf Siedendes Benzol. *Ber. dtsh. Chem. Ges. A/B* **1925**, 58 (2), 285–294. <https://doi.org/10.1002/cber.19250580209>.
- (27) Gelissen, H.; Hermans, P. H. Über Neue Synthesen Mittels Organischer Peroxyde, II.: Die Einwirkung Des Dibenzoylperoxyds Auf Toluol. *Ber. dtsh. Chem. Ges. A/B* **1925**, 58 (3), 476–479. <https://doi.org/10.1002/cber.19250580307>.

- (28) Gelissen, H.; Hermans, P. H. Über Neue Synthesen Mittels Organischer Peroxyde, IV.: Die Einwirkung von Dibenzoylperoxyd Auf Diphenyl. *Ber. dtsh. Chem. Ges. A/B* **1925**, 58 (4), 764–765. <https://doi.org/10.1002/cber.19250580423>.
- (29) Gelissen, H.; Hermans, P. H. Über Neue Synthesen Mittels Organischer Peroxyde, II.: Die Einwirkung Des Dibenzoylperoxyds Auf Toluol. *Ber. dtsh. Chem. Ges. A/B* **1925**, 58 (3), 476–479. <https://doi.org/10.1002/cber.19250580307>.
- (30) Milas, N. A.; McAlevy, A. Studies in Organic Peroxides. I. Peroxides in the Camphoric Acid Series. *J. Am. Chem. Soc.* **1933**, 55 (1), 349–352. <https://doi.org/10.1021/ja01328a048>.
- (31) George, P.; Walsh, A. D. A Note on the Decomposition of Tertiary Alkyl Peroxides. *Transactions of the Faraday Society* **1946**, 42, 94–97.
- (32) Criegee, R. Die Umlagerung Der Dekalin-peroxydester Als Folge von Kationischem Sauerstoff. *Justus Liebigs Ann. Chem.* **1948**, 560 (1), 127–135. <https://doi.org/10.1002/jlac.19485600106>.
- (33) Criegee, R.; Dietrich, H. Darstellung Und Veresterung Tertiärer Hydroperoxyde. *Justus Liebigs Ann. Chem.* **1948**, 560 (1), 135–141. <https://doi.org/10.1002/jlac.19485600107>.
- (34) Criegee, R.; Schnorrenberg, W.; Becke, J. Zur Konstitution von Ketonperoxyden. *Justus Liebigs Ann. Chem.* **1949**, 565 (1), 7–21. <https://doi.org/10.1002/jlac.19495650103>.
- (35) Criegee, R.; Wenner, G. Die Ozonisierung Des 9,10-Oktalins. *Justus Liebigs Ann. Chem.* **1949**, 564 (1), 9–15. <https://doi.org/10.1002/jlac.19495640103>.
- (36) Schönbein, C. F. On the Production of Ozone by Chemical Means. *Philosophical Magazine* **1844**, No. 17, 293–294.
- (37) Harries, C. Ueber Die Einwirkung Des Ozons Auf Organische Verbindungen. *Justus Liebigs Ann. Chem.* **1905**, 343 (2–3), 311–344. <https://doi.org/10.1002/jlac.19053430209>.

- (38) Harries, C. Über Die Einwirkung Des Ozons Auf Organische Verbindungen. [Zweite Abhandlung.]. *Justus Liebigs Ann. Chem.* **1910**, 374 (3), 288–368.
<https://doi.org/10.1002/jlac.19103740303>.
- (39) Harries, C. Über Die Einwirkung Des Ozons Auf Organische Verbindungen. *Justus Liebigs Ann. Chem.* **1912**, 390 (2), 235–268. <https://doi.org/10.1002/jlac.19123900205>.
- (40) Staudinger, H. *Ber Deutsch Chem Ges* **1925**, No. 58, 1088.
- (41) Pummerer, R. *Angewandte Chemie* **1934**, 47, 366.
- (42) Rieche, A.; Meister, R.; Sauthoff, H. Über Ozonoide Und Ihre Spaltung. *Liebigs Ann. Chem.* **1942**, No. 533, 187–249.
- (43) Criegee, R. Mechanism of Ozonolysis. *Angew. Chem. Int. Ed. Engl.* **1975**, 14 (11), 745–752. <https://doi.org/10.1002/anie.197507451>.
- (44) Hawkins, E. G. E. 445. The Reactions of Organic Peroxides. Part I. 2-Phenyl-2-Butyl Hydroperoxide. *J. Chem. Soc.* **1949**, 2076. <https://doi.org/10.1039/jr9490002076>.
- (45) Youngman, E. A.; Rust, F. F.; Coppinger, G. M.; Mare, H. E. D. L. The Autoxidation of Nonvicinal Glycols Ester Formation via Cyclic Ethers and Their Peroxides. *J. Org. Chem.* **1963**, 28 (1), 144–148. <https://doi.org/10.1021/jo01036a033>.
- (46) Kochi, J. K. Chemistry of Alkoxy Radicals: Cleavage Reactions. *J. Am. Chem. Soc.* **1962**, 84 (7), 1193–1197. <https://doi.org/10.1021/ja00866a026>.
- (47) Kharasch, M.; Fono, A. Communications - A New Method of Introducing Peroxy Groups into Organic Molecules. *J. Org. Chem.* **1958**, 23 (2), 324–325.
<https://doi.org/10.1021/jo01096a624>.

- (48) Kharasch, M. S.; Fono, A. New Metal Salt-Induced Homolytic Reactions. II. Modification of Free Radical Reactions by Copper Salts ¹. *J. Org. Chem.* **1959**, *24* (5), 606–614. <https://doi.org/10.1021/jo01087a007>.
- (49) Kharasch, M. S.; Sosnovsky, G. Oxidative Reactions of Nitriles—II. *Tetrahedron* **1958**, *3* (2), 105–112. [https://doi.org/10.1016/0040-4020\(58\)80002-2](https://doi.org/10.1016/0040-4020(58)80002-2).
- (50) Minisci, F.; Portolani, A. Peroxides and Diazonium Salts III. Azides and Nitriles of 1-Hydroxyhydroperoxides. *Gazz. chim. ital* **1959**, *89*, 1941–1949.
- (51) Kochi, J. K.; Mains, H. E. Studies on the Mechanism of the Reaction of Peroxides and Alkenes with Copper Salts ^{*1}. *J. Org. Chem.* **1965**, *30* (6), 1862–1872. <https://doi.org/10.1021/jo01017a036>.
- (52) Kumamoto, J.; De La Mare, H. E.; Rust, F. F. The Use of Cupric and Ferric Chlorides in the Trapping of Radical Intermediates and the Synthesis of Alkyl Chlorides. *J. Am. Chem. Soc.* **1960**, *82* (8), 1935–1939. <https://doi.org/10.1021/ja01493a024>.
- (53) De La Mare, H. E.; Kochi, J. K.; Rust, F. F. The Oxidation and Reduction of Free Radicals by Metal Salts. *J. Am. Chem. Soc.* **1963**, *85* (10), 1437–1449. <https://doi.org/10.1021/ja00893a014>.
- (54) Cekovic, Z.; Green, M. M. Formation of Remote Double Bonds by Ferrous Sulfate-Cupric Acetate Promoted Decomposition of Alkyl Hydroperoxides. *J. Am. Chem. Soc.* **1974**, *96* (9), 3000–3002. <https://doi.org/10.1021/ja00816a059>.
- (55) Čeković, Ž.; Dimttruević, Lj.; Djokić, G.; Srnić, T. Remote Functionalisation by Ferrous Ion-Cupric Ion Induced Decomposition of Alkyl Hydroperoxides. *Tetrahedron* **1979**, *35* (17), 2021–2026. [https://doi.org/10.1016/S0040-4020\(01\)88972-9](https://doi.org/10.1016/S0040-4020(01)88972-9).

- (56) Solomon, E. I.; Heppner, D. E.; Johnston, E. M.; Ginsbach, J. W.; Cirera, J.; Qayyum, M.; Kieber-Emmons, M. T.; Kjaergaard, C. H.; Hadt, R. G.; Tian, L. Copper Active Sites in Biology. *Chem. Rev.* **2014**, *114* (7), 3659–3853. <https://doi.org/10.1021/cr400327t>.
- (57) Glaser, C. Beiträge Zur Kenntniss Des Acetylnylbenzols. *Ber. Dtsch. Chem. Ges.* **1869**, *2* (1), 422–424. <https://doi.org/10.1002/cber.186900201183>.
- (58) Ullmann, F.; Bielecki, J. Ueber Synthesen in Der Biphenylreihe. *Ber. Dtsch. Chem. Ges.* **1901**, *34* (2), 2174–2185. <https://doi.org/10.1002/cber.190103402141>.
- (59) Ullmann, F. Ueber Eine Neue Bildungsweise von Diphenylaminderivaten. *Ber. Dtsch. Chem. Ges.* **1903**, *36* (2), 2382–2384. <https://doi.org/10.1002/cber.190303602174>.
- (60) Ullmann, F.; Sponagel, P. Ueber Die Phenylirung von Phenolen. *Ber. Dtsch. Chem. Ges.* **1905**, *38* (2), 2211–2212. <https://doi.org/10.1002/cber.190503802176>.
- (61) Goldberg, I. Ueber Phenylirungen Bei Gegenwart von Kupfer Als Katalysator. *Ber. Dtsch. Chem. Ges.* **1906**, *39* (2), 1691–1692. <https://doi.org/10.1002/cber.19060390298>.
- (62) Sambigioglio, C.; Marsden, S. P.; Blacker, A. J.; McGowan, P. C. Copper Catalysed Ullmann Type Chemistry: From Mechanistic Aspects to Modern Development. *Chem. Soc. Rev.* **2014**, *43* (10), 3525–3550. <https://doi.org/10.1039/C3CS60289C>.
- (63) Paine, A. J. Mechanisms and Models for Copper Mediated Nucleophilic Aromatic Substitution. 2. Single Catalytic Species from Three Different Oxidation States of Copper in an Ullmann Synthesis of Triarylaminines. *J. Am. Chem. Soc.* **1987**, *109* (5), 1496–1502. <https://doi.org/10.1021/ja00239a032>.
- (64) Chan, D. M. T.; Monaco, K. L.; Wang, R.-P.; Winters, M. P. New N- and O-Arylations with Phenylboronic Acids and Cupric Acetate. *Tetrahedron Letters* **1998**, *39* (19), 2933–2936. [https://doi.org/10.1016/S0040-4039\(98\)00503-6](https://doi.org/10.1016/S0040-4039(98)00503-6).

- (65) Lam, P. Y. S.; Clark, C. G.; Saubern, S.; Adams, J.; Winters, M. P.; Chan, D. M. T.; Combs, A. New Aryl/Heteroaryl C–N Bond Cross-Coupling Reactions via Arylboronic Acid/Cupric Acetate Arylation. *Tetrahedron Letters* **1998**, *39* (19), 2941–2944.
[https://doi.org/10.1016/S0040-4039\(98\)00504-8](https://doi.org/10.1016/S0040-4039(98)00504-8).
- (66) Bryant, R. J.; Sterwin, A. G. Processes for Substitution of Aromatic Compounds. GB 2,089,672, 1982.
https://worldwide.espacenet.com/publicationDetails/originalDocument?FT=D&date=19820630&DB=&locale=en_EP&CC=GB&NR=2089672A&KC=A&ND=2.
- (67) Capdevielle, P.; Maumy, M. Esters Are Effective Co-Catalysts in Copper-Catalyzed Methanolysis of Aryl Bromides. *Tetrahedron Letters* **1993**, *34* (6), 1007–1010.
[https://doi.org/10.1016/S0040-4039\(00\)77477-6](https://doi.org/10.1016/S0040-4039(00)77477-6).
- (68) Goodbrand, H. B.; Hu, N.-X. Ligand-Accelerated Catalysis of the Ullmann Condensation: Application to Hole Conducting Triarylamines. *J. Org. Chem.* **1999**, *64* (2), 670–674. <https://doi.org/10.1021/jo981804o>.
- (69) Kwong, F. Y.; Klapars, A.; Buchwald, S. L. Copper-Catalyzed Coupling of Alkylamines and Aryl Iodides: An Efficient System Even in an Air Atmosphere. *Org. Lett.* **2002**, *4* (4), 581–584. <https://doi.org/10.1021/ol0171867>.
- (70) Shafir, A.; Buchwald, S. L. Highly Selective Room-Temperature Copper-Catalyzed C–N Coupling Reactions. *J. Am. Chem. Soc.* **2006**, *128* (27), 8742–8743.
<https://doi.org/10.1021/ja063063b>.
- (71) Shafir, A.; Lichtor, P. A.; Buchwald, S. L. N- versus O-Arylation of Aminoalcohols: Orthogonal Selectivity in Copper-Based Catalysts. *J. Am. Chem. Soc.* **2007**, *129* (12), 3490–3491. <https://doi.org/10.1021/ja068926f>.

- (72) Klapars, A.; Antilla, J. C.; Huang, X.; Buchwald, S. L. A General and Efficient Copper Catalyst for the Amidation of Aryl Halides and the *N*-Arylation of Nitrogen Heterocycles. *J. Am. Chem. Soc.* **2001**, *123* (31), 7727–7729. <https://doi.org/10.1021/ja016226z>.
- (73) Klapars, A.; Huang, X.; Buchwald, S. L. A General and Efficient Copper Catalyst for the Amidation of Aryl Halides. *J. Am. Chem. Soc.* **2002**, *124* (25), 7421–7428. <https://doi.org/10.1021/ja0260465>.
- (74) Zhu, D.; Wang, R.; Mao, J.; Xu, L.; Wu, F.; Wan, B. Efficient Copper-Catalyzed Amination of Aryl Halides with Amines and NH Heterocycles Using Rac-BINOL as Ligand. *Journal of Molecular Catalysis A: Chemical* **2006**, *256* (1–2), 256–260. <https://doi.org/10.1016/j.molcata.2006.05.005>.
- (75) Bariwal, J.; Van der Eycken, E. C–N Bond Forming Cross-Coupling Reactions: An Overview. *Chem. Soc. Rev.* **2013**, *42* (24), 9283. <https://doi.org/10.1039/c3cs60228a>.
- (76) Tran, B. L.; Li, B.; Driess, M.; Hartwig, J. F. Copper-Catalyzed Intermolecular Amidation and Imidation of Unactivated Alkanes. *J. Am. Chem. Soc.* **2014**, *136* (6), 2555–2563. <https://doi.org/10.1021/ja411912p>.
- (77) Tye, J. W.; Weng, Z.; Johns, A. M.; Incarvito, C. D.; Hartwig, J. F. Copper Complexes of Anionic Nitrogen Ligands in the Amidation and Imidation of Aryl Halides. *J. Am. Chem. Soc.* **2008**, *130* (30), 9971–9983. <https://doi.org/10.1021/ja076668w>.
- (78) Garrett, C. E.; Prasad, K. The Art of Meeting Palladium Specifications in Active Pharmaceutical Ingredients Produced by Pd-Catalyzed Reactions. *Adv Synth Catal* **2004**, *346* (8), 889–900. <https://doi.org/10.1002/adsc.200404071>.

- (79) Kainz, Q. M.; Matier, C. D.; Bartoszewicz, A.; Zultanski, S. L.; Peters, J. C.; Fu, G. C. Asymmetric Copper-Catalyzed C-N Cross-Couplings Induced by Visible Light. *Science* **2016**, *351* (6274), 681–684. <https://doi.org/10.1126/science.aad8313>.
- (80) Evano, G.; Blanchard, N.; Toumi, M. Copper-Mediated Coupling Reactions and Their Applications in Natural Products and Designed Biomolecules Synthesis. *Chem. Rev.* **2008**, *108* (8), 3054–3131. <https://doi.org/10.1021/cr8002505>.
- (81) Bhunia, S.; Pawar, G. G.; Kumar, S. V.; Jiang, Y.; Ma, D. Selected Copper-Based Reactions for C–N, C–O, C–S, and C–C Bond Formation. *Angew Chem Int Ed* **2017**, *56* (51), 16136–16179. <https://doi.org/10.1002/anie.201701690>.
- (82) Zhang, J.; Huan, X.-D.; Wang, X.; Li, G.-Q.; Xiao, W.-J.; Chen, J.-R. Recent Advances in C(Sp³)–N Bond Formation via Metallaphoto-Redox Catalysis. *Chem. Commun.* **2024**, *60* (50), 6340–6361. <https://doi.org/10.1039/D4CC01969E>.
- (83) Zheng, Y.; Zheng, H.; Li, T.; Wei, W. Recent Advances in Copper-Catalyzed C–N Bond Formation Involving N-Centered Radicals. *ChemSusChem* **2021**, *14* (24), 5340–5358. <https://doi.org/10.1002/cssc.202102243>.
- (84) Solladie, G.; Hutt, J. Total Synthesis of Dihydrovitamin DHV3 and Dihydrotachysterol DHT3. Application of the Low-Valent Titanium Induced Reductive Elimination. *J. Org. Chem.* **1987**, *52* (16), 3560–3566. <https://doi.org/10.1021/jo00392a012>.
- (85) Monti, H.; Audran, G.; Monti, J.-P.; Leandri, G. Enantioselective Total Synthesis of (+)-(2*R*,6*R*)-*Trans*- γ -Irone. *J. Org. Chem.* **1996**, *61* (17), 6021–6023. <https://doi.org/10.1021/jo960392l>.

- (86) Ohba, M.; Iizuka, K.; Ishibashi, H.; Fujii, T. Syntheses and Absolute Configurations of the Marine Sponge Purines (+)-Agelasimine-A and (+)-Agelasimine-B. *Tetrahedron* **1997**, *53* (50), 16977–16986. [https://doi.org/10.1016/S0040-4020\(97\)10120-X](https://doi.org/10.1016/S0040-4020(97)10120-X).
- (87) Aubin, Y.; Audran, G.; Monti, H. Improved Enantioselective Synthesis of Natural Striatenic Acid and Its Methyl Ester. *Tetrahedron Letters* **2006**, *47* (22), 3669–3671. <https://doi.org/10.1016/j.tetlet.2006.03.147>.
- (88) Jiang, C.-H.; Bhattacharyya, A.; Sha, C.-K. Enantiospecific Total Synthesis of (–)-Bakkenolide III and Formal Total Synthesis of (–)-Bakkenolides B, C, H, L, V, and X. *Org. Lett.* **2007**, *9* (17), 3241–3243. <https://doi.org/10.1021/ol071124k>.
- (89) Fazakerley, N. J.; Helm, M. D.; Procter, D. J. Total Synthesis of (+)-Pleuromutilin. *Chemistry A European J* **2013**, *19* (21), 6718–6723. <https://doi.org/10.1002/chem.201300968>.
- (90) Zhou, B.-D.; Ren, J.; Liu, X.-C.; Zhu, H.-J. Theoretical and Experimental Study of the Absolute Configuration of Helical Structure of (2R,3S)-Rubiginone A2 Analog. *Tetrahedron* **2013**, *69* (3), 1189–1194. <https://doi.org/10.1016/j.tet.2012.11.050>.
- (91) Muchalski, H.; Xu, L.; Porter, N. A. Tunneling in Tocopherol-Mediated Peroxidation of 7-Dehydrocholesterol. *Org. Biomol. Chem.* **2015**, *13* (4), 1249–1253. <https://doi.org/10.1039/C4OB02377C>.
- (92) Xia, Q.; Liu, X.; Zhang, Y.; Chen, C.; Chen, W. Copper-Catalyzed *N*-Methylation of Amides and *O*-Methylation of Carboxylic Acids by Using Peroxides as the Methylating Reagents. *Org. Lett.* **2013**, *15* (13), 3326–3329. <https://doi.org/10.1021/ol401362k>.

- (93) Kubo, T.; Chatani, N. Dicumyl Peroxide as a Methylating Reagent in the Ni-Catalyzed Methylation of Ortho C–H Bonds in Aromatic Amides. *Org. Lett.* **2016**, *18* (7), 1698–1701. <https://doi.org/10.1021/acs.orglett.6b00658>.
- (94) Rong, G.; Liu, D.; Lu, L.; Yan, H.; Zheng, Y.; Chen, J.; Mao, J. Iron-Catalyzed Decarboxylative Methylation of α,β -Unsaturated Acids under Ligand-Free Conditions. *Tetrahedron* **2014**, *70* (34), 5033–5037. <https://doi.org/10.1016/j.tet.2014.06.014>.
- (95) Zhang, Y.; Feng, J.; Li, C.-J. Palladium-Catalyzed Methylation of Aryl C–H Bond by Using Peroxides. *J. Am. Chem. Soc.* **2008**, *130* (10), 2900–2901. <https://doi.org/10.1021/ja0775063>.
- (96) Teng, F.; Cheng, J.; Yu, J.-T. Copper-Catalyzed N-Methylation/Ethylation of Sulfoximines. *Org. Biomol. Chem.* **2015**, *13* (39), 9934–9937. <https://doi.org/10.1039/C5OB01558H>.
- (97) Sakamoto, R.; Sakurai, S.; Maruoka, K. Alkylsilyl Peroxides as Alkylating Agents in the Copper-Catalyzed Selective Mono- *N*-Alkylation of Primary Amides and Arylamines. *Chemistry A European J* **2017**, *23* (38), 9030–9033. <https://doi.org/10.1002/chem.201702217>.
- (98) Sakurai, S.; Kato, T.; Sakamoto, R.; Maruoka, K. Generation of Alkyl Radicals from Alkylsilyl Peroxides and Their Applications to C–N or C–O Bond Formations. *TETRAHEDRON* **2019**, *75* (2), 172–179. <https://doi.org/10.1016/j.tet.2018.11.048>.
- (99) Sakamoto, R.; Sakurai, S.; Maruoka, K. Bis(Trialkylsilyl) Peroxides as Alkylating Agents in the Copper-Catalyzed Selective Mono-*N*-Alkylation of Primary Amides. *Chem. Commun.* **2017**, *53* (48), 6484–6487. <https://doi.org/10.1039/C7CC02910A>.

- (100) Bao, J.; Tian, H.; Yang, P.; Deng, J.; Gui, J. Modular Synthesis of Functionalized Butenolides by Oxidative Furan Fragmentation. *EUROPEAN JOURNAL OF ORGANIC CHEMISTRY* **2020**, *2020* (3), 339–347. <https://doi.org/10.1002/ejoc.201901613>.
- (101) Liu, S.; Ma, P.; Zhang, L.; Shen, S.; Miao, H.-J.; Liu, L.; Houk, K. N.; Duan, X.-H.; Guo, L.-N. A Cheap Metal Catalyzed Ring Expansion/Cross-Coupling Cascade: A New Route to Functionalized Medium-Sized and Macrolactones. *Chem. Sci.* **2023**, *14* (19), 5220–5225. <https://doi.org/10.1039/D2SC06157K>.
- (102) Tang, Z.-L.; Ouyang, X.-H.; Song, R.-J.; Li, J.-H. Decarboxylative C(Sp³)–N Cross-Coupling of Diacyl Peroxides with Nitrogen Nucleophiles. *Org. Lett.* **2021**, *23* (3), 1000–1004. <https://doi.org/10.1021/acs.orglett.0c04203>.

CHAPTER 2: Aminodealkenylation: Ozonolysis and Copper Catalysis Convert C(sp³)–C(sp²) Bonds to C(sp³)–N Bonds

Zhiqi He.; Jose A. Moreno.; Manisha Swain.; Jason Wu; Ohyun Kwon*

Science **2023**, *381* (6660), 877–886.

2.1. Abstract

Great efforts have been directed toward alkene π -bond amination. In contrast, analogous functionalization of the adjacent C(sp²)–C(sp³) σ -bonds is much rarer. Herein we report how ozonolysis and copper catalysis under mild reaction conditions enable alkene C(sp³)–C(sp²) σ -bond–rupturing cross-coupling reactions for the construction of new C(sp³)–N bonds. We have used this unconventional transformation for late-stage modification of hormones, pharmaceutical reagents, peptides, and nucleosides. Furthermore, we have coupled abundantly available terpenes and terpenoids with nitrogen nucleophiles to access artificial terpenoid-alkaloids and complex chiral amines. In addition, we applied a commodity chemical, α -methylstyrene, as a methylation reagent to prepare methylated nucleosides directly from canonical nucleosides in one synthetic step. Our mechanistic investigation implicates an unusual copper ion-pair cooperative process.

2.2. Introduction

The importance of aliphatic amines and nitrogen-heterocycles is evidenced by their wide representation in natural products, pharmaceuticals, agrochemicals, and other bioactive compounds.¹ The increasing demand in medicinal research for more complex three-dimensional architectures and optically active amines has driven efforts to develop diverse practical methods for C(sp³)–N bond construction.^{2, 3} Conventionally, the electron-rich nature of amino nitrogen atoms renders them strong nucleophiles that can attack the polarized chemical bonds of alkyl halides, alcohol derivatives, and carbonyls, thereby forging new C(sp³)–N bonds. Engaging

ubiquitous and nonpolar C–C bonds in C(sp³)–N bond construction is an intriguing strategy because such transformations can be used to modify molecular skeletons directly and, thereby, access conventionally challenging or inaccessible aliphatic amines.⁴⁻⁶ Classical methods for C–C bond amination, including the Lossen, Hofmann, Curtius, Beckmann, and Schmidt rearrangements, which typically rely on 1,2-migration of an alkyl/aryl group from carbon to nitrogen (Fig. 1A, eqs. 1 and 2), have demonstrated their utility in the syntheses of bioactive molecules and in industrial manufacturing. For example, 5.5 million metric tons of caprolactam, a precursor to Nylon 6, are produced annually through the Beckmann rearrangement of cyclohexanone oxime.⁷ Although these classical transformations are powerful methods for accessing nitrogen insertion products, the sources of the C–C bonds are limited mostly to ketones and carboxylic acids, and the sources of nitrogen atoms are limited to those that insert one N atom, leaving room for incorporation of alternative, perhaps more ubiquitous, chemical functionalities as the sources of both the C–C and C–N bonds.

In the past five years, several important advances have sought to address those limitations in the sources of both the C–C bonds and nitrogen atoms in C–C amination. The Jiao group employed the C–C bonds of alkylarenes, styrenes, and alkynylarenes in a Schmidt-type reaction, although the products were limited to anilines with new C(sp²)–N bonds, due to the preferred migration of the aryl group (Fig. 1A, eq. 3).⁸⁻¹⁰ Fu, Hu, MacMillan, and Martin disclosed deconstructive C(sp³)–N couplings of carboxylic acid and ketone derivatives that overcame the limitation of 1,2-migration chemistry, providing methods to construct C(sp³)–N bonds with various N-heteroarenes, amides, and anilines (Fig. 1A, eq. 4).¹¹⁻¹⁵ Despite these advances, there remains a huge scope for new sources of C–C bonds, beyond carbonyl compounds, for amination.¹⁶⁻²⁰ In particular,

developing methods to exploit a starting material's skeletal complexity to access chiral amine architectures would be highly desirable.

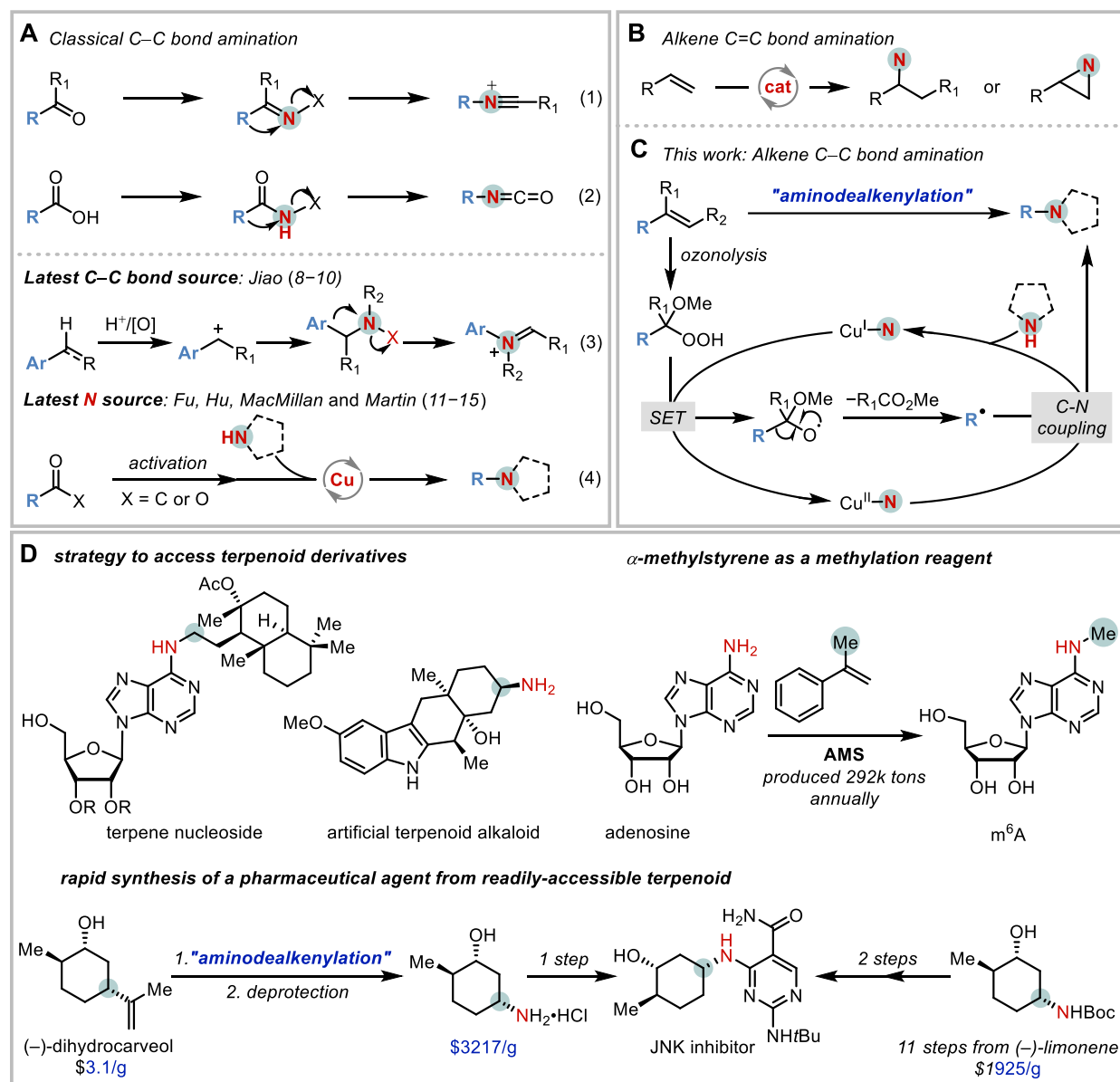


Figure 2.1 Concept and development of dealkenylative C(sp³)–N bond coupling

Alkenes are versatile functional groups that are abundant in natural products and industrial chemicals. In fact, C=C double bonds are the second most frequently encountered functional group in natural products (39.9%), exceeding ketone (15.9%) and carboxylic acid (10.6%)

functionalities.²¹ Because chiral centers are common within natural products, we surmised that the alkene moieties in natural products might serve as ideal C–C bond amination precursors for constructing complex chiral amines from naturally occurring chiral-pool molecules. Most methods for installing nitrogen groups to alkene motifs have focused on addition across the C–C π -bond to produce peripheral amination products (Fig. 1B).³ Conversely, the adjacent C(sp³)–C(sp²) σ -bonds have received less attention for C–N bond construction (Fig. 1C, top). We envisioned that a C–N bond coupling strategy involving unusual C–C bond disconnections would constitute a distinct paradigm for alkyl amine synthesis, with several implications. First, it could access artificial terpenoid alkaloids and complex chiral amine architectures by embedding nitrogen motifs into the natural product precursors (Fig. 1D, top left).²² Second, a commodity chemical, α -methylstyrene, could be applied as an N-methylation reagent (Fig. 1D, top right; for comparison with other N-methylation reagents, see Section 2.6.5.5).²³ Third, such a tool could facilitate the generation of useful value-added compounds that have been challenging to form or inaccessible from readily available starting materials. One such example is (1*R*,2*R*,5*R*)-5-amino-2-methylcyclohexan-1-ol hydrogen chloride, a precursor of a JNK inhibitor. The significant step economy and cost savings from previous approaches indicate the potential utility of this C(sp³)–C(sp²) amination strategy in bioactive reagent synthesis (Fig. 1D, bottom).²⁴

2.3. Reaction Design

To accomplish the conversion of alkene C(sp³)–C(sp²) σ -bonds to C(sp³)–N bonds, we had to address a fundamental challenge: cleavage of a stronger alkene C(sp³)–C(sp²) σ -bond [bond dissociation energy (BDE) = 102 kcal/mol for propene] in preference to an aliphatic alkyl C(sp³)–C(sp³) σ -bond (90 kcal/mol in ethane).²⁵ To realize it, our strategy engaged ozone, widely applied in several industries, to activate alkenes and facilitate their C(sp³)–C(sp²) σ -bond cleavages.^{26, 27}

Ozonolysis of alkenes in alcoholic solvents affords α -alkoxyhydroperoxides *via* the Criegee intermediate.²⁸ The weakness of the O–O bond (44–46 kcal/mol for alkyl hydroperoxides) of an α -alkoxyhydroperoxide can serve as the energetic driving force to promote fragmentation of the robust C–C bond. Previously, we had used Fe(II) salts as single-electron reducing agents to instigate O–O scission. The resulting α -alkoxyalkoxyl radical undergoes β -scission to release an alkyl radical that can be captured by organic radicophiles to provide the functionalization products of seemingly inert C(sp³)–C(sp²) σ -bonds (Fig. 1C, bottom).²⁹⁻³¹

Copper is a redox-active metal that has been used for single electron reduction of peroxide intermediates in both biological processes and synthetic chemistry.³² Recent studies have demonstrated that copper catalysts are efficient at trapping alkyl radicals to afford C(sp³)–N bonds as reductive elimination products.^{12, 13, 33-36} We envisioned sequential reduction of the hydroperoxide intermediate by a copper(I) amido complex and trapping of the resultant alkyl radical by the copper(II) center to induce reductive elimination and, thereby, form the C(sp³)–N bond in an overall redox-neutral process (Fig. 1C, bottom).

2.4. Reaction Scope

To implement our design, we investigated the impact of the copper salt, ligand, and solvent. We discovered that the aminodealkenylation could be performed efficiently under mild reaction conditions when employing CuCl (20 mol%) and 1,10-phenanthroline (20 mol%) in acetonitrile (MeCN) at room temperature (see the Supplementary Materials for details). After determining the reaction conditions, we assessed a diverse array of nitrogen nucleophiles for dealkenylative C–N coupling with (–)-isopulegol as the model alkene substrate (Fig. 2). Our protocol could be employed to install functionalized indoles (**2-1** to **2-7**) into (–)-isopulegol in high yields, producing enantiomerically pure indole derivatives that are promising scaffolds for drug development.³⁷ Two

indole-based natural products, the sleep hormone melatonin (**2-6**) and a protected form of the amino acid tryptophan (**2-7**), were alkylated in high yields with exclusive regioselectivity in the presence of secondary amide N–H bonds. Other pharmaceutically important substituted heterocyclic compounds, including azaindoles (**2-8** to **2-10**), indazoles (**2-11** and **2-12**), carbazole (**2-13**), pyrazoles (**2-14** and **2-15**), and pyrrole (**2-16**), were successfully coupled with (–)-isopulegol in good yields. 6-Chloro-7-iodo-7-deazapurine (**2-17**), a privileged scaffold in antitumor and antiviral drugs, was also a competent alkylation substrate. We obtained high yields when coupling it with phthalimide (**2-18**), and this process could be scaled (50 mmol) with a slightly decreased yield. In addition to azacycles, we found that 2-aminopyrimidine (**2-19**), substituted anilines (**2-20** and **2-21**), and 2-aminopyridine (**2-22**) also underwent the dealkenylative C–N coupling efficiently. Less-nucleophilic amide (**2-23**) and sulfonamide (**2-24**) substrates also provided their coupling products in good yields. Notably, aryl halides were unaffected under the reaction conditions and might be employed as functional handles for further derivatization.

To demonstrate the utility of this protocol in drug discovery, we applied our dealkenylative C–N coupling strategy to the late-stage functionalization of complex bioactive molecules. An *N*-tosyl prolinamide (**2-25**) and a dexibuprofen amide (**2-26**) were decorated with chiral 2-hydroxy-4-methylcyclohexyl groups in good yields. Two known pharmaceuticals, the nonsteroidal anti-inflammatory celecoxib (**2-27**) and the antiretroviral lamivudine (**2-28**), were also *N*-alkylated effectively. Encouraged by the exclusive alkylation of the indole nitrogen atom of tryptophan, we explored the potential for indole *N*-functionalization of the tryptophan residue in the context of peptides featuring several amide N–H bonds. Gratifyingly, both the tripeptide **2-29** and an endogenous opioid neurotransmitter, the endomorphin precursor **2-30**, underwent the site-selective

C–N couplings in good yields with gentle heating. We also tested aliphatic amines, including benzylamine, dibenzylamine, and 1-phenylpiperazine, but none of them afforded desired C–N

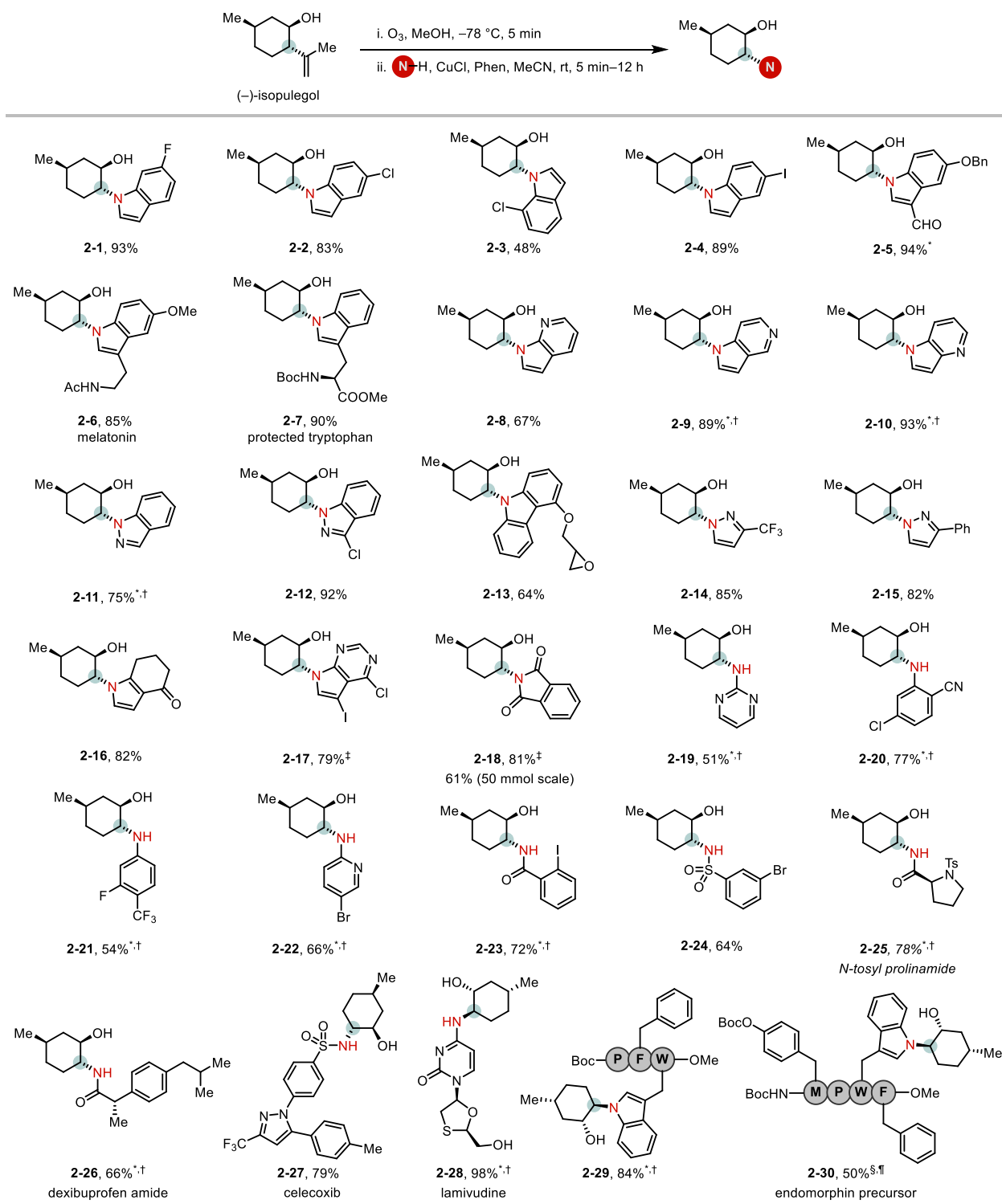


Figure 2.2 Substrate scope of nitrogen nucleophiles.

coupling products. We surmise that aliphatic amines serve as strongly donating ligands on copper, thereby influencing the coordination structures and redox potentials of the copper complexes **3-7/3-8**, in turn leading to inefficient regeneration of copper(I) species (see Section 3.8 of Chapter 3 for details).

Beyond (–)-isopulegol, we subjected an array of terpenes, terpenoids, and their derivatives to our deconstructive C–N coupling protocol to afford various artificial terpenoid alkaloids (Fig. 3). Most of these substrates are single enantiomers derived from natural products or are natural products themselves. (+)-Nootkatone and a eudesmane-type sesquiterpenoid underwent fragmentative C–N couplings with 3-chloroindazole and phthalimide to give the products **2-31a/31b** and **2-32a/32b**, respectively, in good yields with excellent diastereoselectivities. The bridged cyclic ketoester **2-33** was obtained in moderate yield and diastereoselectivity from the synthetic intermediate leading to (+)-seychellene. While good yields could be obtained regardless of substrate, the diastereoselectivity varied widely, especially when engaging the monocyclic terpenoids (–)-limonene-1,2-diol, (+)-dihydrocarvone ethylene glycol acetal, *cis*-(+)-limonene oxide, (+)-dihydrocarveol, (–)-perillyl alcohol oxide, (–)-carveol oxide, and (–)-*O*-benzoyl isopulegol (**2-34** to **2-40**). The observed diastereoselectivities are consistent with stereoselectivity trends commonly encountered in reactions with cyclic radicals, in which the stereoselectivity of the addition is dictated by a combination of torsional and steric effects.^{38, 39} All of the diastereoisomers [except two: the diastereoisomers of the minor regioisomers, **2-57a/57b**, from the aminodealkenylation of (–)- β -pinene] were separable through silica-column flash chromatography—a particularly relevant feature for lead compound discovery because diastereoisomers often exhibit dramatically different bioactivities. Simple cyclohexyl and 4-piperidinyl radicals worked well when applied to the functionalization of

melatonin (**2-41**) and tryptophan (**2-42**), respectively. We evaluated substrates bearing gem-disubstituted olefins, beyond the isopropenyl group, in the reaction and found that they provided primary alkyl-substituted amines in a facile manner (**2-43** to **2-47**). The epoxy indazole **2-43** was obtained in 83% yield from a (\pm)- α -ionone oxide derivative. A (–)-sclareol–derived alkene underwent smooth dealkenylative amination with 3-chloroindazole to afford the drimane meroterpenoid derivative **2-44** in 61% yield. Drimane meroterpenoids possess diverse bioactivities and our protocol provides a strategy toward N-heterocycles substituted with these terpenoid analogues.⁴⁰ We used (*R*)-2,4-dimethylpent-4-en-1-ol, which can be accessed readily from Evans' auxiliary (*ca.* \$3/g for *R*- or *S*-enantiomer) and 2-methyl chloride, to synthesize (*R*)-3-(3-chloroindazolyl)-2-methylpropanol *O*-acetate (**2-45**), a precursor of muscarinic agonists, in 74% yield.⁴¹ Enantiopure 3-indazolyl-2-methylpropanols appear in 22 international patents and two U.S. patents and were prepared from the corresponding (+)- and (–)-3-bromo-2-methyl-1-propanols (*ca.* \$190/g from Sigma–Aldrich), which have previously been prepared from camphor sulfonic acids in five synthetic steps.⁴² Primary alkyl radicals from functionalized alkenes underwent efficient amination (**2-46** and **2-47**). Mono-substituted alkenes were also competent substrates for our Cu-catalyzed dealkenylative C–N coupling (R = R' = H); in contrast, these alkenes performed only moderately in Fe(II)-mediated dealkenylative radical couplings.²⁹ In the event, we obtained a 73% isolated yield of the dealkenylative C–N coupling product **2-48** from (\pm)-dihydromyrcenol. Mono-substituted alkenes derived from (–)- β -citronellol and (+)-geraniol oxide *O*-acetate derivatives afforded the fragmented C–N coupling products **2-49a/49b**, and **2-50** in good yields. 1-Decene, which is produced from the Ziegler process or through cracking in the petroleum industry, worked well as a substrate to generate 3-

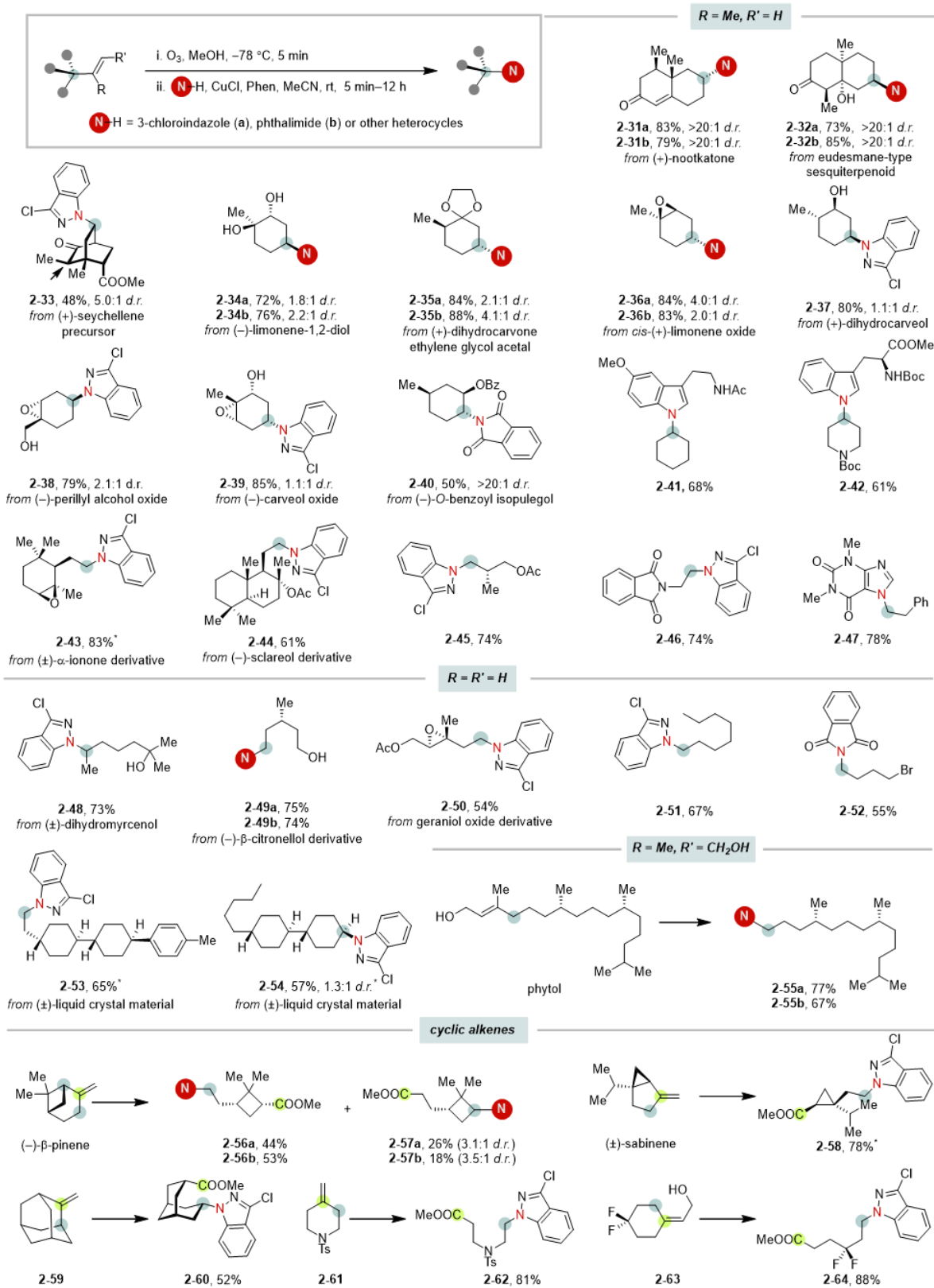


Figure 2.3 Scope of Alkenes

chloro-1-octylindazole (**2-51**) in 67% yield. We found that an alkyl bromide, which could serve

as a radical precursor, was tolerated under our conditions to produce *N*-(4-bromobutyl)phthalimide (**2-52**) in 55% yield.

We also applied our deconstructive C–N coupling protocol to the modification of molecules of interest to materials science. The vinyl groups of chiral molecules used in liquid crystals were replaced by 3-chloroindazole in good yields (**2-53** and **2-54**). Another natural product, phytol, containing a trisubstituted alkene unit, underwent regioselective C(sp³)–C(sp²) σ -bond cleavage to afford the coupling products **2-55a** and **2-55b** in good yields. Compounds **2-55a** and **2-55b** could be considered azacycle analogues of vitamin E, where the benzopyran unit is substituted by chloroindazole and phthalimide moieties, respectively.

Alkylidenecycloalkanes were also suitable substrates for the dealkenylative C–N coupling process. (–)- β -Pinene provided the synthetically valuable chiral cyclobutanes **2-56a/57a** and **2-56b/57b** as 1.7:1 and 2.9:1 mixtures of regioisomers, respectively. In contrast, (\pm)-sabinene afforded the cyclopropane **2-58** as a single regioisomer in 78% yield. Methyleneadamantane (**2-59**) provided the equatorial amination product **2-60** exclusively. The β -amino acid derivative **2-62** was formed smoothly from the corresponding 4-methylenepiperidine **2-61**. The copper-catalyzed amination also converted the trisubstituted alkene **2-63** into the corresponding dealkenylated C–N coupling product **2-64** in 88% yield.

2.5. Applications of aminodealkenylation: Chiral primary amines, N-methylation protocol, and terpene-nucleosides

The ability to use aminodealkenylation to install phthalimide units into chiral-pool molecules provided an opportunity to synthesize chiral primary amines. For example, we prepared the primary amine **2-65** in 75% yield from the phytol-derived phthalimide **2-55b**. Chiral amino alcohols are common in nature, and such bioactive compounds often serve as auxiliaries in organic

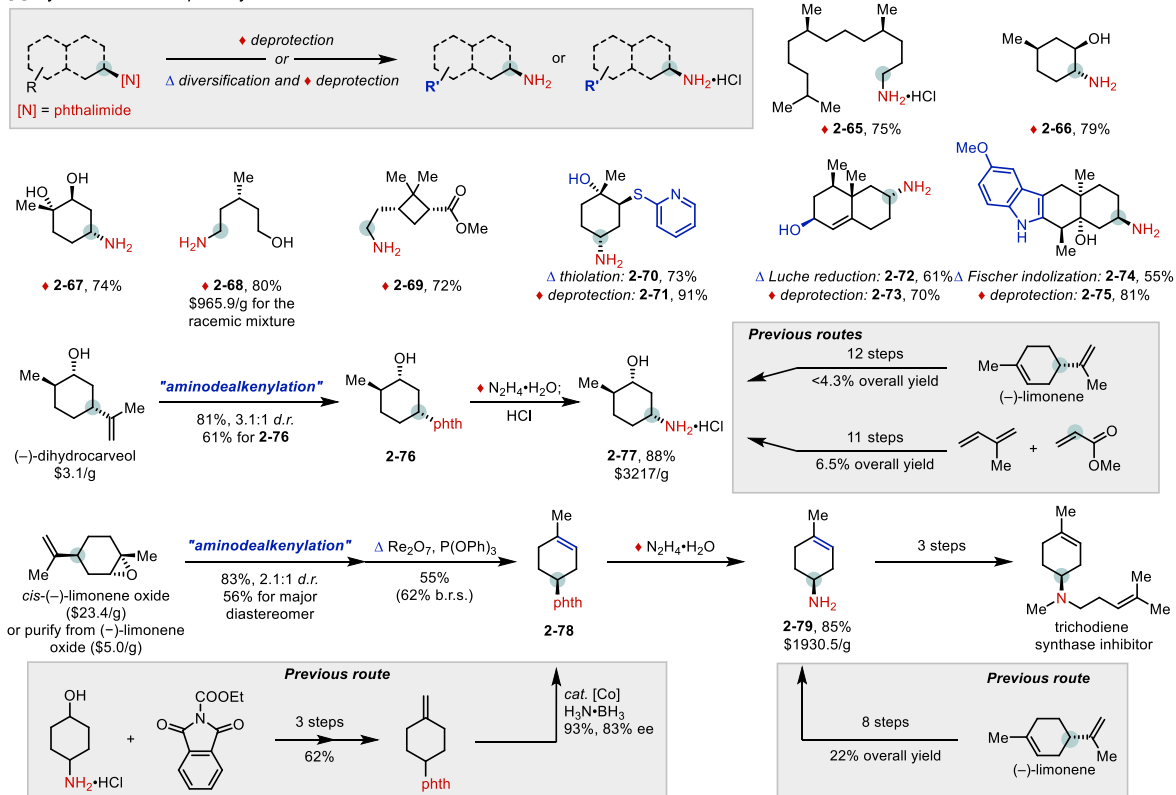
synthesis. 1,2-Aminocyclohexanol is an important motif in organic synthesis and medicinal chemistry; we prepared its unusual 5-methylated analogue **2-66** in 79% yield upon hydrazine-mediated deprotection of the phthalimide **2-18**. Similarly, we synthesized the aminocyclohexandiol **2-67** from the opposite enantiomer of **2-34b** (major diastereoisomer). Although 5-amino-3-methylpentan-1-ol is a useful building block, no asymmetric synthesis has been reported previously and its racemic form costs \$965.90/g. We obtained (*R*)-**2-68** upon deprotection of the phthalimide **2-49b** derived from (–)- β -citronellol. The chiral amino acid ester **2-69** can be synthesized from (–)- β -pinene. The abundant functional groups in terpenoids also facilitated the synthesis of more-elaborate amino alcohols through diversification. For example, we prepared the amino alcohol **2-71** from *cis*-(–)-limonene oxide through aminodealkenylation, thiolation, and deprotection. We obtained the amino alcohol **2-73**, bearing a nootkatol skeleton, through the Luche reduction of **2-31b**, followed by deprotection. We synthesized the artificial indole alkaloid **2-75** through sequential Fischer indolization of **2-32b** with 4-methoxyphenylhydrazine and deprotection. (1*R*,2*R*,5*R*)-5-Amino-2-methylcyclohexanol (**2-77**) is a synthetic intermediate leading to a JNK inhibitor (Fig 1D)^{24, 43}; previous routes to its synthesis have involved 12 steps from (–)-limonene and 11 steps from the Diels–Alder reaction of isoprene and methyl acrylate. Using our deconstructive C–N coupling strategy with commercially available (–)-dihydrocarveol (\$3.1/g) and phthalimide, followed by deprotection using hydrazine monohydrate, afforded **2-77** in two steps in 54% overall yield. Chiral 4-substituted-1-methylcyclohexenes are synthetically challenging molecules and serve as key intermediates in the syntheses of various pharmaceuticals and natural products.⁴⁴ (*S*)-1-Methylcyclohexenyl-4-amine (**2-79**, \$1930.5/g) has been a precursor in the synthesis of a trichodiene synthase inhibitor. The previous route to **2-79** involved eight steps from chiral limonenes.⁴⁵ The enantioenriched

phthalimide **2-78** was prepared recently by Liu and co-workers in four steps, including an alkene desymmetrization strategy employing a chiral cobalt(II) complex catalyst, which was prepared in six steps from L-alaninol.⁴⁴ Our strategy engaged commercially available *cis*-(-)-limonene oxide for dealkenylative amination. In the event, the C–N coupling products were produced in 83% yield with 2.1:1 *d.r.*, with the desired diastereoisomer (isolated in 56% yield), after subsequent deoxygenation, affording the chiral phthalimide **2-78** in 55% yield. The deprotection proceeded smoothly to afford the primary amine **2-79** in 85% yield (29% overall yield over three steps). Considering the capability of copper-catalyzed coupling with various nucleophiles, our strategy might provide facile access to chiral 4-substituted-1-methylcyclohexenes. α -Methylstyrene (AMS), a by-product of the cumene process, is produced in over 292k tons annually.⁴⁶ Because of the relative stability of the methyl radical (BDE: 105.0 kcal/mol for Me–H) over the phenyl radical (BDE: 112.9 kcal/mol for Ph–H)²⁵, we surmised that the Criegee ozonolysis product of AMS, upon exposure to the Cu(I) complex, should produce methyl radicals and, thereby, methylated amines.²³ Indeed, we found that reactions with AMS readily generated 1-methyl-3-chloroindazole (**2-80**) and caffeine (from theophylline) under our protocol, in yields of 84 and 67%, respectively. We methylated zidovudine, an anti-HIV drug, at the N3 atom of the thymidine moiety to afford 3-methylzidovudine, without protecting the 5'-hydroxyl group. Particularly useful methylations were those of canonical nucleosides. *N*⁶-Methyladenosine (**m⁶A**) is the most abundantly modified nucleoside in eukaryotic mRNAs; it plays a crucial role in controlling gene expression in cellular, developmental, and disease processes.⁴⁷

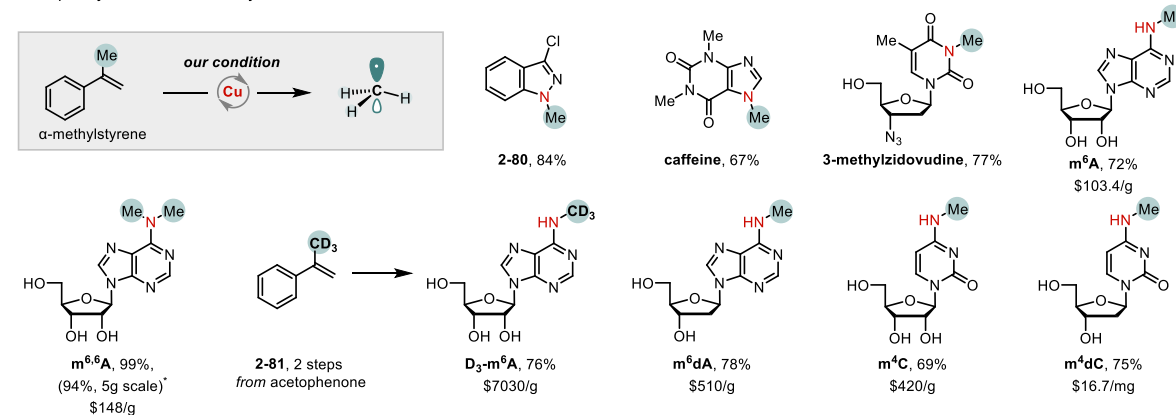
When using our protocol, adenosine (\$0.097/g) can be methylated directly to **m⁶A** (\$103.4/g) in 72% isolated yield in a single step, compared with the two or three steps in previous reports. We achieved another common RNA modification, **m^{6,6}A** (\$148/g), in nearly quantitative yield when

using an additional equivalent of AMS (*cf.* the two steps in a previous report). We also performed the reaction on a 5-gram scale, providing a pure sample without the need for silica-column

A Synthesis of chiral primary amines



B Rapid synthesis of *N*-methylated nucleosides from canonical nucleosides



C Synthesis of terpene nucleosides

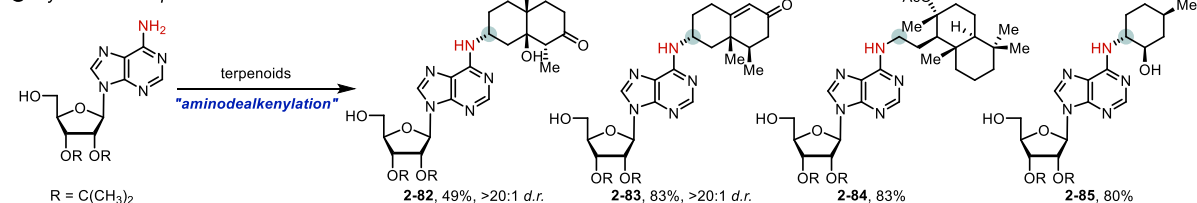


Figure 2.4 Application of dealkenylative C(sp³)-N bond coupling in bioactive compound

purification. We used the deuterium-labeled α -trideuteromethylstyrene (**2-81**), obtained from acetophenone and deuterium oxide in two steps, to generate isotopically labeled **D₃-m⁶A** (\$7030/g). We prepared other common methylated nucleosides, namely **m⁶dA** (\$510/g), **m⁴C** (\$420/g), and **m⁴dC** (\$16.7/mg), from the corresponding canonical deoxyadenosine, cytidine, and deoxycytidine, respectively, in good yields, where multiple synthetic steps or low yields were previously necessary (see Section 2.6.5.8 Additional information on prices and previous syntheses of compounds that appear in the main text for previous routes).

Encouraged by the successful nucleoside methylation, we employed aminodealkenylation for the rapid construction of terpene nucleosides. Terpene nucleoside natural products are generated through the adenosine processing of sesquiterpenoids or diterpenoids. They are found in bacterial metabolites and exhibit significant biofunctionality and bioactivity—for example, as an antacid signaling molecule or as a component in the cell wall of mycobacterium tuberculosis.⁴⁸ Furthermore, an adenosine-processed eudesmane-type sesquiterpenoid isolated from the myxobacterium *Sorangium cellulosum* exhibited moderate antibacterial activity against a wide range of bacterial strains.⁴⁹ Pleasingly, we used the eudesmane-type sesquiterpenoid (**2-82**), (+)-nootkatone (**2-83**), drimane sesquiterpenoid (**2-84**), and the monoterpene (–)-isopulegol (**2-85**) to prepare terpene nucleosides in moderate to good yields. Analogues of terpene nucleosides can be applied as chemical probes of biological function, while their innate bioactivity might also provide a platform for developing lead compounds in medicinal research.

Given the straightforward nature of the modular introduction of nitrogen moieties through the unusual disconnection of alkene skeletons, we anticipate that our copper-catalyzed dealkenylation C–N coupling will find applications in the preparation of complex bioactive three-dimensional

molecules and optically active amines of great interest in organic synthesis and medicinal chemistry.

2.6. Experimental

2.6.1. Materials and Methods

Unless otherwise stated, reactions were performed in flame-dried glassware fitted with rubber septa, under an argon atmosphere, and stirred with Teflon-coated magnetic stirring bars. Liquid reagents and solvents were transferred via syringe using standard Schlenk techniques. Methanol (MeOH) was distilled over magnesium under an argon atmosphere. Dichloromethane (DCM), acetonitrile (MeCN), and triethylamine were distilled over calcium hydride under an argon atmosphere. Tetrahydrofuran (THF), benzene, toluene, and diethyl ether were distilled over sodium/benzophenone ketyl under an argon atmosphere. All other solvents and reagents were used as received from commercial sources, unless otherwise noted. Reaction temperatures above 23 °C refer to oil bath temperatures. Thin layer chromatography (TLC) was performed using SiliCycle silica gel 60 F-254 precoated plates (0.25 mm) and visualized under UV irradiation, with a cerium ammonium molybdate (CAM) stain or a potassium permanganate (KMnO₄) stain. SiliCycle Silica-P silica gel (particle size 40–63 μm) was used for flash column chromatography (FCC). ¹H and ¹³C NMR spectra were recorded using Bruker AV-500, AV-400, and AV-300 MHz spectrometers, with ¹³C NMR spectroscopic operating frequencies of 125, 100, and 75 MHz, respectively. Chemical shifts (δ) are reported in parts per million (ppm) relative to the residual protonated solvent signal: CDCl₃ (δ = 7.26 for ¹H NMR; δ = 77.16 for ¹³C NMR), CD₃OD (δ = 3.31 for ¹H NMR; δ = 49.00 for ¹³C NMR), DMSO-d₆ (δ = 2.50 for ¹H NMR; δ = 39.52 for ¹³C NMR), CD₂Cl₂ (δ = 5.32 for ¹H NMR; δ = 53.84 for ¹³C NMR), (CD₃)₂CO (δ = 2.05 for ¹H NMR; δ = 206.26, 29.84 for ¹³C NMR), and CD₃CN (δ = 1.94 for ¹H NMR; δ = 118.26, 1.32 for ¹³C NMR).

Data for ^1H NMR spectra are reported as follows: chemical shift, multiplicity, coupling constant(s) (Hz), and number of hydrogen atoms. Data for ^{13}C NMR spectra are reported in terms of chemical shift. The following abbreviations are used to describe the multiplicities: s = singlet; d = doublet; t = triplet; q = quartet; quint = quintet; m = multiplet; br = broad. Melting points (MP) are uncorrected and were recorded using an Electrothermal® capillary melting point apparatus. IR spectra were recorded using a Jasco FTIR4100 spectrometer with an ATR attachment; the selected signals are reported in units of cm^{-1} . Optical rotations were recorded using an Autopol IV polarimeter and a 100 mm cell, at concentrations close to 1 g/100 mL. HRMS (ESI) was performed using a Waters LCT Premier spectrometer equipped with an ACQUITY UPLC system and autosampler. HRMS (DART) was performed using a Thermo Fisher Scientific Exactive Plus spectrometer equipped with an IonSense ID CUBE DART source. Ozonolysis was performed using a Globalozone GO-D3G (3 g/h) ozone generator (2.0 L/min, 50% power, O₂ feed gas). In situ FTIR spectroscopic reaction monitoring was performed using a Mettler Toledo ReactIR 702L apparatus, and the data were analyzed using iC IR 7.1 software.

Caution: Ozone is an extremely toxic and reactive oxidant that can react with some compounds to form explosive and shock-sensitive products. Although we have not encountered any ozone-related safety issues in our laboratory, reactions with ozone should be performed only by properly trained individuals in a well-ventilated fume hood (use of a blast-shield is also recommended, especially for reactions performed on larger scales).

2.6.2. Substrate Preparation

The alkenes (–)-isopulegol, nootkatone, **2-94**, **2-95**, **2-106**, **2-109**, **2-110**, **2-111**, **2-112**, phytol, (–)- β -pinene, and (\pm) sabinene in Fig. 2.5, and the amines in Figs. 2.2 and 2.3 and Figs. 2.4B and 2.4C, were commercially available and used as received. Compounds **2-86**,⁵⁹ **2-87**,⁶⁰ **2-88**,⁶¹ **2-**

89,⁶¹ 2-90,⁶² 2-91,⁶³ 2-34,⁶⁴ 2-93,⁶⁵ 2-96,⁶⁶ 2-97,⁶⁷ 2-99,⁶⁸ 2-100,⁶⁹ 2-101,⁷⁰ 2-102,⁷⁰ 2-103,⁷¹ 2-104,⁷² 2-105,⁷² 2-107,⁷³ 2-108,^{73, 74} 2-59,⁷⁵ 2-61,⁷⁶ and 2-81,^{77, 78} were synthesized according to the previously reported procedures (Figure 2.5).

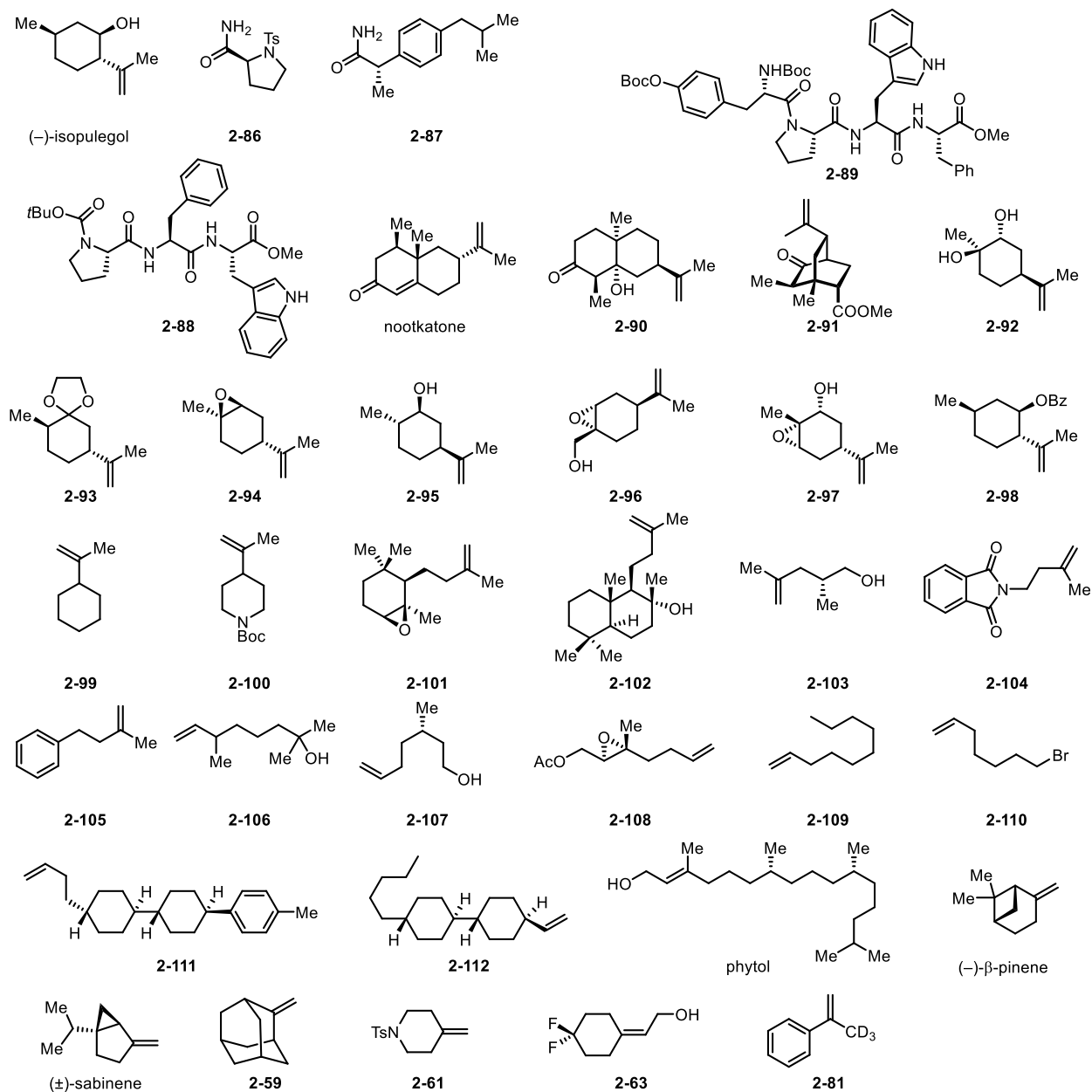
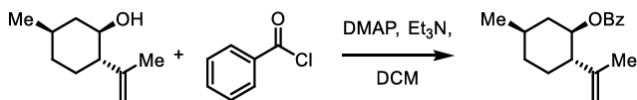


Figure 2.5: Substrates used in aminodealkenylation reactions

Compounds 2-98 and 2-63 were prepared according to the following procedures:



Benzoyl chloride (11.6 mL, 100 mmol, 1.25 equiv) was added slowly to a cooled (0 °C) mixture of (-)- isopulegol (12.3 g, 80.0 mmol, 1.0 equiv), triethylamine (13.2 mL, 100 mmol, 1.25 equiv), and *N,N* dimethylpyridin-4-amine (0.980 g, 8.00 mmol, 0.1 equiv) in DCM (1 L). The resulting mixture was stirred at 0 °C for 30 min, then at room temperature overnight. This mixture was washed with sat. aqueous NaHCO₃ (2 × 300 mL), sat. aqueous NH₄Cl (2 × 300 mL), and brine (300 mL). The organic layer was dried (Na₂SO₄) and filtered. Evaporation of all volatiles under reduced pressure and purification through

FCC (*R_f* = 0.83; hexanes/EtOAc, 9:1) yielded the benzoate **2-98** as a colorless oil (11.9 g, 53% yield). ¹H NMR (400 MHz, CDCl₃) δ 8.03–7.97 (m, 2H), 7.56–7.49 (m, 1H), 7.44–7.37 (m, 2H), 5.02 (td, *J* = 10.9, 4.4 Hz, 1H), 4.82–4.77 (m, 1H), 4.72 (p, *J* = 1.5 Hz, 1H), 2.35–2.25 (m, 1H), 2.21–2.11 (m, 1H), 1.81–1.70 (m, 2H), 1.70–1.68 (m, 3H), 1.68–1.57 (m, 1H), 1.53–1.40 (m, 1H), 1.20–1.09 (m, 1H), 1.09–0.98 (m, 1H), 0.96 (d, *J* = 6.5 Hz, 3H).

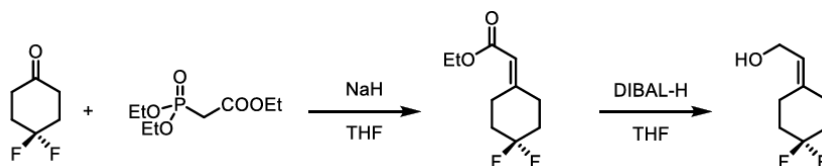
¹³C NMR (100 MHz, CDCl₃) δ 166.01, 146.16, 132.61, 130.89, 129.55, 128.23, 111.94, 74.32, 50.92, 40.51, 34.20, 31.45, 30.51, 22.07, 19.51.

IR (neat, ATR): ν_{max} 3073, 2951, 2926, 2868, 1714, 1647, 1451, 1313, 1287, 1271, 1175, 1110, 1069, 1026, 975, 966, 890, 709 cm⁻¹.

HRMS (DART): [M+H]⁺ calcd for [C₁₇H₂₃O₂]⁺ *m/z* 259.1693, found 259.1693.

Optical Rotation: [α]_D²⁵ = -28.38 (*c* 0.39, CHCl₃)

The alkene **2-63** was synthesized according to the literature procedure.⁷⁹



Methyl or ethyl diethylphosphonoacetate (1.23 g, 5.50 mmol, 1.1 equiv) was added to a cooled (0 °C) suspension of NaH (240 mg, 60 wt% in mineral oil, 6.00 mmol, 1.2 equiv) in THF (0.1 M). The resulting mixture was stirred at 0 °C for 30 min. A solution of 4,4-difluorocyclohexan-1-one (671 mg, 5.00 mmol, 1.0 equiv) in THF (10 mL) was added to the mixture, which was then stirred at room temperature until full conversion of the ketone was detected (TLC). The reaction was quenched through the addition of sat. aqueous NaHCO₃ (100 mL) and then the aqueous phase was extracted with Et₂O (2 × 100 mL). The combined organic layers were washed with brine, dried (Na₂SO₄), and filtered. Evaporation of all volatiles under reduced pressure and purification through FCC (*R*_f = 0.49; hexane/EtOAc, 20:1) yielded the enone product as a colorless oil (956 mg, 94% yield).

DIBAL-H (1.2 M in toluene, 10 mL, 12 mmol) was added to a cooled (-78 °C) solution of the unsaturated ester (956 mg, 4.7 mmol) in THF (50 mL). When the reduction was complete (TLC), the reaction was quenched through the addition of water (2 mL) and sat. potassium sodium tartrate (10 mL) and stirring overnight. The suspension was filtered off and extracted with EtOAc (3 × 30 mL). The combined organic layers were dried (Na₂SO₄) and concentrated under reduced pressure. The crude material was purified through FCC on silica gel to afford **2-63** (*R*_f = 0.57; hexanes/EtOAc, 1:1) as a white solid (720 mg, 95% yield).

¹H NMR (400 MHz, CDCl₃) δ 5.48 (t, *J* = 6.9 Hz, 1H), 4.14 (d, *J* = 7.0 Hz, 2H), 2.39–2.32 (m, 2H), 2.32–2.23 (m, 2H), 2.02–1.86 (m, 4H), 1.65 (brs, 1H).

^{13}C NMR (100 MHz, CDCl_3) δ 138.50, 123.57, 123.14 (t, $J = 239.5\text{ Hz}$), 58.58, 34.79 (t, $J = 23.6\text{ Hz}$), 34.25 (t, $J = 24.0\text{ Hz}$), 32.09 (t, $J = 5.3\text{ Hz}$), 23.99 (t, $J = 5.4\text{ Hz}$).

IR (neat, ATR): ν_{max} 3343 (br), 2970, 2945, 2917, 2888, 2856, 1675, 1440, 1362, 1276, 1267, 1113, 1105, 1070, 1002, 965, 951, 931, 740, 678 cm^{-1} .

HRMS (DART): $[\text{M}+\text{Na}]^+$ calcd for $[\text{C}_8\text{H}_{12}\text{F}_2\text{NaO}]^+$ m/z 185.0748, found 185.0721. **M.p.:** 32–35 $^\circ\text{C}$.

2.6.3. Detection of side products under unoptimized conditions

An oven-dried 8-mL Schlenk tube equipped with a magnetic stirrer bar was charged with phthalimide (44.1 mg, 0.300 mmol, 1.5 equiv), $\text{Cu}(\text{MeCN})_4\text{PF}_6$ (14.9 mg, 0.0400 mmol, 20 mol %), and 3,4,7,8-tetramethyl-1,10-phenanthroline **L1** (14.2 mg, 0.0600 mmol, 30 mol %). The tube was purged with argon three times and then dry MeCN (2 mL) was added. This mixture was stirred at room temperature for 10 min. Another 50-mL round-bottom flask equipped with a magnetic stirrer bar was charged with (–)-*O*-benzoylisopulegol (**2-98**, 258 mg, 1.00 mmol, 1.0 equiv) and MeOH (20 mL, 0.05 M), then cooled to $-78\text{ }^\circ\text{C}$ in a dry-ice/acetone bath. Ozone was bubbled through the solution until complete consumption of the starting material (as indicated by TLC and/or a blue color in the reaction mixture). The solution was sparged with argon for 5 min to expel excess ozone and then the reaction mixture was warmed to room temperature and the MeOH evaporated *in vacuo*. The residue was dissolved in benzene (10 mL) and the solution concentrated *in vacuo* to azeotrope off traces of water. The residue was dissolved in MeOH (4.8 mL) to form a 0.2 M solution. A portion (1.0 mL) of this MeOH solution was transferred into the Schlenk tube *via* syringe. The reaction vessel was stirred at room temperature for 12 h, followed by the addition of 1-chloro 2,4-dinitrobenzene (40.5 mg, 0.2 mmol, 1.0 equiv) as an internal standard. The reaction mixture concentrated *in vacuo*. The residue was passed through a short plug

of silica gel to remove the copper salts and then the filtrate was concentrated *in vacuo*. The crude material was analyzed using NMR spectroscopy.

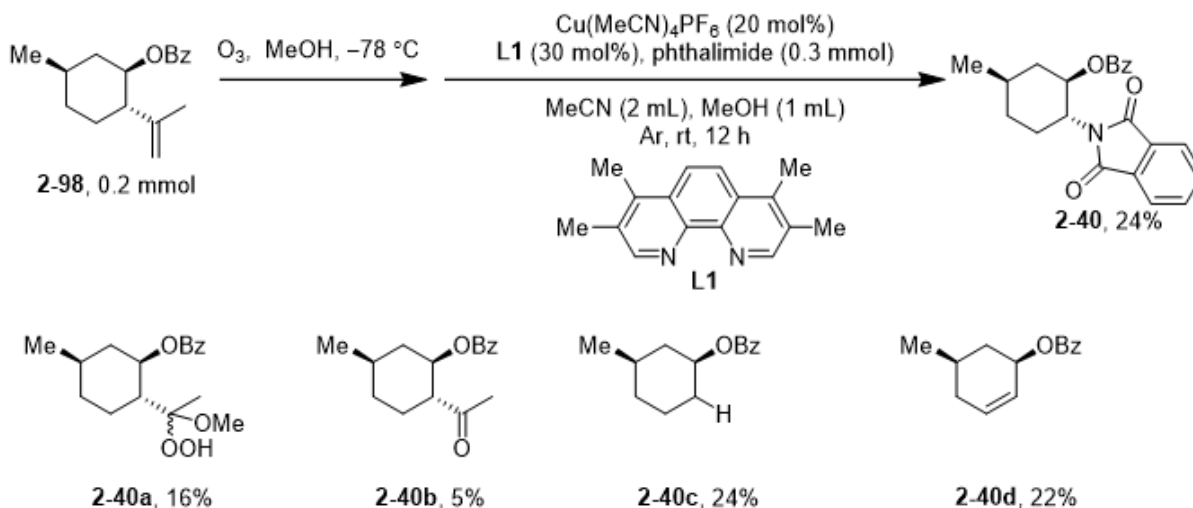
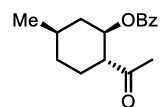


Figure 2.6 Preliminary results and side products of copper-catalyzed aminodealkenylation

After 12 h, the desired C–N coupling product **2-40** was obtained in 24% yield. Most of **2-98** had been consumed, with a 16% recovery. Major byproducts were the ketone **2-40b**, the alkane **2-40c**, and the alkene **2-40d**.



2-40b

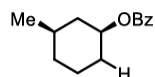
$^1\text{H NMR}$ (400 MHz, CDCl_3) δ 8.02–7.86 (m, 2H), 7.63–7.50 (m, 1H), 7.41 (t, $J = 7.7$ Hz, 2H), 5.23 (td, $J = 11.0, 4.5$ Hz, 1H), 2.74 (ddd, $J = 12.6, 10.7, 3.8$ Hz, 1H), 2.32–2.21 (m, 1H), 2.17 (s, 3H), 1.96 (dq, $J = 13.4, 3.5$ Hz, 1H), 1.87–1.72 (m, 1H), 1.71–1.63 (m, 1H), 1.49 (qd, $J = 13.2, 3.7$ Hz, 1H), 1.14–0.98 (m, 2H), 0.96 (d, $J = 6.6$ Hz, 3H).

$^{13}\text{C NMR}$ (100 MHz, CDCl_3) δ 209.86, 165.57, 132.92, 130.29, 129.52, 128.33, 74.06, 55.82, 39.56, 33.42, 30.95, 29.03, 27.88, 21.86.

HRMS (DART): $[\text{M}+\text{Na}]^+$ calcd for $[\text{C}_{16}\text{H}_{20}\text{NaO}_3]^+$ m/z 283.1305, found 283.1305.

IR (neat, ATR): ν_{max} 3021, 2955, 2928, 2871, 2856, 1715, 1451, 1355, 1314, 1284, 1274, 1216, 1110, 1096 cm^{-1}

Optical Rotation: $[\alpha]_{\text{D}}^{25} = -34.44$ (c 0.3, CHCl_3)



2-40c

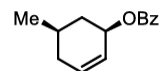
^1H NMR (400 MHz, CDCl_3) δ 8.06–7.99 (m, 2H), 7.58–7.49 (m, 1H), 7.47–7.37 (m, 2H), 5.00–4.88 (m, 1H), 2.14–2.02 (m, 2H), 1.88–1.78 (m, 1H), 1.71–1.63 (m, 1H), 1.63–1.49 (m, 1H), 1.48–1.29 (m, 2H), 1.13 (q, $J = 12.1$ Hz, 1H), 0.96 (d, $J = 6.6$ Hz, 3H), 0.88 (qd, $J = 12.7, 3.8$ Hz, 1H).

^{13}C NMR (100 MHz, CDCl_3) δ 166.07, 132.66, 130.96, 129.52, 128.24, 73.87, 40.59, 34.08, 31.62, 31.40, 24.02, 22.33.

IR (neat, ATR): ν_{max} 2949, 2931, 2862, 1714, 1451, 1315, 1275, 1255, 1174, 1112, 1069, 1040, 1026, 972, 710 cm^{-1} .

HRMS (DART): $[\text{M}+\text{Na}]^+$ calcd for $[\text{C}_{14}\text{H}_{18}\text{NaO}_2]^+$ m/z 241.1190, found 241.1190.

Optical Rotation: $[\alpha]_{\text{D}}^{24} = -4.05$ (c 0.2, CHCl_3)



2-40d

^1H NMR (400 MHz, CDCl_3) δ 8.15–7.97 (m, 2H), 7.60–7.49 (m, 1H), 7.48–7.37 (m, 2H), 5.89 (ddt, $J = 9.5, 4.7, 2.1$ Hz, 1H), 5.77–5.69 (m, 1H), 5.64 (dddq, $J = 10.0, 5.8, 4.1, 2.1$ Hz, 1H), 2.27–2.04 (m, 2H), 1.89 (dttt, $J = 11.5, 9.2, 5.0, 2.7$ Hz, 1H), 1.74 (dddd, $J = 16.3, 10.2, 6.0, 2.8$ Hz, 1H), 1.42 (td, $J = 12.2, 9.8$ Hz, 1H), 1.03 (d, $J = 6.6$ Hz, 3H).

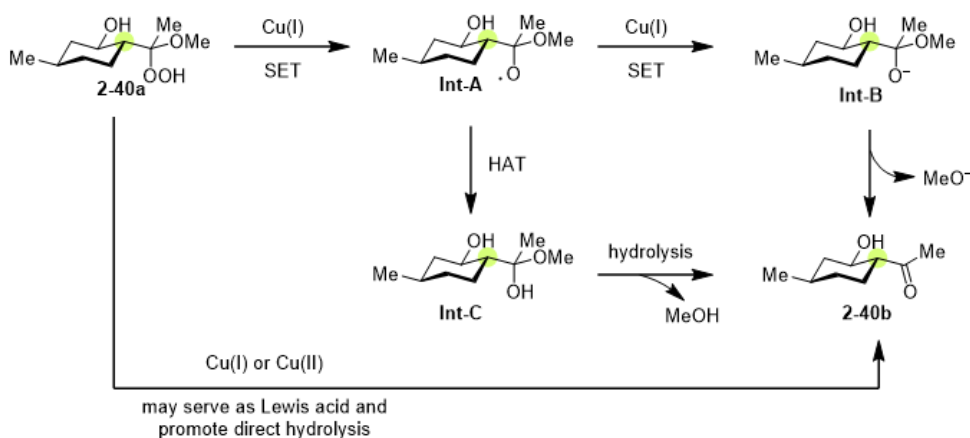
^{13}C NMR (100 MHz, CDCl_3) δ 166.31, 132.79, 130.70, 129.60, 128.28, 126.90, 71.29, 36.83, 33.55, 27.86, 21.88.

IR (neat, ATR): ν_{max} 3064, 3034, 2952, 2926, 2908, 2879, 2872, 2830, 1714, 1451, 1274, 1112, 1069, 1026, 953, 710 cm^{-1} .

HRMS (DART): $[\text{M}+\text{H}]^+$ calcd for $[\text{C}_{14}\text{H}_{17}\text{O}_2]^+$ m/z 217.1223, found 217.1223.

Optical Rotation: $[\alpha]_{\text{D}}^{24} = 48.76$ (c 0.43, CHCl_3)

A. Proposed pathways for ketone formation



B. Proposed pathways for alkane and alkene formation

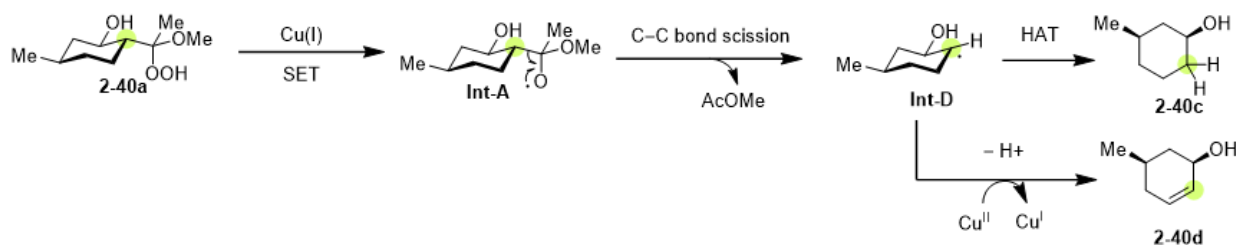


Figure 2.7 Preliminary mechanistic explanation for the formation of the byproducts

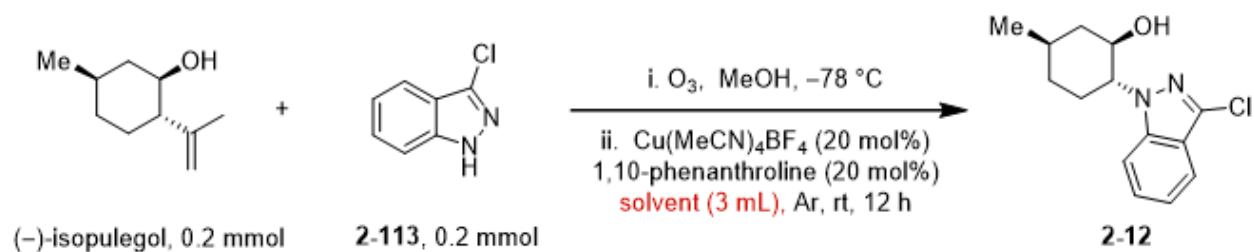
2.6.4. Reaction Optimization

Solvent Screen

Procedure: An oven-dried 8-mL Schlenk tube equipped with a magnetic stirrer bar was charged with 3-chloroindazole (**2-113**, 30.5 mg, 0.200 mmol, 1.0 equiv), tetrakis(MeCN)copper(I) tetrafluoroborate (12.6 mg, 0.0400 mmol, 20 mol %), and 1,10-phenanthroline (7.20 mg, 0.0400

mmol, 20 mol %). The tube was purged with argon three times and then a dry solvent (2 mL) was added to make *Solution A*. This mixture was stirred at room temperature for 10 min.

Another 25-mL round-bottom flask equipped with a magnetic stirrer bar was charged with (–)-isopulegol (154.3 mg, 1.0 mmol) and MeOH (5 mL, 0.2 M), then cooled to –78 °C in a dry-ice/acetone bath with two 250-mL waste gas traps equipped with 20 wt% aqueous KI (200 mL). Ozone was bubbled through the solution until complete consumption of the starting material (as indicated by TLC and/or a blue color in the reaction mixture). The solution was sparged with argon for 5 min to expel excess ozone and then the reaction mixture was warmed to room temperature. For the experiments indicated in Table S1, entries 1–5, this solution was used directly: by transferring a portion (1.0 mL) of this hydroperoxide solution into *Solution A* in the Schlenk tube *via* syringe. For entries 6–9, the hydroperoxide solution was concentrated *in vacuo*. The residue was dissolved in benzene (10 mL) and concentrated *in vacuo* to remove adventitious water. The residue was dissolved in the corresponding solvents (4.8 mL) to give a 0.2 M solution of the hydroperoxide. A portion (1.0 mL) of this hydroperoxide solution was transferred into *Solution A* in the Schlenk tube *via* syringe. The reaction vessel was stirred at room temperature for 12 h, followed by the addition of 1-chloro-2,4-dinitrobenzene (40.5 mg, 0.200 mmol, 1.0 equiv) as an internal standard. The reaction mixture was concentrated *in vacuo*. The residue was passed through a short plug of silica gel to remove copper salts and then the filtrate was concentrated *in vacuo*. The crude materials were analyzed using NMR spectroscopy.



Entry	Solvent	2-12 (%)
1	MeCN/MeOH (2:1)	23
2	acetone/MeOH (2:1)	22
3	DMF/MeOH (2:1)	18
4	DMSO/MeOH (2:1)	23
5	THF/MeOH (2:1)	17
6	MeOH	18
7	MeCN	27
8	DMF	< 5
9	DMSO	< 5

Table 2.1 Survey of the reaction solvents

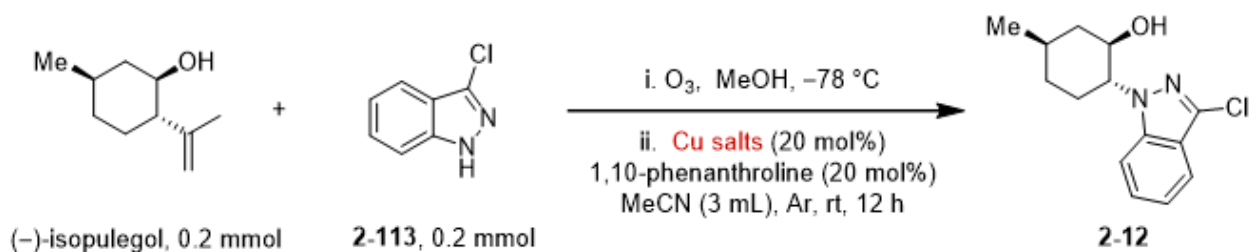
Summary of Table 2.1: We started our screening by adding a MeOH solution of the peroxide directly into *Solution A*—an operationally simpler way to set up the reaction. We found, however, that all of the reactions performed similarly, with poor yields (entries 1 to 5). We then screened single solvents and found that the reaction worked best in MeCN (entry 7). Although we could obtain the product when using DMF or DMSO as a co-solvent with MeOH, the single solvents afforded poor results. MeOH was the best solvent for the methylation of nucleosides (see Section 2.6.5.5).

Cu salt screen

Procedure: An oven-dried 8-mL Schlenk tube equipped with a magnetic stir bar was charged with 3- chloroindazole (**2-113**, 30.5 mg, 0.200 mmol, 1.0 equiv), a copper salt (0.0400 mmol, 20 mol %), and 1,10- phenanthroline (7.20 mg, 0.0400 mmol, 20 mol %). The tube was purged with argon three times and then dry MeCN (2 mL) was added to make *Solution A*. This mixture was stirred at room temperature for 10 min.

Another 25-mL round-bottom flask equipped with a magnetic stirrer bar was charged with (–)-isopulegol (154.3 mg, 1.0 mmol) and MeOH (5 mL, 0.2 M), then cooled to –78 °C in a dry-

ice/acetone bath with two 250-mL waste gas traps equipped with 20 wt% aqueous KI (200 mL). Ozone was bubbled through the solution until complete consumption of the starting material (as indicated by TLC and/or a blue color in the reaction mixture). The solution was sparged with argon for 5 min to expel excess ozone and then the reaction mixture was warmed to room temperature. The hydroperoxide solution was concentrated *in vacuo*. The residue was dissolved in benzene (10 mL) and the solution concentrated *in vacuo* to remove adventitious water. The residue was dissolved in MeCN (4.8 mL) to form a 0.2 M solution of the hydroperoxide. A portion (1.0 mL) of this hydroperoxide solution was transferred into *Solution A* in the Schlenk tube via syringe. The reaction vessel was stirred at room temperature for 12 h, followed by the addition of 1-chloro-2,4-dinitrobenzene (40.5 mg, 0.200 mmol, 1.0 equiv) as an internal standard. The reaction mixture was concentrated *in vacuo*. The residue was passed through a short plug of silica gel to remove copper salts and then the filtrate was concentrated *in vacuo*. The crude materials were analyzed using NMR spectroscopy.



Entry	Cu salt	2-12 (%)
1	CuCl	51
2	CuBr	46
3	CuI	44
4	CuOAc	49
5	Cu(MeCN) ₄ BF ₄	27
6	CuCl ₂	28
7	Cu(OAc) ₂	30
8	Cu(OTf) ₂	Trace

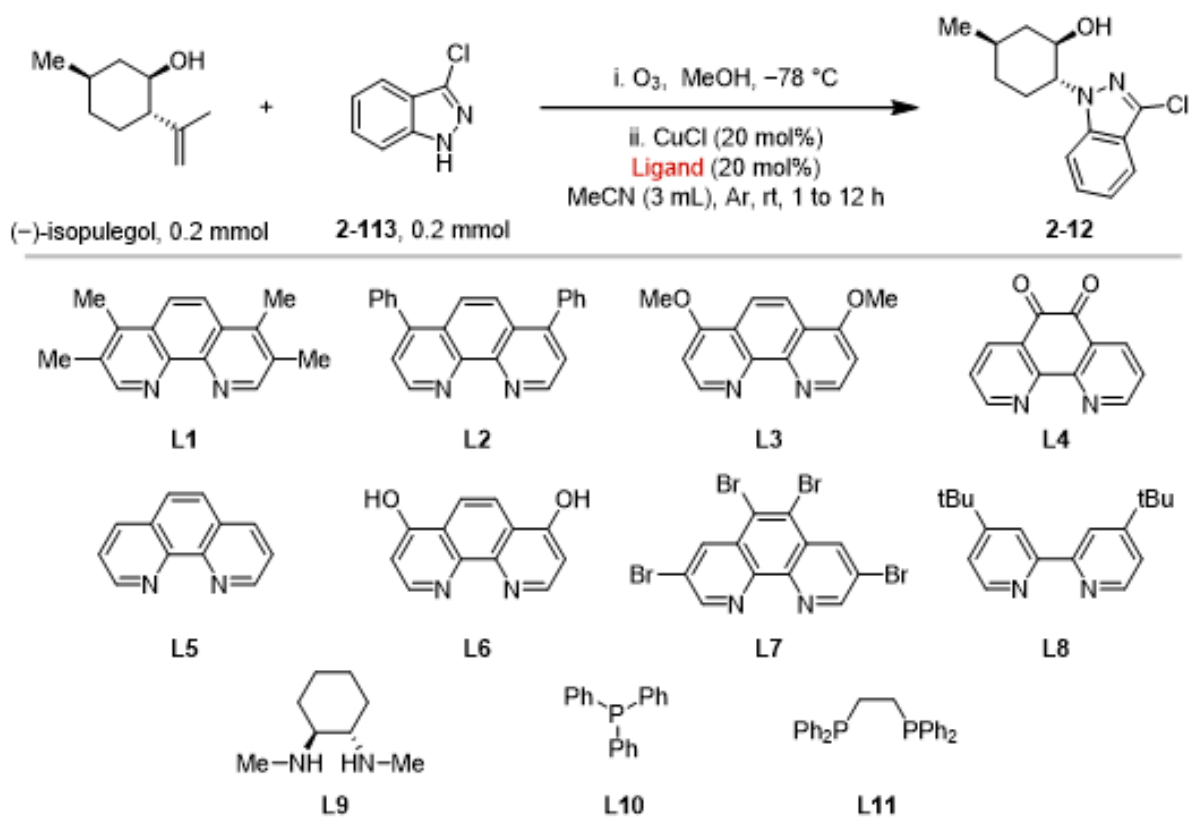
Table 2.2 Survey of the copper salts

Summary of Table 2.2: We found that Cu(I) species needed an anionic ligand to neutralize the Lewis acidity. A cationic Cu(I) species [*e.g.*, Cu(MeCN)₄BF₄] might afford a lower yield because it might promote hydrolysis of the hydroperoxide intermediate. A stronger Lewis acid [*e.g.*, a Cu(II) species] also lowered the yield, and the use of Cu(OTf)₂ afforded the ketone byproduct in 90% yield. When using Cu(I), the reaction was very fast. For example, the reaction was finished within 1 min when using CuCl. In contrast, when using CuCl₂, the reaction was slow (12 h, entry 6).

Ligand Screen

Procedure: An oven-dried 8-mL Schlenk tube equipped with a magnetic stir bar was charged with 3-chloroindazole (**2-113**, 30.5 mg, 0.2 mmol, 1.0 equiv), copper(I) chloride (4.00 mg, 0.0400 mmol, 20 mol %), and a ligand (0.0400 mmol, 20 mol %). The tube was purged with argon three times and then dry MeCN (2 mL) was added to make *Solution A*. This mixture was stirred at room temperature for 10 min. Another 25-mL round-bottom flask equipped with a magnetic stirrer bar was charged with (–)-isopulegol (154.3 mg, 1.0 mmol) and MeOH (5 mL, 0.2 M), then cooled to –78 °C in a dry-ice/acetone bath with two 250-mL waste gas traps equipped with 20 wt% aqueous KI (200 mL). Ozone was bubbled through the solution until complete consumption of the starting

material (as indicated by TLC and/or a blue color in the reaction mixture). The solution was sparged with argon for 5 min to expel excess ozone and then the reaction mixture was warmed to room temperature. The hydroperoxide solution was concentrated *in vacuo*. The residue was dissolved in benzene (10 mL) and the solution concentrated *in vacuo* to remove adventitious water. The residue was dissolved in MeCN (4.8 mL) to form a 0.2 M solution of the hydroperoxide. A portion (1.0 mL) of this hydroperoxide solution was transferred into *Solution A* in the Schlenk tube *via* syringe. The reaction vessel was stirred at room temperature for 1 or 12 h, followed by the addition of 1-chloro-2,4-dinitrobenzene (40.5 mg, 0.200 mmol, 1.0 equiv) as an internal standard. The reaction mixture was concentrated *in vacuo*. The residue was passed through a short plug of silica gel to remove copper salts and then the filtrate was concentrated *in vacuo*. The crude material was analyzed using NMR spectroscopy.

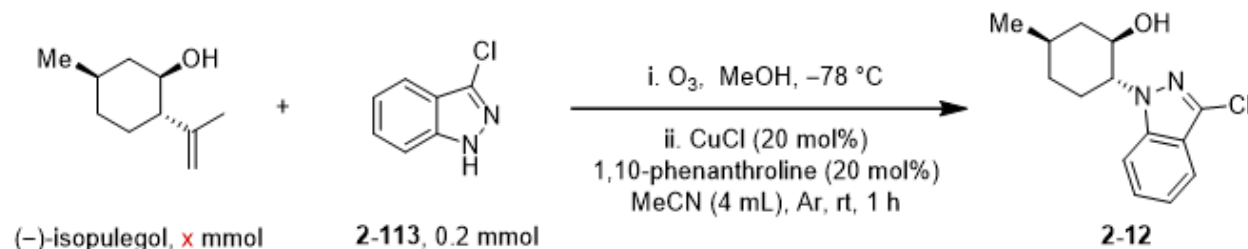


Entry	Ligand	2-12 (%)
1	L1	51
2	L2	49
3	L3	44
4	L4	13
5	L5	51
6	L6	9
7	L7	13
8	L8	52
9 ^a	L9	24
10 ^{a,b}	L10	7
11 ^a	L11	30

Table 2.3 Ligand Survey

Summary of Table 2.3: Phenanthroline, bipyridine, diamine, and phosphine ligands were tested. Phenanthroline and bipyridine ligands (**L1**, **L2**, **L5**, **L8**) worked well. The phenanthroline ligands bearing moderately electron-donating substituents (**L1**, **L2**, **L5**) afforded the best yields. Lower yields were obtained when using electron-rich or -poor phenanthroline ligands (**L3**, **L4**, **L6**, **L7**). The reactions were sluggish when using diamine and phosphine ligands (entries 9–11). Although **L1**, **L2**, **L5**, and **L8** exhibited similar reactivities for the coupling reactions between (–)-isopulegol and **2-113**, their behaviors were different in the coupling reactions between (–)-dihydrocarveol and phthalimide (**2-114**) (see Table 2.6). The simplest and least expensive ligand, 1,10-phenanthroline (**L5**), worked well in both reactions.

Alkene to amine ratio screen



Entry	<i>X</i>	Ratio (-)-isopulegol/2-113	2-12 (%)
1	0.24	1.2/1	63
2	0.3	1.5/1	78
3	0.4	2/1	98 (92% isolated)
4 ^a	0.2	1/1.5	53

^a 0.3 mmol of 2-113 was used.

Table 2.4 Alkene to amine ratio screen

Procedure: An oven-dried 8-mL Schlenk tube equipped with a magnetic stirrer bar was charged with 3- chloroindazole (2-113, 30.5 mg, 0.200 mmol, 1.0 equiv), copper(I) chloride (4.00 mg, 0.0400 mmol, 20 mol %), and 1,10-phenanthroline (7.20 mg, 0.0400 mmol, 20 mol %). The tube was purged with argon three times before dry MeCN [2.8 mL (entry 1), 2.5 mL (entry 2), 2.0 mL (entry 3), or 3.0 mL (entry 4)] was added to make *Solution A*. This mixture was stirred at room temperature for 10 min.

Another 25-mL round-bottom flask equipped with a magnetic stirrer bar was charged with (-)-isopulegol (154.3 mg, 1.0 mmol) and MeOH (5 mL, 0.2 M), then cooled to -78 °C in a dry-ice/acetone bath with two 250-mL waste gas traps equipped with 20 wt% aqueous KI (200 mL). Ozone was bubbled through the solution until complete consumption of the starting material (as indicated by TLC and/or a blue color in the reaction mixture). The solution was sparged with argon for 5 min to expel excess ozone and then the reaction mixture was warmed to room temperature. The hydroperoxide solution was concentrated *in vacuo*. The residue was dissolved

in benzene (10 mL) and then the solution was concentrated *in vacuo* to remove adventitious water. The residue was dissolved in MeCN (4.8 mL) to form a 0.2 M solution of the hydroperoxide. A portion [1.2 mL (entry 1), 1.5 mL (entry 2), 2.0 (entry 3) mL, or 1.0 mL (entry 4)] of this hydroperoxide solution was transferred into *Solution A* in the Schlenk tube *via* syringe. The reaction vessel was stirred at room temperature for 1 h, followed by the addition of 1-chloro 2,4-dinitrobenzene (40.5 mg, 0.200 mmol, 1.0 equiv) as an internal standard. The reaction mixture was concentrated *in vacuo*. The residue was passed through a short plug of silica gel to remove copper salts and then the filtrate was concentrated *in vacuo*. The crude materials were analyzed using NMR spectroscopy.

Summary of

Entry	<i>X</i>	Ratio (-)-isopulegol/ 2-113	2-12 (%)
1	0.24	1.2/1	63
2	0.3	1.5/1	78
3	0.4	2/1	98 (92% isolated)
4a	0.2	1/1.5	53

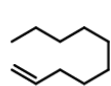
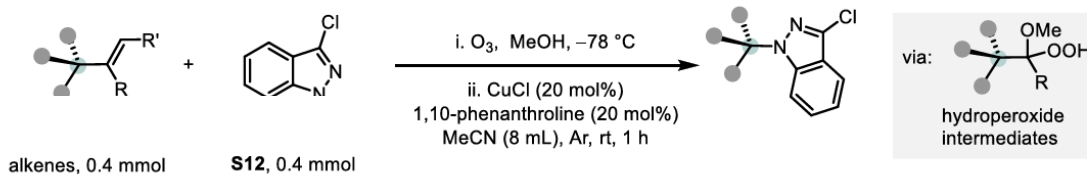
^a 0.3 mmol of **2-113** was used.

Table 2.4: The product yield increased upon increasing the amount of peroxide, while increasing the amount of indazole had little effect.

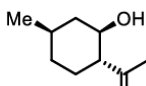
Relationship between the Criegee ozonolysis and the overall product yield

Procedure: An oven-dried 25-mL round bottom flask equipped with a magnetic stirrer bar was charged with 3-chloroindazole (**2-113**, 71.0 mg, 0.400 mmol, 1.0 equiv), copper(I) chloride (8.00 mg, 0.0800 mmol, 20 mol %), and 1,10-phenanthroline (14.40 mg, 0.0800 mmol, 20 mol %). The flask was purged with argon three times and then dry MeCN (4 mL) was added to make *Solution A*. This mixture was stirred at room temperature for 10 min.

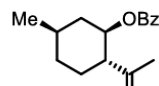
Another 25-mL round-bottom flask equipped with a magnetic stirrer bar was charged with alkene (1.0 mmol) and MeOH (10 mL, 0.1 M), then cooled to $-78\text{ }^{\circ}\text{C}$ in a dry-ice/acetone bath with two 250-mL waste gas traps equipped with 20 wt% aqueous KI (200 mL). Ozone was bubbled through the solution until complete consumption of the starting material (as indicated by TLC and/or a blue color in the reaction mixture). The solution was sparged with argon for 5 min to expel excess ozone and then the reaction mixture was warmed to room temperature. The hydroperoxide solution was concentrated *in vacuo*. The residue was dissolved in benzene (10 mL) and then the solution was concentrated *in vacuo* to remove adventitious water. The residue was dissolved in



1-decene



(-)-isopulegol



(-)-O-benzoyl-isopulegol

Entry	Alkene	Hydroperoxide intermediates (%)	C–N coupling product (%)
1	1-decene	90	30
2	(-)-isopulegol	92	52
3	(-)-O-benzoyl isopulegol	89	57

MeCN (9.8 mL) of form a 0.1 M solution of the hydroperoxide. A portion (4.0 mL) of this hydroperoxide solution was transferred into *Suspension A* in the Schlenk tube *via* syringe. The reaction vessel was stirred at room temperature for 1 h, followed by the addition of 1-chloro-2,4-dinitrobenzene (40.5 mg, 0.200 mmol, 0.5 equiv) as an internal standard. The reaction mixture was concentrated *in vacuo*. The residue was passed through a short plug of silica gel to remove copper salts and then the filtrate was concentrated *in vacuo*. The crude materials were analyzed using NMR spectroscopy.

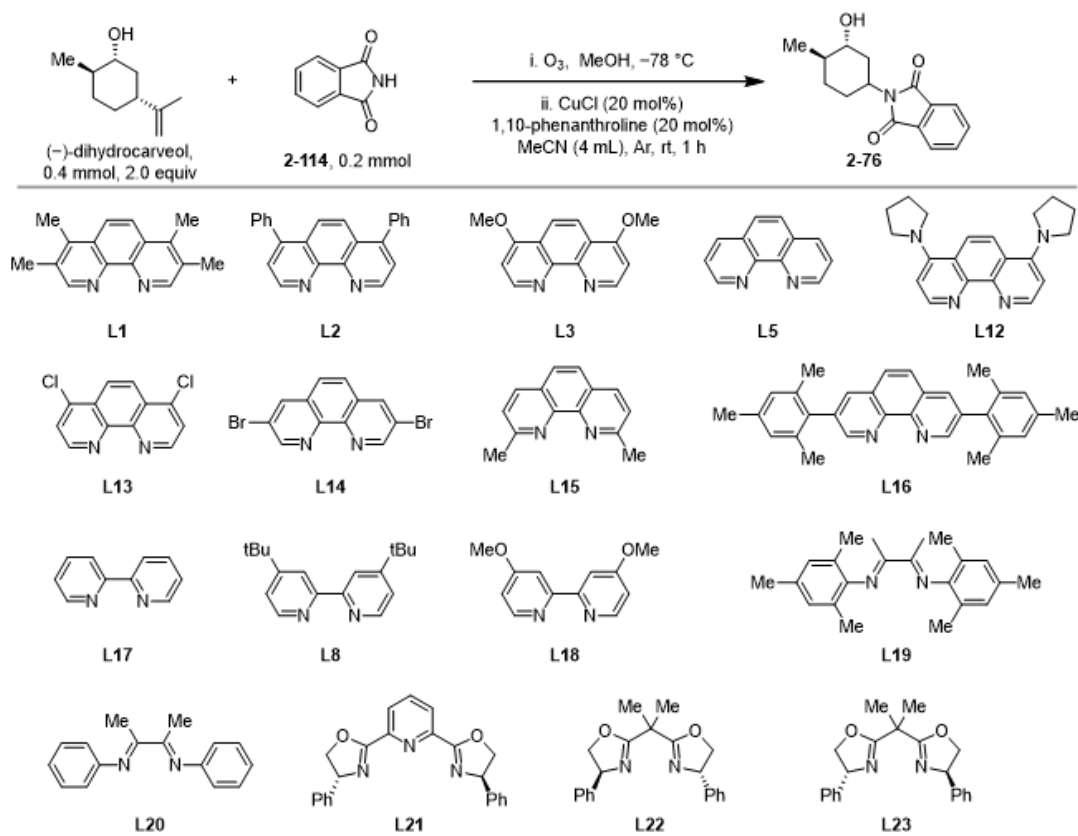
Table 2.5 Relationship between the Criegee ozonolysis and the overall product yield

Summary of Table 2.5: We found that the regioselectivity for the Criegee ozonolysis of 1-decene was better than 4:1, providing the corresponding α -methoxyhydroperoxide in 90% yield. The yield of the C(sp³)-N coupling product was 30% when we used a 1:1 mixture of 1-decene and 3-chloroindazole. The yields for the α -methoxyhydroperoxides from (-)-isopulegol and (-)-*O*-benzoylisopulegol were 92 and 89%, respectively, while the C-N coupling yields using 3-chloroindazole were 52 and 57%, respectively. These results indicate that the yields of the C-N coupling products were not proportional to the observed amounts of the α -methoxyhydroperoxides. Also note that our typical reaction conditions employed 2 equiv of the alkene to consume all of the amine. In the experiments described above, we employed limiting amounts of the alkene to better gauge its influence on the overall yield of the reaction.

Impact of ligands on diastereoselectivity

Procedure: An oven-dried 8-mL Schlenk tube equipped with a magnetic stirrer bar was charged with phthalimide (**2-114**, 29.4 mg, 0.200 mmol, 1.0 equiv), copper(I) chloride (4.00 mg, 0.0400 mmol, 20 mol %), and a ligand (0.0400 mmol, 20 mol %). The tube was purged with argon three times and then dry MeCN (2 mL) was added to make *Suspension A*. This mixture was stirred at room temperature for 10 min. Another 25-mL round-bottom flask equipped with a magnetic stirrer bar was charged with (-)- dihydrocarveol (154 mg, 1.0 mmol) and MeOH (5 mL, 0.2 M), then cooled to -78 °C in a dry-ice/acetone bath with two 250-mL waste gas traps equipped with 20 wt% aqueous KI (200 mL). Ozone was bubbled through the solution until complete consumption of the starting material (as indicated by TLC and/or a blue color in the reaction mixture). The solution was sparged with argon for 5 min to expel excess ozone and then the reaction mixture was warmed to room temperature. The hydroperoxide solution was concentrated *in vacuo*. The

residue was dissolved in benzene (10 mL) and then the solution was concentrated *in vacuo* to remove adventitious water. The residue was dissolved in MeCN (4.8 mL) to form a 0.2 M solution of the hydroperoxide. A portion (2.0 mL) of this hydroperoxide solution was transferred into *Suspension A* in the Schlenk tube *via* syringe. The reaction vessel was stirred at room temperature for 1 h, followed by the addition of 1-chloro-2,4-dinitrobenzene (40.5 mg, 0.200 mmol, 1.0 equiv) as an internal standard. The reaction mixture was concentrated *in vacuo*. The residue was passed through a short plug of silica gel to remove copper salts and then the filtrate was concentrated *in vacuo*. The crude materials were analyzed using NMR spectroscopy.



Entry	Ligand	2-76 (%)	<i>d.r.</i>
1	L1	65	5.9:1
2	L2	85	3.0:1

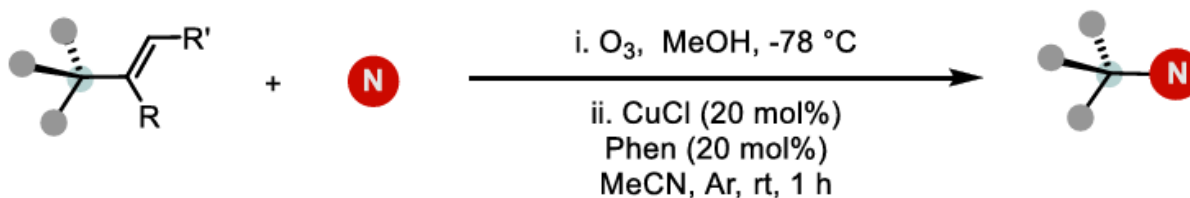
3	L3	26	4.4:1
4	L5	90	2.9:1
5	L12	<5	N.D.
6	L13	86	2.7:1
7	L14	78	2.0:1
8	L15	87	2.8:1
9	L16	86	2.8:1
10	L17	44	2.7:1
11	L8	47	3.7:1
12	L18	37	6.8:1
13	L19	<5	N.D.
14	L20	<5	N.D.
15	L21	<5	N.D.
16	L22	<5	N.D.
17	L23	<5	N.D.
18 ^a	L5	91	2.7:1
19 ^a	L1	74	5.4:1

Table 2.6 Impact of ligands on diastereoselectivity

Summary of Table 2.6: All of the phenanthroline ligands afforded good yields (entries 1–9), except for the 1,8-dimethoxy– and 1,8-dipyrrolidinyl–substituted phenanthrolines (entries 3 and 5). The bipyridine ligands provided moderate yields. Yields of less than 5% were obtained when using diimine (entries 10–12) and bisoxazoline (entries 13–17) ligands. Slightly better diastereoselectivities were obtained when using electron-rich phenanthrolines, compared with electron-poor phenanthrolines (**L1** and **L3** vs **L13** and **L14**), but the yields diminished when using the electron-rich ligands. As a result, although **L5** afforded lower *d.r.*, the yield of the major diastereoisomer was the highest.

2.6.5. Experimental Procedures and Characterization Data

2.6.5.1. General Procedures



General procedure A: An oven-dried 25-mL round-bottom flask equipped with a magnetic stirrer bar was charged with an N-nucleophile (0.20 mmol, 1.0 equiv), copper(I) chloride (4.0 mg, 0.040 mmol, 20 mol %), and 1,10-phenanthroline (7.2 mg, 0.040 mmol, 20 mol %). The flask was purged with argon three times and then dry MeCN (2.0 mL) was added. This mixture was stirred at room temperature for 10 min to make a *Solution A* or *Suspension A*.

Another 25-mL round-bottom flask equipped with a magnetic stirrer bar was charged with an alkene (0.40 mmol, 2.0 equiv) and MeOH (15 mL), then cooled to -78 °C in a dry-ice/acetone bath with two 250-mL waste gas traps equipped with 20 wt% aqueous KI (200 mL). If the alkene did not dissolve completely in MeOH, DCM/MeOH (ranging from 1:1 to 10:1) was used to dissolve the alkene at -78 °C. Ozone was bubbled through the solution until complete consumption of the starting material (as indicated by TLC and/or a blue color in the reaction mixture). The solution was sparged with argon for 5 min to expel excess ozone, the reaction mixture was warmed to room temperature, and the MeOH was evaporated *in vacuo*. The residue was dissolved or suspended in benzene (10 mL) and then the solvent was evaporated *in vacuo* to remove adventitious water. The residue was redissolved in MeCN (1.0 mL) and transferred and kept in a syringe. The round-bottom flask was washed with MeCN (2 × 0.5 mL) and then the solutions were transferred, and kept, in the syringe to make *Solution B*. This MeCN solution of

the hydroperoxide (*Solution B*) was added into the copper mixture (*Solution A*) via syringe. The reaction vessel was stirred at room temperature for a period of time ranging from 10 min to 12 h. Upon completion of the reaction (TLC), the reaction mixture was concentrated *in vacuo*. The residue was redissolved in DCM (5 mL) and silica gel (*ca.* 4 g) was added. The mixture was carefully concentrated and then purified directly through silica gel column chromatography via dry load to afford the desired product.

Note: This procedure was applied when the hydroperoxide displayed good solubility in MeCN.

General procedure B: An oven-dried 10-mL round-bottom flask equipped with a magnetic stirrer bar was charged with an N-nucleophile (0.20 mmol, 1.0 equiv), copper(I) chloride (4.0 mg, 0.040 mmol, 20 mol %), and 1,10-phenanthroline (7.2 mg, 0.040 mmol, 20 mol %). The flask was purged with argon three times and then dry MeCN (2.0 mL) was added. This mixture was stirred at room temperature for 10 min to give *Solution A*.

Another 25-mL round-bottom flask equipped with a magnetic stirrer bar was charged with an alkene (2.0 equiv) and MeOH (15 mL), then cooled to $-78\text{ }^{\circ}\text{C}$ in a dry-ice/acetone bath with two 250-mL waste gas traps equipped with 20 wt% aqueous KI (200 mL). If the alkene did not dissolve completely in MeOH, DCM/MeOH (ranging from 1:1 to 10:1) was used to dissolve the alkene at $-78\text{ }^{\circ}\text{C}$. Ozone was bubbled through the solution until complete consumption of the starting material (as indicated by TLC and/or a blue color in the reaction mixture). The solution was sparged with argon for 5 min to expel excess ozone and then the reaction mixture was warmed to room temperature and the MeOH was evaporated *in vacuo*. The residue was dissolved or suspended in benzene (10 mL) and then the solvent was evaporated *in vacuo* to remove adventitious water, followed by a purge with argon (three times). Acetonitrile (2 mL) was added to this residue to form a suspension (*Suspension B*). The MeCN solution of copper, ligand, and N-

nucleophile (*Solution A*) was transferred into the hydroperoxide suspension (*Suspension B*) via syringe and washed with MeCN (2×0.5 mL). The reaction vessel was stirred at room temperature for 1–12 h.

Upon completion of the reaction (TLC), the reaction mixture was concentrated *in vacuo*. The residue was redissolved in DCM (5 mL) and silica gel (*ca.* 4 g) was added. The mixture was carefully concentrated and then purified directly through silica gel column chromatography *via* dry load to afford the desired product.

Note: This procedure was applied when hydroperoxide did not fully dissolve in MeCN. Some non-polar alkene substrates may require the use of DCM and MeOH as a co-solvent for ozonolysis and benzene as a co-solvent to prepare Suspension B.

General procedure C: An oven-dried 10-mL round-bottom flask equipped with a magnetic stirrer bar was charged with copper(I) chloride (4.0 mg, 0.040 mmol, 20 mol %) and 1,10-phenanthroline (7.2 mg, 0.040 mmol, 20 mol %). The flask was purged with argon three times and then dry MeCN (2 mL) was added. This mixture was stirred at room temperature for 10 min to give *Solution C*. Another 25-mL round-bottom flask equipped with a magnetic stirrer bar was charged with an alkene (2.0 equiv) and MeOH (15 mL), then cooled to -78 °C in a dry-ice/acetone bath with two 250-mL waste gas traps equipped with 20 wt% aqueous KI (200 mL). If the alkene did not dissolve completely in MeOH, DCM /MeOH (ranging from 1:1 to 10:1) was used to dissolve the alkene at -78 °C. Ozone was bubbled through the solution until complete consumption of the starting material (as indicated by TLC and/or a blue color in the reaction mixture). The solution was sparged with argon for 5 min to expel excess ozone and then the reaction mixture was warmed to room temperature and the MeOH was evaporated *in vacuo*. The residue was dissolved or suspended in benzene (10 mL) and then the solvent was evaporated *in vacuo* to remove

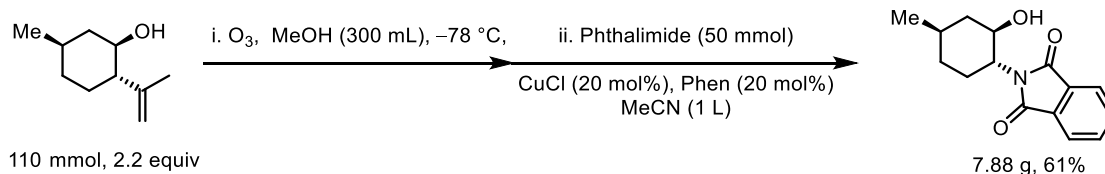
adventitious water. The N-nucleophile (1.0 equiv) was added to this crude hydroperoxide residue. The flask was purged with argon three times and then dry MeCN (2 mL) was added (*Suspension C*). The MeCN solution of copper and ligand (*Solution C*) was added into this mixture of hydroperoxide and N-nucleophile (*Suspension C*) via syringe and washed with MeCN (2×0.5 mL). The reaction vessel was stirred at room temperature for 1–12 h.

Upon completion of the reaction (TLC), the reaction mixture was concentrated *in vacuo*. The residue was redissolved in DCM (5 mL) and silica gel (*ca.* 4 g) was added. The mixture was carefully concentrated and then purified directly through silica gel column chromatography via dry load to afford the desired product.

Note: This procedure was applied when both the hydroperoxide and the N-nucleophile did not fully dissolve in MeCN.

Catalyst loading: We found that the optimal catalyst loading varied depending on both the nature of the alkene and amine starting materials. For example, while 30 mol% of catalyst was essential to obtain a high yield for the coupling reaction between isopulegol and lamivudine (compound **2-29**), a mere 2 mol% of catalyst afforded a 73% yield of the product **2-32b** when coupling the eudesmane-type sesquiterpenoid with phthalimide. We found, in general, that a catalyst loading of 20 mol% was good for most of the substrates. Furthermore, 20 mol% of catalyst (4.0 mg of CuCl and 7.2 mg of phenanthroline) could be weighed more accurately than 5 mol% (1.0 mg of CuCl). Consequently, we adopted 20 mol% of copper chloride and phenanthroline as our general amination condition.

2.6.5.2. Procedures for a 50-mmol-scale reaction and a graphical guide



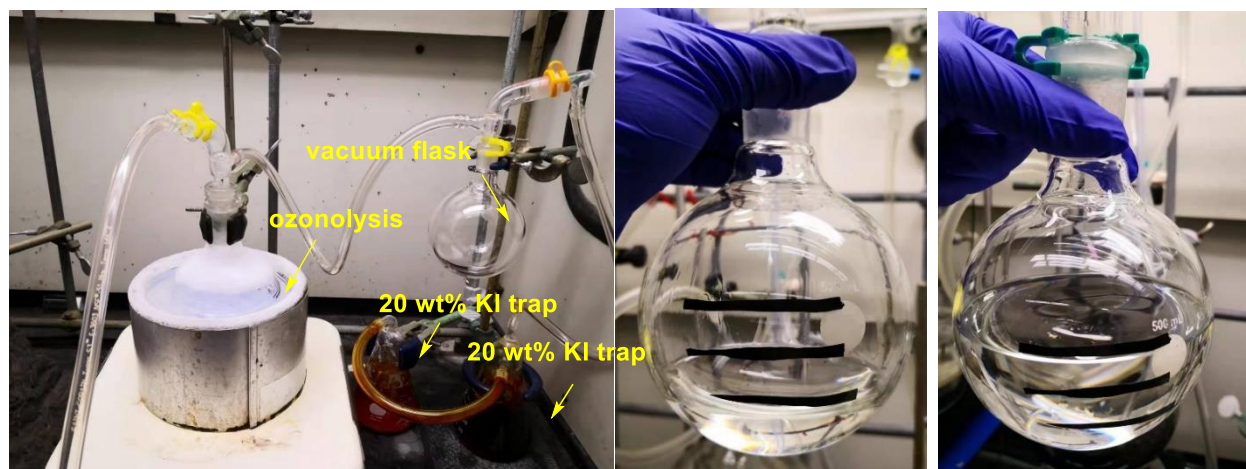
Procedure: An oven-dried 2-L round-bottom flask equipped with a magnetic stirrer bar was charged with phthalimide (7.36 g, 50.0 mmol, 1.0 equiv), copper(I) chloride (990 mg, 10.0 mmol, 20 mol %), and 1,10-phenanthroline (1.80 g, 20.0 mmol, 20 mol %). The flask was purged with argon three times and then dry MeCN (600 mL) was added. This mixture was stirred at room temperature for 10 min to give *Solution A*.

Another 500-mL round-bottom flask equipped with a magnetic stirrer bar was charged with (-)-isopulegol (17.0 g, 110 mmol, 2.2 equiv) and MeOH (300 mL), then cooled to -78 °C in a dry-ice/acetone bath with two 250-mL waste gas traps equipped with 20 wt% aqueous KI (200 mL). Ozone was bubbled through the solution until complete consumption of the starting material (as indicated by TLC and/or a blue color in the reaction mixture). The solution was sparged with argon for 10 min to expel excess ozone and then the reaction mixture was warmed to room temperature and the MeOH was evaporated *in vacuo* until approximately 70–80 mL was left (**for safety concerns, the concentration of the hydroperoxide solution should be less than 1.5 M**). MeCN (230 mL) was added to the residue, followed by evaporation *in vacuo* until approximately 70–80 mL was left. Acetonitrile was added to the residue to make *Solution B* (330 mL). This MeCN solution of hydroperoxide (*Solution B*) was transferred into the copper mixture (*Solution A*) via cannula and rinsed with MeCN (2 × 35 mL). The reaction vessel was stirred at room temperature for 1.5 h.

Upon completion of the reaction (TLC), the reaction mixture was concentrated *in vacuo*. The residue was redissolved in DCM (100 mL) and silica gel (*ca.* 50 g) was added. The mixture was carefully concentrated and purified directly through silica gel column chromatography *via* dry load to afford the desired product (7.88 g, 61% yield) as a white solid.

The characterization data is provided, *vide infra*.

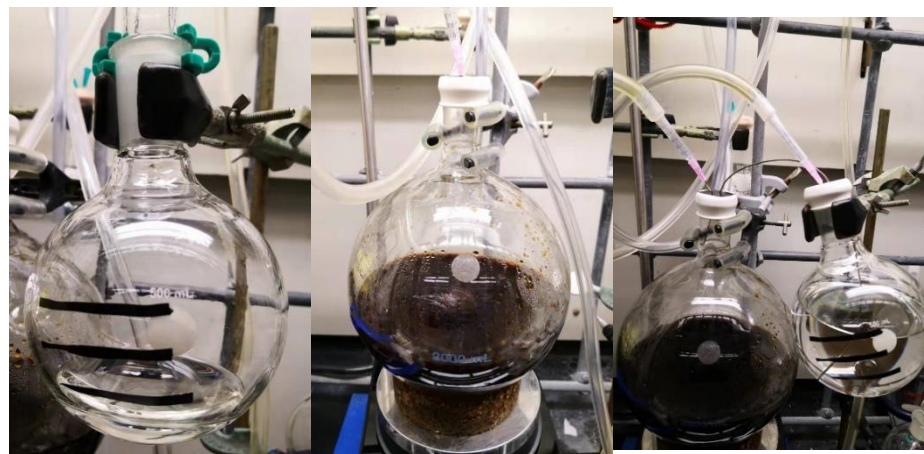
Figure 2.8 Graphical guide for a large-scale reaction



1. Ozonolysis at $-78\text{ }^{\circ}\text{C}$

2. MeOH was evaporated under rotavap until 70–80 mL was left

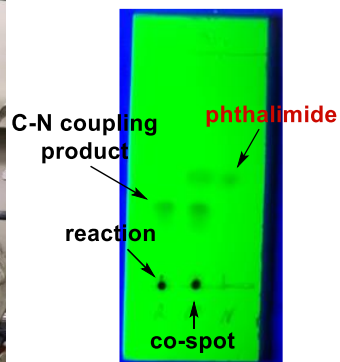
3. MeCN (230 mL) was added to the ozonolysis product



4. Solvent was evaporated under rotavap again until 70–80 mL was left

5. Mixture of phthalimide, phen, and CuCl in MeCN (600 mL)

6. MeCN (330 mL) was added to ozonolysis product, which was cannulated to the solution containing the Cu complex



7. TLC of the reaction

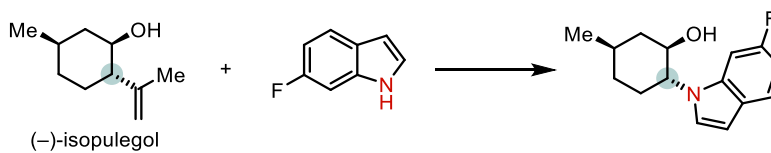


8. Solvent was evaporated under rotavap

9. Crude product was purified through FCC

10. White solid was obtained

2.6.5.3. Details and characterization data of substrates shown in Figure 2.5 and 2.2



Prepared following **General procedure A** using 6-fluoro-1*H*-indole (27.0 mg, 0.200 mmol, 1.0 equiv), copper(I) chloride (4.00 mg, 0.0400 mmol, 20 mol %), 1,10-phenanthroline (7.20 mg, 0.0400 mmol, 20 mol %), and MeCN (2 mL) to make *Solution A*. (-)-Isopulegol (61.7 mg, 0.400 mmol, 2.0 equiv) was used for ozonolysis and MeCN (2 mL) was used to make *Solution B*. The crude product was purified through FCC to give **2-1** ($R_f = 0.38$; hexanes/EtOAc, 4:1) as a white solid (45.8 mg, 93% yield).

$^1\text{H NMR}$ (400 MHz, CDCl_3) δ 7.51 (dd, $J = 8.7, 5.4$ Hz, 1H), 7.14–7.10 (m, 2H), 6.88 (ddd, $J = 9.5, 8.6, 2.3$ Hz, 1H), 6.51 (d, $J = 3.2$ Hz, 1H), 3.99–3.78 (m, 2H), 2.10 (ddd, $J = 12.8, 5.9, 4.0$ Hz, 1H), 2.00 (ddt, $J = 10.6, 4.2, 2.6$ Hz, 1H), 1.87–1.79 (m, 2H), 1.72–1.60 (m, 1H), 1.30–1.10 (m, 2H), 1.03 (d, $J = 6.5$ Hz, 3H).

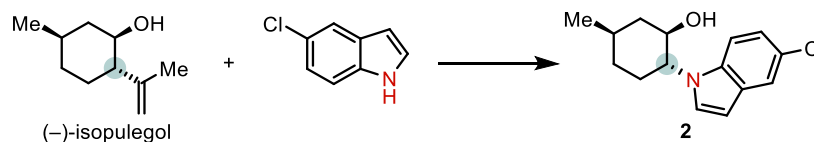
^{13}C NMR (100 MHz, CDCl_3) δ 159.79 (d, $J = 236$ Hz), 136.86 (d, $J = 12$ Hz), 124.81, 124.34 (d, $J = 3$ Hz), 121.59 (d, $J = 10$ Hz), 108.45 (d, $J = 24$ Hz), 102.51, 96.42 (d, $J = 26$ Hz), 73.03, 62.08, 42.10, 33.84, 31.15, 31.03, 21.83.

HRMS (ESI-TOF): $[\text{M}+\text{H}]^+$ calcd for $[\text{C}_{15}\text{H}_{19}\text{FNO}]^+$ m/z 248.1445, found 248.1447.

IR (neat, ATR): ν_{max} 3425 (br), 3070, 2979, 2950, 2937, 2928, 2910, 2887, 2859, 1622, 1514, 1488, 1458, 1332, 1222, 1198, 1177, 1093, 1052, 1006, 933, 852, 803, 754, 716, 624, 529 cm^{-1} .

Optical Rotation: $[\alpha]_{\text{D}}^{27} = 4.96$ (c 1.0, CHCl_3).

M.p.: 170–171 $^{\circ}\text{C}$.



Prepared following **General procedure A** using 5-chloro-1H-indole (30.3 mg, 0.299 mmol, 1.0 equiv), copper(I) chloride (4.09 mg, 0.0400 mmol, 20 mol %), 1,10-phenanthroline (7.20 mg, 0.0400 mmol, 20 mol %), and MeCN (2 mL) to make *Solution A*. (-)-Isopulegol (61.7 mg, 0.400 mmol, 2.0 equiv) was used for ozonolysis and MeCN (2 mL) was used to make *Solution B*. The crude product was purified through FCC to give **2-2** ($R_f = 0.37$; hexanes/EtOAc, 3:1) as a white solid (43.9 mg, 83% yield).

^1H NMR (500 MHz, CDCl_3) δ 7.57 (d, $J = 2.0$ Hz, 1H), 7.34 (d, $J = 8.8$ Hz, 1H), 7.18–7.12 (m, 2H), 6.46 (d, $J = 3.0$ Hz, 1H), 3.97 (ddd, $J = 12.0, 9.7, 4.2$ Hz, 1H), 3.77 (ddd, $J = 11.0, 9.7, 4.5$ Hz, 1H), 2.09–2.02 (m, 1H), 2.02–1.95 (m, 1H), 1.86–1.78 (m, 2H), 1.76 (s, 1H), 1.70–1.60 (m, 1H), 1.25–1.11 (m, 2H), 1.02 (d, $J = 6.6$ Hz, 3H).

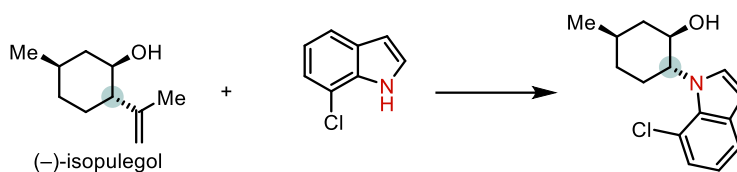
^{13}C NMR (125 MHz, CDCl_3) δ 135.28, 129.31, 125.23, 121.90, 120.26, 110.93, 101.93, 73.22, 61.95, 42.08, 33.83, 31.13, 31.10, 21.83.

HRMS (ESI-TOF): $[\text{M}+\text{H}]^+$ calcd for $[\text{C}_{15}\text{H}_{19}\text{ClNO}]^+$ m/z 264.1150, found 264.1161.

IR (neat, ATR): ν_{max} 3397 (br), 2949, 2926, 2867, 2851, 1505, 1456, 1335, 1307, 1270, 1203, 1099, 1065, 1049, 1007, 937, 907, 868, 793, 753, 718 cm^{-1} .

Optical Rotation: $[\alpha]_{\text{D}}^{26} = 8.57$ (c 1.0, CHCl_3)

M.p.: 153–154 $^{\circ}\text{C}$.



Prepared following **General procedure A** using 7-chloro-1H-indole (30.3 mg, 0.200 mmol, 1.0 equiv), copper(I) chloride (4.00 mg, 0.0400 mmol, 20 mol %), 1,10-phenanthroline (7.20 mg, 0.0400 mmol, 20 mol %), and MeCN (2 mL) to make *Solution A*. (-)-Isopulegol (61.7 mg, 0.400 mmol, 2.0 equiv) was used for ozonolysis and MeCN (2 mL) was used to make *Solution B*. The crude product was purified through FCC to give **2-3** ($R_f = 0.36$; hexanes/EtOAc, 4:1) as a colorless oil (25.5 mg, 48% yield).

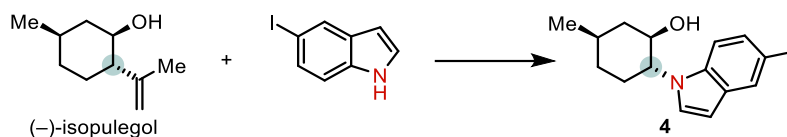
^1H NMR (400 MHz, CDCl_3) δ 7.51 (dd, $J = 7.8, 1.1$ Hz, 1H), 7.26 (d, $J = 3.0$ Hz, 1H), 7.17 (dd, $J = 7.6, 1.1$ Hz, 1H), 7.00 (t, $J = 7.7$ Hz, 1H), 6.59 (d, $J = 3.3$ Hz, 1H), 5.30 (ddd, $J = 12.1, 9.8, 4.0$ Hz, 1H), 3.91 (td, $J = 10.4, 4.4$ Hz, 1H), 2.16 (ddt, $J = 14.5, 7.1, 3.7$ Hz, 2H), 1.79 (ddt, $J = 12.9, 6.2, 3.4$ Hz, 2H), 1.72–1.58 (m, 2H), 1.33–1.15 (m, 3H), 1.03 (d, $J = 6.5$ Hz, 3H).

^{13}C NMR (100 MHz, CDCl_3) δ 132.18, 131.57, 124.83, 124.25, 120.13, 119.89, 116.54, 103.44, 72.96, 61.82, 42.69, 33.71, 32.96, 31.26, 21.82.

HRMS (DART): $[\text{M}+\text{H}]^+$ calcd for $[\text{C}_{15}\text{H}_{19}\text{ClNO}]^+$ m/z 264.1150, found 264.1150.

IR (neat, ATR): ν_{\max} 3623 (br), 3020, 2945, 1633, 1444, 1375, 1039, 919, 759 cm^{-1} .

Optical Rotation: $[\alpha]_{\text{D}}^{24} = -21.67$ (c 0.1, CHCl_3)



Prepared following **General procedure A** using 5-iodo-1*H*-indole (48.6 mg, 0.200 mmol, 1.0 equiv), copper(I) chloride (4.00 mg, 0.0400 mmol, 20 mol %), 1,10-phenanthroline (7.20 mg, 0.0400 mmol, 20 mol %), and MeCN (2 mL) to make *Solution A*. (-)-Isopulegol (61.7 mg, 0.400 mmol, 2.0 equiv) was used for ozonolysis and MeCN (2 mL) was used to make *Solution B*. The crude product was purified through FCC to give **2-4** ($R_f = 0.35$; 15% EtOAc in hexanes) as a yellow solid (63.0 mg, 89% yield).

$^1\text{H NMR}$ (400 MHz, CDCl_3) δ 7.95 (d, $J = 1.5$ Hz, 1H), 7.44 (dd, $J = 8.7, 1.7$ Hz, 1H), 7.24 (t, $J = 8.6$, 1H), 7.13 (d, $J = 3.2$ Hz, 1H), 6.48 (d, $J = 3.2$ Hz, 1H), 3.99 (ddd, $J = 12.0, 9.8, 4.3$ Hz, 1H), 3.84 (td, $J = 10.4, 4.4$ Hz, 1H), 2.15–2.06 (m, 1H), 2.05–1.96 (m, 1H), 1.89–1.77 (m, 2H), 1.74–1.61 (m, 2H), 1.37–1.10 (m, 2H), 1.03 (d, $J = 6.6$ Hz, 3H).

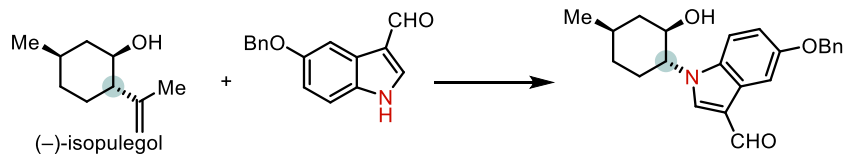
$^{13}\text{C NMR}$ (100 MHz, CDCl_3) δ 136.01, 130.94, 129.87, 129.76, 124.72, 111.92, 101.66, 82.98, 73.23, 61.92, 42.13, 33.84, 31.14, 31.09, 21.84.

HRMS (ESI-TOF): $[\text{M}+\text{H}]^+$ calcd for $[\text{C}_{15}\text{H}_{19}\text{INO}]^+$ m/z 356.0506, found 356.0515.

IR (neat, ATR): ν_{\max} 3393 (br), 2947, 2925, 2864, 2849, 1461, 1453, 1327, 1305, 1271, 1220, 1207, 1099, 1048, 1007, 937, 793, 773, 756, 753, 720, 485 cm^{-1}

Optical Rotation: $[\alpha]_{\text{D}}^{25} = 9.83$ (c 0.2, CHCl_3)

M.p.: 171–172 $^{\circ}\text{C}$.



Prepared following **General procedure A** using 5-(benzyloxy)-1*H*-indole-3-carbaldehyde (50.3 mg, 0.200 mmol, 1.0 equiv), copper(I) chloride (4.00 mg, 0.0400 mmol, 20 mol %), 1,10-phenanthroline (7.20 mg, 0.0400 mmol, 20 mol %), and MeCN (2 mL) to make *Solution A*. (-)-Isopulegol (61.7 mg, 0.400 mmol, 2.0 equiv) was used for ozonolysis and MeCN (2 mL) was used to make *Solution B*. After 1 h, additional (-)-isopulegol (30.9 mg, 0.200 mmol, 1.0 equiv) was used to prepare *Solution B* and added into the reaction mixture. The crude product was purified through FCC to give **2-5** ($R_f = 0.40$; hexanes/EtOAc, 2:3) as a pale-yellow solid (68.2 mg, 94% yield).

$^1\text{H NMR}$ (500 MHz, CDCl_3) δ 9.57 (s, 1H), 7.70 (d, $J = 2.5$ Hz, 1H), 7.65 (s, 1H), 7.50–7.44 (m, 2H), 7.42–7.35 (m, 3H), 7.35–7.29 (m, 1H), 7.00 (dd, $J = 9.0, 2.6$ Hz, 1H), 5.07 (s, 2H), 4.02 (ddd, $J = 11.9, 9.7, 4.1$ Hz, 1H), 3.94 (td, $J = 10.4, 4.4$ Hz, 1H), 2.84 (brs, 1H), 2.16–2.12 (m, 1H), 2.10–2.01 (m, 1H), 1.91–1.78 (m, 2H), 1.73–1.63 (m, 1H), 1.27 (td, $J = 12.6, 10.7$ Hz, 1H), 1.18 (qd, $J = 12.0, 10.7, 5.3$ Hz, 1H), 1.04 (d, $J = 6.5$ Hz, 3H).

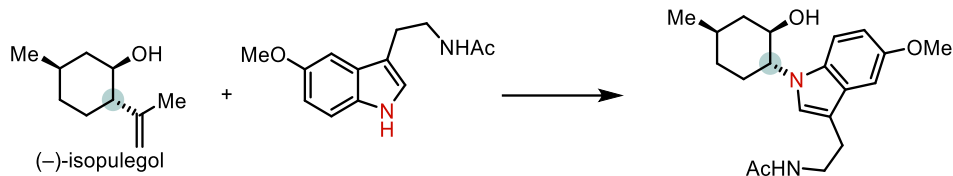
$^{13}\text{C NMR}$ (125 MHz, CDCl_3) δ 184.34, 155.72, 137.25, 136.20, 133.03, 128.53, 127.86, 127.66, 125.88, 118.12, 114.91, 111.73, 104.51, 72.72, 70.41, 63.10, 42.67, 33.64, 31.25, 31.18, 21.76

HRMS (ESI-TOF): $[\text{M}+\text{H}]^+$ calcd for $[\text{C}_{23}\text{H}_{26}\text{NO}_3]^+$ m/z 364.1907, found 364.1915.

IR (neat, ATR): ν_{max} 3373 (br), 3111, 3016, 2956, 2921, 2861, 1644, 1617, 1525, 1463, 1417, 1257, 1218, 1262, 1173, 1039, 1011, 748, 724, 696, 636 cm^{-1} .

Optical Rotation: $[\alpha]_{\text{D}}^{28} = -12.87$ (c 0.5, CHCl_3)

M.p.: 88–89 $^{\circ}\text{C}$.



Prepared following **General procedure A** using melatonin (46.5 mg, 0.200 mmol, 1.0 equiv), copper(I) chloride (4.00 mg, 0.0400 mmol, 20 mol %), 1,10-phenanthroline (7.20 mg, 0.0400 mmol, 20 mol %), and MeCN (2 mL) to make *Solution A*. (-)-Isopulegol (61.7 mg, 0.400 mmol, 2.0 equiv) was used for ozonolysis and MeCN (2 mL) was used to make *Solution B*. The crude product was purified through FCC to give **2-6** ($R_f = 0.53$; DCM/toluene/MeOH, 2:2:1) as a white solid (58.9 mg, 85% yield).

$^1\text{H NMR}$ (400 MHz, CDCl_3) δ 7.30 (d, $J = 8.9$ Hz, 1H), 6.99 (d, $J = 2.7$ Hz, 2H), 6.85 (dd, $J = 8.9$, 2.4 Hz, 1H), 5.91 (s, 1H), 3.96–3.84 (m, 5H), 3.59–3.45 (m, 2H), 2.89 (t, $J = 6.7$ Hz, 2H), 2.09 (d, $J = 11.5$ Hz, 1H), 2.00–1.96 (m, 1H), 1.90–1.70 (m, 5H), 1.68–1.61 (m, 1H), 1.26–1.09 (m, 2H), 1.02 (d, $J = 6.5$ Hz, 3H).

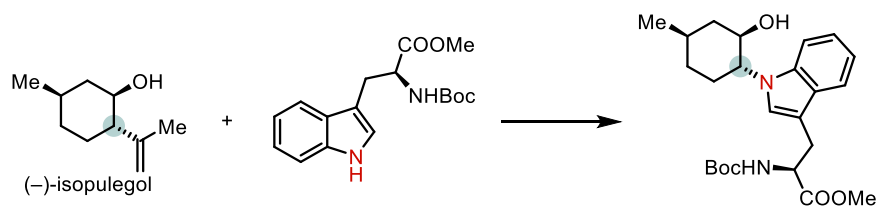
$^{13}\text{C NMR}$ (100 MHz, CDCl_3) δ 170.41, 153.91, 132.49, 128.11, 122.78, 112.05, 111.96, 110.79, 100.61, 72.94, 61.89, 56.00, 42.32, 39.86, 33.92, 31.27, 31.18, 25.39, 23.21, 21.87.

HRMS (ESI-TOF): $[\text{M}+\text{H}]^+$ calcd for $[\text{C}_{20}\text{H}_{29}\text{N}_2\text{O}_3]^+$ m/z 345.2173, found 345.2177.

IR (neat, ATR): ν_{max} 3300 (br), 2926, 2869, 1649, 1552, 1485, 1454, 1372, 1235, 1218, 1179, 1097, 1049, 757 cm^{-1} .

Optical Rotation: $[\alpha]_{\text{D}}^{28} = 0.80$ (c 0.5, CHCl_3)

M.p.: 68–70 $^{\circ}\text{C}$.



Prepared following **General procedure A** using methyl (*tert*-butoxycarbonyl)-L-tryptophanate (63.7 mg, 0.200 mmol, 1.0 equiv), copper(I) chloride (4.00 mg, 0.0400 mmol, 20 mol %), 1,10-phenanthroline (7.20 mg, 0.0400 mmol, 20 mol %), and MeCN (2 mL) to make *Solution A*. (-)-Isopulegol (61.7 mg, 0.400 mmol, 2.0 equiv) was used for ozonolysis and MeCN (2 mL) was used to make *Solution B*. The crude product was purified through FCC to give **2-7** ($R_f = 0.34$; DCM/EtOAc, 9:1) as an off-white solid (77.3 mg, 90% yield).

$^1\text{H NMR}$ (400 MHz, CDCl_3) δ 7.54 (d, $J = 7.9$ Hz, 1H), 7.41 (d, $J = 8.3$ Hz, 1H), 7.20 (ddd, $J = 8.2, 6.9, 1.2$ Hz, 1H), 7.10 (td, $J = 7.4, 6.9, 0.9$ Hz, 1H), 6.99 (s, 1H), 5.08 (d, $J = 8.4$ Hz, 1H), 4.70–4.54 (m, 1H), 4.00 (ddd, $J = 12.0, 9.6, 4.2$ Hz, 1H), 3.88 (td, $J = 10.3, 4.3$ Hz, 1H), 3.67 (s, 3H), 3.34–2.98 (m, 2H), 2.12 (d, $J = 12.5$ Hz, 1H), 2.07–1.90 (m, 2H), 1.82 (d, $J = 12.7$ Hz, 2H), 1.73–1.63 (m, 1H), 1.41 (s, 9H), 1.30–1.11 (m, 3H), 1.03 (d, $J = 6.5$ Hz, 3H).

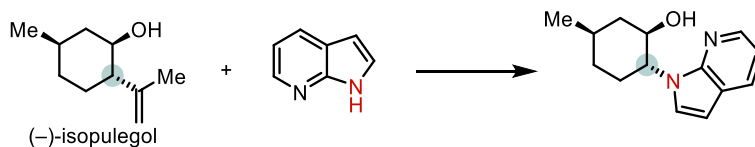
$^{13}\text{C NMR}$ (100 MHz, CDCl_3) δ 172.82, 155.18, 137.04, 128.27, 122.78, 121.84, 119.45, 118.96, 110.17, 110.00, 79.81, 77.28, 72.96, 61.88, 54.42, 52.24, 42.10, 33.91, 31.19 (overlap), 28.34, 21.89.

HRMS (ESI-TOF): $[\text{M}+\text{Na}]^+$ calcd for $[\text{C}_{24}\text{H}_{34}\text{N}_2\text{NaO}_5]^+$ m/z 453.2360, found 453.2366.

IR (neat, ATR): ν_{max} 3409 (br), 2949, 2936, 2867, 1740, 1704, 1505, 1462, 1439, 1366, 1278, 1249, 1222, 1261, 1166, 1053, 1015, 752, 740 cm^{-1} .

Optical Rotation: $[\alpha]_{\text{D}}^{25} = 15.87$ (c 1.0, CHCl_3)

M.p.: 94–96 °C.



Prepared following **General procedure A** using methyl 1*H*-pyrrolo[2,3-*b*]pyridine (23.6 mg, 0.200 mmol, 1.0 equiv), copper(I) chloride (4.00 mg, 0.0400 mmol, 20 mol %), 1,10-phenanthroline (7.20 mg, 0.0400 mmol, 20 mol %), and MeCN (2 mL) to make *Solution A*. (–)-Isopulegol (61.7 mg, 0.400 mmol, 2.0 equiv) was used for ozonolysis and MeCN (2 mL) was used to make *Solution B*. The crude product was purified through FCC to give **2-8** ($R_f = 0.65$; hexanes/EtOAc, 1:2) as a white solid (30.9 mg, 67% yield).

$^1\text{H NMR}$ (400 MHz, CDCl_3) δ 8.26 (dd, $J = 4.4, 1.2$ Hz, 1H), 7.89 (dd, $J = 7.8, 1.6$ Hz, 1H), 7.28 (d, $J = 3.6$ Hz, 1H), 7.04 (dd, $J = 7.8, 4.8$ Hz, 1H), 6.48 (d, $J = 3.6$ Hz, 1H), 4.59 (ddd, $J = 12.3, 9.9, 4.3$ Hz, 1H), 3.94 (td, $J = 10.6, 4.5$ Hz, 1H), 2.72 (brs, 1H), 2.19–2.08 (m, 1H), 2.04 (dq, $J = 12.8, 3.8$ Hz, 1H), 1.92 (qd, $J = 12.8, 3.7$ Hz, 1H), 1.81 (dp, $J = 13.0, 3.4$ Hz, 1H), 1.73–1.61 (m, 1H), 1.35–1.15 (m, 2H), 1.01 (d, $J = 6.5$ Hz, 3H).

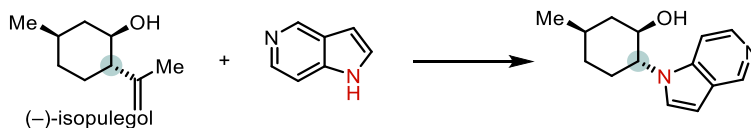
$^{13}\text{C NMR}$ (100 MHz, CDCl_3) δ 148.26, 142.48, 129.09, 125.01, 120.90, 115.93, 100.29, 73.39, 59.98, 43.10, 33.76, 31.20, 31.19, 21.86.

HRMS (ESI-TOF): $[\text{M}+\text{H}]^+$ calcd for $[\text{C}_{14}\text{H}_{19}\text{N}_2\text{O}]^+$ m/z 231.1492, found 231.1494.

IR (neat, ATR): ν_{max} 3324 (br), 3113, 3095, 3049, 3017, 2947, 2909, 2865, 2848, 1595, 1573, 1511, 1459, 1429, 1416, 1354, 1306, 1272, 1215, 1119, 1098, 1054, 937, 897, 795, 770, 753, 725 cm^{-1} .

M.p.: 173–174 °C.

Optical Rotation: $[\alpha]_{\text{D}}^{27} = 18.47$ (c 1.0, CHCl_3)



Prepared following **General procedure A** using methyl 1*H*-pyrrolo[3,2-*c*]pyridine (118 mg, 1.00 mmol, 1.0 equiv), copper(I) chloride (29.7 mg, 0.300 mmol, 30 mol %), 1,10-phenanthroline (54.0 mg, 0.300 mmol, 30 mol %), and MeCN (10 mL) to make *Solution A*. (–)-Isopulegol (462.8 mg, 3.00 mmol, 3.0 equiv) was used for ozonolysis and MeCN (15 mL) was used to make *Solution B*. The crude product was purified through FCC to give **2-9** ($R_f = 0.38$; DCM/toluene/MeOH, 2:2:1) as a pale-yellow solid (204.0 mg, 89% yield).

¹H NMR (500 MHz, CD₃OD) δ 7.62 (s, 1H), 6.85–6.60 (m, 1H), 4.17 (q, $J = 9.3$ Hz, 1H), 3.94 (td, $J = 10.6, 4.4$ Hz, 1H), 2.13–2.05 (m, 1H), 2.03–1.91 (m, 2H), 1.86–1.78 (m, 1H), 1.78–1.66 (m, 1H), 1.31–1.19 (m, 2H), 1.03 (d, $J = 6.5$ Hz, 3H).

¹³C NMR (125 MHz, CD₃OD) δ 140.83 (br), 137.32 (br), 127.67, 102.33 (br), 78.08, 71.85, 61.66, 43.12, 33.33, 31.00, 30.88, 20.83.

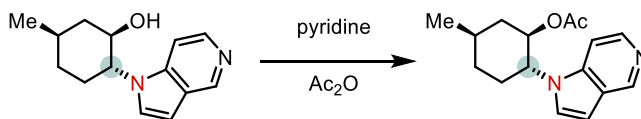
HRMS (ESI-TOF): $[M+H]^+$ calcd for $[C_{14}H_{19}N_2O]^+$ m/z 231.1492, found 231.1495.

IR (neat, ATR): ν_{max} 3277 (br), 2948, 2926, 2867, 1604, 1473, 1450, 1320, 1208, 1055, 897, 772, 751, 728 cm^{-1} .

Optical Rotation: $[\alpha]_D^{24} = 20.33$ (c 1.0, CHCl₃)

M.p.: 193–195 °C.

Note: Some of the ¹H and ¹³C NMR spectral signals of compound 9 were not evident. We characterized the O-acetate-protected product to confirm its structure.



A 10-mL vial equipped with a magnetic stirrer bar was charged with **9** (30 mg, 0.13 mmol), pyridine (1 mL), and acetic anhydride (0.3 mL). The mixture was stirred at room temperature for 12 h. The reaction mixture was diluted with EtOAc (10 mL) and washed with aqueous 1 M HCl (2 × 5 mL), sat. aqueous NaHCO₃ (5 mL), and brine (5 mL). The organic layer was dried (Na₂SO₄) and concentrated. The residue was purified through silica gel column chromatography to afford **2-9-Ac** (*R*_f = 0.47; EtOAc/Et₃N/MeOH, 100:3:5) as a pale-yellow oil (20.5 mg, 58% yield).

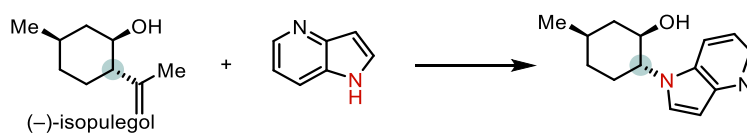
¹H NMR (400 MHz, CD₃OD) δ 8.72 (s, 1H), 8.14 (d, *J* = 6.0 Hz, 1H), 7.56 (d, *J* = 6.1 Hz, 1H), 7.48 (d, *J* = 3.4 Hz, 1H), 6.65 (d, *J* = 3.4 Hz, 1H), 5.13 (td, *J* = 11.0, 4.6 Hz, 1H), 4.44 (ddd, *J* = 12.0, 10.4, 4.6 Hz, 1H), 2.20–2.01 (m, 3H), 1.85 (ddt, *J* = 15.6, 6.1, 2.5 Hz, 1H), 1.82–1.70 (m, 1H), 1.45 (s, 3H), 1.40–1.23 (m, 2H), 1.02 (d, *J* = 6.5 Hz, 3H).

¹³C NMR (100 MHz, CD₃OD) δ 169.81, 142.17, 140.77, 138.36, 126.65, 125.35, 105.75, 101.55, 74.52, 58.05, 39.30, 32.99, 30.68, 30.31, 20.60, 19.04.

HRMS (ESI-TOF): [M+H]⁺ calcd for [C₁₆H₂₁N₂O₂]⁺ *m/z* 273.1598, found 273.1597.

IR (neat, ATR): ν_{max} 2952, 2930, 2869, 1737, 1602, 1471, 1457, 1374, 1320, 1243, 1213, 1041, 1029, 892, 729 cm⁻¹.

Optical Rotation: [α]_D²⁵ = 51.50 (*c* 0.2, CH₂Cl₂)



Prepared following **General procedure A** using methyl 1*H*-pyrrolo[3,2-*b*]pyridine (118 mg, 1.00 mmol, 1.0 equiv), copper(I) chloride (29.7 mg, 0.300 mmol, 30 mol %), 1,10-phenanthroline (54.0 mg, 0.300 mmol, 30 mol %), and MeCN (10 mL) to make *Solution A*. (–)-Isopulegol (462.8 mg, 3.00 mmol, 3.0 equiv) was used for ozonolysis and MeCN (15 mL) was used to make *Solution B*.

The crude product was purified through FCC to give **2-10** ($R_f = 0.41$; EtOAc/Et₃N/MeOH, 10:1:1) as a light-yellow solid (214.0 mg, 93% yield).

¹H NMR (500 MHz, CDCl₃) δ 8.32 (brs, 1H), 7.72 (d, $J = 7.0$ Hz, 1H), 7.29 (s, 1H), 7.04 (brs, 1H), 6.44 (brs, 1H), 4.03–3.83 (m, 2H), 3.28 (brs, 1H), 2.13 (d, $J = 11.8$ Hz, 1H), 2.03–1.93 (m, 1H), 1.93–1.78 (m, 2H), 1.74–1.59 (m, 1H), 1.25 (q, $J = 12.2$ Hz, 1H), 1.16 (qd, $J = 13.1, 3.3$ Hz, 1H), 1.02 (d, $J = 6.5$ Hz, 3H).

¹³C NMR (125 MHz, CDCl₃) δ 127.92, 117.44, 102.73, 72.70, 62.63, 42.58, 33.82, 31.21, 30.97, 21.84.

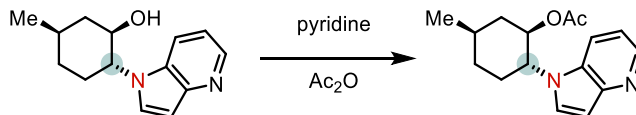
HRMS (ESI-TOF): $[M+H]^+$ calcd for [C₁₄H₁₉N₂O]⁺ m/z 231.1492, found 231.1491.

IR (neat, ATR): ν_{\max} 3139 (br), 2950, 2926, 2863, 1605, 1507, 1449, 1419, 1287, 1220, 1103, 1053, 937, 771, 743 cm⁻¹.

Optical Rotation: $[\alpha]_D^{24} = 15.53$ (c 0.5, CHCl₃)

M.p.: 165–167 °C.

Note: Some of the ¹H and ¹³C NMR spectral signals of compound 2-10 were not evident. We characterized the O-acetate-protected product to confirm its structure.



A 10-mL vial equipped with a magnetic stirrer bar was charged with **2-10** (30 mg, 0.13 mmol), pyridine (1 mL), and acetic anhydride (0.3 mL). The mixture was stirred at room temperature for 12 h. The reaction mixture was diluted with EtOAc (10 mL) and washed with aqueous 1 M HCl (2 × 5 mL), sat. aqueous NaHCO₃ (5 mL), and brine (5 mL). The organic layer was dried (Na₂SO₄)

and concentrated. The residue was purified through silica gel column chromatography to afford **2-10-Ac** ($R_f = 0.47$; EtOAc/Et₃N, 50:1) as a pale-yellow oil (27.3 mg, 78% yield).

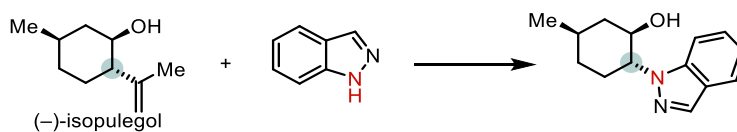
¹H NMR (400 MHz, CD₃OD) δ 8.26 (dd, $J = 4.7, 1.2$ Hz, 1H), 7.97 (dt, $J = 8.3, 0.9$ Hz, 1H), 7.65 (d, $J = 3.4$ Hz, 1H), 7.16 (dd, $J = 8.4, 4.7$ Hz, 1H), 6.64–6.52 (m, 1H), 5.12 (td, $J = 11.0, 4.6$ Hz, 1H), 4.41 (ddd, $J = 12.1, 10.4, 4.6$ Hz, 1H), 2.19–1.99 (m, 3H), 1.85 (dh, $J = 12.5, 3.5, 3.1$ Hz, 1H), 1.76 (dddd, $J = 15.1, 9.8, 6.5, 3.1$ Hz, 1H), 1.45 (s, 3H), 1.39–1.21 (m, 2H), 1.01 (d, $J = 6.5$ Hz, 3H).

¹³C NMR (100 MHz, CD₃OD) δ 169.80, 145.52, 141.60, 130.29, 128.75, 118.19, 115.86, 101.29, 74.63, 58.10, 39.35, 33.05, 30.68, 30.29, 20.61, 19.08.

HRMS (ESI-TOF): $[M+H]^+$ calcd for $[C_{16}H_{21}N_2O_2]^+$ m/z 273.1598, found 273.1600.

IR (neat, ATR): ν_{max} 2952, 2929, 2669, 2854, 1738, 1507, 1417, 1373, 1287, 1243, 1234, 1046, 1030, 775 cm⁻¹.

Optical Rotation: $[\alpha]_D^{25} = 55.17$ (c 0.2, CH₂Cl₂)



Prepared following **General procedure A** using methyl 1H-indazole (23.6 mg, 0.200 mmol, 1.0 equiv), copper(I) chloride (5.90 mg, 0.0600 mmol, 30 mol %), 1,10-phenanthroline (10.8 mg, 0.0600 mmol, 30 mol %), and MeCN (2 mL) to make *Solution A*. (-)-Isopulegol (92.6 mg, 0.600 mmol, 3.0 equiv) was used for ozonolysis and MeCN (3 mL) was used to make *Solution B*. The crude product was purified through FCC to give **2-11** ($R_f = 0.45$; hexanes/EtOAc, 3:1) as a white solid (34.5 mg, 75% yield).

¹H NMR (400 MHz, CDCl₃) δ 8.03 (s, 1H), 7.73 (dt, *J* = 8.1, 1.0 Hz, 1H), 7.48 (dd, *J* = 8.6, 0.8 Hz, 1H), 7.41–7.34 (m, 1H), 7.15 (ddd, *J* = 7.9, 6.8, 0.9 Hz, 1H), 4.36 (ddd, *J* = 11.2, 9.5, 4.4 Hz, 1H), 4.22 (ddd, *J* = 11.9, 9.5, 4.4 Hz, 1H), 2.23–2.13 (m, 1H), 2.10–2.02 (m, 2H), 1.96 (tdd, *J* = 13.3, 12.0, 3.7 Hz, 1H), 1.83 (dp, *J* = 12.9, 3.5 Hz, 1H), 1.78–1.66 (m, 1H), 1.34–1.24 (m, 1H), 1.24–1.13 (m, 1H), 1.04 (d, *J* = 6.5 Hz, 3H).

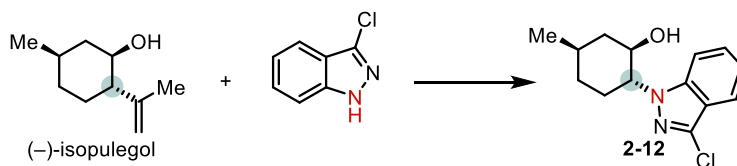
¹³C NMR (100 MHz, CDCl₃) δ 140.18, 133.39, 126.35, 123.93, 121.13, 120.80, 109.31, 71.75, 64.30, 41.91, 33.63, 31.07, 30.57, 21.94.

HRMS (ESI-TOF): [M+H]⁺ calcd for [C₁₄H₁₉N₂O]⁺ *m/z* 231.1492, found 231.1494.

IR (neat, ATR): ν_{\max} 3369 (br), 3055, 2948, 2922, 2856, 1615, 1498, 1453, 1423, 1320, 1183, 1088, 1051, 1007, 942, 832, 742 cm⁻¹.

Optical Rotation: $[\alpha]_{\text{D}}^{28} = -35.13$ (*c* 0.25, CHCl₃)

M.p.: 160–163 °C.



Prepared following **General procedure A** using methyl 3-chloro-1*H*-indazole (30.5 mg, 0.200 mmol, 1.0 equiv), copper(I) chloride (4.00 mg, 0.0400 mmol, 20 mol %), 1,10-phenanthroline (7.20 mg, 0.0400 mmol, 20 mol %), and MeCN (2 mL) to make *Solution A*. (–)-Isopulegol (61.7 mg, 0.400 mmol, 2.0 equiv) was used for ozonolysis and MeCN (2 mL) was used to make *Solution B*. The crude product was purified through FCC to give **2-12** (*R*_f = 0.39; hexanes/EtOAc, 4:1) as a white solid (48.9 mg, 92% yield).

¹H NMR (500 MHz, CDCl₃) δ 7.66 (d, *J* = 8.2 Hz, 1H), 7.47–7.37 (m, 2H), 7.19 (t, *J* = 7.3 Hz, 1H), 4.27 (td, 10.5, 4.5 Hz, 1H), 4.19–4.11 (m, 1H), 2.18–2.10 (m, 1H), 2.04 (brs, 1H), 1.99 (q, *J*

= 6.4 Hz, 2H), 1.82 (dt, $J = 13.6, 3.2$ Hz, 1H), 1.73–1.65 (m, 1H), 1.25 (q, $J = 12.1$ Hz, 1H), 1.21–1.09 (m, 1H), 1.02 (d, $J = 6.5$ Hz, 3H).

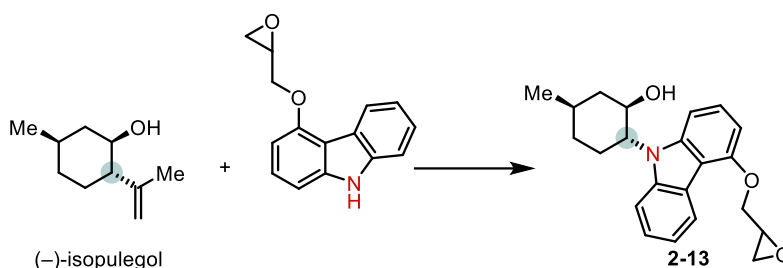
^{13}C NMR (125 MHz, CDCl_3) δ 141.64, 133.27, 127.49, 121.41, 120.96, 119.75, 109.64, 71.68, 64.59, 42.03, 33.55, 30.96, 30.53, 21.89.

HRMS (ESI-TOF): $[\text{M}+\text{H}]^+$ calcd for $[\text{C}_{14}\text{H}_{18}\text{ClN}_2\text{O}]^+$ m/z 265.1102, found 265.1105.

IR (neat, ATR): ν_{max} 3326 (br), 3061, 2952, 2944, 2926, 2917, 2862, 1617, 1494, 1467, 1455, 1339, 1196, 1009, 745 cm^{-1} .

Optical Rotation: $[\alpha]_{\text{D}}^{28} = -24.50$ (c 1.0, CHCl_3)

M.p.: 155–156 $^{\circ}\text{C}$.



Prepared following **General procedure A** using methyl 4-(oxiran-2-ylmethoxy)-9H-carbazole (47.9 mg, 0.200 mmol, 1.0 equiv), copper(I) chloride (4.00 mg, 0.0400 mmol, 20 mol %), 1,10-phenanthroline (7.20 mg, 0.0400 mmol, 20 mol %), and MeCN (2 mL) to make *Solution A*. (-)-Isopulegol (92.6 mg, 0.600 mmol, 3.0 equiv) was used for ozonolysis and MeCN (3 mL) was used to make *Solution B*. The crude product was purified through FCC to give **2-13** ($R_f = 0.50$; hexanes/EtOAc, 2:1) as a white solid (45.0 mg, 64% yield).

^1H NMR (400 MHz, CDCl_3) δ 8.42 (dd, $J = 14.7, 7.5$ Hz, 1H), 7.56 (d, $J = 8.0$ Hz, 0.5 \times 1H, one of the rotamer), 7.51–7.42 (m, 1H), 7.41–7.33 (m, 2H), 7.33–7.23 (m, 1.5 H, overlap with one of the rotamer), 7.21 (d, $J = 8.3$ Hz, 0.5 \times 1H), 7.14 (d, $J = 8.4$ Hz, 0.5 \times 1H), 6.66 (d, $J = 7.9$ Hz, 1H),

4.57–4.40 (m, 2H), 4.40–4.19 (m, 2H), 3.56–3.51 (m, 1H), 2.98 (t, $J = 4.8$ Hz, 1H), 2.87 (dd, $J = 4.9, 2.7$ Hz, 1H), 2.56–2.35 (m, 1H), 2.24–2.10 (m, 1H), 1.98–1.83 (m, 3H), 1.81–1.74 (m, 1H), 1.33–1.18 (m, 2H), 1.07 (d, $J = 6.5$ Hz, 3H).

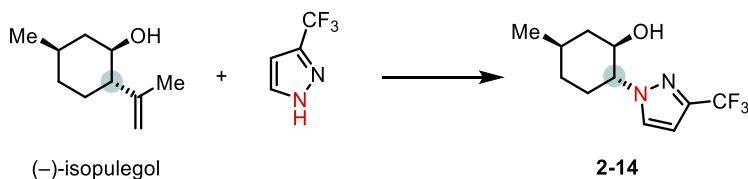
^{13}C NMR (100 MHz, CDCl_3) δ 155.34, 155.02, 143.39, 141.10, 139.99, 137.80, 128.36, 126.47, 125.99, 125.13, 124.52, 123.75, 123.55, 123.28, 122.08, 119.53, 119.40, 113.63, 112.22, 111.00, 108.62, 105.09, 102.70, 101.13, 101.09, 69.61, 69.61, 69.53, 69.52, 68.89, 68.88, 68.85, 62.41, 62.11, 50.37, 44.87, 42.44, 34.24, 31.33, 28.20, 28.16, 22.02.

HRMS (ESI-TOF): $[\text{M}+\text{H}]^+$ calcd for $[\text{C}_{22}\text{H}_{26}\text{NO}_3]^+$ m/z 352.1907, found 352.1912.

IR (neat, ATR): ν_{max} 3416 (br), 3056, 3007, 2951, 2926, 2873, 1623, 1595, 1581, 1502, 1484, 1453, 1439, 1337, 1268, 1157, 1111, 1052, 783, 751, 718 cm^{-1} .

Optical Rotation: $[\alpha]_{\text{D}}^{24} = 17.50$ (c 1.0, CHCl_3)

M.p.: 78–81 °C.



Prepared following **General procedure A** using 3-(trifluoromethyl)-1*H*-pyrazole (27.2 mg, 0.200 mmol, 1.0 equiv), copper(I) chloride (4.00 mg, 0.0400 mmol, 20 mol %), 1,10-phenanthroline (7.20 mg, 0.0400 mmol, 20 mol %), and MeCN (2 mL) to make *Solution A*. (–)-Isopulegol (61.7 mg, 0.400 mmol, 2.0 equiv) was used for ozonolysis and MeCN (2 mL) was used to make *Solution B*. The crude product was purified through FCC to give **2-14** ($R_f = 0.22$; hexanes/EtOAc, 4:1) as a white solid (42.1 mg, 85% yield).

¹H NMR (500 MHz, CDCl₃) δ 7.49 (s, 1H), 6.52 (d, *J* = 2.3 Hz, 1H), 3.97 (td, *J* = 10.5, 4.4 Hz, 1H), 3.89 (ddd, *J* = 13.6, 9.6, 4.2 Hz, 1H), 2.76 (s, 1H), 2.11–2.07 (m, 2H), 1.89 (qd, *J* = 13.2, 3.8 Hz, 1H), 1.81 (ddd, *J* = 13.5, 5.8, 3.0 Hz, 1H), 1.68–1.58 (m, 1H), 1.21–1.03 (m, 2H), 0.99 (d, *J* = 6.6 Hz, 3H).

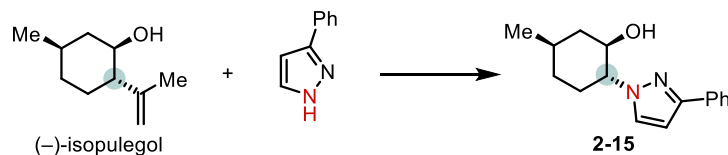
¹³C NMR (125 MHz, CDCl₃) δ 142.33 (q, *J* = 37.9 Hz), 130.21, 121.27 (q, *J* = 266.7 Hz), 103.99 (q, *J* = 1.9 Hz), 72.09, 67.84, 41.95, 33.11, 30.77, 30.71, 21.68.

HRMS (ESI-TOF): [M+H]⁺ calcd for [C₁₁H₁₆F₃N₂O]⁺ *m/z* 249.1209, found 249.1211.

IR (neat, ATR): ν_{max} 3370 (brs), 2953, 2932, 2871, 2855, 1491, 1390, 1372, 1237, 1167, 1130, 1055, 1009, 967, 770 cm⁻¹.

Optical Rotation: [α]_D²⁶ = -10.83 (*c* 0.2, CHCl₃)

M.p.: 56–57 °C.



Prepared following **General procedure A** using 3-phenyl-1*H*-pyrazole (28.8 mg, 0.200 mmol, 1.0 equiv), copper(I) chloride (4.00 mg, 0.0400 mmol, 20 mol %), 1,10-phenanthroline (7.20 mg, 0.0400 mmol, 20 mol %), and MeCN (2 mL) to make *Solution A*. (-)-Isopulegol (61.7 mg, 0.400 mmol, 2.0 equiv) was used for ozonolysis and MeCN (2 mL) was used to make *Solution B*. The crude product was purified through FCC to give **2-15** (*R*_f = 0.29; hexanes/EtOAc, 4:1) as a white solid (42.0 mg, 82% yield).

¹H NMR (400 MHz, CDCl₃) δ 7.81–7.79 (m, 2H), 7.49 (d, *J* = 2.4 Hz, 1H), 7.44–7.34 (m, 2H), 7.34–7.27 (m, 1H), 6.58 (d, *J* = 2.4 Hz, 1H), 4.00–3.85 (m, 2H), 2.24–2.17 (m, 1H), 2.16–2.06 (m, 1H), 1.94–1.79 (m, 2H), 1.57–1.70 (m, 1H), 1.26–1.08 (m, 2H), 1.01 (d, *J* = 6.6 Hz, 3H).

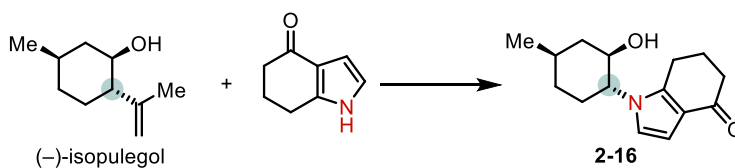
^{13}C NMR (100 MHz, CDCl_3) δ 151.28, 133.22, 129.25, 128.61, 127.74, 125.62, 102.49, 72.89, 66.41, 41.55, 33.23, 30.70, 30.15, 21.80.

HRMS (ESI-TOF): $[\text{M}+\text{H}]^+$ calcd for $[\text{C}_{16}\text{H}_{21}\text{N}_2\text{O}]^+$ m/z 257.1648, found 257.1656.

IR (neat, ATR): ν_{max} 3365 (br), 2948, 2924, 2867, 2854, 1605, 1498, 1455, 1359, 1226, 1099, 1074, 1049, 1024, 1009, 938, 749, 693 cm^{-1} .

Optical Rotation: $[\alpha]_{\text{D}}^{26} = 7.26$ (c 1.0, CHCl_3)

M.p.: 100–101 $^{\circ}\text{C}$.



Prepared following **General procedure A** using 1,5,6,7-tetrahydro-4H-indol-4-one (27.0 mg, 0.200 mmol, 1.0 equiv), copper(I) chloride (4.00 mg, 0.0400 mmol, 20 mol %), 1,10-phenanthroline (7.20 mg, 0.0400 mmol, 20 mol %), and MeCN (2 mL) to make *Solution A*. (-)-Isopulegol (61.7 mg, 0.400 mmol, 2.0 equiv) was used for ozonolysis and MeCN (2 mL) was used to make *Solution B*. The crude product was purified through FCC to give **2-16** ($R_f = 0.32$; EtOAc) as a white solid (40.6 mg, 82% yield).

^1H NMR (400 MHz, CDCl_3) δ 6.62 (d, $J = 3.2$ Hz, 1H), 6.51 (d, $J = 3.2$ Hz, 1H), 3.75 (td, $J = 10.2, 4.5$ Hz, 1H), 3.64 (ddd, $J = 13.6, 9.6, 4.1$ Hz, 1H), 2.84 (dt, $J = 16.2, 6.4$ Hz, 1H), 2.68 (dt, $J = 16.3, 6.0$ Hz, 2H), 2.43–2.28 (m, 2H), 2.11–2.04 (m, 3H), 1.99–1.89 (m, 1H), 1.85–1.55 (m, 3H), 1.23–1.03 (m, 2H), 0.99 (d, $J = 6.5$ Hz, 3H).

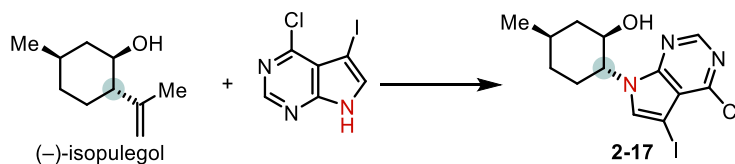
^{13}C NMR (100 MHz, CDCl_3) δ 194.59, 144.90, 120.26, 118.27, 106.39, 72.85, 62.18, 42.50, 37.68, 33.61, 31.42, 31.15, 23.57, 22.12, 21.79.

HRMS (ESI-TOF): $[\text{M}+\text{H}]^+$ calcd for $[\text{C}_{15}\text{H}_{22}\text{NO}_2]^+$ m/z 248.1645, found 248.1648.

IR (neat, ATR): ν_{\max} 3369 (br), 2948, 2928, 2866, 1631, 1501, 1471, 1417, 1384, 1255, 1228, 1190, 1111, 1054, 936, 753, 705 cm^{-1} .

Optical Rotation: $[\alpha]_{\text{D}}^{26} = -4.93$ (c 1.0, CHCl_3)

M.p.: 160–163 $^{\circ}\text{C}$.



Prepared following **General procedure A** using 4-chloro-5-iodo-7*H*-pyrrolo[2,3-*d*]pyrimidine (55.9 mg, 0.200 mmol, 1.0 equiv), copper(I) chloride (4.00 mg, 0.0400 mmol, 20 mol %), 1,10-phenanthroline (7.20 mg, 0.0400 mmol, 20 mol %), and MeCN (2 mL) to make *Solution A*. (-)-Isopulegol (61.7 mg, 0.400 mmol, 2.0 equiv) was used for ozonolysis and MeCN (2 mL) was used to make *Solution B*. The crude product was purified through FCC to give **2-17** ($R_f = 0.52$; DCM/MeOH, 10:1) as a white solid (62.0 mg, 79% yield).

^1H NMR (400 MHz, CDCl_3) δ 8.52 (s, 1H), 7.45 (s, 1H), 4.49 (ddd, $J = 12.1, 10.2, 4.4$ Hz, 1H), 3.96 (td, $J = 10.7, 4.5$ Hz, 1H), 2.17–2.10 (m, 1H), 2.05–1.99 (m, 1H), 1.95 (td, $J = 12.7, 3.7$ Hz, 1H), 1.87–1.81 (m, 1H), 1.75–1.62 (m, 1H), 1.31–1.12 (m, 2H), 1.02 (d, $J = 6.5$ Hz, 3H).

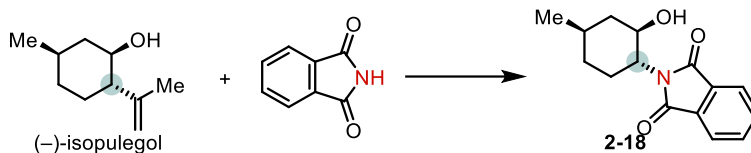
^{13}C NMR (100 MHz, CDCl_3) δ 152.66, 151.30, 150.47, 132.49, 117.10, 72.50, 61.64, 51.29, 43.32, 33.46, 31.16, 30.97, 21.71.

HRMS (ESI-TOF): $[\text{M}+\text{H}]^+$ calcd for $[\text{C}_{13}\text{H}_{16}\text{ClIN}_3\text{O}]^+$ m/z 392.0021, found 392.0020.

IR (neat, ATR): ν_{\max} 3369 (br), 2948, 2928, 2866, 1631, 1501, 1471, 1417, 1384, 1255, 1228, 1190, 1111, 1054, 936, 753, 705 cm^{-1} .

Optical Rotation: $[\alpha]_{\text{D}}^{26} = -3.67$ (c 0.2, CHCl_3)

M.p.: 160 °C (decomposition)



Prepared following **General procedure A** using phthalimide (147 mg, 1.00 mmol, 1.0 equiv), copper(I) chloride (19.8 mg, 0.200 mmol, 20 mol %), 1,10-phenanthroline (36.0 mg, 0.200 mmol, 20 mol %), and MeCN (10 mL) to make *Solution A*. (-)-Isopulegol (386 mg, 2.50 mmol, 2.5 equiv) was used for ozonolysis and MeCN (12.5 mL) was used to make *Solution B*. The crude product was purified through FCC to give **2-18** ($R_f = 0.27$; hexanes/EtOAc, 2:1) as a white solid (211.0 mg, 81% yield).

$^1\text{H NMR}$ (400 MHz, CDCl_3) δ 7.78 (dd, $J = 5.4, 3.1$ Hz, 2H), 7.67 (dd, $J = 5.4, 3.1$ Hz, 2H), 4.32 (td, $J = 10.7, 4.5$ Hz, 1H), 3.92 (ddd, $J = 12.6, 10.2, 4.0$ Hz, 1H), 2.21 (qd, $J = 12.4, 3.5$ Hz, 1H), 2.14–2.03 (m, 1H), 1.80–1.71 (m, 2H), 1.71–1.60 (m, 1H), 1.15–1.00 (m, 2H), 0.97 (d, $J = 6.5$ Hz, 3H).

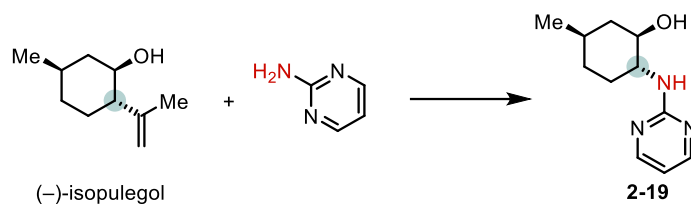
$^{13}\text{C NMR}$ (100 MHz, CDCl_3) δ 168.87, 133.83, 131.97, 123.11, 69.07, 57.32, 43.88, 33.77, 31.12, 28.13, 21.88.

HRMS (DART): $[\text{M}+\text{H}]^+$ calcd for $[\text{C}_{15}\text{H}_{18}\text{NO}_3]^+$ m/z 260.1281, found 260.1281.

IR (neat, ATR): ν_{max} 3523 (br), 2947, 2928, 2871, 2850, 1763, 1700, 1393, 1379, 1074, 1028, 1008, 887, 717 cm^{-1} .

Optical Rotation: $[\alpha]_{\text{D}}^{26} = -15.23$ (c 1.0, CHCl_3)

M.p.: 171–174 °C.



Prepared following **General procedure A** using pyrimidin-2-amine (19.0 mg, 0.200 mmol, 1.0 equiv), copper(I) chloride (5.90 mg, 0.0600 mmol, 30 mol %), 1,10-phenanthroline (10.8 mg, 0.0600 mmol, 30 mol %), and MeCN (2 mL) to make *Solution A*. (-)-Isopulegol (92.6 mg, 0.600 mmol, 3.0 equiv) was used for ozonolysis and MeCN (3 mL) was used to make *Solution B*. The crude product was purified through FCC to give **2-19** ($R_f = 0.21$; DCM/toluene/MeOH, 5:5:1) as a colorless oil (21.1 mg, 51% yield).

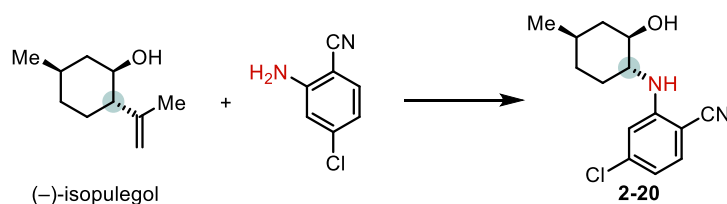
$^1\text{H NMR}$ (400 MHz, CDCl_3) δ 8.23 (d, $J = 4.4$ Hz, 2H), 6.53 (t, $J = 4.8$ Hz, 1H), 5.44 (d, $J = 5.4$ Hz, 1H), 3.64 (dtd, $J = 13.9, 6.6, 3.3$ Hz, 1H), 3.47 (ddd, $J = 10.9, 9.6, 4.5$ Hz, 1H), 2.06–1.98 (m, 2H), 1.68 (dp, $J = 12.9, 3.4$ Hz, 1H), 1.56–1.43 (m, 1H), 1.32 (qd, $J = 13.0, 3.8$ Hz, 1H), 1.17–0.98 (m, 2H), 0.94 (d, $J = 6.6$ Hz, 3H).

$^{13}\text{C NMR}$ (100 MHz, CDCl_3) δ 162.73, 157.91, 110.92, 75.88, 57.17, 43.11, 33.38, 31.56, 30.77, 21.82.

HRMS (ESI-TOF): $[\text{M}+\text{H}]^+$ calcd for $[\text{C}_{11}\text{H}_{18}\text{N}_3\text{O}]^+$ m/z 208.1444, found 208.1451.

IR (neat, ATR): ν_{max} 3274 (br), 2948, 2925, 2853, 1589, 1530, 1452, 1417, 1361, 1240, 1051, 800, 776 cm^{-1} .

Optical Rotation: $[\alpha]_{\text{D}}^{28} = 13.77$ (c 1.0, CHCl_3)



Prepared following **General procedure A** using 2-amino-4-chlorobenzonitrile (61.0 mg, 0.400 mmol, 1.0 equiv), copper(I) chloride (11.9 mg, 0.120 mmol, 30 mol %), 1,10-phenanthroline (21.6 mg, 0.120 mmol, 30 mol %), and MeCN (4 mL) to make *Solution A*. (–)-Isopulegol (185 mg, 1.20 mmol, 3.0 equiv) was used for ozonolysis and MeCN (6 mL) was used to make *Solution B*. The crude product was purified through FCC to give **2-20** ($R_f = 0.24$; toluene/EtOAc, 15:1) as a pale-yellow solid (81.5 mg, 77% yield).

$^1\text{H NMR}$ (400 MHz, CDCl_3) δ 7.27 (d, $J = 8.3$ Hz, 1H), 6.82 (d, $J = 1.8$ Hz, 1H), 6.63 (dd, $J = 8.3$, 1.8 Hz, 1H), 3.51 (ddd, $J = 11.0$, 9.3, 4.4 Hz, 1H), 3.18 (ddd, $J = 11.6$, 9.3, 4.2 Hz, 1H), 2.04 (dq, $J = 13.0$, 3.2 Hz, 2H), 1.72 (dp, $J = 12.8$, 3.3 Hz, 1H), 1.63–1.50 (m, 1H), 1.31–1.00 (m, 3H), 0.97 (d, $J = 6.6$ Hz, 3H).

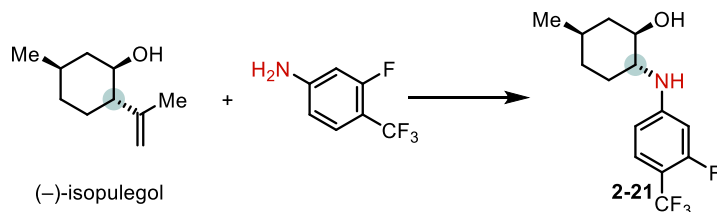
$^{13}\text{C NMR}$ (100 MHz, CDCl_3) δ 151.19, 140.87, 133.73, 117.41, 117.28, 111.84, 94.80, 73.98, 59.21, 42.28, 33.24, 31.07, 31.00, 21.81.

HRMS (ESI-TOF): $[\text{M}+\text{H}]^+$ calcd for $[\text{C}_{14}\text{H}_{18}\text{ClN}_2\text{O}]^+$ m/z 265.1102, found 265.1108.

IR (neat, ATR): ν_{max} 3386 (br), 2948, 2926, 2868, 2215, 1601, 1571, 1507, 1434, 1282, 1105, 1048, 912 cm^{-1} .

Optical Rotation: $[\alpha]_{\text{D}}^{24} = -2.10$ (c 1.0, CHCl_3)

M.p.: 114–117 $^{\circ}\text{C}$.



Prepared following **General procedure A** using 3-fluoro-4-(trifluoromethyl)aniline (71.6 mg, 0.400 mmol, 1.0 equiv), copper(I) chloride (11.9 mg, 0.120 mmol, 30 mol %), 1,10-phenanthroline

(21.6 mg, 0.120 mmol, 30 mol %), and MeCN (4 mL) to make *Solution A*. (–)-Isopulegol (185 mg, 1.20 mmol, 3.0 equiv) was used for ozonolysis and MeCN (6 mL) was used to make *Solution B*. The crude product was purified through FCC to give **2-21** ($R_f = 0.16$; toluene/EtOAc, 15:1) as a white solid (62.9 mg, 54% yield).

$^1\text{H NMR}$ (400 MHz, CDCl_3) δ 7.30 (t, $J = 8.3$ Hz, 1H), 6.44 (s, 1H), 6.41 (s, 1H), 3.43 (ddd, $J = 10.9, 9.5, 4.4$ Hz, 1H), 3.15–3.05 (m, 1H), 2.11–2.00 (m, 2H), 1.71 (dp, $J = 12.6, 3.3, 2.9$ Hz, 1H), 1.61–1.49 (m, 1H), 1.21–1.01 (m, 3H), 0.97 (d, $J = 6.6$ Hz, 3H).

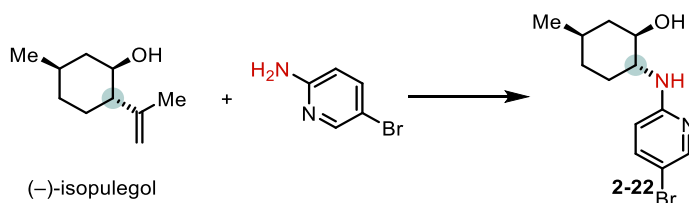
$^{13}\text{C NMR}$ (125 MHz, CDCl_3) δ 161.21 (dq, $J = 252.4, 2.0$ Hz), 152.65 (d, $J = 11.2$ Hz), 127.92 (p, $J = 4.3$ Hz), 123.33 (qd, $J = 268.33, 0.75$ Hz), 108.65 (d, $J = 2.3$ Hz), 106.68 (qd, $J = 33.3, 13.0$ Hz), 100.50 (d, $J = 24.5$ Hz). 74.21, 59.47, 42.19, 33.25, 31.10, 30.93, 21.79.

HRMS (ESI-TOF): $[\text{M}+\text{H}]^+$ calcd for $[\text{C}_{14}\text{H}_{18}\text{F}_4\text{NO}]^+$ m/z 292.1319, found 292.1317.

IR (neat, ATR): ν_{max} 3385, 2952, 2928, 2871, 2858, 1632, 1587, 1534, 1352, 1323, 1194, 1158, 1121, 1045 cm^{-1} .

Optical Rotation: $[\alpha]_{\text{D}}^{26} = -17.17$ (c 0.2, CHCl_3)

M.p.: 113–115 $^{\circ}\text{C}$.



Prepared following **General procedure A** using 5-bromopyridin-2-amine (69.2 mg, 0.400 mmol, 1.0 equiv), copper(I) chloride (11.9 mg, 0.120 mmol, 30 mol %), 1,10-phenanthroline (21.6 mg, 0.120 mmol, 30 mol %), and MeCN (4 mL) to make *Solution A*. (–)-Isopulegol (185 mg, 1.20 mmol, 3.0 equiv) was used for ozonolysis and MeCN (6 mL) was used to make *Solution B*. The

crude product was purified through FCC to give **2-22** ($R_f = 0.35$; toluene/EtOAc, 3:1) as a white solid (75.1 mg, 66% yield).

^1H NMR (400 MHz, CDCl_3) δ 8.02 (d, $J = 2.4$ Hz, 1H), 7.44 (dd, $J = 8.8, 2.5$ Hz, 1H), 6.38 (d, $J = 8.9$ Hz, 1H), 4.42 (d, $J = 5.6$ Hz, 1H), 3.53–3.35 (m, 2H), 2.04 (dq, $J = 12.7, 3.6$ Hz, 1H), 1.98 (dq, $J = 12.7, 3.6$ Hz, 1H), 1.69 (dp, $J = 12.8, 3.3$ Hz, 1H), 1.57–1.42 (m, 1H), 1.35–1.22 (m, 1H), 1.18–0.98 (m, 2H), 0.95 (d, $J = 6.5$ Hz, 3H).

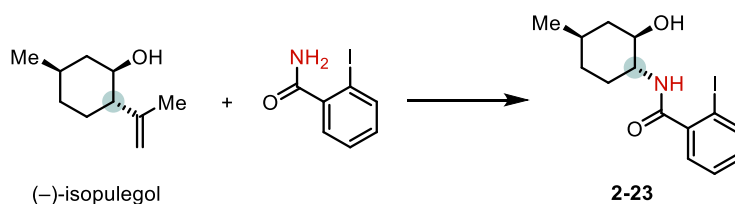
^{13}C NMR (100 MHz, CDCl_3) δ 157.56, 147.72, 140.01, 110.23, 107.31, 75.91, 57.95, 42.96, 33.45, 31.72, 30.80, 21.81.

HRMS (ESI-TOF): $[\text{M}+\text{H}]^+$ calcd for $[\text{C}_{12}\text{H}_{18}\text{BrN}_2\text{O}]^+$ m/z 285.0597, found 285.0595.

IR (neat, ATR): ν_{max} 3329, 2951, 2924, 2868, 2832, 1596, 1505, 1581, 1456, 1390, 1377, 1049 cm^{-1} .

Optical Rotation: $[\alpha]_{\text{D}}^{25} = 22.00$ (c 0.1, CHCl_3).

M.p.: 66–69 °C.



Prepared following **General procedure A** using 2-iodobenzamide (49.4 mg, 0.200 mmol, 1.0 equiv), copper(I) chloride (5.90 mg, 0.0600 mmol, 30 mol %), 1,10-phenanthroline (10.8 mg, 0.0600 mmol, 30 mol %), and MeCN (3 mL) to make *Solution A*. (-)-Isopulegol (92.6 mg, 0.600 mmol, 3.0 equiv) was used for ozonolysis and MeCN (3 mL) was used to make *Solution B*. The crude product was purified through FCC to give **2-23** ($R_f = 0.38$; toluene/EtOAc, 1:1) as a white solid (51.6 mg, 72% yield).

¹H NMR (400 MHz, CDCl₃) δ 7.85 (dd, *J* = 8.0, 1.1 Hz, 1H), 7.47–7.33 (m, 2H), 7.10 (td, *J* = 7.6, 1.9 Hz, 1H), 5.80 (d, *J* = 6.2 Hz, 1H), 3.82 (dddd, *J* = 11.9, 9.8, 7.7, 4.4 Hz, 1H), 3.48 (td, *J* = 10.6, 4.4 Hz, 1H), 2.46 (brs, 2H), 2.13 (dq, *J* = 12.6, 3.5 Hz, 1H), 2.06 (ddd, *J* = 12.8, 6.0, 4.3 Hz, 1H), 1.77–1.66 (m, 1H), 1.56–1.44 (m, 1H), 1.33 (qd, *J* = 12.9, 3.7 Hz, 1H), 1.20–1.02 (m, 2H), 0.97 (d, *J* = 6.5 Hz, 3H).

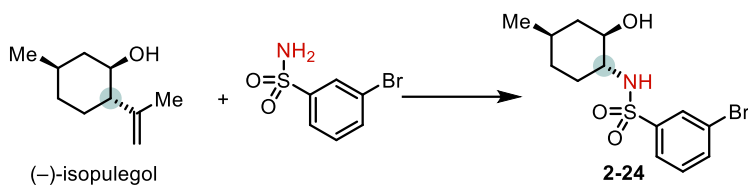
¹³C NMR (100 MHz, CDCl₃) δ 170.85, 141.95, 139.81, 131.30, 128.49, 128.28, 92.45, 74.68, 56.44, 42.92, 33.12, 30.89, 30.85, 21.75.

HRMS (ESI-TOF): [M+H]⁺ calcd for [C₁₄H₁₉INO₂]⁺ *m/z* 360.0455, found 360.04561.

IR (neat, ATR): ν_{max} 3250, 2945, 2921, 2865, 2847, 1633, 1541, 1452, 1336, 1060, 1050, 1015, 851, 769, 732, 686 cm⁻¹.

Optical Rotation: [α]_D²⁴ = -28.27 (*c* 1.0, CHCl₃).

M.p.: 215–218 °C.



Prepared following **General procedure A** using 3-bromobenzenesulfonamide (47.2 mg, 0.200 mmol, 1.0 equiv), copper(I) chloride (4.00 mg, 0.0400 mmol, 20 mol %), 1,10-phenanthroline (7.20 mg, 0.0400 mmol, 20 mol %), and MeCN (2 mL) to make *Solution A*. (-)-Isopulegol (61.7 mg, 0.400 mmol, 2.0 equiv) was used for ozonolysis and MeCN (2 mL) was used to make *Solution B*. The crude product was purified through FCC to give **2-24** (*R*_f = 0.24; hexanes/EtOAc, 2:1) as a pale-yellow oil (44.6 mg, 64% yield).

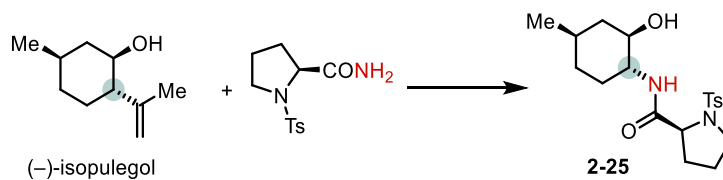
¹H NMR (400 MHz, CDCl₃) δ 8.06 (t, *J* = 1.8 Hz, 1H), 7.84 (ddd, *J* = 7.9, 1.8, 1.0 Hz, 1H), 7.70 (ddd, *J* = 8.0, 1.8, 0.9 Hz, 1H), 7.40 (t, *J* = 7.9 Hz, 1H), 5.29 (d, *J* = 6.7 Hz, 1H), 3.36 (ddd, *J* = 11.1, 9.6, 4.4 Hz, 1H), 2.92–2.84 (m, 1H), 1.97 (ddd, *J* = 12.6, 6.5, 4.1 Hz, 1H), 1.75 (dq, *J* = 13.0, 3.5 Hz, 1H), 1.56 (dp, *J* = 12.8, 3.2 Hz, 1H), 1.51–1.38 (m, 1H), 1.19 (qd, *J* = 13.8, 4.3 Hz, 1H), 1.05–0.94 (m, 1H), 0.93–0.79 (m, 4H).

¹³C NMR (100 MHz, CDCl₃) δ 142.53, 135.77, 130.69, 130.01, 125.63, 123.04, 72.81, 59.85, 42.13, 33.10, 31.41, 30.76, 21.66.

HRMS (ESI-TOF): [M+Na]⁺ calcd for [C₁₃H₁₈BrNNaO₃S]⁺ *m/z* 370.0083, found 370.0081.

IR (neat, ATR): ν_{max} 3496 (br), 3274 (br), 2949, 2926, 2868, 1571, 1459, 1407, 1328, 1295, 1160, 1100, 1070, 1052, 904, 786, 768, 679, 658, 605, 576 cm⁻¹.

Optical Rotation: [α]_D²⁹ = -4.83 (*c* 1.0, CHCl₃).



Prepared following **General procedure A** using (S)-1-tosylpyrrolidine-2-carboxamide (107 mg, 0.400 mmol, 1.0 equiv), copper(I) chloride (11.9 mg, 0.120 mmol, 30 mol %), 1,10-phenanthroline (21.6 mg, 0.120 mmol, 30 mol %), and MeCN (4 mL) to make *Solution A*. (-)-Isopulegol (185 mg, 1.20 mmol, 3.0 equiv) was used for ozonolysis and MeCN (6 mL) was used to make *Solution B*. The crude product was purified through FCC to give **2-25** (*R*_f = 0.43; DCM/MeOH, 20:1) as a white solid (118.2 mg, 78% yield).

¹H NMR (400 MHz, CDCl₃) δ 7.77–7.65 (m, 2H), 7.34 (d, *J* = 8.0 Hz, 2H), 6.86 (d, *J* = 7.0 Hz, 1H), 4.02 (dd, *J* = 8.8, 3.1 Hz, 1H), 3.65–3.52 (m, 2H), 3.46–3.35 (m, 1H), 3.16 (td, *J* = 9.8, 6.5

Hz, 1H), 2.44 (s, 3H), 2.16 (ddt, $J = 12.1, 6.3, 2.9$ Hz, 1H), 2.08–1.92 (m, 2H), 1.83–1.65 (m, 2H), 1.64–1.53 (m, 2H), 1.49 (dddd, $J = 11.9, 8.5, 6.5, 3.3$ Hz, 1H), 1.39 (qd, $J = 13.1, 3.8$ Hz, 1H), 1.13–0.96 (m, 2H), 0.94 (d, $J = 6.6$ Hz, 3H).

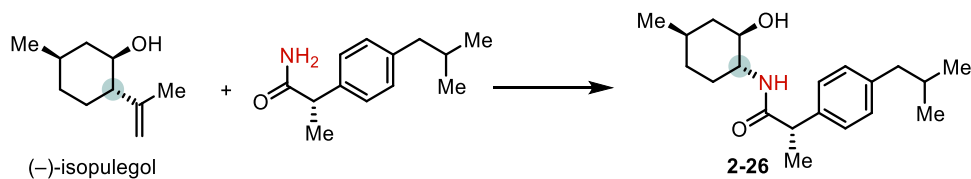
^{13}C NMR (100 MHz, CDCl_3) δ 173.19, 144.55, 132.54, 130.04, 127.90, 74.84, 62.68, 56.14, 50.09, 43.13, 33.15, 30.86, 30.56, 30.44, 24.30, 21.76, 21.60.

HRMS (DART): $[\text{M}+\text{H}]^+$ calcd for $[\text{C}_{19}\text{H}_{29}\text{N}_2\text{O}_4\text{S}]^+$ m/z 381.1843 found 381.1842.

IR (neat, ATR): ν_{max} 3519 (br), 3393 (br), 2950, 2926, 2869, 1651, 1531, 1344, 1159, 1093, 1052, 754, 664 cm^{-1} .

Optical Rotation: $[\alpha]_{\text{D}}^{24} = -55.00$ (c 0.34, CHCl_3).

M.p.: 169–172 $^{\circ}\text{C}$.



Prepared following **General procedure A** using (*S*)-2-(4-isobutylphenyl)propanamide (82.1 mg, 0.400 mmol, 1.0 equiv), copper(I) chloride (11.9 mg, 0.120 mmol, 30 mol %), 1,10-phenanthroline (21.6 mg, 0.120 mmol, 30 mol %), and MeCN (4 mL) to make *Solution A*. (–)-Isopulegol (185 mg, 1.20 mmol, 3.0 equiv) was used for ozonolysis and MeCN (6 mL) was used to make *Solution B*. The crude product was purified through FCC to give **2-26** ($R_f = 0.29$; Et_2O) as a white solid (39.9 mg) and also as an impure material. The fractions containing the impure material were concentrated and subjected again to FCC to give another 43.9 mg of **2-26**. Combined, 83.8 mg of **2-26** was obtained, giving an isolated yield of 66%.

¹H NMR (400 MHz, CDCl₃) δ 7.21–7.13 (m, 2H), 7.13–7.05 (m, 2H), 5.41 (d, *J* = 7.0 Hz, 1H), 3.63 (brs, 1H) 3.61–3.39 (m, 2H), 3.34–3.19 (m, 1H), 2.44 (d, *J* = 7.2 Hz, 2H), 2.06–1.93 (m, 1H), 1.84 (dp, *J* = 13.6, 6.8 Hz, 1H), 1.74 (ddd, *J* = 11.7, 7.2, 3.0 Hz, 1H), 1.58 (dp, *J* = 12.5, 2.9 Hz, 1H), 1.49 (d, *J* = 7.2 Hz, 3H), 1.38 (dddq, *J* = 15.0, 9.7, 6.4, 3.2 Hz, 1H), 1.11–0.99 (m, 2H), 0.99–0.92 (m, 1H), 0.92–0.85 (m, 9H).

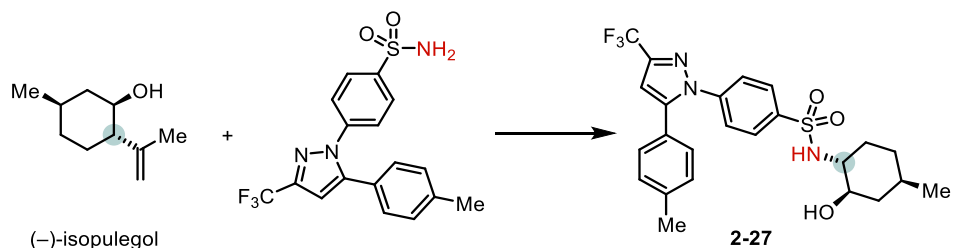
¹³C NMR (100 MHz, CDCl₃) δ 176.64, 140.80, 138.38, 129.67, 127.26, 75.04, 55.83, 46.62, 45.01, 43.07, 33.04, 30.75, 30.69, 30.16, 22.38, 22.37, 21.70, 18.57.

HRMS (DART): [M+H]⁺ calcd for [C₂₀H₃₂NO₂]⁺ *m/z* 318.2428, found 318.2428.

IR (neat, ATR): ν_{max} 3325, 3298, 2960, 2944, 2932, 2906, 2866, 2846, 1646, 1547, 1459, 1048 cm⁻¹.

Optical Rotation: [α]_D²⁴ = 11.17 (*c* 0.1, CHCl₃).

M.p.: 167–169 °C.



Prepared following **General procedure A** using celecoxib (153 mg, 0.400 mmol, 1.0 equiv), copper(I) chloride (7.90 mg, 0.0800 mmol, 20 mol %), 1,10-phenanthroline (14.4 mg, 0.0800 mmol, 20 mol %), and MeCN (4 mL) to make *Solution A*. (–)-Isopulegol (123 mg, 0.800 mmol, 2.0 equiv) was used for ozonolysis and MeCN (4 mL) was used to make *Solution B*. The crude product was purified through FCC to give **2-27** (*R*_f = 0.26; hexanes/EtOAc, 3:2) as a white solid (155.9 mg, 79% yield).

¹H NMR (400 MHz, CDCl₃) δ 7.94–7.85 (m, 2H), 7.51–7.41 (m, 2H), 7.15 (d, *J* = 8.0 Hz, 2H), 7.08 (d, *J* = 8.2 Hz, 2H), 6.74 (s, 1H), 5.34 (d, *J* = 6.9 Hz, 1H), 3.33 (td, *J* = 10.9, 4.4 Hz, 1H), 2.83 (tdd, *J* = 13.9, 7.9, 3.3 Hz, 2H), 2.36 (s, 3H), 2.01–1.89 (m, 1H), 1.70 (dq, *J* = 12.8, 3.4 Hz, 1H), 1.60–1.51 (m, 1H), 1.49–1.37 (m, 1H), 1.17 (qd, *J* = 13.1, 3.7 Hz, 1H), 0.96 (q, *J* = 12.1 Hz, 1H), 0.88 (d, *J* = 6.5 Hz, 3H), 0.81 (td, *J* = 13.3, 12.6, 3.4 Hz, 1H).

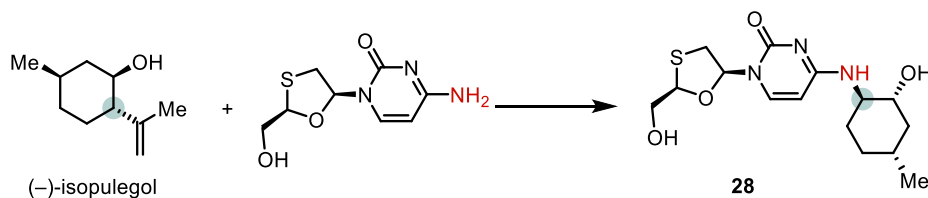
¹³C NMR (100 MHz, CDCl₃) δ 145.36, 144.05 (q, *J* = 38.6 Hz), 142.42, 140.14, 139.80, 129.73, 128.72, 128.16, 125.67, 125.64, 121.06 (q, *J* = 269.1 Hz), 106.25 (q, *J* = 2.0 Hz), 72.72, 59.84, 42.13, 33.14, 31.29, 30.75, 21.66, 21.32.

HRMS (ESI-TOF): [M+H]⁺ calcd for [C₂₄H₂₇F₃N₃O₃S]⁺ *m/z* 494.1720, found 494.1720.

IR (neat, ATR): ν_{max} 3487 (br), 3269 (br), 2950, 2927, 2871, 1598, 1472, 1450, 1374, 1332, 1272, 1237, 1161, 1136, 1096, 976, 843, 760, 633 cm⁻¹.

Optical Rotation: [α]_D²⁵ = -4.50 (*c* 0.4, CHCl₃).

M.p.: 171–181 °C.



Prepared following **General procedure A** using lamivudine (91.7 mg, 0.400 mmol, 1.0 equiv), copper(I) chloride (11.9 mg, 0.120 mmol, 30 mol %), 1,10-phenanthroline (21.6 mg, 0.120 mmol, 30 mol %), MeCN (4 mL), and MeOH (4 mL) to make *Solution A*. (-)-Isopulegol (185 mg, 1.20 mmol, 3.0 equiv) was used for ozonolysis and MeCN (6 mL) was used to make *Solution B*. The crude product was purified through FCC to give **2-28** (*R*_f = 0.41; DCM/MeOH, 4:1) as a yellow solid (133.8 mg, 98% yield).

¹H NMR (400 MHz, DMSO-d₆) δ 7.69 (d, *J* = 7.5 Hz, 1H), 7.63 (d, *J* = 7.6 Hz, 1H), 6.16 (t, *J* = 5.2 Hz, 1H), 5.73 (d, *J* = 7.5 Hz, 1H), 5.26 (t, *J* = 5.8 Hz, 1H), 5.12 (t, *J* = 4.6 Hz, 1H), 4.64 (d, *J* = 4.5 Hz, 1H), 3.68 (h, *J* = 7.1 Hz, 2H), 3.62–3.54 (m, 1H), 3.35 (dd, *J* = 11.6, 5.5 Hz, 1H), 3.27–3.23 (m, 1H), 2.98 (dd, *J* = 11.6, 5.0 Hz, 1H), 1.92–1.74 (m, 2H), 1.54 (d, *J* = 12.7 Hz, 1H), 1.44–1.32 (m, 1H), 1.06 (qd, *J* = 13.0, 3.1 Hz, 1H), 0.99–0.77 (m, 5H).

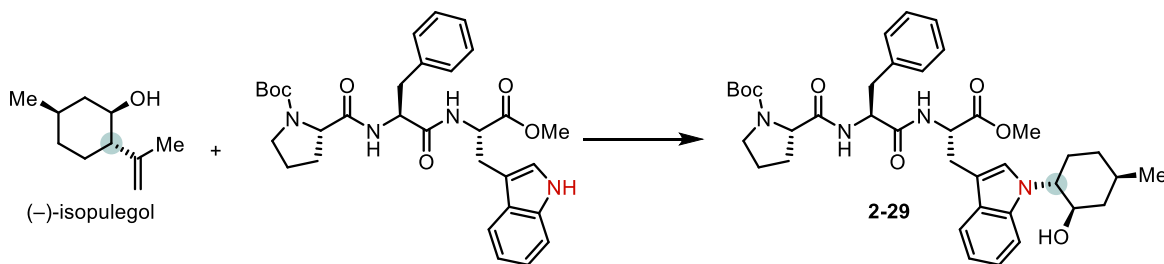
¹³C NMR (100 MHz, DMSO-d₆) δ 163.91, 155.09, 139.85, 95.54, 87.01, 86.16, 71.81, 63.37, 55.76, 43.95, 36.66, 33.39, 31.13, 30.92, 22.38.

HRMS (ESI-TOF): [M+Na]⁺ calcd for [C₁₅H₂₃N₃NaO₄S]⁺ *m/z* 364.1301, found 364.1307.

IR (neat, ATR): ν_{max} 3277 (br), 3134, 2950, 2925, 2862, 1643, 1579, 1502, 1337, 1269, 1051, 755 cm⁻¹.

Optical Rotation: [α]_D²⁵ = -10.50 (*c* 0.2, CHCl₃).

M.p.: 131–134 °C.



Prepared following **General procedure A** using the peptide **2-88** (113 mg, 0.200 mmol, 1.0 equiv), copper(I) chloride (5.90 mg, 0.0600 mmol, 30 mol %), 1,10-phenanthroline (10.8 mg, 0.0600 mmol, 30 mol %), and MeCN (2 mL) to make *Solution A*. (-)-Isopulegol (92.6 mg, 0.600 mmol, 3.0 equiv) was used for ozonolysis and MeCN (3 mL) was used to make *Solution B*. The crude product was purified through FCC to give **2-29** (*R*_f = 0.47; EtOAc/hexanes, 2:1) as a pale-yellow solid (113.1 mg, 84% yield).

¹H NMR (400 MHz, CDCl₃) δ 7.46 (d, *J* = 7.8 Hz, 1H), 7.40 (d, *J* = 8.3 Hz, 1H), 7.25–7.08 (m, 6H), 7.08–7.00 (m, 2H), 6.87–6.10 (m, 2H), 4.64 (q, *J* = 6.7 Hz, 1H), 4.52 (br, 1H), 3.99 (tt, *J* = 12.9, 7.8 Hz, 2H), 3.73 (m, 4H), 3.34 (dd, *J* = 14.8, 5.1 Hz, 1H), 3.29–2.97 (m, 4H), 2.86 (s, 1H), 2.13 (d, *J* = 12.5 Hz, 1H), 1.96 (dt, *J* = 11.0, 3.6 Hz, 1H), 1.90–1.76 (m, 3H), 1.76–1.55 (m, 4H), 1.29 (s, 9H), 1.21–1.80 (m, 3H), 1.02 (d, *J* = 6.5 Hz, 3H).

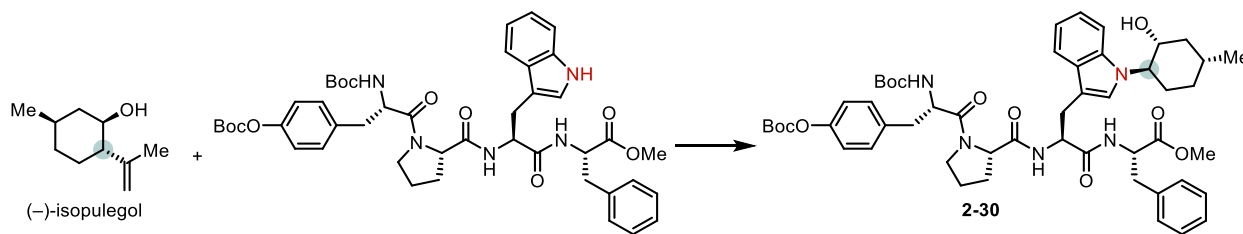
¹³C NMR (100 MHz, CDCl₃) δ 172.40, 172.02, 170.46, 155.64, 137.32, 136.62, 129.17, 128.50, 127.73, 126.85, 123.28, 121.56, 119.13, 118.55, 110.04, 109.13, 80.79, 72.44, 61.81, 60.30, 53.40, 52.86, 52.37, 46.93, 42.49, 36.68, 34.00, 31.36, 31.20, 30.29, 28.66, 28.21, 27.55, 27.03, 24.29, 23.20, 21.96.

HRMS (DART): [M+H]⁺ calcd for [C₃₈H₅₁N₄O₇]⁺ *m/z* 675.3752, found 675.3763.

IR (neat, ATR): ν_{\max} 3310 (br), 2952, 2926, 2853, 1743, 1670, 1522, 1463, 1401, 1366, 1248, 1215, 1163, 1128, 756 cm⁻¹.

Optical Rotation: $[\alpha]_{\text{D}}^{25} = -20.39$ (*c* 0.2, CHCl₃).

M.p.: 101–132 °C.



Prepared following **General procedure A** using the peptide **2-89** (165 mg, 0.200 mmol, 1.0 equiv), tetrakis(acetonitrile)copper(I) tetrafluoroborate (18.9 mg, 0.0600 mmol, 30 mol %), 1,10-phenanthroline (10.8 mg, 0.0600 mmol, 30 mol %), and MeCN (5 mL) to make *Solution A* and (-)-isopulegol (154 mg, 1.00 mmol, 5.0 equiv) and MeCN (5 mL) to make *Solution B*. The crude

product was purified through FCC to give **2-30** ($R_f = 0.46$; EtOAc/hexanes, 7:3) as a fine white solid (149.5 mg, 80% yield).

$^1\text{H NMR}$ (400 MHz, CD_3OD) δ 7.63–7.48 (m, 1H), 7.45–7.35 (m, 1H), 7.29–6.93 (m, 12H), 4.69–4.32 (m, 4H), 4.12–3.90 (m, 2H), 3.67–3.47 (m, 4H), 3.27–2.88 (m, 5H), 2.87–2.55 (m, 2H), 2.16–1.57 (m, 9H), 1.54–1.40 (m, 11H), 1.39–1.11 (m, 11H), 1.01 (d, $J = 6.0$ Hz, 3H).

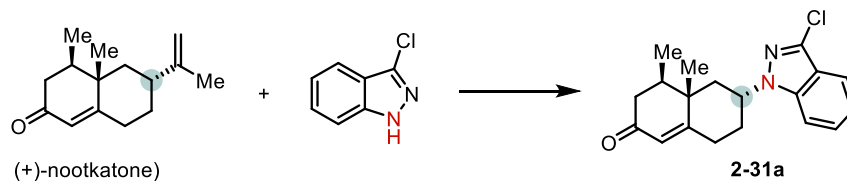
$^{13}\text{C NMR}$ (125 MHz, CD_3OD) δ 173.79, 173.65, 173.33, 173.18, 173.11, 172.89, 157.65, 157.45, 153.39, 151.77, 151.37, 138.77, 138.67, 137.91, 137.86, 135.84, 134.98, 131.61, 130.34, 130.31, 129.49, 129.48, 129.25, 127.88, 124.75, 124.55, 122.69, 122.34, 122.13, 120.09, 119.89, 119.53, 111.08, 110.97, 110.92, 110.75, 84.28, 84.14, 80.77, 80.65, 73.28, 62.49, 62.33, 61.66, 61.44, 56.77, 55.42, 55.34, 55.24, 55.01, 52.69, 44.48, 44.20, 39.18, 38.75, 38.48, 37.94, 35.01, 34.95, 32.87, 32.66, 32.52, 30.01, 29.04, 28.83, 28.68, 27.91, 25.93, 22.44, 22.38, 22.31.

HRMS (DART): $[\text{M}-\text{Boc}+2\text{H}]^+$ calcd for $[\text{C}_{47}\text{H}_{60}\text{N}_5\text{O}_9]^+$ m/z 838.4386, found 838.4356.

IR (neat, ATR): ν_{max} 3347 (br), 2952, 2933, 2861, 1757, 1651, 1512, 1449, 1368, 1273, 1256, 1150 cm^{-1} .

Optical Rotation: $[\alpha]_{\text{D}}^{26} = -10.00$ (c 0.2, MeOH).

M.p.: 119–130 °C.



Prepared following **General procedure B** using 3-chloro-1H-indazole (30.5 mg, 0.200 mmol, 1.0 equiv), copper(I) chloride (4.00 mg, 0.0400 mmol, 20 mol %), 1,10-phenanthroline (7.20 mg, 0.0400 mmol, 20 mol %), and MeCN (2 mL) to make *Solution A*. (+)-Nootkatone (87.3 mg, 0.400

mmol, 2.0 equiv) was used for ozonolysis and MeCN (2 mL) was used to make *Suspension B*. The crude product was purified through FCC to give **2-31a** ($R_f = 0.34$; hexanes/EtOAc, 2:1) as a colorless oil (54.4 mg, 83% yield).

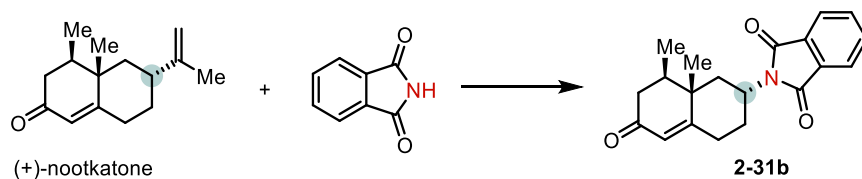
^1H NMR (400 MHz, CDCl_3) δ 7.67 (d, $J = 8.1$ Hz, 1H), 7.44 (d, $J = 3.5$ Hz, 2H), 7.34 (s, 1H), 7.21 (dt, $J = 7.9, 3.9$ Hz, 1H), 5.85 (d, $J = 1.4$ Hz, 1H), 4.87–4.69 (m, 1H), 2.76–2.67 (m, 1H), 2.55 (dt, $J = 15.5, 3.4$ Hz, 1H), 2.32–2.17 (m, 5H), 2.16–2.08 (m, 1H), 2.01 (t, $J = 12.8$ Hz, 1H), 1.26 (s, 3H), 0.93 (d, $J = 6.7$ Hz, 3H).

^{13}C NMR (100 MHz, CDCl_3) δ 199.05, 167.03, 140.10, 132.92, 128.33, 127.46, 125.56, 121.44, 121.15, 120.04, 109.04, 54.15, 43.59, 41.66, 40.25, 39.76, 31.83, 31.81, 16.99, 14.89.

HRMS (ESI-TOF): $[\text{M}+\text{H}]^+$ calcd for $[\text{C}_{19}\text{H}_{22}\text{ClN}_2\text{O}]^+$ m/z 329.1415, found 329.1425.

IR (neat, ATR): ν_{max} 2966, 2942, 2876, 1664, 1617, 1494, 1465, 1337, 1206, 983, 765, 745 cm^{-1} .

Optical Rotation: $[\alpha]_{\text{D}}^{25} = 48.1$ (c 1.0, CHCl_3).



Prepared following **General procedure A** using phthalimide (368 mg, 2.50 mmol, 1.0 equiv), copper(I) chloride (49.5 mg, 0.500 mmol, 20 mol %), 1,10-phenanthroline (90.1 mg, 0.500 mmol, 20 mol %), and MeCN (25 mL) to make *Solution A*. (+)-Nootkatone (1.09 g, 5.00 mmol, 2.0 equiv) was used for ozonolysis and MeCN (50 mL) was used to make *Solution B*. The crude product was purified through FCC to give **2-31b** ($R_f = 0.34$; toluene/Et₂O, 3:1) as a yellow oil (638 mg, 79% yield).

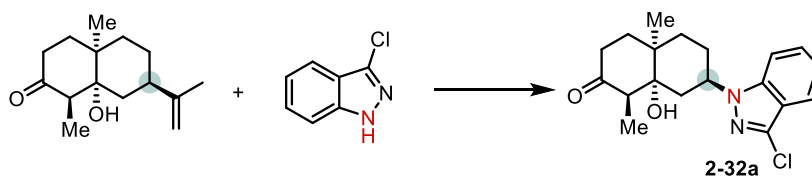
¹H NMR (600 MHz, CDCl₃) δ 7.94–7.76 (m, 2H), 7.76–7.60 (m, 2H), 5.83 (s, 1H), 4.58 (tt, *J* = 12.6, 3.4 Hz, 1H), 3.57–3.41 (m, 1H), 2.63 (td, *J* = 14.7, 4.4 Hz, 1H), 2.55–2.40 (m, 2H), 2.32–2.18 (m, 3H), 2.18–2.09 (m, 1H), 1.98–1.86 (m, 2H), 1.24–1.15 (m, 4H), 0.94 (d, *J* = 6.6 Hz, 3H).

¹³C NMR (100 MHz, CDCl₃) δ 199.11, 168.23, 167.49, 134.04, 131.84, 125.41, 123.19, 46.66, 41.67, 40.84, 40.25, 39.83, 32.19, 29.16, 16.67, 14.84.

HRMS (DART): [M+H]⁺ calcd for [C₂₀H₂₂NO₃]⁺ *m/z* 324.1594, found 324.1588.

IR (neat, ATR): ν_{\max} 2965, 2940, 2881, 1768, 1708, 1664, 1615, 1375, 1288, 1081, 979, 722 cm⁻¹.

Optical Rotation: $[\alpha]_{\text{D}}^{25} = 46.50$ (*c* 0.2, CH₂Cl₂).



Prepared following **General procedure A** using 3-chloro-1*H*-indazole (30.5 mg, 0.200 mmol, 1.0 equiv), copper(I) chloride (4.00 mg, 0.0400 mmol, 20 mol %), 1,10-phenanthroline (7.20 mg, 0.0400 mmol, 20 mol %), and MeCN (2 mL) to make *Solution A*. The alkene **2-90** (94.5 mg, 0.400 mmol, 2.0 equiv) was used for ozonolysis and MeCN (2 mL) was used to make *Solution B*. The crude product was purified through FCC to give **2-32a** (*R*_f = 0.28; hexanes/EtOAc, 2:1) as a white solid (50.8 mg, 73% yield).

¹H NMR (400 MHz, CDCl₃) δ 7.64 (dt, *J* = 8.2, 1.0 Hz, 1H), 7.45–7.31 (m, 2H), 7.17 (ddd, *J* = 8.0, 6.1, 1.6 Hz, 1H), 4.79 (dddd, *J* = 12.1, 10.6, 6.1, 4.5 Hz, 1H), 2.81 (q, *J* = 6.6 Hz, 1H), 2.67–2.51 (m, 1H), 2.46–2.32 (m, 2H), 2.27 (td, *J* = 12.9, 3.9 Hz, 1H), 2.11 (td, *J* = 14.0, 4.0 Hz, 1H), 1.92–1.80 (m, 3H), 1.50–1.59 (m, 2H), 1.30 (s, 3H), 1.00 (d, *J* = 6.7 Hz, 3H).

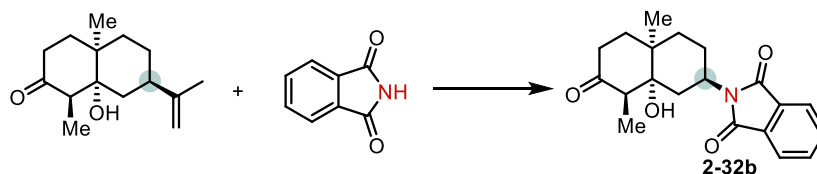
^{13}C NMR (100 MHz, CDCl_3) δ 209.31, 140.15, 132.66, 127.19, 121.21, 120.93, 119.81, 109.21, 78.72, 54.07, 51.94, 37.50, 34.58, 34.52, 31.32, 26.89, 21.32, 6.57.

HRMS (ESI-TOF): $[\text{M}+\text{H}]^+$ calcd for $[\text{C}_{19}\text{H}_{24}\text{ClN}_2\text{O}_2]^+$ m/z 347.1521, found 347.1532.

IR (neat, ATR): ν_{max} 3432(br), 2990, 2976, 2958, 2949, 2929, 2912, 1709, 1619, 1496, 1462, 1338, 1202, 1190, 1146, 1054, 988, 772, 766, 743 cm^{-1} .

Optical Rotation: $[\alpha]_{\text{D}}^{25} = 15.70$ (c 1.0, CHCl_3).

M.p.: 207 $^{\circ}\text{C}$ (decomposition)



Prepared following **General procedure A** using phthalimide (147 mg, 1.00 mmol, 1.0 equiv), copper(I) chloride (19.8 mg, 0.200 mmol, 20 mol %), 1,10-phenanthroline (36.0 mg, 0.200 mmol, 20 mol %), and MeCN (10 mL) to make *Solution A*. The alkene **2-90** (473 mg, 2.00 mmol, 2.0 equiv) was used for ozonolysis and MeCN (10 mL) was used to make *Solution B*. The crude product was purified through FCC to give **2-32b** ($R_f = 0.27$; hexanes/EtOAc, 2:1) as a white solid (290.2 mg, 85% yield).

^1H NMR (400 MHz, CDCl_3) δ 7.82–7.73 (m, 2H), 7.73–7.63 (m, 2H), 4.53 (tt, $J = 12.7, 4.6$ Hz, 1H), 2.83 (q, $J = 6.6$ Hz, 1H), 2.65–2.32 (m, 4H), 2.19–1.98 (m, 2H), 1.91 (s, 1H), 1.63–1.41 (m, 4H), 1.26 (s, 3H), 1.00 (d, $J = 6.6$ Hz, 3H).

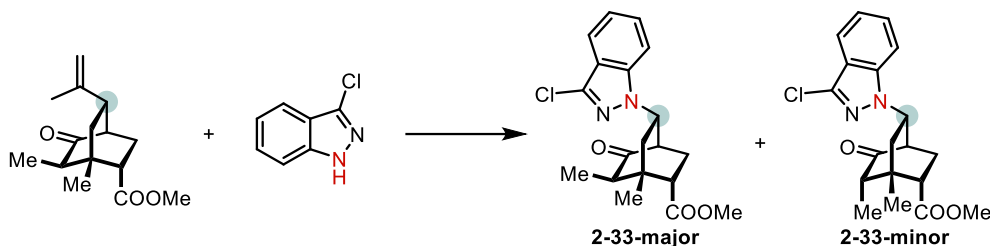
^{13}C NMR (100 MHz, CDCl_3) δ 209.80, 168.32, 133.91, 131.92, 123.10, 78.37, 51.87, 46.36, 37.51, 37.31, 34.49, 31.88, 31.23, 23.68, 21.22, 6.56.

HRMS (DART): $[\text{M}+\text{H}]^+$ calcd for $[\text{C}_{20}\text{H}_{24}\text{NO}_4]^+$ m/z 342.1700, found 342.1708.

IR (neat, ATR): ν_{\max} 3531 (brs), 2934, 2926, 2878, 2857, 1769, 1705, 1467, 1397, 1376, 1096, 991, 882, cm^{-1} .

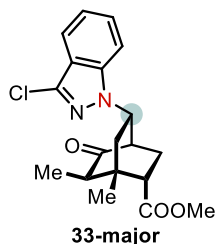
Optical Rotation: $[\alpha]_{\text{D}}^{24} = 14.50$ (c 0.1, CHCl_3).

M.p.: 232–234 °C.



Prepared following **General procedure A** using 3-chloro-1H-indazole (61.0 mg, 0.400 mmol, 1.0 equiv), copper(I) chloride (11.9 mg, 0.120 mmol, 30 mol %), 1,10-phenanthroline (21.6 mg, 0.120 mmol, 30 mol %), and MeCN (4 mL) to make *Solution A*. The alkene **2-91** (300 mg, 1.20 mmol, 3 equiv) was used for ozonolysis and MeCN (6 mL) was used to make *Solution B*. The crude product was purified through FCC to give **2-33-major** ($R_f = 0.55$; hexanes/ Et_2O , 1:4) as a white solid (58.2 mg, 40% yield) and **2-33-minor** ($R_f = 0.50$; hexanes/ Et_2O , 1:4) as a colorless oil (11.6 mg, 8.0% yield).

Note: 2-35-minor arose from impure 2-91. The alkene 2-91 could not be prepared in pure form. The literature procedure⁵⁷ also mentions not being able to separate the diastereoisomers.



¹H NMR (400 MHz, CDCl₃) δ 7.63 (d, *J* = 8.2 Hz, 1H), 7.40 (ddd, *J* = 8.0, 6.9, 0.9 Hz, 1H), 7.31 (d, *J* = 8.5 Hz, 1H), 7.23–7.14 (m, 1H), 4.89 (ddd, *J* = 10.6, 6.5, 2.2 Hz, 1H), 3.73 (s, 3H), 2.86 (qd, *J* = 7.3, 2.0 Hz, 1H), 2.81–2.73 (m, 2H), 2.54 (dt, *J* = 3.5, 2.3 Hz, 1H), 2.33–2.17 (m, 2H), 1.96 (ddd, *J* = 14.2, 10.7, 2.2 Hz, 1H), 1.33 (d, *J* = 7.4 Hz, 3H), 1.06 (s, 3H).

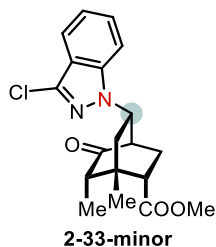
¹³C NMR (100 MHz, CDCl₃) δ 213.50, 174.76, 140.39, 133.20, 127.45, 121.77, 121.54, 120.15, 108.77, 56.28, 51.88, 48.20, 46.63, 45.67, 38.38, 34.88, 26.35, 22.10, 9.52.

HRMS (DART): [M+H]⁺ calcd for [C₁₉H₂₂ClN₂O₃]⁺ *m/z* 361.1313, found 361.1314.

IR (neat, ATR): ν_{max} 2947, 2879, 1616, 1466, 1365, 1337, 1169, 1061, 1033, 765, 747 cm⁻¹.

Optical Rotation: [α]_D²⁴ = -1.00 (*c* 0.2, CHCl₃).

M.p.: 142–144 °C.



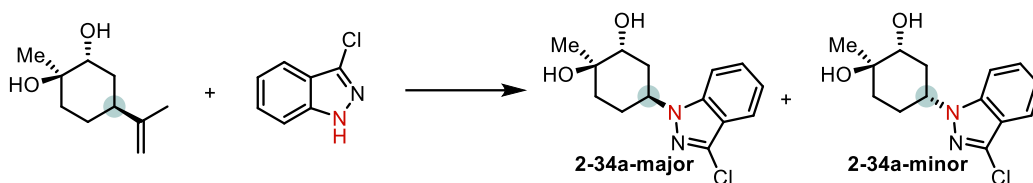
¹H NMR (400 MHz, CDCl₃) δ 7.65 (dt, *J* = 8.2, 0.9 Hz, 1H), 7.42 (ddd, *J* = 8.4, 6.8, 1.1 Hz, 1H), 7.34 (d, *J* = 8.6 Hz, 1H), 7.20 (ddd, *J* = 7.8, 6.8, 0.9 Hz, 1H), 4.93 (ddd, *J* = 10.9, 4.8, 2.7 Hz, 1H), 3.73 (s, 3H), 2.74 (q, *J* = 7.5 Hz, 1H), 2.65 (q, *J* = 2.9 Hz, 1H), 2.63–2.59 (m, 1H), 2.55 (ddd, *J* = 14.4, 6.7, 2.9 Hz, 1H), 2.48 (dd, *J* = 14.3, 4.9 Hz, 1H), 2.31 (dd, *J* = 14.2, 10.9 Hz, 1H), 2.20 (ddd, *J* = 14.0, 10.3, 3.3 Hz, 1H), 1.27 (s, 3H), 1.15 (d, *J* = 7.6 Hz, 3H).

¹³C NMR (100 MHz, CDCl₃) δ 212.78, 174.31, 140.50, 133.44, 127.57, 121.62, 121.57, 120.16, 108.75, 54.84, 51.98, 51.48, 47.91, 44.53, 43.82, 39.80, 26.93, 23.01, 10.41.

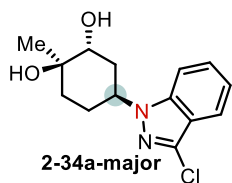
HRMS (DART): [M+H]⁺ calcd for [C₁₉H₂₂ClN₂O₃]⁺ *m/z* 361.1313, found 361.1313.

IR (neat, ATR): ν_{\max} 2950, 1731, 1616, 1494, 1465, 1339, 1203, 1176, 1021, 761, 748 cm^{-1} .

Optical Rotation: $[\alpha]_{\text{D}}^{25} = 1.00$ (c 0.1, CHCl_3).



Prepared following **General procedure A** using 3-chloro-1H-indazole (30.5 mg, 0.200 mmol, 1.0 equiv), copper(I) chloride (4.00 mg, 0.0400 mmol, 20 mol %), 1,10-phenanthroline (7.20 mg, 0.0400 mmol, 20 mol %), and MeCN (2 mL) to make *Solution A*. The alkene **2-92** (68.1 mg, 0.400 mmol, 2.0 equiv) was used for ozonolysis and MeCN (2 mL) was used to make *Solution B*. The crude product was purified through FCC to give **2-34a-major** ($R_f = 0.68$; EtOAc) with impurity and **2-34a-minor** ($R_f = 0.29$; EtOAc) as a white solid (14.4 mg, 26% yield). The impure material of **2-34a-major** was purified again through FCC to give pure **2-34a-major** ($R_f = 0.51$; DCM/MeOH, 50:3) as a white solid (26.0 mg, 46% yield).



$^1\text{H NMR}$ (400 MHz, CDCl_3) δ 7.69–7.61 (m, 1H), 7.47 (d, $J = 8.6$ Hz, 1H), 7.42–7.35 (m, 1H), 7.21–7.14 (m, 1H), 4.84 (tt, $J = 11.4, 4.1$ Hz, 1H), 3.92 (s, 1H), 2.74 (ddd, $J = 14.1, 11.6, 2.8$ Hz, 1H), 2.37 (qd, $J = 12.9, 4.1$ Hz, 1H), 2.11 (brs, 1H), 2.08–1.94 (m, 4H), 1.91–1.80 (m, 1H), 1.74 (ddd, $J = 11.2, 3.8, 1.9$ Hz, 1H), 1.37 (s, 3H).

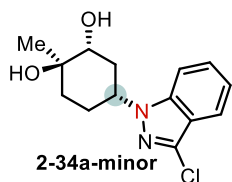
$^{13}\text{C NMR}$ (100 MHz, CDCl_3) δ 140.21, 132.36, 127.18, 121.20, 120.99, 119.79, 109.58, 77.35, 77.03, 76.72, 74.11, 70.76, 52.62, 34.80, 32.80, 27.22, 26.37.

HRMS (DART): $[M+H]^+$ calcd for $[C_{14}H_{18}ClN_2O_2]^+$ m/z 281.1051, found 281.1051.

IR (neat, ATR): ν_{\max} 3401 (br), 2965, 2932, 1618, 1496, 1466, 1340, 1198, 1046, 1033, 871, 766, 743 cm^{-1} .

Optical Rotation: $[\alpha]_D^{24} = -4.33$ (c 0.1, CHCl_3).

M.p.: 158–160 $^{\circ}\text{C}$.



^1H NMR (400 MHz, CDCl_3) δ 7.67 (d, $J = 8.2$ Hz, 1H), 7.49–7.34 (m, 2H), 7.20 (ddd, $J = 7.8$, 6.4, 1.2 Hz, 1H), 4.56 (tt, $J = 10.2$, 4.7 Hz, 1H), 3.73 (dd, $J = 10.6$, 4.6 Hz, 1H), 2.41 (brs, 2H), 2.29 (dt, $J = 12.8$, 3.8 Hz, 1H), 2.25–2.15 (m, 1H), 2.15–1.97 (m, 2H), 1.92 (dt, $J = 13.5$, 4.2 Hz, 1H), 1.61 (td, $J = 13.0$, 4.4 Hz, 1H), 1.38 (s, 3H).

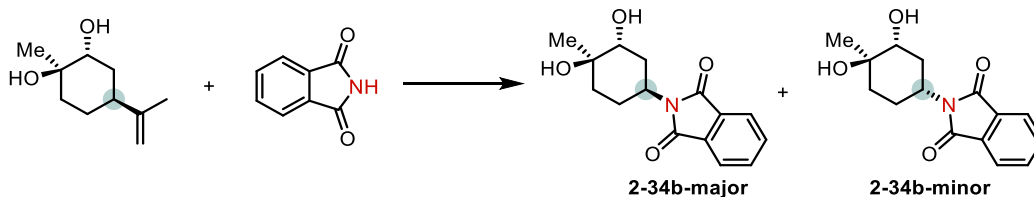
^{13}C NMR (100 MHz, CDCl_3) δ 140.05, 132.65, 127.51, 121.42, 121.07, 119.98, 109.19, 75.01, 73.27, 55.58, 35.83, 35.29, 28.88, 20.35.

HRMS (ESI-TOF): $[M+H]^+$ calcd for $[C_{14}H_{18}ClN_2O_2]^+$ m/z 281.1051, found 281.1051.

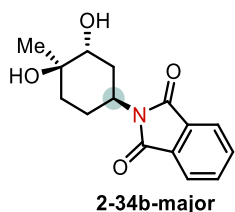
IR (neat, ATR): ν_{\max} 3393 (br), 2978, 2943, 2871, 1618, 1494, 1465, 1338, 1196, 1143, 1130, 1093, 1071, 994, 767, 743 cm^{-1} .

Optical Rotation: $[\alpha]_D^{24} = -3.00$ (c 0.1, CHCl_3).

M.p.: 164–166 $^{\circ}\text{C}$.



Prepared following **General procedure A** using phthalimide (147 mg, 1.00 mmol, 1.0 equiv), copper(I) chloride (19.8 mg, 0.200 mmol, 20 mol %), 1,10-phenanthroline (36.0 mg, 0.200 mmol, 20 mol %), and MeCN (10 mL) to make *Solution A*. The alkene **2-92** (681 mg, 4.00 mmol, 4.0 equiv) was used for ozonolysis and MeCN (10 mL) was used to make *Solution B*. The crude product was purified through FCC (1% MeOH/DCM) to remove most of the impurity. The mixture was purified again through FCC to afford **2-34b-major** ($R_f = 0.56$; EtOAc/hexanes, 1:1) as a white solid (136.0 mg, 53% yield) and **2-34b-minor** ($R_f = 0.23$; EtOAc/hexanes, 1:1) as a white solid (61.8 mg, 23% yield).



$^1\text{H NMR}$ (500 MHz, CDCl_3) δ 7.85–7.78 (m, 2H), 7.73–7.66 (m, 2H), 4.56 (tt, $J = 12.6, 4.1$ Hz, 1H), 3.77 (s, 1H), 2.95 (td, $J = 13.3, 2.7$ Hz, 1H), 2.61–2.45 (m, 1H), 1.96 (td, $J = 13.8, 4.0$ Hz, 1H), 1.74–1.65 (m, 2H), 1.65–1.55 (m, 3H), 1.32 (s, 3H).

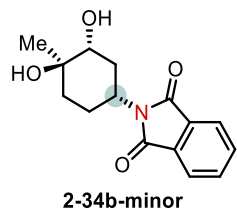
$^{13}\text{C NMR}$ (125 MHz, CDCl_3) δ 168.43, 133.83, 132.02, 123.08, 74.16, 70.28, 44.57, 32.73, 32.25, 27.02, 24.46.

HRMS (DART): $[\text{M}+\text{H}]^+$ calcd for $[\text{C}_{15}\text{H}_{18}\text{NO}_4]^+$ m/z 276.1230, found 276.1232.

IR (neat, ATR): ν_{max} 3441 (br), 2956, 2926, 2852, 1768, 1707, 1398, 1377, 1088, 884, 718 cm^{-1} .

Optical Rotation: $[\alpha]_{\text{D}}^{26} = -14.00$ (c 0.2, MeOH).

M.p.: 231–234 $^{\circ}\text{C}$.



¹H NMR (500 MHz, CDCl₃) δ 7.86–7.78 (m, 2H), 7.76–7.67 (m, 2H), 4.29 (tt, *J* = 12.6, 4.6 Hz, 1H), 3.62 (dd, *J* = 12.0, 4.5 Hz, 1H), 2.46–2.28 (m, 2H), 2.17 (s, 1H), 2.20–1.89 (m, 2H), 1.85 (dt, *J* = 13.2, 3.5 Hz, 1H), 1.66 (dtd, *J* = 13.4, 4.3, 2.2 Hz, 1H), 1.55 (td, *J* = 13.6, 4.1 Hz, 1H), 1.37 (s, 3H).

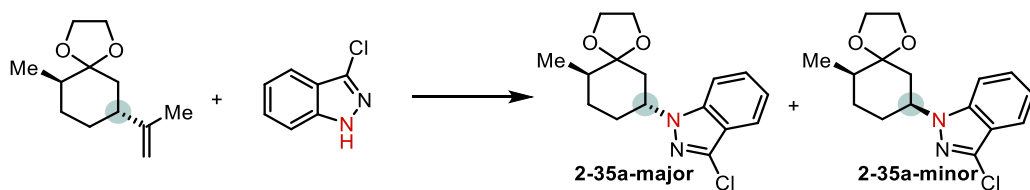
¹³C NMR (125 MHz, CDCl₃) δ 168.14, 134.02, 131.85, 123.22, 75.74, 73.38, 47.85, 36.63, 33.65, 26.40, 18.83.

HRMS (DART): [M+H]⁺ calcd for [C₁₅H₁₈NO₄]⁺ *m/z* 276.1230, found 276.1233.

IR (neat, ATR): ν_{max} 3405 (brs), 2925, 2852, 1762, 1709, 1467, 1379, 1113, 1974, 1045, 719 cm⁻¹.

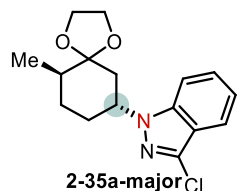
Optical Rotation: [α]_D²⁵ = -0.94 (*c* 0.2, CHCl₃)

M.p.: 232–234 °C.



Prepared following **General procedure A** using 3-chloro-1*H*-indazole (61.0 mg, 0.400 mmol, 1.0 equiv), copper(I) chloride (7.90 mg, 0.0800 mmol, 20 mol %), 1,10-phenanthroline (14.4 mg, 0.0800 mmol, 20 mol %), and MeCN (4 mL) to make *Solution A*. The alkene **2-93** (157 mg, 0.800 mmol, 2.0 equiv) was used for ozonolysis and MeCN (4 mL) was used to make *Solution B*. The

crude product was purified through FCC to give **2-35a-major** ($R_f = 0.46$; hexanes/Et₂O, 5:1) as a white solid (69.8 mg, 57% yield) and **2-35a-minor** ($R_f = 0.38$; hexanes/Et₂O, 5:1) as a colorless oil (33.5 mg, 27% yield).



¹H NMR (400 MHz, CDCl₃) δ 7.65 (dt, $J = 8.2, 1.0$ Hz, 1H), 7.41 (tdd, $J = 8.6, 6.8, 1.0$ Hz, 2H), 7.22–7.13 (m, 1H), 4.66–4.54 (m, 1H), 4.05–3.91 (m, 4H), 2.22 (t, $J = 12.4$ Hz, 1H), 2.16–2.08 (m, 1H), 2.08–1.97 (m, 2H), 1.94–1.77 (m, 2H), 1.60–1.46 (m, 1H), 0.94 (d, $J = 6.5$ Hz, 3H).

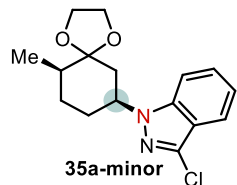
¹³C NMR (100 MHz, CDCl₃) δ 140.07, 132.54, 127.17, 121.18, 120.95, 119.79, 110.17, 109.31, 65.51, 65.09, 56.12, 41.17, 39.00, 31.64, 30.09, 13.55.

HRMS (DART): $[M+H]^+$ calcd for $[C_{16}H_{20}ClN_2O_2]^+$ m/z 307.1208 found 307.1208.

IR (neat, ATR): ν_{max} 2975, 2963, 2934, 2884, 1616, 1494, 1466, 1337, 1173, 1161, 1094, 1023, 987, 944, 925, 767, 744 cm⁻¹.

Optical Rotation: $[\alpha]_D^{24} = -3.00$ (c 0.2, CHCl₃)

M.p.: 107–110 °C.



¹H NMR (400 MHz, CDCl₃) δ 7.66 (d, $J = 8.2$ Hz, 1H), 7.49–7.36 (m, 2H), 7.18 (ddd, $J = 7.9, 6.5, 1.1$ Hz, 1H), 4.64 (tt, $J = 12.3, 4.1$ Hz, 1H), 4.05–3.88 (m, 4H), 2.46 (t, $J = 12.6$ Hz, 1H), 2.19

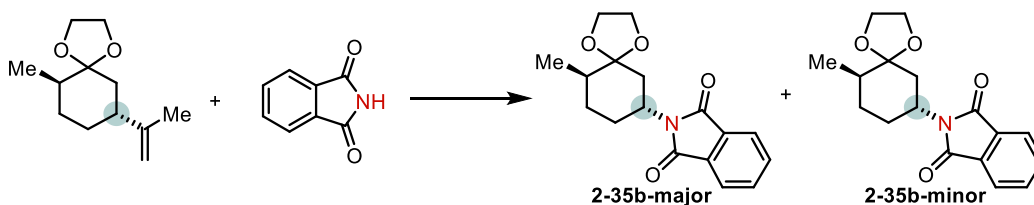
(qd, $J = 12.9, 4.0$ Hz, 1H), 2.05–1.85 (m, 3H), 1.85–1.75 (m, 1H), 1.71–1.63 (m, 1H), 1.16 (d, $J = 7.2$ Hz, 3H).

^{13}C NMR (100 MHz, CDCl_3) δ 140.09, 132.52, 127.14, 121.16, 120.96, 119.78, 111.23, 109.33, 64.47, 64.46, 56.15, 35.94, 35.63, 27.84, 25.73, 14.58.

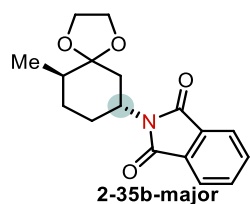
HRMS (DART): $[\text{M}+\text{H}]^+$ calcd for $[\text{C}_{16}\text{H}_{20}\text{ClN}_2\text{O}_2]^+$ m/z 307.1208 found 307.1208.

IR (neat, ATR): ν_{max} 2965, 2935, 2878, 1616, 1495, 1466, 1339, 1195, 1171, 1153, 1098, 1032, 1006, 957, 846, 766, 744 cm^{-1} .

Optical Rotation: $[\alpha]_{\text{D}}^{25} = -6.48$ (c 0.1, CHCl_3)



Prepared following **General procedure A** using phthalimide (294 mg, 2.00 mmol, 1.0 equiv), copper(I) chloride (39.6 mg, 0.400 mmol, 20 mol %), 1,10-phenanthroline (72.1 mg, 0.400 mmol, 20 mol %), and MeCN (20 mL) to make *Solution A*. The alkene **2-93** (785 mg, 4.00 mmol, 2.0 equiv) was used for ozonolysis and MeCN (20 mL) to make *Solution B*. The crude product was purified through FCC to give **2-35b-major** ($R_f = 0.24$; hexanes/EtOAc, 4:1) as a white solid (531.4 mg, 88% yield, 4.1:1 *d.r.* determined by NMR). Pure **2-35b-major** was obtained through recrystallization (DCM/hexanes). The mother liquor was concentrated *in vacuo*. Repeating the recrystallization afforded another fraction of pure **2-35b-major**. This mother liquor was concentrated *in vacuo* to afford a 1:1 mixture of **2-35b-major** and **2-35b-minor**.



¹H NMR (400 MHz, CD₃CN) δ 7.82–7.67 (m, 4H), 4.24 (tt, *J* = 12.7, 3.9 Hz, 1H), 3.99–3.83 (m, 4H), 2.26 (t, *J* = 12.7 Hz, 1H), 2.21–2.10 (m, 1H), 1.88 (ddd, *J* = 12.5, 3.9, 2.0 Hz, 1H), 1.83–1.66 (m, 3H), 1.43–1.29 (m, 1H), 0.86 (d, *J* = 6.5 Hz, 3H).

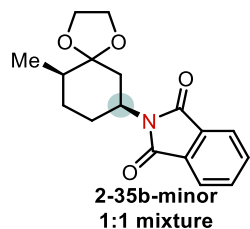
¹³C NMR (100 MHz, CD₃CN) δ 169.17, 135.02, 133.02, 123.65, 110.72, 66.20, 65.79, 49.27, 39.87, 39.28, 31.18, 29.64, 13.93.

HRMS (DART): [M+H]⁺ calcd for [C₁₇H₂₀NO₄]⁺ *m/z* 302.1387 found 302.1384.

IR (neat, ATR): ν_{max} 2976, 2920, 2881, 1710, 1376, 1236, 1089, 1887 cm⁻¹.

Optical Rotation: [α]_D²⁵ = -3.00 (*c* 0.2, CH₂Cl₂).

M.p.: 157–159 °C.



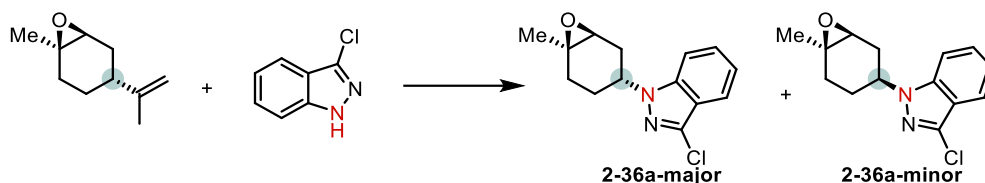
¹H NMR (500 MHz, CDCl₃) δ 7.87–7.76 (m, 0.5×2H), 7.74–7.61 (m, 0.5×2H), 4.47–4.34 (m, 0.5×1H), 4.05–3.86 (m, 0.5×4H), 2.69 (t, *J* = 12.7 Hz, 0.5×1H), 2.37 (qd, *J* = 13.0, 4.2 Hz, 0.5×1H), 1.94–1.80 (m, 0.5×2H), 1.63–1.55 (m, 0.5×2H), 1.16 (d, *J* = 7.2 Hz, 0.5×3H).

¹³C NMR (125 MHz, CDCl₃) δ 168.32, 133.92, 132.07, 123.13, 111.17, 64.47, 64.46, 48.32, 35.67, 32.96, 27.96, 22.77, 14.51.

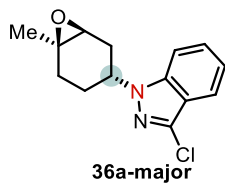
HRMS (DART): [M+H]⁺ calcd for [C₁₇H₂₀NO₄]⁺ *m/z* 302.1387 found 302.1386.

IR (neat, ATR): ν_{\max} 2975, 2940, 2881, 1709, 1372, 1173, 1118, 1030 cm^{-1} .

Optical Rotation: $[\alpha]_{\text{D}}^{27} = -0.65$ (c 0.31, CH_2Cl_2).



Prepared following **General procedure A** using 3-chloro-1*H*-indazole (76.3 mg, 0.500 mmol, 1.0 equiv), copper(I) chloride (9.90 mg, 0.100 mmol, 20 mol %), 1,10-phenanthroline (18.0 mg, 0.100 mmol, 20 mol %), and MeCN (5 mL) to make *Solution A*. The alkene **2-94** (152 mg, 1.00 mmol, 2.0 equiv) was used for ozonolysis and MeCN (5 mL) to make *Solution B*. The crude product was purified through FCC to give **2-36a-major** ($R_f = 0.57$; CHCl_3) as a white solid (88.1 mg, 67% yield) and **2-36a-minor** ($R_f = 0.40$; CHCl_3) as a white solid (22.0 mg, 17 % yield).



^1H NMR (400 MHz, CDCl_3) δ 7.65 (d, $J = 8.2$ Hz, 1H), 7.44–7.32 (m, 2H), 7.18 (ddd, $J = 7.9$, 5.6, 2.1 Hz, 1H), 4.63 (dddd, $J = 9.8$, 8.3, 5.2, 2.8 Hz, 1H), 3.26 (s, 1H), 2.57 (ddd, $J = 14.9$, 8.6, 2.5 Hz, 1H), 2.46 (dd, $J = 14.8$, 5.2 Hz, 1H), 2.10–1.91 (m, 2H), 1.91–1.82 (m, 1H), 1.82–1.74 (m, 1H), 1.38 (s, 3H).

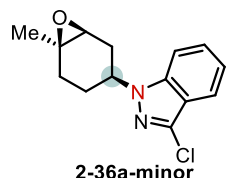
^{13}C NMR (100 MHz, CDCl_3) δ 140.29, 132.52, 127.27, 121.27, 121.06, 119.78, 109.30, 60.50, 57.41, 51.41, 30.91, 27.76, 26.91, 23.85.

HRMS (ESI-TOF): $[\text{M}+\text{H}]^+$ calcd for $[\text{C}_{14}\text{H}_{16}\text{ClN}_2\text{O}]^+$ m/z 263.0946, found 263.0950.

IR (neat, ATR): ν_{\max} 3062, 2978, 2956, 2924, 2861, 1616, 1493, 1465, 1379, 1336, 1210, 1192, 1174, 1128, 1971, 1040, 1033, 1018, 1006, 985, 961, 849, 832, 743 cm^{-1} .

Optical Rotation: $[\alpha]_{\text{D}}^{23} = -7.33$ (c 0.1, CHCl_3)

M.p.: 75–77 °C.



^1H NMR (400 MHz, CDCl_3) δ 7.65 (d, $J = 8.2$ Hz, 1H), 7.45–7.32 (m, 2H), 7.18 (ddd, $J = 8.0$, 5.4, 2.3 Hz, 1H), 4.47–4.31 (m, 1H), 3.07 (d, $J = 5.1$ Hz, 1H), 2.56 (dd, $J = 15.3$, 11.2 Hz, 1H), 2.37 (dddd, $J = 15.2$, 6.9, 5.2, 1.7 Hz, 1H), 2.33–2.17 (m, 2H), 2.01–1.89 (m, 1H), 1.74–1.65 (m, 1H), 1.40 (s, 3H).

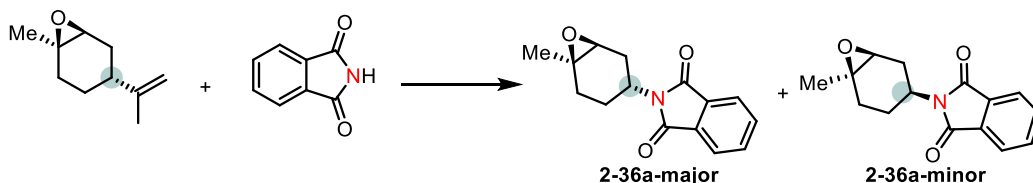
^{13}C NMR (100 MHz, CDCl_3) δ 139.92, 132.59, 127.21, 121.38, 121.23, 119.97, 109.42, 58.14, 57.21, 54.79, 29.96, 29.94, 25.45, 22.75.

HRMS (ESI-TOF): $[\text{M}+\text{H}]^+$ calcd for $[\text{C}_{14}\text{H}_{16}\text{ClN}_2\text{O}]^+$ m/z 263.0946, found 263.0945.

IR (neat, ATR): ν_{\max} 3059, 2978, 2960, 2923, 2862, 1616, 1494, 1466, 1435, 1380, 1337, 1233, 1212, 1194, 1129, 1023, 1006, 985, 839, 769, 744 cm^{-1} .

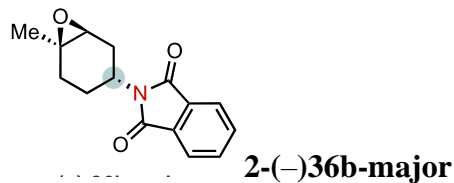
Optical Rotation: $[\alpha]_{\text{D}}^{24} = -11.00$ (c 0.2, CHCl_3)

M.p.: 82–84 °C.



Prepared following **General procedure A** using phthalimide (368 mg, 2.50 mmol, 1.0 equiv), copper(I) chloride (49.5 mg, 0.500 mmol, 20 mol %), 1,10-phenanthroline (90.1 mg, 0.500 mmol,

20 mol %), and MeCN (25 mL) to make *Solution A*. The alkene (+)-**2-94** (761 mg, 5.00 mmol, 2.0 equiv) was used for ozonolysis and MeCN (25 mL) to make *Solution B*. The crude product was purified through FCC to give **2-(-)-36b-major** ($R_f = 0.55$; EtOAc/hexanes, 1:2) as a white solid (357.2 mg, 55% yield) and **2-(-)-36b-minor** ($R_f = 0.51$; EtOAc/hexanes, 1:2) as a white solid (175.9 mg, 27 % yield).



$^1\text{H NMR}$ (400 MHz, CDCl_3) δ 7.88–7.75 (m, 2H), 7.75–7.63 (m, 2H), 4.48–4.29 (m, 1H), 3.17 (s, 1H), 2.67 (ddd, $J = 14.5, 9.8, 2.3$ Hz, 1H), 2.26–2.18 (m, 1H), 2.18–1.98 (m, 2H), 1.97–1.86 (m, 1H), 1.61–1.48 (m, 1H), 1.37 (s, 3H).

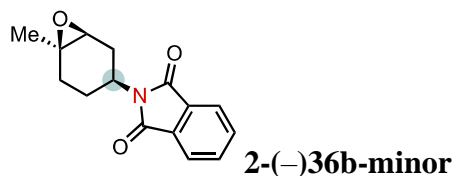
$^{13}\text{C NMR}$ (100 MHz, CDCl_3) δ 168.43, 133.91, 131.95, 123.10, 60.77, 57.08, 44.19, 28.23, 28.13, 25.01, 24.01.

HRMS (DART): $[\text{M}+\text{H}]^+$ calcd for $[\text{C}_{15}\text{H}_{16}\text{NO}_3]^+$ m/z 258.1125, found 258.1126.

IR (neat, ATR): ν_{max} 2926, 2856, 1772, 1719, 1701, 1400, 1376, 1102, 879 cm^{-1} .

Optical Rotation: $[\alpha]_{\text{D}}^{25} = -2.00$ (c 0.2, CHCl_3)

M.p.: 146–149 $^{\circ}\text{C}$.



$^1\text{H NMR}$ (400 MHz, CDCl_3) δ 7.89–7.76 (m, 2H), 7.74–7.65 (m, 2H), 4.10 (dddd, $J = 12.8, 11.9, 6.6, 3.0$ Hz, 1H), 3.05–2.92 (m, 1H), 2.60–2.39 (m, 2H), 2.20–2.04 (m, 2H), 1.87 (ddd, $J = 14.8, 12.8, 5.0$ Hz, 1H), 1.44–1.36 (m, 1H), 1.35 (s, 3H).

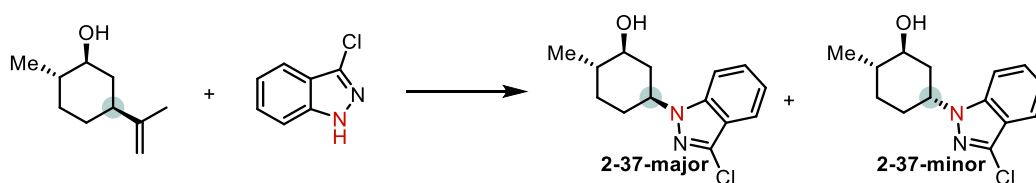
^{13}C NMR (100 MHz, CDCl_3) δ 168.08, 133.91, 131.94, 123.14, 58.39, 56.97, 46.40, 30.42, 27.92, 23.43, 22.83.

HRMS (DART): $[\text{M}+\text{H}]^+$ calcd for $[\text{C}_{15}\text{H}_{16}\text{NO}_3]^+$ m/z 258.1125, found 258.1126.

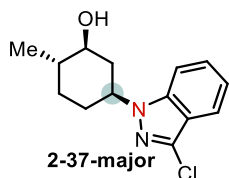
IR (neat, ATR): ν_{max} 2925, 2857, 1701, 11396, 1377, 1075 cm^{-1} .

Optical Rotation: $[\alpha]_{\text{D}}^{25} = -15.30$ (c 0.2, CHCl_3)

M.p.: 187–190 $^{\circ}\text{C}$.



Prepared following **General procedure A** using 3-chloro-1H-indazole (61.0 mg, 0.400 mmol, 1.0 equiv), copper(I) chloride (7.90 mg, 0.0800 mmol, 20 mol %), 1,10-phenanthroline (14.4 mg, 0.0800 mmol, 20 mol %), and MeCN (4 mL) to make *Solution A*. The alkene **2-95** (123 mg, 0.800 mmol, 2.0 equiv) was used for ozonolysis and MeCN (4 mL) to make *Solution B*. The crude product was purified through FCC to give **2-37-major** ($R_f = 0.32$; $\text{CHCl}_3/\text{MeOH}$, 100:1) as a pale-yellow oil (44.7 mg, 42%) and **2-37-minor** ($R_f = 0.47$; $\text{CHCl}_3/\text{MeOH}$, 100:1) as a pale-yellow oil (40.1 mg, 38 % yield).



^1H NMR (400 MHz, CDCl_3) δ 7.65 (d, $J = 8.2$ Hz, 1H), 7.42–7.36 (m, 2H), 7.18 (ddd, $J = 7.9$, 4.8, 2.9 Hz, 1H), 4.43 (tt, $J = 11.7$, 4.2 Hz, 1H), 3.35 (ddd, $J = 11.0$, 9.9, 4.2 Hz, 1H), 2.33 (dtd, J

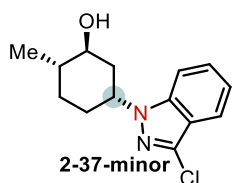
= 12.0, 4.0, 1.8 Hz, 1H), 2.17–2.07 (m, 1H), 2.07–1.93 (m, 3H), 1.89 (dq, $J = 13.8, 3.6$ Hz, 1H), 1.47 (dddq, $J = 14.5, 8.9, 6.2, 3.1, 2.4$ Hz, 1H), 1.25–1.13 (m, 1H), 1.09 (d, $J = 6.4$ Hz, 3H).

^{13}C NMR (100 MHz, CDCl_3) δ 139.98, 132.58, 127.27, 121.24, 121.04, 119.88, 109.25, 74.86, 56.73, 40.85, 39.33, 31.63, 31.08, 18.03.

HRMS (ESI-TOF): $[\text{M}+\text{H}]^+$ calcd for $[\text{C}_{14}\text{H}_{18}\text{ClN}_2\text{O}]^+$ m/z 265.1102, found 265.1105.

IR (neat, ATR): ν_{max} 3380 (br), 2949, 2932, 2871, 1616, 1494, 1465, 1338, 1191, 1128, 1049, 1015, 1006, 987, 767, 743 cm^{-1} .

Optical Rotation: $[\alpha]_{\text{D}}^{25} = -4.00$ (c 0.4, CHCl_3)



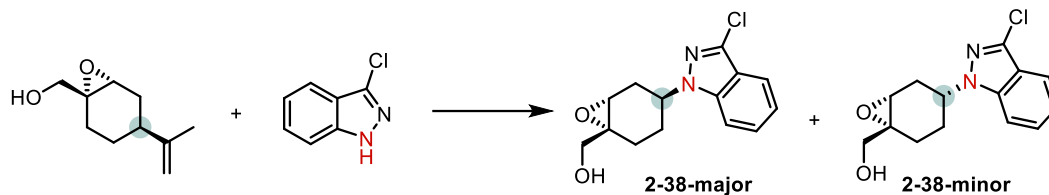
^1H NMR (400 MHz, CDCl_3) δ 7.65 (d, $J = 8.2$ Hz, 1H), 7.46–7.35 (m, 2H), 7.18 (ddd, $J = 7.8, 6.5, 1.1$ Hz, 1H), 4.86 (tt, $J = 9.4, 4.2$ Hz, 1H), 4.12–4.01 (m, 1H), 2.44 (ddd, $J = 13.1, 9.7, 3.0$ Hz, 1H), 2.23–2.10 (m, 1H), 2.02 (ddt, $J = 15.3, 11.2, 4.1$ Hz, 1H), 1.93 (dt, $J = 13.7, 4.4$ Hz, 1H), 1.88–1.75 (m, 4H), 1.56 (dq, $J = 13.7, 4.4$ Hz, 1H), 1.11 (d, $J = 7.1$ Hz, 3H).

^{13}C NMR (100 MHz, CDCl_3) δ 140.20, 132.16, 127.08, 121.13, 120.94, 119.73, 109.49, 72.20, 53.65, 35.48, 35.03, 27.59, 26.27, 16.99.

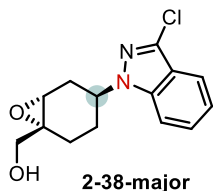
HRMS (ESI-TOF): $[\text{M}+\text{H}]^+$ calcd for $[\text{C}_{14}\text{H}_{18}\text{ClN}_2\text{O}]^+$ m/z 265.1102, found 265.1107.

IR (neat, ATR): ν_{max} 3381 (br), 2954, 2931, 2873, 1616, 1494, 1465, 1339, 1267, 1244, 1192, 1181, 1130, 10058, 1017, 981, 965, 766, 743 cm^{-1} .

Optical Rotation: $[\alpha]_{\text{D}}^{24} = 3.50$ (c 0.2, CHCl_3)



Prepared following **General procedure A** using 3-chloro-1*H*-indazole (153 mg, 1.00 mmol, 1.0 equiv), copper(I) chloride (19.8 mg, 0.200 mmol, 20 mol %), 1,10-phenanthroline (36.0 mg, 0.200 mmol, 20 mol %), and MeCN (10 mL) to make *Solution A*. The alkene **2-95** (337 mg, 2.00 mmol, 2.0 equiv) was used for ozonolysis and MeCN (10 mL) to make *Solution B*. The crude product was purified through FCC to give **2-38-major** ($R_f = 0.30$; hexanes/EtOAc, 2:3) containing impurities and **2-38-minor** ($R_f = 0.15$; hexanes/EtOAc, 2:3) containing impurities. The crude **2-38-major** was purified again through FCC to give **2-38-major** ($R_f = 0.53$; Et₂O) as a white solid (148.6 mg, 54% yield). The crude **2-38-minor** was purified again through FCC to give **2-38-minor** ($R_f = 0.23$; toluene/EtOAc, 3:2) as a white solid (71.8 mg, 26% yield).



¹H NMR (400 MHz, CDCl₃) δ 7.65 (dt, $J = 8.2, 0.8$ Hz, 1H), 7.45–7.34 (m, 2H), 7.19 (ddd, $J = 7.9, 6.0, 1.7$ Hz, 1H), 4.67 (dq, $J = 9.5, 5.4, 2.6$ Hz, 1H), 3.79–3.63 (m, 2H), 3.54 (t, $J = 2.0$ Hz, 1H), 2.57 (ddd, $J = 15.0, 8.5, 2.5$ Hz, 1H), 2.50 (dd, $J = 15.0, 5.4$ Hz, 1H), 2.09–1.97 (m, 3H), 1.97–1.90 (m, 1H), 1.90–1.82 (m, 1H).

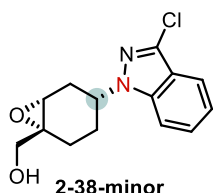
¹³C NMR (100 MHz, CDCl₃) δ 140.28, 132.74, 127.41, 121.38, 121.06, 119.86, 109.22, 64.38, 59.87, 56.89, 51.69, 30.49, 26.65, 23.60.

HRMS (ESI-TOF): $[M+H]^+$ calcd for $[C_{14}H_{16}ClN_2O_2]^+$ m/z 279.0895, found 279.0897.

IR (neat, ATR): ν_{\max} 3417 (br), 2929, 2865, 1616, 1494, 1466, 1338, 1197, 1052, 1006, 768, 743 cm^{-1} .

Optical Rotation: $[\alpha]_{\text{D}}^{24} = 8.00$ (c 0.1, CHCl_3)

M.p.: 130–132 °C.



^1H NMR [400 MHz, $(\text{CD}_3)_2\text{CO}$] δ 7.66 (d, $J = 8.6$ Hz, 1H), 7.62 (d, $J = 8.2$ Hz, 1H), 7.52–7.37 (m, 1H), 7.21 (t, $J = 7.3$ Hz, 1H), 4.68 (dtd, $J = 10.5, 8.0, 3.8$ Hz, 1H), 3.70–3.50 (m, 2H), 3.20 (d, $J = 3.9$ Hz, 1H), 2.48–2.31 (m, 2H), 2.23–2.04 (m, 3H), 1.76–1.62 (m, 1H).

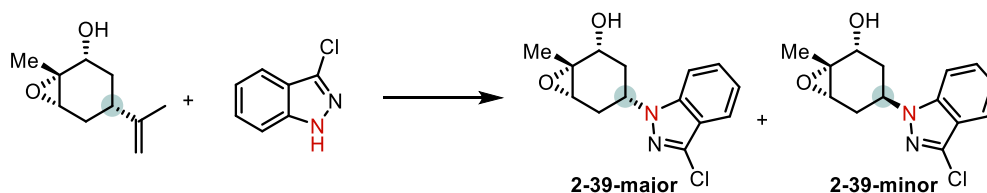
^{13}C NMR [100 MHz, $(\text{CD}_3)_2\text{CO}$] δ 140.38, 131.60, 127.25, 121.46, 120.72, 119.05, 109.92, 65.00, 64.88, 59.91, 54.57, 53.77, 29.78, 25.24, 24.60.

HRMS (DART): $[\text{M}+\text{H}]^+$ calcd for $[\text{C}_{14}\text{H}_{16}\text{ClN}_2\text{O}_2]^+$ m/z 279.0895, found 279.0895.

IR (neat, ATR): ν_{\max} 3426 (br), 2926, 2858, 1616, 1495, 1466, 1338, 1194, 1056, 1007, 761, 744 cm^{-1} .

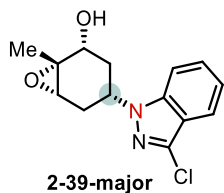
Optical Rotation: $[\alpha]_{\text{D}}^{24} = 22.77$ (c 0.1, CHCl_3)

M.p.: 115–116 °C.



Prepared following **General procedure A** using 3-chloro-1H-indazole (30.5 mg, 0.200 mmol, 1.0 equiv), copper(I) chloride (4.00 mg, 0.0400 mmol, 20 mol %), 1,10-phenanthroline (7.20 mg,

0.0400 mmol, 20 mol %), and MeCN (2 mL) to make *Solution A*. The alkene **2-97** (67.3 mg, 0.400 mmol, 2.0 equiv) was used for ozonolysis and MeCN (2 mL) to make *Solution B*. The crude product was purified through FCC to give **2-39-major** ($R_f = 0.21$; CHCl₃/Et₂O, 3/2) as a white solid (24.6 mg, 44% yield) and **2-39-minor** ($R_f = 0.37$; CHCl₃/Et₂O, 3/2) as a colorless oil (22.6 mg, 41% yield).



¹H NMR (400 MHz, CDCl₃) δ 7.66 (d, $J = 8.2$ Hz, 1H), 7.46–7.35 (m, 2H), 7.20 (ddd, $J = 7.8$, 6.4, 1.3 Hz, 1H), 4.53–4.37 (m, 1H), 4.15–4.05 (m, 1H), 3.21 (d, $J = 5.0$ Hz, 1H), 2.51 (dd, $J = 15.2$, 11.1 Hz, 1H), 2.34 (dddd, $J = 15.2$, 6.7, 5.1, 1.8 Hz, 1H), 2.23 (td, $J = 12.3$, 10.7 Hz, 1H), 2.16–2.08 (m, 1H), 1.95 (d, $J = 9.6$ Hz, 1H), 1.53 (s, 3H).

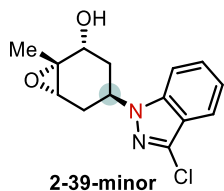
¹³C NMR (100 MHz, CDCl₃) δ 139.87, 133.00, 127.50, 121.44, 121.39, 120.08, 109.19, 70.97, 60.32, 59.96, 53.40, 34.87, 29.51, 18.87.

HRMS (ESI-TOF): $[M+H]^+$ calcd for [C₁₄H₁₆ClN₂O₂]⁺ m/z 279.0895, found 279.0895.

IR (neat, ATR): ν_{\max} 3412 (br), 2982, 2930, 1616, 1494, 1466, 1337, 1319, 1195, 1129, 1049, 1009, 850, 768, 744 cm⁻¹.

Optical Rotation: $[\alpha]_D^{23} = -3.56$ (c 0.1, CHCl₃)

M.p.: 145–148 °C.



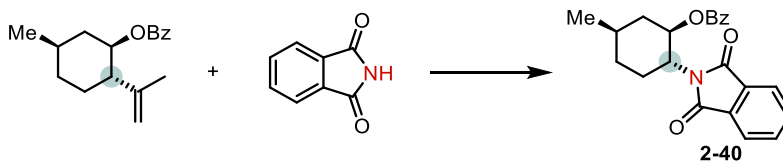
¹H NMR (400 MHz, CDCl₃) δ 7.65 (d, *J* = 8.2 Hz, 1H), 7.49–7.35 (m, 2H), 7.19 (ddd, *J* = 7.9, 5.8, 1.8 Hz, 1H), 4.73 (dddd, *J* = 11.1, 8.6, 5.7, 2.9 Hz, 1H), 4.03 (s, 1H), 3.48 (t, *J* = 2.1 Hz, 1H), 2.60–2.45 (m, 2H), 2.40–2.28 (brs, 1H), 2.15 (ddd, *J* = 13.8, 10.9, 5.0 Hz, 1H), 1.98–1.88 (m, 1H), 1.52 (s, 3H).

¹³C NMR (100 MHz, CDCl₃) δ 140.36, 132.95, 127.50, 121.47, 121.10, 119.85, 109.20, 68.21, 63.25, 60.18, 48.54, 36.85, 30.46, 21.07.

HRMS (ESI-TOF): [M+H]⁺ calcd for [C₁₄H₁₆ClN₂O₂]⁺ *m/z* 279.0895, found 279.0893.

IR (neat, ATR): *v*_{max} 3417 (br), 2978, 2962, 2926, 1617, 1494, 1466, 1337, 1192, 1060, 1039, 1032, 845, 766, 745 cm⁻¹.

Optical Rotation: [α]_D²⁴ = 4.00 (*c* 0.2, CHCl₃)



Prepared following **General procedure A** using phthalimide (**2-114**, 58.8 mg, 0.400 mmol, 1.0 equiv), copper(I) chloride (7.90 mg, 0.0800 mmol, 20 mol %), 1,10-phenanthroline (14.4 mg, 0.0800 mmol, 20 mol %), and MeCN (4 mL) to make *Solution A*. The alkene **2-98** (207 mg, 0.800 mmol, 2.0 equiv) was used for ozonolysis and MeCN (4 mL) was used to make *Solution B*. The crude product was purified through FCC to give **2-40** (*R*_f = 0.49; toluene/DCM, 1:1) as a pale-yellow oil (72.7 mg, 50% yield).

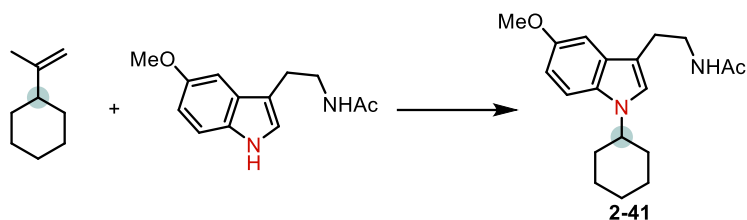
¹H NMR (400 MHz, CDCl₃) δ 7.96–7.80 (m, 2H), 7.76 (dd, *J* = 5.4, 3.0 Hz, 2H), 7.62 (dd, *J* = 5.5, 3.0 Hz, 2H), 7.45 (tt, *J* = 7.0, 1.2 Hz, 1H), 7.32 (t, *J* = 7.7 Hz, 2H), 5.70 (td, *J* = 10.9, 4.7 Hz, 1H), 4.38 (ddd, *J* = 12.7, 10.6, 4.3 Hz, 1H), 2.51 (qd, *J* = 13.9, 13.4, 3.9 Hz, 1H), 2.39–2.27 (m, 1H), 1.91–1.75 (m, 3H), 1.37–1.09 (m, 2H), 1.00 (d, *J* = 6.4 Hz, 3H).

^{13}C NMR (100 MHz, CDCl_3) δ 168.28, 165.63, 133.86, 132.80, 130.05, 129.54, 128.26, 123.19, 72.21, 53.48, 39.90, 33.62, 30.67, 27.84, 21.75.

HRMS (DART): $[\text{M}+\text{H}]^+$ calcd for $[\text{C}_{22}\text{H}_{22}\text{NO}_4]^+$ m/z 364.1543, found 364.1541

IR (neat, ATR): ν_{max} 2954, 2931, 2870, 2853, 1174, 1722, 1468, 1453, 1382, 1295, 1272, 1114, 1099, 1070, 714 cm^{-1} .

Optical Rotation: $[\alpha]_{\text{D}}^{24} = -52.72$ (c 0.2, CHCl_3)



Prepared following **General procedure A** using melatonin (**S6**, 46.5 mg, 0.200 mmol, 1.0 equiv), copper(I) chloride (4.00 mg, 0.0400 mmol, 20 mol %), 1,10-phenanthroline (7.20 mg, 0.0400 mmol, 20 mol %), and MeCN (2 mL) to make *Solution A*. The alkene **2-99** (62.1 mg, 0.500 mmol, 2.0 equiv) was used for ozonolysis and MeCN (2 mL) to make *Solution B*. The crude product was purified through FCC to give **2-41** ($R_f = 0.26$; EtOAc) as an off-white solid (42.8 mg, 68% yield).

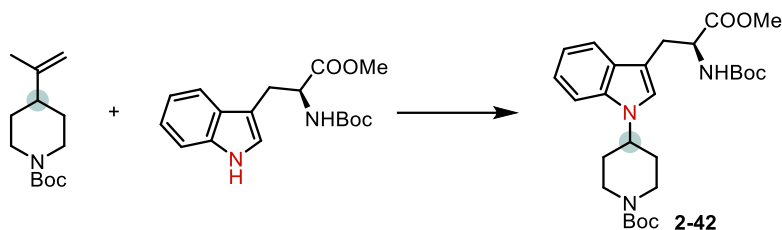
^1H NMR (400 MHz, CDCl_3) δ 7.25 (d, $J = 8.9$ Hz, 1H), 7.08–6.99 (m, 2H), 6.87 (dd, $J = 8.9, 2.5$ Hz, 1H), 5.72 (brs, 1H), 4.11 (tt, $J = 11.8, 3.7$ Hz, 1H), 3.85 (s, 3H), 3.57 (q, $J = 6.7$ Hz, 2H), 2.93 (t, $J = 6.8$ Hz, 2H), 2.10 (dd, $J = 12.9, 2.1$ Hz, 2H), 1.94–1.91 (m, 5H), 1.84–1.73 (m, 1H), 1.66 (qd, $J = 12.5, 3.4$ Hz, 2H), 1.48 (qt, $J = 13.1, 3.4$ Hz, 2H), 1.27 (qt, $J = 13.1, 3.7$ Hz, 1H).

^{13}C NMR (100 MHz, CDCl_3) δ 170.11, 153.77, 131.31, 127.93, 122.68, 111.71, 110.87, 110.35, 100.59, 56.01, 55.19, 39.99, 33.63, 25.97, 25.65, 25.39, 23.39.

HRMS (ESI-TOF): $[\text{M}+\text{H}]^+$ calcd for $[\text{C}_{19}\text{H}_{27}\text{N}_2\text{O}_2]^+$ m/z 315.2067, found 315.2075.

IR (neat, ATR): ν_{max} 3250, 3075, 3000, 2928, 2849, 1636, 1553, 1484, 1452, 1373, 1301, 1231, 1210, 1180, 1107, 1036, 852, 785, 749 cm^{-1} .

M.p.: 112–115 °C.



Prepared following **General procedure A** using **2-115** (63.7 mg, 0.200 mmol, 1.0 equiv), copper(I) chloride (4.00 mg, 0.0400 mmol, 20 mol %), 1,10-phenanthroline (7.20 mg, 0.0400 mmol, 20 mol %), and MeCN (2 mL) to make *Solution A*. The alkene **2-100** (90.1 mg, 0.400 mmol, 2.0 equiv) was used for ozonolysis and MeCN (2 mL) to make *Solution B*. The crude product was purified through FCC to give **2-42** ($R_f = 0.47$; hexanes/EtOAc, 2:1) as a pale-yellow oil (61.4 mg, 61% yield).

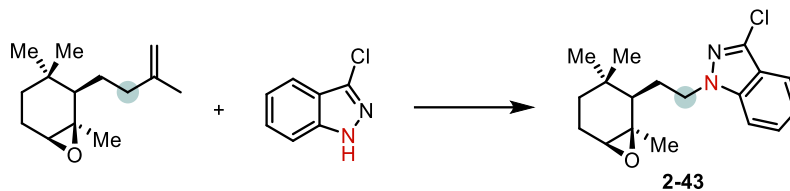
^1H NMR (400 MHz, CDCl_3) δ 7.54 (d, $J = 7.9$ Hz, 1H), 7.33 (d, $J = 8.3$ Hz, 1H), 7.24–7.16 (m, 1H), 7.11 (t, $J = 7.3$ Hz, 1H), 6.97 (s, 1H), 5.04 (d, $J = 8.1$ Hz, 1H), 4.64 (q, $J = 5.5$ Hz, 1H), 4.35–4.29 (m, 3H), 3.68 (s, 3H), 3.31–3.20 (m, 2H), 2.90 (t, $J = 12.6$ Hz, 2H), 2.05 (d, 2H), 1.86 (qd, $J = 12.5, 3.8$ Hz, 2H), 1.50 (s, 9H), 1.43 (s, 9H).

^{13}C NMR (100 MHz, CDCl_3) δ 172.75, 155.21, 154.62, 135.72, 128.31, 122.44, 121.71, 119.42, 119.16, 109.52, 109.21, 79.99, 79.81, 54.24, 53.38, 52.23, 32.39, 28.46, 28.39, 28.36, 28.15.

HRMS (DART): $[\text{M}+\text{H}]^+$ calcd for $[\text{C}_{27}\text{H}_{44}\text{N}_3\text{O}_6]^+$ m/z 502.2912, found 502.2914.

IR (neat, ATR): ν_{max} 3349 (br), 2967, 2952, 2931, 2862, 1744, 1693, 1463, 1426, 1365, 1245, 1165, 742 cm^{-1} .

Optical Rotation: $[\alpha]_{\text{D}}^{24} = 10.10$ (c 1.0, CHCl_3)



Prepared following **General procedure A** using **2-113** (61.0 mg, 0.400 mmol, 1.0 equiv), copper(I) chloride (7.90 mg, 0.0800 mmol, 20 mol %), 1,10-phenanthroline (14.4 mg, 0.0800 mmol, 20 mol %), and MeCN (4 mL) to make *Solution A*. The alkene **2-101** (166 mg, 0.800 mmol, 2.0 equiv) was used for ozonolysis and MeCN (4 mL) to make *Solution B*. The crude product was purified through FCC to give **2-43** ($R_f = 0.60$; hexanes/EtOAc, 4:1) as a white solid (105.9 mg, 83% yield).

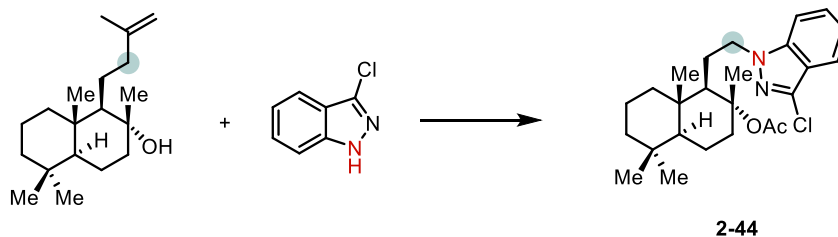
$^1\text{H NMR}$ (400 MHz, CDCl_3) δ 7.66 (dt, $J = 8.2, 0.9$ Hz, 1H), 7.53 (dt, $J = 8.5, 0.7$ Hz, 1H), 7.47–7.38 (m, 1H), 7.23–7.13 (m, 1H), 4.61 (ddd, $J = 13.6, 10.6, 5.7$ Hz, 1H), 4.39 (ddd, $J = 13.6, 10.6, 5.6$ Hz, 1H), 3.03 (s, 1H), 2.05–1.80 (m, 4H), 1.57–1.46 (m, 1H), 1.35 (s, 3H), 1.25 (td, $J = 12.9, 6.2$ Hz, 1H), 0.91 (s, 3H), 0.88–0.79 (m, 4H).

$^{13}\text{C NMR}$ (100 MHz, CDCl_3) δ 140.56, 132.24, 127.37, 121.08, 121.02, 119.67, 109.83, 60.34, 59.13, 49.15, 44.71, 31.38, 28.01, 27.69, 27.09, 26.76, 26.68, 21.96.

HRMS (ESI-TOF): $[\text{M}+\text{H}]^+$ calcd for $[\text{C}_{18}\text{H}_{24}\text{ClN}_2\text{O}]^+$ m/z 319.1572, found 319.1578.

IR (neat, ATR): ν_{max} 2959, 2932, 2870, 1616, 1495, 1468, 1378, 1337, 1246, 1175, 1127, 1007, 985, 896, 743 cm^{-1} .

M.p.: 70–71 $^\circ\text{C}$.



Prepared following **modified General procedure B** using **2-113** (61.0 mg, 0.400 mmol, 1.0 equiv), copper(I) chloride (7.90 mg, 0.0800 mmol, 20 mol %), 1,10-phenanthroline (14.4 mg, 0.0800 mmol, 20 mol %), and MeCN (4 mL) to make *Solution A*. The alkene **2-102** (334 mg, 1.20 mmol, 3 equiv) was dissolved in DCM (10 mL) for ozonolysis. MeCN (6 mL) was used to make *Suspension B*. The crude product was purified through FCC to give **2-44** ($R_f = 0.44$; toluene/DCM, 1:1) as a white solid (105.1 mg, 61% yield).

$^1\text{H NMR}$ (400 MHz, CDCl_3) δ 7.67 (dt, $J = 8.2, 1.0$ Hz, 1H), 7.42 (ddd, $J = 7.8, 6.8, 1.0$ Hz, 1H), 7.34 (d, $J = 8.5$ Hz, 1H), 7.19 (ddd, $J = 7.9, 6.8, 0.8$ Hz, 1H), 4.42 (ddd, $J = 13.9, 10.4, 6.1$ Hz, 1H), 4.30 (ddd, $J = 13.9, 10.6, 5.9$ Hz, 1H), 2.76 (dt, $J = 12.1, 3.0$ Hz, 1H), 2.03–1.82 (m, 5H), 1.79–1.54 (m, 5H), 1.52–1.43 (m, 4H), 1.43–1.35 (m, 1H), 1.34–1.23 (m, 1H), 1.16 (td, $J = 13.4, 4.1$ Hz, 1H), 1.04–0.90 (m, 2H), 0.87 (s, 3H), 0.82 (s, 3H), 0.78 (s, 3H).

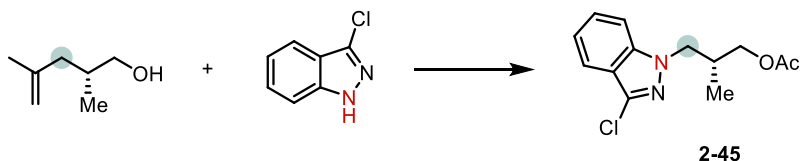
$^{13}\text{C NMR}$ (100 MHz, CDCl_3) δ 169.98, 140.40, 132.31, 127.34, 121.05, 119.91, 109.16, 87.69, 56.45, 55.65, 51.20, 41.78, 39.60, 39.30, 38.86, 33.31, 33.14, 26.46, 23.05, 21.41, 20.20, 19.91, 18.29, 15.65.

HRMS (ESI-TOF): $[\text{M}-\text{OAc}]^+$ calcd for $[\text{C}_{23}\text{H}_{32}\text{ClN}_2]^+$ m/z 371.2249, found 371.2262.

IR (neat, ATR): ν_{max} 2992, 2950, 2938, 2929, 2871, 2848, 1729, 1467, 1390, 1365, 1337, 1248, 1174, 1126, 1043, 1018, 773, 769, 743 cm^{-1} .

Optical Rotation: $[\alpha]_{\text{D}}^{23} = -7.00$ (c 0.1, CHCl_3)

M.p.: 118–121 $^\circ\text{C}$.



Prepared following **General procedure A** using **2-113** (61.0 mg, 0.400 mmol, 1.0 equiv), copper(I) chloride (7.90 mg, 0.0800 mmol, 20 mol %), 1,10-phenanthroline (14.4 mg, 0.0800 mmol, 20 mol %), and MeCN (4 mL) to make *Solution A*. The alkene **2-103** (114 mg, 1.00 mmol, 2.5 equiv) was used for ozonolysis. MeCN (4 mL) was used to make *Solution B*. The crude product was purified through FCC to give **2-45** ($R_f = 0.39$; hexanes/EtOAc, 4:1) as a pale-yellow oil (79.0 mg, 74% yield).

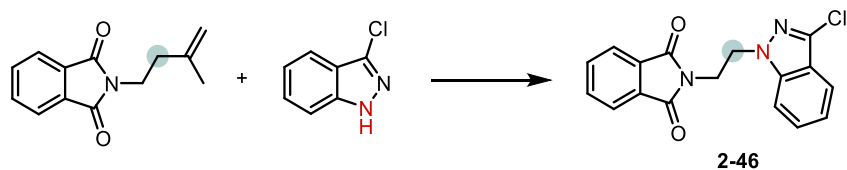
^1H NMR (400 MHz, CDCl_3) δ 7.65 (dt, $J = 8.2, 0.9$ Hz, 1H), 7.41 (ddd, $J = 8.5, 6.7, 1.1$ Hz, 1H), 7.34 (dt, $J = 8.6, 0.8$ Hz, 1H), 7.21–7.13 (m, 1H), 4.35 (dd, $J = 14.2, 6.9$ Hz, 1H), 4.19 (dd, $J = 14.2, 7.2$ Hz, 1H), 4.02–3.88 (m, 2H), 2.57 (dtd, $J = 13.3, 6.9, 5.1$ Hz, 1H), 2.01 (s, 3H), 0.97 (d, $J = 6.9$ Hz, 3H).

^{13}C NMR (100 MHz, CDCl_3) δ 170.85, 141.31, 133.02, 127.56, 121.24, 120.93, 119.85, 109.20, 66.42, 51.85, 33.87, 20.80, 14.87.

HRMS (ESI-TOF): $[\text{M}+\text{H}]^+$ calcd for $[\text{C}_{13}\text{H}_{16}\text{ClN}_2\text{O}_2]^+$ m/z 267.0895, found 267.0894.

IR (neat, ATR): ν_{max} 2964, 2933, 2879, 1739, 1617, 1496, 1468, 1393, 1367, 1338, 1236, 1192, 1128, 1051, 1039, 987, 765, 745 cm^{-1} .

Optical Rotation: $[\alpha]_{\text{D}}^{23} = 6.50$ (c 0.2, CHCl_3)



Prepared following **General procedure A** using **2-113** (30.5 mg, 0.200 mmol, 1.0 equiv), copper(I) chloride (4.00 mg, 0.0400 mmol, 20 mol %), 1,10-phenanthroline (7.20 mg, 0.0400 mmol, 20 mol %), and MeCN (2 mL) to make *Solution A*. The alkene **2-104** (86.1 mg, 0.400 mmol,

2.0 equiv) was used for ozonolysis and MeCN (2 mL) to make *Solution B*. The crude product was purified through FCC to give **2-46** ($R_f = 0.18$; hexanes/EtOAc, 4:1) as a white solid (48.2 mg, 74% yield).

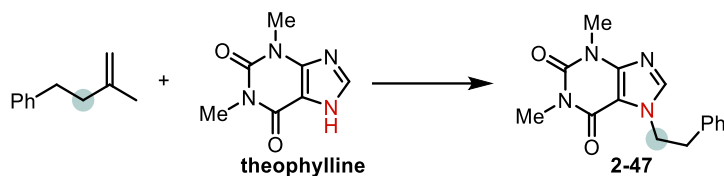
$^1\text{H NMR}$ (400 MHz, CDCl_3) δ 7.75 (dd, $J = 5.6, 3.0$ Hz, 2H), 7.67 (dd, $J = 5.5, 3.0$ Hz, 2H), 7.61 (dt, $J = 8.2, 1.0$ Hz, 1H), 7.35–7.26 (m, 2H), 7.11 (ddd, $J = 8.0, 6.5, 1.2$ Hz, 1H), 4.62 (t, $J = 6.2$ Hz, 2H), 4.12 (t, $J = 6.2$ Hz, 2H).

$^{13}\text{C NMR}$ (100 MHz, CDCl_3) δ 167.75, 141.13, 134.06, 133.82, 131.79, 127.69, 123.34, 121.36, 121.32, 119.95, 108.78, 46.73, 37.35.

HRMS (ESI-TOF): $[\text{M}+\text{H}]^+$ calcd for $[\text{C}_{17}\text{H}_{13}\text{ClN}_3\text{O}_2]^+$ m/z 326.0691, found 326.0693.

IR (neat, ATR): ν_{max} 3067, 3028, 2953, 1773, 1705, 1617, 1467, 1393, 1336, 1265, 1010, 745, 717 cm^{-1} .

M.p.: 167–170 $^\circ\text{C}$.



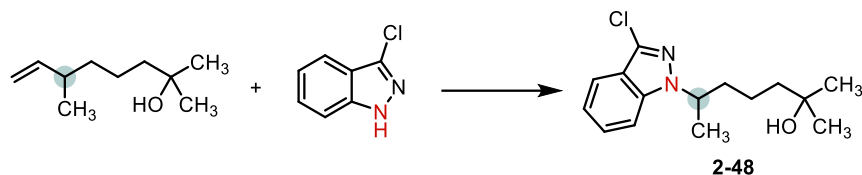
Prepared following **General procedure A** using theophylline (72.0 mg, 0.400 mmol, 1.0 equiv), $\text{Cu}(\text{MeCN})_4\text{BF}_4$ (25.2 mg, 0.0800 mmol, 20 mol %), 1,10-phenanthroline (14.4 mg, 0.0800 mmol, 20 mol %), and MeCN (4 mL) to make *Solution A*. The alkene **2-105** (175 mg, 1.20 mmol, 3.0 equiv) was used for ozonolysis and MeCN (6 mL) to make *Solution B*. The crude product was purified through FCC to give **2-47** ($R_f = 0.45$; EtOAc) as a pale-yellow oil (88.6 mg, 78% yield).

$^1\text{H NMR}$ (400 MHz, CDCl_3) δ 7.30–7.19 (m, 3H), 7.15 (s, 1H), 7.11–7.03 (m, 2H), 4.47 (t, $J = 7.0$ Hz, 2H), 3.56 (s, 3H), 3.43 (s, 3H), 3.13 (t, $J = 7.0$ Hz, 2H).

^{13}C NMR (100 MHz, CDCl_3) δ 155.18, 151.71, 149.00, 141.05, 137.05, 128.82, 127.08, 106.61, 48.83, 37.31, 29.81, 28.04.

HRMS (ESI-TOF): $[\text{M}+\text{H}]^+$ calcd for $[\text{C}_{15}\text{H}_{17}\text{N}_4\text{O}_2]^+$ m/z 285.1346, found 285.1345.

IR (neat, ATR): ν_{max} 1703, 1657, 1604, 1547, 1475, 1456, 1429, 1407, 1375, 1237, 1221, 1028, 772, 764 cm^{-1} .



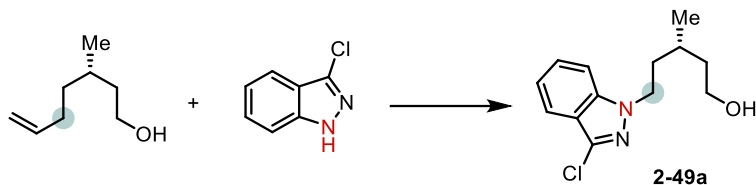
Prepared following **General procedure A** using **2-113** (30.5 mg, 0.200 mmol, 1.0 equiv), copper(I) chloride (4.00 mg, 0.0400 mmol, 20 mol %), 1,10-phenanthroline (7.20 mg, 0.0400 mmol, 20 mol %), and MeCN (2 mL) to make *Solution A*. The alkene **2-106** (78.1 mg, 0.500 mmol, 2.5 equiv) was used for ozonolysis and MeCN (2 mL) to make *Solution B*. The crude product was purified through FCC to give **2-48** with small amount of impurities ($R_f = 0.14$; hexanes/EtOAc, 4:1). The crude material was purified again through FCC to give **2-48** ($R_f = 0.35$; toluene/ $\text{CHCl}_3/\text{Et}_2\text{O}$, 2:2:1) as a colorless oil (41.2 mg, 73% yield).

^1H NMR (400 MHz, CDCl_3) δ 7.66 (dt, $J = 8.2, 0.9$ Hz, 1H), 7.39 (dd, $J = 4.2, 0.8$ Hz, 2H), 7.21–7.13 (m, 1H), 4.66–4.52 (m, 1H), 2.20–2.05 (m, 1H), 1.82 (ddt, $J = 13.8, 9.9, 5.7$ Hz, 1H), 1.54 (d, $J = 6.7$ Hz, 3H), 1.51–1.14 (m, 6H), 1.09 (d, $J = 6.3$ Hz, 6H).

^{13}C NMR (100 MHz, CDCl_3) δ 140.60, 132.52, 127.15, 121.06, 120.87, 119.84, 109.31, 70.79, 55.23, 43.32, 36.74, 29.23, 29.14, 21.22, 20.85.

HRMS (ESI-TOF): $[\text{M}-\text{OH}]^+$ calcd for $[\text{C}_{15}\text{H}_{20}\text{ClN}_2]^+$ m/z 263.1310, found 263.1310.

IR (neat, ATR): ν_{max} 3377 (br), 3060, 2971, 2935, 2865, 1616, 1495, 1463, 1377, 1337, 1197, 1154, 1120, 768, 742 cm^{-1} .



Prepared following **General procedure A** using **2-113** (61.0 mg, 0.400 mmol, 1.0 equiv), copper(I) chloride (7.90 mg, 0.0800 mmol, 20 mol %), 1,10-phenanthroline (14.4 mg, 0.0800 mmol, 20 mol %), and MeCN (4 mL) to make *Solution A*. The alkene **2-107** (128 mg, 1.00 mmol, 2.5 equiv) was used for ozonolysis and MeCN (4 mL) to make *Solution B*. The crude product was purified through FCC to give **2-49a** ($R_f = 0.52$; toluene/EtOAc/DCM, 2:1:1) as a pale-yellow oil (76.0 mg, 74% yield).

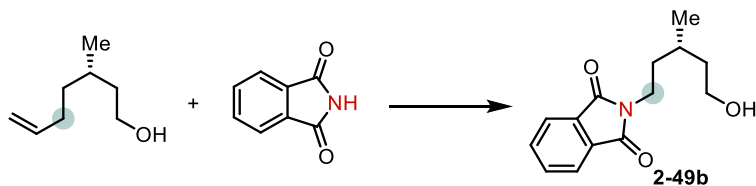
$^1\text{H NMR}$ (400 MHz, CDCl_3) δ 7.64 (d, $J = 8.2$ Hz, 1H), 7.45–7.30 (m, 2H), 7.17 (ddd, $J = 7.9$, 6.5, 1.1 Hz, 1H), 4.41–4.26 (m, 2H), 3.75–3.57 (m, 2H), 2.01–1.91 (m, 1H), 1.80–1.58 (m, 3H), 1.51–1.39 (m, 1H), 0.98 (d, $J = 6.4$ Hz, 3H).

$^{13}\text{C NMR}$ (100 MHz, CDCl_3) δ 140.64, 132.44, 127.44, 121.15, 120.97, 119.84, 109.27, 60.55, 47.20, 39.41, 36.54, 27.20, 19.60.

HRMS (ESI-TOF): $[\text{M}+\text{H}]^+$ calcd for $[\text{C}_{13}\text{H}_{18}\text{ClN}_2\text{O}]^+$ m/z 253.1102, found 253.1102.

IR (neat, ATR): ν_{max} 3370 (br), 2956, 2931, 2926, 2876, 1617, 1496, 1338, 1176, 1063, 1006, 768, 743 cm^{-1} .

Optical Rotation: $[\alpha]_{\text{D}}^{25} = -3.00$ (c 0.4, CHCl_3)



Prepared following **General procedure A** using phthalimide (**2-114**, 29.4 mg, 0.200 mmol, 1.0 equiv), copper(I) chloride (4.00 mg, 0.0400 mmol, 20 mol %), 1,10-phenanthroline (7.20 mg, 0.0400 mmol, 20 mol %), and MeCN (2 mL) to make *Solution A*. (*S*)-3-Methylhept-6-en-1-ol (**2-107**, 103 mg, 0.800 mmol, 4.0 equiv) was used for ozonolysis and MeCN (2 mL) to make *Solution B*. The crude reaction mixture was dry-loaded onto SiO₂ and purified through FCC (EtOAc/hexanes/Et₂O/toluene, 1:1:1.5:1.5) to provide a clear oil (*R*_f = 0.34; Et₂O/toluene, 1.85:1) that was recrystallized (pentanes) to provide **2-49b** as a white solid (36.6 mg, 74% yield).

¹H NMR (500 MHz, CDCl₃) δ 7.81 (dd, *J* = 5.4, 3.1 Hz, 2H), 7.68 (dd, *J* = 5.5, 3.1 Hz, 2H), 3.84–3.56 (m, 4H), 1.83–1.58 (m, 4H), 1.52 (dq, *J* = 13.3, 6.9, 6.4 Hz, 1H), 1.41 (dq, *J* = 13.0, 6.5 Hz, 1H), 0.98 (d, *J* = 6.3 Hz, 3H).

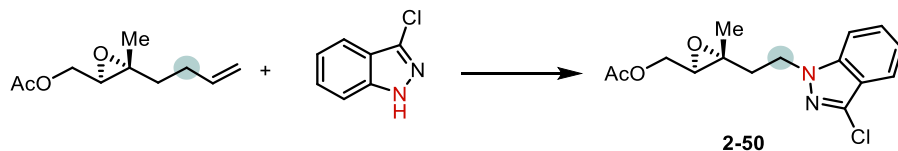
¹³C NMR (125 MHz, CDCl₃) δ 168.50, 133.89, 132.11, 123.18, 60.65, 39.34, 36.06, 35.61, 27.20, 19.46.

HRMS (ESI-TOF): [M+H]⁺ calcd for [C₁₄H₁₈NO₃]⁺ *m/z* 248.1281, found 248.1282.

IR (neat, ATR): ν_{max} 3413 (brs), 2955, 2930, 2872, 1772, 1714, 1400, 1373, 1173, 1061 cm⁻¹.

Optical Rotation: [α]_D²⁶ = -4.00 (*c* 0.2, CHCl₃).

M.p.: 53–55 °C.



Prepared following **General procedure A** using **2-113** (61.0 mg, 0.400 mmol, 1.0 equiv), copper(I) chloride (7.90 mg, 0.0800 mmol, 20 mol %), 1,10-phenanthroline (14.4 mg, 0.0800 mmol, 20 mol %), and MeCN (4 mL) to make *Solution A*. The alkene **2-108** (147 mg, 0.800 mmol, 2.0 equiv) and MeCN (4 mL) were used to make *Solution B*. The crude product was purified

through FCC to give **2-50** ($R_f = 0.35$; Et₂O/CHCl₃/DCM/toluene, 1:1:3:5) as a pale-yellow oil (66.7 mg, 54% yield).

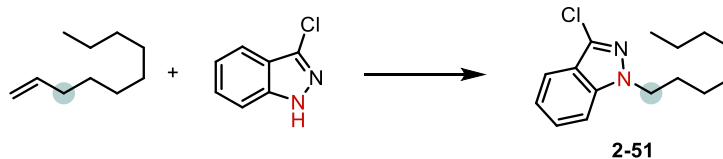
¹H NMR (400 MHz, CDCl₃) δ 7.66 (d, $J = 8.2$ Hz, 1H), 7.48–7.33 (m, 2H), 7.24–7.14 (m, 1H), 4.51–4.37 (m, 2H), 4.12 (dd, $J = 12.2, 4.2$ Hz, 1H), 3.95 (dd, $J = 12.2, 6.8$ Hz, 1H), 2.73 (dd, $J = 6.8, 4.2$ Hz, 1H), 2.25–2.07 (m, 2H), 2.03 (s, 3H), 1.34 (s, 3H).

¹³C NMR ¹³C NMR (100 MHz, CDCl₃) δ 170.70, 140.67, 132.99, 127.68, 121.38, 121.14, 119.95, 109.12, 62.91, 59.52, 58.62, 45.10, 37.91, 20.72, 16.94.

HRMS (DART): [M+H]⁺ calcd for [C₁₅H₁₈ClN₂O₃]⁺ m/z 309.1000, found 309.1001.

IR (neat, ATR): ν_{\max} 3064, 2994, 2947, 1617, 1497, 1468, 1375, 1338, 1176, 1038, 766, 746 cm⁻¹.

Optical Rotation: $[\alpha]_D^{25} = 9.82$ (c 0.56, CHCl₃)



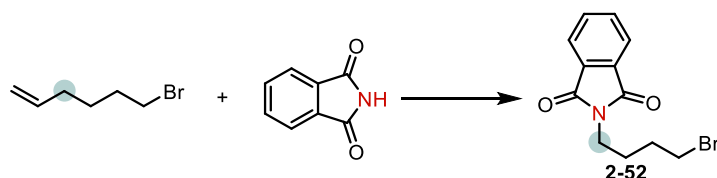
Prepared following **General procedure A** using **2-113** (30.5 mg, 0.200 mmol, 1.0 equiv), copper(I) chloride (4.00 mg, 0.0400 mmol, 20 mol %), 1,10-phenanthroline (7.20 mg, 0.0400 mmol, 20 mol %), and MeCN (2 mL) to make *Solution A*. The alkene **2-109** (56.1 mg, 0.400 mmol, 2.0 equiv) was used for ozonolysis and MeCN (2 mL) to make *Solution B*. The crude product was purified through FCC to give **2-51** ($R_f = 0.47$; hexanes/EtOAc, 40:1) with a little amount of impurities. This impure material was purified again through FCC to give pure **2-51** ($R_f = 0.36$; hexanes/toluene, 5:2) as a colorless oil (35.4 mg, 67% yield).

¹H NMR (400 MHz, CDCl₃) δ 7.66 (dt, *J* = 8.2, 0.8 Hz, 1H), 7.45–7.32 (m, 2H), 7.18 (ddd, *J* = 7.9, 6.5, 1.1 Hz, 1H), 4.30 (t, *J* = 7.2 Hz, 2H), 1.90 (p, *J* = 7.3 Hz, 2H), 1.37–1.17 (m, 10H), 0.86 (t, *J* = 6.9 Hz, 3H).

¹³C NMR (100 MHz, CDCl₃) δ 140.77, 132.35, 127.26, 121.00, 120.96, 119.79, 109.34, 49.32, 31.76, 29.82, 29.15, 29.11, 26.80, 22.62, 14.08.

HRMS (ESI-TOF): [M+H]⁺ calcd for [C₁₅H₂₂ClN₂]⁺ *m/z* 265.1466, found 265.1473.

IR (neat, ATR): *v*_{max} 3063, 2953, 2925, 2854, 1617, 1495, 1467, 1336, 1173, 1125, 1005, 982, 766, 740 cm⁻¹.



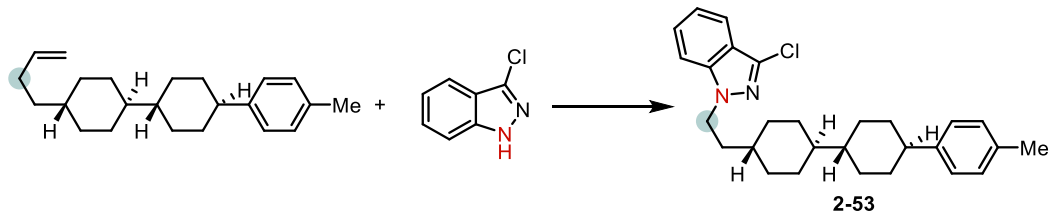
Prepared following **General procedure A** using **2-114** (58.8 mg, 0.400 mmol, 1.0 equiv), copper(I) chloride (7.9- mg, 0.0800 mmol, 20 mol %), 1,10-phenanthroline (14.4 mg, 0.0800 mmol, 20 mol %), and MeCN (4 mL) to make *Solution A*. The alkene **2-110** (130.4 mg, 0.8 mmol, 2.0 equiv) was used for ozonolysis and MeCN (4 mL) to make *Solution B*. The crude product was purified through FCC to give **2-52** (*R*_f = 0.51; hexanes/EtOAc, 3:1) as a colorless oil (61.4 mg, 55% yield).

¹H NMR (400 MHz, CDCl₃) δ 7.84 (td, *J* = 5.3, 2.1 Hz, 2H), 7.76–7.68 (m, 2H), 3.72 (t, *J* = 6.7 Hz, 2H), 3.44 (t, *J* = 6.4 Hz, 2H), 1.96–1.80 (m, 4H).

¹³C NMR (100 MHz, CDCl₃) δ 168.38, 134.00, 132.05, 123.28, 36.97, 32.80, 29.85, 27.26.

HRMS (DART): [M+H]⁺ calcd for [C₁₂H₁₃BrNO₂]⁺ *m/z* 282.0124, found 282.0124.

IR (neat, ATR): *v*_{max} 2939, 2868, 1770, 1703, 1436, 1394, 1371, 1359, 1256, 1188, 1086, 1023, 716, 529 cm⁻¹.



Prepared following **General procedure B** using **2-113** (61.0 mg, 0.400 mmol, 1.0 equiv), copper(I) chloride (7.90 mg, 0.0800 mmol, 20 mol %), 1,10-phenanthroline (14.4 mg, 0.0800 mmol, 20 mol %), and MeCN (4 mL) to make *Solution A*. The alkene **2-111** (248 mg, 0.800 mmol, 2.0 equiv) was dissolved in MeOH (4 mL) and DCM (20 mL) for ozonolysis. MeCN (6 mL) and benzene (4 mL) were used to make *Solution B*. The crude product was purified through FCC to give **2-53** ($R_f = 0.25$; hexanes/EtOAc, 40:1) as a white solid (113.0 mg, 65% yield).

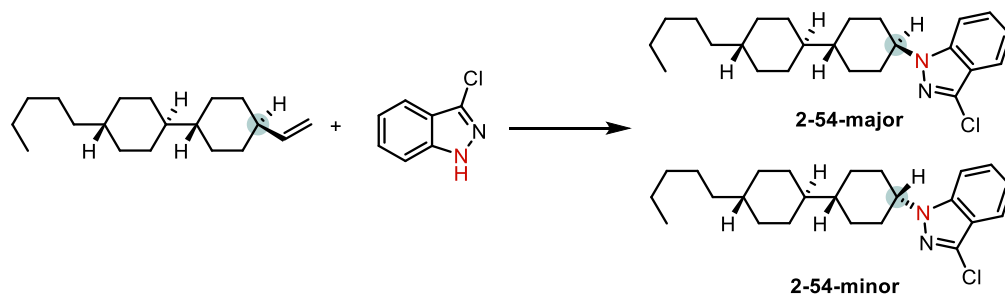
$^1\text{H NMR}$ (400 MHz, CDCl_3) δ 7.69 (d, $J = 8.2$ Hz, 1H), 7.47–7.35 (m, 2H), 7.20 (ddd, $J = 7.9, 6.6, 1.0$ Hz, 1H), 7.11 (s, 4H), 4.42–4.28 (m, 2H), 2.42 (tt, $J = 12.1, 3.3$ Hz, 1H), 2.33 (s, 3H), 1.97–1.72 (m, 10H), 1.51–1.35 (m, 2H), 1.30–0.93 (m, 9H).

$^{13}\text{C NMR}$ (100 MHz, CDCl_3) δ 144.86, 140.65, 135.21, 132.32, 128.98, 127.28, 126.69, 121.04, 119.84, 109.30, 47.30, 44.23, 43.22, 42.85, 37.14, 35.48, 34.69, 33.34, 30.41, 29.84, 21.02.

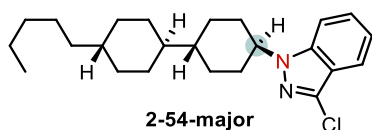
HRMS (ESI-TOF): $[\text{M}+\text{H}]^+$ calcd for $[\text{C}_{28}\text{H}_{36}\text{ClN}_2]^+$ m/z 435.2562, found 435.2561.

IR (neat, ATR): ν_{max} 2918, 2849, 1617, 1514, 1495, 1467, 1446, 1336, 1174, 980, 812, 767, 742 cm^{-1} .

M.p.: 115–118 $^\circ\text{C}$.



Prepared following **General procedure B** using **2-113** (15.3 mg, 0.100 mmol, 1.0 equiv), copper(I) chloride (2.00 mg, 0.0200 mmol, 20 mol %), 1,10-phenanthroline (3.6 mg, 0.0800 mmol, 20 mol %), and MeCN (2 mL) to make *Solution A*. The alkene **2-112** (52.5 mg, 0.200 mmol, 2.0 equiv) was dissolved in MeOH (1 mL) and DCM (10 mL) for ozonolysis. MeCN (1 mL) and benzene (3 mL) were used to make *Solution B*. The crude product was purified through FCC to give **2-54-major** ($R_f = 0.43$; hexanes/toluene, 4:1) as a white solid (12.5 mg, 32% yield) and **2-54-minor** ($R_f = 0.56$; hexanes/toluene, 4:1) as a white solid (9.6 mg, 25% yield).



$^1\text{H NMR}$ (400 MHz, CDCl_3) δ 7.65 (d, $J = 8.2$ Hz, 1H), 7.48–7.33 (m, 2H), 7.17 (ddd, $J = 7.9$, 6.2, 1.4 Hz, 1H), 4.31 (tt, $J = 10.4$, 6.6 Hz, 1H), 2.12–1.98 (m, 4H), 1.97–1.87 (m, 2H), 1.76 (t, $J = 12.4$ Hz, 4H), 1.37–1.20 (m, 9H), 1.19–1.07 (m, 4H), 1.02 (qd, $J = 12.6$, 11.6, 3.4 Hz, 2H), 0.93–0.81 (m, 5H).

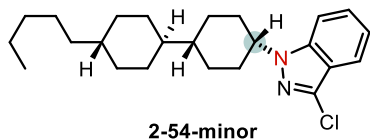
$^{13}\text{C NMR}$ (100 MHz, CDCl_3) δ 140.05, 132.12, 126.94, 120.98, 119.79, 109.44, 58.79, 43.03, 42.22, 37.87, 37.45, 33.58, 32.44, 32.25, 30.16, 29.15, 26.69, 22.74, 14.14.

HRMS (DART): $[\text{M}+\text{H}]^+$ calcd for $[\text{C}_{24}\text{H}_{36}\text{ClN}_2]^+$ m/z 387.2562, found 387.2555

IR (neat, ATR): ν_{max} 2921, 2851, 1616, 1494, 1465, 1449, 1337, 1194, 1005, 990, 765, 742 cm^{-1} .

1.

M.p.: 73–74 °C.



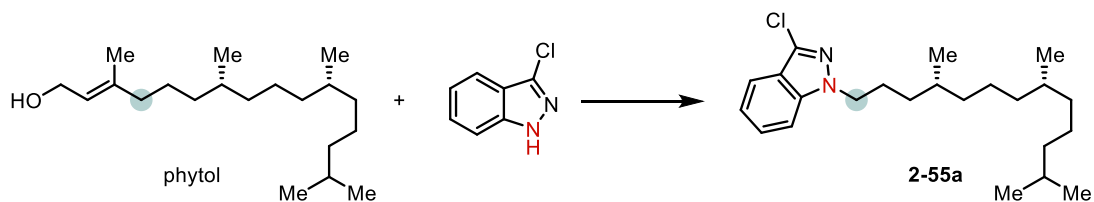
¹H NMR (400 MHz, CDCl₃) δ 7.66 (d, *J* = 8.2 Hz, 1H), 7.46–7.34 (m, 2H), 7.18 (ddd, *J* = 7.9, 5.3, 2.4 Hz, 1H), 4.44 (tt, *J* = 9.3, 4.0 Hz, 1H), 2.26–2.09 (m, 2H), 2.04–1.93 (m, 2H), 1.93–1.86 (m, 2H), 1.86–1.70 (m, 4H), 1.62–1.39 (m, 3H), 1.35–1.21 (m, 7H), 1.21–1.07 (m, 3H), 0.97–0.77 (m, 7H).

¹³C NMR (100 MHz, CDCl₃) δ 140.11, 131.92, 126.91, 120.98, 120.95, 119.76, 109.50, 57.65, 39.14, 37.69, 37.44, 36.68, 33.37, 32.27, 30.94, 28.34, 26.70, 26.66, 22.75, 14.15.

HRMS (DART): [M+H]⁺ calcd for [C₂₄H₃₆ClN₂]⁺ *m/z* 387.2562, found 387.2558

IR (neat, ATR): ν_{max} 2951, 2921, 2870, 2851, 1616, 1493, 1464, 1447, 1337, 1188, 764, 743 cm⁻¹.

M.p.: 73–74 °C.



Prepared following **General procedure B** using **2-113** (61.0 mg, 0.400 mmol, 1.0 equiv), copper(I) chloride (7.90 mg, 0.0800 mmol, 20 mol %), 1,10-phenanthroline (14.4 mg, 0.0800 mmol, 20 mol %), and MeCN (4 mL) to make *Solution A*. Phytol (237 mg, 0.800 mmol, 2.0 equiv), MeOH (2 mL), and DCM (10 mL) were used for ozonolysis. When the ozonolysis was complete, the ozonolysis mixture was diluted with DCM (70 mL). The solution was filtered through silica

gel (50 g) and washed with DCM/MeOH (40:1, 100 mL) and then the filtrate was concentrated. The residue was treated with MeCN (8 mL) to make *Solution B*. The crude product was purified through FCC to give **2-55a** ($R_f = 0.28$; hexanes/EtOAc, 60:1) as a colorless oil (116.0 mg, 77% yield).

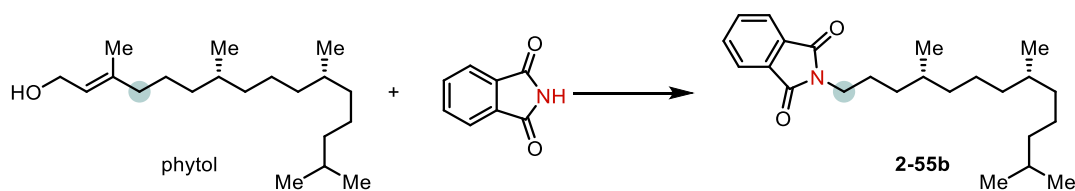
$^1\text{H NMR}$ (400 MHz, CDCl_3) δ 7.66 (d, $J = 8.2$ Hz, 1H), 7.46–7.32 (m, 2H), 7.18 (ddd, $J = 7.8, 6.5, 1.1$ Hz, 1H), 4.29 (t, $J = 7.3$ Hz, 2H), 2.02–1.80 (m, 2H), 1.52 (dp, $J = 13.2, 6.6$ Hz, 1H), 1.45–1.00 (m, 16H), 0.90–0.78 (m, 12H).

$^{13}\text{C NMR}$ (100 MHz, CDCl_3) δ 140.75, 132.36, 127.26, 121.00, 120.97, 119.80, 109.34, 49.63, 39.38, 37.36, 37.28, 37.16, 33.94, 32.78, 32.49, 28.00, 27.40, 24.81, 24.42, 22.75, 22.65, 19.74, 19.61.

HRMS (ESI-TOF): $[\text{M}+\text{H}]^+$ calcd for $[\text{C}_{23}\text{H}_{38}\text{ClN}_2]^+$ m/z 377.2718, found 377.2717.

IR (neat, ATR): ν_{max} 2953, 2926, 2867, 1617, 1496, 1467, 1376, 1337, 1174, 1126, 1006, 767, 742 cm^{-1} .

Optical Rotation: $[\alpha]_{\text{D}}^{25} = -1.17$ (c 0.2, CHCl_3)



Prepared following **General procedure A** using **2-114** (101 mg, 0.689 mmol, 1.0 equiv), copper(I) chloride (13.6 mg, 0.137 mmol, 20 mol %), 1,10-phenanthroline (24.9 mg, 0.137 mmol, 20 mol %), and MeCN (10 mL) to make *Solution A*. Phytol (297 mg, 1.00 mmol, 2.0 equiv), MeOH (3 mL), and DCM (15 mL) were used for ozonolysis. When the ozonolysis was complete, the ozonolysis mixture was diluted with DCM (100 mL). The solution was filtered through silica gel

(50 g) and washed with DCM/MeOH (40:1, 100 mL) and then the filtrate was concentrated. The residue was treated with MeCN (10 mL) to make *Solution B*. The crude product was purified through FCC to give **2-55b** ($R_f = 0.58$; hexanes/EtOAc, 9:1) as a colorless oil (white foam) (205.0 mg, 80% yield).

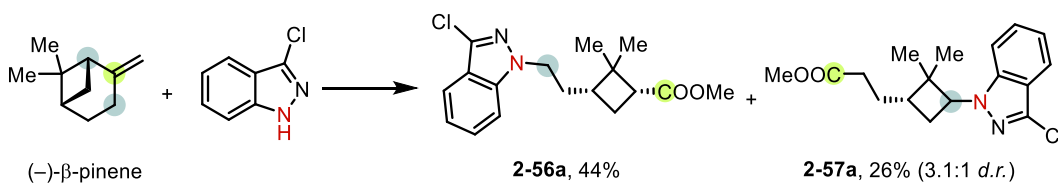
$^1\text{H NMR}$ (500 MHz, CDCl_3) δ 7.85–7.76 (m, 2H), 7.72–7.64 (m, 2H), 3.63 (t, $J = 7.5$ Hz, 2H), 1.75–1.56 (m, 2H), 1.49 (dp, $J = 13.3, 6.6$ Hz, 1H), 1.41 (dt, $J = 12.3, 6.2$ Hz, 1H), 1.38–1.27 (m, 3H), 1.27–1.07 (m, 9H), 1.07–0.97 (m, 3H), 0.87–0.81 (m, 9H), 0.80 (d, $J = 6.6$ Hz, 3H).

$^{13}\text{C NMR}$ (100 MHz, CDCl_3) δ 168.38, 133.77, 132.20, 123.10, 39.35, 38.36, 37.36, 37.26, 37.23, 34.03, 32.75, 32.51, 27.96, 26.20, 24.78, 24.43, 22.72, 22.62, 19.71, 19.57.

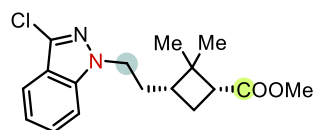
HRMS (DART): $[\text{M}+\text{H}]^+$ calcd for $[\text{C}_{24}\text{H}_{38}\text{NO}_2]^+$ m/z 373.2898, found 373.2895.

IR (neat, ATR): ν_{max} 2953, 2926, 2868, 1776, 1717, 1467, 1396, 1370 cm^{-1} .

Optical Rotation: $[\alpha]_{\text{D}}^{25} = 1.00$ (c 0.2, CHCl_3)



Prepared following **General procedure A** using **2-113** (76.3 mg, 0.500 mmol, 1.0 equiv), copper(I) chloride (9.90 mg, 0.100 mmol, 20 mol %), 1,10-phenanthroline (18.0 mg, 0.100 mmol, 20 mol %), and MeCN (5 mL) to make *Solution A*. $(-)\text{-}\beta\text{-Pinene}$ (136 mg, 1.00 mmol, 2.0 equiv) was used for ozonolysis and MeCN (5 mL) to make *Solution B*. The crude product was purified through FCC to give **2-56a** ($R_f = 0.59$; hexanes/EtOAc, 4:1) as a pale-yellow oil (70.0 mg, 44% yield) and **2-57b** ($R_f = 0.53$; hexanes/EtOAc, 4:1) as a pale-yellow oil (42.0 mg, 26% yield).



2-56a, 44%

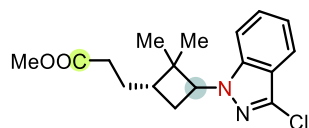
¹H NMR (400 MHz, CDCl₃) δ 7.66 (dt, *J* = 8.2, 1.0 Hz, 1H), 7.41 (ddd, *J* = 8.5, 6.8, 1.1 Hz, 1H), 7.34 (dt, *J* = 8.6, 0.8 Hz, 1H), 7.22–7.14 (m, 1H), 4.28–4.15 (m, 2H), 3.64 (s, 3H), 2.71–2.62 (m, 1H), 2.07–1.77 (m, 5H), 1.16 (s, 3H), 0.92 (s, 3H).

¹³C NMR (100 MHz, CDCl₃) δ 173.24, 140.63, 132.55, 127.40, 121.11, 121.02, 119.86, 109.17, 51.19, 47.40, 46.00, 42.56, 39.70, 30.37, 30.17, 24.32, 17.72.

HRMS (DART): [M+H]⁺ calcd for [C₁₇H₂₂ClN₂O₂]⁺ *m/z* 321.1364, found 321.1365.

IR (neat, ATR): ν_{\max} 2951, 2924, 2854, 1732, 1617, 1496, 1467, 1436, 1385, 1370, 1338, 1235, 1194, 1176, 767, 743 cm⁻¹.

Optical Rotation: $[\alpha]_{\text{D}}^{26} = 6.33$ (*c* 0.1, CHCl₃).



2-57a, 26% (3.1:1 *d.r.*)

¹H NMR (400 MHz, CDCl₃) **major:** δ 7.65 (dq, *J* = 8.1, 1.0 Hz, 0.75×1H), 7.43–7.29 (m, 0.75×2H), 7.22–7.13 (m, 0.75×1H), 4.53 (dd, *J* = 9.7, 8.1 Hz, 0.75×1H), 3.69 (s, 0.75×3H), 2.81 (q, *J* = 10.6 Hz, 0.75×1H), 2.48 (dt, *J* = 11.2, 7.8 Hz, 0.75×1H), 2.41–2.22 (m, 0.75×2H), 2.00–1.65 (m, 0.75×3H), 1.29 (s, 0.75×3H), 1.23 (s, 1H), 0.70 (s, 0.75×2H).

¹³C NMR (100 MHz, CDCl₃) **major:** δ 173.86, 141.02, 132.22, 127.22, 121.37, 121.25, 119.71, 109.58, 59.17, 51.60, 45.39, 38.31, 32.23, 29.52, 27.45, 25.34, 15.90.

¹H NMR (400 MHz, CDCl₃) **minor:** δ 7.65 (dq, *J* = 8.1, 1.0 Hz, 0.25×1H), 7.43–7.29 (m, 0.25×2H), 7.22–7.13 (m, 0.25×1H), 4.66 (dd, *J* = 8.1, 6.5 Hz, 0.25×1H), 3.69 (s, 0.25×3H), 3.21

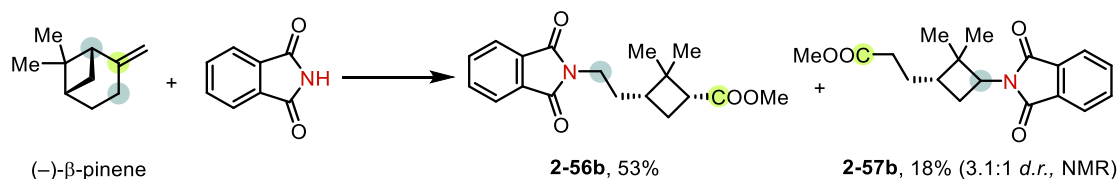
(tdd, $J = 11.4, 7.7, 4.5$ Hz, $0.25 \times 1\text{H}$), 2.41–2.22 (m, $0.25 \times 2\text{H}$), 2.22–2.09 (m, $0.25 \times 2\text{H}$), 2.00–1.65 (m, $0.25 \times 3\text{H}$), 1.23 (s, $0.25 \times 3\text{H}$), 0.69 (s, $0.25 \times 3\text{H}$).

^{13}C NMR (100 MHz, CDCl_3) **minor**: δ 174.02, 141.38, 132.26, 127.20, 121.30, 121.22, 119.71, 109.51, 59.78, 51.63, 43.56, 39.45, 32.48, 26.88, 26.34, 23.40, 23.28.

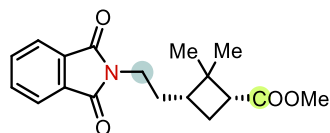
HRMS (DART): $[\text{M}+\text{H}]^+$ calcd for $[\text{C}_{17}\text{H}_{22}\text{ClN}_2\text{O}_2]^+$ m/z 321.1364, found 321.1364.

IR (neat, ATR): ν_{max} 2952, 2924, 28533, 1739, 1616, 1493, 1465, 1438, 1370, 1340, 1221, 1175, 768, 744 cm^{-1} .

Optical Rotation: $[\alpha]_{\text{D}}^{25} = 21.44$ (c 0.1, CHCl_3).



Prepared following **General procedure A** using phthalimide (29.4 mg, 0.200 mmol, 1.0 equiv), copper(I) chloride (4.00 mg, 0.0400 mmol, 20 mol %), 1,10-phenanthroline (7.20 mg, 0.0400 mmol, 20 mol %), and MeCN (2 mL) to make *Solution A*. (-)-β-Pinene (54.5 mg, 0.400 mmol, 2.0 equiv) was used for ozonolysis. After evaporation of MeOH *in vacuo*, the remaining residue had the smell of an artificial berry. MeCN (2 mL) was used to make *Solution B*. The crude product was dry-loaded onto SiO_2 and purified through FCC (Et_2O /toluene, from 0 to 5%) to provide a 3.1:1 ratio of regioisomers, with **2-57b** present as an inseparable mixture of diastereoisomers (ratio of 3.5:1), as determined by ^1H NMR spectroscopy with 1,3,5-trimethoxybenzene (33.6 mg, 0.2 mmol) as an internal standard. **2-56b** ($R_f = 0.52$; EtOAc/hexanes, 1:3) and **2-57b** ($R_f = 0.54$; EtOAc/hexanes, 1:3) were obtained as clear oils (**2-56b**: 33.0 mg, 53% yield).



2-56b

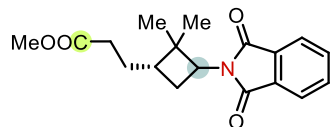
$^1\text{H NMR}$ (500 MHz, CDCl_3) δ 7.86–7.81 (m, 2H), 7.73–7.67 (m, 2H), 3.67–3.53 (m, 5H), 2.75–2.64 (m, 1H), 2.07–2.00 (m, 1H), 1.98–1.85 (m, 2H), 1.77–1.69 (m, 1H), 1.67–1.57 (m, 1H), 1.18 (s, 3H), 0.92 (s, 3H).

$^{13}\text{C NMR}$ (125 MHz, CDCl_3) δ 173.31, 168.33, 133.90, 132.12, 123.19, 51.16, 46.08, 42.60, 39.96, 36.33, 30.21, 29.26, 24.49, 17.52.

HRMS (DART): $[\text{M}+\text{H}]^+$ calcd for $[\text{C}_{18}\text{H}_{22}\text{NO}_4]^+$ m/z 316.1543, found 316.1544.

IR (neat, ATR): ν_{max} 2952, 2869, 1714, 1436, 1398, 1195, 1088, 1034 cm^{-1} .

Optical Rotation: $[\alpha]_{\text{D}}^{27} = 8.15$ (c 0.27, MeOH).



2-57b, (3.1:1 *d.r.*, NMR)

$^1\text{H NMR}$ (500 MHz, CD_3CN) **major:** δ 7.83–7.70 (m, 0.72 \times 4H), 4.13 (*dd*, $J = 10.5, 8.4$ Hz, 0.72 \times 1H), 3.62 (s, 0.72 \times 3H), 3.01 (*q*, $J = 10.6$ Hz, 0.72 \times 1H), 2.25 (*t*, $J = 7.8$ Hz, 0.72 \times 2H), 2.15 (*d*, $J = 8.2$ Hz, 0.72 \times 2H), 1.78–1.67 (m, 0.72 \times 1H), 1.68–1.59 (m, 0.72 \times 1H), 1.15 (s, 0.72 \times 3H), 0.96 (s, 0.72 \times 3H).

$^{13}\text{C NMR}$ (125 MHz, CD_3CN) **major:** δ 173.61, 169.40, 134.08, 131.87, 122.62, 52.88, 50.95, 45.37, 39.52, 31.82, 28.63, 25.86, 25.20, 15.93.

$^1\text{H NMR}$ (500 MHz, CD_3CN) **minor:** δ 7.83–7.70 (m, 0.28 \times 4H), 4.37–4.27 (m, 0.28 \times 1H), 3.62 (s, 0.28 \times 3H), 3.29 (*ddd*, $J = 12.0, 9.3, 5.4$ Hz, 0.28 \times 1H), 2.25 (*t*, $J = 7.8$ Hz, 0.28 \times 2H), 2.15 (*d*, J

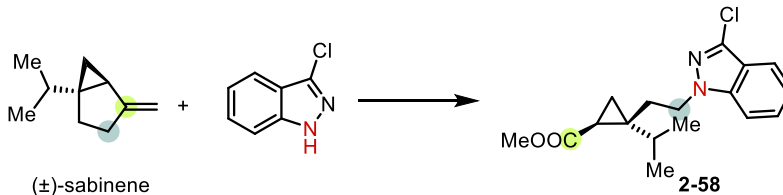
= 8.2 Hz, 0.28×2H), 1.78–1.67 (m, 0.28×1H), 1.68–1.59 (m, 0.28×1H), 1.10 (s, 0.28×3H), 1.00 (s, 0.28×3H),.

¹³C NMR (125 MHz, CD₃CN) **minor**: δ 173.69, 169.21, 134.11, 131.87, 122.68, 53.14, 50.95, 43.02, 40.07, 31.98, 25.84, 24.36, 23.73, 22.61.

HRMS (DART): [M+H]⁺ calcd for [C₁₈H₂₂NO₄]⁺ *m/z* 316.1543, found 316.1541.

IR (neat, ATR): ν_{max} 2952, 2869, 1736, 1612, 1467, 1370, 1173, 1089, 1051, 1017 cm⁻¹.

Optical Rotation: [α]_D²⁷ = 11.15 (*c* 0.52, MeOH).



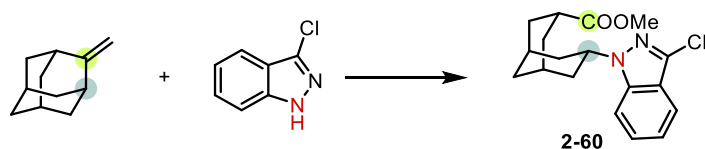
Prepared following **General procedure A** using **2-113** (76.3 mg, 0.500 mmol, 1.0 equiv), copper(I) chloride (9.90 mg, 0.100 mmol, 20 mol %), 1,10-phenanthroline (18.0 mg, 0.100 mmol, 20 mol %), and MeCN (4 mL) to make *Solution A*. (±)-Sabinene (136 mg, 1.00 mmol, 2 equiv) was used for ozonolysis and MeCN (4 mL) to make *Solution B*. The crude product was purified through FCC to give **2-58** (*R*_f = 0.63; hexanes/EtOAc, 4:1) as a pale-yellow oil (124.5 mg, 78% yield).

¹H NMR (500 MHz, CDCl₃) δ 7.64 (d, *J* = 8.2 Hz, 1H), 7.47–7.38 (m, 2H), 7.17 (ddd, *J* = 7.9, 6.4, 1.2 Hz, 1H), 4.42 (ddd, *J* = 13.9, 10.3, 6.1 Hz, 1H), 4.27 (ddd, *J* = 13.9, 10.4, 6.0 Hz, 1H), 3.67 (s, 3H), 2.18–2.04 (m, 2H), 1.62 (dd, *J* = 8.3, 5.7 Hz, 1H), 1.45 (hept, *J* = 6.8 Hz, 1H), 1.15–1.09 (m, 1H), 1.00–0.95 (m, 4H), 0.93 (d, *J* = 6.9 Hz, 3H).

¹³C NMR (125 MHz, CDCl₃) δ 173.23, 140.50, 132.28, 127.36, 121.07, 121.04, 119.66, 109.60, 51.82, 48.10, 34.50, 33.52, 27.71, 24.36, 19.45, 19.28, 18.97.

HRMS (DART): $[M+H]^+$ calcd for $[C_{17}H_{22}ClN_2O_2]^+$ m/z for 321.1364, found 321.1364

IR (neat, ATR): ν_{\max} 2959, 2879, 1725, 1618, 1496, 1468, 1438, 1390, 1338, 1194, 1174, 766, 746 cm^{-1} .



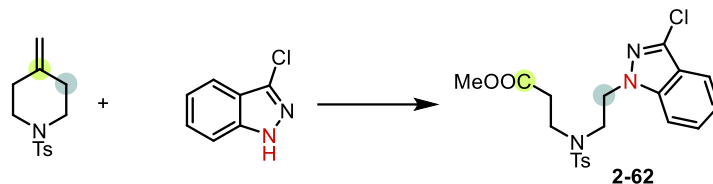
Prepared following **General procedure A** using **2-113** (61.0 mg, 0.400 mmol, 1.0 equiv), copper(I) chloride (7.90 mg, 0.0800 mmol, 20 mol %), 1,10-phenanthroline (14.4 mg, 0.0800 mmol, 20 mol %), and MeCN (4 mL) to make *Solution A*. The alkene **2-59** (119 mg, 0.800 mmol, 2.0 equiv) was used for ozonolysis and MeCN (4 mL) to make *Solution B*. The crude product was purified through FCC to give **2-60** ($R_f = 0.29$; toluene) as a colorless oil (68.9 mg, 52% yield).

^1H NMR (400 MHz, CDCl_3) δ 7.64 (dt, $J = 8.2, 0.9$ Hz, 1H), 7.47 (d, $J = 8.6$ Hz, 1H), 7.44–7.35 (m, 1H), 7.17 (ddd, $J = 8.0, 6.7, 0.9$ Hz, 1H), 4.83 (tt, $J = 12.2, 4.8$ Hz, 1H), 3.73 (s, 3H), 2.64 (tt, $J = 11.5, 6.6$ Hz, 1H), 2.41–2.32 (m, 2H), 2.32–2.21 (m, 2H), 2.17 (td, $J = 13.0, 3.6$ Hz, 2H), 1.94–1.83 (m, 2H), 1.76–1.63 (m, 3H), 1.40 (dt, $J = 13.1, 2.2$ Hz, 1H).

^{13}C NMR (100 MHz, CDCl_3) δ 177.10, 140.23, 132.28, 127.15, 121.17, 120.93, 119.75, 109.36, 51.86, 50.98, 38.70, 35.48, 29.48, 28.31, 25.61.

HRMS (DART): $[M+H]^+$ calcd for $[C_{18}H_{22}ClN_2O_2]^+$ m/z 333.1364, found 333.1362

IR (neat, ATR): ν_{\max} 2948, 2924, 2870, 1731, 1616, 1494, 1466, 1337, 1298, 1280, 1222, 1192, 1174, 743 cm^{-1} .



Prepared following **General procedure A** using **2-113** (61.0 mg, 0.400 mmol, 1.0 equiv), copper(I) chloride (7.90 mg, 0.0800 mmol, 20 mol %), 1,10-phenanthroline (14.4 mg, 0.0800 mmol, 20 mol %), and MeCN (4 mL) to make *Solution A*. The alkene **2-61** (201 mg, 0.800 mmol, 2.0 equiv) was used for ozonolysis and MeCN (4 mL) to make *Solution B*. The crude product was purified through FCC to give **2-62** ($R_f = 0.45$; toluene/Et₂O, 10:1) as a white solid (141.7 mg, 81% yield).

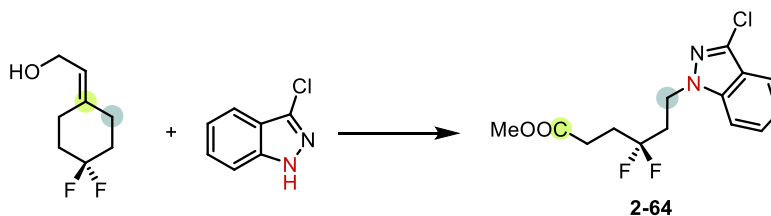
¹H NMR (400 MHz, CDCl₃) δ 7.67–7.59 (m, 3H), 7.53 (d, $J = 8.6$ Hz, 1H), 7.50–7.42 (m, 1H), 7.27–7.17 (m, 3H), 4.58 (t, $J = 6.5$ Hz, 2H), 3.60 (s, 3H), 3.53 (t, $J = 6.5$ Hz, 2H), 3.30 (t, $J = 14.8$, 2H), 2.40 (s, 3H), 2.30 (t, $J = 14.8$, 2H).

¹³C NMR (100 MHz, CDCl₃) δ 171.39, 143.86, 141.45, 135.28, 133.59, 129.86, 128.01, 127.20, 121.55, 120.98, 119.64, 109.70, 51.83, 48.96, 48.86, 45.91, 33.69, 21.54.

HRMS (DART): $[M+H]^+$ calcd for [C₂₀H₂₃ClN₃O₄S]⁺ m/z 436.1092, found 436.1091.

IR (neat, ATR): ν_{\max} 2954, 1737, 1619, 1599, 1497, 1468, 1438, 1338, 1258, 1205, 1160, 1090, 816, 766, 747 cm⁻¹.

M.p.: 83–85 °C.

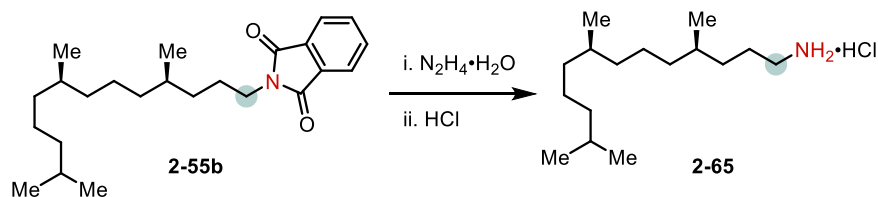


Prepared following **General procedure B** using **2-113** (30.5 mg, 0.200 mmol, 1.0 equiv), copper(I) chloride (4.00 mg, 0.0400 mmol, 20 mol %), 1,10-phenanthroline (7.20 mg, 0.0400 mmol, 20 mol %), and MeCN (2 mL) to make *Solution A*. **2-63** (64.9 mg, 0.400 mmol, 2.0 equiv), MeOH (4 mL), and DCM (10 mL) were used for ozonolysis. When ozonolysis was complete, DCM (150 mL) was added to dilute the ozonolysis mixture. The mixture was filtered through silica gel (50 g) and washed with DCM/MeOH (40:1, 400 mL) and then the filtrate was concentrated. The residue was treated with MeCN (2 mL) to make *Solution B*. The crude product was purified through FCC to give **2-64** ($R_f = 0.44$; hexanes/EtOAc, 4:1) as a colorless oil (55.9 mg, 88% yield). $^1\text{H NMR}$ (400 MHz, CDCl_3) δ 7.66 (dt, $J = 8.2, 1.0$ Hz, 1H), 7.48–7.34 (m, 2H), 7.20 (ddd, $J = 8.2, 6.7, 1.0$ Hz, 1H), 4.59–4.46 (m, 2H), 3.67 (s, 3H), 2.58–2.41 (m, 4H), 2.27–2.11 (m, 2H). $^{13}\text{C NMR}$ (100 MHz, CDCl_3) δ 172.50, 140.78, 133.36, 127.75, 122.97, 121.44 (t, $J = 240.5$ Hz), 121.13, 119.89, 109.17, 51.96, 42.38 (t, $J = 5.7$ Hz), 36.42 (t, $J = 24.7$ Hz), 32.11 (t, $J = 25.2$ Hz), 26.79 (t, $J = 4.8$ Hz).

HRMS (DART): $[\text{M}+\text{H}]^+$ calcd for $[\text{C}_{14}\text{H}_{16}\text{ClF}_2\text{N}_2\text{O}_2]^+$ m/z 317.0863, found 317.0863.

IR (neat, ATR): ν_{max} 2953, 1739, 1618, 1497, 1469, 1439, 1337, 1202, 1178, 1130, 932, 767, 744 cm^{-1} .

2.6.5.4. Synthesis of chiral amines



The ammonium chloride **2-65** was synthesized according to a literature procedure.⁷⁴ The phthalimide **2-55b** (186 mg, 0.500 mmol) was dissolved in 0.3 M methanolic hydrazine hydrate (10 mL) and heated under reflux for 3 h. The reaction mixture was concentrated and DCM (10

mL) was added. The resulting suspension was filtered and the filtrate concentrated. The residue was acidified (pH < 2) by adding 1.0 M HCl and extracted twice with DCM. The organic phase was washed with brine, dried (Na₂SO₄), and concentrated. The residue was purified through FCC (*R*_f = 0.56; MeOH/EtOAc, 1:10) to give **2-65** as an off-white solid (85.5 mg, 75% yield).

¹H NMR (500 MHz, CDCl₃) δ 8.21 (brs, 3H), 2.96 (h, *J* = 12.7 Hz, 2H), 1.89–1.61 (m, 2H), 1.51 (dp, *J* = 13.1, 6.6 Hz, 1H), 1.44–1.31 (m, 3H), 1.31–1.09 (m, 10H), 1.09–0.98 (m, 3H), 0.91–0.75 (m, 12H).

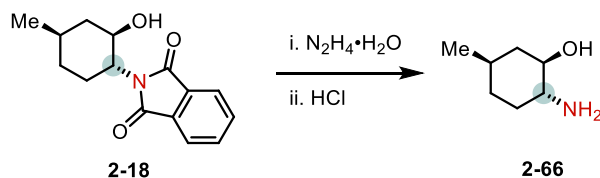
¹³C NMR (125 MHz, CDCl₃) 40.34, 39.37, 37.39, 37.30, 37.27, 33.82, 32.83, 32.39, 27.98, 25.33, 24.81, 24.49, 22.74, 22.64, 19.72, 19.38.

HRMS (DART): [M–Cl]⁺ calcd for [C₁₆H₃₆N]⁺ *m/z* 242.2842, found 242.2840.

IR (neat, ATR): ν_{max} 3429 (br), 2958, 2925, 2870, 2852, 1610, 1509, 1468, 1380, 1259 cm⁻¹.

Optical Rotation: [α]_D²⁶ = 0.50 (*c* 0.2, CH₂Cl₂).

M.p.: 69–72 °C.



The ammonium salt **2-66** was synthesized according to a literature procedure.⁷⁴ The phthalimide **2-18** (130 mg, 0.500 mmol) was dissolved in 0.3 M methanolic hydrazine hydrate (5 mL). After the mixture had stirred for 0.5 h at room temperature, 5% HCl (2 mL) was added and the reaction mixture was stirred for an additional 12 h. The resulting suspension was filtered and then the filtrate was diluted with an equal amount of water, acidified (pH < 2), and washed with DCM. The organic phase was discarded. The aqueous phase was basified with solid KOH (pH >10) and then

extracted with ether (2×15 mL). The combined ethereal layers were washed with brine, dried (Na_2SO_4), and concentrated. The residue was dissolved in DCM (5 mL) and the insoluble solid removed through filtration. The filtrate was concentrated to give the off-white solid, which was washed with cool pentane to give **2-66** as an off-white solid (51.1 mg, 79% yield).

^1H NMR (400 MHz, CDCl_3) δ 3.23–3.03 (m, 1H), 2.37 (t, $J = 7.4$ Hz, 1H), 2.15–1.68 (m, 5H), 1.63 (d, $J = 13.0$ Hz, 1H), 1.51 (ttt, $J = 12.9, 6.5, 3.4$ Hz, 1H), 1.14 (qd, $J = 13.0, 3.5$ Hz, 1H), 1.04–0.84 (m, 5H).

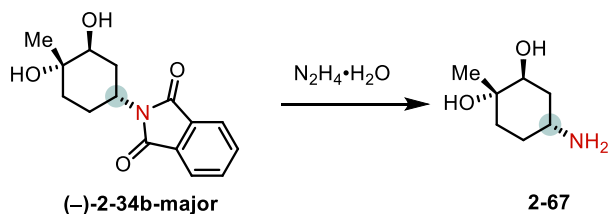
^{13}C NMR (125 MHz, CDCl_3) δ 75.55, 56.89, 42.13, 34.63, 33.83, 31.43, 22.00.

HRMS (DART): $[\text{M}+\text{H}]^+$ calcd for $[\text{C}_7\text{H}_{16}\text{NO}]^+$ m/z 130.1226, found 130.1223.

IR (neat, ATR): ν_{max} 3288 (br), 2950, 2925, 2867, 2854, 1581, 1456, 1048 cm^{-1} .

Optical Rotation: $[\alpha]_{\text{D}}^{25} = -17.00$ (c 0.1, CH_2Cl_2).

M.p.: 76–78 $^\circ\text{C}$.



The phthalimide **2-34b** (71.6 mg, 0.260 mmol) was dissolved in 0.3 M methanolic hydrazine hydrate (3 mL). After heating under reflux for 1 h, the reaction mixture was concentrated *in vacuo*. The residue was purified through silica gel FCC ($R_f = 0.38$; 7 N NH_3 in MeOH solution/DCM, 2:5) to afford **2-67** as a yellow solid (27.8 mg, 74% yield).

^1H NMR (500 MHz, CD_3OD) δ 3.56 (t, $J = 3.3$ Hz, 1H), 3.00 (tt, $J = 9.9, 4.8$ Hz, 1H), 1.86–1.66 (m, 3H), 1.66–1.58 (m, 1H), 1.58–1.45 (m, 2H), 1.19 (s, 3H).

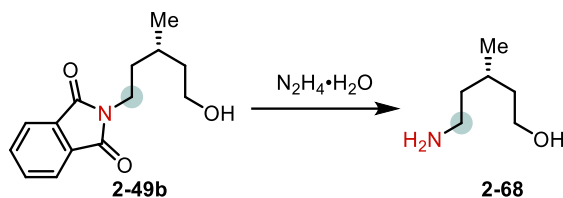
^{13}C NMR (125 MHz, CD_3OD) δ 73.06, 70.02, 44.27, 37.20, 31.92, 29.54, 25.33.

HRMS (DART): $[\text{M}+\text{H}]^+$ calcd for $[\text{C}_7\text{H}_{16}\text{NO}_2]^+$ m/z 146.1176, found 146.1175.

IR (neat, ATR): ν_{\max} 3341 (br), 3289 (br), 2927, 2869, 1634, 1598, 1563, 1454, 1376, 1181, 1133, 1042 cm^{-1} .

Optical Rotation: $[\alpha]_{\text{D}}^{27} = 12.50$ (c 0.2, MeOH).

M.p.: 137–140 $^{\circ}\text{C}$.



The phthalimide **2-49b** (170 mg, 0.690 mmol) was dissolved in 0.2 M methanolic hydrazine hydrate (10 mL). After heating under reflux for 5 h, the reaction mixture was concentrated *in vacuo*. DCM (10 mL) was added to the residue and the resulting suspension was filtered. The filtrate was concentrated and the residue purified through silica gel FCC ($R_f = 0.29$; 7 N NH_3 in MeOH solution/DCM, 1:5) to give a yellow oil. DCM (5 mL) was added and the resulting suspension was filtered to remove the silica that had dissolved in the eluent. The DCM solution was concentrated to afford **2-68** as a yellow oil (64.1 mg, 80% yield).

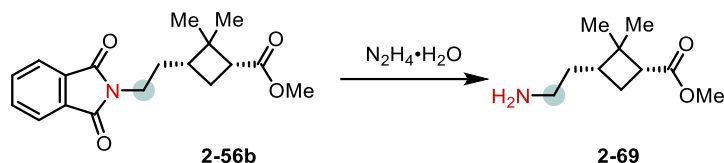
^1H NMR (400 MHz, CD_3OD) δ 3.64–3.51 (m, 2H), 2.83–2.44 (m, 2H), 1.69–1.43 (m, 3H), 1.39–1.25 (m, 2H), 0.90 (d, $J = 6.6$ Hz, 3H).

^{13}C NMR (75 MHz, CDCl_3) δ 60.66, 40.37, 39.90, 39.81, 27.22, 20.19.

HRMS (DART): $[\text{M}+\text{H}]^+$ calcd for $[\text{C}_6\text{H}_{16}\text{NO}]^+$ m/z 118.1226, found 118.1226.

IR (neat, ATR): ν_{\max} 3315 (br), 2957, 2925, 2871, 1565, 1469, 1383, 1324, 1088, 883 cm^{-1} .

Optical Rotation: $[\alpha]_{\text{D}}^{25} = -3.50$ (c 0.2, CH_2Cl_2).



A round-bottom flask was charged with a stirrer bar, the ester **2-55b** (78.8 mg, 0.250 mmol), and of 0.5 M hydrazine (2.2 equiv) in MeOH (1.1 mL). The mixture was heated under reflux. After 45 min [when the starting material was fully consumed (TLC)], the reaction mixture was allowed to cool and the solvent was evaporated *in vacuo*. The residue was treated with minimal MeOH to form a homogenous solution, which was dry-loaded onto a SiO₂ column and subjected to FCC to obtain **2-69** (*R*_f = 0.41; DCM/7 N NH₃ in MeOH, 12:1) as a clear oil (33.5 mg, 72% yield).

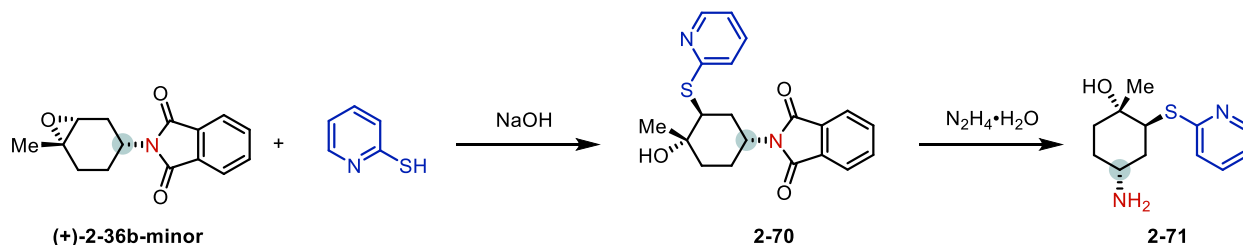
¹H NMR (400 MHz, CDCl₃) δ 3.62 (s, 3H), 2.74–2.41 (m, 3H), 2.04–1.76 (m, 3H), 1.48 (dq, *J* = 14.1, 7.8, 7.0 Hz, 1H), 1.35 (dq, *J* = 14.4, 8.1 Hz, 1H), 1.24–1.13 (m, 4H), 0.88 (s, 3H).

¹³C NMR (125 MHz, CDCl₃) δ 173.46, 1.09, 46.08, 42.67, 40.38, 40.06, 34.59, 30.25, 24.59, 17.51.

HRMS (DART): [M+H]⁺ calcd for [C₁₀H₂₀NO₂]⁺ *m/z* 186.1489, found 186.1495.

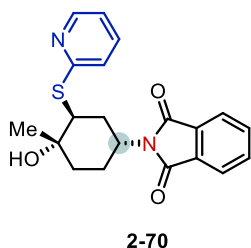
IR (neat, ATR): ν_{max} 3305 (br), 2952, 2926, 2872, 1732, 1574, 1463, 1435, 1324, 1195, 1178 cm⁻¹.

Optical Rotation: [α]_D²⁷ = -1.60 (*c* 0.25, MeOH).



A 20-mL vial was equipped with a stirrer bar and charged with sodium hydroxide (400 mg, 10.0 mmol) and ethanol (12 mL) to form a solution (0.83 M). An 8-mL Schlenk tube was charged with

the phthalimide **2-(+)-36b-minor** (88.1 mg, 0.340 mmol, 1.0 equiv) and 2-mercaptopyridine (128 mg, 1.15 mmol, 3.0 equiv) and then capped with a stopper. The reaction vessel was purged with argon three times before the NaOH solution (0.41 mL, 1.0 equiv) and ethanol (1.6 mL) were added. The reaction vessel was stirred at 50 °C for 12 h and then EtOAc (5 mL) was added. This mixture was washed with sat. aqueous NH₄Cl (2 × 10 mL) and brine (10 mL). The organic phase was dried (Na₂SO₄) and filtered. Evaporation of all volatiles under reduced pressure and purification of the residue through FCC (*R*_f = 0.42; hexanes/EtOAc, 1:1) yielded **2-70** as a pale-yellow solid (93.0 mg, 73% yield).



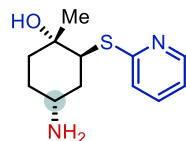
¹H NMR (500 MHz, CDCl₃) δ 8.37 (ddd, *J* = 4.9, 1.8, 0.9 Hz, 1H), 7.85–7.74 (m, 2H), 7.72–7.64 (m, 2H), 7.51–7.42 (m, 1H), 7.20 (dt, *J* = 8.1, 0.8 Hz, 1H), 6.96 (ddd, *J* = 7.3, 4.9, 1.0 Hz, 1H), 4.57 (tt, *J* = 12.1, 4.2 Hz, 1H), 4.45 (q, *J* = 3.5 Hz, 1H), 3.27 (ddd, *J* = 13.3, 12.2, 4.0 Hz, 1H), 2.60 (qd, *J* = 12.7, 4.7 Hz, 1H), 2.12 (s, 1H), 1.92–1.73 (m, 3H), 1.68–1.57 (m, 1H), 1.41 (s, 3H).
¹³C NMR (125 MHz, CDCl₃) δ 168.31, 157.86, 149.27, 136.06, 133.81, 131.99, 123.07, 123.02, 119.70, 71.39, 49.81, 46.54, 35.10, 31.03, 28.44, 24.73.

HRMS (DART): [M+H]⁺ calcd for [C₂₀H₂₁N₂O₃S]⁺ *m/z* 369.1267, found 369.1267.

IR (neat, ATR): ν_{max} 3471 (br), 3057, 2964, 2928, 2868, 1709, 1579, 1376, 1122, 1085 cm⁻¹.

Optical Rotation: [α]_D²⁶ = 64.00 (*c* 0.2, CH₂Cl₂).

M.p.: 183–185 °C.



2-71

The phthalimide **2-70** (73.6 mg, 0.2 mmol) was dissolved in 0.3 M methanolic hydrazine hydrate (2 mL). After heating under reflux for 1 h, the reaction mixture was concentrated *in vacuo*. DCM (10 mL) was added to the residue and the resulting suspension was filtered. The filtrate was concentrated and the residue was purified through silica gel FCC ($R_f = 0.46$; 7 N NH_3 in MeOH/DCM, 1:10) to give an off-white solid. DCM (2 mL) was added and the resulting suspension was filtered to remove silica that had dissolved in the eluent. The DCM solution was concentrated to afford **2-71** as an off-white solid (43.4 mg, 91% yield).

$^1\text{H NMR}$ (500 MHz, CDCl_3) δ 8.34 (ddd, $J = 5.0, 1.8, 0.9$ Hz, 1H), 7.46 (ddd, $J = 8.1, 7.4, 1.9$ Hz, 1H), 7.22 (dt, $J = 8.1, 1.0$ Hz, 1H), 6.98 (ddd, $J = 7.3, 5.0, 1.0$ Hz, 1H), 4.15 (dd, $J = 11.4, 4.0$ Hz, 1H), 3.33–3.14 (m, 1H), 1.98 (dtd, $J = 13.6, 4.3, 1.8$ Hz, 1H), 1.91 (td, $J = 13.3, 4.3$ Hz, 1H), 1.86–1.73 (m, 2H), 1.70–1.61 (m, 1H), 1.61–1.52 (m, 1H), 1.26 (s, 3H).

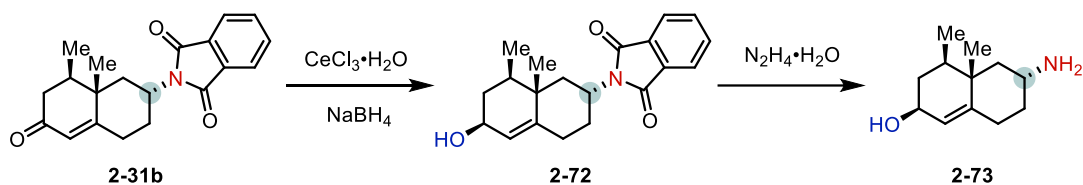
$^{13}\text{C NMR}$ (125 MHz, CDCl_3) δ 159.16, 148.80, 136.35, 122.90, 119.83, 72.42, 50.22, 46.05, 38.67, 35.47, 30.70, 22.79.

HRMS (DART): $[\text{M}+\text{H}]^+$ calcd for $[\text{C}_{12}\text{H}_{19}\text{N}_2\text{OS}]^+$ m/z 239.1213, found 239.1213.

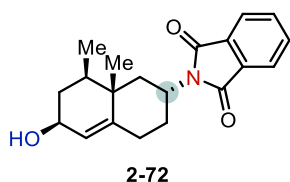
IR (neat, ATR): ν_{max} 3253 (br), 2929, 2869, 1579, 1453, 1414, 1121 cm^{-1} .

Optical Rotation: $[\alpha]_{\text{D}}^{25} = 28.50$ (c 0.2, CH_2Cl_2).

M.p.: 127–128 $^{\circ}\text{C}$.



$\text{CeCl}_3 \cdot \text{H}_2\text{O}$ (196 mg, 0.520 mmol) was added to a stirred solution of the enone **2-31b** (163 mg, 0.500 mmol) in EtOH (5 mL) while cooling in an ice bath. NaBH_4 (37.8 mg, 1.00 mmol) was added slowly. After 10 min, the reaction was quenched through the addition of aq. NH_4Cl (10 mL). The aqueous phase was extracted with DCM three times. The combined organics were washed with brine, dried (Na_2SO_4), and concentrated *in vacuo*. The residue was purified through silica gel FCC ($R_f = 0.25$; EtOAc/hexanes, 3:7) to furnish **2-72** as a white foam (99.1 mg, 61% yield).



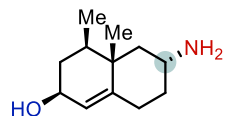
$^1\text{H NMR}$ (500 MHz, CDCl_3) δ 7.81 (dd, $J = 5.2, 3.1$ Hz, 2H), 7.69 (dd, $J = 5.3, 3.1$ Hz, 2H), 5.41 (s, 1H), 4.50 (tt, $J = 12.6, 3.6$ Hz, 1H), 4.34–4.24 (m, 1H), 2.43 (t, $J = 13.6$ Hz, 1H), 2.35–2.19 (m, 2H), 2.02 (t, $J = 12.7$ Hz, 1H), 1.89–1.74 (m, 3H), 1.63 (dq, $J = 15.3, 8.6, 7.8$ Hz, 2H), 1.09 (s, 3H), 0.86 (d, $J = 6.9$ Hz, 3H).

$^{13}\text{C NMR}$ (125 MHz, CDCl_3) δ 168.43, 143.56, 133.86, 131.97, 125.56, 123.07, 67.88, 47.37, 41.61, 39.02, 38.70, 36.82, 31.55, 30.43, 17.99, 15.33.

HRMS (DART): $[\text{M}+\text{H}]^+$ calcd for $[\text{C}_{20}\text{H}_{24}\text{NO}_3]^+$ m/z 326.1751, found 326.1754.

IR (neat, ATR): ν_{max} 3408 (br), 2956, 2928, 2857, 1767, 1709, 1376, 721 cm^{-1} .

Optical Rotation: $[\alpha]_{\text{D}}^{24} = 19.50$ (c 0.2, CHCl_3)



2-73

The alcohol **2-72** (80.0 mg, 0.220 mmol) was dissolved in 0.3 M methanolic hydrazine hydrate (5 mL). After heating under reflux for 6 h, the reaction mixture was concentrated *in vacuo*. DCM (10 mL) was added to the residue and the resulting suspension was filtered. The filtrate was concentrated and the residue purified through silica gel FCC ($R_f = 0.43$; 7 N NH_3 in MeOH/MeOH/DCM, 1:1:10) to provide an off-white solid. DCM (2 mL) was added and the resulting suspension was filtered to remove the silica that had dissolved in eluent. The DCM solution was concentrated to afford **2-73** as an off-white solid (33.4 mg, 70% yield).

^1H NMR (400 MHz, CDCl_3) δ 5.31 (d, $J = 1.6$ Hz, 1H), 4.20 (ddt, $J = 10.0, 6.3, 2.2$ Hz, 1H), 2.95 (s, 1H), 2.29 (tdt, $J = 14.1, 4.3, 2.1$ Hz, 1H), 2.06 (ddd, $J = 14.3, 4.2, 2.6$ Hz, 1H), 1.97 (dt, $J = 12.5, 2.9$ Hz, 1H), 1.94–1.83 (m, 1H), 1.73 (ddt, $J = 12.3, 6.4, 2.0$ Hz, 1H), 1.60 (s, 2H), 1.48 (dq, $J = 13.6, 6.9, 2.2$ Hz, 1H), 1.32 (td, $J = 12.6, 9.9$ Hz, 1H), 1.02 (dtd, $J = 13.9, 11.9, 4.3$ Hz, 1H), 0.94 (s, 3H), 0.87 (d, $J = 6.9$ Hz, 3H), 0.77 (t, $J = 12.1$ Hz, 1H).

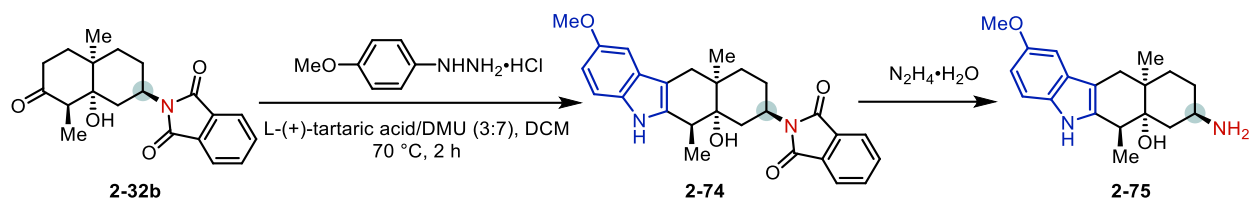
^{13}C NMR (100 MHz, CDCl_3) δ 144.70, 124.98, 67.66, 49.49, 46.76, 39.22, 38.41, 38.01, 36.90, 31.37, 18.52, 15.39.

HRMS (DART): $[\text{M}+\text{H}]^+$ calcd for $[\text{C}_{12}\text{H}_{22}\text{NO}]^+$ m/z 196.1696, found 196.1695.

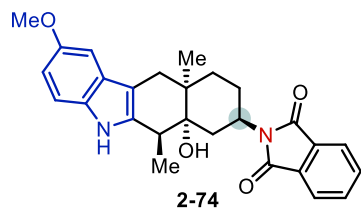
IR (neat, ATR): ν_{max} 3304 (br), 2965, 2925, 2854, 1582, 1459, 1328, 1148, 1086, 1028 cm^{-1} .

Optical Rotation: $[\alpha]_{\text{D}}^{25} = 39.00$ (c 0.1, CH_2Cl_2).

M.p.: 123–126 $^{\circ}\text{C}$.



The indole **2-74** was synthesized following a modification of the procedure reported in the literature.⁷⁵ A mixture of L-(+)-tartaric acid and DMU (30:70; 6.00 g) was heated at 90 °C to obtain a clear melt. 4-Methoxyphenylhydrazine hydrochloride (140 mg, 0.800 mmol) was added to the melt. Once the hydrazine hydrochloride had dissolved, the melt was cooled to 70 °C. The ketone **2-32b** (205 mg, 0.600 mmol) was dissolved in a minimum of DCM and added to the melt mixture at 70 °C. The mixture was stirred at 70 °C for 2 h, then cooled to room temperature and treated with water (10 mL) and EtOAc (10 mL). The aqueous phase was extracted with EtOAc (2 × 10 mL). The organic phase was washed with brine (10 mL), dried (Na₂SO₄), and concentrated under reduced pressure. The residue was purified through silica gel FCC (*R_f* = 0.46; EtOAc/hexanes, 1:1) to give **2-74** as a yellow solid (145.4 mg, 55% yield).



¹H NMR (400 MHz, CD₃CN) δ 8.77 (s, 1H), 7.76–7.63 (m, 4H), 7.23–7.17 (m, 1H), 6.95 (d, *J* = 2.5 Hz, 1H), 6.71 (dd, *J* = 8.7, 2.4 Hz, 1H), 4.60 (tt, *J* = 12.7, 4.9 Hz, 1H), 3.82 (s, 3H), 3.24 (dd, *J* = 16.2, 2.0 Hz, 1H), 3.04 (q, *J* = 6.9, 6.2 Hz, 1H), 2.84–2.67 (m, 1H), 2.54 (qd, *J* = 13.3, 4.8 Hz, 1H), 2.36 (d, *J* = 16.1 Hz, 1H), 2.16–1.98 (m, 2H), 1.96 (s, 1H), 1.67–1.54 (m, 2H), 1.42 (ddd, *J* = 13.6, 4.6, 2.1 Hz, 1H), 1.26 (d, *J* = 7.1 Hz, 3H), 0.97 (s, 3H).

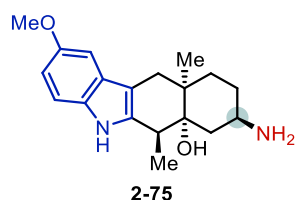
^{13}C NMR (100 MHz, CD_3CN) δ 169.33, 154.73, 137.57, 134.89, 133.02, 132.64, 129.18, 123.54, 112.26, 111.35, 106.58, 100.68, 76.65, 56.20, 46.85, 38.32, 38.07, 34.60, 30.99, 30.65, 24.93, 22.22, 11.55.

HRMS (DART): $[\text{M}+\text{H}]^+$ calcd for $[\text{C}_{27}\text{H}_{29}\text{N}_2\text{O}_4]^+$ m/z 440.2122, found 440.2109.

IR (neat, ATR): ν_{max} 3537 (br), 3413 (br), 2936, 2851, 1702, 1482, 1467, 1396, 1374, 1216, 1145, 1083 cm^{-1} .

Optical Rotation: $[\alpha]_{\text{D}}^{25} = 140.00$ (c 0.1, CH_2Cl_2).

M.p.: 154 $^\circ\text{C}$ (decomposition).



The indole **2-74** (88.9 mg, 0.200 mmol) was dissolved in 0.3 M methanolic hydrazine hydrate (5 mL). After heating under reflux for 2 h under argon, the reaction mixture was concentrated *in vacuo*. DCM (10 mL) was added to the residue and the resulting suspension was filtered. The filtrate was concentrated and the residue purified through silica gel FCC ($R_f = 0.18$; 7 N NH_3 in MeOH/DCM, 1:10) to give the off-white solid. DCM (2 mL) was added and the resulting suspension was filtered to remove the silica that had dissolved in the eluent. The DCM solution was concentrated to afford **2-75** as an off-white solid (50.8 mg, 81% yield).

^1H NMR (400 MHz, CD_3OD) δ 7.16 (d, $J = 8.7$ Hz, 1H), 6.85 (d, $J = 2.5$ Hz, 1H), 6.67 (dd, $J = 8.7, 2.4$ Hz, 1H), 3.79 (s, 3H), 3.20–2.98 (m, 3H), 2.28 (d, $J = 15.6$ Hz, 1H), 2.01 (td, $J = 13.7, 4.2$ Hz, 1H), 1.84–1.73 (m, 2H), 1.58 (qd, $J = 13.1, 4.2$ Hz, 1H), 1.43–1.31 (m, 4H), 1.12 (t, $J = 12.6$ Hz, 1H), 0.97 (s, 3H).

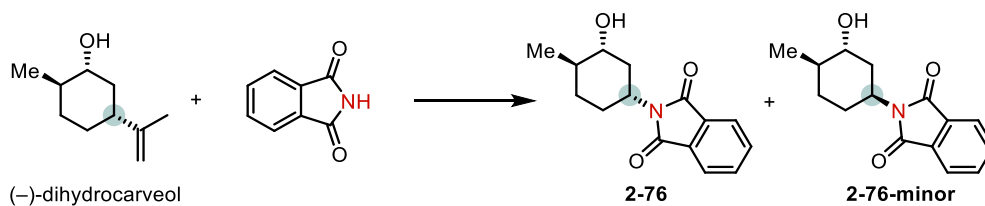
^{13}C NMR (100 MHz, CD_3OD) δ 154.80, 137.79, 133.58, 129.42, 112.21, 111.10, 106.37, 101.00, 77.19, 56.36, 47.03, 38.51, 38.45, 36.66, 34.98, 31.17, 30.94, 22.56, 11.69.

HRMS (DART): $[\text{M}+\text{H}]^+$ calcd for $[\text{C}_{19}\text{H}_{27}\text{N}_2\text{O}_2]^+$ m/z 315.2067, found 315.2061.

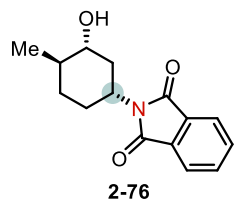
IR (neat, ATR): ν_{max} 3386 (br), 2979, 2917, 2857, 1468, 1236, 1089, 926, 885 cm^{-1} .

Optical Rotation: $[\alpha]_{\text{D}}^{26} = 62.00$ (c 0.1, MeOH).

M.p.: 144 $^{\circ}\text{C}$ (decomposition).



Prepared following **General procedure A** using phthalimide (294 mg, 2.00 mmol, 1.0 equiv), copper(I) chloride (39.6 mg, 0.400 mmol, 20 mol %), 1,10-phenanthroline (72.1 mg, 0.400 mmol, 20 mol %), and MeCN (20 mL) to make *Solution A* and (-)-dihydrocarveol (771 mg, 5.00 mmol, 2.5 equiv) and MeCN (20 mL) to make *Solution B*. The crude product was purified through FCC to give **2-76** ($R_f = 0.34$; hexanes/ Et_2O , 1:3) as a white solid (315.8 mg, 61% yield) and **2-76-minor** ($R_f = 0.39$; hexanes/ Et_2O , 1:3) as a white solid (104.9 mg, 20% yield).



^1H NMR (500 MHz, CDCl_3) δ 7.81 (dt, $J = 7.3, 3.6$ Hz, 2H), 7.69 (dd, $J = 5.4, 3.0$ Hz, 2H), 4.18 (tt, $J = 12.5, 3.9$ Hz, 1H), 3.24 (td, $J = 10.6, 4.3$ Hz, 1H), 2.36–2.17 (m, 2H), 2.03 (dtd, $J = 11.6, 4.0, 2.2$ Hz, 1H), 1.82 (dq, $J = 13.8, 3.5$ Hz, 1H), 1.67 (ddt, $J = 12.5, 6.3, 3.6$ Hz, 1H), 1.49–1.39 (m, 1H), 1.16–1.08 (m, 1H), 1.06 (d, $J = 6.4$ Hz, 3H).

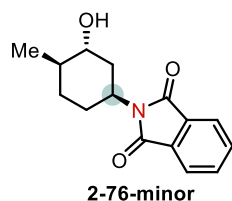
^{13}C NMR (125 MHz, CDCl_3) δ 168.26, 133.90, 131.92, 123.14, 75.13, 48.80, 39.17, 38.30, 31.44, 29.00, 18.01.

HRMS (DART): $[\text{M}+\text{H}]^+$ calcd for $[\text{C}_{15}\text{H}_{18}\text{NO}_3]^+$ m/z 260.1281, found 260.1281.

IR (neat, ATR): ν_{max} 3458 (br), 2929, 2873, 1772, 1708, 1466, 1397, 1389, 1376, 1335, 1105, 1056, 1043, 720 cm^{-1} .

Optical Rotation: $[\alpha]_{\text{D}}^{24} = -3.50$ (c 0.1, CHCl_3).

M.p.: 152–156 $^{\circ}\text{C}$.



^1H NMR (400 MHz, CDCl_3) δ 7.79 (td, $J = 5.2, 2.1$ Hz, 2H), 7.69 (td, $J = 5.2, 2.1$ Hz, 2H), 4.58 (tt, $J = 12.6, 4.2$ Hz, 1H), 4.04–3.91 (m, 1H), 2.65 (td, $J = 13.4, 2.7$ Hz, 1H), 2.39 (qd, $J = 14.3, 13.5, 4.3$ Hz, 1H), 2.06 (tt, $J = 13.4, 4.5$ Hz, 1H), 1.99–1.87 (m, 1H), 1.66 (d, $J = 13.6$ Hz, 1H), 1.57–1.42 (m, 2H), 1.10 (d, $J = 7.3$ Hz, 3H).

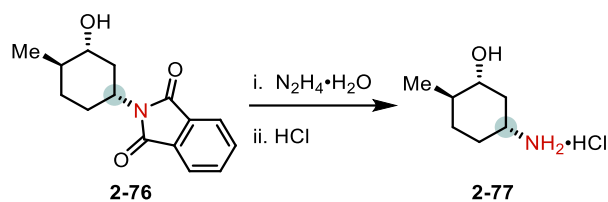
^{13}C NMR (100 MHz, CDCl_3) δ 168.53, 133.82, 132.04, 123.03, 72.12, 45.67, 33.56, 31.12, 25.45, 23.72, 16.40.

HRMS (DART): $[\text{M}+\text{H}]^+$ calcd for $[\text{C}_{15}\text{H}_{18}\text{NO}_3]^+$ m/z 260.1281, found 260.1281.

IR (neat, ATR): ν_{max} 3487 (br), 2961, 2934, 2875, 1766, 1713, 1468, 1396, 1373, 1335, 1147, 1054, 1026, 967, 717 cm^{-1} .

Optical Rotation: $[\alpha]_{\text{D}}^{25} = -7.67$ (c 0.1, CHCl_3).

M.p.: 142–144 $^{\circ}\text{C}$.



The ammonium salt **2-77** was synthesized according to a literature procedure.⁷⁴ The phthalimide **2-76** (130 mg, 0.500 mmol) was dissolved in 0.3 M methanolic hydrazine hydrate (5 mL). After the mixture had been stirred for 0.5 h at room temperature, 5% HCl (2 mL) was added and the mixture was stirred for an additional 12 h. The resulting suspension was filtered and then the filtrate was diluted with an equal amount of water, acidified (pH < 2), and washed with diethyl ether. The organic phase was discarded. The aqueous phase was basified with solid KOH (pH > 10) and then extracted with diethyl ether (2 × 15 mL). The combined ethereal layers were washed with brine, dried (Na₂SO₄), and concentrated. The residue was dissolved in DCM (5 mL). 4 M HCl in dioxane was added while cooling in an ice bath and then the mixture was stirred for 4 h at room temperature. Concentrating and washing with DCM provided **2-77** as a white crystal (73.2 mg, 88% yield).

¹H NMR (400 MHz, CD₃OD) δ 3.18–3.03 (m, 2H), 2.22 (dtd, *J* = 11.6, 4.0, 2.4 Hz, 1H), 1.94 (ddt, *J* = 12.9, 6.2, 3.5 Hz, 1H), 1.79 (dq, *J* = 13.9, 3.6 Hz, 1H), 1.41–1.21 (m, 3H), 1.15–1.02 (m, 1H), 1.00 (d, *J* = 6.4 Hz, 3H).

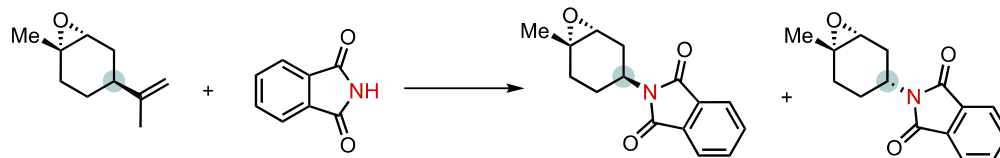
¹³C NMR (100 MHz, CD₃OD) δ 72.67, 48.71, 38.95, 38.63, 29.72, 16.77.

HRMS (DART): [M–Cl]⁺ calcd for [C₇H₁₆NO]⁺ *m/z* 130.1226, found 130.1226.

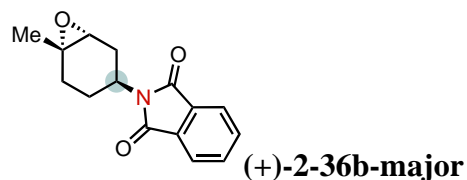
IR (neat, ATR): ν_{max} 3358 (br), 2952, 2876, 1637 cm⁻¹.

Optical Rotation: [α]_D²⁵ = –14.00 (*c* 0.1, MeOH).

M.p.: 186 °C (decomposition).



Prepared following **General procedure A** using phthalimide (368 mg, 2.50 mmol, 1.0 equiv), copper(I) chloride (49.5 mg, 0.500 mmol, 20 mol %), 1,10-phenanthroline (90.1 mg, 0.500 mmol, 20 mol %), and MeCN (25 mL) to make *Solution A*. The alkene (–)-**2-94** (761 mg, 5.00 mmol, 2.0 equiv) was used for ozonolysis and MeCN (25 mL) to make *Solution B*. The crude product was purified through FCC to give **2-(+)-36b-major** ($R_f = 0.55$; EtOAc/hexanes, 1:2) as a white solid (360.8 mg, 56% yield) and **(+)-36b-minor** ($R_f = 0.51$; EtOAc/hexanes, 1:2) as a white solid (172.5 mg, 27 % yield).



$^1\text{H NMR}$ (400 MHz, CDCl_3) δ 7.86–7.75 (m, 2H), 7.74–7.62 (m, 2H), 4.46–4.30 (m, 1H), 3.17 (s, 1H), 2.67 (ddd, $J = 14.5, 9.8, 2.3$ Hz, 1H), 2.22 (ddt, $J = 14.5, 5.2, 1.6$ Hz, 1H), 2.18–1.97 (m, 2H), 1.92 (ddd, $J = 15.2, 6.4, 3.8$ Hz, 1H), 1.59–1.51 (m, 1H), 1.37 (s, 3H).

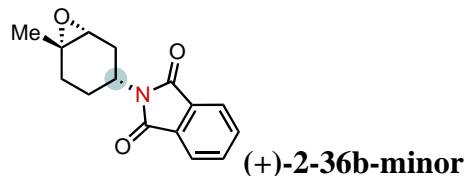
$^{13}\text{C NMR}$ (100 MHz, CDCl_3) δ 168.43, 133.91, 131.95, 123.11, 60.78, 57.08, 44.20, 28.24, 28.13, 25.01, 24.01.

HRMS (DART): $[\text{M}+\text{H}]^+$ calcd for $[\text{C}_{15}\text{H}_{16}\text{NO}_3]^+$ m/z 258.1125, found 258.1125.

IR (neat, ATR): ν_{max} 2926, 2855, 1773, 1716, 1701, 1399, 1377, 1103, 878 cm^{-1} .

Optical Rotation: $[\alpha]_{\text{D}}^{25} = 3.50$ (c 0.2, CHCl_3).

M.p.: 146–149 $^{\circ}\text{C}$.



¹H NMR (400 MHz, CDCl₃) δ 7.86–7.75 (m, 2H), 7.74–7.64 (m, 2H), 4.10 (dddd, *J* = 12.9, 11.7, 6.6, 3.0 Hz, 1H), 3.01 (d, *J* = 5.3 Hz, 1H), 2.63–2.37 (m, 2H), 2.22–1.99 (m, 2H), 1.87 (ddd, *J* = 14.8, 12.8, 4.9 Hz, 1H), 1.44–1.37 (m, 1H), 1.35 (s, 3H).

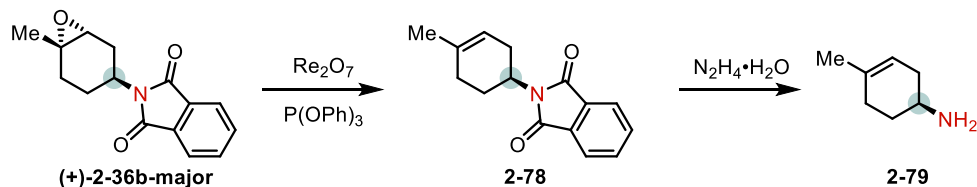
¹³C NMR (100 MHz, CDCl₃) δ 168.08, 133.90, 131.94, 123.14, 58.39, 56.98, 46.40, 30.42, 27.93, 23.43, 22.84.

HRMS (DART): [M+H]⁺ calcd for [C₁₅H₁₆NO₃]⁺ *m/z* 258.1125, found 258.1125.

IR (neat, ATR): ν_{max} 2926, 2853, 1763, 1708, 1396, 1376, 1128, 1075, 718 cm⁻¹.

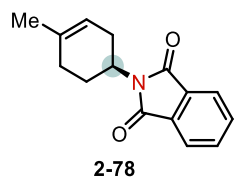
Optical Rotation: [α]_D²⁵ = 18.00 (*c* 0.2, CHCl₃).

M.p.: 187–190 °C.



Deoxygenation was performed according to the literature.⁷⁶ The epoxide **(+)-2-36b-major** (257 mg, 1.00 mmol), triphenyl phosphite (466 mg, 1.50 mmol), and rhenium(VII) oxide (2.40 mg, 0.5 mol %) were added in sequence to a 50-mL round-bottom flask in a glove box. The flask was capped with a rubber septum and removed from the glove box, followed by the addition of 10 mL of toluene. The mixture was stirred at 100 °C for 48 h and then cooled to room temperature. The mixture was concentrated and the residue purified through FCC to give **2-78** (*R*_f = 0.27;

EtOAc/hexanes, 1:20) as a white solid (132.6 mg, 55% yield). The starting material epoxide (+)-**2-36b-major** (29.2 mg, 11% yield) was also recovered (62% yield b.r.s.).



¹H NMR (400 MHz, CDCl₃) δ 7.85–7.77 (m, 2H), 7.72–7.65 (m, 2H), 5.37 (d, *J* = 4.5 Hz, 1H), 4.35 (dddd, *J* = 12.9, 11.3, 5.5, 3.2 Hz, 1H), 2.83 (dddt, *J* = 15.8, 8.8, 4.1, 2.2 Hz, 1H), 2.55 (ddt, *J* = 18.3, 12.3, 5.9 Hz, 1H), 2.28–2.15 (m, 1H), 2.15–2.00 (m, 2H), 1.78 (dddt, *J* = 12.4, 5.0, 3.3, 1.7 Hz, 1H), 1.69 (s, 3H).

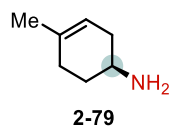
¹³C NMR (100 MHz, CDCl₃) δ 168.46, 133.79, 133.74, 132.10, 123.03, 119.23, 47.70, 30.52, 28.58, 26.47, 23.30.

HRMS (DART): [M+H]⁺ calcd for [C₁₅H₁₆NO₂]⁺ *m/z* 242.1176, found 242.1173.

IR (neat, ATR): ν_{\max} 2958, 2915, 2852, 1699, 1612, 1464, 1394, 1380, 1107, 926, 876 cm⁻¹.

Optical Rotation: $[\alpha]_{\text{D}}^{25} = -3.00$ (*c* 0.1, CH₂Cl₂).

M.p.: 147–150 °C.



The alkene **2-78** (113 mg, 0.470 mmol) was dissolved in 0.3 M methanolic hydrazine hydrate (5 mL). The mixture was heated under reflux under argon for 3 h, then cooled to room temperature and diluted with DCM (20 mL). The suspension was filtered and the filtrate concentrated *in vacuo* at 0 °C. The residue was diluted with DCM (10 mL), the resulting suspension was filtered, and the filtrate concentrated *in vacuo* at 0 °C again. The residue was diluted with DCM (5 mL) and

subjected to silica FCC (7 N NH₃ in MeOH/DCM, 1:30) to afford 2-**79** (*R*_f = 0.24; 7 N NH₃ in MeOH/DCM, 1:20) as a pale-yellow oil (44.5 mg, 85% yield).

¹H NMR (400 MHz, CD₂Cl₂) δ 5.31–5.26 (m, 1H), 2.88 (dddd, *J* = 10.1, 8.5, 5.2, 3.2 Hz, 1H), 2.19 (ddtd, *J* = 16.6, 6.7, 3.5, 1.7 Hz, 1H), 2.10–1.92 (m, 2H), 1.81–1.65 (m, 2H), 1.65–1.59 (m, 3H), 1.43–1.31 (m, 3H).

¹³C NMR (100 MHz, CD₂Cl₂) δ 134.24, 119.77, 47.30, 36.03, 33.34, 29.78, 23.61.

HRMS (DART): [M+H]⁺ calcd for [C₇H₁₄N]⁺ *m/z* 112.1121, found 112.1116.

IR (neat, ATR): ν_{max} 3325 (br), 2930, 2835, 2857, 1572, 1448, 1383, 1333, 1276 cm⁻¹.

Optical Rotation: [α]_D²⁵ = -50.33 (*c* 0.2, CH₂Cl₂).

2.6.5.5. N-Methylation reaction

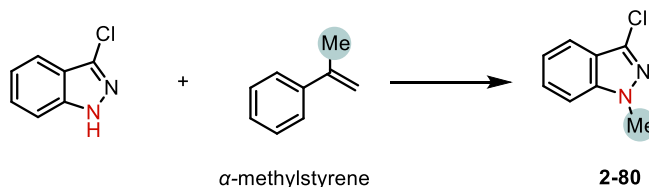
α-Methylstyrene (AMS) is an industrial by-product of the cumene–phenol process. The world market for AMS is 220k ton/year and is worth \$120m. As mentioned in the main text, AMS is less expensive (\$5.1/mol) than other common methylation reagents. Other commercially available sources of Me⁺ and/or Me• include CH(OMe)₃ (\$10.4/mol), *t*-BuOOH (\$8.9/mol), Me₂SO₄ (\$6.1/mol), trimethyl phosphate (\$12.6/mol), MeOTs (\$26.3/mol), di-*tert*-butylperoxide (\$39.3/mol), MeI (\$42.6/mol), di-cumylperoxide (\$80.4/mol), *tert*-butylperacetate (\$33.6/mol), PhI(OAc)₂ (\$331.6/mol), and MesI(OAc)₂ (\$4,340.9/mol). In a recent report, the Doyle group used trimethyl orthoformate (as the reaction solvent; 180 equiv) as the Me• source for the Ni/Ir-catalyzed methylation of (het)aryl chlorides.⁷⁷ Methane would be the most atom-economical methylating agent, but its use would require a high-pressure photoreactor operating under at 50 bar.⁷⁸ MeOH would be another atom-economical methylating agent, but not as a source of Me•, but rather HOCH₂•, which eventually methylates aza-aromatics.^{79, 80} MeOH has also been used in

the methylation of hydrocarbons in a flange reactor containing gallium nitride nanowires illuminated by a Xe lamp;⁸¹ here, MeOH is the source of methyl carbene. All of these examples, however, involve the formation of C–C bonds. One exception would be the use of MeOH in a precious metal–catalyzed hydrogen-borrowing strategy (hydrogen autotransfer),^{82–86} but this process has not been used in the N-methylation of N-heteroarenes. For instance, the formaldehyde formed through the dehydration of MeOH undergoes C3 hydroxymethylation, eventually resulting in the 3-methylindole.⁸⁷ In all cases, MeOH has been used as a (co)solvent (100–250 equiv). Recently, the MacMillan group reported an alcohol deoxygenative sp^3 – sp^2 cross-coupling enabled by metallaphotoredox catalysis where MeOH was used as a Me• precursor.⁸⁸ A stoichiometric amount of NHC was, however, needed for activation. Acetic acid would be another atom-economical methylating agent, but the direct decarboxylation of an acid often favors the alkyl radical generated with adjacent stabilizing substituents. Methyl radical generation from acetic acid is often challenging⁸⁹ and, thus, excess amounts of acetic acid and oxidants are often employed.⁹⁰ For example, 5 equiv of acetic acid and 10 equiv of AgNO₃ have been used in the methylation of acridine and 4-cyanopyridine (Minisci reaction).⁹¹ In 2020, the Nocera group reported a photocatalyzed hydromethylation of active alkenes using acetic acid as a Me• precursor.⁸⁹ This reaction is efficient and good yields were obtained when using only 3 equiv of acetic acid. Formation of an activated acetate ester intermediate is another strategy to engage acetic acid as a Me• precursor; for example, using PhI(OAc)₂,¹³ or *N*-acetyloxyphthalimide,⁹² which need stoichiometric activation reagents and an additional synthetic step.

Notably, the by-product from our protocol—methyl benzoate (\$5.6/mol)—is another value-added compound. It is relatively nonpolar and runs with the solvent front of the eluent during FCC;

therefore, it is easy to recover. In an industrial setting, it would be readily separable from crystalline amino products.

Note: The prices were checked from Thermo Scientific Chemicals on 02/06/2023. The price of MesI(OAc)₂ was checked from TCI.

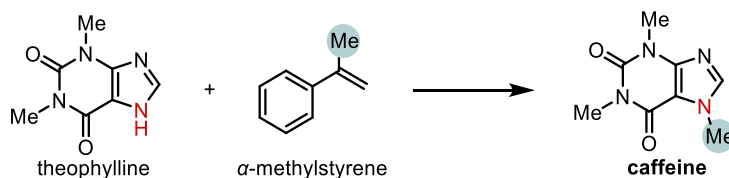


Prepared following **General procedure A** using **2-113** (61.0 mg, 0.400 mmol, 1.0 equiv), copper(I) chloride (7.90 mg, 0.0800 mmol, 20 mol %), 1,10-phenanthroline (14.4 mg, 0.0800 mmol, 20 mol %), and MeCN (4 mL) to make *Solution A*. AMS (94.6 mg, 0.800 mmol, 2.0 equiv) was used for ozonolysis and MeCN (4 mL) to make *Solution B*. The crude product was purified through FCC to give **2-80** ($R_f = 0.45$; toluene/EtOAc, 2:1) as a colorless oil (56.2 mg, 84% yield). ¹H NMR (400 MHz, CDCl₃) δ 7.66 (d, $J = 8.2$ Hz, 1H), 7.43 (ddd, $J = 7.9, 6.8, 1.0$ Hz, 1H), 7.35 (d, $J = 8.5$ Hz, 1H), 7.19 (ddd, $J = 7.8, 6.8, 0.8$ Hz, 1H), 4.02 (s, 3H).

¹³C NMR (100 MHz, CDCl₃) δ 141.22, 132.38, 127.45, 121.11, 121.05, 119.74, 109.26, 35.79.

HRMS (ESI-TOF): [M+H]⁺ calcd for [C₈H₈ClN₂]⁺ m/z 167.0371, found 167.0378.

IR (neat, ATR): ν_{\max} 3061, 2936, 1618, 1498, 1470, 1383, 1366, 1231, 1165, 1121, 1030, 977, 742, 629, 595 cm⁻¹.



Prepared following **General procedure A** using theophylline (36.0 mg, 0.200 mmol, 1.0 equiv), copper(I) chloride (4.00 mg, 0.0400 mmol, 20 mol %), 1,10-phenanthroline (7.20 mg, 0.0400 mmol, 20 mol %), and MeOH (20 mL) to make *Solution A*. AMS (47.3 mg, 0.400 mmol, 4.0 equiv) was used for ozonolysis and MeCN (4 mL) to make *Solution B*. The crude product was purified through FCC to give **caffeine** ($R_f = 0.27$; toluene/MeOH, 10:1) as a white solid (26.1 mg, 67% yield).

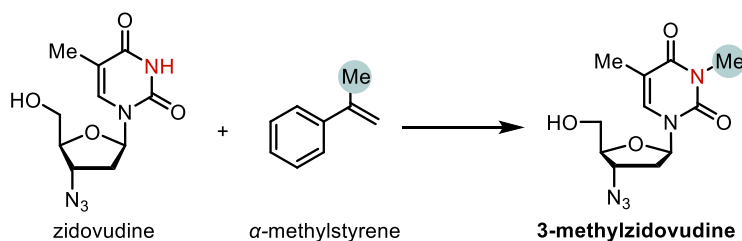
$^1\text{H NMR}$ (400 MHz, DMSO- d_6) δ 7.97–7.91 (m, 1H), 3.85–3.78 (m, 3H), 3.34 (s, 3H), 3.15 (s, 3H).

$^{13}\text{C NMR}$ (100 MHz, DMSO- d_6) δ 154.95, 151.45, 148.52, 143.21, 107.01, 33.57, 29.80, 27.91.

HRMS (DART): $[\text{M}+\text{H}]^+$ calcd for $[\text{C}_8\text{H}_{11}\text{N}_4\text{O}_2]^+$ m/z 195.0877, found 195.0878.

IR (neat, ATR): ν_{max} 3111, 2959, 1697, 1651, 1599, 1548, 1485, 1455, 1429, 1402, 1359, 1285, 1237, 1025, 973, 744 609, 482 cm^{-1} .

M.p.: 234–235 $^\circ\text{C}$.



Prepared following **General procedure A** using zidovudine (56.3 mg, 0.200 mmol, 1.0 equiv), copper(I) chloride (9.90 mg, 0.100 mmol, 50 mol %), 1,10-phenanthroline (18.0 mg, 0.100 mmol, 50 mol %), and MeOH (20 mL) to make *Solution A*. AMS (94.6 mg, 0.800 mmol, 4.0 equiv) was used for ozonolysis and MeCN (4 mL) to make *Solution B*. The crude product was purified through FCC to give **3-methylzidovudine** ($R_f = 0.24$; EtOAc/hexanes, 2:1) as a colorless oil (43.4 mg, 77% yield).

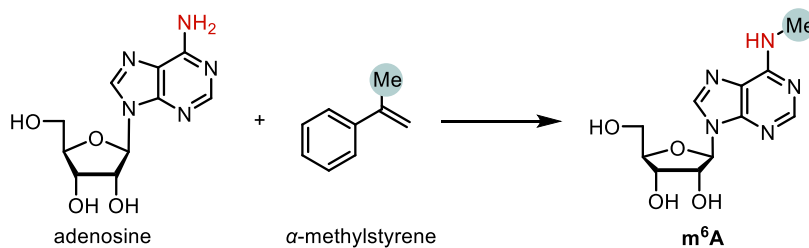
¹H NMR (500 MHz, CDCl₃) δ 7.43 (d, *J* = 1.6 Hz, 1H), 6.06 (t, *J* = 6.4 Hz, 1H), 4.37 (dt, *J* = 7.5, 5.0 Hz, 1H), 4.00–3.89 (m, 2H), 3.84–3.73 (m, 1H), 3.30 (s, 3H), 2.84 (brs, 1H), 2.50 (dt, *J* = 13.7, 6.8 Hz, 1H), 2.38 (ddd, *J* = 13.9, 6.8, 5.2 Hz, 1H), 1.90 (s, 3H).

¹³C NMR (125 MHz, CDCl₃) δ 163.63, 150.95, 134.68, 110.13, 87.29, 84.58, 61.90, 59.93, 37.45, 27.88, 13.28.

HRMS (DART): [M+H]⁺ calcd for [C₁₁H₁₆N₅O₄]⁺ *m/z* 282.1197, found 282.1198.

IR (neat, ATR): ν_{max} 3429 (br), 2932, 2102, 1697, 1666, 1629, 1474, 1296, 1257, 1101, 1060, 768 cm⁻¹.

Optical Rotation: [α]_D²⁵ = 22.20 (*c* 1.0, CHCl₃)



Prepared following **General procedure A** using adenosine (107 mg, 0.400 mmol, 1.0 equiv), copper(I) chloride (7.90 mg, 0.0800 mmol, 20 mol %), 1,10-phenanthroline (14.4 mg, 0.0800 mmol, 20 mol %), and MeOH (20 mL) to make *Solution A*. AMS (94.6 mg, 0.800 mmol, 2.0 equiv) was used for ozonolysis and MeCN (4 mL) to make *Solution B*. The crude product was purified through FCC to give m⁶A (*R*_f = 0.23; DCM/MeOH, 10:1) as a white solid (81.4 mg, 72 % yield).

¹H NMR (500 MHz, DMSO-d₆) δ 8.32 (s, 1H), 8.21 (s, 1H), 7.80 (s, 1H), 5.86 (d, *J* = 6.2 Hz, 1H), 5.41 (t, *J* = 6.9 Hz, 2H), 5.16 (d, *J* = 4.6 Hz, 1H), 4.59 (q, *J* = 6.0 Hz, 1H), 4.12 (q, *J* = 4.5 Hz, 1H), 3.94 (d, *J* = 3.0 Hz, 1H), 3.65 (dt, *J* = 11.9, 3.9 Hz, 1H), 3.53 (ddd, *J* = 11.7, 7.3, 3.5 Hz, 1H), 2.93 (brs, 3H).

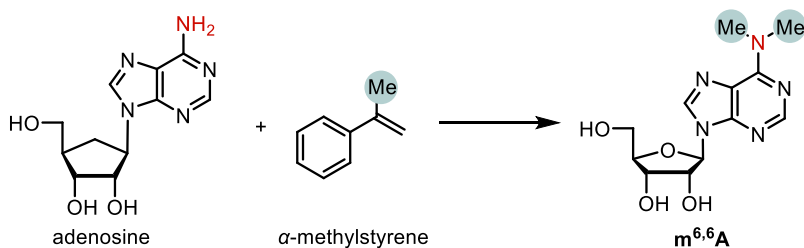
^{13}C NMR (125 MHz, DMSO- d_6) δ 155.53, 152.88, 148.51, 140.11, 120.35, 88.37, 86.36, 73.93, 71.12, 62.14, 27.45 (br).

HRMS (ESI-TOF): $[\text{M}+\text{H}]^+$ calcd for $[\text{C}_{11}\text{H}_{16}\text{N}_5\text{O}_4]^+$ m/z 282.1197, found 282.1198.

IR (neat, ATR): ν_{max} 3237 (br), 2931, 1633, 1376, 1334, 1228, 1093, 1084, 1055 cm^{-1} .

Optical Rotation: $[\alpha]_{\text{D}}^{24} = -33.67$ (c 0.1, MeOH).

M.p.: 162 $^{\circ}\text{C}$ (decomposition).



Prepared following **General procedure A** using adenosine (53.4 mg, 0.200 mmol, 1.0 equiv), copper(I) chloride (4.00 mg, 0.0400 mmol, 20 mol %), 1,10-phenanthroline (7.20 mg, 0.0400 mmol, 20 mol %), and MeOH (10 mL) to make *Solution A*. AMS (118 mg, 1.00 mmol, 5.0 equiv) was used for ozonolysis and MeCN (2 mL) to make *Solution B*. The crude product was purified through FCC to give $m^{6,6}\text{A}$ ($R_f = 0.35$; DCM/MeOH, 10:1) as a white solid (58.2 mg, 99% yield).

^1H NMR (500 MHz, CD_3OD) δ 8.19 (s, 1H), 8.17 (s, 1H), 5.94 (d, $J = 6.4$ Hz, 1H), 4.73 (t, $J = 5.8$ Hz, 1H), 4.31 (dd, $J = 4.7, 2.2$ Hz, 1H), 4.16 (d, $J = 2.1$ Hz, 1H), 3.87 (dd, $J = 12.5, 1.9$ Hz, 1H), 3.73 (dd, $J = 12.5, 2.1$ Hz, 1H), 3.49 (brs, 6H).

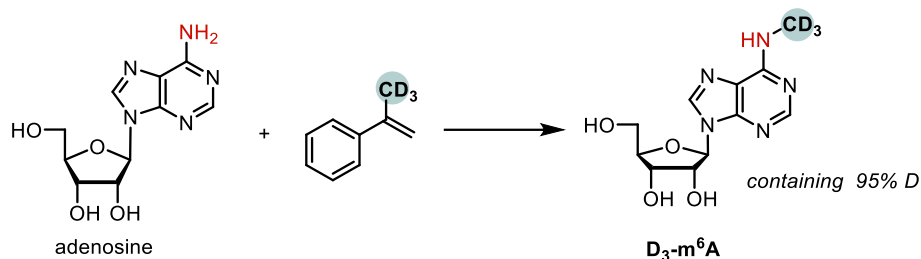
^{13}C NMR (125 MHz, CD_3OD) δ 154.83, 151.24, 149.25, 138.78, 120.59, 89.80, 86.73, 73.82, 71.28, 62.11, 37.62 (br).

HRMS (ESI-TOF): $[\text{M}+\text{H}]^+$ calcd for $[\text{C}_{12}\text{H}_{18}\text{N}_5\text{O}_4]^+$ m/z 296.1353, found 296.1361.

IR (neat, ATR): ν_{\max} 3251 (br), 2926, 2870, 1598, 1568, 1487, 1426, 1341, 1300, 1276, 1221, 1122, 1082, 1038, 791, 697, 648 cm^{-1} .

Optical Rotation: $[\alpha]_{\text{D}}^{26} = -29.50(c\ 0.2, \text{MeOH})$

M.p.: 107–110 °C.



Prepared following **General procedure A** using adenosine (53.4 mg, 0.200 mmol, 1.0 equiv), copper(I) chloride (4.00 mg, 0.0400 mmol, 20 mol %), 1,10-phenanthroline (7.20 mg, 0.0400 mmol, 20 mol %), and MeOH (10 mL) to make *Solution A*. $\text{D}_3\text{-AMS}$ (48.5 mg, 0.400 mmol, 2.0 equiv) was used for ozonolysis and MeCN (2 mL) to make *Solution B*. The crude product was purified through FCC to give $\text{D}_3\text{-m}^6\text{A}$ ($R_f = 0.23$; DCM/MeOH, 10:1) as a white solid (43.0 mg, 76% yield).

$^1\text{H NMR}$ (400 MHz, CD_3OD) δ 8.20 (s, 1H), 8.18 (s, 1H), 5.92 (d, $J = 6.5$ Hz, 1H), 4.73 (dd, $J = 6.5, 5.1$ Hz, 1H), 4.30 (dd, $J = 5.1, 2.5$ Hz, 1H), 4.15 (q, $J = 2.5$ Hz, 1H), 3.86 (dd, $J = 12.6, 2.5$ Hz, 1H), 3.72 (dd, $J = 12.5, 2.7$ Hz, 1H), 3.03 (s, $5.3\% \times 3\text{H}$).

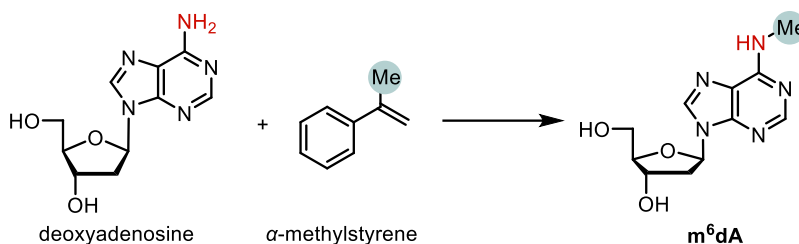
$^{13}\text{C NMR}$ (125 MHz, CD_3OD) δ 155.45, 152.06, 147.36, 140.03, 120.19, 89.86, 86.80, 74.04, 71.32, 62.11, 25.72 (br).

HRMS (ESI-TOF): $[\text{M}+\text{H}]^+$ calcd for $[\text{C}_{11}\text{H}_{13}\text{D}_3\text{N}_5\text{O}_4]^+$ m/z 285.1385, found 285.1387.

IR (neat, ATR): ν_{\max} 3201 (br), 2935, 1617, 1480, 1335, 1298, 1226, 1091, 1052, 983, 861, 813, 791, 755, 703, 641 cm^{-1} .

Optical Rotation: $[\alpha]_D^{24} = -27.00$ (*c* 0.1, MeOH)

M.p.: 138 °C (decomposition).



Prepared following **General procedure A** using deoxyadenosine (50.2 mg, 0.200 mmol, 1.0 equiv), copper(I) chloride (4.00 mg, 0.0400 mmol, 20 mol %), 1,10-phenanthroline (7.20 mg, 0.0400 mmol, 20 mol %), and MeOH (10 mL) to make *Solution A*. AMS (47.3 mg, 0.400 mmol, 2.0 equiv) was used for ozonolysis and MeCN (2 mL) to make *Solution B*. The crude product was purified through FCC to give m^6dA ($R_f = 0.24$; DCM/MeOH, 10:1) as a white solid (41.3 mg, 78% yield).

1H NMR (500 MHz, CD_3OD) δ 8.24 (s, 1H), 8.21 (s, 1H), 6.49–6.34 (m, 1H), 4.62–4.52 (m, 1H), 4.12–4.01 (m, 1H), 3.84 (dd, $J = 12.3, 2.5$ Hz, 1H), 3.73 (dd, $J = 12.3, 3.0$ Hz, 1H), 3.09 (s, 3H), 2.80 (dt, $J = 13.6, 6.0$ Hz, 1H), 2.39 (ddd, $J = 13.4, 5.8, 2.2$ Hz, 1H).

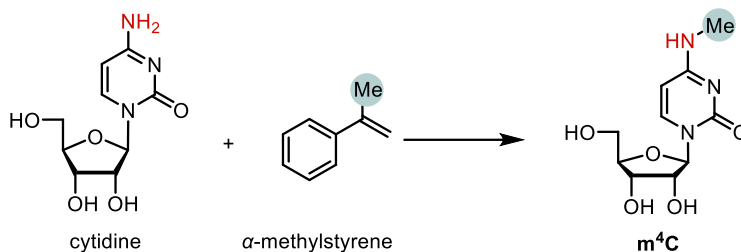
^{13}C NMR (125 MHz, CD_3OD) δ 155.43, 152.05, 147.41, 139.60, 120.09, 88.51, 85.80, 71.70, 62.29, 40.18, 26.27.

HRMS (ESI-TOF): $[M+H]^+$ calcd for $[C_{11}H_{16}N_5O_3]^+$ m/z 266.1248, found 266.1251.

IR (neat, ATR): ν_{max} cm^{-1} . 3300 (br), 3097, 1632, 1622, 1381, 1319, 1246, 1082, 1071, 1027, 976, 929, 889, 851, 797, 654 cm^{-1} .

Optical Rotation: $[\alpha]_D^{24} = -11.33$ (*c* 0.1, MeOH)

M.p.: 201–204 °C.



Prepared following **General procedure A** using deoxyadenosine (97.3 mg, 0.400 mmol, 1.0 equiv), copper(I) chloride (7.90 mg, 0.0800 mmol, 20 mol %), 1,10-phenanthroline (14.4 mg, 0.0800 mmol, 20 mol %), and MeOH (20 mL) to make *Solution A*. AMS (94.6 mg, 0.800 mmol, 2.0 equiv) was used for ozonolysis and MeCN (4 mL) to make *Solution B*. The crude product was purified through FCC to give m⁴C ($R_f = 0.14$; DCM/MeOH, 2:1) as a white solid (71.4 mg, 69% yield).

¹H NMR (500 MHz, CD₃OD) δ 7.90 (d, $J = 7.6$ Hz, 1H), 5.84 (d, $J = 3.2$ Hz, 1H), 5.81 (d, $J = 7.5$ Hz, 1H), 4.16–4.09 (m, 2H), 4.00 (dt, $J = 5.5, 3.0$ Hz, 1H), 3.86 (dd, $J = 12.3, 2.6$ Hz, 1H), 3.73 (dd, $J = 12.3, 3.2$ Hz, 1H), 2.88 (s, 3H).

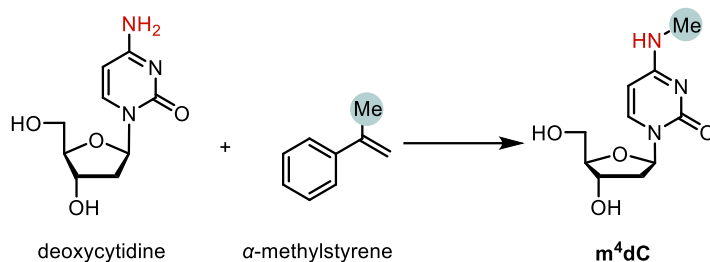
¹³C NMR (125 MHz, CD₃OD) δ 164.59, 157.46, 139.91, 95.42, 90.87, 84.34, 74.68, 69.38, 60.62, 26.38.

HRMS (ESI-TOF): $[M+Na]^+$ calcd for $[C_{10}H_{15}N_3NaO_5]^+$ m/z 280.0904, found 280.0905.

IR (neat, ATR): ν_{max} 3163, 2927, 1633, 1617, 1539, 1500, 1401, 1291, 1107, 1090, 1055, 1020, 1004, 786, 779, 767 cm^{-1} .

Optical Rotation: $[\alpha]_D^{24} = 20.00$ (c 0.1, MeOH)

M.p.: 213–214 °C.



Prepared following **General procedure A** using deoxyadenosine (90.9 mg, 0.400 mmol, 1.0 equiv), copper(I) chloride (7.90 mg, 0.0800 mmol, 20 mol %), 1,10-phenanthroline (14.4 mg, 0.0800 mmol, 20 mol %), and MeOH (20 mL) to make *Solution A*. AMS (94.6 mg, 0.800 mmol, 2.0 equiv) was used for ozonolysis and MeCN (4 mL) to make *Solution B*. The crude product was purified through FCC to give **m⁴dC** ($R_f = 0.45$; DCM/MeOH, 2:1) as a white solid (71.9 mg, 75% yield).

¹H NMR (400 MHz, CD₃OD) δ 7.85 (d, $J = 7.5$ Hz, 1H), 6.24 (t, $J = 6.6$ Hz, 1H), 5.81 (d, $J = 7.6$ Hz, 1H), 4.33 (dt, $J = 6.7, 3.6$ Hz, 1H), 3.89 (q, $J = 3.6$ Hz, 1H), 3.75 (dd, $J = 12.0, 3.3$ Hz, 1H), 3.69 (dd, $J = 12.0, 3.9$ Hz, 1H), 2.86 (s, 3H), 2.30 (ddd, $J = 13.5, 6.1, 3.7$ Hz, 1H), 2.10 (dt, $J = 13.5, 6.6$ Hz, 1H).

¹³C NMR (100 MHz, CD₃OD) δ 164.55, 157.22, 139.43, 95.57, 87.34, 85.98, 70.69, 61.43, 40.51, 26.37.

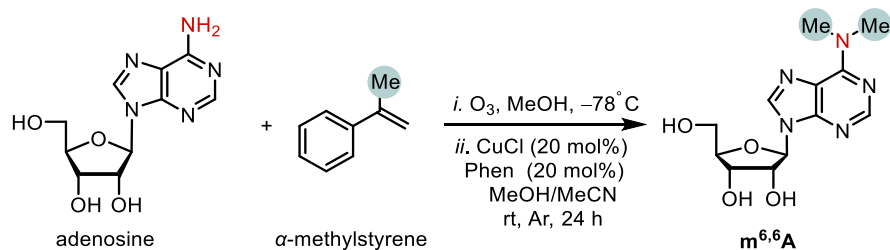
HRMS (ESI-TOF): $[M+Na]^+$ calcd for $[C_{10}H_{15}N_3NaO_4]^+$ m/z 264.0955, found 264.0960.

IR (neat, ATR): ν_{max} 3266 (br), 3135, 1626, 1620, 1573, 1519, 1403, 1337, 1290, 1089, 1060, 1039, 1029, 954, 790, 776, 743, 664 cm^{-1} .

Optical Rotation: $[\alpha]_D^{24} = 35.00$ (c 0.1, MeOH)

M.p.: 199–201 °C.

2.6.5.6. Preparation of m^{6,6}A on 20-mmol-scale with a graphical guide

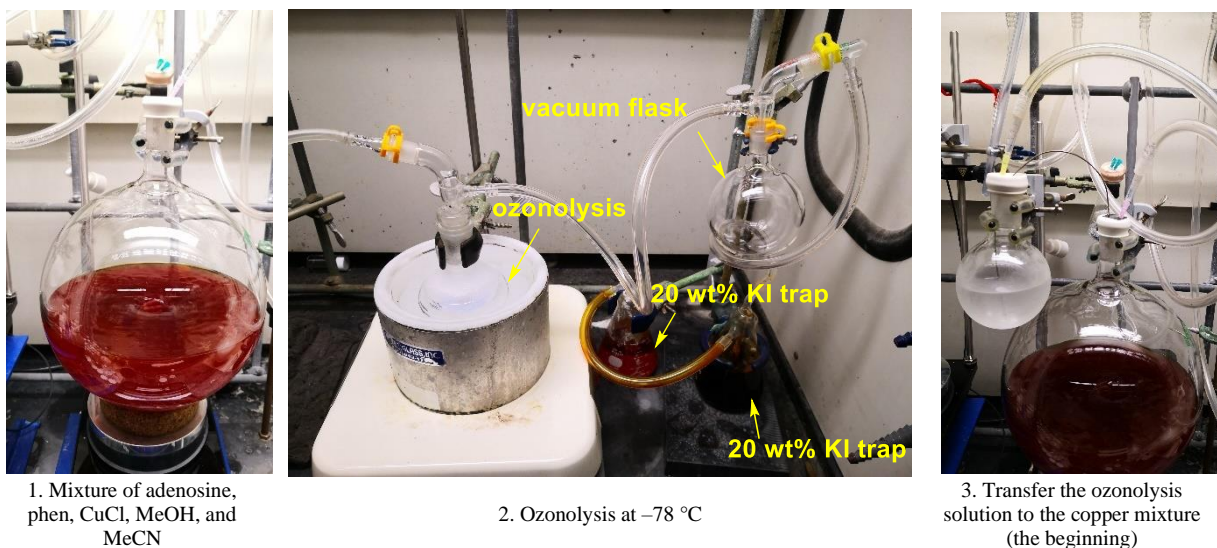


An oven-dried 5-L round-bottom flask equipped with a magnetic stirrer bar was charged with adenosine (5.34 g, 20.0 mmol, 1.0 equiv), 1,10-phenanthroline (720 mg, 4.00 mmol, 20 mol %), HPLC-grade MeOH (1.85 L), and HPLC-grade MeCN (400 mL). The suspension was sparged with argon for 30 min to expel air and capped with a sleeve stopper. This mixture was stirred at room temperature for 20 min to form a suspension. The stirring was stopped and copper(I) chloride (396 mg, 4.0 mmol, 20 mol %) was added quickly. The mixture was sparged with argon for 30 min and stirred for 2 h.

Another 250-mL round-bottom flask equipped with a magnetic stirrer bar was charged with AMS (11.8 g, 100 mmol, 5.0 equiv) and HPLC-grade MeOH (150 mL), then cooled to -78 °C in a dry-ice/acetone bath with two 250-mL waste gas traps equipped with 20 wt% aqueous KI (200 mL). Ozone was bubbled through the solution through a long needle until complete consumption of the starting material had occurred (as indicated by TLC and/or a blue color in the reaction mixture). The solution was sparged with argon for 30 min to expel excess ozone and oxygen, and then the reaction mixture was warmed to room temperature. This MeOH solution of the hydroperoxide was added into the copper mixture *via* cannula and washed with additional MeOH (2 × 10 mL). The reaction vessel was stirred at room temperature for 24 h.

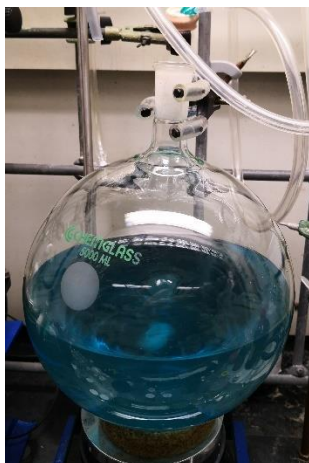
Upon completion of the reaction (TLC), the mixture was concentrated to approximately 150 mL. The residue was transferred into a 500-mL round-bottom flask and diluted with DCM (200 mL). Silica gel (*ca.* 100 g) was added into the solution and the blue copper(II) salt absorbed onto it. The mixture was filtered through silica gel and washed with MeOH/DCM (1:2, v/v; 2 × 500 mL). The combined solutions were evaporated *in vacuo* and the residue was washed with DCM (3 × 30 mL) to afford a white solid. The DCM washings were combined and concentrated. This residue was washed with DCM (3 × 15 mL) to provide a small amount of white solid. The combined white solids were dried under high vacuum at 60 °C for 2 h to give **m^{6,6}A** as a white solid (5.55 g, 94% yield).

Figure 2.9 Graphical guide for the 20-mmol-scale synthesis of m^{6,6}A

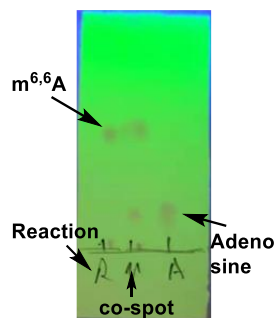




4. Transfer the ozonolysis solution to the copper mixture (the end)



5. The mixture after 24 h



6. TLC of the reaction mixture



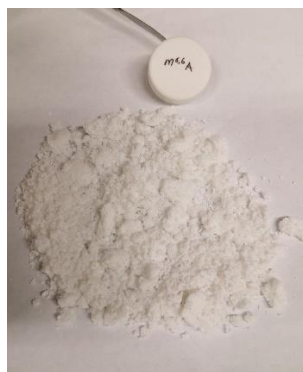
7. Concentration and silica addition



8. Filtration



9. Concentration and DCM wash

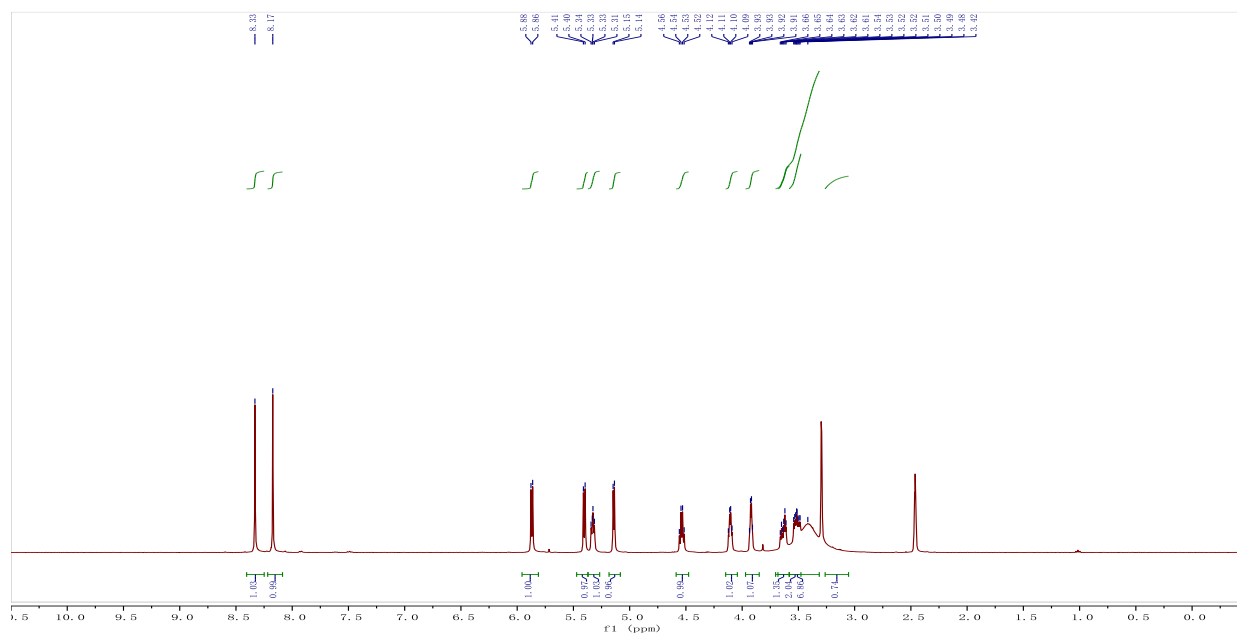


10. Combined white solids

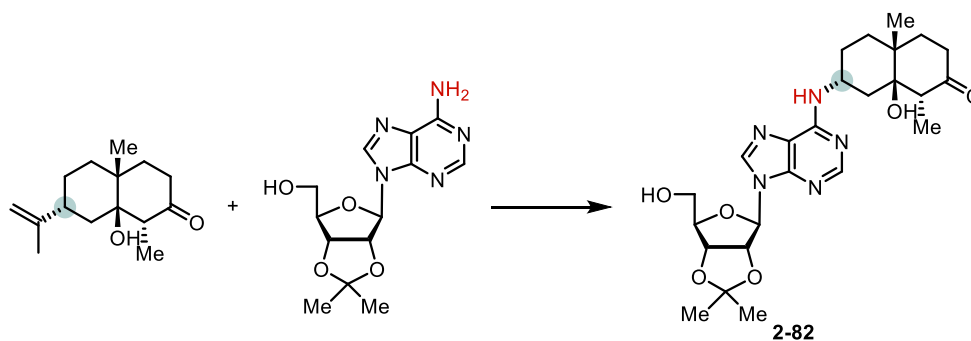


11. Dry under high vacuum at 60 °C

Figure 2.10 ^1H NMR spectrum of the $m^{6,6}\text{A}$ sample prepared without column chromatography



2.6.5.7. Synthesis of terpene nucleoside analogs



Prepared following **General procedure A** using 2',3'-*O*-isopropylideneadenosine (61.5 mg, 0.200 mmol, 1.0 equiv) copper(I) chloride (5.90 mg, 0.0600 mmol, 30 mol %), 1,10-phenanthroline (10.8 mg, 0.0600 mmol, 30 mol %), and MeCN (5 mL) to make *Solution A*. The alkene **2-90** (236 mg, 1.00 mmol, 5.0 equiv) was used for ozonolysis and MeCN (5 mL) to make *Solution B*. The crude product was purified through FCC to give **2-82** ($R_f = 0.38$; EtOAc) as a white solid (49.2 mg, 49% yield).

¹H NMR (400 MHz, CD₃OD) δ 8.22 (s, 1H), 8.18 (s, 1H), 6.09 (d, *J* = 3.6 Hz, 1H), 5.23 (dd, *J* = 6.0, 3.6 Hz, 1H), 5.00 (dd, *J* = 6.1, 2.2 Hz, 1H), 4.33 (q, *J* = 3.5 Hz, 2H), 3.76 (dd, *J* = 12.1, 3.4 Hz, 1H), 3.68 (dd, *J* = 12.1, 3.9 Hz, 1H), 2.92 (q, *J* = 6.6 Hz, 1H), 2.66 (td, *J* = 13.2, 12.5, 7.0 Hz, 1H), 2.27–2.09 (m, 2H), 2.09–1.99 (m, 1H), 1.98–1.90 (m, 1H), 1.83 (d, *J* = 12.8 Hz, 1H), 1.66–1.52 (m, 4H), 1.46–1.31 (m, 5H), 1.23 (s, 3H), 1.18–1.09 (m, 1H), 0.96 (d, *J* = 6.7 Hz, 3H).

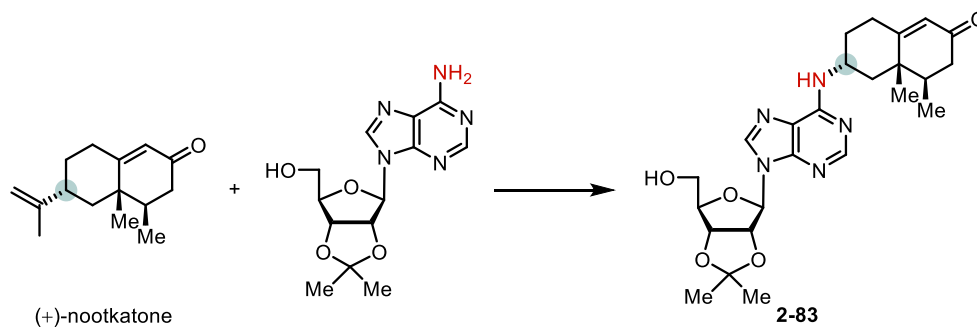
¹³C NMR (100 MHz, CD₃OD) δ 212.05, 153.90, 152.25, 147.70, 139.85, 119.55, 113.82, 91.48, 86.62, 83.85, 81.54, 78.00, 62.18, 51.59, 45.87, 37.27, 37.16, 33.95, 31.19, 29.33, 26.87, 26.24, 24.17, 20.44, 5.65.

HRMS (DART): [M+H]⁺ calcd for [C₂₅H₃₆N₅O₆]⁺ *m/z* 502.2660, found 502.2661.

IR (neat, ATR): ν_{max} 3368 (br) 2982, 2932, 2873, 1702, 1622, 1479, 1376, 1217, 1097, 1082, 1058, 851 cm⁻¹.

Optical Rotation: [α]_D²³ = -2.78 (*c* 0.3, CHCl₃)

M.p.: 146 °C (decomposition).



Prepared following **General procedure C** using copper(I) chloride (5.90 mg, 0.0600 mmol, 30 mol %), 1,10-phenanthroline (10.8 mg, 0.0600 mmol, 30 mol %), and MeCN (4 mL) to make *Solution C*. (+)-Nootkatone (218 mg, 1.00 mmol, 5.0 equiv) was used for ozonolysis. 2',3'-O-Isopropylideneadenosine (61.5 mg, 0.200 mmol, 1.0 equiv) and MeCN (9 mL) were added to make

Suspension C. The crude product was purified through FCC to give **2-69** ($R_f = 0.38$; EtOAc) as a white solid (80.3 mg, 83% yield).

$^1\text{H NMR}$ (400 MHz, CDCl_3) δ 8.30 (s, 1H), 7.79 (s, 1H), 6.66 (brs, 1H), 6.03 (brs, 1H), 5.83 (d, $J = 4.8$ Hz, 1H), 5.80–5.73 (m, 1H), 5.17 (t, $J = 5.3$ Hz, 1H), 5.11–4.99 (m, 1H), 4.58 (brs, 1H), 4.51 (s, 1H), 3.94 (dd, $J = 12.8, 1.3$ Hz, 1H), 3.83–3.68 (m, 1H), 2.75–2.58 (m, 1H), 2.46–2.36 (m, 1H), 2.35–2.27 (m, 2H), 2.22 (d, $J = 4.4$ Hz, 1H), 2.00 (tt, $J = 13.1, 6.0$ Hz, 1H), 1.61 (s, 3H), 1.35 (s, 4H), 1.29–1.11 (m, 5H), 0.93 (d, $J = 6.8$ Hz, 3H).

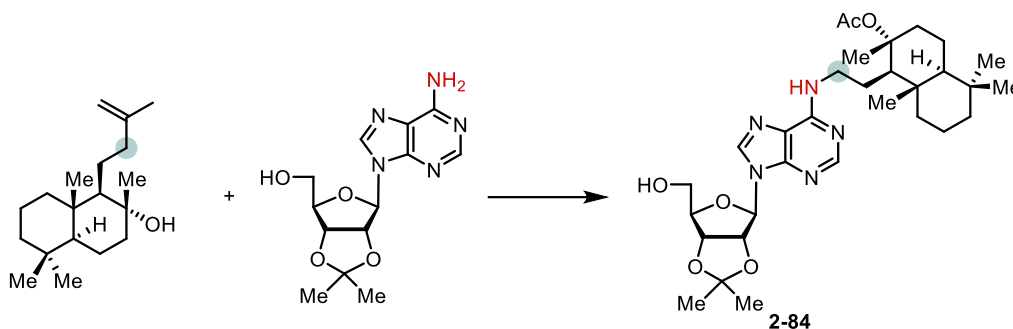
$^{13}\text{C NMR}$ (100 MHz, CDCl_3) δ 199.24, 174.91, 168.23, 154.32, 152.85, 139.62, 125.18, 113.97, 94.30, 86.07, 83.00, 81.72, 63.39, 45.67, 44.71, 41.69, 40.42, 39.73, 32.81, 31.64, 27.66, 25.26, 21.07, 16.99, 14.91.

HRMS (DART): $[\text{M}+\text{H}]^+$ calcd for $[\text{C}_{25}\text{H}_{34}\text{N}_5\text{O}_5]^+$ m/z 484.2554, found 484.2554.

IR (neat, ATR): ν_{max} 3314 (br) 2976, 2940, 1661, 1619, 1477, 1375, 1295, 1217, 1112, 1084, 851, 758 cm^{-1} .

Optical Rotation: $[\alpha]_{\text{D}}^{25} = 4.36$ (c 0.2, CHCl_3)

M.p.: 77 °C (decomposition).



Prepared following **General procedure C** using copper(I) chloride (3.00 mg, 0.0300 mmol, 30 mol %), 1,10-phenanthroline (5.40 mg, 0.0300 mmol, 30 mol %), and MeCN (2 mL) to make *Solution C*. The alkene **2-102** (139 mg, 0.500 mmol, 5.0 equiv) was used for ozonolysis. 2',3'-*O*-

Isopropylideneadenosine (30.7 mg, 0.100 mmol, 1.0 equiv) and MeCN (5 mL) were used to make *Suspension C*. The crude product was purified through FCC to give **2-84** ($R_f = 0.27$; hexanes/EtOAc, 1:1) as a white solid (48.6 mg, 83% yield).

$^1\text{H NMR}$ (400 MHz, CDCl_3) δ 8.30 (s, 1H), 7.74 (s, 1H), 6.82 (brs, 1H), 6.22 (s, 1H), 5.81 (d, $J = 4.9$ Hz, 1H), 5.18 (t, $J = 5.4$ Hz, 1H), 5.09 (d, $J = 5.8$ Hz, 1H), 4.51 (s, 1H), 4.00–3.86 (m, 1H), 3.76 (d, $J = 12.8$ Hz, 1H), 3.64 (d, $J = 27.9$ Hz, 2H), 2.88–2.69 (m, 1H), 2.05 (s, 3H), 1.80–1.51 (m, 10H), 1.49 (s, 3H), 1.46–1.38 (m, 1H), 1.35 (s, 4H), 1.25 (q, $J = 15.0, 13.6$ Hz, 1H), 1.12 (td, $J = 13.3, 3.8$ Hz, 1H), 1.05–0.92 (m, 2H), 0.84 (s, 3H), 0.83 (s, 3H), 0.76 (s, 3H).

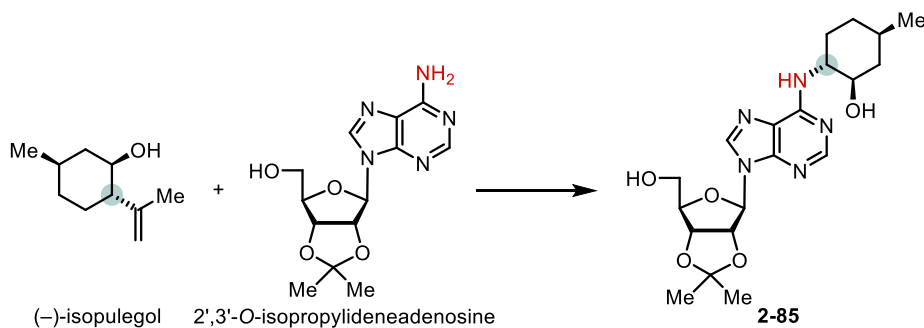
$^{13}\text{C NMR}$ (100 MHz, CDCl_3) δ 170.30, 155.27, 152.82, 147.12, 139.30, 121.34, 113.89, 94.40, 87.49, 86.01, 82.96, 81.76, 63.47, 56.22, 55.56, 42.36, 41.76, 39.61, 39.30, 38.92, 33.29, 33.09, 27.69, 25.37, 25.26, 23.09, 21.41, 20.02, 19.92, 18.24, 15.62.

HRMS (DART): $[\text{M}-\text{OAc}]^+$ calcd for $[\text{C}_{29}\text{H}_{44}\text{N}_5\text{O}_4]^+$ m/z 526.3388, found 526.3388.

IR (neat, ATR): ν_{max} 3243 (br), 2991, 2939, 2871, 1723, 1622, 1476, 1387, 1297, 1252, 1114, 1081, 851, 754 cm^{-1} .

Optical Rotation: $[\alpha]_{\text{D}}^{25} = -23.83$ (c 0.2, CHCl_3)

M.p.: 78 °C (decomposition).



Prepared following **General procedure A** using 2',3'-O-isopropylideneadenosine (61.5 mg, 0.200 mmol, 1.0 equiv), copper(I) chloride (4.00 mg, 0.400 mmol, 20 mol %), 1,10-phenanthroline (7.20

mg, 0.200 mmol, 50 mol %), and MeOH (5 mL) to make *Solution A*. (–)-Isopulegol (92.5 mg, 0.600 mmol, 3.0 equiv) was used for ozonolysis and MeCN (2 mL) to make *Solution B*. The crude product was purified through FCC to give **2-85** ($R_f = 0.26$; EtOAc/MeOH, 20:1) as a white solid (67.1 mg, 80% yield).

$^1\text{H NMR}$ (400 MHz, CDCl_3) δ 8.05 (s, 1H), 7.69 (s, 1H), 7.41 (brs, 1H), 6.42 (brs, 1H), 5.74 (d, $J = 5.0$ Hz, 1H), 5.19 (t, $J = 5.4$ Hz, 1H), 5.11 (d, $J = 5.9$ Hz, 1H), 3.98 (brs, 1H), 3.87 (d, $J = 12.5$ Hz, 1H), 3.77–3.55 (m, 2H), 2.23–2.11 (m, 1H), 2.10–1.96 (m, 1H), 1.72–1.61 (m, 4H), 1.60–1.50 (m, 1H), 1.46 (s, 3H), 1.38–1.26 (m, 1H), 1.26–1.07 (m, 2H), 0.98 (d, $J = 6.5$ Hz, 3H).

$^{13}\text{C NMR}$ (100 MHz, CDCl_3) δ 154.59, 152.44, 146.26, 138.89, 120.07, 114.08, 94.61, 86.25, 82.78, 81.66, 74.00, 63.31, 56.06, 44.33, 33.14, 31.63, 31.16, 27.83, 25.25, 21.93.

HRMS (ESI-TOF): $[\text{M}+\text{H}]^+$ calcd for $[\text{C}_{20}\text{H}_{30}\text{N}_5\text{O}_5]^+$ m/z 420.2241, found 420.2242.

IR (neat, ATR): ν_{max} 3321 (br), 2926, 2855, 1623, 1588, 1479, 1376, 1337, 1298, 1216, 1113, 1083, 851, 761 cm^{-1} .

Optical Rotation: $[\alpha]_{\text{D}}^{25} = -30.00$ (c 0.1, CHCl_3)

M.p.: 64 °C (decomposition).

2.6.5.8. Additional information on prices and previous syntheses of compounds that appear in the main text

Figure 2.11 Previous routes for the synthesis of enantiopure 3-indazolyl-2-methylpropanols

The search of the following structure afforded 2663 reactions and 22 international patents in SciFinder®.

Reaction Structure substructure with limiters > reactions (2663) > get references (26)

REFERENCES

Research Topic
Author Name
Company Name
Document Identifier
Journal
Patent
Tags

SUBSTANCES

Chemical Structure
Markush
Molecular Formula
Property
Substance Identifier

REACTIONS

Reaction Structure

REACTIONS: REACTION STRUCTURE

Structure Editor

Click image to change structure or view detail.

Import CxF

Search

Reaction Structure substructure with limiters > reactions (2663) > get references (26)

REFERENCES

Get Substances
Get Reactions
Get Relations
Citations

Analyze Refine Categorize

Sort by: Accession Number

0 of 26 References Selected

1. Preparation of aryl ether compounds as TE PATENTPAK
By Lim, Jongwon; Simov, Vladimir; Vara, Brandon A
From PCT Int. Appl. (2022), WO 2022177869 A1 20
The present invention is directed compds. I | and the A² ring may contain ≥1 heteroatoms 1H-inden-5-yl or cyclohexyl; Ring D = Ph or p

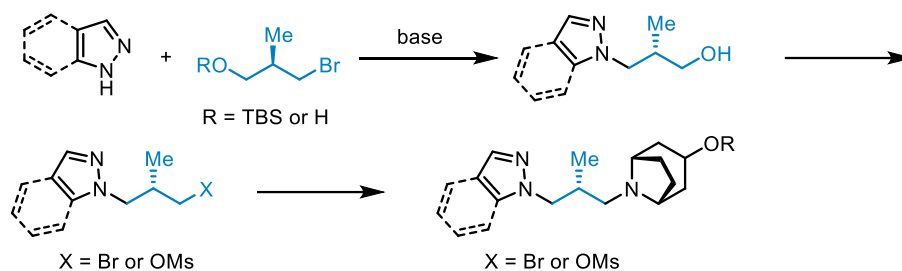
2. Pyrazoles as casein kinase 1 delta modulat PATENTPAK
By Lebold, Terry Patrick; Previllo, Cathy; Samant, Ai
From PCT Int. Appl. (2022), WO 2022058920 A1 20
A compd. of formula 1, pharmaceutical com^y casein kinase 1 delta (CSNK1D) modulation fluorouridilidyl rvaazolyl at^r: R² is (m)subst

U.S. Pat. Appl. Publ. 22
Faming Zhanli Shengqing 1
Jpn. Kokai Tokkyo Koho 1

Show More

Synthesis of muscarinic agonists

International Patent WO 2014/152144 A1, Sep. 25, 2014.



Synthesis of (R)-3-bromo-2-methylpropan-1-ol

J. Org. Chem. **2015**, *80*, 1610–1617.

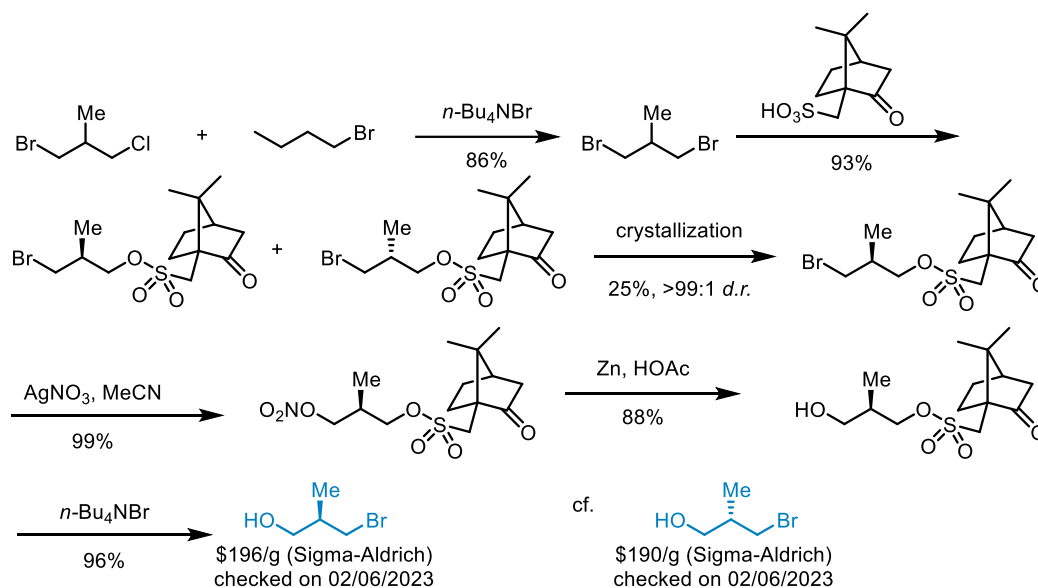
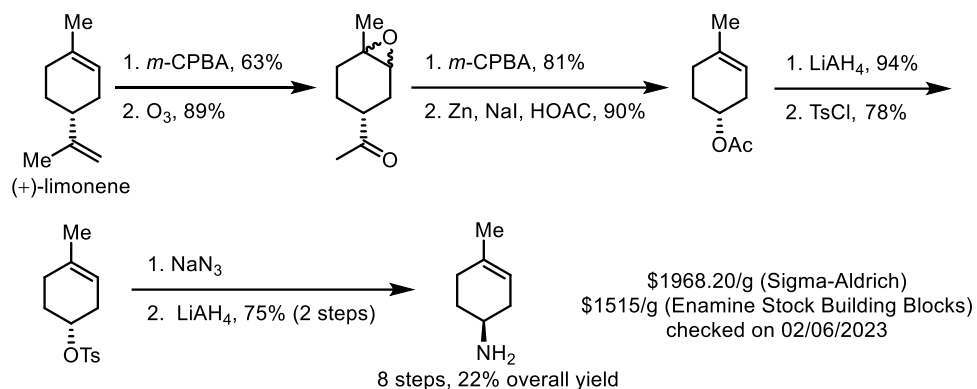


Figure 2.12 Previous routes for the synthesis of enantiopure 4-methyl-3-cyclohexenamine

Synthesis of (-)-(1S)-4-methyl-3-cyclohexenamine

J. Org. Chem. **1992**, *57*, 3454–3462.



Synthesis of (+)-(1*R*)-4-methyl-3-cyclohexenamine

J. Org. Chem. **1992**, *57*, 3454–3462.

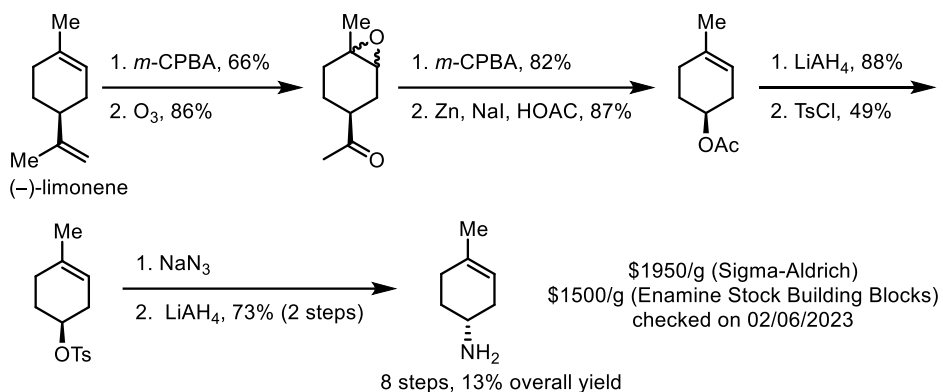
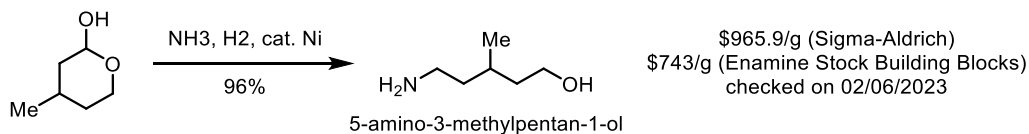


Figure 2.13 Previous route for the synthesis of 5-amino-3-methylpentan-1-ol

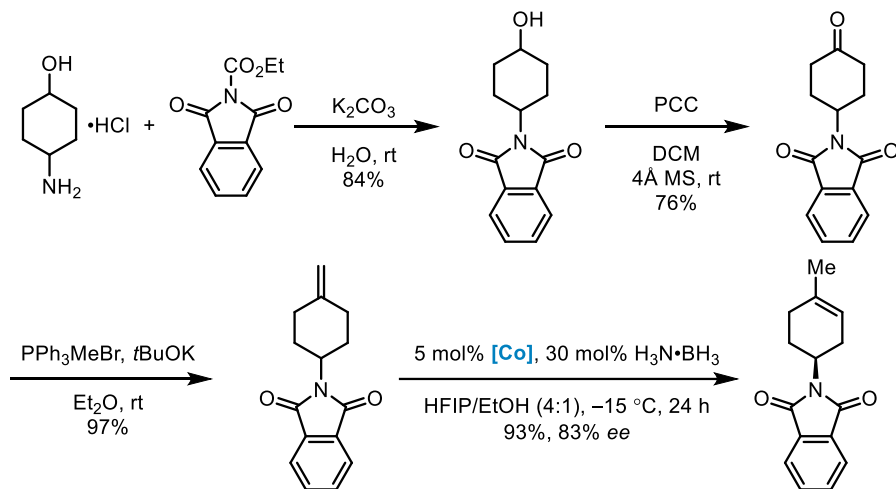
European Patent Application, 1074541, 07 Feb 2001



No known synthesis of an enantiopure sample

Figure 2.14 Previous route for the synthesis of (*S*)-2-(4-methylcyclohex-3-en-1-yl)isoindoline-1,3-dione

J. Am. Chem. Soc. **2021**, *143*, 20633–20639.



Synthesis of [Co]:

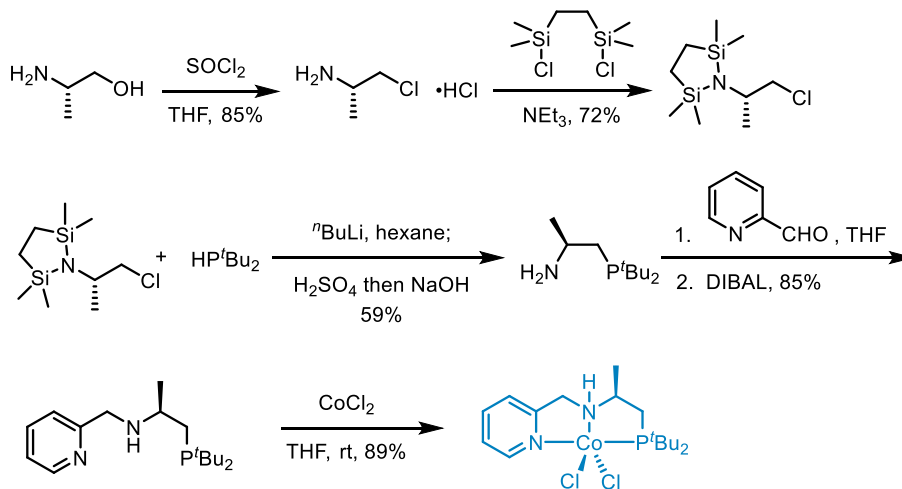
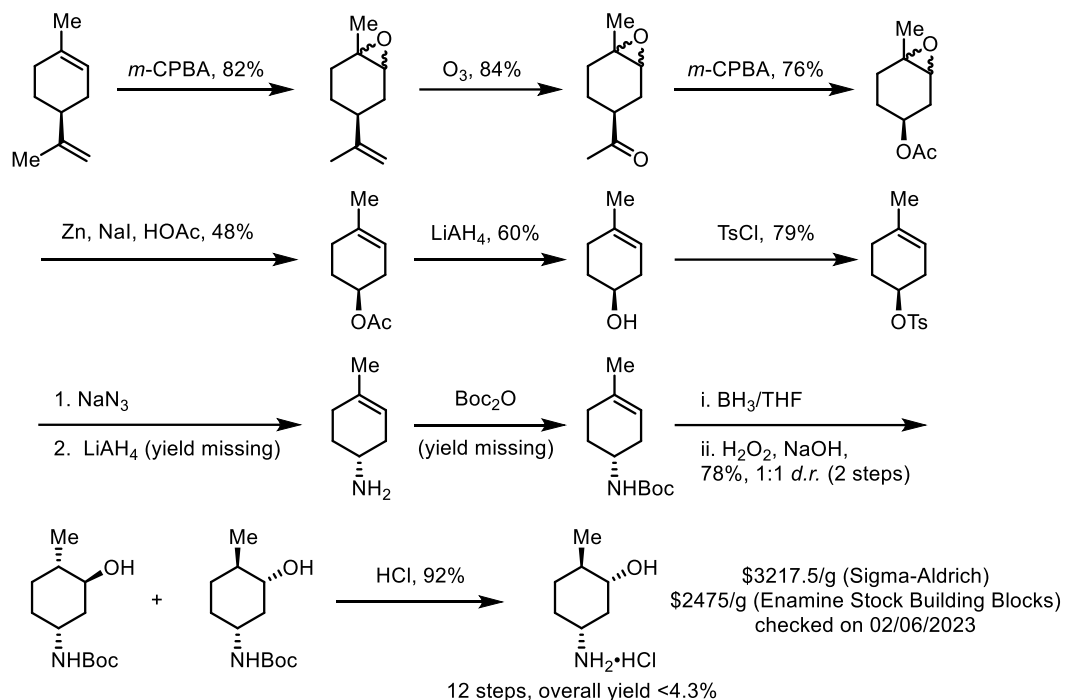


Figure 2.15 Previous routes for the synthesis of (1*R*,3*R*,4*R*)-3-hydroxy-4-methylcyclohexan-1-aminium chloride

U.S. Patent US 9365524 B2, Jun. 14, 2016.



International Patent WO 2017/019487 A1, Feb. 2, 2017.

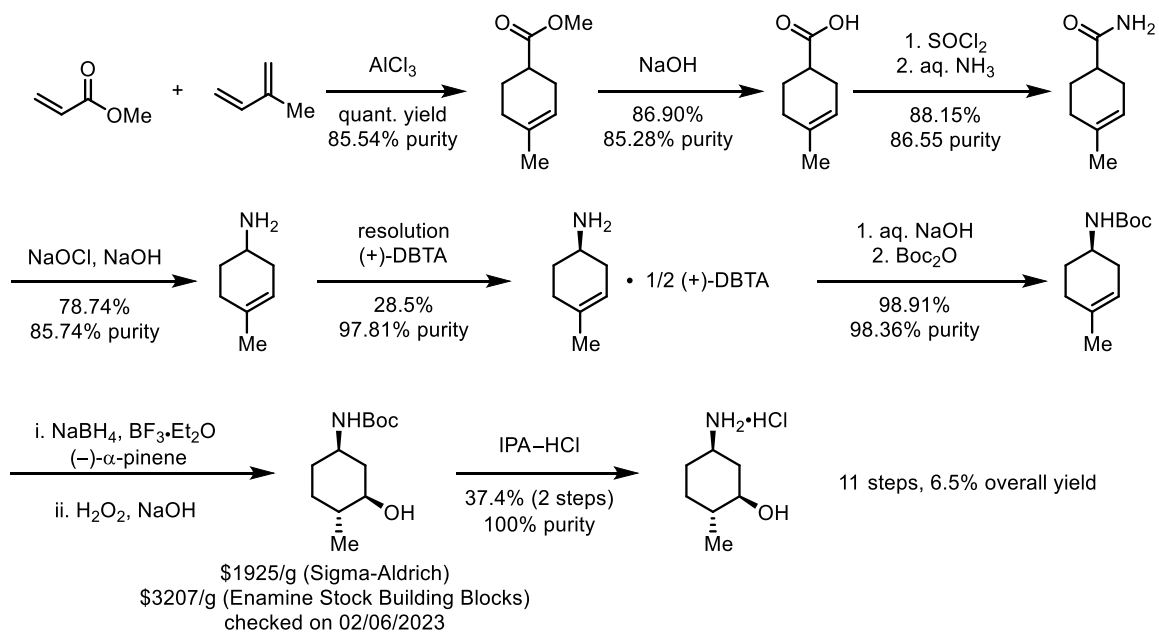
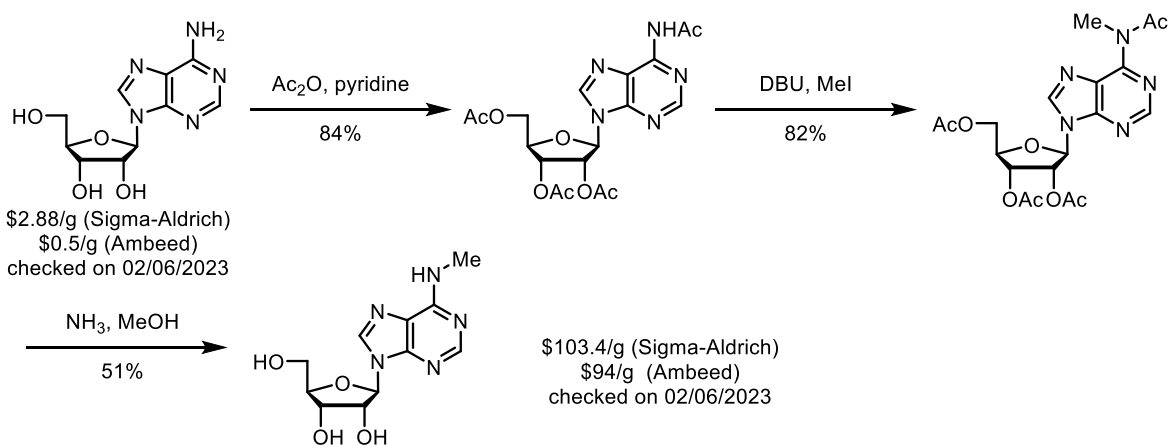
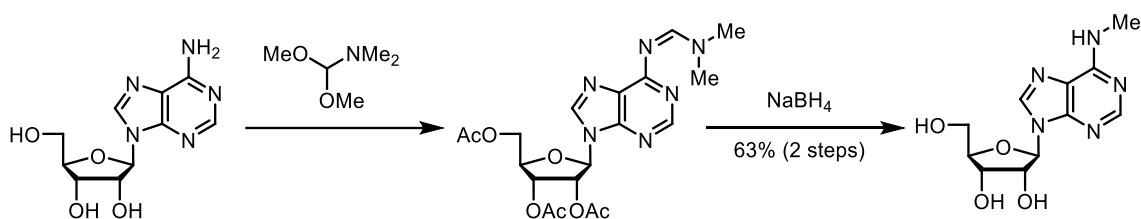


Figure 2.16 Previous routes for the synthesis of m⁶A and D₃-m⁶A

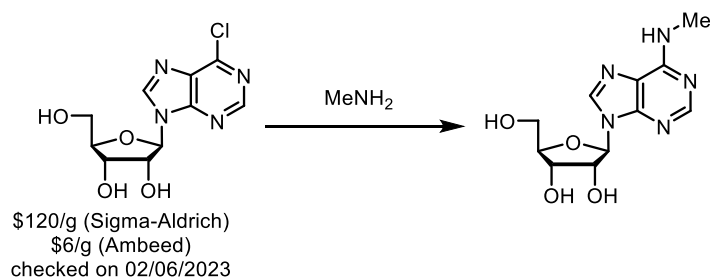
Bioorg. Med. Chem. **2019**, 27, 1099–1109; *ACS Chem. Biol.* **2015**, 10, 1450–1455; *Synthesis* **2011**, 15, 2483–2489.



Synlett, **2001**, 5, 643–645.



Eight references using this method:



We did not find any synthesis of D₃-m⁶A.

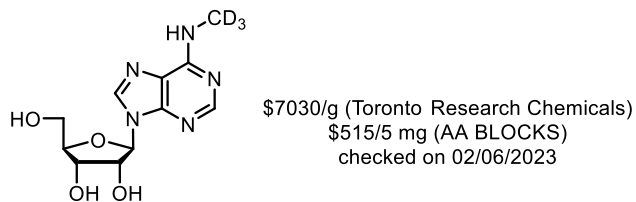
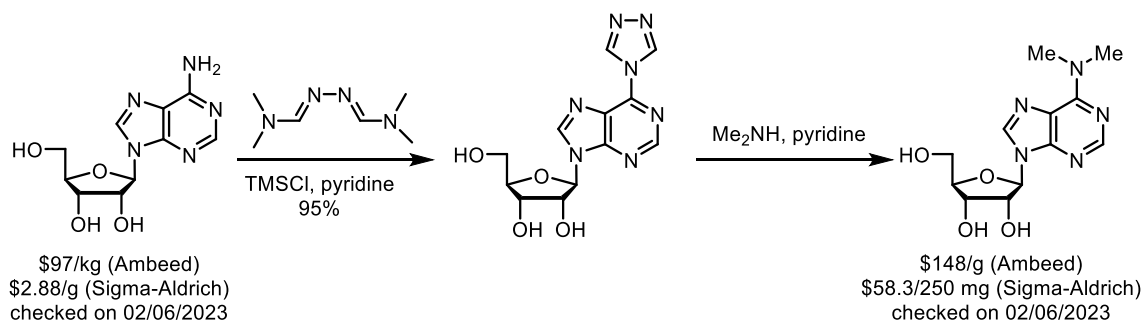


Figure 2.17 Previous routes for the synthesis of m⁶,6A

J. Am. Chem. Soc. **1995**, *117*, 5951–5957.



10 references using this method

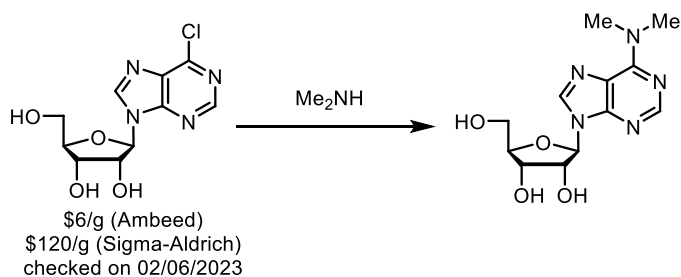
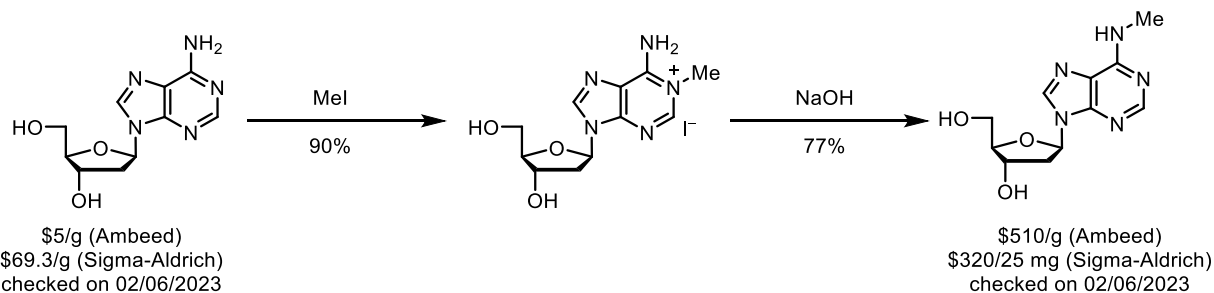
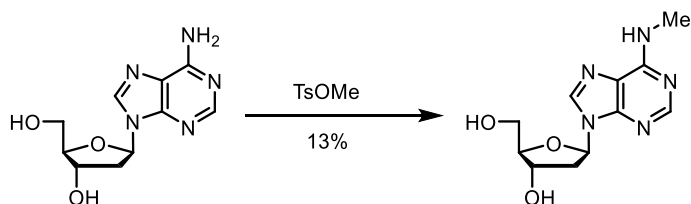


Figure 2.18 Previous routes for m⁶dA synthesis

Helv. Chim. Acta. **1986**, *69*, 1034–1040.



Angew. Chem. Int. Ed. **2017**, *56*, 11268–11271.



Acta. Chem. Scand B, **1986**, *B40*, 806–816.

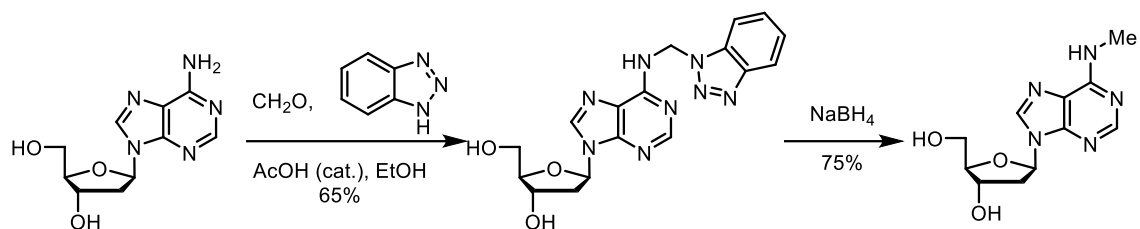
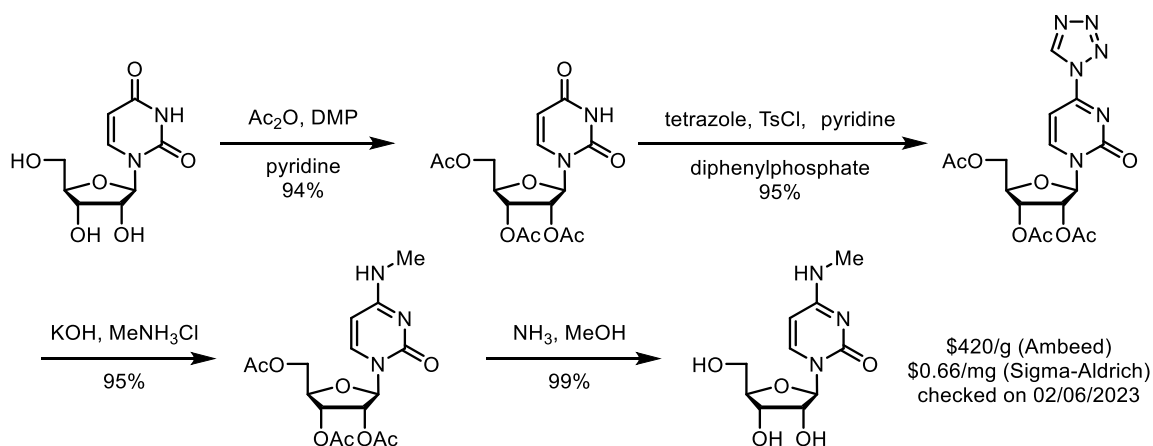
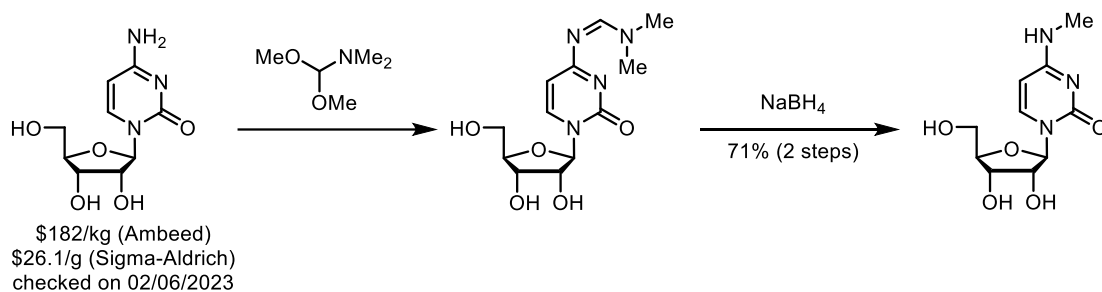


Figure 2.19 Previous routes for the synthesis of m⁴C

Bioorg. Med. Chem. **2008**, *16*, 8795–8800.



Synlett, **2001**, *5*, 643–645.



Nucleosides Nucleotides **1997**, *16*, 53–65.

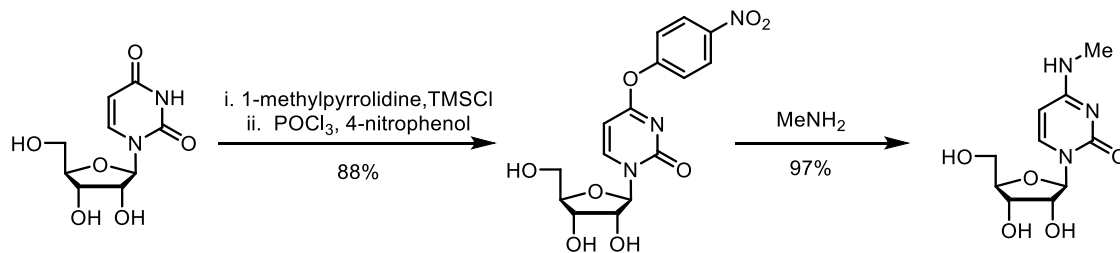
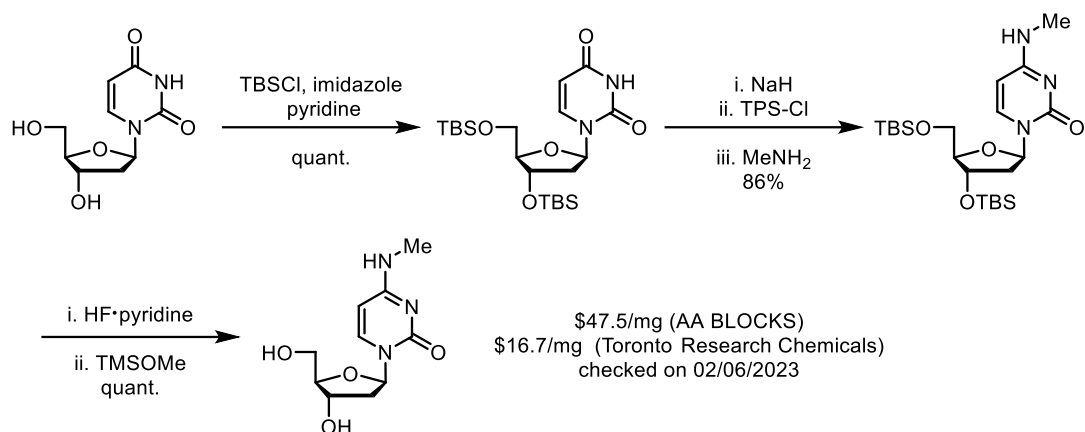
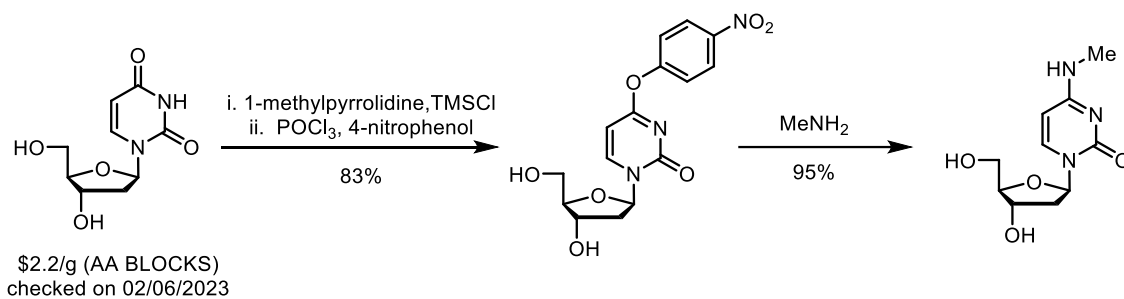


Figure 2.20 Previous routes for the synthesis of **m⁴dC**

Angew. Chem. Int. Ed. **2017**, *56*, 11268–11271.

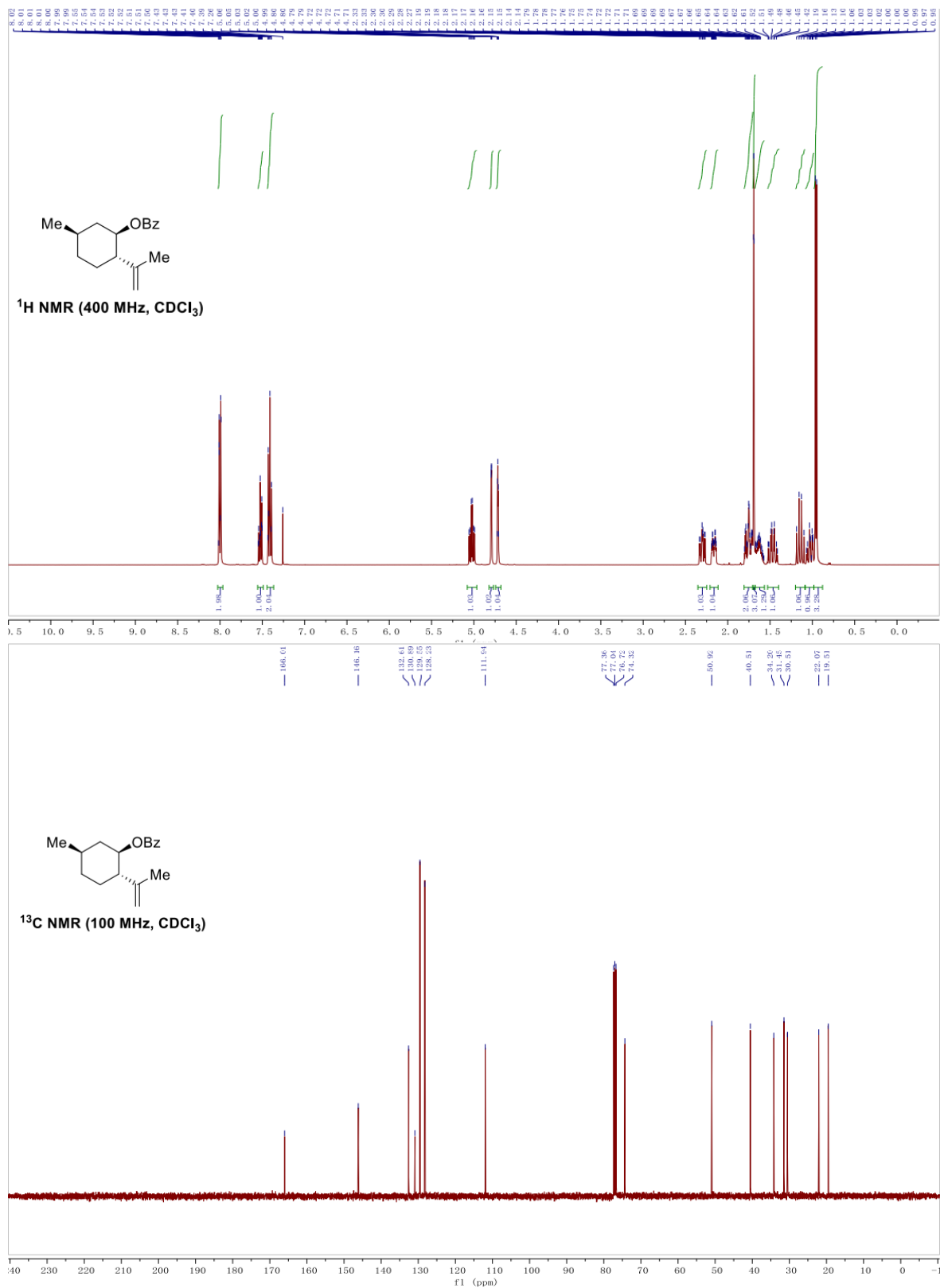


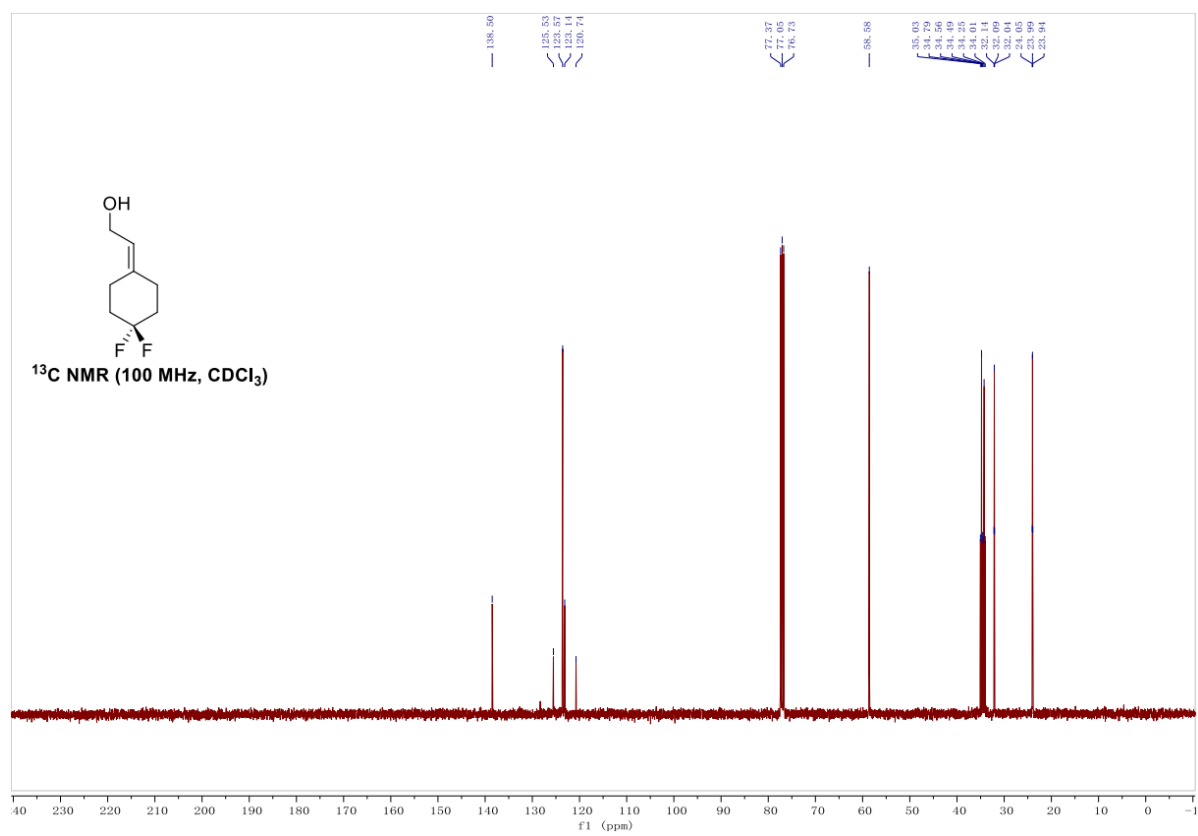
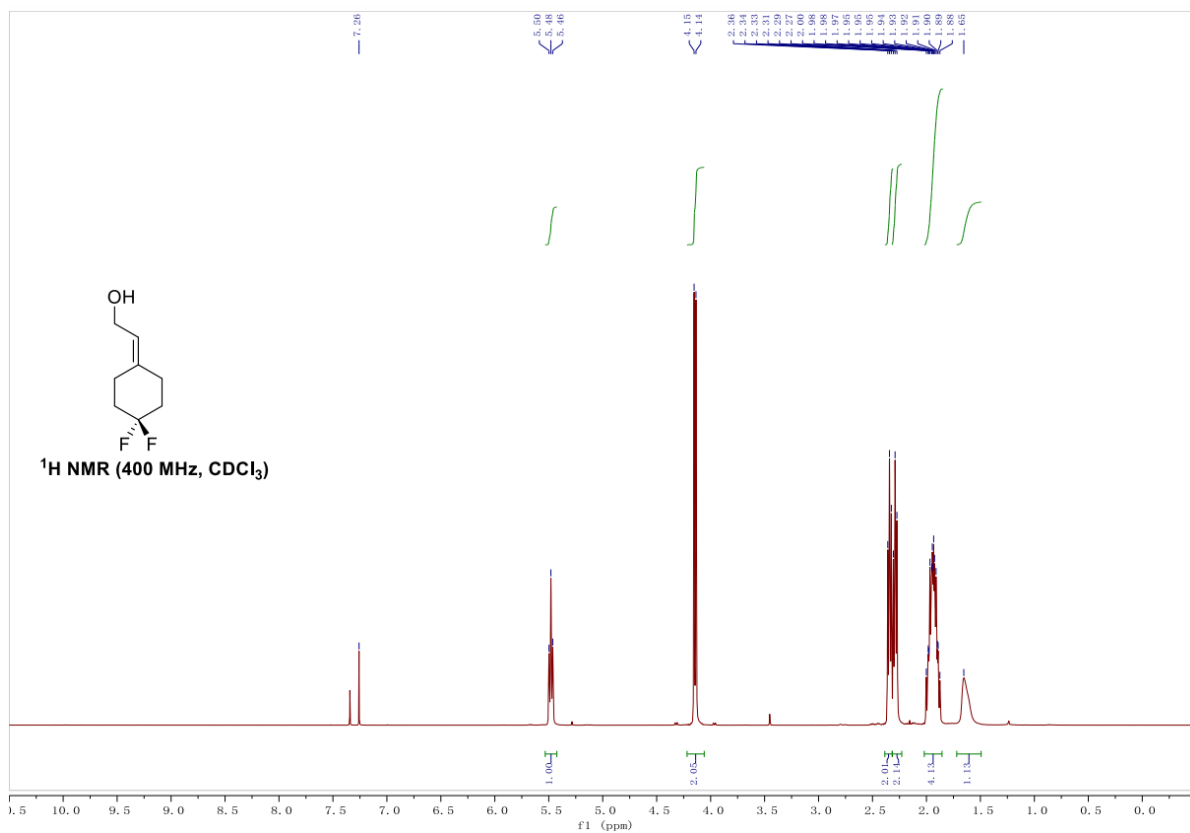
Nucleosides Nucleotides **1997**, *16*, 53–65.

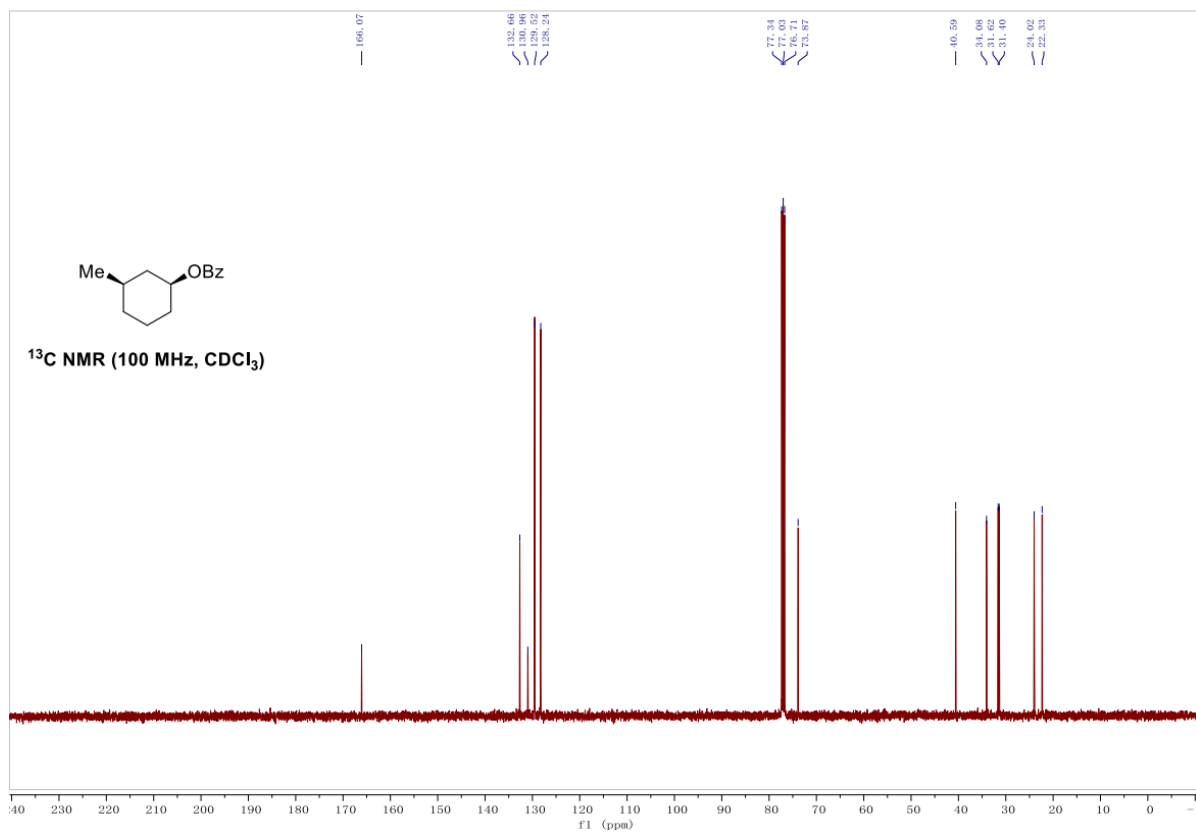
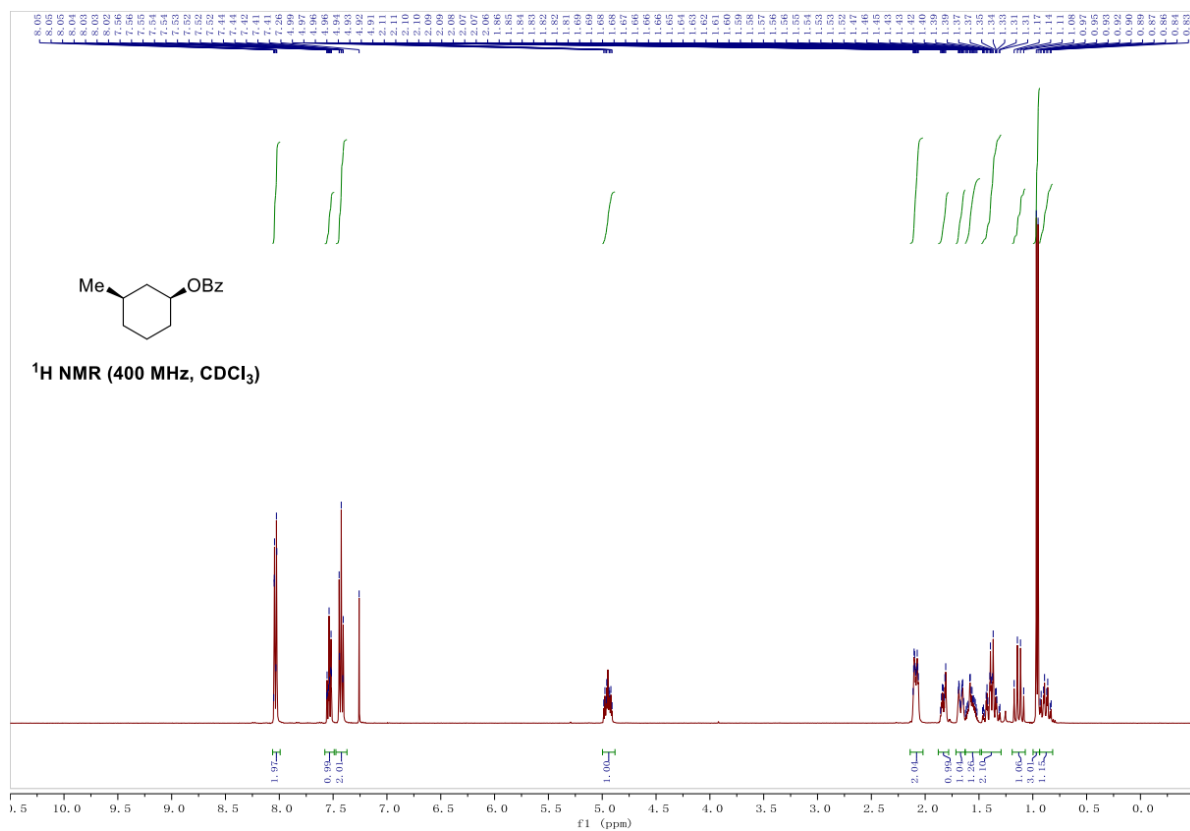


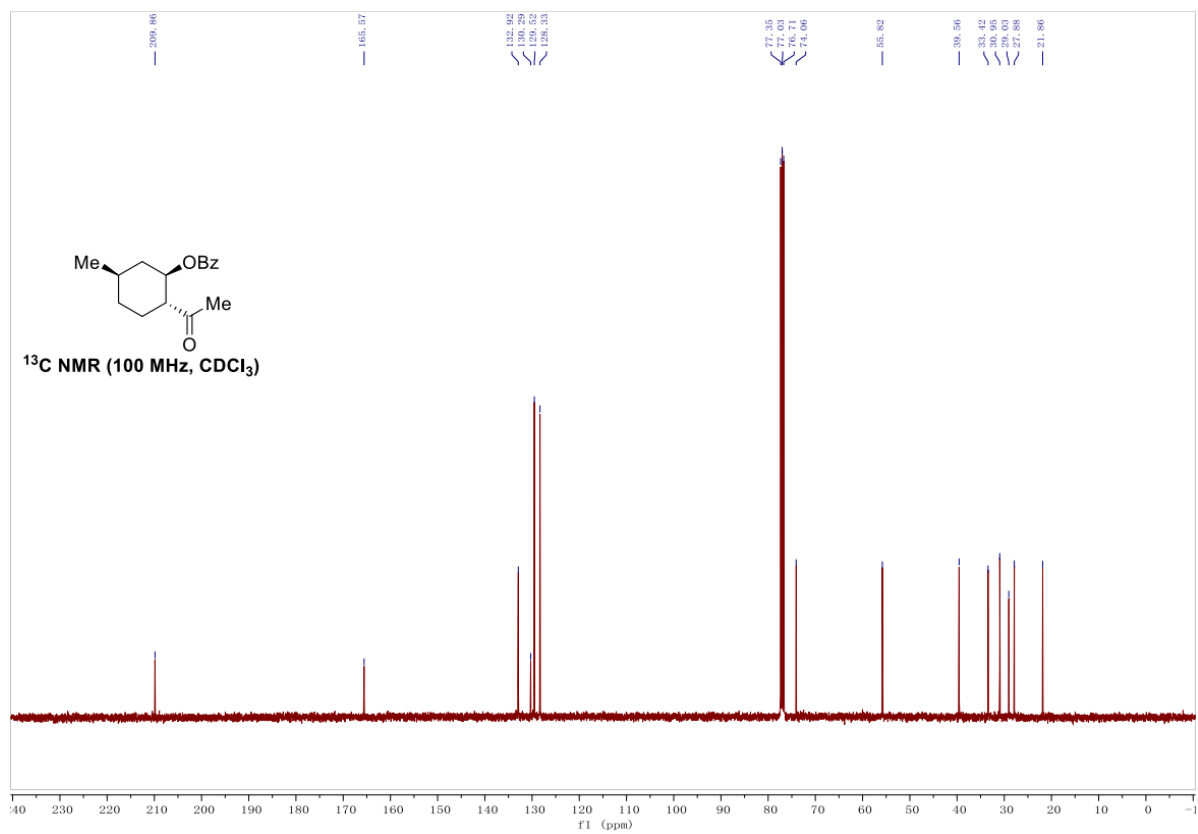
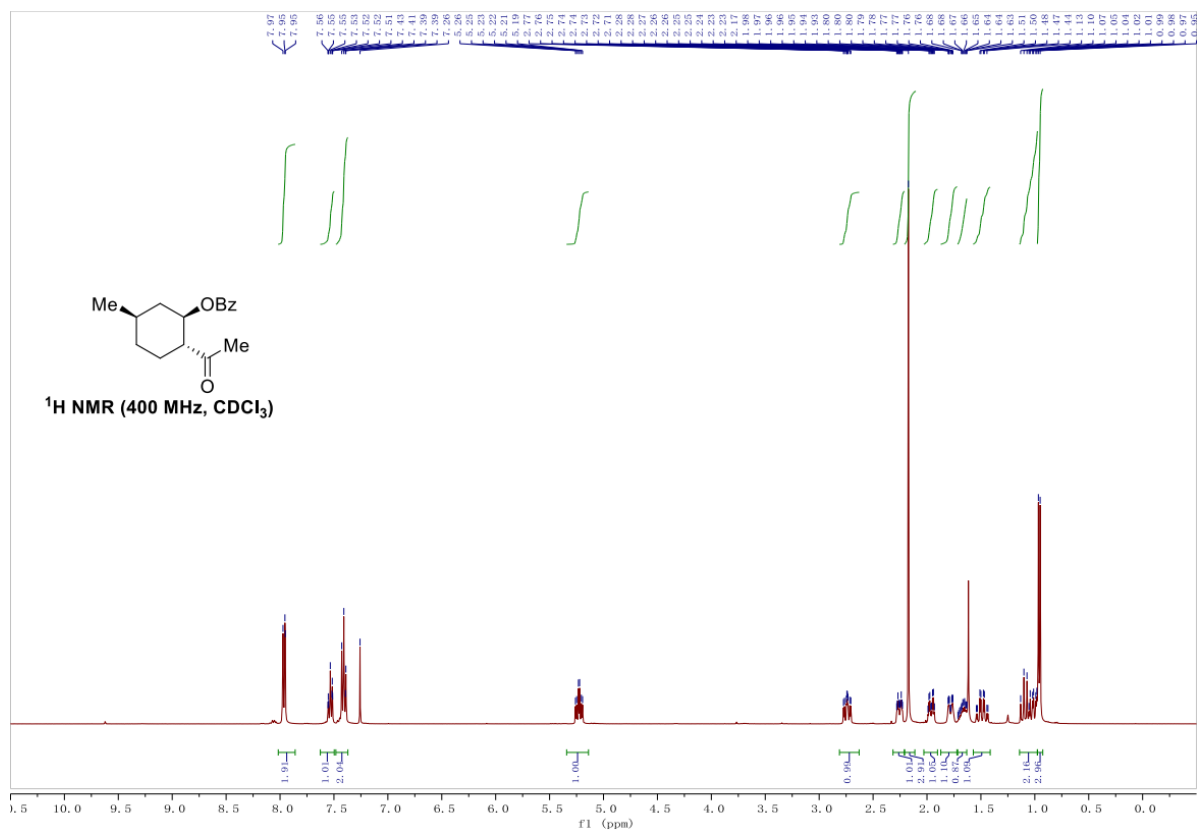
Note: No known syntheses of **m⁴dC** have started from deoxycytidine.

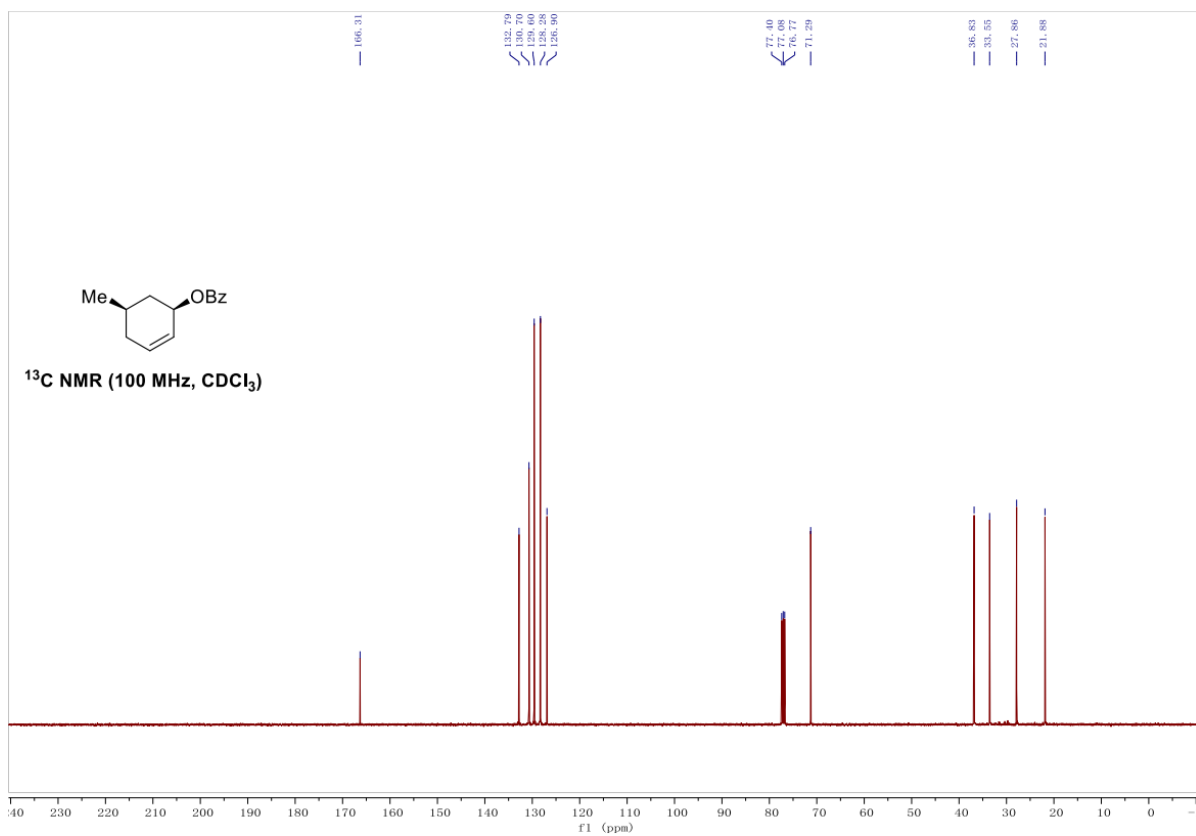
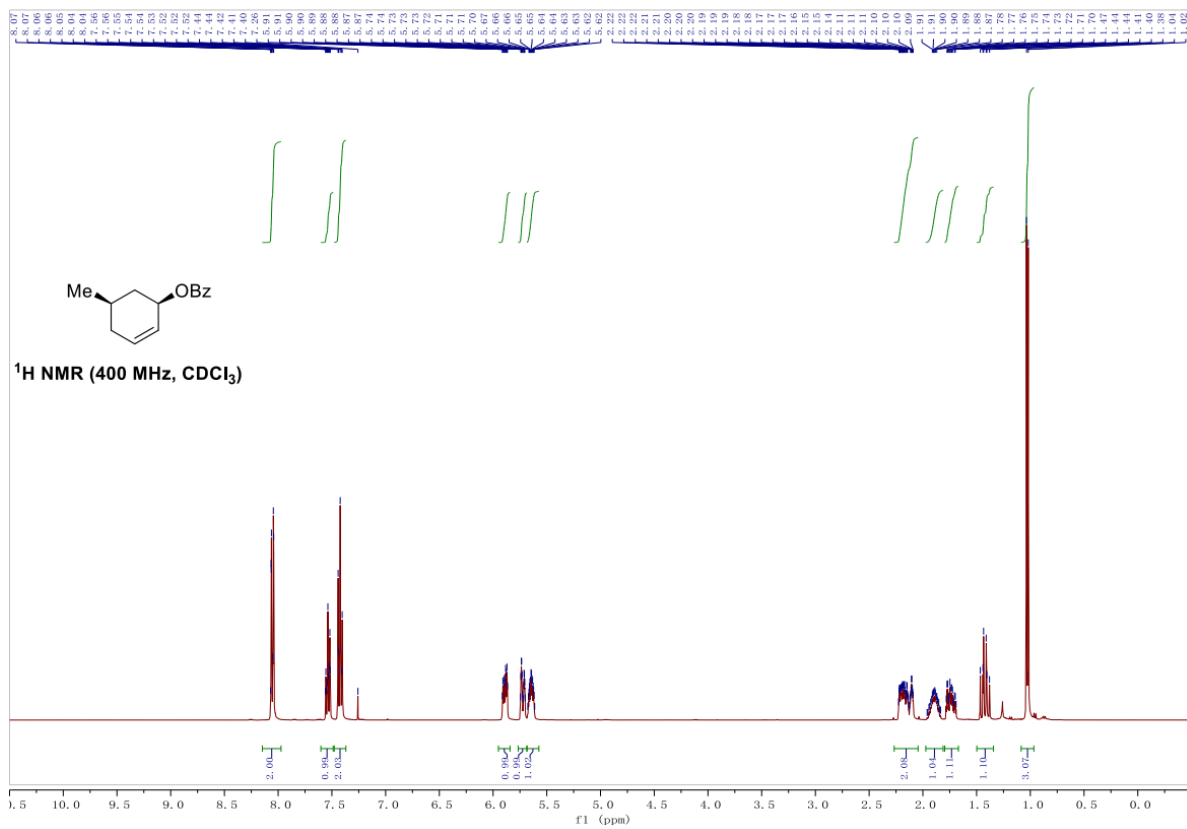
2.6.6. NMR Spectra Relevant to Chapter 2

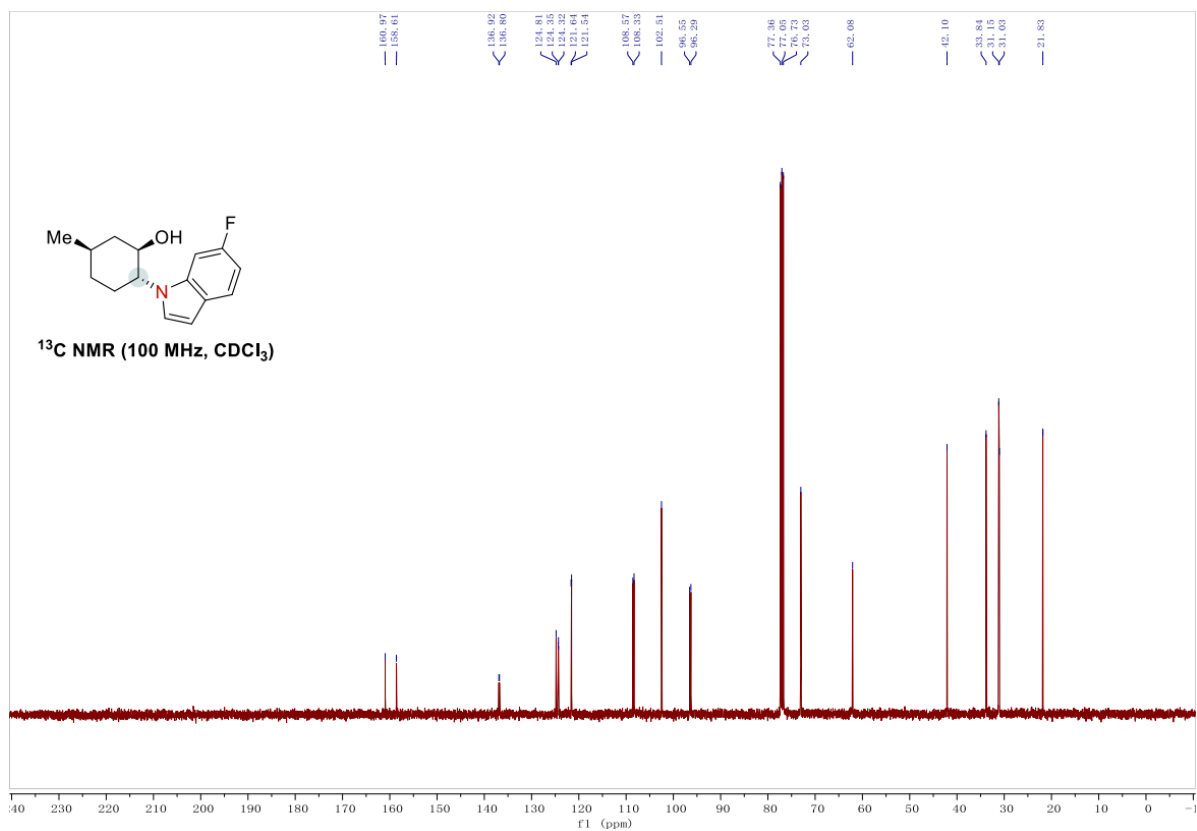
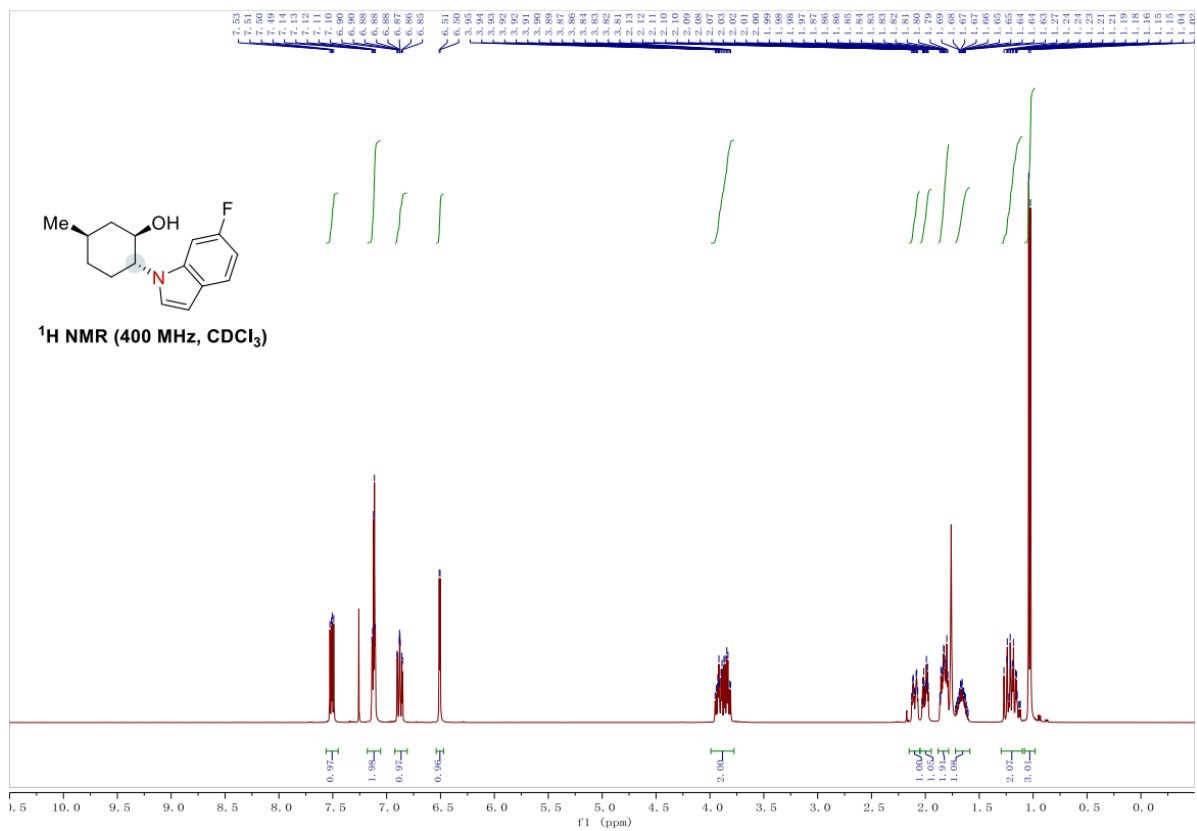


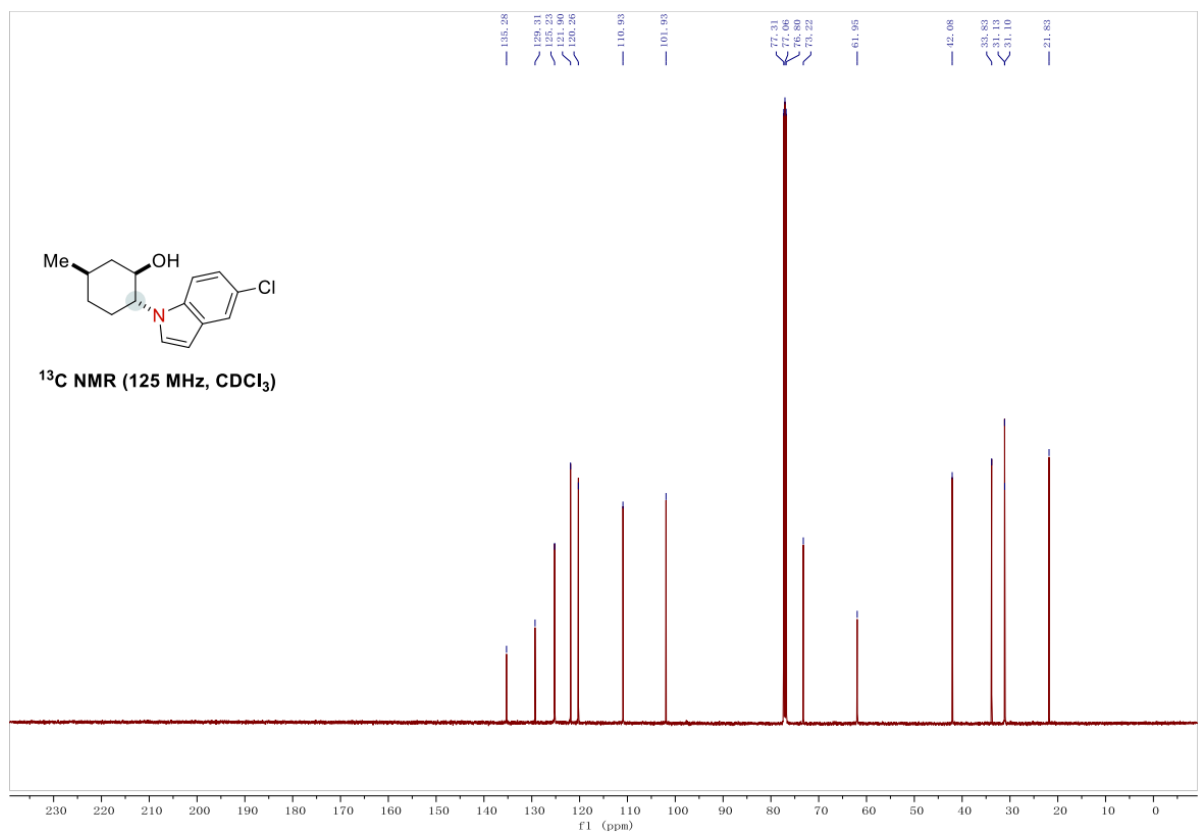
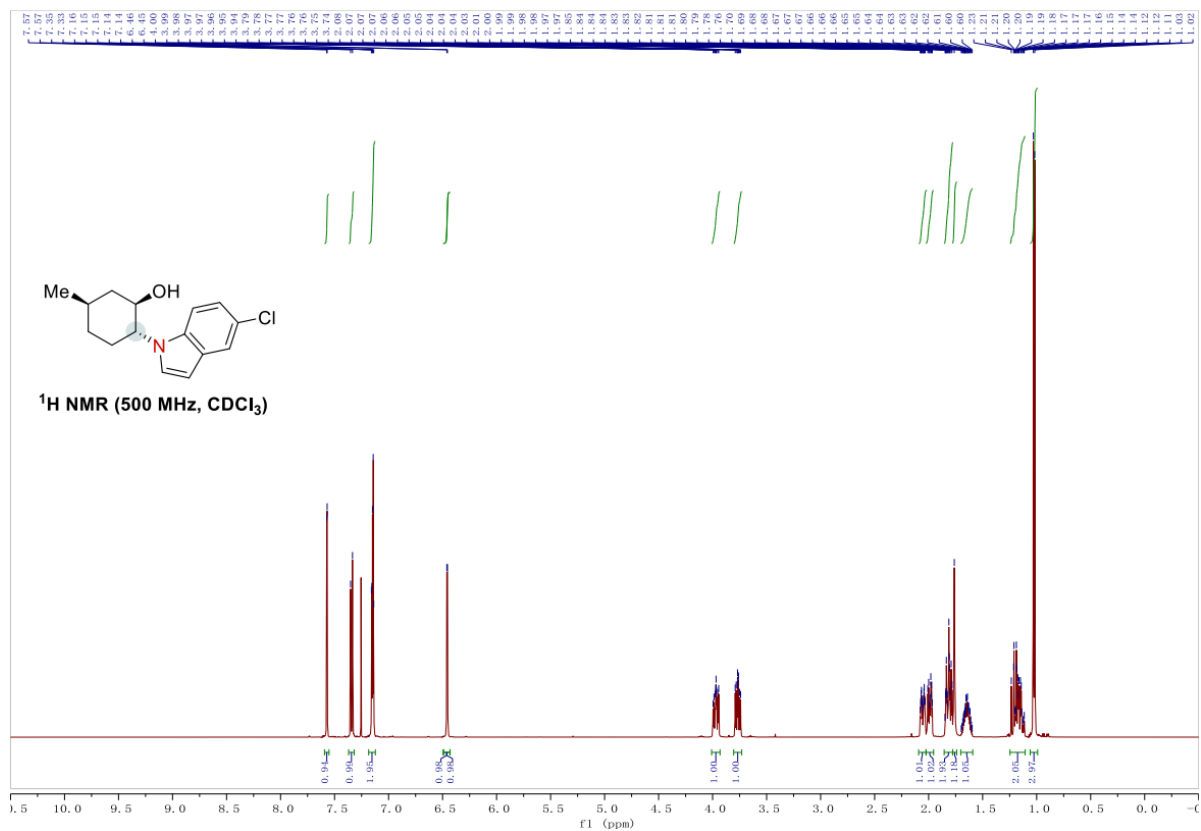


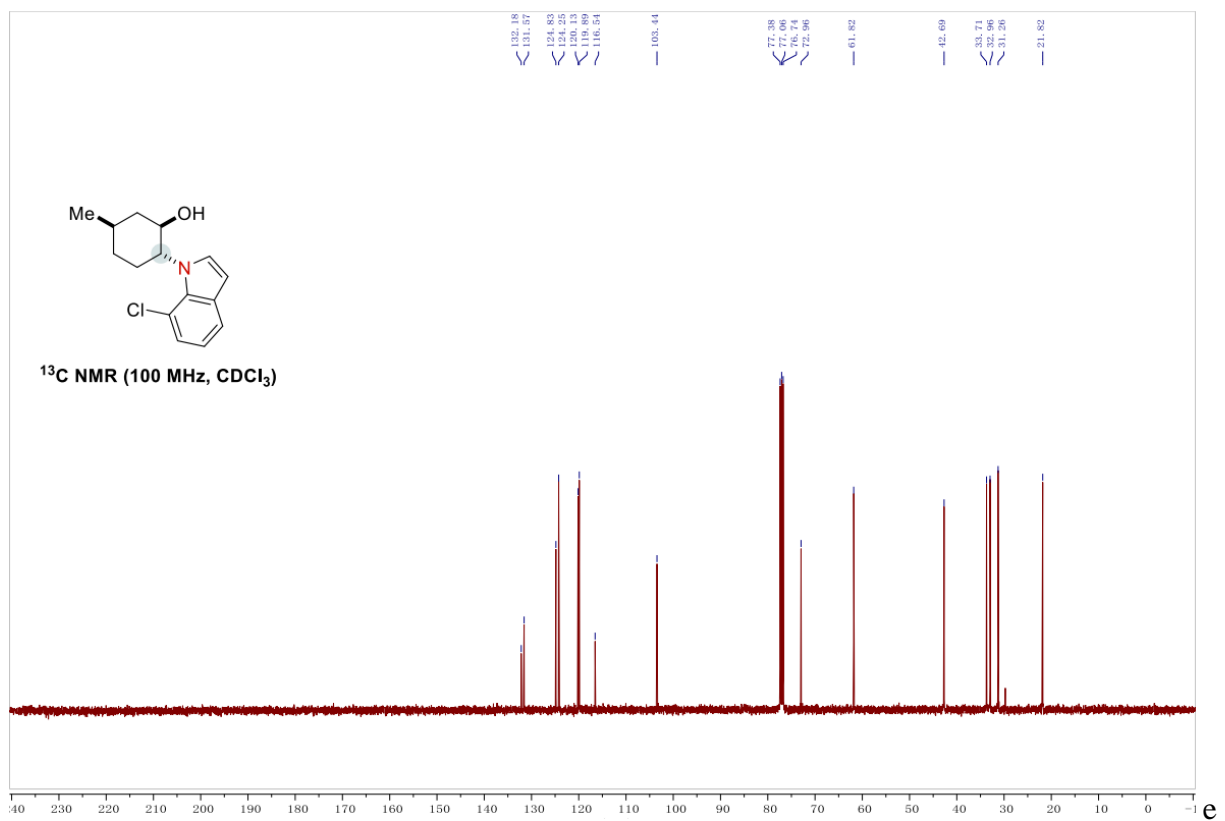
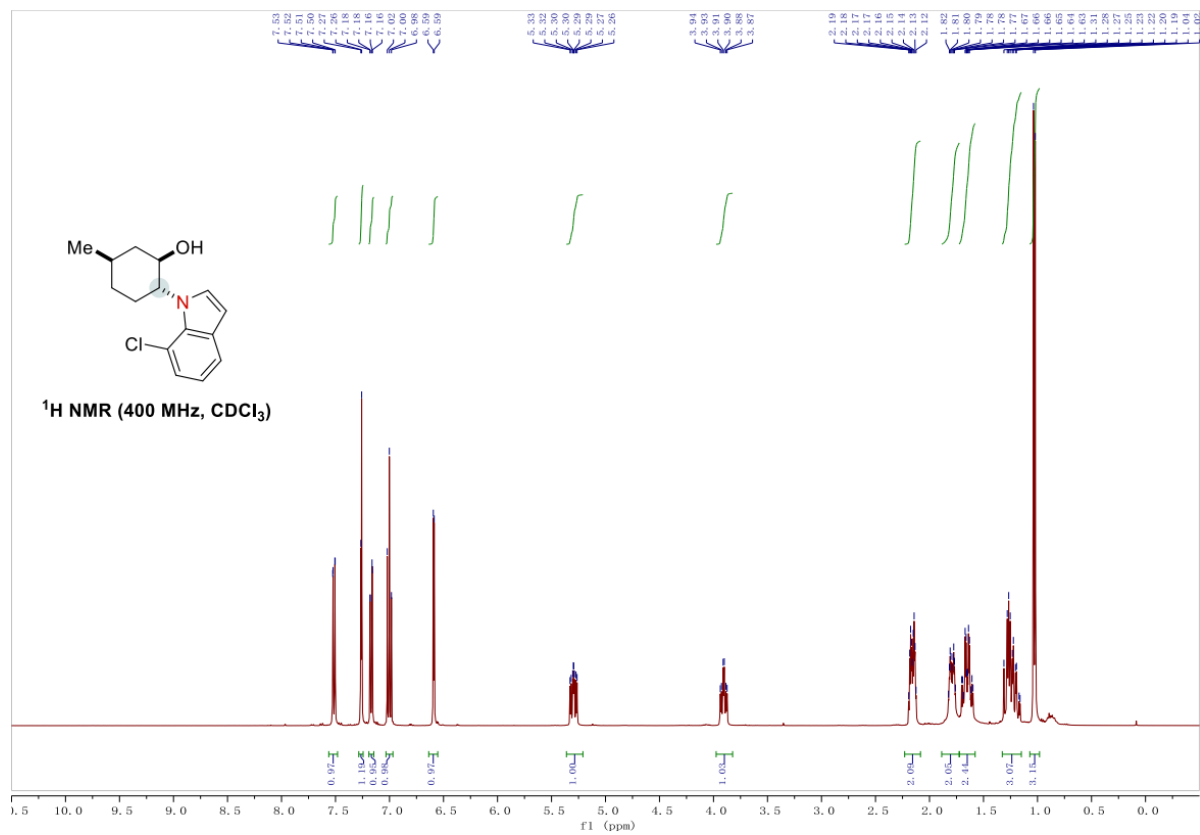


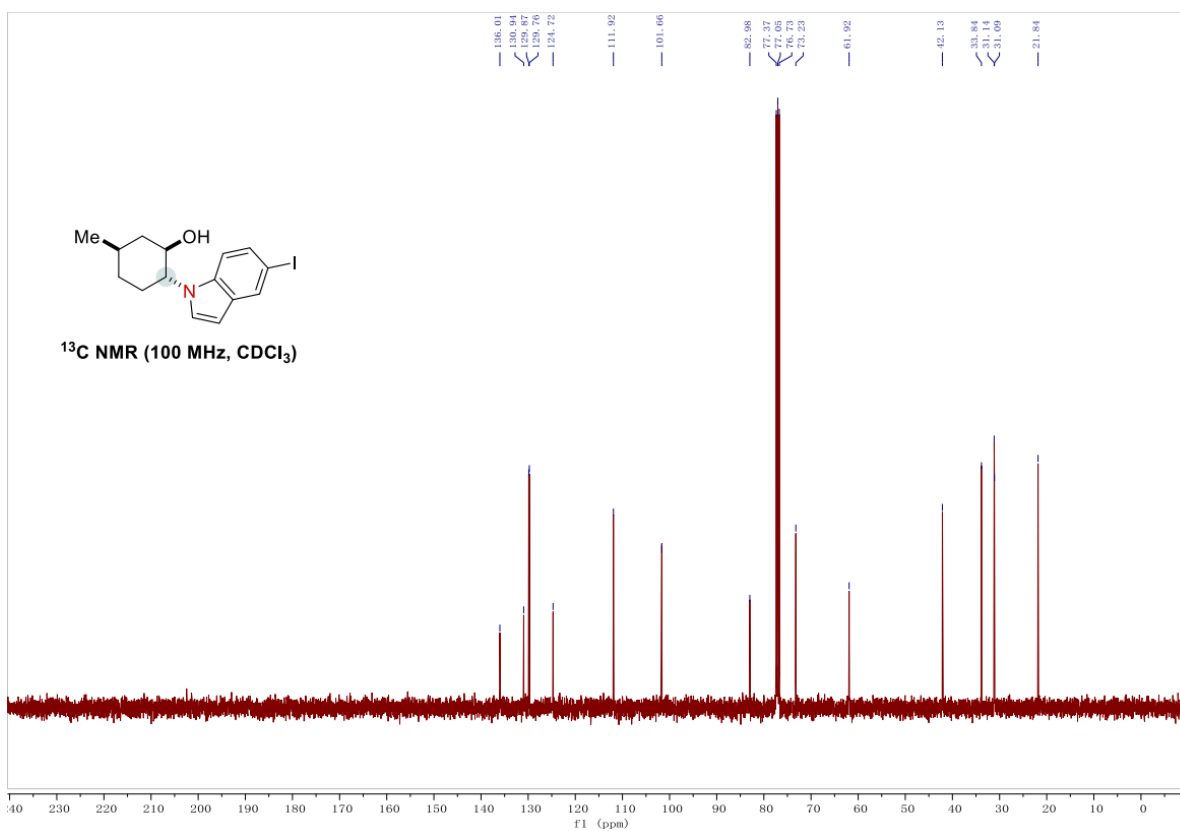
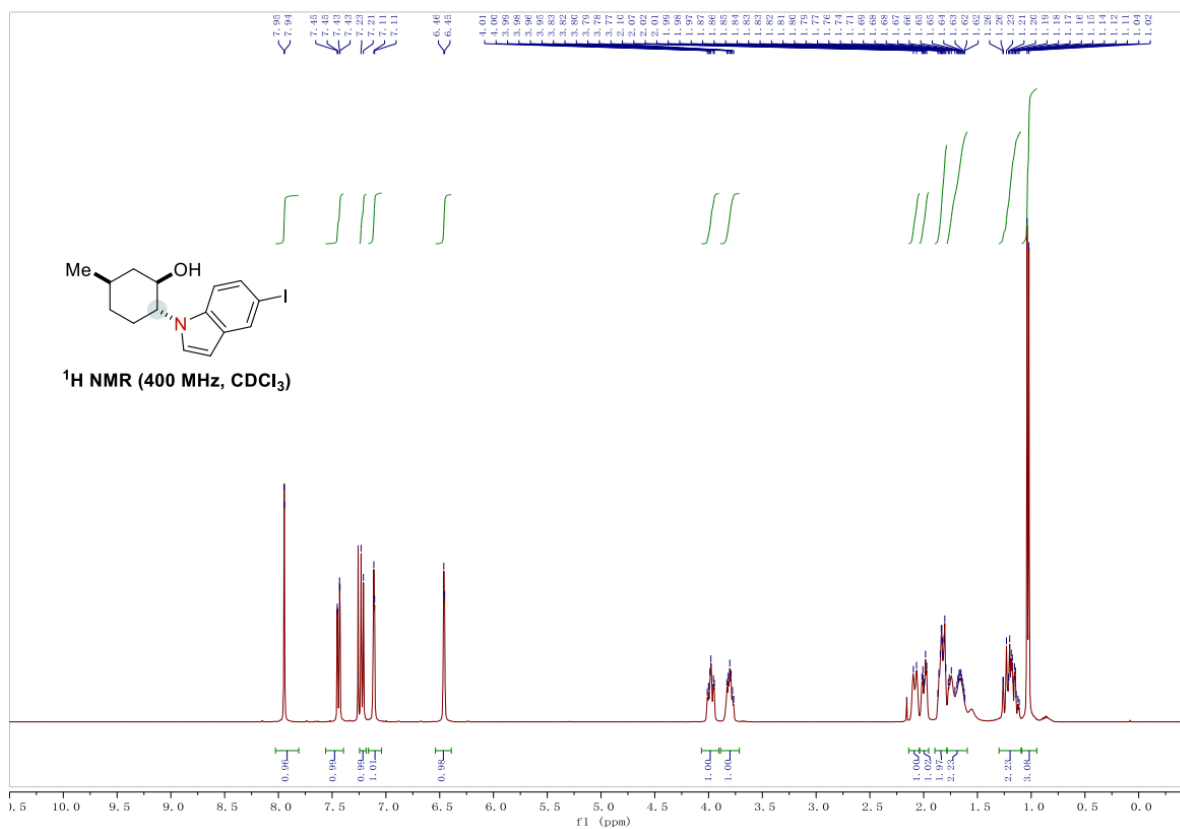


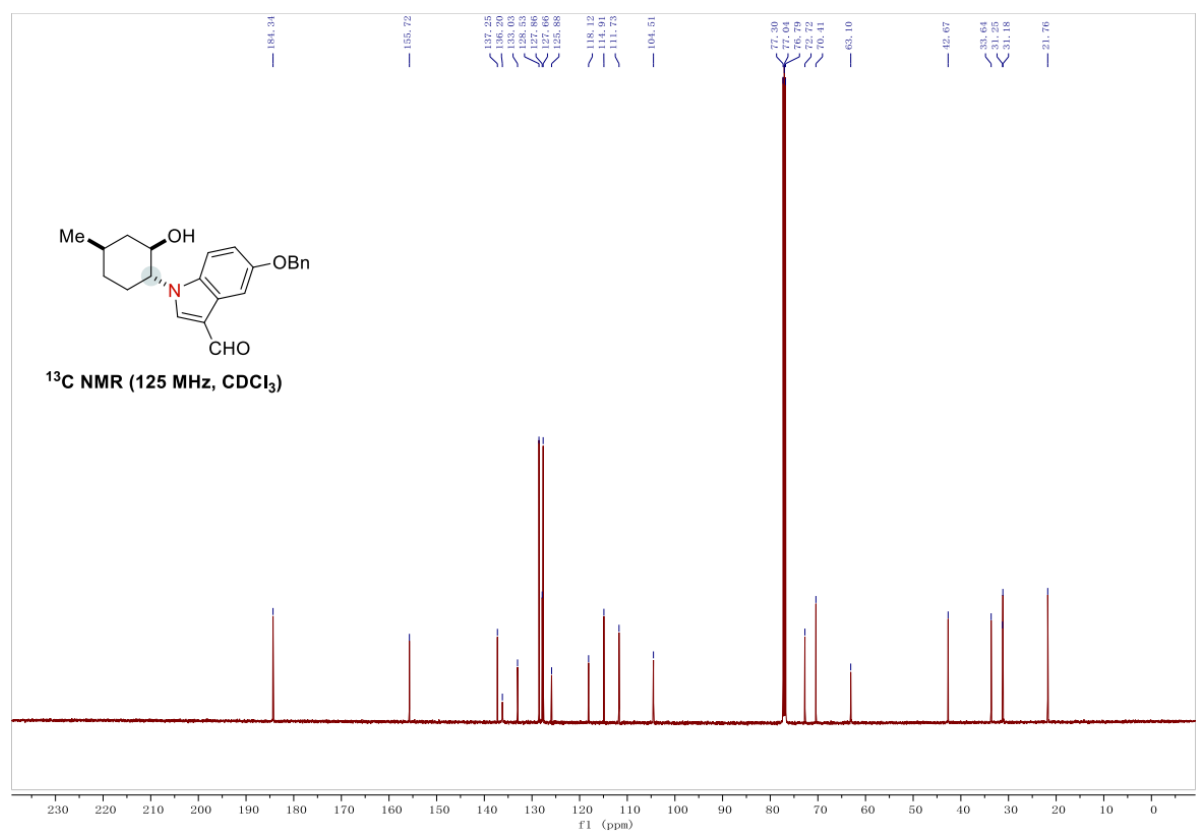
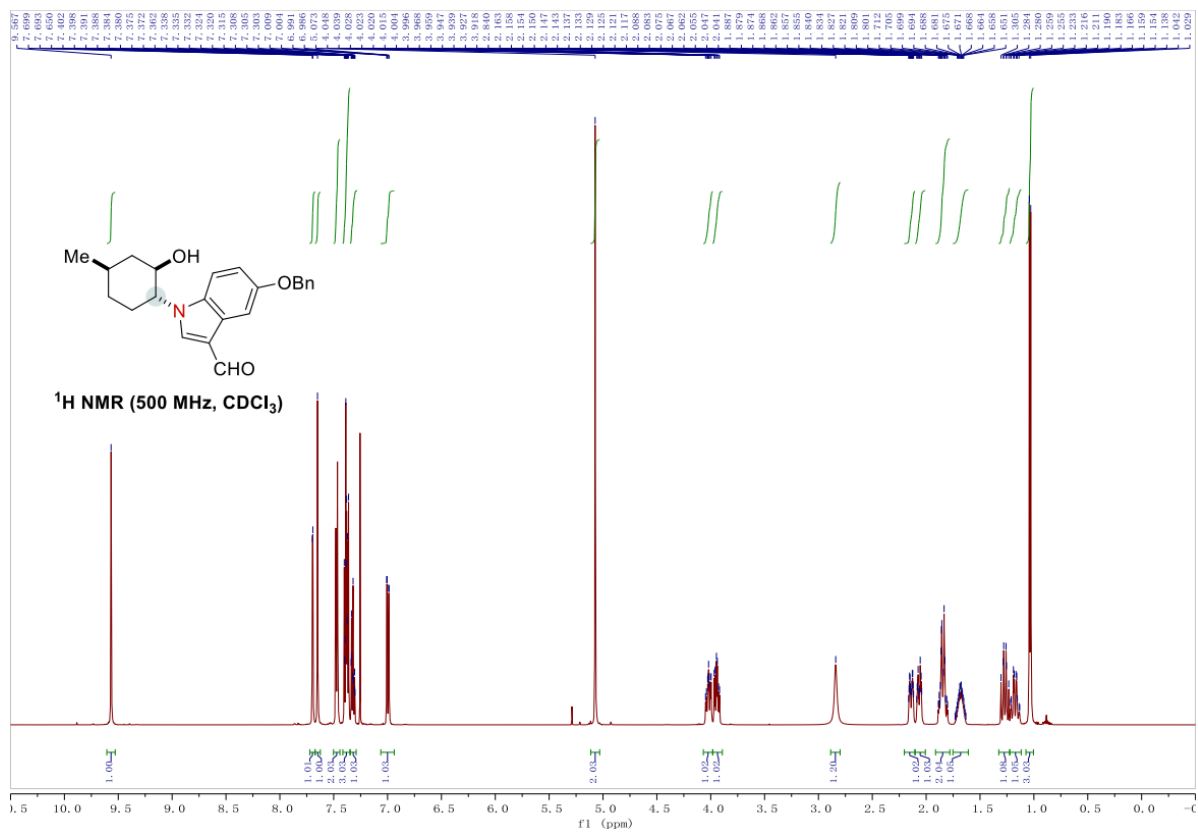


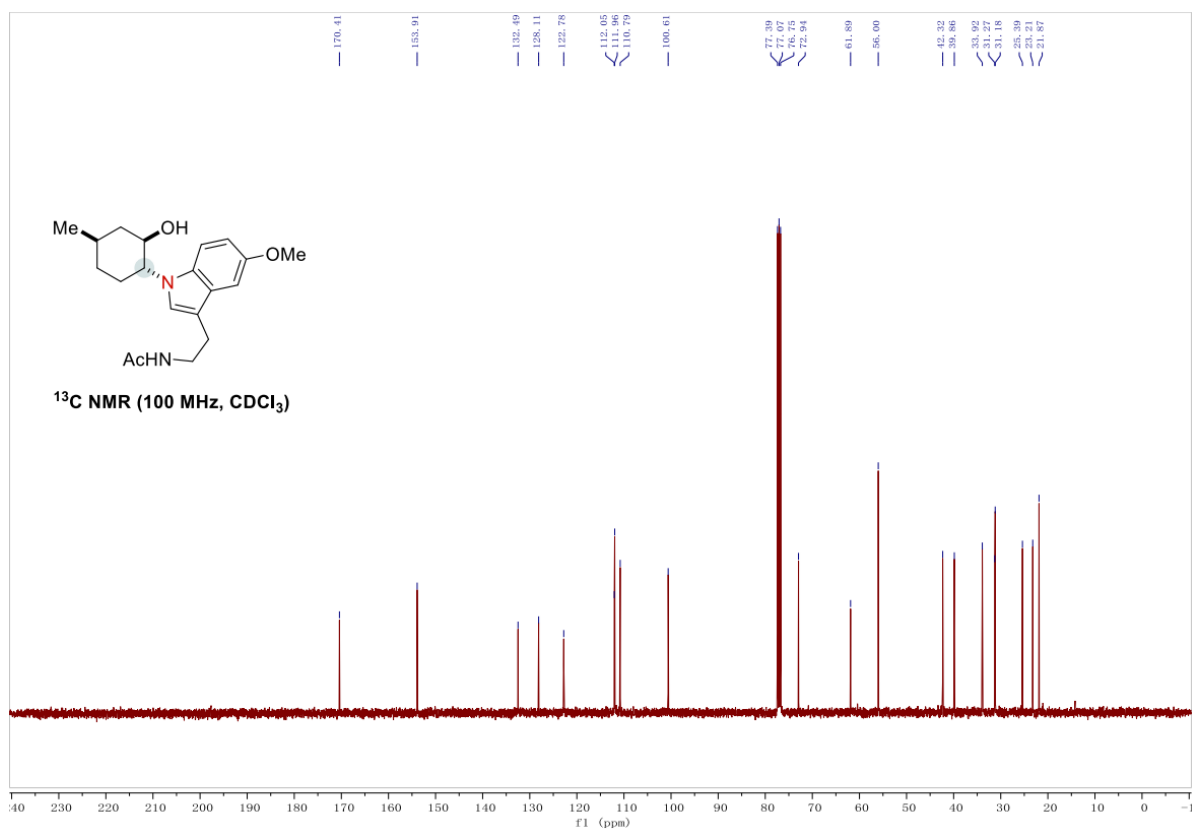
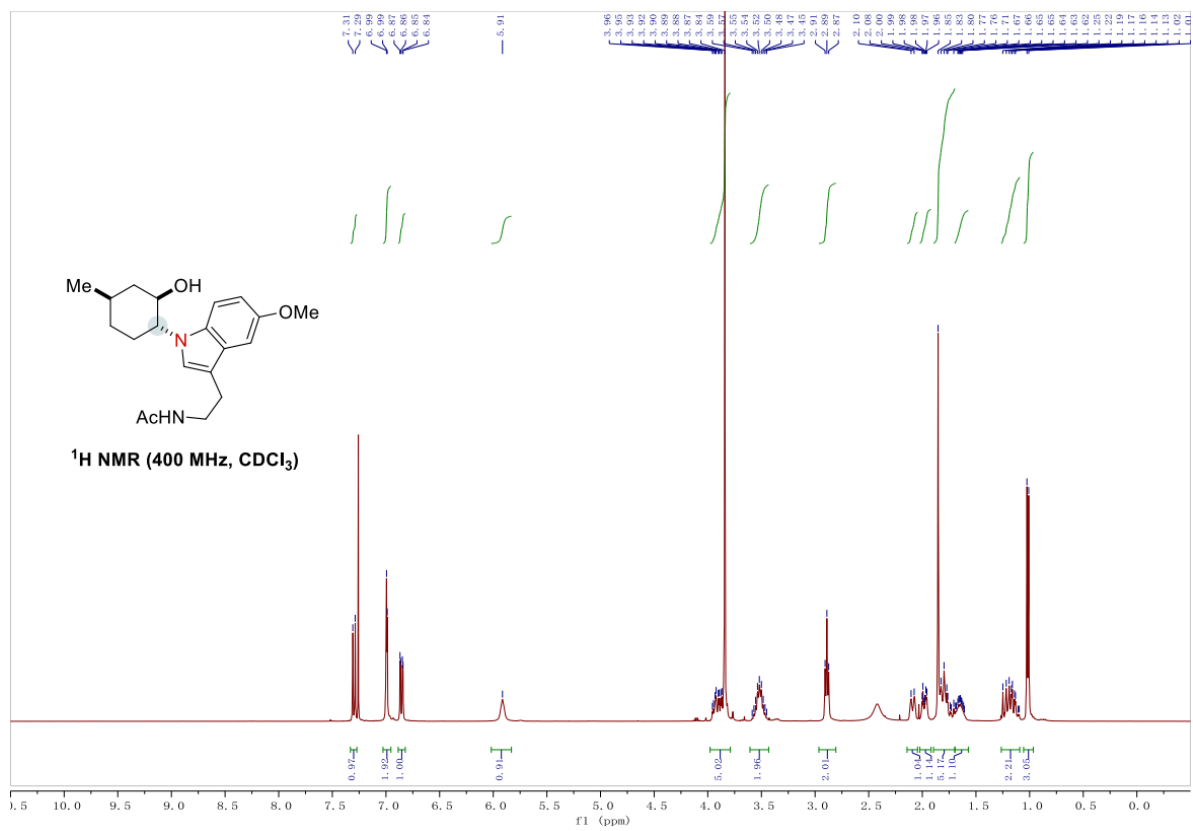


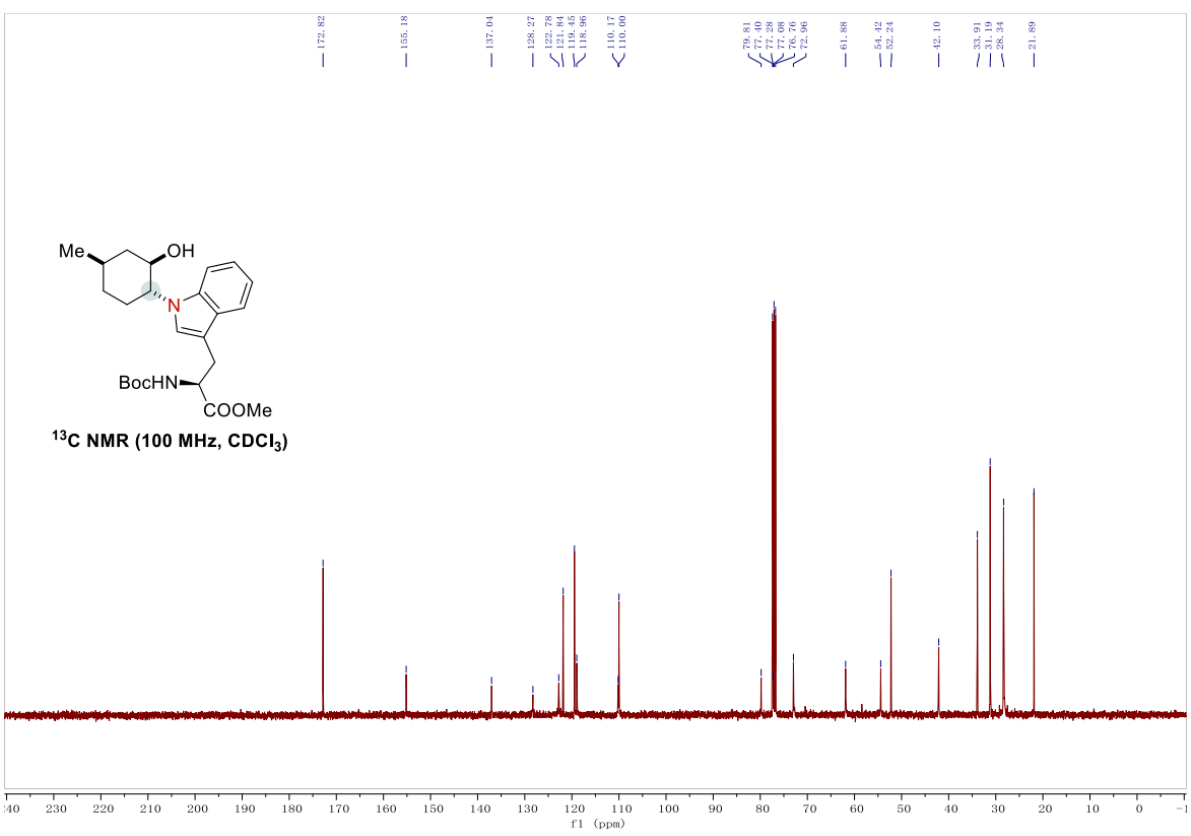
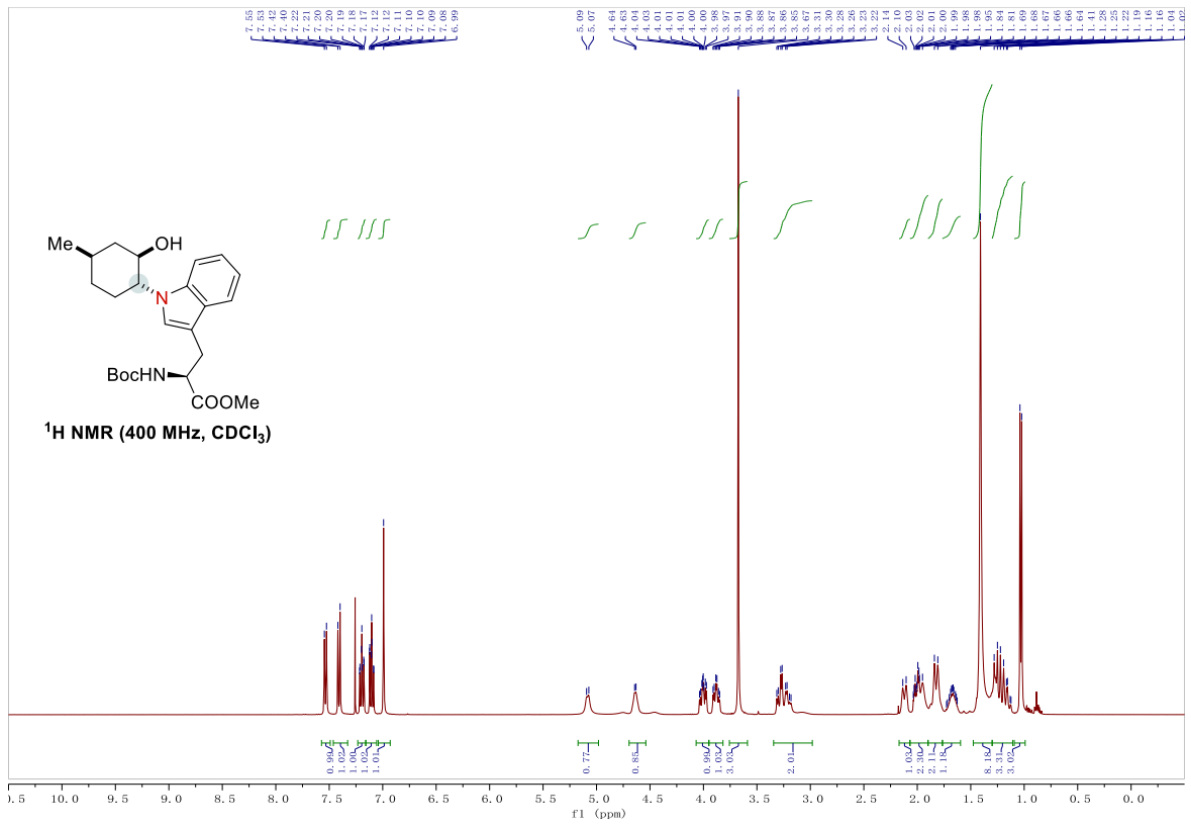


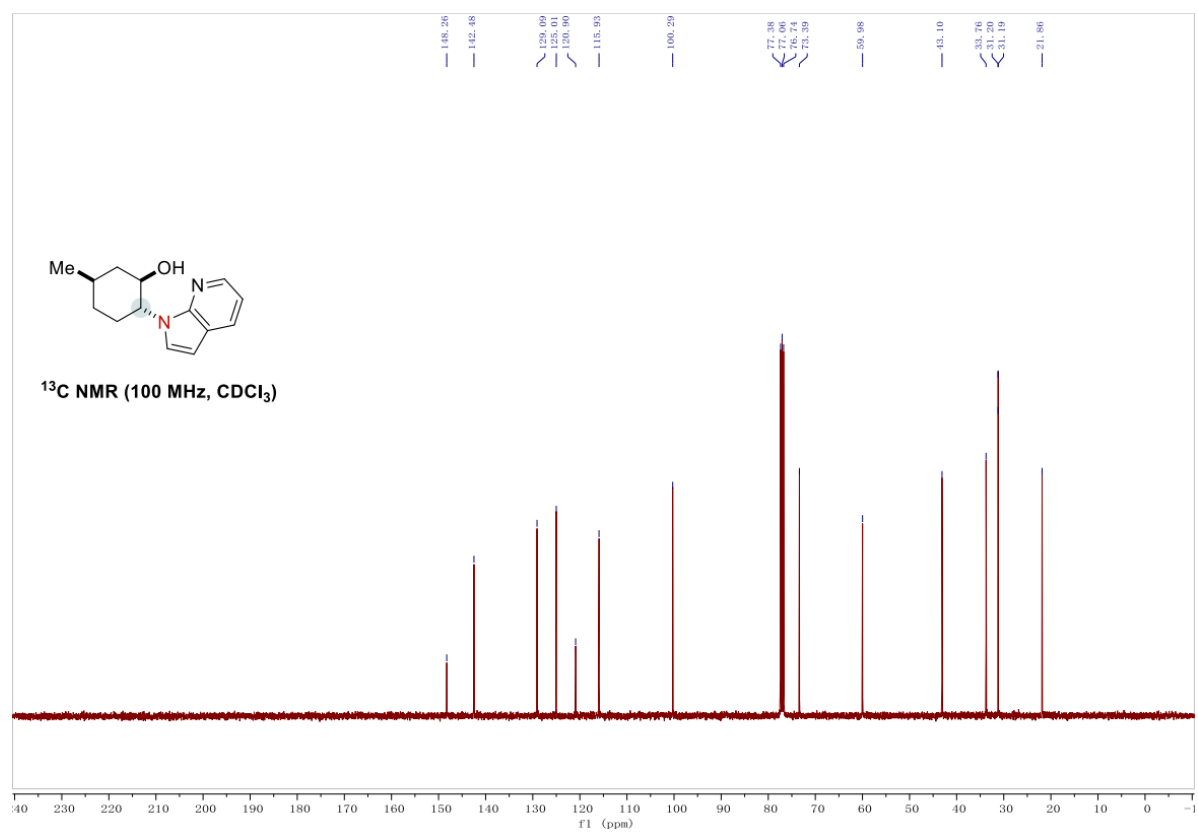
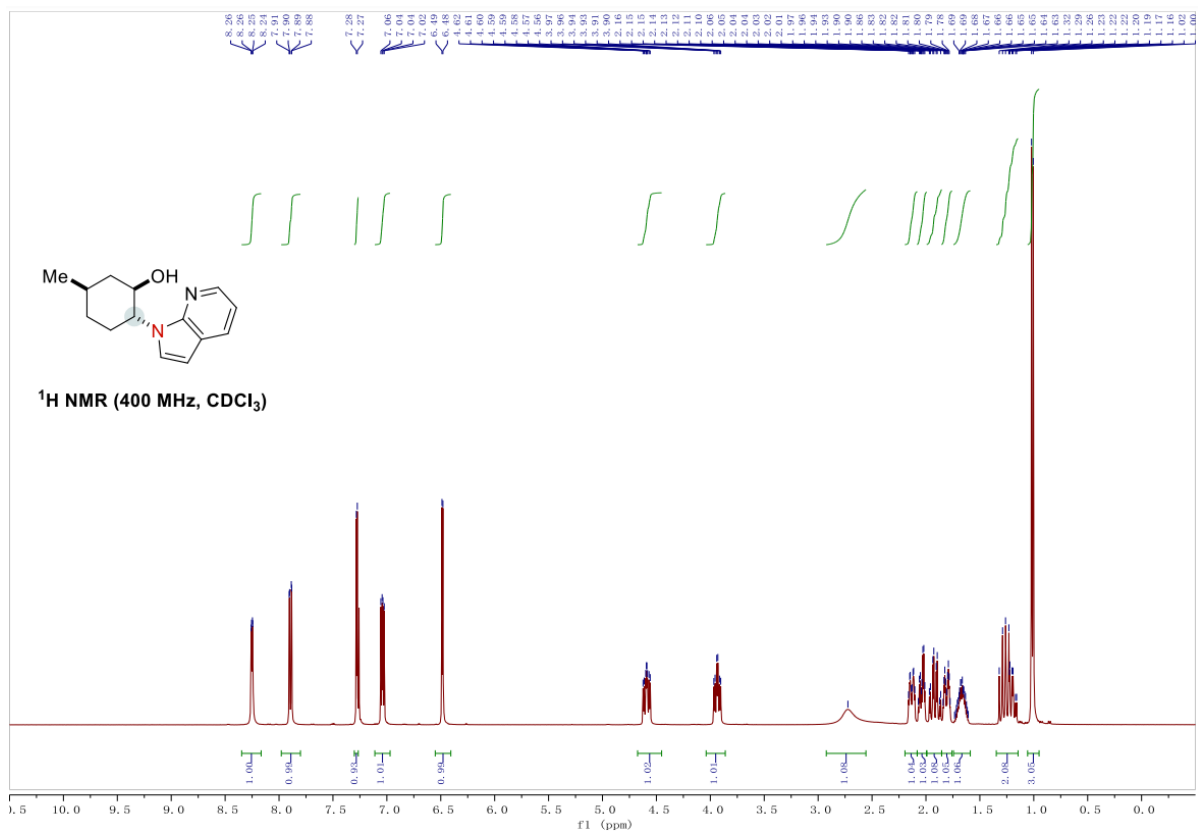


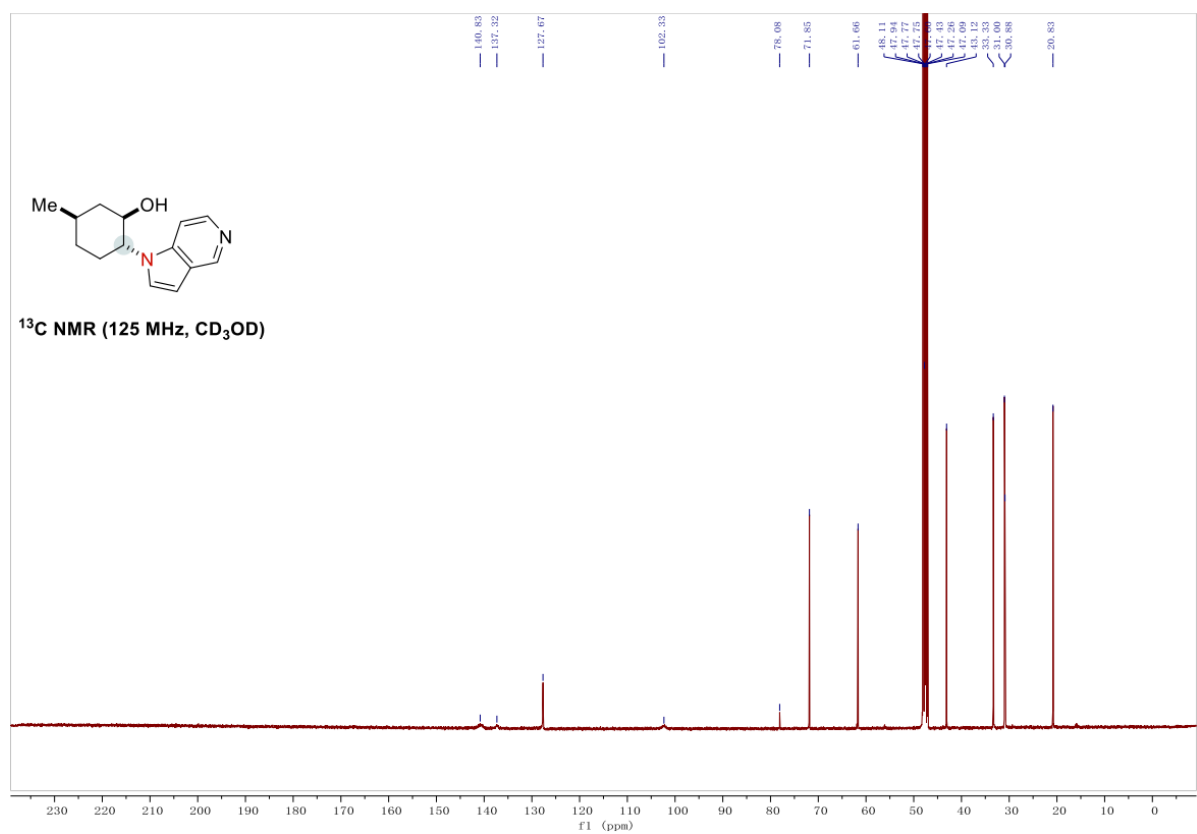
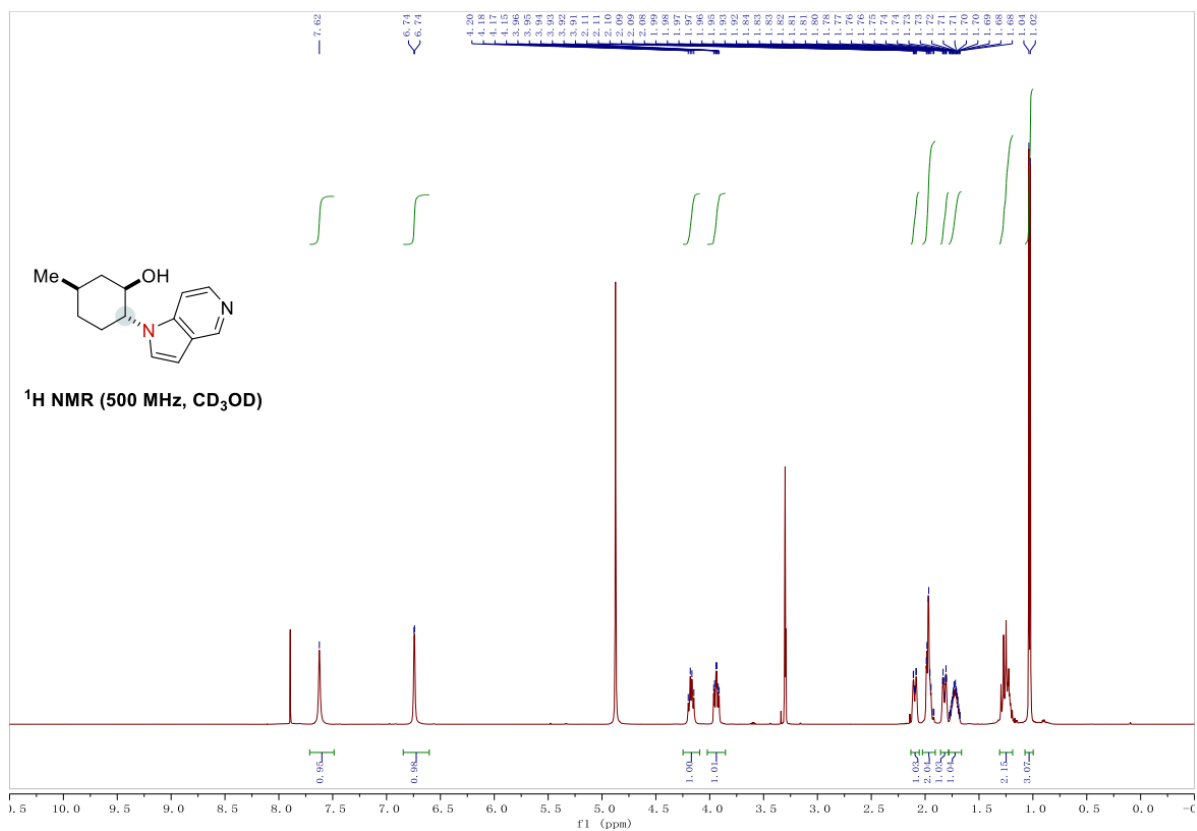


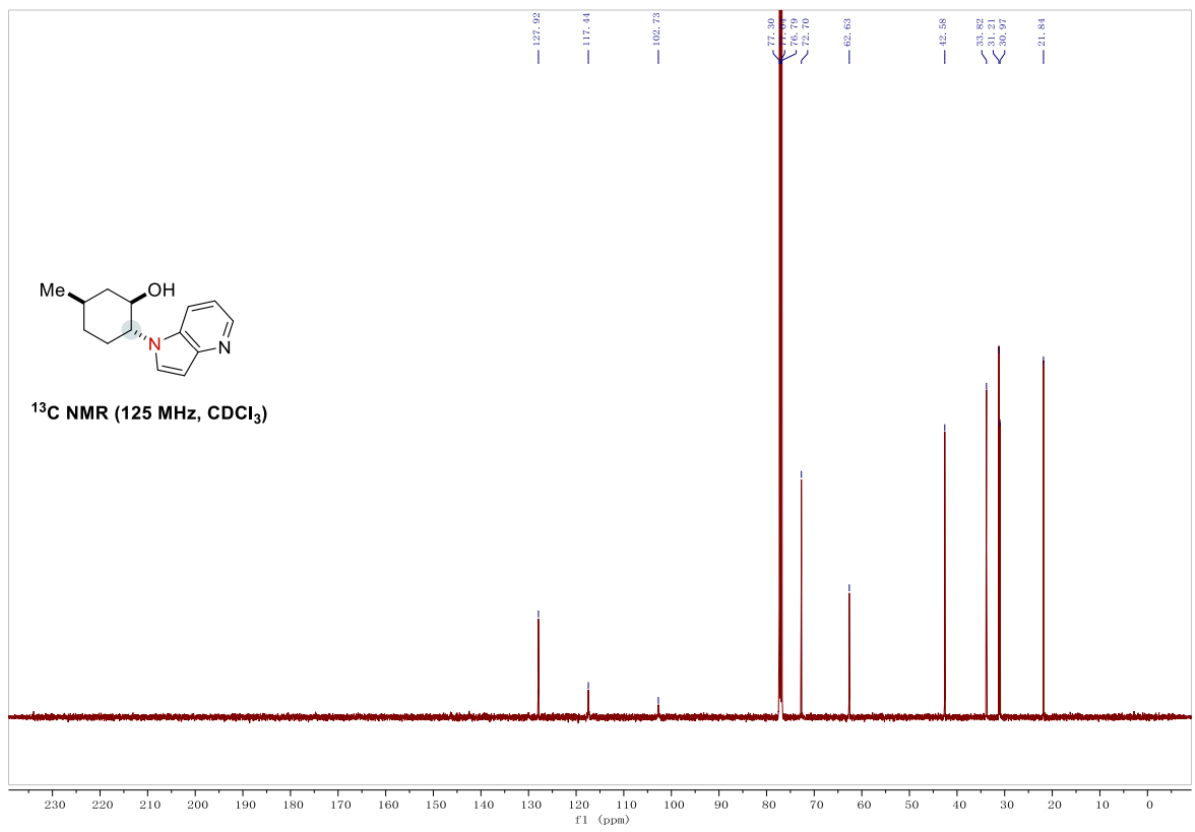
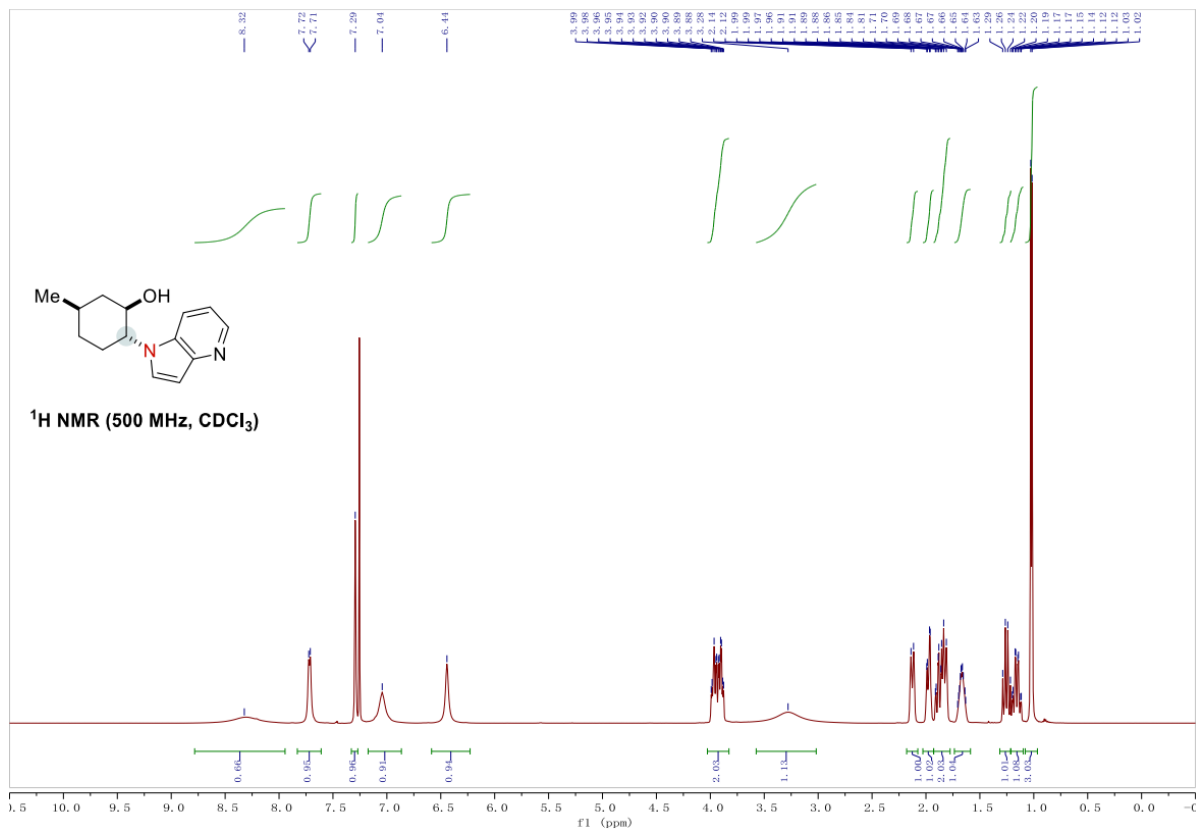


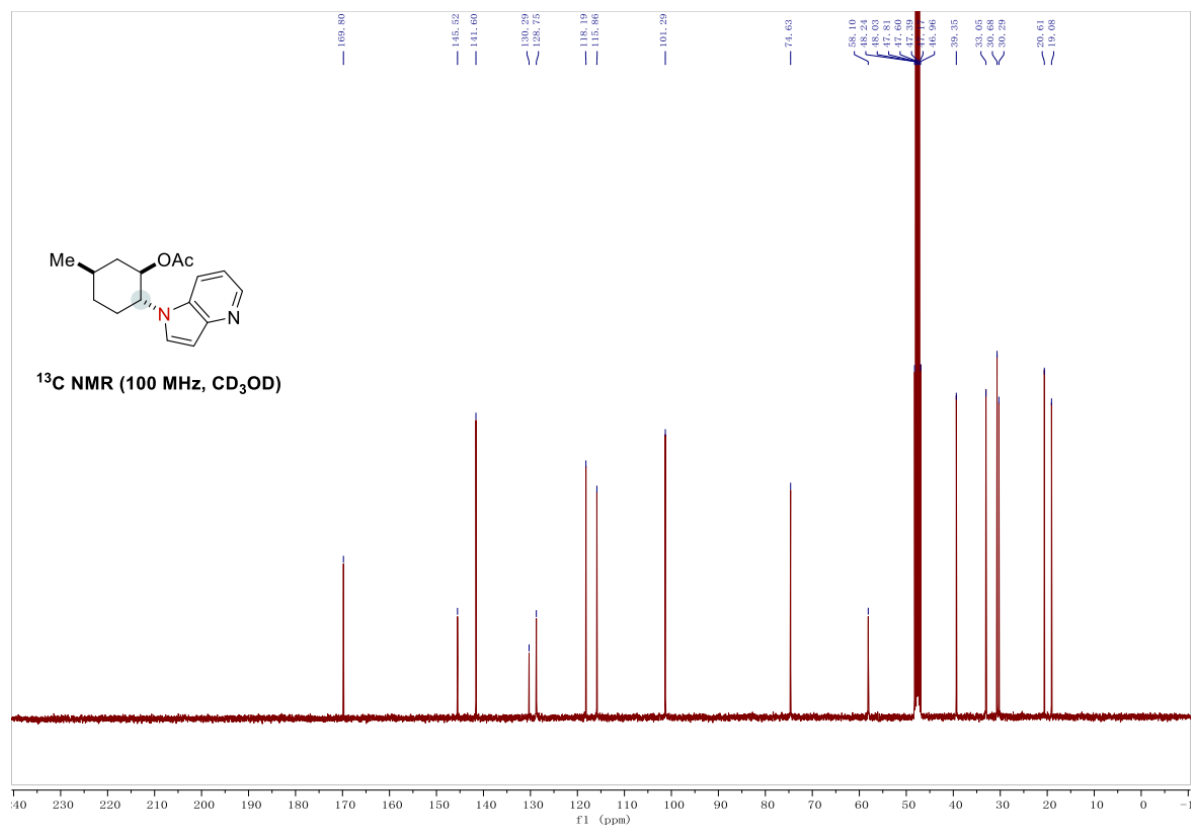
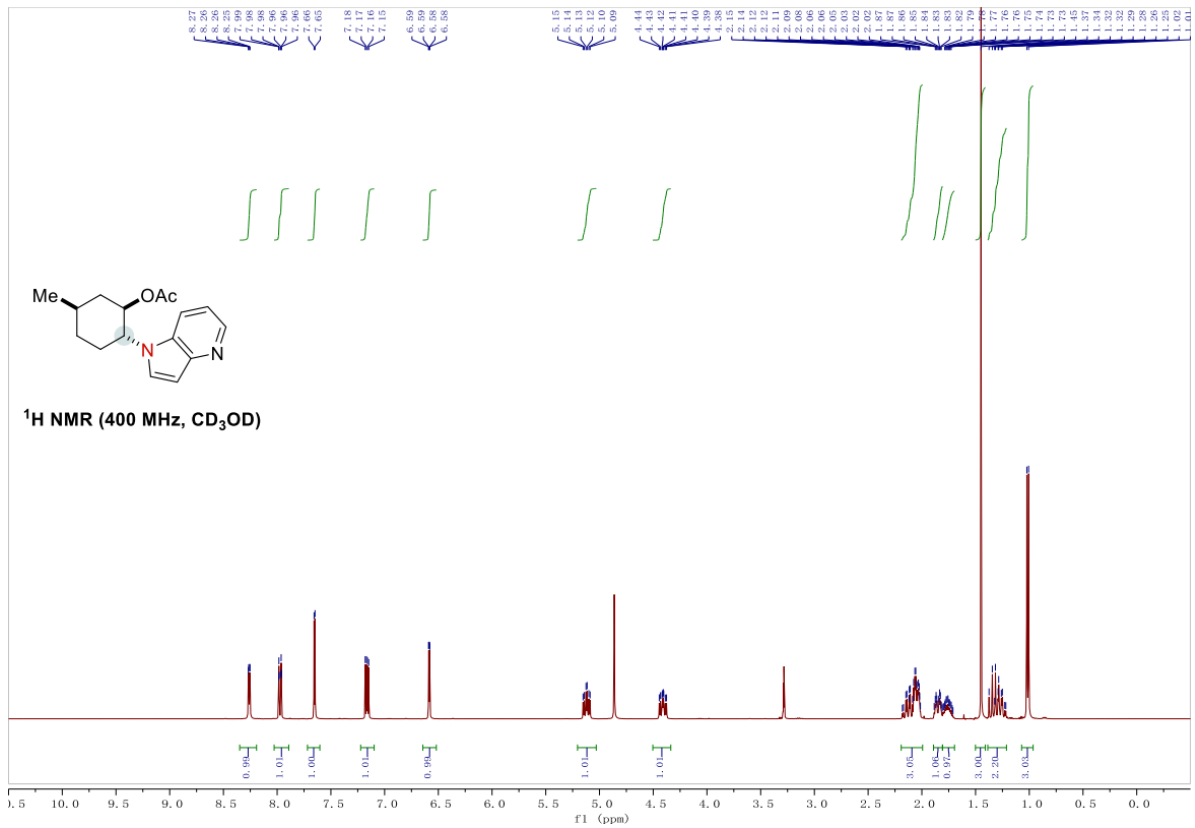


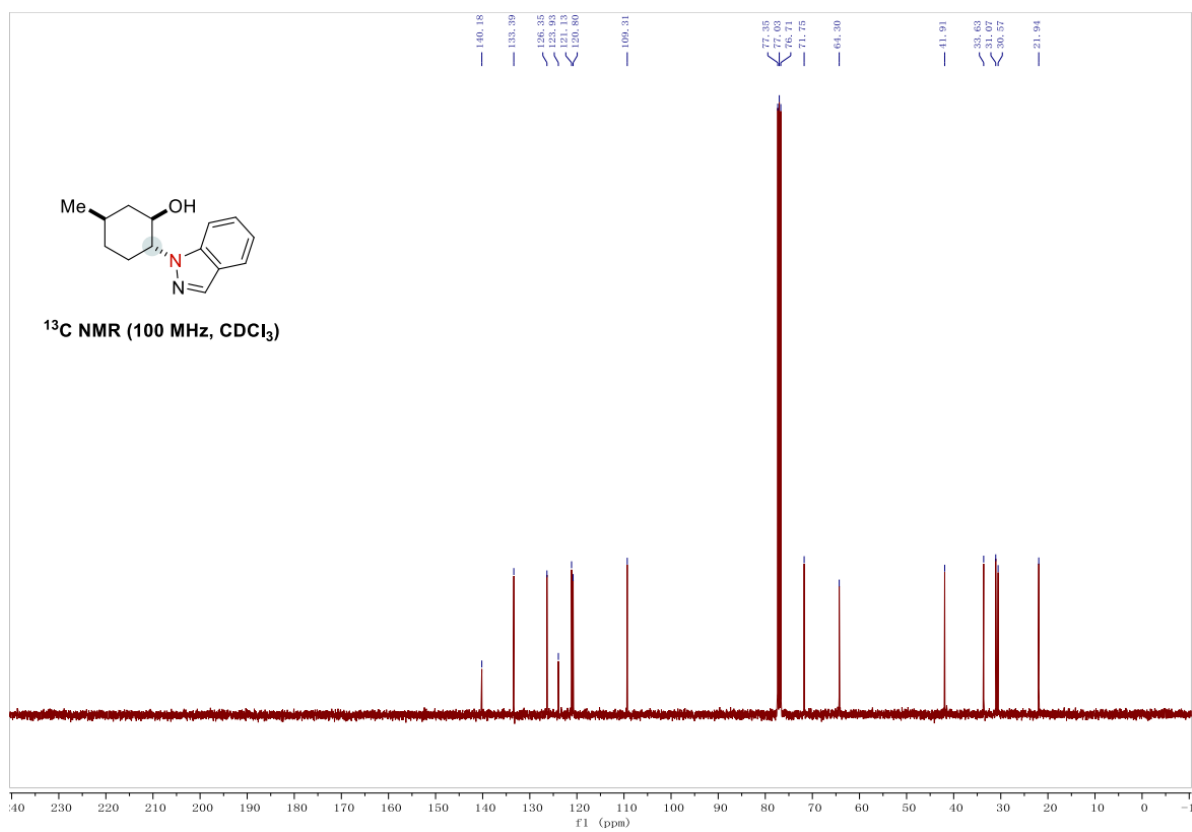
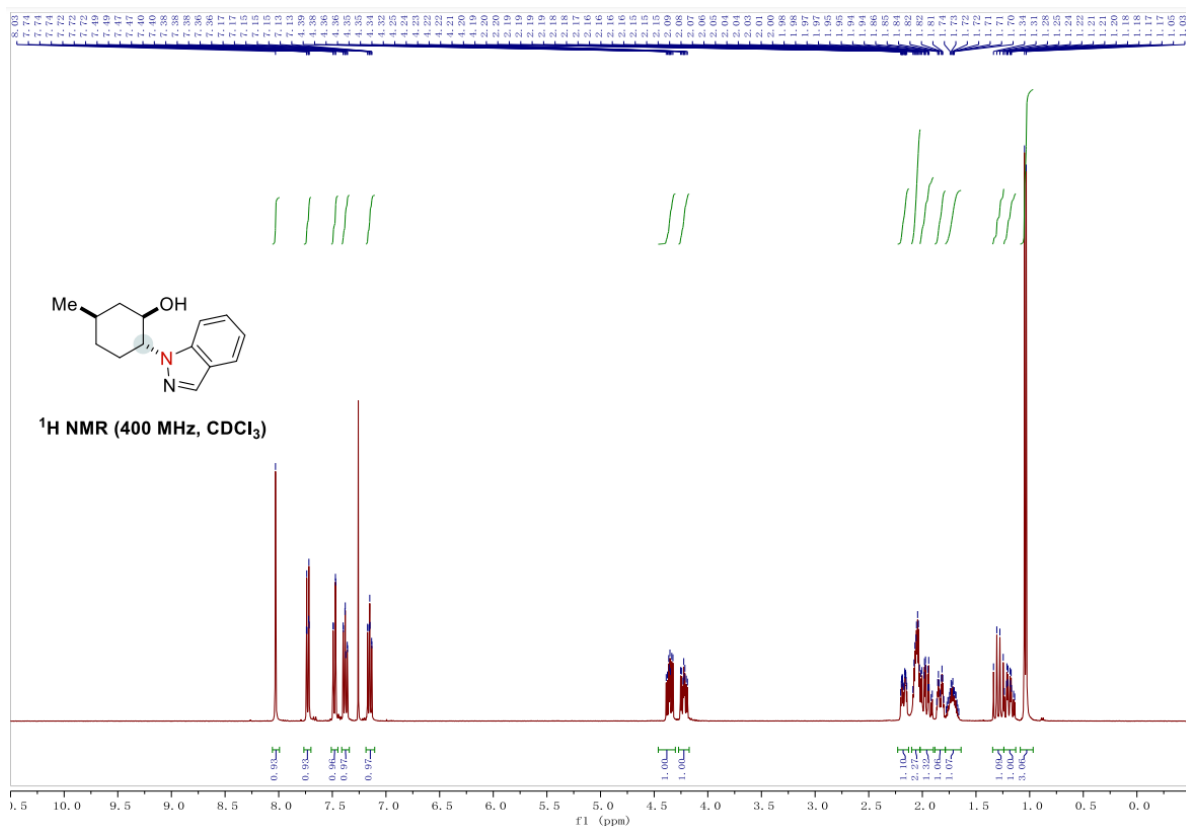


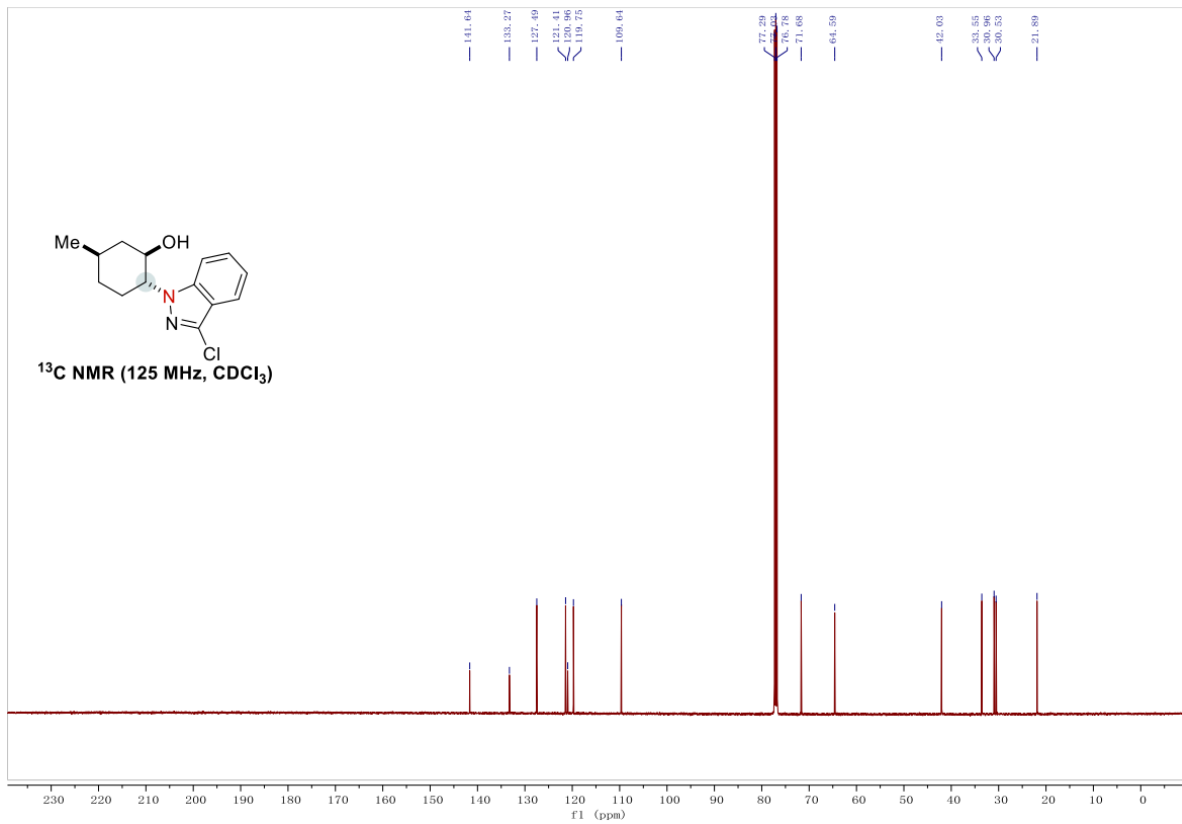
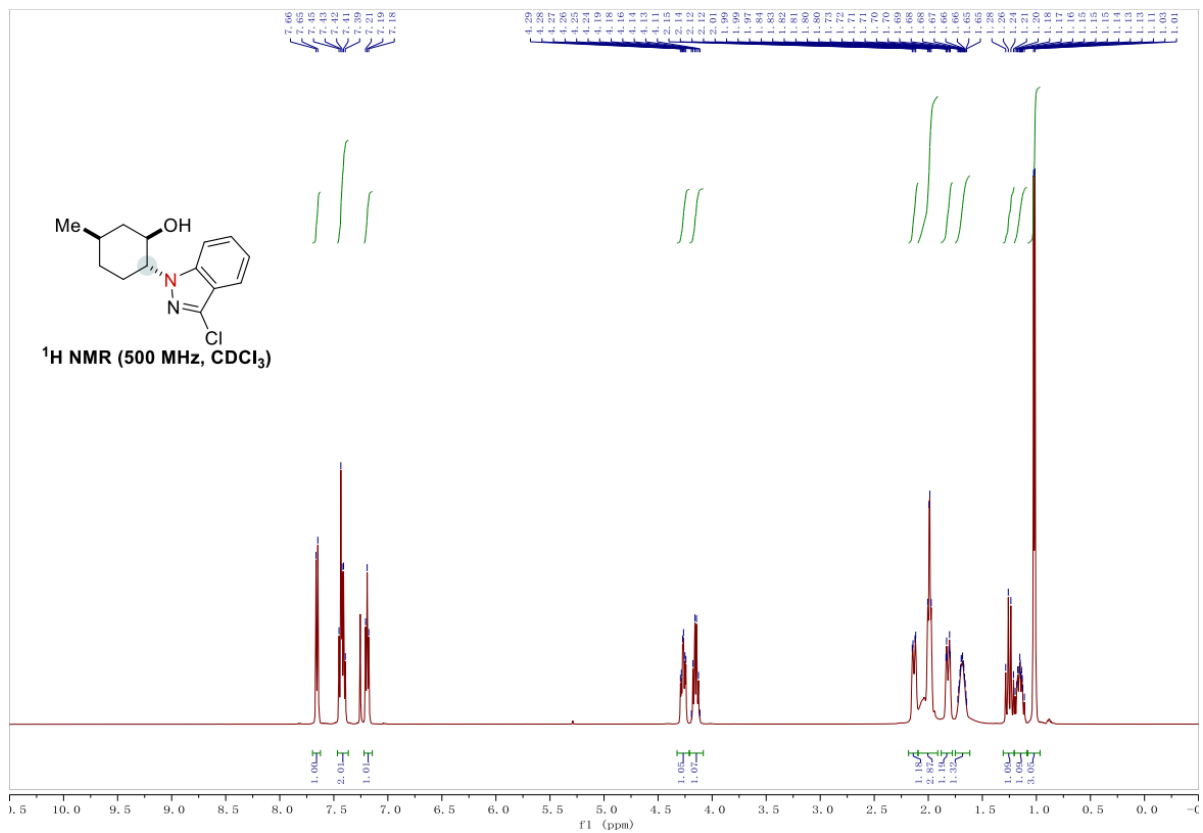


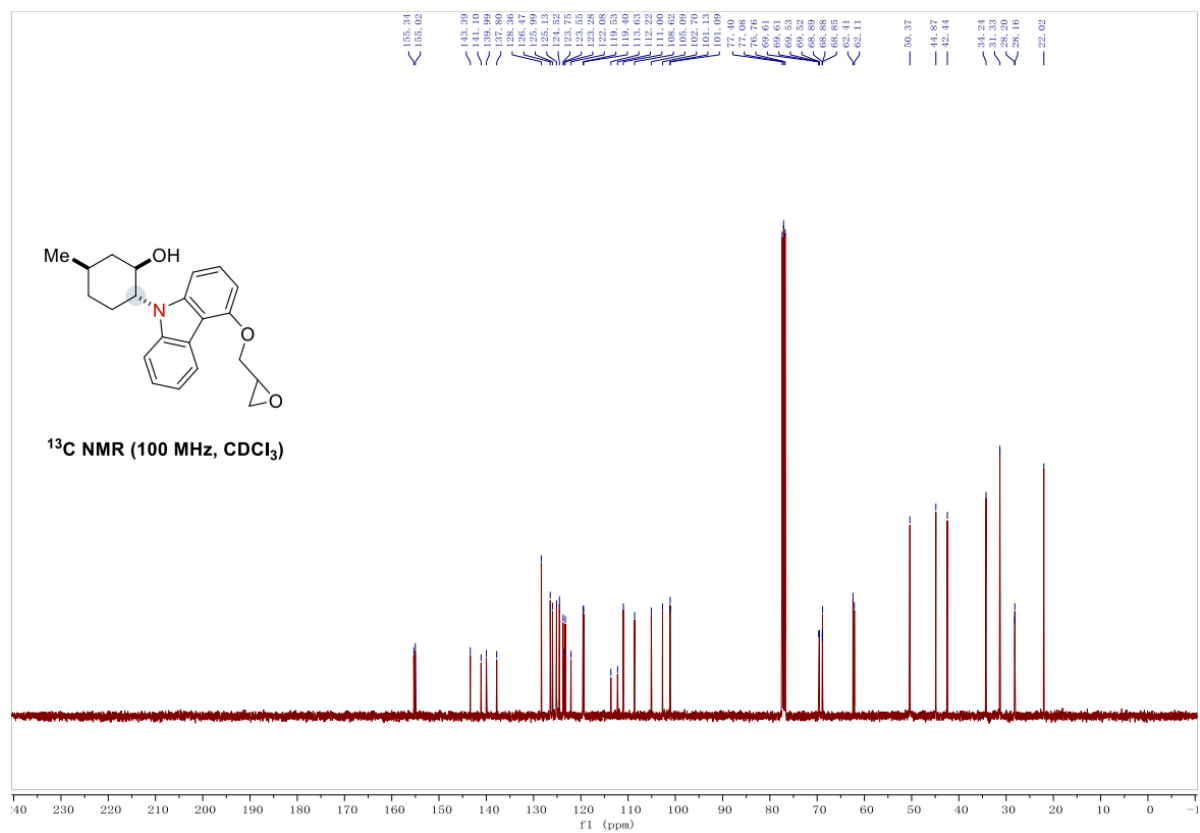
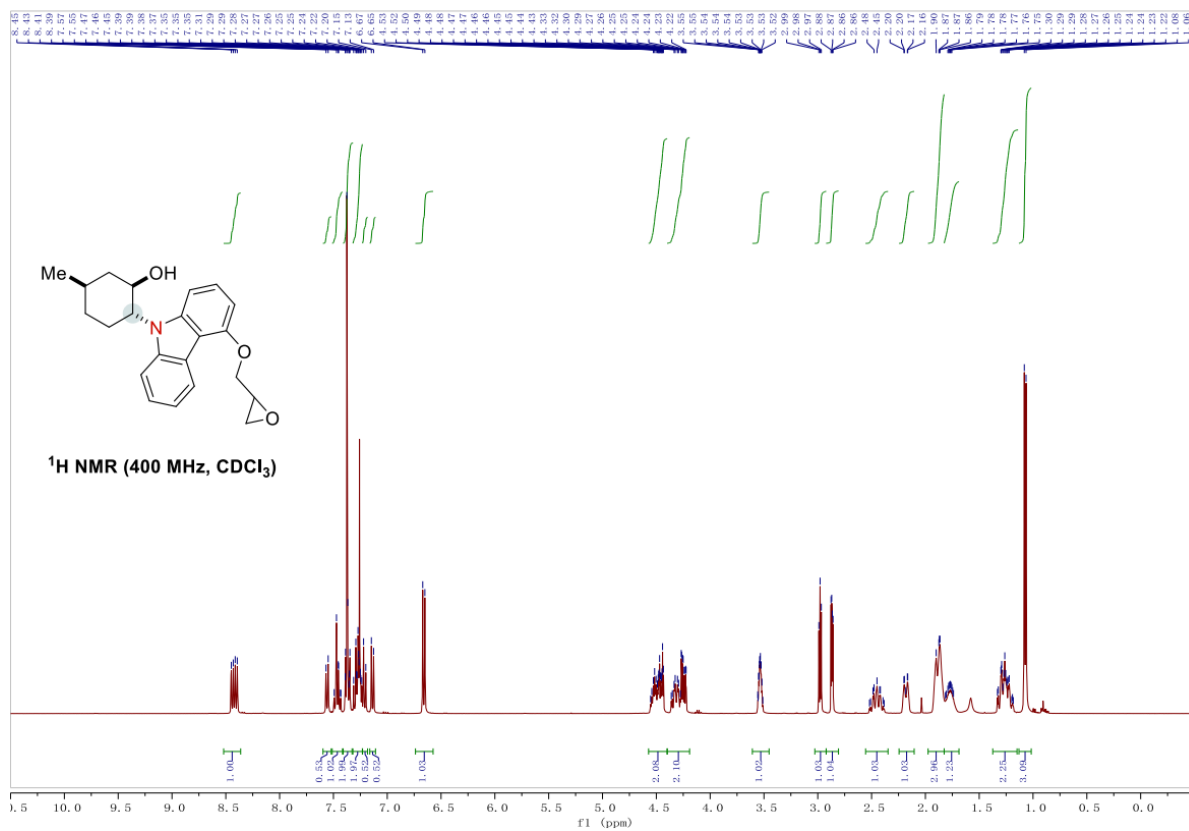


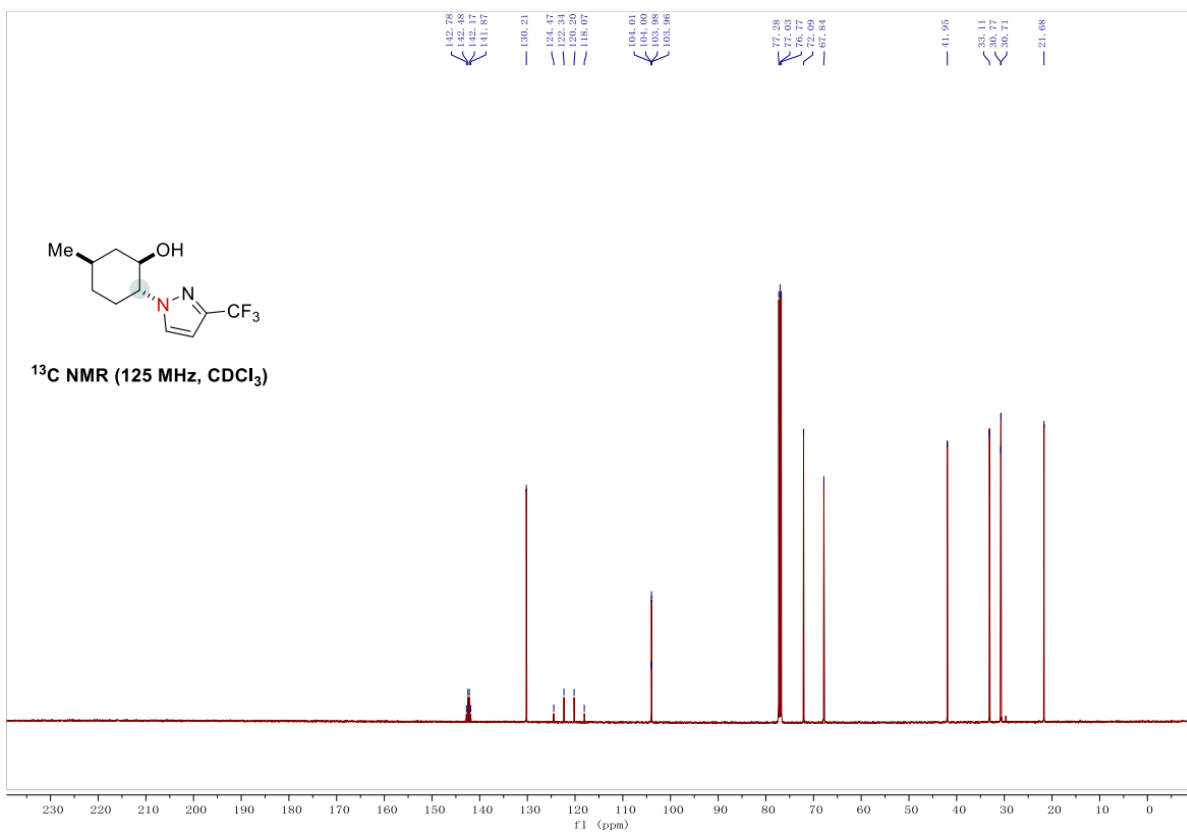
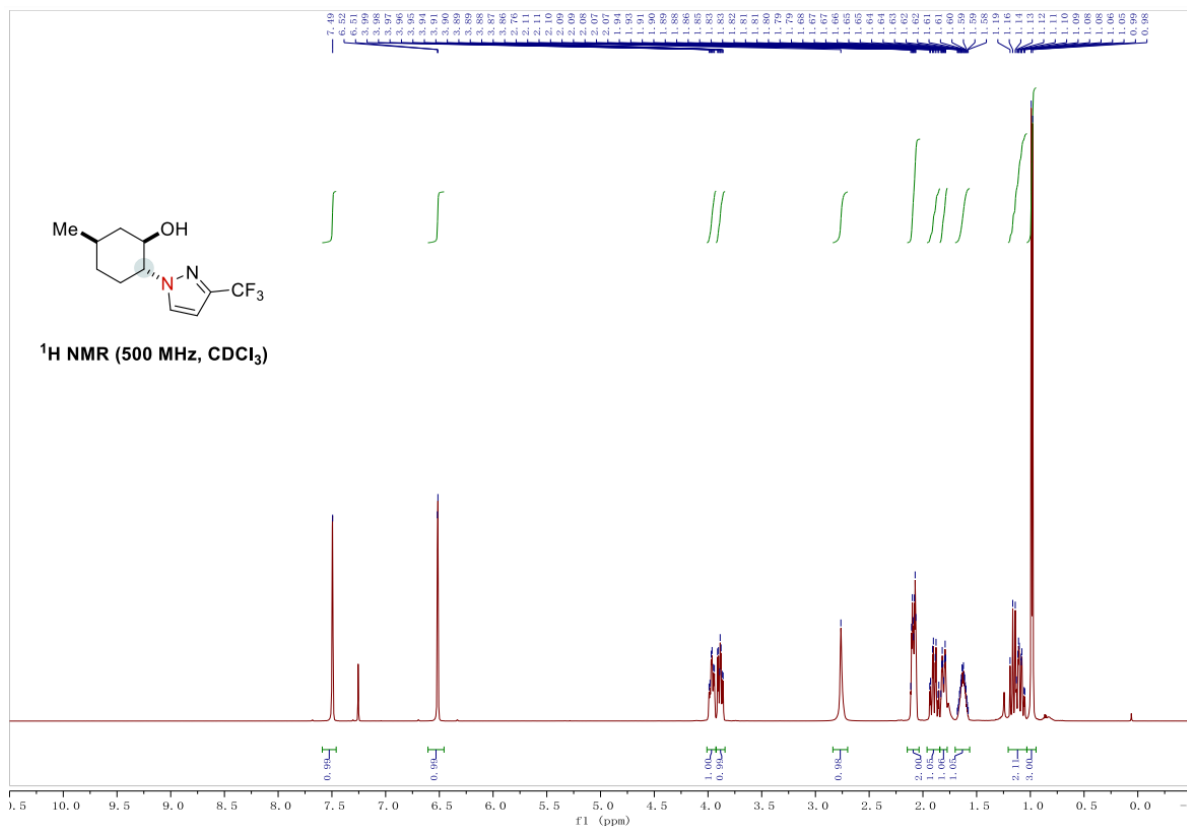


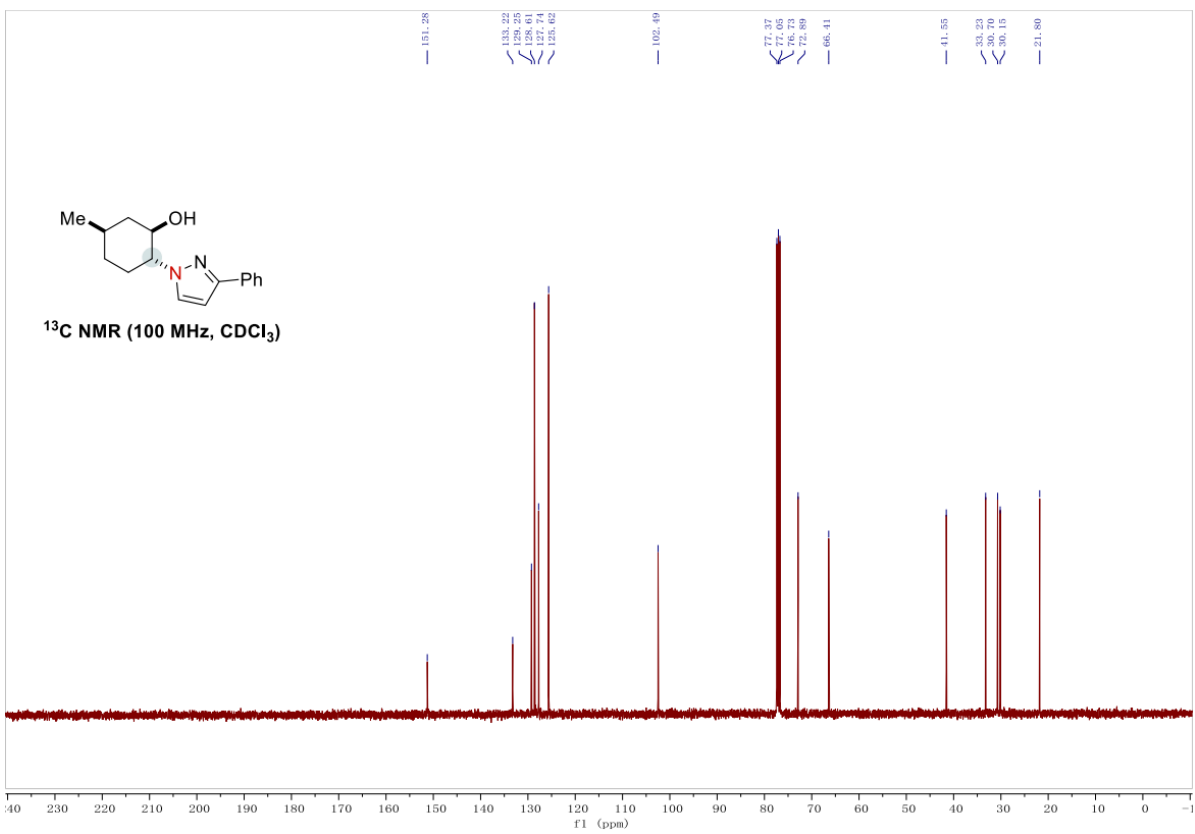
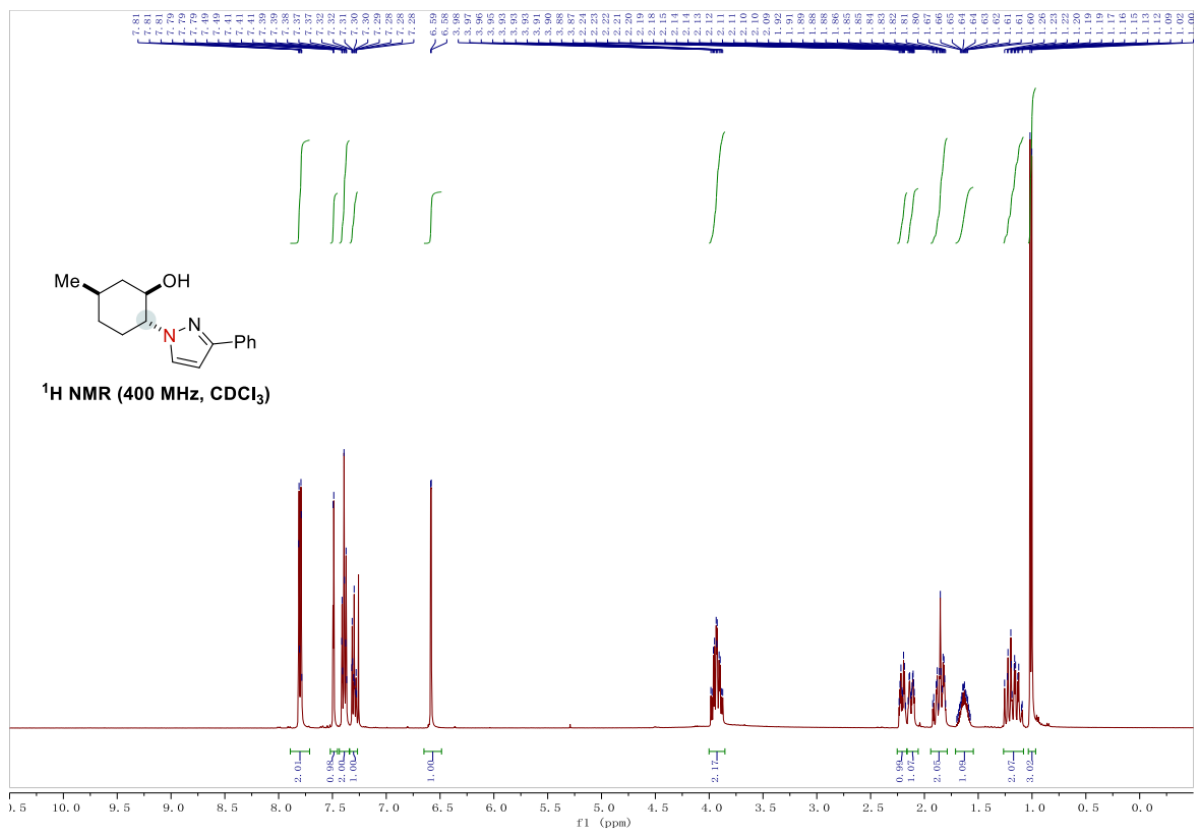


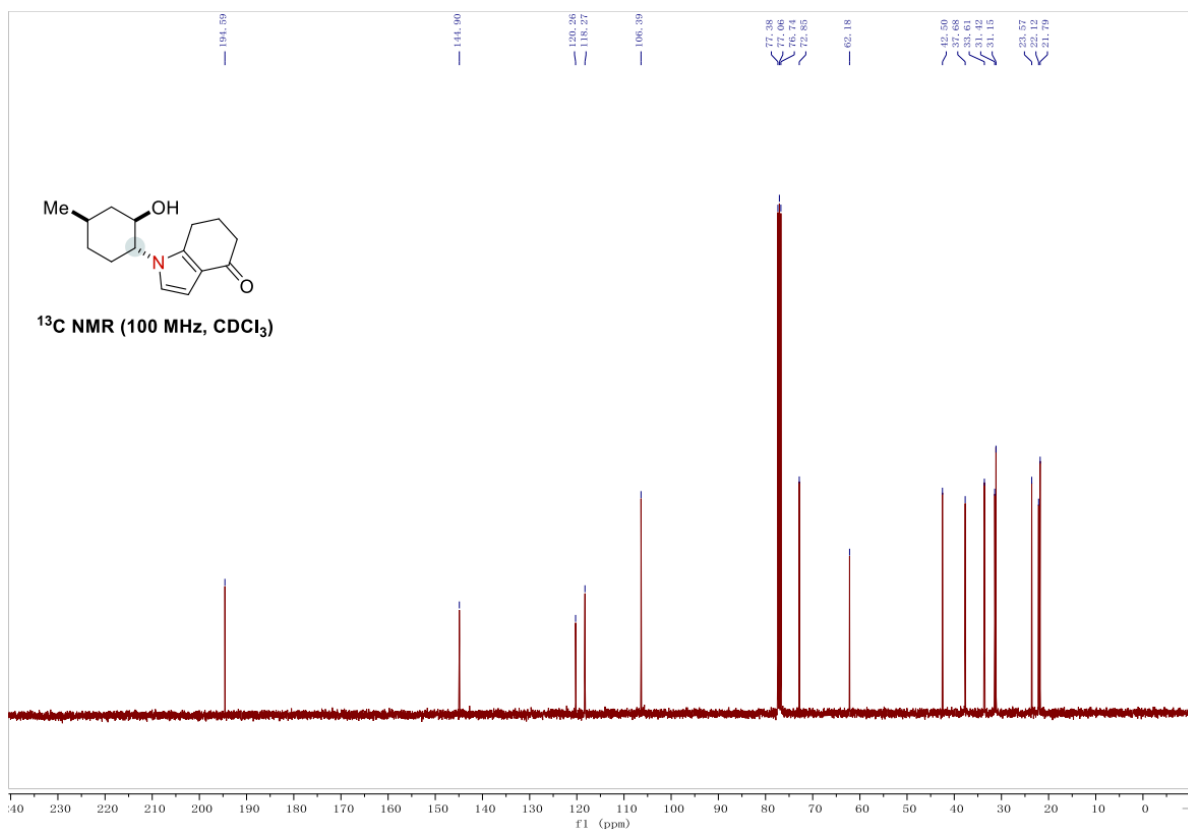
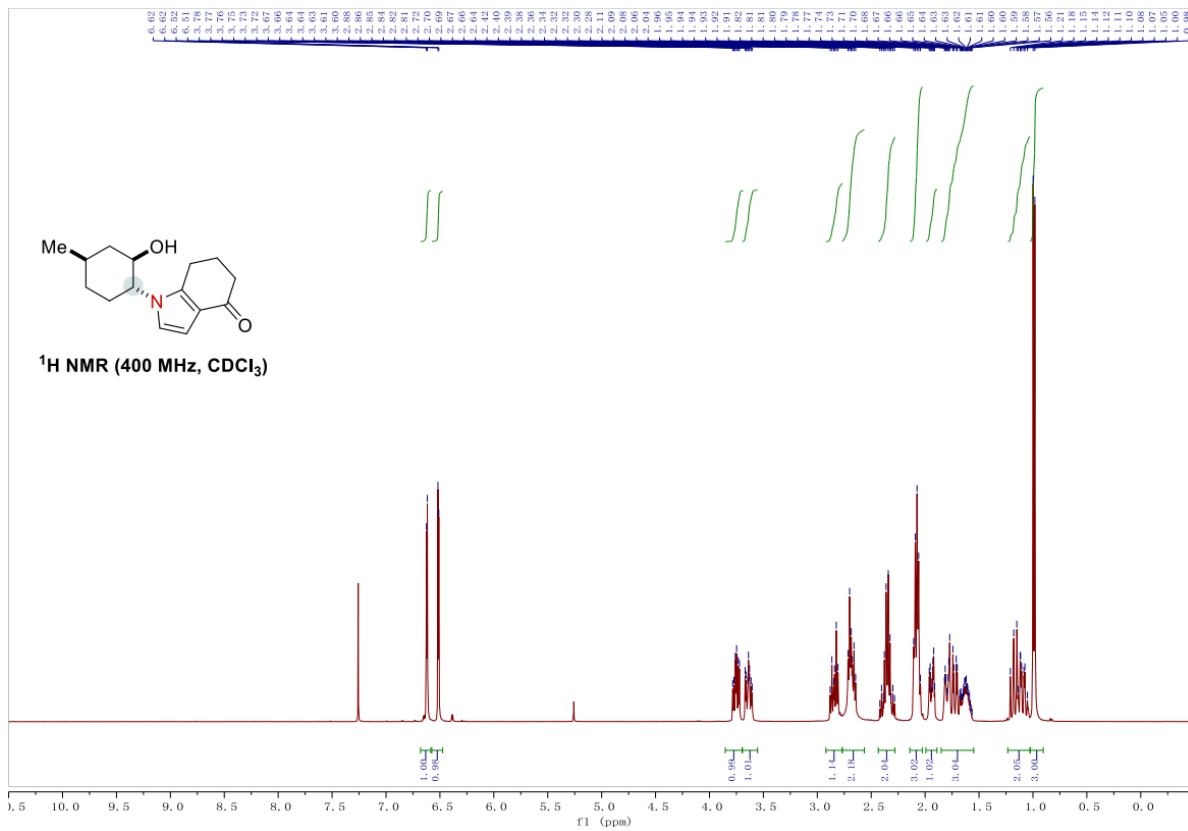


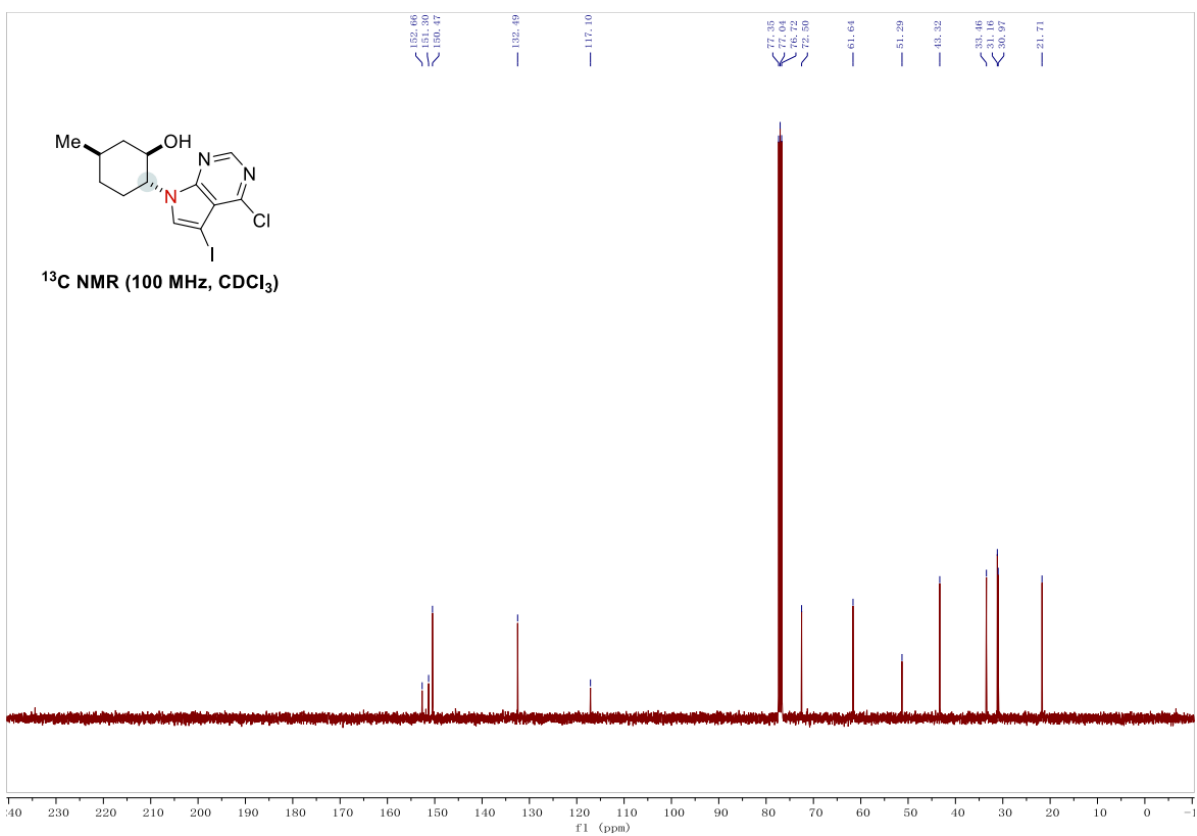
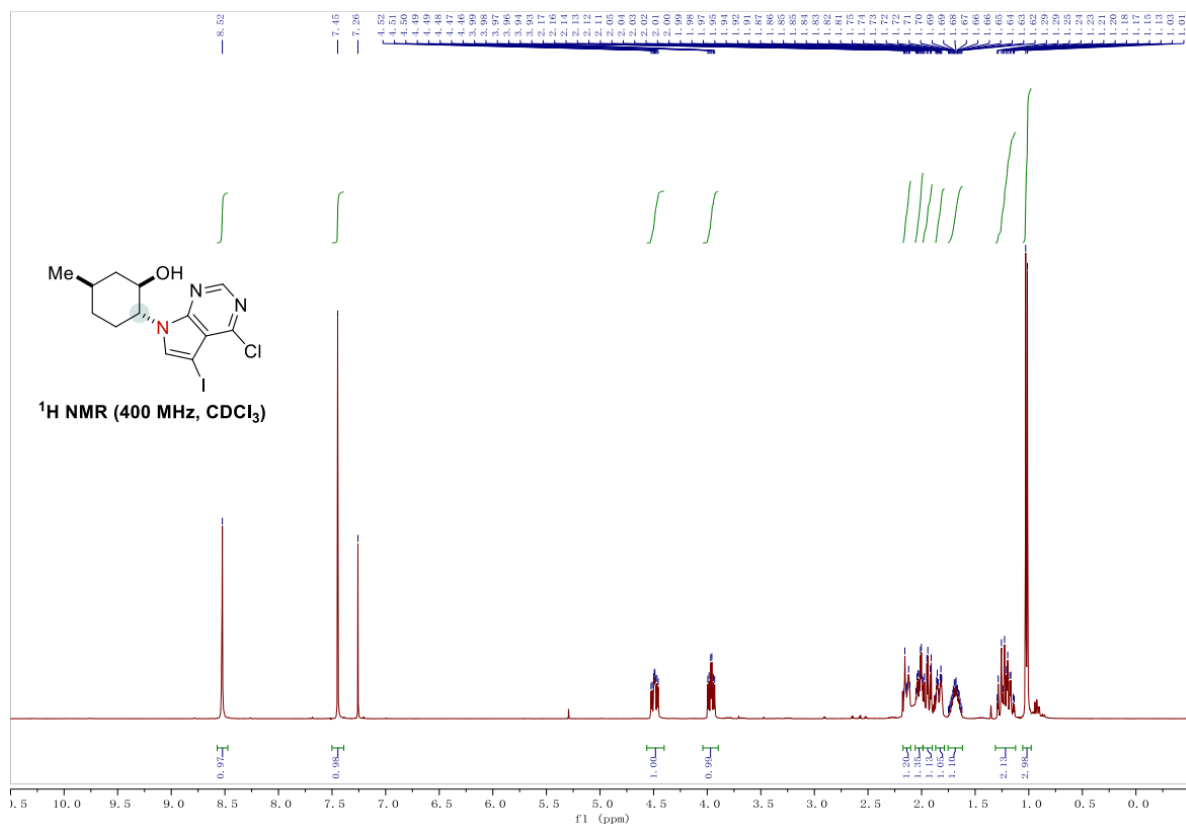


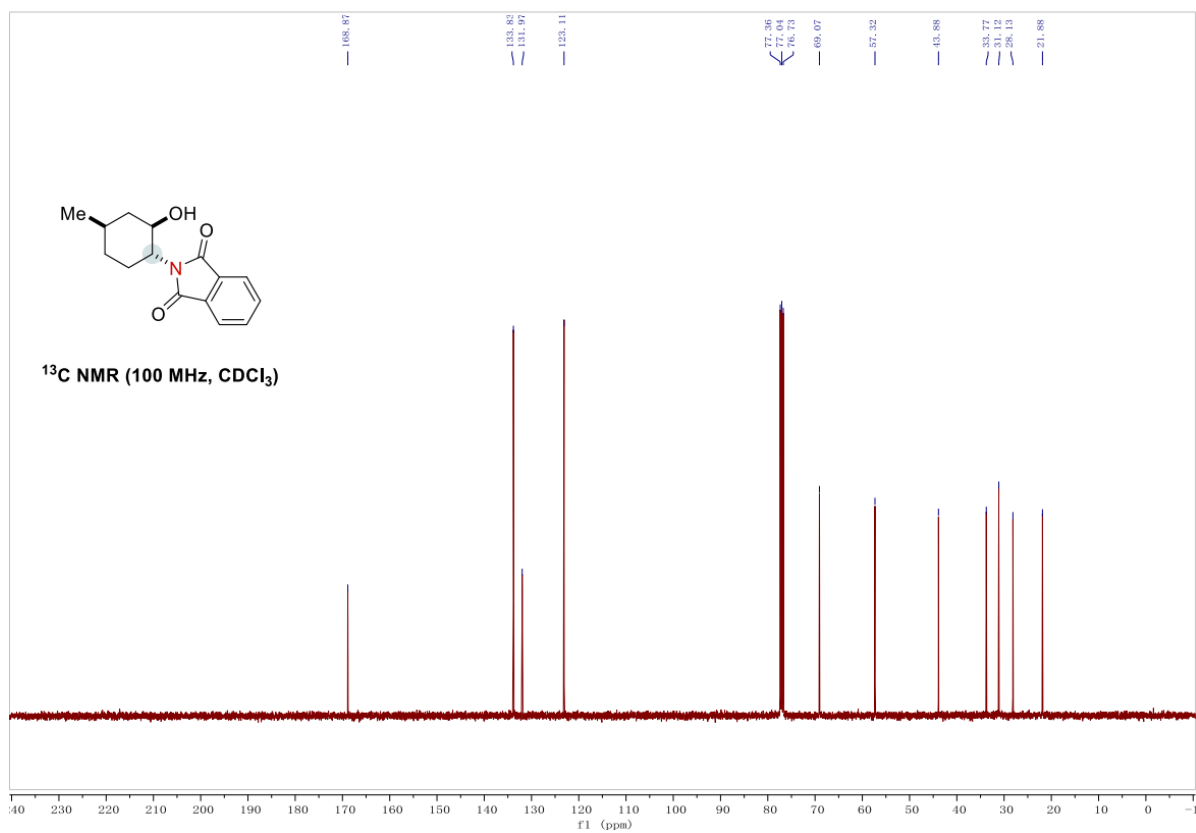
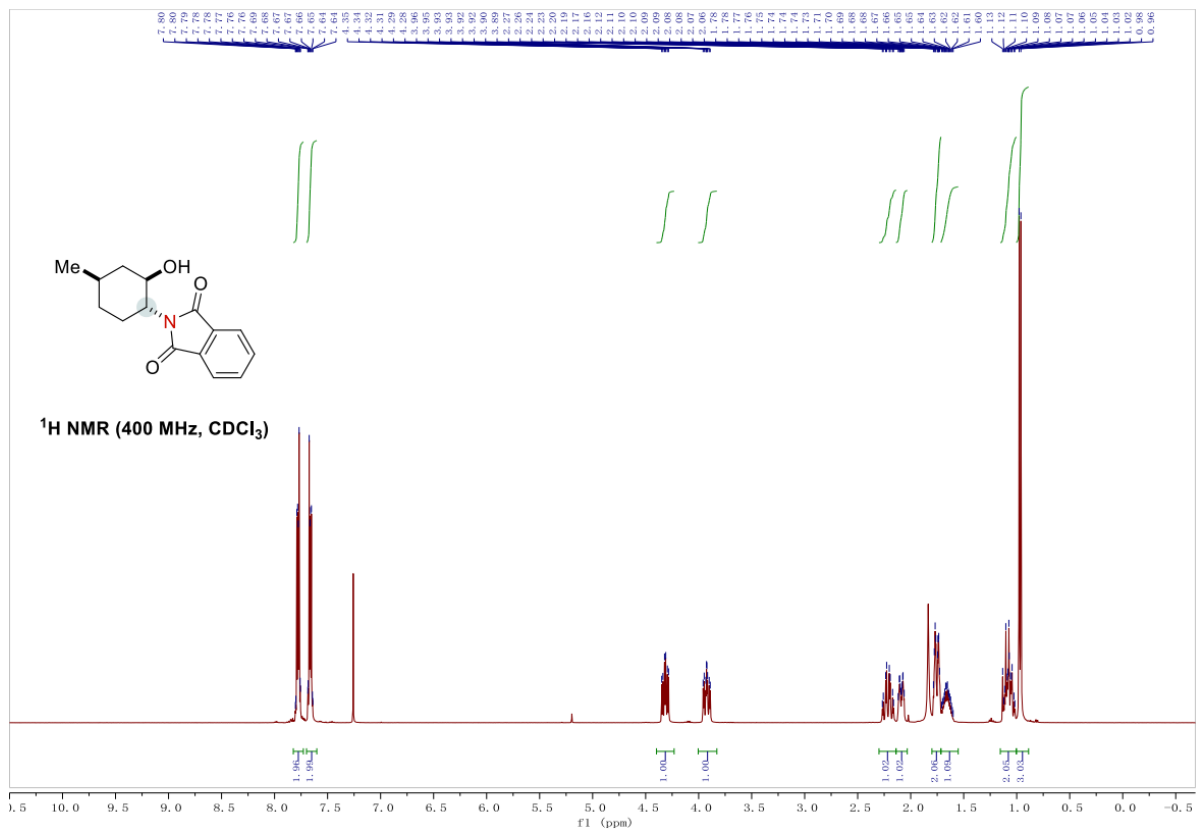


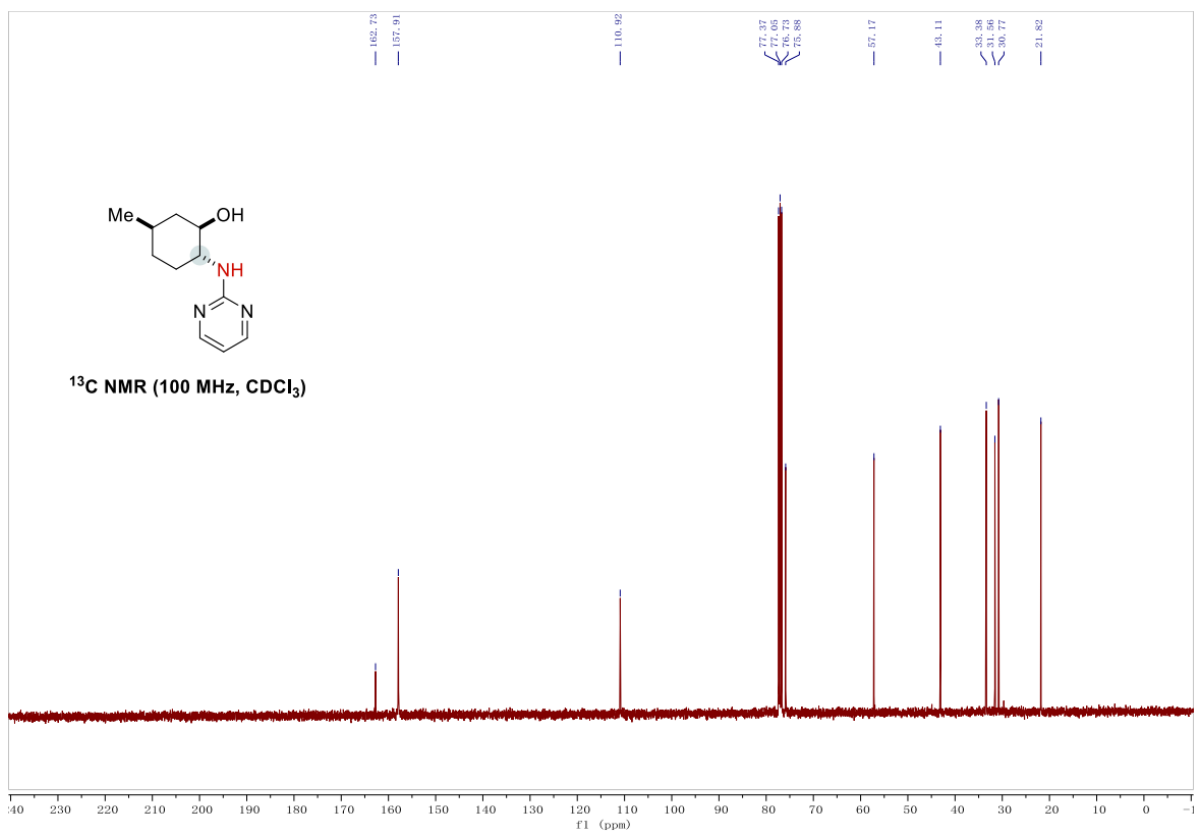
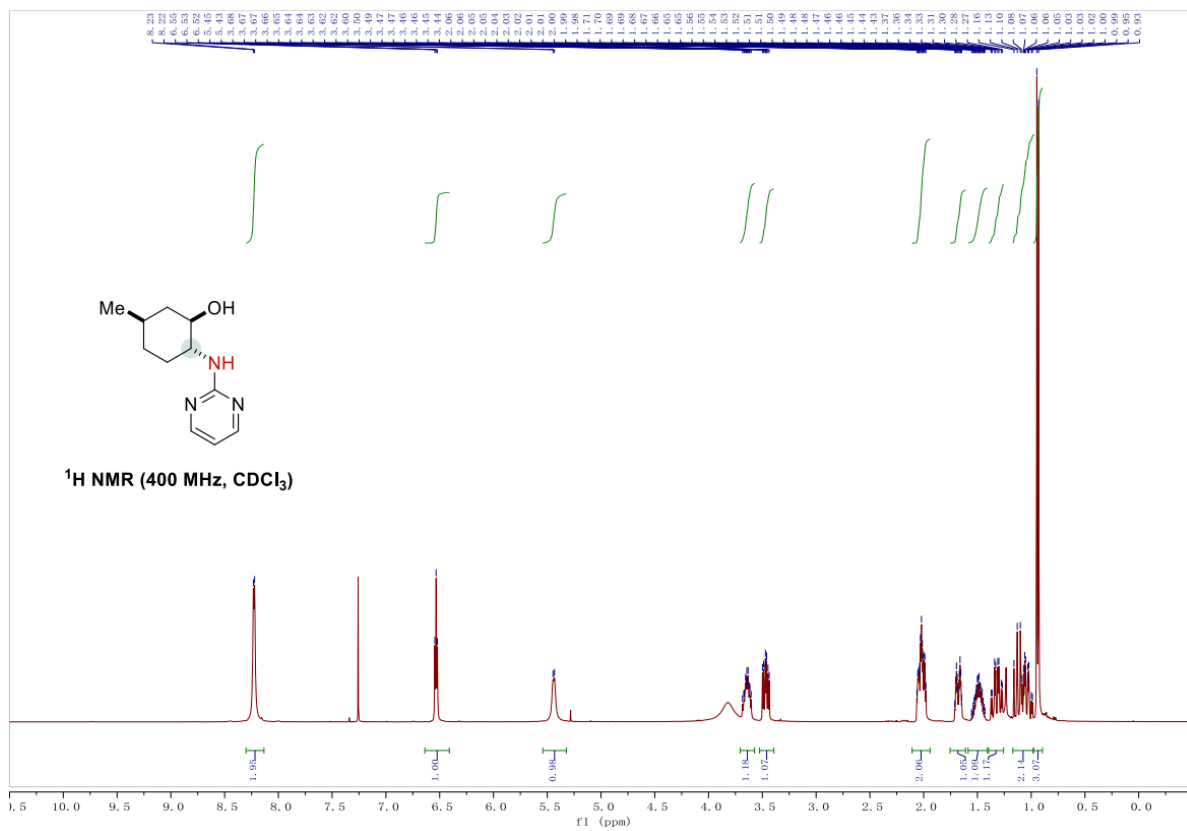


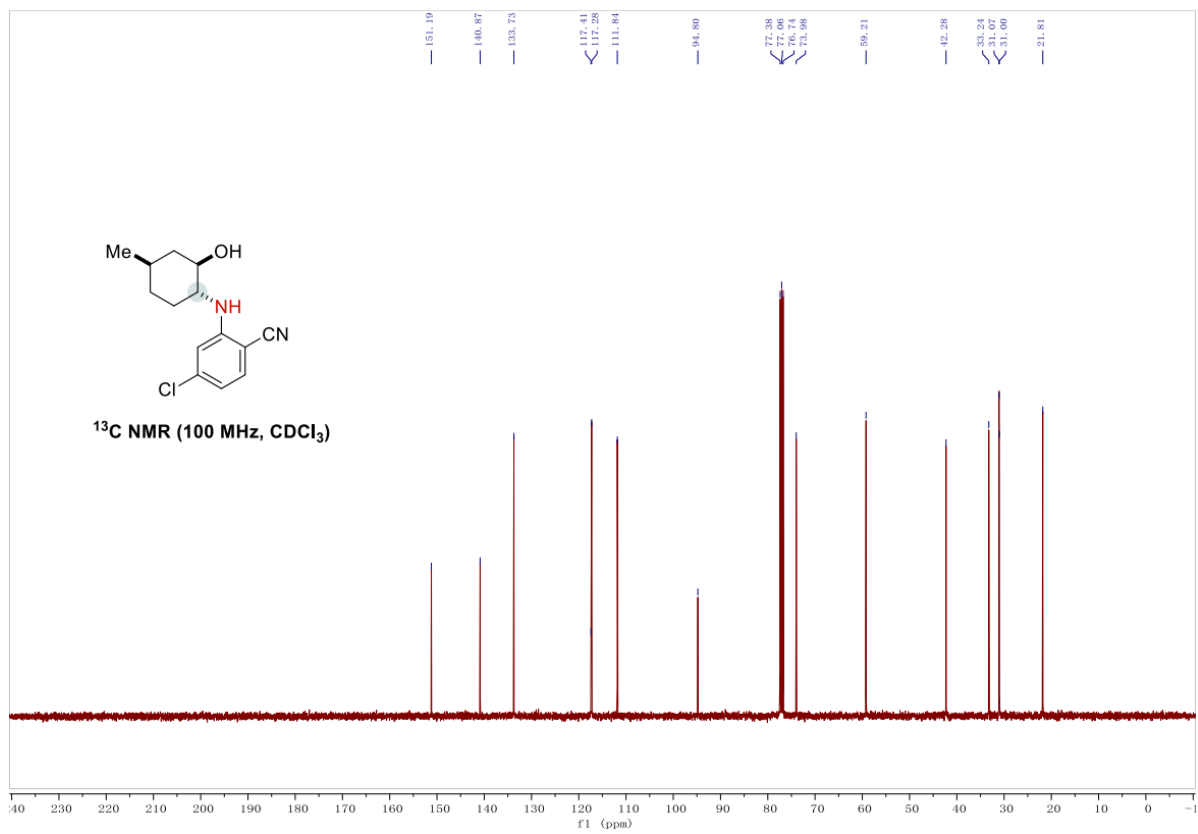
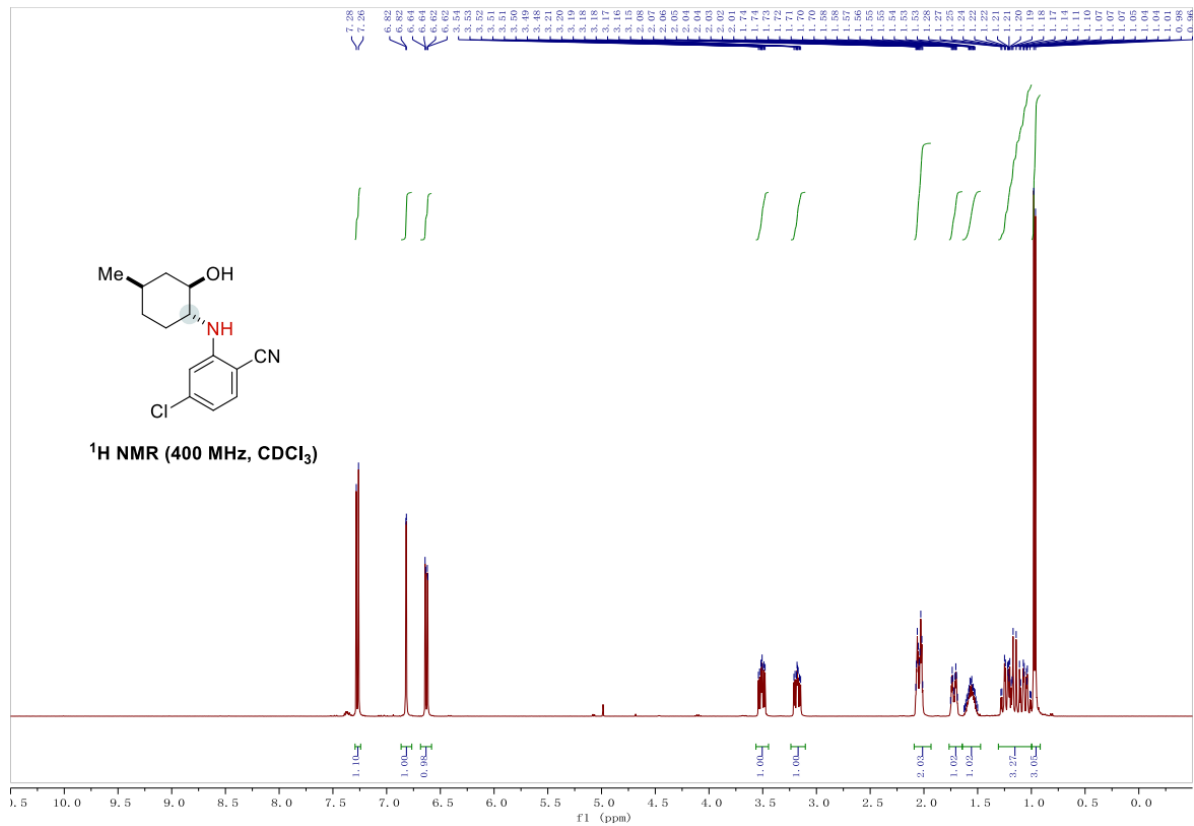


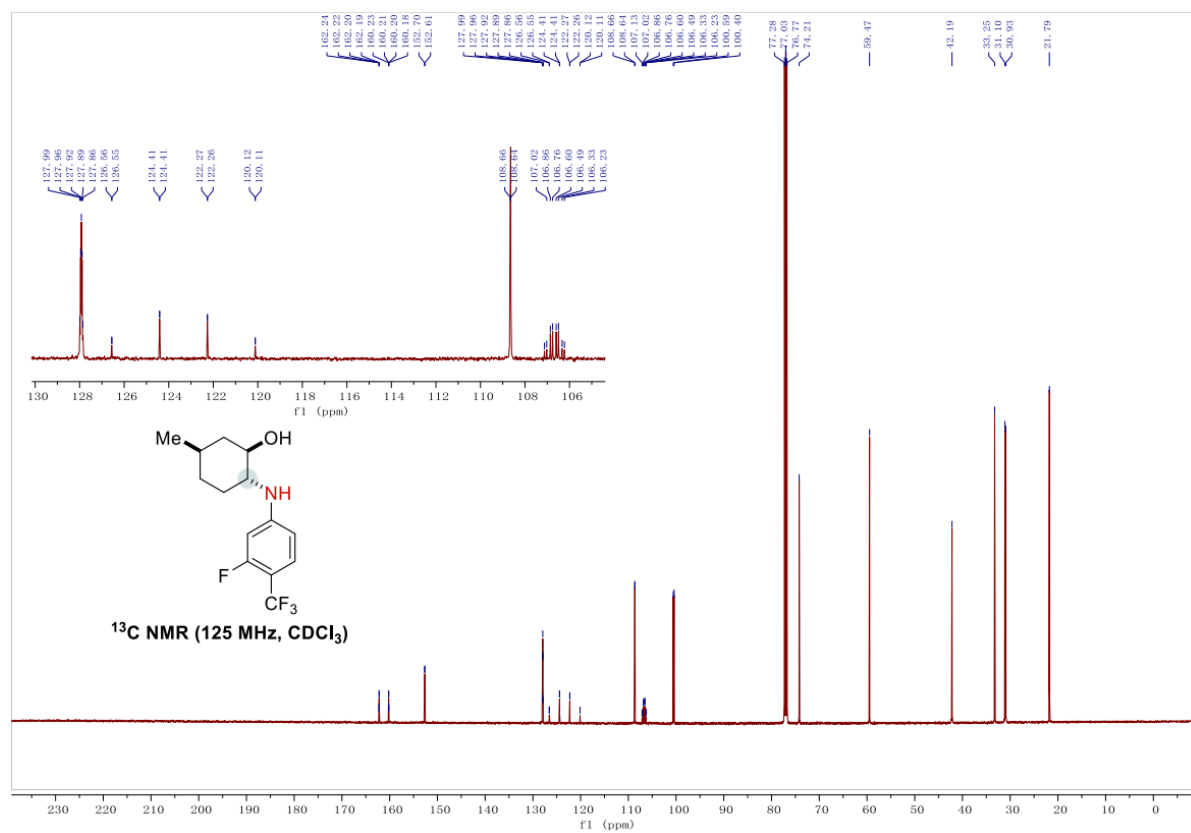
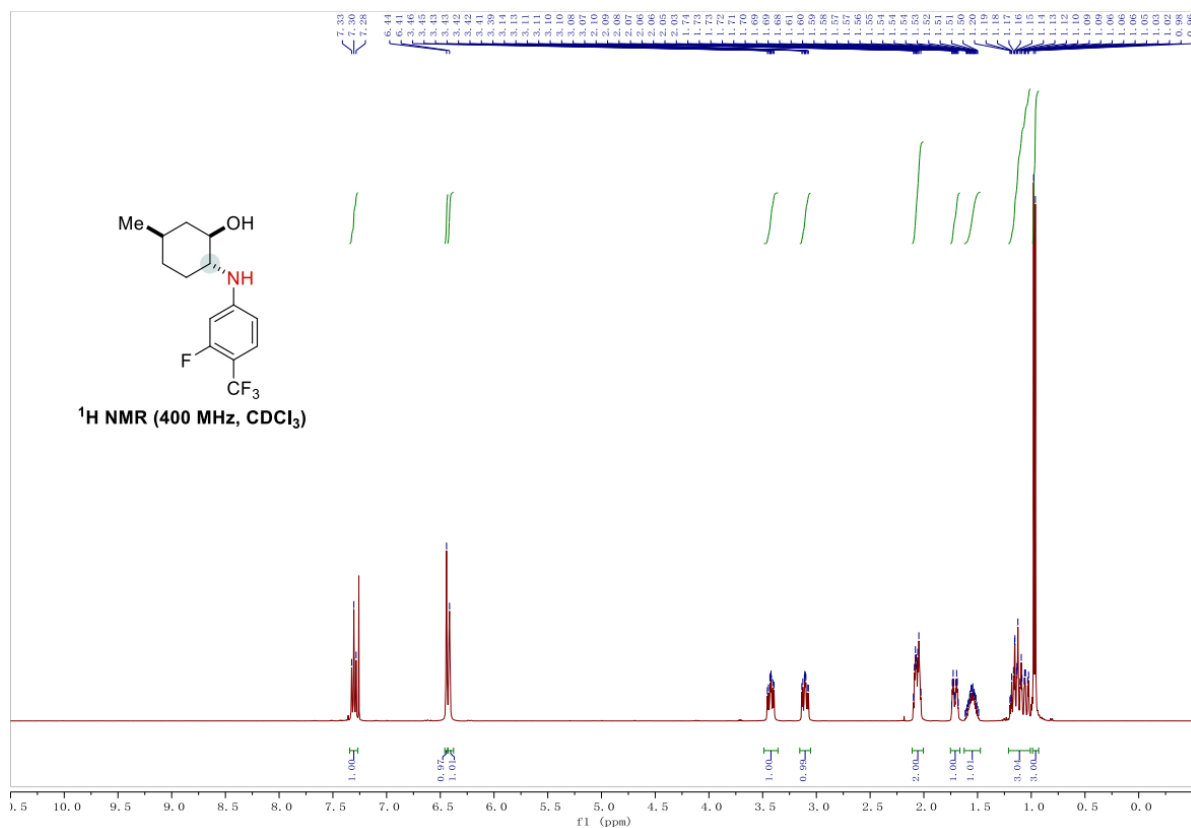


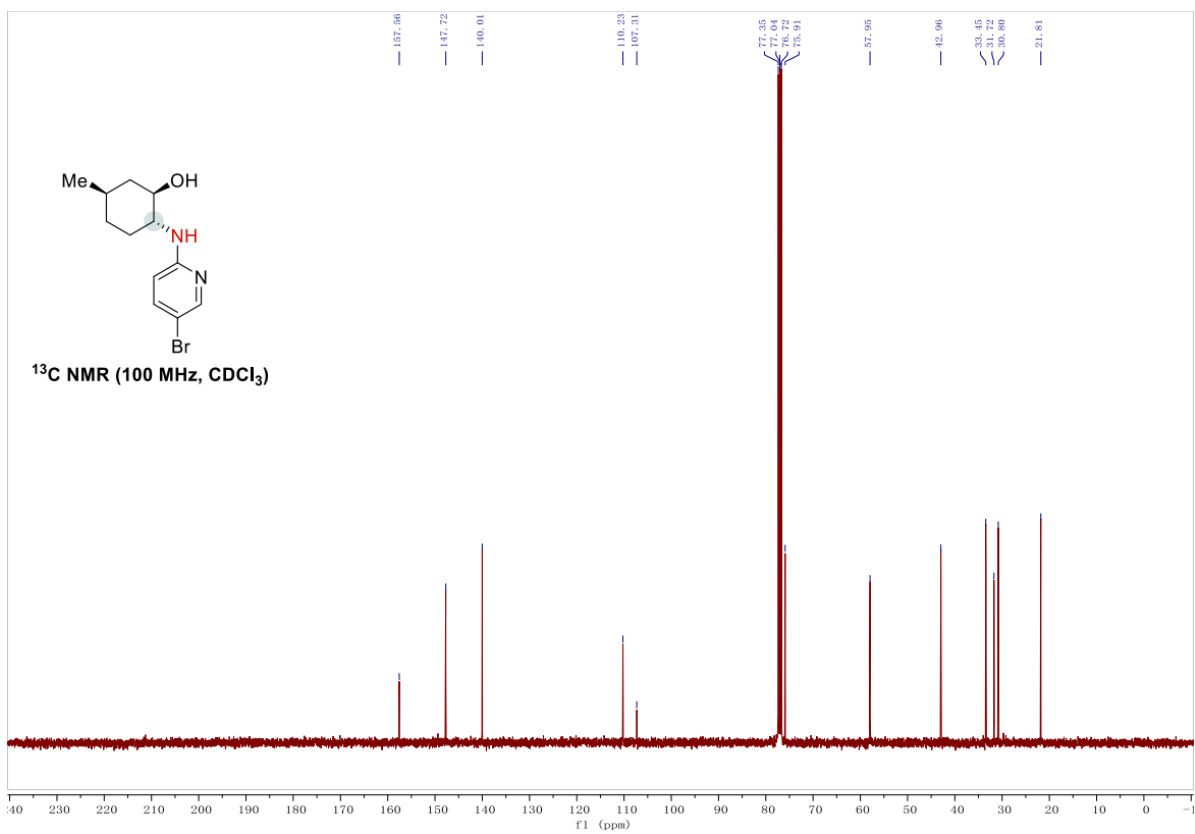
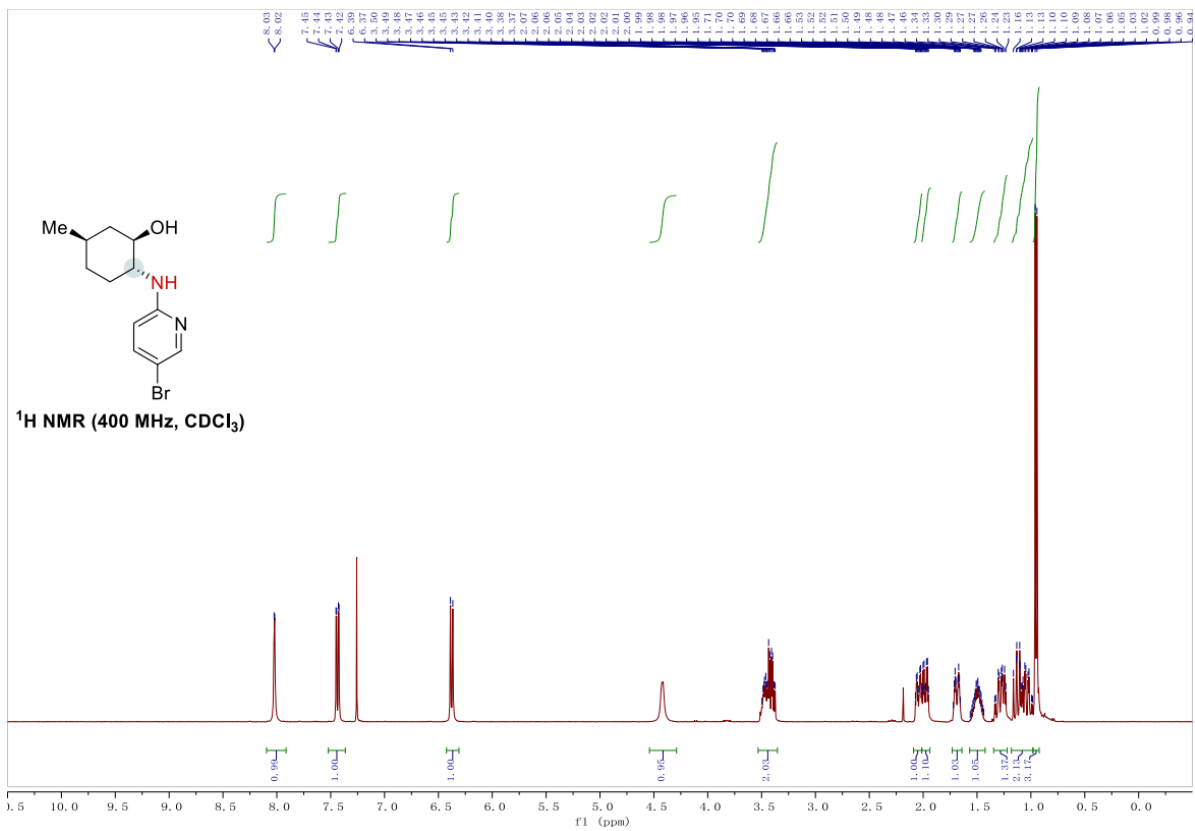


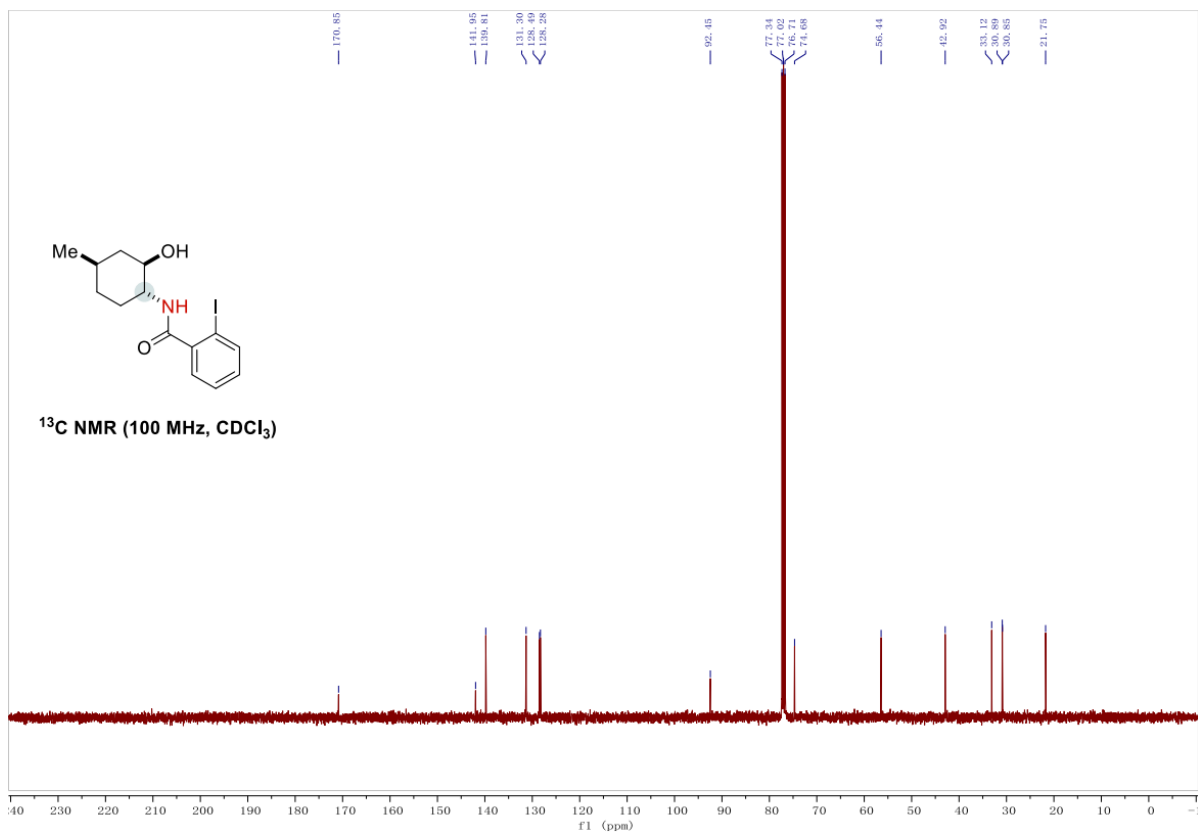
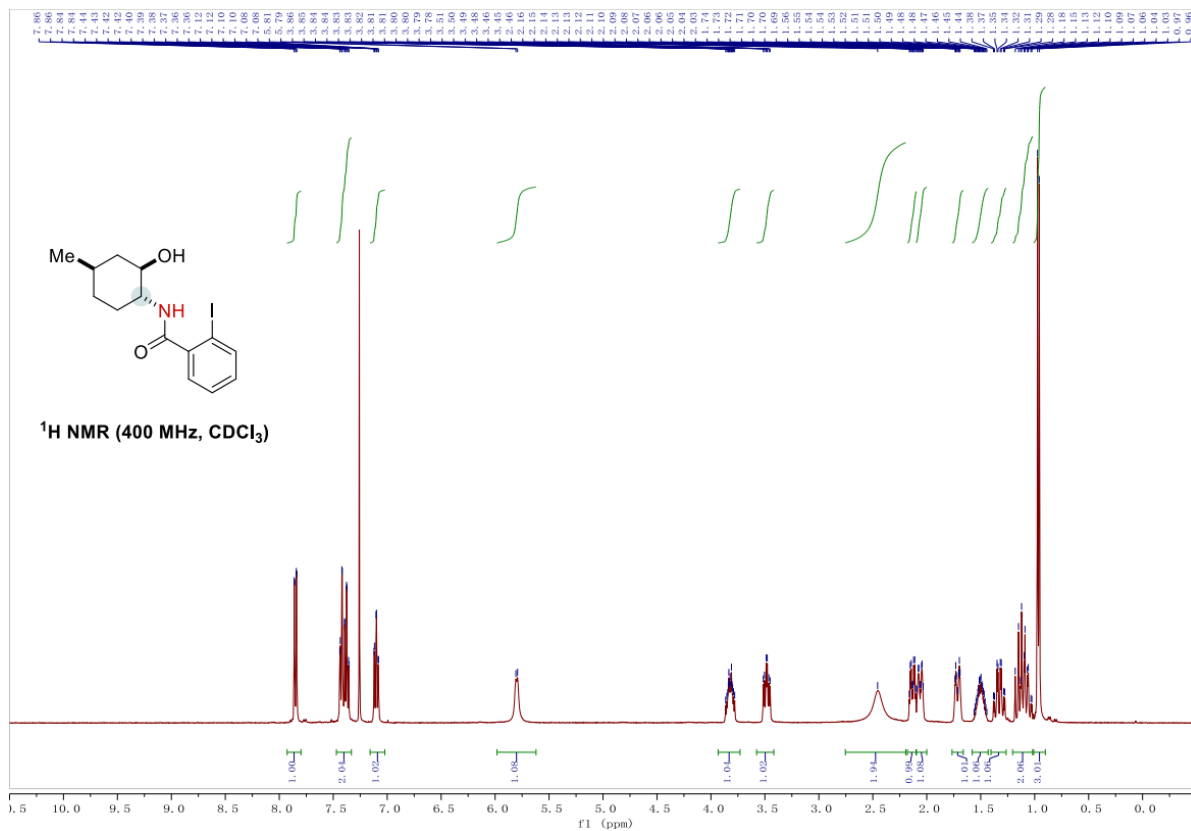


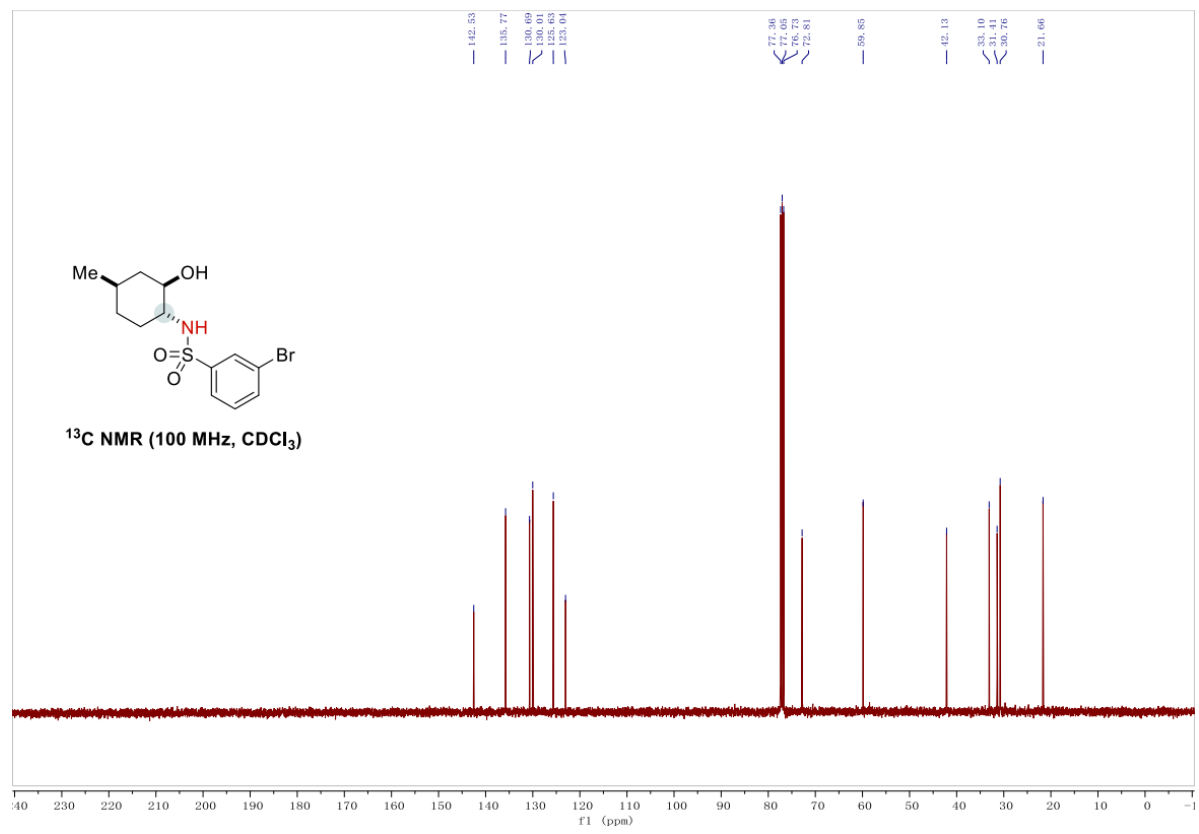
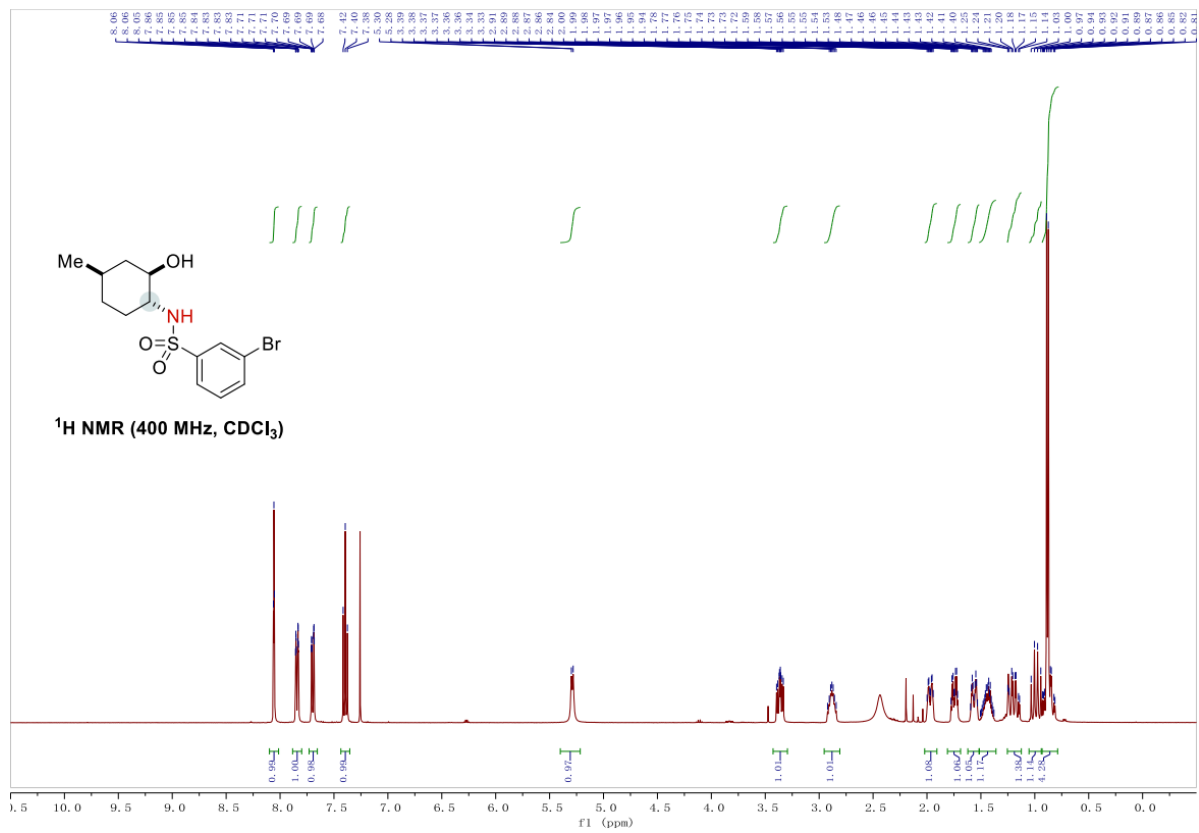


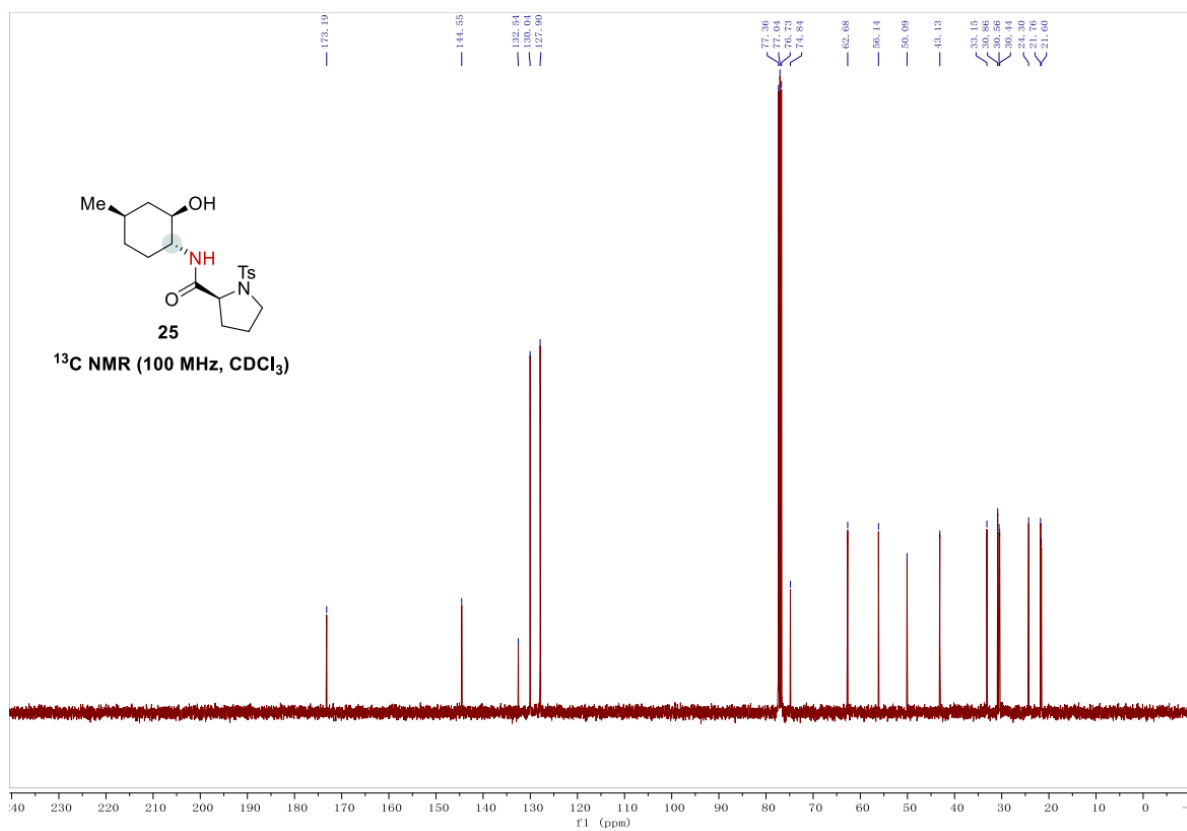
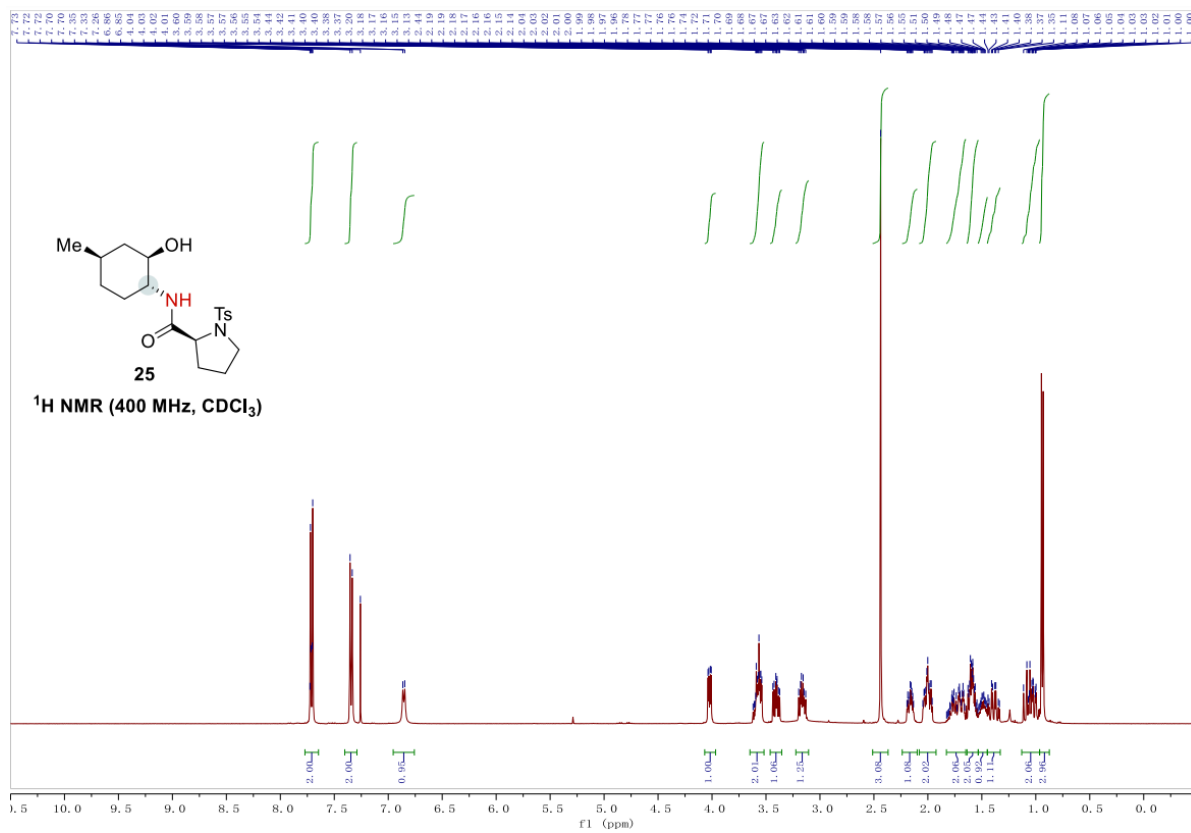


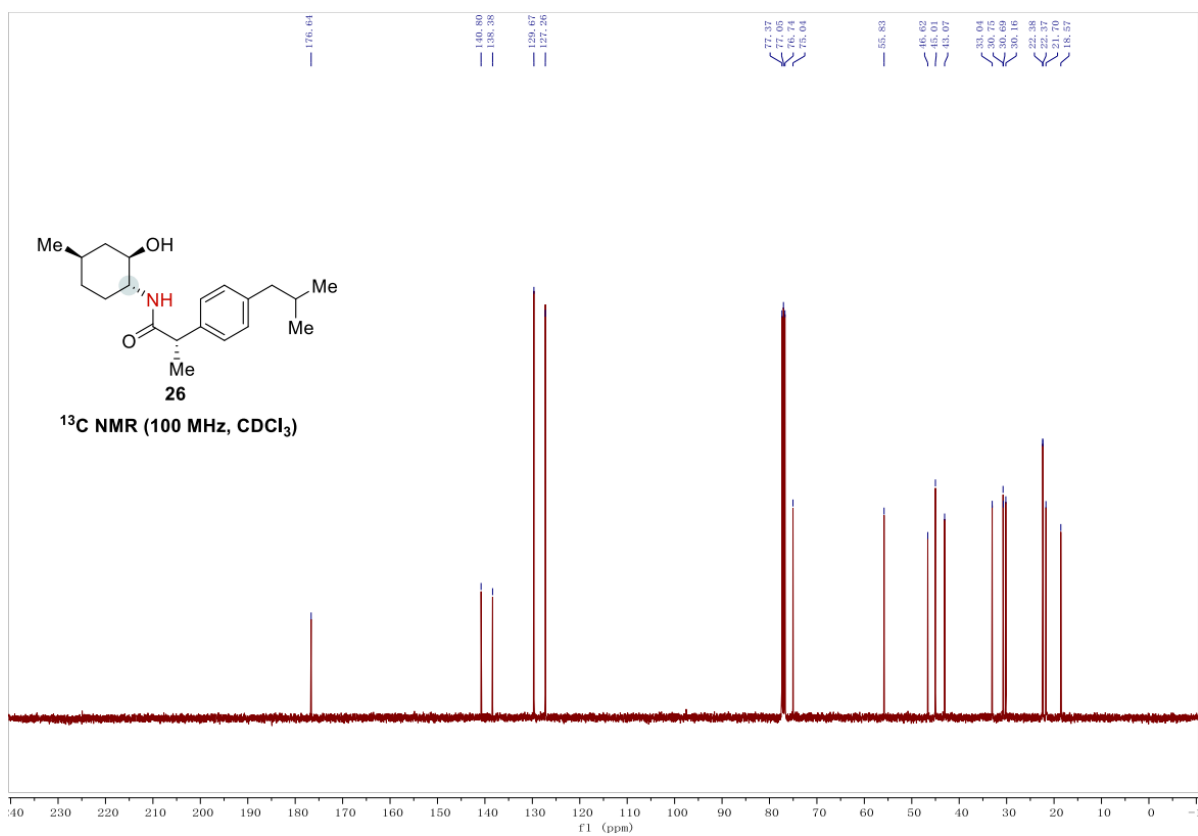
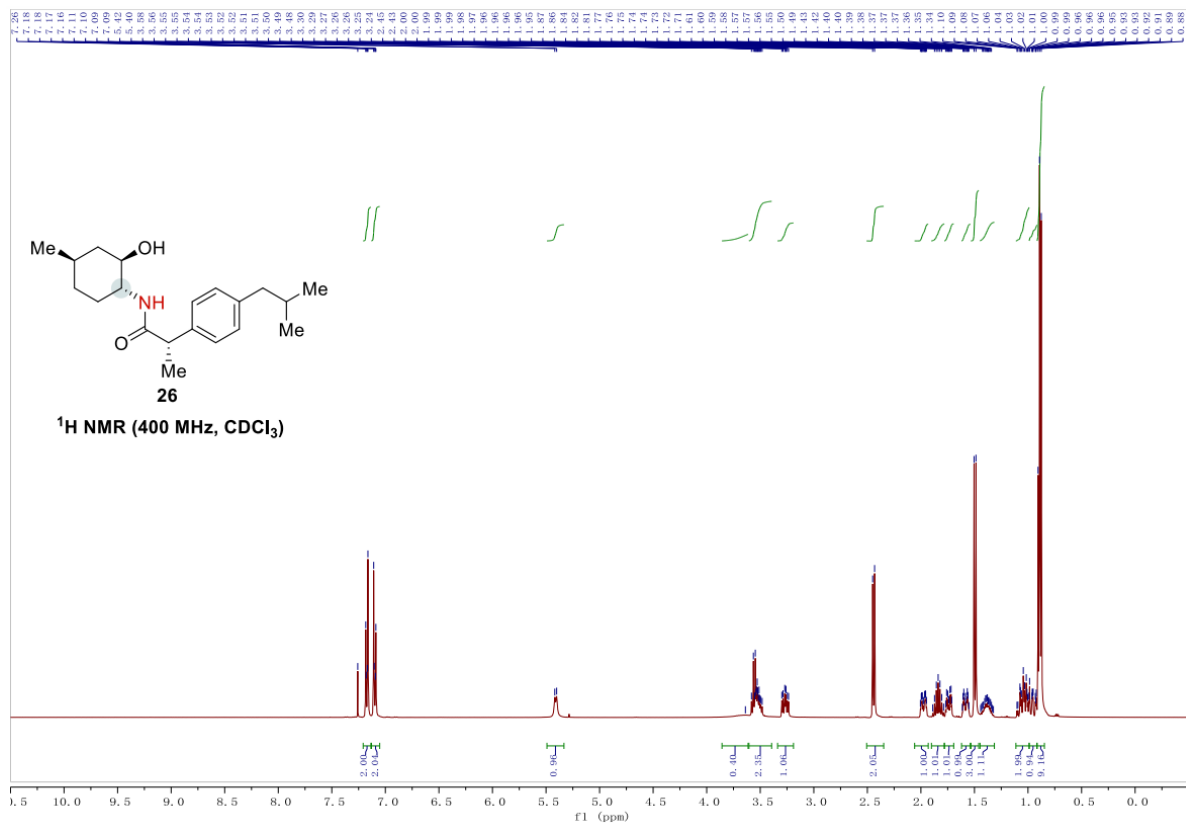


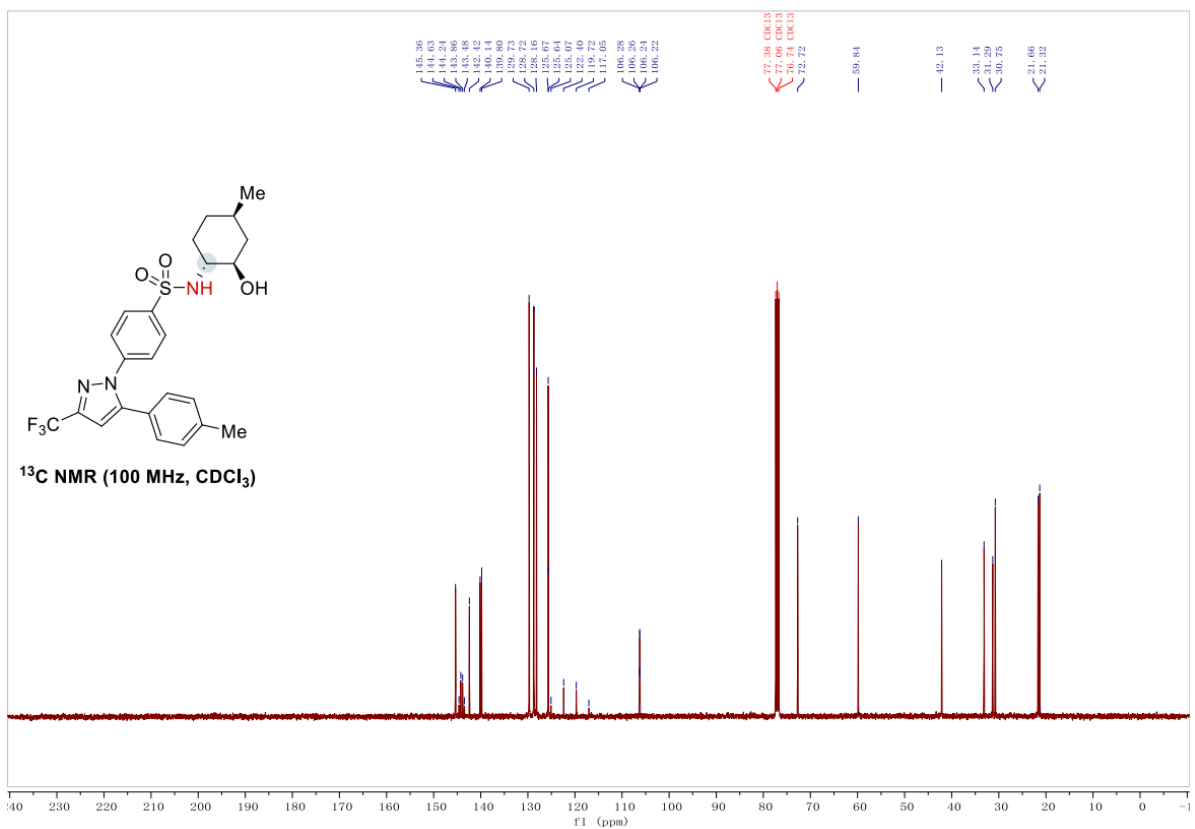
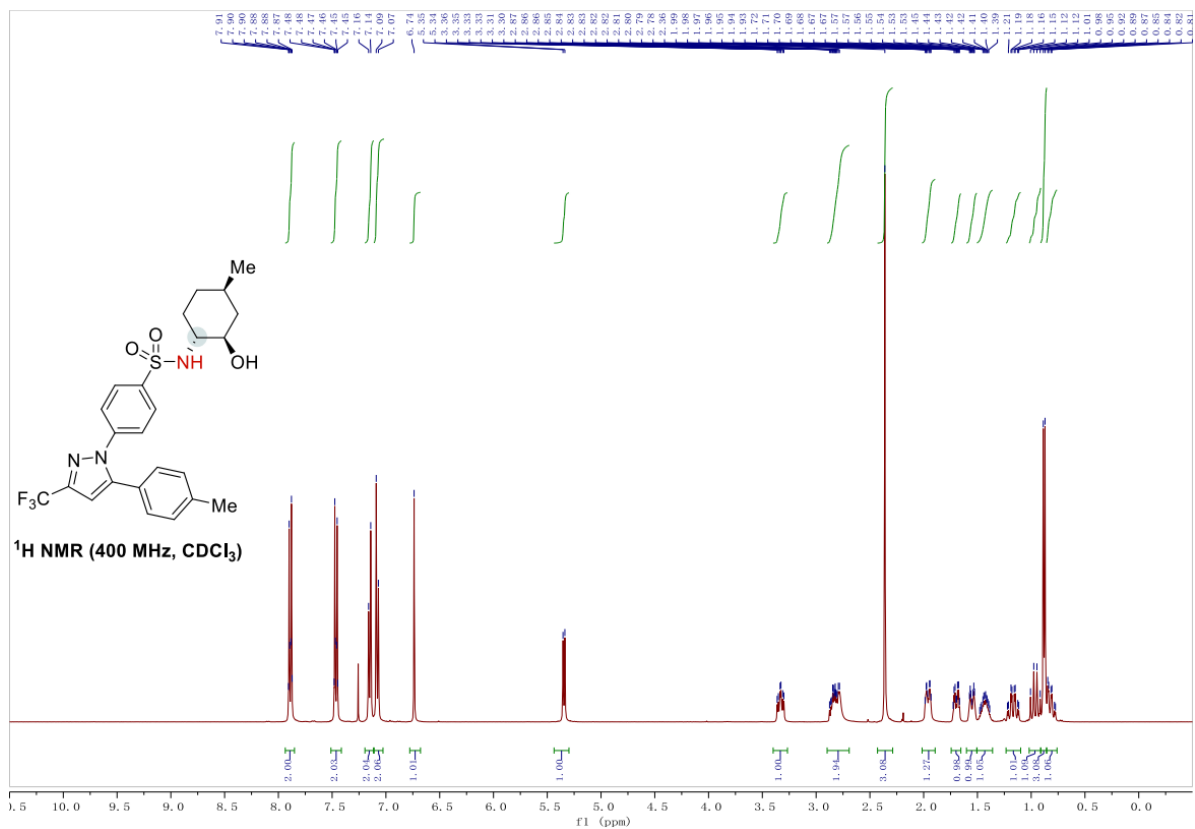


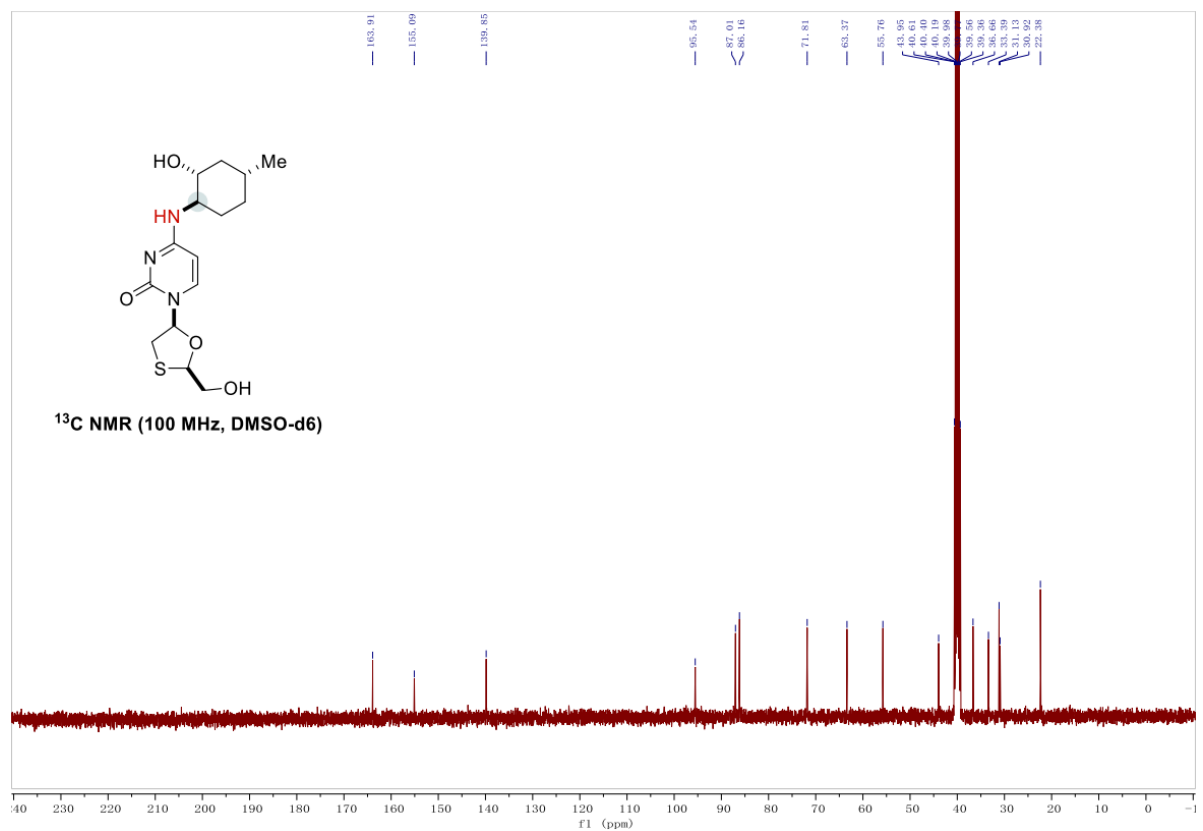
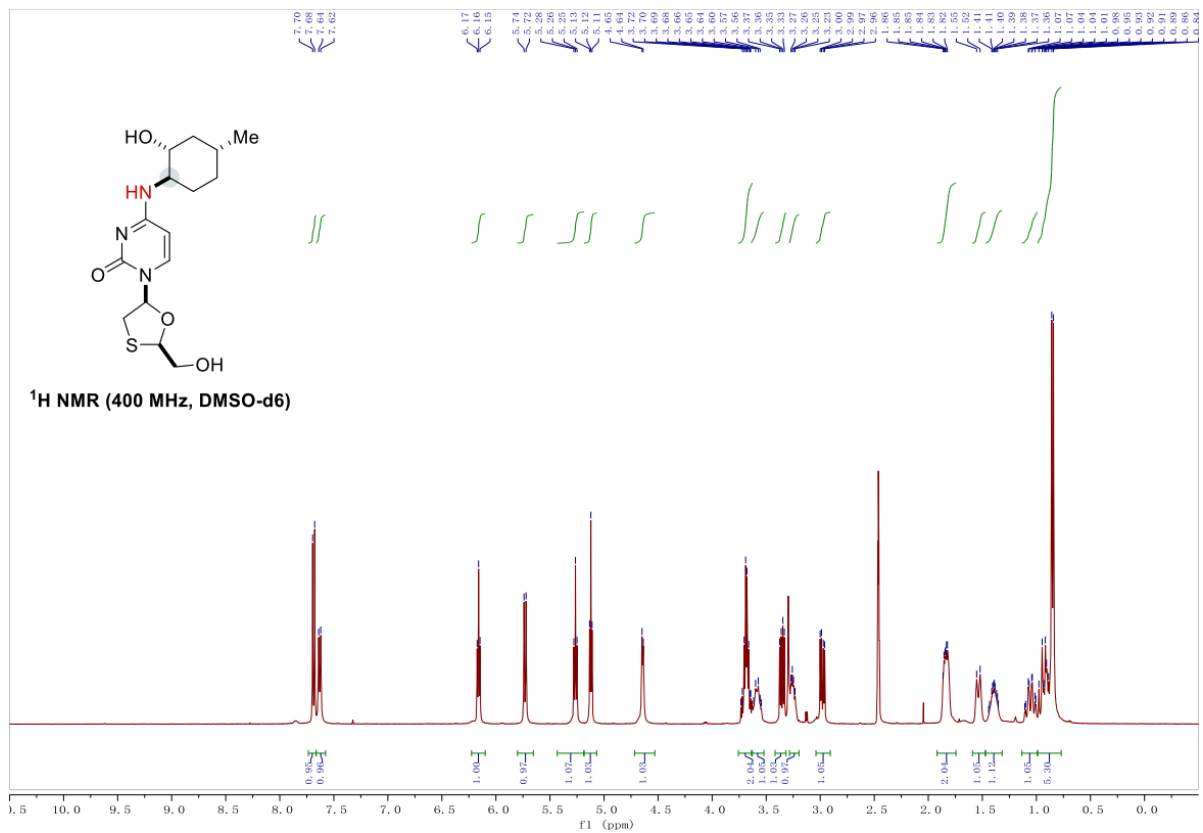


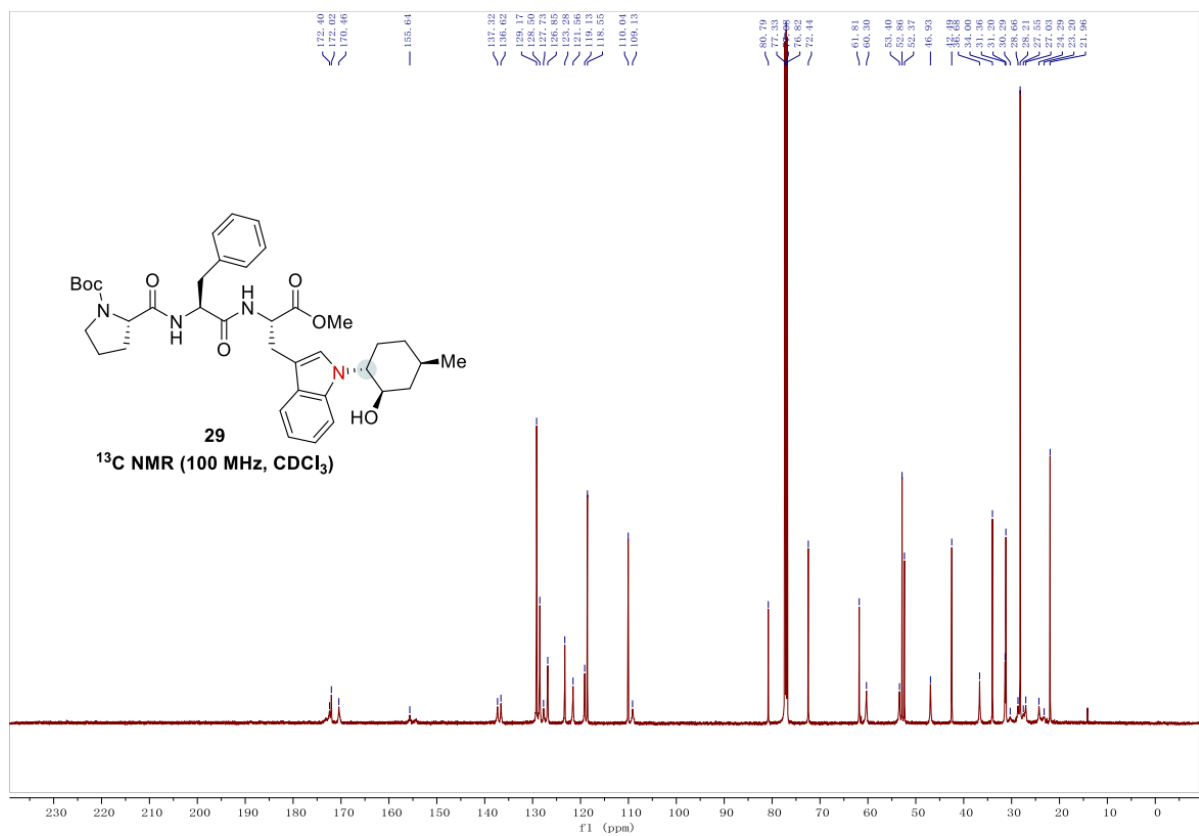
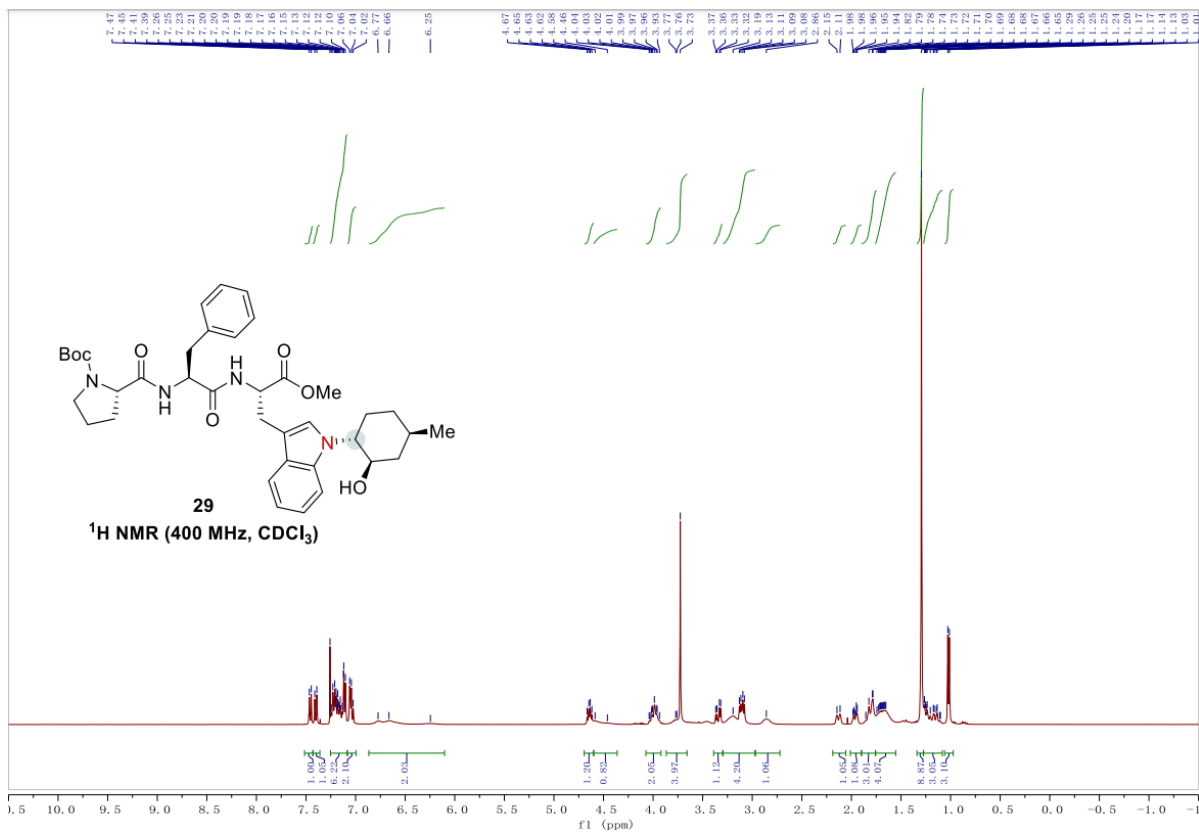


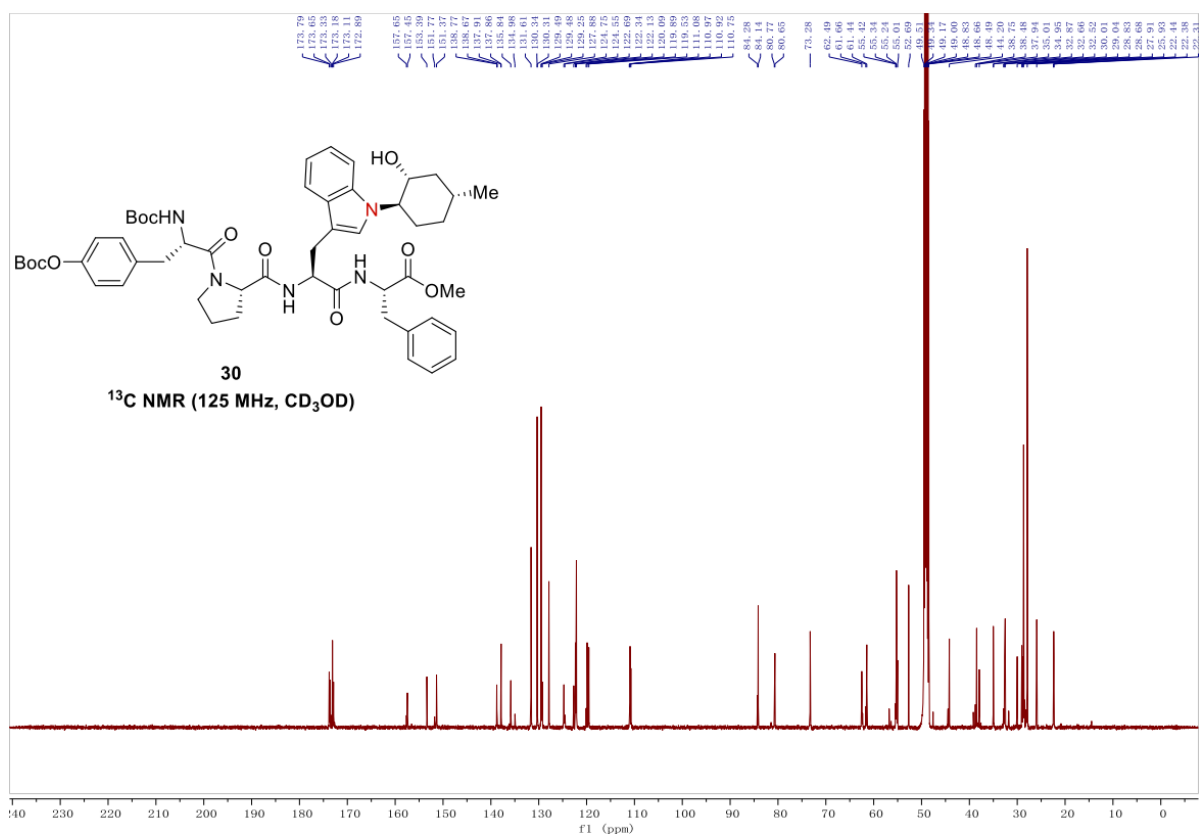
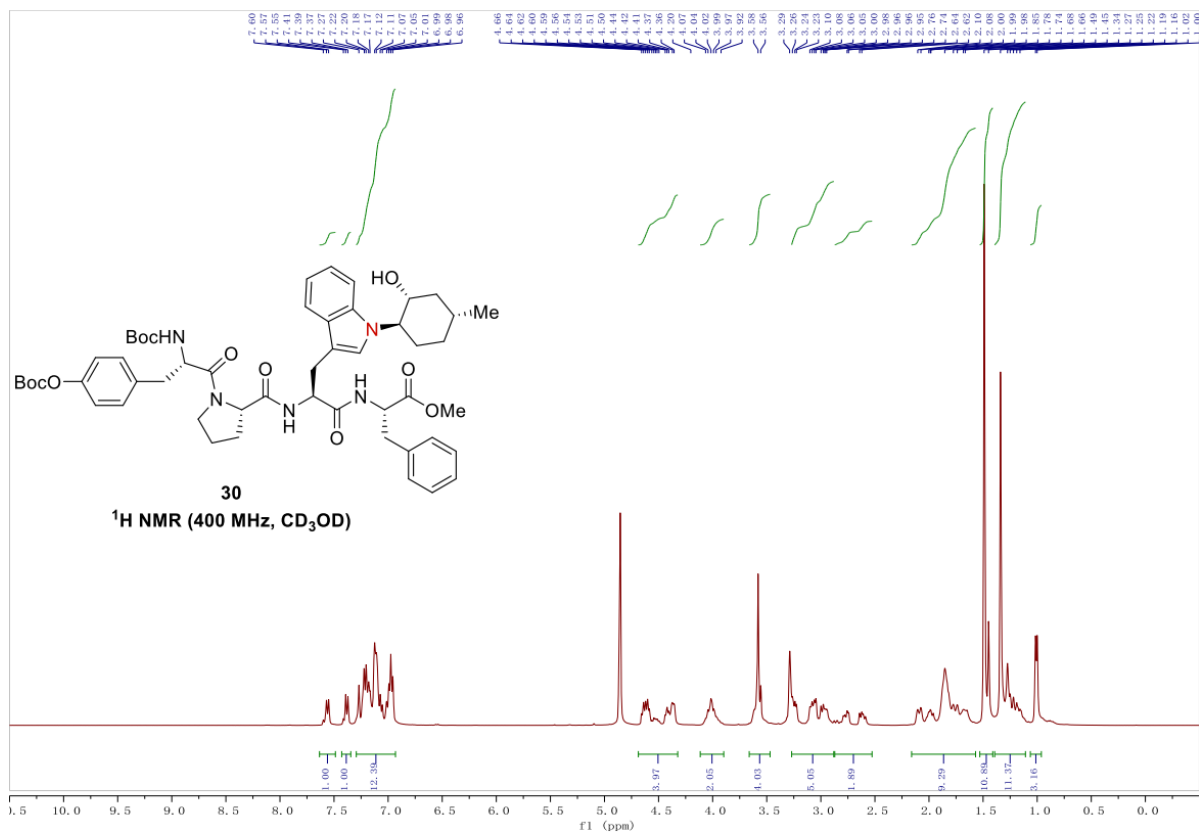


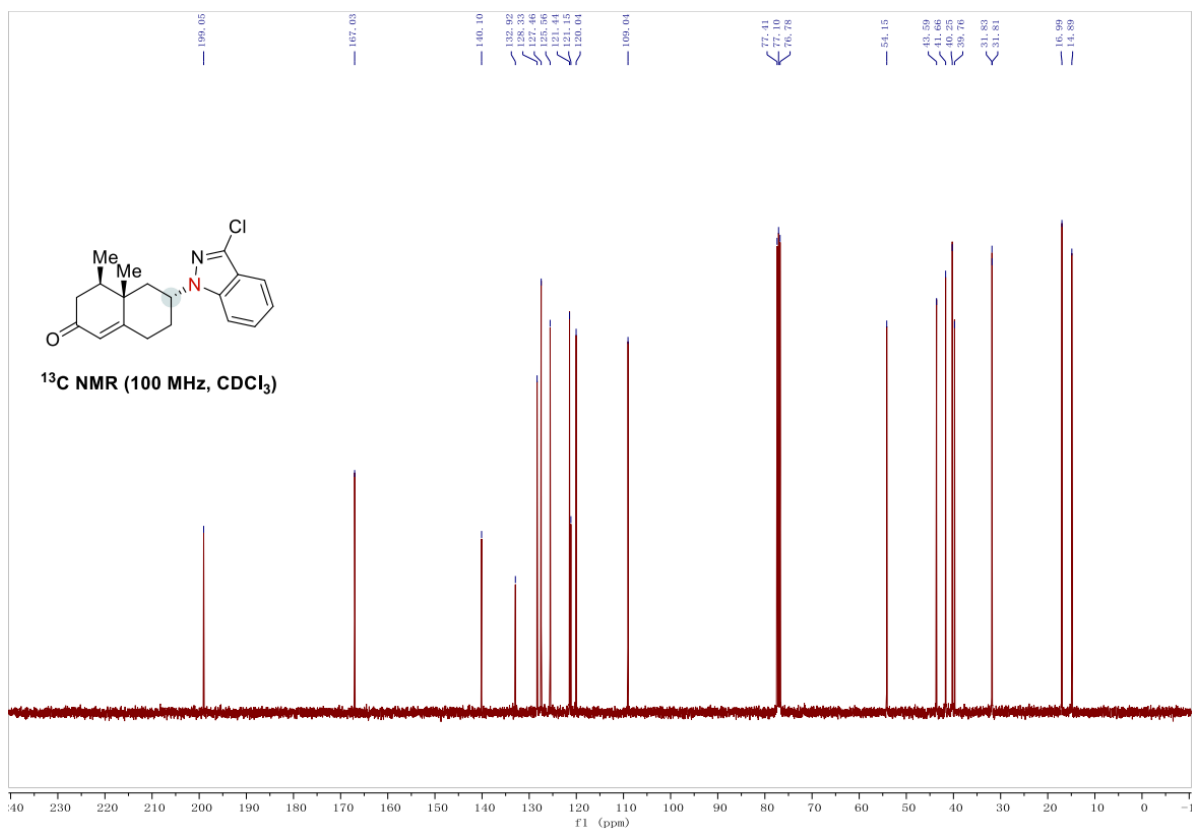
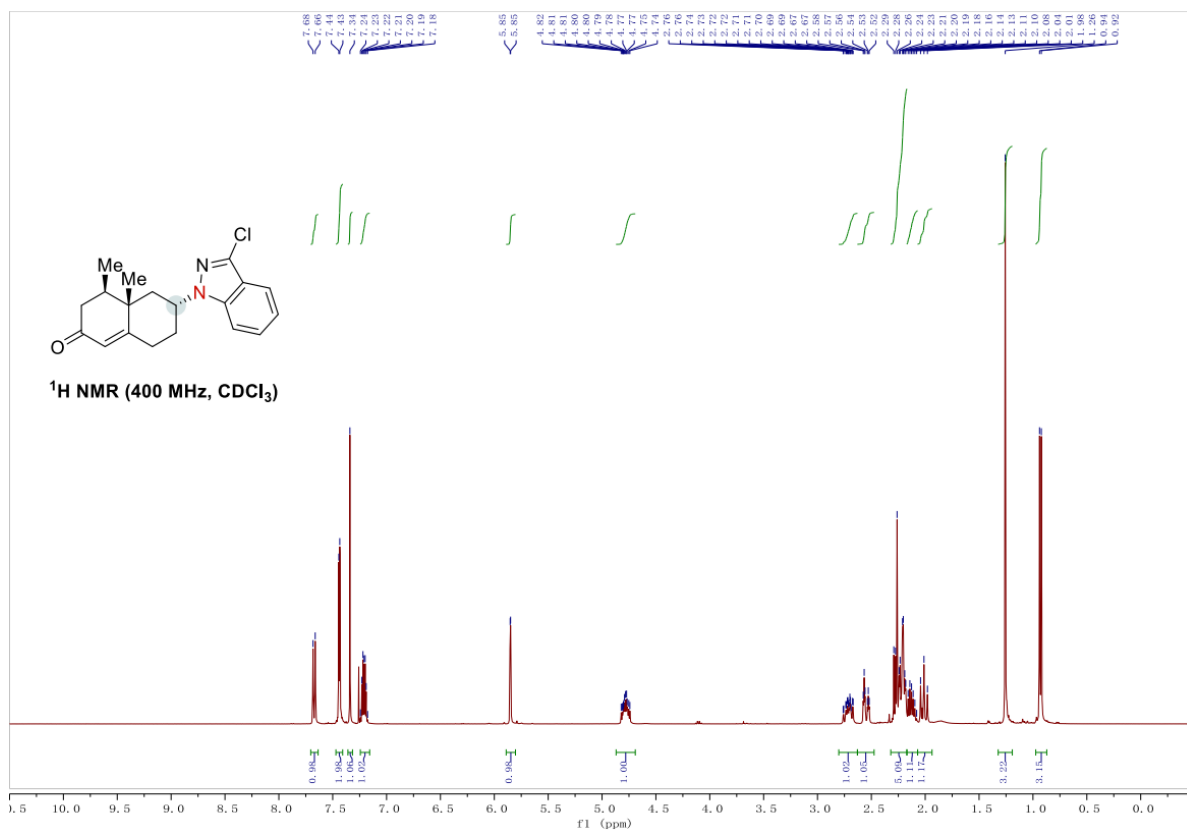


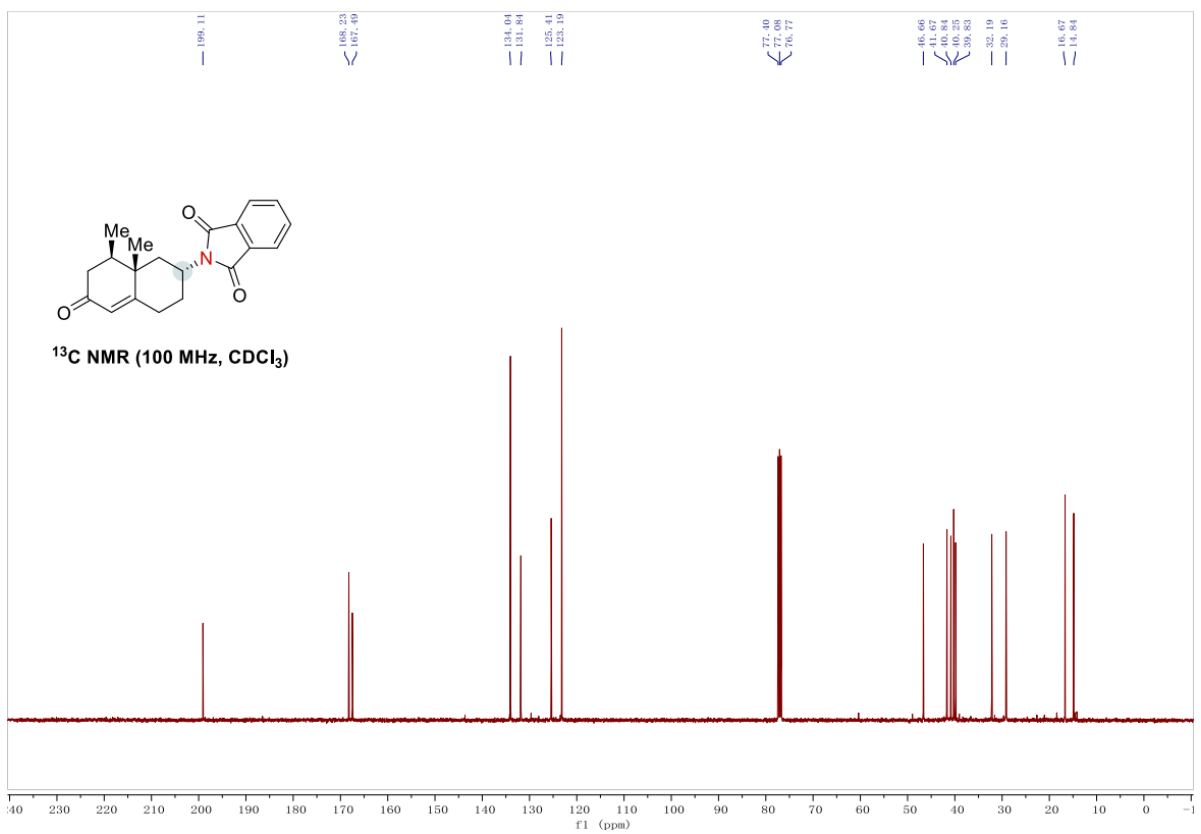
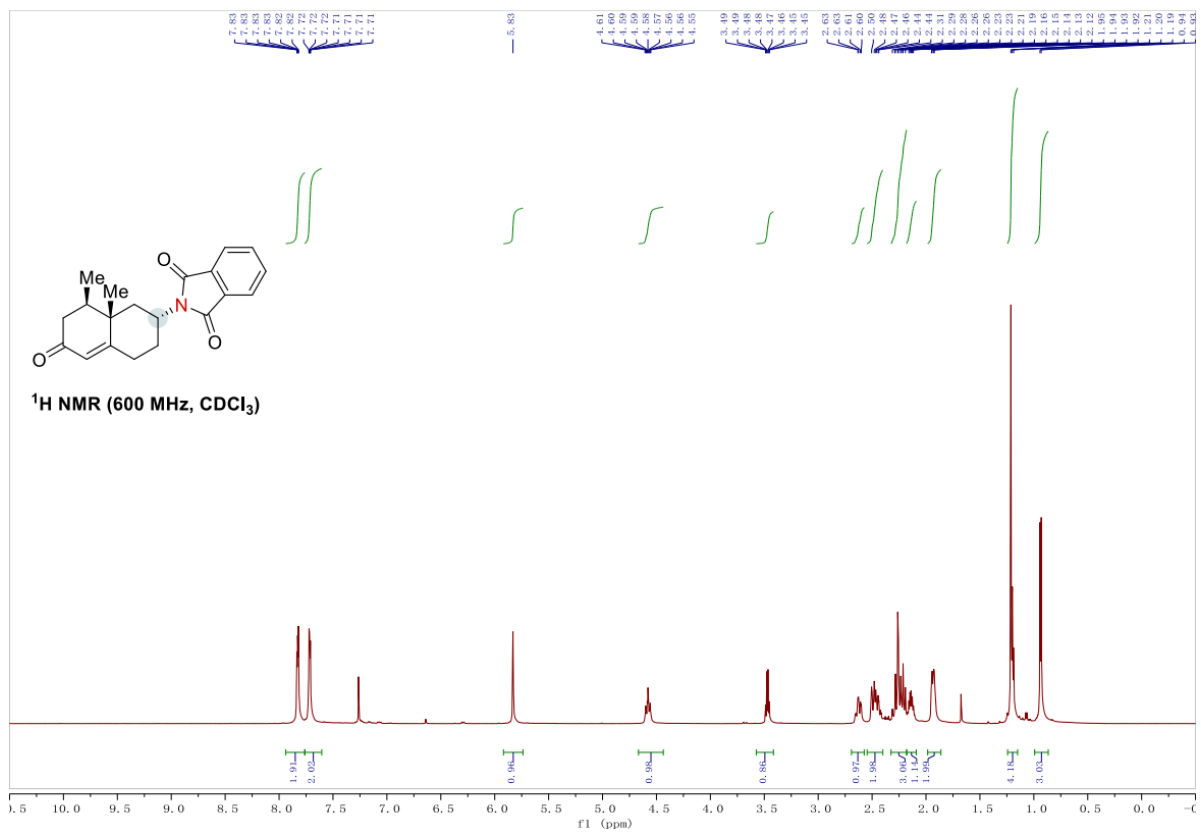


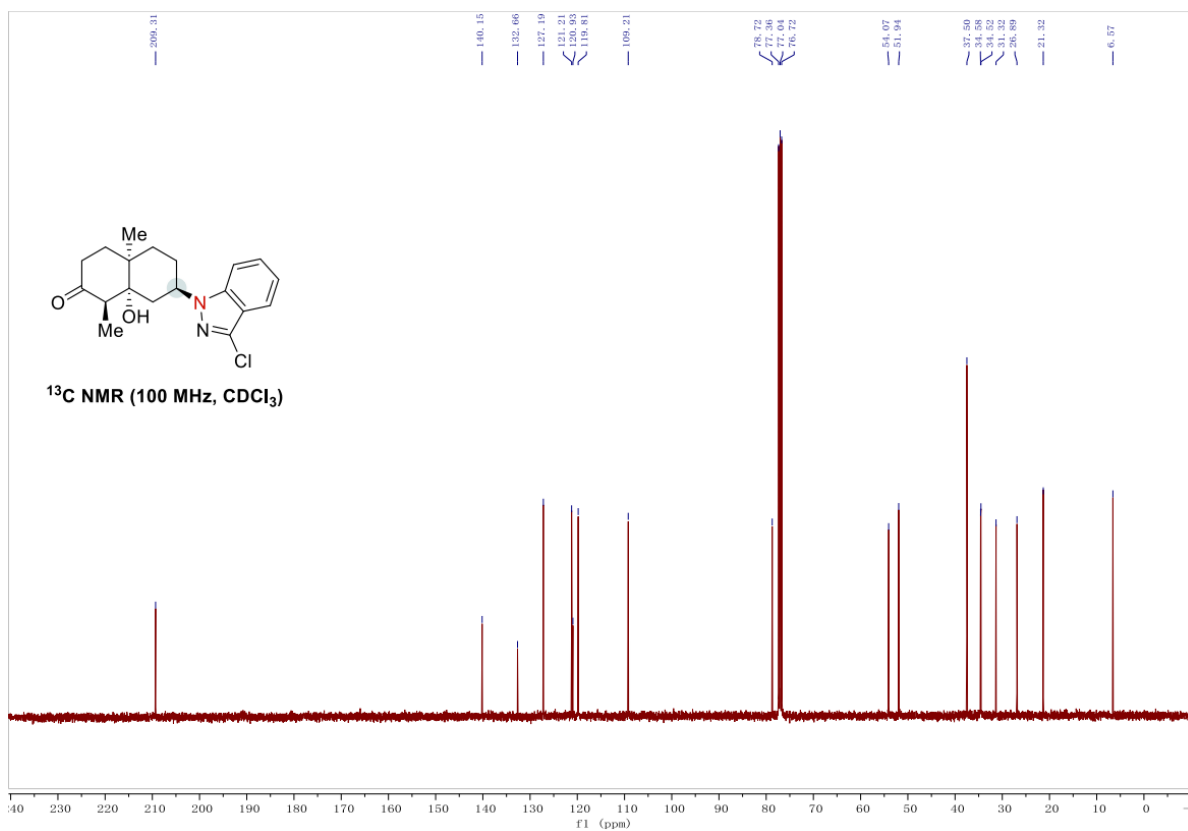
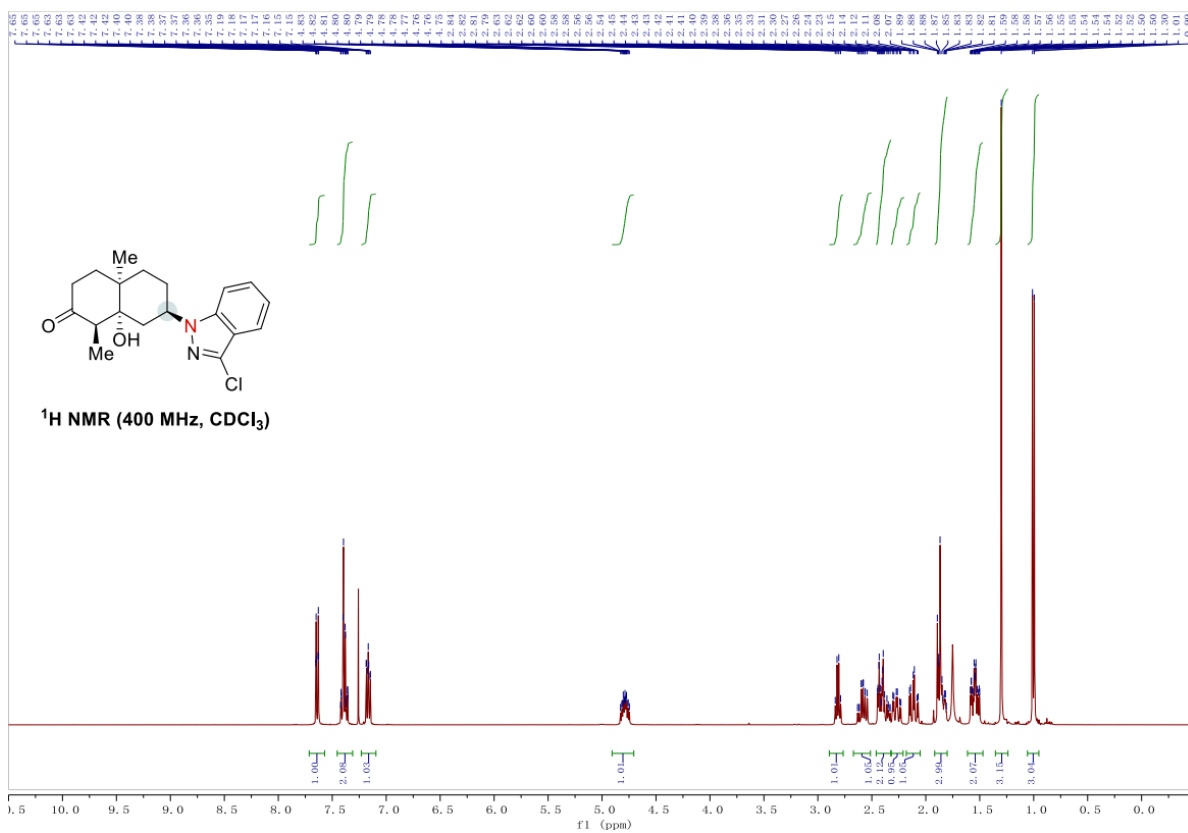


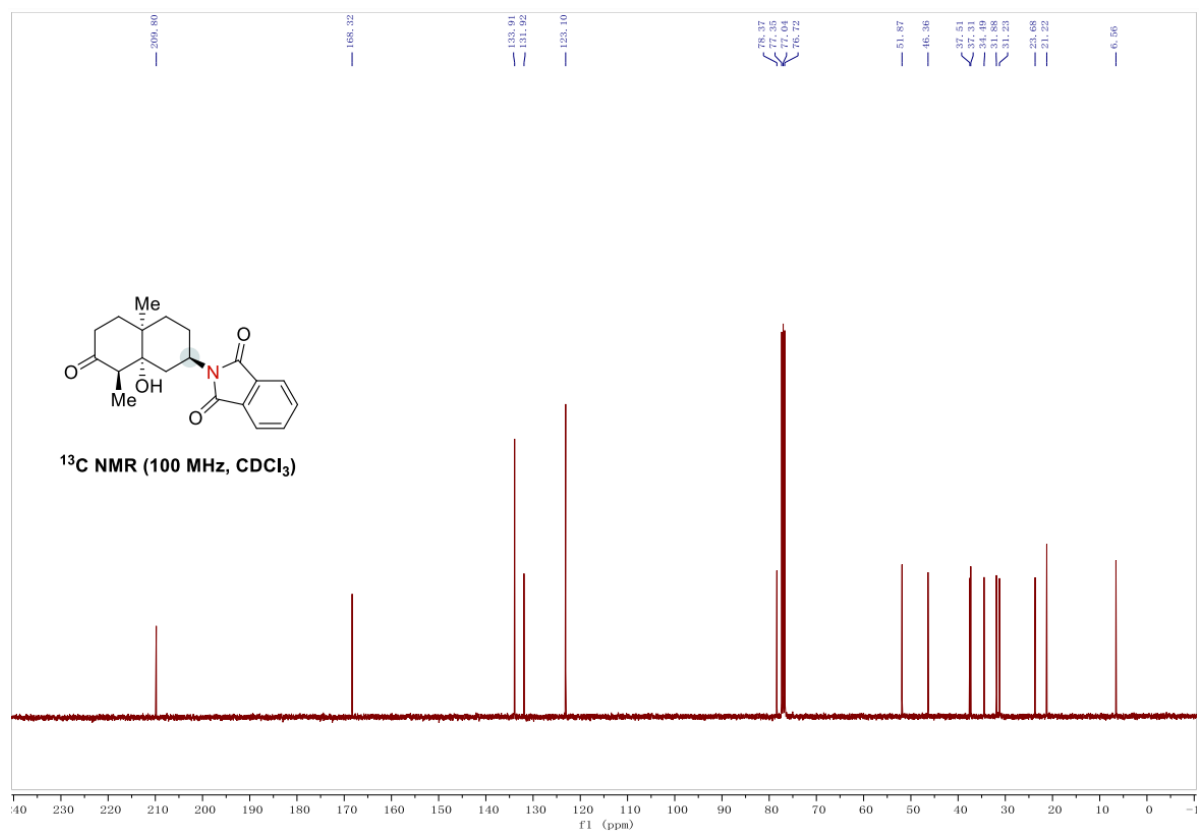
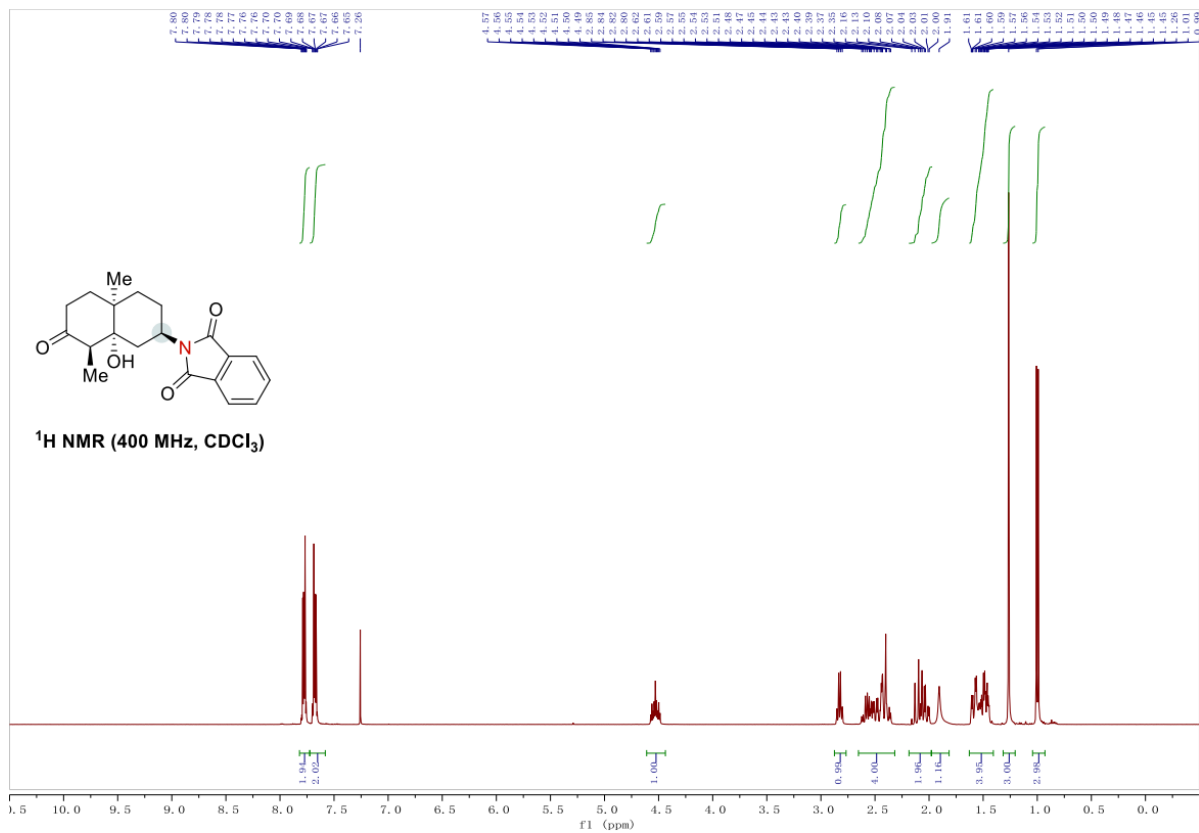


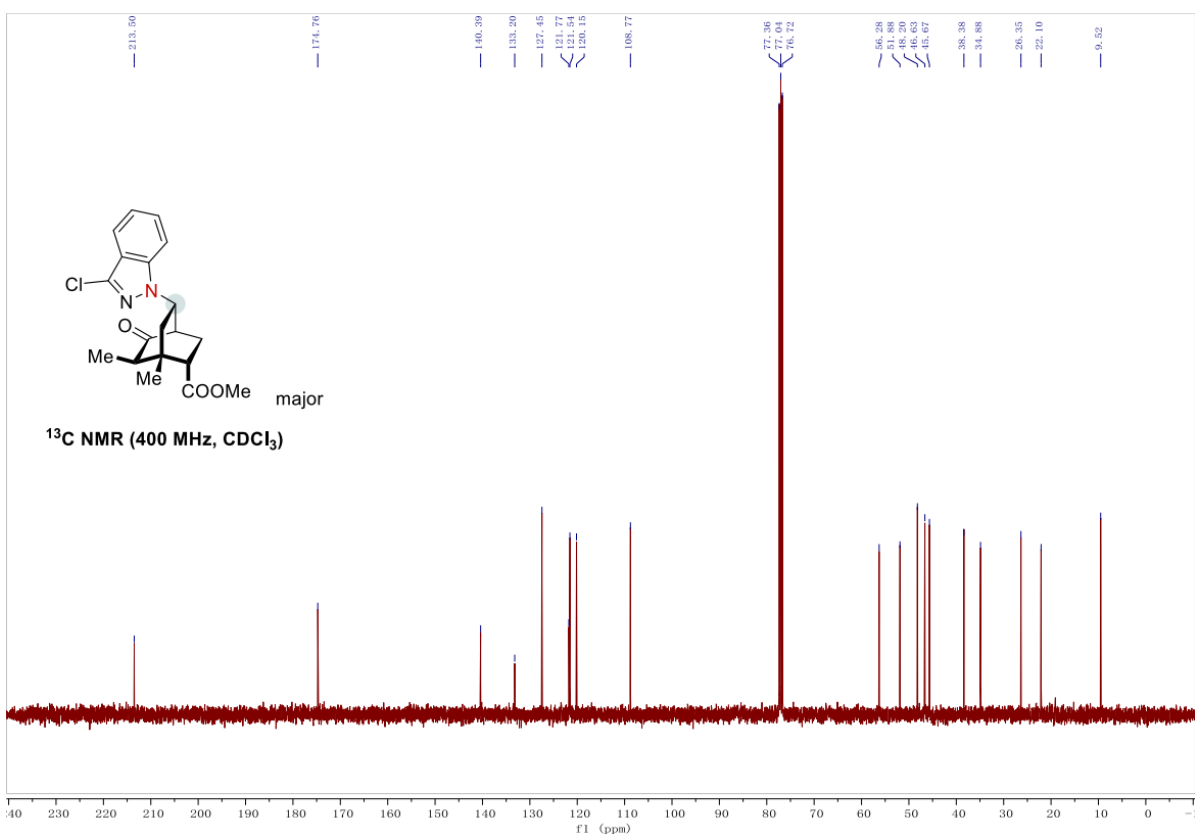
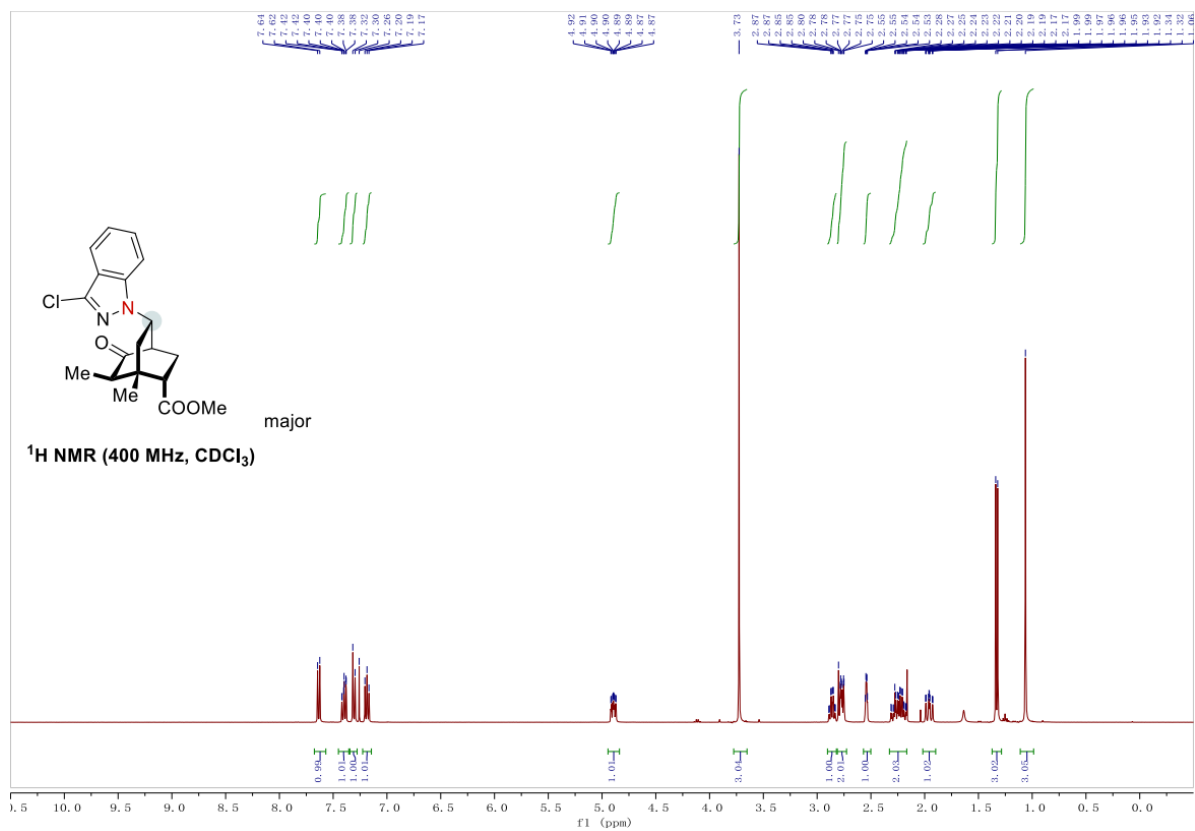


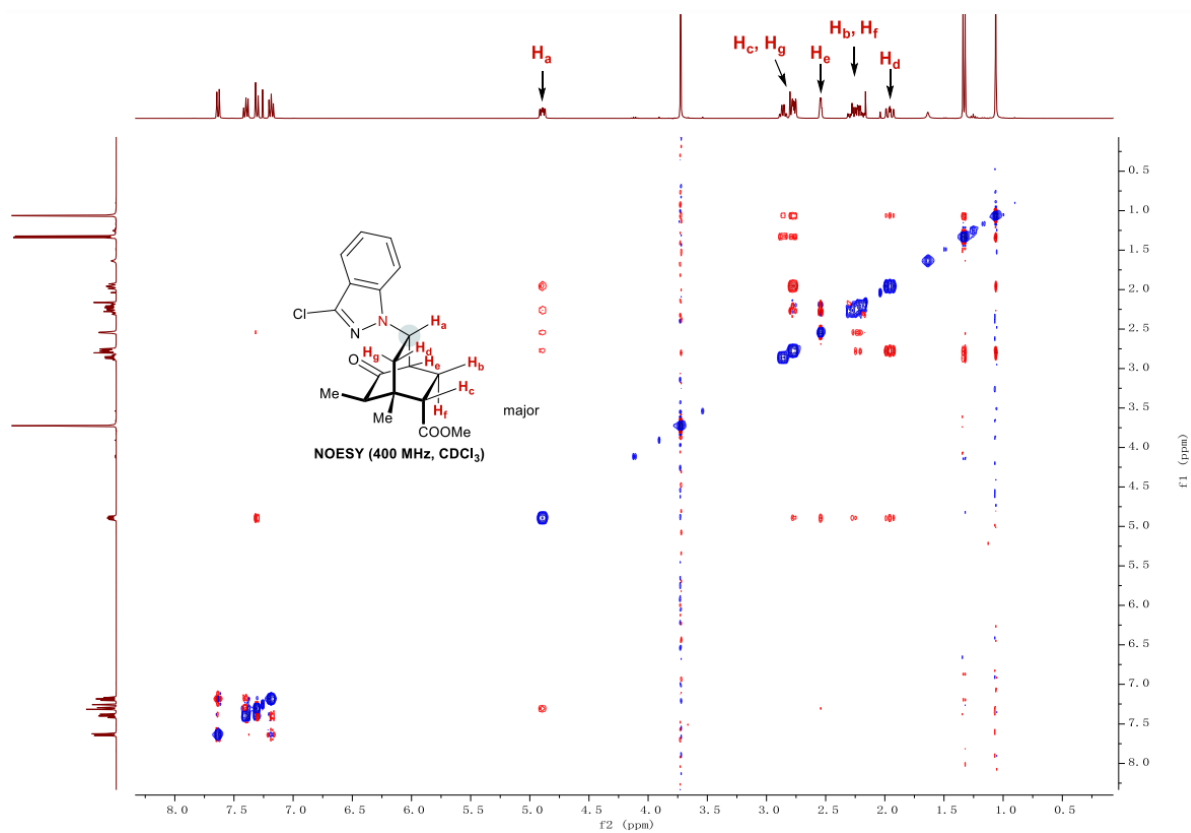
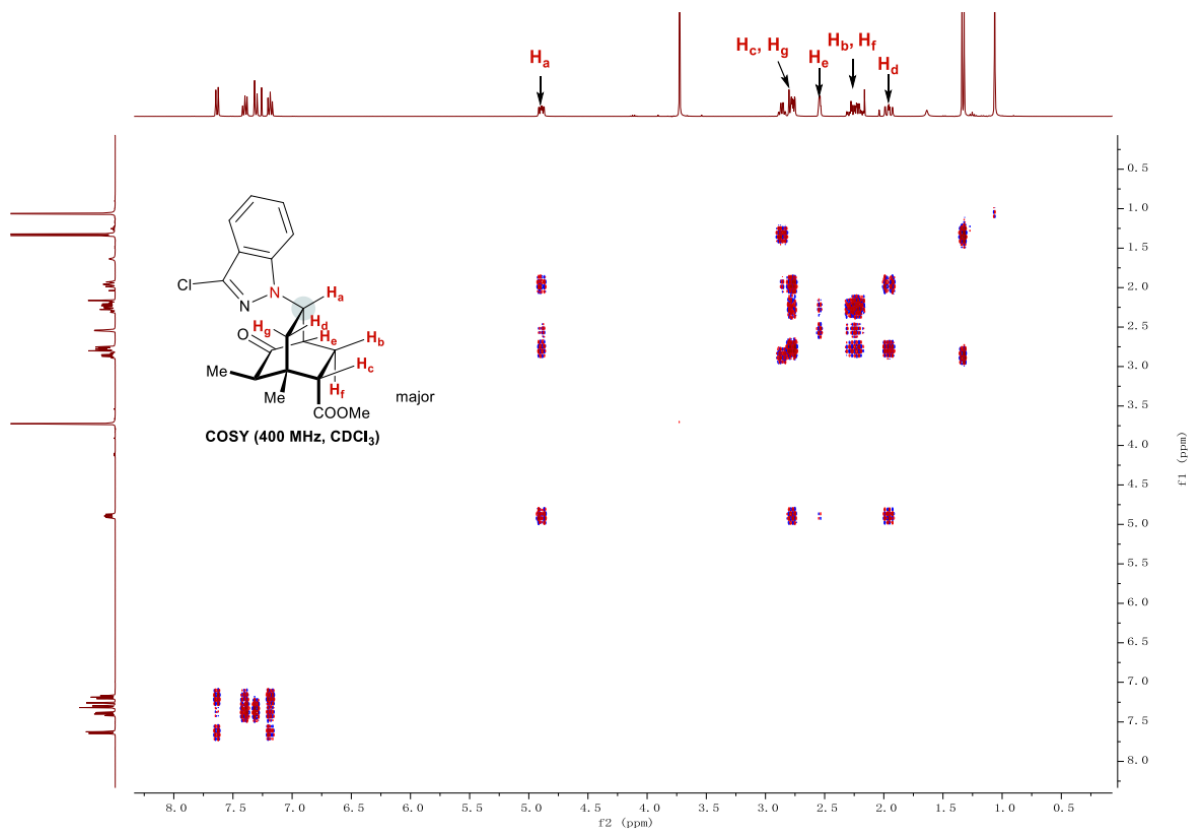


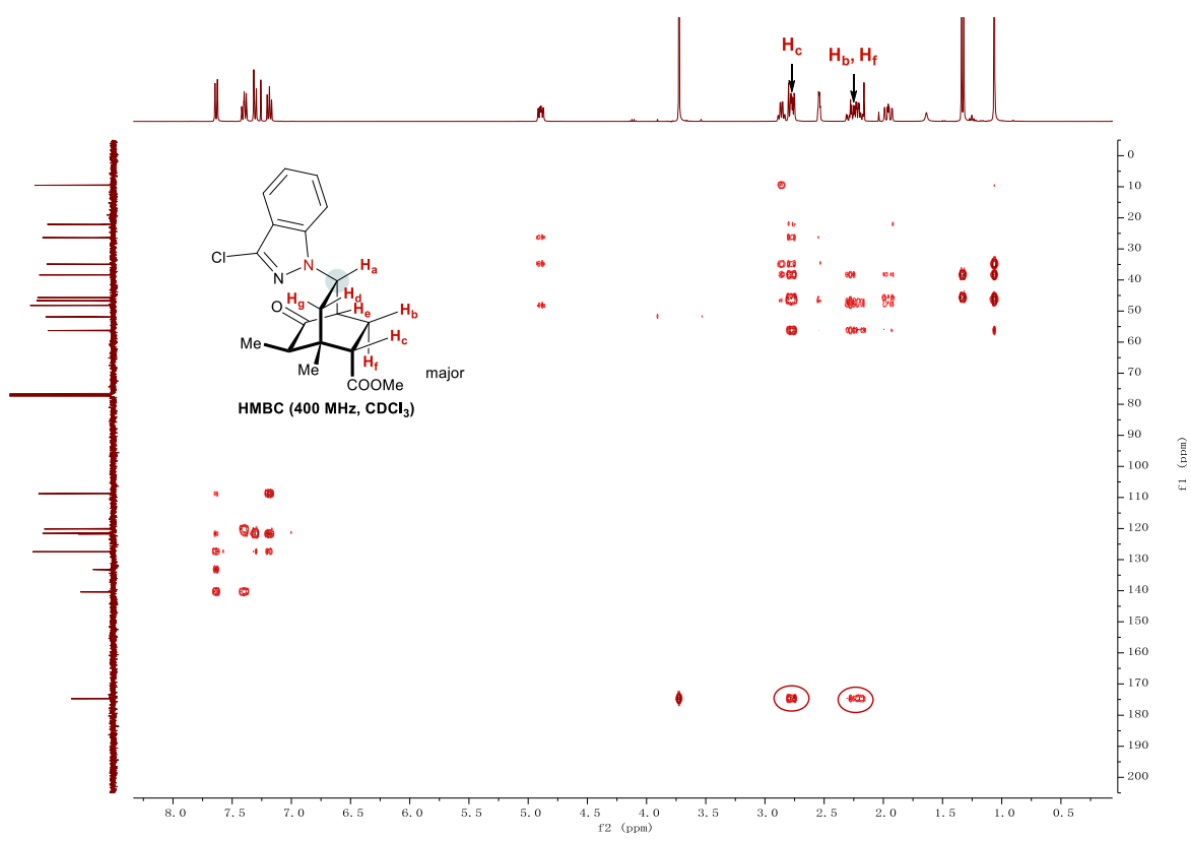
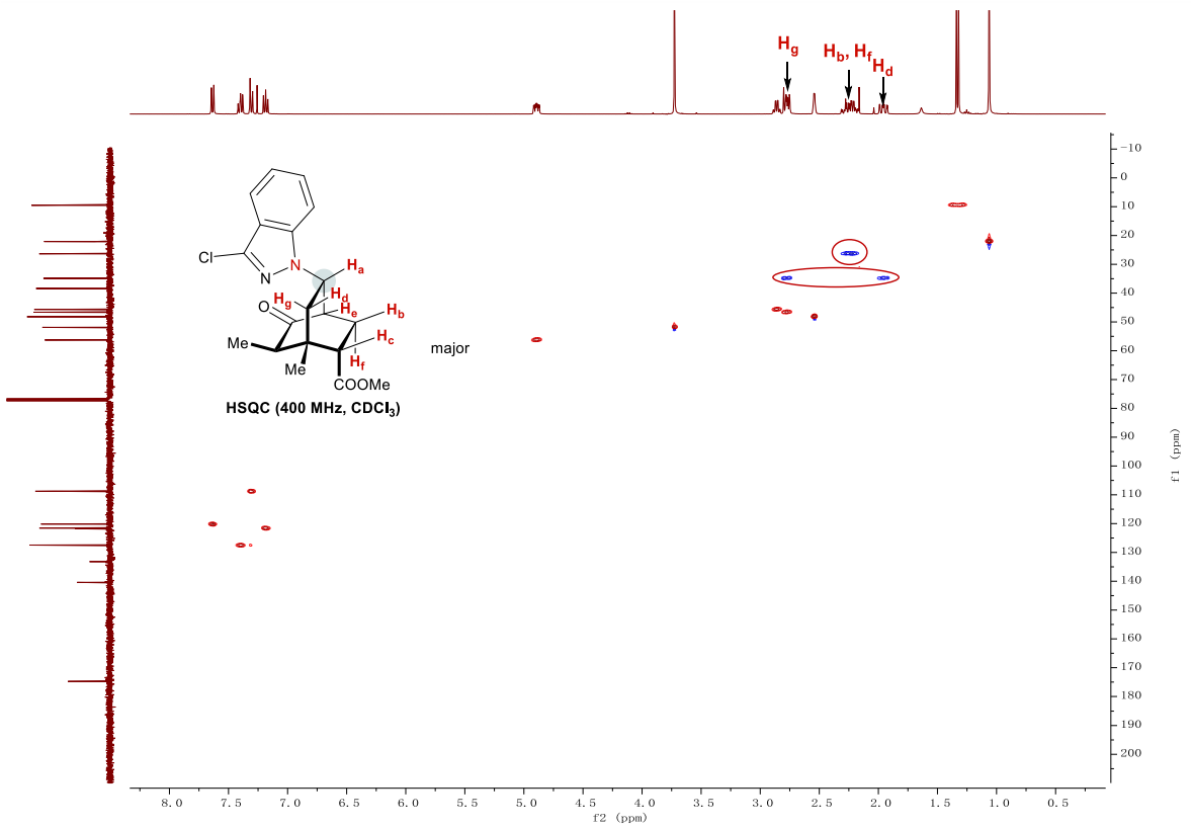


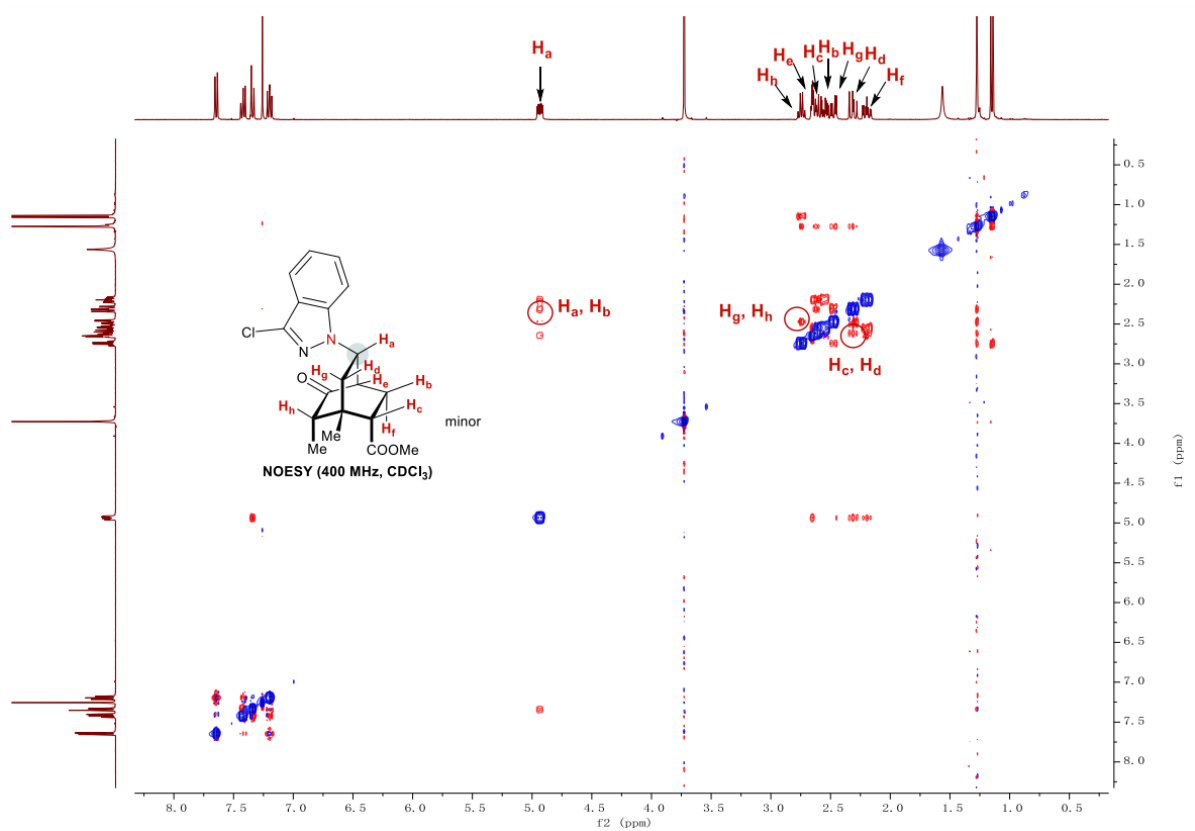
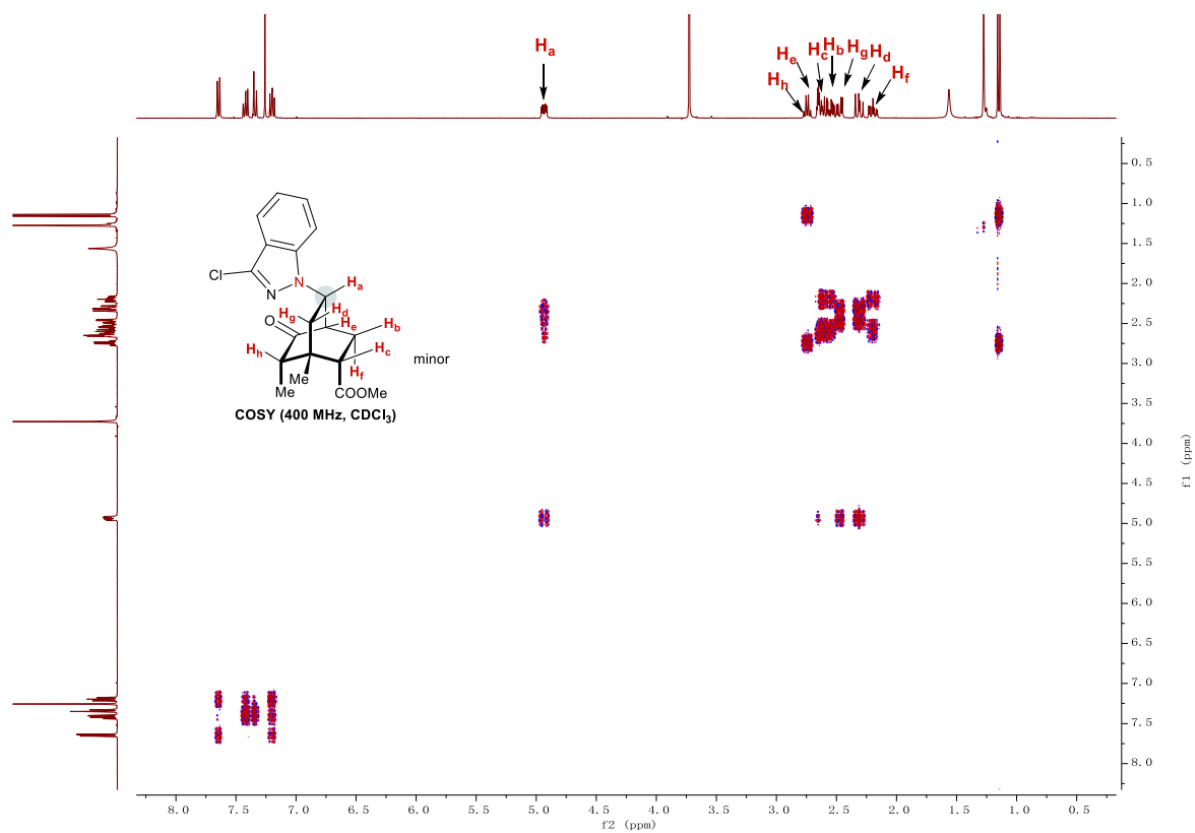


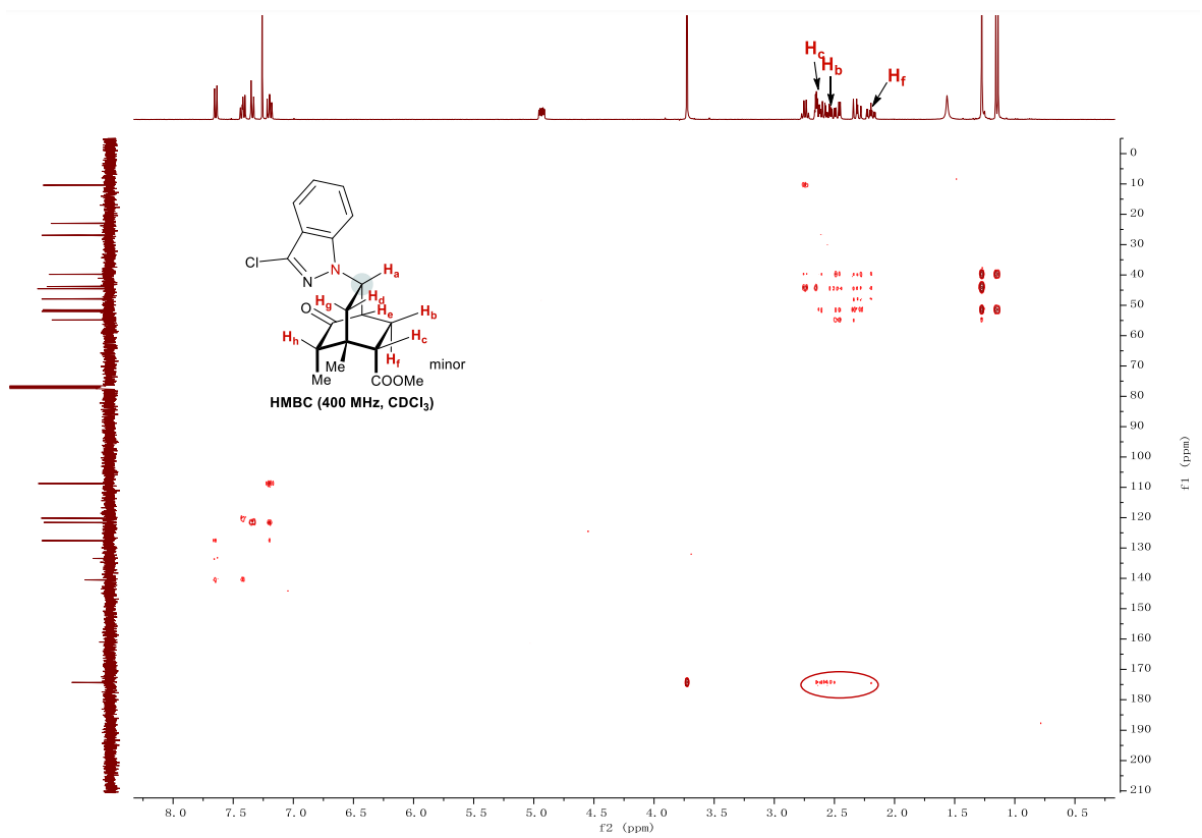
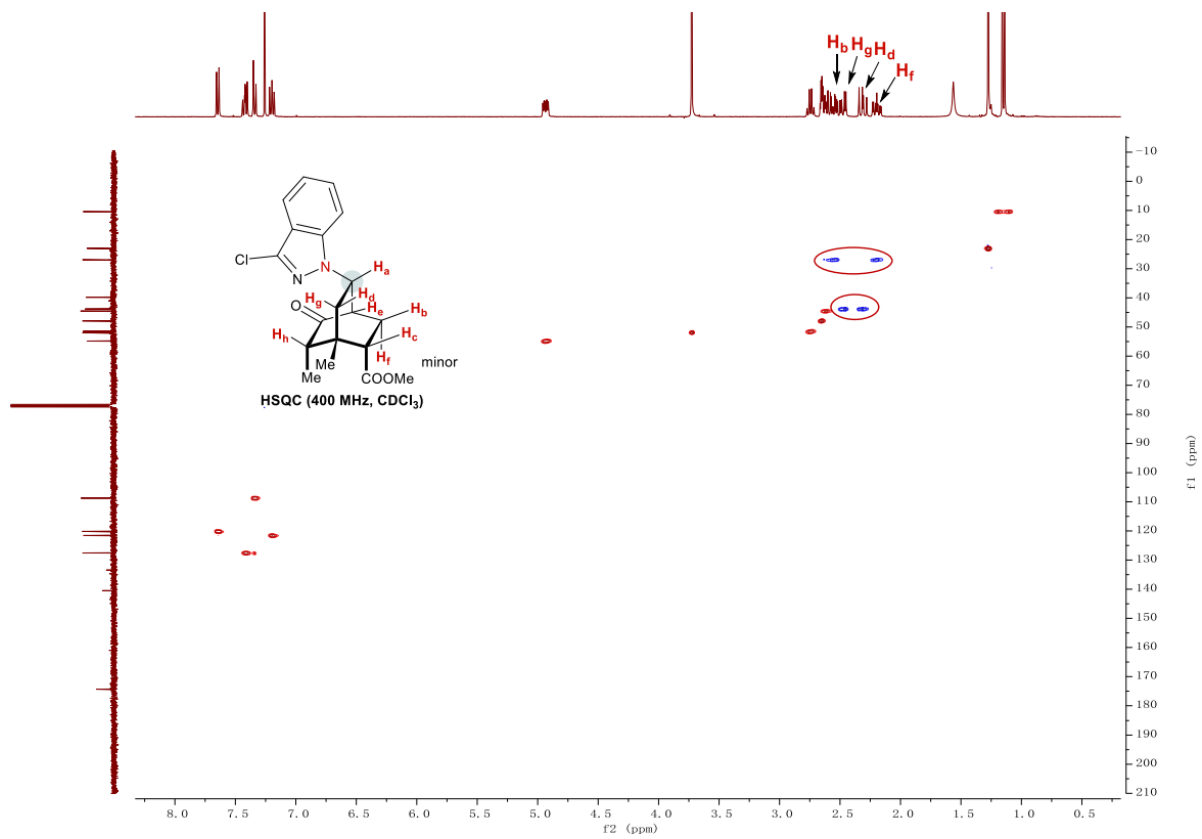


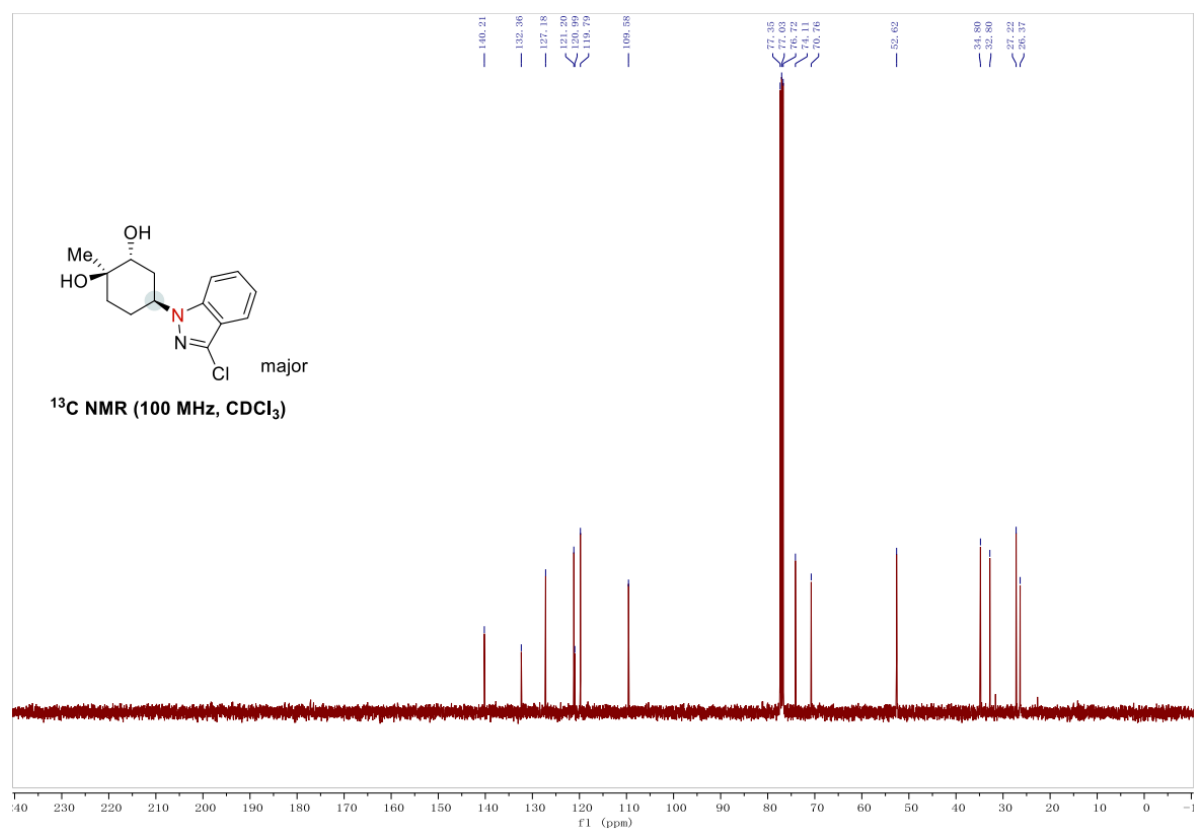
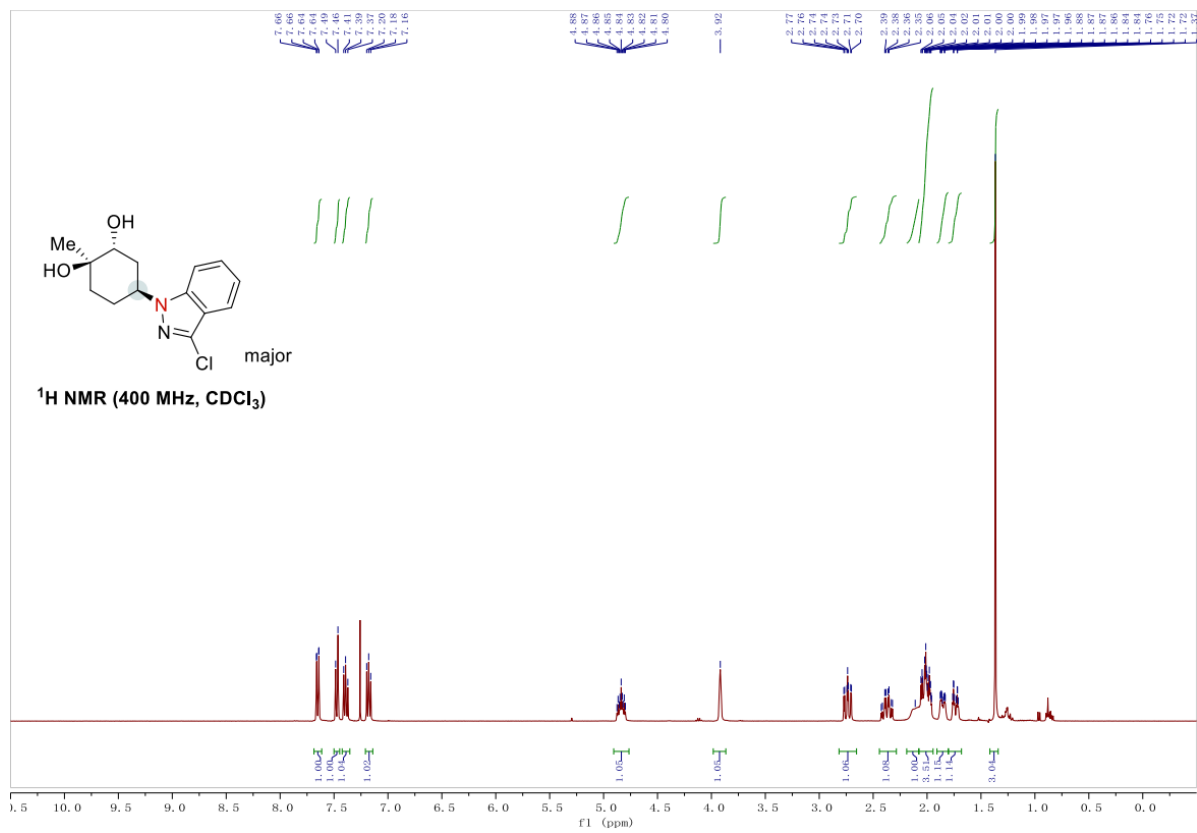


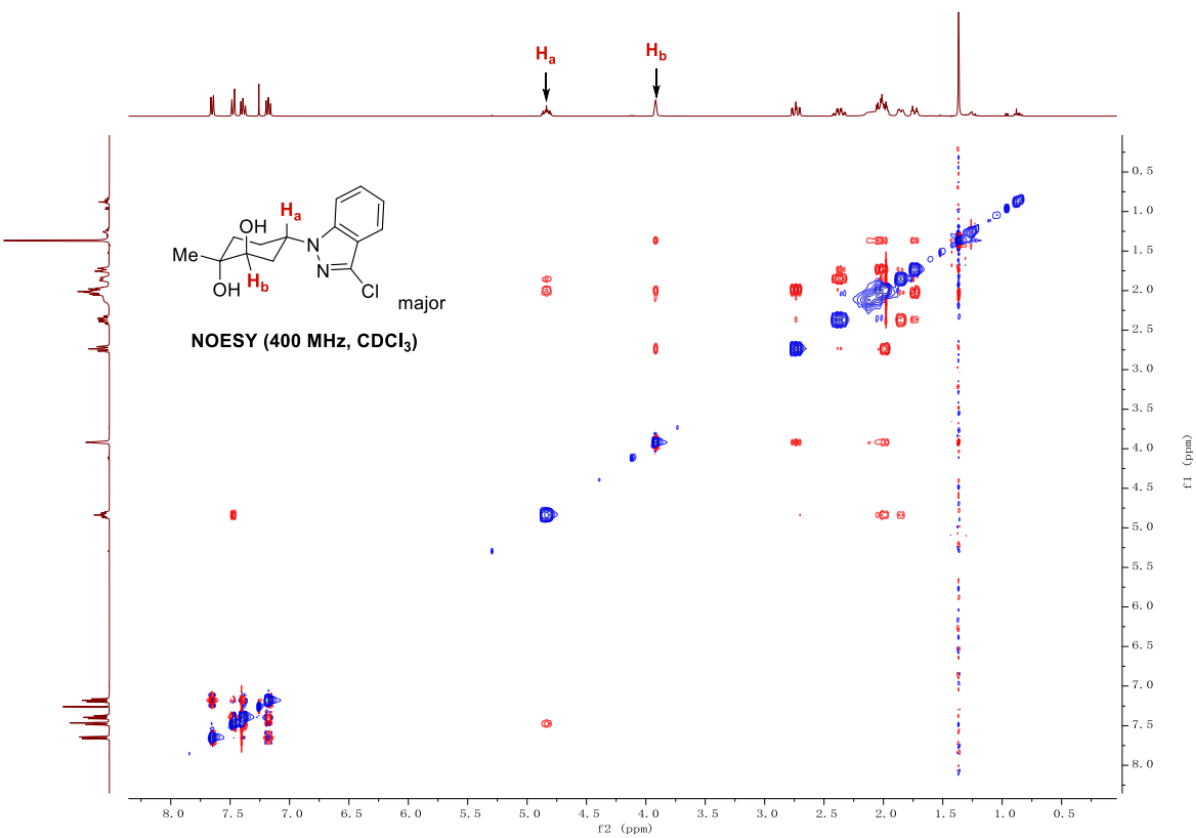
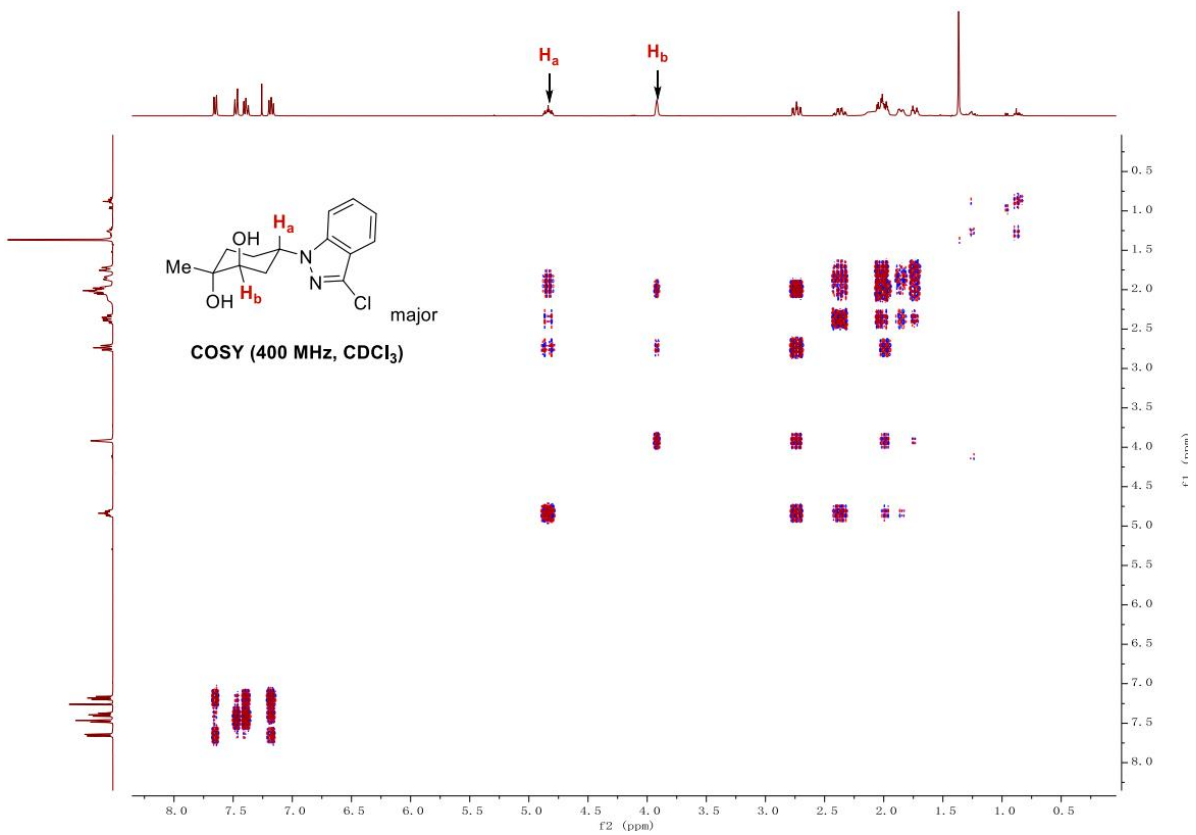


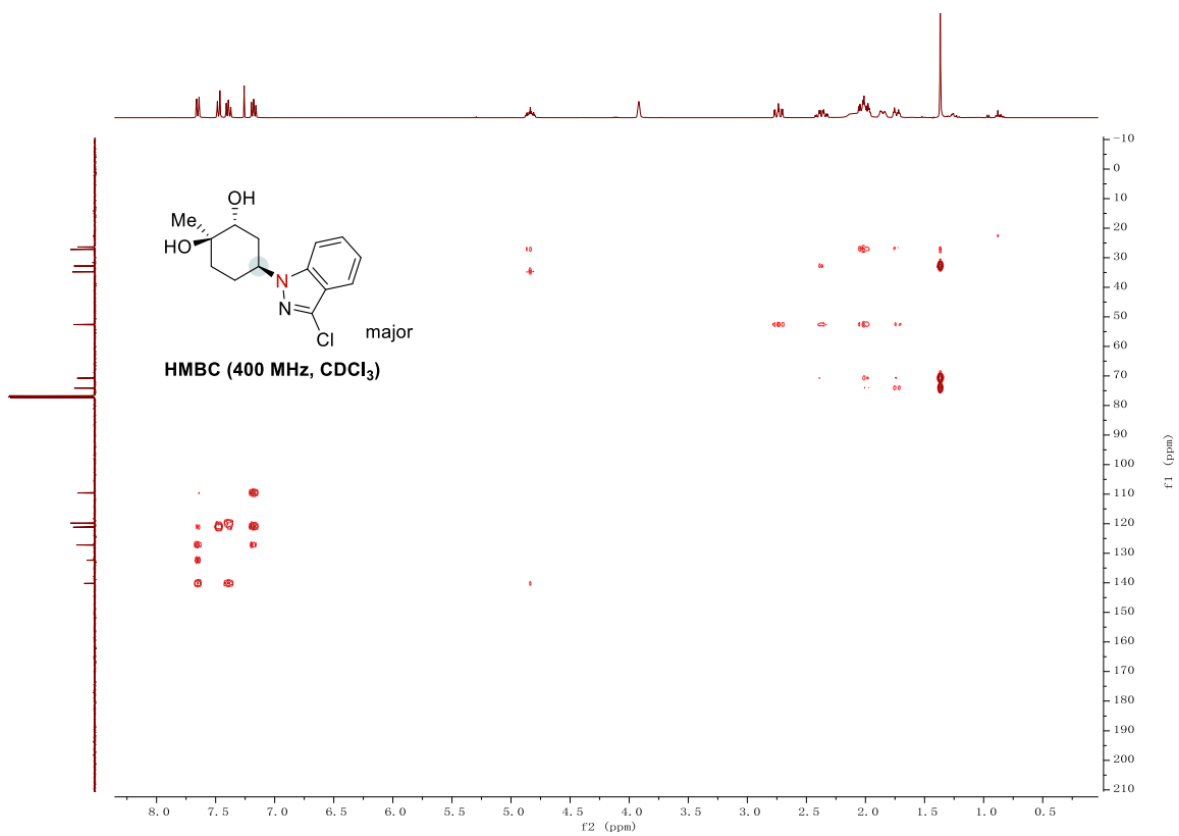
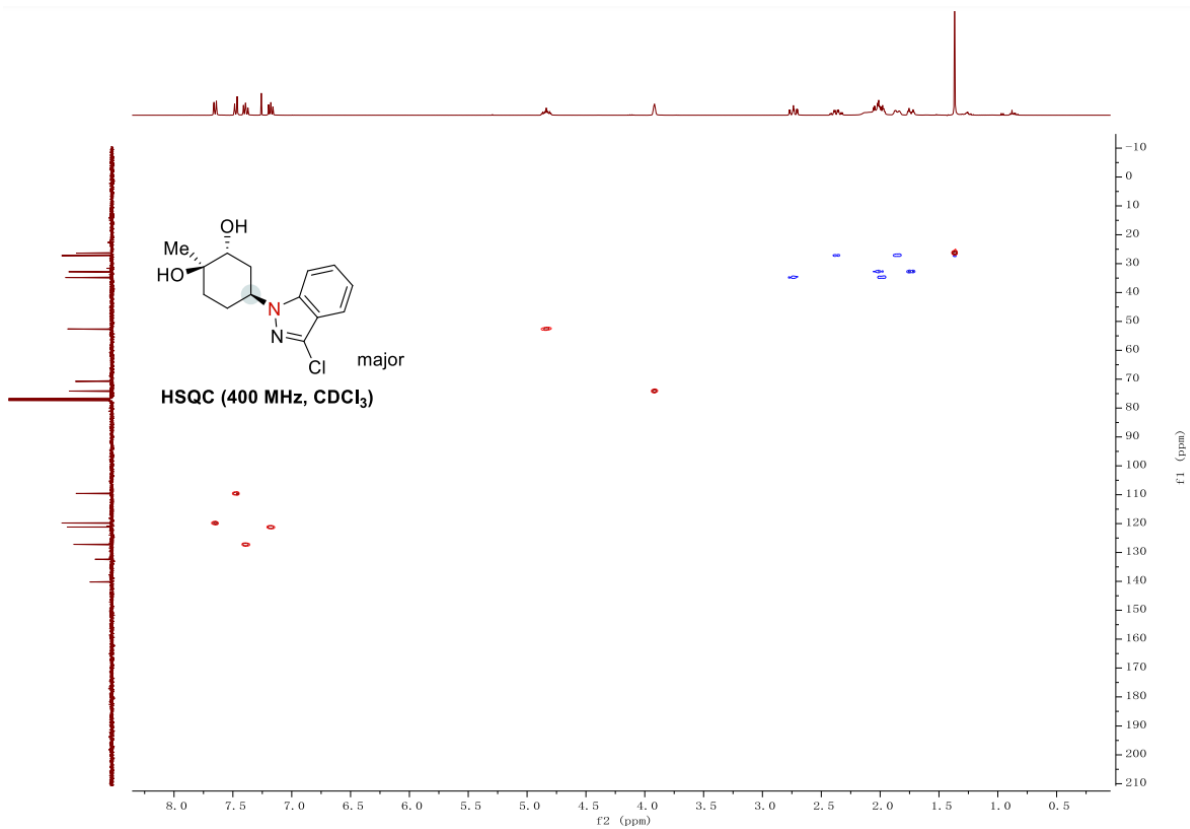


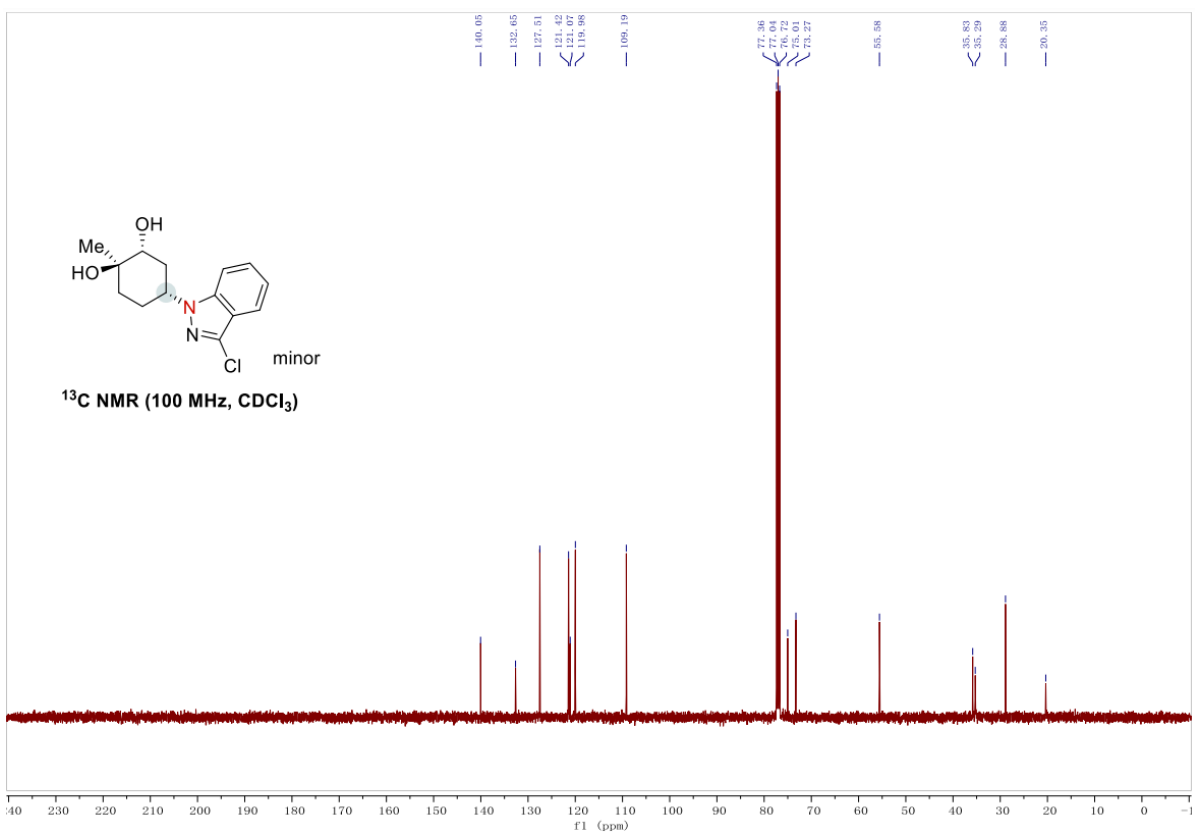
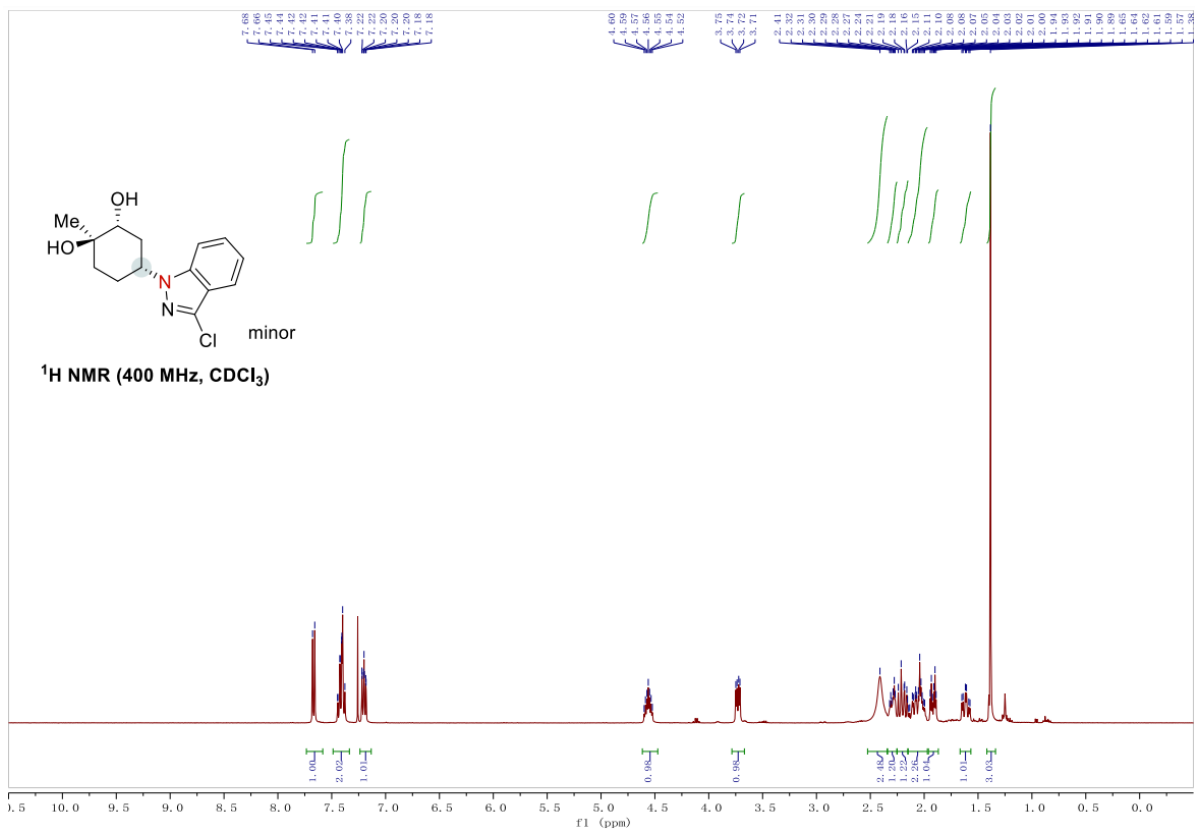


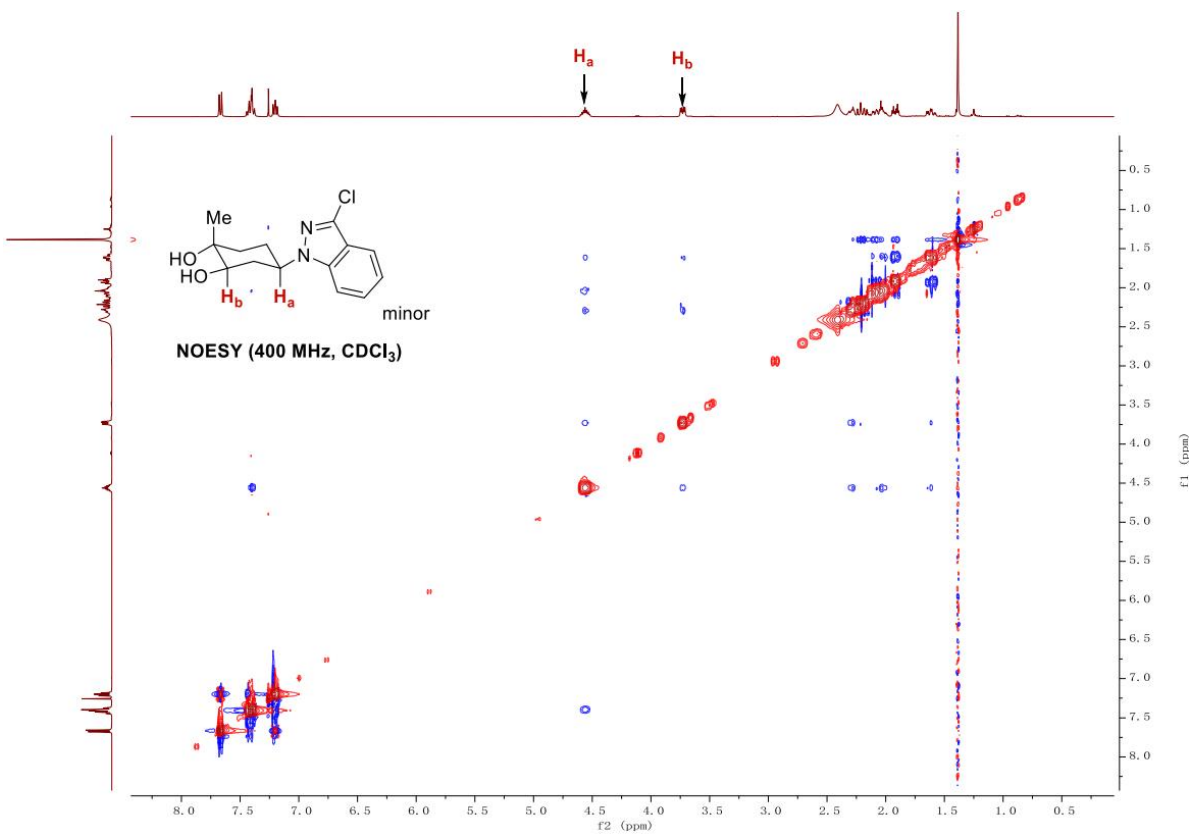
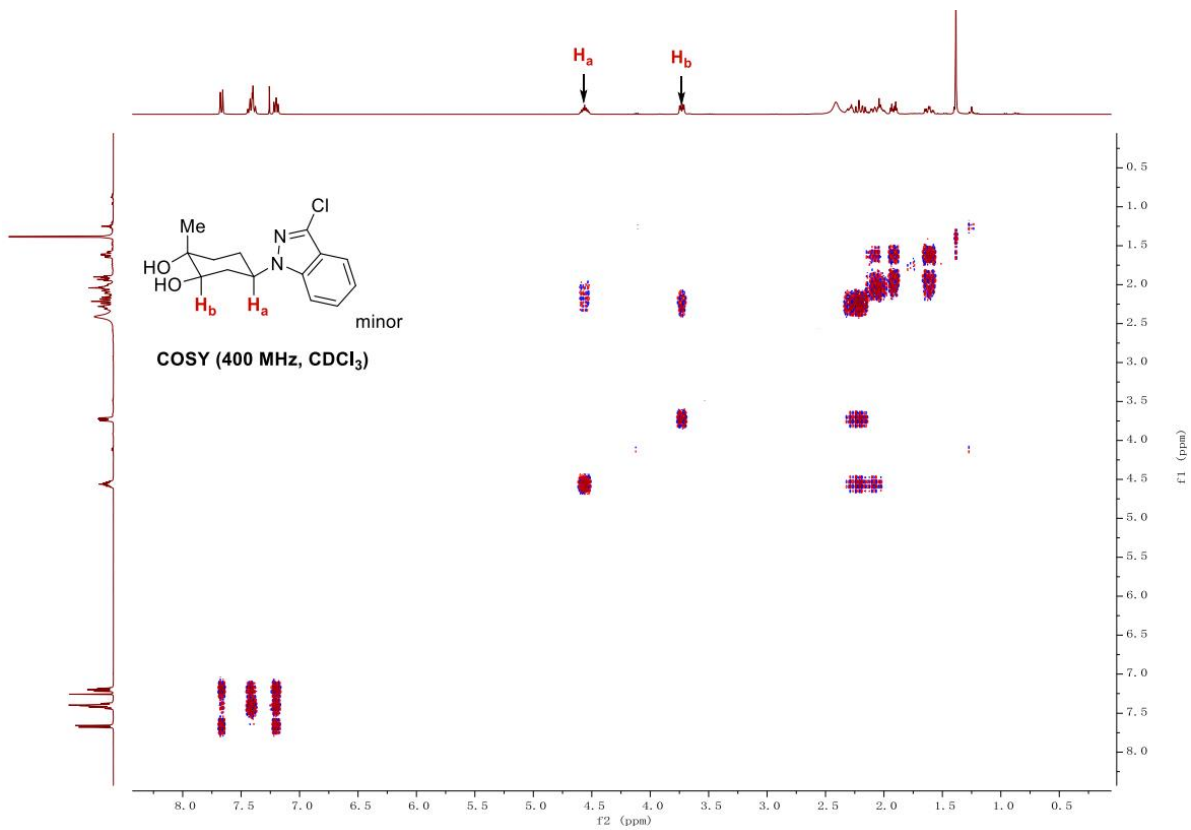


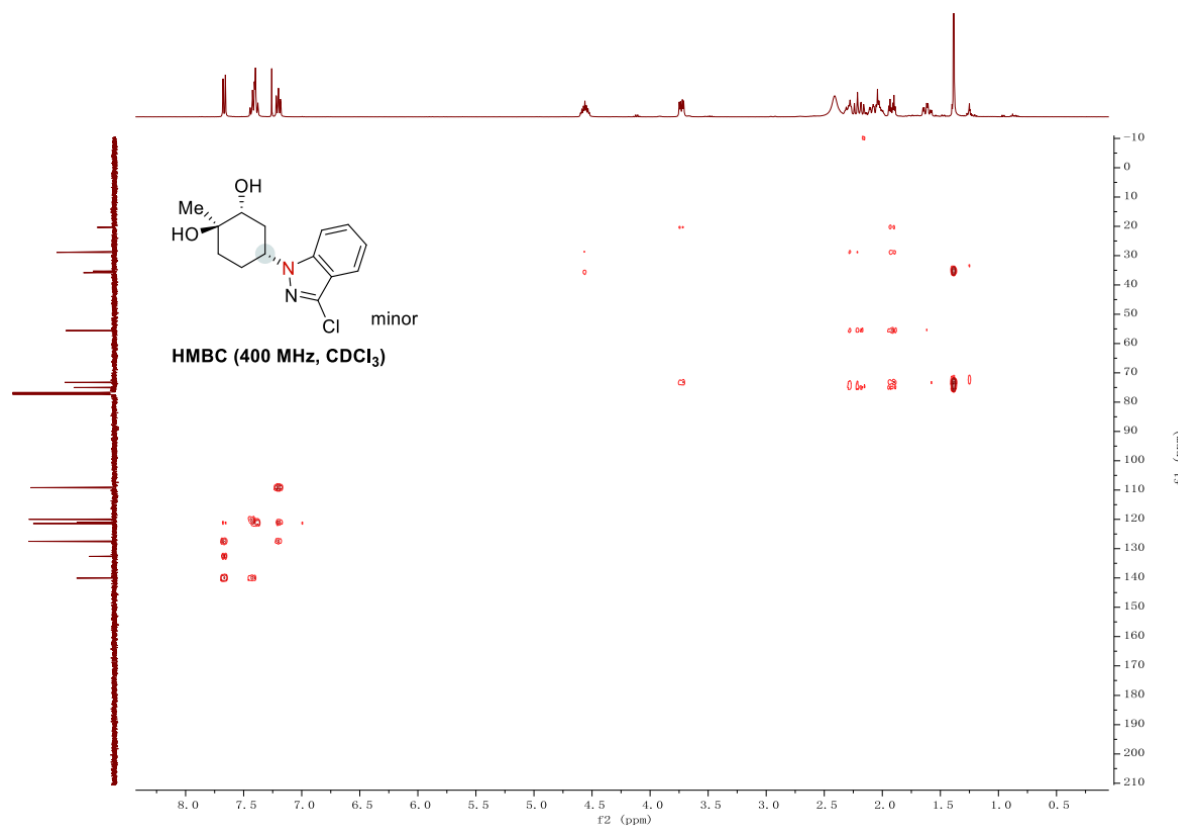
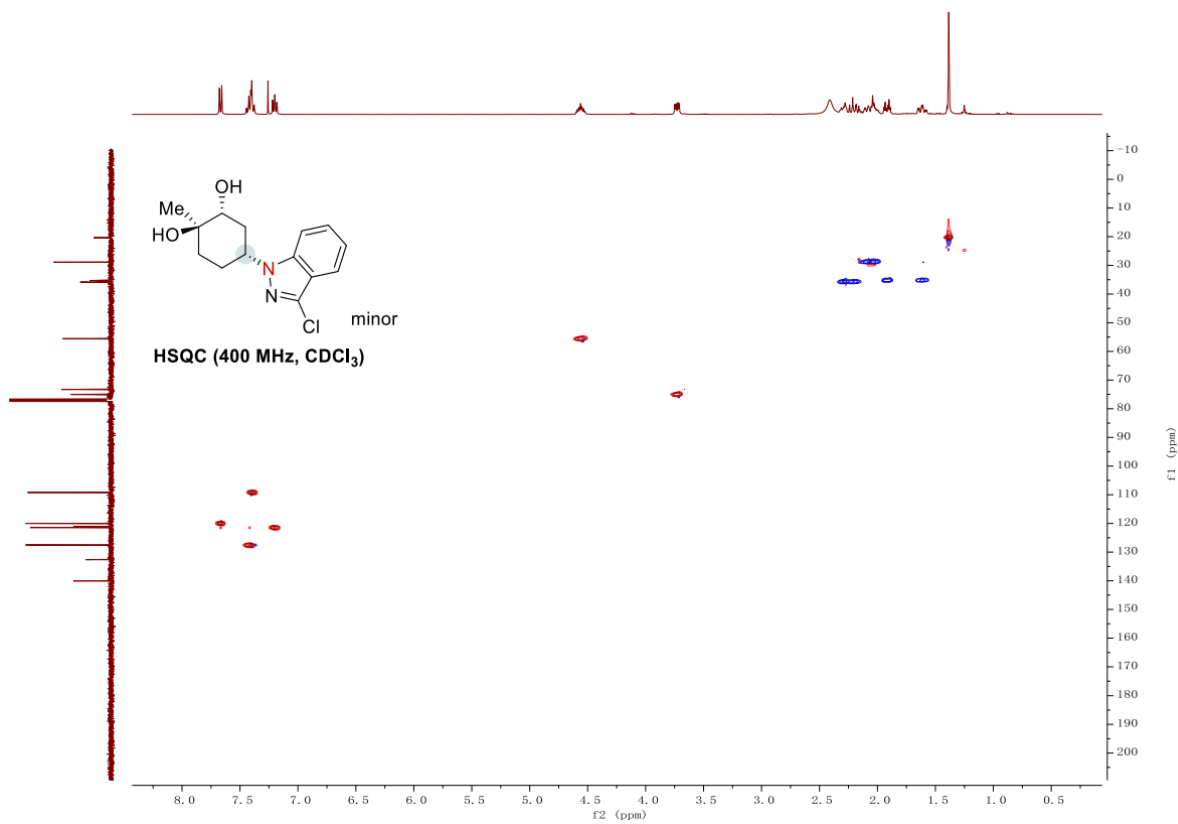


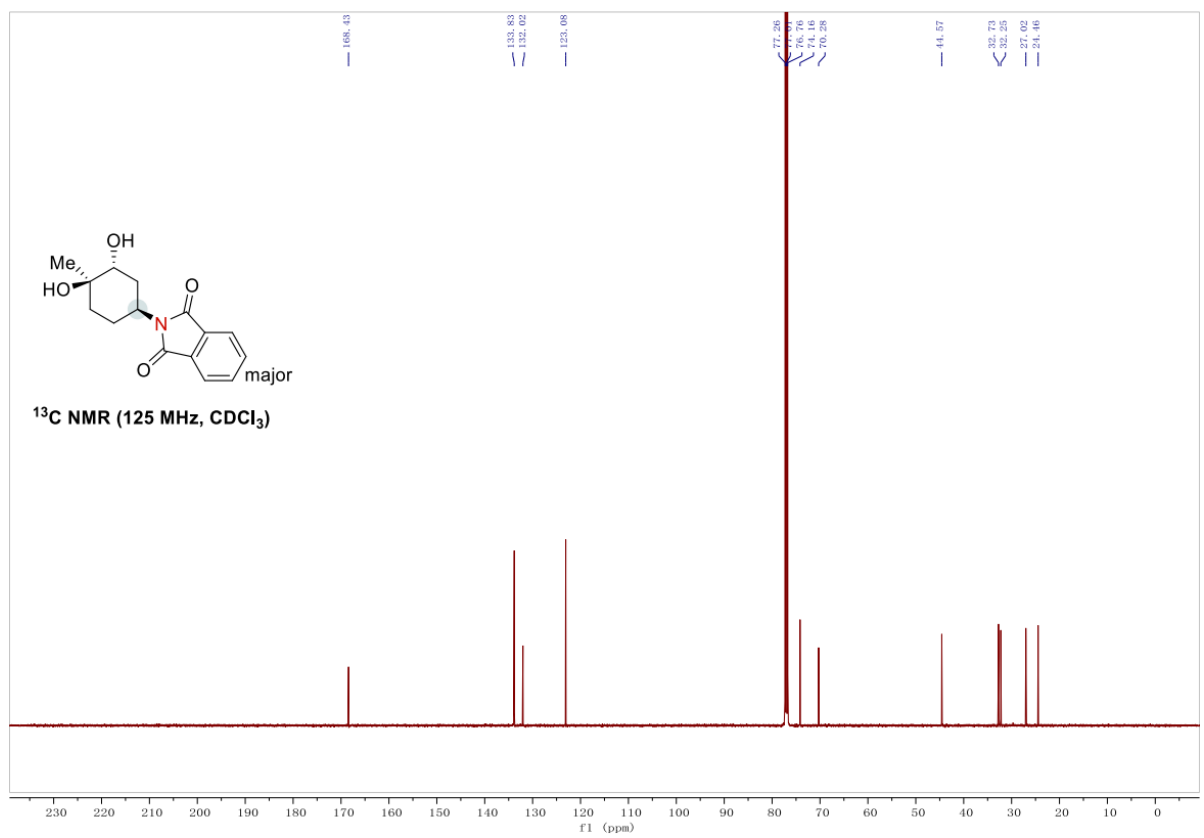
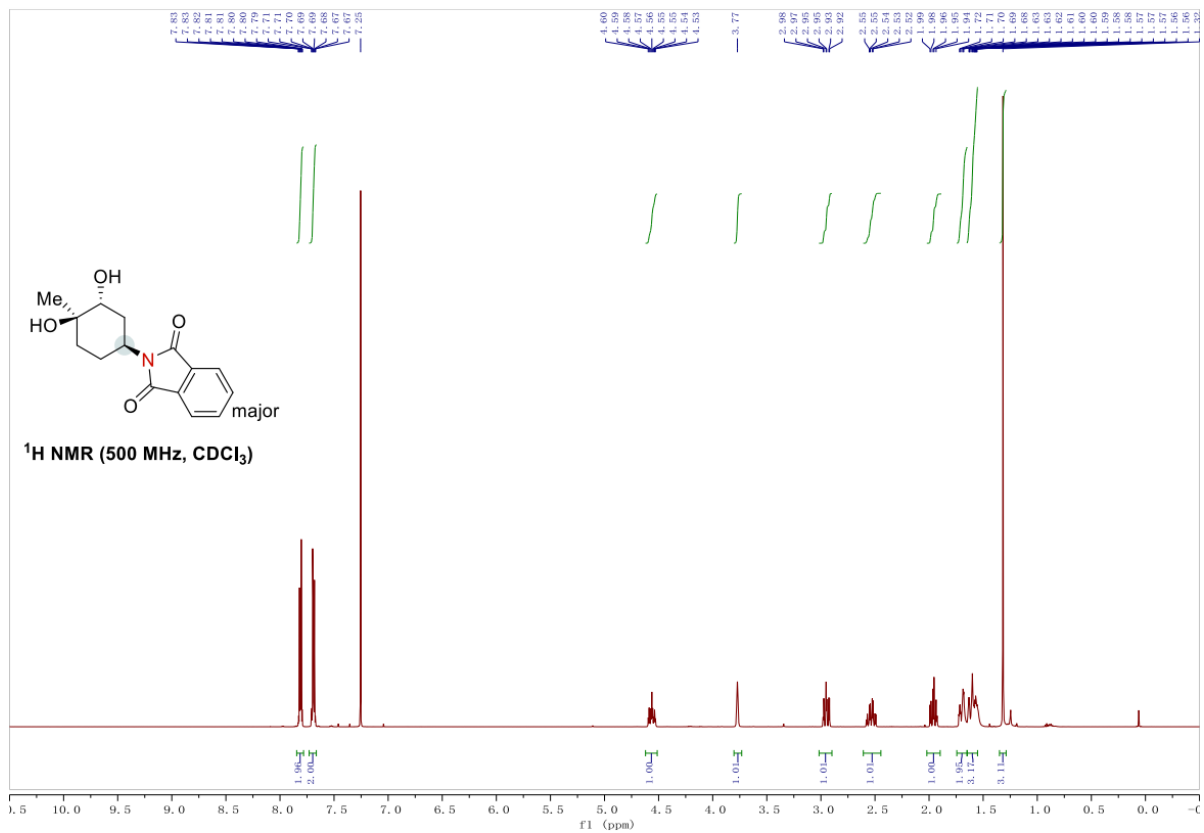


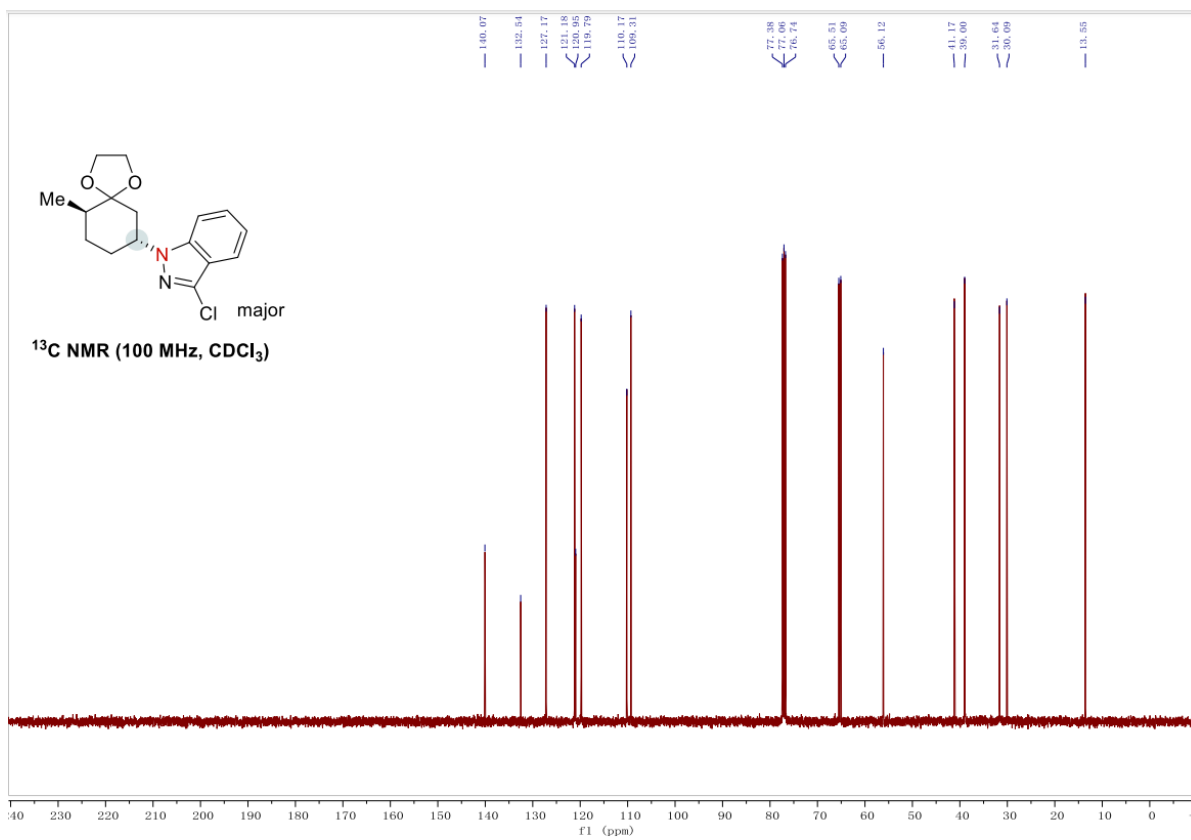
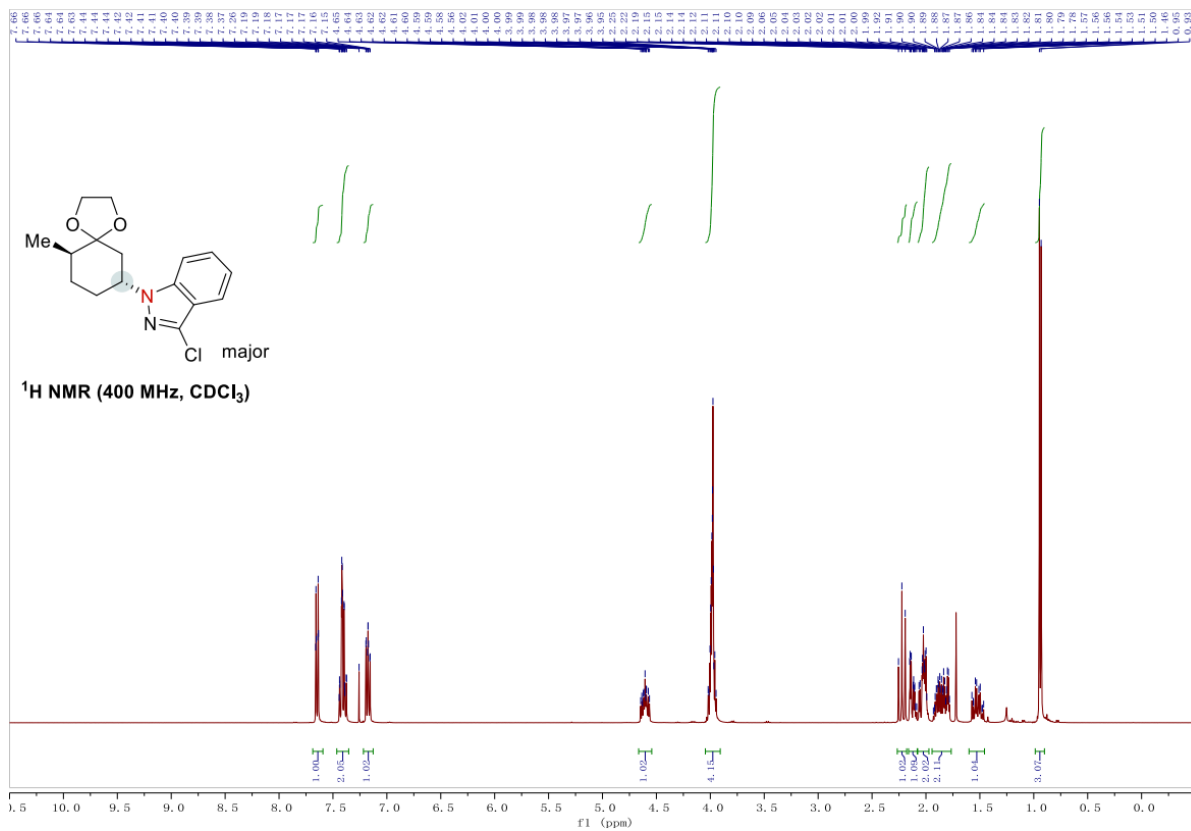


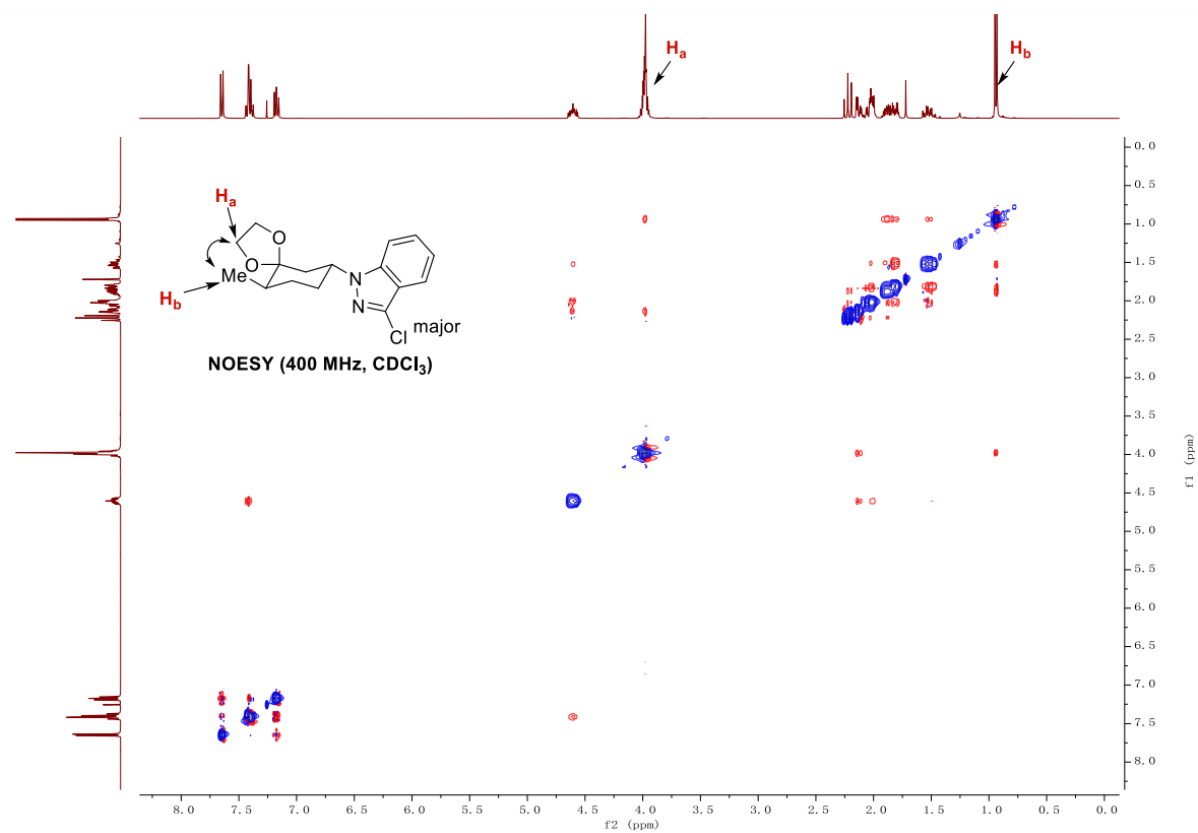
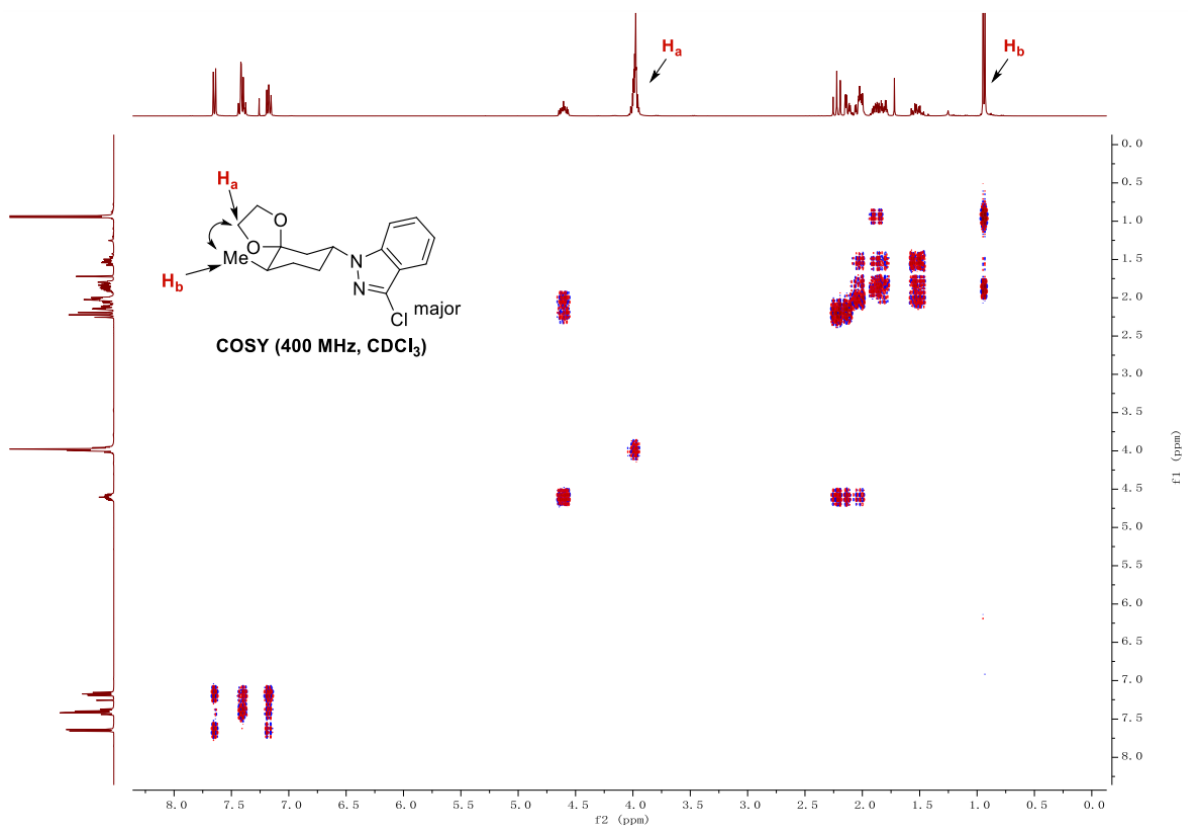


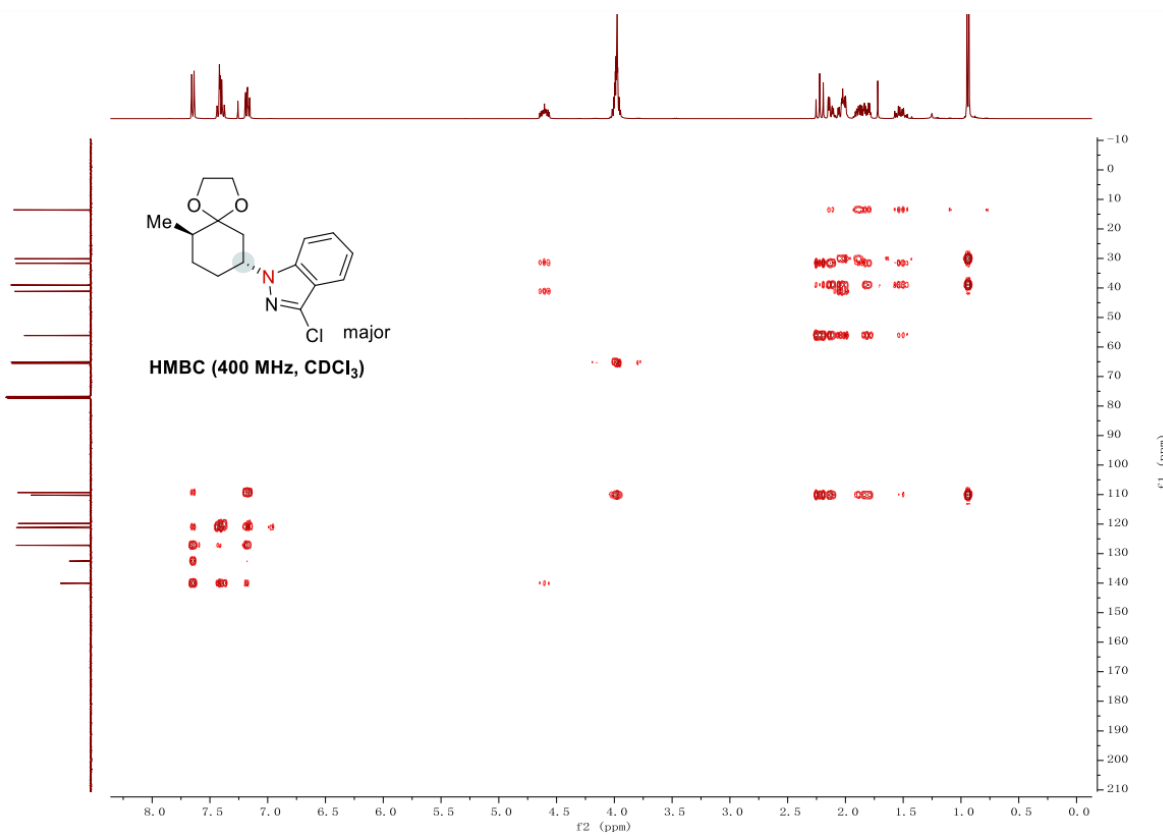
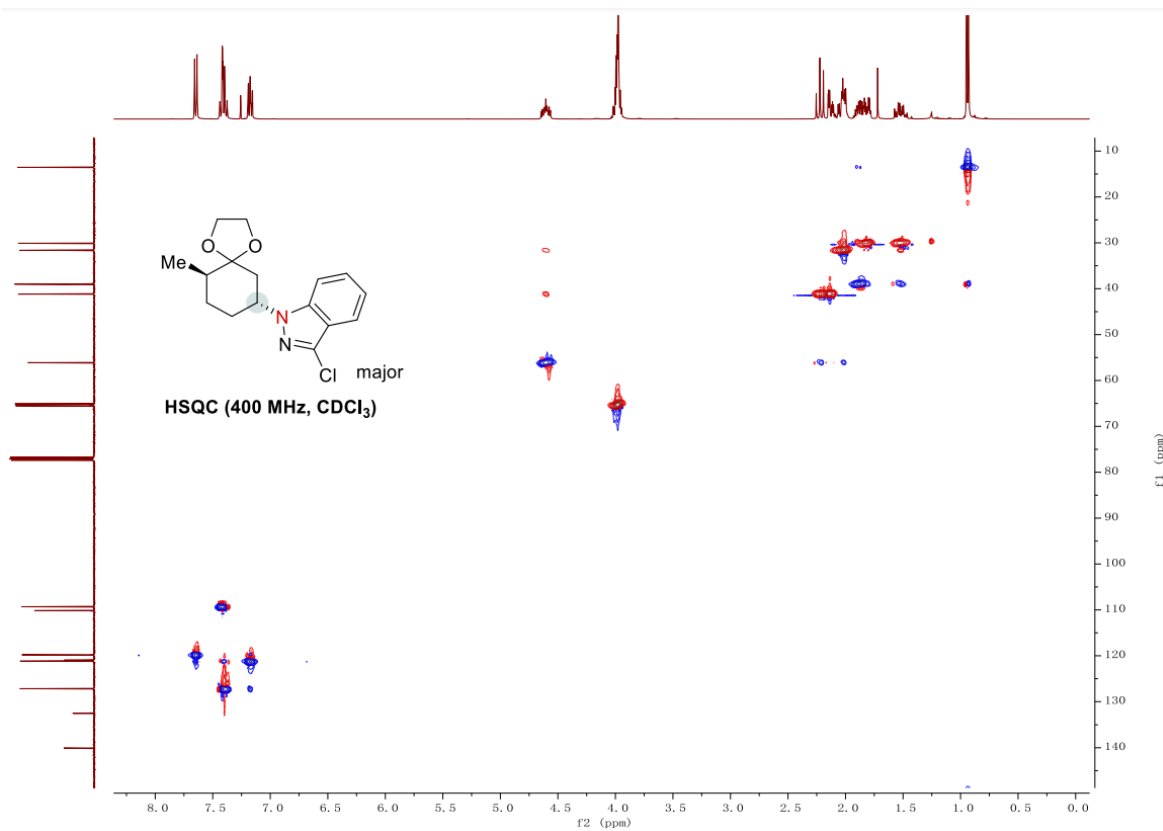


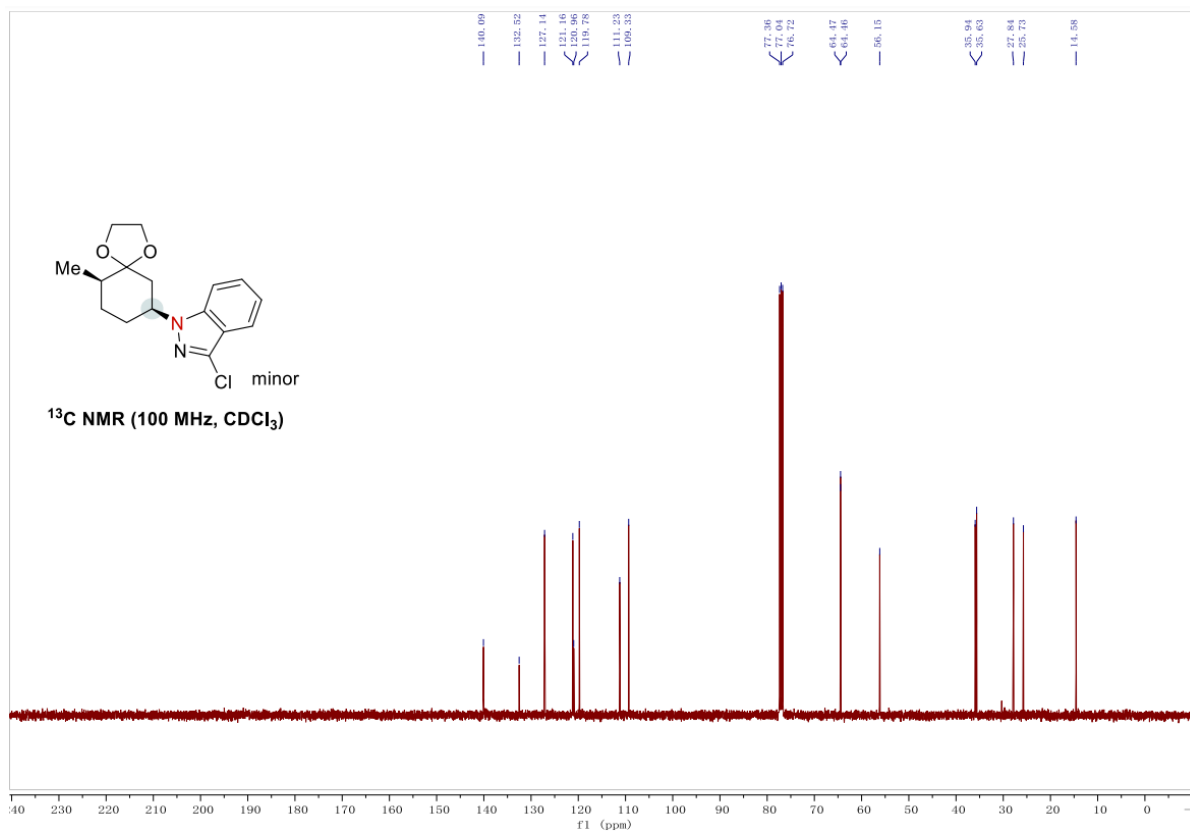
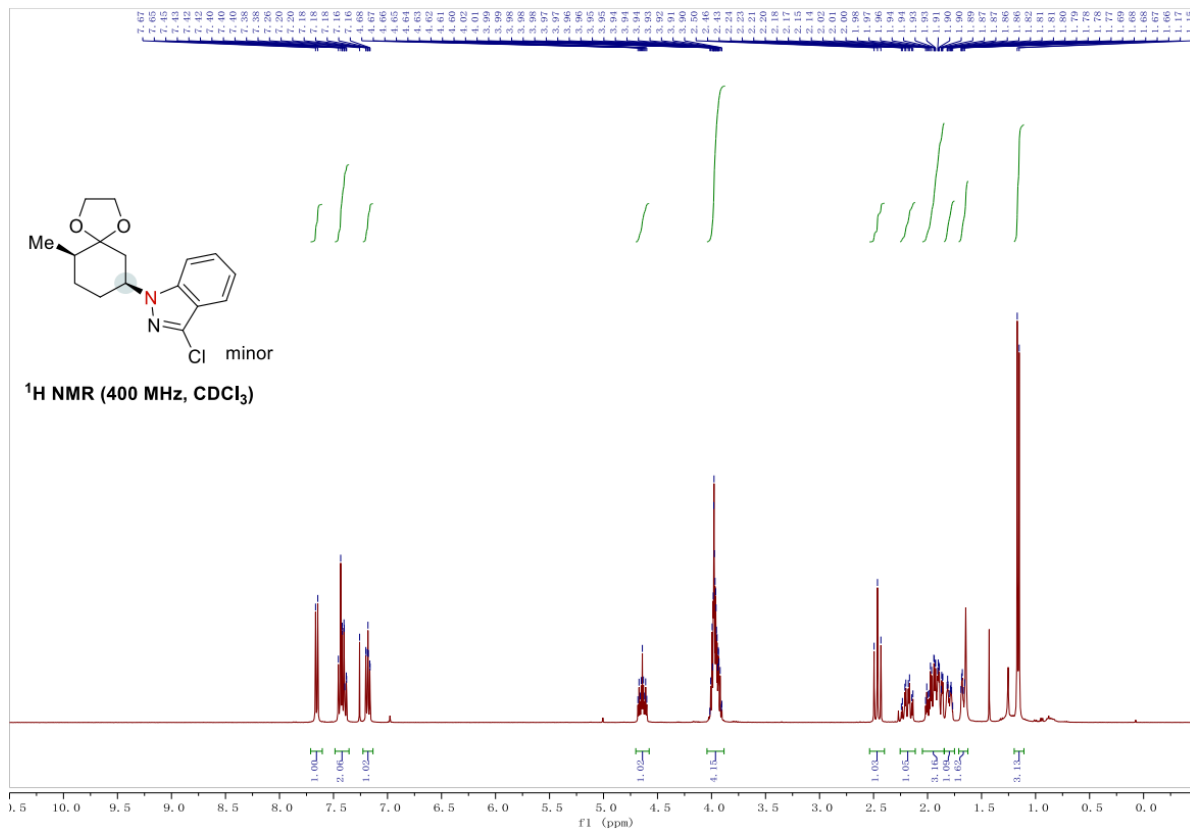


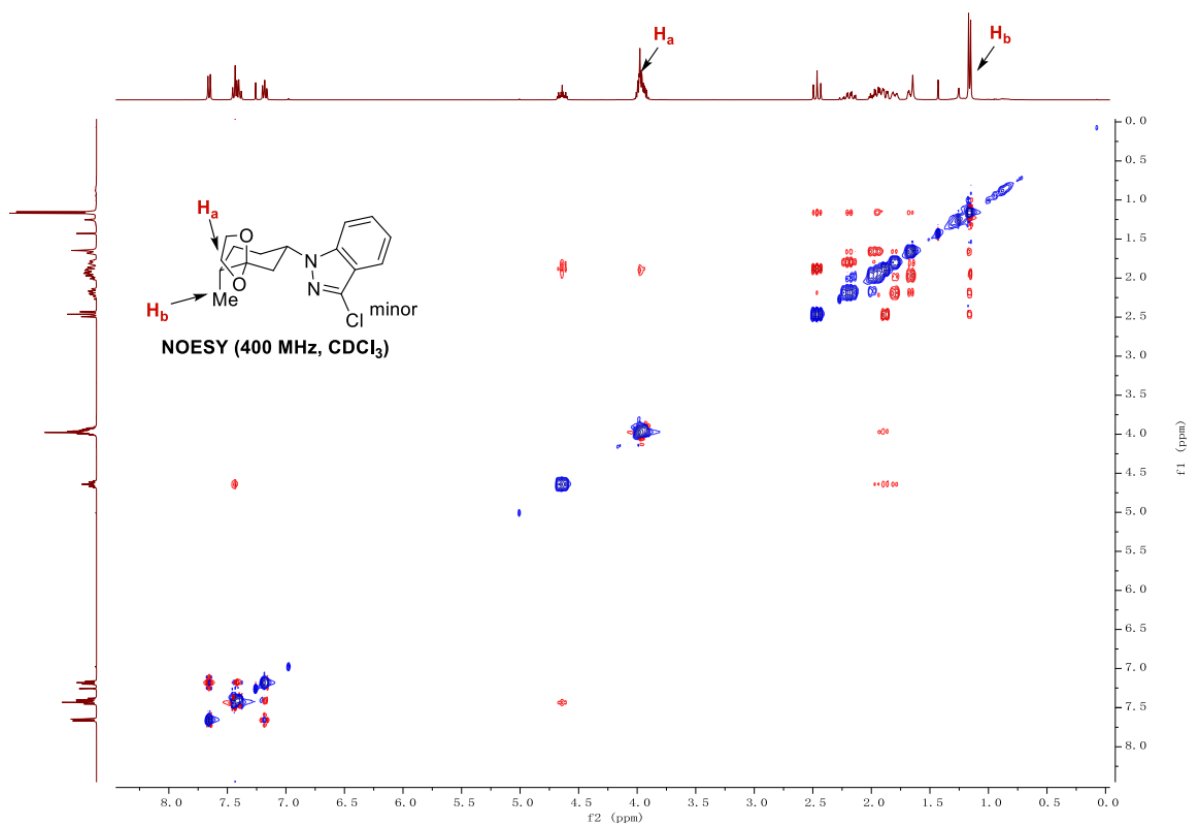
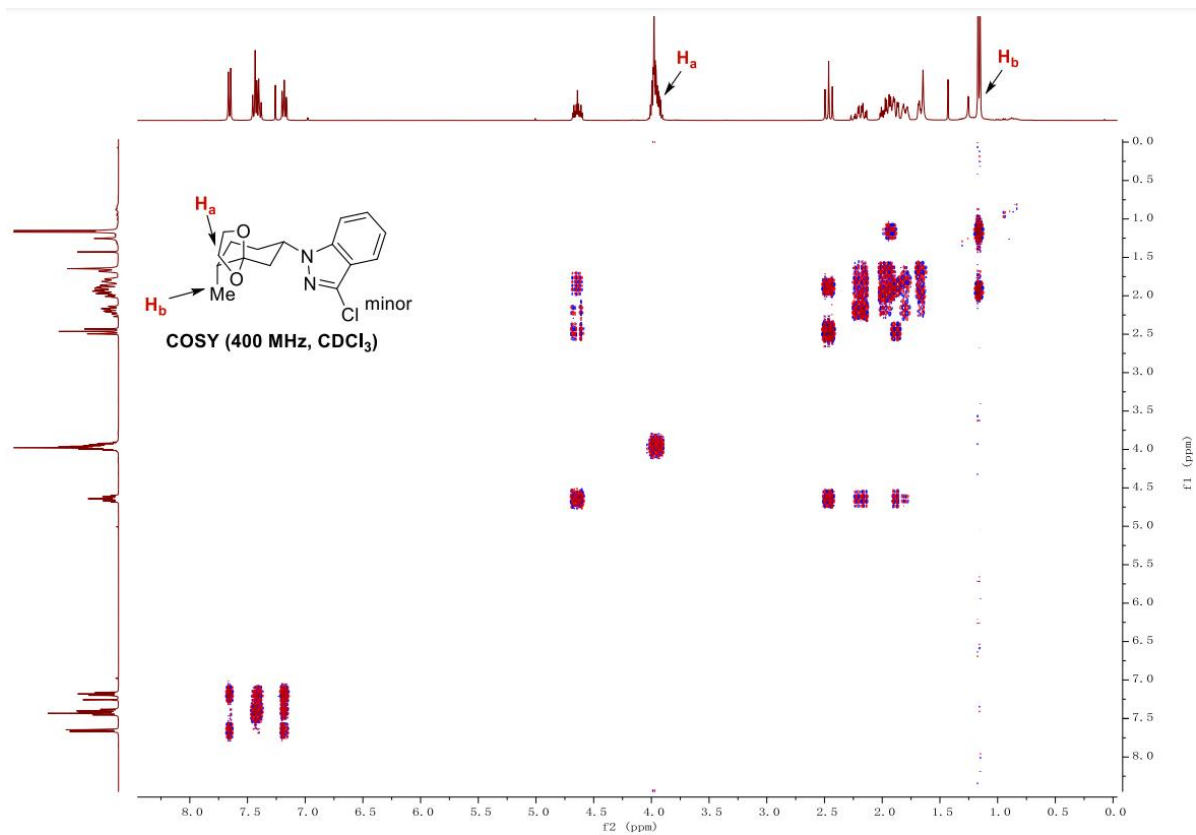


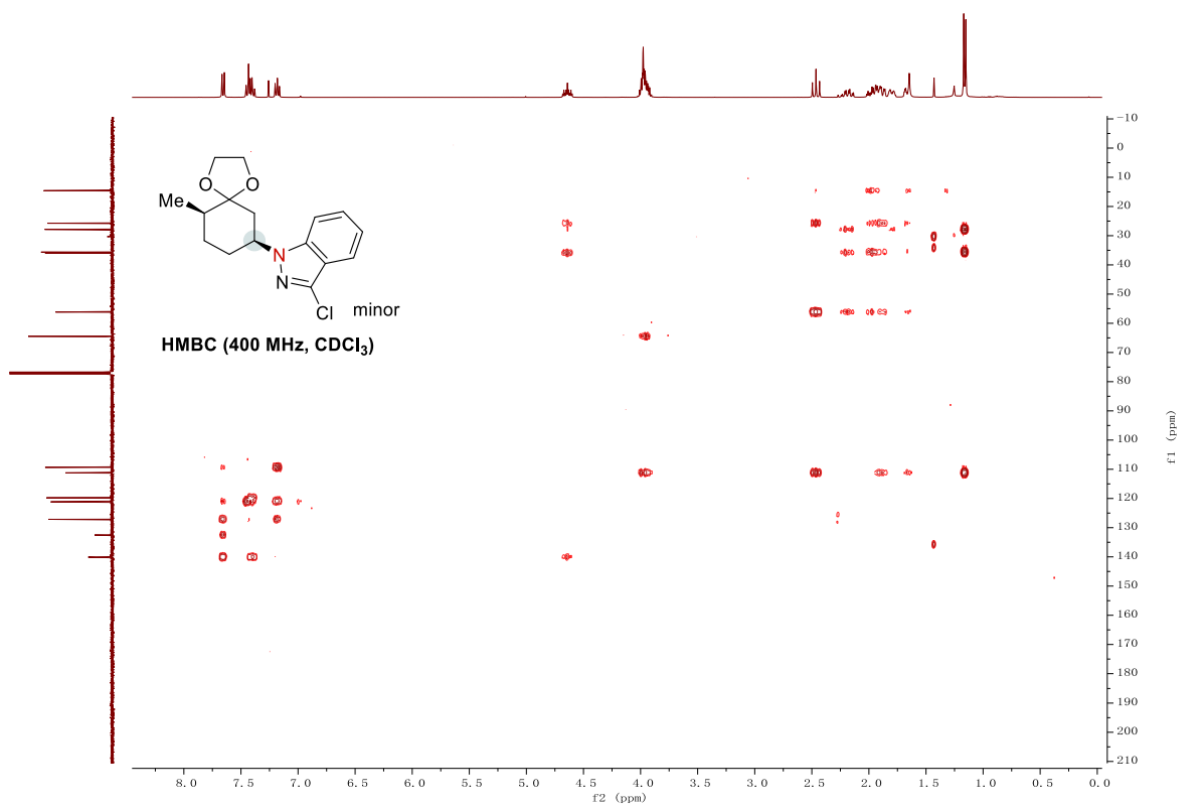
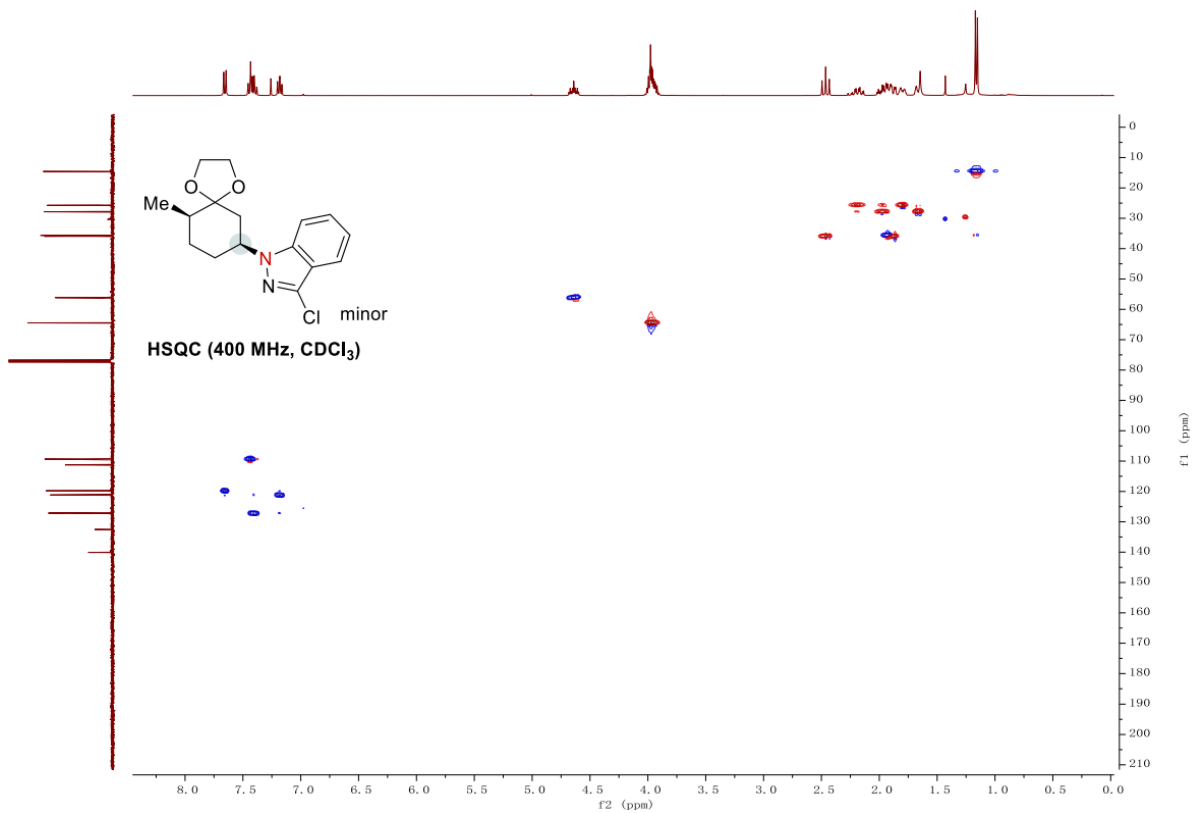


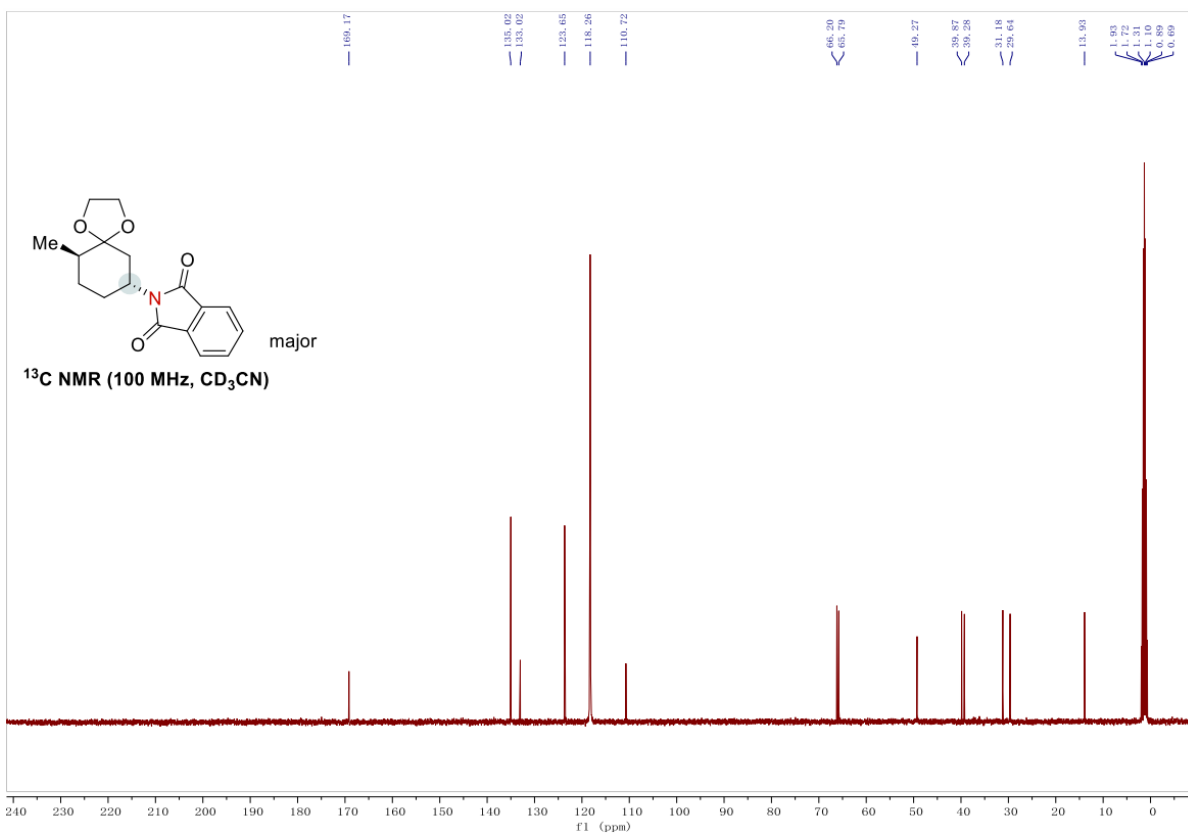
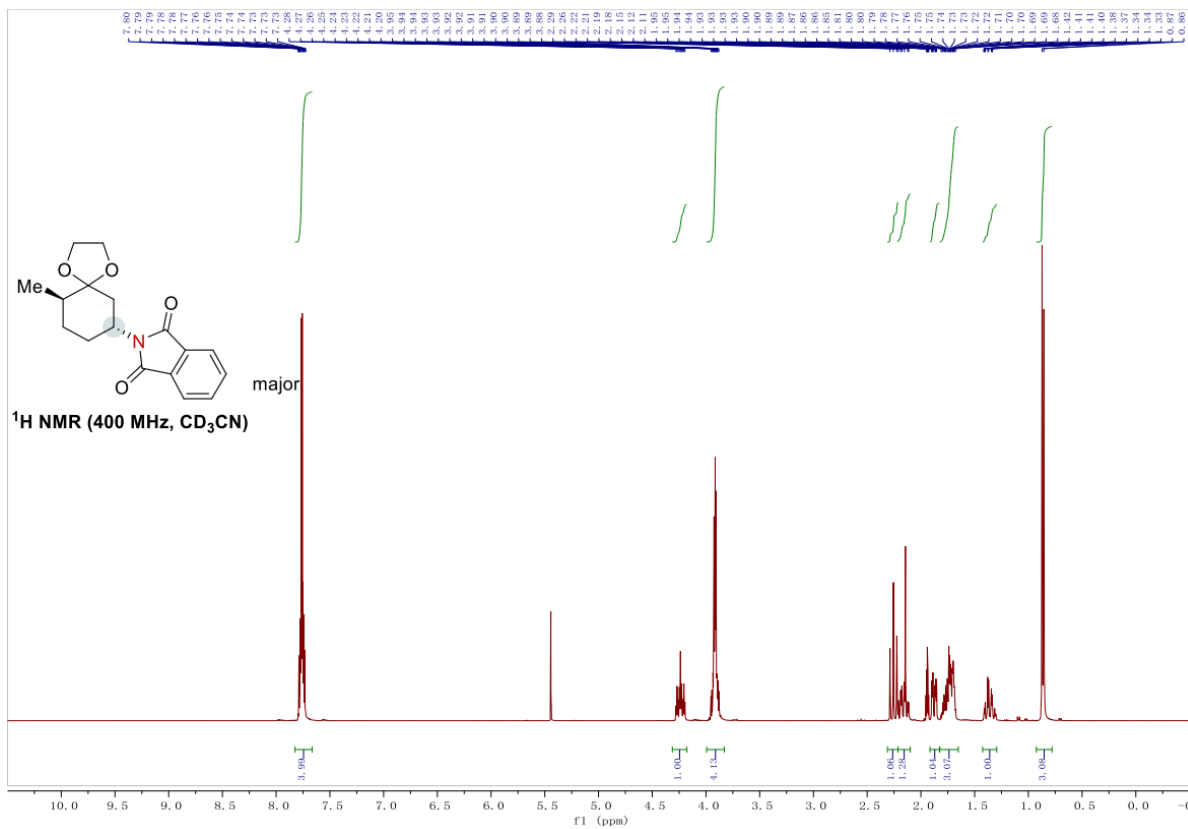


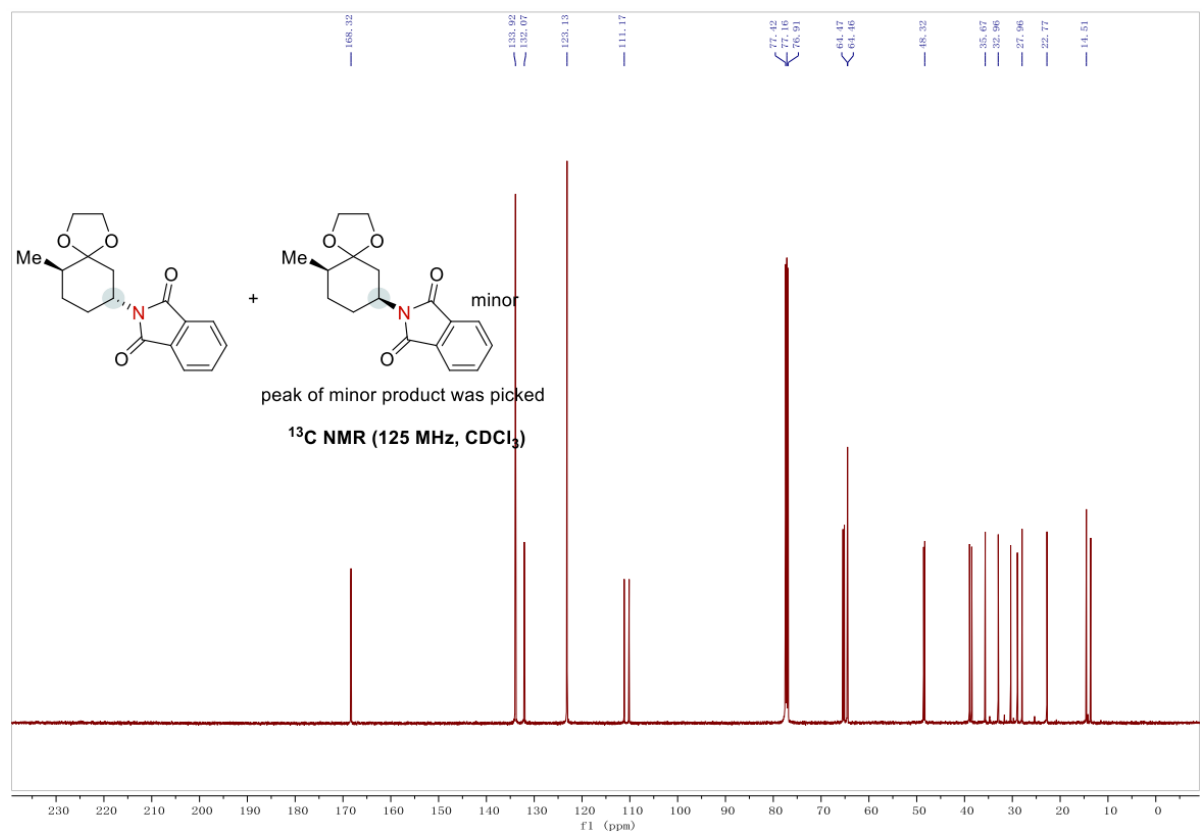
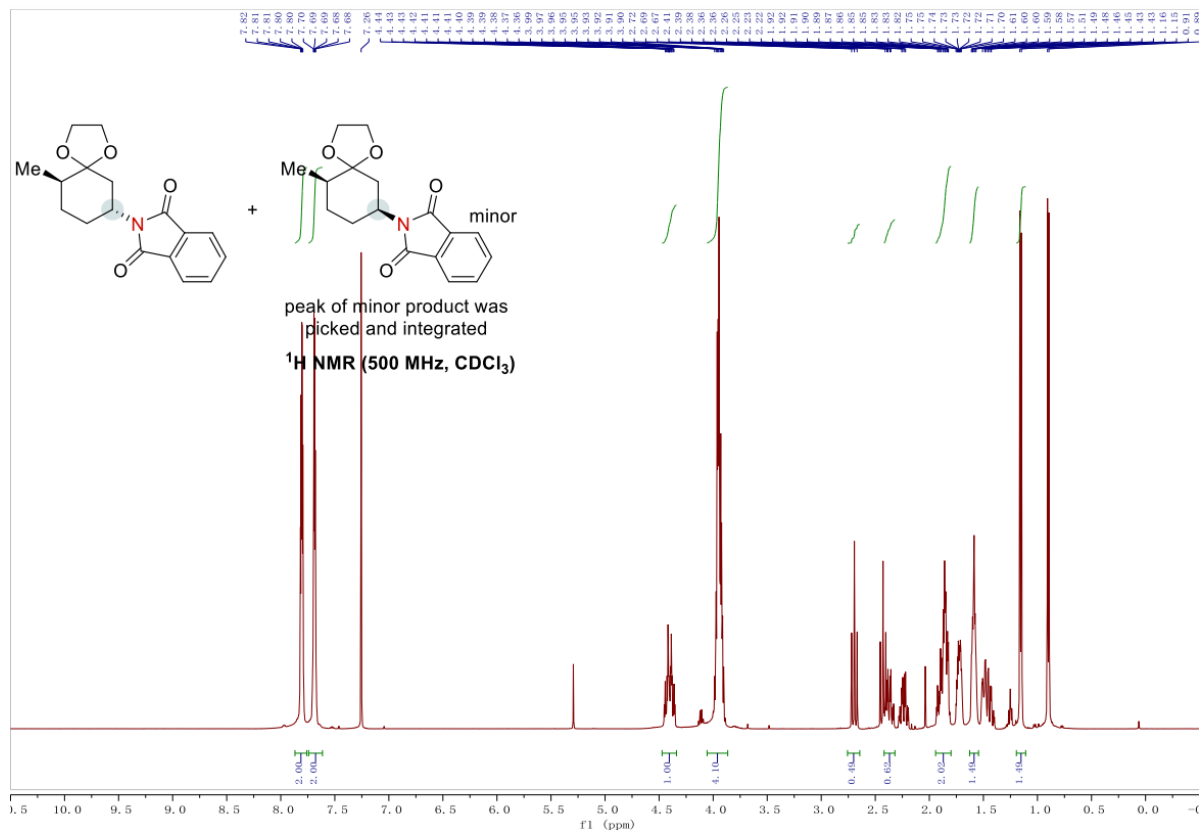


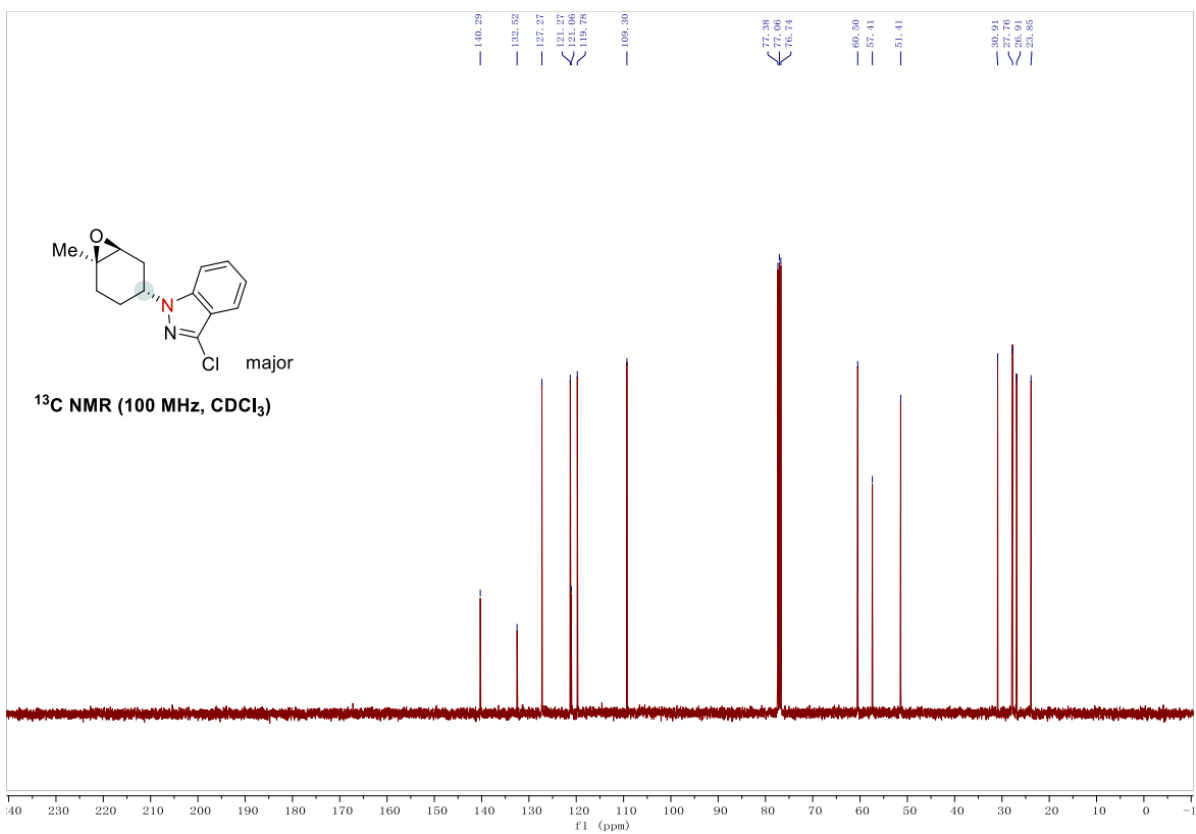
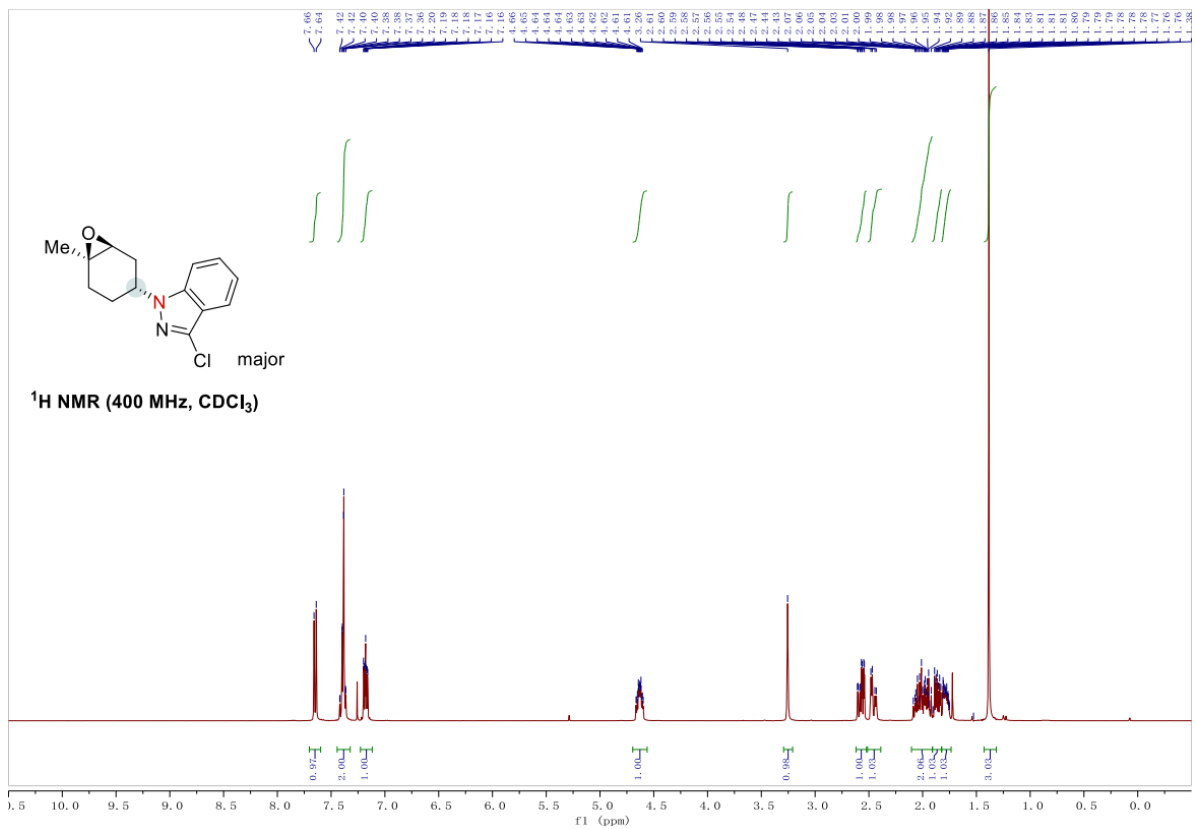


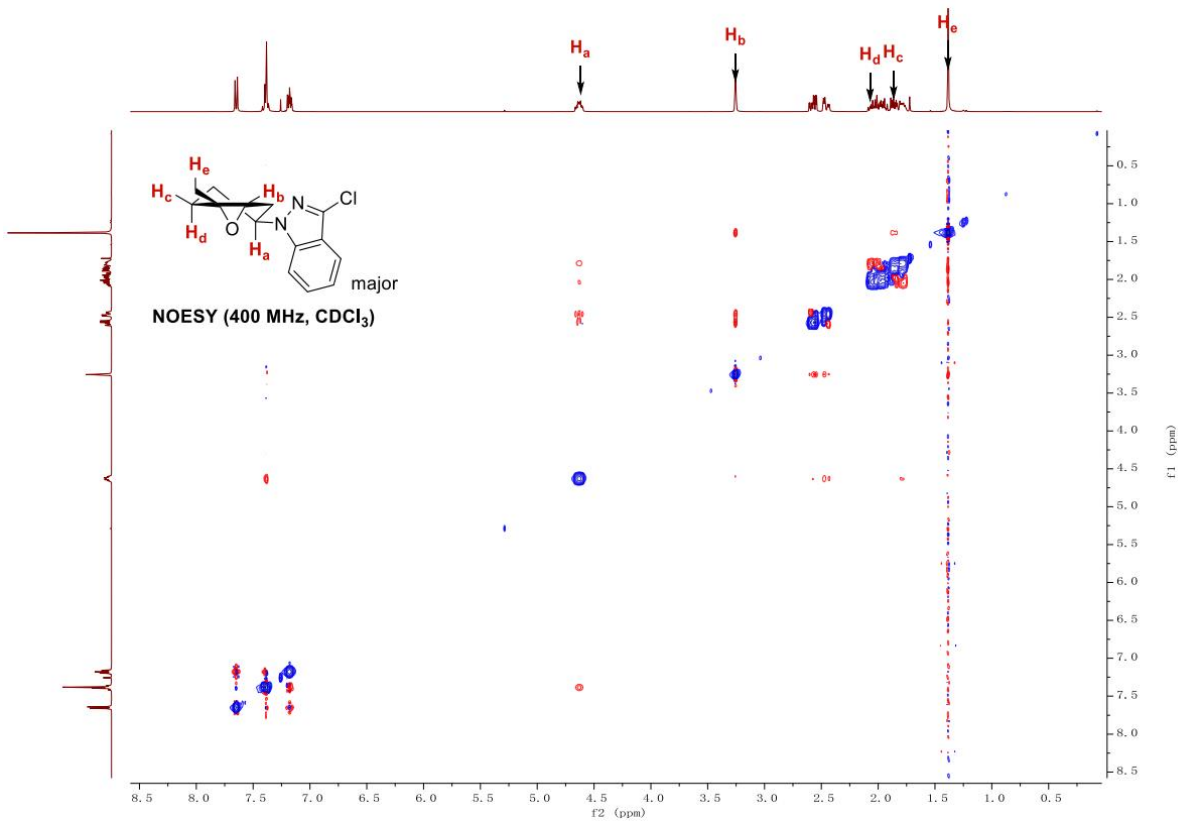
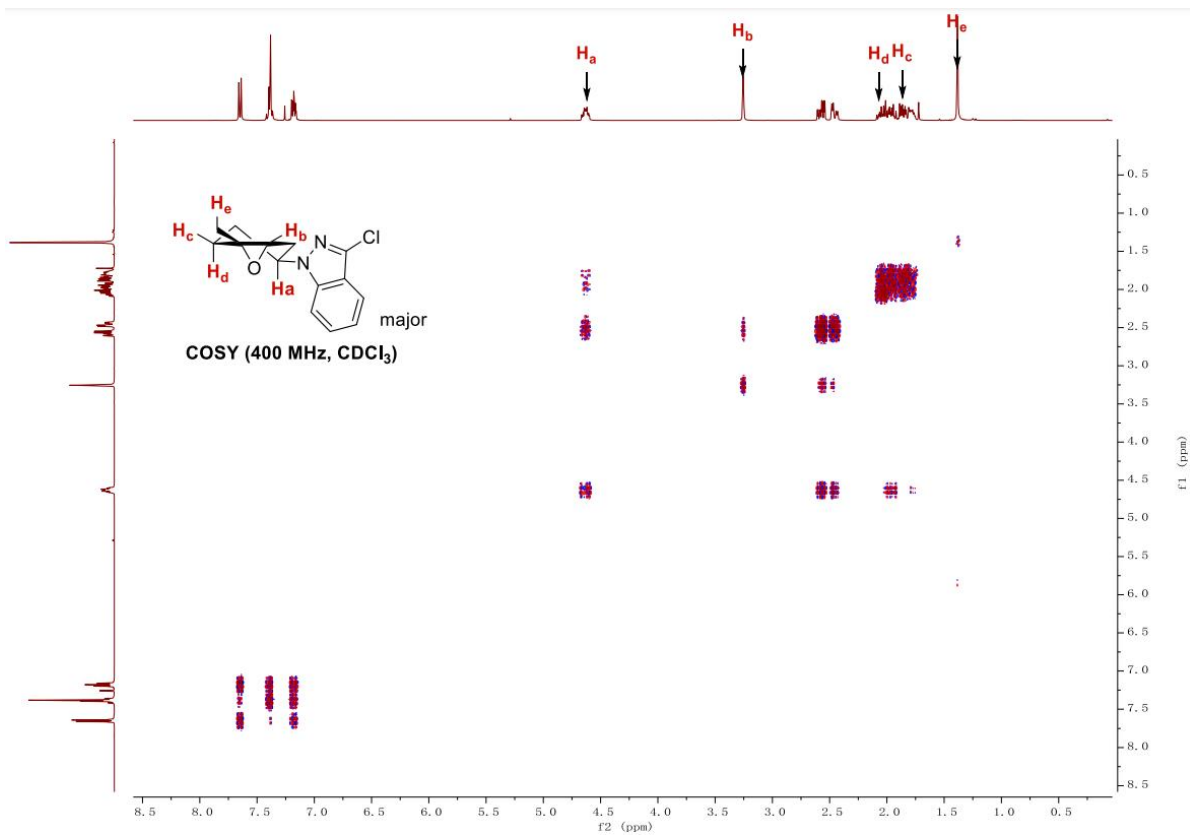


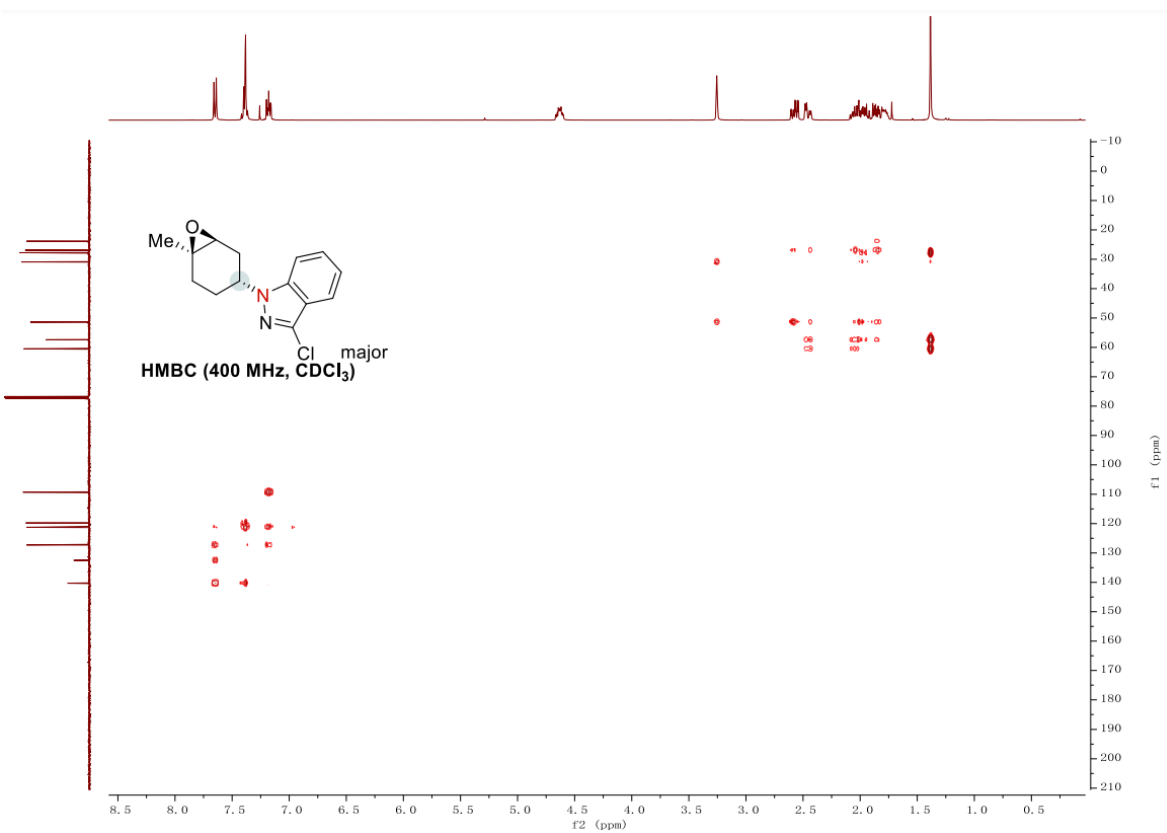
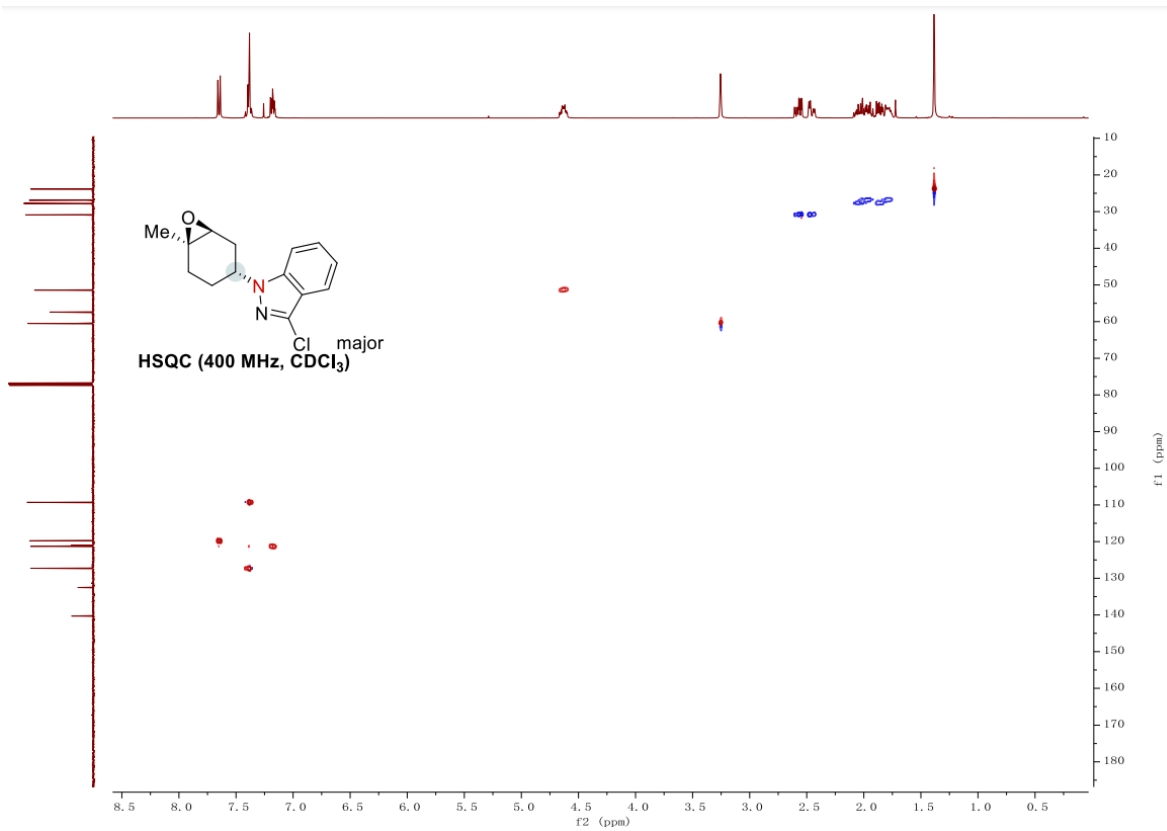


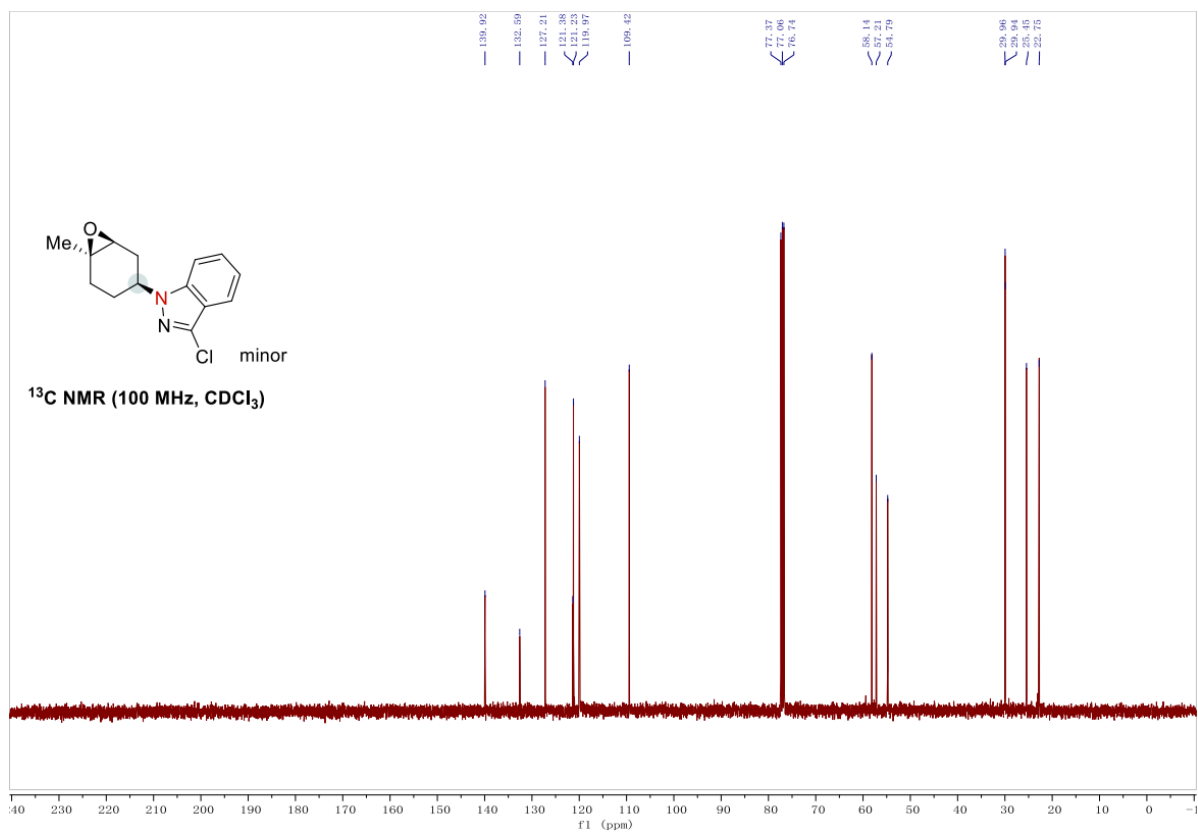
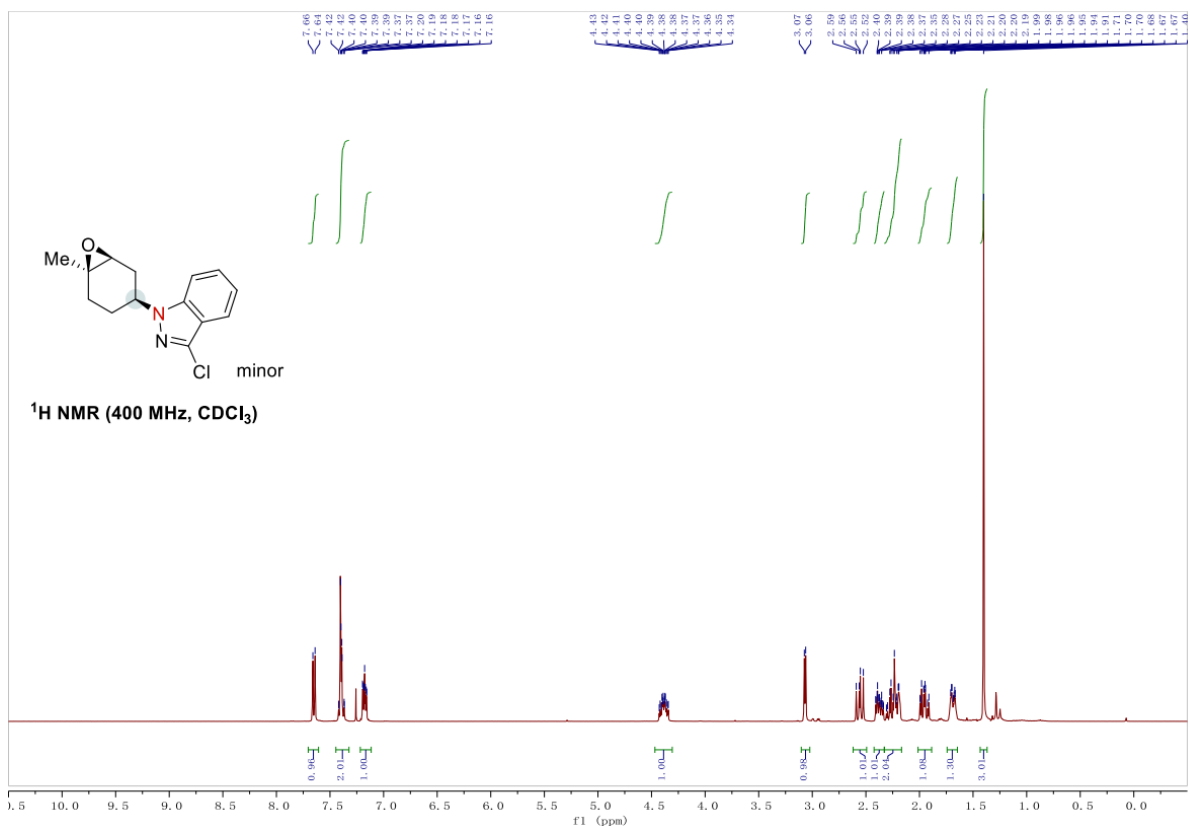


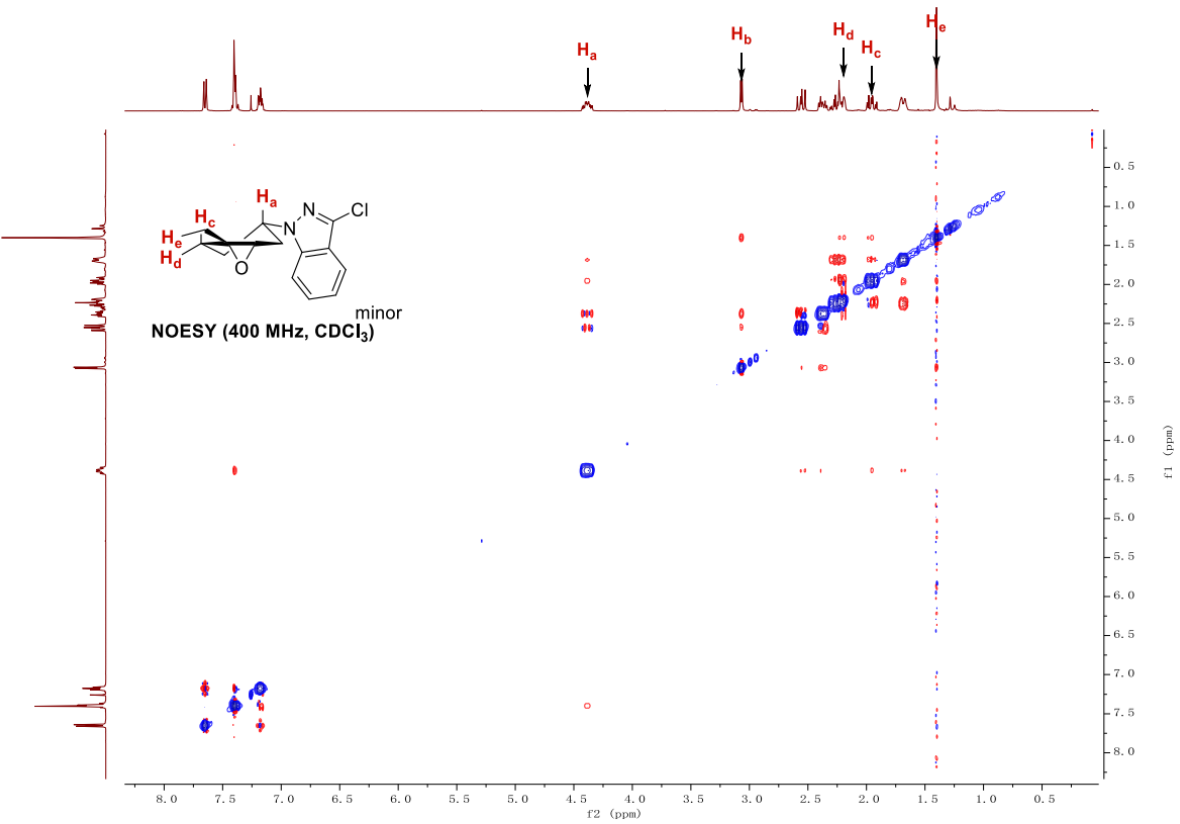
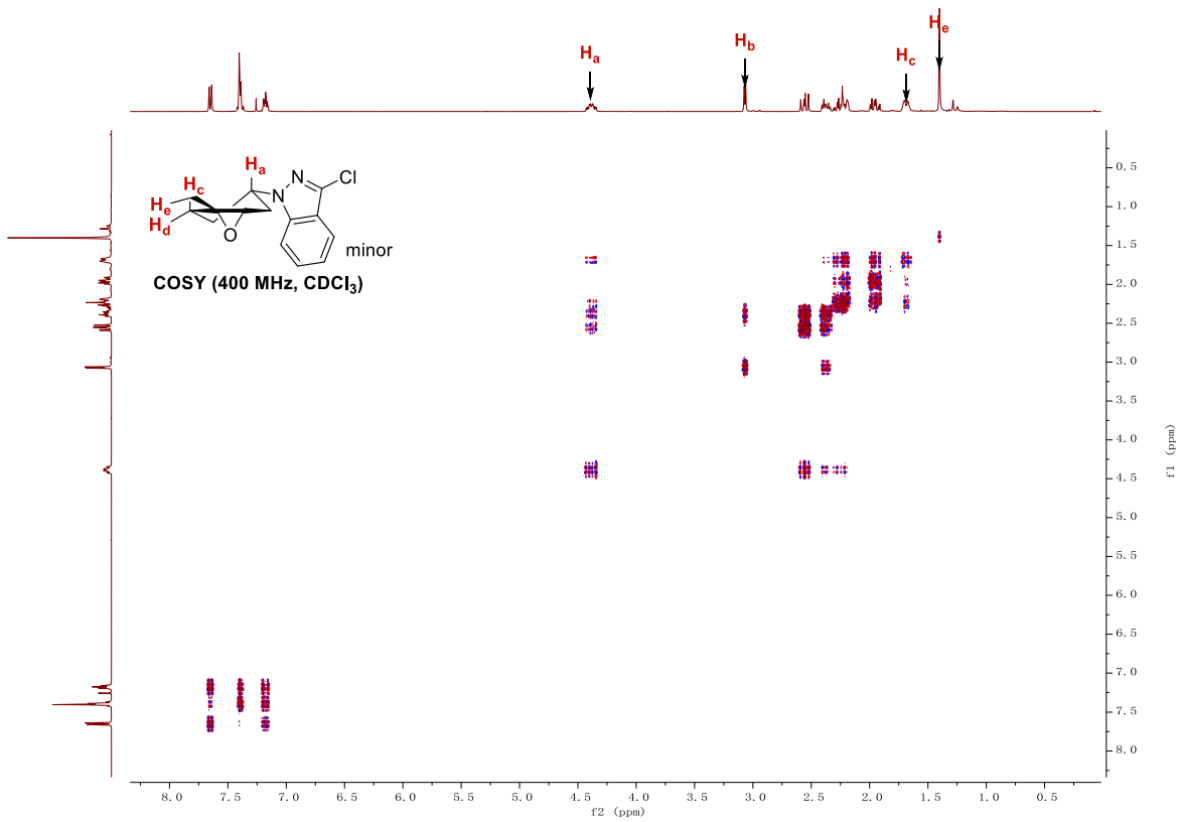


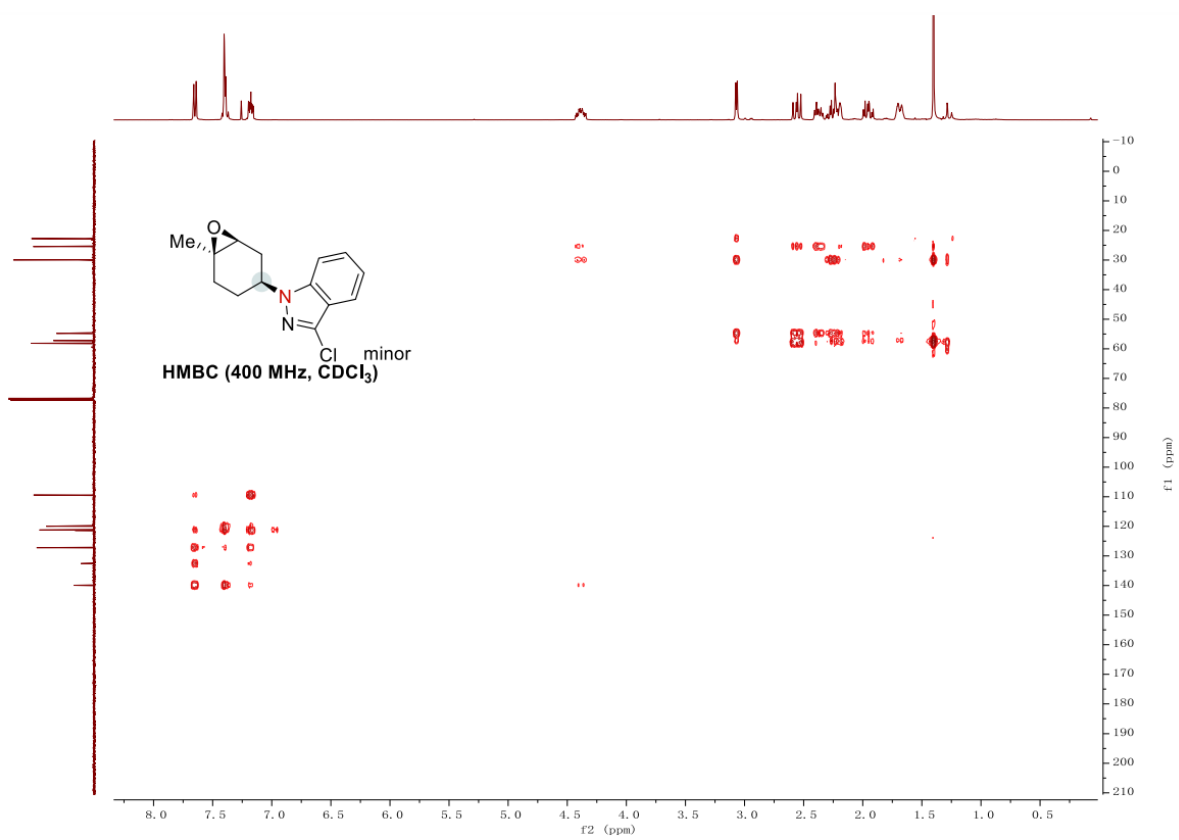
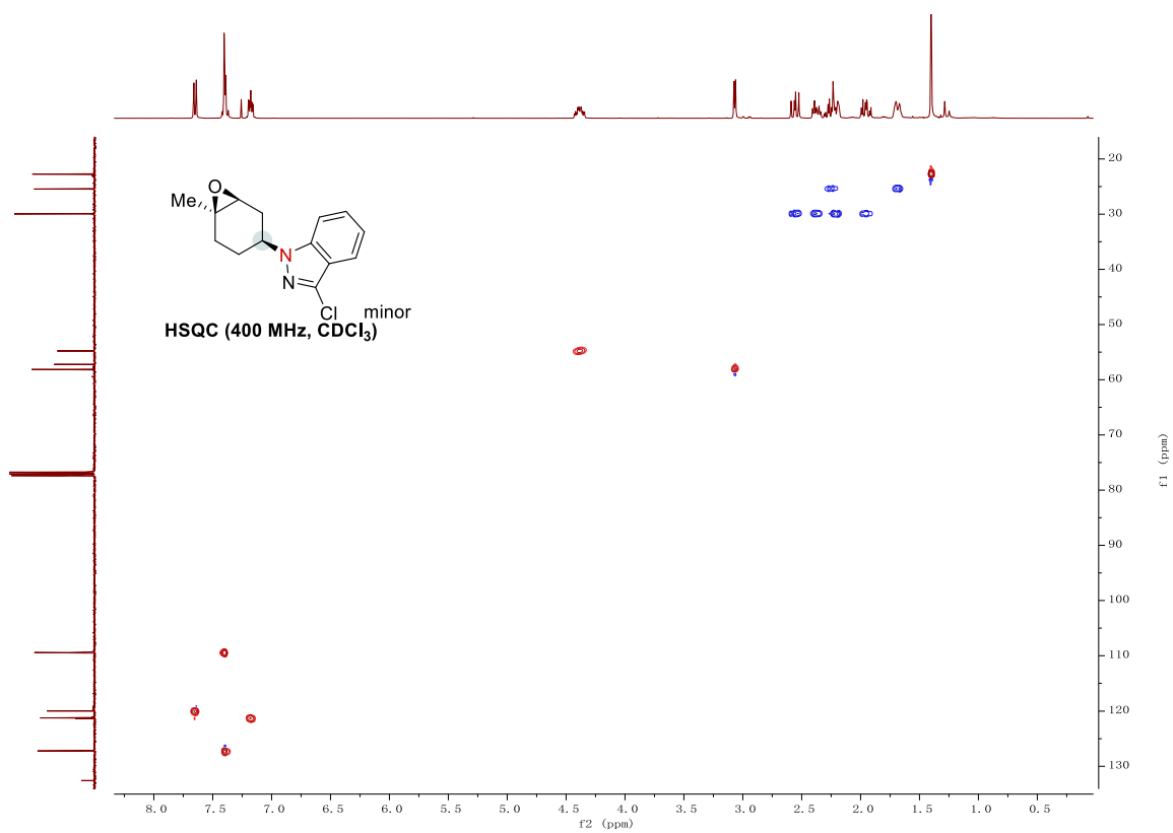


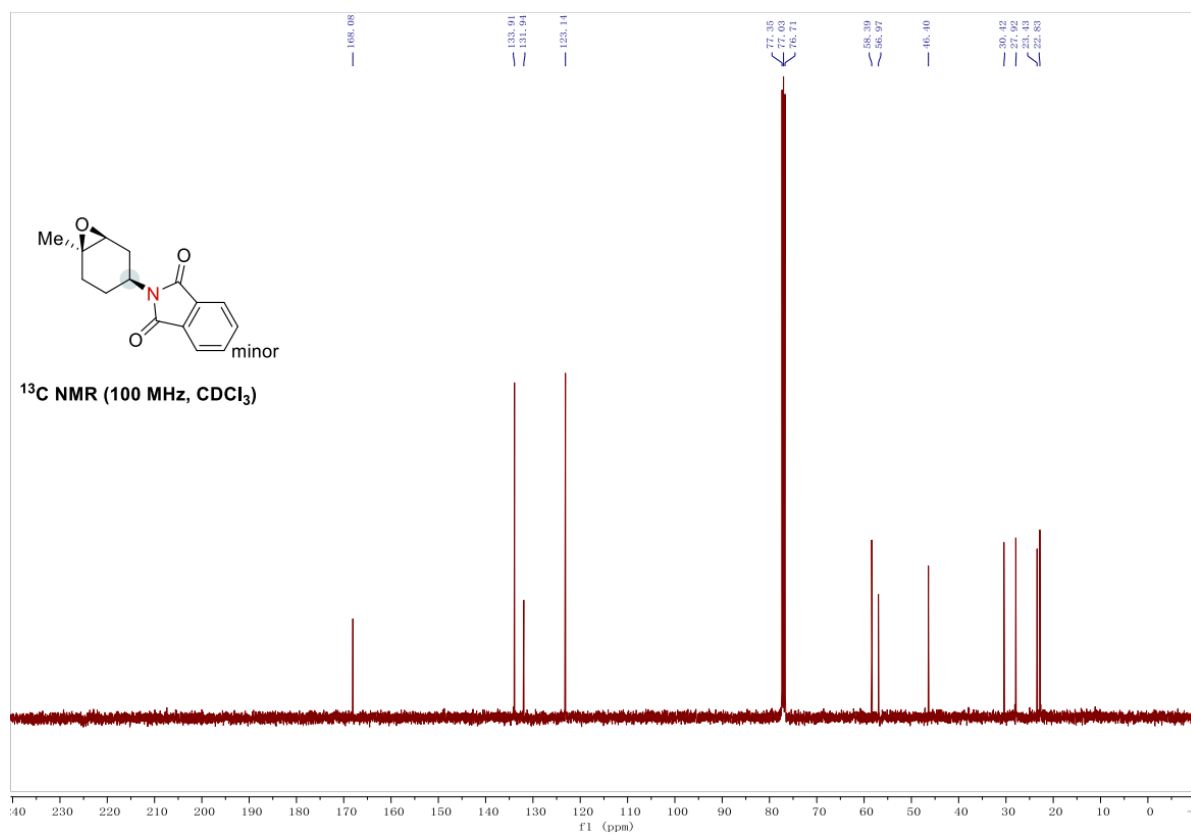
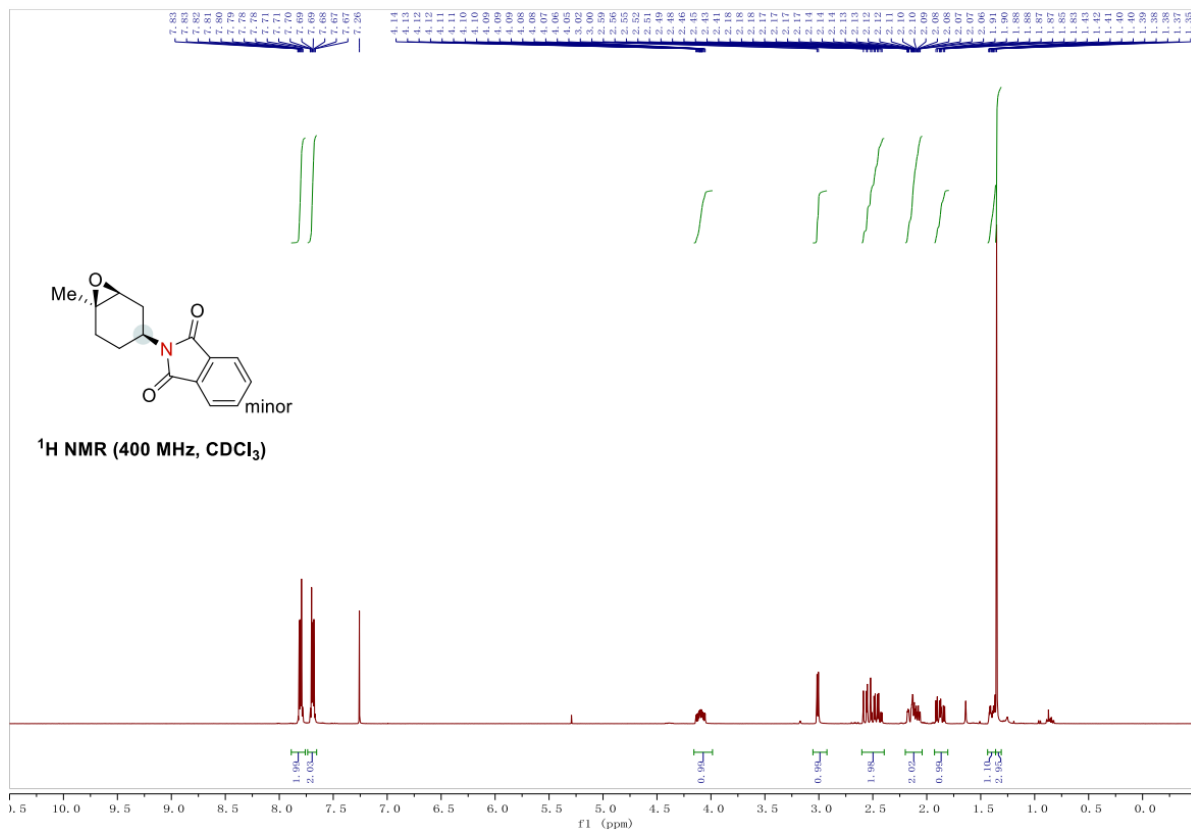


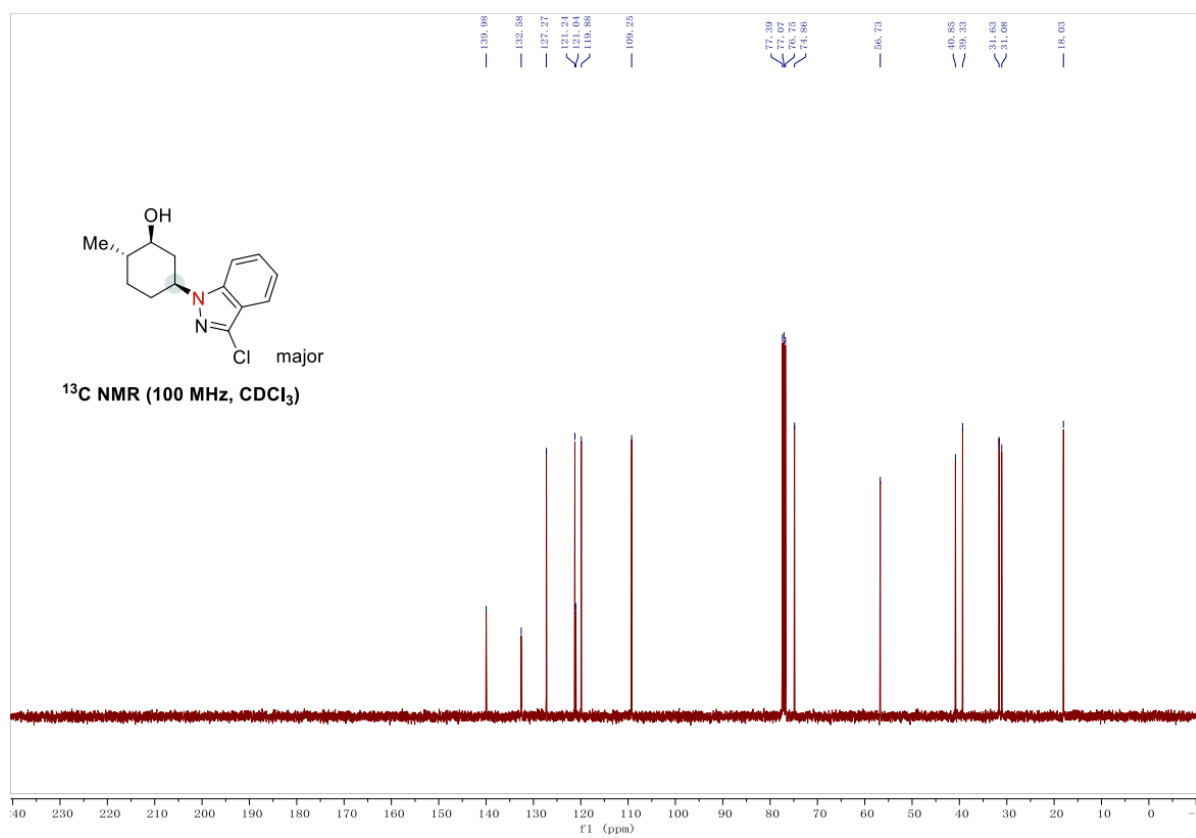
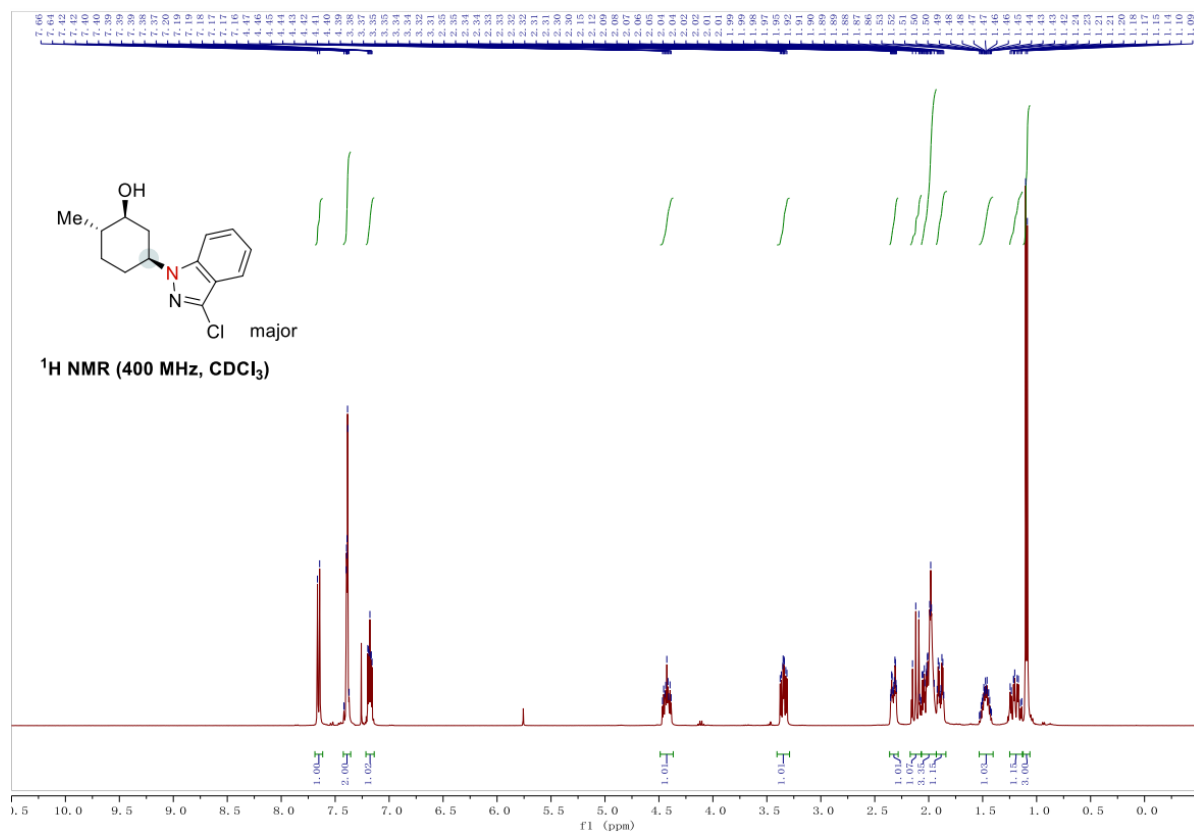


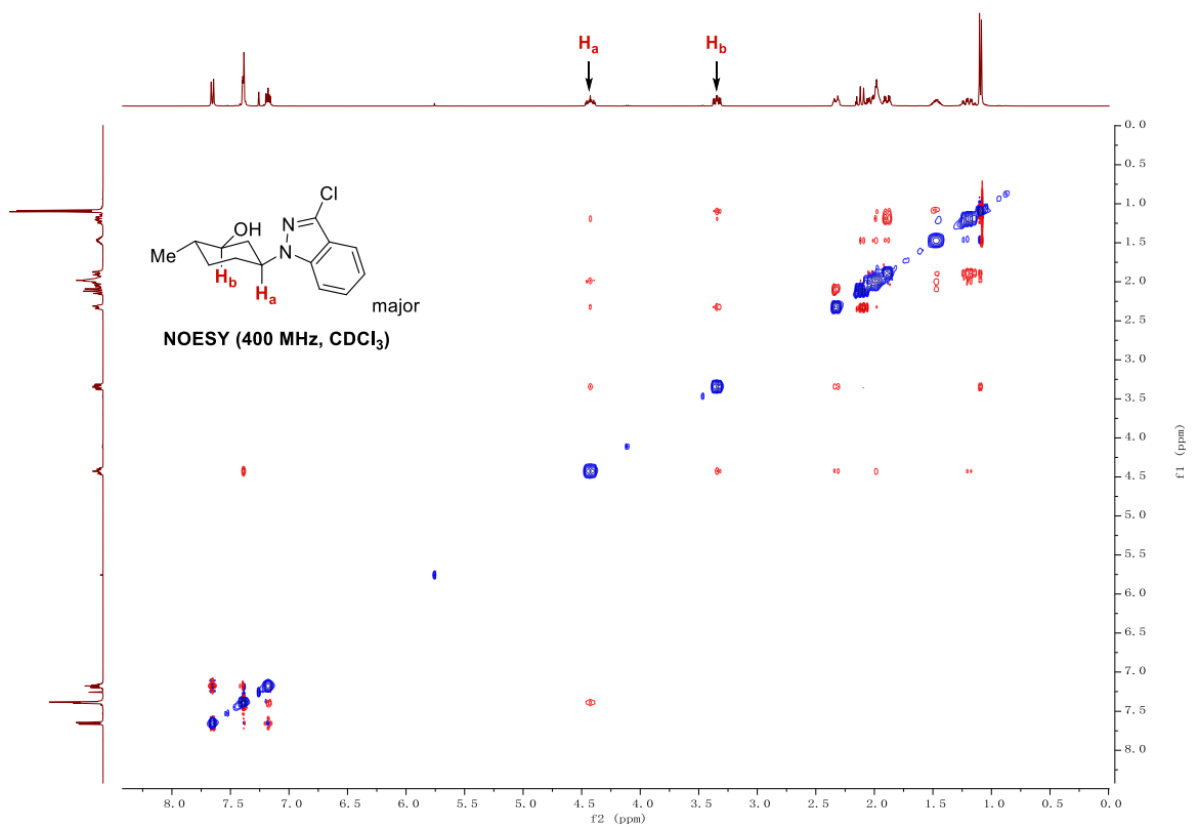
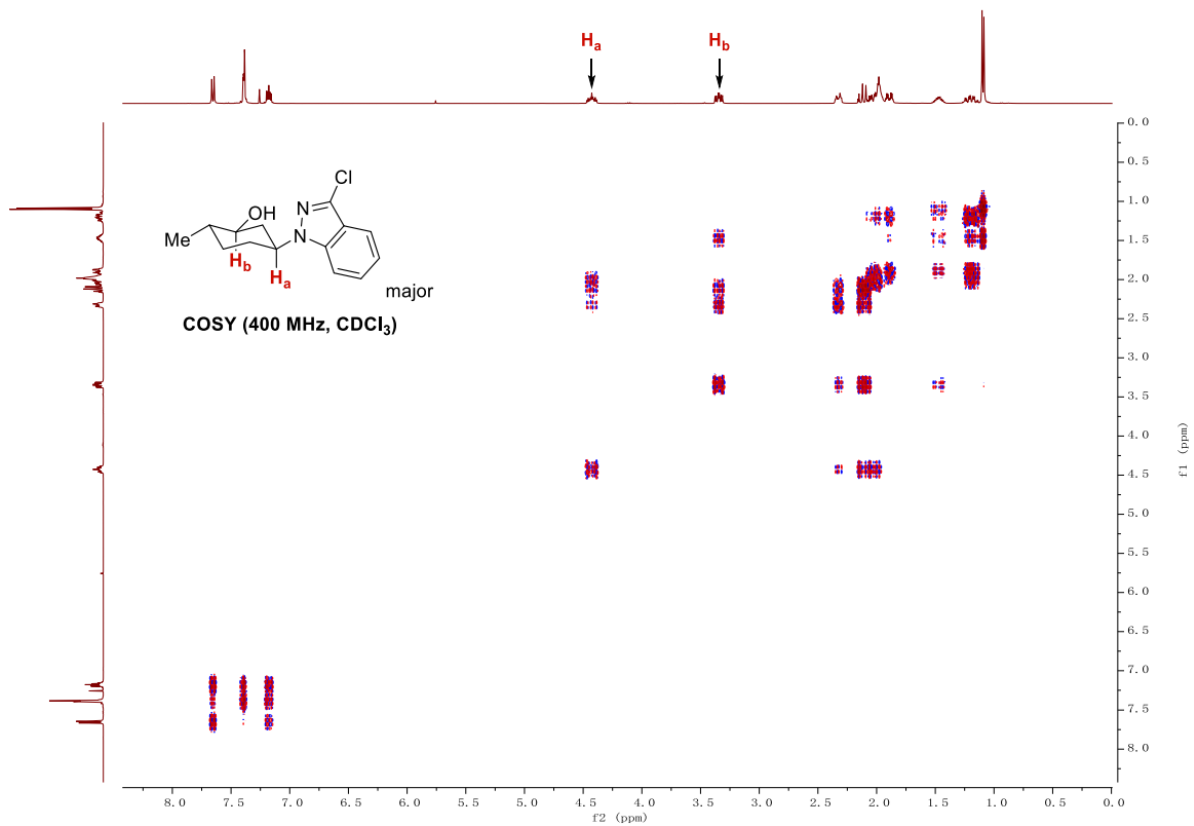


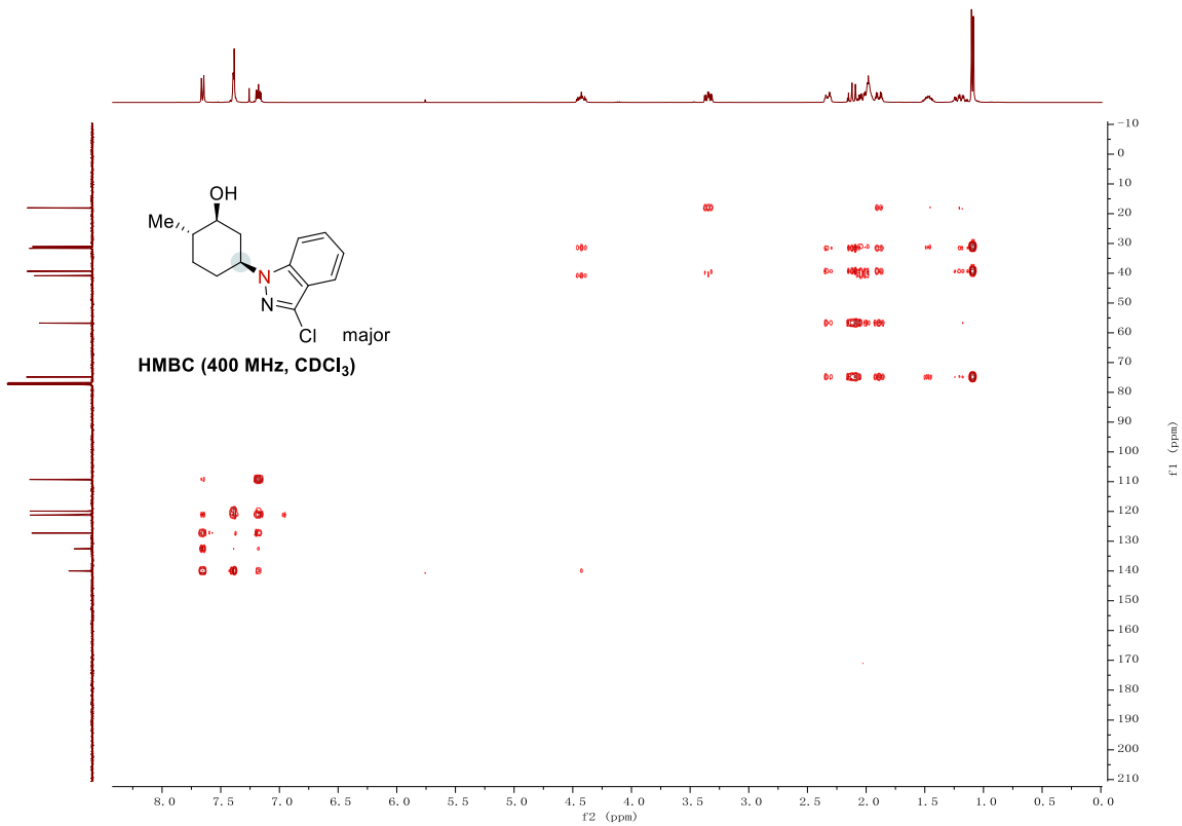
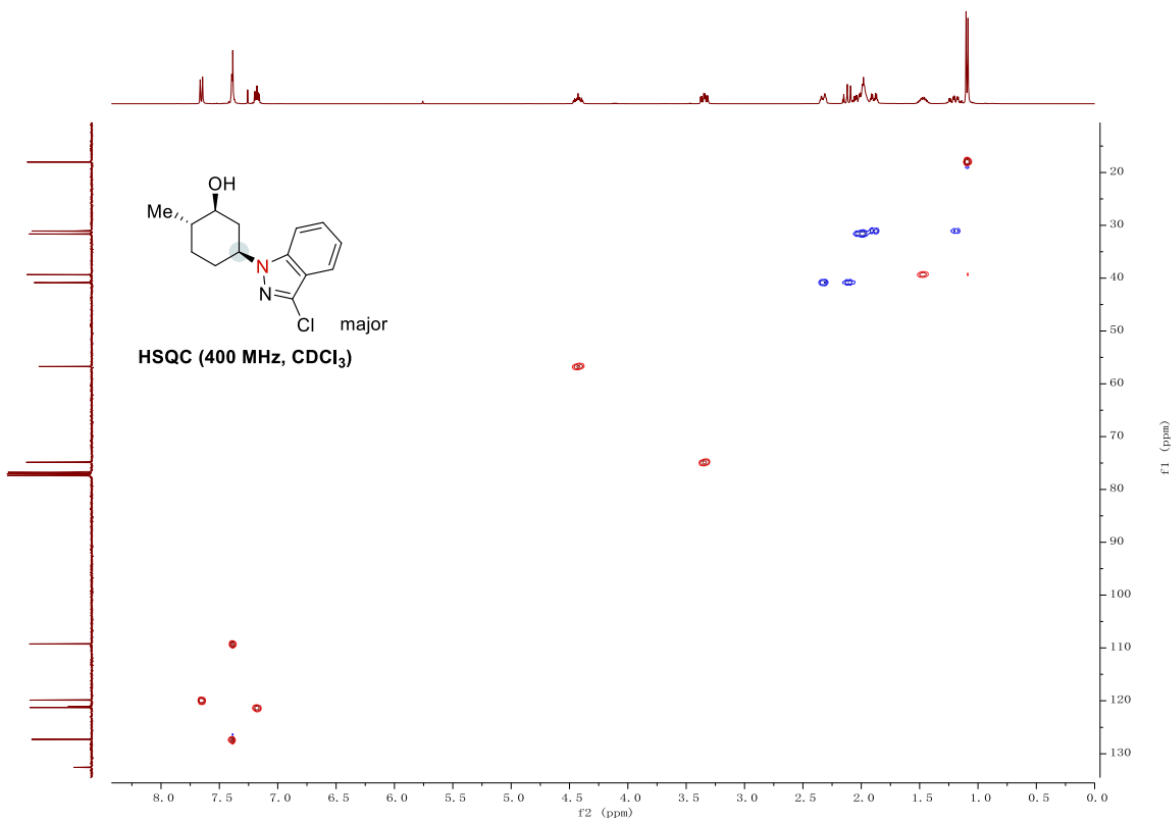


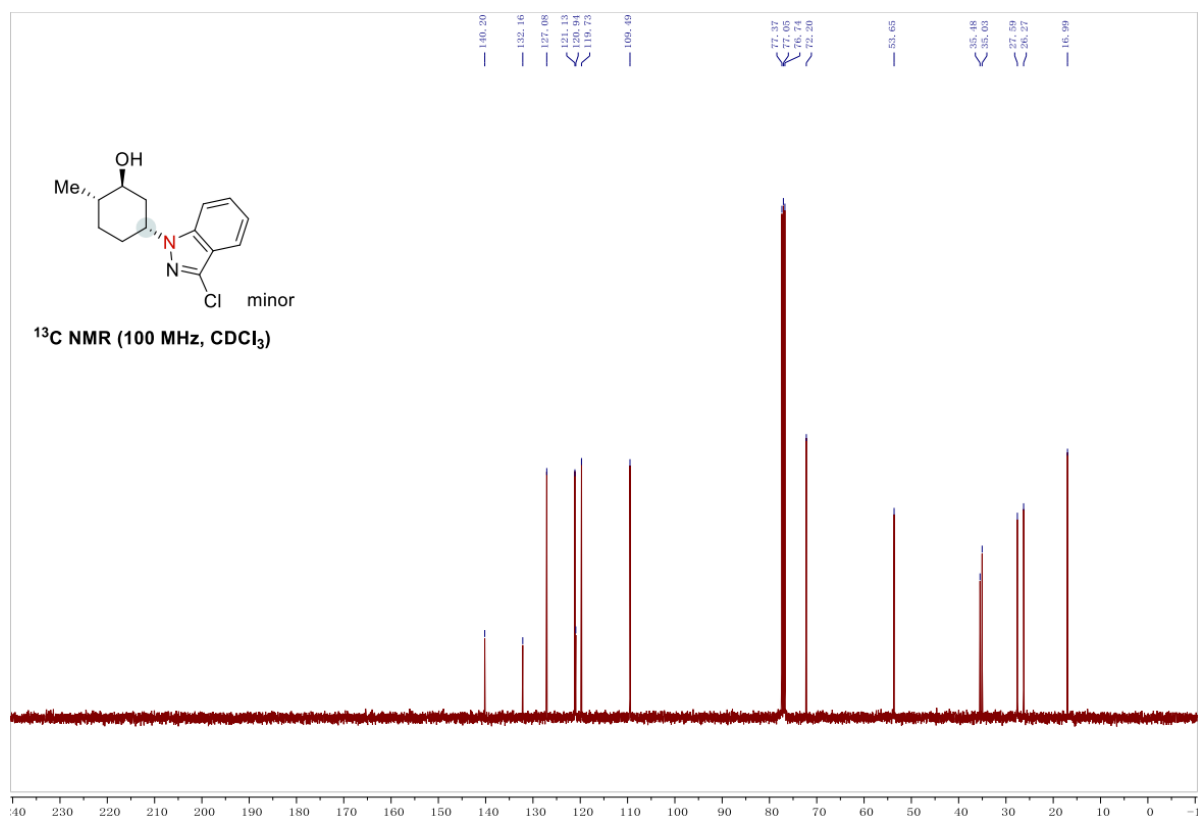
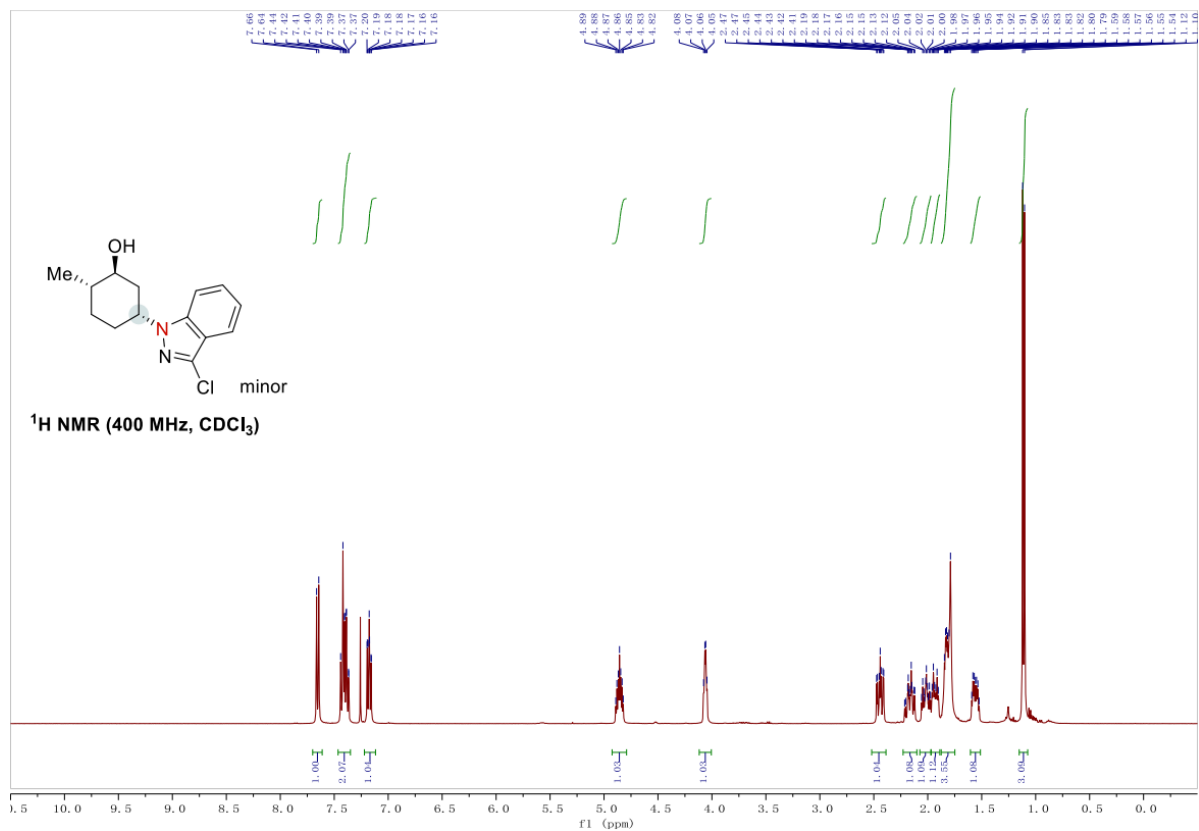


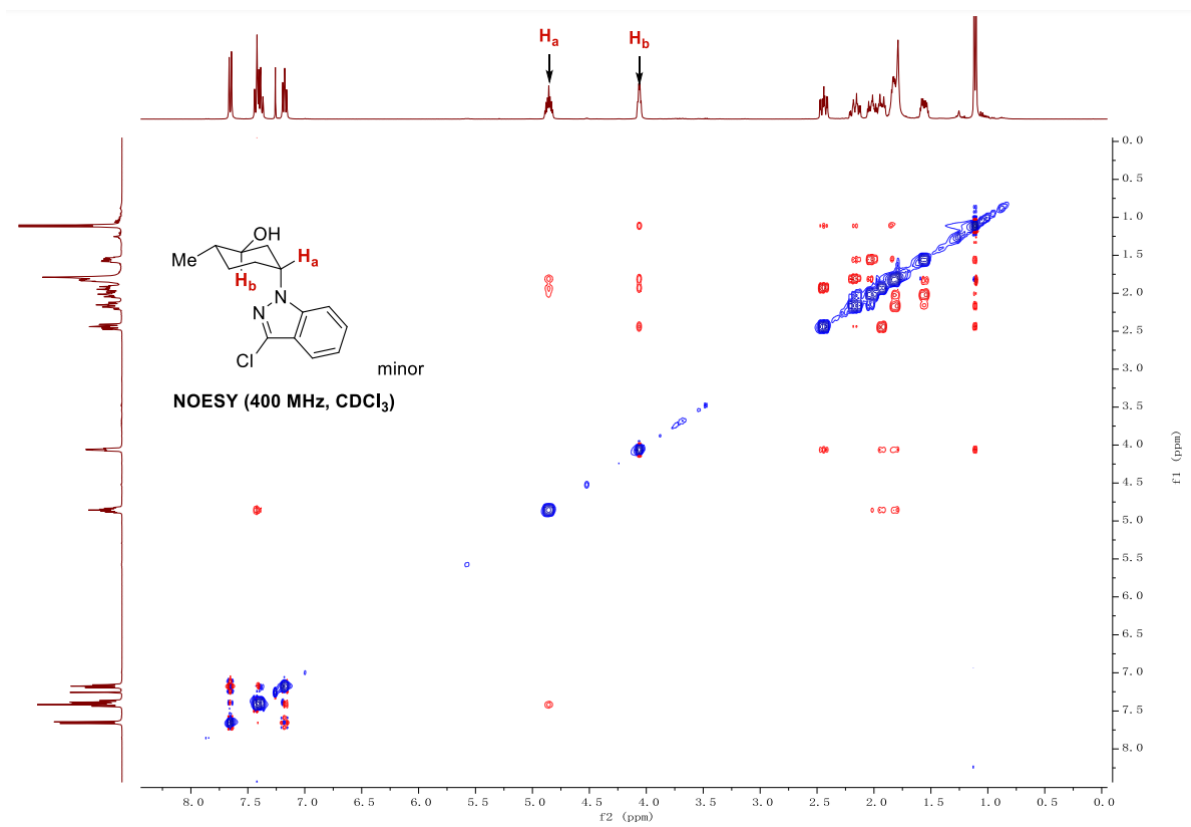
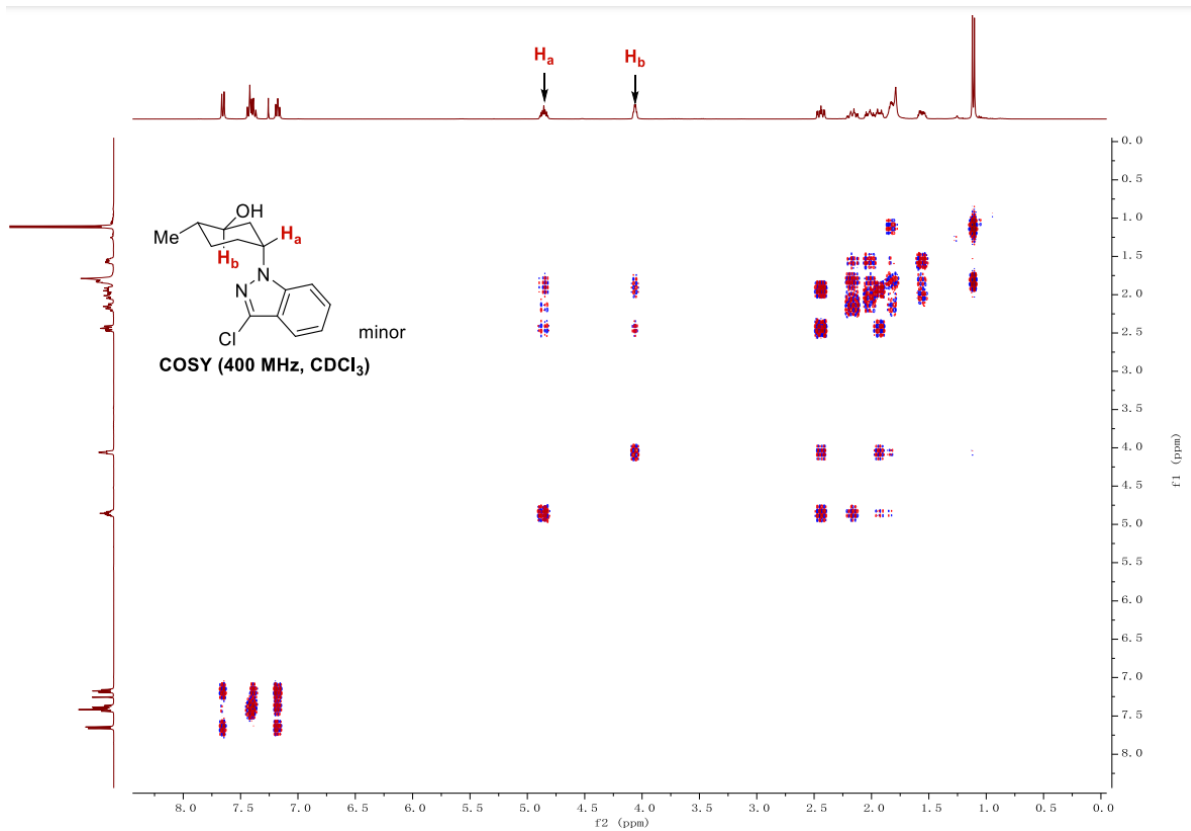


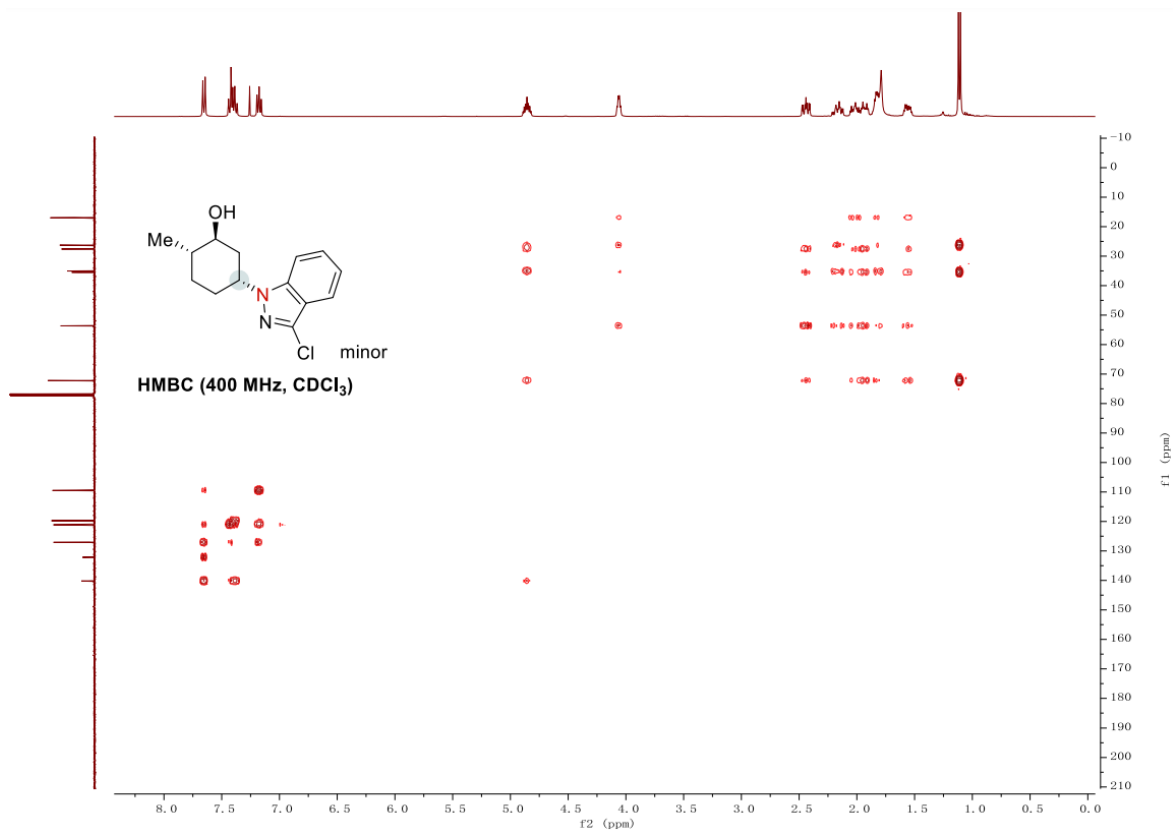
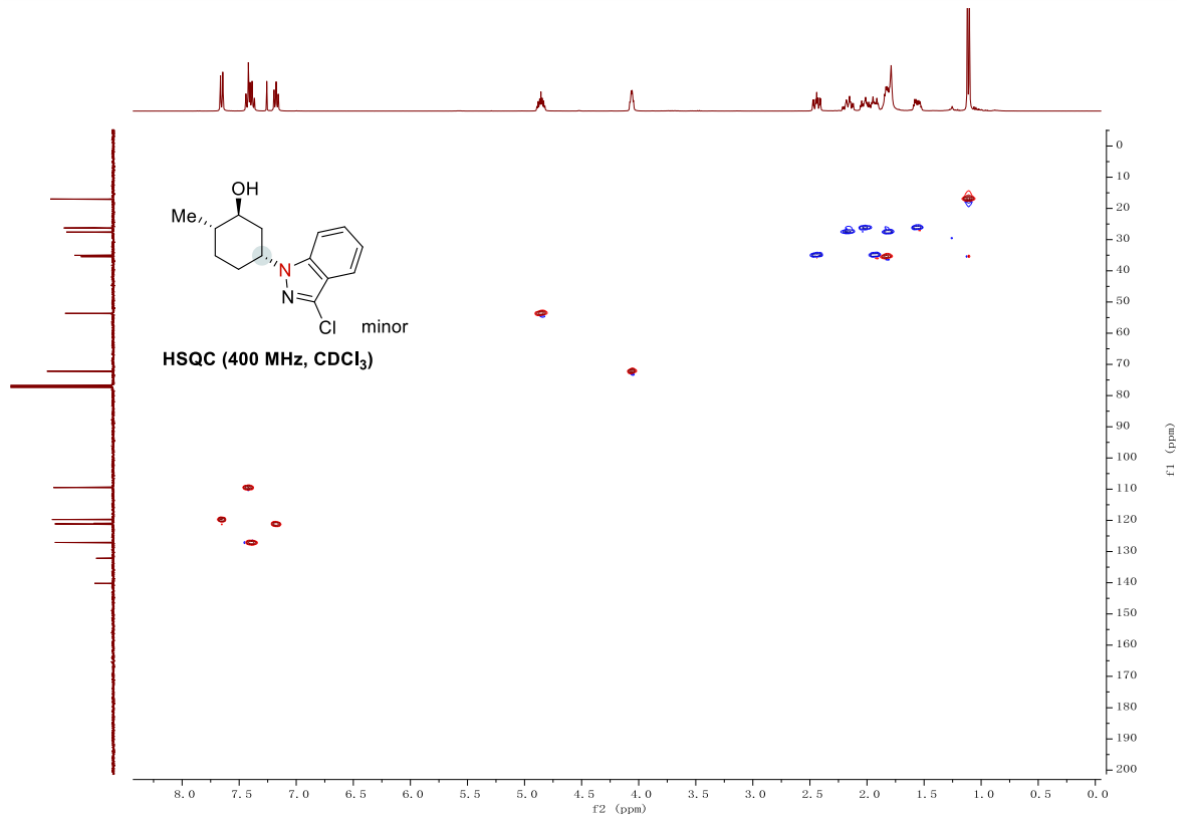


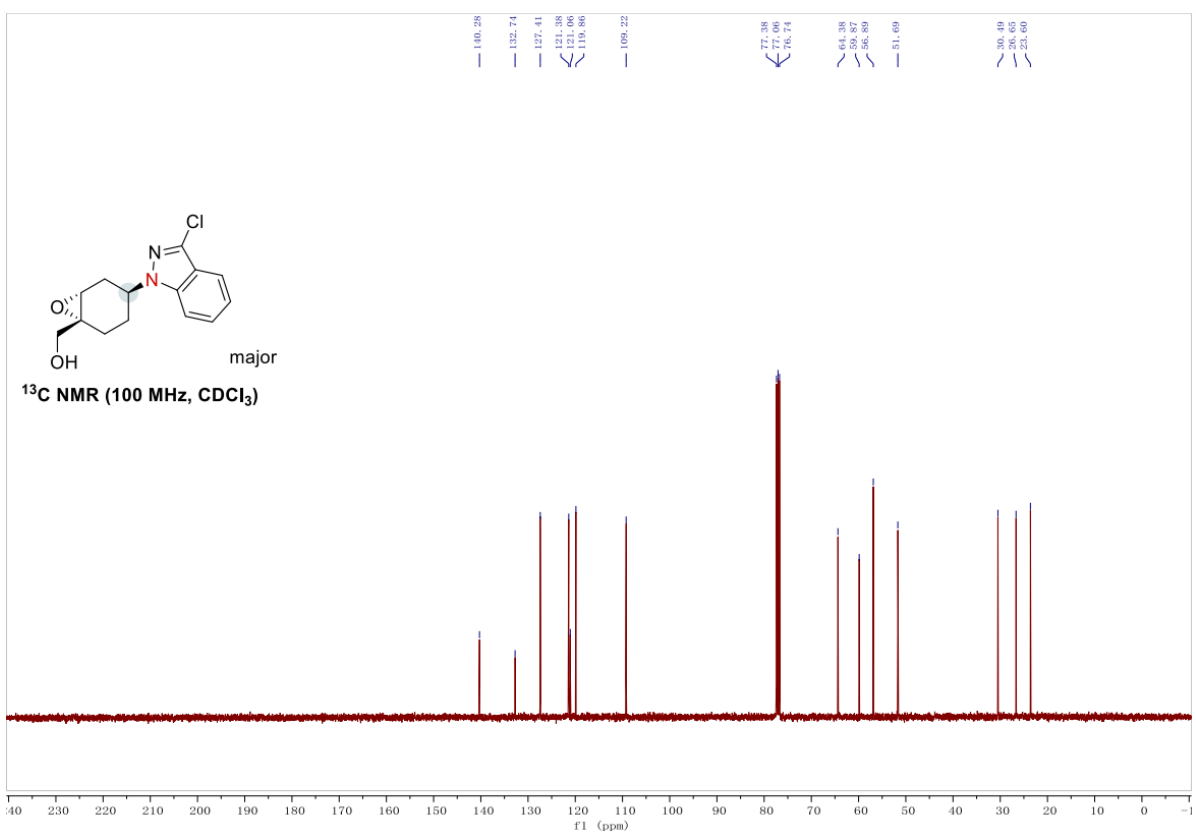
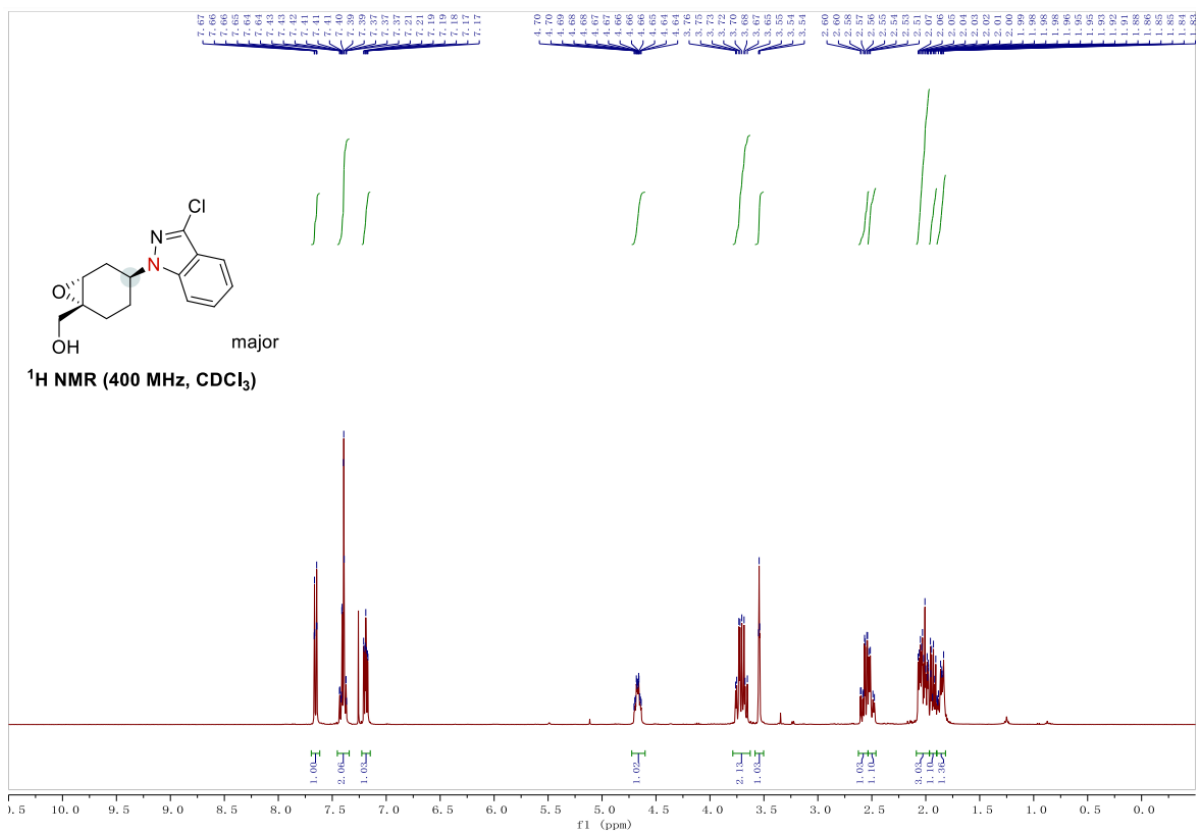


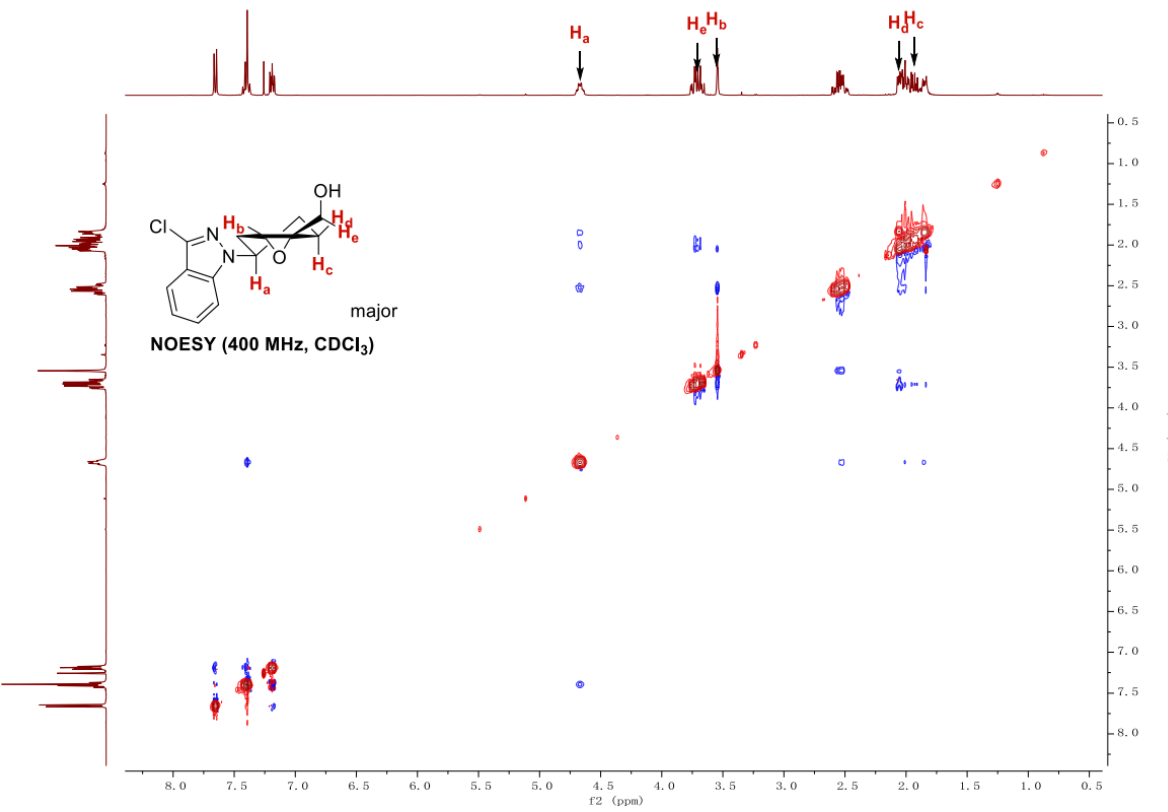
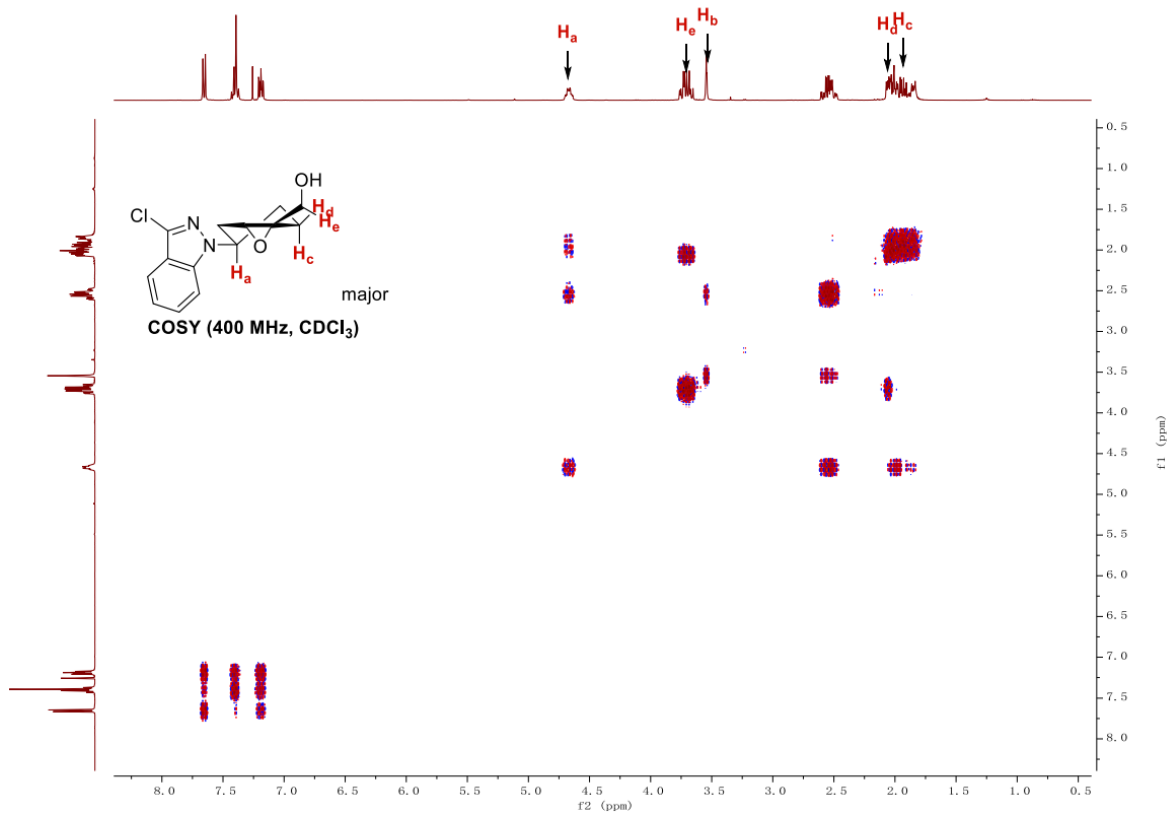


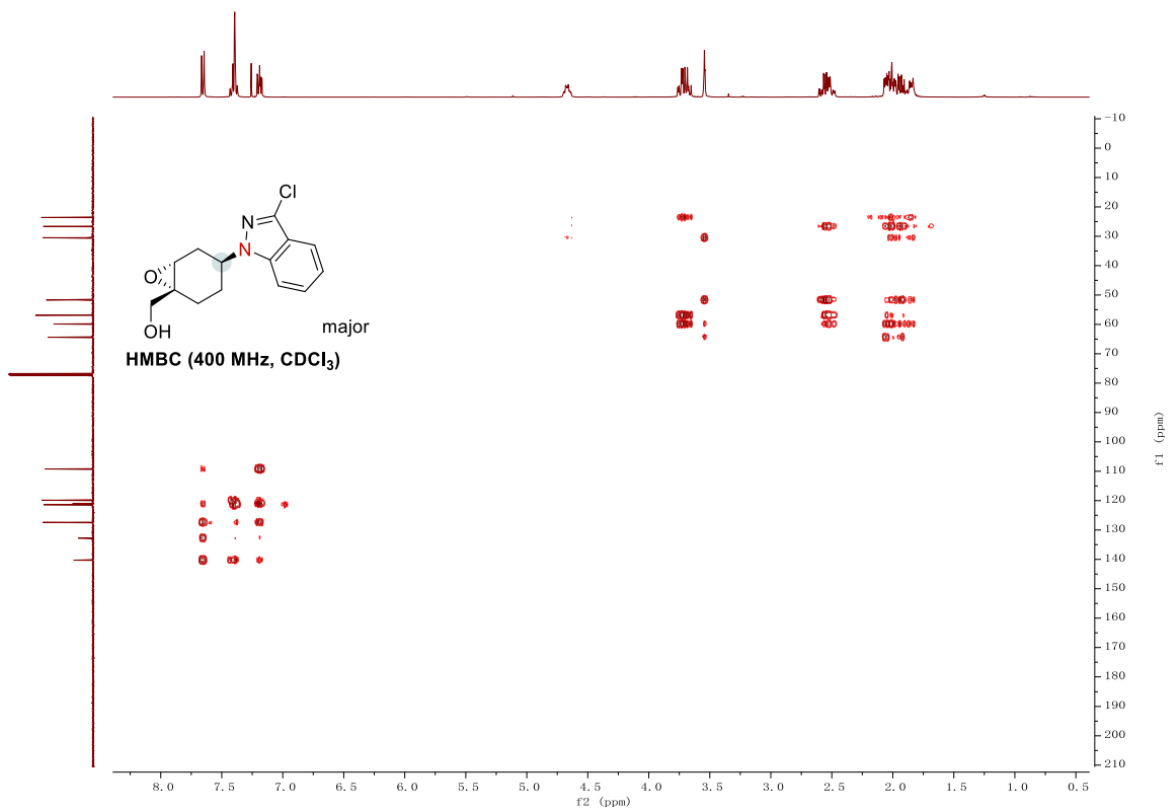
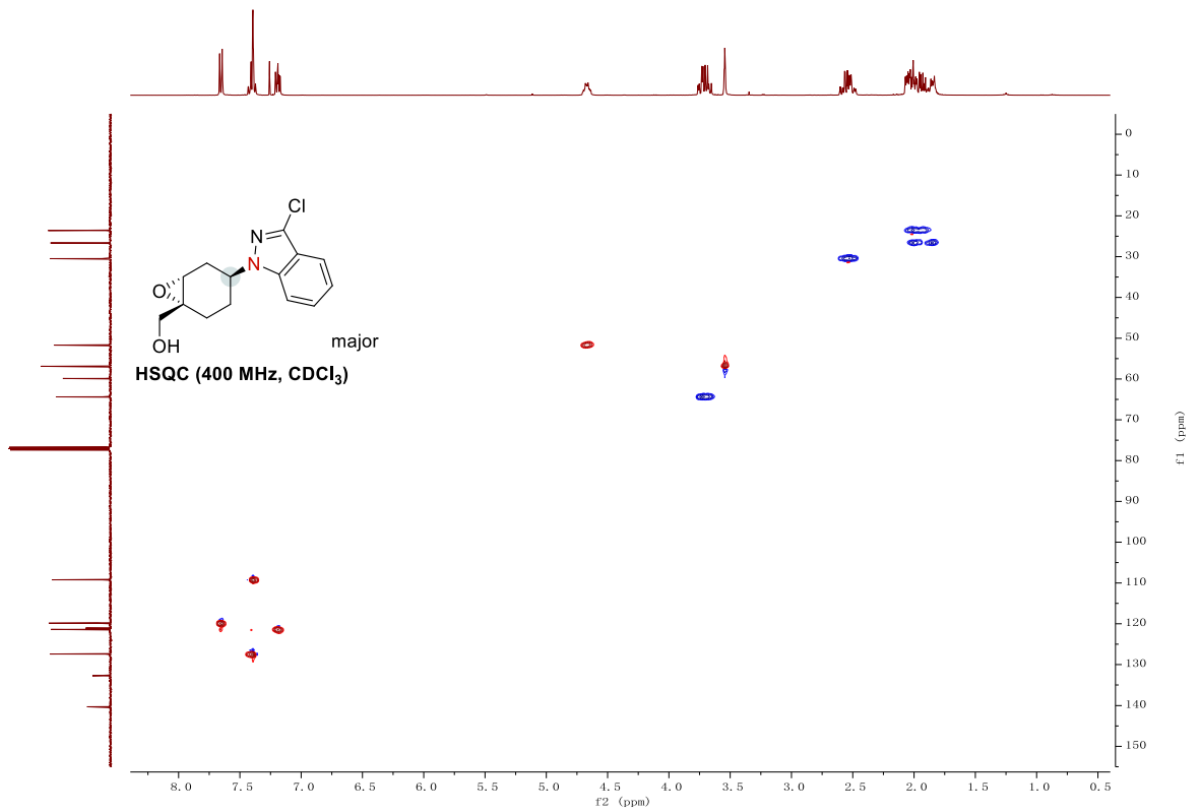


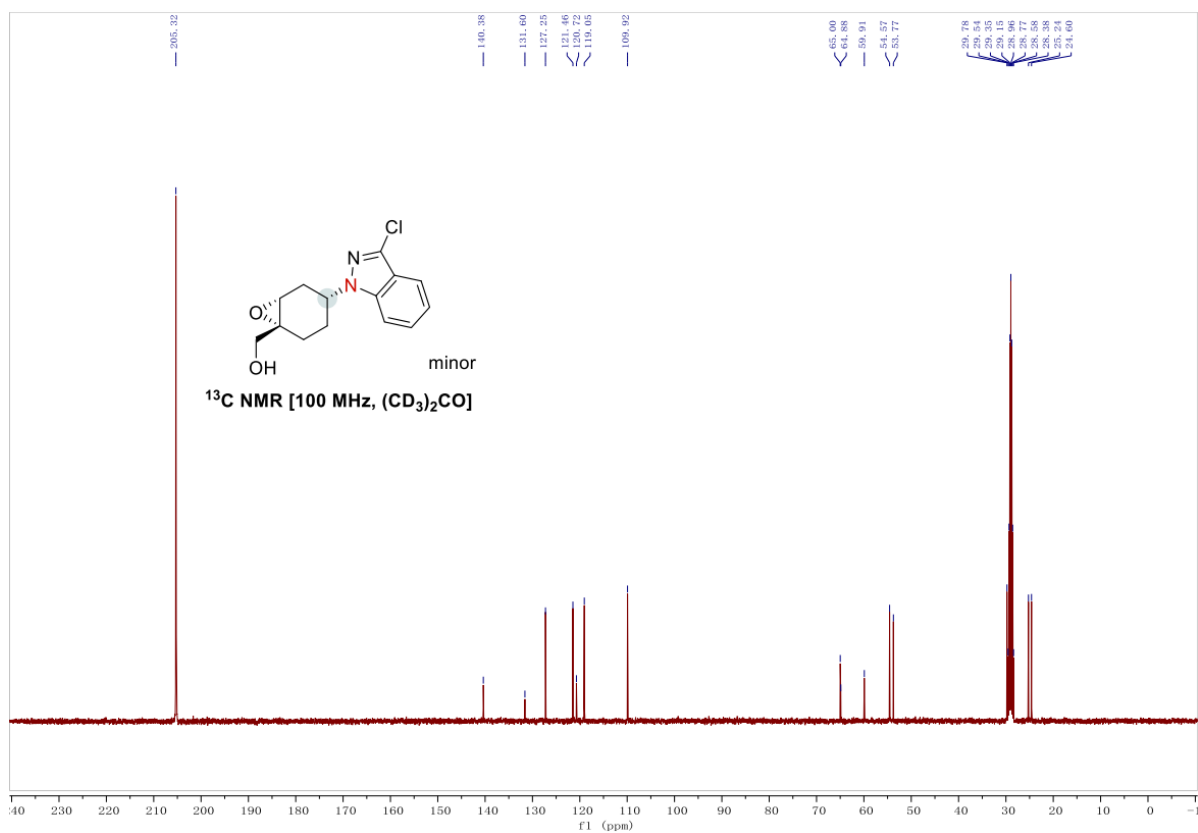
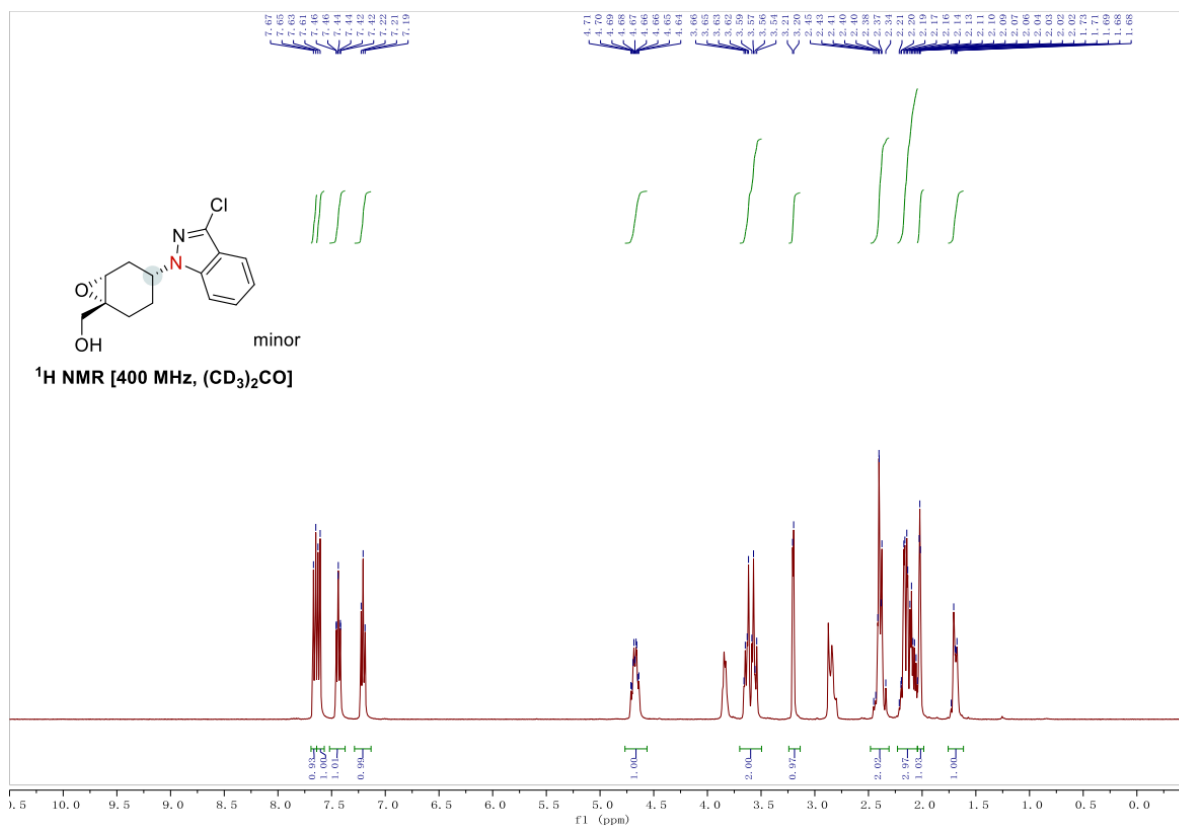


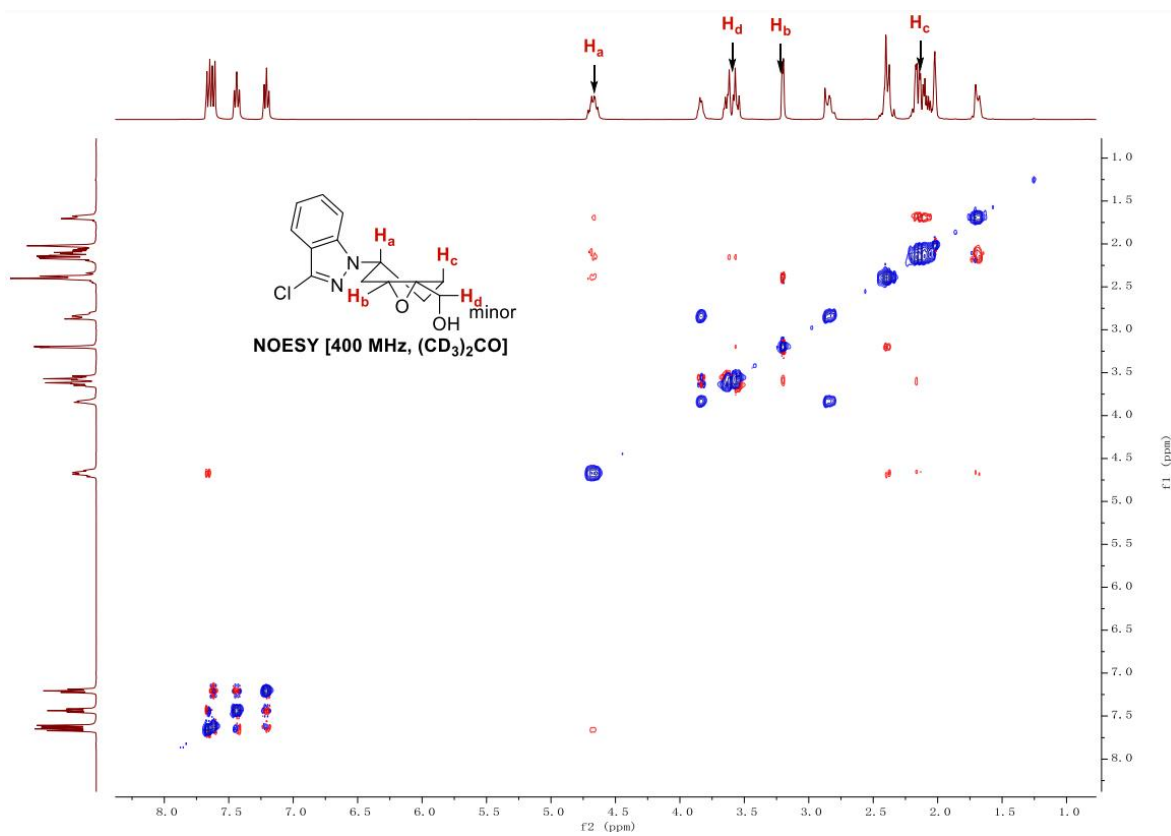
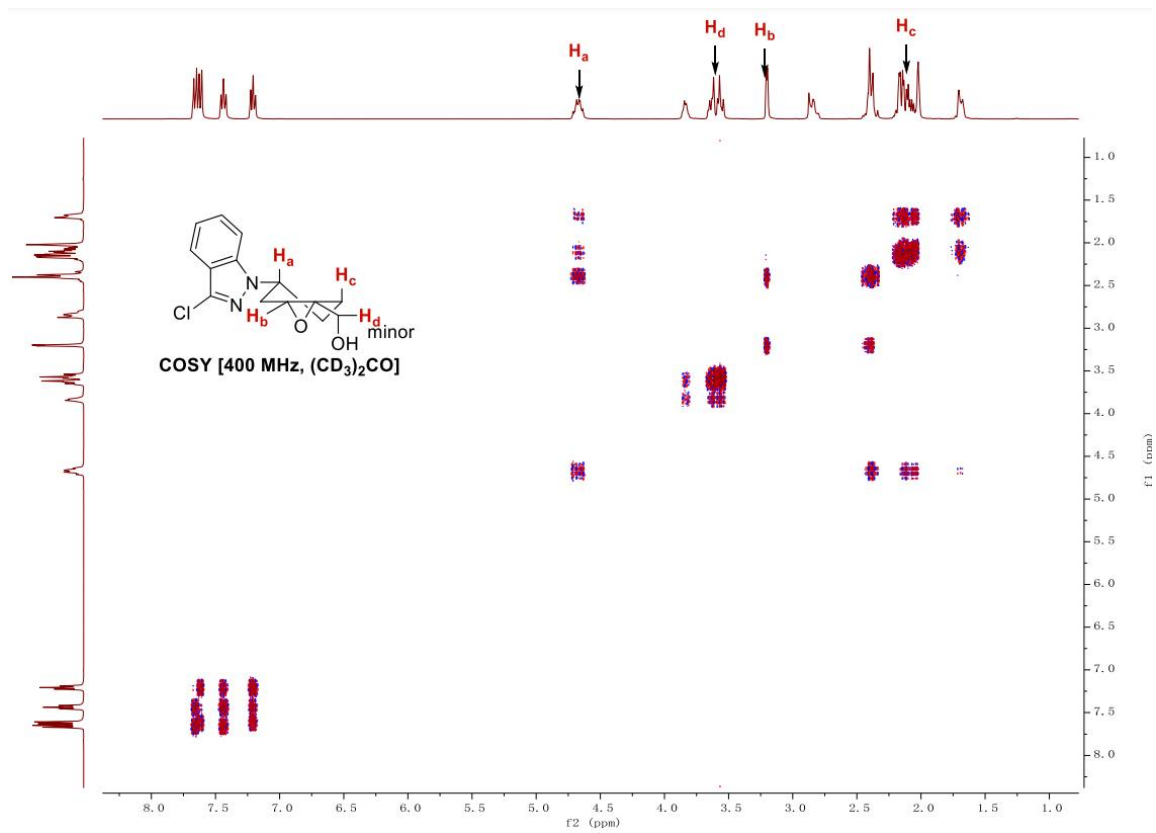


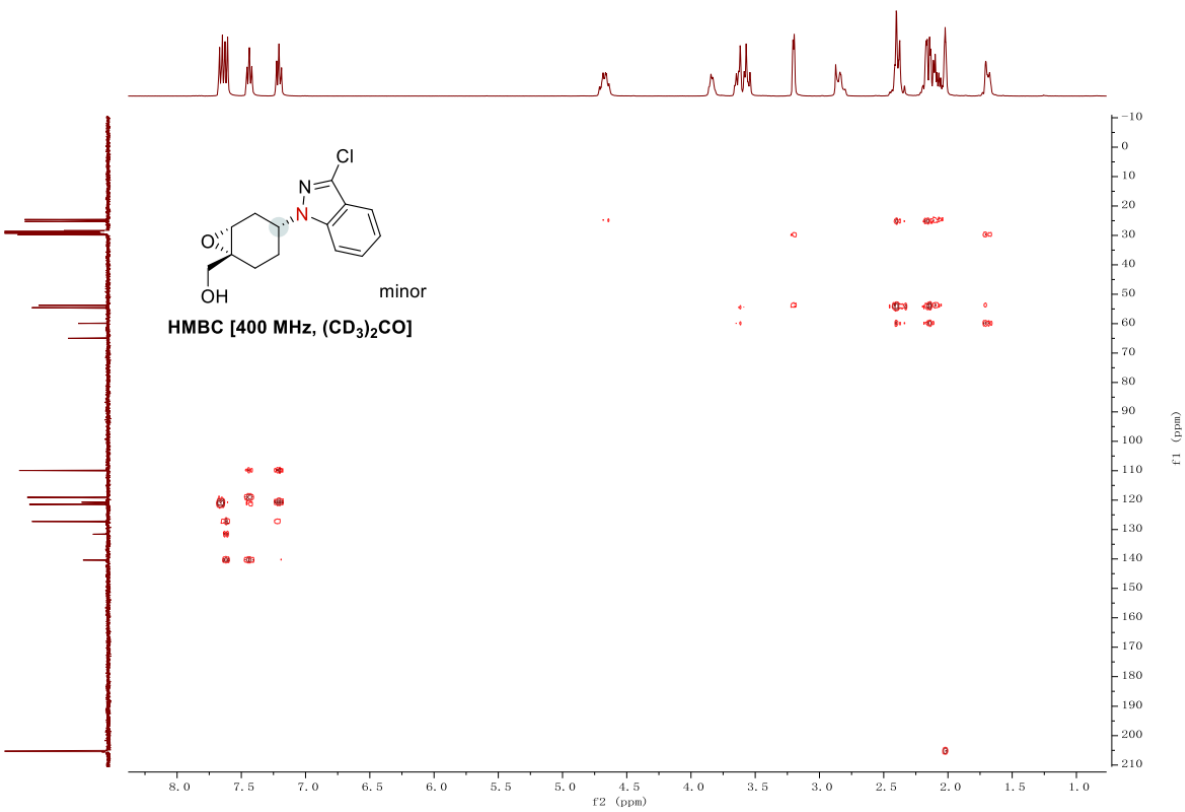
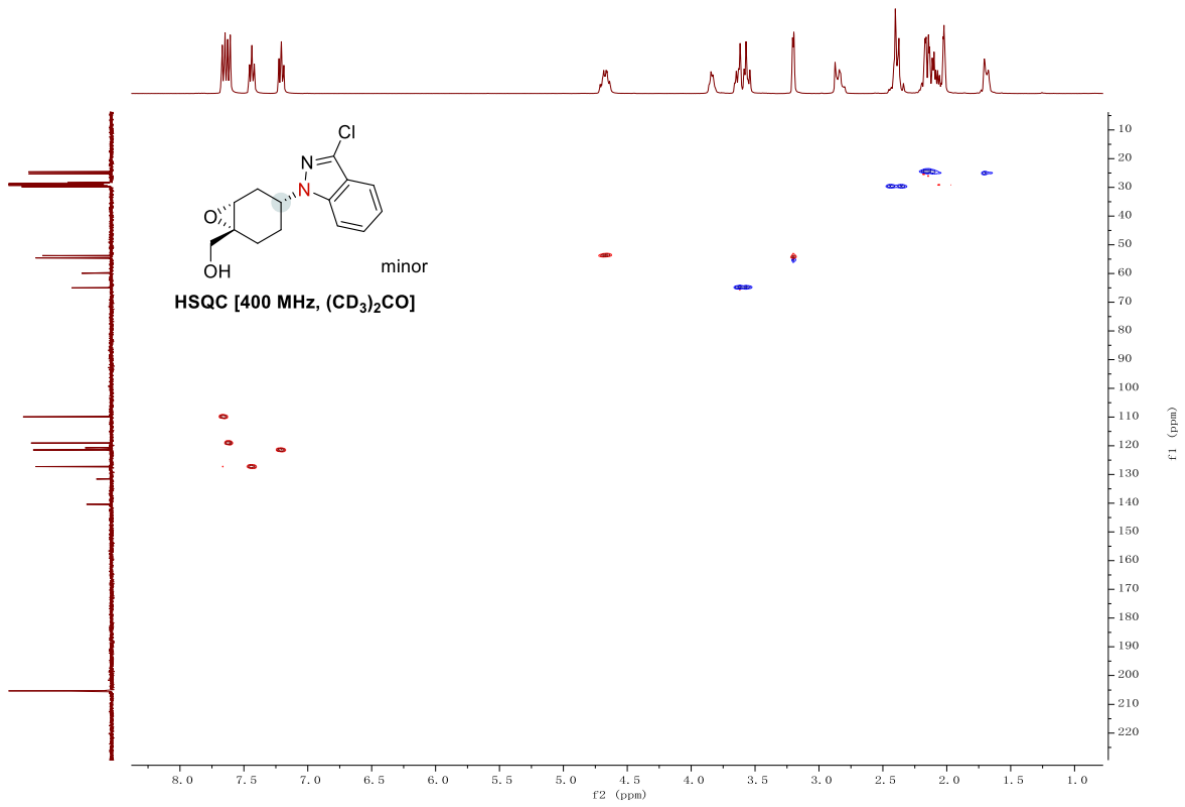


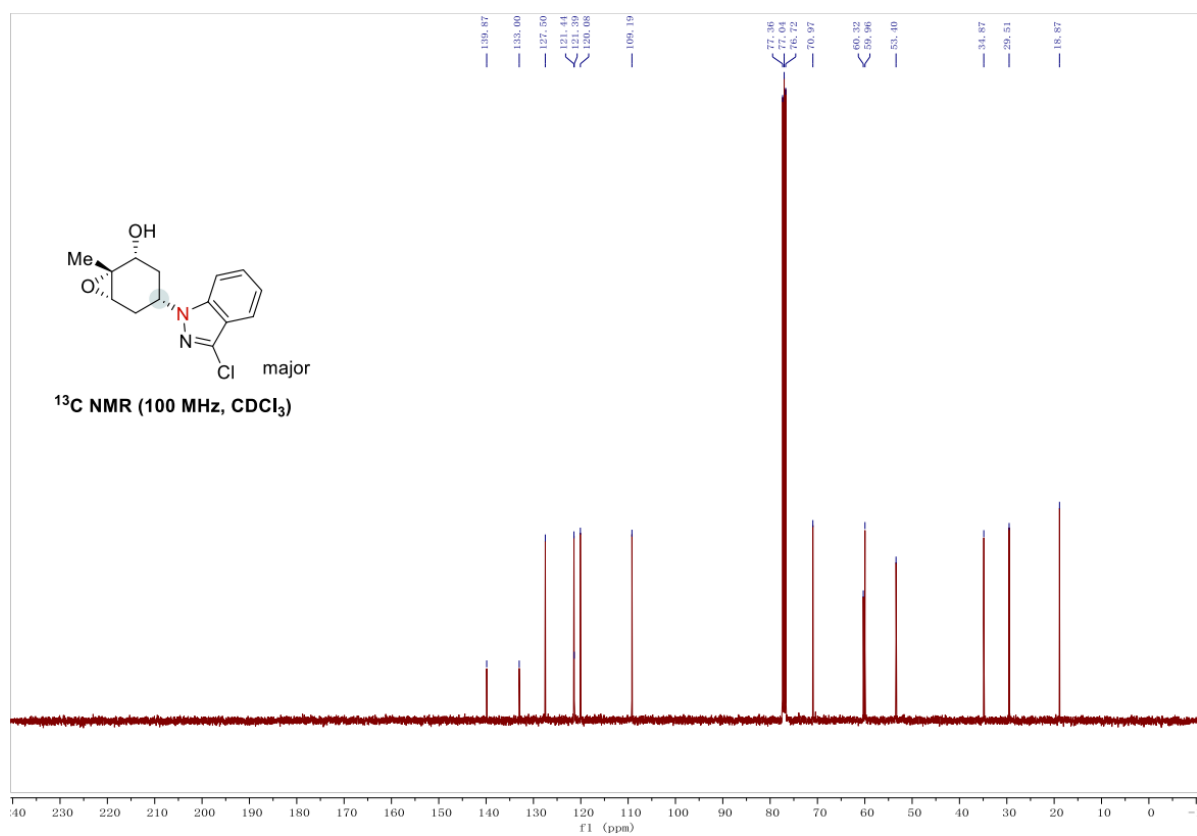
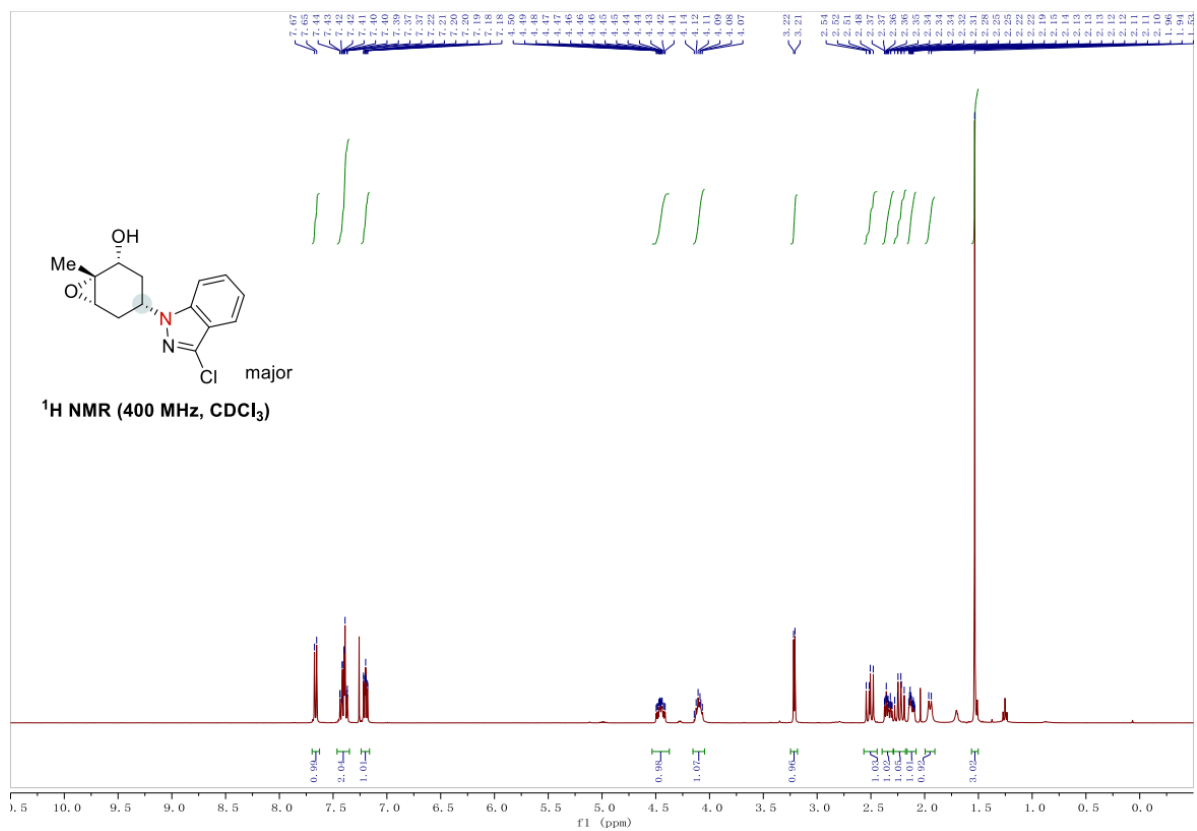


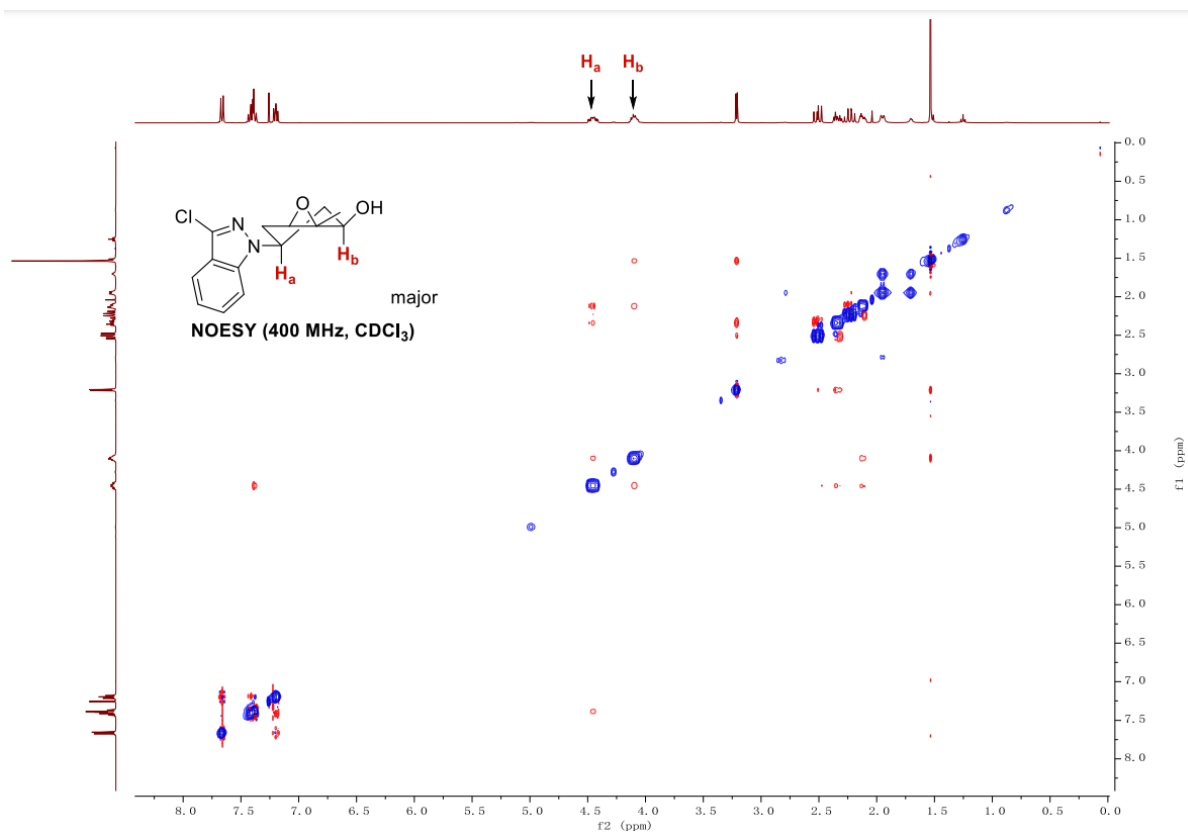
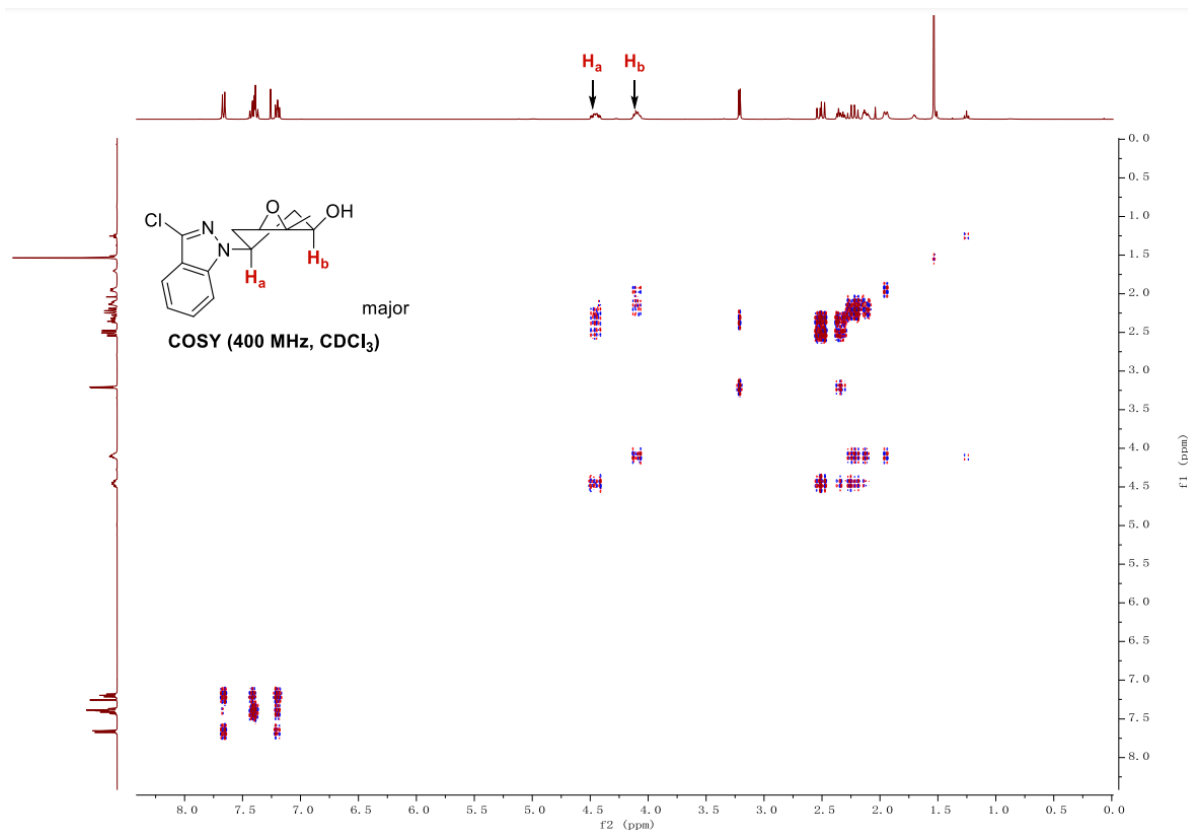


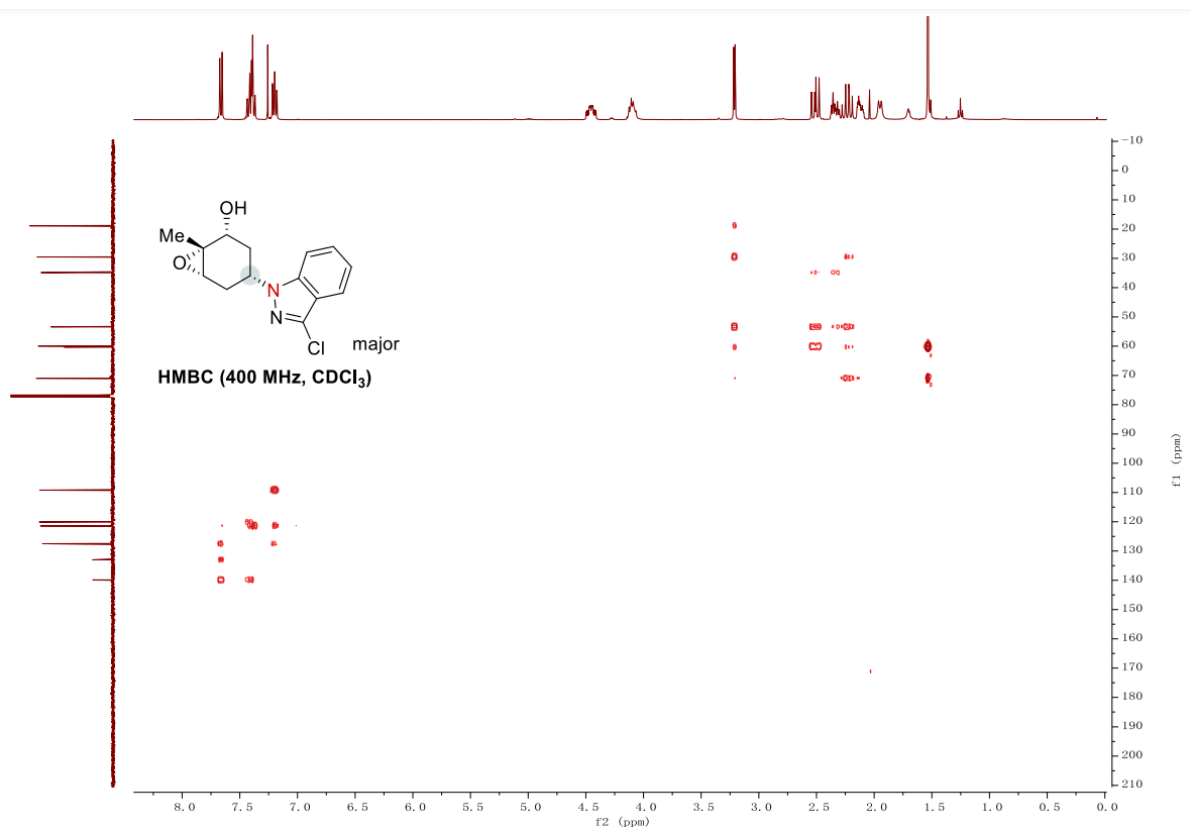
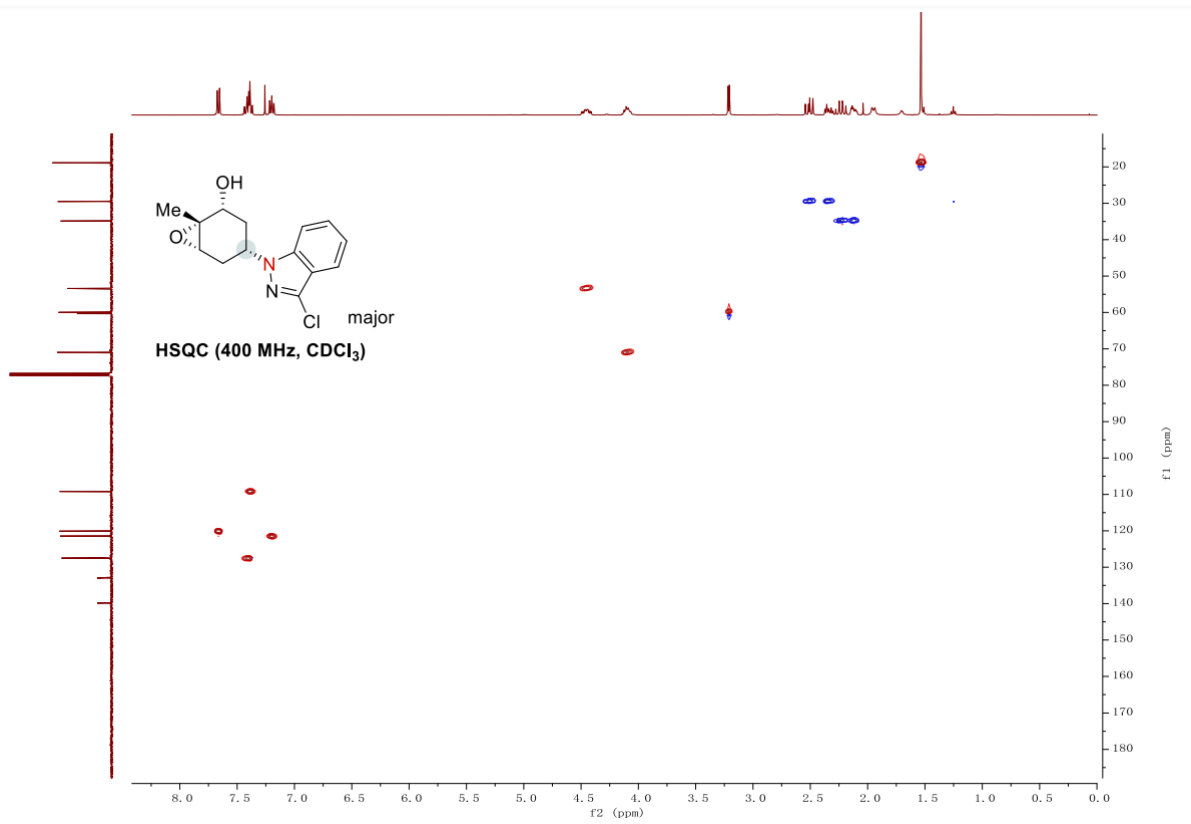


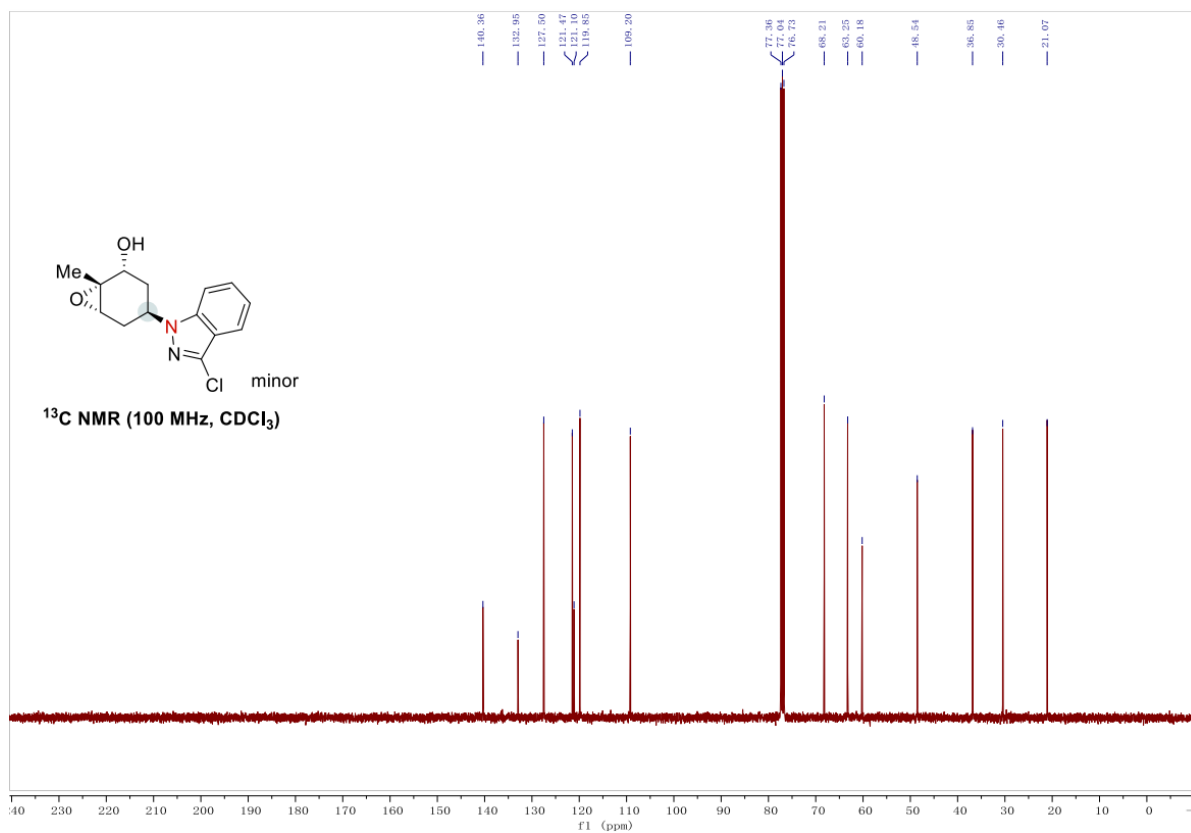
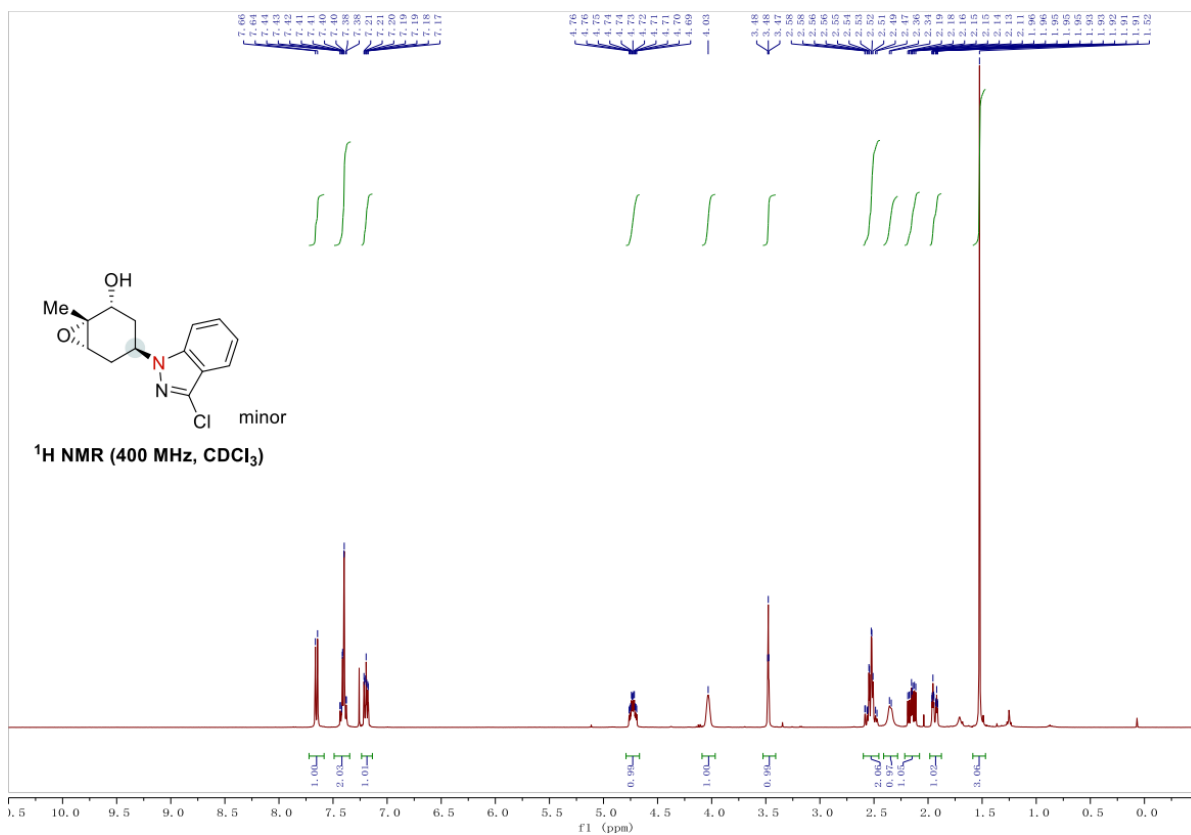


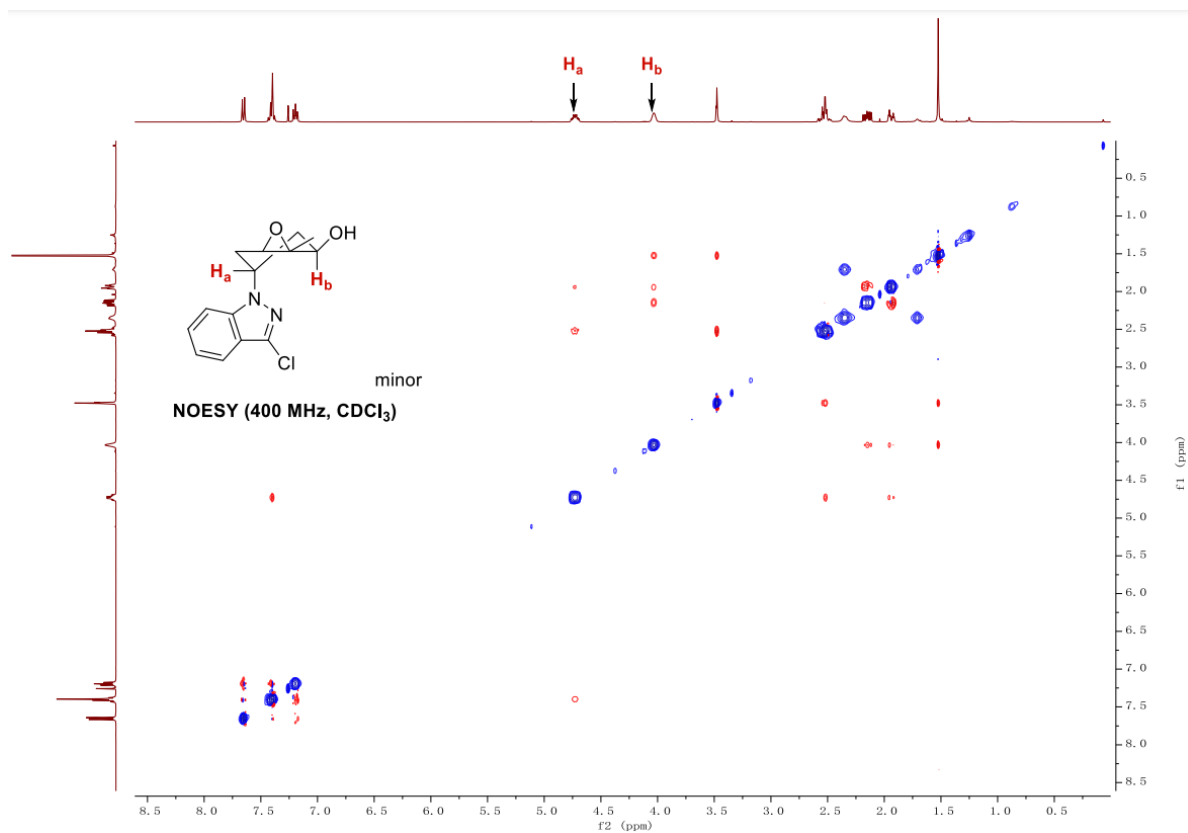
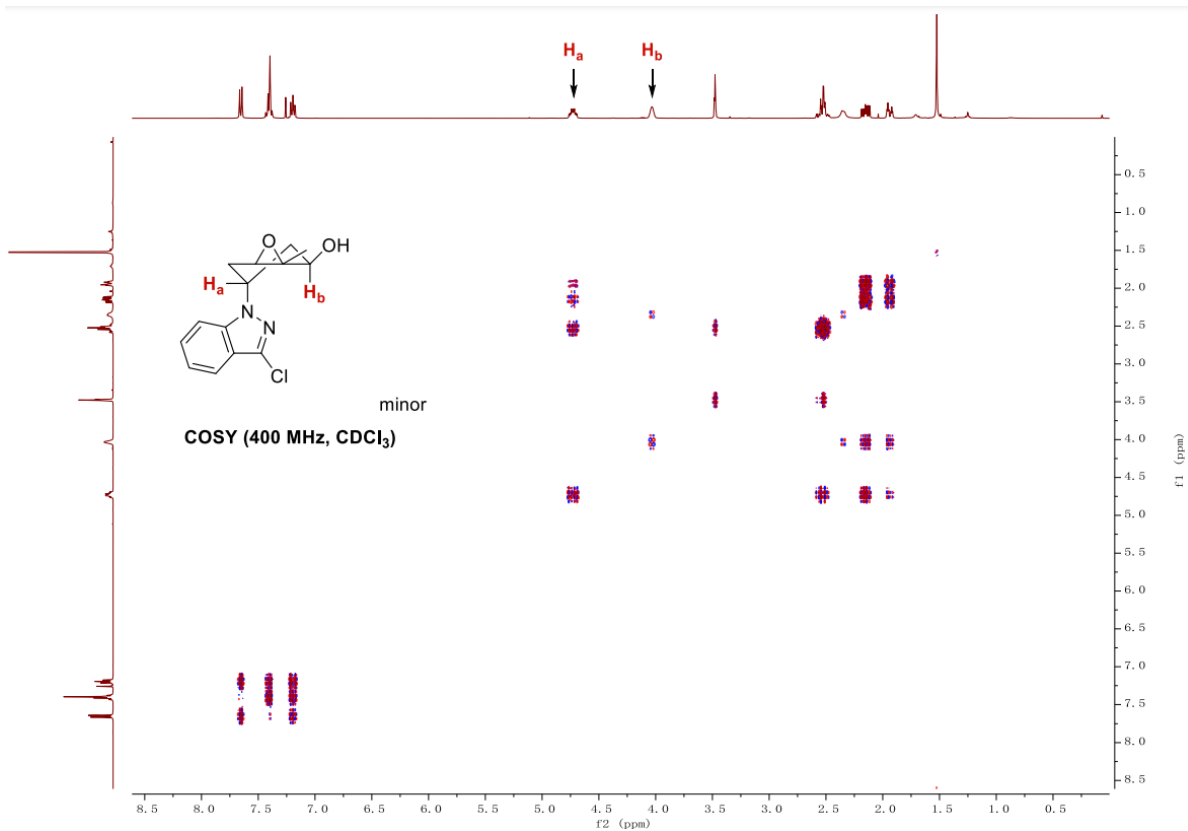


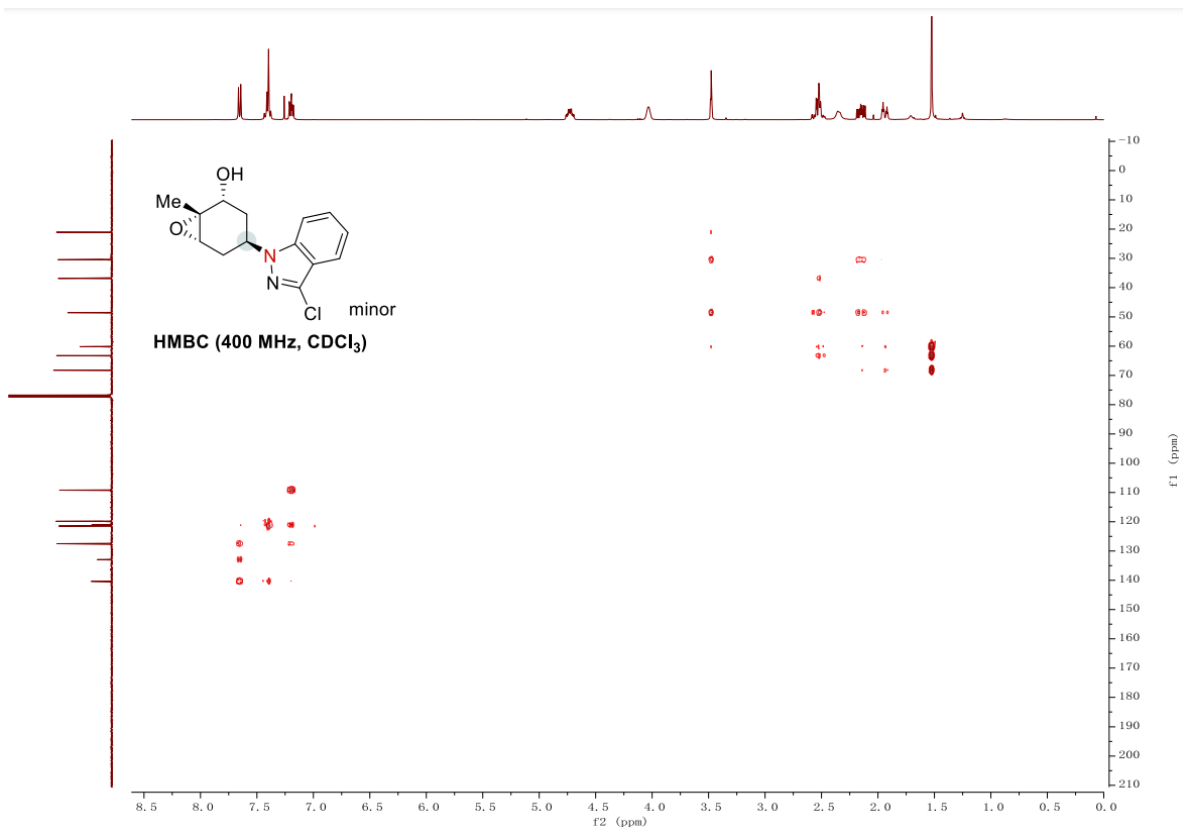
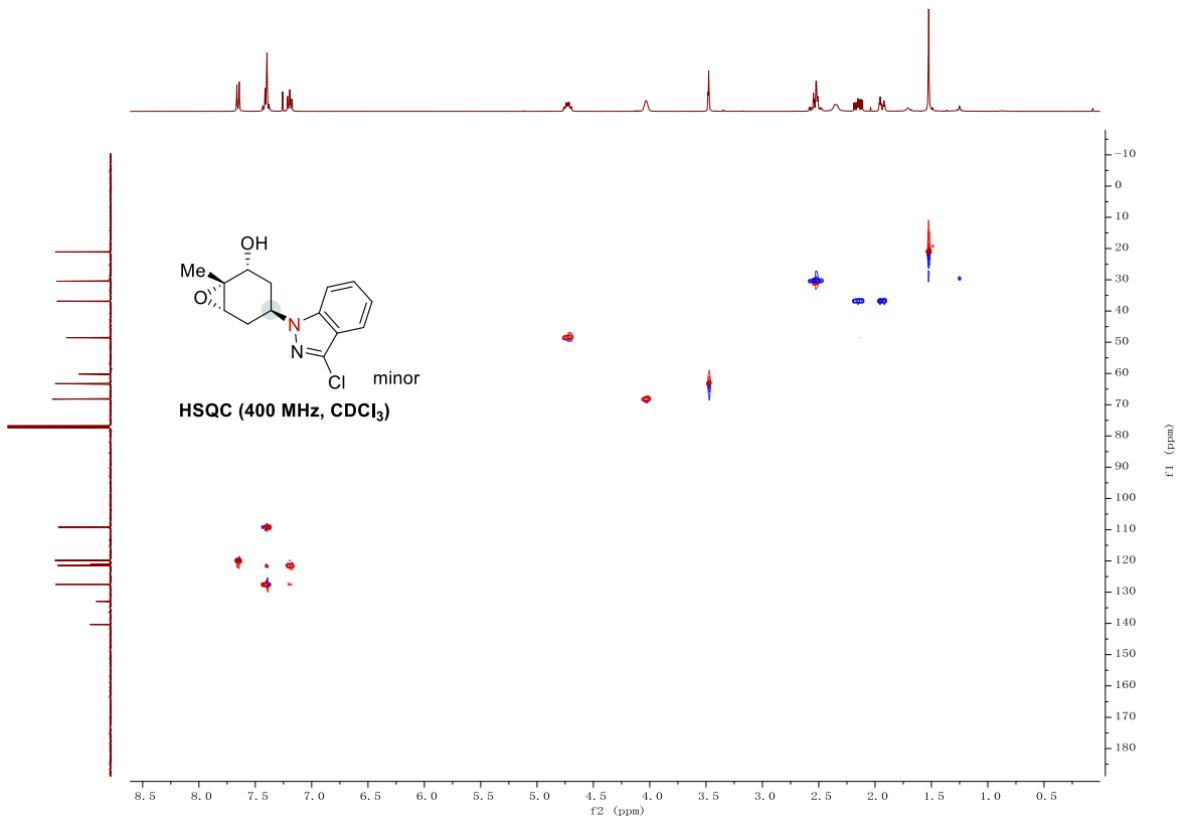


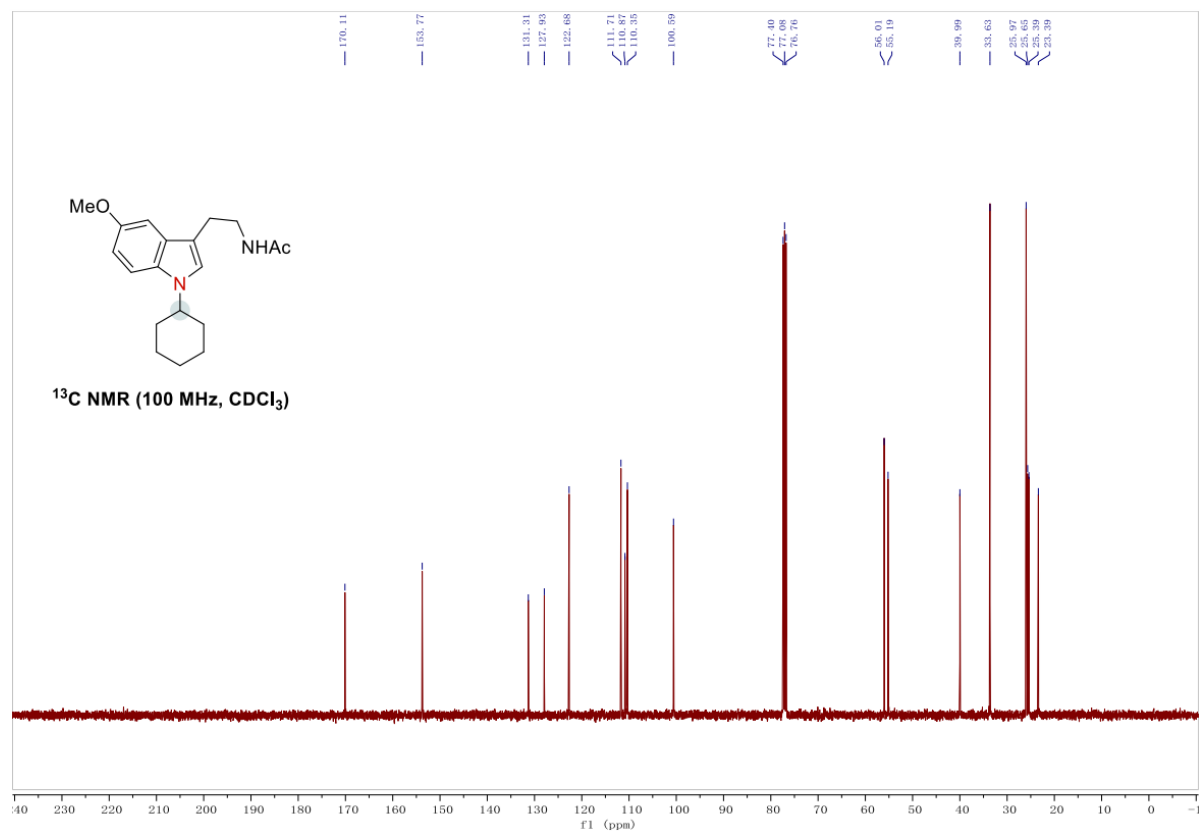
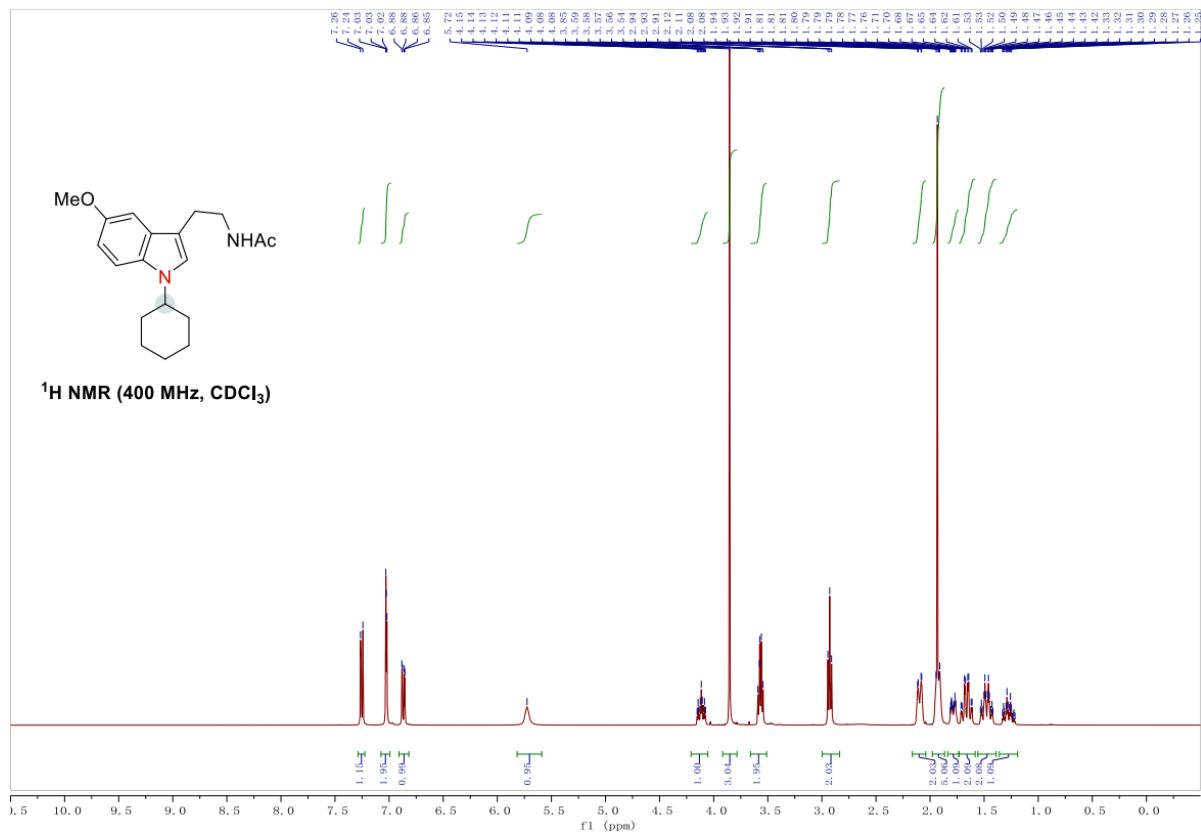


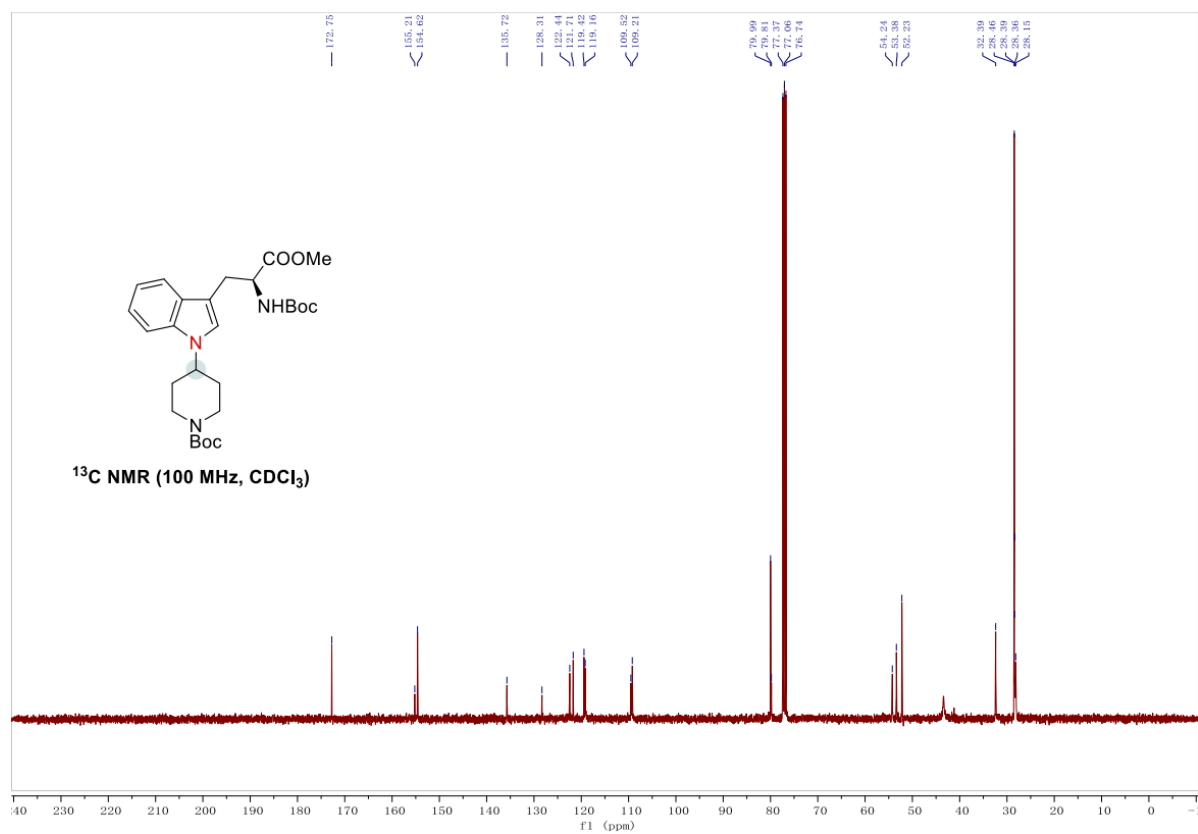
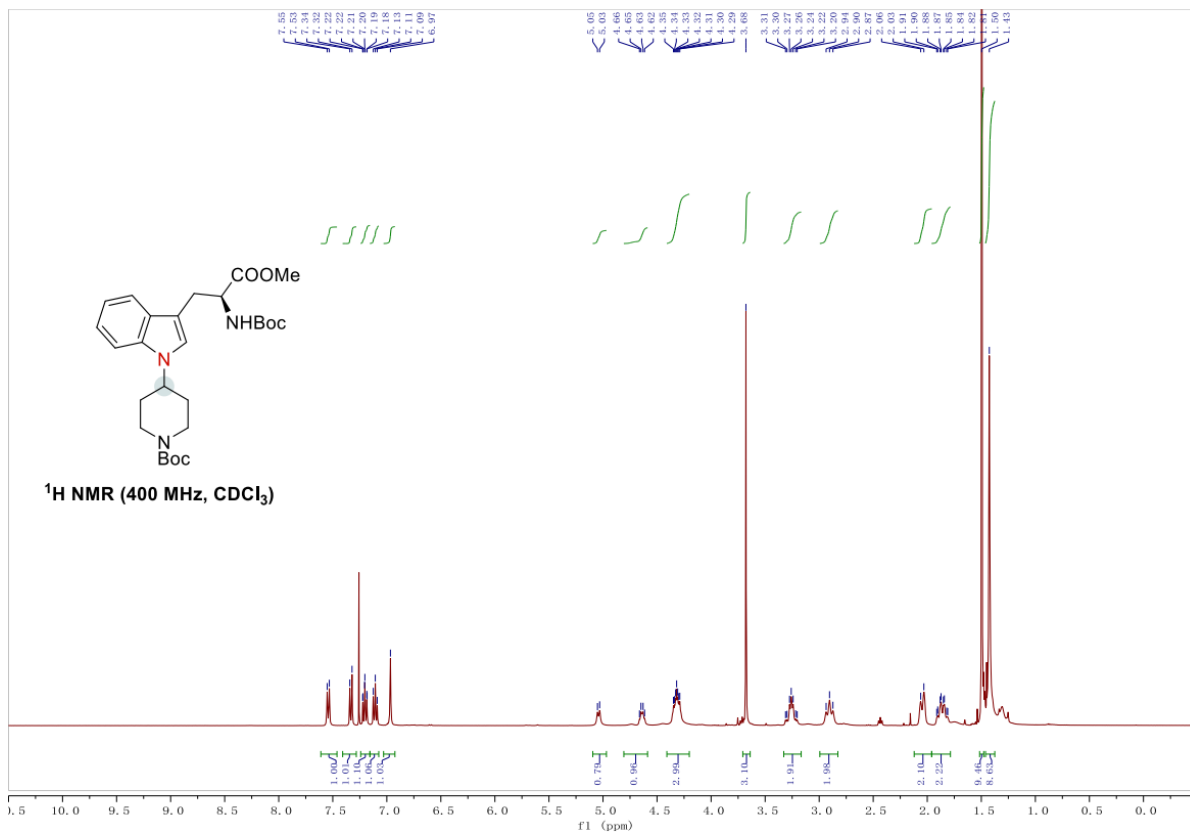


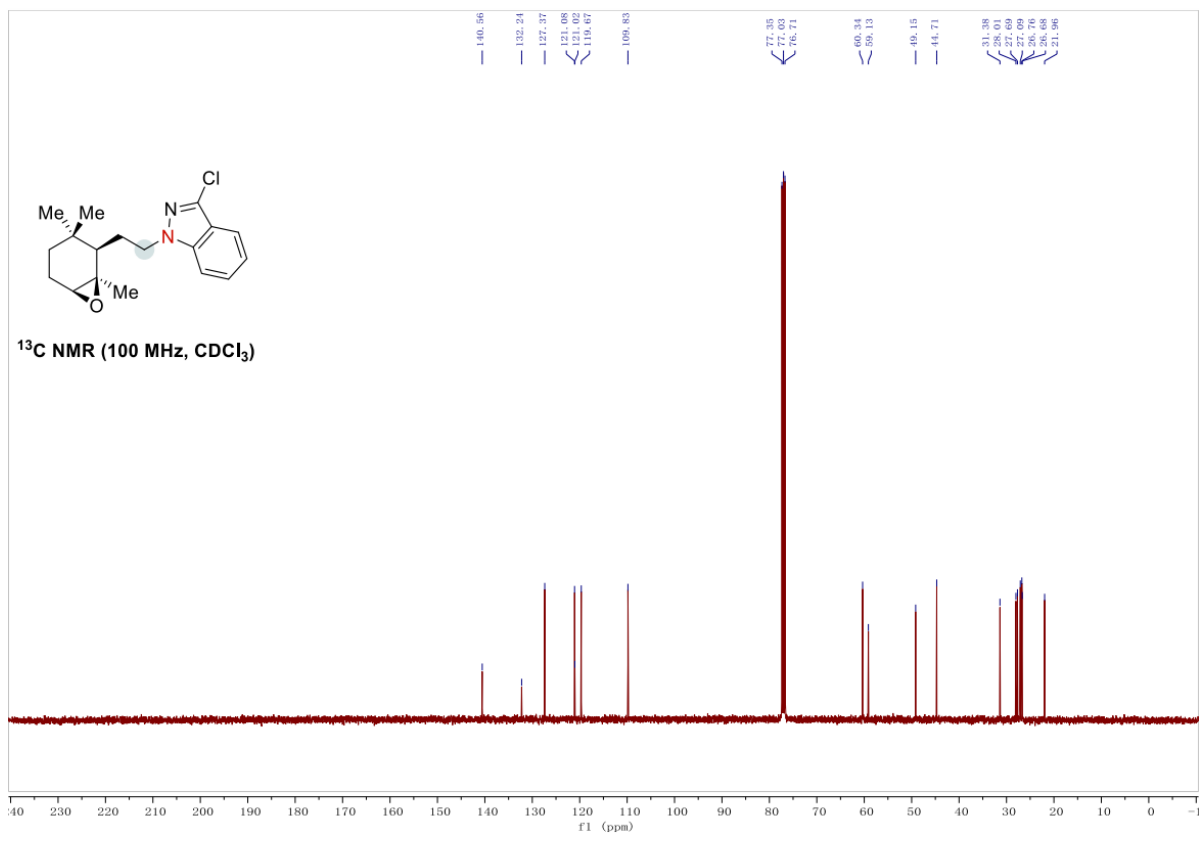
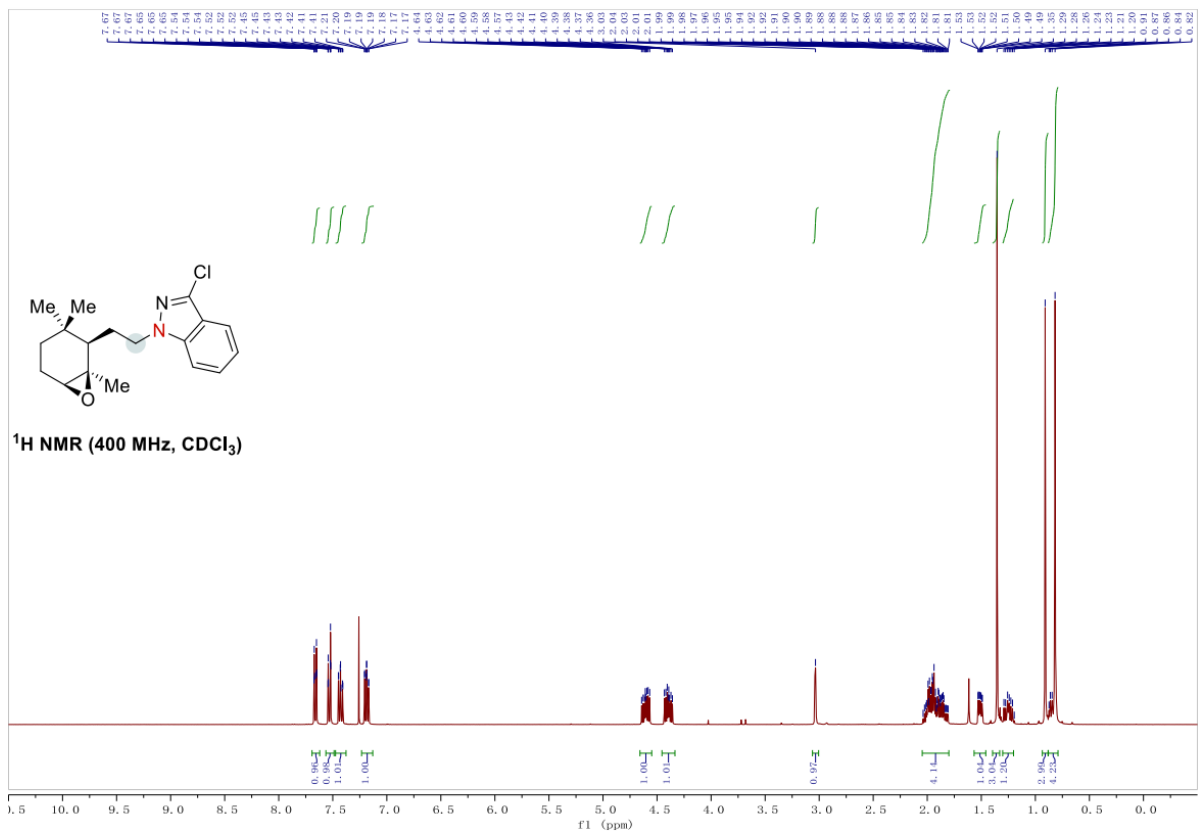


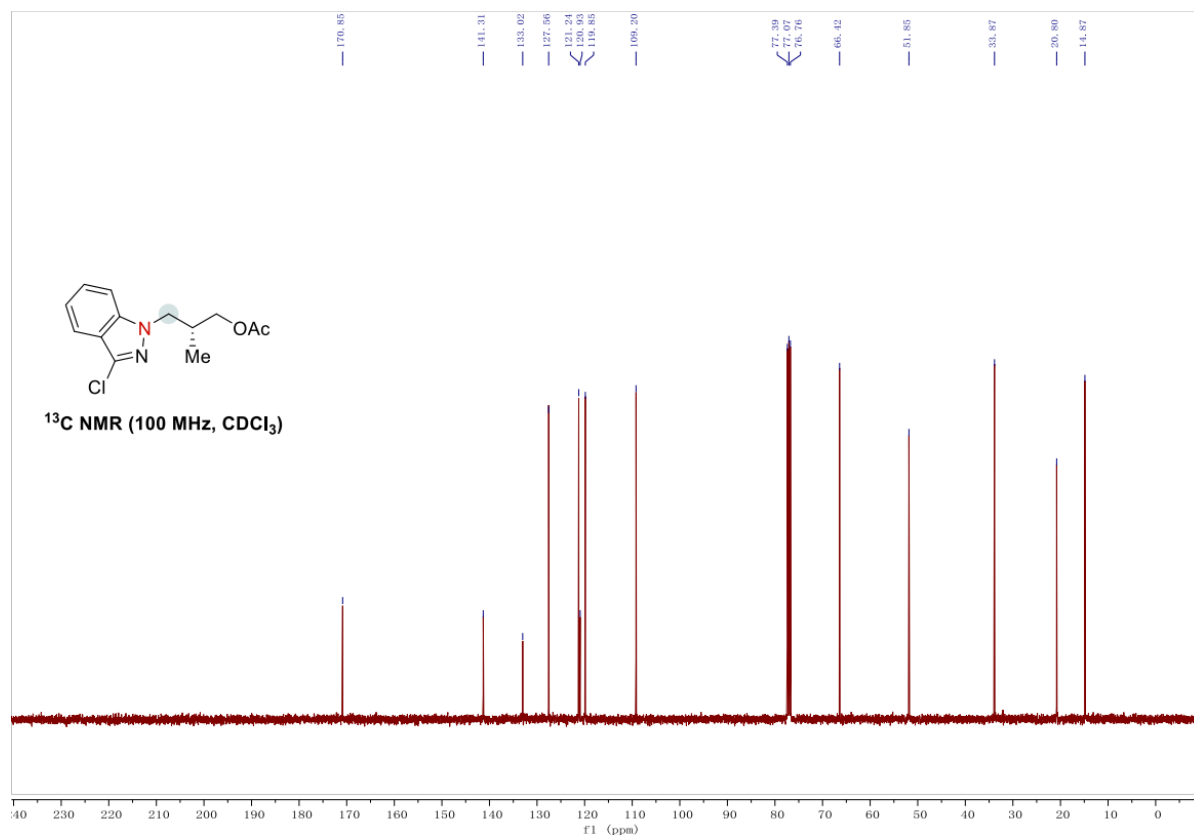
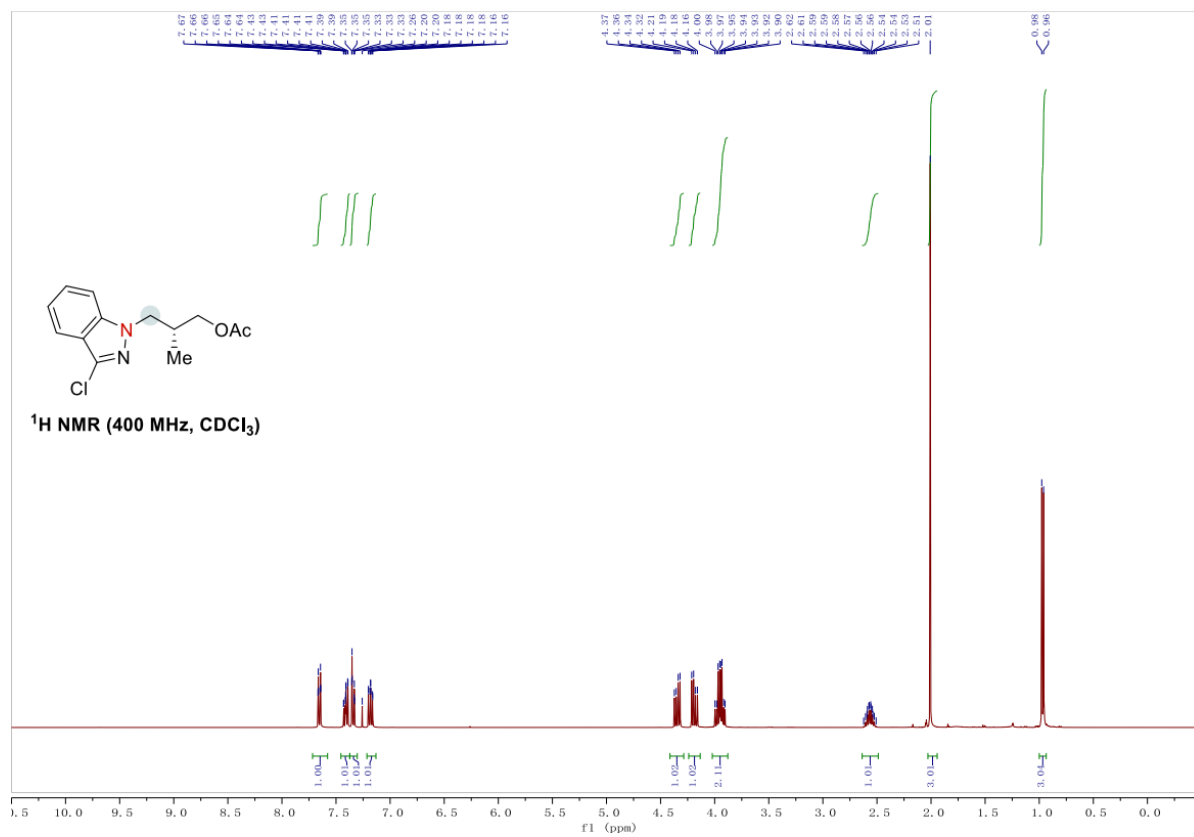


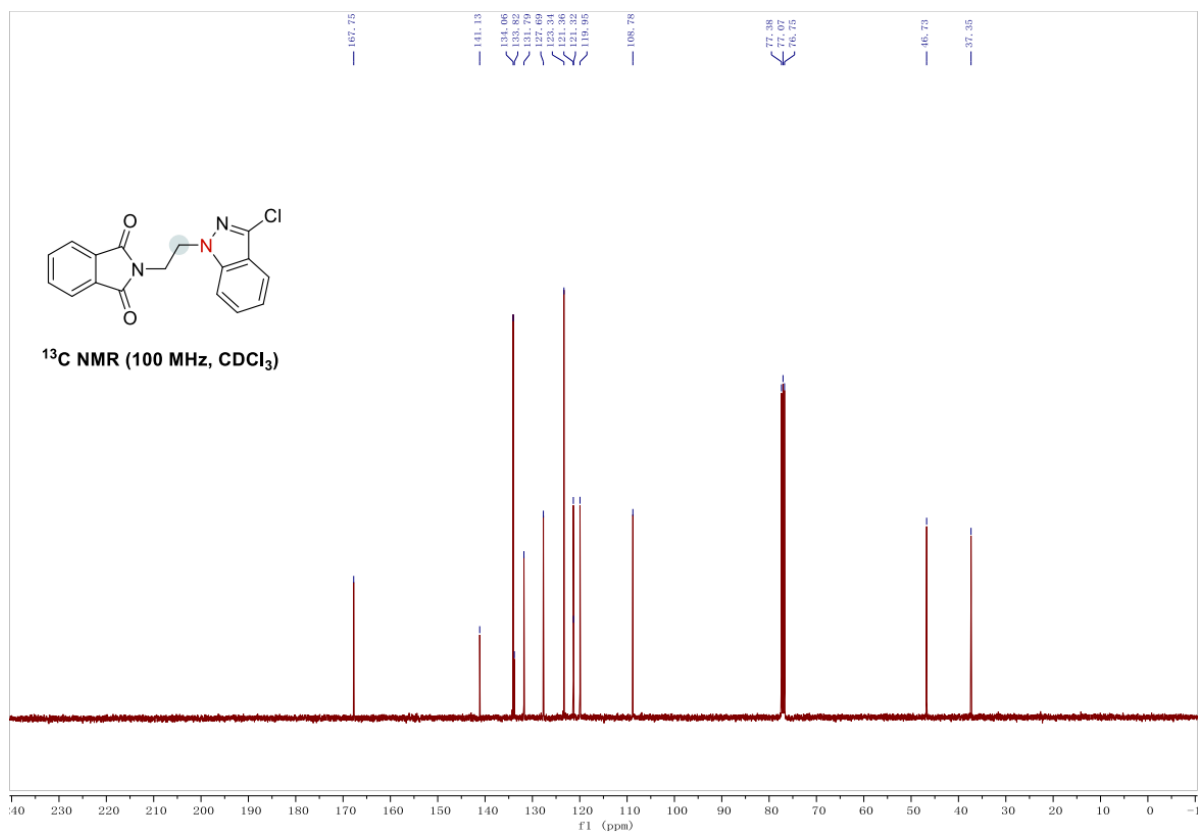
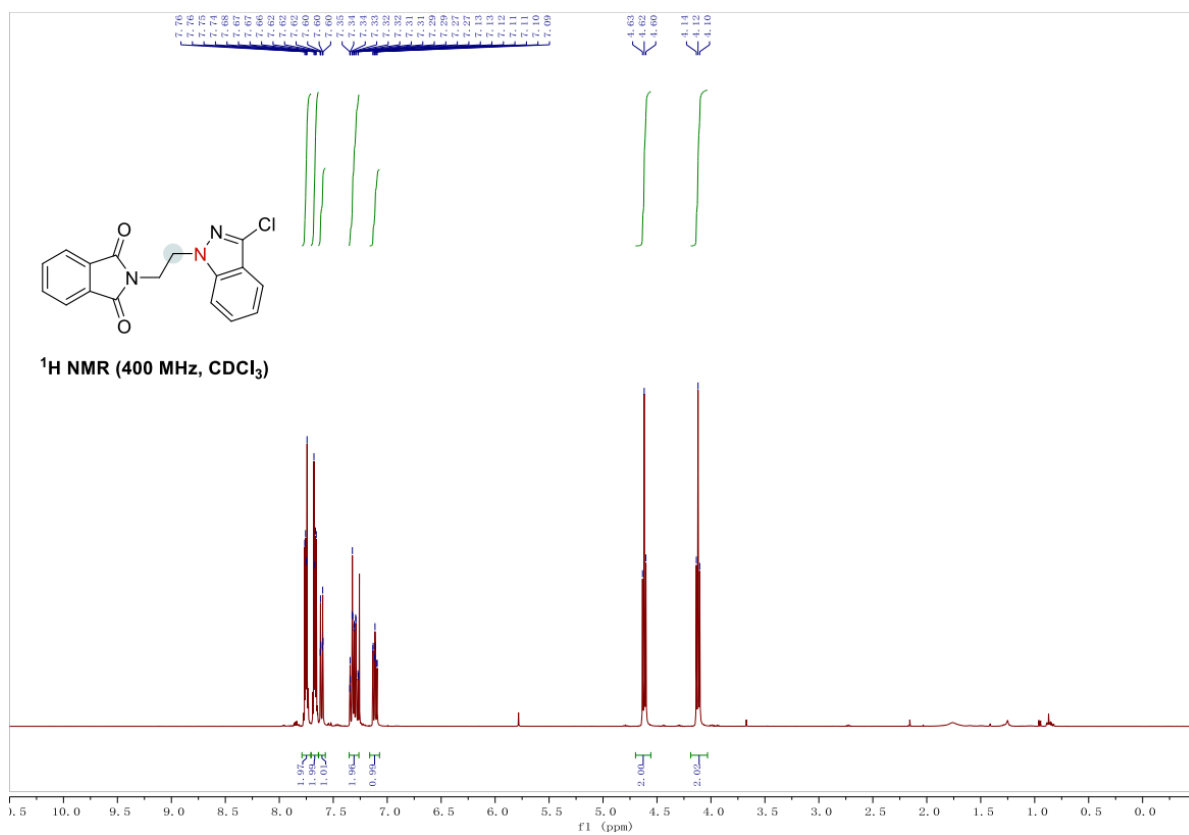


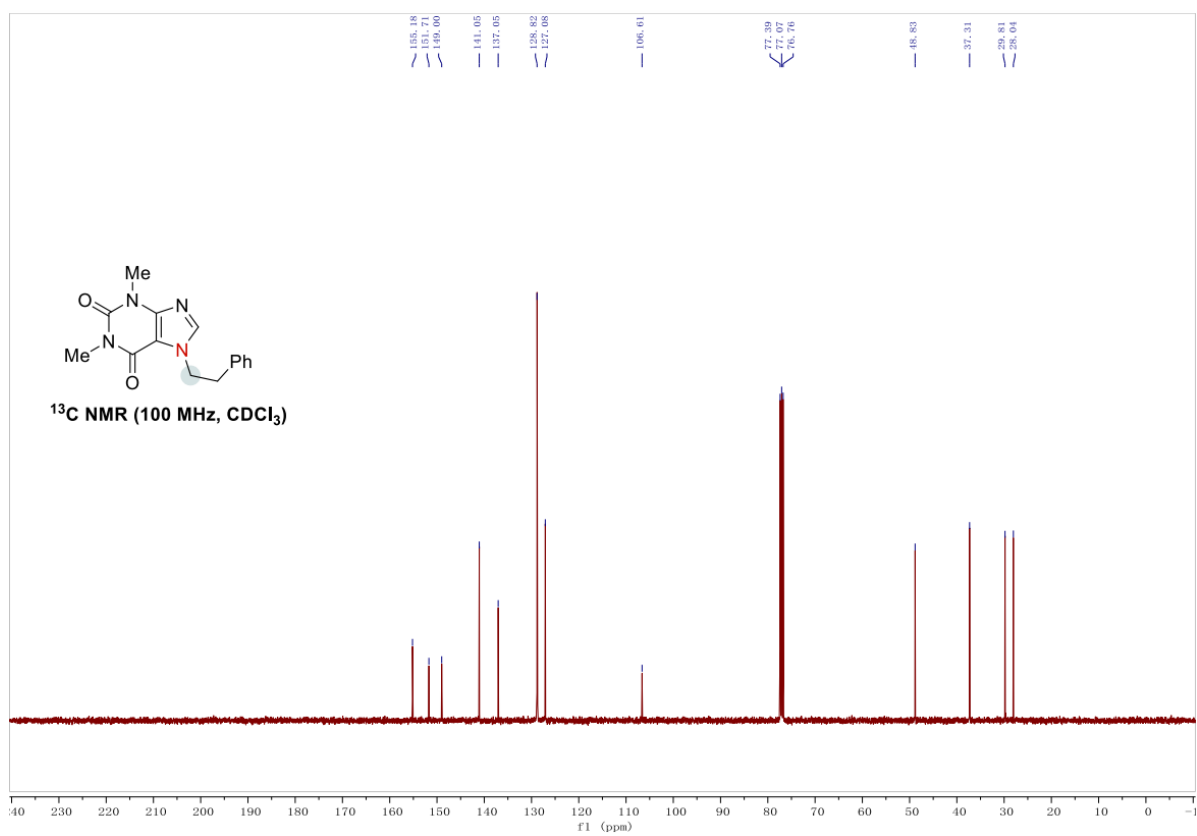
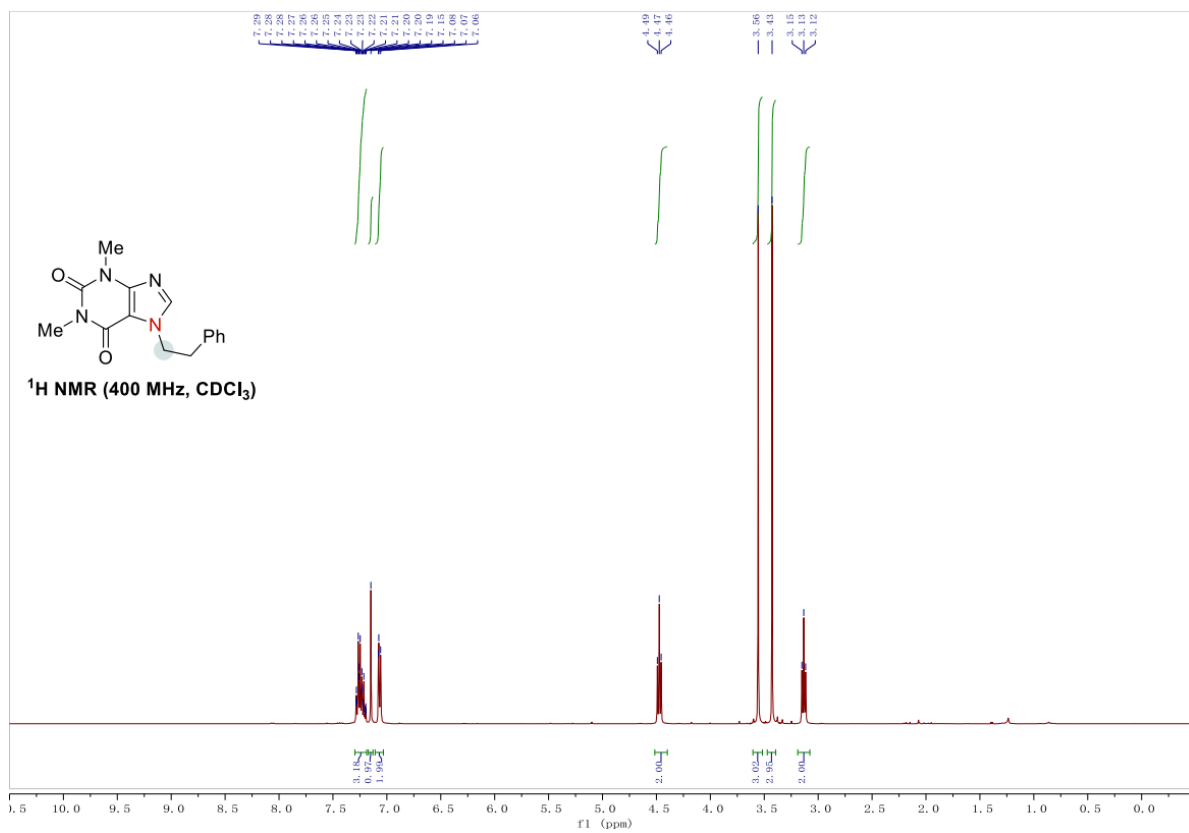


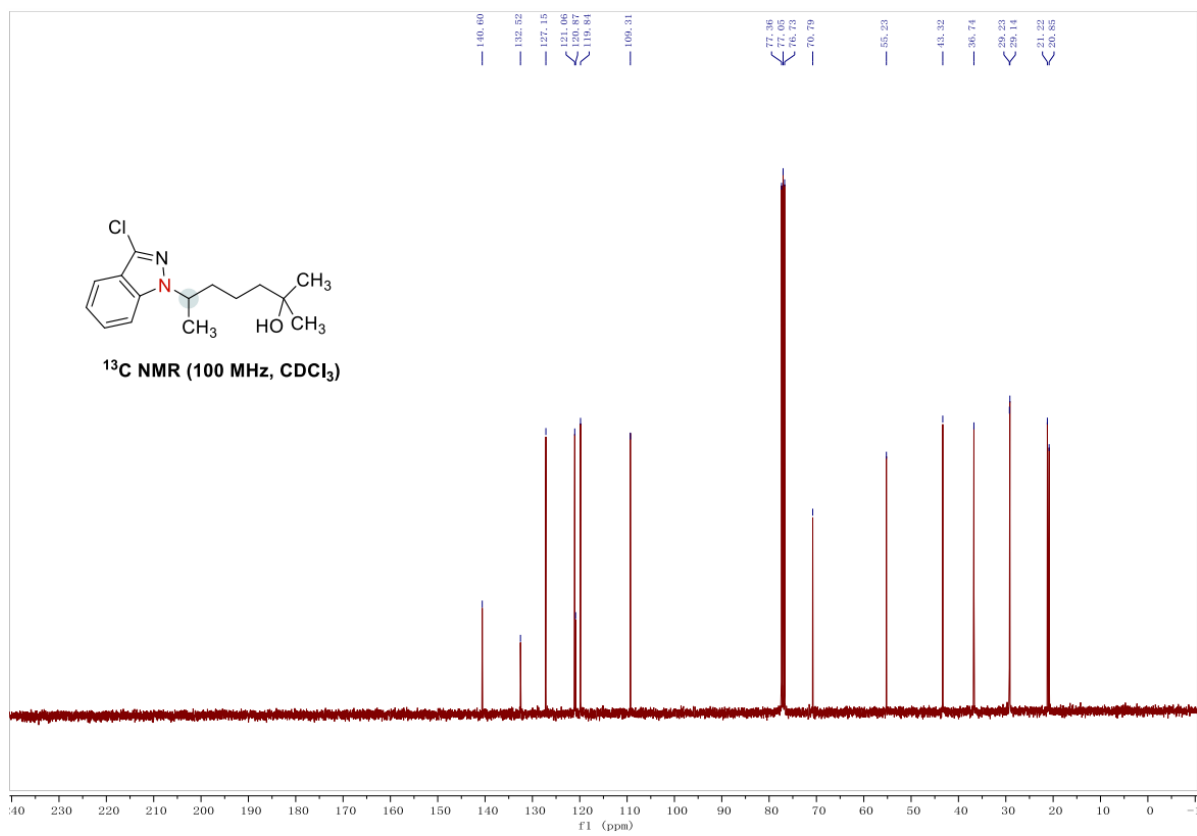
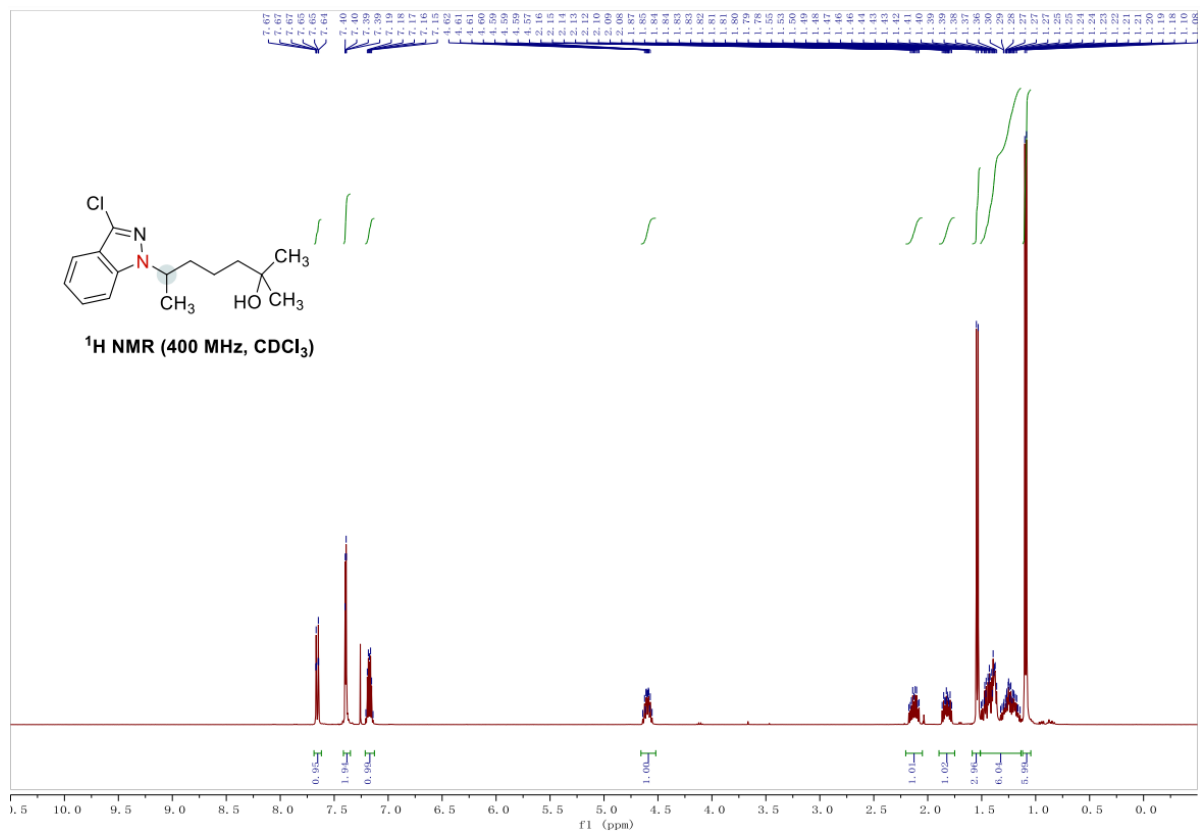


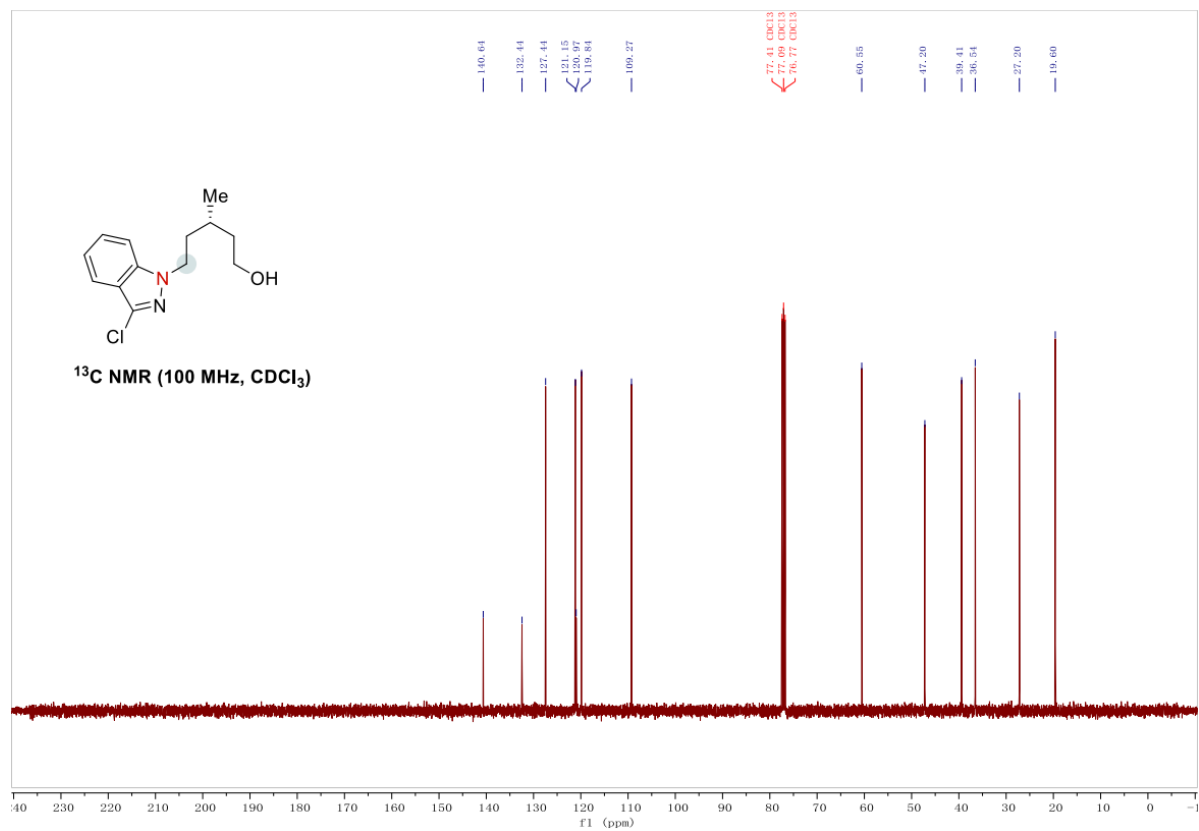
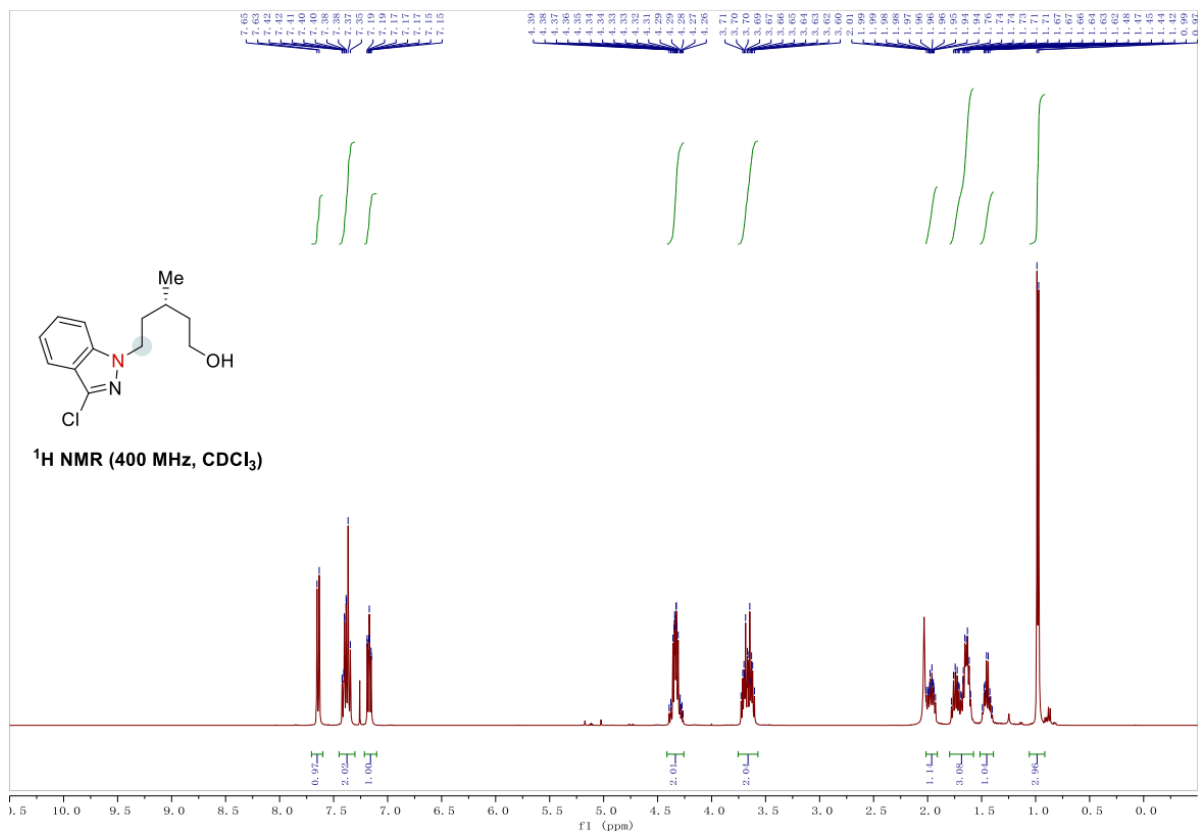


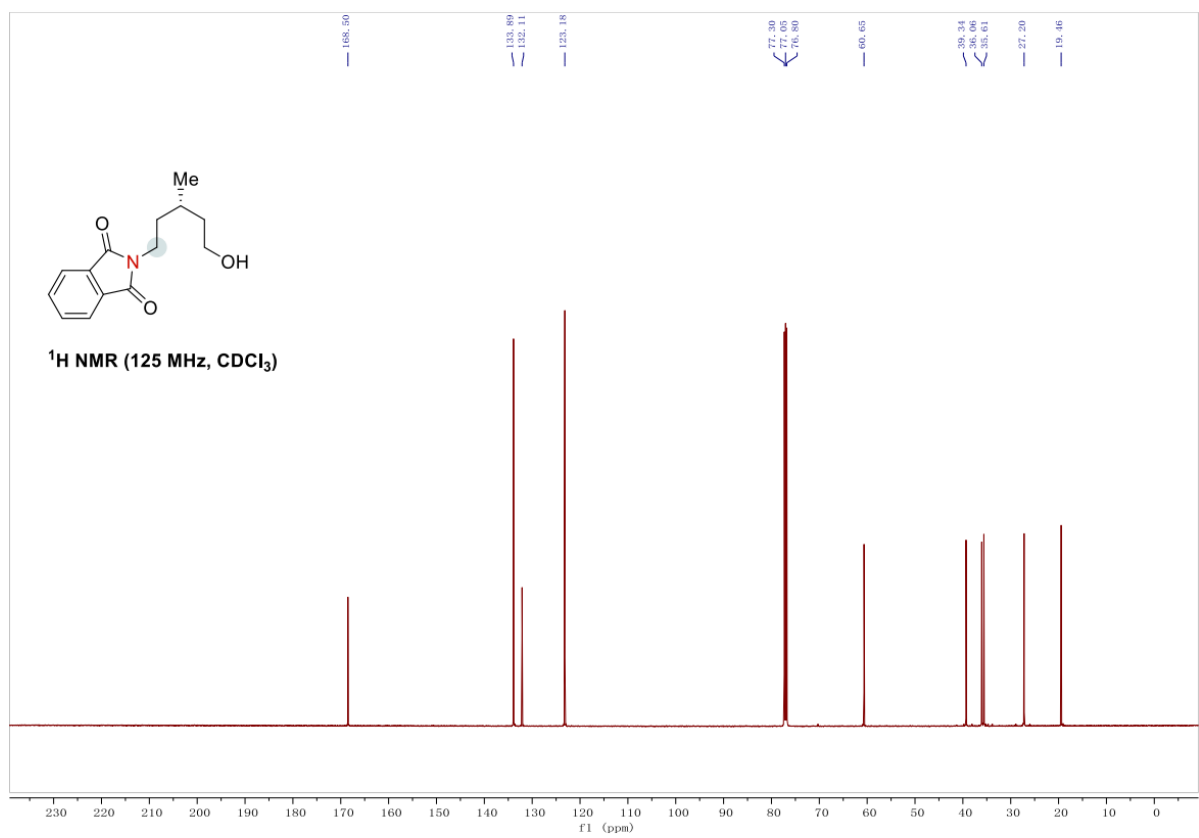
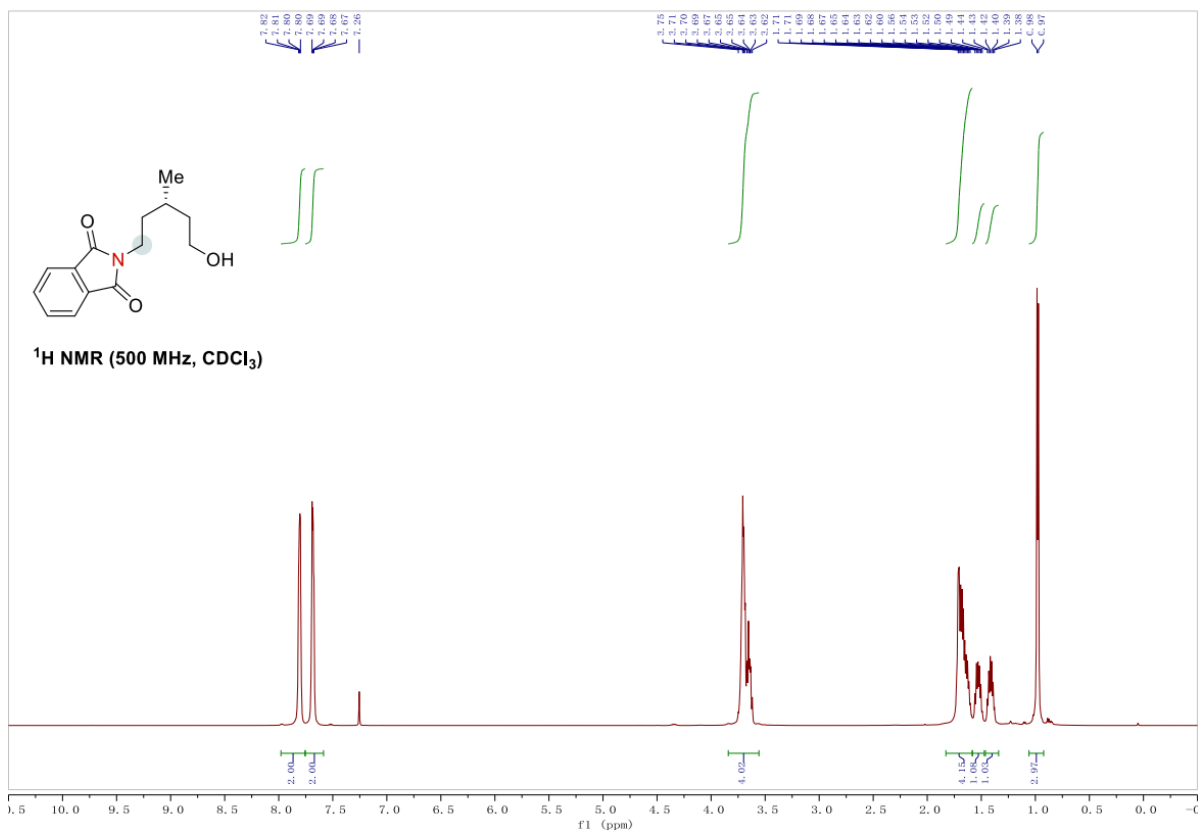


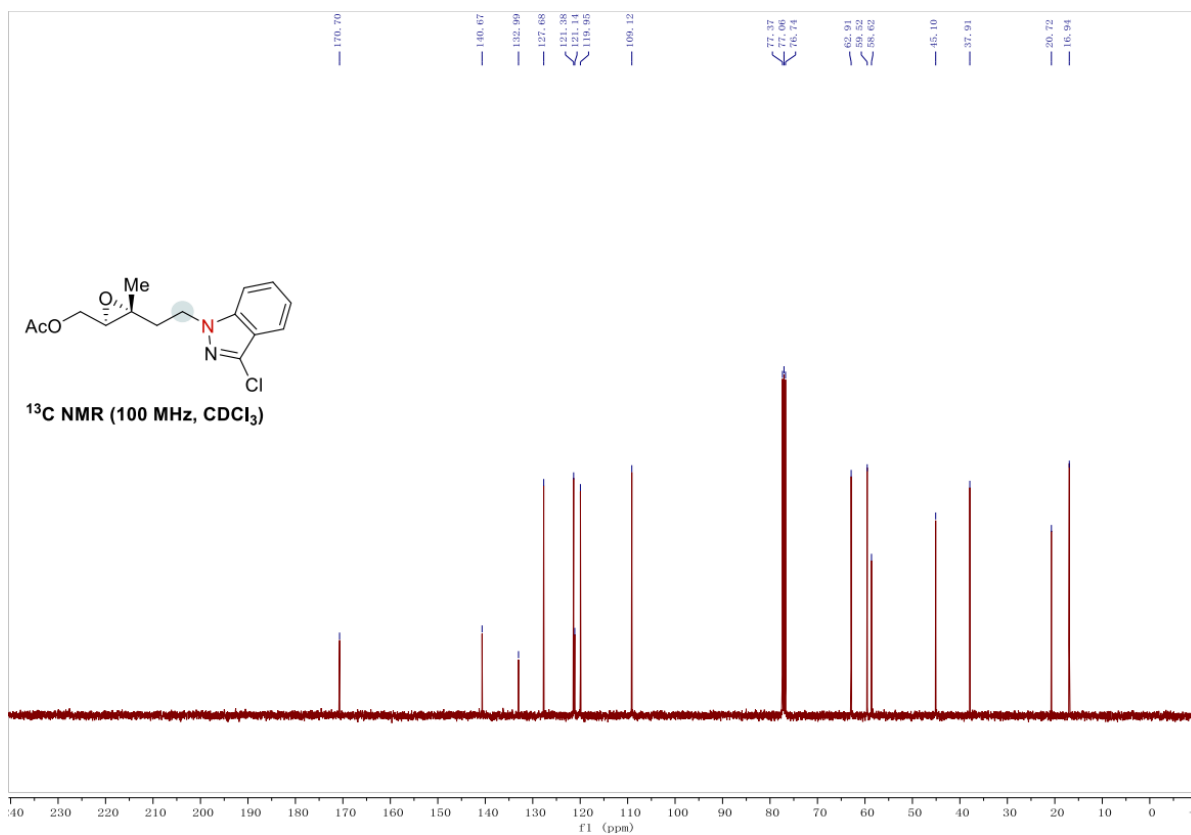
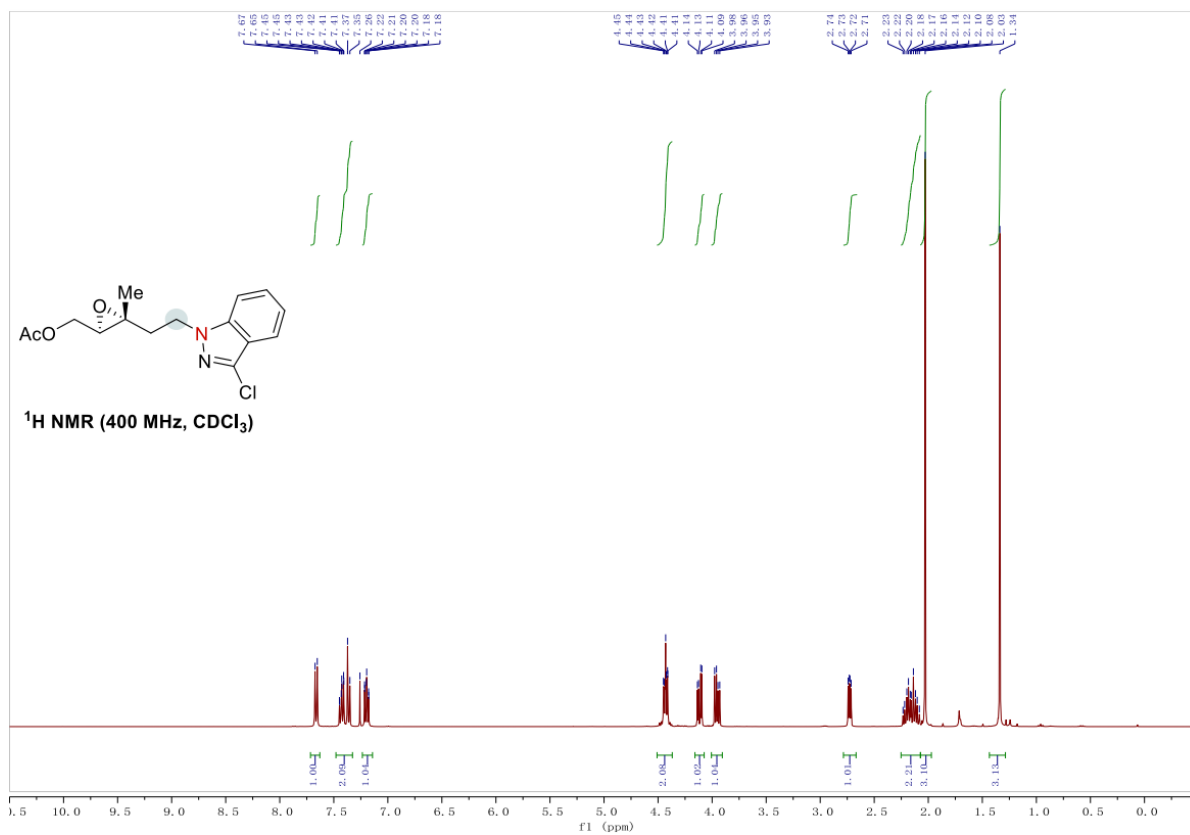


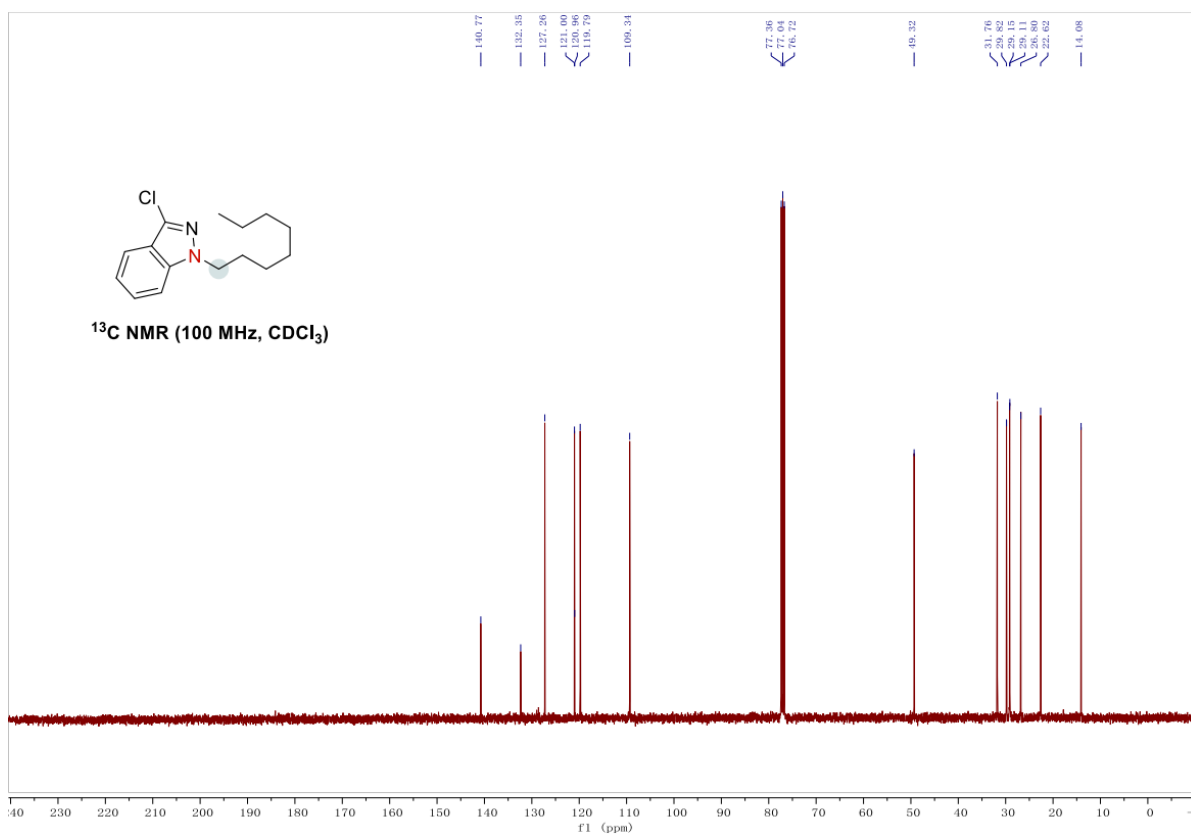
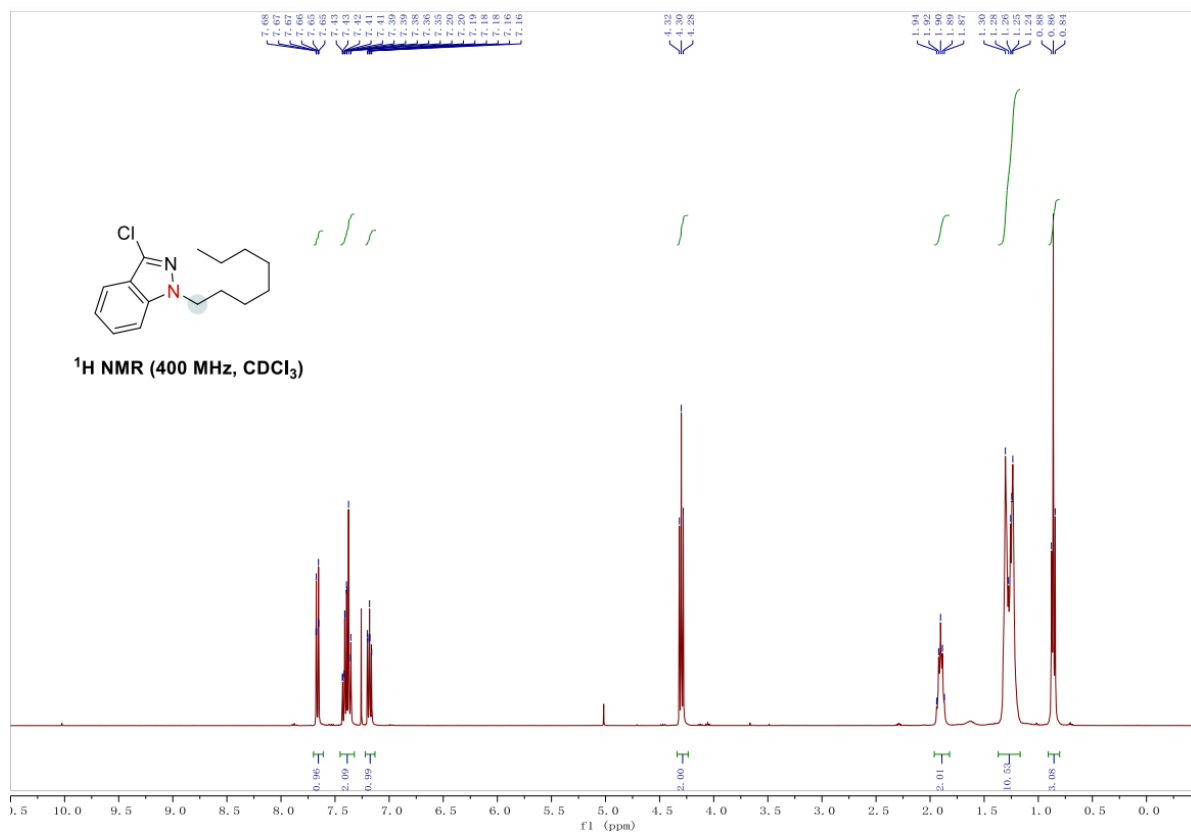


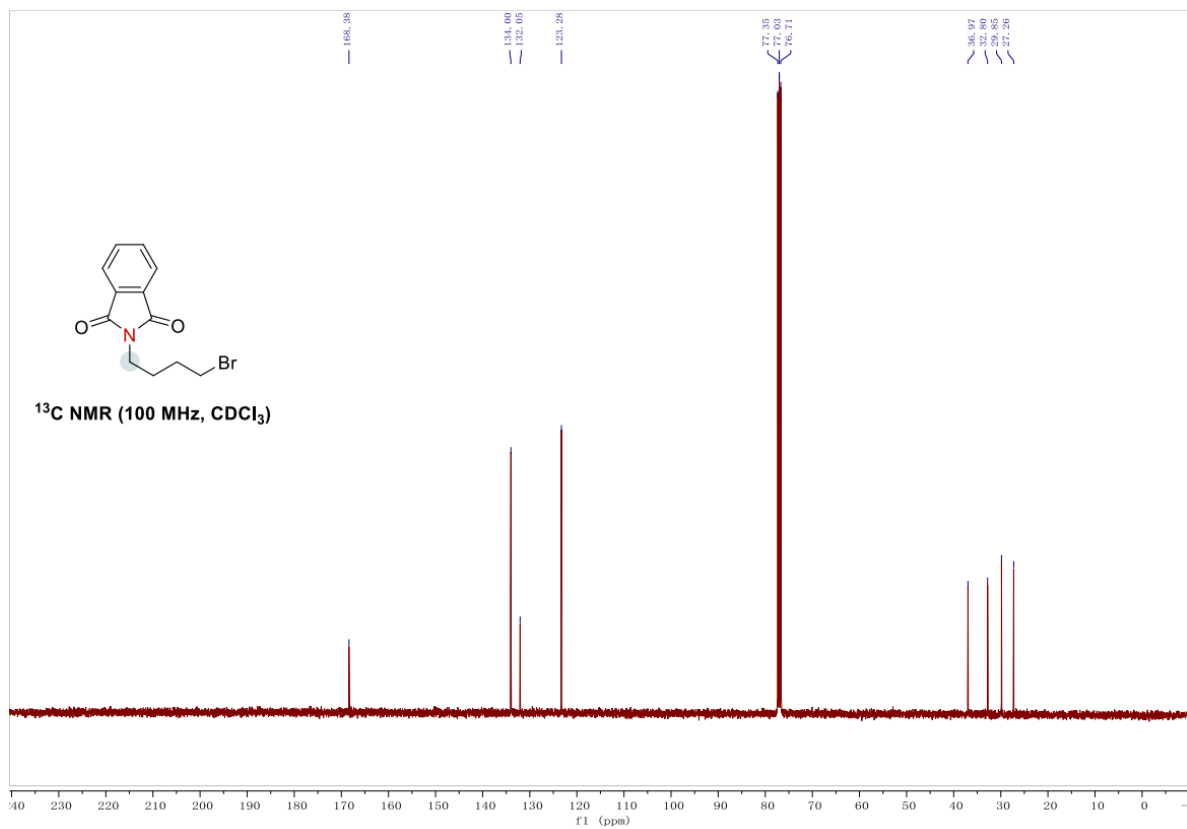
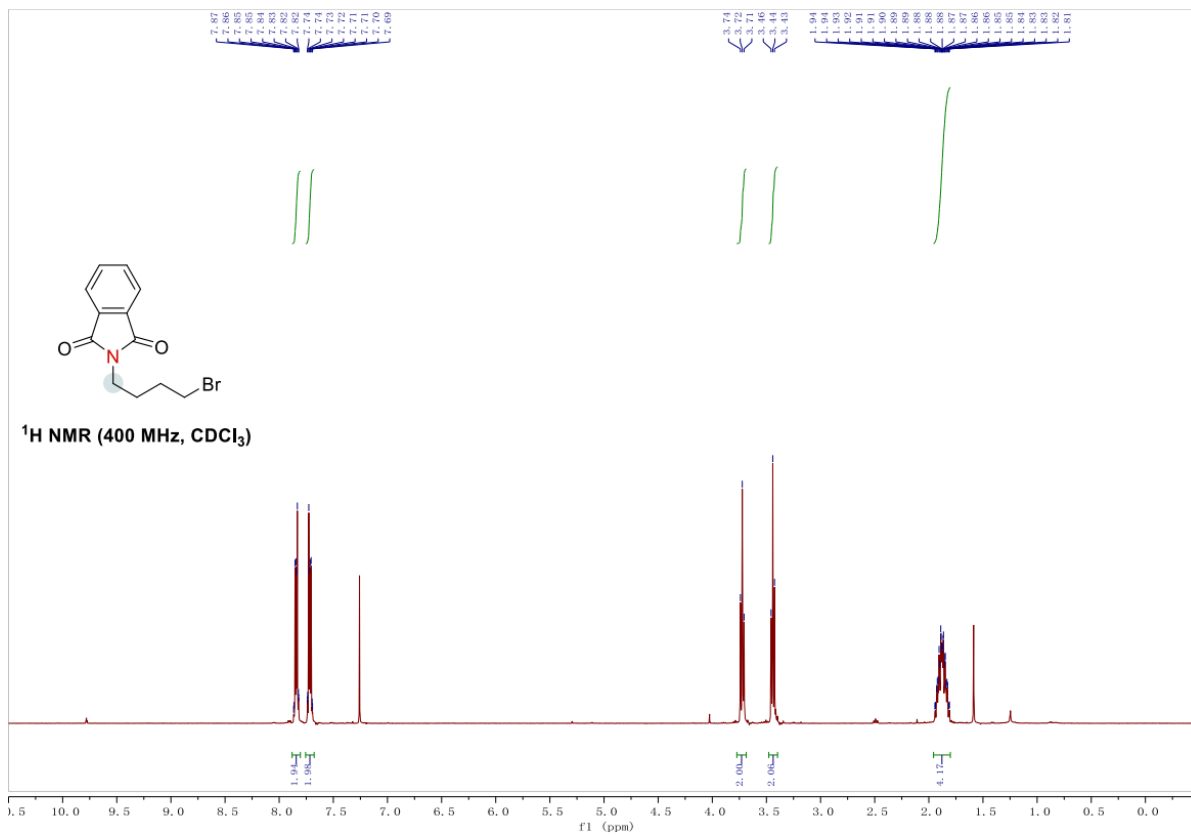


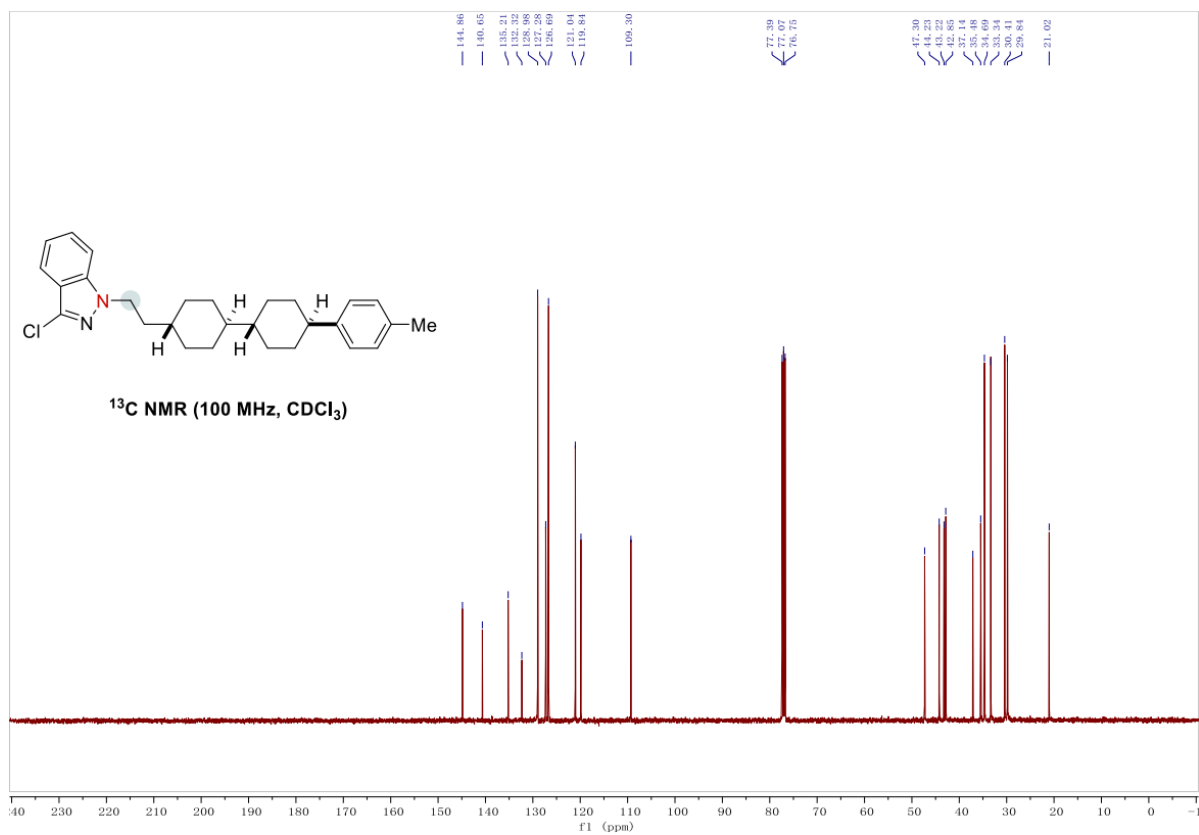
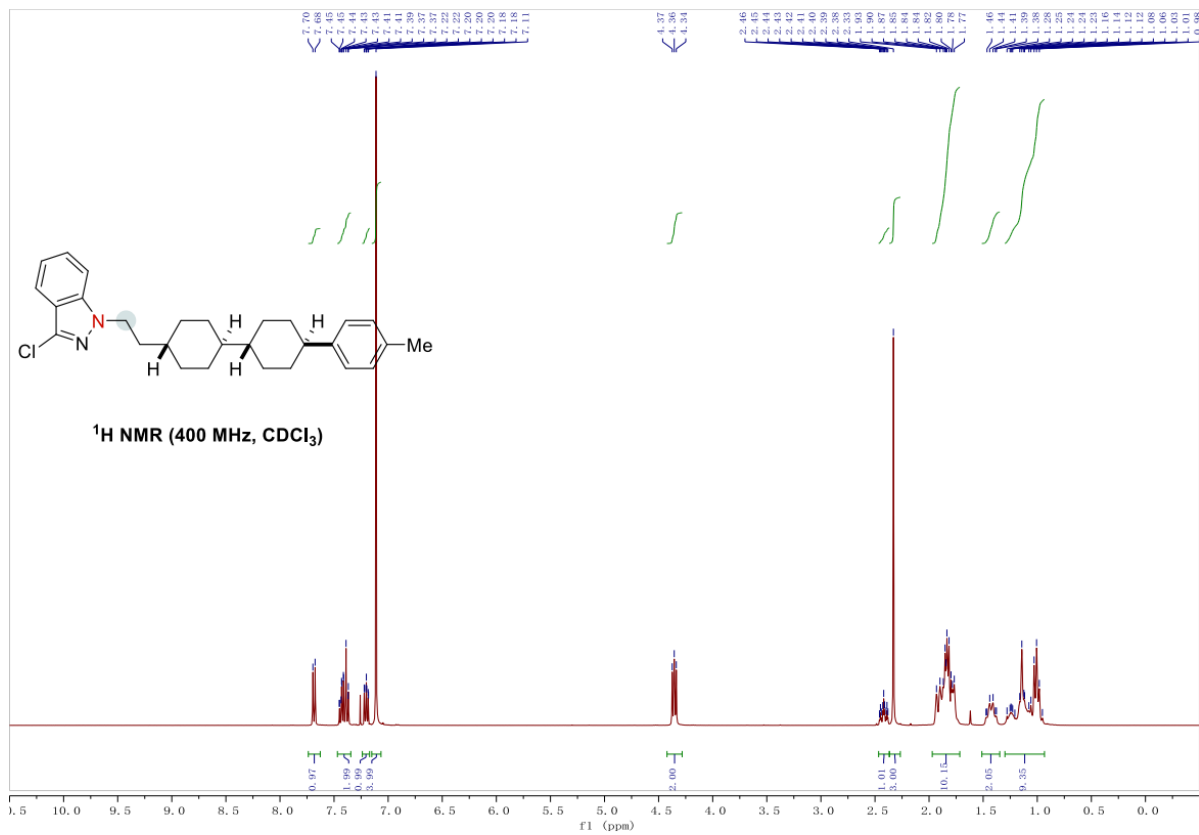


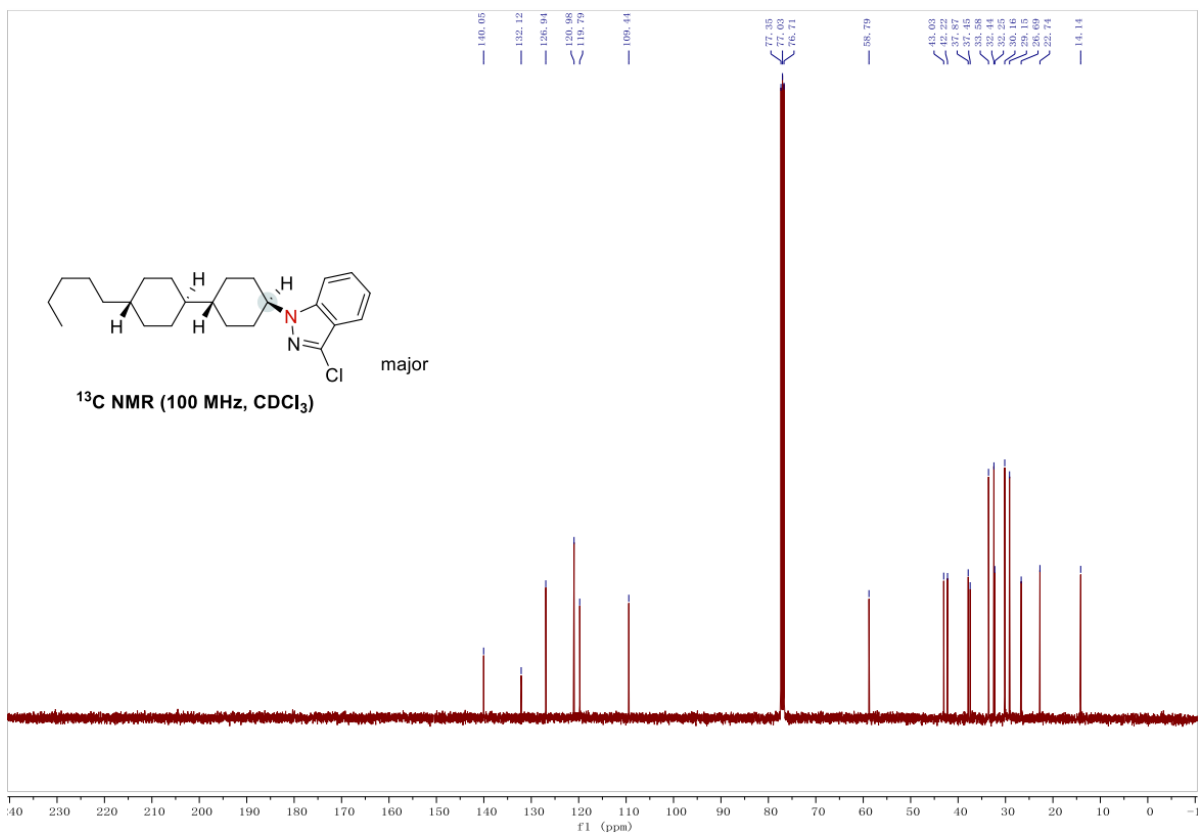
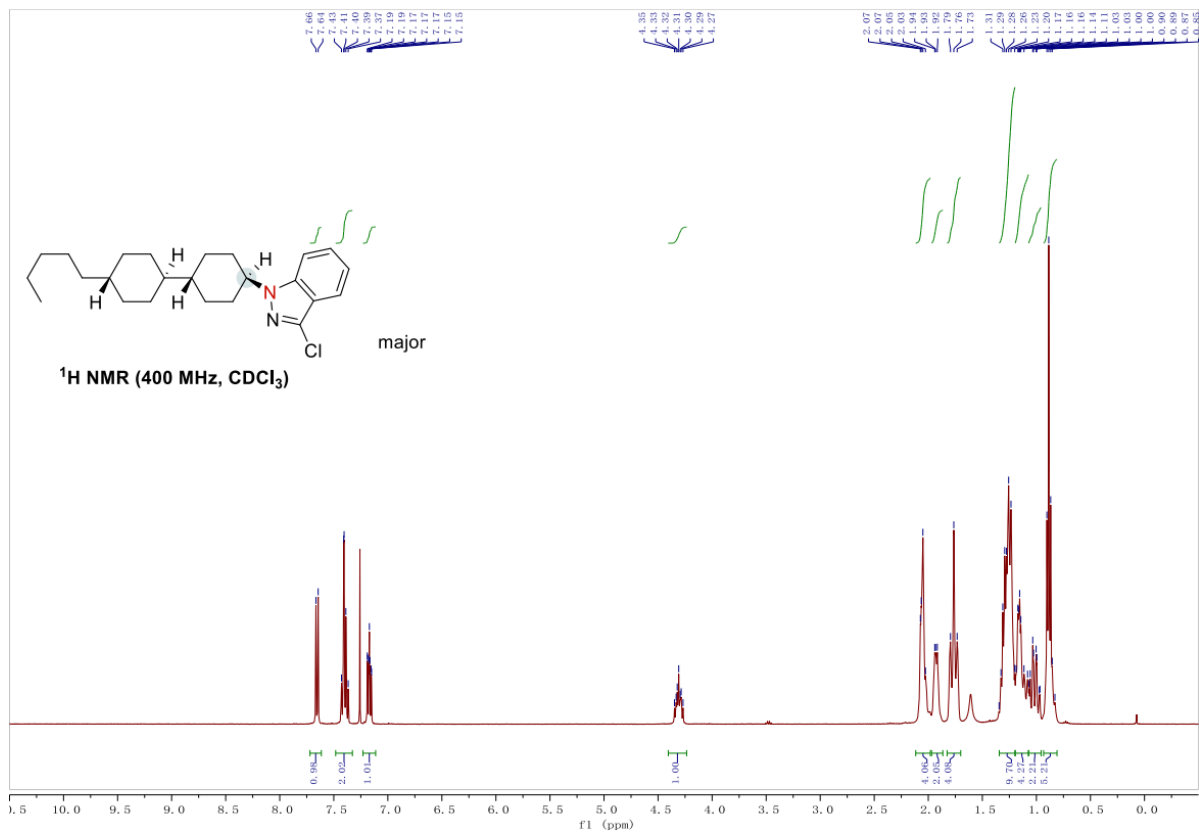


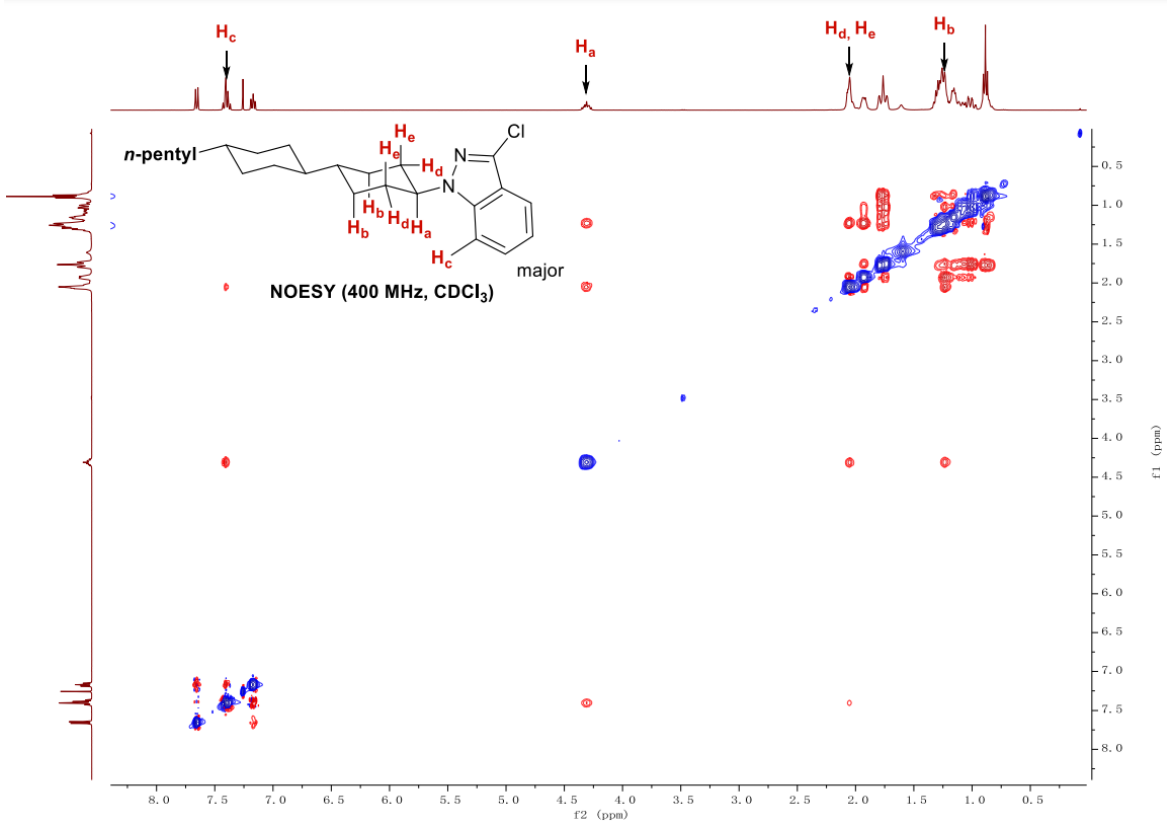
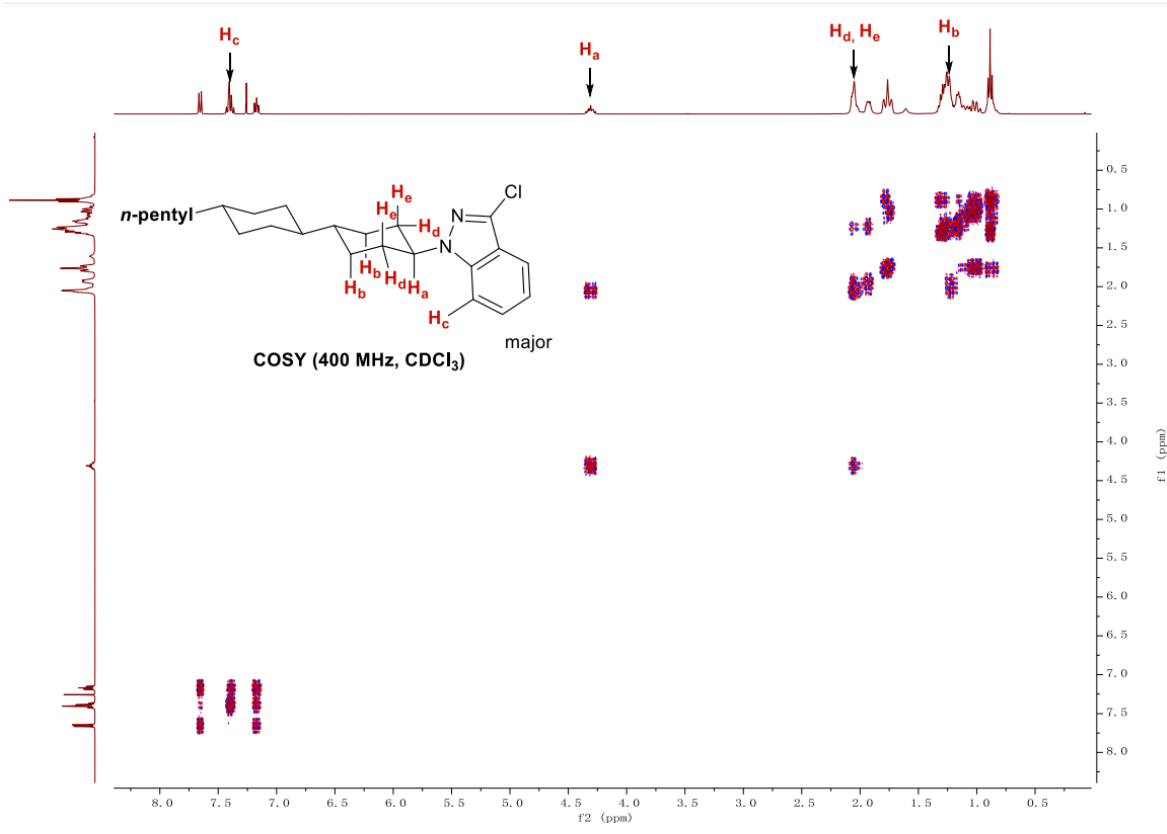


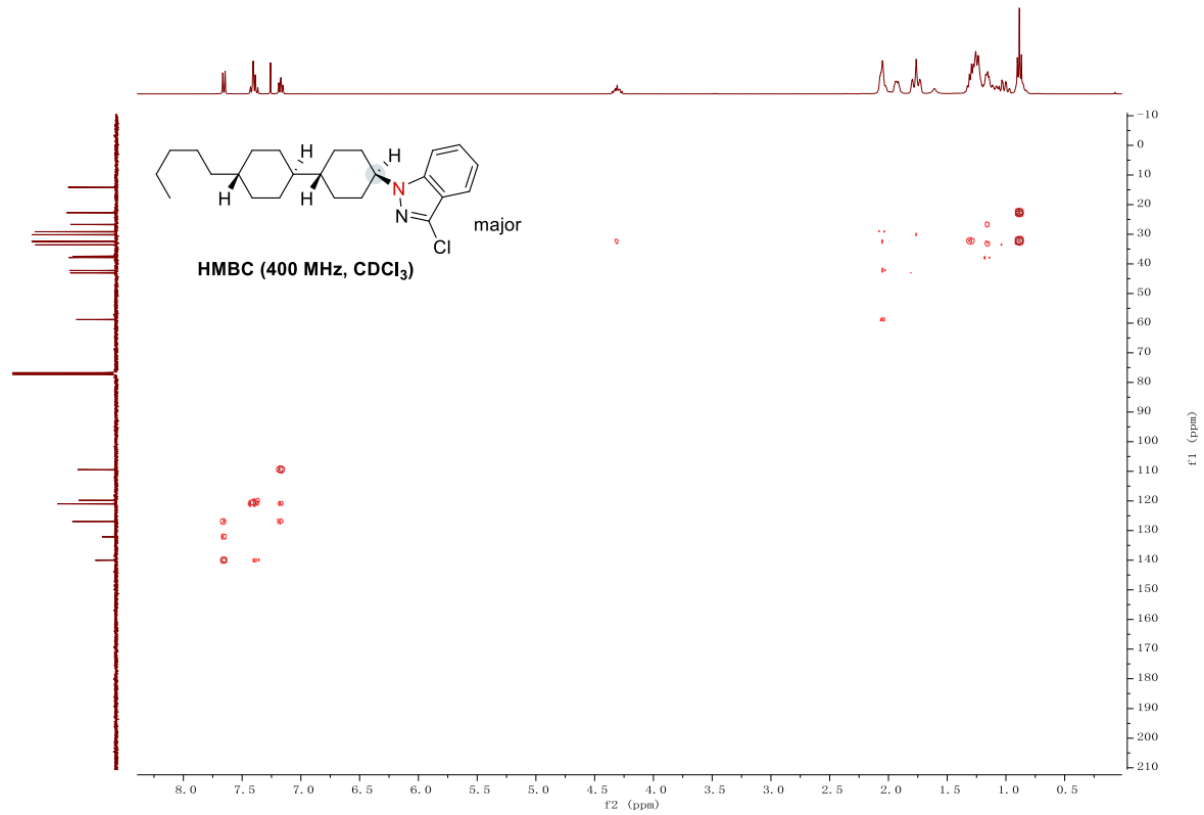
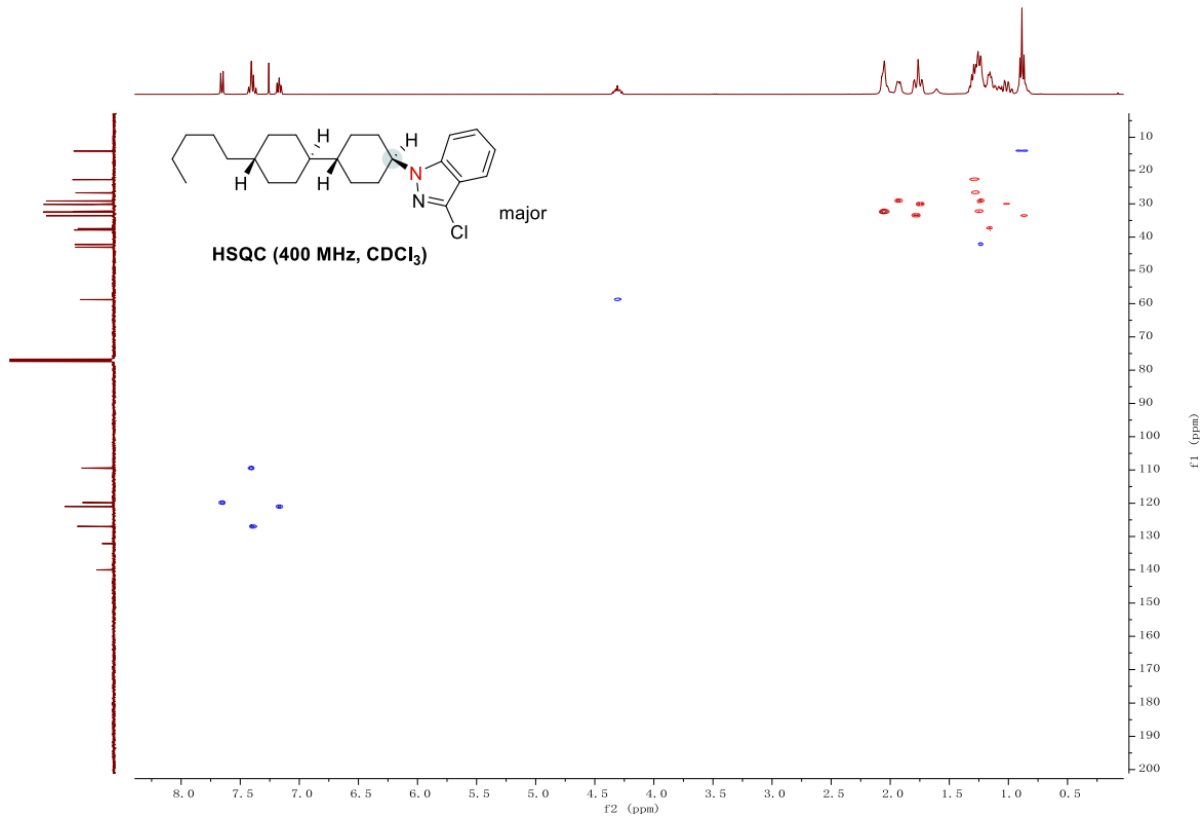


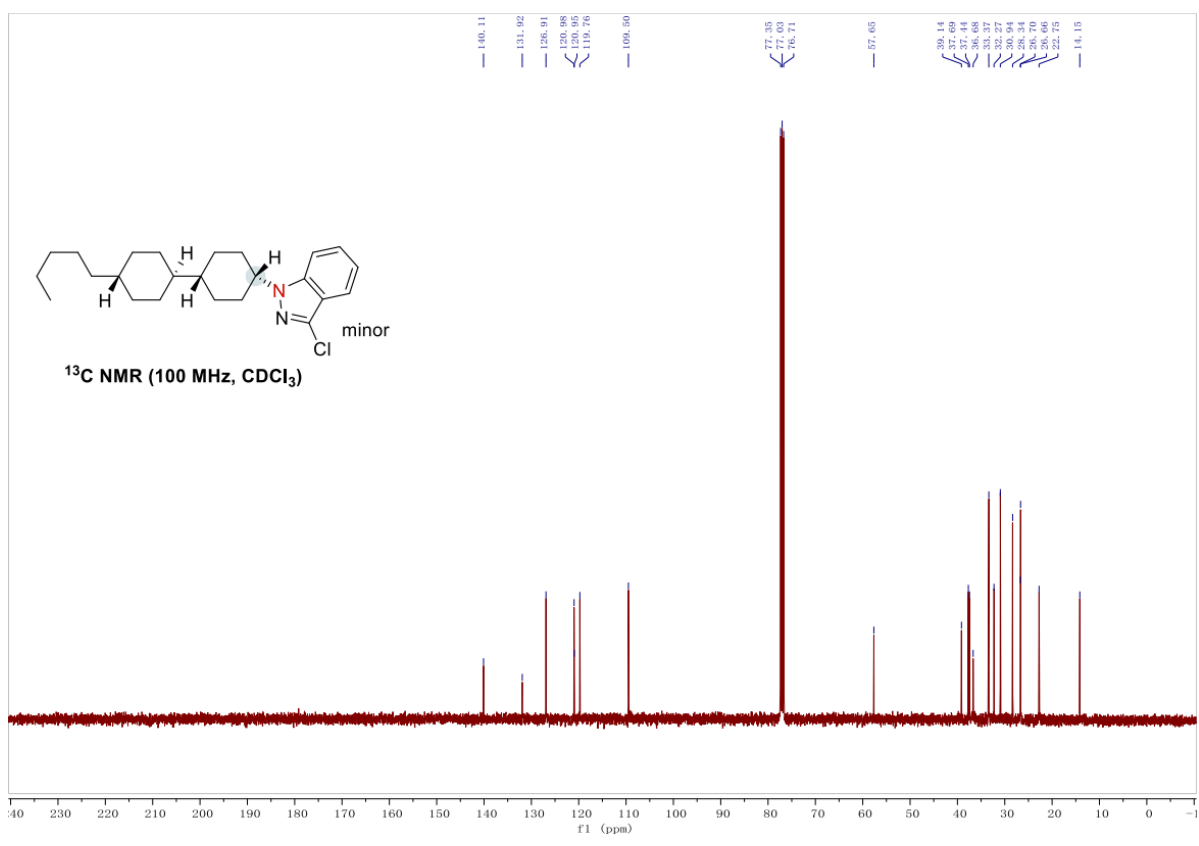
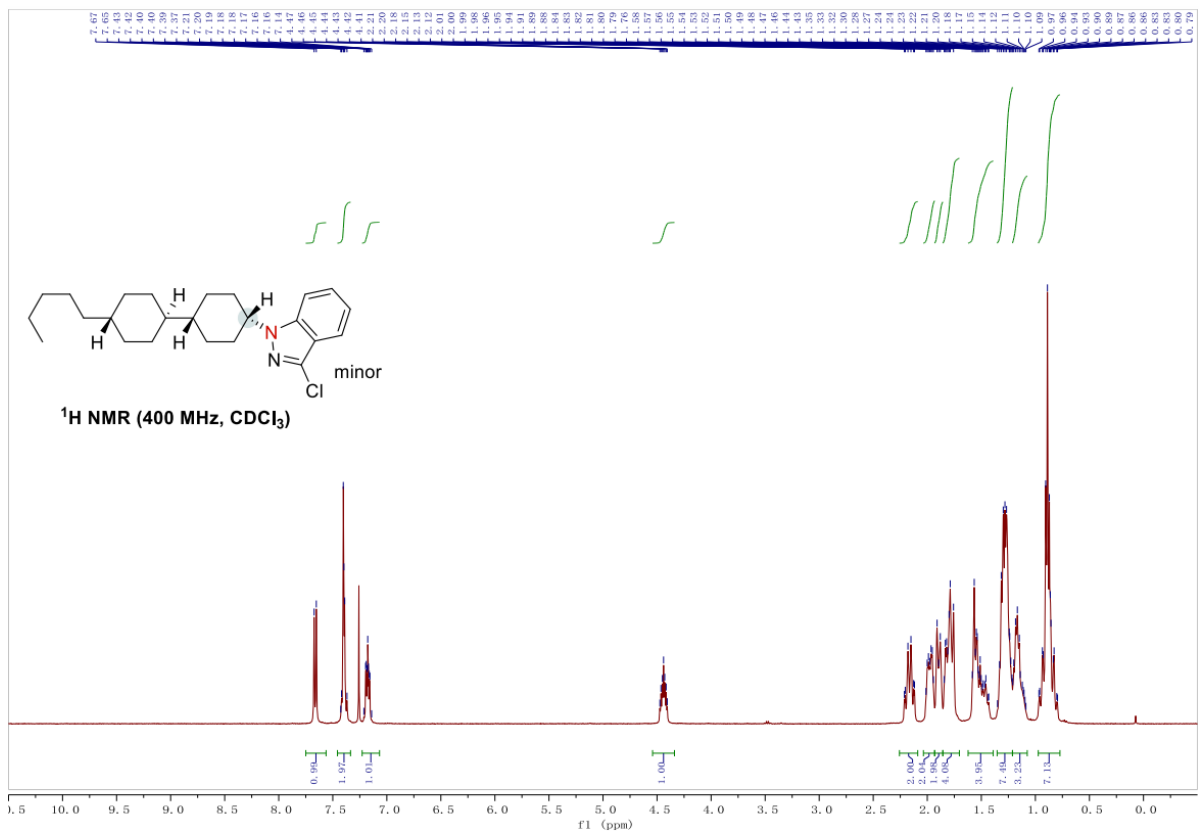


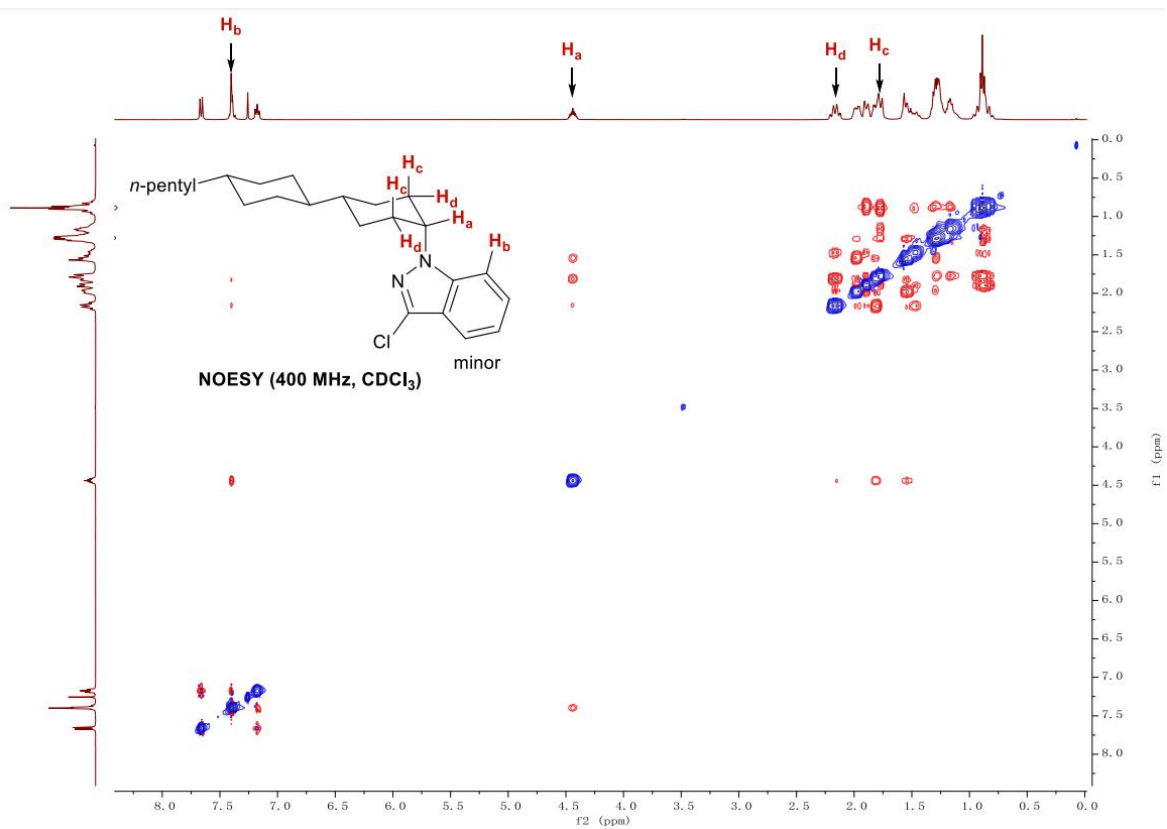
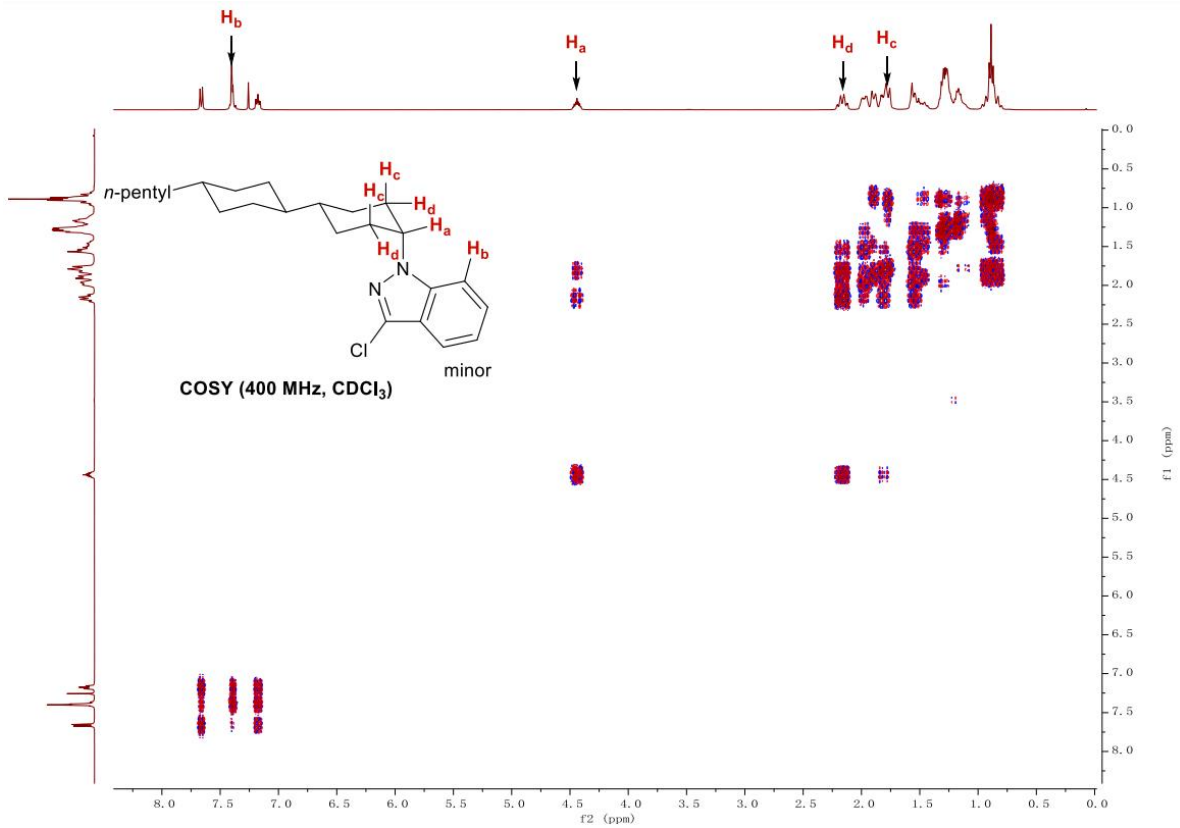


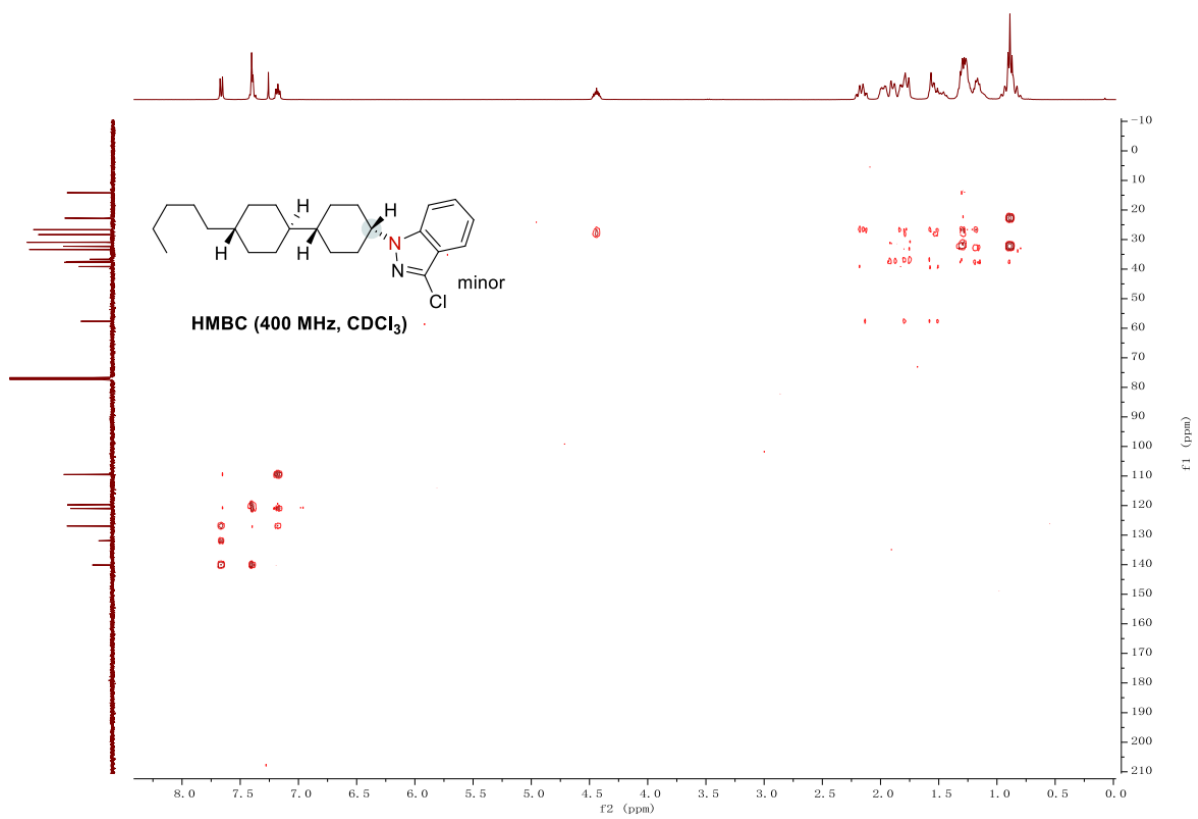
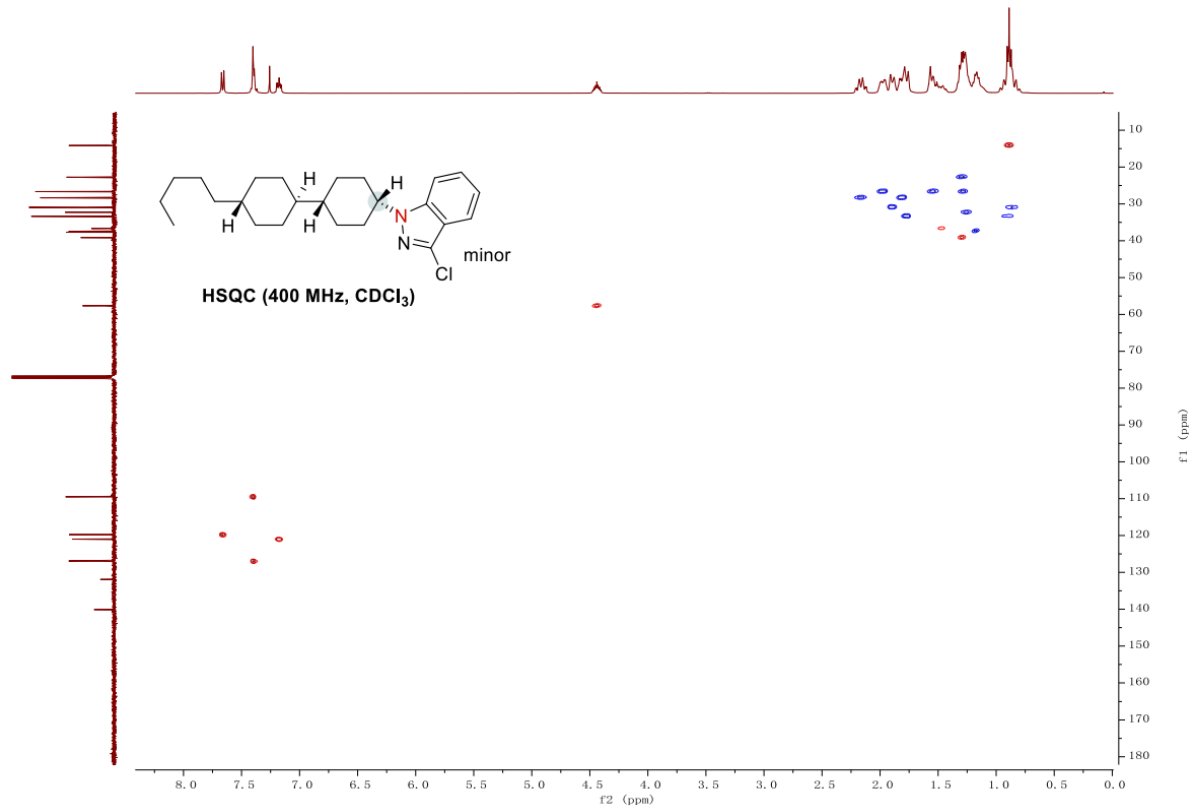


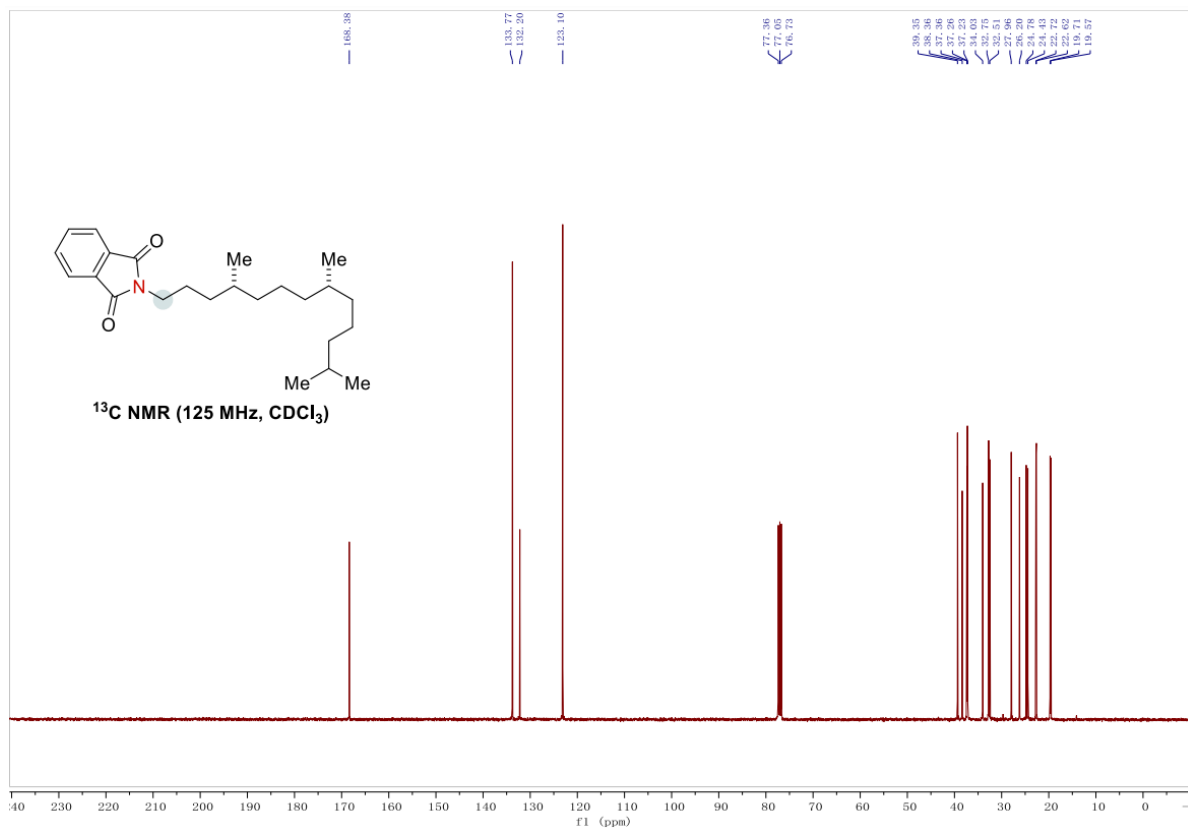
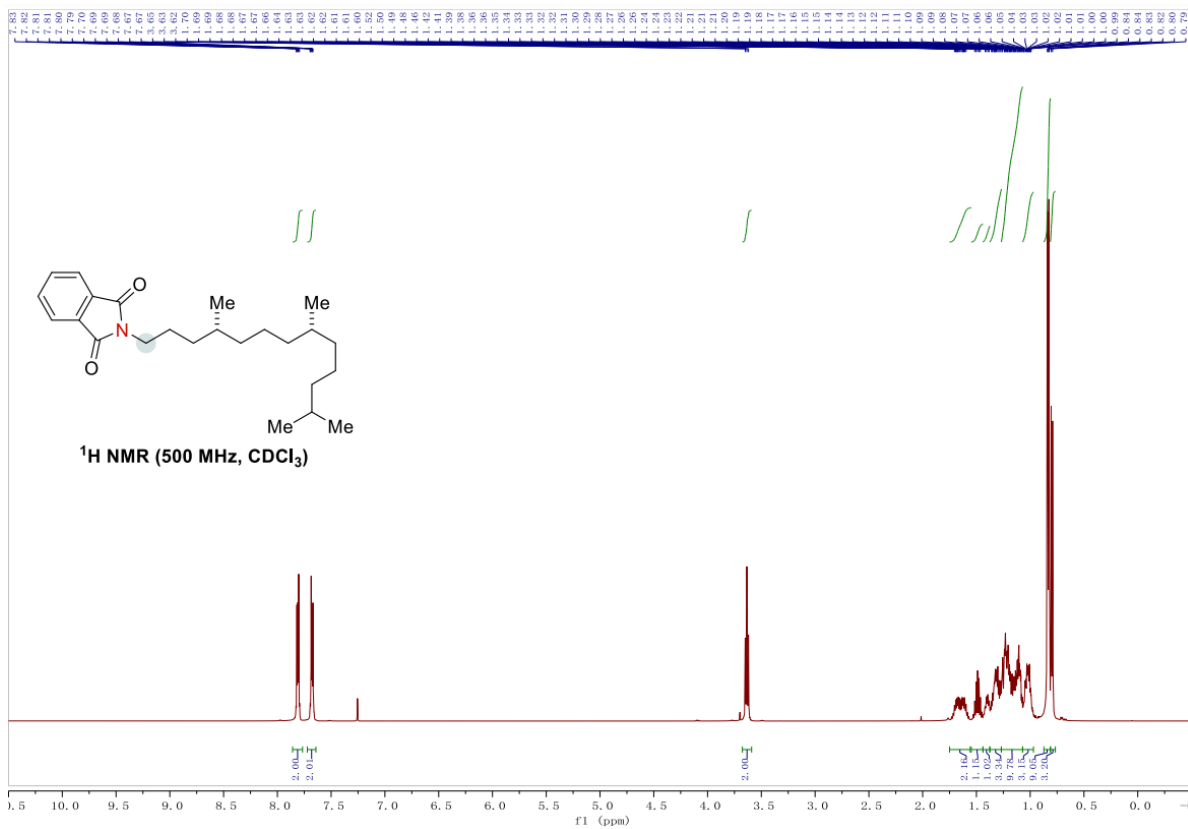


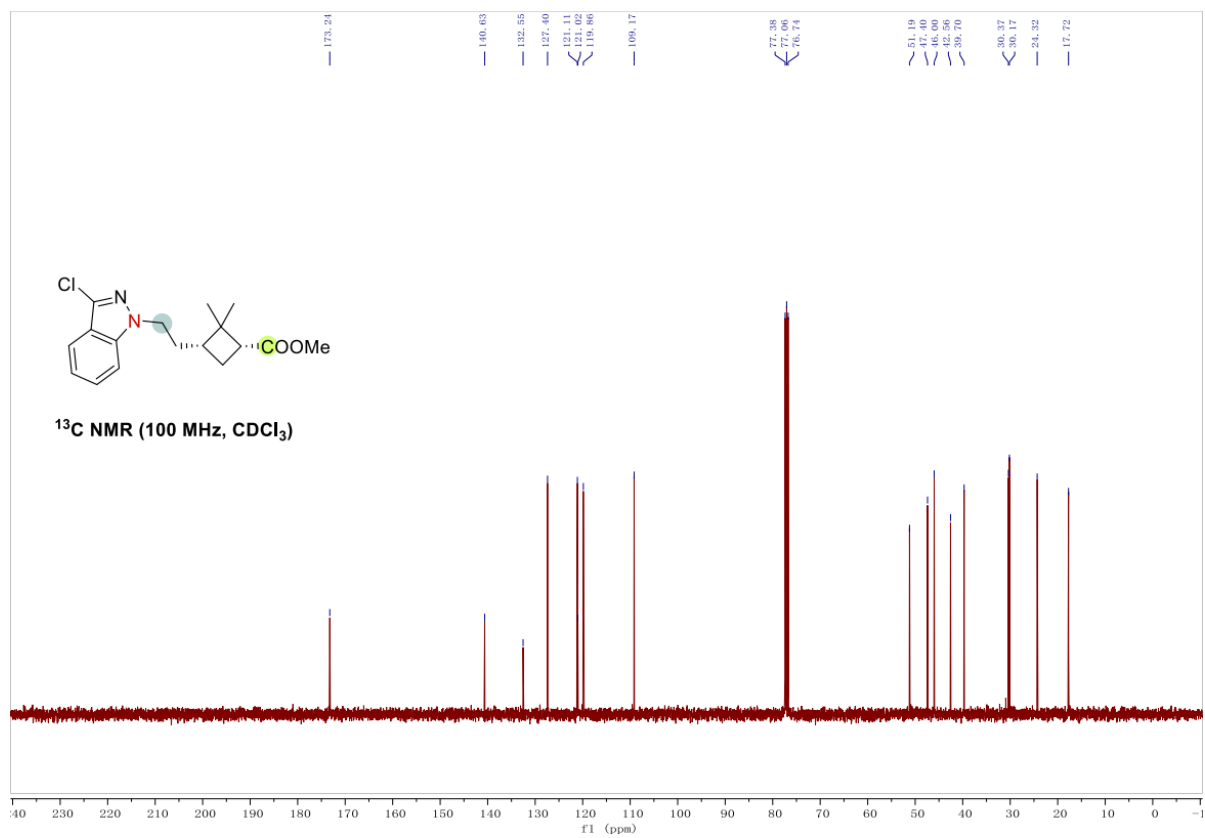
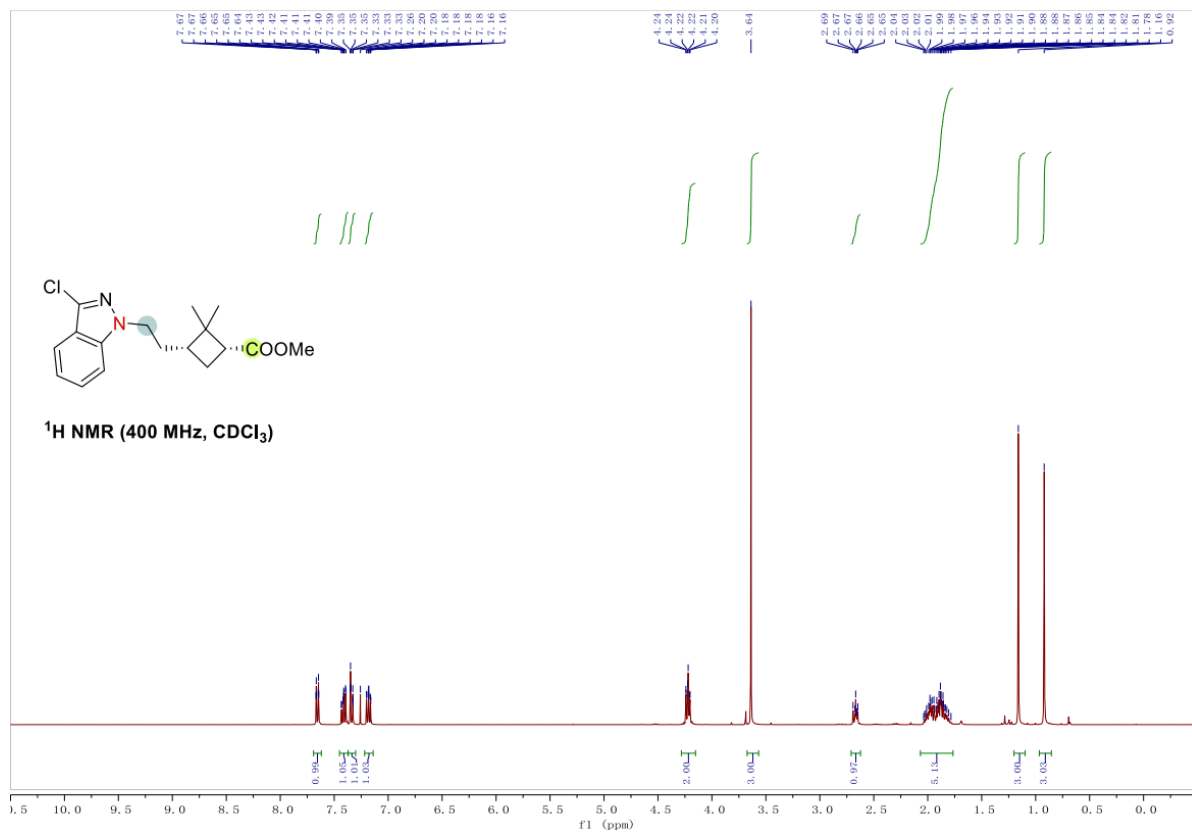


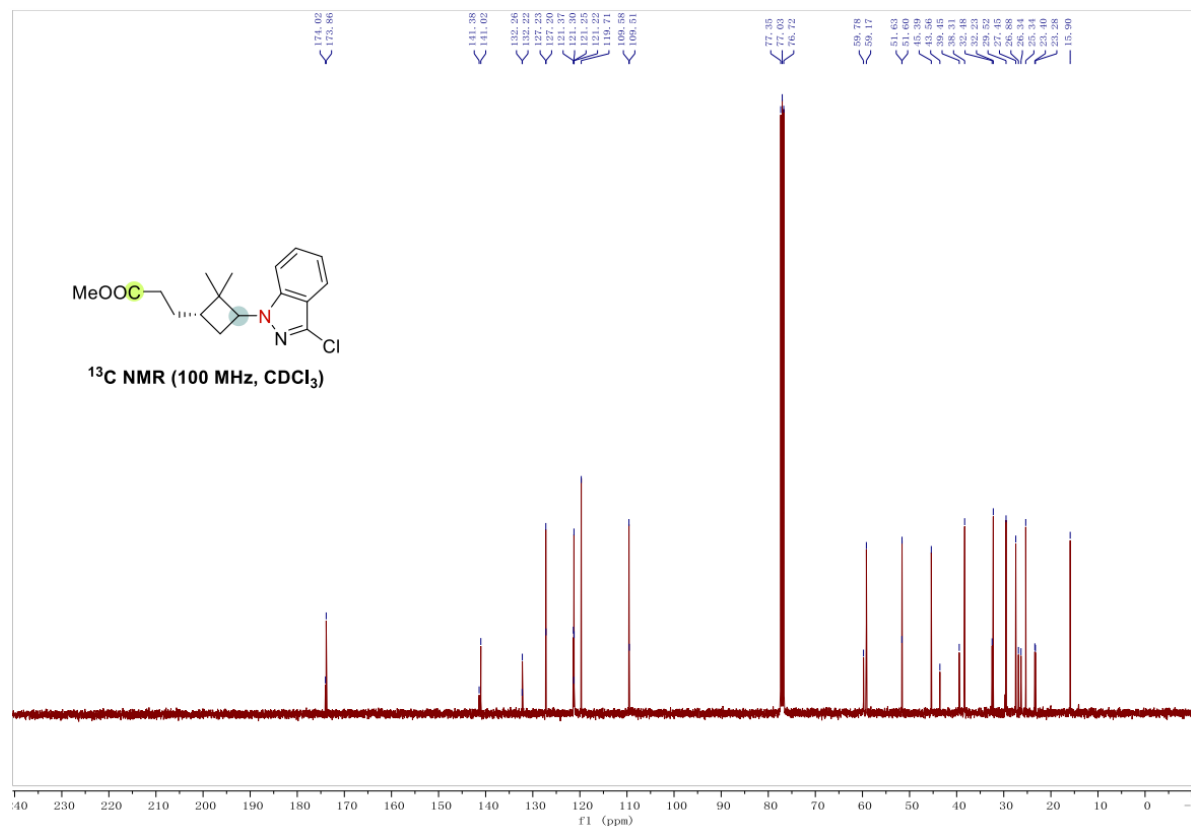
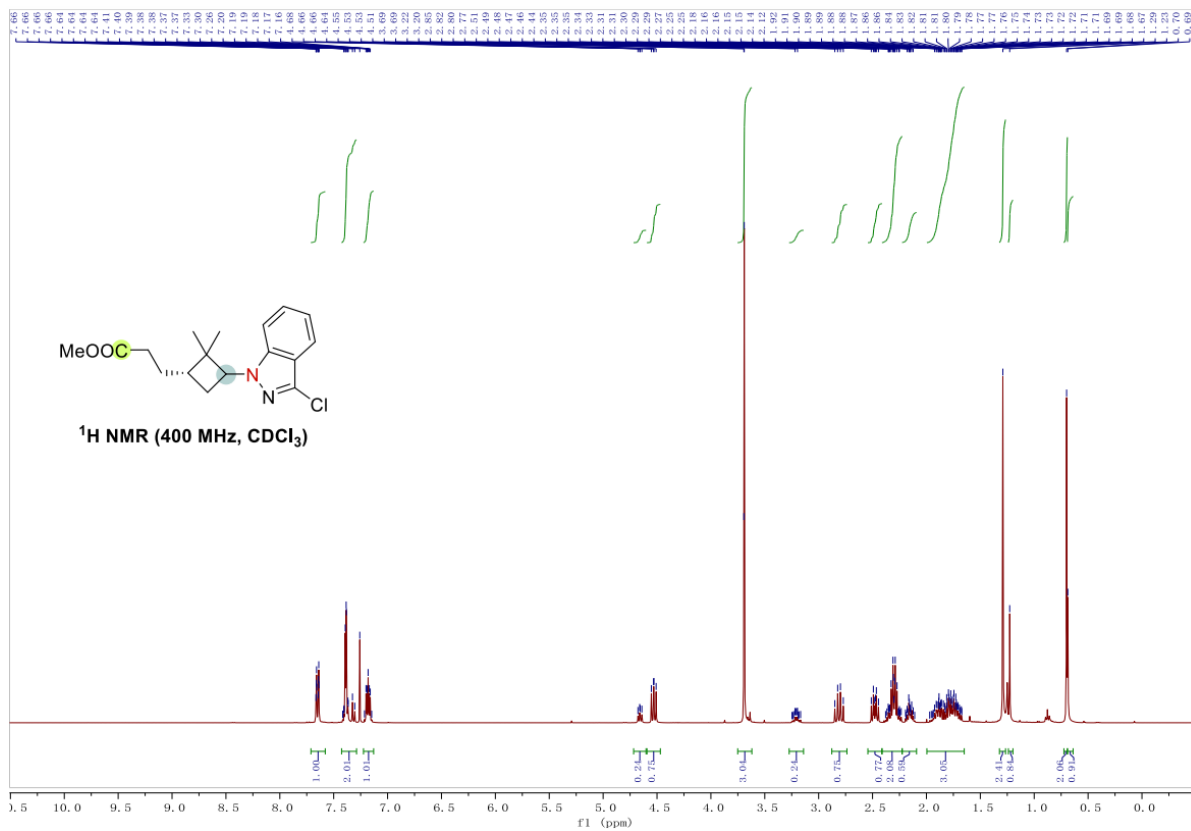


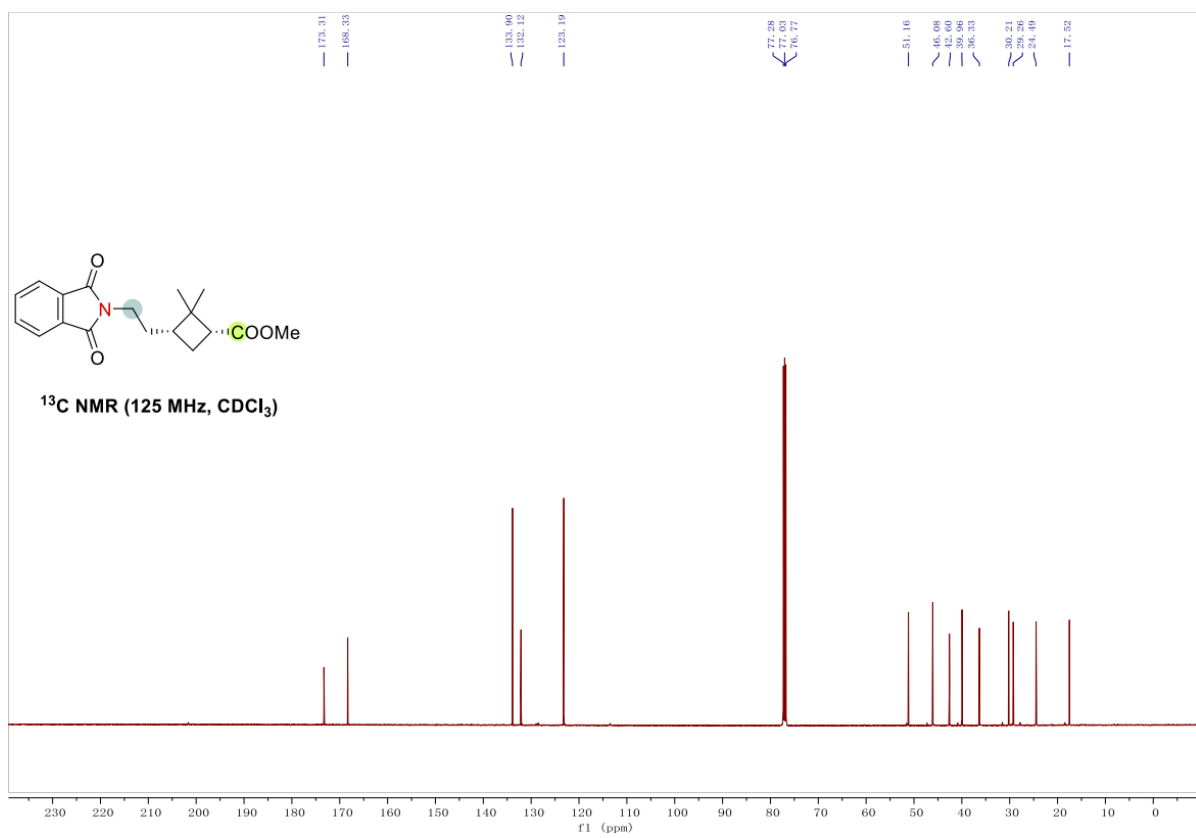
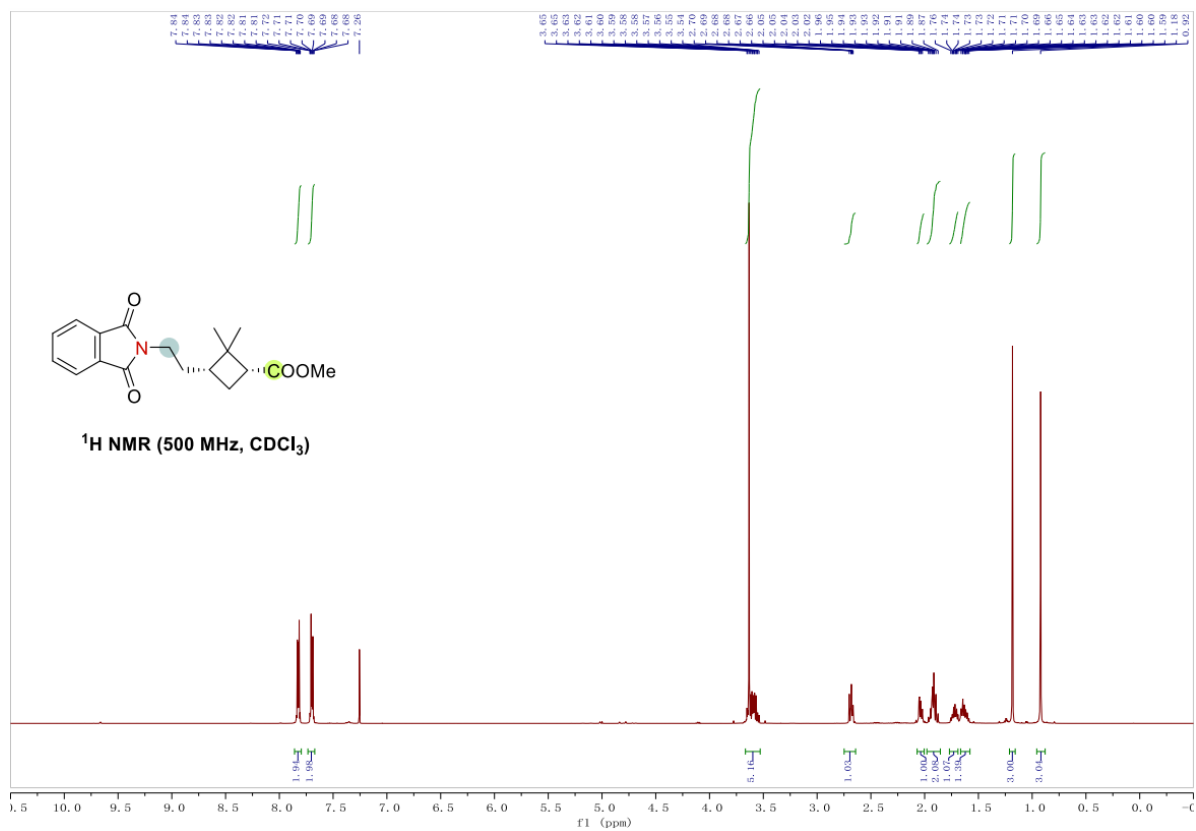


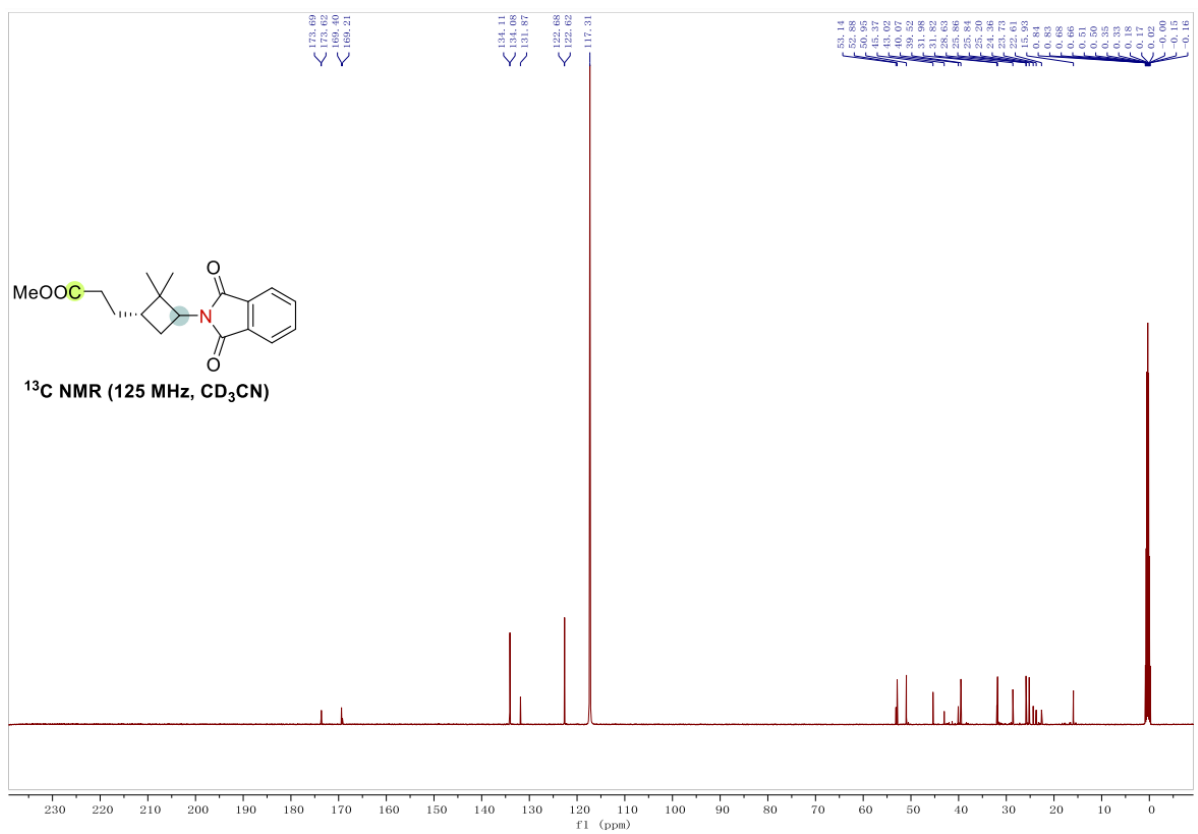
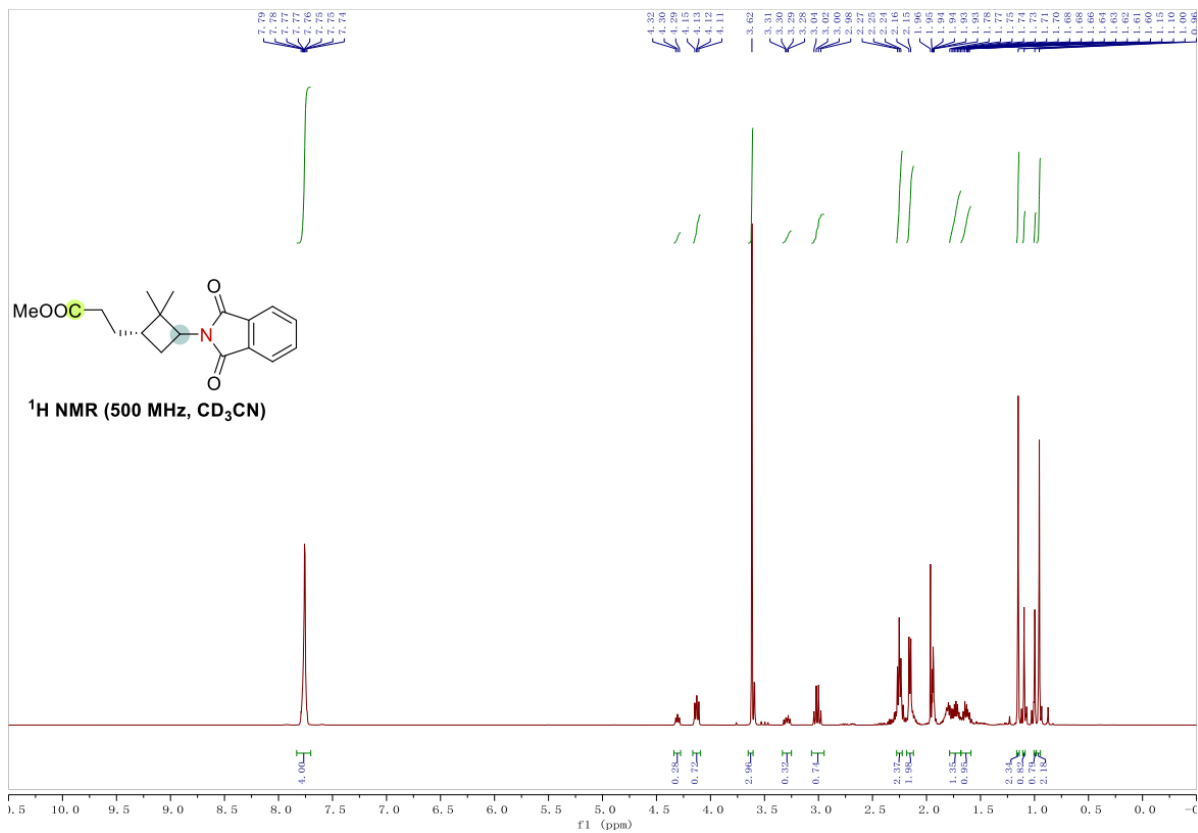


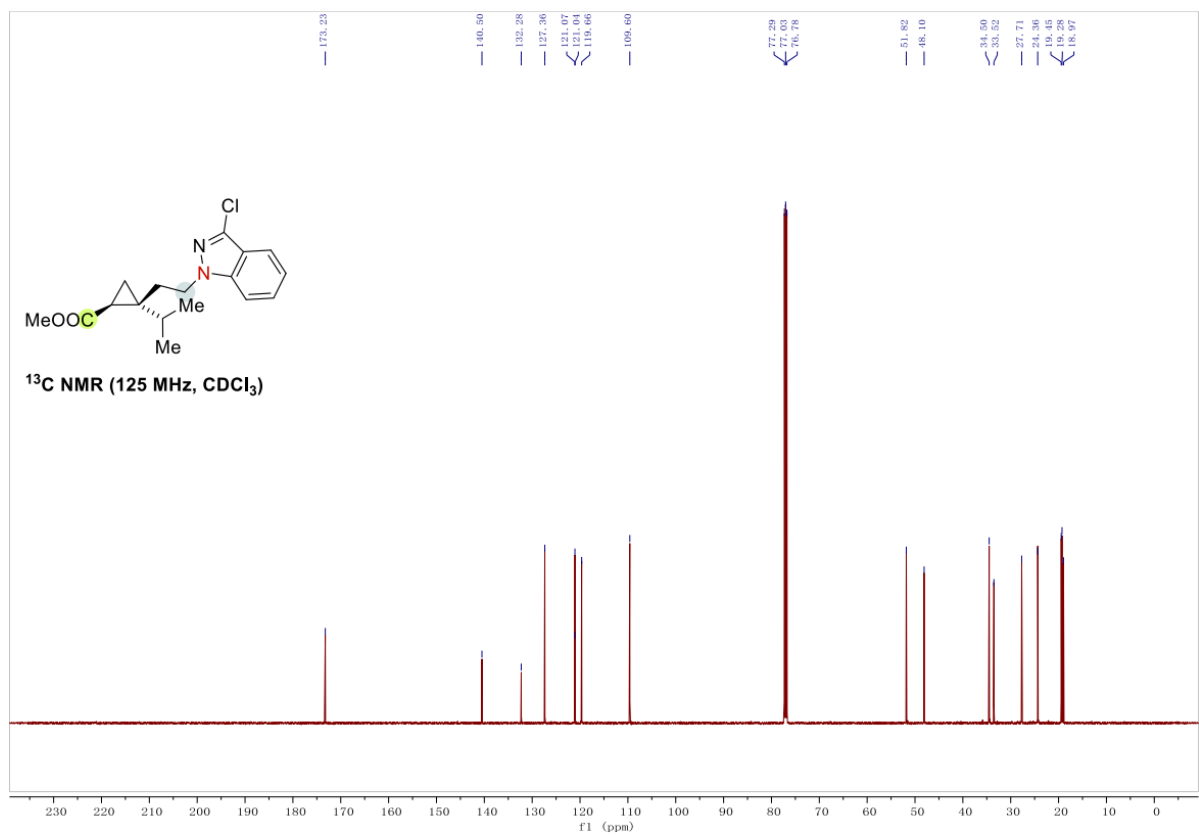
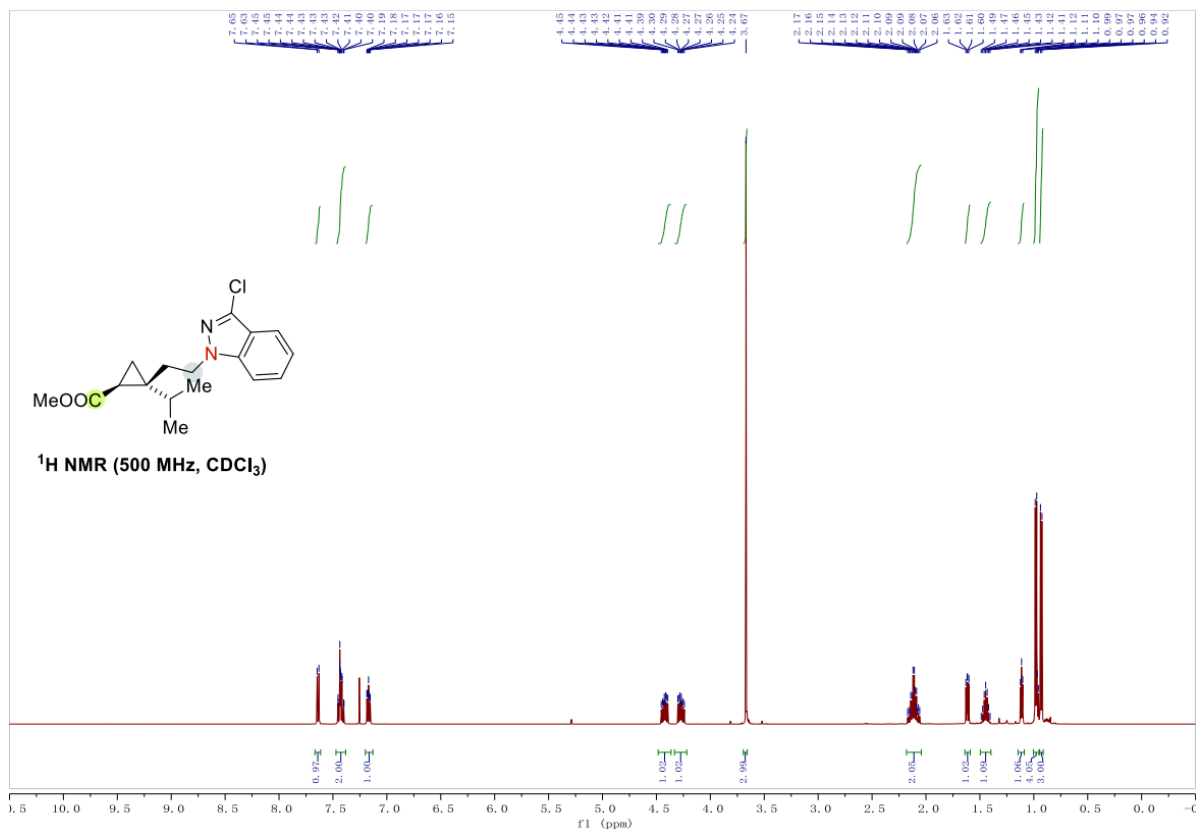


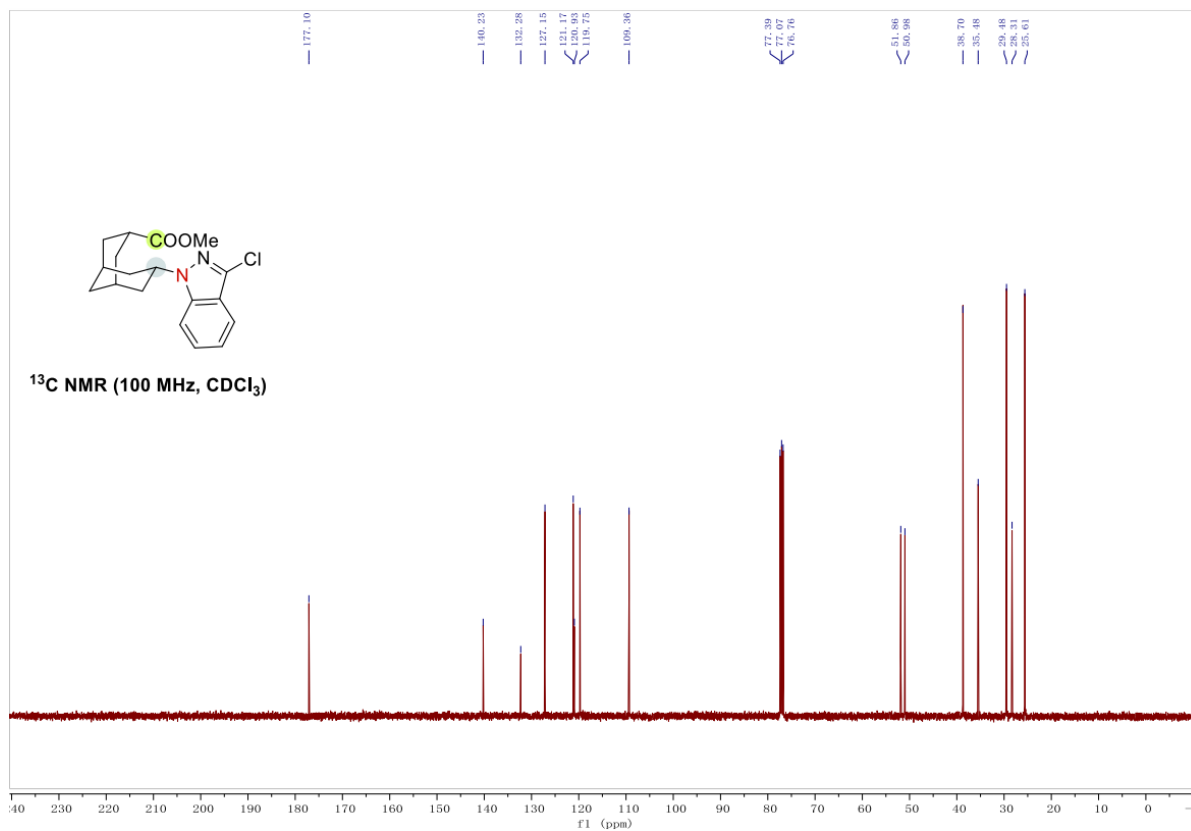
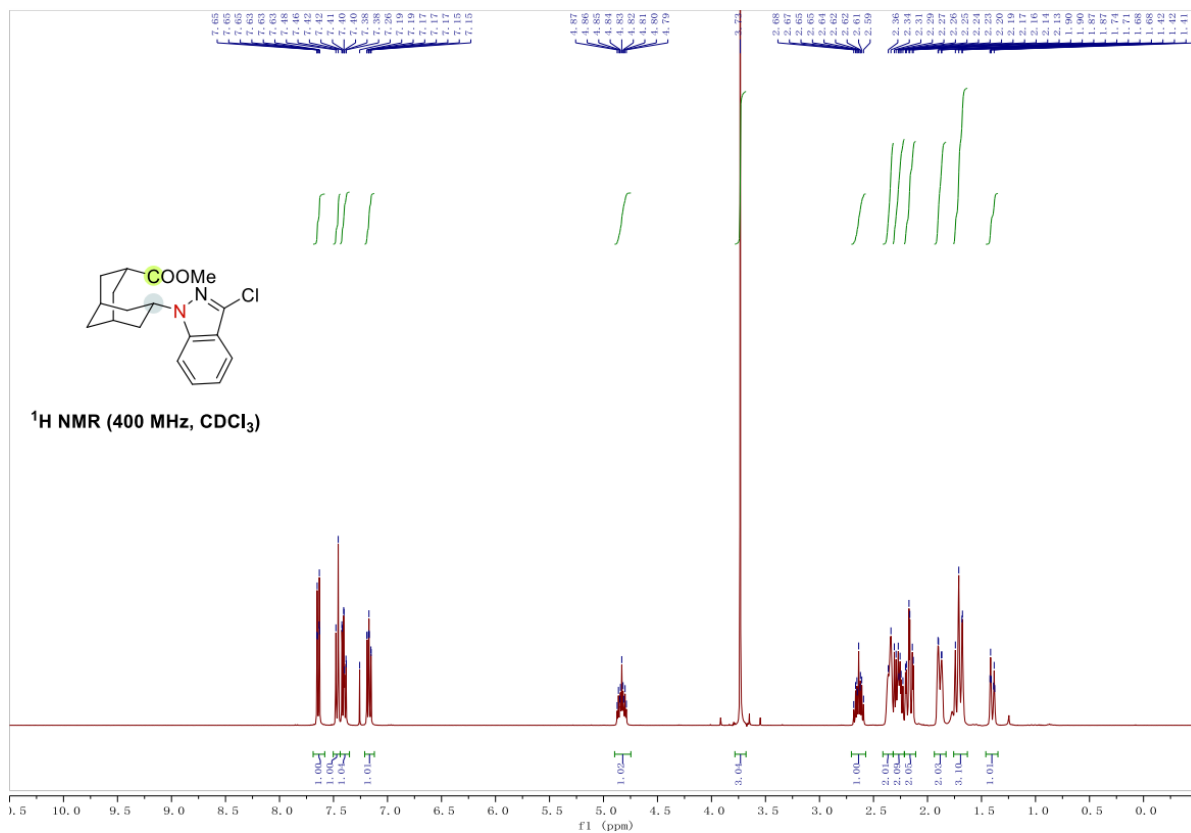


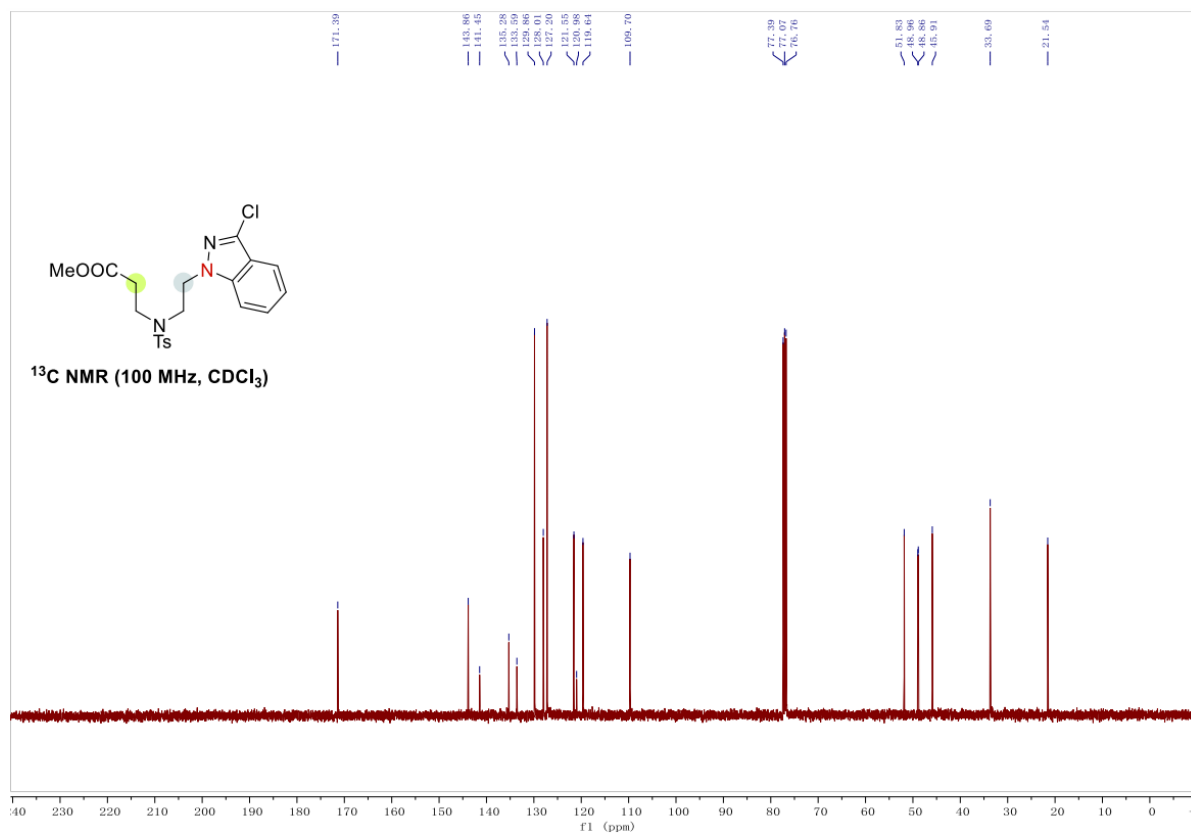
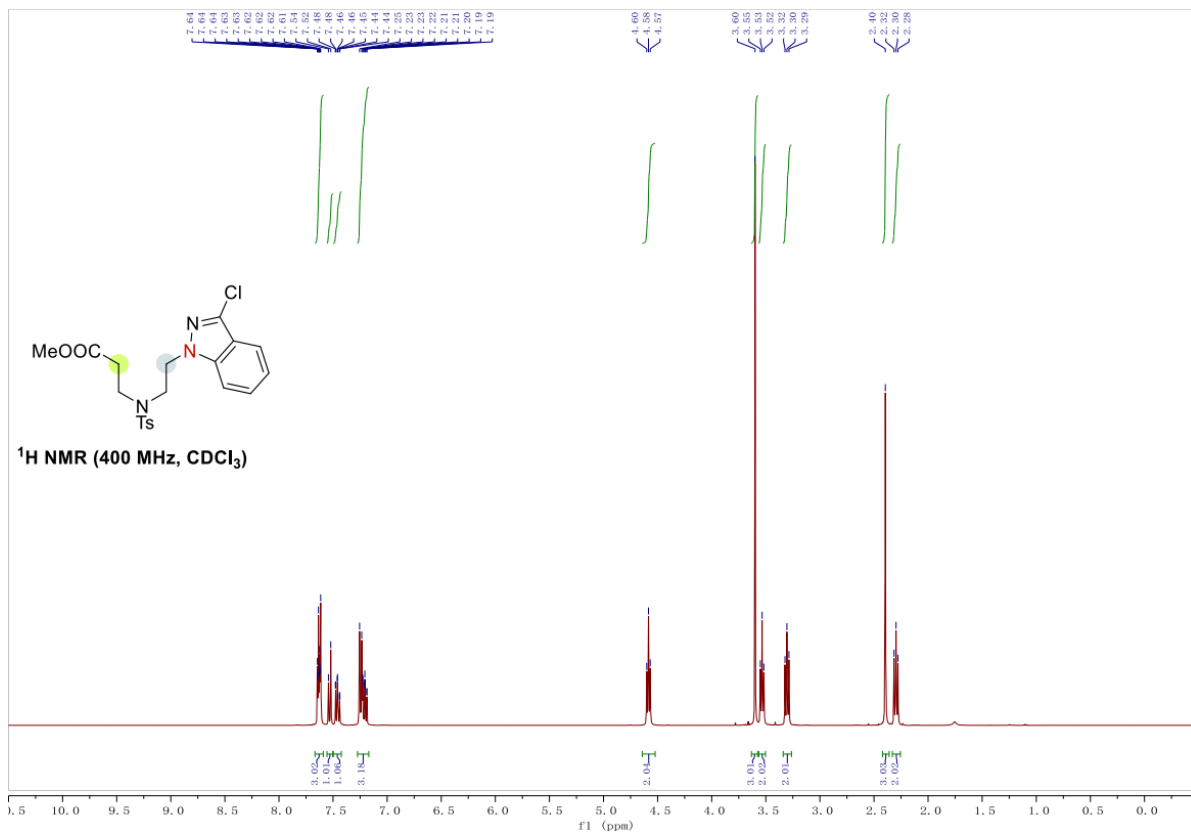


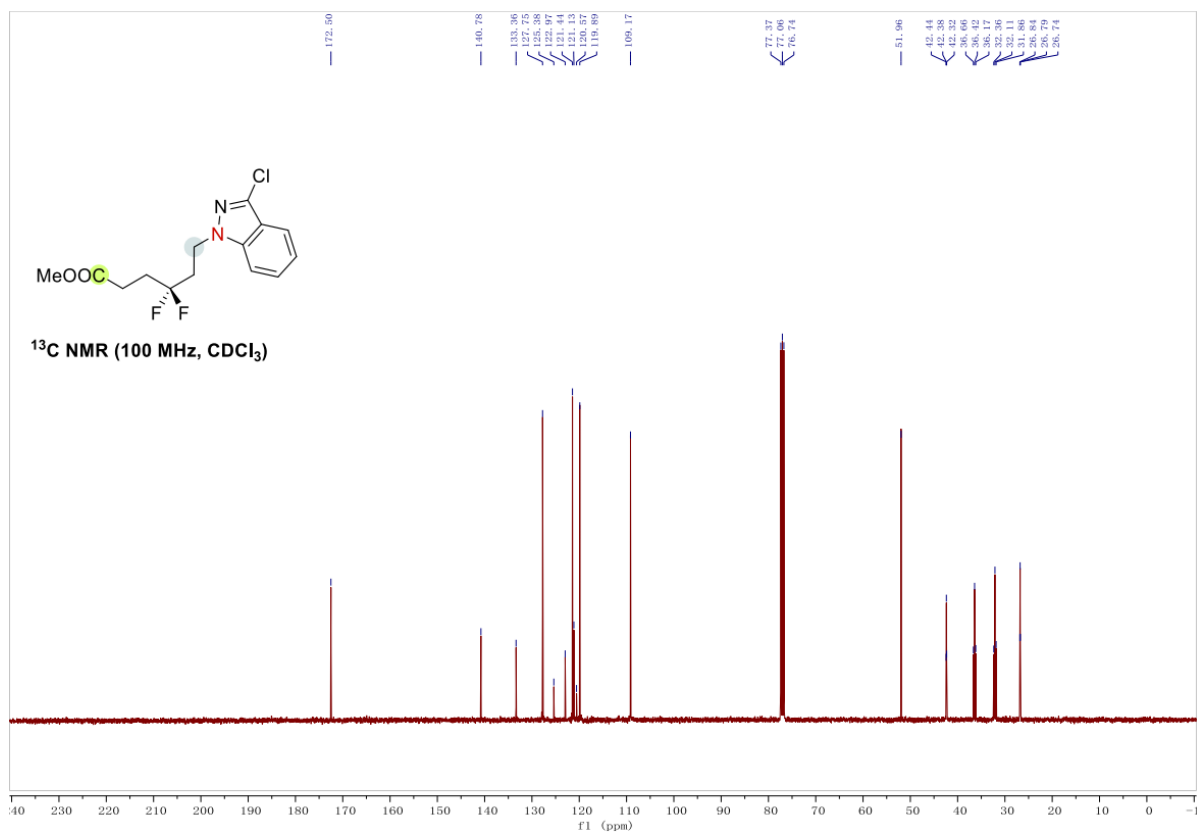
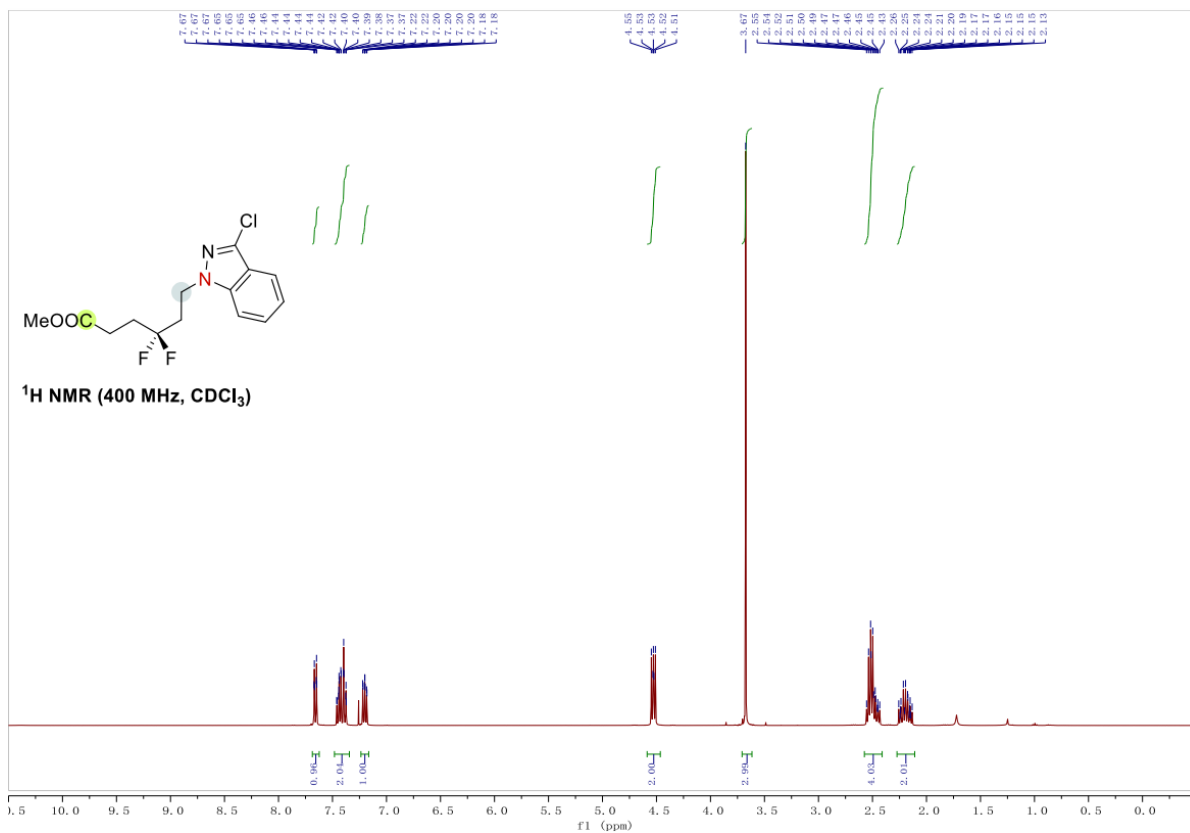


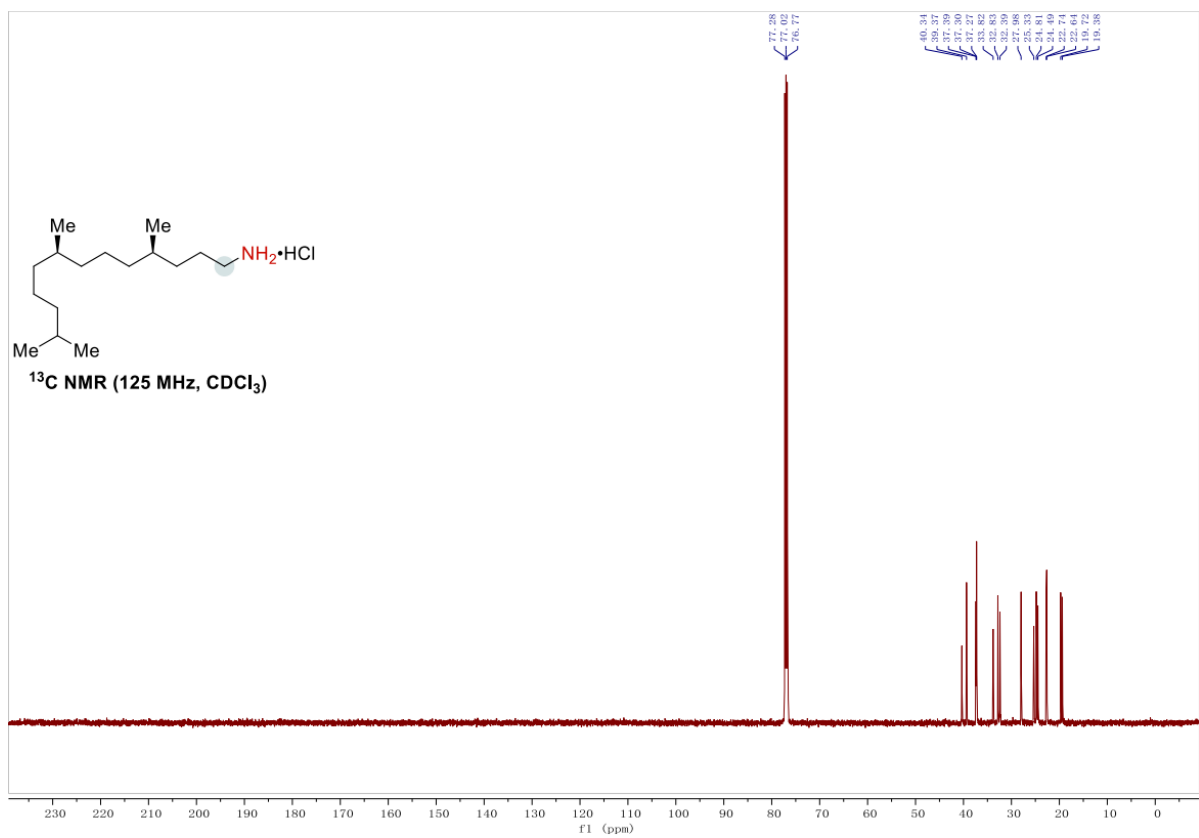
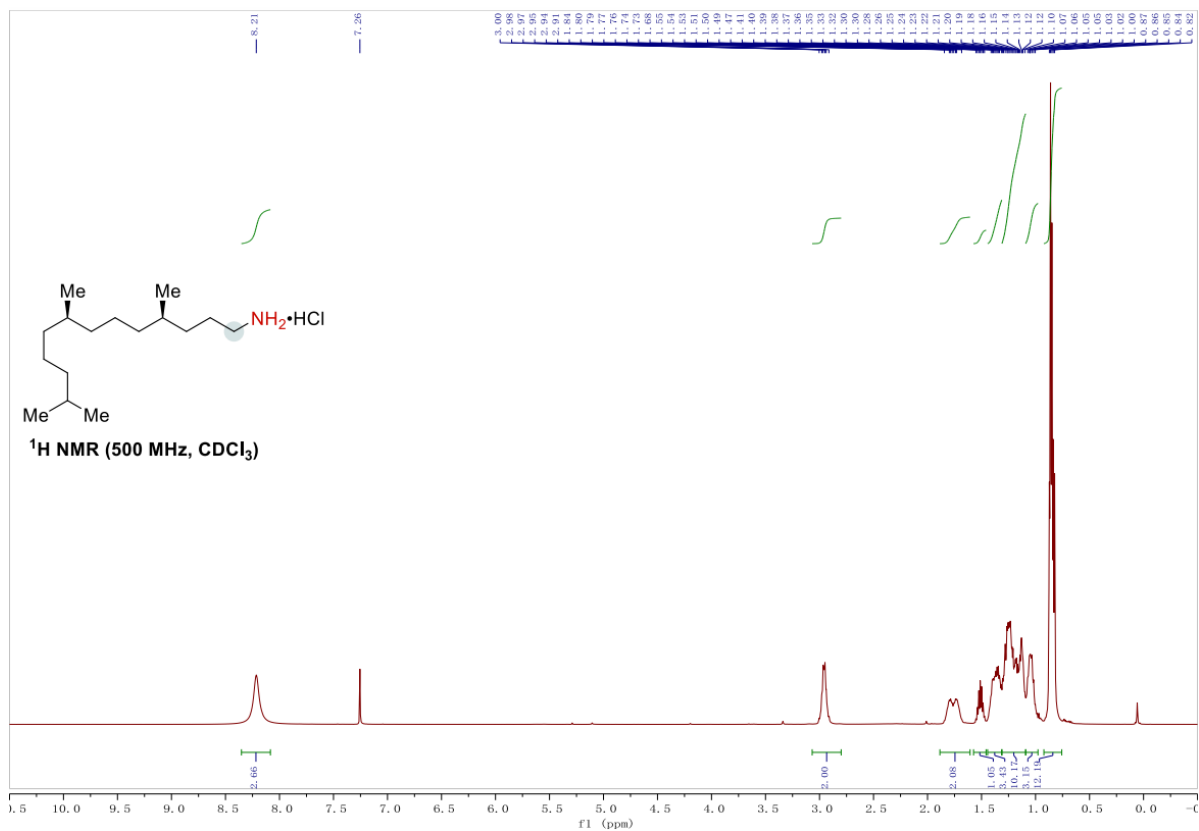


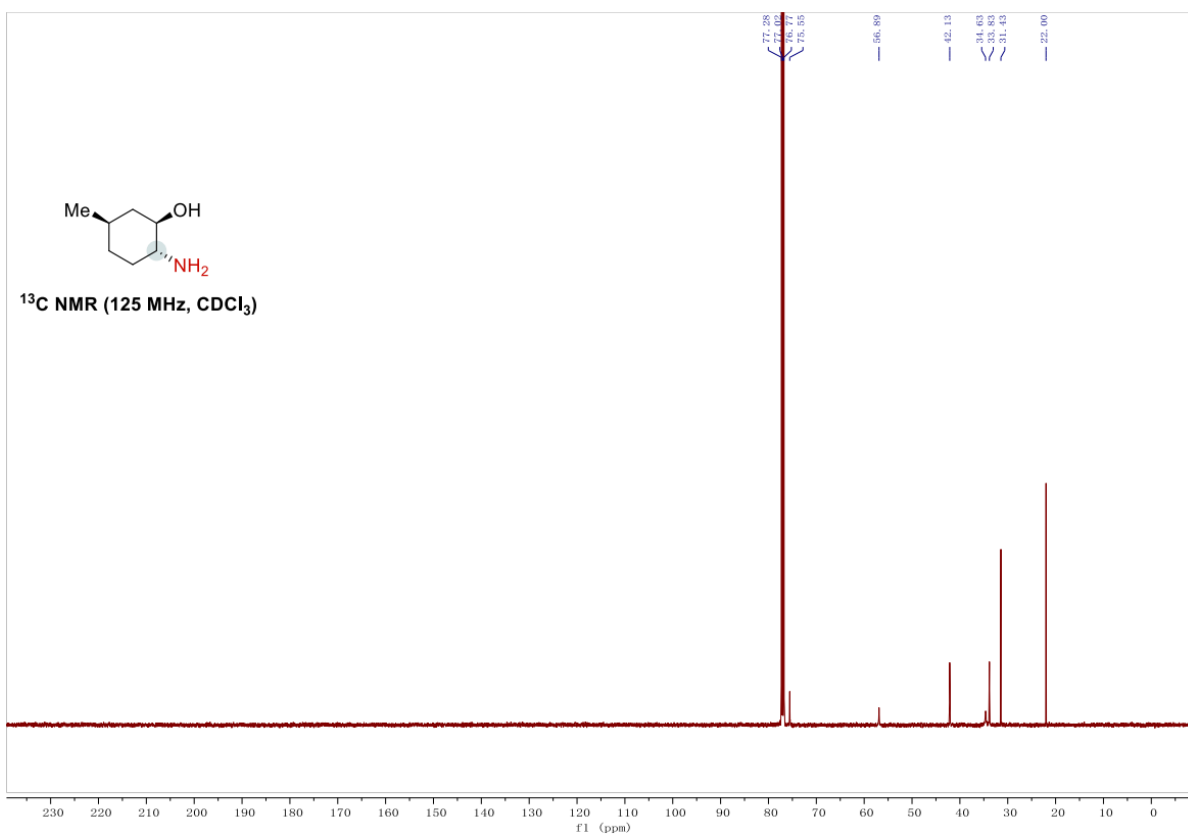
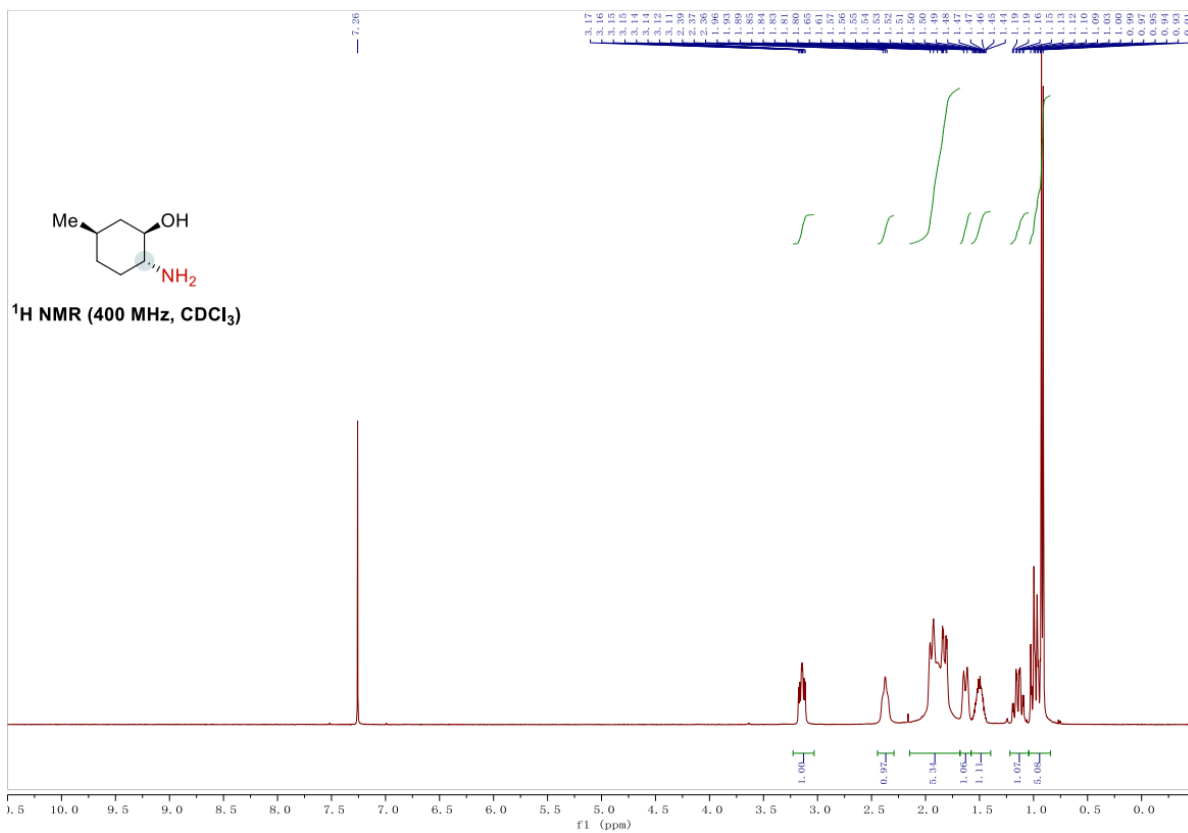


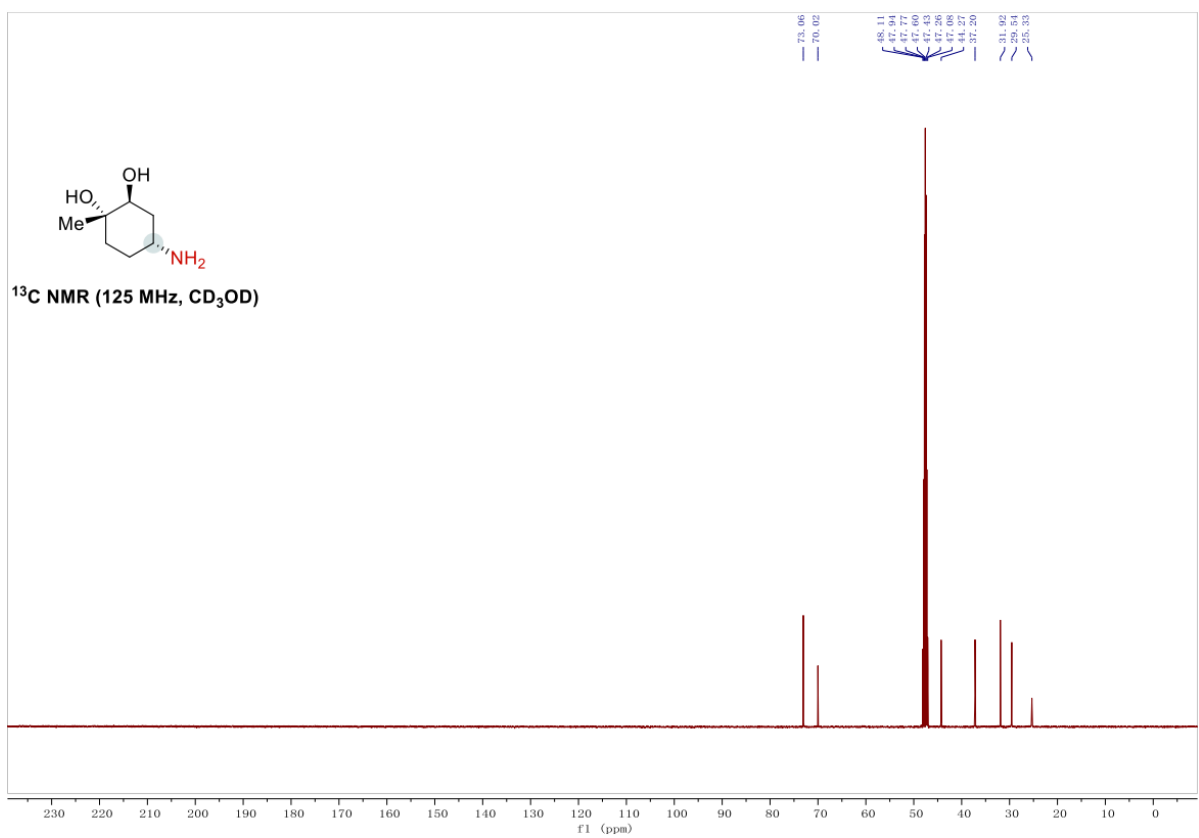
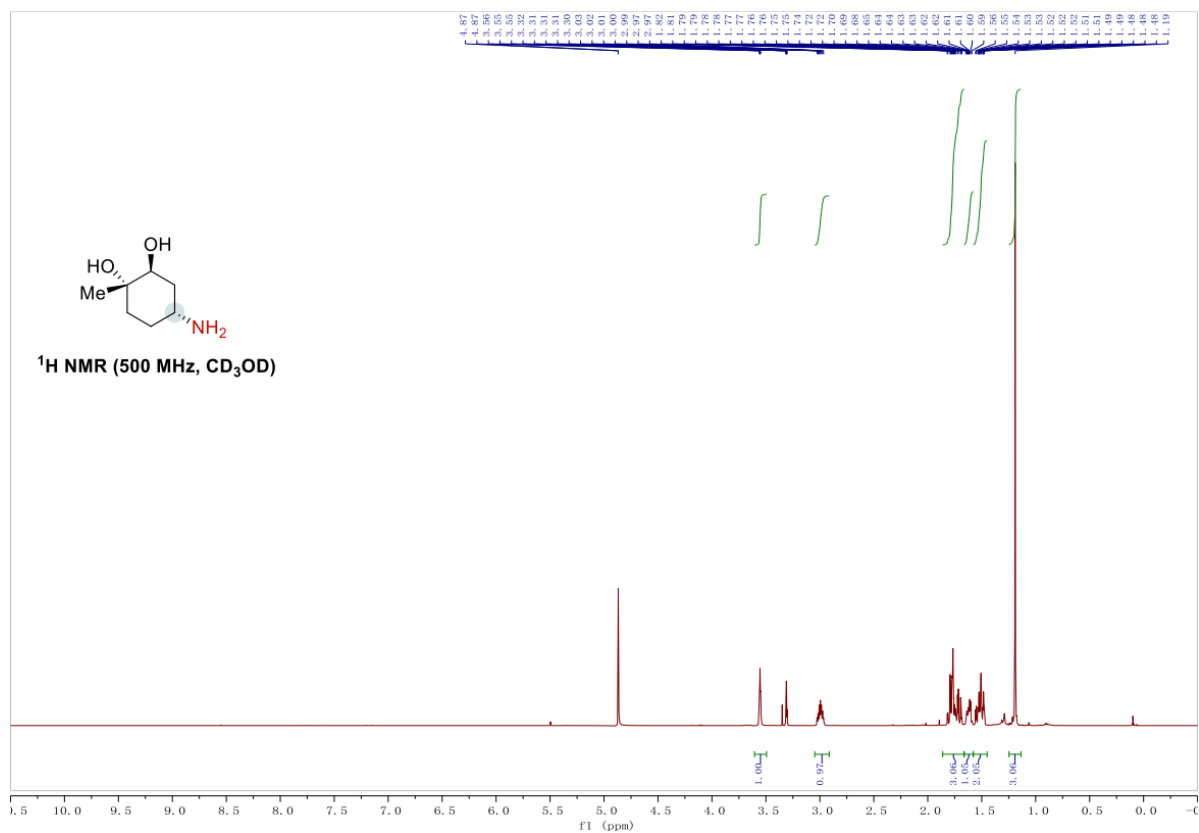


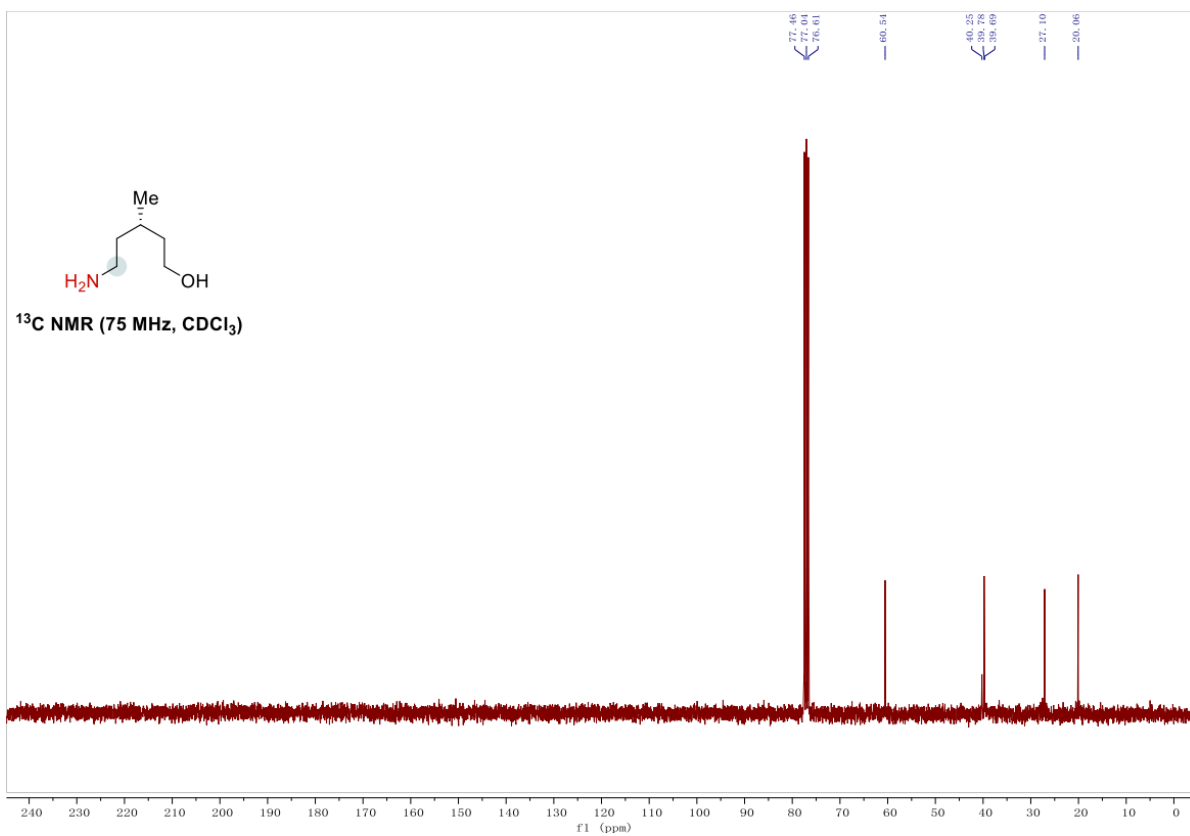
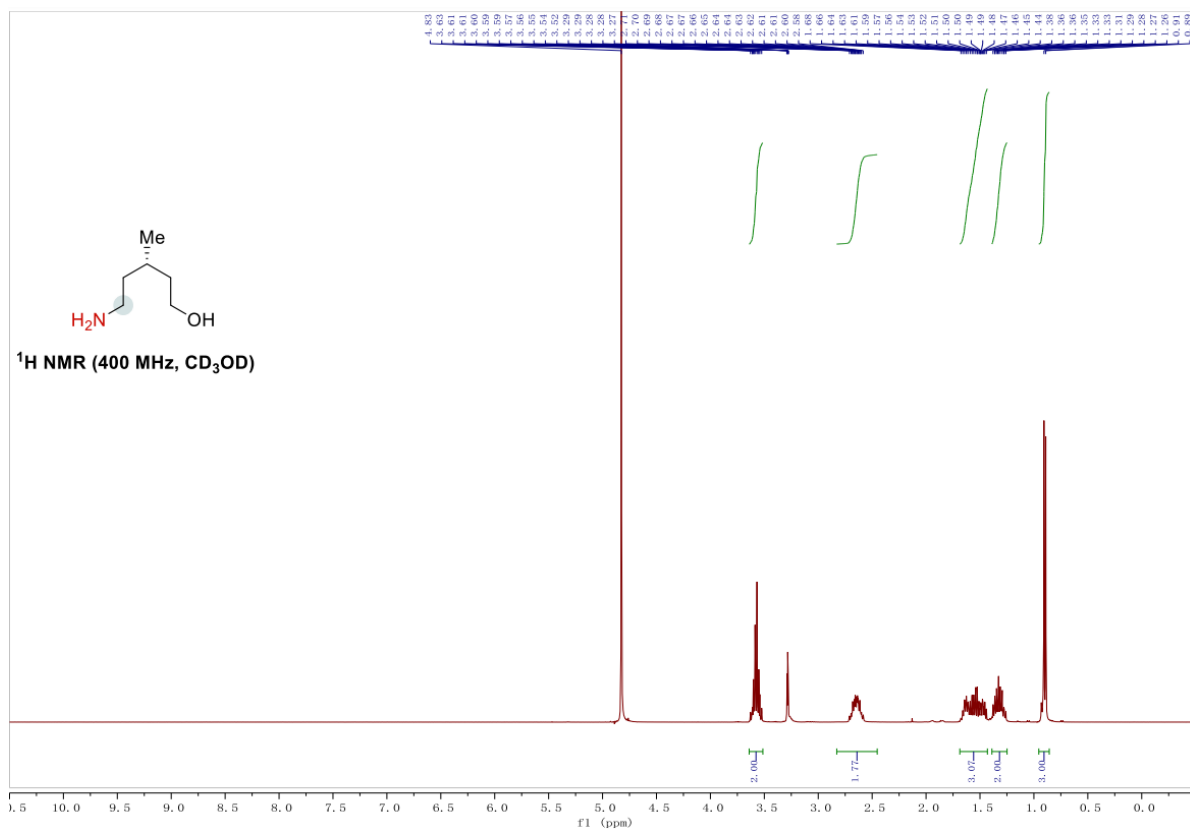


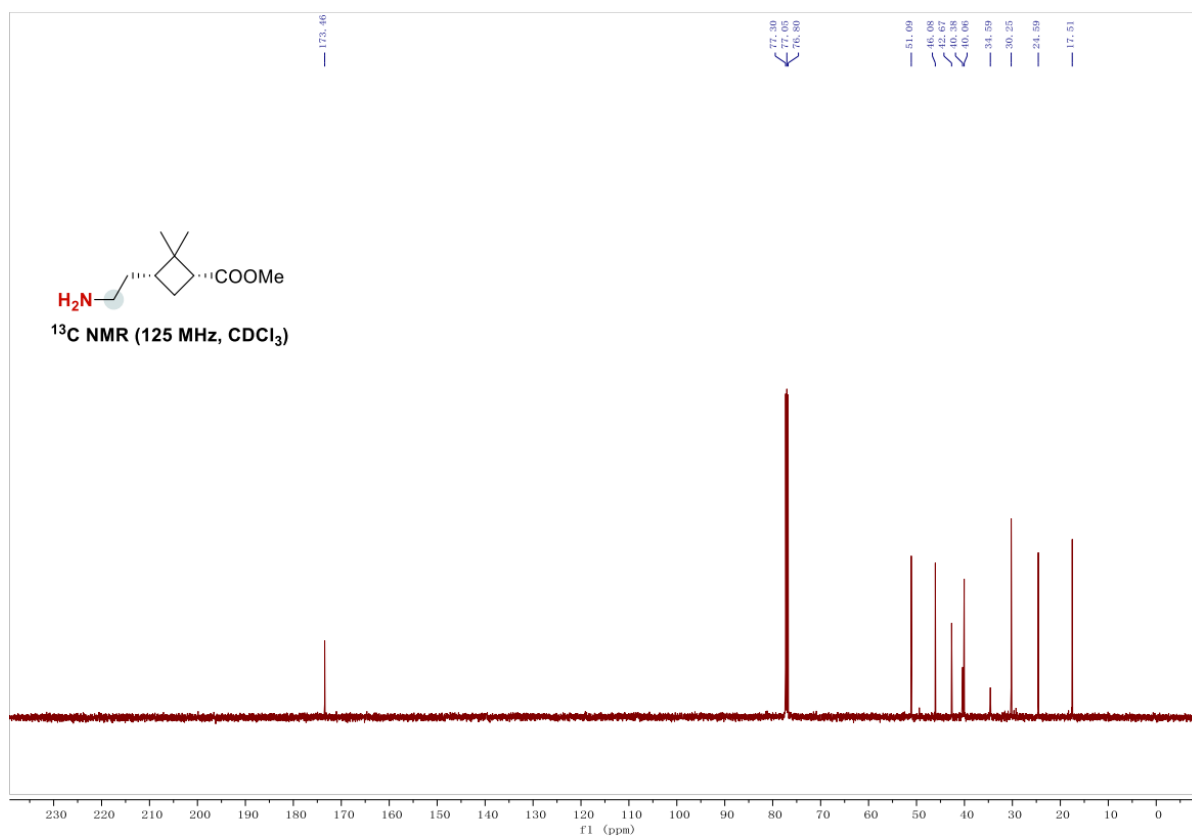
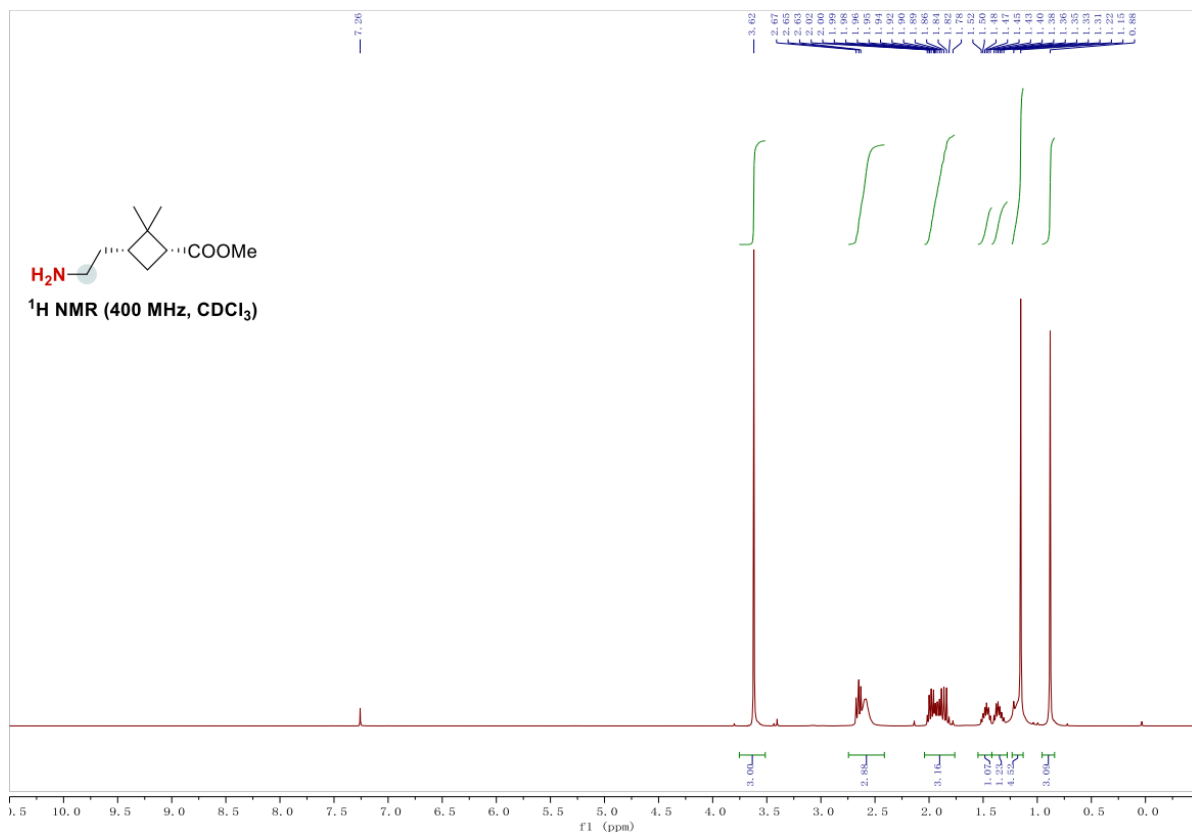


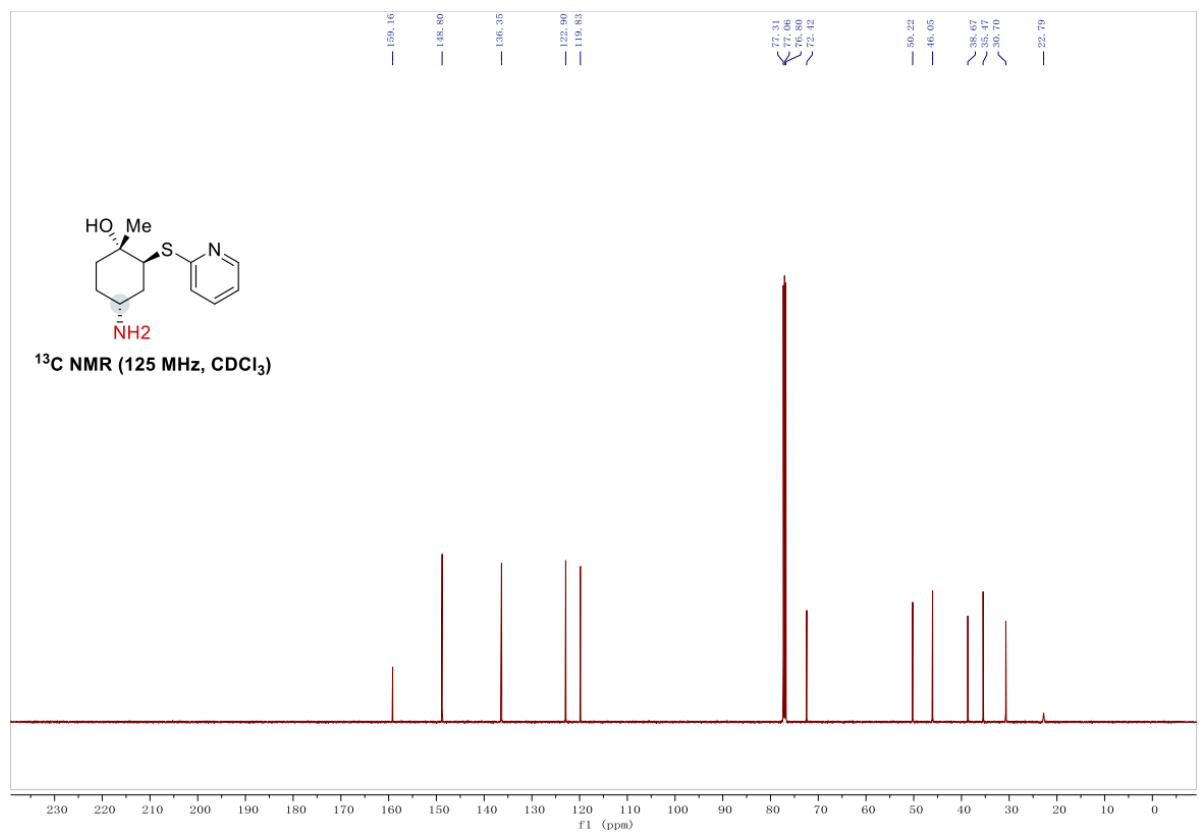
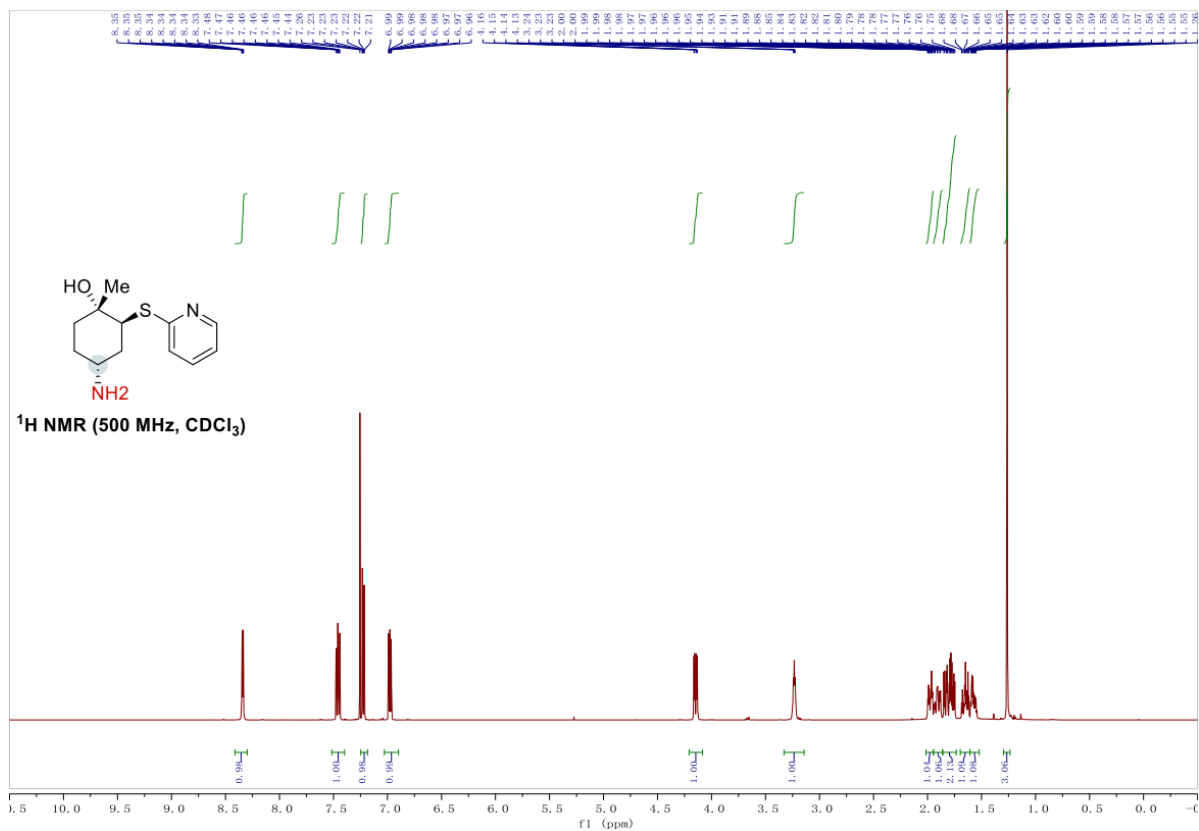


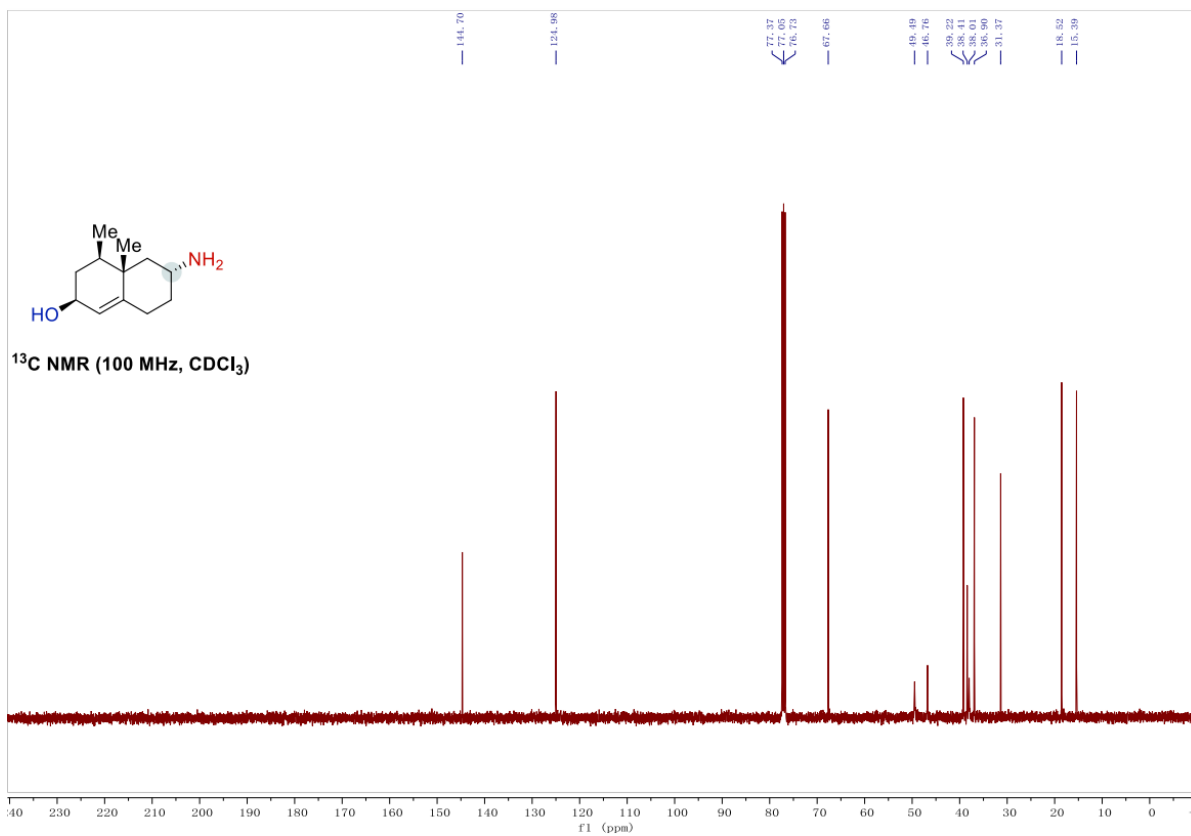
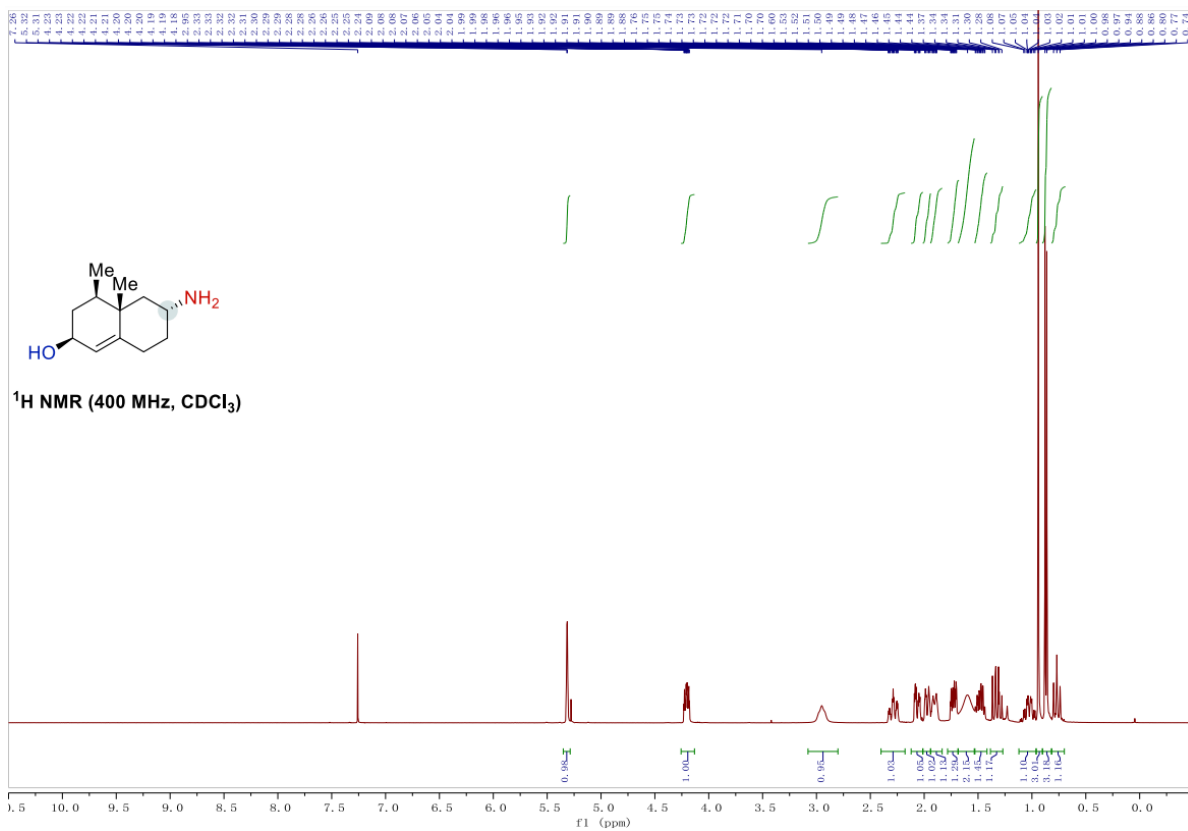


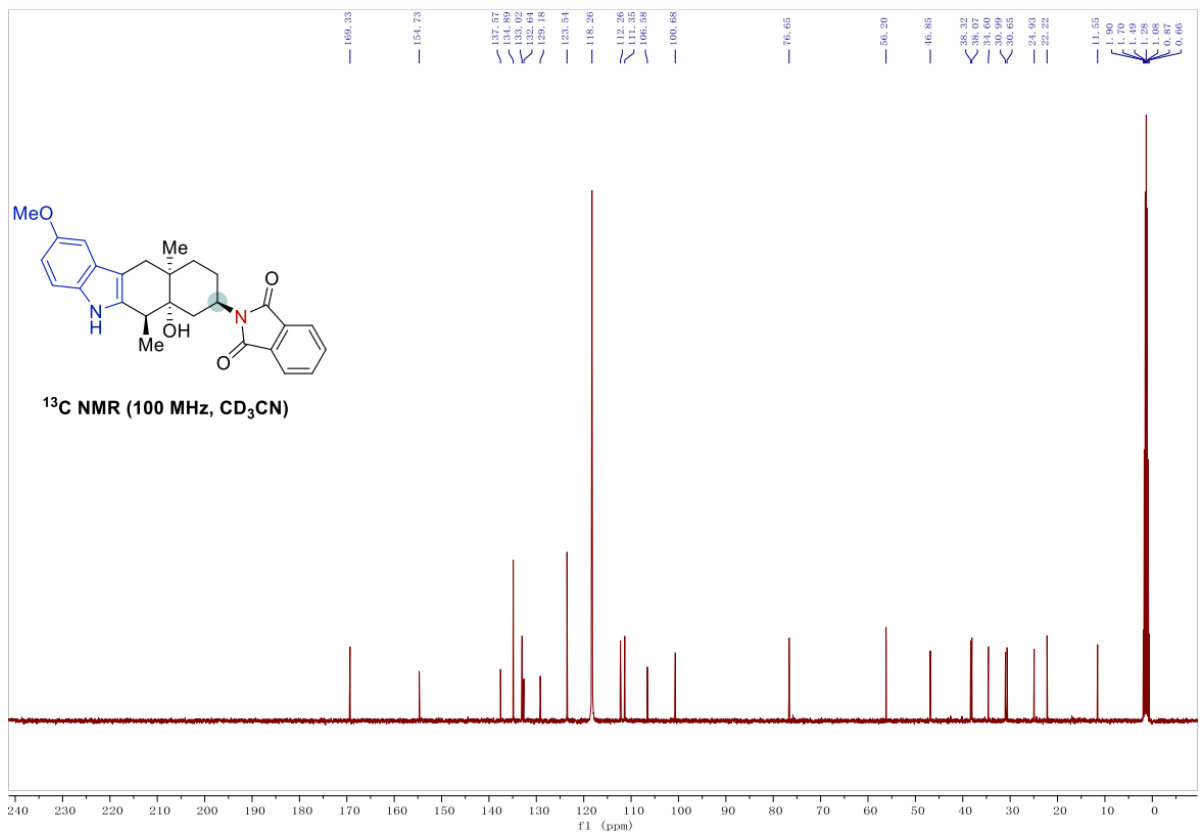
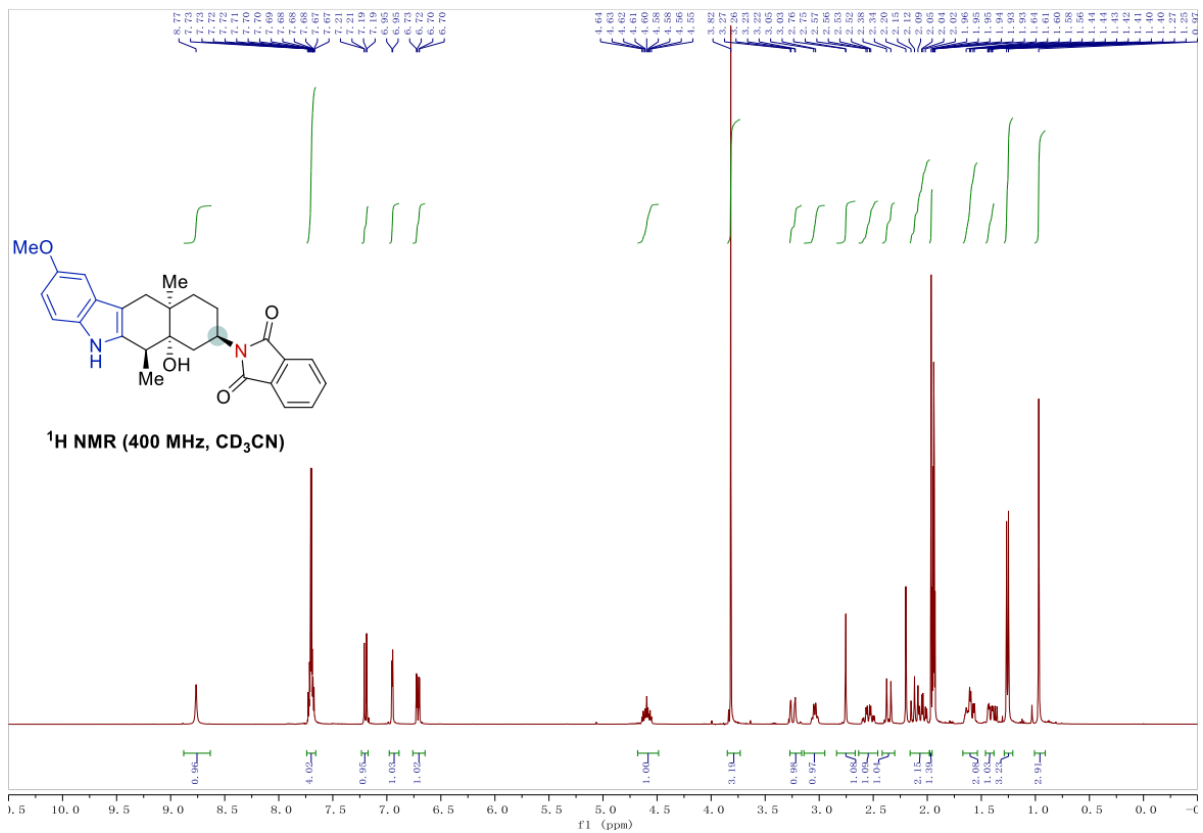


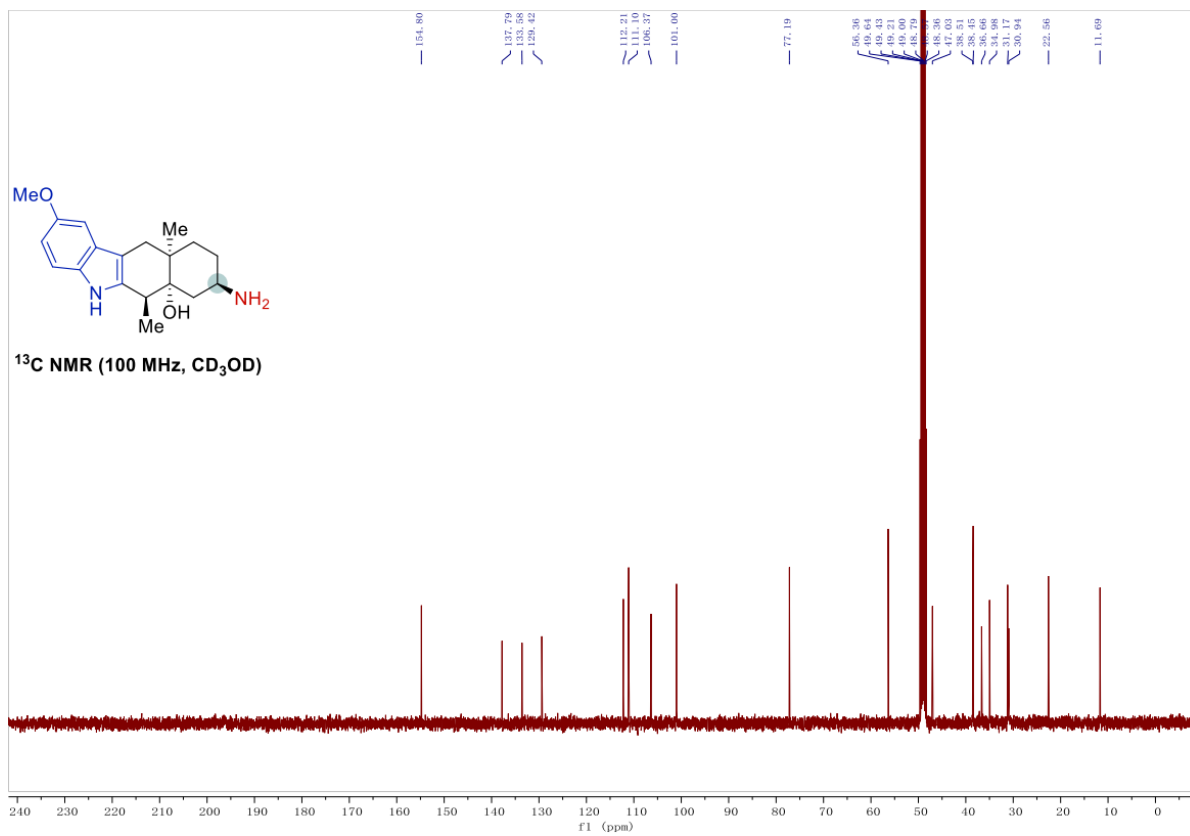
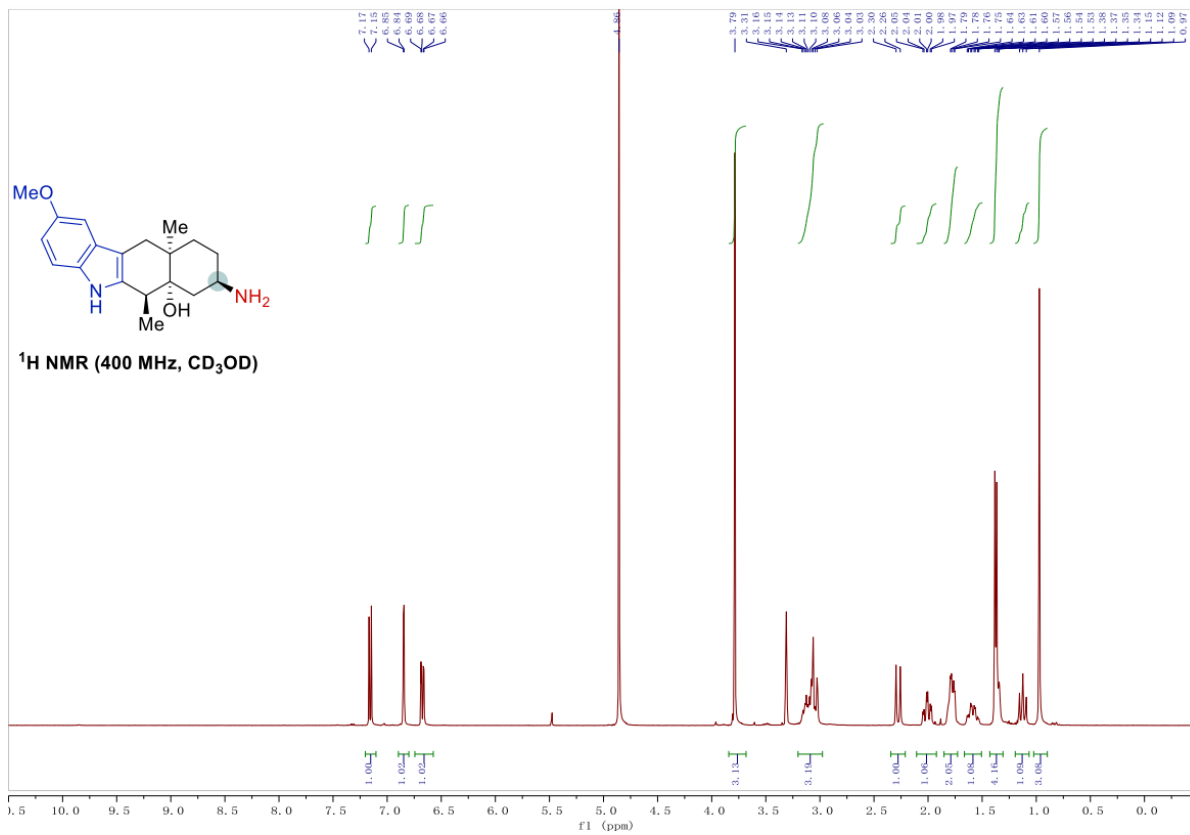


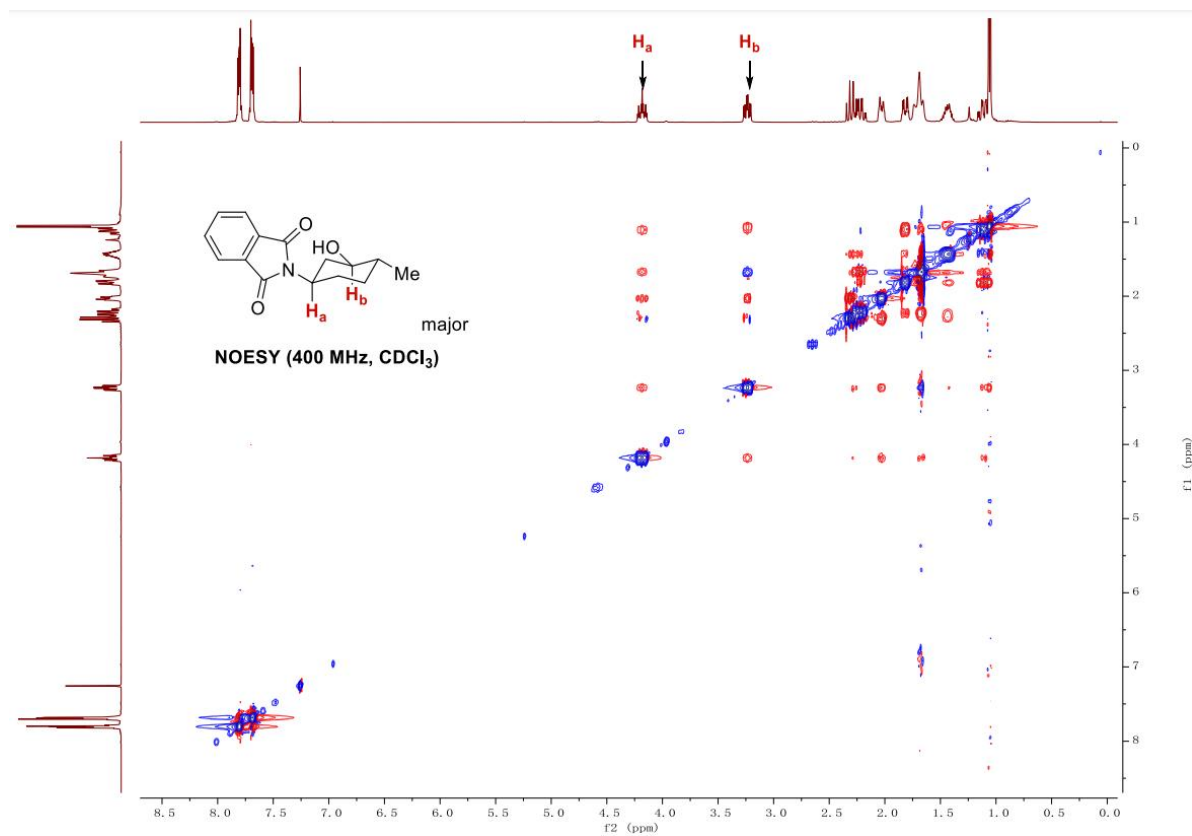
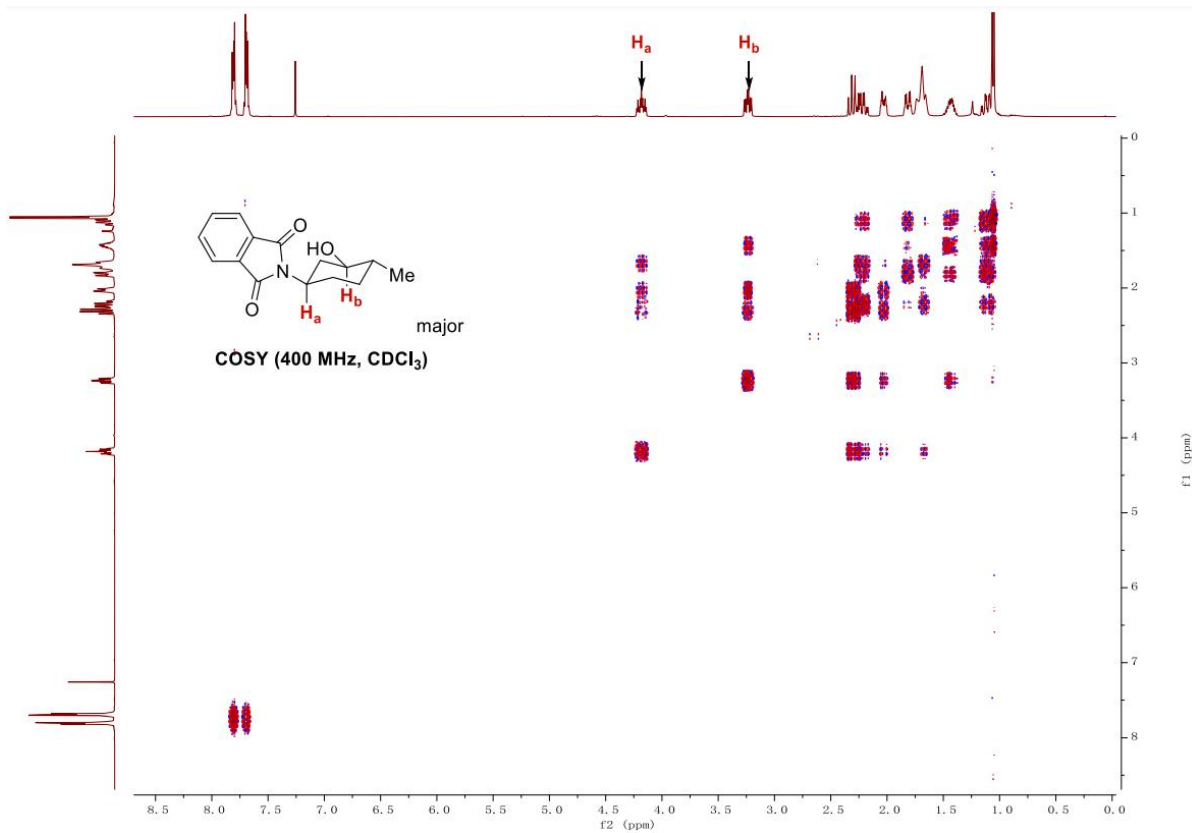


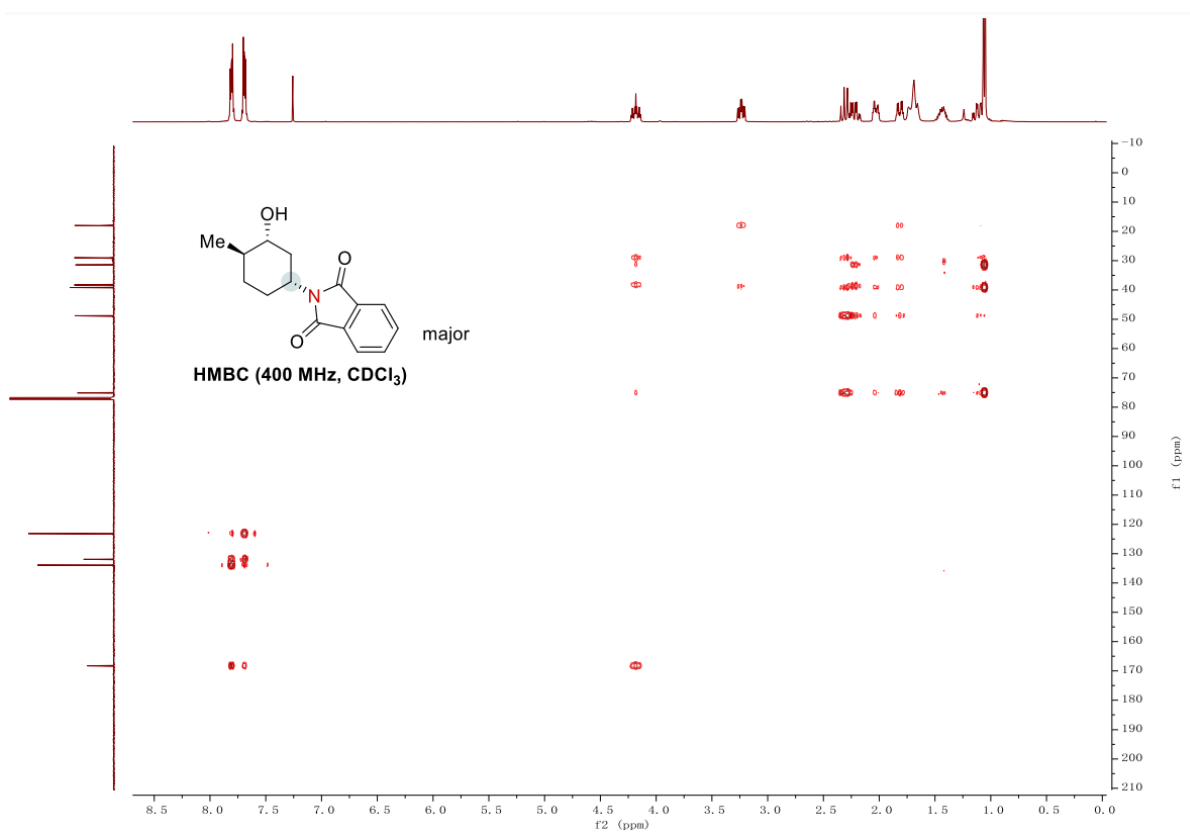
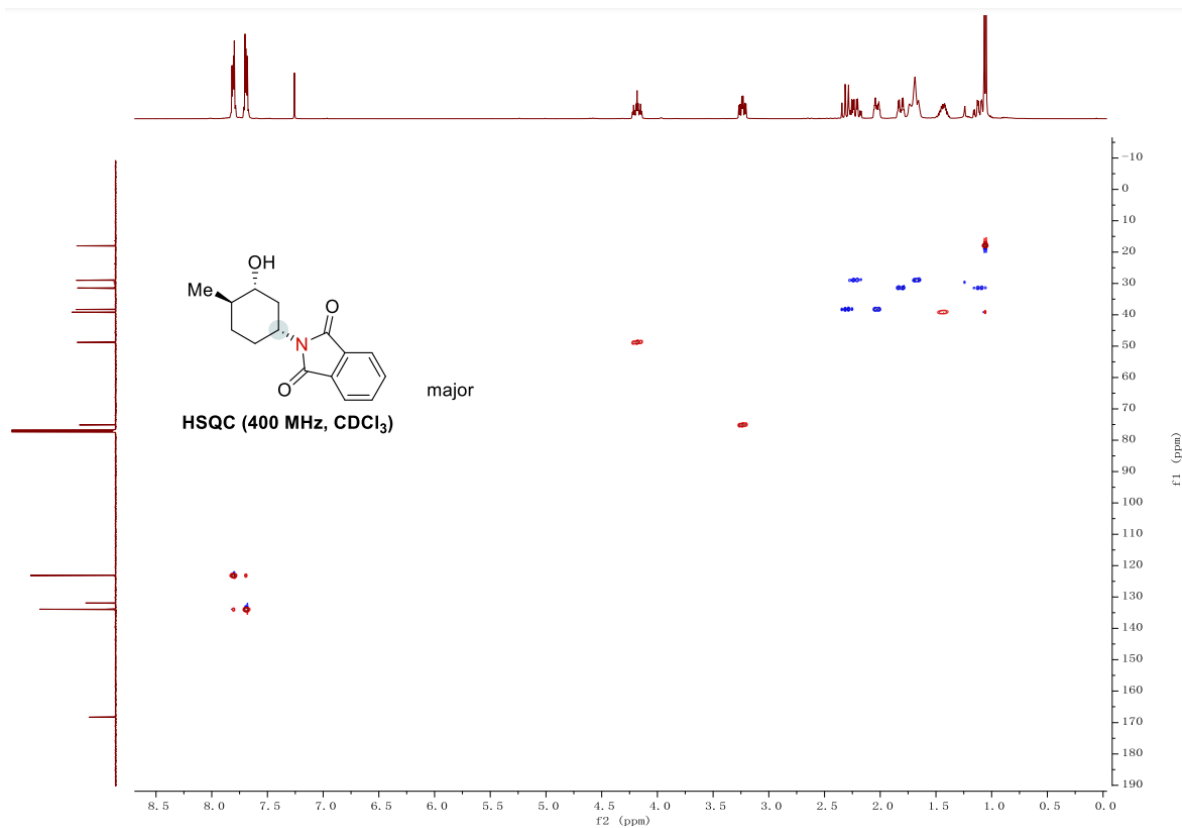


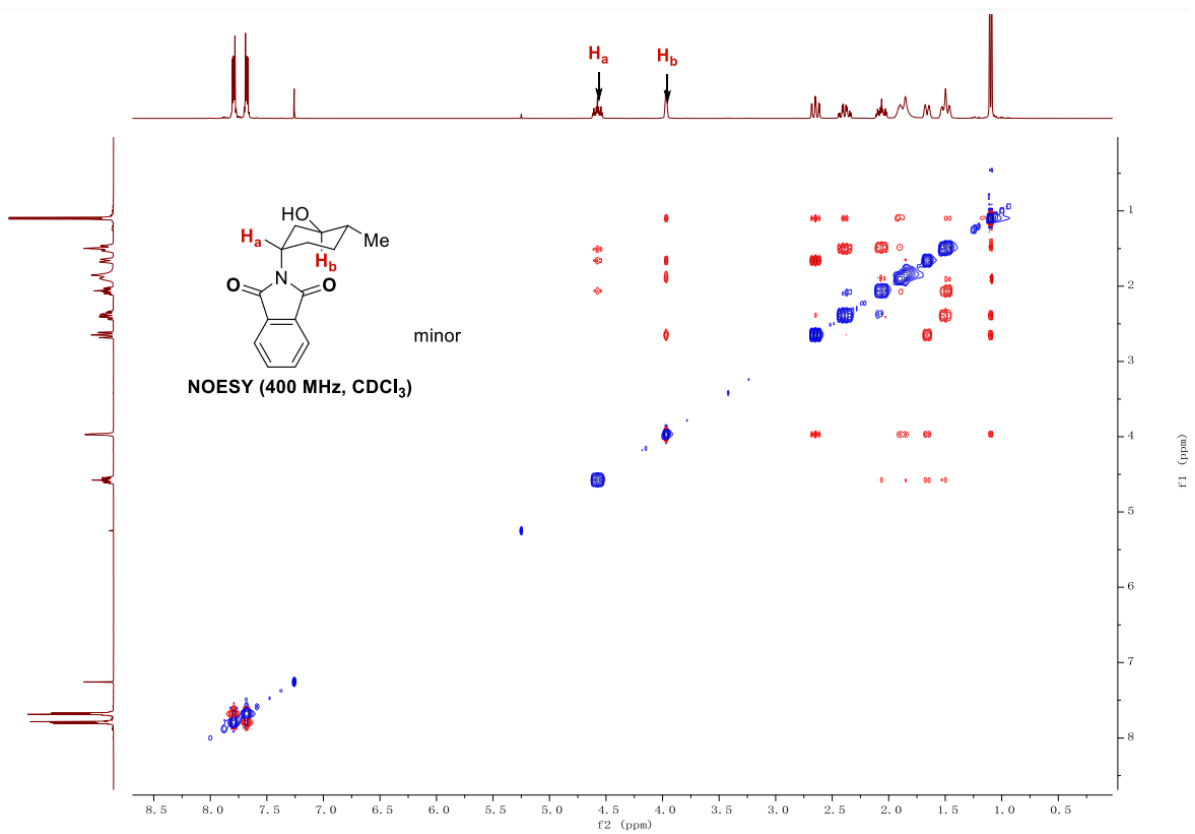
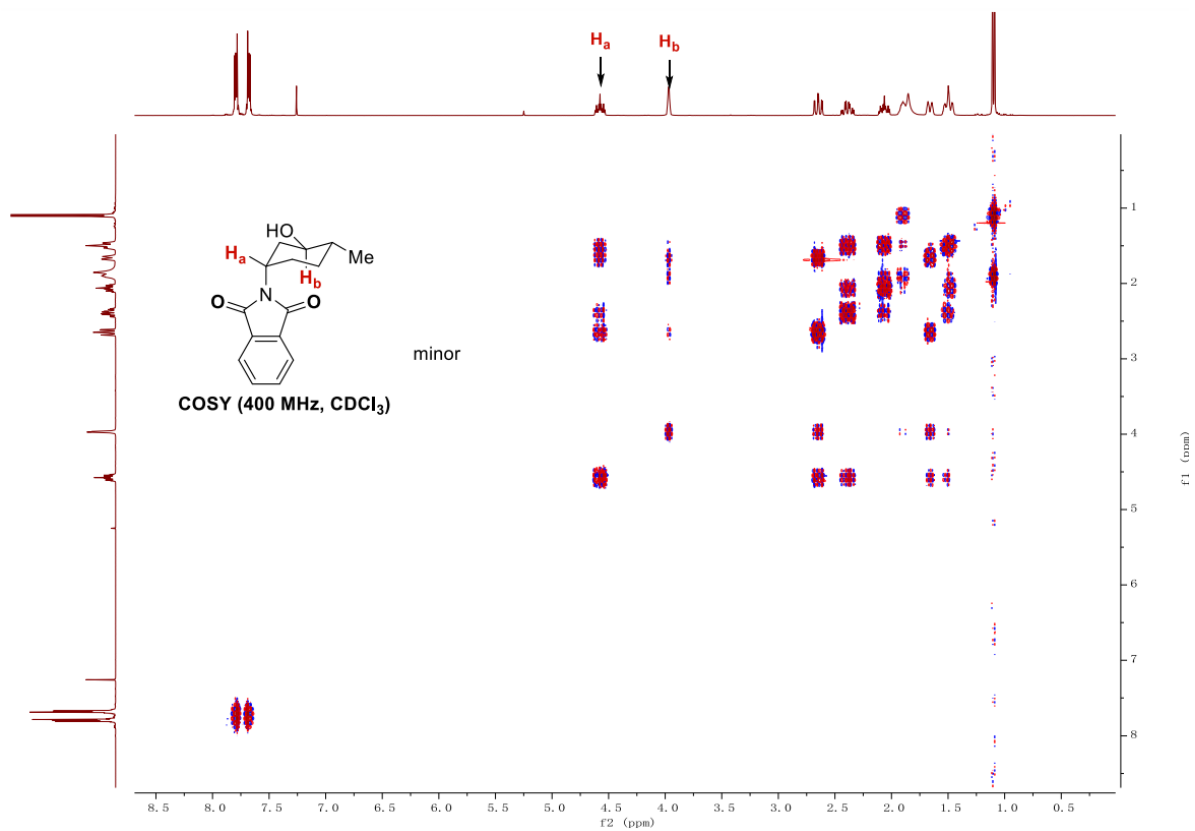


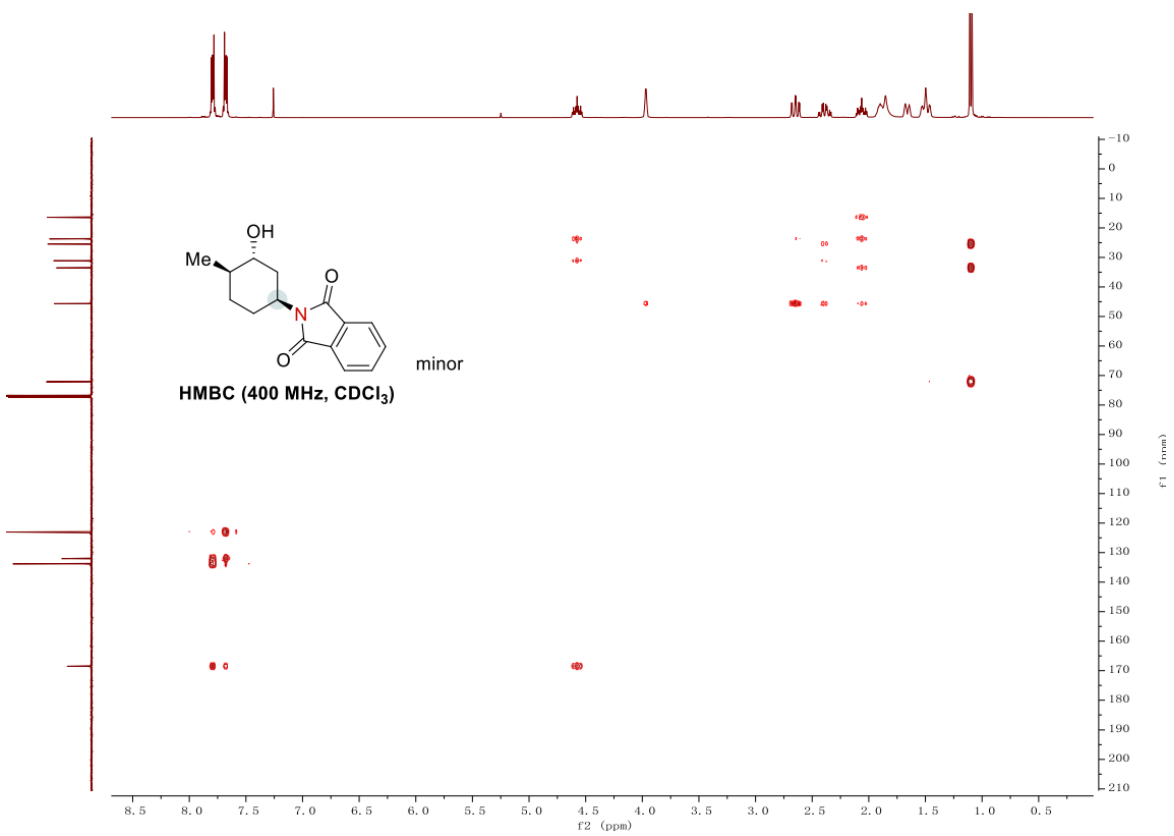
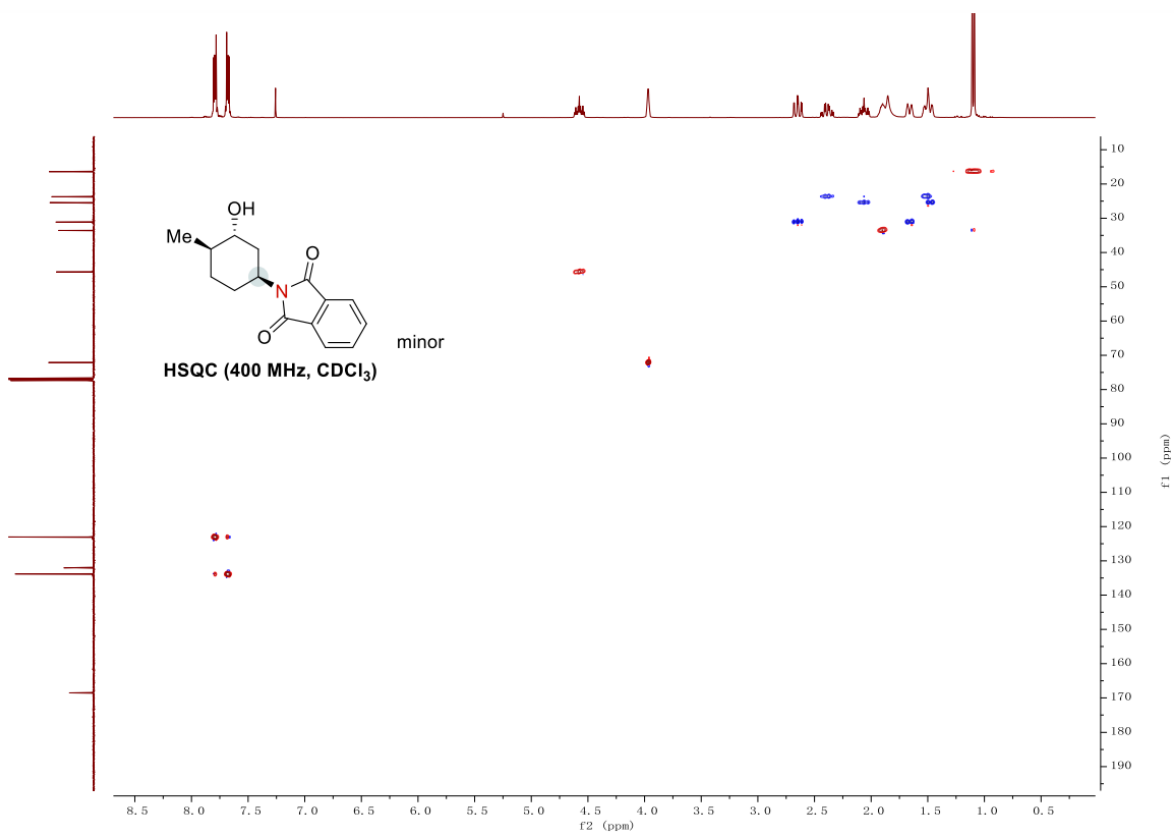


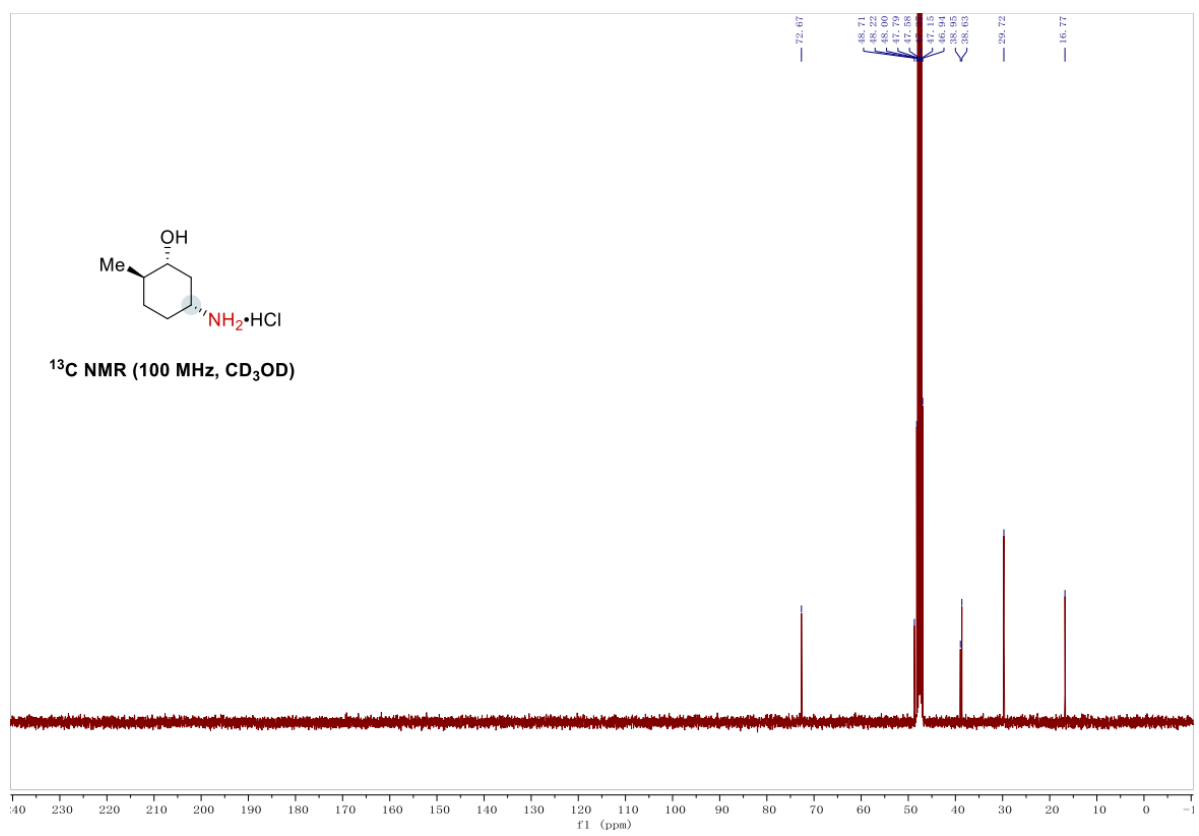
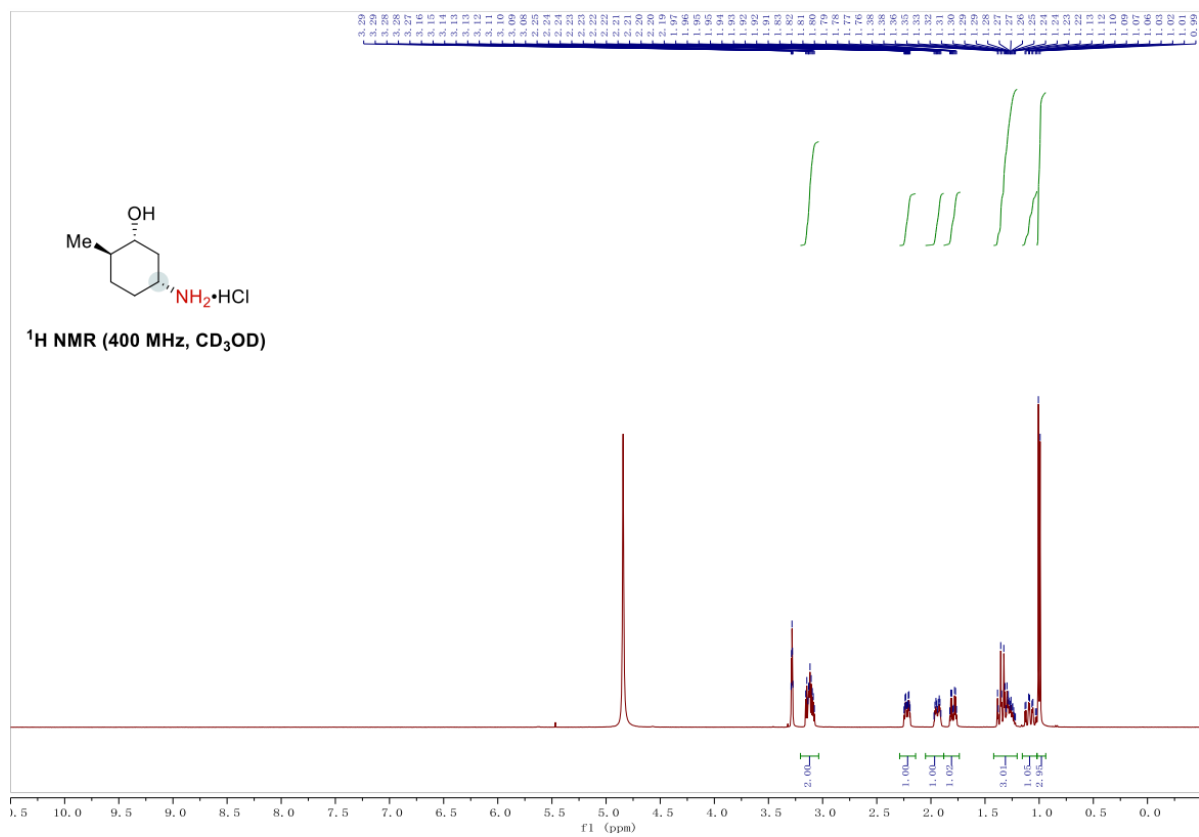


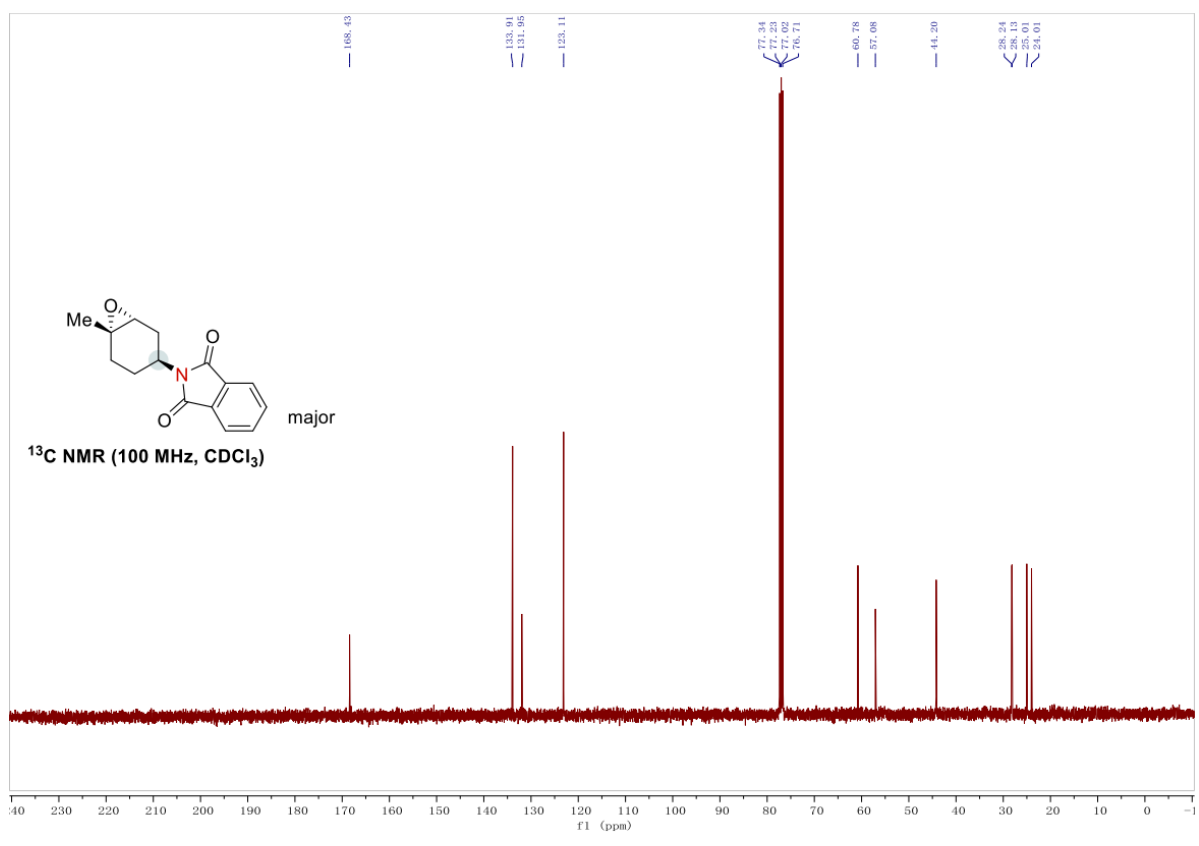
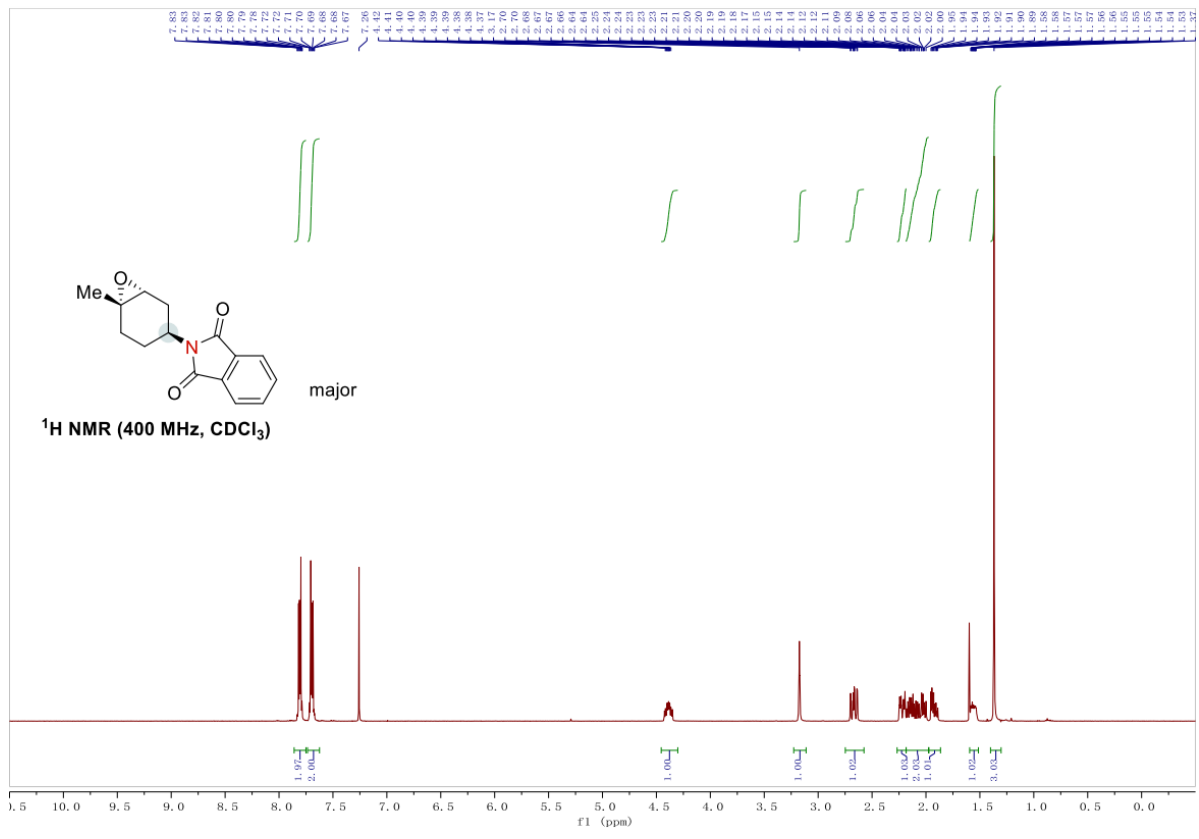


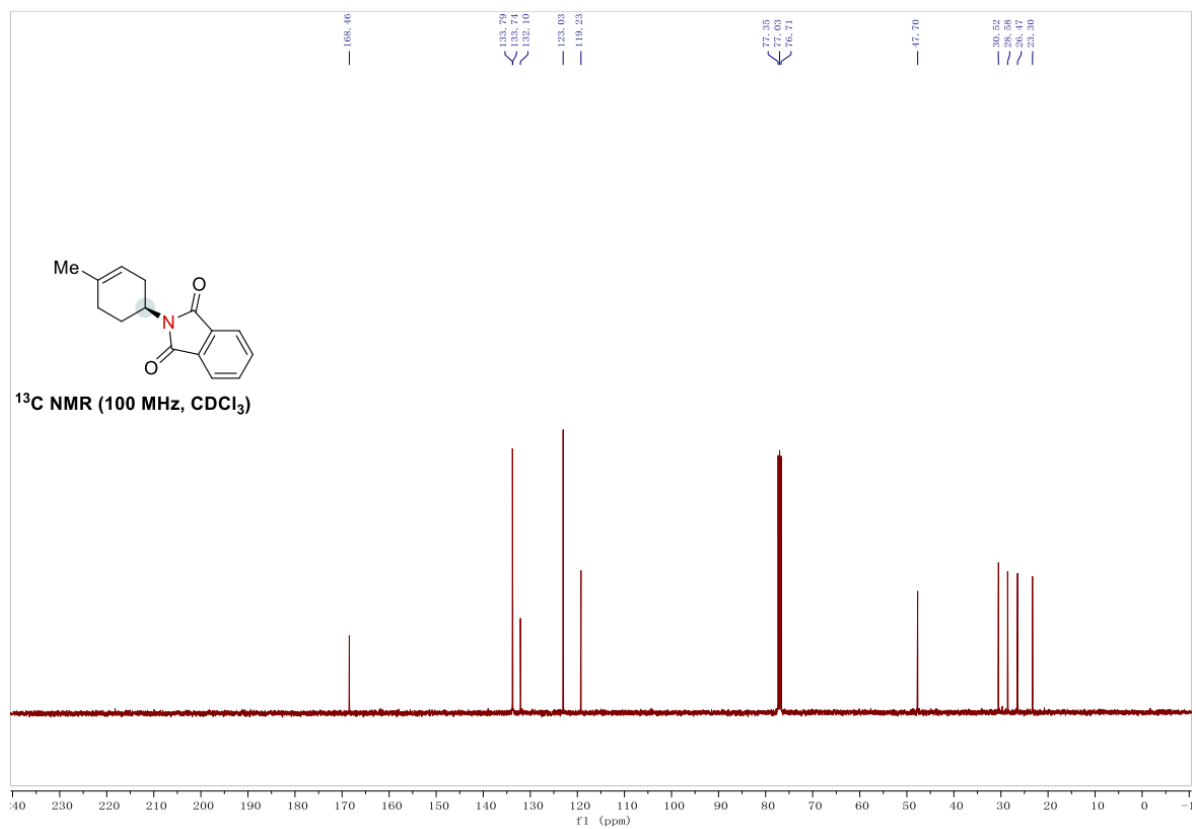
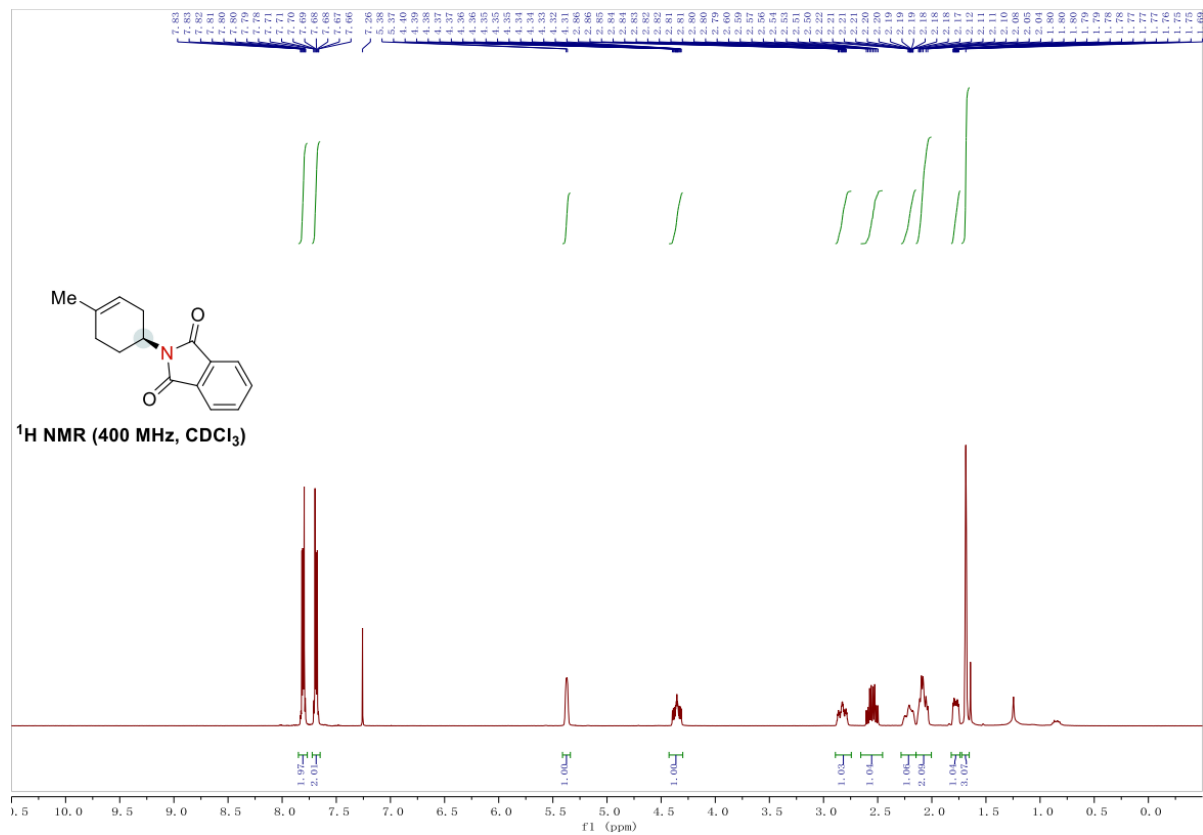


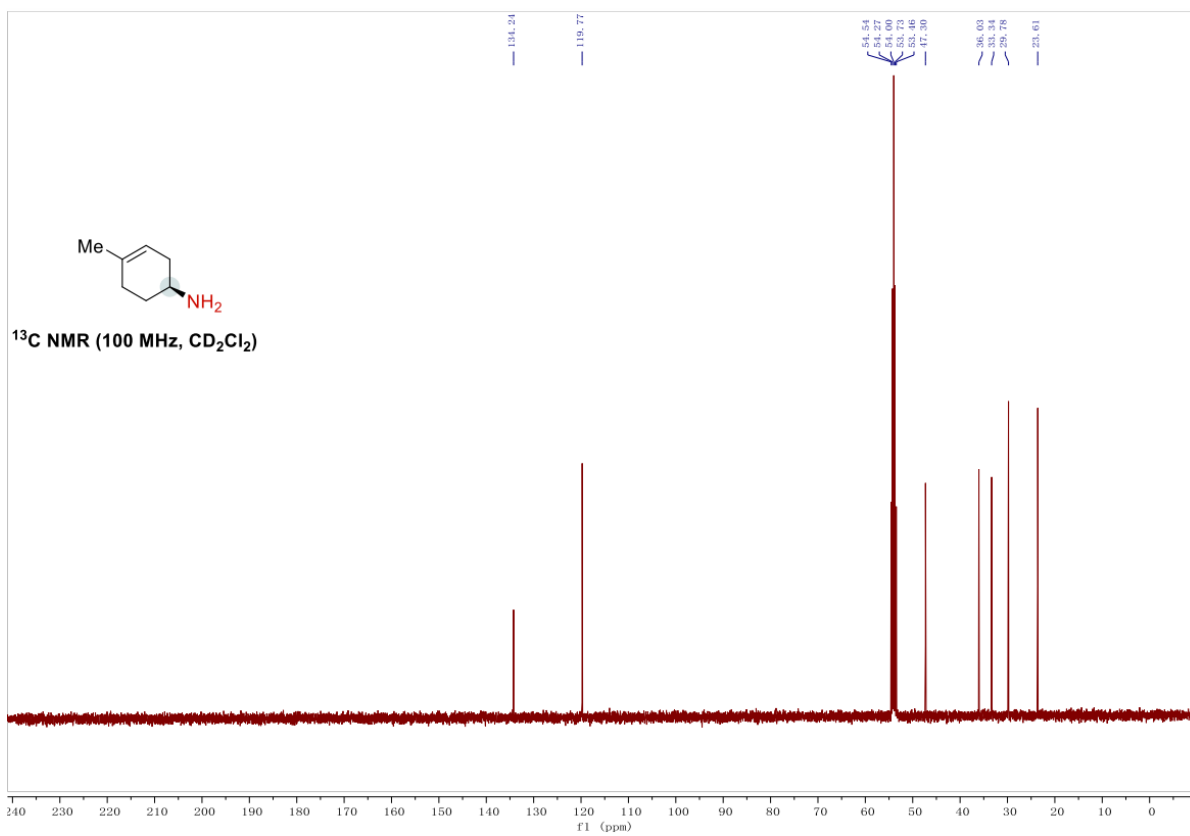
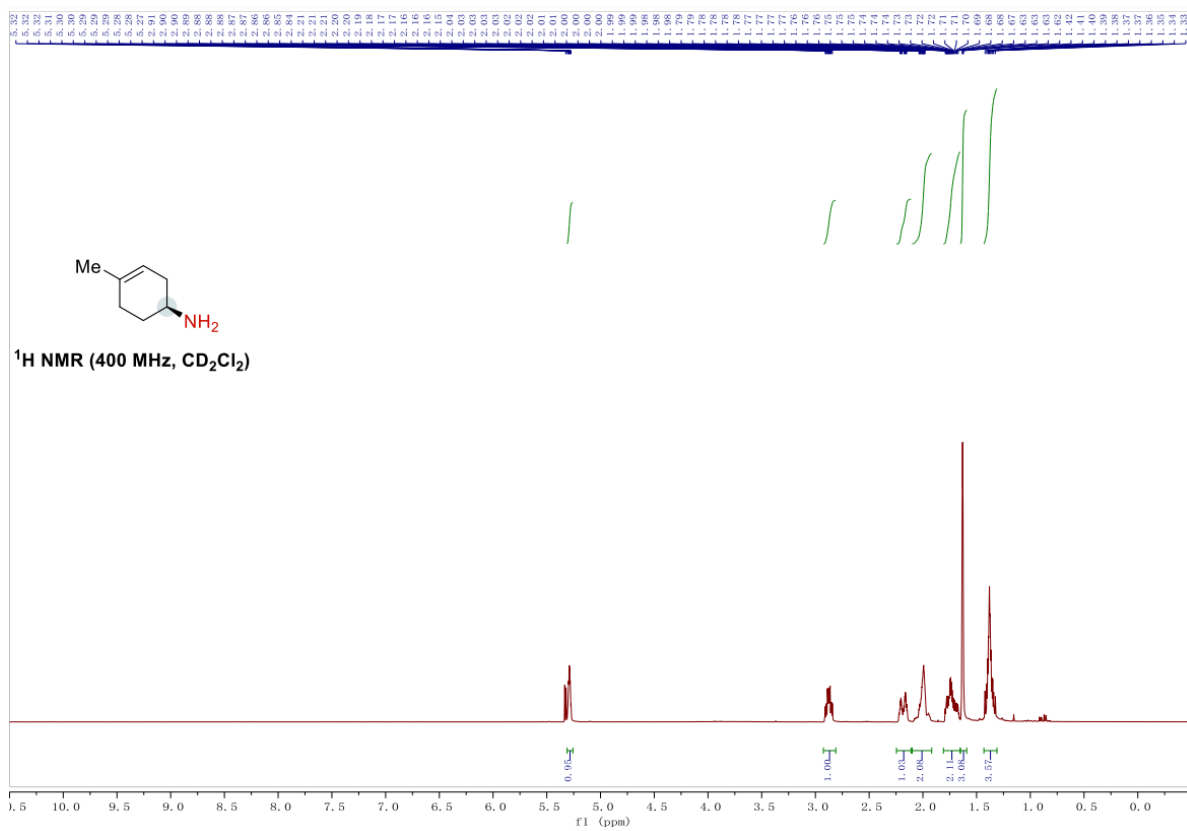


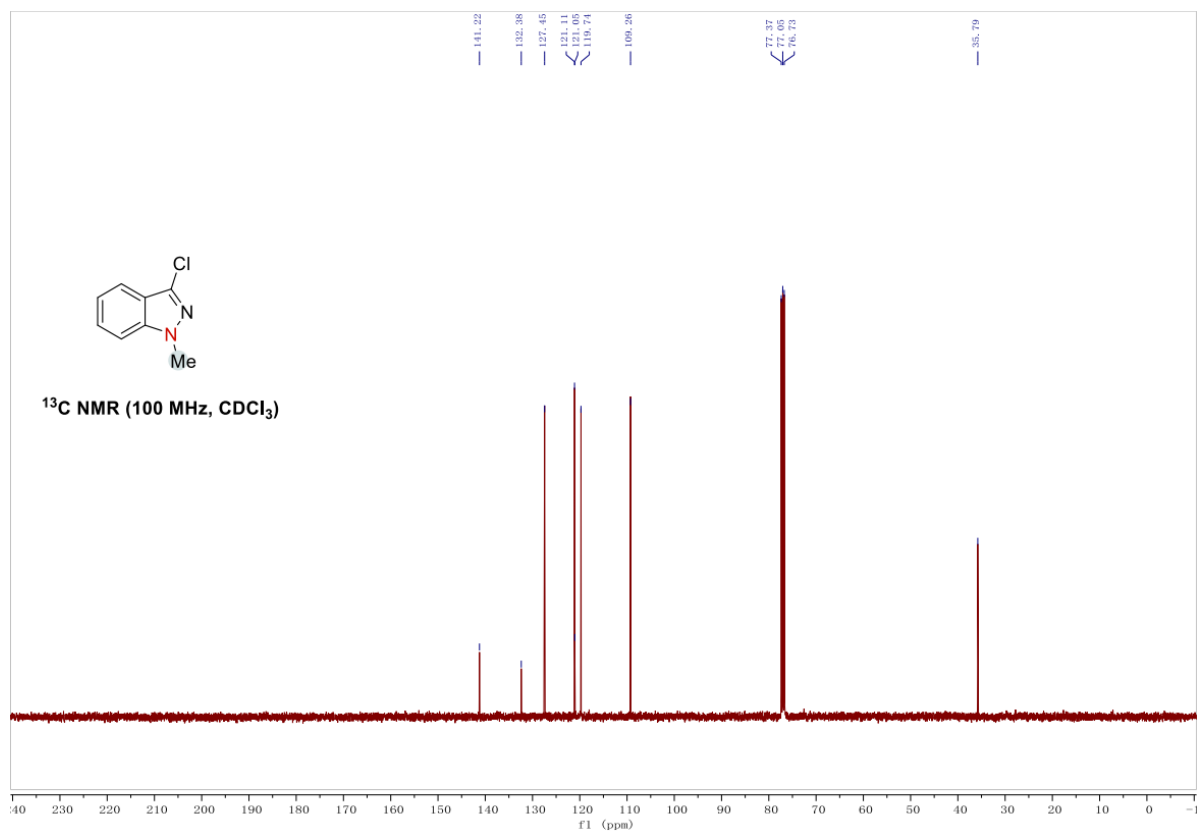
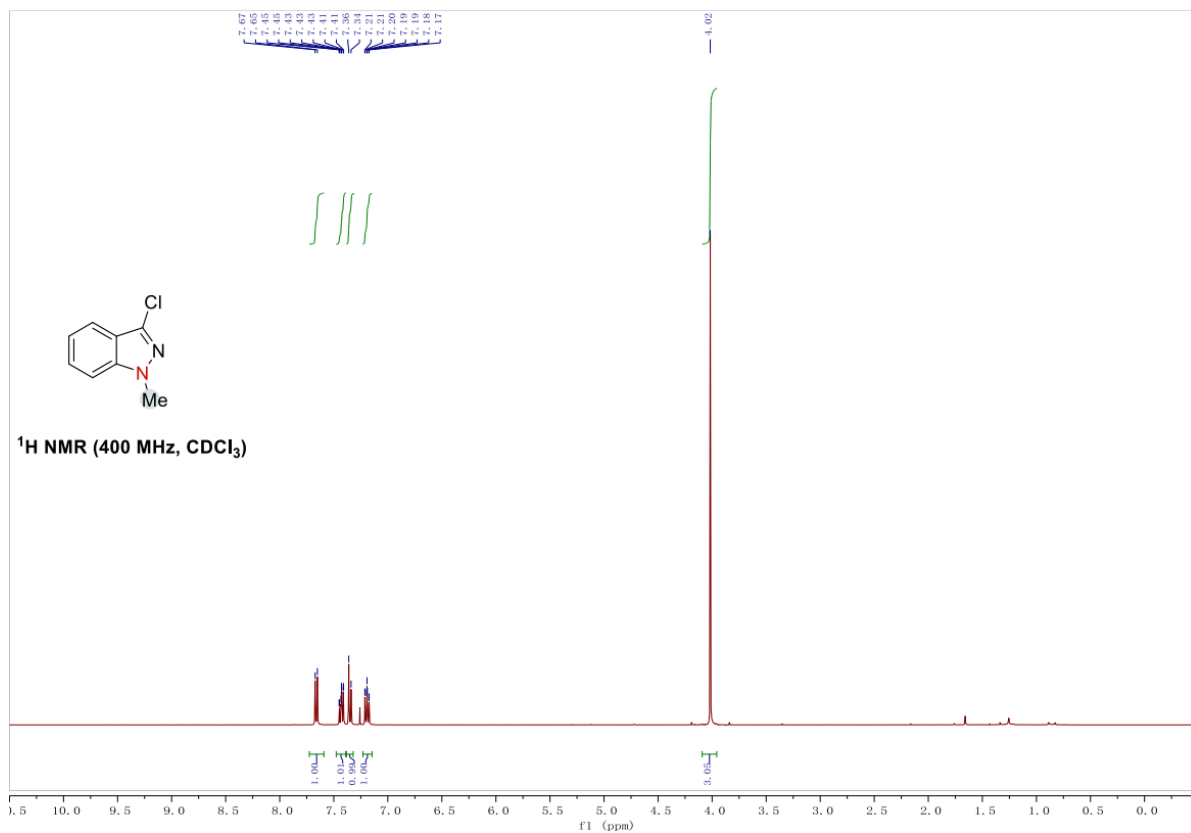


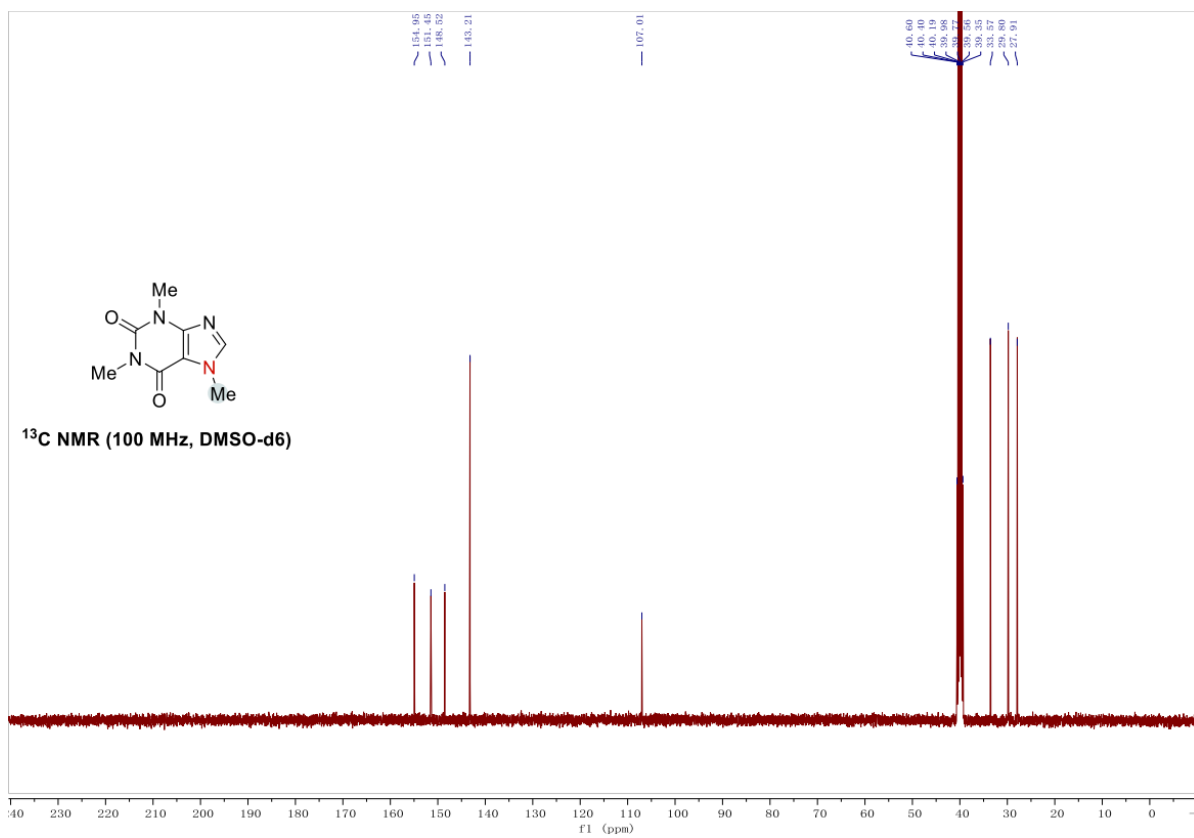
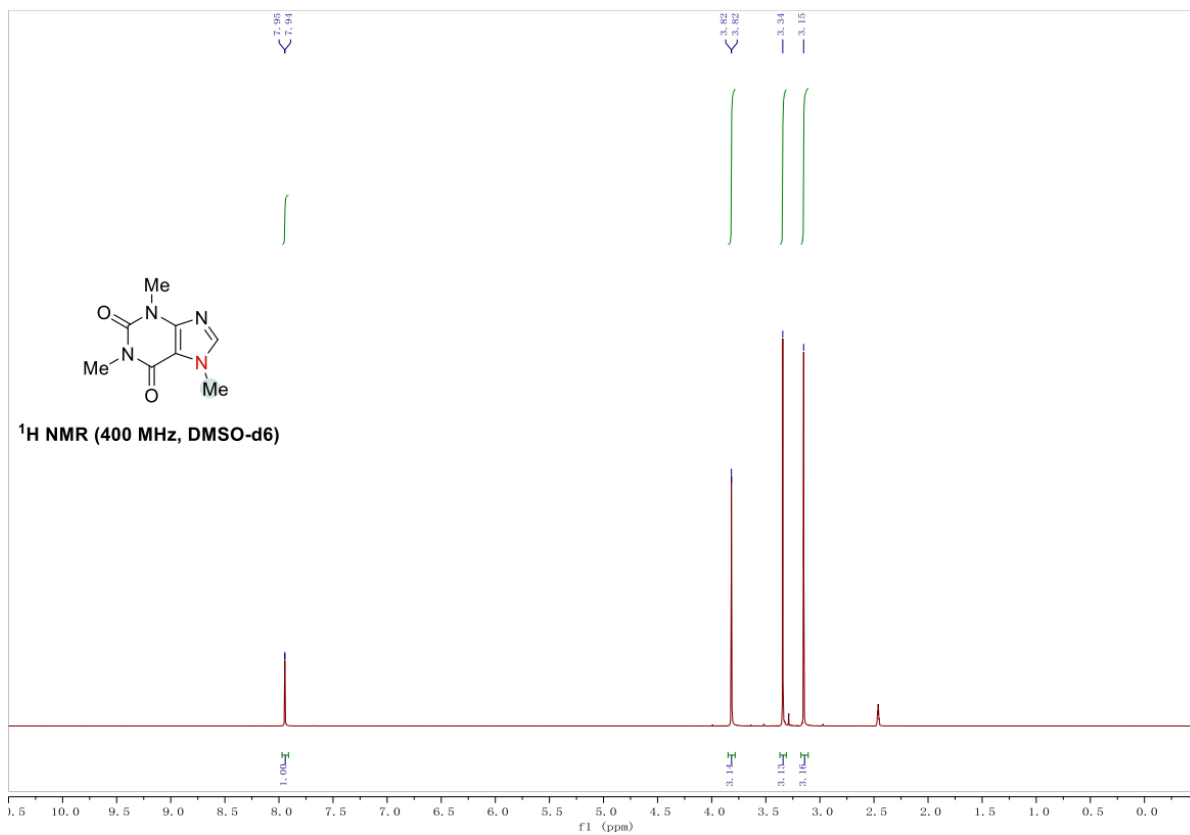


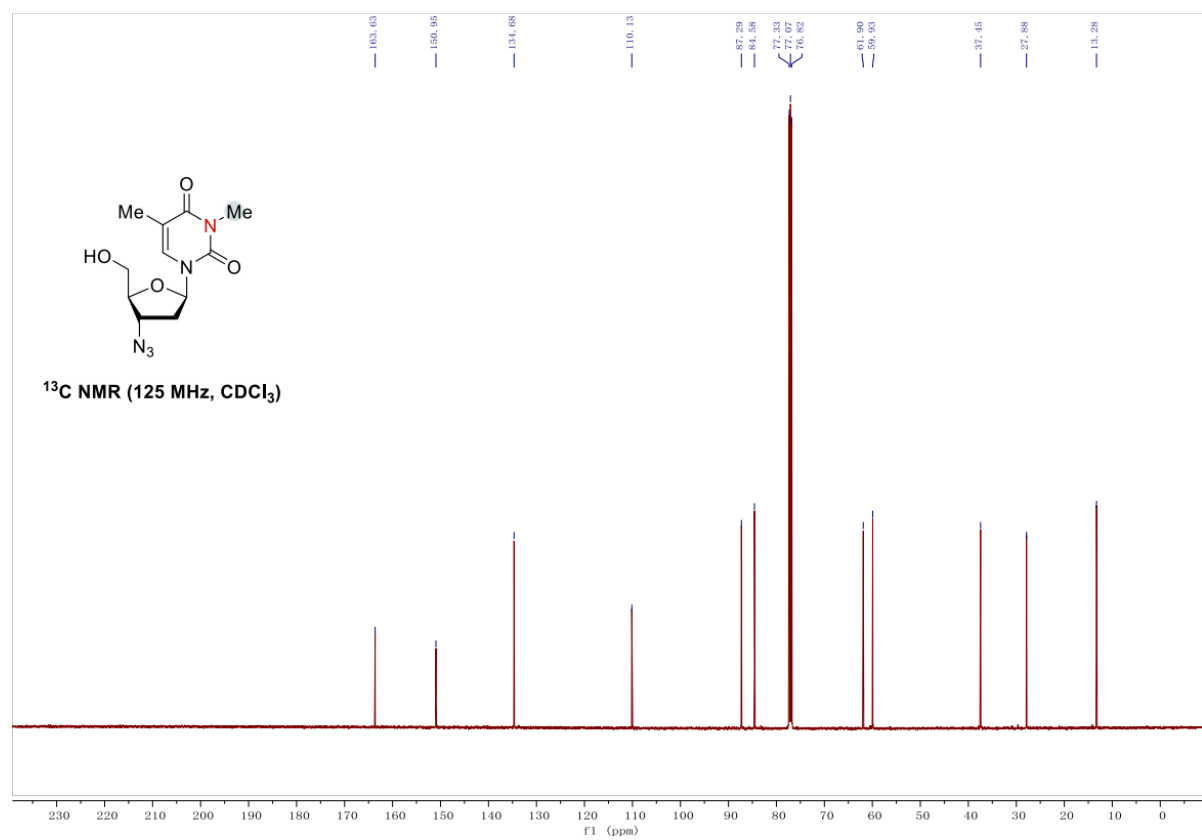
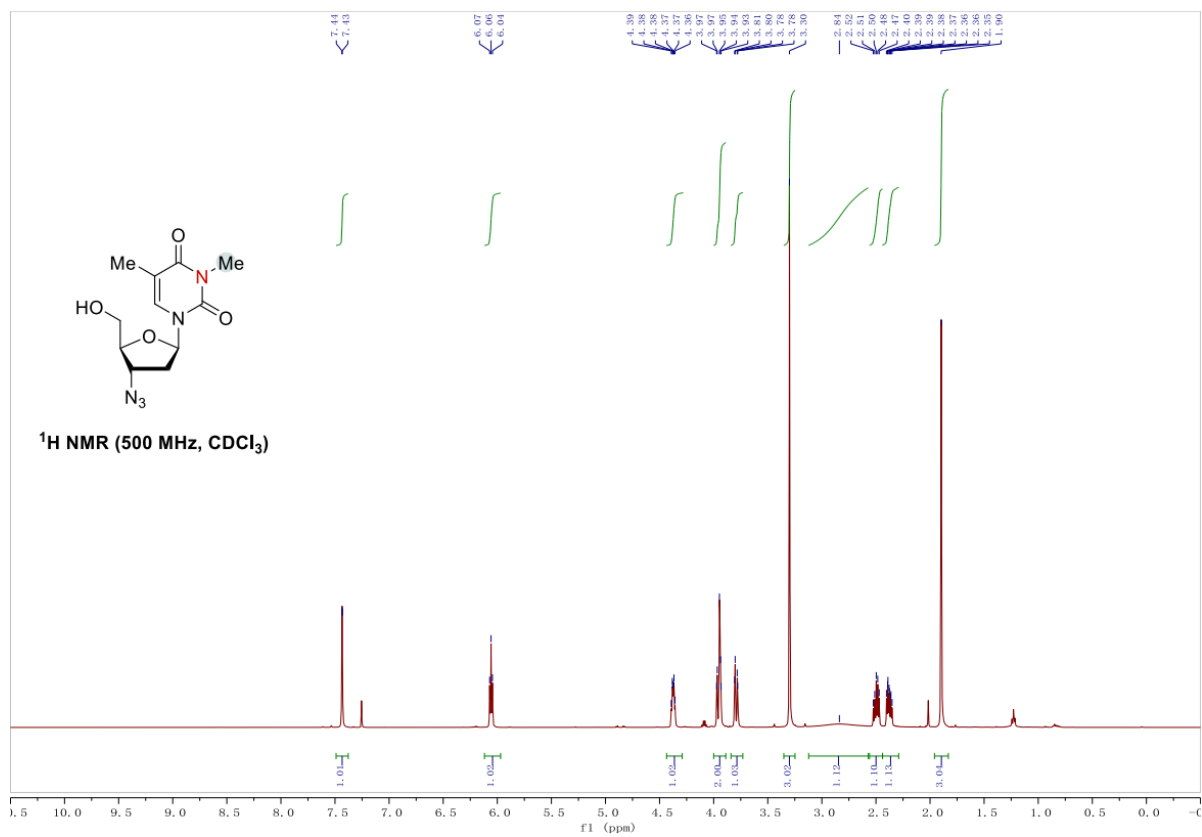


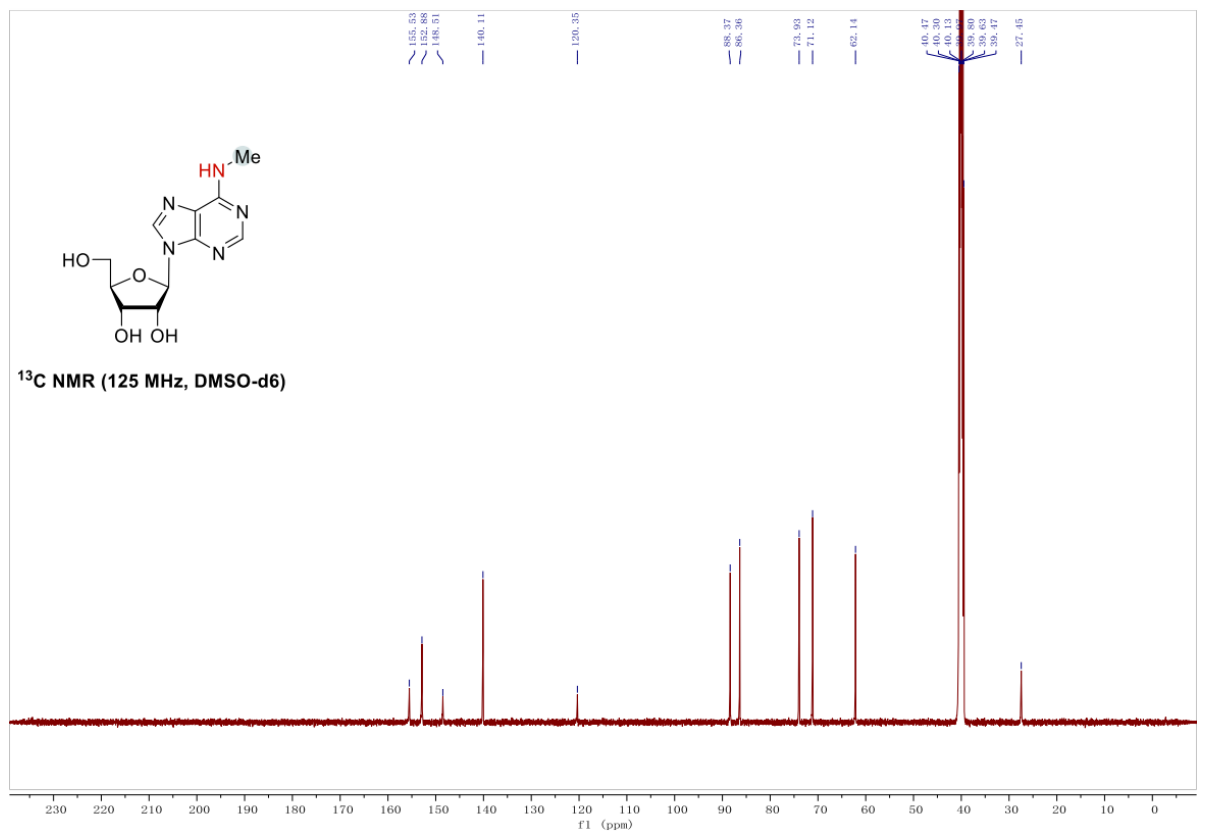
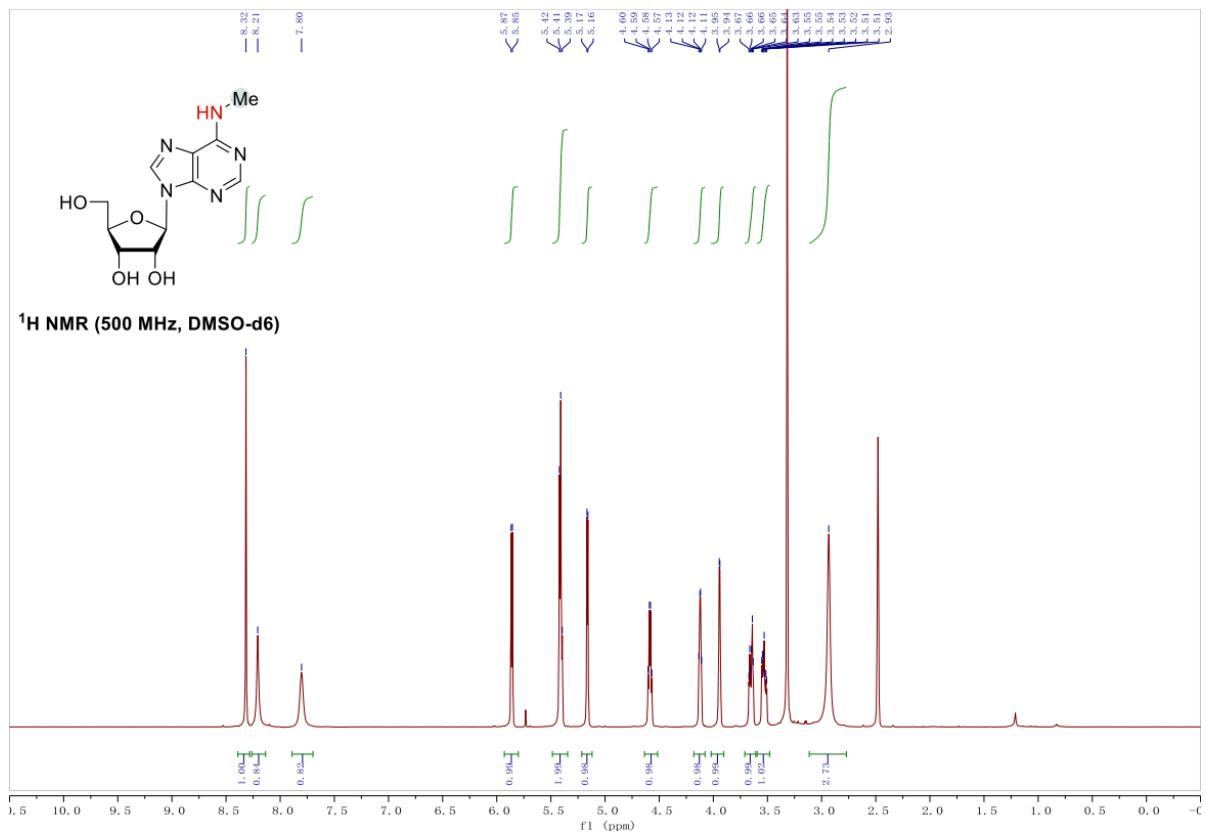


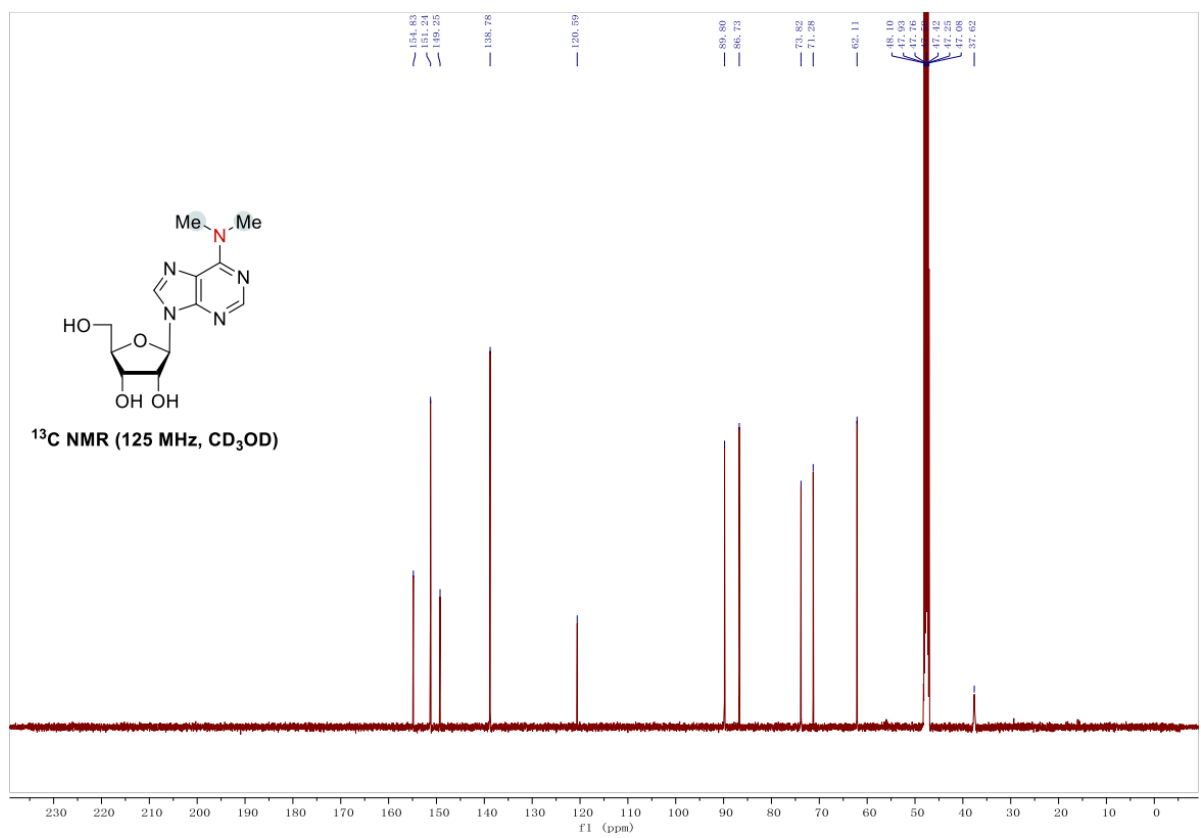
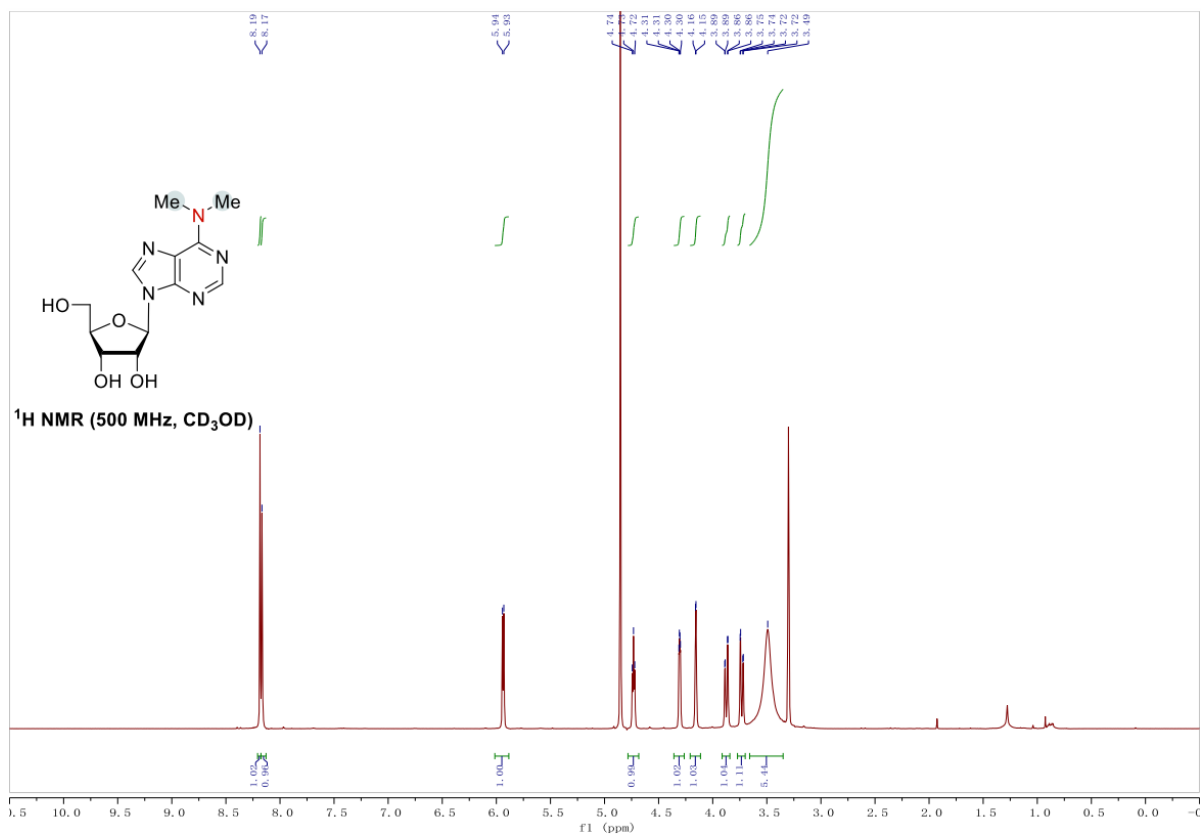


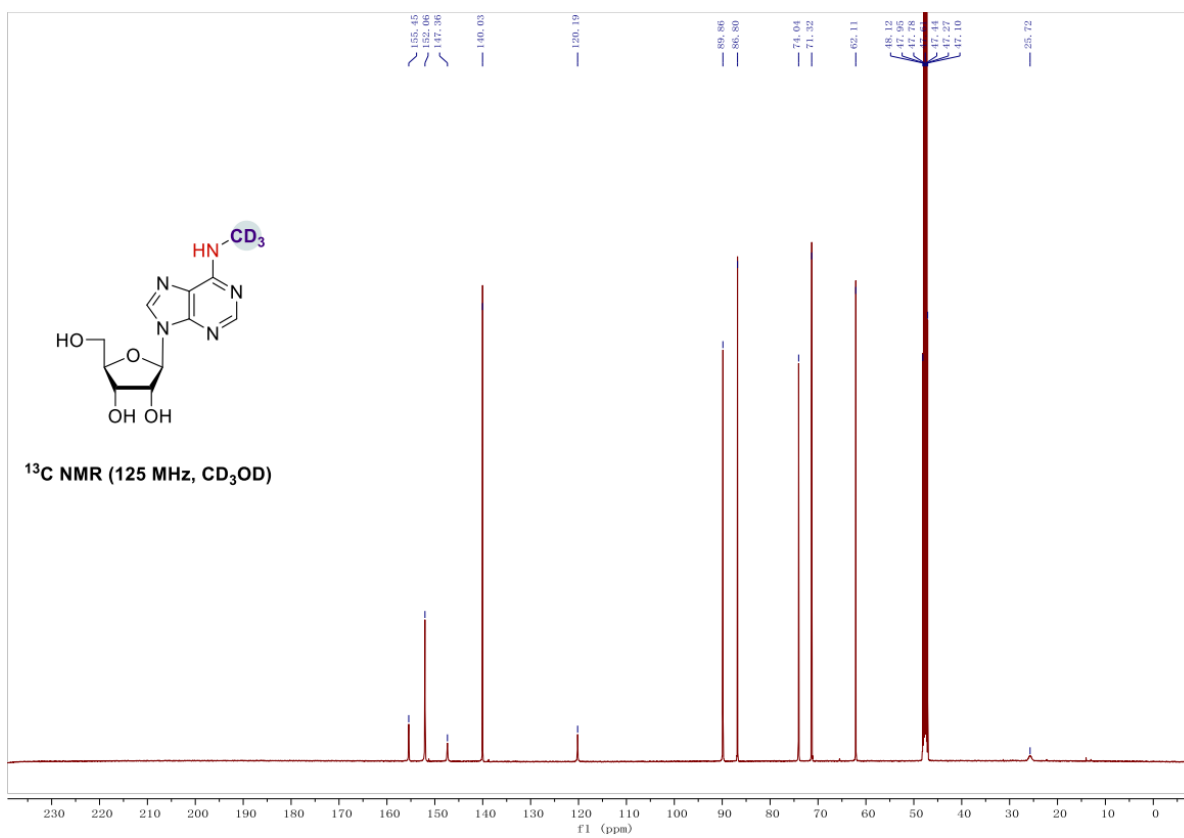
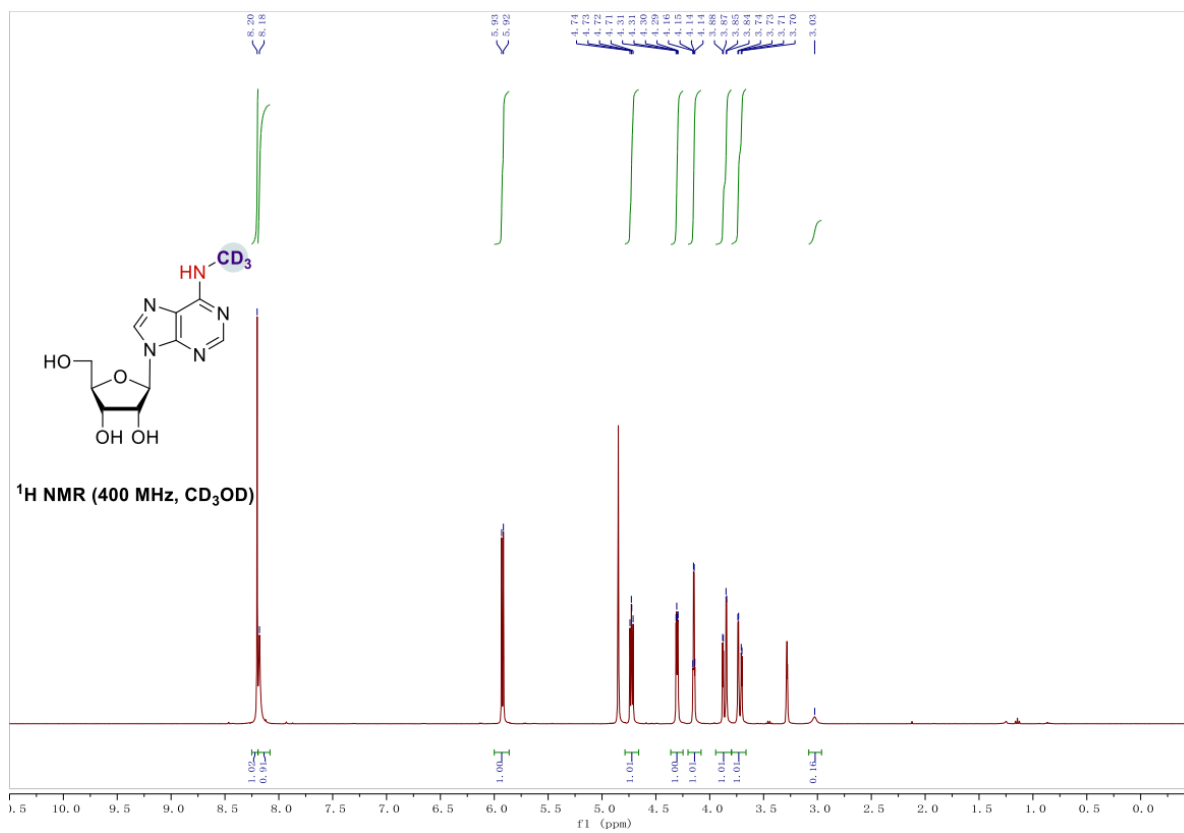


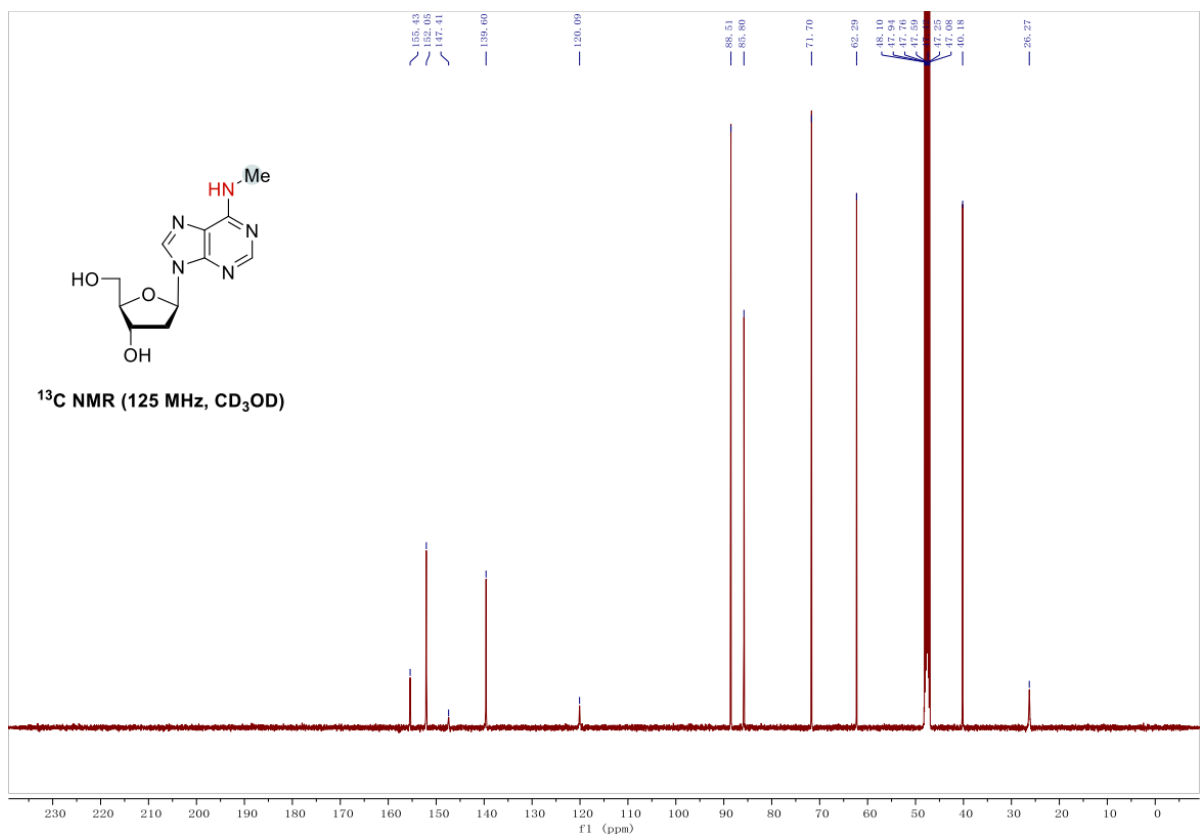
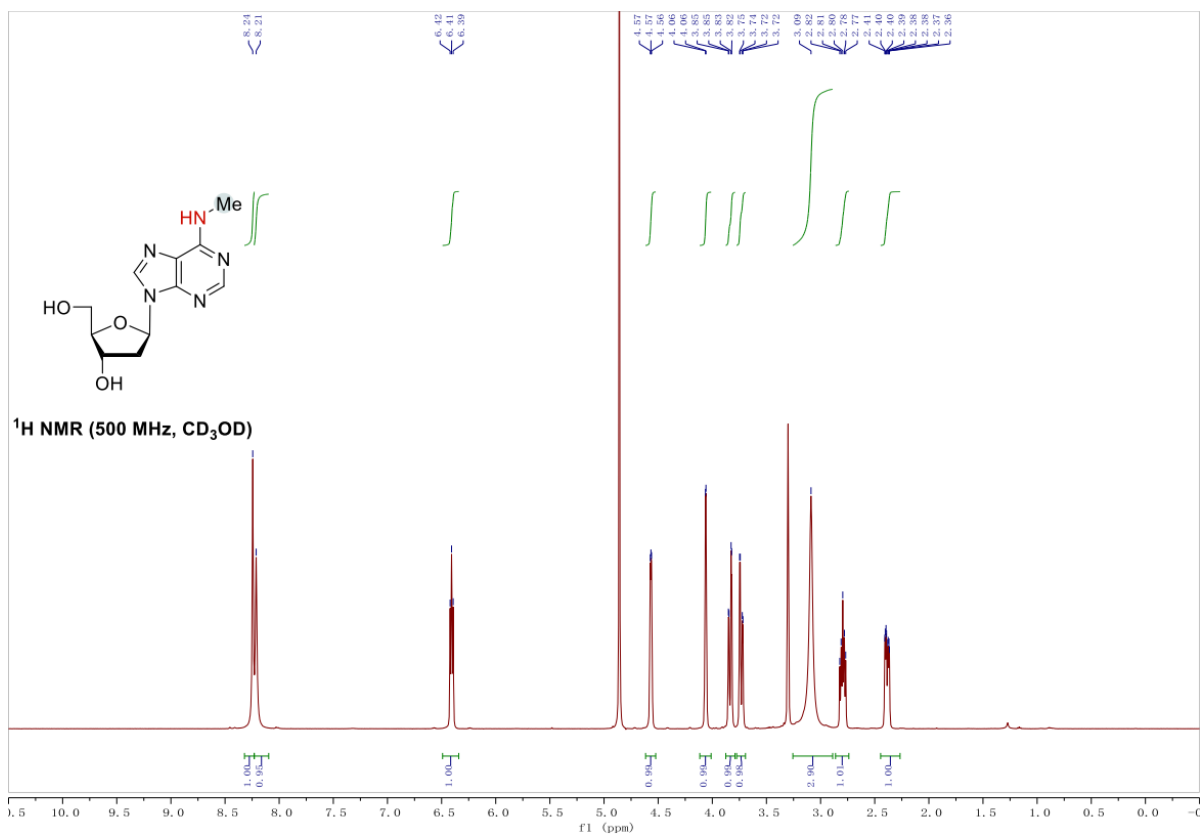


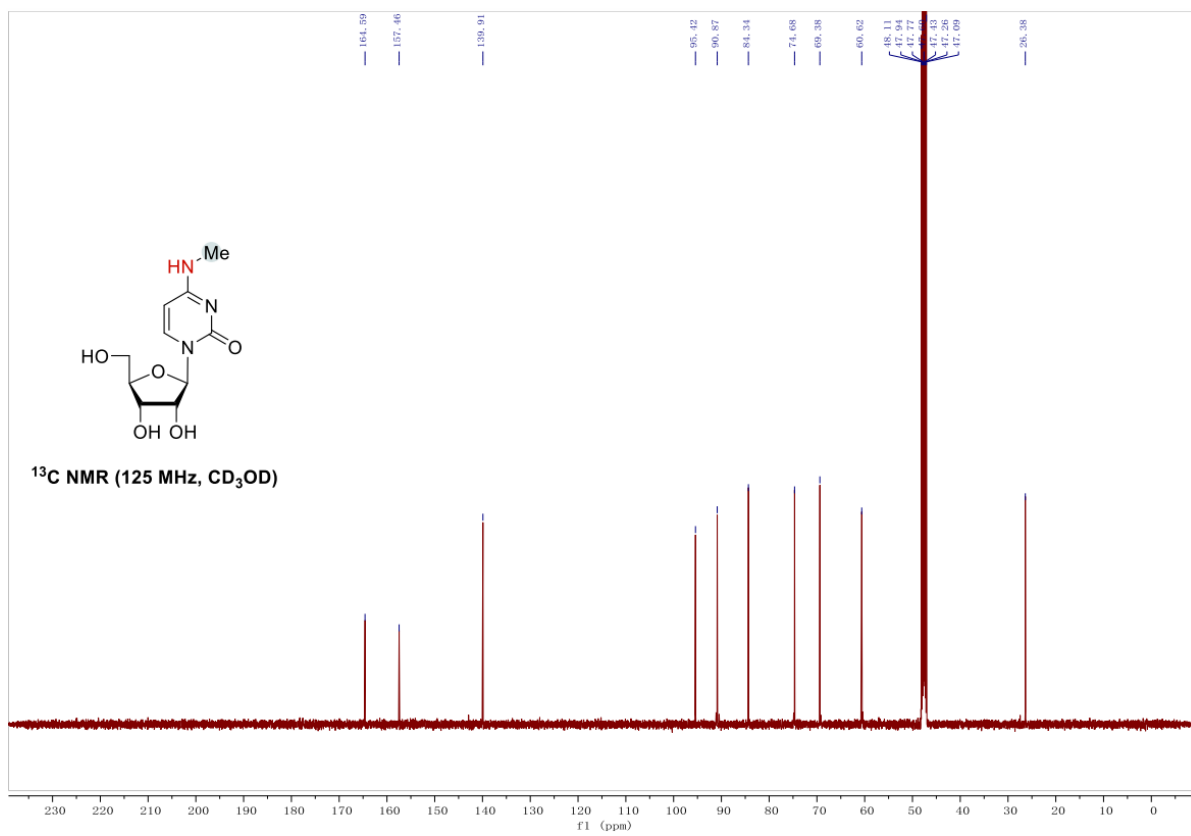
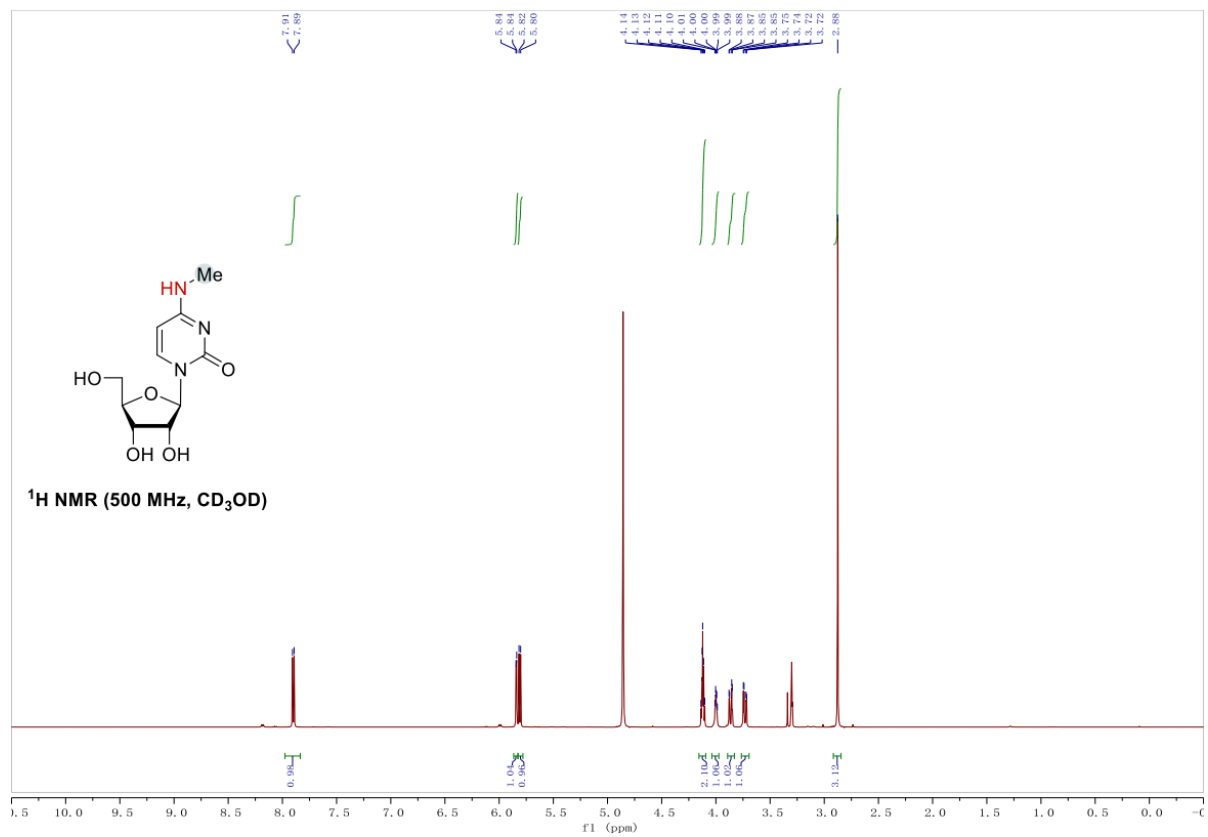


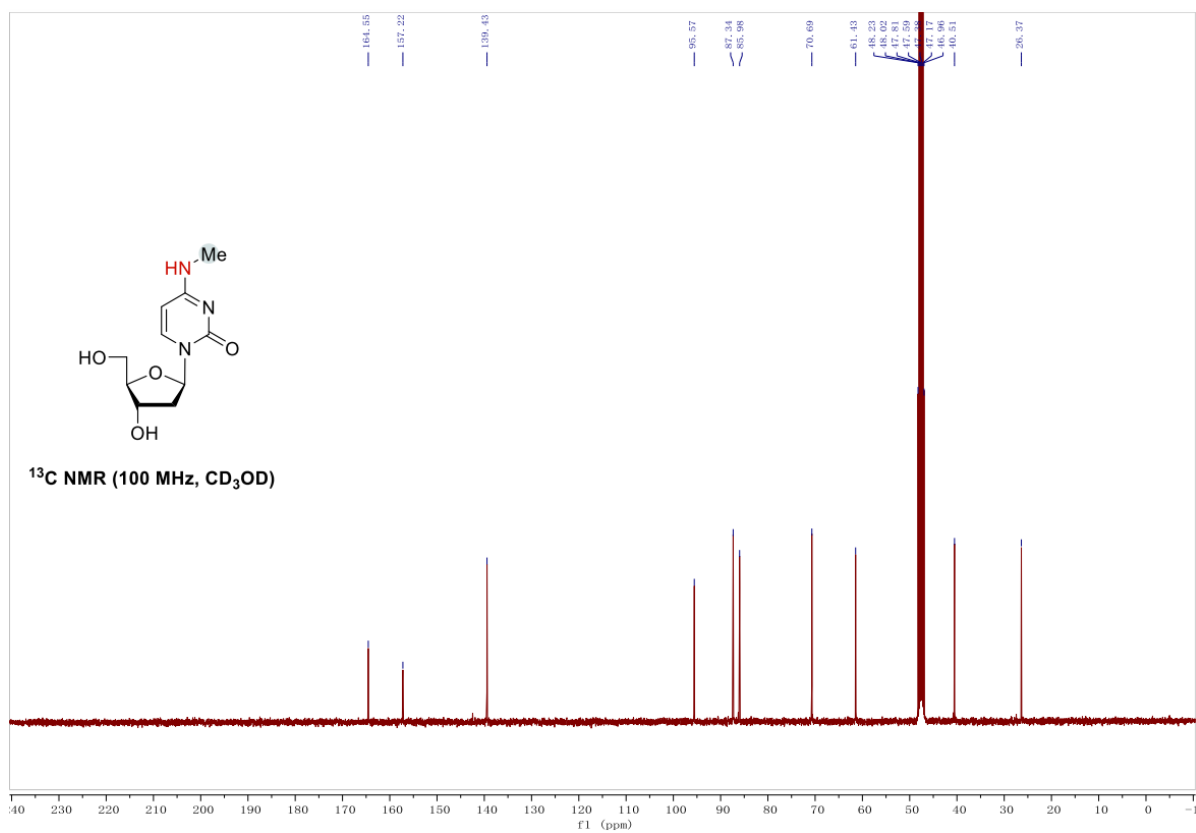
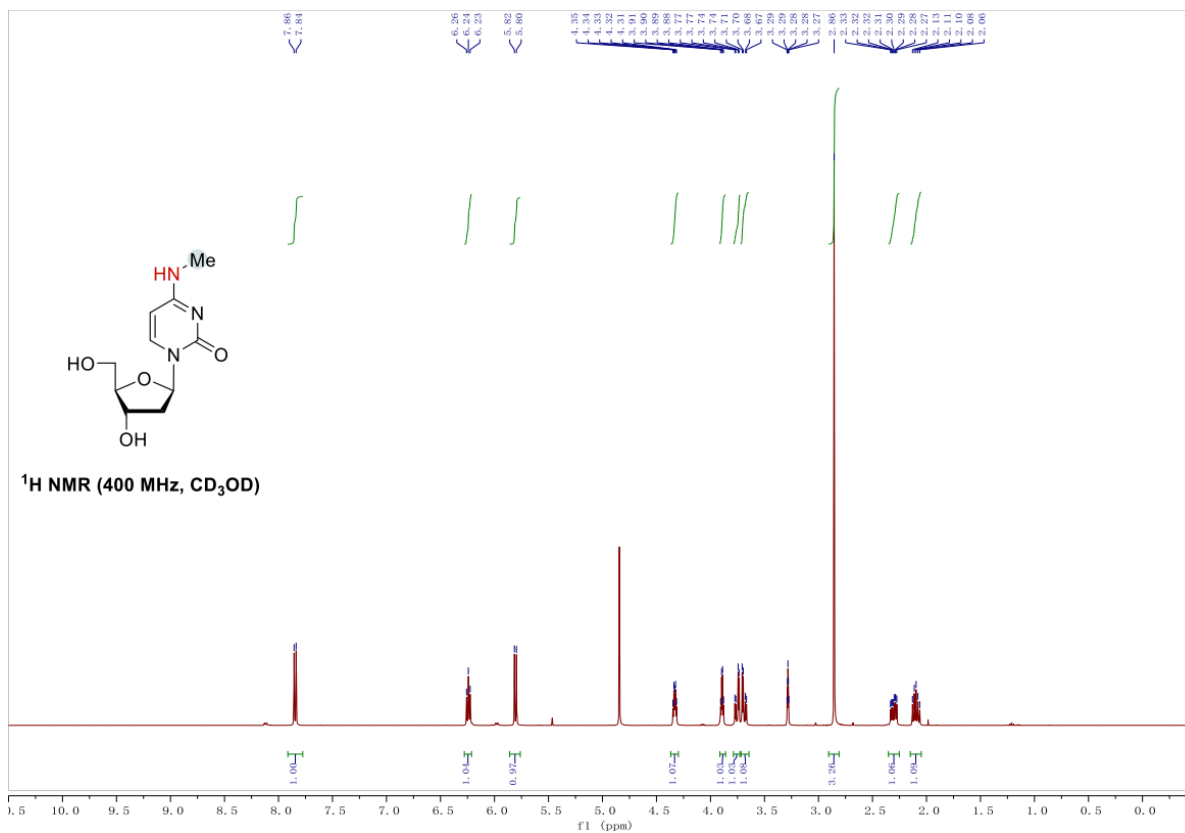


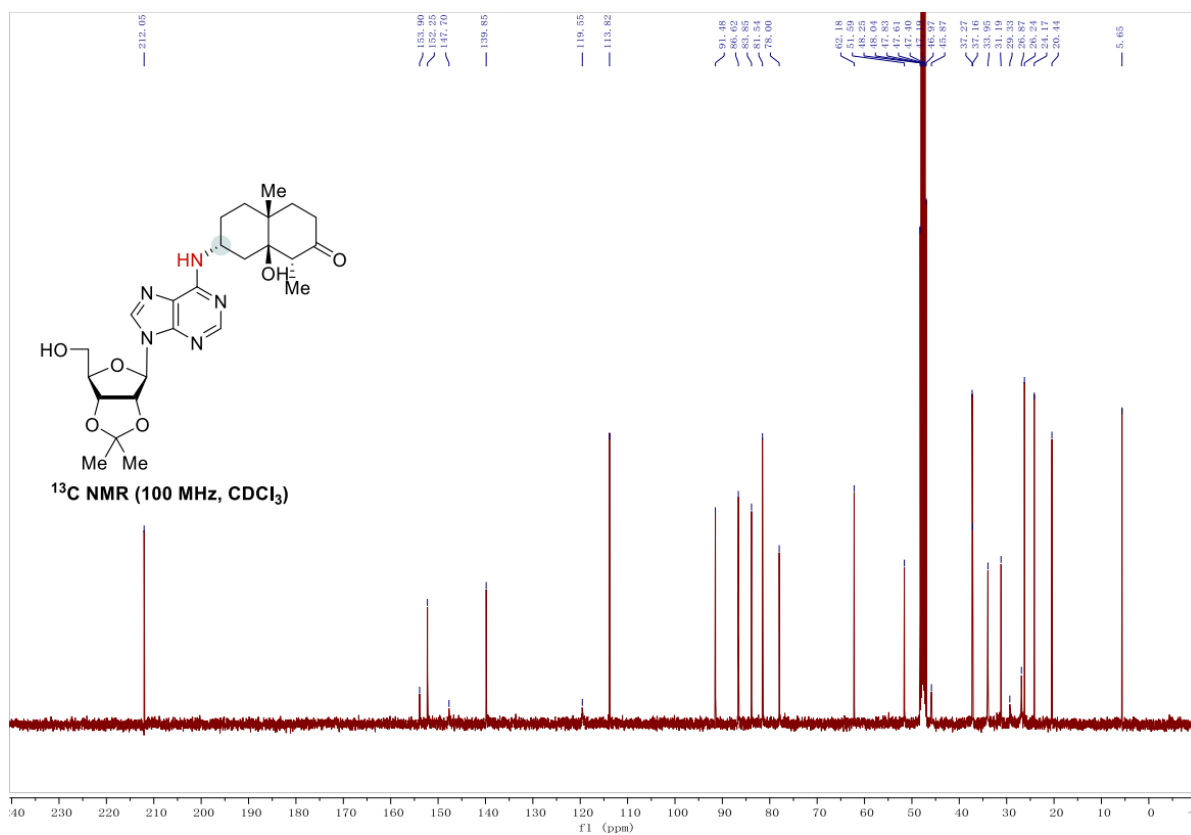
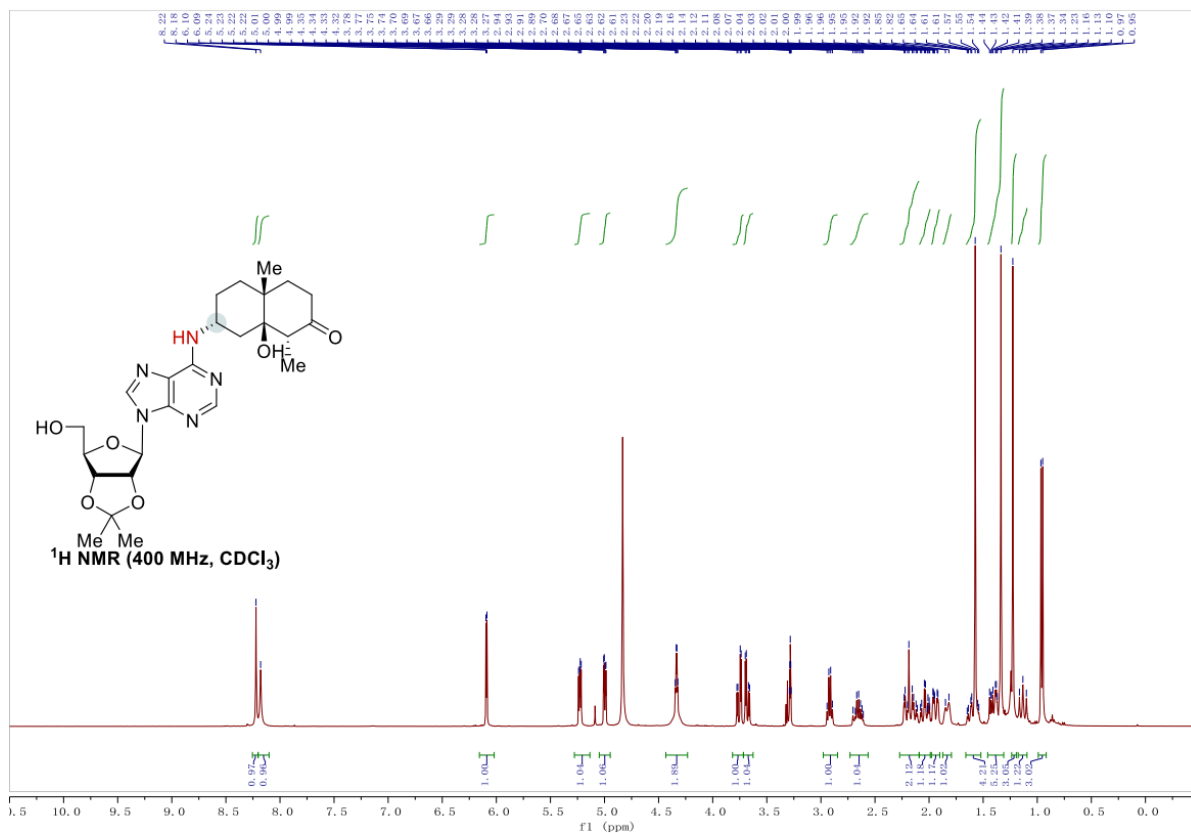


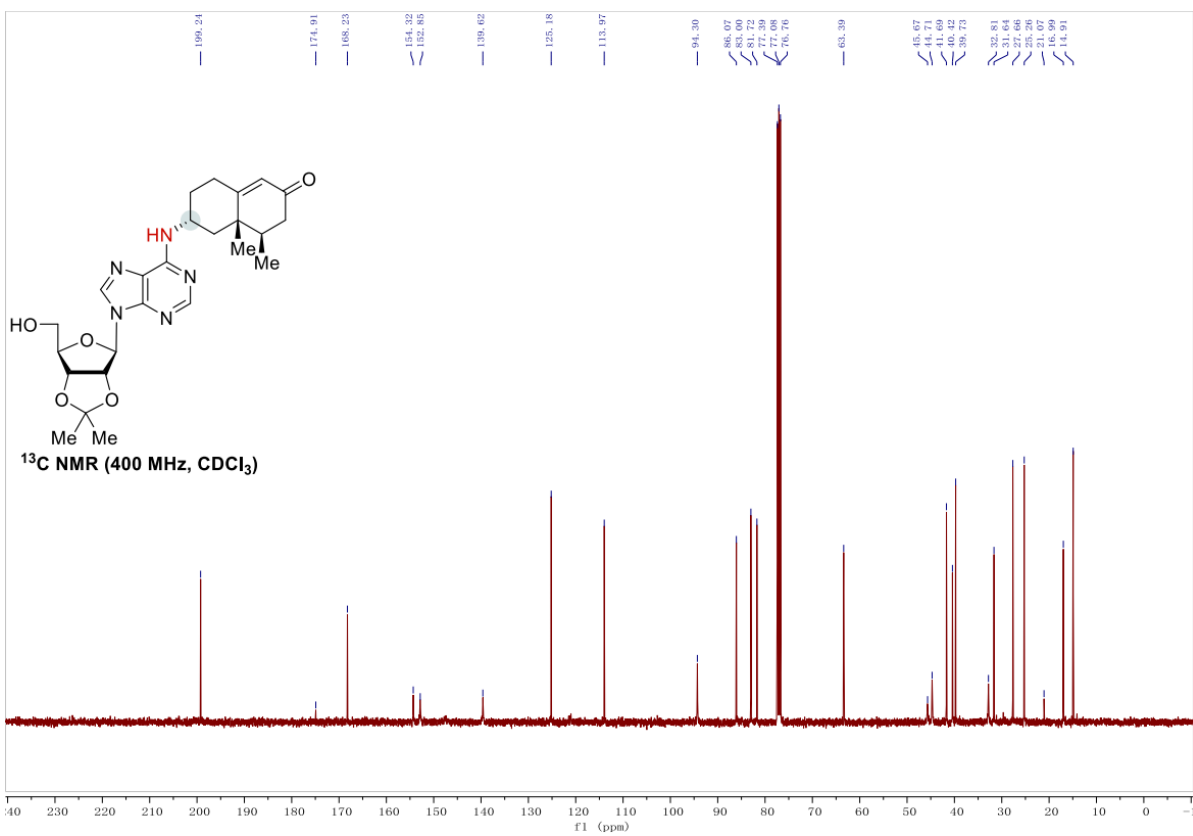
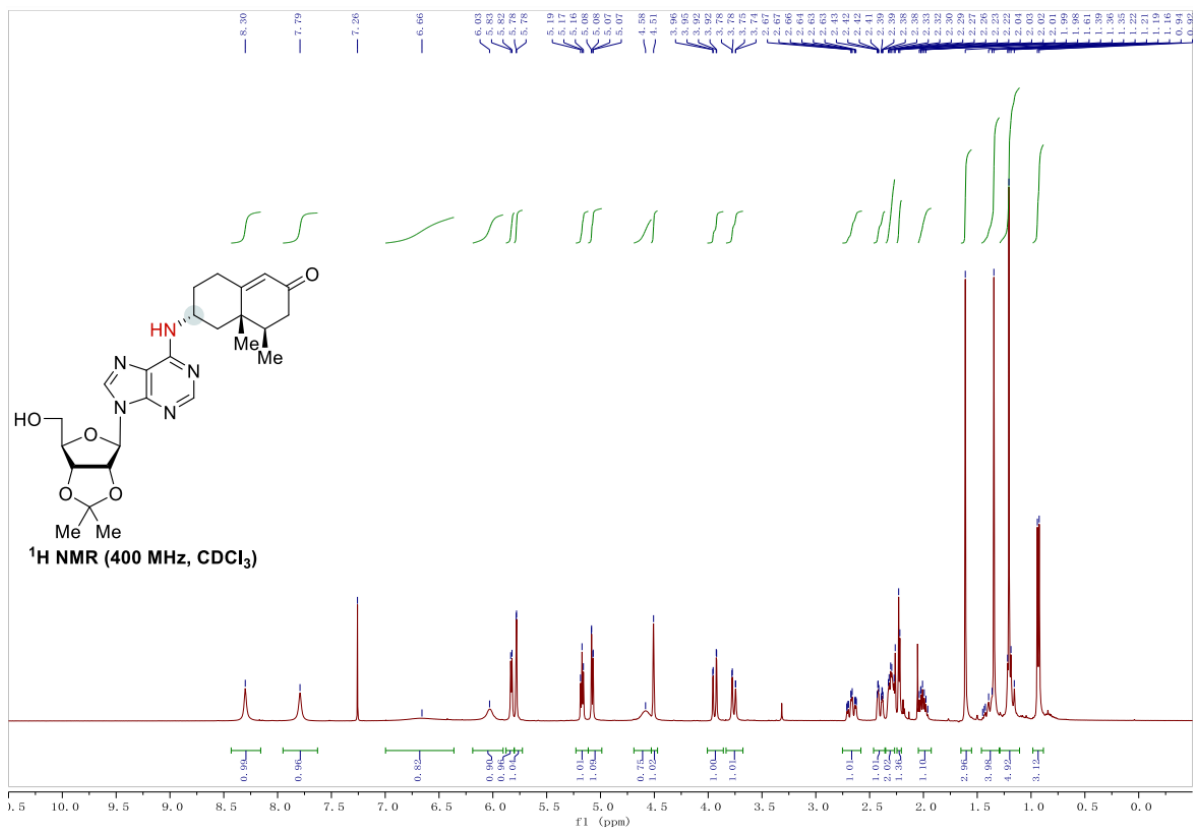


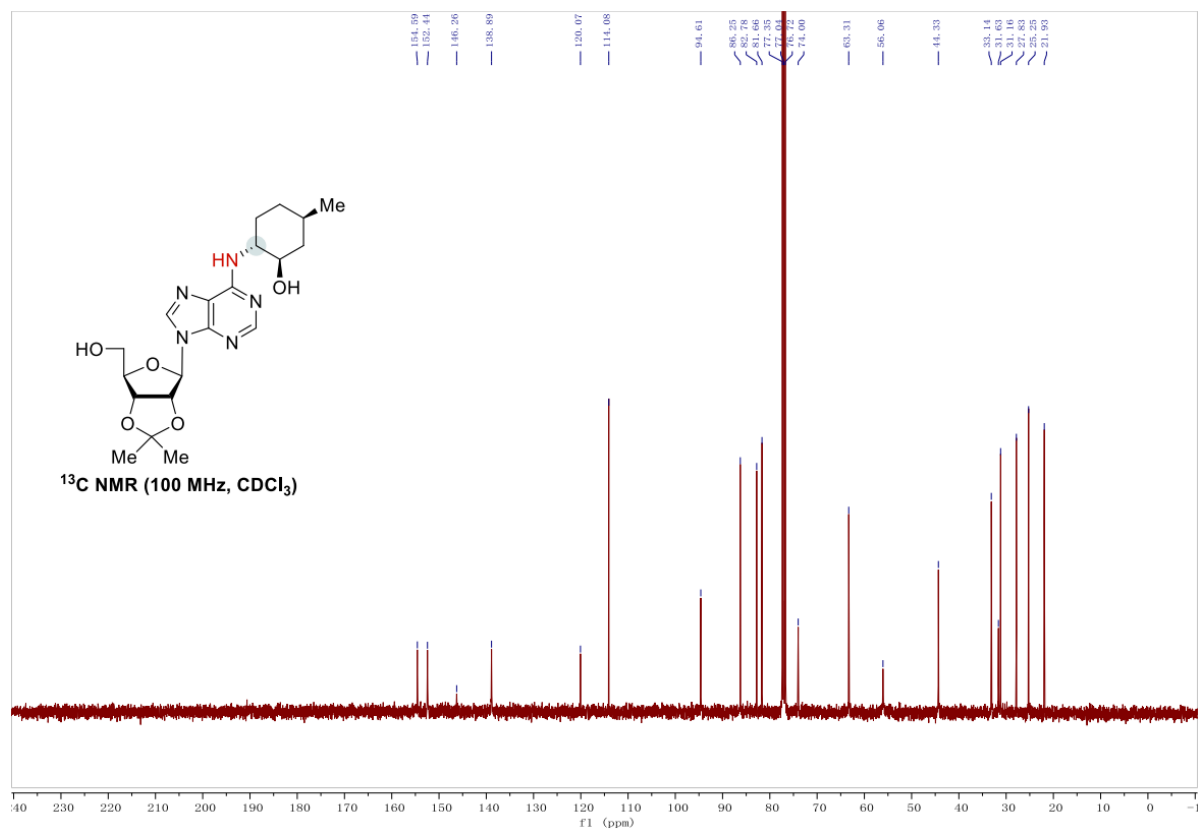
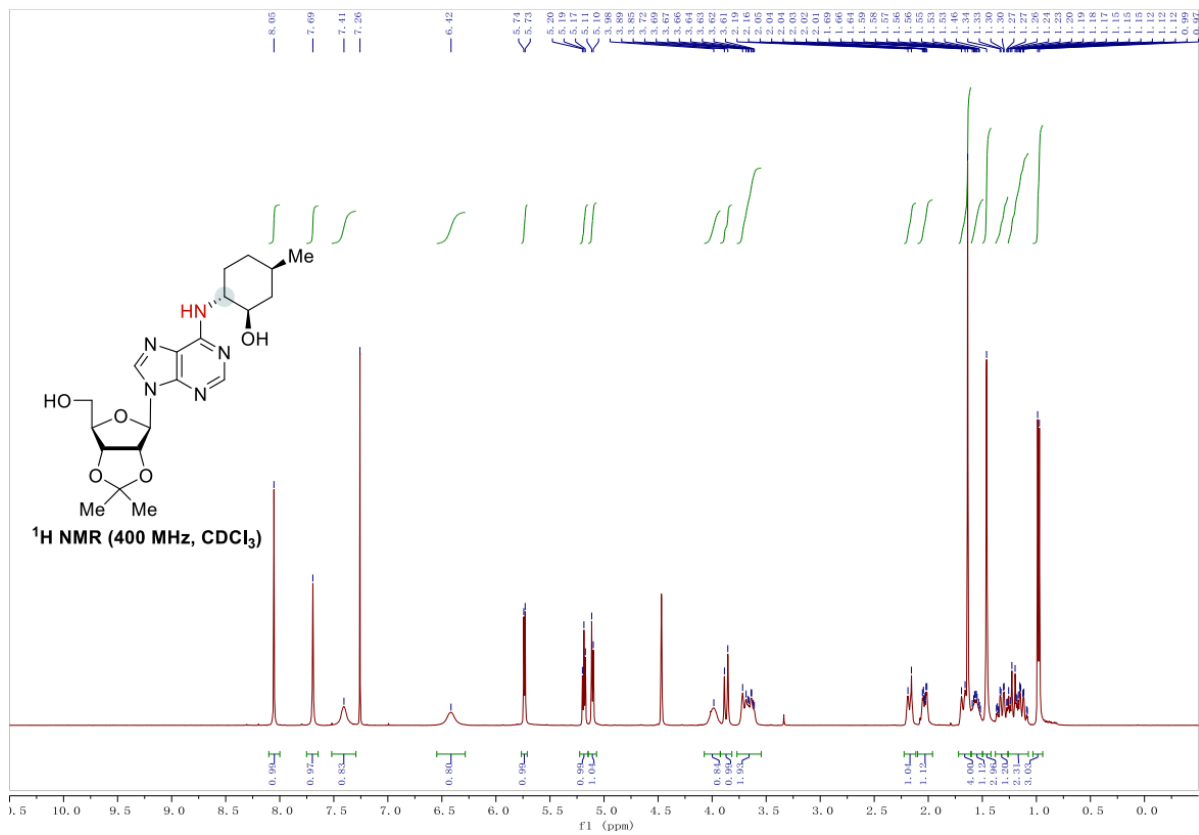












2.7. References

- (1) E. Vitaku, D. T. Smith, J. T. Njardarson, Analysis of the structural diversity, substitution patterns, and frequency of nitrogen heterocycles among U.S. FDA approved pharmaceuticals. *J. Med. Chem.* **57**, 10257–10274 (2014).
- (2) D. G. Brown, J. Boström, Analysis of past and present synthetic methodologies on medicinal chemistry: Where have all the new reactions gone? *J. Med. Chem.* **59**, 4443–4458 (2016).
- (3) A. Trowbridge, S. M. Walton, M. J. Gaunt, New strategies for the transition-metal catalyzed synthesis of aliphatic amines. *Chem. Rev.* **120**, 2613–2692 (2020).
- (4) F. Chen, T. Wang, N. Jiao, Recent advances in transition-metal-catalyzed functionalization of unstrained carbon–carbon bonds. *Chem. Rev.* **114**, 8613–8661 (2014).
- (5) Y. Xia, G. Dong, Temporary or removable directing groups enable activation of unstrained C–C bonds. *Nat. Rev. Chem.* **4**, 600–614 (2020).
- (6) J. B. Roque, Y. Kuroda, L. T. Göttemann, R. Sarpong, Deconstructive diversification of cyclic amines. *Nature* **564**, 244–248 (2018).
- (7) J. Tinge, M. Groothaert, H. op het Veld, J. Ritz, H. Fuchs, H. Kieczka, W. C. Moran, Caprolactam. *Ullmann's Encyclopedia of Industrial Chemistry*, 1–31 (2018).
- (8) J. Liu, X. Qiu, X. Huang, X. Lou, C. Zhang, J. Wei, J. Pan, Y. Liang, Y. Zhu, Q. Qin, S. Song, N. Jiao, From alkylarenes to anilines via site-directed carbon–carbon amination. *Nat. Chem.* **11**, 71–77 (2019).
- (9) J. Liu, C. Zhang, Z. Zhang, X. Wen, X. Dou, J. Wei, X. Qiu, S. Song, N. Jiao, Nitromethane as a nitrogen donor in Schmidt-type formation of amides and nitriles. *Science* **367**, 281–285 (2020).

- (10) J. Liu, J. Pan, Xi. Luo, X. Qiu, C. Zhang, N. Jiao, Selective dealkenylative functionalization of styrenes via C–C bond cleavage, *Research* **2020**, 7947029 (2020).
- (11) W. Zhao, R. P. Wurz, J. C. Peters, G. C. Fu, Photoinduced, copper-catalyzed decarboxylative C–N coupling to generate protected amines: An alternative to the Curtius rearrangement. *J. Am. Chem. Soc.* **139**, 12153–12156 (2017).
- (12) R. Mao, A. Frey, J. Balon, X. Hu, Decarboxylative C(sp³)–N cross-coupling via synergetic photoredox and copper catalysis. *Nat. Catal.* **1**, 120–126 (2018).
- (13) Y. Liang, X. Zhang, D. W. C. MacMillan, Decarboxylative sp³ C–N coupling via dual copper and photoredox catalysis. *Nature* **559**, 83–88 (2018).
- (14) X. Hu, Y. Shao, H. Xie, X. Chen, F. Chen, Z. Ke, H. Jiang, W. Zeng, Direct carbon–carbon σ bond amination of unstrained arylalkylketones. *ACS Catal.* **10**, 8402–8408 (2020).
- (15) X.-Y. Lv, R. Abrams, R. Martin, Copper-catalyzed C(sp³)-amination of ketone-derived dihydroquinazolinones by aromatization-driven C–C bond scission. *Angew. Chem. Int. Ed.* e202217386 (2023).
- (16) G. P. Chiusoli, F. Minisci, Radical reactions of nitric oxide. Nitrated acids from nitric oxide and peroxide. *Gazz. Chim. Ital.* **88**, 261–270 (1958).
- (17) B. L. Tran, B. Li, M. Driess, J. F. Hartwig, Copper-catalyzed intermolecular amidation and imidation of unactivated alkanes. *J. Am. Chem. Soc.* **136**, 2555–2563 (2014).
- (18) J.-J. Guo, A. Hu, Y. Chen, J. Sun, H. Tang, Z. Zuo, Photocatalytic C–C bond cleavage and amination of cycloalkanols by cerium(III) chloride complex. *Angew. Chem. Int. Ed.* **55**, 15319–15322 (2016).

- (19) S. Sakurai, T. Kato, R. Sakamoto, K. Maruoka, Generation of alkyl radicals from alkylsilyl peroxides and their applications to C–N or C–O bond formations. *Tetrahedron*, **75**, 172–179 (2019).
- (20) J. Bao, H. Tian, P. Yang, J. Deng, J. Gui, Modular synthesis of functionalized butenolides by oxidative furan fragmentation. *Eur. J. Org. Chem.* **2020**, 339–347 (2020).
- (21) P. Ertl, T. Schuhmann, A systematic cheminformatics analysis of functional groups occurring in natural products. *J. Nat. Prod.* **82**, 1258–1263 (2019).
- (22) T. C. Nugent, Ed. *Chiral Amine Synthesis: Methods, Developments and Applications* (Wiley-VCH: Weinheim, 1–479, 2010).
- (23) F. Ospina, K. H. Schülke, J. Soler, A. Klein, B. Prosenc, M. Garcia-Borràs, S. C. Hammer, Selective biocatalytic N-methylation of unsaturated heterocycles. *Angew. Chem. Int. Ed.* **61**, e2022130 (2022).
- (24) H.-W. Man *et al.*, Solid forms of 2-(*tert*-butylamino)-4-((1*R*,3*R*,4*R*)-3-hydroxy-4-methylcyclohexylamino)-pyrimidine-5-carboxamide, compositions thereof and methods of their use. U.S. Patent US 9365524 B2, Jun. 14, 2016.
- (25) Y.-R. Luo, *Comprehensive Handbook of Chemical Bond Energies* (CRC Press: Boca Raton, FL, 2007).
- (26) T. J. Fisher, P. H. Dussault, Alkene ozonolysis. *Tetrahedron* **73**, 4233–4258 (2017).
- (27) E. I. Epelle, A. Macfarlane, M. Gusack, A. Burns, J. A. Okolie, W. Mackay, M. Rateb, M. Yaseen, Ozone application in different industries: A review of recent developments. *Chem. Eng. J.* **454**, 140188 (2023).

- (28) R. Criegee, G. Wenner, Die Ozonisierung des 9,10-Oktalins. *Justus Liebigs Ann. Chem.* **564**, 9–15 (1949).
- (29) A. J. Smaligo, M. Swain, J. C. Quintana, M. F. Tan, D. A. Kim, O. Kwon, Hydrodealkenylative C(sp³)–C(sp²) bond fragmentation. *Science* **364**, 681–685 (2019).
- (30) J. H. Dworkin, B. D. Dehnert, O. Kwon, When all C–C breaks LO–Ose. *Trends Chem.* **5**, 174–200 (2023).
- (31) B. D. Dehnert, J. H. Dworkin, O. Kwon, Dealkenylative functionalizations: Conversion of alkene C(sp³)–C(sp²) bonds into C(sp³)–X bonds via redox-based radical processes. *Synthesis* DOI: 10.1055/a-2044-4571 (2023).
- (32) R. Trammell, K. Rajabimoghadam, I. Garcia-Bosch, Copper-promoted functionalization of organic molecules: From biologically relevant Cu/O₂ model systems to organometallic transformations. *Chem. Rev.* **119**, 2954–3031 (2019).
- (33) A. C. Bissember, R. J. Lundgren, S. E. Creutz, J. C. Peters, G. C. Fu, Transition-metal-catalyzed alkylations of amines with alkyl halides: Photoinduced, copper-catalyzed couplings of carbazoles. *Angew. Chem. Int. Ed.* **52**, 5129–5133 (2013).
- (34) C. Chen, J. C. Peters, G. C. Fu, Photoinduced copper-catalysed asymmetric amidation via ligand cooperativity. *Nature* **596**, 250–256 (2021).
- (35) B. Górski, A.-L. Barthelemy, J. J. Douglas, F. Juliá, D. Leonori, Copper-catalysed amination of alkyl iodides enabled by halogen-atom transfer. *Nat. Catal.* **4**, 623–630 (2021).
- (36) N. W. Dow, A. Cabré, D. W. C. MacMillan, A general *N*-alkylation platform via copper metallaphotoredox and silyl radical activation of alkyl halides. *Chem* **7**, 1827–1842 (2021).

- (37) T. V. Sravanthi, S. L. Manju, Indoles: A promising scaffold for drug development. *Eur. J. Pharm. Sci.* **91**, 1–10 (2016).
- (38) B. Giese, The stereoselectivity of intermolecular free radical reactions. *Angew. Chem. Int. Ed.* **28**, 969–1146 (1989)
- (39) G. Bar, A. F. Parsons, Stereoselective radical reactions. *Chem. Soc. Rev* **32**, 251–263 (2003).
- (40) D. D. Dixon, J. W. Lockner, Q. Zhou, P. S. Baran, Scalable, divergent synthesis of meroterpenoids via “boronosclareolide.” *J. Am. Chem. Soc.* **134**, 8432–8435 (2012).
- (41) E. S. Burstein, *et al.*, Preparation of indazole compounds as muscarinic agonists. International Patent WO 2014/152144 A1, Sep. 25, 2014.
- (42) S. Mekala, R. C. Hahn, A scalable, nonenzymatic synthesis of highly stereopure difunctional C4 secondary methyl linchpin synthons. *J. Org. Chem.* **80**, 1610–1617 (2015).
- (43) T. J. Connolly *et al.*, Methods of synthesis of (1*R*,2*R*,5*R*)-5-amino-2-methylcyclohexanol hydrochloride and intermediates useful therein. International Patent WO 2017/019487 A1, Feb. 2, 2017.
- (44) X. Liu, X. Rong, S. Liu, Y. Lan, Q. Liu, Cobalt-catalyzed desymmetric isomerization of exocyclic olefins. *J. Am. Chem. Soc.* **143**, 20633–20639 (2021).
- (45) D. E. Cane, G. Yang, R. M. Coates, H. J. Pyun, T. M. Hohn, Trichodiene synthase. Synergistic inhibition by inorganic pyrophosphate and aza analogs of the bisabolylyl cation. *J. Org. Chem.* **57**, 3454–3462 (1992).

- (46) <https://www.globenewswire.com/news-release/2019/05/27/1850397/0/en/542-9-Mn-Alpha-Methylstyrene-Market-Global-Forecast-to-2024.html>. The price of each chemical in this study was checked on 02/06/2023. See the Supplementary Materials for details.
- (47) S. Zaccara, R. J. Ries, S. R. Jaffrey, Reading, writing and erasing mRNA methylation. *Nat. Rev. Mol. Cell. Biol.* **20**, 608–624 (2019).
- (48) M. Holzheimer, J. Buter, A. J. Minnaard, Chemical synthesis of cell wall constituents of *Mycobacterium tuberculosis*. *Chem. Rev.* **121**, 9554–9643 (2021).
- (49) J.-W. Ahn, K. H. Jang, S.-C. Chung, K.-B. Oh, J. Shin, Sorangiadenosine, a new sesquiterpene adenoside from the myxobacterium *Sorangium cellulosum*. *Org. Lett.* **10**, 1167–1169 (2008).
- (50) A. J. Pallenberg, K. S. Koenig, D. M. Barnhart, Synthesis and characterization of some copper(I) phenanthroline complexes. *Inorg. Chem.* **34**, 2833–2840 (1995).
- (51) J. W. Tye, Z. Weng, A. M. Johns, C. D. Incarvito, J. F. Hartwig, Copper complexes of anionic nitrogen ligands in the amidation and imidation of aryl halides. *J. Am. Chem. Soc.* **130**, 9971–9983 (2008).
- (52) M. Masarwa, H. Cohen, D. Meyerstein, D. L. Hickman, A. Bakac, J. H. Espenson, Reactions of low-valent transition-metal complexes with hydrogen peroxide. Are they “Fenton-like” or not? 1. The case of Cu^+_{aq} and $\text{Cr}^{2+}_{\text{aq}}$. *J. Am. Chem. Soc.* **110**, 4293–4297 (1988).
- (53) K. V. Ponganis, M. A. De Araujo, H. L. Hodges, Electron-transfer reactions of copper complexes. 1. A kinetic investigation of the oxidation of bis(1,10-phenanthroline)copper(I) by

- hydrogen peroxide in aqueous and sodium dodecyl sulfate solution. *Inorg. Chem.* **19**, 2704–2709 (1980).
- (54) J. Burés, A simple graphical method to determine the order in catalyst. *Angew. Chem. Int. Ed.* **55**, 2028–2031 (2016).
- (55) D. G. Blackmond, Kinetic profiling of catalytic organic reactions as a mechanistic tool. *J. Am. Chem. Soc.* **137**, 10852–10866 (2015).
- (56) C. Alamillo-Ferrer, G. Hutchinson, J. Burés, Mechanistic interpretation of orders in catalyst greater than one. *Nat. Rev. Chem.* **7**, 26–34 (2023).
- (57) J. W. Moffett, R. G. Zika, Reaction kinetics of hydrogen peroxide with copper and iron in seawater. *Environ. Sci. Technol.* **21**, 804–810 (1987)
- (58) H. Lee, J. M. Ahn, P. H. Oyala, C. Citek, H. Yin, G. C. Fu, J. C. Peters, Investigation of the C–N bond-forming step in a photoinduced, copper-catalyzed enantioconvergent N-alkylation: Characterization and application of a stabilized organic radical as a mechanistic probe. *J. Am. Chem. Soc.* **144**, 4114–4123 (2022).
- (59) A. A. Nikolin, E. P. Kramarova, A. G. Shipov, Y. I. Baukov, V. V. Negrebetsky, D. E. Arkhipov, A. A. Korlyukov, A. A. Lagunin, S. Yu. Bylikin, A. R. Bassindale, P. G. Taylor, *N,N*-Bis-(dimethylfluorosilylmethyl)amides of *N*-organosulfonylproline and sarcosine: Synthesis, structure, stereodynamic behaviour and *in silico* studies. *RSC Adv.* **6**, 75315–75327 (2016).
- (60) M. Tomassettia, M. Fanì, G. Bianchini, S. Giuli, A. Aramini, S. Colagioia, G. Nano, S. Lillini, Retention of stereochemistry in the microwave assisted synthesis of 1*H*-tetrazole

- bioisosteric moiety from chiral phenyl-acetic acid derivatives. *Tetrahedron Lett.* **54**, 6247–6250 (2013).
- (61) M. Hu, M. A. Giulianotti, J. P. McLaughlin, J. Shao, G. Debevec, L. E. Maida, P. Geer, M. Cazares, J. Misler, L. Li, C. Dooley, M. L. Ganno, S. O. Eans, E. Mizrachi, R. G. Santos, A. B. Yongye, R. A. Houghten, Y. Yu, Synthesis and biological evaluations of novel endomorphin analogues containing α -hydroxy- β -phenylalanine (AHPBA) displaying mixed μ/δ opioid receptor agonist and δ opioid receptor antagonist activities. *Eur. J. Med. Chem.* **92**, 270–281 (2015).
- (62) [54] D. Huang, A. W. Schuppe, M. Z. Liang, T. R. Newhouse, Scalable procedure for the fragmentation of hydroperoxides mediated by copper and iron tetrafluoroborate salts. *Org. Biomol. Chem.* **14**, 6197–6200 (2016).
- (63) A. Srikrishna, G. Ravi, A stereoselective total synthesis of (–)-seychellene. *Tetrahedron* **64**, 2565–2571 (2008).
- (64) M. Blair, P. C. Andrews, B. H. Fraser, C. M. Forsyth, P. C. Junk, M. Massi, K. L. Tuck, Facile methods for the separation of the *cis*- and *trans*-diastereomers of limonene 1,2-oxide and convenient routes to diequatorial and diaxial 1,2-diols. *Synthesis* **10**, 1523–1527 (2007).
- (65) G. Solladie, J. Hutt, Total synthesis of dihydrovitamin DHV3 and dihydrotachysterol DHT3. Application of the low-valent titanium induced reductive elimination. *J. Org. Chem.* **52**, 3560–3566 (1987).
- (66) J. M. Schomaker, V. R. Pulgam, B. Borhan, Synthesis of diastereomerically and enantiomerically pure 2,3-disubstituted tetrahydrofurans using a sulfoxonium ylide. *J. Am. Chem. Soc.* **126**, 13600–13601 (2004).

- (67) K. Tanveer, S.-J. Kim, M. S. Taylor, Borinic acid/halide co-catalyzed semipinacol rearrangements of 2,3-epoxy alcohols. *Org. Lett.* **20**, 5327–5331 (2018).
- (68) W. B. Reid, D. A. Watson, Synthesis of trisubstituted alkenyl boronic esters from alkenes using the boryl-Heck reaction. *Org. Lett.* **20**, 6832–6835 (2018).
- (69) L. Gonnard, A. Guérinot, J. Cossy, Cobalt-catalyzed cross-coupling of 3- and 4-iodopiperidines with Grignard reagents. *Chem. Eur. J.* **21**, 12797–12803 (2015).
- (70) A. Torres, P. Gutierrez, R. Alvarez-Manzaneda, R. Chahboun, E. Alvarez-Manzaneda, Preparation of oxocene terpenes. The first enantiospecific synthesis of cytotoxic arenaran A. *Org. Biomol. Chem.* **14**, 9836–9845 (2016).
- (71) A. B. Smith, E. F. Mesaros, E. A. Meyer, Evolution of a total synthesis of (–)-kendomycin exploiting a Petasis–Ferrier rearrangement/ring-closing olefin metathesis strategy. *J. Am. Chem. Soc.* **128**, 5292–5299 (2006).
- (72) J. C. Siu, J. B. Parry, S. Lin, Aminoxyl-catalyzed electrochemical diazidation of alkenes mediated by a metastable charge-transfer complex. *J. Am. Chem. Soc.* **141**, 2825–2831 (2019).
- (73) H. Hagiwara, T. Katsumi, V. P. Kamat, T. Hoshi, T. Suzuki, M. Ando, Application of ring closing metathesis to the first total synthesis of (R)-(+)-muscopyridine: Determination of absolute stereochemistry. *J. Org. Chem.* **65**, 7231–7234 (2000).
- (74) J. Yu, Y. Zhou, Z. Lin, R. Tong, Regioselective and stereospecific copper-catalyzed deoxygenation of epoxides to alkenes. *Org. Lett.* **18**, 4734–4737 (2016).
- (75) T.-H. Yan, C.-C. Tsai, C.-T. Chien, C.-C. Cho, P.-C. Huang, Dichloromethane activation. Direct methylenation of ketones and aldehydes with CH₂Cl₂ promoted by Mg/TiCl₄/THF. *Org. Lett.* **6**, 4961–4963 (2004).

- (76) F. Romanov-Michailidis, K. F. Sedillo, J. M. Neely, T. Rovis, Expedient access to 2,3-dihydropyridines from unsaturated oximes by Rh(III)-catalyzed C–H activation. *J. Am. Chem. Soc.* **137**, 8892–8895 (2015).
- (77) Y.-F. Liang, X.-F. Zhou, S.-Y. Tang, Y.-B. Huang, Y.-S. Feng, H.-J. Xu, Lithium *tert*-butoxide mediated α -alkylation of ketones with primary alcohols under transition-metal-free conditions. *RSC Adv.* **3**, 7739–7742 (2013).
- (78) Q.-J. Liang, C. Yang, F.-F. Meng, B. Jiang, Y.-H. Xu, T.-P. Loh, Chelation versus non-chelation control in the stereoselective alkenyl sp^2 C–H bond functionalization reaction. *Angew. Chem. Int. Ed.* **56**, 5091–5095 (2017).
- (79) B. Xu, U. K. Tambar, Copper-catalyzed enantio-, diastereo-, and regioselective [2,3]-rearrangements of iodonium ylides. *Angew. Chem. Int. Ed.* **56**, 9868–9871 (2017).
- (80) S. E. Sen, S. L. Roach, A convenient two-step procedure for the synthesis of substituted allylic amines from allylic alcohols. *Synthesis* **1995**, 756–758 (1995).
- (81) S. Gore, S. Baskaran, B. König, Fischer indole synthesis in low melting mixtures. *Org. Lett.* **14**, 4568–4571 (2012).
- (82) T. Nakagiri, M. Murai, K. Takai, Stereospecific deoxygenation of aliphatic epoxides to alkenes under rhenium catalysis. *Org. Lett.* **17**, 3346–3349 (2015).
- (83) S. K. Kariofillis, B. J. Shields, M. A. Tekle-Smith, M. J. Zacuto, A. G. Doyle, Nickel/photoredox-catalyzed methylation of (hetero)aryl chlorides using trimethyl orthoformate as a methyl radical source. *J. Am. Chem. Soc.* **142**, 7683–7689 (2020).
- (84) A. Hu, J.-J. Guo, H. Pan, Z. Zuo, Selective functionalization of methane, ethane, and higher alkanes by cerium photocatalysis. *Science* **361**, 668–672 (2018).

- (85) J. Jin, D. W. C. MacMillan, Alcohols as alkylating agents in heteroarene C–H functionalization. *Nature* **525**, 87–90 (2015).
- (86) W. Liu, X. Yang, Z.-Z. Zhou, C.-J. Li, Simple and clean photo-induced methylation of heteroarenes with MeOH. *Chem* **2**, 688–702 (2017).
- (87) M. Liu, Z. Qiu, L. Tan, R. T. Rashid, S. Chu, Y. Cen, Z. Luo, R. Z. Khaliullin, Z. Mi, C.-J. Li, Photocatalytic methylation of nonactivated sp³ and sp² C–H bonds using methanol on GaN. *ACS Catal.* **10**, 6248–6253 (2020).
- (88) R. Grigg, T. R. B. Mitchell, S. Sutthivaiyakit, N. Tongpenyai, Oxidation of alcohols by transition metal complexes. Part V. Selective catalytic monoalkylation of arylcaetonitriles by alcohols. *Tetrahedron Lett.* **22**, 4107–4110 (1981).
- (89) M. H. S. A. Hamid, P. A. Slatford, J. M. J. Williams, Borrowing hydrogen in the activation of alcohols. *Adv. Synth. Catal.* **349**, 1555–1575 (2007).
- (90) G. E. Dobereiner, R. H. Crabtree, Dehydrogenation as a substrate-activating strategy in homogeneous transition-metal catalysis. *Chem. Rev.* **110**, 681–703 (2010).
- (91) G. Guillena, D. J. Ramón, M. Yus, Hydrogen autotransfer in the N-alkylation of amines and related compounds using alcohols and amines as electrophiles. *Chem. Rev.* **110**, 1611–1641 (2010).
- (92) C. Gunanathan, D. Milstein, Applications of acceptorless dehydrogenation and related transformations in chemical synthesis. *Science* **341**, 1229712 (2013).
- (93) S.-J. Chen, G.-P. Lu, C. Cai, Iridium-catalyzed methylation of indoles and pyrroles using methanol as feedstock. *RSC Adv.* **5**, 70329–70332 (2015).
- (94) Z. Dong, D. W. C. MacMillan, Metallaphotoredox-enabled deoxygenative arylation of alcohols, *Nature* **598**, 451–456 (2021).

- (95) Q. Zhu, D. G. Nocera, Photocatalytic hydromethylation and hydroalkylation of olefins enabled by titanium dioxide mediated decarboxylation. *J. Am. Chem. Soc.* **142**, 17913–17918 (2020).
- (96) Proctor, R. S. J.; Phipps, R. J. Recent advances in Minisci-type reactions. *Angew. Chem. Int. Ed.* **58**, 13666–13699 (2019).
- (97) F. Minisci, R. Bernardi, F. Bertini, R. Galli, M. Perchinummo, Nucleophilic character of alkyl radicals–VI. A new convenient selective alkylation of heteroaromatic bases. *Tetrahedron* **27**, 3575–3579 (1971).
- (98) E. Mao, D. W.C. MacMillan, Late-stage C(sp³)–H methylation of drug molecules. *J. Am. Chem. Soc.* 10.1021/jacs.2c13396 (2023).
- (99) L. N. Schneider, E.-M. Tanzer Krauel, C. Deutsch, K. Urbahns, T. Bischof, K. A. M. Maibom, J. Landmann, F. Keppner, C. Kerpen, M. Hailmann, L. Zapf, T. Knuplez, R. Bertermann, N. V. Ignat'ev, M. Finze, Stable and storable N(CF₃)₂ transfer reagents. *Chem. Eur. J.* **27**, 10973–10978.
- (100) M. Ruthkosky, F. N. Castellano, G. J. Meyer, Photodriven electron and energy transfer from copper phenanthroline excited states. *Inorg. Chem.* **35**, 6406–6412 (1996).
- (101) H. L. Hodges, M. A. De Araujo, Kinetic investigation of the equilibrium between mono- and bis(1,10-phenanthroline)copper(I) in aqueous and sodium dodecyl sulfate solution. *Inorg. Chem.* **21**, 3236–3239 (1982).
- (102) U. M. Frei, G. Geier. Lewis-base-catalyzed diimine-ligand-substitution reactions at copper(I). *Inorg. Chem.* **31**, 3132–3137 (1992).
- (103) R. G. Pearson, R. D. Lanier, Rates of rapid ligand exchange reactions by nuclear magnetic resonance line broadening studies. *J. Am. Chem. Soc.* **86**, 765–771 (1964).

- (104) M. Eigen, R. G. Wilkins, The kinetics and mechanism of formation of metal complexes. *Adv. Chem.* **49**, 55–80 (1965).
- (105) D. C. Weatherburn, Kinetics of ligand exchange reactions of copper(II) complexes *Inorg. Chim. Acta* **21**, 209–215 (1977).
- (106) L. Helm, A. E. Merbach, Inorganic and bioinorganic solvent exchange mechanisms. *Chem. Rev.* **105**, 1923–1959 (2005).
- (107) D. T. Richens, Ligand substitution reactions at inorganic centers. *Chem. Rev.* **105**, 1961–2002 (2005).
- (108) A. S. Mereshchenko, S. K. Pal, K. E. Karabaeva, P. Z. El-Khoury, A. N. Tarnovsky, Photochemistry of monochloro complexes of copper(II) in methanol probed by ultrafast transient absorption. *J. Phys. Chem. A* **116**, 2791–2799 (2012).
- (109) A. S. Mereshchenko, P. K. Olshin, K. E. Karabaeva, M. S. Panov, R. Marshall Wilson, V. A. Kochemirovsky, M. Yu. Skripkin, Y. S. Tveryanovich, A. N. Tarnovsky, Mechanism of formation of copper(II) chloro complexes revealed by transient absorption spectroscopy and DFT/TDDFT calculations. *J. Phys. Chem. B* **119**, 8754–8763 (2015).
- (110) J. Catalan, J. Carlos del Valle, R. M. Claramunt, G. Boyer, J. Laynez, J. Gomez, P. Jimenez, F. Tomas, J. Elguero, Acidity and basicity of indazole and its N-methyl derivatives in the ground and in the excited state. *J. Phys. Chem.* **98**, 10606–10612 (1994).
- (111) M. Swain, T. B. Bunnell, J. Kim, O. Kwon, Dealkenylative alkynylation using catalytic Fe^{II} and vitamin C. *J. Am. Chem. Soc.* **144**, 14828–14837 (2022).
- (112) J. K. Kochi, R. V. Subramanian, Kinetics of electron-transfer oxidation of alkyl radicals by copper(II) complexes. *J. Am. Chem. Soc.* **87**, 4855–4866 (1965).

- (113) N. Navon, G. Golub, H. Cohen, D. Meyerstein, Kinetics and reaction mechanisms of copper(I) complexes with aliphatic free radicals in aqueous solutions. A pulse-radiolysis study. *Organometallics* **14**, 5670–5676 (1995).
- (114) C. Mansano-Weiss, D. M. Epstein, H. Cohen, A. Masarwa, D. Meyerstein, Mechanism of reaction of alkyl radicals with copper(II)(glycylglycylglycine) in aqueous solutions. *Inorg. Chim. Acta* **339** 283–291 (2002).
- (115) X. Zhao, Y. Liu, R. Zhu, C. Liu, D. Zhang, Mechanistic study on the decarboxylative sp^3 C–N cross-coupling between alkyl carboxylic acids and nitrogen nucleophiles via dual copper and photoredox catalysis. *Inorg. Chem.* **58**, 12669–12677 (2019).
- (116) M. McConnell, H. E. Weaver, Jr., Rate of electron exchange between cuprous and cupric ions in hydrochloric acid solutions by nuclear magnetic resonance *J. Chem. Phys.* **25**, 307 (1956).
- (117) M. McConnell, S. B. Berger, Rates of paramagnetic pulse reactions by nuclear magnetic resonance. *J. Chem. Phys.* **27**, 230 (1957).
- (118) G. S. Yoneda, G. L. Blackmer, R. A. Holwerda, Kinetics of the oxidation of $\text{Cu}(\text{phen})_2^{2+}$ and $\text{Cu}(\text{bpy})_2^{2+}$ by aminopoly carboxylatocobalt (III) complexes. *Inorg. Chem.* **16**, 3376–3378 (1977).
- (119) C. W. Lee, F. C. Anson, Electron exchange between $\text{Cu}(\text{I})(\text{phen})_2^+$ adsorbed on graphite and $\text{Cu}(\text{phen})_2^{2+}$ in solution. *Inorg. Chem.* **23**, 837–844 (1984).
- (120) D. B. Rorabacher, Electron transfer by copper centers. *Chem. Rev.* **104**, 651–698 (2004).
- (121) F. J. Millero, V. K. Sharma, B. Karn, The rate of reduction of copper(II) with hydrogen peroxide in seawater. *Marine Chem.* **36**, 71–83 (1991).

- (122) H. Zhao, J. Chang, A. Boika, A. J. Bard, Electrochemistry of high concentration copper chloride complexes. *Anal. Chem.* **85**, 7696–7703 (2013).
- (123) J. D. Cope, H. U. Valle, R. S. Hall, K. M. Riley, E. Goel, S. Biswas, M. P. Hendrich, D. O. Wipf, S. L. Stokes, J. P. Emerson, Tuning the copper(II)/copper(I) redox potential for more robust copper-catalyzed C–N bond forming reactions. *Eur. J. Inorg. Chem.* **2020**, 1278–1285 (2020).
- (124) J. Qiu, K. Matyjaszewski, L. Thouin, C. Amatore, Cyclic voltammetric studies of copper complexes catalyzing atom transfer radical polymerization. *Macromol. Chem. Phys.* **201**, 1625–1631 (2000).
- (125) G. Laus, Kinetics of acetonitrile-assisted oxidation of tertiary amines by hydrogen peroxide. *J. Chem. Soc., Perkin Trans.* **2**, 864–868 (2001).
- (126) A. J., Smaligo, O. Kwon, Dealkenylative thiylation of C(sp³)–C(sp²) bonds. *Org. Lett.* **21**, 8592–8597 (2019).
- (127) M. Swain, G. Sadykhov, R. Wang, O. Kwon, Dealkenylative alkenylation: Formal σ -bond metathesis of olefins. *Angew. Chem. Int. Ed.* **59**, 17565–17571 (2020).
- (128) W. H. Koppenol, Oxyradical reactions: From bond-dissociation energies to reduction potentials. *FEBS Lett.* **264**, 165–167 (1990).
- (129) R. T. Gephart, C. L. McMullin, N. G. Sapiezynski, E. S. Jang, M. J. B. Aguilá, T. R. Cundari, T. H. Warren, Reaction of Cu^I with Dialkyl Peroxides: Cu^{II}-Alkoxides, Alkoxy Radicals, and Catalytic C–H Etherification. *J. Am. Chem. Soc.* **134**, 17350–17353 (2012).

CHAPTER 3: Mechanism of aminodealkenylation: the unexpected role of CuCl 1,10-phenanthroline complex as a cooperative ion pair catalyst system

Adapted from: Aminodealkenylation: Ozonolysis and Copper Catalysis Convert C(sp³)–C(sp²) Bonds to C(sp³)–N Bonds by Zhiqi He.; Jose A. Moreno.; Manisha Swain.; Jason Wu; Ohyun Kwon* *Science* **2023**, 381 (6660), 877–886.

3.1. Abstract

Central to the understanding and development of a novel catalytic method is a detailed understanding of the underlying mechanism. Herein we describe the results of several experiments, including spectroscopic and kinetic studies, to probe the nature of the copper catalyst throughout its cycle in the aminodealkenylation reaction. Consistent with the results of these studies, it was determined that the catalyst system, copper (I) chloride and 1,10-phenanthroline, operates as a cooperative ion pair consisting of the ionic species copper (I) di-1,10-phenanthroline cation and copper (I) dichloride anion. The data suggests the cationic species is primarily responsible for the C–N coupling event while the anionic portion is involved in the reduction of the hydroperoxyacetal and oxidizing the reduced cationic species to propagate the catalytic cycle.

3.2. Mechanism studies

We conducted several experiments to gain insight into the reaction mechanism. Copper halides and phenanthroline are known to form tight ion pairs [(Phen)₂Cu]⁺[CuX₂][–] instead of neutral complexes [(Phen)CuX] in polar solvents^{1,2}, and our ultraviolet–visible spectroscopic measurements indicated that the ion pair complex [(Phen)₂Cu]⁺[CuCl₂][–] was the dominant species in MeCN (see Section 3.5 for more details). Previous mechanistic studies have suggested that the neutral complex is the active species in the C–N coupling reaction, due to inefficient oxidative addition of ionic copper complexes to aryl halides^{1,3}. However, in contrast to oxidative addition,

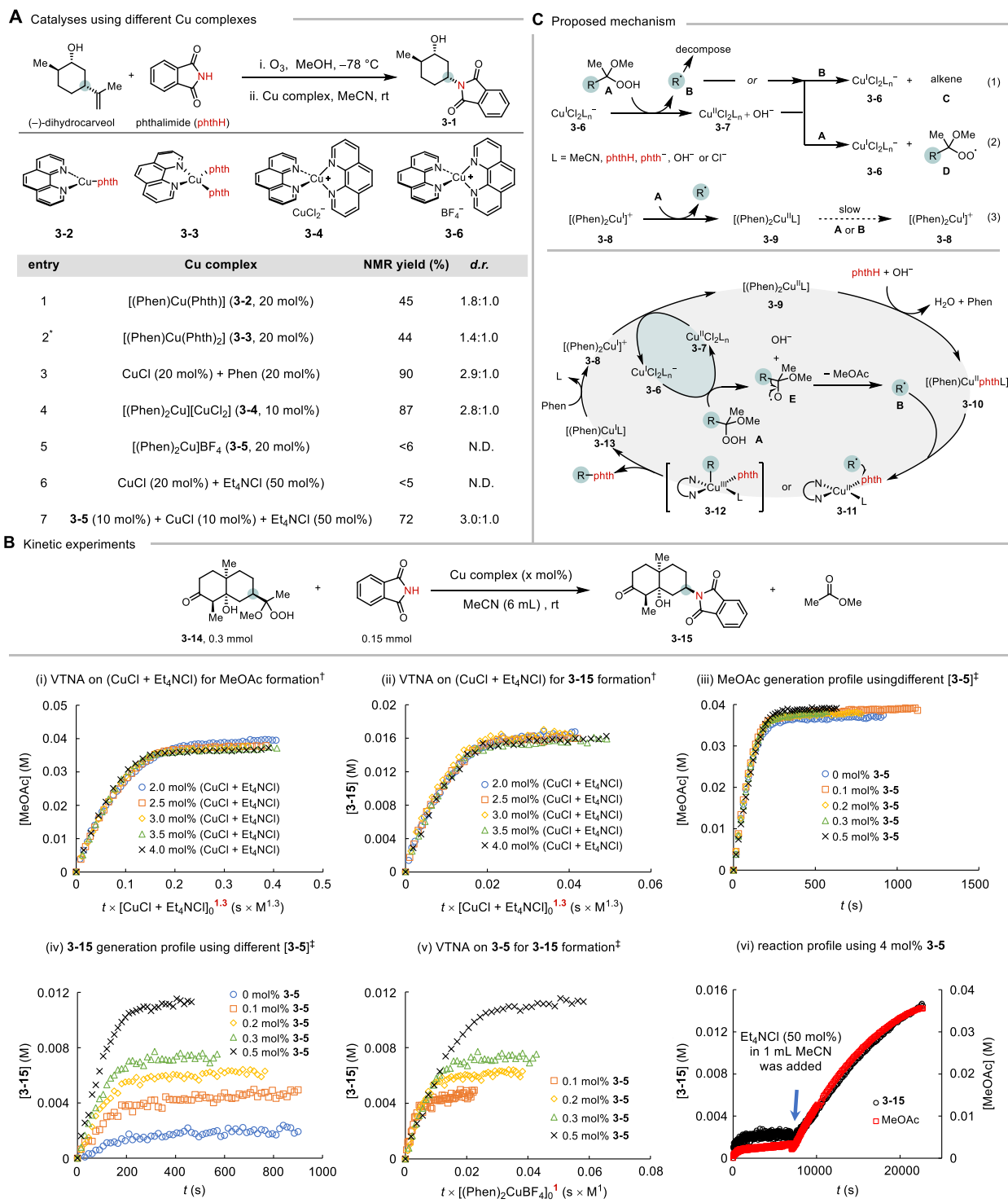
single electron transfer (SET) between hydroperoxide and either $[(\text{Phen})_2\text{Cu}]^+$ or $[\text{CuCl}_2]^-$ is rapid (rate constant (k) $\approx 4 \times 10^3 \text{ M}^{-1} \text{ s}^{-1}$) and can trigger peroxide fragmentation.^{4,5}

In attempts to directly probe the nature of the reactive copper species, we prepared a series of copper complexes (Fig. 3.1) and compared their performance in the aminodealkenylation between (–)-dihydrocarveol and phthalimide. When the prototypical mixture of 1:1 CuCl and phenanthroline was replaced with a neutral phthalimido copper complex $\{[(\text{Phen})\text{Cu}(\text{phth})]\}$ (**3-2**) or $[(\text{Phen})\text{Cu}(\text{phth})_2]$ (**3-3**), which had been proposed previously as a reactive intermediate^{3,6}, both the product yields (45 and 25%, respectively) and diastereoisomeric ratios (*d.r.*; 1.8:1.0 and 1.5:1.0, respectively) deteriorated significantly when compared with those of the standard reaction (90% NMR yield, 2.9:1.0 *d.r.*) (entries 1–3). Using the ion pair $[(\text{Phen})_2\text{Cu}]^+[\text{CuCl}_2]^-$ (**3-4**) directly afforded a reaction similar to the prototypical aminodealkenylation (87% yield, 2.8:1.0 *d.r.*), indicating that the ion pair might have been the active catalytic species. Reactions employing either $[(\text{Phen})_2\text{Cu}]^+$ (**3-5**) or $[\text{CuCl}_2]^-$ (CuCl + Et₄NCl) were extremely sluggish (entries 5 and 6), while the combination of independently prepared $[(\text{Phen})_2\text{Cu}]^+$ and $[\text{CuCl}_2]^-$ afforded a product similar to that from the parent reaction (entries 4 and 7), but with a slightly diminished yield.

To gain further insight into the mechanism of the copper-catalyzed amination, we conducted kinetic studies through variable time normalization analysis (VTNA)⁷. Using ReactIR, we collected the concentration–time profiles for both the C–C scission product [methyl acetate (MeOAc)] and the C–N coupling product (**3-15**). The formation of MeOAc displayed 0.3-, zero-, and 1.3-order dependences with respect to **3-14**, phthalimide, and the catalyst (CuCl + Phen), respectively, while the coupling product **3-15** displayed 0.3-, 0.3-, and 1.3-order dependences (Figs. 3.6–3.11). The zero- and pseudo-zero-order dependences on both peroxide and the amine implied that there existed an off-cycle catalyst resting state^{8,9}. Because both $[(\text{Phen})_2\text{Cu}]^+$ and

$[\text{CuCl}_2]^-$ are readily oxidized by peroxides, we surmised that the resting states of the catalyst were

Figure 3.1 (A) Comparison of different copper complexes. (B) Kinetic studies. (C) Proposed mechanism



the corresponding copper(II) species **3-7** and **3-9** (Fig. 3.1C, eqs. 1–3). The kinetic order of 1.3 with respect to catalyst indicates a scenario in which two catalytic species were operating on-cycle (Fig. 3.1C).

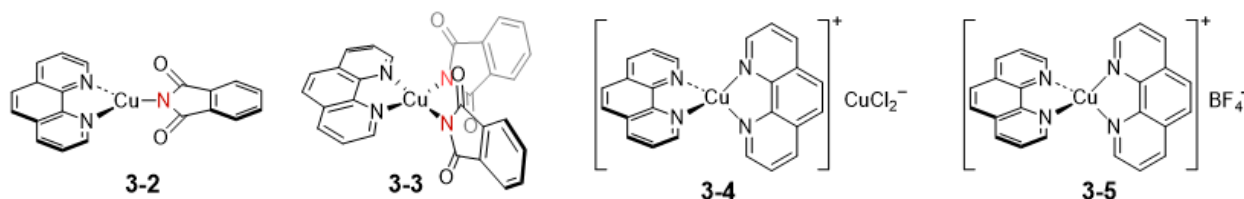
To tease out the roles of the cation and anion complexes in the catalytic cycle, we investigated the kinetics of $[(\text{Phen})_2\text{Cu}]^+$ (**3-5**) and $[\text{CuCl}_2]^-$ (1:1 mixture of $\text{CuCl} + \text{Et}_4\text{NCl}$) separately. Both the C–C scission and C–N coupling events exhibited a kinetic order of 1.3 in $[\text{CuCl}_2]^-$ in the presence of 2 mol% **3-5** (Figs. 3.1B, i and ii; Figs. 3.16 and 3.17) and a kinetic order of 2 in the presence of 0.5 mol% **3-5** (Figs. 3.18 and 3.19). Moreover, although $[\text{CuCl}_2]^-$ alone could catalyze the generation of MeOAc (Fig. 3.1B, iii), the formation of **3-15** was sluggish in the absence of $[(\text{Phen})_2\text{Cu}]^+$ (Fig. 3.1B, iv; Fig. 3.1A, entry 6). In sum, the C–C scission and C–N coupling steps displayed zero- and first-order dependences on $[(\text{Phen})_2\text{Cu}]^+$ at low concentrations (0.1–0.5 mmol%, Figs. 3.1B, iii and v) and saturation kinetics at higher concentrations (0.5–2.0 mol%), respectively, each in the presence of 2.0 mol% $[\text{CuCl}_2]^-$ (Figs. 3.12–3.15). The amount of **3-5** did not affect C–C scission, generating MeOAc even in its absence (Fig. 3.1B, iii), while both the production rate and yield of **3-15** were dependent on the concentration of **3-5** (Fig. 3.1B, iv). Complex **3-5** alone, however, could not generate significant amounts of MeOAc and **3-15**, both of which were generated steadily upon addition of Et_4NCl (Fig. 3.1B, vi). We surmise that $[(\text{Phen})_2\text{Cu}]^{2+}$ (**3-9**) was a stable cation whose reduction back to Cu(I) species was sluggish. Therefore, once $[(\text{Phen})_2\text{Cu}]^+$ was oxidized, the reaction stalled (Fig. 3.1C, eq. 3). Nevertheless, the addition of chloride replenished some $\text{Cu(II)Cl}_m\text{L}_n$ species that could oxidize the peroxide **A** and the radical **B** and return to the Cu(I) species (Fig. 3.1C, eqs. 1 and 2)¹⁰. The disparate reaction kinetics of $[\text{CuCl}_2]^-$ and $[(\text{Phen})_2\text{Cu}]^+$ indicate that $[\text{CuCl}_2]^-$ was involved in hydroperoxide decomposition, while $[(\text{Phen})_2\text{Cu}]^+$ participated in the C–N coupling. Because C–C scission

occurred prior to C–N coupling, $[\text{CuCl}_2]^-$ influenced both the C–C scission and C–N coupling processes (Figs. 3.18 and 3.19).

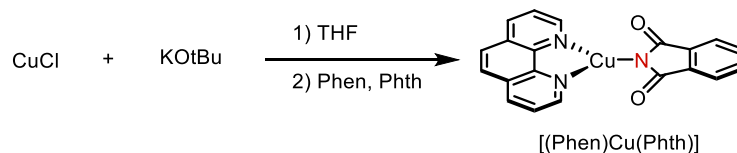
Taken together, we propose the involvement of $[\text{CuCl}_2]^- - [(\text{Phen})_2\text{Cu}]^+$ cooperative catalysis (Fig. 3.1C). SET between complex **3-6** and the peroxide **A** affords the alkoxy radical **E**, which undergoes β -scission to generate the alkyl radical **B**. The cationic Cu(I) complex **3-8** is oxidized by peroxide **A** to afford a copper(II) complex **3-9**. Deprotonated phthalimide associates with complex **3-9**, followed by dissociation of Phen, to afford the phthalimido copper(II) complex **3-10**. Complex **3-10** traps the alkyl radical **B** to afford the C–N coupling product and the copper(I) complex **3-13** through either an outer sphere (**3-11**) or inner sphere (**3-12**) pathway¹¹. Ligand exchange on the Cu(I) complex **3-13** affords **3-8**. Subsequent electron transfer between **3-7** and **3-8** regenerates **3-6** and **3-9**, completing a catalytic cycle. Alternatively, electron transfer between **3-13** and **3-7** is also possible to regenerate **3-6**. Deprotonated phthalimide associates with the resulting Cu(II) complex from **3-13** to regenerate **3-10**, completing the catalytic cycle.

3.3. Synthesis of Cu Complexes

The copper complexes **3-2**², **3-3**³, **3-4**¹², and **3-5**¹³ were synthesized according to previously reported procedures.



The complex **3-2** was prepared using the following procedure.



The copper(I) complex $[(\text{Phen})\text{Cu}(\text{Phth})]$ (**3-2**) was synthesized using a modification of a procedure reported in the literature². An oven-dried 50-mL round-bottom flask equipped with a

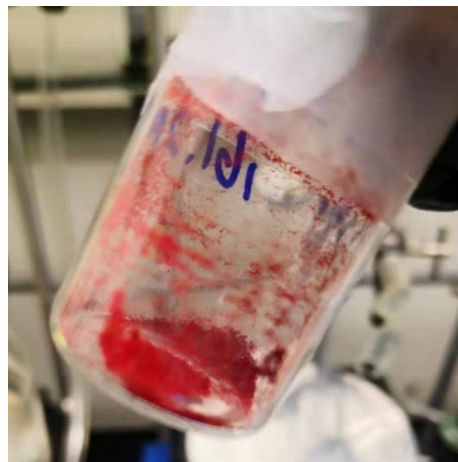
magnetic stirrer bar was treated with CuCl (119 mg, 1.20 mmol, 1.04 equiv) and potassium tert-butoxide (135 mg, 1.20 mmol, 1.04 equiv). The flask was purged with argon three times and then THF (10 mL) was added. The mixture was stirred at room temperature for 6 h and then 1,10-phenanthroline (207 mg, 1.15 mmol, 1.0 equiv) was added quickly. The flask was degassed and refilled with argon three times and then stirred for 20 min. Phthalimide (176 mg, 1.20 mmol, 1.04 equiv) was added into the mixture quickly. The flask was degassed and refilled with argon three times and then stirred for 20 min. The mixture was concentrated in vacuo and refilled with argon to afford a solid; the flask was capped with a septa. This solid was dissolved in a mixture of DMSO (4 mL) and THF (1 mL), added via syringe, and then Et₂O (15 mL) was added slowly and carefully via syringe to afford a bilayer solution. Red crystals had formed after standing for 2 days. The liquid phase was removed by syringe and the solid was washed with THF (5 × 1.5 mL, using syringe for adding and removing) under an argon atmosphere. The solid was dried in vacuo. The crude red solid was washed with DI water (3 × 3 mL) under an argon atmosphere and then benzene (10 mL) was added. The benzene was evaporated in vacuo to remove water; this procedure was repeated four times to give [(Phen)Cu(Phth)] as red crystals (162.1 mg, 35% yield).

¹H NMR (400 MHz, DMSO-d₆) δ 9.07 (br s, 2H), 8.79 (d, J = 7.3 Hz, 2H), 8.25 (br s, 2H), 8.02 (s, 2H), 7.68–7.47 (m, 4H), matching the literature data¹⁴.

Figure 3.2 Crystals of complex 3-2



Recrystallization by layering a THF/DMSO solution with Et₂O



The red crystalline product

3.4. Control Experiments

General procedure

An oven-dried 8-mL Schlenk tube equipped with a magnetic stirrer bar was charged with phthalimide (29.4 mg, 0.200 mmol, 1.0 equiv) and a copper catalyst (0.0400 mmol for total amount of copper, 20 mol %) [and tetraethylaminonium chloride (TEACl) (0.1 mmol, 50 mol %) when appropriate]. The tube was purged with argon three times before dry MeCN (2 mL) was added. [Note: When complex **3-3** was used, dry MeOH (0.4 mL) and dry MeCN (1.6 mL) was used.] This mixture was stirred at room temperature for 10 min to make *Suspension A*.

Another 50-mL round-bottom flask equipped with a magnetic stirrer bar was charged with (–)-dihydrocarveol (154 mg, 1.00 mmol) and MeOH (20 mL, 0.05 M) and cooled to –78 °C in a dry-ice/acetone bath with two 250-mL waste gas traps equipped with 20 wt% aqueous KI (200 mL). Ozone was bubbled through the solution until complete consumption of the starting material (as indicated by TLC and/or a bluish color in the reaction mixture). The solution was sparged with argon for 5 min to expel excess ozone and then the mixture was warmed to room temperature and the MeOH was evaporated *in vacuo*. The residue was dissolved in benzene (10 mL) followed by

evaporation *in vacuo* to remove adventitious water. The residue was dissolved in MeCN to form a 0.2 M solution of the hydroperoxide. A portion (2.0 mL) of this hydroperoxide solution was transferred into *Suspension A* in the Schlenk tube *via* syringe. The reaction vessel was stirred at room temperature for 1 h, followed by adding 1-chloro-2,4-dinitrobenzene (40.5 mg, 0.200 mmol, 1.0 equiv) as an internal standard. The mixture was concentrated *in vacuo*. The residue was passed through a short plug of silica gel to remove copper salts prior to concentration *in vacuo*. The crude materials were analyzed using NMR spectroscopy.

Table 3.1 Comparison of different Cu complexes

entry	catalyst and salt	yield (%)	<i>d.r.</i>
1	Phen (20 mol %) + CuCl (20 mol %)	90	2.9:1.0
2	[(Phen)Cu(Phth)] (3-2) (20 mol %)	45	1.8:1.0
3 ^a	[(Phen)Cu(Phth) ₂] (3-3) (20 mol %)	44	1.4:1.0
4	[(Phen) ₂ Cu][CuCl ₂] (3-4) (10 mol %)	87	2.8:1.0
5	[(Phen) ₂ Cu]BF ₄ (3-5) (20 mol %)	<6	N.D.
6	CuCl (20 mol %) + TEACl (50 mol %)	<5	N.D.
7	[(Phen) ₂ Cu]BF ₄ (10 mol %) + CuCl (10 mol %) + TEACl (50 mol %)	72	3.0:1.0
8	[(Phen) ₂ Cu]BF ₄ (3-5) (20 mol %) + TEACl (50 mol %)	74	2.9:1.0
9	Phen (20 mol %) + CuCl (20 mol %) + TEACl (50 mol %)	75	3.2:1.0
10	Phen (20 mol %) + CuCl (20 mol %) + TBABF ₄ (50 mol %)	72	2.9:1.0

^a MeOH/MeCN (1:9, v/v) was used as the solvent because this complex did not dissolve in MeCN

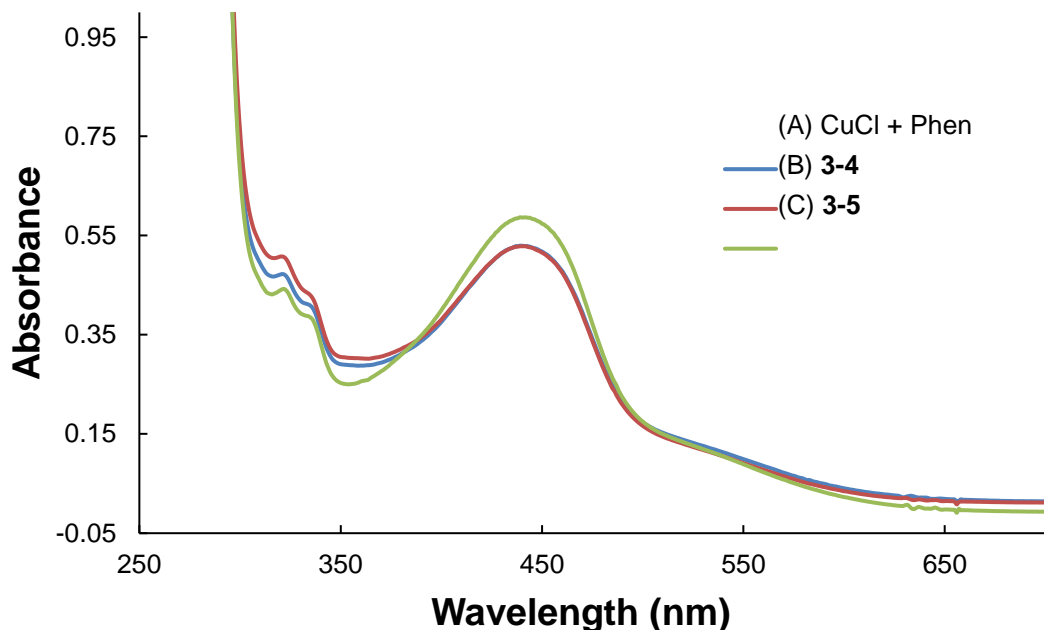
Summary of Table 3.1: In attempts to directly probe the nature of the reactive copper species, a series of copper complexes were prepared (Fig. S17). To compare the performance of each putative copper species, we employed them in the aminodealkenylation between (–)-dihydrocarveol and phthalimide. When the prototypical mixture of 1:1 CuCl and phenanthroline were replaced by neutral copper imidate complexes [(Phen)Cu(phth)] (**3-2**) and [(Phen)Cu(phth)₂] (**3-3**), which had been proposed previously as catalytic intermediates^{3,6,14}, both the product yields (45% and 44%, respectively) and diastereoisomeric ratios (*d.r.*) (1.8:1.0 and 1.4:1.0, respectively) deviated significantly from those of the standard reaction (90% NMR yield, 2.9:1.0 *d.r.*) (entries 1–3). Using the ion pair [(Phen)₂Cu]⁺[CuCl₂][–] (**3-4**) directly afforded a reaction similar to that of the prototypical aminodealkenylation (87% yield, 2.8:1.0 *d.r.*) (entry 4), indicating that the ion pair might be the active catalytic species. Reactions employing either [(Phen)₂Cu]⁺ (**3-5**) or [CuCl₂][–] (CuCl + Et₄NCl) were extremely sluggish (entries 5 and 6), while the combination of independently prepared [(Phen)₂Cu]⁺ and [CuCl₂][–] afforded a reaction similar to that of the parent reaction (entries 7–10) but with slightly diminished yield.

3.5. UV–Vis Spectroscopy

The absorbance of the CuCl and Phen mixture (trail A) almost overlaps with the absorbance of the complex **3-4** (trail B). This observation indicates that a 1:1 mixture of CuCl and Phen in MeCN forms the ion pair complex **3-4** predominantly, in agreement with a previous literature report¹⁵. All of the trails have the same fingerprint absorbances at 324, 337, and 442 nm, which are the absorbances of [(Phen)₂Cu]⁺, although trail C does not overlap perfectly with trails A and B. We propose that the shape and size of the counter anion (CuCl₂[–]: linear and small; BF₄[–]: tetrahedral and bulky) impacts the interactions between the cations and anions, particularly for these tight ion pairs. As a result, the absorbances of [(Phen)₂Cu]⁺ are slightly different.

Figure 3.3 UV–Vis absorption spectra of copper complexes

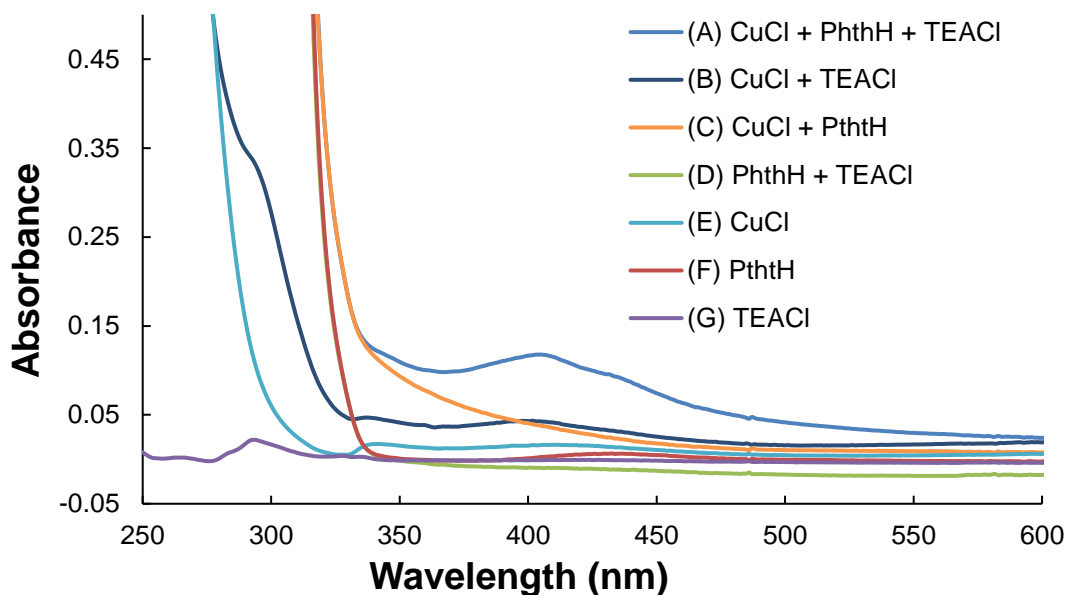
Measurements done in MeCN at 23 °C of (A) a 1:1 mixture of CuCl + Phen (0.2 mM), (B)



Tetraethylammonium chloride (TEACl) barely has any absorbances in the range from 250 to 600 nm (trail G). The absorbance of phthalimide (trail F) overlaps with the absorbance of a TEACl and phthalimide mixture (trail D), indicating that no interactions occurred between TEACl and phthalimide, and that the absorbance of the mixture was contributed solely by phthalimide. In contrast, a new peak at 295 nm appeared for the mixture of CuCl and TEACl (trail B), when compared with those of CuCl (trail E) and TEACl (trail G) individually. We believe that this new signal indicates that chloride coordinated with CuCl to form CuCl_2^- . The signal in the mixture of CuCl and phthalimide (trail C) exhibited a red-shift when compared with that of phthalimide (trail F), indicative of chelation between CuCl and phthalimide. For the mixture of CuCl, phthalimide, and TEACl (trail A), the red-shift was observed and a new peak appeared at 410 nm that must have been caused by the complex formed between CuCl_2^- and phthalimide.

Figure 3.4 UV–Vis absorption spectra of copper salt, phthalimide and ammonium salts

Experiments conducted in MeCN at 23 °C of (A) a 1:1:1 mixture of CuCl + PhthH + TEACl (10.0 mM), (B) a 1:1 mixture of CuCl + TEACl (10.0 mM), (C) a 1:1 mixture of CuCl + PhthH (10.0 mM), (D) a 1:1 mixture of PhthH + TEACl (10.0 mM), (E) CuCl (10.0 mM), (F) PhthH (10.0 mM), (G) TEACl (10.0 mM). PhthH = phthalimide; TEACl = tetraethylammonium chloride.

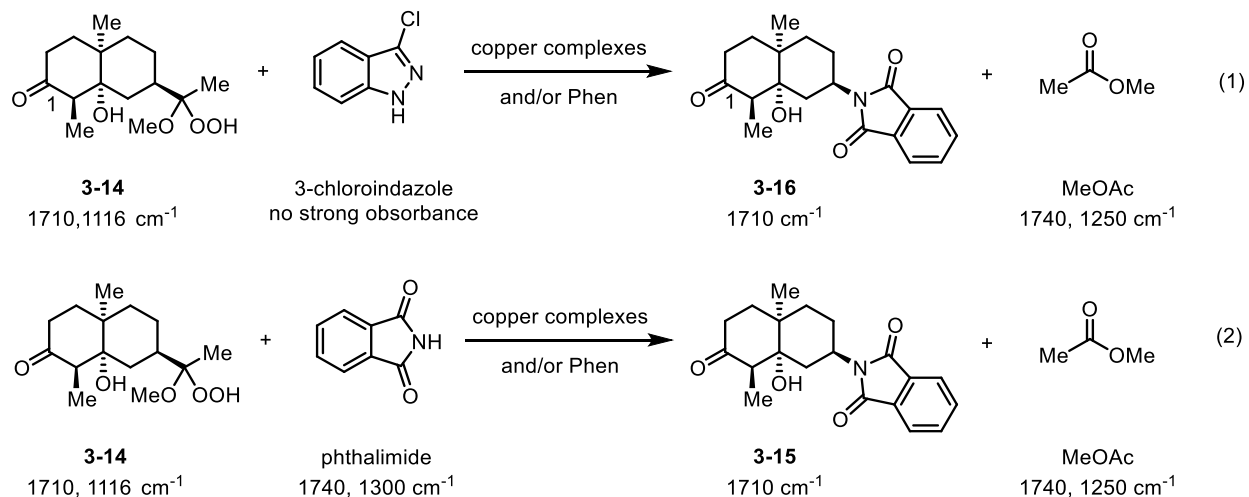


3.6. Kinetic Studies

3.6.1. General considerations and procedures for the ReactIR reaction setup

During the reaction between the peroxide and the amine, the copper catalyst participates in both the C–C scission and C–N coupling events. To gain insight into the kinetic behavior of different copper species in these two steps, we monitored the formation of both methyl acetate (MeOAc) and the coupling product as proxies for the C–C scission and the C–N coupling events, respectively. Initially, we considered the amination between the peroxide **3-14** and 3-chloroindazole because in a previous study we demonstrated that **3-14** could be generated quantitatively and was relatively stable (eq. 1)¹⁶. While MeOAc displays well-resolved strong absorbances at 1250 and 1740 cm^{-1} , the strong carbonyl absorbance of the coupling product **3-16** at 1710 cm^{-1} is identical to that of **3-14** and this intensity remained constant during the reaction.

The product **3-16** does not have any other well-resolved or strong peaks to follow. With anticipation of a change in its carbonyl absorbance, we adopted phthalimide instead (eq. 2). Interestingly, the phthalimide carbonyl absorbance changed from 1740 to 1710 cm^{-1} , the latter overlapping with the carbonyl signals of **3-14** and **3-15**; the intensity of the peak at 1710 cm^{-1} increased, however, in proportion to the formation of **3-15** because the intensities of the carbonyl signals of both **3-14** and **3-15** were almost identical. The carbonyl absorptions of MeOAc and phthalimide overlapped (1740 cm^{-1}), so we used the peaks at 1116 and 1300 cm^{-1} to monitor the consumption of **3-14** and phthalimide, respectively. The ReactIR data were analyzed using iC IR 7.1 software. We applied variable time normalization analysis (VTNA) for kinetic analysis. When the exponent was equal to 0, the VTNA analysis diagram represented the reaction profile.



An oven-dried 25-mL three-neck flask equipped with a magnetic stirrer bar was capped with a rubber septum on the left neck. The ReactIR probe was equipped on the middle neck. The right neck was connected to the Schlenk line. The flask was purged with argon three times. Freshly prepared solutions of phthalimide, phenanthroline, copper, and peroxide were added into the three-

neck flask sequentially *via* syringe. For the exact procedures for the preparation of solutions, see each section.

Note:

1. The reaction vessel should be sealed carefully because the copper(I) species are highly O₂-sensitive. The juncture between the probe and probe adapter was sealed with Teflon tape. The bottom part of the stopper and the probe adapter were twined by Teflon tape prior to being capped on the flask. Parafilm was used to seal the outside of the juncture. The right neck was sealed with high-vacuum grease.
2. MeCN was freshly distilled, followed by three freeze/pump/thaw deoxygenation cycles prior to use.
3. All of the materials were dissolved in deoxygenated MeCN and should be used as a solution.
4. The junctures between the syringes and needles were sealed with Parafilm and the syringes and needles were purged with argon three times prior to use.
5. To prevent the peroxide from slowly decomposing at room temperature (actually, we found it was stable in MeCN at room temperature for a few hours), once made, the peroxide solution was kept at $-78\text{ }^{\circ}\text{C}$ and warmed to room temperature in a water bath prior to use.

before degassed MeCN (30 mL) was added. The flask was shaken gently until the entire white solid had dissolved.

B. Copper(I) chloride solution (0.015 M): A 50-mL round-bottom flask was charged with copper(I) chloride (29.7 mg, 0.300 mmol). The flask was capped with a Telfon tape–twined stopper and further sealed with Parafilm wrapping around the joints. The flask was purged with argon three times before degassed MeCN (20 mL) was added. The flask was shaken gently until the entire white solid had dissolved.

C. Phenanthroline solution (0.015 M): A 50-mL round-bottom flask was charged with phenanthroline (54.1 mg, 0.300 mmol). The flask was capped with a Telfon tape–twined stopper and further sealed with Parafilm wrapping around the joints. The flask was purged with argon three times before degassed MeCN (20 mL) was added. The flask was shaken gently until the entire white solid was dissolved.

D. Peroxide solution (0.3 M): A 50-mL round-bottom flask equipped with a magnetic stirrer bar was charged with the alkene (319 mmol, 1.35 mmol) and MeOH (30 mL, 0.045 M) and then cooled to $-78\text{ }^{\circ}\text{C}$ in a dry-ice/acetone bath with two 250-mL waste gas traps equipped with 20 wt% aqueous KI (200 mL). Ozone was bubbled through the solution until complete consumption of the starting material had occurred (as indicated by TLC and/or a blue color in the reaction mixture). The solution was sparged with argon for 5 min to expel excess ozone and then the mixture was warmed to room temperature and the MeOH evaporated *in vacuo*. The residue was dissolved in benzene (15 mL) followed by concentration *in vacuo* to remove adventitious water; this step was repeated one more time. The flask was capped with a Telfon tape–twined stopper and further sealed with Parafilm wrapping around the joints. The flask

was purged with argon three times before degassed MeCN (usually *ca.* 4.2 mL) was added to give a solution having a total volume of 4.5 mL.

The phthalimide solution, phenanthroline solution, degassed MeCN, CuCl solution, and peroxide solution were added into a three-neck round-bottom flask sequentially. Volumes are indicated in the Table below.

Experiments	Phthalimide (mL)	Phenanthroline (mL)	MeCN (mL)	CuCl (mL)	Peroxide (mL)
2 mol % (CuCl + Phen)	3.0	0.2	1.6	0.2	1.0
4 mol % (CuCl + Phen)	3.0	0.4	1.2	0.4	1.0
6 mol % (CuCl + Phen)	3.0	0.6	0.8	0.6	1.0
8 mol % (CuCl + Phen)	3.0	0.8	0.4	0.8	1.0

Figure 3.6 VTNA to determine the reaction order of (CuCl + Phen) on 3-15 generation

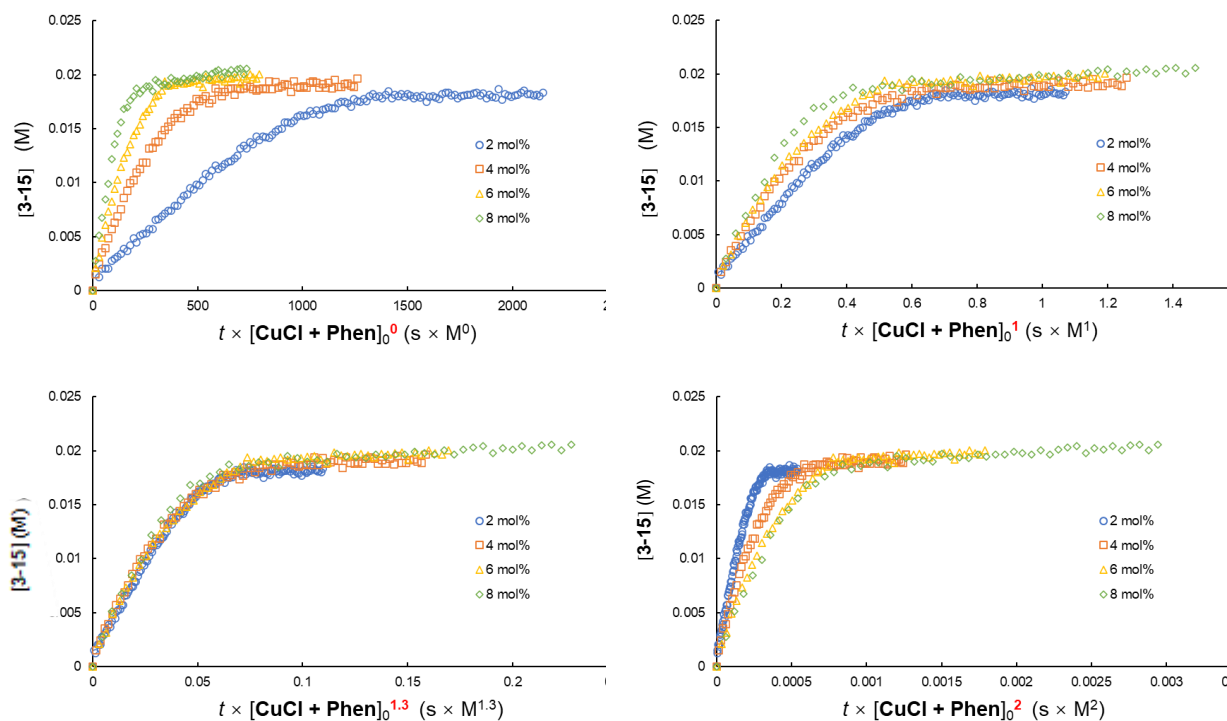
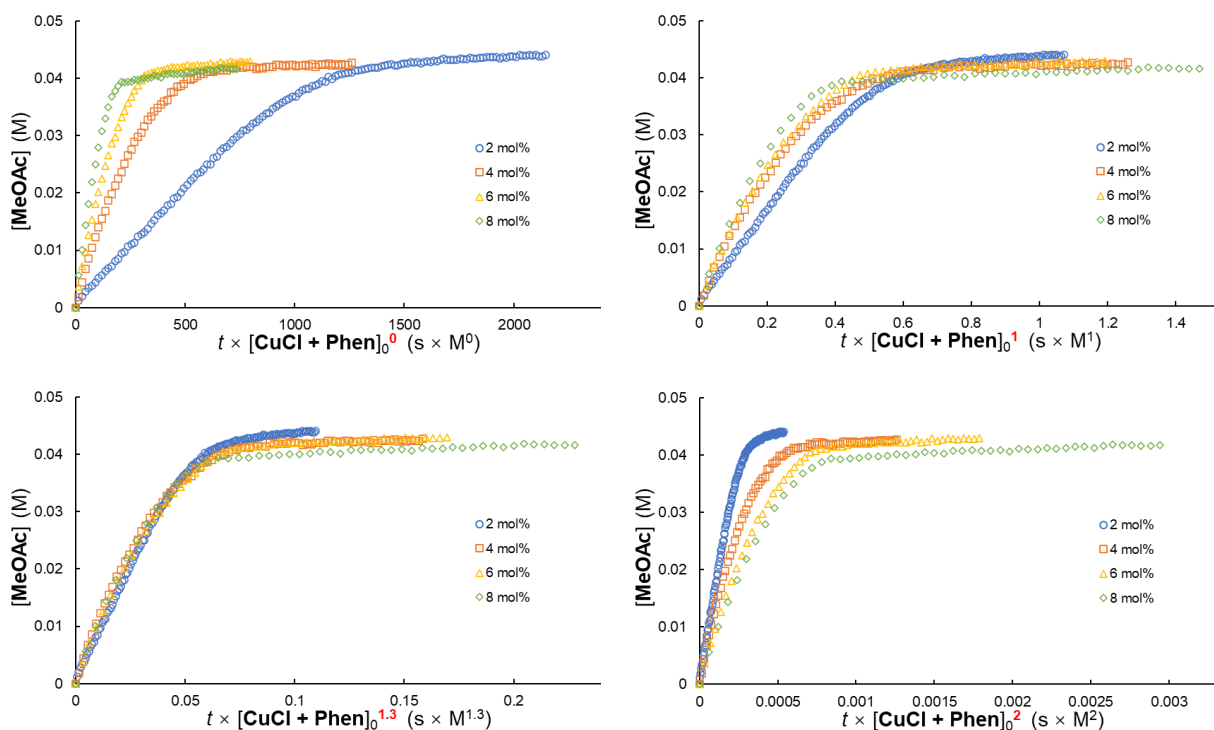


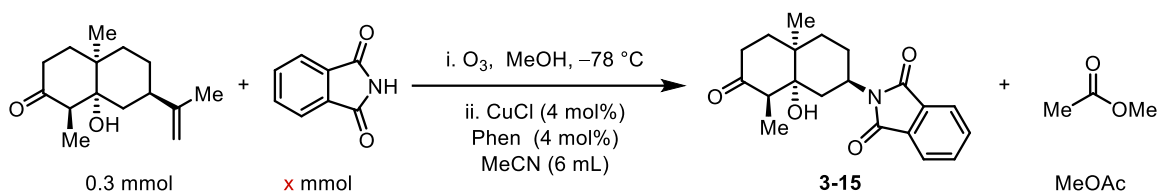
Figure 3.7 VTNA to determine the reaction order of (CuCl+ Phen) on MeOAc generation.



Summary of Section 3.6.2: The amination between **3-14** and phthalimide using 20 mol % of CuCl and Phen was rapid and complete within 2 min, even at 0 °C; therefore, we could not collect a sufficient number of data points. In addition, it is generally suggested to use less than 10 mol % of a catalyst for kinetic studies¹. Consequently, we used 2.0–8.0 mol % of (CuCl + Phen) catalyst for the kinetic measurements. The reaction using 4 mol % of catalyst was complete within approximately 10 min, an optimal period for operation. As a result, we used 4 mol % of catalyst for determination of the reaction orders of peroxide and phthalimide (Sections 3.6.3 and 3.6.4). The kinetic studies of $[\text{CuCl}_2]^-$ and $[(\text{Phen})_2\text{Cu}]^+$ were based on, and varied from, the 4 mol % Cu(I) loading conditions.

The rates of **3-15** and MeOAc generation both decreased when we decreased the concentration of the catalyst from 8 to 2 mol % (Figs. 3.6 and 3.7, top left). The reaction traces did not overlap for both the first order and second order for **3-15** and MeOAc (Figs. 3.6 and 3.7, top and bottom right). We found that orders of 1.3 for the generation of both **3-15** and MeOAc afforded the best overlap (Figs. 3.6 and 3.7, bottom left). This unusual 1.3-order-dependence on the (CuCl + Phen) catalyst for both C–C scission (MeOAc generation) and C–N coupling (**3-15** generation) indicates bimolecular catalysis, in contrast to the results of previous studies^{3,6,14}.

3.6.3. Determination of the reaction order of phthalimide



Preparation of the solutions:

- A. Phthalimide solution (0.05 M):** A 50-mL round-bottom flask was charged with phthalimide (221 mg, 1.50 mmol). The flask was capped with a Teflon tape–twined stopper and further sealed with Parafilm wrapping around the joints. The flask was purged with argon three times before degassed MeCN (30 mL) was added. The flask was shaken gently until the entire white solid had dissolved.
- B. Copper(I) chloride solution (0.015 M):** A 50-mL round-bottom flask was charged with copper(I) chloride (29.7 mg, 0.300 mmol). The flask was capped with a Teflon tape–twined stopper and further sealed with Parafilm wrapping around the joints. The flask was purged with argon three times before degassed MeCN (20 mL) was added. The flask was shaken gently until the entire white solid had dissolved.

C. Phenanthroline solution (0.015 M): A 50-mL round-bottom flask was charged with phenanthroline (54.1 mg, 0.3 mmol). The flask was capped with a Telfon tape–twined stopper and further sealed with Parafilm wrapping around the joints. The flask was purged with argon three times before degassed MeCN (20 mL) was added. The flask was shaken gently until the entire white solid had dissolved.

D. Peroxide solution (0.3 M): A 50-mL round-bottom flask equipped with a magnetic stirrer bar was charged with the alkene (319 mmol, 1.35 mmol) and MeOH (30 mL, 0.045 M) and then it was cooled to $-78\text{ }^{\circ}\text{C}$ in a dry-ice/acetone bath with two 250-mL waste gas traps equipped with 20 wt% aqueous KI (200 mL). Ozone was bubbled through the solution until complete consumption of the starting material had occurred (as indicated by TLC and/or a blue color in the reaction mixture). The solution was sparged with argon for 5 min to expel excess ozone and then the mixture was warmed to room temperature and the MeOH was evaporated *in vacuo*. The residue was dissolved in benzene (15 mL) followed by evaporation *in vacuo* to remove adventitious water; this step was repeated one more time. The flask was capped with a Telfon tape–twined stopper and further sealed with Parafilm wrapping around the joints. The flask was purged with argon three times before degassed MeCN (usually *ca.* 4.2 mL) was added to give a solution having a total volume of 4.5 mL.

The phthalimide solution, phenanthroline solution, degassed MeCN, CuCl solution, and peroxide solution were added into a three-neck round-bottom flask sequentially. Volumes are indicated in the Table below.

Experiment	Phthalimide (mL)	Phenanthroline (mL)	MeCN (mL)	CuCl (mL)	Peroxide (mL)
0.0125 M (0.075 mmol)	1.5	0.4	2.7	0.4	1.0

0.0167 M (0.10 mmol)	2.0	0.4	2.2	0.4	1.0
0.0208 M (0.125 mmol)	2.5	0.4	1.7	0.4	1.0
0.0250 M (0.15 mmol)	3.0	0.4	1.2	0.4	1.0
0.0317 M (0.19 mmol)	3.8	0.4	0.4	0.4	1.0

Figure 3.8 VTNA to determine the reaction order of phthalimide on 3-15 generation.

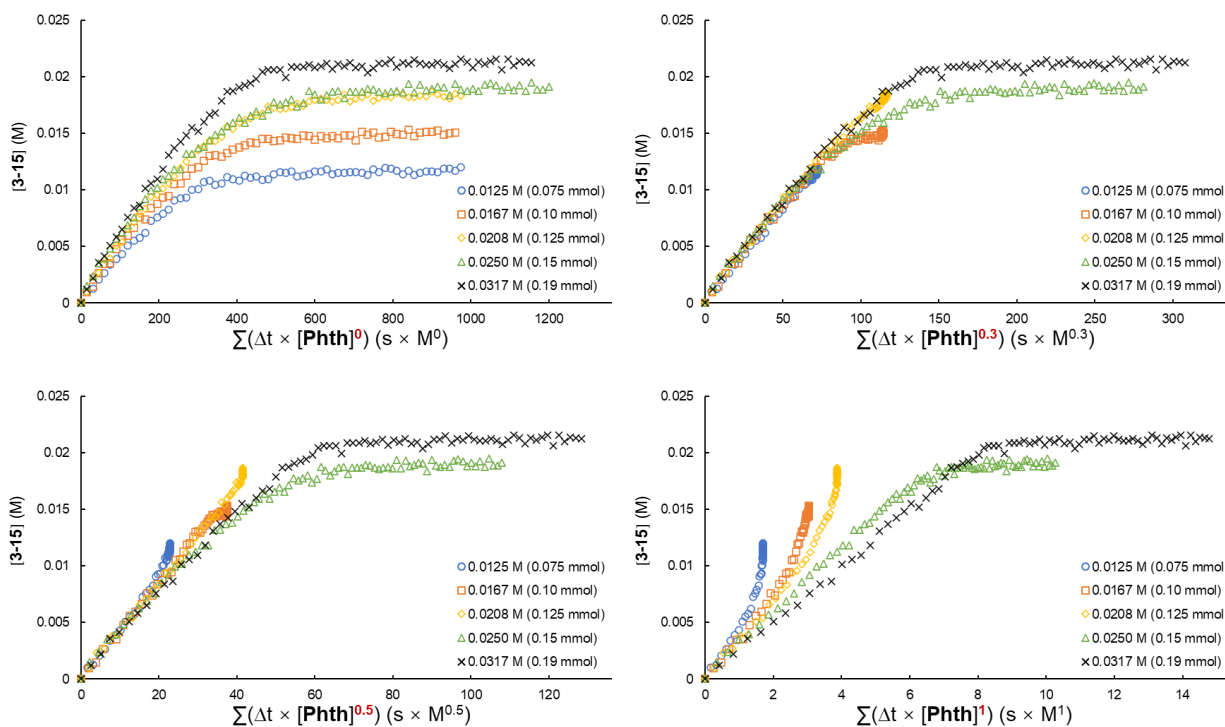
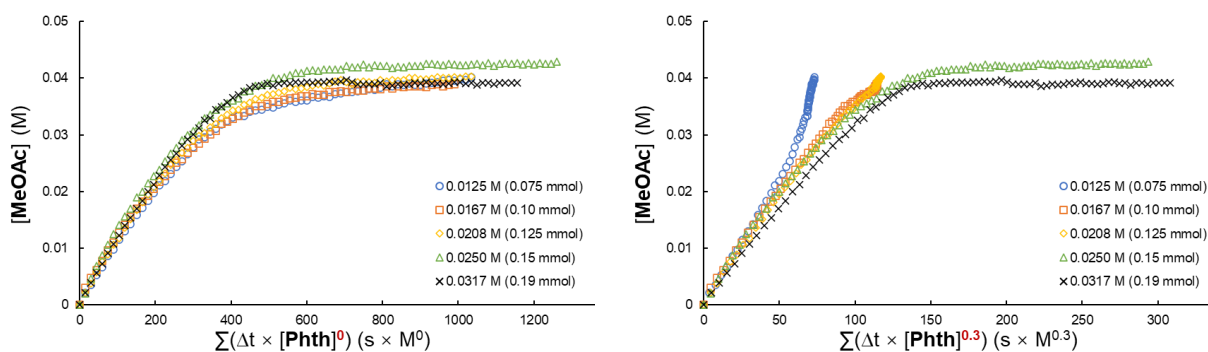
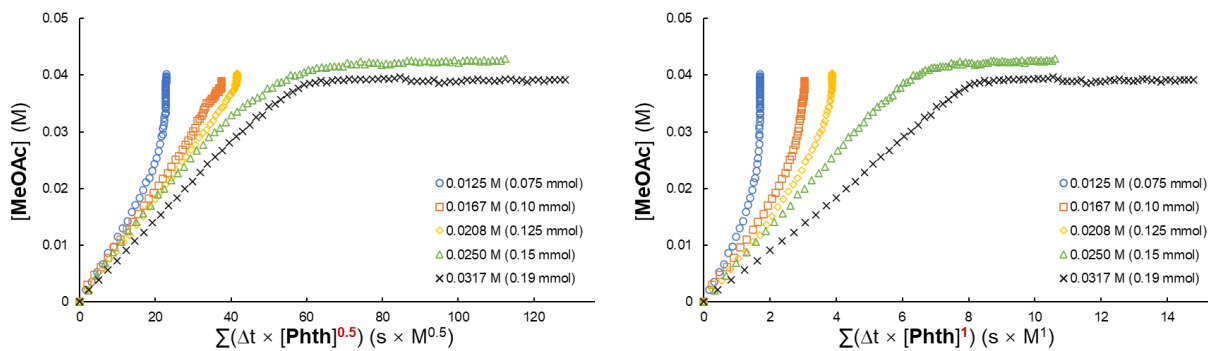


Figure 3.9 VTNA to determine the reaction order of phthalimide on MeOAc generation.

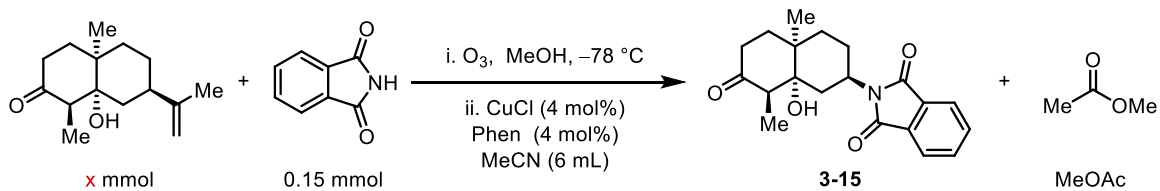




Summary of Section 3.6.3: A lower amount of peroxide led to a lower yield and shorter reaction time. To obtain a significant product peak intensity and sufficient data points, a half amount of phthalimide [0.075 mmol, compared with the standard condition (0.15 mmol)] was selected as the lowest concentration. Consequently, 0.075, 0.10, 0.125, 0.15, and 0.19 mmol of phthalimide were used to determine the reaction order.

We found that the rates of **3-15** generation decreased slightly upon decreasing the concentration of phthalimide (Fig. 3.8, top left). The traces of **3-15** generation overlapped the best when applying an order of 0.3 on phthalimide (Fig. 3.9, top right). Other reaction orders, including 0.5 and 1, did not afford such a good overlap (Fig. 3.9, bottom). In contrast, the rates of MeOAc generation were almost identical when using different concentrations of phthalimide (Fig. 3.9, top left). Other reaction orders did not afford such a good overlap (Fig. 3.9, top right and bottom). Therefore, the generation of **3-15** was 0.3-order (pseudo-zero-order)-dependent on phthalimide. The generation of MeOAc was zero-order-dependent on phthalimide.

3.6.4. Determination of the reaction order of peroxide (alkene)



Preparation of the solutions:

- A. Phthalimide solution (0.05 M):** A 50-mL round-bottom flask was charged with phthalimide (221 mg, 1.50 mmol). The flask was capped with a Teflon tape–twined stopper and further sealed with Parafilm wrapping around the joints. The flask was purged with argon three times before degassed MeCN (30 mL) was added. The flask was shaken gently until the entire white solid had dissolved.
- B. Copper(I) chloride solution (0.015 M):** A 50-mL round-bottom flask was charged with copper(I) chloride (29.7 mg, 0.300 mmol). The flask was capped with a Teflon tape–twined stopper and further sealed with Parafilm wrapping around the joints. The flask was purged with argon three times before degassed MeCN (20 mL) was added. The flask was shaken gently until the entire white solid had dissolved.
- C. Phenanthroline solution (0.015 M):** A 50-mL round-bottom flask was charged with phenanthroline (54.1 mg, 0.300 mmol). The flask was capped with a Teflon tape–twined stopper and further sealed with Parafilm wrapping around the joints. The flask was purged with argon three times before degassed MeCN (20 mL) was added. The flask was shaken gently until the entire white solid had dissolved.
- D. Peroxide solution (0.3 M):** A 50-mL round-bottom flask equipped with a magnetic stirrer bar was charged with the alkene (330 mmol, 1.35 mmol) and MeOH (30 mL, 0.045 M) and then cooled to $-78\text{ }^\circ\text{C}$ in a dry-ice/acetone bath with two 250-mL waste gas traps equipped with 20 wt% aqueous KI (200 mL). Ozone was bubbled through the solution until complete

consumption of the starting material had occurred (as indicated by TLC and/or a blue color in the reaction mixture). The solution was sparged with argon for 5 min to expel excess ozone and then the mixture was warmed to room temperature and the MeOH was evaporated *in vacuo*. The residue was dissolved in benzene (15 mL) followed by concentration *in vacuo* to remove adventitious water; this step was repeated one more time. The flask was capped with a Telfon tape–twined stopper and further sealed with Parafilm wrapping around the joints. The flask was purged with argon three times before degassed MeCN (usually about 4.2 mL) was added to give a solution having a total volume of 4.5 mL.

The phthalimide solution, phenanthroline solution, degassed MeCN, CuCl solution, and peroxide solution were added into a three-neck round-bottom flask sequentially. Volumes are indicated in the Table below.

Experiment	Phthalimide (mL)	Phenanthroline (mL)	MeCN (mL)	CuCl (mL)	Peroxide (mL)
0.030 M (0.18 mmol)	3.0	0.4	1.6	0.4	0.6
0.035 M (0.21 mmol)	3.0	0.4	1.5	0.4	0.7
0.050 M (0.30 mmol)	3.0	0.4	1.2	0.4	1.0
0.060 M (0.36 mmol)	3.0	0.4	1.0	0.4	1.2
0.070 M (0.42 mmol)	3.0	0.4	0.8	0.4	1.4

Figure 3.10 VTNA to determine the reaction order of peroxide on 3-15 generation.

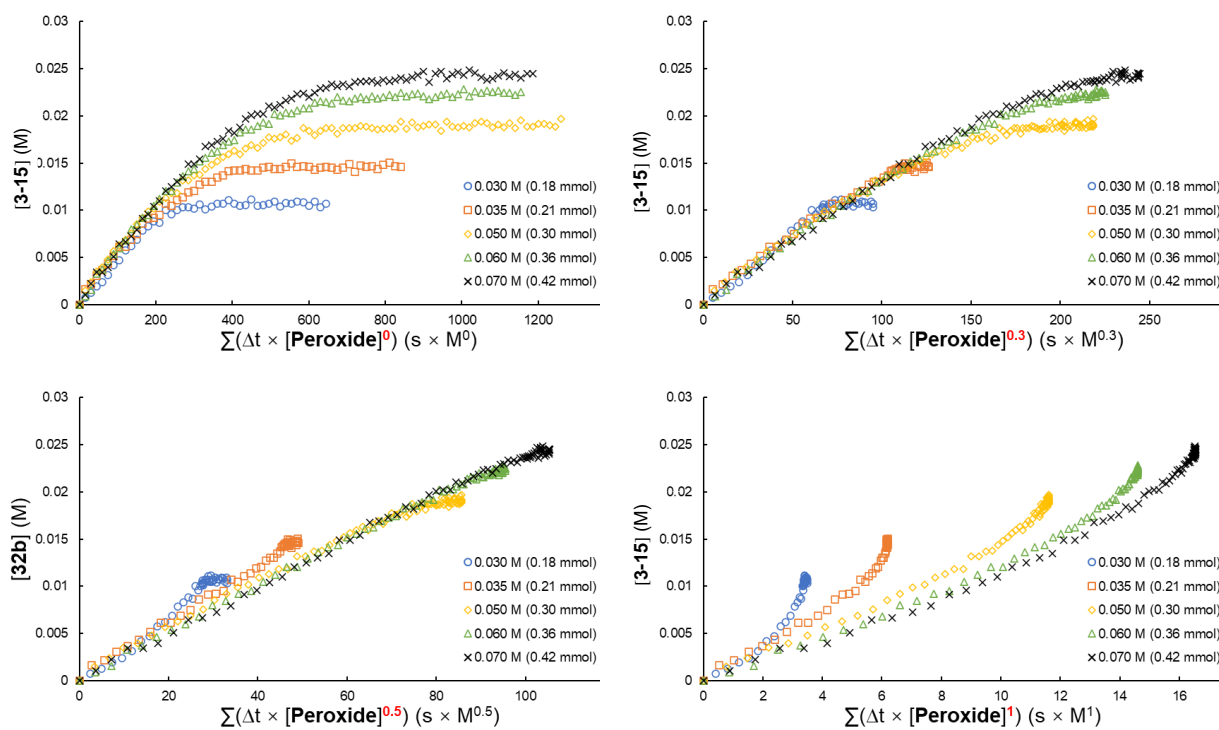
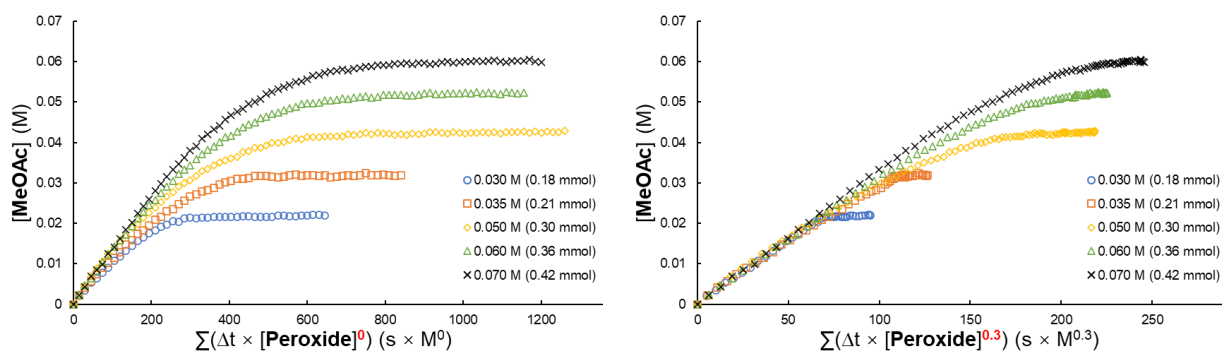
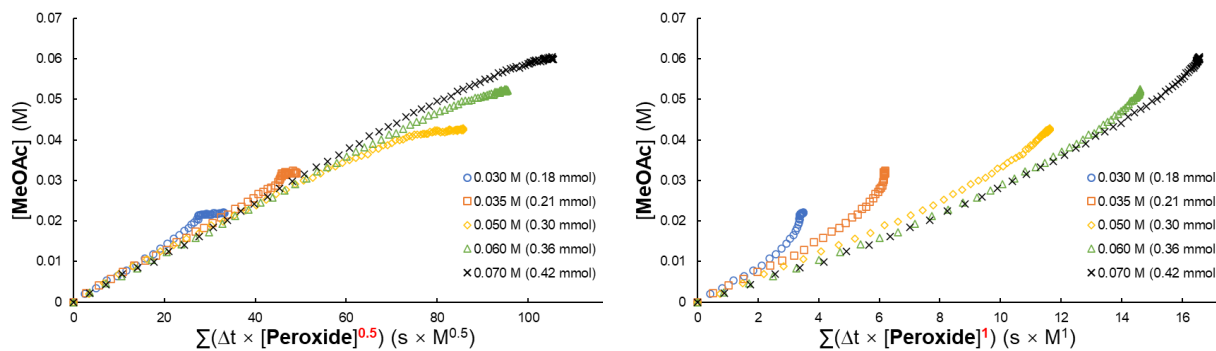


Figure 3.11. VTNA to determine the reaction order of peroxide on MeOAc generation.

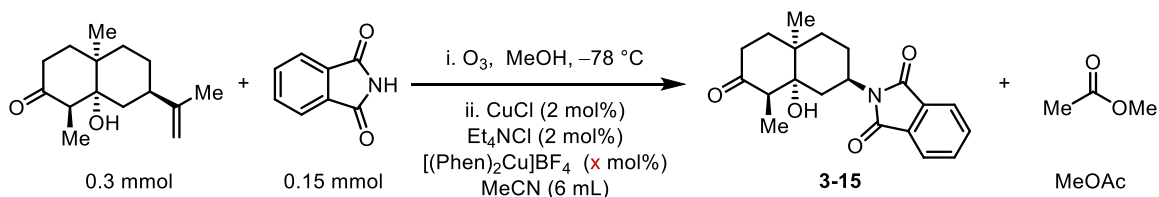




Summary of Section 3.6.4: A lower amount of peroxide led to a lower yield and shorter reaction time. To obtain a significant product peak intensity and sufficient data points, we selected a 60% amount of peroxide [0.18 mmol, compared with the standard condition (0.30 mmol)] as the lowest concentration. Consequently, we used 0.18, 0.21, 0.30, 0.36, and 0.42 mmol of phthalimide to determine the reaction order.

We found that the rates of generation of **3-15** and MeOAc both decreased slightly upon decreasing the concentration of peroxide (Figs. 3.10 and 3.11, top left). The traces for **3-15** and MeOAc generation both overlapped best when applying an order of 0.3 (Figs. 3.10 and 3.11, top right). Other reaction orders, including 0.5 and 1, did not afford such a good fit (Figs. 3.10 and 3.11, bottom). Therefore, the generations of **3-15** and MeOAc were both 0.3-order (pseudo-zero-order)–dependent on peroxide.

3.6.5. Determination of the reaction order of $[(\text{Phen})_2\text{Cu}]\text{BF}_4$



Preparation of the solutions:

A. Phthalimide solution (0.05 M): A 50-mL round-bottom flask was charged with phthalimide (221 mg, 1.50 mmol). The flask was capped with a Telfon tape–twined stopper and further sealed with Parafilm wrapping around the joints. The flask was purged with argon three times before degassed MeCN (30 mL) was added. The flask was shaken gently until the entire white solid had dissolved.

B. Et₄NCl solution (0.0075 M): A 50-mL round-bottom flask was charged with Et₄NCl (37.3 mg, 0.225 mmol) in a glove box. The flask was capped with a Telfon tape–twined stopper and then removed from the glove box, followed by sealing with Parafilm wrapping around the joints. Degassed MeCN (30 mL) was then added. The flask was shaken gently until the entire white solid had dissolved.

C. [Copper(I) chloride + Et₄NCl] solution (0.0075 M): A 50-mL round-bottom flask was charged with copper(I) chloride (14.9 mg, 0.15 mmol). The flask was capped with a Telfon tape–twined stopper and further sealed with Parafilm wrapping around the joints. The flask was purged with argon three times before Et₄NCl solution (20 mL) was added. The flask was shaken gently until the entire white solid had dissolved.

D. [(Phen)₂Cu]BF₄ solutions:

Solution A (3.75 mM): A 50-mL round-bottom flask was charged with [(Phen)₂Cu]BF₄ (19.2 mg, 0.0375 mmol). The flask was capped with a Telfon tape–twined stopper and further sealed with Parafilm wrapping around the joints. The flask was purged with argon three times before degassed MeCN (10 mL) was added. The flask was shaken gently until the entire dark-red solid had dissolved.

Solution B (0.375 mM): A 25-mL round-bottom flask was capped with a Telfon tape–twined

stopper and further sealed with Parafilm wrapping around the joints. The flask was purged with argon three times before **Solution A** (1 mL) and degassed MeCN (9 mL) were added to afford **Solution B**.

E. Peroxide solution (0.3 M): A 50-mL round-bottom flask equipped with a magnetic stirrer bar was charged with the alkene (319 mmol, 1.35 mmol) and MeOH (30 mL, 0.045 M) and then it was cooled to $-78\text{ }^{\circ}\text{C}$ in a dry-ice/acetone bath with two 250-mL waste gas traps equipped with 20 wt% aqueous KI (200 mL). Ozone was bubbled through the solution until complete consumption of the starting material had occurred (as indicated by TLC and/or a blue color in the reaction mixture). The solution was sparged with argon for 5 min to expel excess ozone and then the mixture was warmed to room temperature and the MeOH was evaporated *in vacuo*. The residue was dissolved in benzene (15 mL) followed by concentration *in vacuo* to remove adventitious water; this step was repeated one more time. The flask was capped with a Telfon tape-twined stopper and further sealed with Parafilm wrapping around the joints. The flask was purged with argon three times before degassed MeCN (usually *ca.* 4.2 mL) was added to give a solution having a total volume of 4.5 mL.

The phthalimide solution, phenanthroline solution, degassed MeCN, CuCl solution, and peroxide solution were added into a three-neck round-bottom flask sequentially. Volumes are indicated in the Table below.

Experiment	Phthalimide (mL)	Complex 3-5 (mL)	MeCN (mL)	(CuCl + Et ₄ NCl) (mL)	Peroxide (mL)
0 mol % 3-5	3.0	0 (Solution B)	1.6	0.4	1.0
0.1 mol % 3-5	3.0	0.4 (Solution B)	1.2	0.4	1.0
0.2 mol % 3-5	3.0	0.8 (Solution B)	0.8	0.4	1.0
0.3 mol % 3-5	3.0	1.2 (Solution B)	0.4	0.4	1.0
0.5 mol % 3-5	3.0	0.2 (Solution A)	1.4	0.4	1.0

1.0 mol % 3-5	3.0	0.4 (Solution A)	1.2	0.4	1.0
1.5 mol % 3-5	3.0	0.6 (Solution A)	1.0	0.4	1.0
2.0 mol % 3-5	3.0	0.8 (Solution A)	0.8	0.4	1.0
4.0 mol % 3-5	3.0	1.6 (Solution A)	0	0.4	1.0

Figure 3.12 VTNA to determine the reaction order of complex 3-5 on 3-15 generation (from 0.5 mol % to 4.0 mol %) using 2.0 mol % of (CuCl + TEACl).

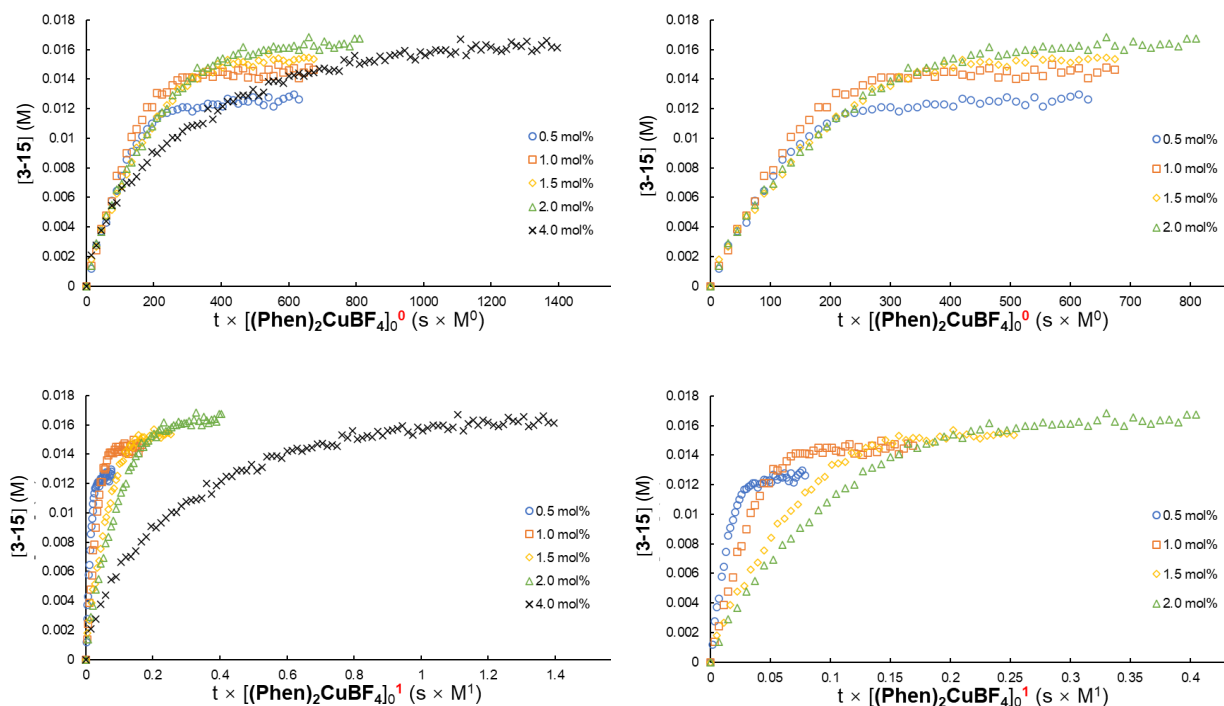
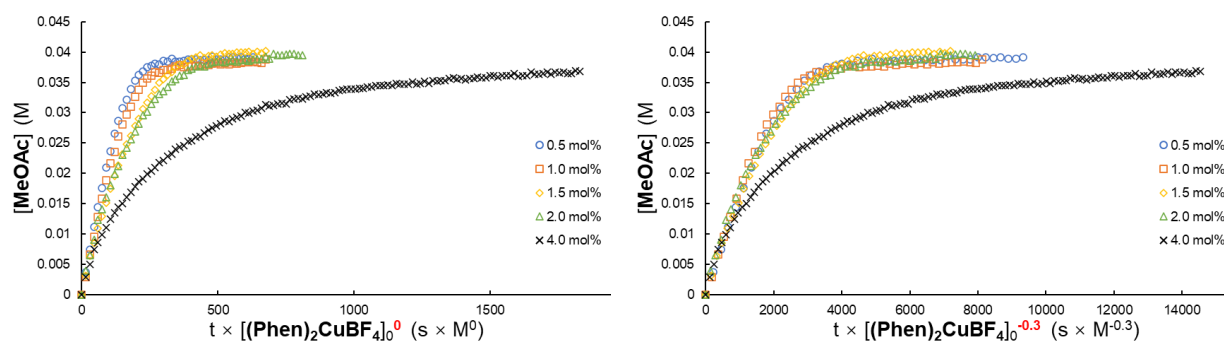


Figure 3.13 VTNA to determine the reaction order of complex 3-5 on MeOAc generation (from 0.5 to 4.0 mol %) using 2.0 mol % of (CuCl + TEACl)



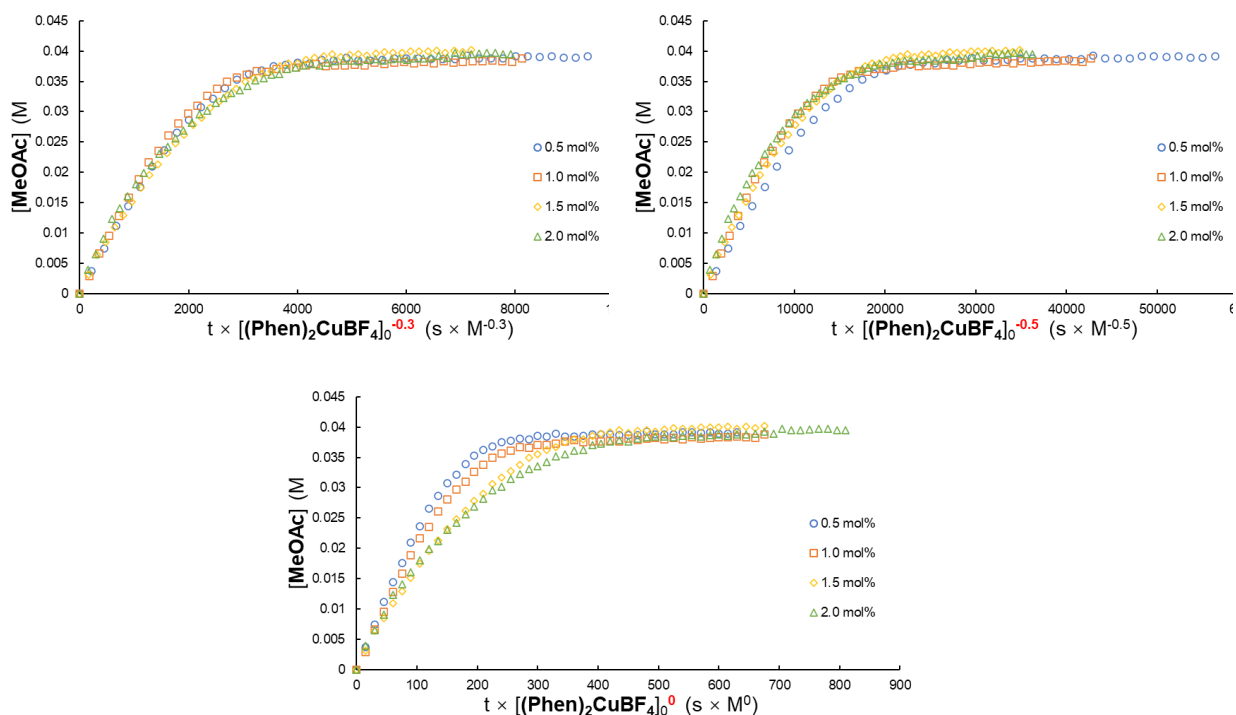
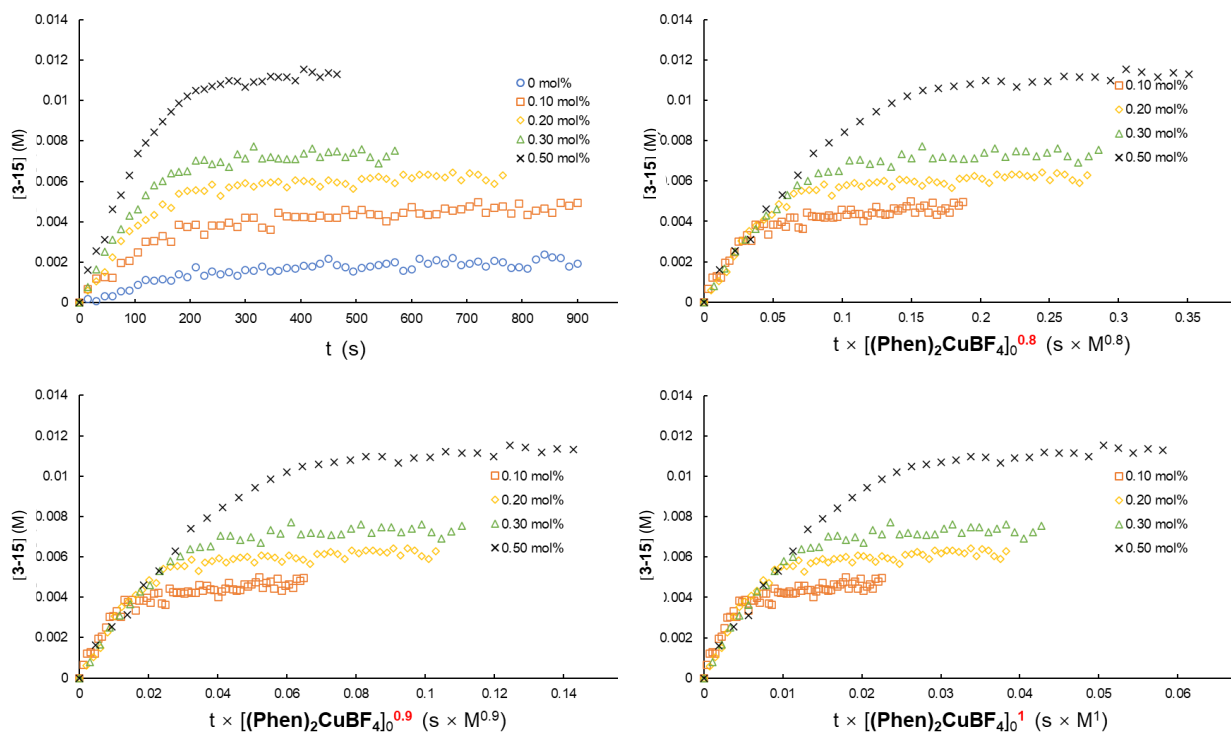


Figure 3.14 VTNA to determine the reaction order of complex 3-5 on 3-15 generation (from 0 to 0.5 mol %) using 2.0 mol % of (CuCl + TEACl).



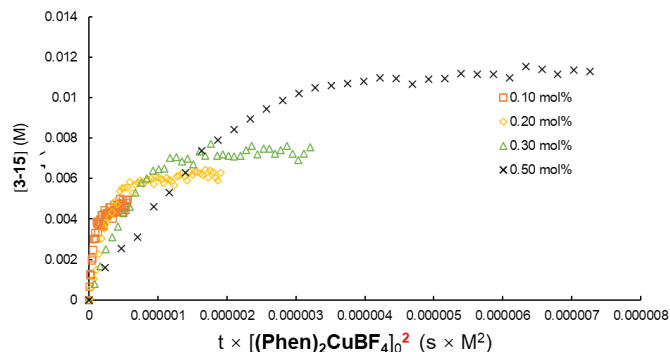
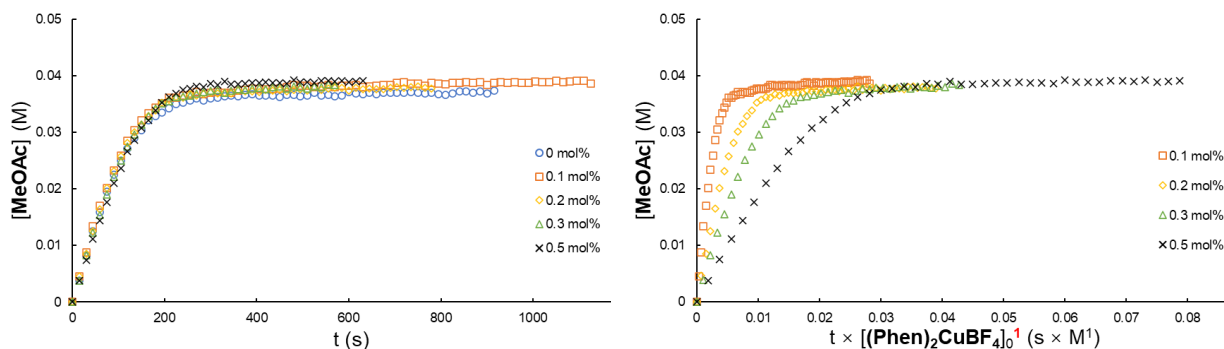


Figure 3.15 VTNA to determine the reaction order of complex **3-5** on MeOAc generation (from 0 to 0.5 mol %) using 2.0 mol % of (CuCl + TEACl).



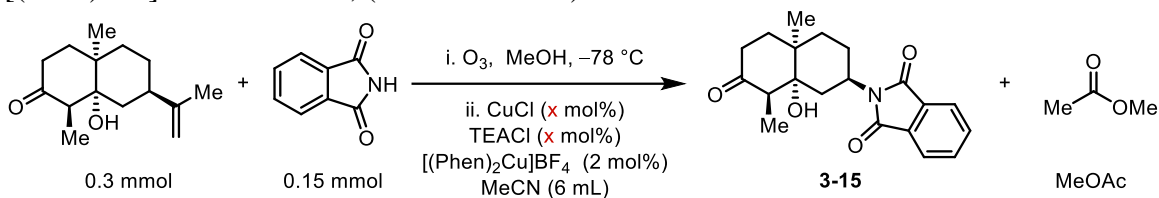
Summary of Section 3.6.5: Because control experiments (Section 3.4) suggested cooperative catalysis between $[(\text{Phen})_2\text{Cu}]^+$ and $[\text{CuCl}_2]^-$ and the reaction displayed a 1.3-order-dependence on the (CuCl + Phen) catalyst, we studied the roles and kinetics of $[(\text{Phen})_2\text{Cu}]^+$ and $[\text{CuCl}_2]^-$ separately. For our preliminary kinetic study of $[(\text{Phen})_2\text{Cu}]\text{BF}_4$, we chose concentrations ranging from 0.5 to 4 mol %. We found, firstly, when using 4 mol % of $[(\text{Phen})_2\text{Cu}]^+$ (the concentration of $[(\text{Phen})_2\text{Cu}]^+$ was higher than that of $[\text{CuCl}_2]^-$), the rates of **3-15** and MeOAc generation both decreased significantly (Figs. 3.12 and 3.13, top left). We posited that Phen could dissociate from the $[(\text{Phen})_2\text{Cu}]^{2+}$ complex and coordinate to $[\text{CuCl}_2\text{L}]$, significantly decreasing the concentration of $[\text{CuCl}_2\text{L}]$ and, as the consequence, slowing down the peroxide decomposition (see Section 3.8 for details). This observation also fits with the kinetic study of phenanthroline (see Section 3.6.7).

Secondly, the reaction traces for **3-15** generation overlapped best when applying a zero order (Fig. 3.12, top right). In contrast, the rate of MeOAc generation decreased slightly upon increasing the concentration of $[(\text{Phen})_2\text{Cu}]\text{BF}_4$ from 0.5 to 2.0 mol %. We surmised that this rate decrease was also due to Phen dissociation from $[(\text{Phen})_2\text{Cu}]^{2+}$. The reaction traces overlapped best when applying a -0.3 order (Fig. 3.13, middle right). Therefore, the generation of **3-15** was zero-order-dependent on $[(\text{Phen})_2\text{Cu}]\text{BF}_4$ in the range from 0.5 to 2 mol % and the generation of MeOAc was -0.3 -order (pseudo-zero-order)-dependent on $[(\text{Phen})_2\text{Cu}]\text{BF}_4$ in the range from 0.5 to 2 mol %. Our previous control experiments indicated that $<5\%$ of **3-15** was obtained when using CuCl and TEACl alone as the catalyst (Section 3.4, Table 3.1). In fact, a mere 0.5 mol % of $[(\text{Phen})_2\text{Cu}]\text{BF}_4$ produced a product yield of approximately 50% (see Fig. 3.12, top). Therefore, we suspected that experiments using 0.5–2.0 mol % $[(\text{Phen})_2\text{Cu}]\text{BF}_4$ might exhibit saturation kinetics. Consequently, we conducted additional kinetic measurements using lower concentrations (0–0.5 mol %) of $[(\text{Phen})_2\text{Cu}]\text{BF}_4$.

Indeed, as described in the main text, both the rate and yield of **3-15** formation decreased upon decreasing the amount of $[(\text{Phen})_2\text{Cu}]\text{BF}_4$ (Fig. 3.14, top left). The traces overlapped the best when applying an almost first order (0.8 or 0.9 might have been the best). The rate and yield of MeOAc formation were not affected by the concentration of $[(\text{Phen})_2\text{Cu}]\text{BF}_4$. In particular, MeOAc was generated at the same rate even in the absence of $[(\text{Phen})_2\text{Cu}]\text{BF}_4$. The traces overlapped the best when applying a zero order (Fig. 3.15). In all, the generation of **3-15** was first-order-dependent on $[(\text{Phen})_2\text{Cu}]\text{BF}_4$ in the range from 0.1 to 0.5 mol %. The generation of MeOAc was zero-order-dependent on $[(\text{Phen})_2\text{Cu}]\text{BF}_4$ in the same range.

3.6.6. Determination of the reaction order of (CuCl + Et₄NCl)

(1) [(Phen)₂Cu]BF₄ 2.0 mol %, (CuCl + Et₄NCl) from 2.0 to 4.0 mol %



Preparation of the solutions:

- A. Phthalimide solution (0.05 M):** A 50-mL round-bottom flask was charged with phthalimide (221 mg, 1.50 mmol). The flask was capped with a Teflon tape-twined stopper and further sealed with Parafilm wrapping around the joints. The flask was purged with argon three times before degassed MeCN (30 mL) was added. The flask was shaken gently until the entire white solid had dissolved.
- B. Et₄NCl solution (0.0075 M):** A 50-mL round-bottom flask was charged with Et₄NCl (37.3 mg, 0.225 mmol) in glove box. The flask was capped with a Teflon tape-twined stopper, removed from the glove box, and sealed with Parafilm wrapping around the joints. Degassed MeCN (30 mL) was added. The flask was shaken gently until the entire white solid had dissolved.
- C. (Copper(I) chloride + Et₄NCl) solution (0.0075 M):** A 50-mL round-bottom flask was charged with copper(I) chloride (14.9 mg, 0.150 mmol). The flask was capped with a Teflon tape-twined stopper and further sealed with Parafilm wrapping around the joints. The flask was purged with argon three times before Et₄NCl solution (20 mL) was added. The flask was shaken gently until the entire white solid had dissolved.
- D. [(Phen)₂Cu]BF₄ solution (3.75 mM):** A 50-mL round-bottom flask was charged with [(Phen)₂Cu]BF₄ (19.2 mg, 0.0375 mmol). The flask was capped with a Teflon tape-twined stopper and further sealed with Parafilm wrapping around the joints. The flask was purged with

argon three times before degassed MeCN (10 mL) was added. The flask was shaken gently until the entire dark-red solid had dissolved.

E. Peroxide solution (0.3 M): A 50-mL round-bottom flask equipped with a magnetic stirrer bar was charged with the alkene (319 mmol, 1.35 mmol) and MeOH (30 mL, 0.045 M) and then it was cooled to $-78\text{ }^{\circ}\text{C}$ in a dry-ice/acetone bath with two 250-mL waste gas traps equipped with 20 wt% aqueous KI (200 mL). Ozone was bubbled through the solution until complete consumption of the starting material had occurred (as indicated by TLC and/or a blue color in the reaction mixture). The solution was sparged with argon for 5 min to expel excess ozone and then the mixture was warmed to room temperature and the MeOH evaporated *in vacuo*. The residue was dissolved in benzene (15 mL) followed by concentration *in vacuo* to remove adventitious water; this step was repeated one more time. The flask was capped with a Telfon tape-twined stopper and further sealed with Parafilm wrapping around the joints. The flask was purged with argon three times before degassed MeCN (usually *ca.* 4.2 mL) was added to make a solution having a total volume of 4.5 mL.

The phthalimide solution, phenanthroline solution, degassed MeCN, CuCl solution, and peroxide solution were added into a three-neck round-bottom flask sequentially. Volumes are indicated in the Table below.

Experiment	Phthalimide (mL)	Complex 3-5 (mL)	MeCN (mL)	(CuCl + Et ₄ NCl) (mL)	Peroxide (mL)
2.0 mol % (CuCl + Et ₄ NCl)	3.0	0.8	0.8	0.4	1.0
2.5 mol % (CuCl + Et ₄ NCl)	3.0	0.8	0.7	0.5	1.0
3.0 mol % (CuCl + Et ₄ NCl)	3.0	0.8	0.6	0.6	1.0
3.5 mol % (CuCl + Et ₄ NCl)	3.0	0.8	0.5	0.7	1.0

4.0 mol % (CuCl + Et ₄ NCl)	3.0	0.8	0.4	0.8	1.0
---	-----	-----	-----	-----	-----

Figure 3.16 VTNA to determine the reaction order of (CuCl + Et₄NCl) (from 2.0 to 4.0 mol %) on 3-15 generation using 2.0 mol % of [(Phen)₂Cu]BF₄.

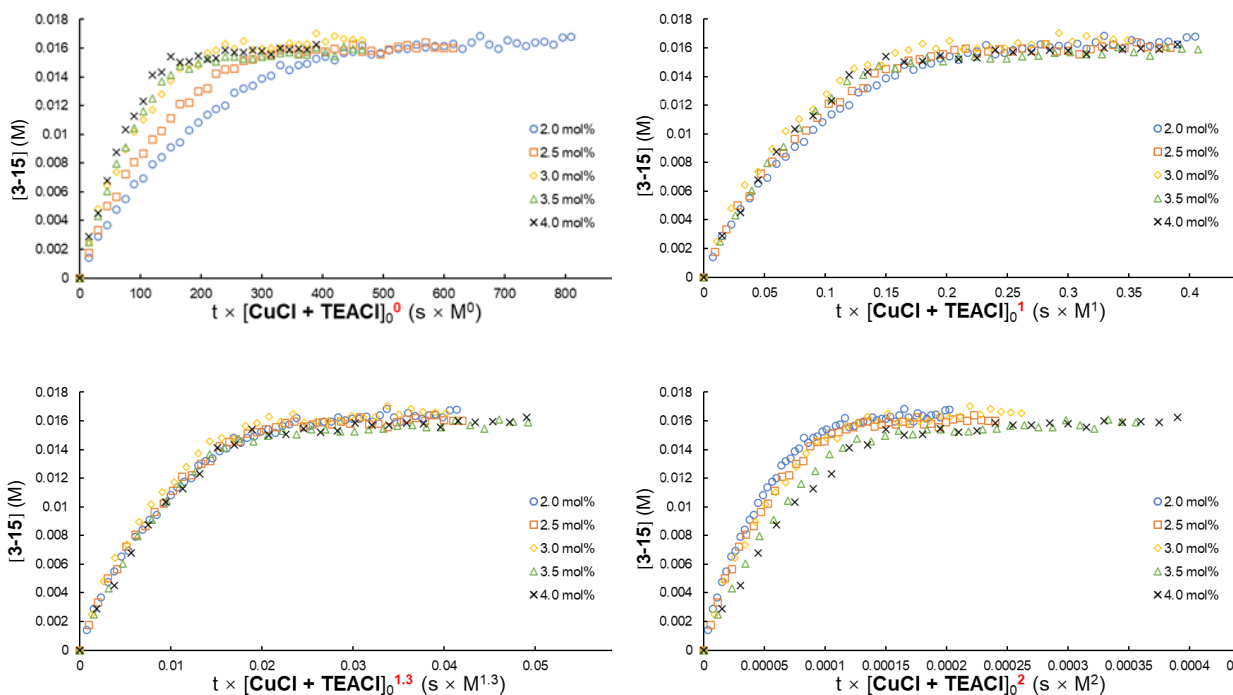
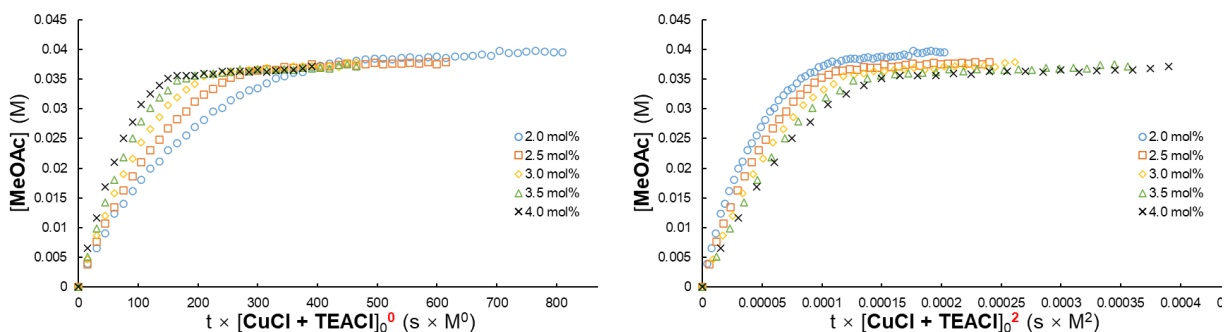
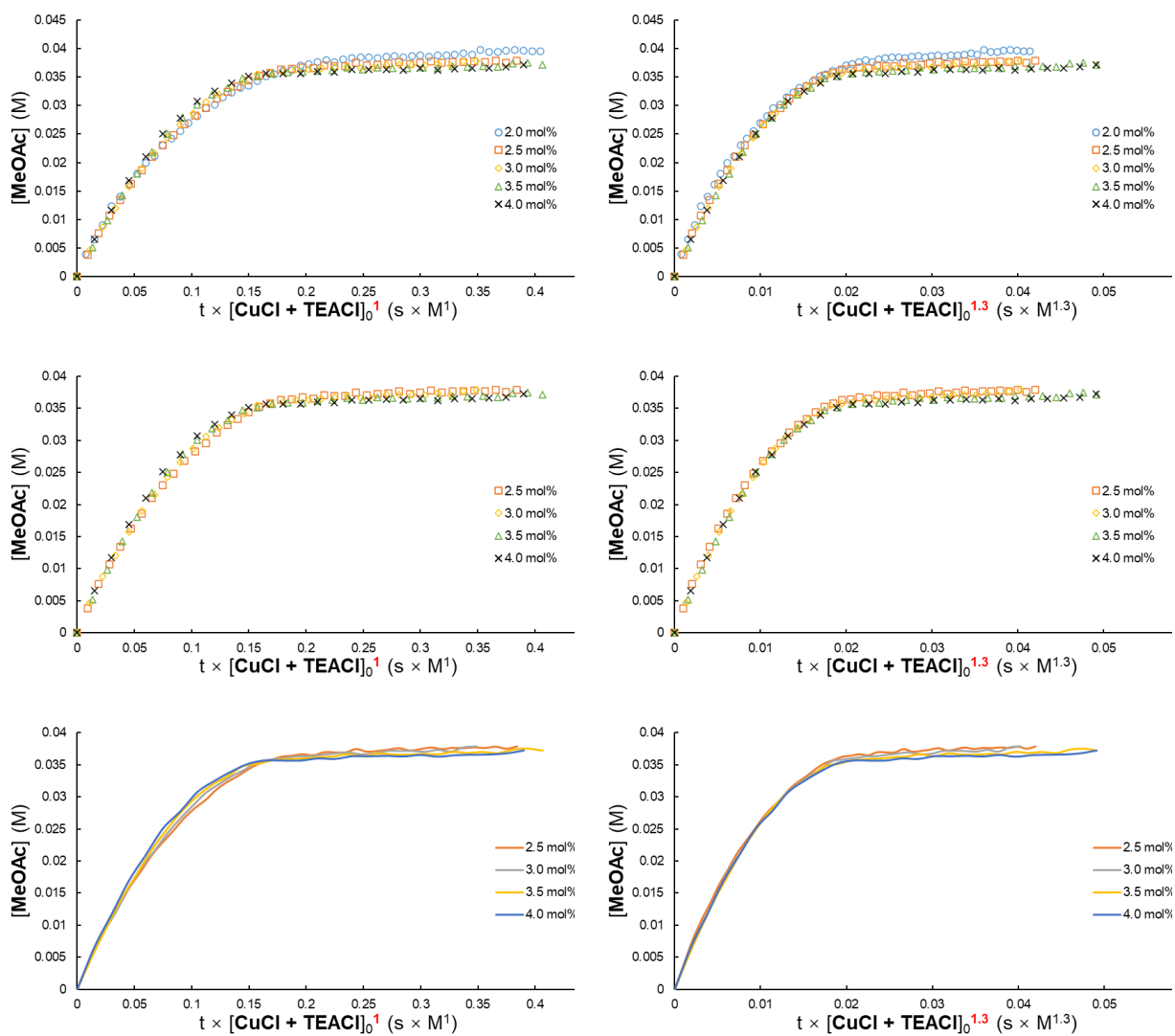
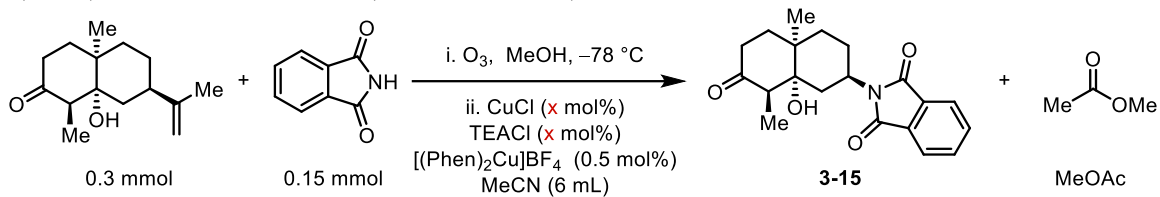


Figure 3.17 VTNA to determine the reaction order of (CuCl + Et₄NCl) (from 2.0 to 4.0 mol %) on MeOAc generation using 2.0 mol % of [(Phen)₂Cu]BF₄.





(2) [(Phen)₂Cu]BF₄ 0.5 mol %, (CuCl + Et₄NCl) from 1.0 to 2.0 mol %



Experiment	Phthalimide (mL)	Complex 3-5 (mL)	MeCN (mL)	(CuCl + Et ₄ NCl) (mL)	Peroxide (mL)
1.0 mol % (CuCl + Et ₄ NCl)	3.0	0.2	1.6	0.2	1.0

1.5 mol % (CuCl + Et ₄ NCl)	3.0	0.2	1.5	0.3	1.0
2.0 mol % (CuCl + Et ₄ NCl)	3.0	0.2	1.4	0.4	1.0

Figure 3.18 VTNA to determine the reaction order of (CuCl + Et₄NCl) (from 1.0 to 2.0 mol %) on 3-15 generation using 0.5 mol % of [(Phen)₂Cu]BF₄.

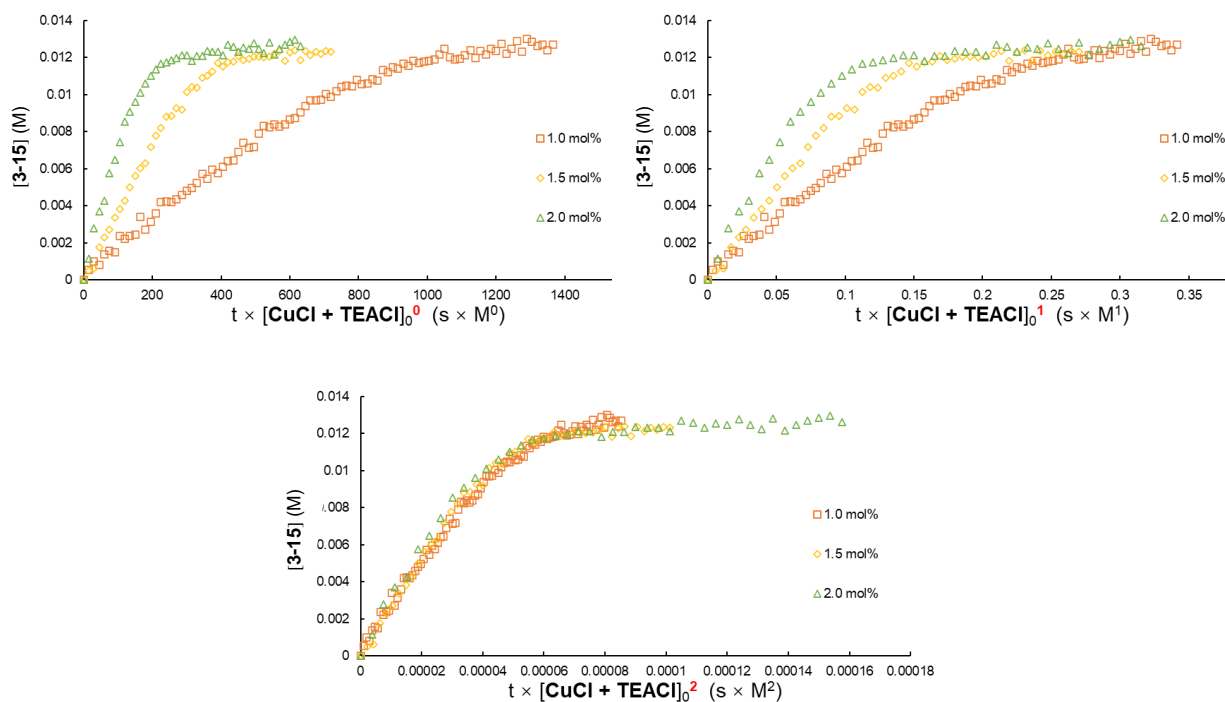
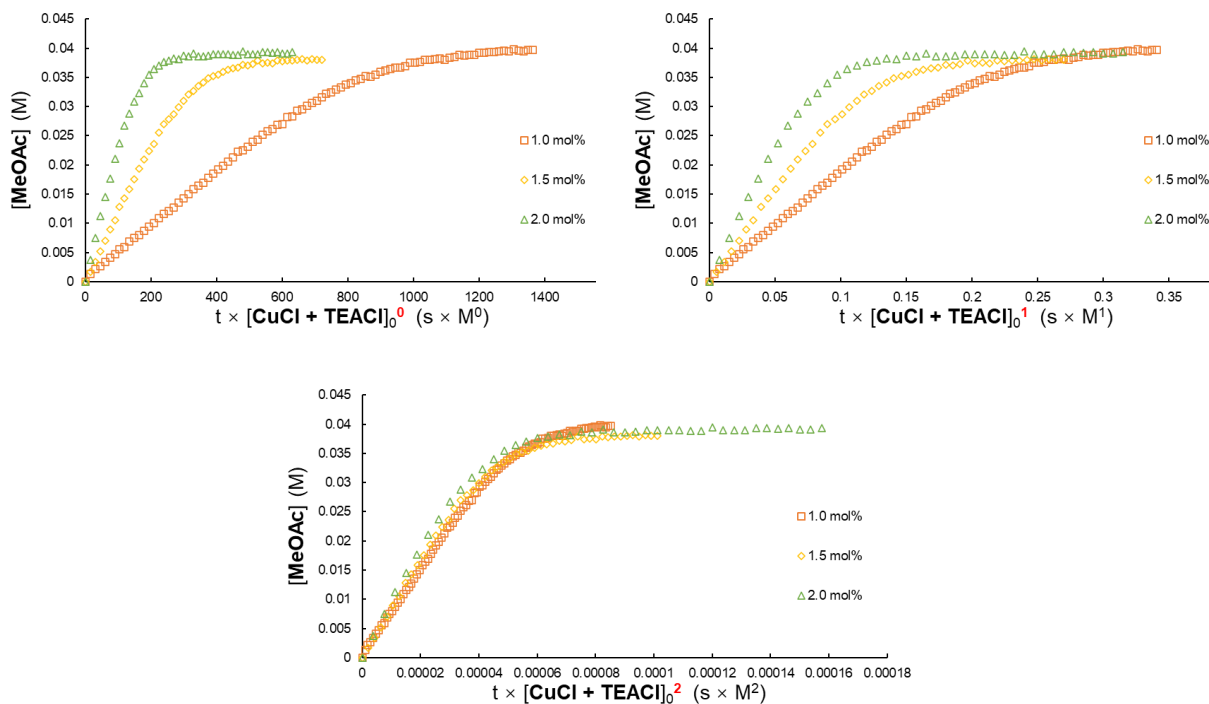


Figure 3.19 VTNA to determine the reaction order of (CuCl + Et₄NCl) (from 1.0 to 2.0 mol %) on MeOAc generation using 0.5 mol % of [(Phen)₂Cu]BF₄.



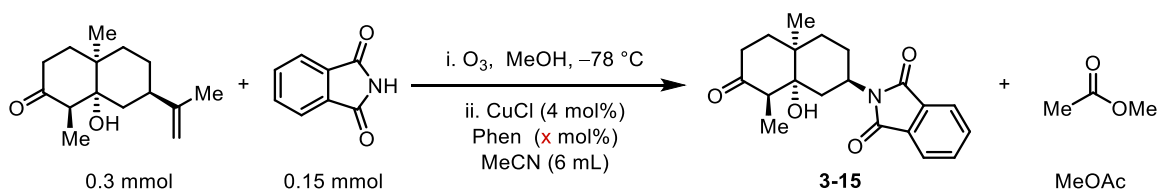
Summary of Section 3.6.6: After obtaining the kinetic data for [(Phen)₂Cu]⁺, we conducted a kinetic study for [CuCl₂]⁻. We used a 1:1 mixture of (CuCl + Et₄NCl) to mimic a [CuCl₂]⁻ species. In the preliminary kinetic study of (CuCl + Et₄NCl), we chose concentrations ranging from 2.0 to 4.0 mol % in the presence of 2.0 mol % [(Phen)₂Cu]BF₄ because the kinetics would change significantly if the concentration of [(Phen)₂Cu]BF₄ were higher than that of (CuCl + Et₄NCl).

The rates of **3-15** and MeOAc generation both became slow upon decreasing the concentration of (CuCl + Et₄NCl) from 4.0 to 2.0 mol % (Figs. 3.16 and 3.17, top left). The **3-15** generation traces overlapped the best when applying an order of 1.3 (Fig. 3.16, bottom left). The MeOAc generation traces overlapped similarly when applying an order of either 1 or 1.3 (Fig. 3.17, second row). We

carefully compared each chart and found that the trace for 2.0 mol % was slightly above all of the others. This trace was obtained from the set of experiments conducted in Section 3.6.5. We reasoned that the concentration of each solution made in Section 3.6.6 might have been slightly different, so we removed the 2.0 mol % (Fig. 3.17, third row) and used a line graph instead of a scatter plot (Fig. 3.17, bottom row). The MeOAc generation traces overlapped best when applying an order of 1.3 (Fig. 3.17, bottom right). Thus, the rate of **3-15** and MeOAc generation were both 1.3-order-dependent on (CuCl + Et₄NCl) when [(Phen)₂Cu]⁺ exhibited saturation kinetics (from 0.5 to 2.0 mol %).

Because the kinetic behavior of [(Phen)₂Cu]⁺ was roughly divided into two parts (Section 3.6.5), next we set up kinetic experiments for [CuCl₂]⁻ species in the first-order region of [(Phen)₂Cu]⁺ (0.1 to 0.5 mol %). The concentration of [(Phen)₂Cu]BF₄ was selected to be 0.5 mol % because a further decrease in its concentration led to a low yield of **3-15** and a low absorbance. The rates of **3-15** and MeOAc generation both decreased dramatically upon decreasing the concentration of (CuCl + Et₄NCl) from 2 to 1 mol % (Figs. 3.18 and 3.19, top left). The traces of **3-15** and MeOAc generation both overlapped best when applying a second order (Figs. 3.18 and 3.19, bottom). Therefore, the rate of **3-15** and MeOAc generation were both second-order-dependent on (CuCl + Et₄NCl) in the presence of a limited amount of [(Phen)₂Cu]⁺, at which point it exhibits first-order kinetics for the C–N coupling step (from 0.1 to 0.5 mol %).

3.6.7. Determination of the reaction order of phenanthroline



Preparation of the solutions:

- A. Phthalimide solution (0.05 M):** A 50-mL round-bottom flask was charged with phthalimide (221 mg, 1.50 mmol). The flask was capped with a Telfon tape–twined stopper and further sealed with Parafilm wrapping around the joints. The flask was purged with argon three times before degassed MeCN (30 mL) was added. The flask was shaken gently until the entire white solid had dissolved.
- B. Copper(I) chloride solution (0.015 M):** A 50-mL round-bottom flask was charged with copper(I) chloride (29.7 mg, 0.300 mmol). The flask was capped with a Telfon tape–twined stopper and further sealed with Parafilm wrapping around the joints. The flask was purged with argon three times before degassed MeCN (20 mL) was added. The flask was shaken gently until the entire white solid had dissolved.
- C. Phenanthroline solution (0.0075 M):** A 50-mL round-bottom flask was charged with phenanthroline (27.1 mg, 0.150 mmol). The flask was capped with a Telfon tape–twined stopper and further sealed with Parafilm wrapping around the joints. The flask was purged with argon three times before degassed MeCN (20 mL) was added. The flask was shaken gently until the entire white solid had dissolved.
- D. Peroxide solution (0.3 M):** A 50-mL round-bottom flask equipped with a magnetic stirrer bar was charged with the alkene (319 mmol, 1.35 mmol) and MeOH (30 mL, 0.045 M) and then it was cooled to $-78\text{ }^{\circ}\text{C}$ in a dry-ice/acetone bath with two 250-mL waste gas traps equipped with 20 wt% aqueous KI (200 mL). Ozone was bubbled through the solution until complete consumption of the starting material had occurred (as indicated by TLC and/or a blue color in the reaction mixture). The solution was sparged with argon for 5 min to expel excess ozone and then the mixture was warmed to room temperature and the MeOH evaporated *in vacuo*. The residue was dissolved in benzene (15 mL) followed by concentration *in vacuo* to remove

adventitious water; this step was repeated one more time. The flask was capped with a Telfon tape–twined stopper and further sealed with Parafilm wrapping around the joints. The flask was purged with argon three times before degassed MeCN (usually *ca.* 4.2 mL) was added to make a solution having a total volume of 4.5 mL.

The phthalimide solution, phenanthroline solution, degassed MeCN, CuCl solution, and peroxide solution were added into a three-neck round-bottom flask sequentially. Volumes are indicated in the Table below.

Experiemts	Phthalimide (mL)	Phenanthroline (mL)	MeCN (mL)	CuCl (mL)	Peroxide (mL)
2.0 mol% Phen	3.0	0.4	1.2	0.4	1.0
2.5 mol% Phen	3.0	0.5	1.1	0.4	1.0
3.0 mol% Phen	3.0	0.6	1.2	0.4	1.0
3.5 mol% Phen	3.0	0.7	0.9	0.4	1.0
4.5 mol% Phen	3.0	0.9	0.7	0.4	1.0
5.0 mol% Phen	3.0	1.0	0.6	0.4	1.0
6.0 mol% Phen	3.0	1.2	0.4	0.4	1.0
7.0 mol% Phen	3.0	1.4	0.2	0.4	1.0
8.0 mol% Phen	3.0	1.6	0	0.4	1.0

Figure 3.20 VTNA to determine the reaction order of phenanthroline (from 2.0 to 4.0 mol %) on 3-15 generation using 4.0 mol % of CuCl.

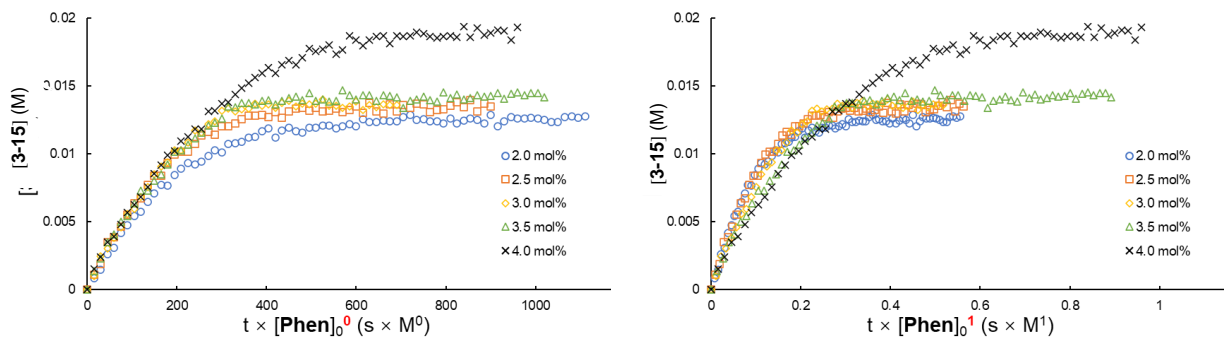


Figure 3.21 VTNA to determine the reaction order of phenanthroline (from 2.0 to 4.0 mol %) on MeOAc generation using 4.0 mol % of CuCl.

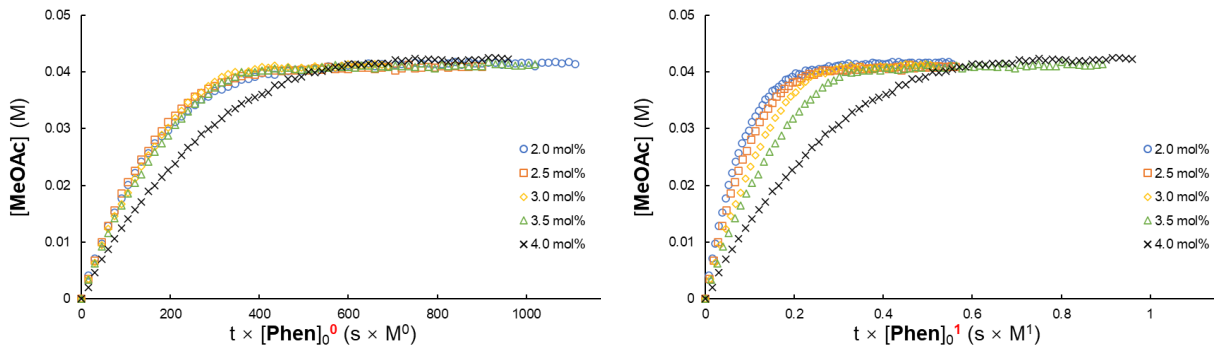
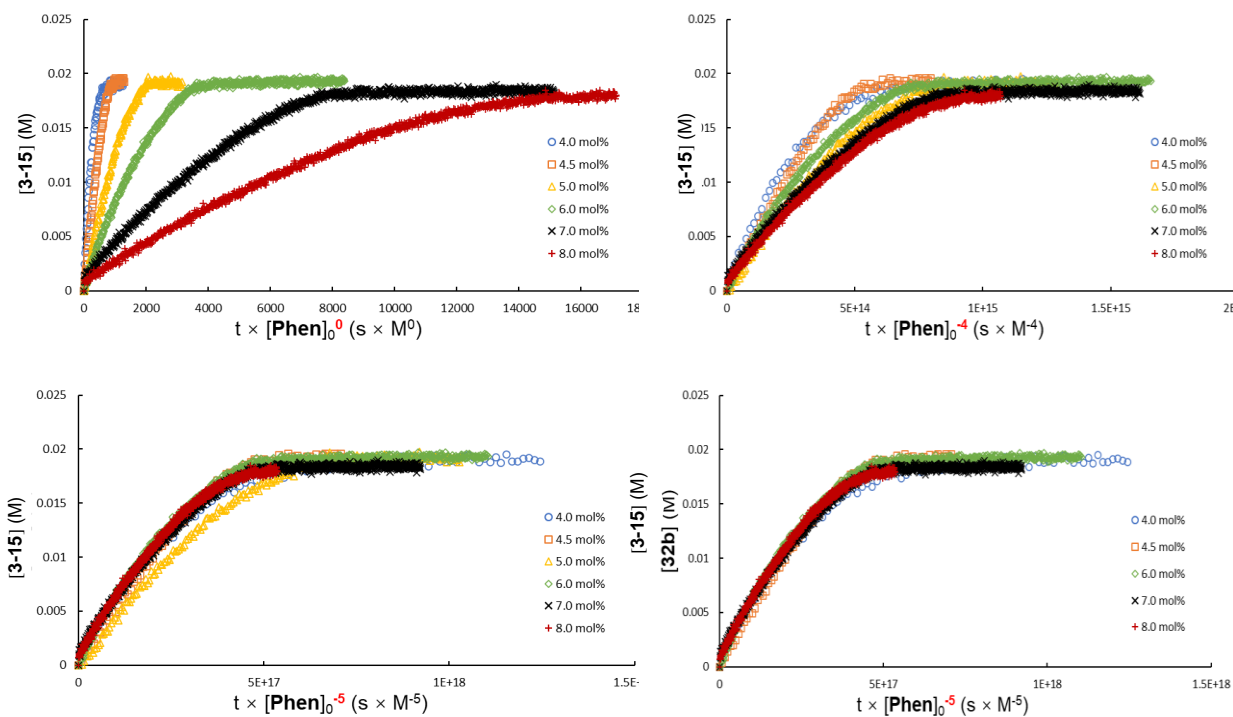


Figure 3.22 VTNA to determine the reaction order of phenanthroline (from 4.0 to 8.0 mol %) on 3-15 generation using 4.0 mol % of CuCl.



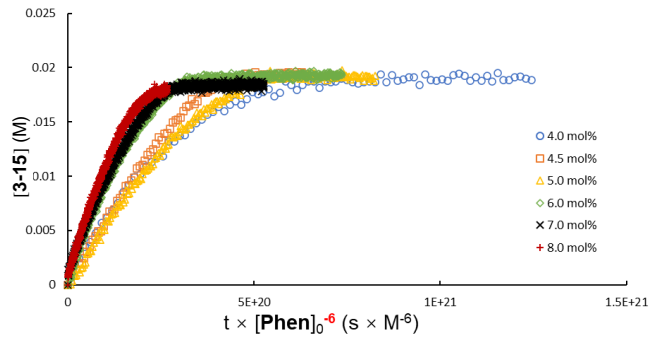
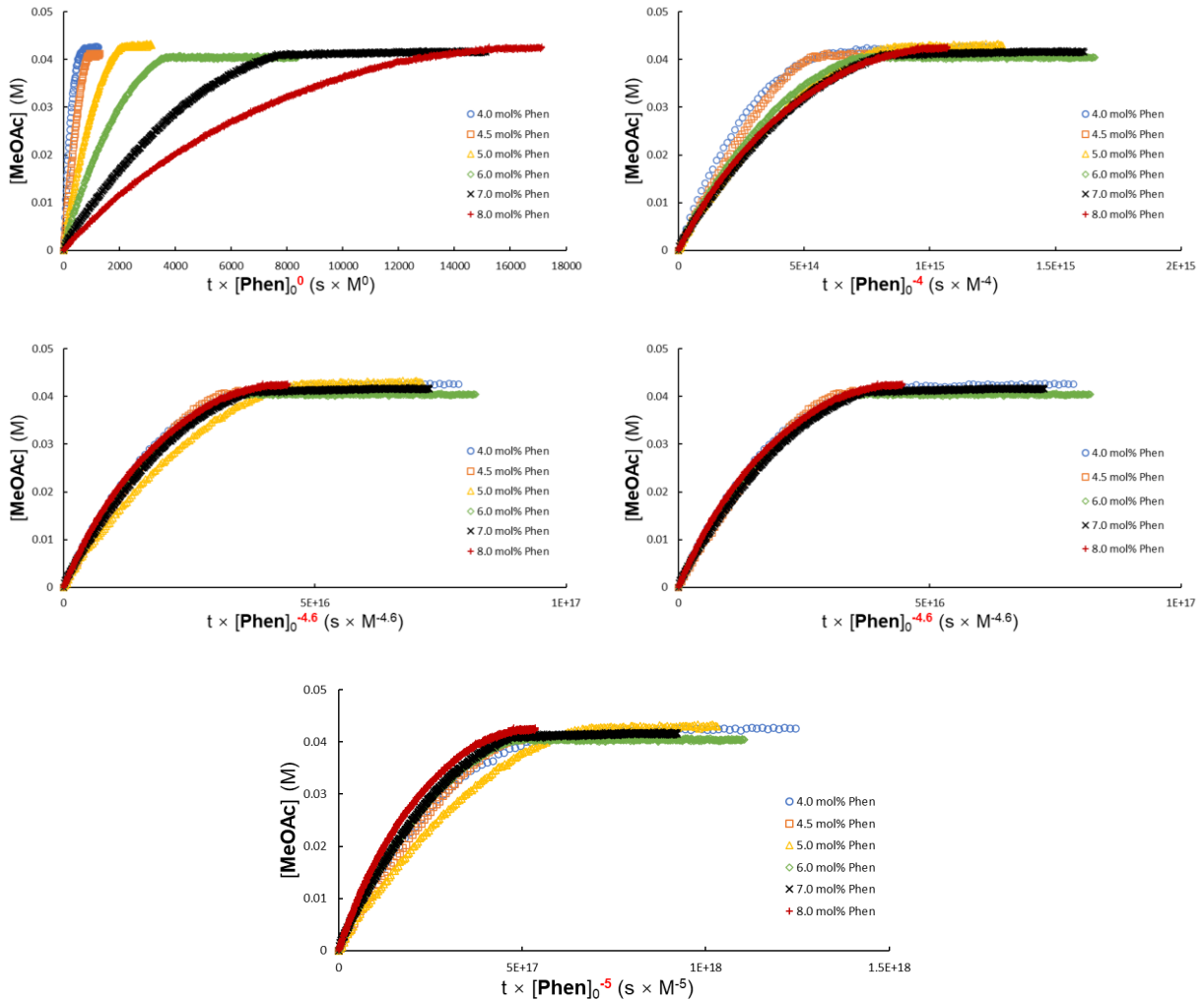


Figure 3.23 VTNA to determine the reaction order of phenanthroline (from 4.0 to 8.0 mol %) on MeOAc generation using 4.0 mol % of CuCl.

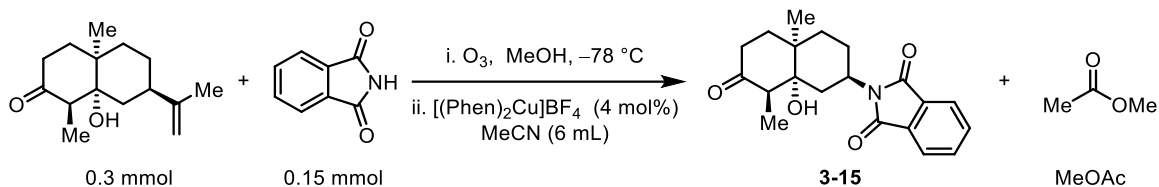


Summary of Section 3.6.7: We also studied the kinetics of phenanthroline as supplementary kinetic experiments. The idea was that a ratio of Phen:CuCl of less than 1:1 might generate a lower amount of $[\text{CuCl}_2]^-$, and the resulting excess CuCl could react with $[\text{CuCl}_2]^-$ to form a cluster $[\text{Cu}_x\text{Cl}_y]^{x-y}$. Indeed, when using 4 mol % of CuCl, although the yield of the coupling product **3-15** decreased upon decreasing the amount of phenanthroline from 4.0 to 2.0 mol %, the rates of **3-15** formation remained similar. VTNA analysis revealed the best fit when applying an order of zero (Fig. 3.20). The MeOAc generation traces also overlapped the best when applying an order of zero (Fig. 3.21). Therefore, the rates of **3-15** and MeOAc generation were both zero-order-dependent on phenanthroline (from 2.0 to 4.0 mol %).

Because we observed a dramatic decrease in the reaction rate when the concentration of $[(\text{Phen})_2\text{Cu}]^+$ was higher than that of $[\text{CuCl}_2]^-$ (Section 3.6.5), we also monitored the reactions under conditions in which a greater mole-percentage of phenanthroline (to CuCl) was present.

Indeed, we observed that the rates of **3-15** and MeOAc generation both decreased dramatically when the amount of Phen ranged from 4.0 to 8.0 mol % in the presence of 4.0 mol % of CuCl (Figs. 3.22 and 3.23, top left), although the overall yields remained almost identical. The trails of **3-15** and MeOAc generation overlapped the best when applying orders of -5 and -4.6 , respectively (Figs. 3.22 and 3.23, second row). We suspect an error might have occurred during the experiment performed using 5 mol % of Phen, because its trace deviated from the others (Fig. 3.23, middle left). We removed this trace and found that the other traces fit well. Therefore, the rates of **3-15** and MeOAc generation displayed -5 - and -4.6 -order-dependence on Phen, respectively (from 4.0 to 8.0 mol %) in the presence of 4.0 mol % of CuCl.

3.6.8. Effect of chloride



Preparation of the solutions:

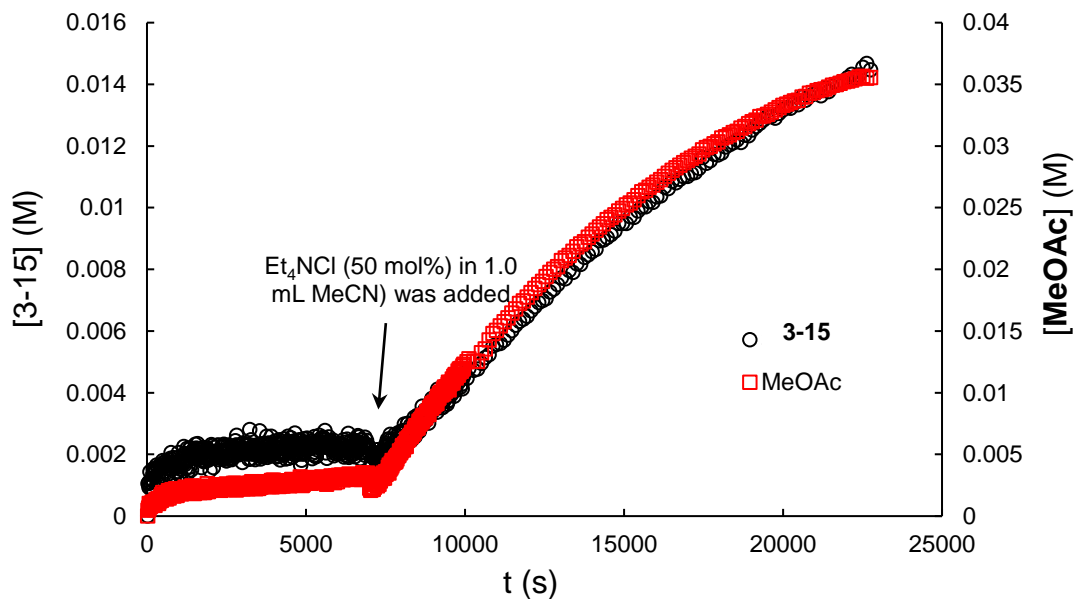
- A. Phthalimide solution (0.05 M):** A 50-mL round-bottom flask was charged with phthalimide (221 mg, 1.50 mmol). The flask was capped with a Teflon tape–twined stopper and further sealed with Parafilm wrapping around the joints. The flask was purged with argon three times before degassed MeCN (30 mL) was added. The flask was shaken gently until the entire white solid had dissolved.
- B. Et₄NCl solution (0.075 M):** A 50-mL round-bottom flask was charged with phthalimide (37.3 mg, 0.225 mmol) in a glove box. The flask was capped with a Teflon tape–twined stopper, removed from the glove box, and sealed with Parafilm wrapping around the joints. Degassed MeCN (3 mL) was then added. The flask was shaken gently until the entire white solid had dissolved.
- C. [(Phen)₂Cu]BF₄ solution (3.75 mM):** A 50-mL round-bottom flask was charged with [(Phen)₂Cu]BF₄ (19.2 mg, 0.0375 mmol). The flask was capped with a Teflon tape–twined stopper and further sealed with Parafilm wrapping around the joints. The flask was purged with argon three times before degassed MeCN (10 mL) was added. The flask was shaken gently until the entire dark-red solid had dissolved.
- D. Peroxide solution (0.3 M):** A 50-mL round-bottom flask equipped with a magnetic stirrer bar was charged with the alkene (319 mmol, 1.35 mmol) and MeOH (30 mL, 0.045 M) and then it was cooled to -78 °C in a dry-ice/acetone bath with two 250-mL waste gas traps equipped with 20 wt% aqueous KI (200 mL). Ozone was bubbled through the solution until complete

consumption of the starting material had occurred (as indicated by TLC and/or a blue color in the reaction mixture). The solution was sparged with argon for 5 min to expel excess ozone and then the mixture was warmed to room temperature and the MeOH evaporated *in vacuo*. The residue was dissolved in benzene (15 mL) followed by concentration *in vacuo* to remove adventitious water; this step was repeated one more time. The flask was capped with a Telfon tape-twined stopper and further sealed with Parafilm wrapping around the joints. The flask was purged with argon three times before degassed MeCN (usually *ca.* 4.2 mL) was added to give a solution having a total volume of 4.5 mL.

The phthalimide solution, phenanthroline solution, degassed MeCN, CuCl solution, and peroxide solution were added into a three-neck round-bottom flask sequentially. Volumes are indicated in the Table below.

Phthalimide (mL)	Complex 3-5 (mL)	MeCN (mL)	Peroxide (mL)	Et ₄ NCl (mL)
3.0	1.6	0.4	1.0	1.0

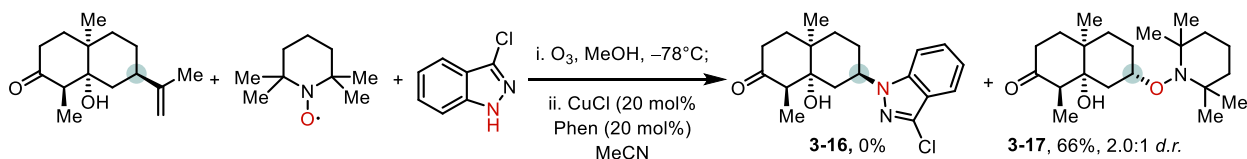
Figure 3.24 Reaction profile using 4.0 mol % of complex 3-5 in the absence and presence of



chloride anions.

Summary of Section 3.6.8: The reaction was sluggish in the absence of chloride, with **3-15** and MeOAc both being generated slowly (Fig. 3.24). Less than 5% of the product was obtained when employing $[(\text{Phen})_2\text{Cu}]\text{BF}_4$ alone as the catalyst (Section 3.4). After 7000 s, 50 mol % of Et_4NCl in 1 mL of MeCN (0.075 mmol) was added and the reaction began to progress slowly, generating both **3-15** and MeOAc. This experiment confirmed the essential role of $[\text{CuCl}_2\text{L}]$ in the reaction (*vide infra*).

3.7. TEMPO Trap Experiment



An oven-dried 25-mL round-bottom flask equipped with a magnetic stirrer bar was charged with 3-chloro-1*H*-indazole (30.5 mg, 0.200 mmol, 1.0 equiv), copper(I) chloride (4.00 mg, 0.0400 mmol, 20 mol %), and 1,10-phenanthroline (7.20 mg, 0.0400 mmol, 20 mol %). The flask was purged with argon three times before dry MeCN (2 mL) was added. This mixture was stirred at room temperature for 10 min to form a deep-red solution.

Another 25-mL round-bottom flask equipped with a magnetic stirrer bar was charged with alkene (94.6 mg, 0.400 mmol, 2.0 equiv) and MeOH (10 mL) and then it was cooled to $-78\text{ }^{\circ}\text{C}$ in a dry-ice/acetone bath with two 250-mL waste gas traps equipped with 20 wt% aqueous KI (200 mL). Ozone was bubbled through the solution until complete consumption of the starting material had occurred (as indicated by TLC and/or a blue color in the reaction mixture). The solution was sparged with argon for 5 min to expel excess ozone and then the mixture was warmed to room temperature and the MeOH evaporated *in vacuo*. The residue was dissolved in benzene (10 mL) followed by concentration *in vacuo* to remove adventitious water. The residue was dissolved in MeCN (2 mL). TEMPO (31.2 mg, 0.200 mmol, 1.0 equiv) was added to this hydroperoxide solution, which was then transferred into the copper mixture *via* syringe and rinsed with MeCN (2 \times 0.5 mL). The reaction vessel was stirred at room temperature for 1 h. The mixture was concentrated *in vacuo*. The residue was passed through a column of silica gel. 10% EtOAc in hexanes was used initially as the eluent to remove TEMPO, then 100% EtOAc was used to wash the column. 1-Chloro-2,4-dinitrobenzene (40.5 mg, 0.200 mmol, 1.0 equiv) was added as an internal standard and then the sample was concentrated *in vacuo*. The crude materials were analyzed using NMR spectroscopy.

Summary of TEMPO trap experiment: Formation of the TEMPO-trap product **3-17** indicated that the alkyl radical was generated after the C–C scission. Interestingly, the TEMPO-trap product was obtained in 66% (NMR) yield when using only 20 mol % of the catalyst. The greater than 20 mol % yield of the TEMPO adduct points to certain alternative pathways for the reduction of Cu(II) species to Cu(I), and supports our proposed mechanism in which the peroxide (and alkyl radical) plays a role in the reduction of Cu(II) to Cu(I) complexes (*vide infra*).

3.8. Mechanistic Discussion

3.8.1. Discussion of the mechanism

All of the elementary reaction steps that occur during the copper-catalyzed aminodealkenylation process are preceded in the literature, and we illustrate the rate constants of each individual step in Fig. 3.25. A 1:1 mixture of CuCl and Phen is known to afford the ion pair $[(\text{Phen})_2\text{Cu}]^+[\text{CuCl}_2]^-$ in MeCN. The anionic complex **3-6** and the cationic complex **3-8** are both highly active at reducing peroxide ($k = ca. 4 \times 10^3 \text{ M}^{-1} \text{ s}^{-1}$)^{4,5}. When compared, however, with other steps, including ligand exchange [$(10^4$ to 10^7 for Cu(I) and 10^6 to 10^9 for Cu(II)]^{17–24}, N–H deprotonation ($1.6 \times 10^6 \text{ M}^{-1} \text{ s}^{-1}$)²⁵, β -scission of alkoxy radical **E** ($6.2 \times 10^8 \text{ s}^{-1}$)²⁶, alkyl radical addition to Cu(II) (10^6 to $10^8 \text{ M}^{-1} \text{ s}^{-1}$)^{27–29}, C(sp³)–N bond formation [we could not find such kinetic data, but the activation energy (ΔG) of this step has been calculated (DFT) to be $0.2 \text{ kcal mol}^{-1}$, indicating that it is very fast]³⁰, and electron transfer between copper complexes (10^5 to $10^8 \text{ M}^{-1} \text{ s}^{-1}$)^{31–34}, the reduction of peroxide is the slowest step. If so, the reaction rate should exhibit a first-order dependence on the peroxide concentration. In contrast, the reaction displayed a pseudo-zero-order dependence on peroxide, as well as on phthalimide (Sections 3.6.3 and 3.6.4), and a 1.3 order on catalyst (CuCl + Phen). These results indicate a complicated mechanistic scenario in which the catalyst exists in an off-cycle resting state. Indeed, we found that the color of the reaction changed from dark-red to

light-yellow immediately after the addition of peroxide to the mixture of CuCl, Phen, and phthalimide in MeCN (Fig. 3.26, A). The cationic complex $[(\text{Phen})_2\text{Cu}]^+$ displays a dark-red color and CuCl_2 is bright yellow. Therefore, the change in the reaction color from dark-red to light-yellow, we surmise, is due to the oxidation of both $[(\text{Phen})_2\text{Cu}]^+$ and $[\text{CuCl}_2]^-$ to $[(\text{Phen})_2\text{CuL}]^{2+}$ and CuCl_2 , respectively. As seen for reaction B in Fig. 3.26, $\text{Et}_4\text{N}^+[\text{CuCl}_2]^-$ is colorless and CuCl_2 is yellow, while $[(\text{Phen})_2\text{Cu}]^+$ is dark-red and $[(\text{Phen})_2\text{CuL}]^{2+}$ is pale-blue (reaction C). While the Cu(II) complex **3-7**, along with a hydroxide anion (ligand) generated during the SET, can be reduced back to the Cu(I) species **3-6** readily by an oxidizing alkyl radical **B** or the peroxide **A** (Fig. 3.25, eqs. 1 and 2)^{3,32}, the reduction of coordinatively saturated $[(\text{Phen})_2\text{CuL}]^{2+}$ (**3-9**) is sluggish, as evidenced by our experiments described in Section 3.6.8 (Fig. 3.25, eq. 3).

From the data provided in Sections 3.4–3.7, we propose a type of $[\text{CuCl}_2]^-$ – $[(\text{Phen})_2\text{Cu}]^+$ cooperative catalysis (Fig. 3.25, bottom). The cationic Cu(I) complex **3-8** is oxidized by the peroxide **A** to afford a copper(II) complex **3-9**. Deprotonated phthalimide associates with the complex **3-9**, followed by Phen dissociation, to afford the imido complex **3-10** (see Fig. 3.30 for details). SET between the complex **3-6** and the peroxide **A** affords the alkoxy radical **E**, which undergoes β -scission to generate the alkyl radical **B**. The complex **3-10** traps the alkyl radical **B** to afford the C–N coupling product and the copper(I) complex **3-13** through either an outer (**3-11**) or inner (**3-12**) sphere pathway¹¹. The coordinatively unsaturated Cu(I) complex **3-13** undergoes ligand exchange with a bidentate ligand (Phen) and dissociates from the monodentate ligand L to afford **3-8**. Subsequent electron transfer between **3-7** and **3-8** regenerates **3-6** and **3-9**, completing a catalytic cycle.

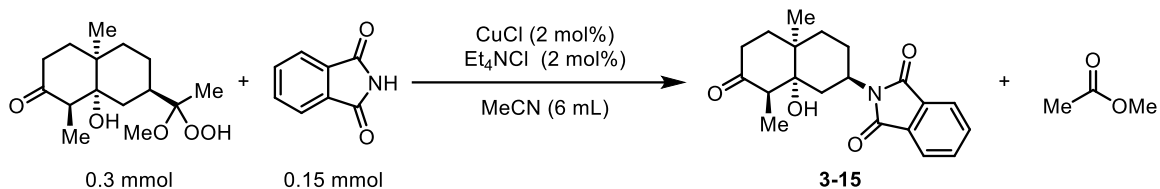


Reaction mixture before adding peroxide



Reaction mixture after adding peroxide

B.

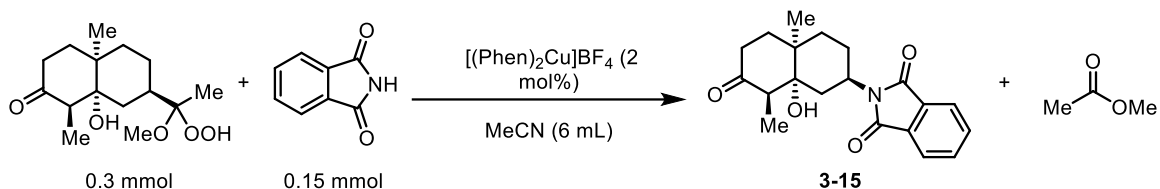


Reaction mixture before adding peroxide



Reaction mixture after adding peroxide

C.



Reaction mixture before adding peroxide

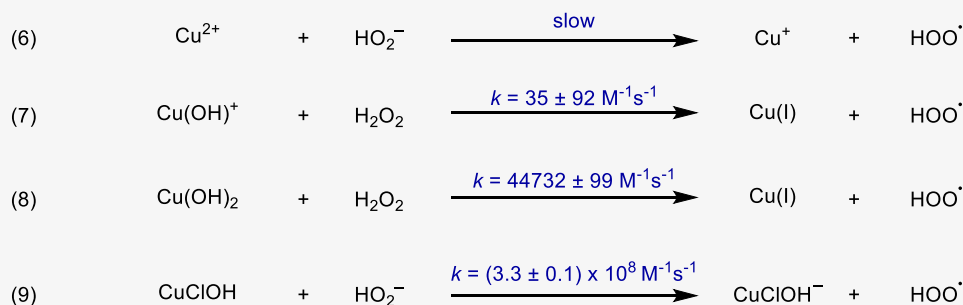
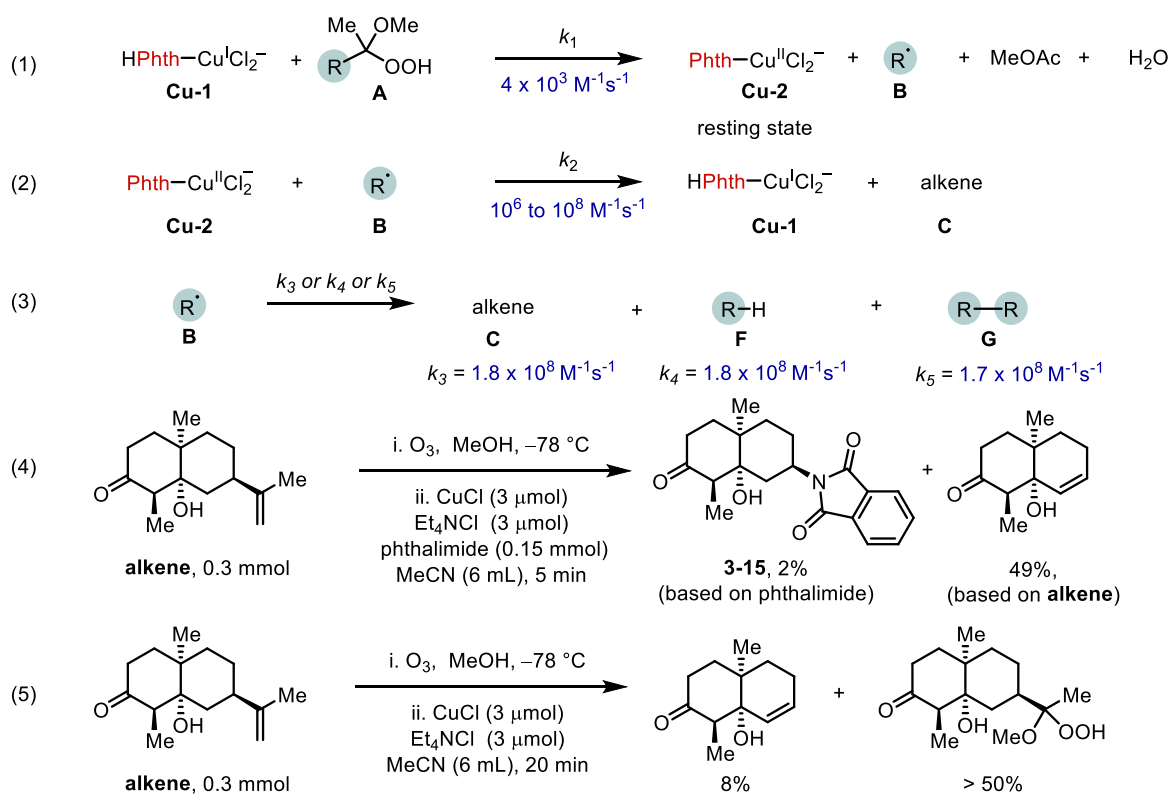


Reaction mixture after adding peroxide

To explain the reaction order of each component of our aminodealkenylation reaction, we established a kinetic model for the copper dichloride–catalyzed peroxide decomposition reaction. Fig. 3.27 delineates more details regarding this process. According to UV–Vis spectral measurements, phthalimide and [CuCl₂][−] form a complex **Cu-1** (Fig. 3.4). The oxidation of **Cu-1**

by the peroxide **A** will afford **Cu-2**, water, and the alkoxy radical **E**, which will generate the alkyl

Figure 3.27 Redox processes between copper dichloride species and peroxides



radical **B** and MeOAc (Fig. 3.27, eq. 1). The deprotonation, ligand addition, and β -scission steps are all much faster than the oxidation step, so we can combine all of these events in one. Although **Cu-2** can be reduced back to **Cu-1** by oxidizing the alkyl radical **B** (Fig. 3.27, eq. 2), not all of **B** will react with **Cu-2** because the radical decomposition processes (the disproportionation to the alkene **C** and the alkane **F**, and the dimerization to **G**) are also very fast ($k_3 \cong k_4 \cong k_5 > 10^8 \text{ M}^{-1}$

s⁻¹, Fig. 3.27, eq. 3)³⁵, as have been discussed in Section 2.6.3. As a result, after a few cycles, all of **Cu-1** will have been oxidized to **Cu-2**. According to the experiments in Section 3.6.5, however, [CuCl₂]⁻ alone can catalyze the decomposition of the peroxide, generating MeOAc in 80% yield (Fig. 3.15, left) and the alkene **C** in 49% yield (Fig. 3.27, eq. 4). (*Note: When the reaction was complete, the concentration of MeOAc was 0.04 M. The concentration of 3-14 was 0.05 M at the onset of the reaction.*) These results demonstrate not only that not all of the alkyl radical was oxidized by **Cu-2** but also that **Cu-2** uses other components in the reaction mixture for its reduction back to **Cu-1**. In fact, the reaction in eq. 4, run in the absence of phthalimide, produced an 8% yield of the alkene with recovery of >50% of the peroxide (*Note: This result was obtained using NMR spectroscopy. Because we needed to work up the reaction, remove the copper salts, concentrate the mixture, and wait to use the NMR spectrometer, as described in Section 3.6, the peroxide decomposed somewhat during the operation. The NMR spectral yield would, therefore, be lower than the actual value.*), indicating that phthalimide served as a crucial ligand in the copper turnover process. Hydroperoxide is known as a moderate reductant that can be oxidized and converted to peroxy radical^{3,32}. According to the literature^{3,32}, Cu(II) species bearing two bases are much more efficient in oxidizing peroxide to generate Cu(I) and peroxy radical (Fig. 3.27, eqs. 6–9). We envision that such a redox process (between copper species bearing two bases and peroxide) should also occur in our aminodealkenylation reaction, and that it would be a crucial pathway for the catalytic decomposition of the peroxide **A**. We surmise that the **Cu-2** complex bearing one base is an inefficient oxidant of the peroxide. Ligand exchange between two **Cu-2** species will generate the doubly-base-chelated-copper(II) complex **Cu-3** and the copper(II) trichloride **Cu-4** (Fig. 3.28, eq. 1). **Cu-3** would be active for oxidizing the peroxide **A** and affording the copper(I) complex **Cu-5**, phthalimide, and the peroxy radical **D** (Fig. 3.28, eq. 2). SET from

Cu-5 to **A** would afford **Cu-6**, the alkyl radical **B**, and MeOAc, in what we believe would be the slowest step. Deprotonation and ligand exchange among **Cu-6**, **Cu-4**, and phthalimide would regenerate two molecules of **Cu-2** species and water. Radical–radical coupling between **B** and **D** would afford the peroxide **H**. We observed evidence for the presence of the peroxide **H** in mass spectra when using (CuCl + Phen) or (CuCl + TEACl) as the catalyst for the reaction (Fig. 3.29).

Figure 3.28 Copper dichloride–catalyzed decomposition of the peroxide

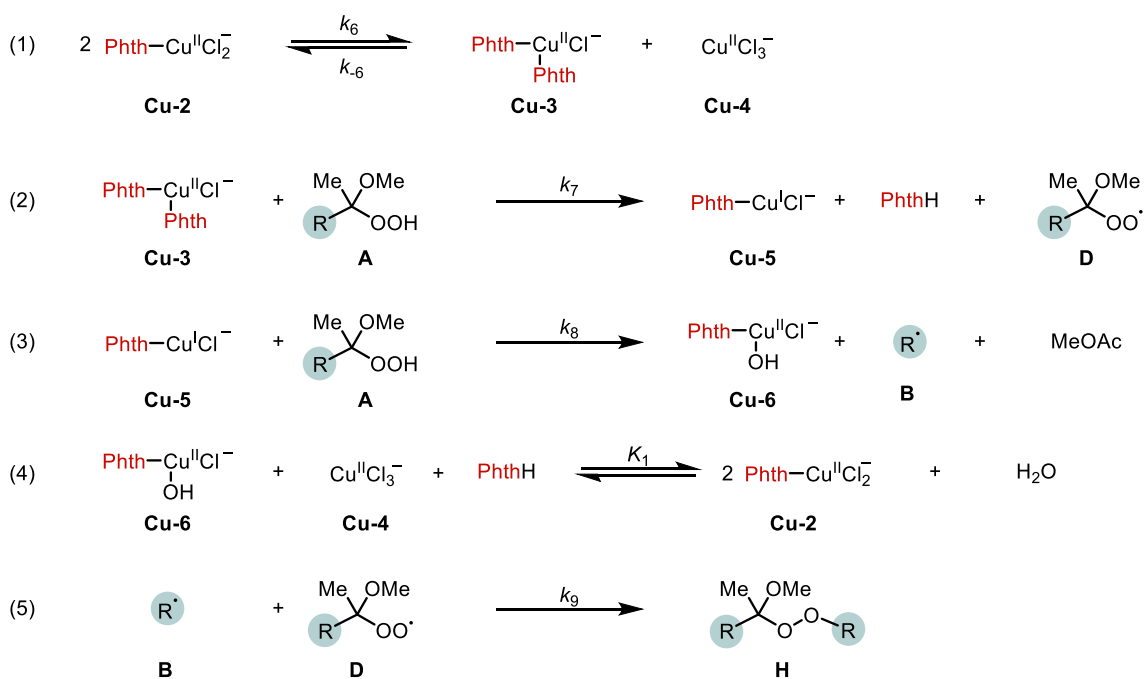
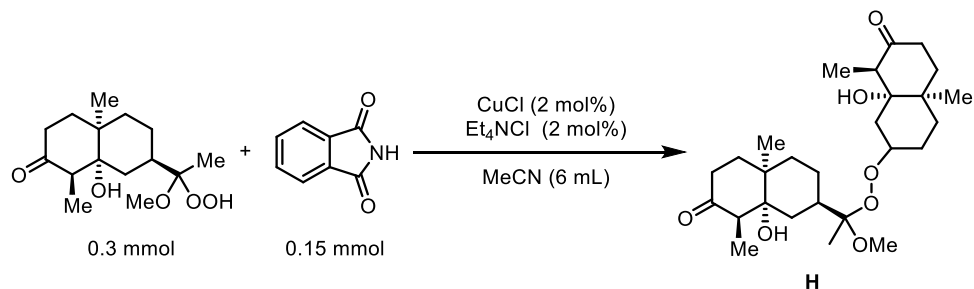
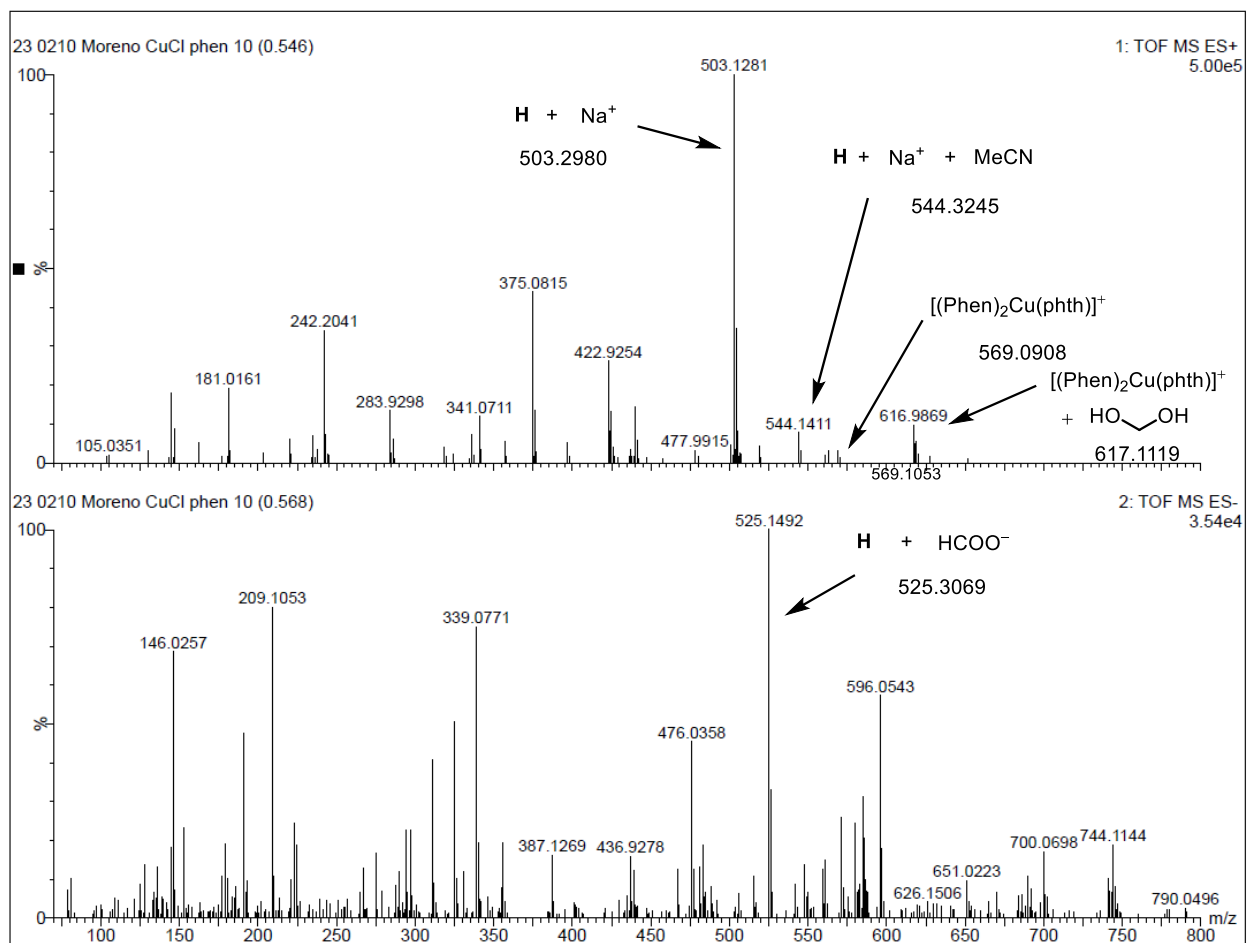
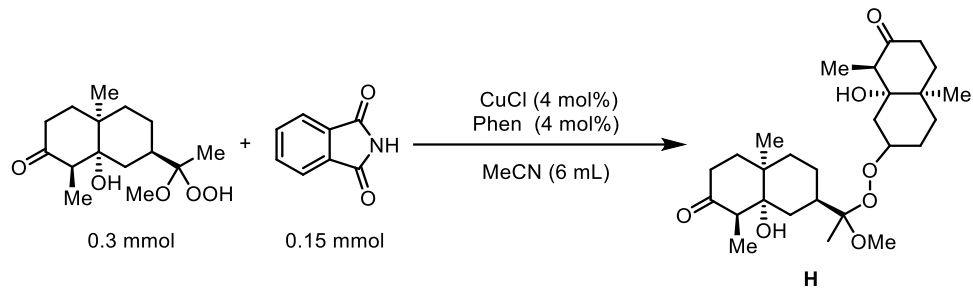
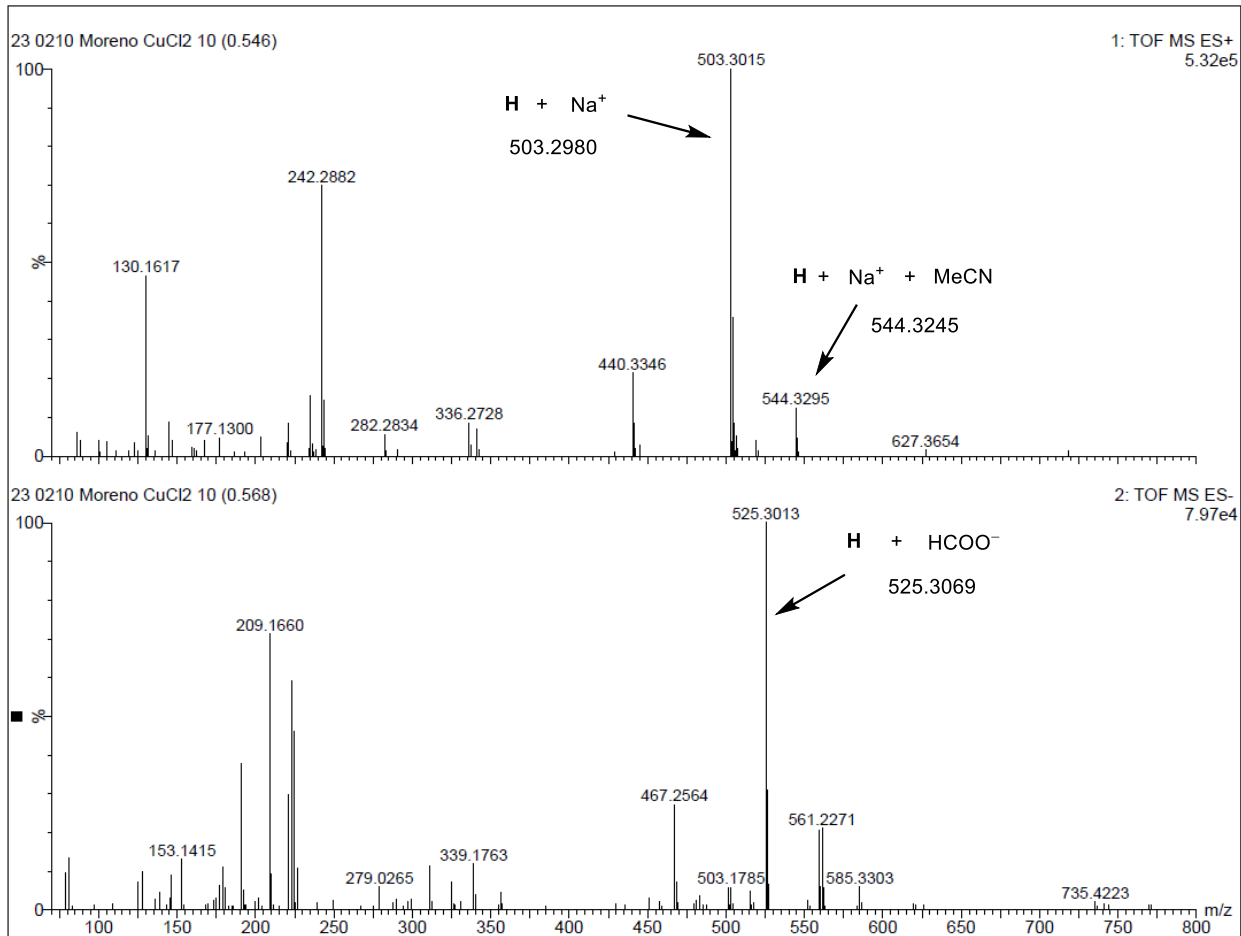


Figure 3.29 Mass spectral (MS) evidence for the generation of the





3.8.2. Rate law derivation and explanation of the reaction orders obtained in Section 3.6

With the said reactions in mind involving the copper dichloride species displayed in Fig. 3.28, we derived the rate law for the generation of MeOAc. Because **Cu-3** is highly reactive in the presence of peroxide, we applied the steady state approximation on **[Cu-3]**:

$$\frac{d[\text{Cu-3}]}{dt} = 0$$

$$k_6[\text{Cu-2}]^2 = k_{-6}[\text{Cu-3}][\text{Cu-4}] + k_7[\text{Cu-3}][\text{A}]$$

eq. 1

$$[\text{Cu-3}] = \frac{k_6[\text{Cu-2}]^2}{k_{-6}[\text{Cu-4}] + k_7[\text{A}]}$$

We also assume that the copper(I) species is not stable in the presence of the peroxide, so we apply the steady state approximation on **Cu-5**:

$$\frac{d[\mathbf{Cu-5}]}{dt} = 0$$

$$k_8[\mathbf{Cu-5}][\mathbf{A}] = k_7[\mathbf{Cu-3}][\mathbf{A}]$$

The formation of MeOAc can be described as

eq. 2

$$\frac{d[\mathbf{MeOAc}]}{dt} = k_8[\mathbf{Cu-5}][\mathbf{A}] = k_7[\mathbf{Cu-3}][\mathbf{A}]$$

Displacing [**Cu-3**] in **eq. 2** and using **eq. 1** affords

eq. 3

$$\frac{d[\mathbf{MeOAc}]}{dt} = \frac{k_6 k_7 [\mathbf{Cu-2}]^2 [\mathbf{A}]}{k_{-6} [\mathbf{Cu-4}] + k_7 [\mathbf{A}]}$$

The alkyl radical **B** is a reactive intermediate that can participate in several transformations (Fig. 3.30, *vide infra*). As discussed above (Fig. 3.27, eq. 2), **Cu-2** can trap **B** to generate the alkene **C** and **Cu-1**. Radical–radical disproportionation will generate the alkene **C** and the alkane **F** (Fig. 3.30, eq. 2). The alkyl radical can also abstract a hydrogen atom to afford another relatively stable radical **J** and the alkane **F** (Fig. 3.30, eq. 3). Radical–radical homocoupling will afford the dimer **G** (Fig. 3.30, eq. 4). Radical–radical coupling between **B** and **D** will afford the peroxide **H**, as discussed above. According to Figs. 3.14 and 3.24, [(Phen)₂Cu]⁺ participates in the alkyl radical trapping process to afford the C–N coupling product. We surmised that [(Phen)₂Cu]⁺ (**3-8**) will also be oxidized to the corresponding bis-phenanthroline Cu(II) species **Cu-7** in the presence of the peroxide. In the presence of phthalimide, ligand exchange will afford **Cu-8**, which we propose as the resting state of the cation moiety (evidence for **Cu-8** was found in the *in situ* mass spectrum

of the reaction, Fig. 3.29). We surmise that **Cu-8** cannot directly trap the alkyl radical **B** and that one phenanthroline ligand must dissociate from the complex **Cu-8**. The resulting mono-phenanthroline Cu(II) complex **3-10** can trap the alkyl radical and, eventually, afford the C–N coupling product **3-15** and the copper(I) species **3-13**.

Because the radical **B** is very reactive, we can apply the steady-state approximation on **[B]**:

$$\frac{d[\mathbf{B}]}{dt} = 0$$

$$k_8[\mathbf{Cu-5}][\mathbf{A}] = k_2[\mathbf{Cu-2}][\mathbf{B}] + k_3[\mathbf{B}]^2 + k_4[\mathbf{B}][\mathbf{I}] + k_5[\mathbf{B}]^2 + k_9[\mathbf{B}][\mathbf{D}] + k_{10}[\mathbf{B}][\mathbf{3-10}]$$

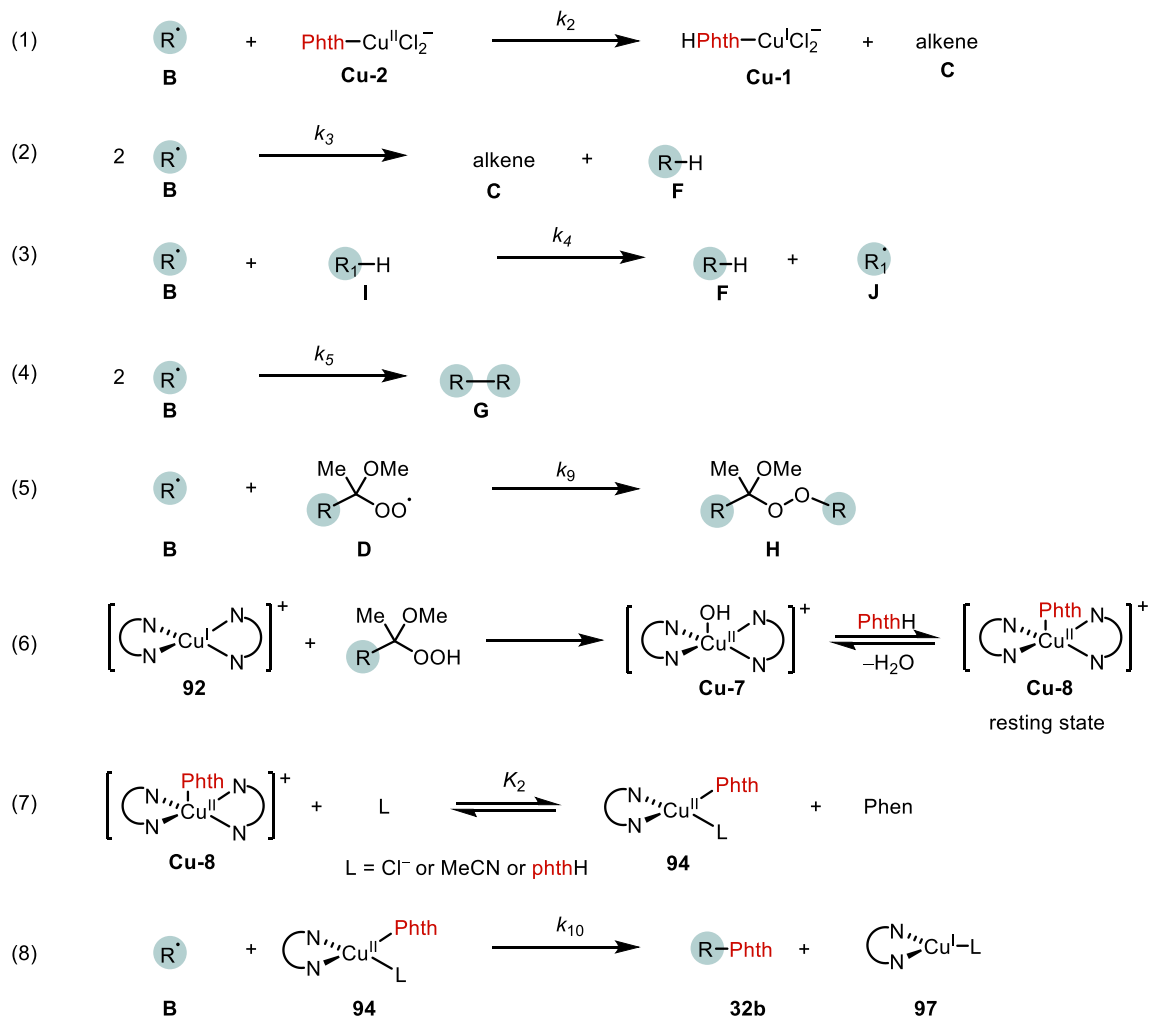
$$[\mathbf{B}] = \frac{k_8[\mathbf{Cu-5}][\mathbf{A}]}{k_2[\mathbf{Cu-2}] + k_3[\mathbf{B}] + k_4[\mathbf{I}] + k_5[\mathbf{B}] + k_9[\mathbf{D}] + k_{10}[\mathbf{3-10}]}$$

The formation of **3-15** can be described as

eq. 4

$$\frac{d[\mathbf{3-15}]}{dt} = k_{10}[\mathbf{B}][\mathbf{3-10}] = \frac{k_{10}[\mathbf{3-10}] \cdot k_8[\mathbf{Cu-5}][\mathbf{A}]}{k_2[\mathbf{Cu-2}] + k_3[\mathbf{B}] + k_4[\mathbf{I}] + k_5[\mathbf{B}] + k_9[\mathbf{D}] + k_{10}[\mathbf{3-10}]}$$

Figure 3.30 Proposed reaction pathways of the alkyl radical B



From eq. 2 and eq. 3,

$$\frac{d[\text{MeOAc}]}{dt} = k_8[\text{Cu-5}][\text{A}] = \frac{k_6 k_7 [\text{Cu-2}]^2 [\text{A}]}{k_{-6} [\text{Cu-4}] + k_7 [\text{A}]}$$

Using eq. 3 to replace $k_8[\text{Cu-5}][\text{A}]$ in eq. 4:

eq. 5

$$\frac{d[\text{3-15}]}{dt} = \frac{k_6 k_7 [\text{Cu-2}]^2 [\text{A}]}{k_{-6} [\text{Cu-4}] + k_7 [\text{A}]} \cdot \frac{k_{10} [\text{3-10}]}{k_2 [\text{Cu-2}] + k_3 [\text{B}] + k_4 [\text{I}] + k_5 [\text{B}] + k_9 [\text{D}] + k_{10} [\text{3-10}]}$$

We can see that **eq. 5** is constructed from two parts. The first part is the rate of MeOAc/radical **B** generation. The second part is the proportion of C–N bond couplings in all of the radical **B** transformations.

Because [**3-10**] cannot be measured, we substitute it with [**Cu-8**]. There is an equilibrium between **Cu-8** and **3-10** (Fig. 3.30, eq. 7):

$$[\mathbf{3-10}] = \frac{K_2[\mathbf{Cu-8}][\mathbf{L}]}{[\mathbf{Phen}]}$$

Then,

eq. 6

$$\frac{d[\mathbf{3-15}]}{dt} = \frac{k_6 k_7 [\mathbf{Cu-2}]^2 [\mathbf{A}]}{k_{-6} [\mathbf{Cu-4}] + k_7 [\mathbf{A}]} \cdot \frac{1}{(k_2 [\mathbf{Cu-2}] + k_3 [\mathbf{B}] + k_4 [\mathbf{I}] + k_5 [\mathbf{B}] + k_9 [\mathbf{D}]) [\mathbf{Phen}] + k_{10} K_2 [\mathbf{Cu-8}] [\mathbf{L}]}$$

Assuming that the concentration of the resting state of copper dichloride species can be approximated to that of the initial concentration of the copper dichloride added $\{[\mathbf{Cu-2}] \approx [(\text{CuCl} + \text{TEACl})_{\text{T}}]\}$, and that the concentration of the resting species **Cu-8** is equal to that of the initially added $[(\text{Phen})_2\text{Cu}]^+$ $\{[\mathbf{Cu-8}] \approx [\mathbf{3-5}_{\text{T}}]\}$, $(k_2 [\mathbf{Cu-2}] + k_3 [\mathbf{B}] + k_4 [\mathbf{I}] + k_5 [\mathbf{B}] + k_9 [\mathbf{D}]) [\mathbf{Phen}] = \alpha \gg k_{10} K_2 [\mathbf{Cu-8}] [\mathbf{L}]$ under the conditions of a low concentration of the complex **3-5** (0–0.5 mol % $[(\text{Phen})_2\text{Cu}]^+$ in Section 3.6.5 and 0.5 mol % $[(\text{Phen})_2\text{Cu}]^+$ in Section 3.6.6).

eq. 3 is approximated to be

$$\frac{d[\mathbf{MeOAc}]}{dt} \approx \frac{k_6 k_7 [(\text{CuCl} + \text{TEACl})_{\text{T}}]^2 [\mathbf{A}]}{k_{-6} [\mathbf{Cu-4}] + k_7 [\mathbf{A}]}$$

eq. 6 is approximated to be

$$\frac{d[\mathbf{3-15}]}{dt} \approx \frac{k_6 k_7 [(\text{CuCl} + \text{TEACl})_{\text{T}}]^2 [\mathbf{A}]}{k_{-6} [\mathbf{Cu-4}] + k_7 [\mathbf{A}]} \cdot \frac{k_{10} K_2 [\mathbf{3-5}_{\text{T}}] [\mathbf{L}]}{\alpha}$$

These equations indicate that the formation of **3-15** and MeOAc should be second-order-dependent on (CuCl + Et₄NCl), which fits with the kinetic studies provided in Figs. 3.18 and 3.19. On the other hand, while the formation of **3-15** exhibited first-order-dependence on the complex **3-5**, the formation of MeOAc was zero-order-dependent, which again fits the kinetic analysis conducted in Figs. 3.14 and 3.15.

For higher concentrations of the complex **3-5** (0.5–2.0 mol % [(Phen)₂Cu]⁺ in Section 3.6.5; 2.0 mol % [(Phen)₂Cu]⁺ in Section 3.6.6), we assume $\alpha \ll k_{10} K_2 [\mathbf{Cu-8}] [\mathbf{L}]$:

eq. 7

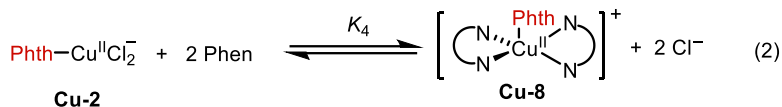
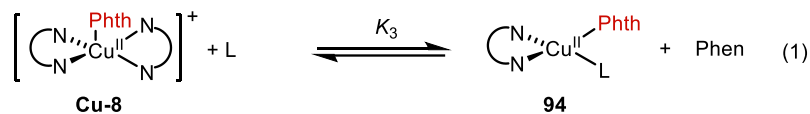
$$\frac{d[\mathbf{3-15}]}{dt} \approx \frac{k_6 k_7 [\mathbf{Cu-2}]^2 [\mathbf{A}]}{k_{-6} [\mathbf{Cu-4}] + k_7 [\mathbf{A}]} \cdot \frac{k_{10} K_2 [\mathbf{Cu-8}] [\mathbf{L}]}{k_{10} K_2 [\mathbf{Cu-8}] [\mathbf{L}]} = \frac{k_6 k_7 [\mathbf{Cu-2}]^2 [\mathbf{A}]}{k_{-6} [\mathbf{Cu-4}] + k_7 [\mathbf{A}]} = \frac{d[\mathbf{MeOAc}]}{dt}$$

When **[A]** is high, **eq.7** can be approximated to be

$$\frac{d[\mathbf{3-15}]}{dt} = \frac{d[\mathbf{MeOAc}]}{dt} \approx \frac{k_6 k_7 [\mathbf{Cu-2}]^2 [\mathbf{A}]}{k_7 [\mathbf{A}]} = k_6 [\mathbf{Cu-2}]^2$$

We propose that phenanthroline can dissociate from complex **Cu-8** (Fig. 3.31, eq. 1). The free phenanthroline can chelate with **Cu-2** and establish an equilibrium (Fig. 3.31, eq. 2). When using a low concentration of **3-5**, we assume that it does not affect the concentration of **[Cu-2]** significantly, but under a higher concentration of **3-5**, this effect cannot be ignored, so the $[\mathbf{Cu-2}] < [(\text{CuCl} + \text{TEACl})_{\text{T}}]$.

Figure 3.31 Proposed phenanthroline dissociation from Cu-8 and association to Cu-2



eq. 8

$$\frac{d[\mathbf{3-15}]}{dt} = \frac{d[\text{MeOAc}]}{dt} = k_6[\text{Cu-2}]^2 = k_6[(\text{CuCl} + \text{TEACl})_{\text{T}}]^{2-n}$$

These equations indicate that the formation of **3-15** and MeOAc will display a less-than-second-order dependence on (CuCl + Et₄NCl), which fits the kinetic data (1.3 order) presented in Figs. 3.6, 3.7, 3.16, and 3.17 {2.0–8.0 mol % of (CuCl + Phen) in Section 3.6.2; 2.0 mol % of [(Phen)₂Cu]⁺ in Section 3.6.6}. On the other hand, the rates of formation of **3-15** and MeOAc both displayed a zero-order-dependence on the complex **3-5** (Figs. 3.12 and 3.13).

These equations also fit our observations for phthalimide (Section 3.6.3) and the peroxide (Section 3.6.4). The rates of generation of **3-15** and MeOAc are both zero- or pseudo-zero-order-dependent on phthalimide and peroxide, because phthalimide and peroxide both contribute nothing to the simplified rate law (eq. 8).

When the concentration of phenanthroline is higher than that of CuCl, we propose the excess Phen can coordinate to **Cu-2** and establish an equilibrium (Fig. 3.31, eq. 2):

eq. 9

$$[\text{Cu-2}] = \frac{[\text{Cu-8}][\text{Cl}^-]^2}{K_4[\text{Phen}]^2}$$

Using **eq. 9** to replace [Cu-2] in **eq. 8**:

$$\frac{d[\mathbf{3-15}]}{dt} = \frac{d[\mathbf{MeOAc}]}{dt} = k_6 \frac{([\mathbf{Cu-8}][\text{Cl}^-]^2)^2}{K_4^2[\text{Phen}]^4}$$

Because $[\text{Phen}]_T = [\text{Phen}] + 2[\mathbf{Cu-8}]$ (to simplify the rate law, we assume the concentration of mono-Phen-substituted copper complexes is low):

eq. 10

$$\begin{aligned} \frac{d[\mathbf{3-15}]}{dt} &= \frac{d[\mathbf{MeOAc}]}{dt} = k_6 \frac{([\mathbf{Cu-8}][\text{Cl}^-]^2)^2}{K_4^2([\text{Phen}]_T - 2[\mathbf{Cu-8}])^4} \\ &= \frac{k_6}{K_4^2} \frac{([\mathbf{Cu-8}][\text{Cl}^-]^2)^2}{[\text{Phen}]_T^4 - 8[\text{Phen}]_T^3[\mathbf{Cu-8}] + 24[\text{Phen}]_T^2[\mathbf{Cu-8}]^2 - 32[\text{Phen}]_T[\mathbf{Cu-8}]^3 + 16[\mathbf{Cu-8}]^4} \end{aligned}$$

Although we currently cannot establish a good model to perfectly fit the results from Section 3.6.7 (the generation of both **3-15** and MeOAc is -5 -order-dependent on $[\text{Phen}]_T$ when using an excess of Phen), eq. 10 might imply a reason for the high negative-order-dependence on $[\text{Phen}]_T$. Equation 10 is a rough estimation because **Cu-2** can also coordinate with 1 equiv of Phen to generate mono-Phen-substituted copper complexes, such as **3-10**, and the value of $[\mathbf{Cu-8}]$ might also change along with that of $[\text{Phen}]_T$ because they are in equilibrium.

3.9. Conclusion

Using reaction kinetic analysis, control experiments with putative catalytic organometallic species, IR, UV-Vis, proton nuclear magnetic resonance and mass spectroscopy enabled the elucidation of the mechanistic details of the copper-peroxide redox enabled C–N coupling reaction, Aminodealkenylation. In-situ IR spectroscopic techniques were used to track the progress of peroxide decomposition and the evolution of the C–N coupling product, helping to determine the resting state of the copper catalyst and uncover the cooperative ion pair catalysis consisting of the ionic species copper (I) di-1,10-phenanthroline cation and copper (I) dichloride anion from the copper(I) chloride–1,10-phenanthroline catalyst system. These comprehensive organometallic

studies and kinetic study of the reaction unveiled the crucial and distinct nature of both ion pairs in initiating peroxide decomposition and propagating the Cu catalyzed C–N coupling. The mechanistic insights gained from this study served to inform a reaction rate law derivation and provide precedent for future developments in copper-catalyzed C–N coupling.

3.10. References

- (1) Pallenberg, A. J.; Koenig, K. S.; Barnhart, D. M. Synthesis and Characterization of Some Copper(I) Phenanthroline Complexes. *Inorg. Chem.* **1995**, *34* (11), 2833–2840.
<https://doi.org/10.1021/ic00115a009>.
- (2) Tye, J. W.; Weng, Z.; Johns, A. M.; Incarvito, C. D.; Hartwig, J. F. Copper Complexes of Anionic Nitrogen Ligands in the Amidation and Imidation of Aryl Halides. *J. Am. Chem. Soc.* **2008**, *130* (30), 9971–9983. <https://doi.org/10.1021/ja076668w>.
- (3) Tran, B. L.; Li, B.; Driess, M.; Hartwig, J. F. Copper-Catalyzed Intermolecular Amidation and Imidation of Unactivated Alkanes. *J. Am. Chem. Soc.* **2014**, *136* (6), 2555–2563.
<https://doi.org/10.1021/ja411912p>.
- (4) Masarwa, M.; Cohen, H.; Meyerstein, D.; Hickman, D.; Bakac, A.; Espenson, J. Reactions Of Low-Valent Transition-Metal Complexes With Hydrogen-Peroxide - Are They Fenton-Like Or Not .1. The Case Of Cu+Aq And Cr-2+Aq. *J. Am. Chem. Soc.* **1988**, *110* (13), 4293–4297. <https://doi.org/10.1021/ja00221a031>.
- (5) Ponganis, K.; Dearaujo, M.; Hodges, H. Electron-Transfer Reactions Of Copper-Complexes .1. A Kinetic Investigation Of The Oxidation Of Bis(1,10-Phenanthroline)Copper(I) By Hydrogen-Peroxide In Aqueous And Sodium Dodecyl-Sulfate Solution. *Inorg. Chem.* **1980**, *19* (9), 2704–2709. <https://doi.org/10.1021/ic50211a044>.
- (6) Lv, X.; Abrams, R.; Martin, R. Copper-Catalyzed C(Sp³)-Amination of Ketone-Derived Dihydroquinazolinones by Aromatization-Driven C-C Bond Scission. *Angew. Chem.-Int. Ed.* **2023**, *62* (8). <https://doi.org/10.1002/anie.202217386>.
- (7) Burés, J. A Simple Graphical Method to Determine the Order in Catalyst. *Angew. Chem.-Int. Ed.* **2016**, *55* (6), 2028–2031. <https://doi.org/10.1002/anie.201508983>.

- (8) Blackmond, D. G. Kinetic Profiling of Catalytic Organic Reactions as a Mechanistic Tool. *J. Am. Chem. Soc.* **2015**, *137* (34), 10852–10866. <https://doi.org/10.1021/jacs.5b05841>.
- (9) Alamillo-Ferrer, C.; Hutchinson, G.; Burés, J. Mechanistic Interpretation of Orders in Catalyst Greater than One. *Nat. Rev. Chem.* **2022**, *7* (1), 26–34. <https://doi.org/10.1038/2-99570-022-00447-w>.
- (10) Moffett, J.; Zika, R. Reaction-Kinetics Of Hydrogen-Peroxide With Copper And Iron In Seawater. *Environ. Sci. Technol.* **1987**, *21* (8), 804–810. <https://doi.org/10.1021/es00162a012>.
- (11) Lee, H.; Ahn, J.; Oyala, P.; Citek, C.; Yin, H.; Fu, G.; Peters, J. Investigation of the C-N Bond-Forming Step in a Photoinduced, Copper-Catalyzed Enantioconvergent N-Alkylation: Characterization and Application of a Stabilized Organic Radical as a Mechanistic Probe. *J. Am. Chem. Soc.* **2022**, *144* (9), 4114–4123. <https://doi.org/10.1021/jacs.1c13151>.
- (12) Schneider, L.; Krauel, E.; Deutsch, C.; Urbahns, K.; Bischof, T.; Maibom, K.; Landmann, J.; Keppner, F.; Kerpen, C.; Hailmann, M.; Zapf, L.; Knuplez, T.; Bertermann, R.; Ignat'ev, N.; Finze, M. Stable and Storable N(CF₃)₂ Transfer Reagents. *Chem. - Eur. J.* **2021**, *27* (42), 10973–10978. <https://doi.org/10.1002/chem.202101436>.
- (13) Ruthkosky, M.; Castellano, F.; Meyer, G. Photodriven Electron and Energy Transfer from Copper Phenanthroline Excited States. *Inorg. Chem.* **1996**, *35* (22), 6406–6412. <https://doi.org/10.1021/ic960503z>.
- (14) Cane, D.; Yang, G.; Coates, R.; Pyun, H.; Hohn, T. Trichodiene Synthase - Synergistic Inhibition By Inorganic Pyrophosphate And Aza Analogs Of The Bisabolylyl Cation. *J. Org. Chem.* **1992**, *57* (12), 3454–3462. <https://doi.org/10.1021/jo00038a040>.

- (15) Liu, X.; Rong, X.; Liu, S.; Lan, Y.; Liu, Q. Cobalt-Catalyzed Desymmetric Isomerization of Exocyclic Olefins. *J. Am. Chem. Soc.* **2021**, *143* (49), 20633–20639. <https://doi.org/10.1021/jacs.1c11343>.
- (16) Dow, N.; Cabré, A.; MacMillan, D. A General N-Alkylation Platform via Copper Metallaphotoredox and Silyl Radical Activation of Alkyl Halides. *CHEM* **2021**, *7* (7), 1827–1842. <https://doi.org/10.1016/j.chempr.2021.05.005>.
- (17) Frei, U.; Geier, G. Lewis-Base-Catalyzed Diimine-Ligand-Substitution Reactions At Copper(I). *Inorg. Chem.* **1992**, *31* (14), 3132–3137. <https://doi.org/10.1021/ic00040a025>.
- (18) Pearson, R.; Lanier, R. Rates Of Rapid Ligand Exchange Reactions By Nuclear Magnetic Resonance Line Broadening Studies. *J. Am. Chem. Soc.* **1964**, *86* (5), 765-. <https://doi.org/10.1021/ja01059a004>.
- (19) *Mechanisms of Inorganic Reactions*; Kleinberg, J., Murmann, R. K., Fraser, R. T. M., Bauman, J., Eds.; Advances in Chemistry; AMERICAN CHEMICAL SOCIETY: WASHINGTON, D.C., 1965; Vol. 49. <https://doi.org/10.1021/ba-1965-0049>.
- (20) Weatherburn, D. Kinetics Of Ligand-Exchange Reactions Of Copper(Ii) Complexes Of Pyridine-2-Aldehyde-2'-Pyridylhydrazone. *INORGANICA Chim. ACTA* **1977**, *21* (2), 209–215. [https://doi.org/10.1016/S0020-1693\(00\)86263-5](https://doi.org/10.1016/S0020-1693(00)86263-5).
- (21) Helm, L.; Merbach, A. Inorganic and Bioinorganic Solvent Exchange Mechanisms. *Chem. Rev.* **2005**, *105* (6), 1923–1959. <https://doi.org/10.1021/cr030726o>.
- (22) Richens, D. Ligand Substitution Reactions at Inorganic Centers. *Chem. Rev.* **2005**, *105* (6), 1961–2002. <https://doi.org/10.1021/cr030705u>.
- (23) Mereshchenko, A.; Pal, S.; Karabaeva, K.; El-Khoury, P.; Tarnovsky, A. Photochemistry of Monochloro Complexes of Copper(II) in Methanol Probed by Ultrafast Transient

Absorption Spectroscopy. *J. Phys. Chem. A* **2012**, *116* (11), 2791–2799.

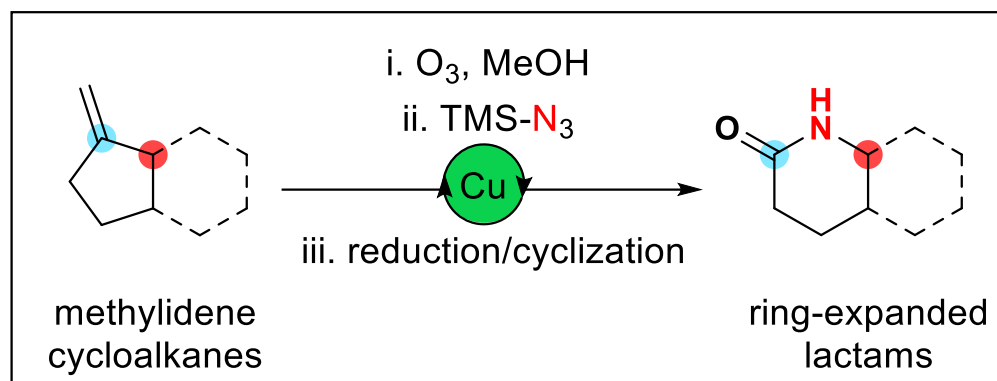
<https://doi.org/10.1021/jp208532u>.

- (24) Mereshchenko, A.; Olshin, P.; Karabaeva, K.; Panov, M.; Wilson, R.; Kochemirovsky, V.; Skripkin, M.; Tveryanovich, Y.; Tarnovsky, A. Mechanism of Formation of Copper(II) Chloro Complexes Revealed by Transient Absorption Spectroscopy and DFT/TDDFT Calculations. *J. Phys. Chem. B* **2015**, *119* (28), 8754–8763.
<https://doi.org/10.1021/acs.jpcc.5b03889>.
- (25) Catalan, J.; Delvalle, J.; Claramunt, R.; Boyer, G.; Laynez, J.; Gomez, J.; Jimenez, P.; Tomas, F.; Elguero, J. Acidity And Basicity Of Indazole And Its N-Methyl Derivatives In The Ground And In The Excited-State. *J. Phys. Chem.* **1994**, *98* (41), 10606–10612.
<https://doi.org/10.1021/j100092a035>.
- (26) Koppel, W. H. Oxyradical Reactions: From Bond-Dissociation Energies to Reduction Potentials. *FEBS Lett.* **1990**, *264* (2), 165–167. [https://doi.org/10.1016/0014-5793\(90\)80239-F](https://doi.org/10.1016/0014-5793(90)80239-F).
- (27) Kochi, J.; Subraman.Rv. Kinetics Of Electron-Transfer Oxidation Of Alkyl Radicals By Copper .2. Complexes. *J. Am. Chem. Soc.* **1965**, *87* (21), 4855-
<https://doi.org/10.1021/ja00949a033>.
- (28) Navon, N.; Golub, G.; Cohen, H.; Meyerstein, D. Kinetics And Reaction-Mechanisms Of Copper(I) Complexes With Aliphatic Free-Radicals In Aqueous-Solutions - A Pulse-Radiolysis Study. *ORGANOMETALLICS* **1995**, *14* (12), 5670–5676.
<https://doi.org/10.1021/om00012a037>.
- (29) Mansano-Weiss, C.; Epstein, D.; Cohen, H.; Masarwa, A.; Meyerstein, D. Mechanism of Reaction of Alkyl Radicals with Copper(II)(Glycylglycylglycine) in Aqueous Solutions.

INORGANICA Chim. ACTA **2002**, 339, 283–291. [https://doi.org/10.1016/S0020-1693\(02\)00950-7](https://doi.org/10.1016/S0020-1693(02)00950-7).

- (30) Zhao, X.; Liu, Y.; Zhu, R.; Liu, C.; Zhang, D. Mechanistic Study on the Decarboxylative Sp³ C-N Cross-Coupling between Alkyl Carboxylic Acids and Nitrogen Nucleophiles via Dual Copper and Photoredox Catalysis. *Inorg. Chem.* **2019**, 58 (19), 12669–12677. <https://doi.org/10.1021/acs.inorgchem.9b01477>.
- (31) McConnell, H.; Weaver, H. Rate Of Electron Exchange Between Cuprous And Cupric Ions In Hydrochloric Acid Solutions By Nuclear Magnetic Resonance. *J. Chem. Phys.* **1956**, 25 (2), 307–311. <https://doi.org/10.1063/1.1742877>.
- (32) Lee, C.; Anson, F. Electron Exchange Between Cu(Phen)²⁺ Adsorbed On Graphite And Cu(Phen)₂²⁺ In Solution. *Inorg. Chem.* **1984**, 23 (7), 837–844. <https://doi.org/10.1021/ic00175a009>.
- (33) Rorabacher, D. Electron Transfer by Copper Centers. *Chem. Rev.* **2004**, 104 (2), 651–697. <https://doi.org/10.1021/cr020630e>.
- (34) Yoneda, G.; Blackmer, G.; Holwerda, R. Kinetics Of Oxidation Of Cu(Phen)₂²⁺ And Cu(Bpy)₂²⁺ By Aminopolycarboxylatocobalt(III) Complexes. *Inorg. Chem.* **1977**, 16 (12), 3376–3378. <https://doi.org/10.1021/ic50178a087>.
- (35) Gephart, R.; McMullin, C.; Sapiezynski, N.; Jang, E.; Aguila, M.; Cundari, T.; Warren, T. Reaction of CuI with Dialkyl Peroxides: CuII-Alkoxides, Alkoxy Radicals, and Catalytic C-H Etherification. *J. Am. Chem. Soc.* **2012**, 134 (42), 17350–17353. <https://doi.org/10.1021/ja3053688>.

CHAPTER 4: Azidodealkenylation



4.1. Abstract

An efficient method for nitrogen atom insertion into carbocyclic frameworks of exomethylenic cyclic alkenes was developed. Leveraging copper(I)-catalyzed decomposition of hydroperoxyacetals, generated by Criegee ozonolysis of the alkene substrates, the carbocyclic skeleton is ruptured at the C(sp²)-C(sp³) bond to concurrently provide an ester at the former most substituted C(sp²) site and, in the presence of TMS-azide, an azido moiety at the C(sp³) site. This strategy was used to produce versatile ester containing primary, secondary or tertiary azides. The azides were subsequently reduced and cyclized onto the ester to provide ring-expanded cyclic lactams, providing rapid access value-added products such as a pharmaceutical intermediate, and a pseudoalkaloid from a terpene precursor.

4.2. Introduction

Organic azides are an important and versatile functional group of interest to many areas of chemical research such as medicinal chemistry, chemical biology, and material science. Azides are often viewed as a masked amine unit, a precursor to amides through rearrangements, imines via the Staudinger and aza-Wittig reactions and a privileged reagent for azaheterocycle synthesis.¹⁻

⁶ Adding to their versatility, azides can be used to access a variety of reactive species such as

isocyanates, and after loss of dinitrogen, electron-deficient nitrenes – which under transition metal catalysis, allow for a host of unique reactivity and enabling transformations.⁷⁻⁹ Furthermore, the azido group serves as a 1,3-dipole which can engage in [3+2] dipolar cycloadditions with a variety of unsaturated partners such as alkynes, alkenes, and nitriles to arrive at 1,2,3-triazoles or tetrazole motifs.^{10,11} The utility of these facile heterocycle syntheses has not gone unnoticed as the azide-alkyne cycloaddition, dubbed “click chemistry” as applied to the biorthogonal ligation of molecular building blocks, was a subject that went on to win the 2022 Nobel Prize in Chemistry.¹² For this and many other reasons, azide chemistry has been intensely studied, especially as they allow access to such a variety of key nitrogenous functional groups.

The introduction of nitrogenous moieties into organic compounds is another intensely studied area of organic synthesis. Nitrogen atoms are present in a majority of FDA approved small molecule therapeutics, highlighting their importance in drug design and discovery.^{13,14} At a time where medicinal chemists are calling for expanded methods to incorporate more C(sp³) character into small molecule pharmaceuticals, novel methods to produce aliphatic azides may provide an answer.^{15,16} To this end, organic azides may prove as a versatile functional handle to access such compounds or may serve as prodrugs and even bioactive compounds themselves (Figure 1a).^{17,18} Classically, azides have been introduced into organic molecules through diazo transfer to an amine, substitution or addition reactions using an alkali metal azide nucleophile, such as sodium azide, and an appropriate electrophile, including alkyl halides, epoxides or aziridines (Figure 1b).² While this approach benefits from well-defined reactivity, chemoselectivity issues may arise if multiple electrophilic centers are present. Additional limitations arise from harsh conditions required for these types of transformations, toxicity of the azide reagents, and the high polarity solvents required to solubilize these strongly ionic azide sources.¹⁹ Modern approaches to circumvent these

limitations include metal catalysis which have been developed as milder azide transfer mediators

capable of employing less toxic azide sources. Another powerful approach is the radical azidation of pi bonds wherein a radical species is produced forming a bond at one terminus of unsaturation and providing another alkyl radical on the other terminus that is then utilized to form another bond (Figure 1b, top right).²¹

There are many recent reports for the 1,2-azido functionalization across alkenes and even alkynes, however they are generally limited by only providing the 1,2-motif.^{22–}

³⁴ As we seek to diversify the types of aliphatic azides we can access, novel protocols employing unique reactivity should be explored.

Many advancements in this area have been made, enabling azidation of complex substrates in natural product settings, as well as of late-stage azidation of pharmaceuticals (Figure 1c, top).²⁰ While these undirected radical C–H azidation

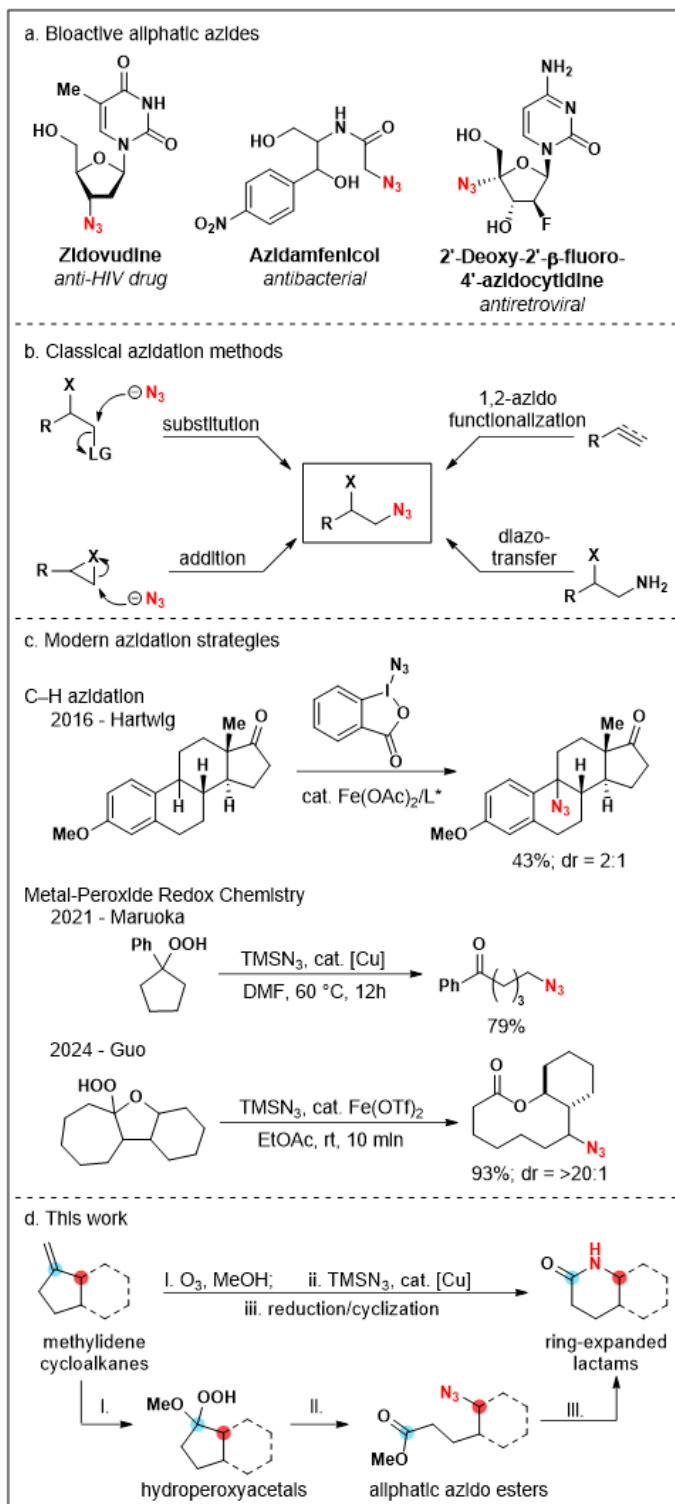


Figure 4.1: a. Medicinally important aliphatic azides b. Traditional azide synthesis c. Modern azide synthesis.

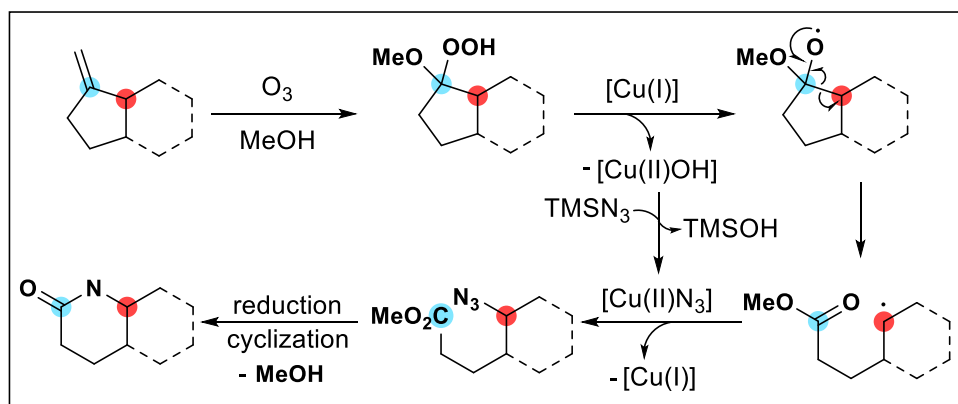
strategies are useful, they are limited in site selectivity by the stability of the carbon radical formed, favoring benzylic or tertiary C–H bonds.

In recent years, an attractive approach to generate alkyl radicals for azidation involves the homolysis of C–C bonds to install C(sp³)–N₃ bonds. To be synthetically useful the substrates of these reactions should be readily accessible and require little to no prefunctionalization. In this vein silver-catalyzed decarboxylative azidation chemistry using aliphatic carboxylic acids and aldehydes has been reported.^{35,36} A study by the company, Novartis, examined the prevalence of functional groups occurring in natural products by a chemoinformatics study of the Open Natural Products collection and found that more prevalent than carboxylic acids (11%) and aldehydes (2%), alkenes were the second most frequent functional group present in nearly 40% of natural products studied.³⁷ Recently, the Kwon lab has been exploring dealkenylative functionalization which ruptures the C(sp³)–C(sp²) bond of alkenes to functionalize the C(sp³) carbon center. This strategy has been applied to a broad range of radicophiles to install H atoms, aryl sulfides, carbonyls, alkenes, alkynes and most recently to couple nitrogen nucleophiles.^{38–43} Disclosed herein is the latest extension of this manifold to couple an azido unit in this fashion using exomethylene cyclic alkenes as substrates.

While peroxide redox azidation chemistry has been known in the literature since 1959⁴⁴, these methods were often low to moderate yielding⁴⁵, relied on photochemistry to form the peroxides⁴⁶, or were narrow in substrate scope, requiring secondary 1,1-aryl alkyl peroxyesters⁴⁷. Recent notable examples of this chemistry include works by Maruoka who demonstrated cyclic alkyl hydroperoxides⁴⁸ and silyl peroxides⁴⁹ can form linear azido carbonyl compounds, and Guo⁵⁰ who used this chemistry with cyclic hemiketal hydroperoxides to synthesize medium-sized azido lactones (Figure 1c, middle and bottom). In light of these works and advancements in our own

work, we realized there was untapped potential of this chemistry to be applied to the rapid generation of pseudoalkaloids in a formal example of skeletal editing. Pseudoalkaloids are a class of natural products bearing a non-proteinogenic nitrogen atom, differentiating them from the true alkaloids. However, similar to true alkaloids, several pseudoalkaloids possess a broad range of bioactivities making them valuable targets for this method.

As seen in Scheme 1, our reaction design for dealkenylative azidation begins with Criegee ozonolysis of an olefin substrate to form a hydroperoxyacetal. When performed on an exomethylene cyclic alkene that is then treated with a copper(I)-1,10-phenanthroline complex in the presence of TMS-azide, the hydroperoxide fragments from a SET event from Cu(I) to provide Cu(II) and an alkoxy radical. The alkoxy radical then undergoes beta-scission to sunder the ring and provide an ester from what was the alkoxy group and an alkyl radical. The alkyl radical is then coupled with a copper(II)-azido complex to produce the azido ester. When the azide group is reduced to the amine, it can nucleophilically add to the ester to provide a n+1 ring-expanded lactam - a formal example of skeletal editing where a nitrogen has been inserted into the carbocyclic ring system.



Scheme 4.1: Reaction design of dealkenylative azidation & reductive cyclization

Lactams are well known pharmacophores with their own broad range of bioactivities.⁵¹

Highlighting the potential of creating pseudoalkaloid lactams with enhanced activity from terpenes

is a recent report from the 2021 where researchers created an additional lactam ring using a 1,2-azidoalkylation of the exo-methylenic double-bond in the tetracyclic terpene *ent*-kaurenoic acid.⁵² SAR testing of these derivatives revealed anti-proliferative effects higher than the well-known drug Cisplatin, as well as promising selectivity profiles for targeting tumor cells. Analogously, when terpene-derived exomethylene alkene substrates are used in our azidodealkenylation-cyclization sequence they produce pseudoalkaloid-like compounds in which the lactam is embedded into the original carbocyclic framework, not additionally appended to the original structure. We believe this unique strategy, enabled by the unique reactivity of our method, will allow for rapid access to a host of interesting and potentially bioactive compounds.

4.3. Results and Discussion

We commenced reaction optimization by using 4-methylene-1-tosylpiperidine (**4-1a**) and (4-methylenecyclohexyl)benzene (**4-2a**) as model substrates. Based on results from our previous dealkenylation amination work and unpublished results from our lab we first explored the use of

Entry	Cu cat	Yield
1	CuCl	47
2	CuI	27
3	CuOTf	53
4	Cu(MeCN) ₄ PF ₆	88
5	Cu(MeCN) ₄ BF ₄	90
6	Cu(MeCN) ₄ OTf	83.5
7	none	0

Table 4.1 Cu(I) Salt Optimization

copper(I) salts and 1,10-phenanthroline ligand scaffold as a catalyst system for this transformation. When copper(I) halides (Table 1, entry 1 & 2) and pseudohalide salts (entry 3) were used, the azido ester (**4-1b**) was attained in moderate to low yields. When copper(I) tetrakisacetonitrile salts were surveyed (entries 4-6), dramatically improved results were observed, with identity of the counter anion having only a small effect on overall yield. From these results copper(I) tetrakisacetonitrile tetrafluoroborate, $\text{Cu}(\text{MeCN})_4\text{BF}_4$, produced the product **4-1b** in 90% yield and was chosen as the optimal copper salt for this transformation. Control experiments indicated that in the absence of a copper catalyst, no product formation was detected. Next the amounts of catalyst complex in the reaction were varied to observe the effects on yield. When the catalyst system amount was halved from 20 mol% to 10 mol% (Table 2, entry 2) the yield of product **4-2** also decreased by roughly half from 90% to 42% yield, respectively. Further lowering the catalyst complex to 5% (entry 1) completely shut down the azidation

Entry	[Cu] mol %	Solvent	Yield
1	5	Acetone	0
2	10	Acetone	42
3	30	Acetone	86
4	20	MeCN	78
5	20	EtOAc	54
6	20	THF	64
7	20	DCE	87

Table 4.2 Optimization of catalyst loading and solvent

reactivity. Further increasing the catalyst loading to 30 mol% (entry 3) slightly diminished the overall yield indicating 20% was the optimal loading. Altering the identity of the solvent from acetone (entries 4-6) did not provide any additional benefit to the reaction efficiency but did reveal that DCE could also serve as a competent solvent in this reaction.

Using exomethylene alkene **4-2a**, impacts on yield based on ligand scaffold were studied (Table 4.3, entries 1-5). These experiments revealed that other N-based ligands aside from 1,10-phen, **L1**, can serve as competent ligands with pyridine, **L2** used in 40 mol% to account for the monodentate binding, (entry 2) providing identical yields as **L1** and diimine ligand **L4** providing only slightly diminished yields. Interestingly, bipyridine dramatically lowered the yield from 98% with **L1** & **L2** to 37% (entry 3). Control experiment in the absence of ligand (entry 5) indicated that while beneficial, ligands are not an essential component of the reaction with the ligandless copper salt the azidated product, **4-2b**, in a synthetically useful 80% yield. It was determined that the dealkenylative azidation is not sensitive to enlarged scales (entries 6 & 7), providing only slightly

Entry	N ₃ Source	Scale (mmol)	Ligand	Yield
1	TMSN ₃	0.4	L1	98%
2	TMSN ₃	0.4	L2 (40 mol%)	98%
3	TMSN ₃	0.4	L3	37%
4	TMSN ₃	0.4	L4	92%
5	TMSN ₃	0.4	none	80%
6	TMSN ₃	0.5	L1	95%
7	TMSN ₃	2.0	L1	93%

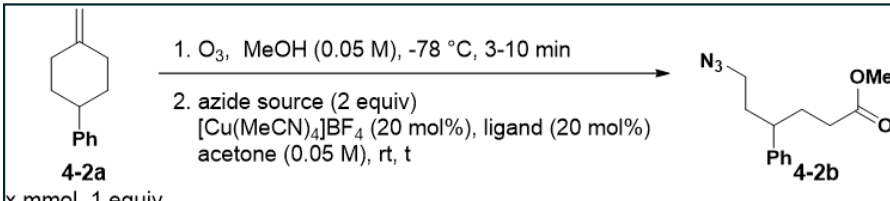
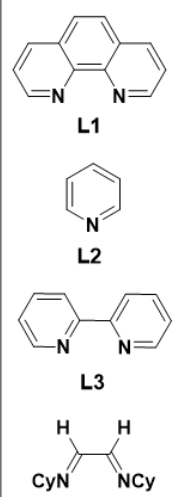
 <p>1. O₃, MeOH (0.05 M), -78 °C, 3-10 min 2. azide source (2 equiv) [Cu(MeCN)₄]BF₄ (20 mol%), ligand (20 mol%) acetone (0.05 M), rt, t</p> <p>4-2a → 4-2b</p>	 <p>L1 L2 L3 L4</p>
---	--

Table 4.3 Impacts of ligand, reaction scale and N₃ source

lower yields when scaled up 5 times from the originally screened reaction scale (entry 7). Finally, it was observed that TMSN_3 is required for fruitful reactivity with NaN_3 as an azide source only providing 19% of the product (entry 8). With these optimal conditions in hand, the substrate scope was then explored.

4.3.1. Scope of exomethylene alkenes

To establish the generality of this method, cyclic exomethylene alkenes were subjected to optimized dealkenylative azidation conditions. Model substrates **4-1a/2a** provided the corresponding azidoesters **4-1b** and **4-2b** in nearly quantitative yield (Figure 4.2). Phenyl substituted alkene **4-2a** was chosen for a large scale reaction and performed with minimal loss in yield to smoothly provide **4-2b** in high yield. The carbocycle **4-3a** was found to be volatile and

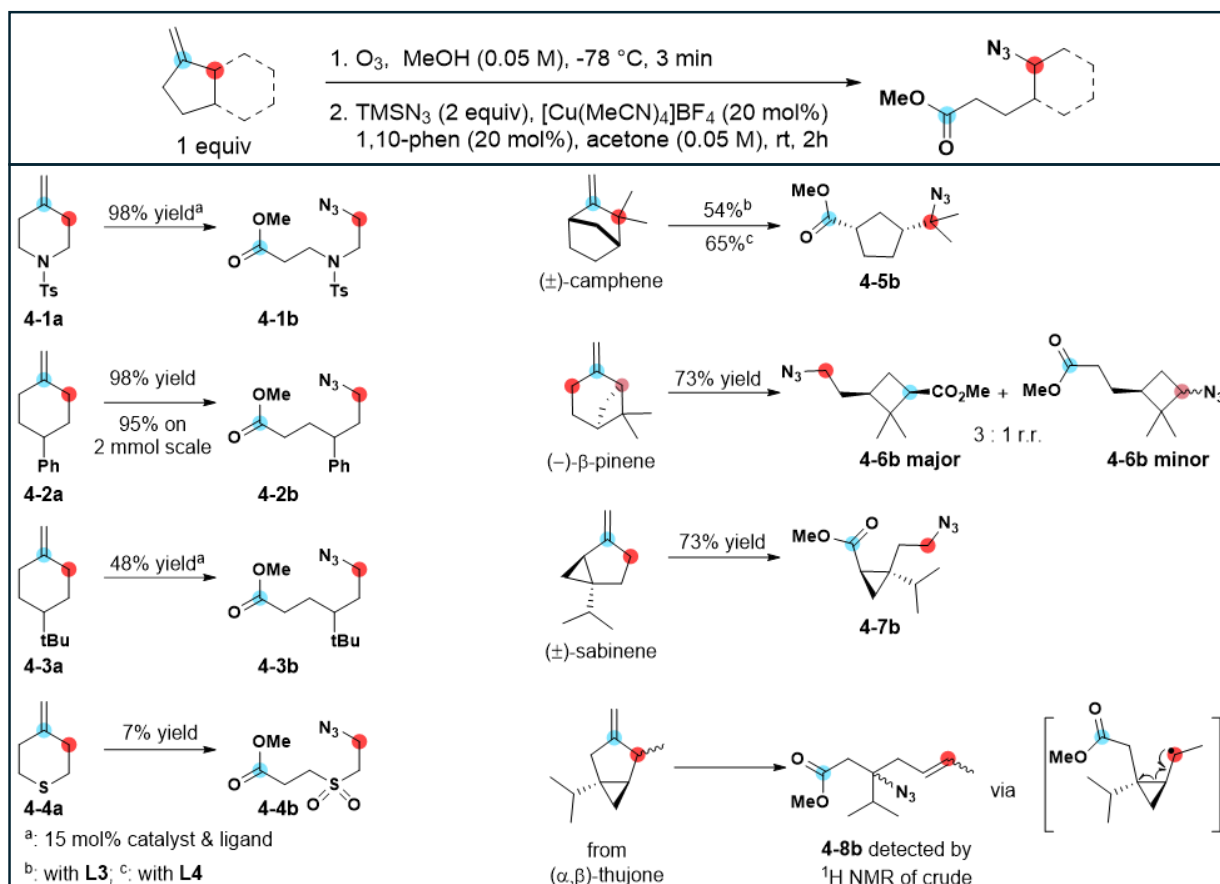


Figure 4.2 Methyldene Cycloalkene Substrate Scope

provided the corresponding product **4-3b** in reduced yield, likely owing to the volatility of the starting material. Interestingly the tetrahydrothiopyran, **4-4a**, provided step economical access to azidoester functionalized sulfone **4-4b**, although in only 7% yield. To investigate the feasibility of using more complex terpene derived exocyclic alkenes, (\pm)-camphene was subjected to the reaction conditions. The results with optimized conditions were initially unsatisfactory, providing low yields of the product. We hypothesized this could be the result of steric crowding by the dimethyl moiety that would bear the tertiary radical to be coupled with the azide. We presumed less rigid ligands could offer more conformational flexibility during the coupling step so 2,2'-bipyridine **L3** and diimine ligand **L4** were employed which gratifyingly provided the cyclopentyl tertiary azide product **4-5b** in 54% and 65% respectively. Inspired by this result the bridged bicyclic terpene, (-)- β -pinene, reacted under standard conditions to provide regioisomeric primary, and secondary cyclobutyl azides as a 3:1 mixture respectively in 73% yield. The minor regioisomer, **4-6b minor** was isolated as an intractable mixture of diastereomers. The fused bicyclic terpene, (\pm)-sabinene provided the primary cyclopropyl azide **4-7b** as the sole product in 73% yield. To probe the suspected intermediacy of the alkyl radical, the cyclopropyl containing terpene, (α,β)-thujone was employed as a radical clock. True to the nature of this reaction, alkene **4-8b** was detected by ^1H NMR as a major product, which arises from the radical alpha to the cyclopropyl ring causing a homolytic cleavage of strained ring, providing support for a radical based mechanism.

4.3.2. Reductive Cyclization of Azidoesters

Having achieved the dealkenylative azidation of several substrates, we began to examine optimal conditions for the reduction of the azides and cyclization onto the ester to produce the target lactams. Among the methods screened included Staudinger reduction with PPh_3 , a one pot

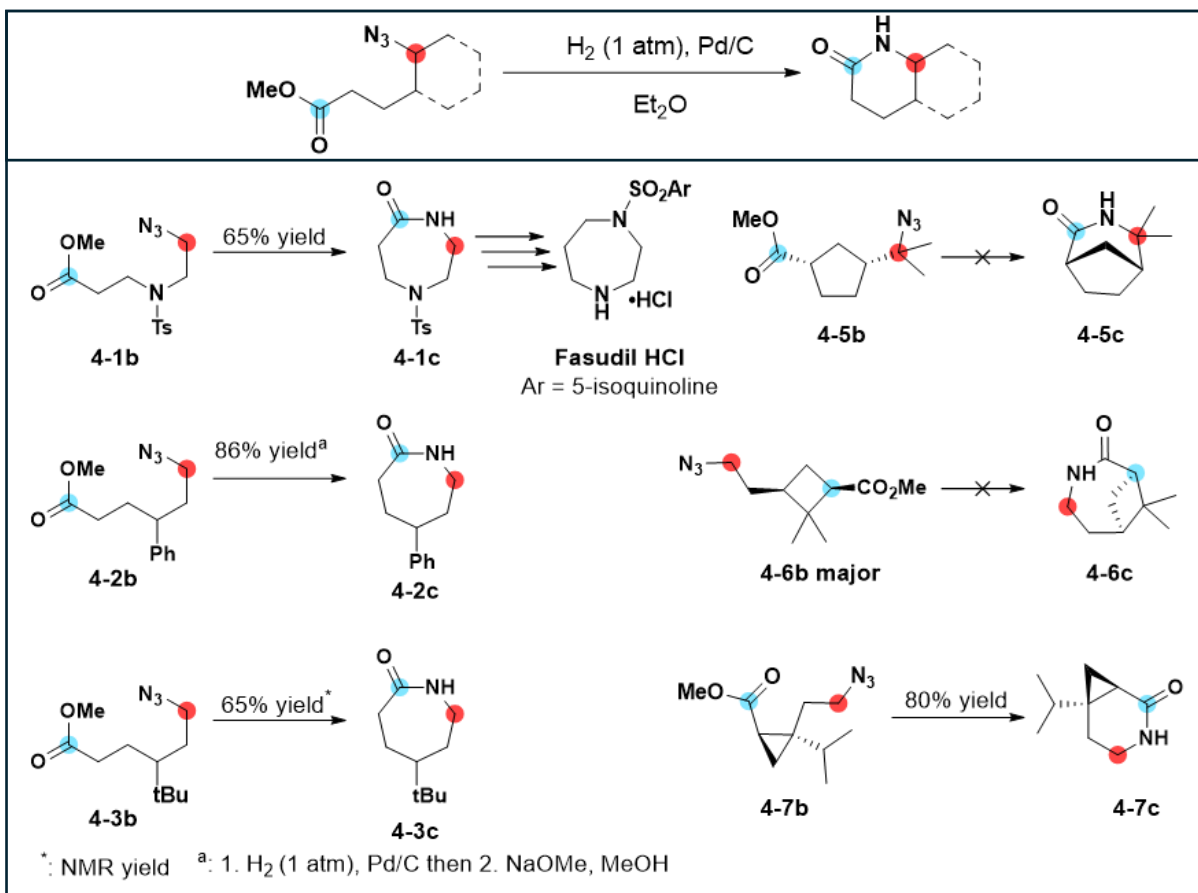


Figure 4.3 Reductive Cyclization of Azidoesters

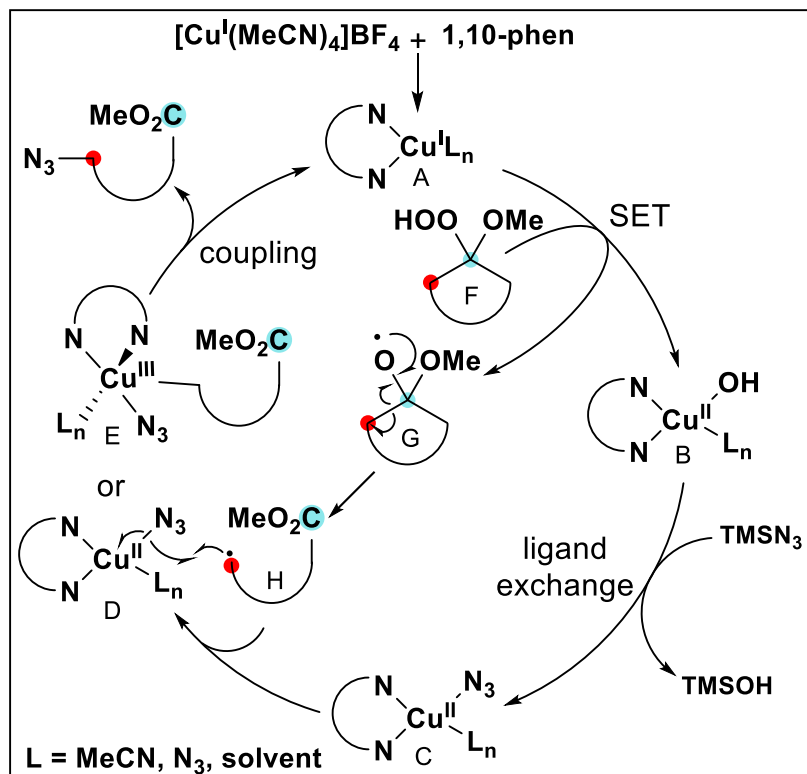
tris(TMS)silane reduction inspired by a 2022 report from Wang and coworkers⁵³, and hydrogenation over palladium on charcoal. The attempts with PPh₃ were met with poor results or no reactivity in the case of silane reduction. However, hydrogenation became the reduction procedure of choice, smoothly converting the azidoesters into aminoesters, many of which spontaneously lactamized during the course of the reaction. These results are summarized in Figure 4.3. The formal nitrogen insertion into the ring system of model substrate N-tosyl piperidine **4-1a** was achieved in 65% yield from the azidoesters. The product of this reaction, the protected 1,4-diazepinone, **4-1c**, is an advanced intermediate and only three synthetic steps away (NaBH₄ reduction, arylsulfonyl chloride coupling, and deprotection/salt formation) from the synthesis of Fasudil HCl. This small molecule therapeutic is a known rho kinase inhibitor clinically used in

Japan since 1995 to treat subarachnoid hemorrhage and is being investigated as a therapeutic for heart ischemia and CNS disorders such as Alzheimer's disease.⁵⁴⁻⁵⁶ The phenyl substituted lactam **4-2c** was achieved in high yield from the corresponding azidoester, requiring treatment with NaOMe for efficient cyclization. The azide **4-3b** spontaneously cyclized to provide the lactam **4-3c**. Despite several attempts the azides **4-5b** and **4-6b** failed to cyclize to the bridged lactams under the reduction conditions employed. In the case of substrate **4-5b** sterics of the tertiary azide and formation of the bridged ring system are likely reasons for inefficient cyclization, even in the presence of base and prolonged heating. The amine of **4-6b** was detected from the reaction mixture, but cyclization failed to occur using the forcing conditions mentioned previously, indicating additional strategies may need to be developed to provide a more general cyclization protocol for bridged systems. Gratifyingly the fused bicyclic sabinalactam **4-7c** was smoothly accessed in 80% yield, showcasing the viability of our approach to insert nitrogen atoms into carbocyclic terpene frameworks.

4.4. Mechanism of dealkenylative azidation

An outline of a possible mechanism for dealkenylative azidation is outlined in Scheme 4.2. A 1:1 mixture of the copper(I) salt and 1,10-phen can form complex **A**. In the presence of hydroperoxyacetal, **F**, obtained from Criegee ozonolysis of an exomethylenic olefin, a single electron transfer event can oxidize **A** to form copper(II) hydroxide complex **B**, and reduce the peroxide to alkoxy radical species **G**. Alkyl radical **H** will be formed upon beta-scission of the alkoxy radical with concomitant formation of the methyl ester. Upon ligand exchange with TMSN₃, copper(II) azido complex **C** can intercept the alkyl radical **H** by way of an outer sphere coupling process, **D**, or through an inner sphere process through a copper(III) intermediate **E**. From

either complex the azido ester product can be obtained and the initial copper(I) complex can be regenerated to propagate the catalytic cycle anew.



Scheme 4.2 Proposed mechanism of dealkenylative

4.5. Conclusion

We have demonstrated the latest expansion of the dealkenylative functionalization platform for the deconstructive radical azidation of exomethylene cyclic alkenes. This method leverages the metal-peroxide redox chemistry of hydroperoxyacetals, generated in-situ through Criegee ozonolysis of exocyclic alkenes and a commercially available and inexpensive copper(I) catalyst system to provide access to synthetically versatile primary, secondary and tertiary azides. In a formal example of skeletal editing the azide group was hydrogenated and cyclized onto the ester moiety, produced from beta-scission of the alkoxy radical, to insert the nitrogen atom into the carbocyclic ring to provide n+1 ring-expanded lactams. This sequence was used to prepare an

intermediate of the clinically used rho kinase inhibitor, Fasudil HCl, the pseudoalkaloid sabinalactam from the terpene sabinene, as well as other ring expanded lactams. Future work may include addressing limitations to the reduction-cyclization sequence to produce bridged bicyclic lactams. This study provides unprecedented access to azido esters by virtue of the unique reactivity enabled by the dealkenylation platform and establishes an approach for rapid synthesis of pseudoalkaloids from readily available terpene precursors which may be of broad interest to the community.

4.6. References

- (1) Bräse, S.; Gil, C.; Knepper, K.; Zimmermann, V. Organic Azides: An Exploding Diversity of a Unique Class of Compounds. *Angew. Chem. Int. Ed.* **2005**, *44* (33), 5188–5240.
<https://doi.org/10.1002/anie.200400657>.
- (2) *Organic Azides: Syntheses and Applications*; Bräse, S., Banert, K., Eds.; John Wiley: Chichester, West Sussex, U.K, 2010.
- (3) Gololobov, Y. G.; Kasukhin, L. F. Recent Advances in the Staudinger Reaction. *Tetrahedron* **1992**, *48* (8), 1353–1406. [https://doi.org/10.1016/S0040-4020\(01\)92229-X](https://doi.org/10.1016/S0040-4020(01)92229-X).
- (4) Huang, D.; Yan, G. Recent Advances in Reactions of Azides. *Adv. Synth. Catal.* **2017**, *359* (10), 1600–1619. <https://doi.org/10.1002/adsc.201700103>.
- (5) Kim, S.; Joe, G. H.; Do, J. Y. Novel Radical Cyclizations of Alkyl Azides. A New Route to N-Heterocycles. *J. Am. Chem. Soc.* **1994**, *116* (12), 5521–5522.
<https://doi.org/10.1021/ja00091a087>.
- (6) Balci, M. Acyl Azides: Versatile Compounds in the Synthesis of Various Heterocycles-. *Synthesis* **2018**, *50* (07), 1373–1401. <https://doi.org/10.1055/s-0036-1589527>.
- (7) *Azides and Nitrenes: Reactivity and Utility*; Scriven, E. F. V., Ed.; Academic Press: Orlando, Fla, 1984.
- (8) Gillaizeau, I.; Gigant, N. Alkyl and Acyl Azide Rearrangements. In *Molecular Rearrangements in Organic Synthesis*; Rojas, C. M., Ed.; Wiley, 2015; pp 85–110.
<https://doi.org/10.1002/9781118939901.ch4>.
- (9) Müller, P.; Fruit, C. Enantioselective Catalytic Aziridinations and Asymmetric Nitrene Insertions into CH Bonds. *Chem. Rev.* **2003**, *103* (8), 2905–2920.
<https://doi.org/10.1021/cr020043t>.

- (10) Beutick, S. E.; Vermeeren, P.; Hamlin, T. A. The 1,3-Dipolar Cycloaddition: From Conception to Quantum Chemical Design. *Chem. – Asian J.* **2022**, *17* (17), e202200553. <https://doi.org/10.1002/asia.202200553>.
- (11) Huisgen, R. 1,3-Dipolar Cycloadditions. Past and Future. *Angew. Chem. Int. Ed. Engl.* **1963**, *2* (10), 565–598. <https://doi.org/10.1002/anie.196305651>.
- (12) Zaia, J. The 2022 Nobel Prize in Chemistry for the Development of Click Chemistry and Bioorthogonal Chemistry. *Anal. Bioanal. Chem.* **2023**, *415* (4), 527–532. <https://doi.org/10.1007/s00216-022-04483-9>.
- (13) Vitaku, E.; Smith, D.; Njardarson, J. Analysis of the Structural Diversity, Substitution Patterns, and Frequency of Nitrogen Heterocycles among US FDA Approved Pharmaceuticals. *J. Med. Chem.* **2014**, *57* (24), 10257–10274. <https://doi.org/10.1021/jm501100b>.
- (14) Pennington, L. D.; Moustakas, D. T. The Necessary Nitrogen Atom: A Versatile High-Impact Design Element for Multiparameter Optimization. *J. Med. Chem.* **2017**, *60* (9), 3552–3579. <https://doi.org/10.1021/acs.jmedchem.6b01807>.
- (15) Wei, W.; Cherukupalli, S.; Jing, L.; Liu, X.; Zhan, P. Fsp3: A New Parameter for Drug-Likeness. *Drug Discov. Today* **2020**, *25* (10), 1839–1845. <https://doi.org/10.1016/j.drudis.2020.07.017>.
- (16) Lovering, F.; Bikker, J.; Humblet, C. Escape from Flatland: Increasing Saturation as an Approach to Improving Clinical Success. *J. Med. Chem.* **2009**, *52* (21), 6752–6756. <https://doi.org/10.1021/jm901241e>.

- (17) Geng, J.; Zhang, Y.; Gao, Q.; Neumann, K.; Dong, H.; Porter, H.; Potter, M.; Ren, H.; Argyle, D.; Bradley, M. Switching on Prodrugs Using Radiotherapy. *Nat. Chem.* **2021**, *13* (8), 805–810. <https://doi.org/10.1038/2-99557-021-00711-4>.
- (18) Fischl, M. A.; Richman, D. D.; Grieco, M. H.; Gottlieb, M. S.; Volberding, P. A.; Laskin, O. L.; Leedom, J. M.; Groopman, J. E.; Mildvan, D.; Schooley, R. T.; Jackson, G. G.; Durack, D. T.; King, D.; The AZT Collaborative Working Group. The Efficacy of Azidothymidine (AZT) in the Treatment of Patients with AIDS and AIDS-Related Complex. *N. Engl. J. Med.* **1987**, *317* (4), 185–191. <https://doi.org/10.1056/NEJM198707233170401>.
- (19) Tat, J.; Heskett, K.; Satomi, S.; Pilz, R. B.; Golomb, B. A.; Boss, G. R. Sodium Azide Poisoning: A Narrative Review. *Clin. Toxicol.* **2021**, *59* (8), 683–697. <https://doi.org/10.1080/15563650.2021.1906888>.
- (20) Karimov, R. R.; Sharma, A.; Hartwig, J. F. Late Stage Azidation of Complex Molecules. *ACS Cent. Sci.* **2016**, *2* (10), 715–724. <https://doi.org/10.1021/acscentsci.6b00214>.
- (21) Ge, L.; Chiou, M.-F.; Li, Y.; Bao, H. Radical Azidation as a Means of Constructing C(Sp³)-N₃ Bonds. *Green Synth. Catal.* **2020**, *1* (2), 86–120. <https://doi.org/10.1016/j.gresc.2020.07.001>.
- (22) Hossain, A.; Vidyasagar, A.; Eichinger, C.; Lankes, C.; Phan, J.; Rehbein, J.; Reiser, O. Visible-Light-Accelerated Copper(II)-Catalyzed Regio- and Chemoselective Oxo-Azidation of Vinyl Arenes. *Angew. Chem. Int. Ed.* **2018**, *57* (27), 8288–8292. <https://doi.org/10.1002/anie.201801678>.
- (23) Ikemoto, Y.; Chiba, S.; Li, Z.; Chen, Q.; Mori, H.; Nishihara, Y. Carboazidation of Terminal Alkenes with Trimethylsilyl Azide and Cyclic Ethers Catalyzed by Copper Powder

- under Oxidative Conditions. *J. Org. Chem.* **2023**, *88* (7), 4472–4480.
<https://doi.org/10.1021/acs.joc.2c03081>.
- (24) Luo, Y.; Lv, L.; Li, Z. Copper-Catalyzed Germyl-Azidation of Alkenes with Germanium Hydrides and Trimethylsilyl Azide. *Org. Lett.* **2022**, *24* (43), 8052–8056.
<https://doi.org/10.1021/acs.orglett.2c03302>.
- (25) Shen, K.; Wang, Q. Copper-Catalyzed Alkene Aminoazidation as a Rapid Entry to 1,2-Diamines and Installation of an Azide Reporter onto Azaheterocycles. *J. Am. Chem. Soc.* **2017**, *139* (37), 13110–13116. <https://doi.org/10.1021/jacs.7b06852>.
- (26) Shen, S.-J.; Zhu, C.-L.; Lu, D.-F.; Xu, H. Iron-Catalyzed Direct Olefin Diazidation via Peroxyester Activation Promoted by Nitrogen-Based Ligands. *ACS Catal.* **2018**, *8* (5), 4473–4482. <https://doi.org/10.1021/acscatal.8b00821>.
- (27) Yang, B.; Lu, Z. Visible-Light-Promoted Metal-Free Aerobic Hydroxyazidation of Alkenes. *ACS Catal.* **2017**, *7* (12), 8362–8365. <https://doi.org/10.1021/acscatal.7b02892>.
- (28) Zhao, D.; Kang, K.; Wan, W.; Jiang, H.; Deng, H.; Chen, Y.; Hao, J. Manganese-Mediated/-Catalyzed Oxidative Carboazidation of Acrylamides. *Org. Chem. Front.* **2017**, *4* (8), 1555–1560. <https://doi.org/10.1039/C7QO00217C>.
- (29) Cai, Y.; Chatterjee, S.; Ritter, T. Photoinduced Copper-Catalyzed Late-Stage Azidoarylation of Alkenes via Arylthianthrenium Salts. *J. Am. Chem. Soc.* **2023**, *145* (25), 13542–13548. <https://doi.org/10.1021/jacs.3c04016>.
- (30) Shen, Y.-T.; Ran, Y.-S.; Jiang, B.; Zhang, C.; Jiang, W.; Li, Y.-M. Azido-Difluoromethylthiolation of Alkenes with TMSN_3 and $\text{PhSO}_2\text{SCF}_2\text{H}$. *Org. Lett.* **2023**, *25* (24), 4525–4529. <https://doi.org/10.1021/acs.orglett.3c01562>.

- (31) Yu, J.; Jiang, M.; Song, Z.; He, T.; Yang, H.; Fu, H. Iron-Catalyzed Azidoalkylthiation of Alkenes with Trimethylsilyl Azide and 1-(Alkylthio)Pyrrolidine-2,5-Diones. *Adv. Synth. Catal.* **2016**, *358* (17), 2806–2810. <https://doi.org/10.1002/adsc.201600133>.
- (32) Zhu, C.-L.; Wang, C.; Qin, Q.-X.; Yruegas, S.; Martin, C. D.; Xu, H. Iron(II)-Catalyzed Azidotrifluoromethylation of Olefins and N-Heterocycles for Expedient Vicinal Trifluoromethyl Amine Synthesis. *ACS Catal.* **2018**, *8* (6), 5032–5037. <https://doi.org/10.1021/acscatal.8b01253>.
- (33) Wei, R.; Xiong, H.; Ye, C.; Li, Y.; Bao, H. Iron-Catalyzed Alkylazidation of 1,1-Disubstituted Alkenes with Diacylperoxides and TMSN₃. *Org. Lett.* **2020**, *22* (8), 3195–3199. <https://doi.org/10.1021/acs.orglett.0c00969>.
- (34) Fu, N.; Sauer, G. S.; Saha, A.; Loo, A.; Lin, S. Metal-Catalyzed Electrochemical Diazidation of Alkenes. *Science* **2017**, *357* (6351), 575–579. <https://doi.org/10.1126/science.aan6206>.
- (35) Liu, C.; Wang, X.; Li, Z.; Cui, L.; Li, C. Silver-Catalyzed Decarboxylative Radical Azidation of Aliphatic Carboxylic Acids in Aqueous Solution. *J. Am. Chem. Soc.* **2015**, *137* (31), 9820–9823. <https://doi.org/10.1021/jacs.5b06821>.
- (36) Wang, R.; Wang, C.-Y.; Liu, P.; Bian, K.-J.; Yang, C.; Wu, B.-B.; Wang, X.-S. Enantioselective Catalytic Radical Decarbonylative Azidation and Cyanation of Aldehydes. *Sci. Adv.* **2023**, *9* (35), eadh5195. <https://doi.org/10.1126/sciadv.adh5195>.
- (37) Ertl, P.; Schuhmann, T. A Systematic Cheminformatics Analysis of Functional Groups Occurring in Natural Products. *J. Nat. Prod.* **2019**, *82* (5), 1258–1263. <https://doi.org/10.1021/acs.jnatprod.8b01022>.

- (38) He, Z.; Moreno, J. A.; Swain, M.; Wu, J.; Kwon, O. Aminodealkenylation: Ozonolysis and Copper Catalysis Convert C(Sp³)-C(Sp²) Bonds to C(Sp³)-N Bonds. *Science* **2023**, *381* (6660), 877–886. <https://doi.org/10.1126/science.adi4758>.
- (39) Swain, M.; Sadykhov, G.; Wang, R.; Kwon, O. Dealkenylative Alkenylation: Formal σ -Bond Metathesis of Olefins. *Angew. Chem. Int. Ed.* **2020**, *59* (40), 17565–17571. <https://doi.org/10.1002/anie.202005267>.
- (40) Swain, M.; Bunnell, T.; Kim, J.; Kwon, O. Dealkenylative Alkynylation Using Catalytic FeII and Vitamin C. *J. Am. Chem. Soc.* **2022**, *144* (32), 14828–14837. <https://doi.org/10.1021/jacs.2c05980>.
- (41) Smaligo, A.; Kwon, O. Dealkenylative Thiylation of C(Sp³)-C(Sp²) Bonds. *Org. Lett.* **2019**, *21* (21), 8592–8597. <https://doi.org/10.1021/acs.orglett.9b03186>.
- (42) Smaligo, A.; Swain, M.; Quintana, J.; Tan, M.; Kim, D.; Kwon, O. Hydrodealkenylative C(Sp³)-C(Sp²) Bond Fragmentation. *SCIENCE* **2019**, *364* (6441), 681-+.
<https://doi.org/10.1126/science.aaw4212>.
- (43) Smaligo, A. J.; Wu, J.; Burton, N. R.; Hacker, A. S.; Shaikh, A. C.; Quintana, J. C.; Wang, R.; Xie, C.; Kwon, O. Oxodealkenylative Cleavage of Alkene C(Sp³)-C(Sp²) Bonds: A Practical Method for Introducing Carbonyls into Chiral Pool Materials. *Angew. Chem. Int. Ed.* **2020**, *59* (3), 1211–1215. <https://doi.org/10.1002/anie.201913201>.
- (44) Minisci, F.; Portolani, A. Peroxides and Diazonium Salts III. Azides and Nitriles of 1-Hydroxyhydroperoxides. *Gazz. Chim Ital* **1959**, *89*, 1941–1949.
- (45) Čeković, Z.; Cvetković, M. Functionallization of the δ -Carbon Atom by the Ferrous Ion Induced Decomposition of Alkyl Hydroperoxides in the Presence of Cupric Salts.

- Tetrahedron Lett.* **1982**, 23 (37), 3791–3794. [https://doi.org/10.1016/S0040-4039\(00\)87708-4](https://doi.org/10.1016/S0040-4039(00)87708-4).
- (46) Bao, J.; Tian, H.; Yang, P.; Deng, J.; Gui, J. Modular Synthesis of Functionalized Butenolides by Oxidative Furan Fragmentation. *Eur. J. Org. Chem.* **2020**, 2020 (3), 339–347. <https://doi.org/10.1002/ejoc.201901613>.
- (47) Wang, K.; Li, Y.; Li, X.; Li, D.; Bao, H. Iron-Catalyzed Asymmetric Decarboxylative Azidation. *Org. Lett.* **2021**, 23 (22), 8847–8851. <https://doi.org/10.1021/acs.orglett.1c03355>.
- (48) Xu, W.; Zhong, W.; Yang, Q.; Kato, T.; Liu, Y.; Maruoka, K. In-Situ-Generation of Alkylsilyl Peroxides from Alkyl Hydroperoxides and Their Subsequent Copper-Catalyzed Functionalization with Organosilicon Compounds. *Tetrahedron Lett.* **2021**, 75, 153144. <https://doi.org/10.1016/j.tetlet.2021.153144>.
- (49) Xu, W.; Liu, Y.; Kato, T.; Maruoka, K. The Formation of C–C or C–N Bonds via the Copper-Catalyzed Coupling of Alkylsilyl Peroxides and Organosilicon Compounds: A Route to Perfluoroalkylation. *Org. Lett.* **2021**, 23 (5), 1809–1813. <https://doi.org/10.1021/acs.orglett.1c00215>.
- (50) Liu, S.; Ma, P.; Zhang, L.; Shen, S.; Miao, H.-J.; Liu, L.; Houk, K. N.; Duan, X.-H.; Guo, L.-N. A Cheap Metal Catalyzed Ring Expansion/Cross-Coupling Cascade: A New Route to Functionalized Medium-Sized and Macrolactones. *Chem. Sci.* **2023**, 14 (19), 5220–5225. <https://doi.org/10.1039/D2SC06157K>.
- (51) Saldívar-González, F. I.; Lenci, E.; Trabocchi, A.; Medina-Franco, J. L. Exploring the Chemical Space and the Bioactivity Profile of Lactams: A Chemoinformatic Study. *RSC Adv.* **2019**, 9 (46), 27105–27116. <https://doi.org/10.1039/C9RA04841C>.

- (52) Pruteanu, E.; Gîrbu, V.; Ungur, N.; Persoons, L.; Daelemans, D.; Renaud, P.; Kulçitki, V. Preparation of Antiproliferative Terpene-Alkaloid Hybrids by Free Radical-Mediated Modification of Ent-Kauranic Derivatives. *Molecules* **2021**, *26* (15), 4549. <https://doi.org/10.3390/molecule2-87154549>.
- (53) Jia, S.-M.; Huang, Y.-H.; Wang, Z.-L.; Fan, F.-X.; Fan, B.-H.; Sun, H.-X.; Wang, H.; Wang, F. Hydroamination of Unactivated Alkenes with Aliphatic Azides. *J. Am. Chem. Soc.* **2022**, *144* (36), 16316–16324. <https://doi.org/10.1021/jacs.2c07643>.
- (54) Ichinomiya, T.; Cho, S.; Higashijima, U.; Matsumoto, S.; Maekawa, T.; Sumikawa, K. High-Dose Fasudil Preserves Postconditioning against Myocardial Infarction under Hyperglycemia in Rats: Role of Mitochondrial KATP Channels. *Cardiovasc. Diabetol.* **2012**, *11* (1), 28. <https://doi.org/10.1186/1475-2840-11-28>.
- (55) Mao, M.; Zeng, W.; Zheng, Y.; Fan, W.; Yao, Y. Fasudil Attenuates Syncytin-1-mediated Activation of Microglia and Impairments of Motor Neurons and Motor Function in Mice. *Drug Dev. Res.* **2024**, *85* (6), e22254. <https://doi.org/10.1002/ddr.22254>.
- (56) Huang, Y.; Wu, J.; Su, T.; Zhang, S.; Lin, X. Fasudil, a Rho-Kinase Inhibitor, Exerts Cardioprotective Function in Animal Models of Myocardial Ischemia/Reperfusion Injury: A Meta-Analysis and Review of Preclinical Evidence and Possible Mechanisms. *Front. Pharmacol.* **2018**, *9*, 1083. <https://doi.org/10.3389/fphar.2018.01083>.
- (57) Suh, S.-E.; Chen, S.-J.; Mandal, M.; Guzei, I. A.; Cramer, C. J.; Stahl, S. S. Site-Selective Copper-Catalyzed Azidation of Benzylic C–H Bonds. *J. Am. Chem. Soc.* **2020**, *142* (26), 11388–11393. <https://doi.org/10.1021/jacs.0c05362>.

4.7. Materials and Methods

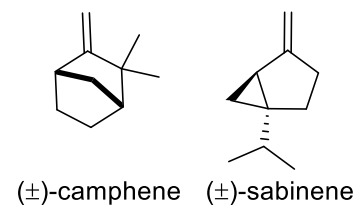
Unless otherwise stated, reactions were performed in flame-dried glassware fitted with rubber septa, under an argon atmosphere, and stirred with Teflon-coated magnetic stirring bars. Liquid reagents and solvents were transferred via syringe using standard Schlenk techniques. Methanol (MeOH) was distilled over magnesium under an argon atmosphere. Dichloromethane (DCM), acetonitrile (MeCN), and triethylamine were distilled over calcium hydride under an argon atmosphere. Tetrahydrofuran (THF), benzene, toluene, and diethyl ether were distilled over sodium/benzophenone ketyl under an argon atmosphere. All other solvents and reagents were used as received from commercial sources, unless otherwise noted. Reaction temperatures above 23 °C refer to oil bath temperatures. Thin layer chromatography (TLC) was performed using SiliCycle silica gel 60 F-254 precoated plates (0.25 mm) and visualized under UV irradiation, with a cerium ammonium molybdate (CAM) stain or a potassium permanganate (KMnO₄) stain. SiliCycle Silica-P silica gel (particle size 40–63 μm) was used for flash column chromatography (FCC). ¹H and ¹³C NMR spectra were recorded using Bruker AV-500, AV-400, and AV-300 MHz spectrometers, with ¹³C NMR spectroscopic operating frequencies of 125, 100, and 75 MHz, respectively. Chemical shifts (δ) are reported in parts per million (ppm) relative to the residual protonated solvent signal: CDCl₃ (δ = 7.26 for ¹H NMR; δ = 77.16 for ¹³C NMR), CD₃OD (δ = 3.31 for ¹H NMR; δ = 49.00 for ¹³C NMR). Data for ¹H NMR spectra are reported as follows: chemical shift, multiplicity, coupling constant(s) (Hz), and number of hydrogen atoms. Data for ¹³C NMR spectra are reported in terms of chemical shift. The following abbreviations are used to describe the multiplicities: s = singlet; d = doublet; t = triplet; q = quartet; quint = quintet; m = multiplet; br = broad. Melting points (MP) are uncorrected and were recorded using an Electrothermal® capillary melting point apparatus. IR spectra were recorded using a Jasco

FTIR4100 spectrometer with an ATR attachment; the selected signals are reported in units of cm^{-1} . Optical rotations were recorded using an Autopol IV polarimeter and a 100-mm cell, at concentrations close to 1 g/100 mL. HRMS (ESI) was performed using a Waters LCT Premier spectrometer equipped with an ACQUITY UPLC system and autosampler. HRMS (DART) was performed using a Thermo Fisher Scientific Exactive Plus spectrometer equipped with an IonSense ID-CUBE DART source. Ozonolysis was performed using a Globalozone GO-D3G (3 g/h) ozone generator (2.0 L/min, 100% power, O_2 feed gas).

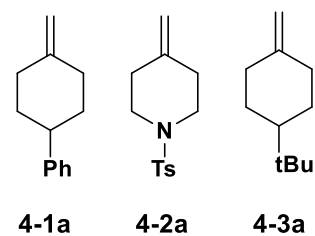
Caution: Ozone is an extremely toxic and reactive oxidant that can react with some compounds to form explosive and shock-sensitive products. Although we have not encountered any ozone-related safety issues in our laboratory, reactions with ozone should be performed only by properly trained individuals in a well-ventilated fume hood (use of a blast-shield is also recommended, especially for reactions performed on larger scales). Furthermore, caution should be taken when preparing solutions of copper salts and azides which could potentially form explosive copper azide complexes. Organic azide waste should be placed in a separate, explicitly labeled container designated solely for azide waste and extra caution must be taken to make certain that azide waste does not come in contact with acid. Acids can protonate the azide ion to form hydrazoic acid which is both acutely toxic (mouse $\text{LD}_{50} = 22 \text{ mg/kg}$) and a powerful explosive. Although the authors have not encountered such hazards under the standard conditions at scales described, adequate safety measures should be taken and reactions should be performed only by properly trained individuals in a well-ventilated fume hood.

4.7.1. Substrate Preparation

The following substrates were purchased from commercial sources and were used as received.



The following known compounds, **4-1a**¹, **4-2a**², **4-3a**³, were prepared according to the following adapted procedure^{1a} from the corresponding ketones. All physical and spectral data is in alignment with known literature data.

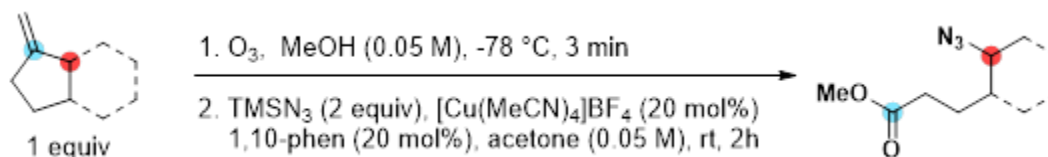


General Olefination Procedure:

To a solution of t-BuOK (1.5 equiv) in dry Et₂O (0.38 M) was added Ph₃PCH₂Br (1.5 equiv) under Ar at rt. The solution turned yellow. The reaction mixture was stirred 30 min. Ketone (1 equiv) in dry Et₂O (0.33 M) was then canulated into the reaction mixture. It was then stirred 1.5 h or until reaction was complete by TLC. The reaction mixture was then diluted with Et₂O and was washed with water. The combined organic layers were dried over MgSO₄, filtered and concentrated under reduced pressure to afford a crude residue. The crude mixture was then purified by flash chromatography on silica gel.

4.8. Experimental Procedures and Characterization Data

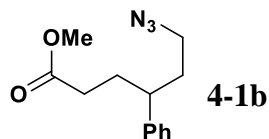
4.8.1. General procedure for azidation



An oven-dried 8-mL Schlenk tube equipped with a magnetic stirrer bar was charged with $\text{Cu}(\text{MeCN})_4\text{BF}_4$ (12.6 mg, 0.0400 mmol, 20 mol %), and 1,10-phenanthroline (7.2 mg, 0.0400 mmol, 20 mol %). The tube was purged with argon three times and then dry acetone (2 mL) was added. This mixture was stirred at room temperature for 10 min. After this time TMS-N_3 (46.1 mg, 0.400 mmol, 2 equiv) was added via Hamilton syringe and the mixture was allowed to stir for another 5 minutes.

A 25-mL round-bottom flask equipped with a magnetic stir bar was charged with alkene (0.200 mmol, 1.0 equiv) and MeOH (8 mL, 0.025 M), then cooled to $-78\text{ }^\circ\text{C}$ in a dry-ice/acetone bath. Ozone was bubbled through the solution until complete consumption of the starting material (as indicated by TLC and/or a blue color in the reaction mixture). The solution was sparged with argon for 5 min to expel excess ozone, then the stir bar was removed and the MeOH evaporated in vacuo. The residue was dissolved in benzene (8 mL) and the solution concentrated in vacuo to azeotrope off any residual water. This residue was dissolved in acetone (2 mL) to form a 0.1 M solution. This solution was transferred into the Schlenk tube via syringe. The reaction vessel was stirred at room temperature for 2 h, or until complete by TLC. After completion the reaction mixture was passed through a short plug of celite to remove the copper salts and then the filtrate was concentrated *in vacuo*. The crude material was then purified by flash column chromatography (FCC) on SiO_2 to afford the title compound.

4.8.2. Characterization data



Yield: 98%

Physical State: colorless oil

¹H NMR (400 MHz, CDCl₃) δ 7.37 – 7.26 (m, 2H), 7.25 – 7.19 (m, 1H), 7.18 – 7.08 (m, 2H), 3.61 (s, 3H), 3.17 (ddd, *J* = 12.6, 7.5, 5.1 Hz, 1H), 3.04 (ddd, *J* = 12.3, 8.2, 7.1 Hz, 1H), 2.68 (sept, *J* = 5.0 Hz, 1H), 2.22 – 2.10 (m, 2H), 2.06 – 1.80 (m, 4H).

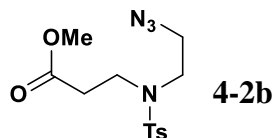
¹³C NMR (126 MHz, CDCl₃) δ 173.82, 142.64, 128.79, 127.64, 126.85, 51.54, 49.42, 42.52, 35.72, 32.04, 31.60.

HRMS (DART): calc'd for C₁₃H₁₈N₃O₂ [M+H]⁺ = 248.1394, Found: 248.13945

IR (neat, ATR): ν_{max} 3028, 2949, 2873, 2094, 1735, 1603, 1453, 1196, 701 cm⁻¹.

R_f = 0.39 (10% EtOAc/hexanes)

Purification: (SiO₂, 0 to 20% EtOAc/hexanes)



*15 mol% catalyst & ligand used

Yield: 88%

Physical State: colorless oil

¹H NMR (400 MHz, CDCl₃) δ 7.76 – 7.64 (m, 2H), 7.39 – 7.27 (m, 2H), 3.68 (s, 3H), 3.50 (t, *J* = 6.3 Hz, 2H), 3.45 (t, *J* = 7.2 Hz, 3H), 3.27 (t, *J* = 6.3 Hz, 2H), 2.69 (t, *J* = 7.3 Hz, 2H), 2.43 (s, 3H).

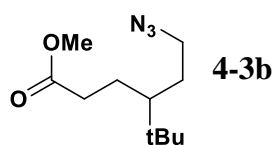
^{13}C NMR (100 MHz, CDCl_3) δ 171.76, 143.88, 135.83, 129.91, 127.27, 51.87, 50.70, 48.60, 45.60, 34.35, 21.54.

HRMS (ESI-TOF): calc'd for $\text{C}_{13}\text{H}_{18}\text{N}_4\text{O}_4\text{SNa}$ $[\text{M}+\text{Na}]^+ = 349.0941$, Found: 349.0944

IR (neat, ATR): ν_{max} 2953, 2927, 2103, 1733, 1594, 1440, 1336, 1305, 1154, 816 cm^{-1} .

Rf = 0.34 (40% EtOAc/hexanes)

Purification: (SiO_2 , 20 to 40% EtOAc/hexanes)



Yield: 48%

Physical State: colorless oil

^1H NMR (400 MHz, CDCl_3) δ 3.67 (s, 3H), 3.41 – 3.15 (m, 2H), 2.45 – 2.23 (m, 2H), 1.93 – 1.74 (m, 2H), 1.39 – 1.25 (m, 2H), 0.99 (sept, $J = 3.6$ Hz, 1H), 0.89 (s, 9H).

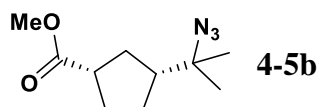
^{13}C NMR (126 MHz, CDCl_3) δ 174.04, 51.59, 51.44, 45.20, 33.99, 33.94, 30.33, 27.50, 26.36.

HRMS (ESI-TOF): calc'd for $\text{C}_{11}\text{H}_{22}\text{N}_3\text{O}_2$ $[\text{M}+\text{H}]^+ = 228.1707$, Found: 228.1713

IR (neat, ATR): ν_{max} 2960, 2873, 2094, 1739, 1473, 1436, 1162 cm^{-1} .

Rf = 0.79 (20% EtOAc/hexanes)

Purification: (SiO_2 , 0 to 5% EtOAc/hexanes)



Yield: 65%

Physical State: colorless oil

¹H NMR (400 MHz, CDCl₃) δ 3.65 (s, 3H), 2.76 (p, *J* = 7.6 Hz, 1H), 2.04 – 1.92 (m, 2H), 1.86 (dd, *J* = 14.5, 8.1 Hz, 2H), 1.71 – 1.59 (m, 3H), 1.18 (d, *J* = 3.7 Hz, 6H).

¹³C NMR (101 MHz, CDCl₃) δ 176.92, 71.64, 51.67, 50.93, 43.76, 31.36, 29.49, 28.18, 28.15, 26.26.

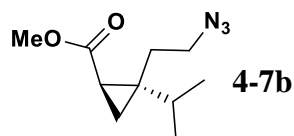
HRMS (ESI-TOF): calc'd for C₁₀H₁₈N₃O₂ [M+H]⁺ = 212.1394, Found:

IR (neat, ATR): ν_{max} 2960, 2873, 2094, 1739, 1473, 1436, 1162 cm⁻¹.

R_f = 0.45 (40% EtOAc/hexanes)

Purification: (SiO₂, 50 to 70% Et₂O/hexanes)

Note: 20 mol% of bipyridine was used as the ligand instead



Yield: 80%

Physical State: colorless oil

¹H NMR (500 MHz, CDCl₃) δ 3.67 (s, 3H), 3.31 (m, 1H), 3.23 (m, 1H), 1.92 – 1.77 (m, 2H), 1.58 (dd, *J* = 8.4, 5.6 Hz, 1H), 1.41 (hept, *J* = 6.8 Hz, 1H), 1.08 (t, *J* = 5.3 Hz, 1H), 0.95 (dd, *J* = 8.3, 4.8 Hz, 1H), 0.91 (dd, *J* = 16.9, 6.9 Hz, 6H).

¹³C NMR (126 MHz, CDCl₃) δ 173.09, 51.74, 49.92, 34.05, 33.29, 27.04, 24.29, 19.33, 19.25, 18.93.

HRMS (ESI-TOF): calc'd for C₁₀H₁₈N₃O₂ [M+H]⁺ = 212.1394, Found: 212.13878

IR (neat, ATR): ν_{max} 2957, 2873, 2147, 1653, 1472, 1443, 1364, 1210 cm⁻¹.

R_f = 0.41 (10% EtOAc/hexanes)

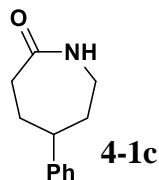
Purification: (SiO₂, 0 to 10% EtOAc/hexanes)

4.8.3. General procedure for reduction

Method A: A round bottomed flask (rbf) was charged with stir bar and was added 10% wt palladium on carbon (0.1000 equiv). The rbf was sealed with a rubber septa and placed under N₂ atmosphere after which Et₂O was added via syringe to produce a 0.3M solution with respect to the azide. To the stirred mixture was added via syringe the azido ester substrate as a 0.1M solution in Et₂O. The N₂ inlet was removed and an H₂ balloon was inserted into the reaction vessel via needle. A smaller gauge needle was briefly pierced through the septa to exchange atmosphere with H₂. The reaction was stirred for 22 hrs or until consumption of starting material was determined by TLC. Once complete, the H₂ balloon was removed, and the reaction was sparged with Ar. The reaction was then diluted with Et₂O and filtered through a celite plug to remove solids and the filtrate was evaporated *in vacuo* at 0° C. The crude material was then purified by FCC on SiO₂ to afford the title compounds.

Method B: As in method A, but the crude amine material from hydrogenation (1 equiv) was placed in rbf and MeOH (0.02M) was added. The rbf was sealed with a rubber septa, placed under N₂ atmosphere and to this mixture was added a 35% solution of NaOMe in MeOH (10 equiv). A reflux condenser was attached to the rbf, sealed with a rubber septa and an N₂ inlet was introduced. The reaction was heated to reflux and allowed to stir for 48h or until conversion of the amine to the lactam was complete as determined by TLC. The reaction was then filtered through a celite plug and the filtrate was evaporated *in vacuo* at 0 °C. The crude material was then purified by FCC on SiO₂ to afford the title compound.

4.8.4. Characterization data



Prepared by method B.

Note: Compound is known, all physical and spectral data are in accordance with the literature.⁴

Yield: 86%

Physical State: white solid

¹H NMR (400 MHz, CDCl₃) δ 7.37 – 7.26 (m, 2H), 7.25 – 7.19 (m, 1H), 7.19 – 7.09 (m, 2H), 6.44 (br s, 1H), 3.47 – 3.23 (m, 2H), 2.77 (tt, *J* = 12.1, 3.4 Hz, 1H), 2.69 – 2.51 (m, 2H), 2.07 – 1.94 (m, 2H), 1.85 – 1.67 (m, 2H).

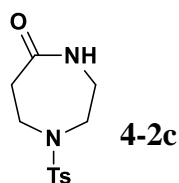
¹³C NMR (101 MHz, CDCl₃) δ 178.33, 146.29, 128.68, 126.66, 126.58, 48.85, 42.21, 37.34, 30.53.

HRMS (DART): calc'd for C₁₂H₁₆NO [M+H]⁺ = 190.1226, Found: 190.12258

IR (neat, ATR): ν_{max} 3411 (br), 3056, 2985, 1659, 1556, 1485, 746 cm⁻¹.

R_f = 0.20 (5% MeOH/DCM)

Purification: (SiO₂, 5% MeOH in DCM)



Prepared by method A with EtOAc used instead of MeOH.

Note: Compound is known, all physical and spectral data are in accordance with the literature.⁵

Yield: 65%

Physical State: white solid

¹H NMR (500 MHz, CDCl₃) δ 7.63 (d, *J* = 8.4 Hz, 2H), 7.35 – 7.30 (m, 2H), 6.01 (br s, 1H), 3.42 – 3.37 (m, 2H), 3.35 – 3.22 (m, 4H), 2.79 – 2.67 (m, 2H), 2.43 (s, 3H).

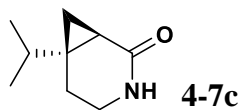
¹³C NMR (126 MHz, CDCl₃) δ 176.13, 144.02, 134.37, 129.96, 127.27, 50.24, 43.69, 42.83, 38.08, 21.55.

HRMS (ESI-TOF): calc'd for C₁₂H₁₇N₂O₃S [M+H]⁺ = 269.0954, Found: 269.0943

IR (neat, ATR): ν_{max} 3213 (br), 3088, 2933, 2899, 1659, 1333, 1317, 1157, 1100, 812, cm⁻¹.

R_f = 0.31 (5% 7N NH₃ in MeOH: DCM)

Purification: (SiO₂, 5% 7N NH₃ in MeOH: DCM)



Prepared by method A.

Note: Compound is known, all physical and spectral data are in accordance with the literature.⁶

Yield: 80%

Physical State: clear oil

¹H NMR (500 MHz, CDCl₃) δ 6.42 (br s, 1H), 3.23 – 3.14 (m, 1H), 3.10 – 2.97 (m, 1H), 1.87 – 1.76 (m, 2H), 1.46 – 1.40 (m, 1H), 1.34 (t, *J* = 4.3 Hz, 1H), 1.17 (q, *J* = 6.9 Hz, 1H), 0.97 (qd, *J* = 7.0, 1.5 Hz, 6H), 0.81 (ddd, *J* = 9.5, 5.4, 1.9 Hz, 1H).

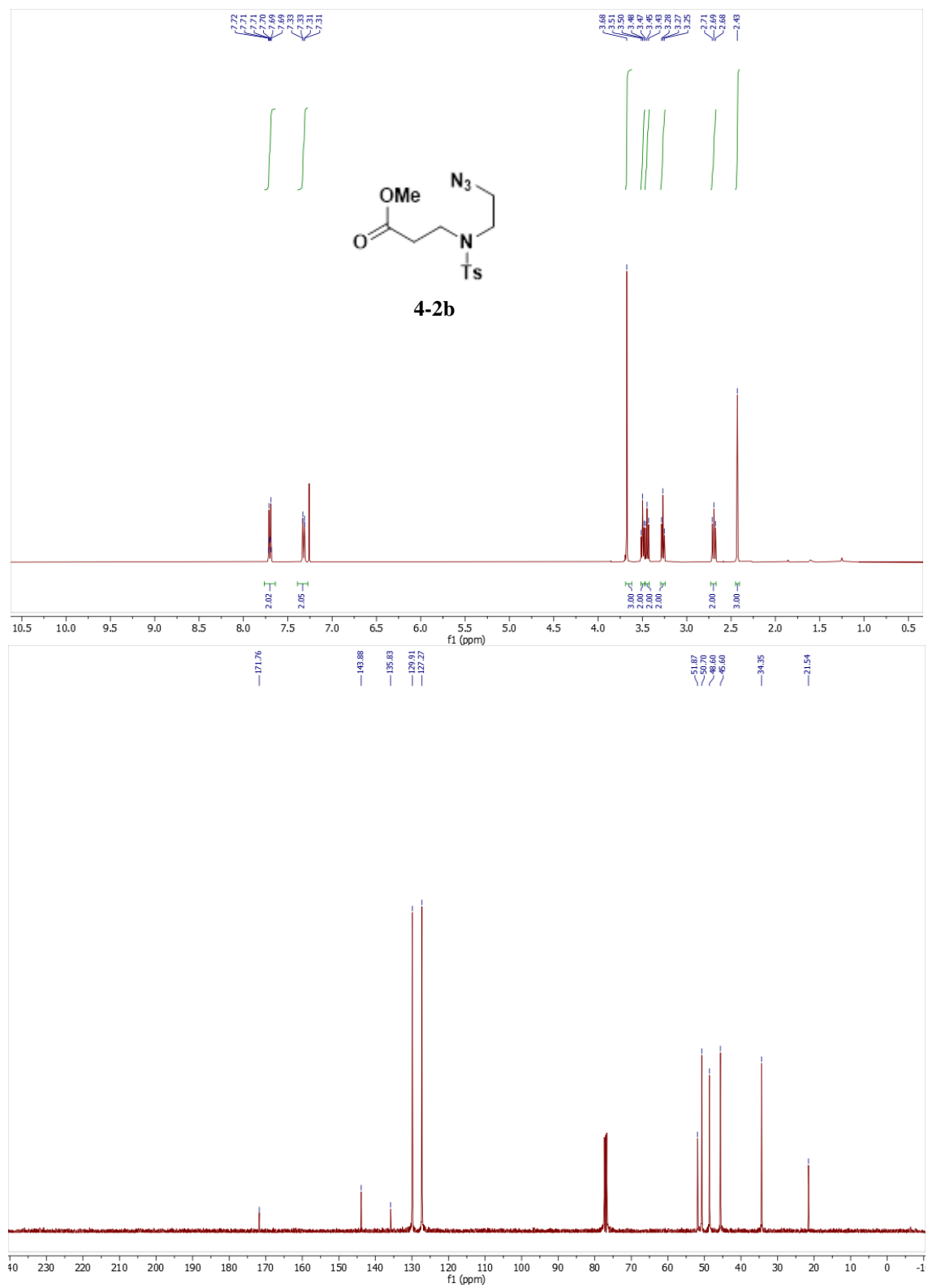
¹³C NMR (126 MHz, CDCl₃) δ 174.15, 37.37, 35.65, 30.66, 23.91, 19.93, 19.25, 19.01, 14.12.

HRMS (ESI-TOF): calc'd for C₉H₁₆NO [M+H]⁺ = 154.1226, Found: 154.1228

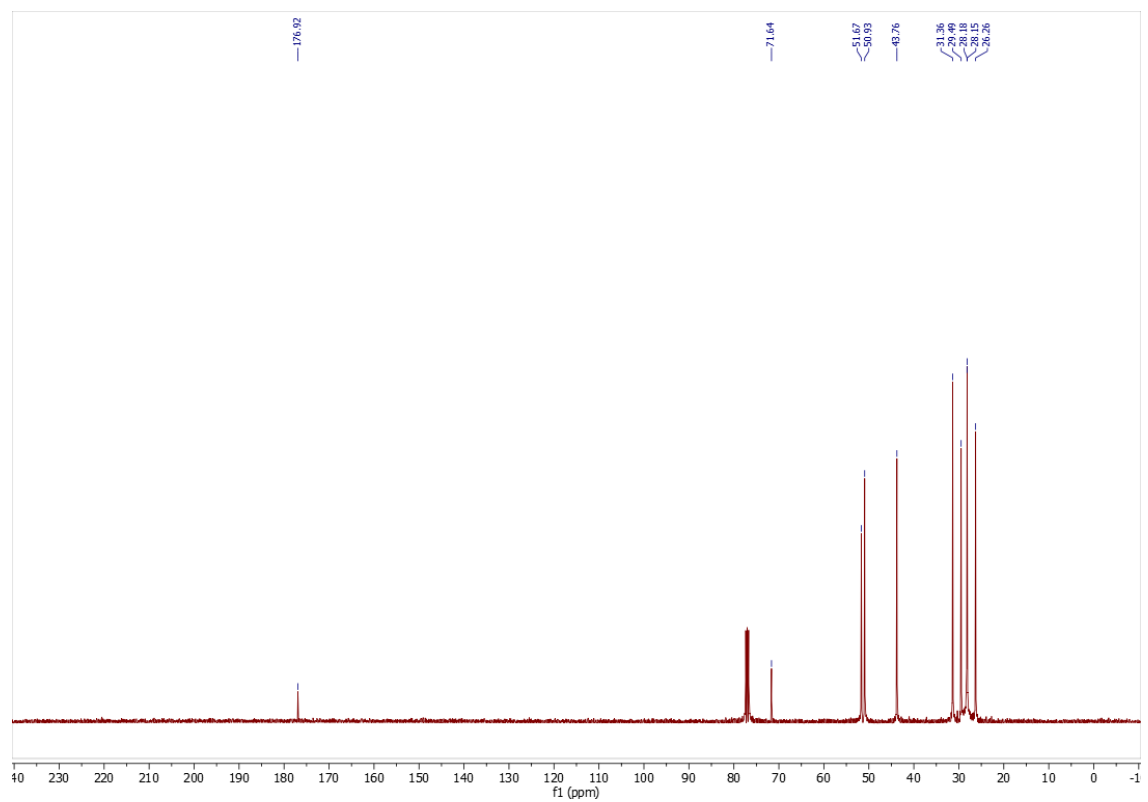
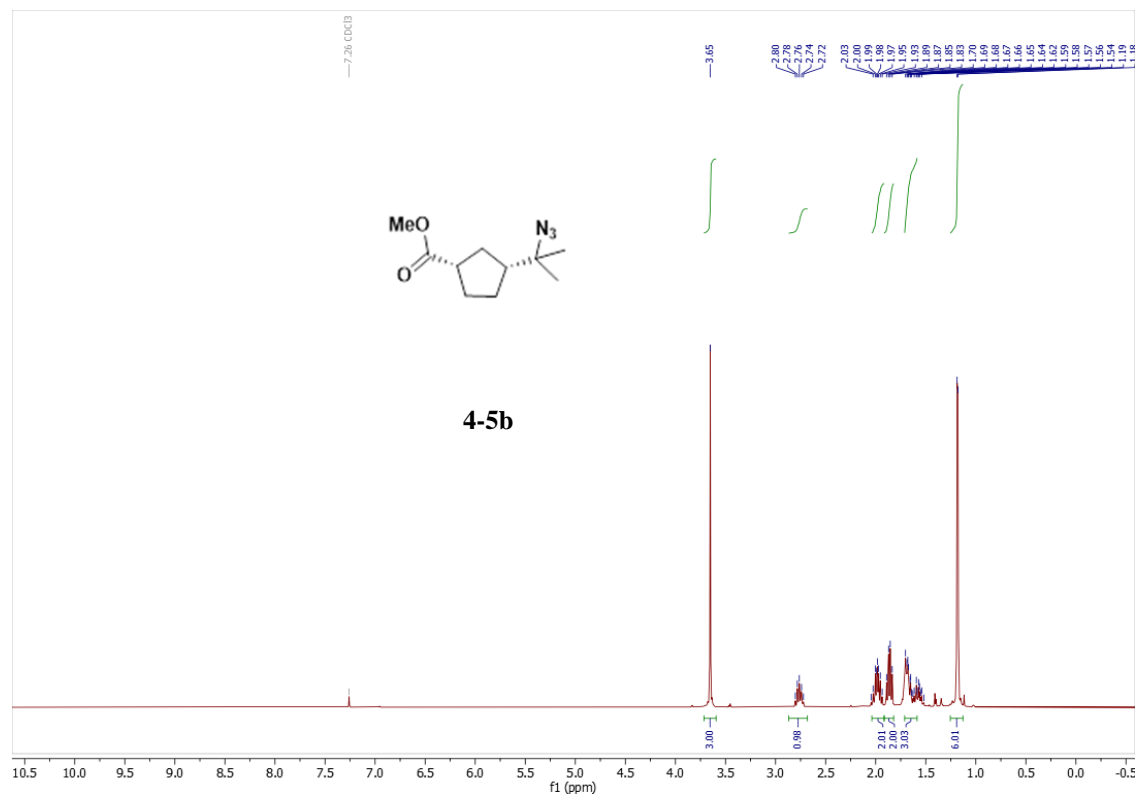
IR (neat, ATR): ν_{max} 3375 (br), 2966, 1655, 1559, 1471, 1361 cm⁻¹.

R_f = 0.20 (33% acetone/hexanes)

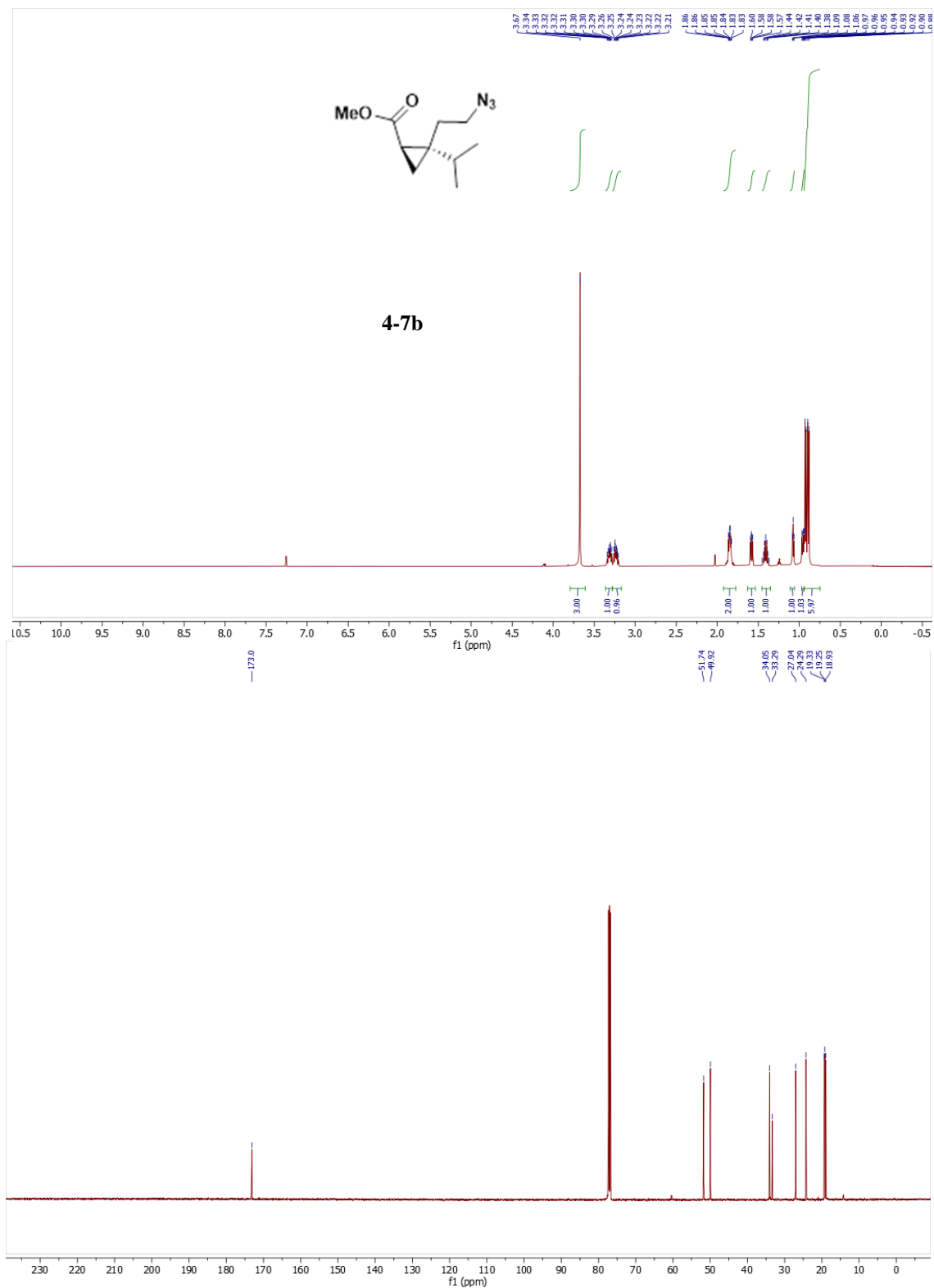
Purification: (SiO₂, 20 to 40% Acetone/hexanes)



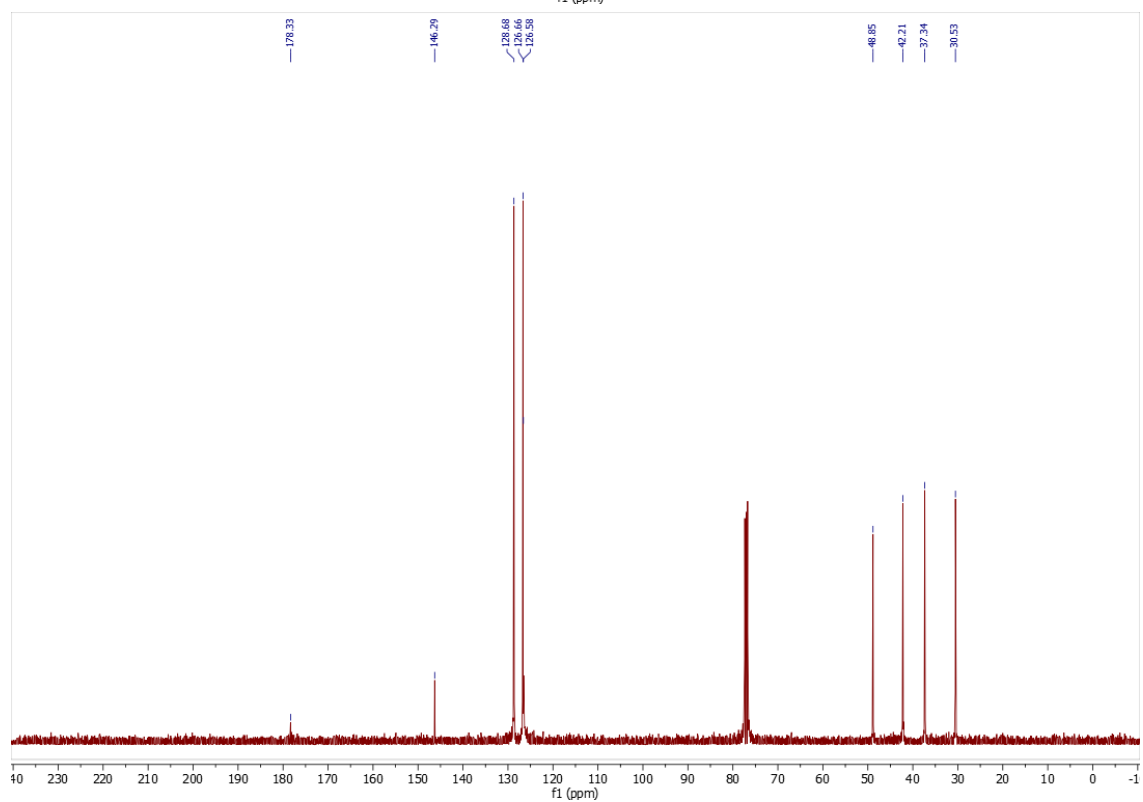
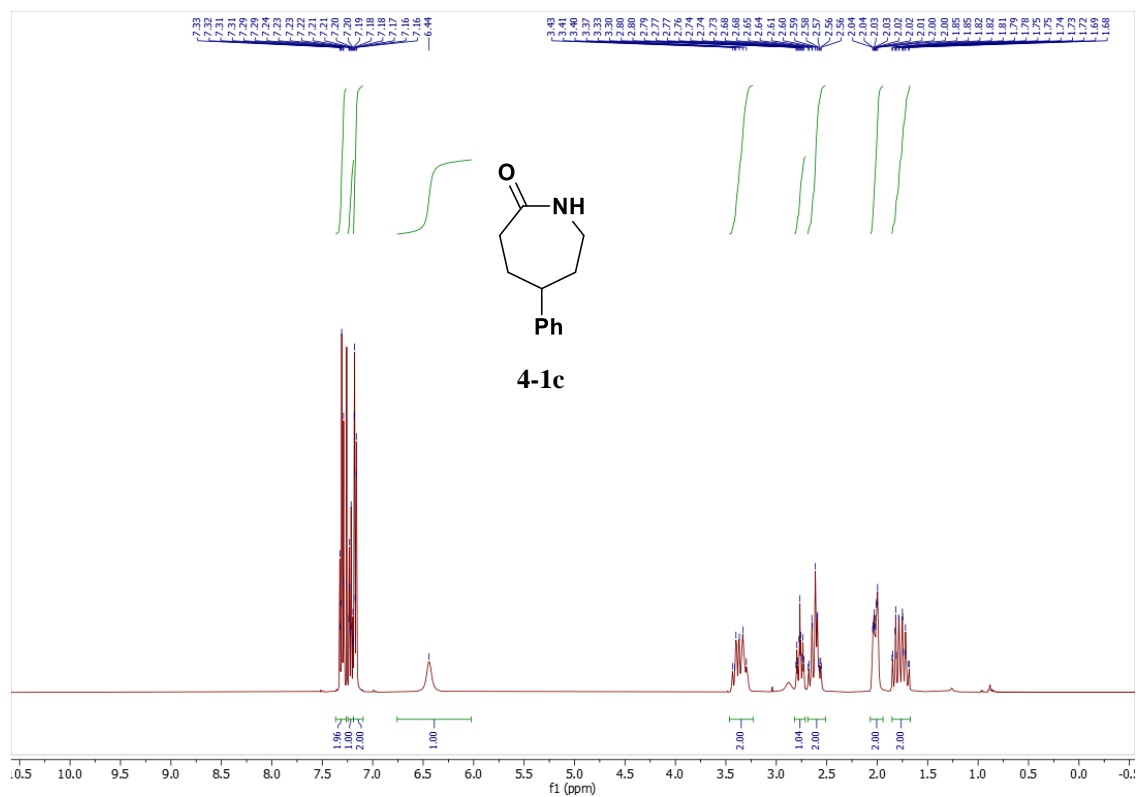
¹H NMR (400 MHz, CDCl₃) & ¹³C NMR (100 MHz, CDCl₃) spectra of **4-2b**



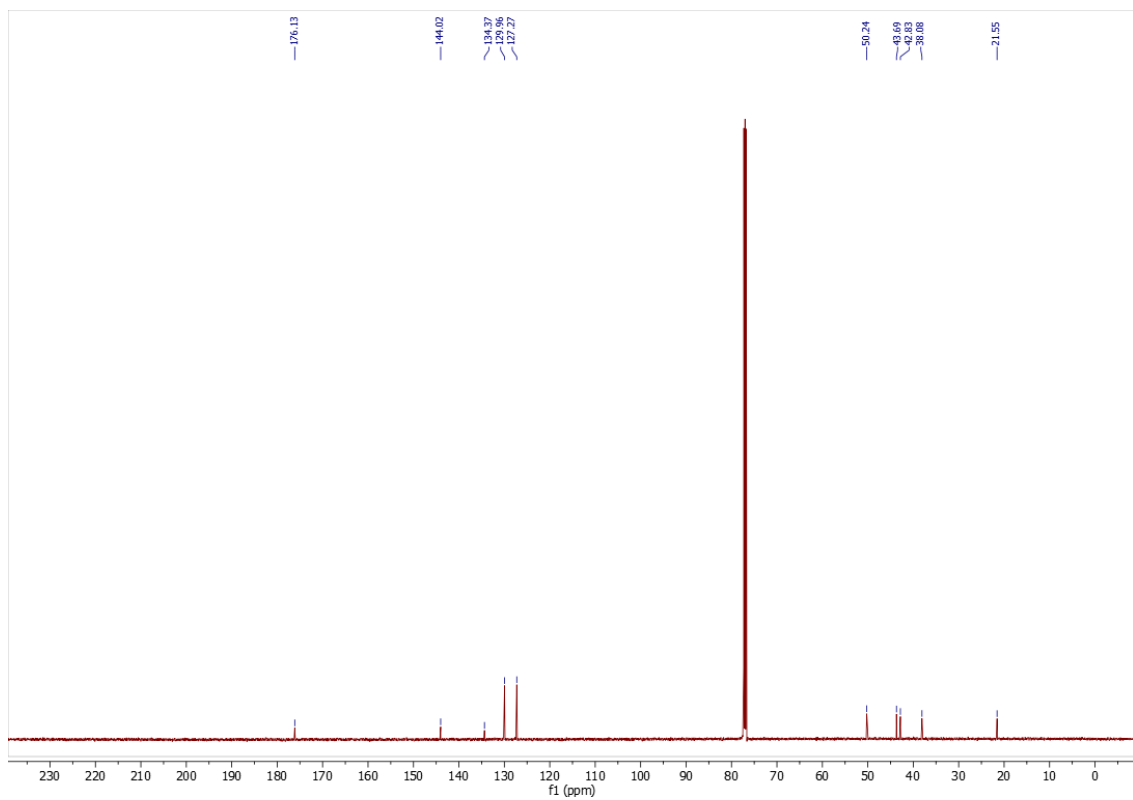
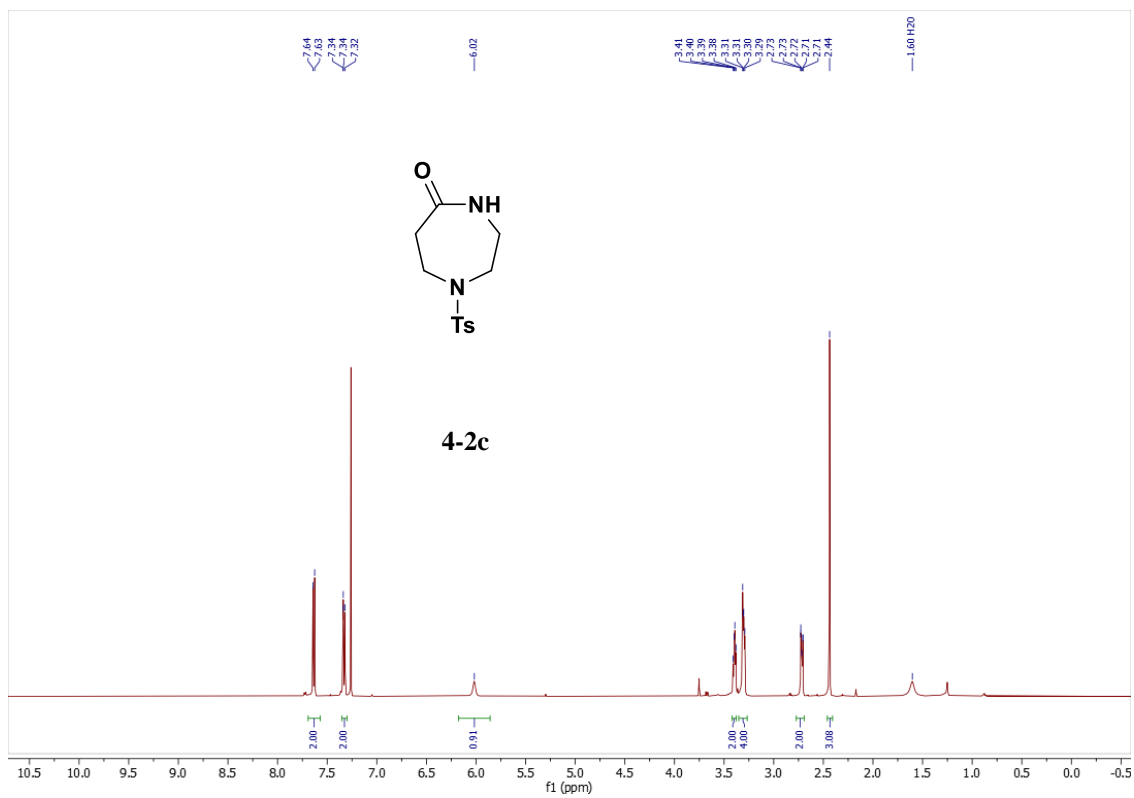
¹H NMR (400 MHz, CDCl₃) & ¹³C NMR (100 MHz, CDCl₃) spectra of **4-5b**



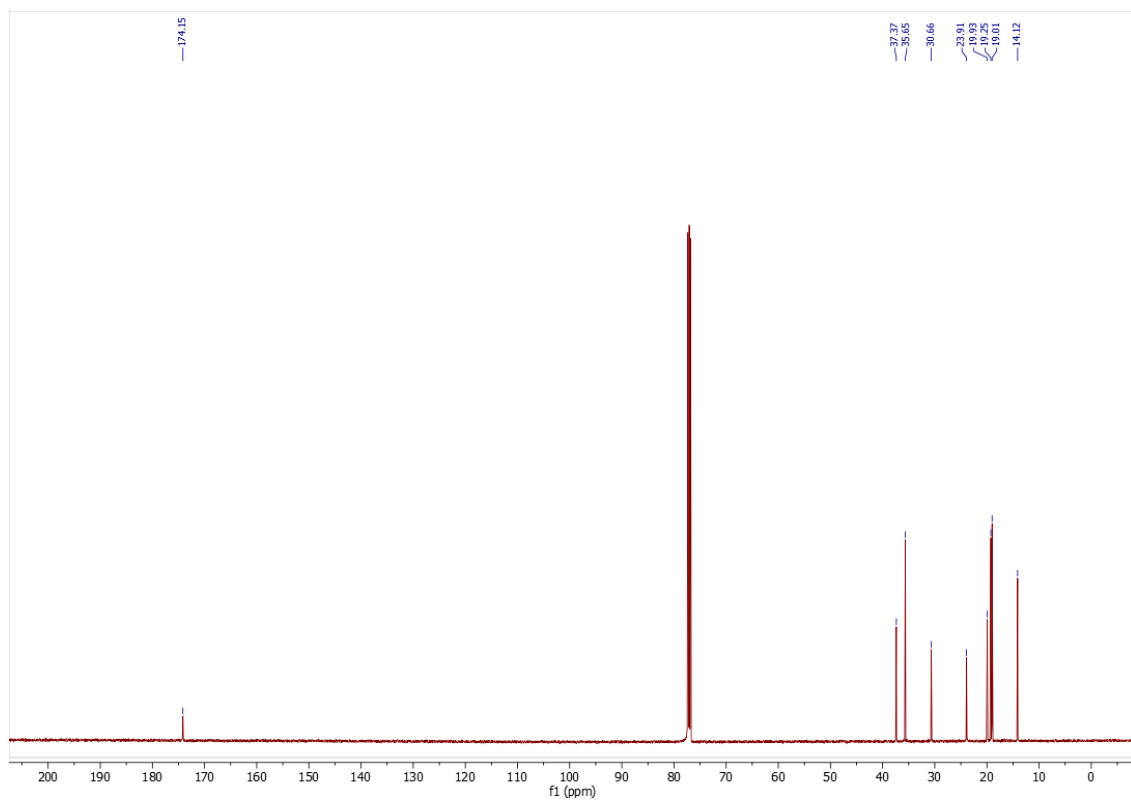
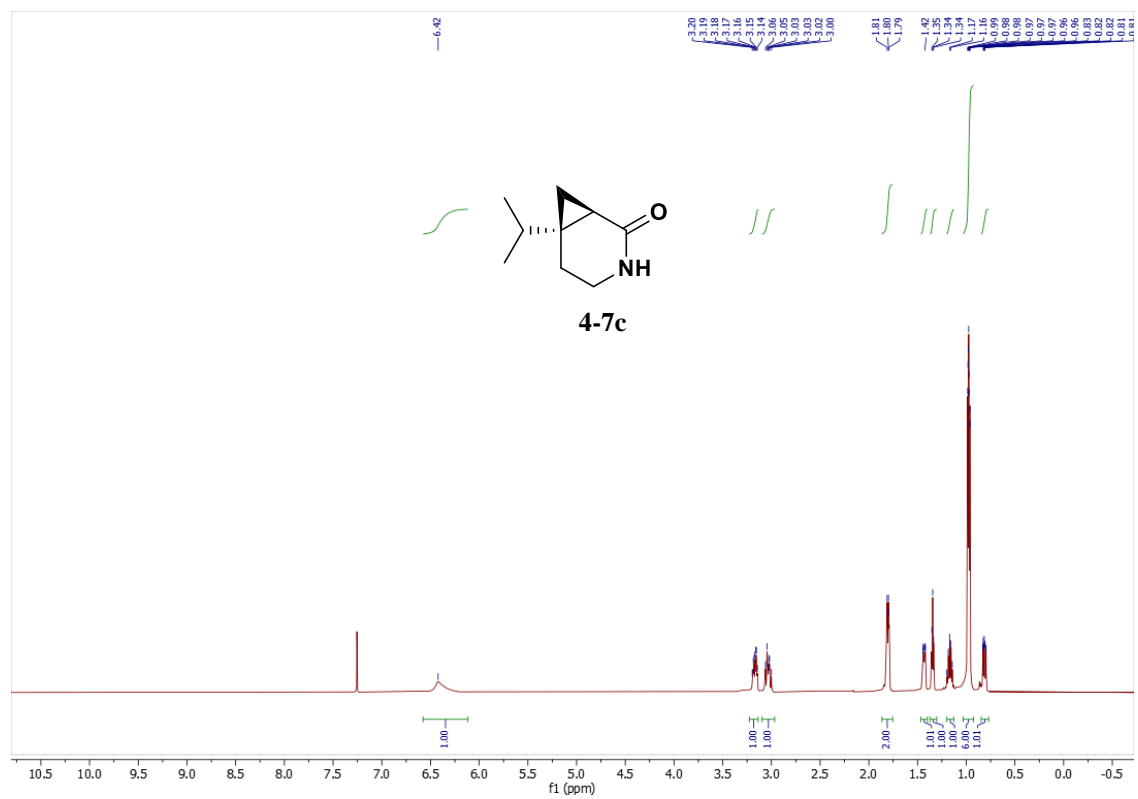
¹H NMR (500 MHz, CDCl₃) & ¹³C NMR (126 MHz, CDCl₃) spectra of 4-7b



¹H NMR (400 MHz, CDCl₃) & ¹³C NMR (101 MHz, CDCl₃) spectra of **4-1c**



¹H NMR (500 MHz, CDCl₃) & ¹³C NMR (126 MHz, CDCl₃) spectra of **4-2c**



¹H NMR (500 MHz, CDCl₃) & ¹³C NMR (126 MHz, CDCl₃) spectra of 4-7c

4.9. References relevant to substrate preparation

- (1) Soulard, V.; Villa, G.; Vollmar, D. P.; Renaud, P. Radical Deuteration with D₂O: Catalysis and Mechanistic Insights. *J. Am. Chem. Soc.* **2018**, *140* (1), 155–158. <https://doi.org/10.1021/jacs.7b12105>.
- (2) Liu, J.; Rong, J.; Wood, D. P.; Wang, Y.; Liang, S. H.; Lin, S. Co-Catalyzed Hydrofluorination of Alkenes: Photocatalytic Method Development and Electroanalytical Mechanistic Investigation. *J. Am. Chem. Soc.* **2024**, *146* (7), 4380–4392. <https://doi.org/10.1021/jacs.3c10989>.
- (3) Albitz, K.; Csókás, D.; Dobi, Z.; Pápai, I.; Soós, T. Late-Stage Formal Double C–H Oxidation of Prenylated Molecules to Alkylidene Oxetanes and Azetidines by Strain-Enabled Cross-Metathesis. *Angew Chem Int Ed* **2023**, *62* (13), e202216879. <https://doi.org/10.1002/anie.202216879>.
- (4) (a) Aube, J.; Wang, Y.; Hammond, M.; Tanol, M.; Takusagawa, F.; Vander Velde, D. Synthetic Aspects of an Asymmetric Nitrogen-Insertion Process: Preparation of Chiral, Non-Racemic Caprolactams and Valerolactams. Total Synthesis of (-)-Alloyohimbane. *J. Am. Chem. Soc.* **1990**, *112* (12), 4879–4891. <https://doi.org/10.1021/ja00168a038>.
(b) Lavinda, O.; Witt, C. H.; Woerpel, K. A. Origin of High Diastereoselectivity in Reactions of Seven-Membered-Ring Enolates. *Angew Chem Int Ed* **2022**, *61* (14), e202114183. <https://doi.org/10.1002/anie.202114183>.
- (5) (a) Gao, J.; Wang, X. L.; Li, Y. Z.; Ye, D.; Xie, C. L. Preparation of fasudil hydrochloride. CN1021207392011. (b) Gao, J.; Wang, X.L.; Li, Y. Z.; Ye, D.; Xie, C. L. Preparation of homopiperazine and its derivatives. CN1021207322011.

(6) Gnilka, R.; Wawrzeńczyk, C. Synthesis of Sabina δ -Lactones and Sabina δ -Lactams from (+)-Sabinene. *Aust. J. Chem.* **2013**, *66* (11), 1399.

<https://doi.org/10.1071/CH13306>.